Food Engineering Series
Series Editor: Gustavo V. Barbosa-Cánovas

Hao Feng
Gustavo V. Barbosa-Cánovas
Jochen Weiss *Editors*

Ultrasound Technologies for Food and Bioprocessing

Springer

Food Engineering Series

Series Editor
Gustavo V. Barbosa-Cánovas, Washington State University

Advisory Board
José Miguel Aguilera, Pontificia Universidad Católica de Chile
Xiao Dong Chen, Monash University
J. Peter Clark, Clark Consulting
Richard W. Hartel, University of Wisconsin
Albert Ibarz, University of Lleida
Jozef Kokini, Rutgers University
Michèle Marcotte, Agriculture & Agri-Food Canada
Michael McCarthy, University of California at Davis
Keshavan Niranjan, University of Reading
Micha Peleg, University of Massachussetts-Amherst
Shafiur Rahman, Sultan Qaboos University
M. Anandha Rao, Cornell University
Yrjö Roos, University College Cork
Walter L. Spiess, Bundesforschungsanstalt
Jorge Welti-Chanes, Instituto Tecnológia y de Estudios Superiores de Monterrey

For further volumes:
http://www.springer.com/series/5996

Hao Feng · Gustavo V. Barbosa-Cánovas ·
Jochen Weiss
Editors

Ultrasound Technologies for Food and Bioprocessing

Springer

Editors
Hao Feng
Department of Food Science and Human Nutrition
University of Illinois at Urbana-Champaign
Urbana, IL 61801, USA
haofeng@illinois.edu

Jochen Weiss
Department of Food Structure and Functionality
Institute of Food Science and Biotechnology
Universität Hohenheim
Garbenstraße 21/25, 70599 Stuttgart
Germany
j.weiss@uni-hohenheim.de

Gustavo V. Barbosa-Cánovas
Department of Biological Systems Engineering
Washington State University
Pullman, WA 99164-6120, USA
barbosa@wsu.edu

ISSN 1571-0297
ISBN 978-1-4419-7471-6 e-ISBN 978-1-4419-7472-3
DOI 10.1007/978-1-4419-7472-3
Springer New York Dordrecht Heidelberg London

© Springer Science+Business Media, LLC 2011
All rights reserved. This work may not be translated or copied in whole or in part without the written permission of the publisher (Springer Science+Business Media, LLC, 233 Spring Street, New York, NY 10013, USA), except for brief excerpts in connection with reviews or scholarly analysis. Use in connection with any form of information storage and retrieval, electronic adaptation, computer software, or by similar or dissimilar methodology now known or hereafter developed is forbidden.
The use in this publication of trade names, trademarks, service marks, and similar terms, even if they are not identified as such, is not to be taken as an expression of opinion as to whether or not they are subject to proprietary rights.

Printed on acid-free paper

Springer is part of Springer Science+Business Media (www.springer.com)

Preface

The use of acoustic energy in food or bioprocessing operations is a relatively new endeavor if compared with other sources of energy, such as mechanical or thermal, which have been utilized for centuries in various applications. There are two important factors that make the current ultrasound-assisted processes possible. One is related with the development in ultrasound generation technology and the other one is the better understanding of interactions between acoustic energy and liquid media, enabling the development of important guidelines for ultrasound-based processes.

In addition to existing applications, there is an increasing list of potential uses of ultrasound in a wide range of industries. For food and bioprocessing purposes, it includes, for example, homogenization, cutting, extraction, inactivation of microorganisms, inactivation/activation of enzymes, drying enhancement, surface cleaning, depolymerization, crystallization, sieving, bio-component separation, peeling, nanoparticle production, particle size reduction, improvement of interface heat and mass transfer, and so on. It is, therefore, the strong belief of the editors that a comprehensive compilation summarizing the fundamentals of ultrasound technology, current developments, new research findings, and more importantly examples of industrial applications is very much needed to further the uses of ultrasound technology.

This book was designed to be an aid to a broad range of scientists and engineers in several fields, including food processing, food safety, chemistry, physics, chemical engineering, material science, agriculture, and bioprocessing-related disciplines. The 25 chapters in the book are organized into three sections. Section I (Chapters 1 to 4) covers fundamental aspects of ultrasound as well as high-intensity ultrasound applications. The basic concepts in acoustics, the theory of acoustic cavitation, and the physical and chemical effects of cavitation on biomaterials are detailed in three chapters. There is also a chapter dealing with the thermodynamic and kinetic aspects of ultrasound. Section II (Chapters 5 to 8) focuses on recent developments in the power ultrasound domain, where the four chapters elucidate important topics, such as how to use variable frequency strategies to enhance an ultrasound treatment and how to avoid the pitting problem in probe-type sonoreactors. This section also

includes non-traditional approaches to generate cavitation, which are very promising. The 17 chapters in Section III (Chapters 9 to 25) are dedicated to current and potential applications of power ultrasound mainly in the food processing and bioprocessing industries. Topics covered in these chapters include ultrasound-assisted unit operations, such as cutting, cleaning, homogenization, extraction, freezing, crystallization, drying, and membrane separation. In addition, the inactivation of microorganisms and enzymes are covered in detail in three chapters. The use of acoustic energy to change the functionality of food components and ingredients is also extensively covered in the two following chapters, and later on, specific applications, such as the utilization of power ultrasound in the dairy industry, are included. At the end, there is a chapter dealing with the sonochemistry of power ultrasound as applied to the production of nanomaterials.

We hope this book will not only prove to be useful in research and development efforts but will also facilitate the industrial adoption of power ultrasound. Finally, we would like to thank all of the authors for their efforts to contribute very stimulating chapters. Many of these authors also participated in reviewing the manuscripts, for which we are grateful. It was indeed a great pleasure to work with such a fine group of professionals.

Urbana, Illinois — Hao Feng
Pullman, Washington — Gustavo V. Barbosa-Cánovas
Stuttgart, Germany — Jochen Weiss

Contents

1 The Physical and Chemical Effects of Ultrasound 1
Sandra Kentish and Muthupandian Ashokkumar

2 Acoustic Cavitation 13
Olivier Louisnard and José González-García

3 Ultrasound Applications in Food Processing 65
Daniela Bermúdez-Aguirre, Tamara Mobbs,
and Gustavo V. Barbosa-Cánovas

4 The Thermodynamic and Kinetic Aspects of Power Ultrasound Processes 107
Hao Feng

5 Wideband Multi-Frequency, Multimode, and Modulated (MMM) Ultrasonic Technology 125
Miodrag Prokic

6 Application of Hydrodynamic Cavitation for Food and Bioprocessing 141
Parag R. Gogate

7 Contamination-Free Sonoreactor for the Food Industry 175
Jean-Luc Dion

8 Controlled Cavitation for Scale-Free Heating, Gum Hydration and Emulsification in Food and Consumer Products . . 191
Douglas G. Mancosky and Paul Milly

9 Ultrasonic Cutting of Foods 211
Yvonne Schneider, Susann Zahn, and Harald Rohm

10 Engineering Food Ingredients with High-Intensity Ultrasound . . . 239
Jochen Weiss, Kristberg Kristbergsson,
and Gunnar Thor Kjartansson

11 Manothermosonication for Microbial Inactivation 287
Santiago Condón, Pilar Mañas, and Guillermo Cebrián

12 Inactivation of Microorganisms 321
Stella Maris Alzamora, Sandra N. Guerrero, Marcela Schenk, Silvia Raffellini, and Aurelio López-Malo

13 Ultrasonic Recovery and Modification of Food Ingredients 345
Kamaljit Vilkhu, Richard Manasseh, Raymond Mawson, and Muthupandian Ashokkumar

14 Ultrasound in Enzyme Activation and Inactivation 369
Raymond Mawson, Mala Gamage, Netsanet Shiferaw Terefe, and Kai Knoerzer

15 Production of Nanomaterials Using Ultrasonic Cavitation – A Simple, Energy Efficient and Technological Approach 405
Sivakumar Manickam and Rohit Kumar Rana

16 Power Ultrasound to Process Dairy Products 445
Daniela Bermúdez-Aguirre and Gustavo V. Barbosa-Cánovas

17 Sonocrystallization and Its Application in Food and Bioprocessing 467
Parag R. Gogate and Aniruddha B. Pandit

18 Ultrasound-Assisted Freezing 495
A.E. Delgado and Da-Wen Sun

19 Ultrasound-Assisted Hot Air Drying of Foods 511
Antonio Mulet, Juan Andrés Cárcel, José Vicente García-Pérez, and Enrique Riera

20 Novel Applications of Power Ultrasonic Spray 535
Ke-ming Quan

21 High-Power Ultrasound in Surface Cleaning and Decontamination 545
Sami B. Awad

22 Effect of Power Ultrasound on Food Quality 559
Hyoungill Lee and Hao Feng

23 Ultrasonic Membrane Processing 583
Sandra Kentish and Muthupandian Ashokkumar

24 Industrial Applications of High Power Ultrasonics 599
Alex Patist and Darren Bates

25 Technologies and Applications of Airborne Power Ultrasound in Food Processing 617
Juan A. Gallego-Juárez and Enrique Riera

Index 643

Contributors

Stella Maris Alzamora Departamento de Industrias, Universidad de Buenos Aires, Ciudad Universitaria, 1428 Buenos Aires, Argentina, smalzamora@gmail.com

Muthupandian Ashokkumar School of Chemistry, University of Melbourne, Melbourne, VIC 3010, Australia, masho@unimelb.edu.au

Sami B. Awad VP Technology, Crest Ultrasonics Corp., Trenton, NJ 08628, USA, sawad@rcn.com

Gustavo V. Barbosa-Cánovas Biological Systems Engineering Department, Center for Nonthermal Processing of Food, Washington State University, Pullman, WA 99164-6120, USA, barbosa@wsu.edu

Darren Bates Cavitus, Queensland, Queensland, QLD 4564, Australia, dbates@cavitus.com

Daniela Bermúdez-Aguirre Biological Systems Engineering Department, Center for Nonthermal Processing of Food, Washington State University, Pullman, WA 99164-6120, USA, daniela@wsu.edu

Juan Andrés Cárcel Grupo de Análisis y Simulación de Procesos Agroalimentarios, Departamento de Tecnología de Alimentos, Universidad Politécnica de Valencia, 46022 Valencia, Spain, jcarcel@tal.upv.es

Guillermo Cebrián Departamento de Producción Animal y Ciencia de los Alimentos, Tecnología de los Alimentos, Facultad de Veterinaria, Universidad de Zaragoza, 50013, Zaragoza, Spain, guiceb@unizar.es

Santiago Condón Departamento de Producción Animal y Ciencia de los Alimentos, Tecnología de los Alimentos, Facultad de Veterinaria, Universidad de Zaragoza, 50013, Zaragoza, Spain, scondon@unizar.es

A.E. Delgado Food Refrigeration and Computerised Food Technology, Agriculture and Food Science Centre, University College Dublin, Belfield, Dublin 4, Ireland, adriana.delgado@ucd.ie

Jean-Luc Dion Département de Génie électrique et Génie informatique, Université du Québec à Trois-Rivières, Trois-Rivières, QC G8Y 3P2, Canada, JL.Dion@cgocable.ca

Hao Feng Department of Food Science and Human Nutrition, University of Illinois at Urbana-Champaign, Urbana, IL 61801, USA, haofeng@illinois.edu

Juan A. Gallego-Juárez Instituto de Acústica, CSIC, 28006 Madrid, Spain, jgallego@ia.cetef.csic.es

Mala Gamage CSIRO Food and Nutritional Sciences, Werribee, VIC 3030, Australia, Thambaramala.Gamage@csiro.au

José Vicente García-Pérez Grupo de Análisis y Simulación de Procesos Agroalimentarios, Departamento de Tecnología de Alimentos, Universidad Politécnica de Valencia, 46022 Valencia, Spain, jogarpe4@tal.upv.es

Parag R. Gogate Chemical Engineering Department, Institute of Chemical Technology, Mumbai, Matunga 400 019, India, pr.gogate@ictmumbai.edu.in

José González-García Departamento de Química Física e Instituto Universitario de Electroquímica, Universidad de Alicante, Alicante, Spain, jose.gonzalez@ua.es

Sandra N. Guerrero Departamento de Industrias, Universidad de Buenos Aires, Ciudad Universitaria, 1428 Buenos Aires, Argentina, sguerrero@di.fcen.uba.ar

Sandra Kentish Department of Chemical and Biomolecular Engineering, Particulate Fluids Processing Centre, University of Melbourne, Melbourne, VIC 3010, Australia, sandraek@unimelb.edu.au

Gunnar Thor Kjartansson Department of Food Science and Human Nutrition, University of Iceland, Reykjavik, Iceland, gkjartan@gmail.com

Kai Knoerzer CSIRO Food and Nutritional Sciences, Werribee, VIC 3030, Australia, Kai.Knoerzer@csiro.au

Kristberg Kristbergsson Department of Food Science and Human Nutrition, University of Iceland, Reykjavik, Iceland, kk@hi.is

Rohit Kumar Rana Nanomaterials Laboratory, Inorganic and Physical Chemistry Division, Indian Institute of Chemical Technology, Hyderabad, 500 007, India, rkrana@iict.res.in

Hyoungill Lee Department of Food Science and Human Nutrition, University of Illinois at Urbana-Champaign, Urbana, IL 61801, USA, hyoungil@illinois.edu

Aurelio López-Malo Departamento de Ingeniería Química y Alimentos, Universidad de las Américas, Puebla 72820, México, aurelio.lopezm@udlap.mx

Olivier Louisnard Centre RAPSODEE, FRE CNRS 3213, Université de Toulouse, Ecole des Mines d'Albi, 81013 ALBI Cedex 09, France, louisnar@enstimac.fr

Pilar Mañas Tecnología de los Alimentos, Departamento de Producción Animal y Ciencia de los Alimentos, Facultad de Veterinaria, Universidad de Zaragoza, 50013 Zaragoza, Spain, manas@unizar.es

Richard Manasseh Faculty of Engineering and Industrial Science (H38), Swinburn University of Technology, PO Box 218, Hawthorn, VIC, 3122, Australia, rmanasseh@swin.edu.au

Douglas G. Mancosky Application Development, Hydro Dynamics, Inc., Rome, GA, USA, dmancosky@hydrodynamics.com

Raymond Mawson CSIRO Food and Nutritional Sciences, Werribee, VIC 3030, Australia, raymond.mawson@csiro.au

Paul Milly Food Scientist and Brewer, 319 N. Broadmoor Ave., West Covina, CA 91790, USA, paulmilly@hotmail.com

Tamara Mobbs Biological Systems Engineering Department, Center for Nonthermal Processing of Food, Washington State University, Pullman, WA 99164-6120, USA, tamamobbs@gmail.com

Antonio Mulet Grupo de Análisis y Simulación de Procesos Agroalimentarios, Departamento de Tecnología de Alimentos, Universidad Politécnica de Valencia, 46022 Valencia, Spain, amulet@tal.upv.es

Aniruddha B. Pandit Chemical Engineering Department, Institute of Chemical Technology, Mumbai, Maharashtra 400 019, India, ab.pandit@ictmumbai.edu.in, dr.pandit@gmail.com

Alex Patist Cargill Research, Wayzata, MN 55391, USA, alex_patist@cargill.com

Miodrag Prokic MP Interconsulting 2400 Le Locle, Switzerland, mpi@bluewin.ch

Ke-ming Quan Procter and Gamble Company, West Chester, OH 45069, USA, quan.k@pg.com

Silvia Raffellini Departamento de Tecnologías, Universidad Nacional de Luján, 6700 Luján (Pcia. de Buenos Aires), Argentina, raf@unlu.edu.ar

Enrique Riera Instituto de Acústica, CSIC, 28006 Madrid, Spain, eriera@ia.cetef.csic.es

Harald Rohm Institute of Food Technology and Bioprocess Engineering, Technische Universität Dresden, 01069 Dresden, Germany, harald.rohm@tu-dresden.de

Marcela Schenk Departamento de Industrias, Universidad de Buenos Aires, Ciudad Universitaria, 1428 Buenos Aires, Argentina, marcelisk@yahoo.com.ar

Yvonne Schneider Institute of Food Technology and Bioprocess Engineering, Technische Universität Dresden, 01069 Dresden, Germany, yvonne.schneider@tu-dresden.de

Sivakumar Manickam Department of Chemical and Environmental Engineering, Faculty of Engineering, University of Nottingham (Malaysia Campus), Semenyih, Selangor, Malaysia, sivakumar.manickam@nottingham.edu.my

Da-Wen Sun Food Refrigeration and Computerised Food Technology, Agriculture and Food Science Centre, University College Dublin, Belfield, Dublin 4, Ireland, dawen.sun@ucd.ie

Netsanet Shiferaw Terefe CSIRO Food and Nutritional Sciences, Werribee, VIC 3030, Australia, Netsanet.Shiferawterefe@csiro.au

Kamaljit Vilkhu Innovative Scientific Solutions, 8 Hayley Street, Hoppers Crossing, VIC, 3029, Australia, kamaljit.vilkhu@yahoo.com

Jochen Weiss Department of Food Structure and Functionality, Institute of Food Science and Biotechnology, Universität Hohenheim, Garbenstraße 21/25, 70599, Stuttgart, Germany, j.weiss@uni-hohenheim.de

Susann Zahn Institute of Food Technology and Bioprocess Engineering, Technische Universität Dresden, 01069 Dresden, Germany, susann.zahn@tu-dresden.de

Chapter 1
The Physical and Chemical Effects of Ultrasound

Sandra Kentish and Muthupandian Ashokkumar

1 Introduction

When a violin string is vibrated by the bow, a pressure wave is generated which travels to the human ear and is perceived as music. All sound waves are similar to this; they are simply longitudinal pressure waves passing through a medium.

The type of sound wave is determined by its frequency (Fig. 1.1). "Infrasound" refers to sound waves of frequency below that detectable by the human ear. This is the zone used by whales and by submarine sonar devices. The range of human hearing is from around 20 Hz to ~20 kHz. The word "ultrasound" refers to sound waves that are at a frequency above this range. This ultrasonic spectrum can itself be divided into two zones. Power ultrasound will be the major focus of this book and refers to the frequency range from 20 kHz to around 1 MHz. Diagnostic ultrasound has a frequency in excess of 1 MHz and is used mainly for medical and industrial imaging purposes.

A major advantage of ultrasound to the food industry is that it is perceived as benign by the general public. Other processing techniques (microwaves, gamma radiation, pulsed electric field) can be considered cautiously by elements of the general population. However, sound waves are generally considered safe, non-toxic, and environmentally friendly – this gives the use of ultrasound a major advantage over other techniques.

So why is ultrasound an effective processing aid for the food and bioprocessing industry? The impact of this phenomenon is generally classified into two categories: physical and chemical effects. These two categories are discussed in more detail in the sections below. The focus is on the use of ultrasound in liquid rather than gaseous media, as this will be the usual situation in such industrial applications.

S. Kentish (✉)
Department of Chemical and Biomolecular Engineering, Particulate Fluids Processing Centre, University of Melbourne, Melbourne, VIC 3010, Australia
e-mail: sandraek@unimelb.edu.au

H. Feng et al. (eds.), *Ultrasound Technologies for Food and Bioprocessing*, Food Engineering Series, DOI 10.1007/978-1-4419-7472-3_1,
© Springer Science+Business Media, LLC 2011

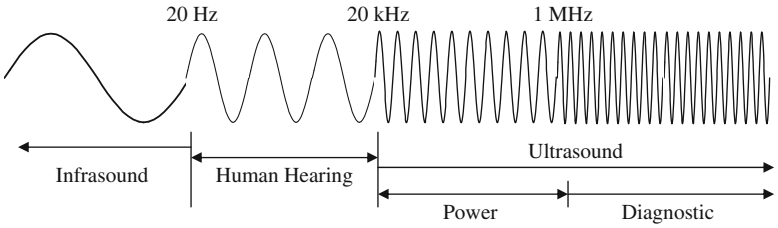

Fig. 1.1 The sound spectrum

2 Physical Effects of Ultrasound

As previously indicated ultrasound simply represents a high-frequency pressure wave. As this pressure wave passes through the medium, regions of high and low pressure are created. The size of these pressure variations, referred to as the amplitude of the pressure wave or the acoustic pressure, is directly proportional to the amount of energy applied to the system. As this wave passes through a viscous medium, be it air or water, it will dissipate this energy in the form of viscous flow. This is referred to as "steady streaming" (Riley, 2001). The flow pattern that results will depend upon the form of the original acoustic wave and whether the pressure wave is reflected from hard surfaces or otherwise interacts with the system boundaries. For example, Rayleigh streaming is the term used to refer to the specific flow patterns that arise from a standing wave pattern between two plane walls (Riley, 2001). Higher frequency ultrasound leads to higher energy absorption and in turn generates greater acoustic streaming flow rates than lower frequencies for the same power intensity (Suslick, 1988a).

In gases such as air, which are compressible fluids, the movement of fluid in streaming patterns is always sufficient to accommodate these pressure variations. However, most liquids are inelastic and incompressible and thus cannot respond as easily in this manner. If the changes in pressure are great enough, then the liquid can literally be "torn" apart under the influence of ultrasound. Microbubbles of gas and vapor form, which relieve the tensile stresses created by the pressure wave. Scientific theory would suggest that the acoustic pressure variation required for this to occur is very large, up to 3,000 MPa (Brennen, 1995). However, in practice, these microbubbles form at relatively mild acoustic pressures. It is generally believed that this is because any liquid already contains cavities of gas or nanobubbles, and that these nuclei assist in the formation of microbubbles. It is interesting that these nanobubbles, which have been the subject of speculation for many decades in the ultrasonic field, have only recently been proven to exist (Zhang et al., 2008) at least at the interface between water and a hydrophobic surface.

The bubble formation process is known as *cavitation.* The lowest acoustic pressure at which it is observed is called the cavitation or the Blake threshold, P_B, and is a function of the solution vapor pressure, P_v, the surface tension (σ), the initial nanobubble radius (R_0), and the system pressure (P_0) (Leighton, 1994):

$$P_B = P_0 - P_v + \frac{4}{3}\sigma \sqrt{\frac{2\sigma}{3\left(P_0 + 2\frac{\sigma}{R_0} - P_v\right)R_0^3}} \tag{1.1}$$

It is much easier to generate an acoustic wave of high amplitude (high acoustic pressure) at lower frequencies. At higher frequencies (>1 MHz), acoustic pressures are lower and this amplitude is more readily dissipated within the fluid. For this reason, the Blake threshold is rarely exceeded at these frequencies in industrial applications and so cavitation is generally not observed.

It should be noted that while cavitation formally refers to the "creation" of a microbubble, most authors in the ultrasound field use this term to encompass the full range of bubble behavior once it has been formed. While the focus of this book is on acoustic cavitation, the hydrodynamic forces around pump impellers or in homogenizers can also create sufficient pressure changes so as to induce cavitation. Later chapters in this book discusses both acoustic cavitation and hydrodynamic cavitation in more detail.

Bubbles formed through cavitation will begin to expand and collapse under the influence of the acoustic field. The expansion/collapse cycle can be sinusoidal, mimicking that of the acoustic wave (Fig. 1.2a). Alternatively, for certain bubble sizes and acoustic pressures, the bubble expansion phase is extended and is followed by a violent collapse back to a smaller bubble size. This is referred to as inertial cavitation. This mode of bubble oscillation can persist for many hundreds of acoustic cycles, in which case it is referred to as stable, or repetitive transient cavitation. An example of this phenomenon is shown in Fig. 1.2b. In this example, a bubble initially of radius 0.5 μm expands to over 30 times this radius before collapsing back to the 0.5 μm size (Yasui, 2002). Alternatively, if the acoustic amplitude is higher, the bubbles grow and collapse spectacularly within a very few acoustic cycles and the collapsed bubble then disintegrates into a mass of smaller bubbles (Leighton, 1994; Yasui, 2002). These daughter bubbles are often small and themselves collapse rapidly so that complete annihilation of the original bubble occurs (Crum and Nordling, 1972; Strasberg, 1959). This is referred to as unstable or transient cavitation (Fig. 1.2c) and is generally observed at low frequencies (20–100 kHz). The size range at which transient cavitation occurs is often referred to as the resonance size. However, Yasui (2002) shows that the bubble size range for transient cavitation is often over an order of magnitude wide and does not necessarily coincide with the linear resonance radius.

A number of other processes may also be occurring within the bubble population, even below the cavitation threshold. If the bubbles are small, they will simply dissolve away (Fig. 1.2a). However, the mass transfer boundary layer is thinner and the interfacial area is greater during bubble expansion than during bubble collapse. This means that more air transfers into the bubble during the expansion phase than leaks out during collapse. This causes larger bubbles to grow over a very large number of acoustic cycles in a process referred to as rectified diffusion (Crum, 1980; Lee et al., 2005a). Larger bubbles may also form through coalescence of smaller bubbles

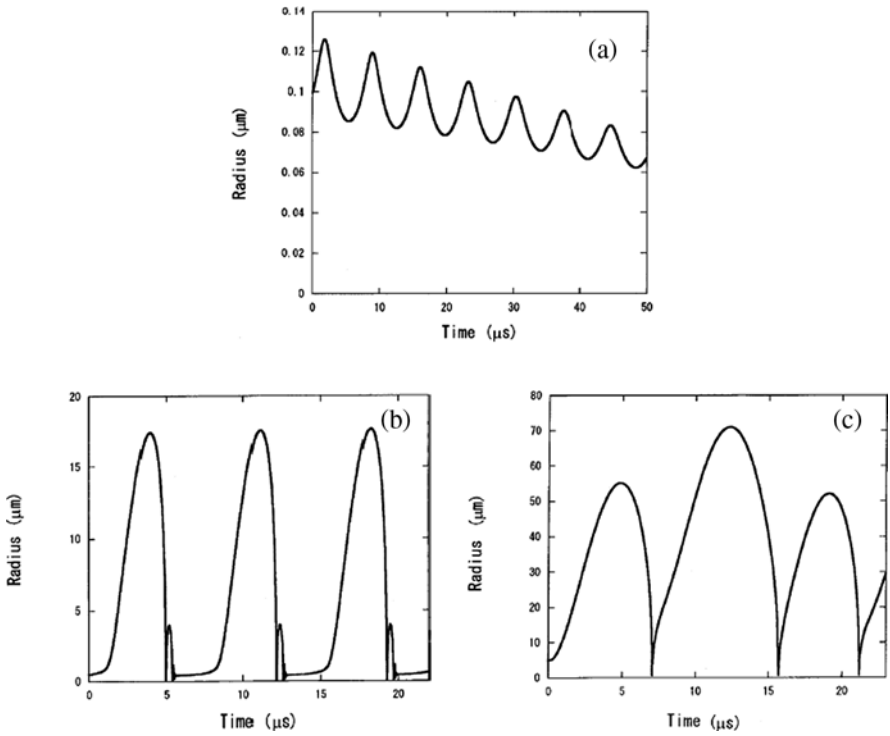

Fig. 1.2 Simulated radius time curves at 140 kHz for (**a**) a dissolving bubble (initial radius 0.1 μm and acoustic pressure 500 kPa), (**b**) a bubble in repetitive transient cavitation (initial radius 0.5 μm and acoustic pressure 250 kPa), and (**c**) a bubble in transient cavitation (initial radius 5 μm and acoustic pressure 500 kPa). This last bubble disintegrates into a mass of smaller bubbles just after the third collapse (t∼22 μs) (reproduced from Yasui (2002) with permission)

(Ashokkumar et al., 2007; Lee et al., 2005b). These coalesced bubbles may eventually be of a size where they simply float away from the sonication zone through the influence of gravity. Further, the oscillating bubble will generate fluctuations in velocity and pressure in the surrounding fluid (see Fig. 1.3). This is referred to as "cavitation microstreaming" (Elder, 1959) and generates turbulence within the fluid on a microscale.

More significantly, the collapse of a bubble during transient or repetitive transient cavitation is a cataclysmic event – extremely high pressures can be generated (70–100 MPa) (Laborde et al., 1998; Suslick, 1988b) that result in outward propagating shockwaves. This propagation causes severe turbulence within the immediate surroundings. These dramatic "micro" events can easily cause polymer chains to break (Price, 1990) or the cell walls of plant and animals to be destroyed (Cioffi and Wolfersberger, 1983; Lin and Thomas James, 2004; Simon, 1974). Hacias et al. (1997) comment that the energy released from a single transient collapse is

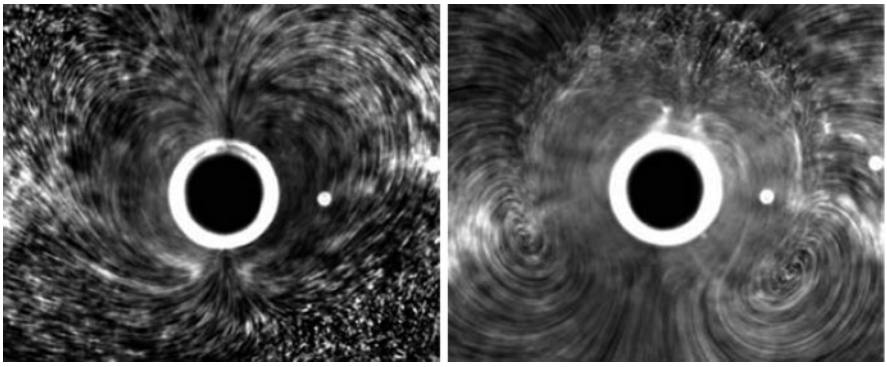

Fig. 1.3 Cavitation microstreaming patterns around a 272 μm radius bubble excited at acoustic frequencies 9 and 11 kHz (reproduced from Tho et al. (2007) with permission)

extremely small, but millions of bubbles collapse every second and the cumulative effect is large.

Of particular relevance to many food applications is the occurrence of transient cavitation within the proximity of a solid surface. In this case, the bubble collapses asymmetrically. In doing so, a microjet of fluid or bubbles (Lee et al., 2007) can be emitted from the bubble (Fig. 1.4). This microjet is directed toward the solid surface and this can lead to pitting and erosion. The surface action can also dislodge particles attached to the surface and break down large aggregates into smaller particles (Hagenson and Doraiswamy, 1997; Suslick, 1988a).

Acoustic standing waves can result from the reflection of sound from a solid surface or an air–liquid interface back into the solution at the same time that a wave is generated at the transducer (Fig. 1.5). At the pressure antinode of such a standing wave pattern, the pressure fluctuates from a maximum to minimum amplitude with time. Conversely, at the pressure node the acoustic pressure is invariant and close to zero. A phenomenon referred to as Bjerknes forces causes smaller bubbles to accumulate at the antinode, while larger bubbles accumulate at the node (Crum and Eller, 1970; Yasui, 2002). In moving to the antinodes, the cavitation bubbles travel in ribbon-like structures (referred to as "streamers") coalescing as they collide. In doing so, a filamentary structure, referred to as an acoustic "Lichtenberg" figure

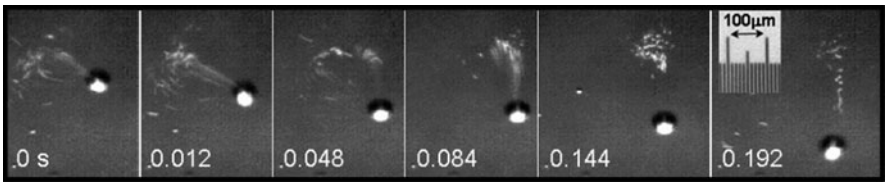

Fig. 1.4 Selected images of the release of a fountain of microbubbles from a parent bubble in water within a confined microspace. Acoustic frequency 59.67 kHz and intensity 0.5–0.7 W/cm^2 (reproduced from Lee et al. (2007) with permission)

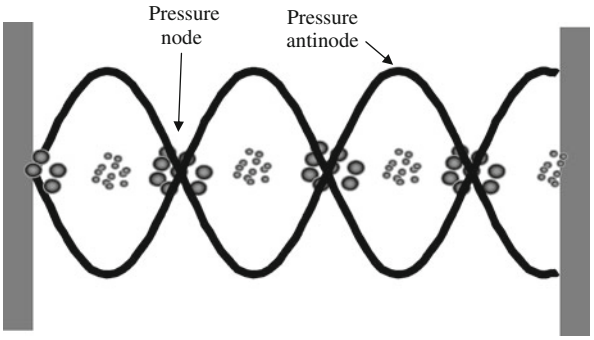

Fig. 1.5 Effects of a standing wave pattern. Bubbles smaller than the resonance size accumulate at the pressure antinodes, larger bubbles accumulate at the nodes

Fig. 1.6 The movement of bubbles toward a solid surface acting as a pressure antinode within an acoustic standing wave pattern

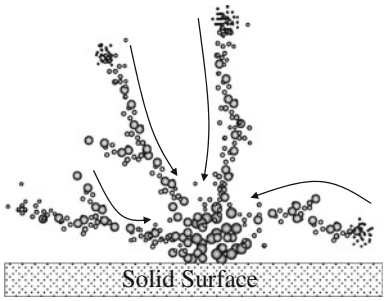

is created (Fig. 1.6) (Mettin et al., 1999). At 20 kHz these bubbles are typically <10 μm in size, about a millimeter apart and traveling at less than 1 μm/s (Luther et al., 2001). This bubble translation is known to dislodge particles from fouled surfaces, in cases where the surface itself acts as the pressure antinode (Lamminen et al., 2004).

Of particular interest to many of the applications discussed in this book is that these physical effects are strongest near to fluid/solid and fluid/fluid boundaries. Specifically, the microjetting that occurs with asymmetric bubble collapse and the acoustic streaming patterns around solid objects are strongest within a few millimeters of the surface. Similarly, the movement of bubbles toward a solid surface acting as a pressure antinode within an acoustic standing wave pattern results in increased turbulence within this same zone. These boundary layer effects are important, because it is usually such boundary layers that offer the greatest resistance to both heat and mass transfer. By concentrating the acoustic energy dissipation in these areas, ultrasound is extremely effective in improving heat and mass transfer kinetics, often proving to be more effective than other less site-specific options such as high-shear mixers or microfluidic devices. Surface effects are also important in emulsification, where interfacial turbulence is associated with droplet formation (Li and Fogler, 1978) and in nebulization, where acoustic streaming effects cause a

"fountain structure" to form at the air/water interface from which microdroplets are ejected (Lang, 1962).

Increasing the external pressure increases the cavitation threshold within an ultrasonic field and thus fewer bubbles form. However, increasing the external pressure also increases the collapse pressure during transient cavitation (Bondy and Sollner, 1935; Suslick, 1988b; Young, 1989). This means that the collapse of the bubbles when cavitation occurs becomes stronger and more violent. This use of "overpressure" is a common feature of many commercial sonoprocessing applications. Conversely, increasing the external temperature increases the water vapor pressure inside the cavitating bubbles. This water vapor "cushions" the bubble collapse and the collapse event is subdued. Hence, ultrasound is less effective at temperatures significantly above ambient levels.

Finally, regardless of the mechanism for dissipation of acoustic energy, be it steady streaming, microstreaming, transient cavitation, or microjetting, the energy is ultimately converted to heat. This means that all applications of ultrasound will result in an increase in temperature unless cooling is simultaneously applied. In most circumstances, the temperature increase is relatively mild, of the order of a few degrees Celsius, but it is dangerous to ignore this effect in system design. Experimentally, the change in temperature can be used to determine the fraction of the electrical energy originally applied to the transducer that is converted to acoustic energy and ultimately to heat. This is referred to as the calorimetric determination of acoustic energy and it is simply determined from an energy balance (Kimura et al., 1996; Ratoarinoro et al., 1995) as

$$Q = mC_p\Delta T \tag{1.2}$$

where Q is the energy input in Watts, m is the sample mass, C_p is the heat capacity of the sample, and ΔT is the change in temperature.

3 Chemical Effects

The violent collapse events that occur during transient and repetitive transient cavitation can also generate enormous temperatures at a localized level (>5,000 K) (Ashokkumar and Mason, 2007). These high temperatures and the violent pressure changes occurring simultaneously can cause a number of chemical changes to occur within both the vapor phase inside the cavitation bubble and in the immediate fluid surrounding it. There are a number of review articles (Luche, 1998; Ashokkumar et al., 2007; Mason and Lorimer, 2002) that provide detailed information on these chemical effects, commonly referred to as sonochemistry. This section summarizes key aspects of this extensive field of research.

Primary radicals are formed as a direct result of the high temperatures inside a collapsing bubble. If water vapor is present, H and OH primary radicals are generated and these can recombine to form molecular products as shown in Reactions (1.3)–(1.6).

$$H_2O \longrightarrow H\bullet + OH\bullet \tag{1.3}$$

$$H\bullet + H\bullet \longrightarrow H_2 \tag{1.4}$$

$$OH\bullet + OH\bullet \rightarrow H_2O_2 \tag{1.5}$$

$$H\bullet + OH\bullet \longrightarrow H_2O \tag{1.6}$$

When a single bubble is considered, the number of radicals generated is high when the temperature inside the collapsing bubble is at a maximum. This temperature can be increased by increasing the sonication power, increasing the external pressure, or decreasing the external (solution) temperature as described above. Changing from an air-saturated medium to one saturated with an inert gas such as argon is also effective. The heavier inert gases have a lower thermal conductivity and hence are less efficient at transferring heat away from the bubble to the surrounding fluid (Ashokkumar et al., 2007; Leighton, 1994).

The amount of heat generated also depends upon the size of the cavitation bubble. A 20 kHz bubble grows to the largest size (60–100 μm) and hence generates a relatively large amount of heat. Thus the amount of primary radicals generated per bubble is higher at 20 kHz compared to that generated at higher frequencies.

In a multibubble field, the total number of primary radicals generated is controlled not only by the bubble temperature, but also by the number of active bubbles generated. In fact, it has been shown that the number of bubbles generated is the dominant factor in controlling the radical yield (Ashokkumar et al., 2007). Thus, for a given liquid volume and acoustic power, a greater number of radicals are generated at higher frequencies and this can dominate over the radical production per bubble (see Fig. 1.7). For this reason, sonochemical effects are generally most dominant at intermediate frequencies (200–500 kHz).

A number of analytical methods have been developed to quantify the number of primary radicals generated during acoustic cavitation (Ashokkumar et al., 2007).

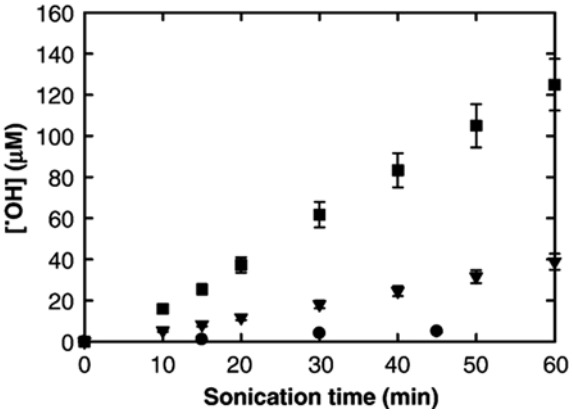

Fig. 1.7 •OH radical yield generated in water upon sonication at different ultrasonic frequencies (0.90 W/cm^2). More radicals form per bubble at low frequencies, but many more bubbles are generated at the higher frequencies. Data shown are means ± SD of three experiments. (■ 358 kHz, ▼ 1062 kHz, ●20 kHz) (reprinted from Ashokkumar et al. (2008) with permission)

These include electron spin resonance trapping and terephthalic acid, luminol, and iodide methods. Among these methods, the iodide method is a simple and common method that can be used to estimate the amount of OH radicals generated. This method is based on the amount of hydrogen peroxide formed due to Reaction (1.5). The actual number of OH• radicals generated may be higher than estimated using this method since some of the OH• radicals recombine with H atoms and form water.

In air-saturated solutions, other reactions involving oxygen and nitrogen occur. In particular, this results in the formation of NO_2, which forms nitric acid in solution. It is for this reason that sonication of air-saturated solutions often leads to a decrease in the pH (Supeno and Kruus, 2000). Some secondary radicals may also be produced by the reaction between the primary radicals and other solute molecules. For example, alcohols and surfactants readily adsorb at the bubble/solution interface and generate highly reactive secondary reducing radicals. A variety of chemical reactions have been studied that use the primary and secondary radicals generated during acoustic cavitation (Ashokkumar et al., 2007).

The high temperatures within the bubble can also result in a range of pyrolysis reactions if organic solutes are present. Further, the primary and secondary radicals generated during the bubble collapse can be consumed in a range of secondary reactions that may occur within the bulk fluid and some distance from the bubble itself. For example, the OH• radicals generated within the bubbles have been used to oxidize organic pollutants (Inazu et al., 1993; Kotronarou et al., 1992), and the H• atoms and other secondary reducing radicals have been used to reduce metal ions to generate metal nanoparticles (Hyeon et al., 1996; Suslick et al., 1996). Of particular importance in food applications, Suslick and Grinstaff (1990) proposed that the superoxide species (HO_2•) formed from primary radicals may induce disulfide cross-linkage between proteins. These effects have been used to generate both gas- and liquid-filled protein microspheres that have applications for drug delivery (Dibbern et al., 2006; Toublan et al., 2006) and medical imaging (Webb et al., 1996). Similarly, Ashokkumar et al. (2008) propose that hydroxyl radicals generated during sonication can be used to enhance the degree of hydroxylation in food materials and hence increase the antioxidant activity of foods.

It should be noted that the generation of OH• radicals may affect the quality of some foods by reducing the antioxidant capacity (Ashokkumar et al., 2008). Intense sonication is also known to generate off-flavors. Riener et al. (2009) showed that extended sonication of milk generated a range of volatile organic compounds that might be responsible for a “rubbery” aroma. They related these compounds to both pyrolysis reactions inside the cavitating bubbles and to free radical-induced lipid oxidation resulting from the decomposition of unsaturated fatty acid hydroperoxides. In these applications, it may be important to minimize sonochemical reactions by either utilizing a low frequency, where free radical formation is very low (20 kHz), or by the addition of a free radical scavenger such as ascorbic acid (Ashokkumar et al., 2008).

Finally, the bubble collapse is also accompanied by light emission known as sonoluminescence (Fig. 1.8). The high-temperature conditions generated on bubble collapse are responsible for the light emission (Ashokkumar and Grieser, 2004). In

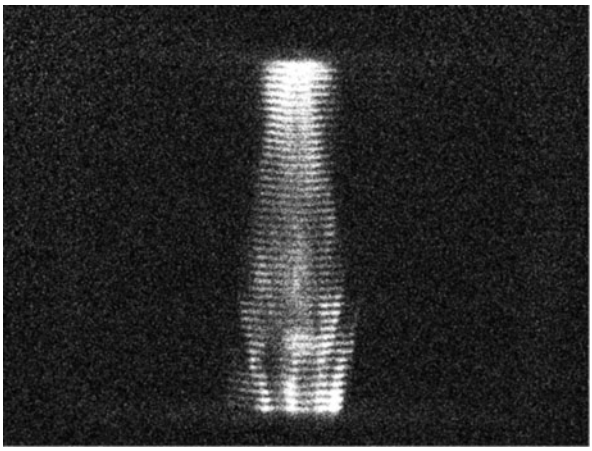

Fig. 1.8 Multibubble sonoluminescence observed at 440 kHz and 30 W in a rectangular Pyrex cell containing 1,000 mL water with a piezoelectric transducer attached at the bottom of the cell. The photograph is taken with a total exposure time of 30 s. The light emitting cavitation bubbles are located at several antinodes in a standing wave pattern

Fig. 1.8, the sonoluminescence observed in a multibubble standing wave field is shown. Since the topic of this book is concerned with physical effects and chemical reactions of ultrasound, further discussion on sonoluminescence is not provided; however, interested readers may refer to the literature (Young, 2005).

4 Conclusions

Most of the applications to be considered in the remainder of this book will focus on the physical effects of ultrasound which dominate at lower frequencies of around 20 kHz. The physical effects of ultrasound can be generally summarized as increased turbulence throughout the medium but with the strongest effects in the vicinity of system boundaries and interfaces. At lower frequencies (20–100 kHz), this increased turbulence results primarily from transient cavitation, that is, the catastrophic collapse of microbubbles throughout the fluid.

At intermediate frequencies, say between 200 and 500 kHz, chemical effects are more dominant as the number of active bubbles generated is higher. Transient cavitation events are less frequent and hence the strong physical effects experienced at 20 kHz are weaker here, although they are still present.

At higher frequencies (>1 MHz), cavitation and the associated chemical effects are less likely and acoustic streaming effects are more dominant. Thus for example, ultrasound in the MHz range is used in the electronics industry to clean sensitive components such as silicon wafers and disk drive parts without risking the erosive damage that might occur in the cavitational frequency range.

References

Ashokkumar, M., and Grieser, F. (2004). Single bubble sonoluminescence-a chemist's overview. *ChemPhysChem*, 5(4), 439–448.

Ashokkumar, M., Lee, J., Kentish, S., and Grieser, F. (2007). Bubbles in an acoustic field: An overview. *Ultrasonics Sonochemistry*, 14(4), 470–475.

Ashokkumar, M., and Mason, T. J. (2007). *Sonochemistry. Kirk-Othmer Encyclopedia of Chemical Technology*. New York, NY, Wiley.

Ashokkumar, M., Sunartio, D., Kentish, S., Mawson, R., Simons, L., Vilkhu, K., and Versteeg, C. (2008). Modification of food ingredients by ultrasound to improve functionality: A preliminary study on a model system. *Innovative Food Science and Emerging Technologies*, 9(2), 155–160.

Bondy, C., and Sollner, K. (1935). On the mechanism of emulsification by ultrasonic waves. *Transactions of the Faraday Society*, 31, 835–842.

Brennen, C. E. (1995). *Cavitation and Bubble Dynamics*. New York, NY, Oxford University Press.

Cioffi, M., and Wolfersberger, M. G. (1983). Isolation of separate apical, lateral and basal plasma membrane from cells of an insect epithelium. A procedure based on tissue organization and ultrastructure. *Tissue and Cell*, 15(5), 781–803.

Crum, L. A. (1980). Measurements of the growth of air bubbles by rectified diffusion. *Journal of the Acoustical Society of America*, 68, 203–211.

Crum, L. A., and Eller, A. I. (1970). Motion of bubbles in a stationary sound field. *Journal of the Acoustical Society of America*, 48, 181–189.

Crum, L. A., and Nordling, D. A. (1972). Velocity of transient cavities in an acoustic stationary wave. *Journal of the Acoustical Society of America*, 52(1), 294–301.

Dibbern, E. M., Toublan, F. J., and Suslick, K. S. J. (2006). Formation and characterization of polyglutamate core-shell microspheres. *Journal of the American Chemical Society*, 128(20), 6540–6541.

Elder, S. A. (1959). Cavitation microstreaming. *Journal of the Acoustical Society of America*, 31, 54–64.

Hagenson, L. C., and Doraiswamy, L. K. (1997). Comparison of the effects of ultrasound and mechanical agitation on a reacting solid-liquid system. *Chemical Engineering Science*, 53(1), 131–148.

Hyeon, T., Fang, M., and Suslick, K. S. (1996). Nanostructured molybdenum carbide: Sonochemical synthesis and catalytic properties. *Journal of the American Chemical Society*, 118(23), 5492–5493.

Hacias, K.J., Cormier, G.J., Nourie, S.M., and Kubel, E.J. (1997). *Guide to Acid, Alkaline, Emulsion, and Ultrasonic Cleaning*. ASM International, Ohio, USA.

Inazu, K., Nagata, Y., and Maeda, Y. (1993). Decomposition of chlorinated hydrocarbons in aqueous solutions by ultrasonic irradiation. *Chemistry Letters*, 1, 57–60.

Kimura, T., Sakamoto, T., Leveque, J.-M., Sohmiya, H., Fujita, M., and Ikeda, S. (1996). Standardization of ultrasonic power for sonochemical reaction. *Ultrasonics Sonochemistry*, 3(3), S157–S161.

Kotronarou, A., Mills, G., and Hoffmann, M. R. (1992). Decomposition of parathion in aqueous solution by ultrasonic irradiation. *Environmental Science and Technology*, 26(7), 1460–1462.

Laborde, J. L., Bouyer, C., Caltagirone, J. P., and Gerard, A. (1998). Acoustic bubble cavitation at low frequencies. *Ultrasonics*, 36(1–5), 589–594.

Lamminen, M. O., Walker, H. W., and Weavers, L. K. (2004). Mechanisms and factors influencing the ultrasonic cleaning of particle-fouled ceramic membranes. *Journal of Membrane Science*, 237(1–2), 213–223.

Lang, R. J. (1962). Ultrasonic atomization of liquids. *Journal of the Acoustic Society of America*, 34, 6–9.

Lee, J., Kentish, S., and Ashokkumar, M. (2005a). Effect of surfactants on the rate of growth of an air bubble by rectified diffusion. *Journal of Physical Chemistry B*, 109(30), 14595–14598.

Lee, J., Kentish, S. E., and Ashokkumar, M. (2005b). The effect of surface-active solutes on bubble coalescence in the presence of ultrasound. *Journal of Physical Chemistry B*, 109(11), 5095–5099.

Lee, J., Tuziuti, T., Yasui, K., Kentish, S., Grieser, F., Ashokkumar, M., and Iida, Y. (2007). Influence of surface-active solutes on the coalescence, clustering, and fragmentation of acoustic bubbles confined in a microspace. *Journal of Physical Chemistry C*, 111(51), 19015–19023.

Leighton, T. G. (1994). *The acoustic bubble*. San Diego, CA, Academic.

Li, M. K., and Fogler, H. S. (1978). Acoustic emulsification. Part 1. The instability of the oil-water interface to form the initial droplets. *Journal of Fluid Mechanics*, 88(3), 499–511.

Lin, H.-Y., and Thomas James, L. (2004). Factors affecting responsivity of unilamellar liposomes to 20 kHz ultrasound. *Langmuir: The ACS Journal of Surfaces and Colloids*, 20(15), 6100–6106.

Luche, J. L. (1998). *Synthetic organic sonochemistry*. New York, NY, Plenum Press.

Luther, S., Mettin, R., Koch, P., and Lauterborn, W. (2001). Observation of acoustic cavitation bubbles at 2250 frames per second. *Ultrasonics Sonochemistry*, 8(3), 159–162.

Mason, T. J., and Lorimer, J. P. (2002). *Applied sonochemistry*. Weinheim, Wiley–VCH.

Mettin, R., Luther, S., Ohl, C.-D., and Lauterborn, W. (1999). Acoustic cavitation structures and simulations by a particle model. *Journal of Histochemistry and Cytochemistry*, 47(5), 25–29.

Price, G. J. (1990). The use of ultrasound for the controlled degradation of polymer solutions. *Advances in Sonochemistry*, 1, 231–287.

Ratoarinoro, C. F., Wilhelm, A. M., Berlan, J., and Delmas, H. (1995). Power measurement in sonochemistry. *Ultrasonics Sonochemistry*, 2(1), S43–S47.

Riener, J., Noci, F., Cronin, D. A., Morgan, D. J., and Lyng, J. G. (2009). Characterisation of volatile compounds generated in milk by high intensity ultrasound. *International Dairy Journal*, 19, 269–272.

Riley, N. (2001). Steady streaming. *Annual Review of Fluid Mechanics*, 33, 43–65.

Simon, R. D. (1974). The use of an ultrasonic bath to disrupt cells suspended in volumes of less than 100 micro liters. *Analytical Biochemistry*, 60(1), 51–58.

Strasberg, M. (1959). Onset of ultrasonic cavitation in tap water. *Journal of the Acoustical Society of America*, 31(2), 163–176.

Supeno, X., and Kruus, P. (2000). Sonochemical formation of nitrate and nitrite in water. *Ultrasonics Sonochemistry*, 7(3), 109–113.

Suslick, K. E. (1988a). *Ultrasound*. Weinheim, VCH.

Suslick, K. S. (1988b). *Ultrasound: Its Chemical Physical and Biological Effects*. New York, NY, VCH.

Suslick, K. S., Fang, M., and Hyeon, T. (1996). Sonochemical synthesis of iron colloids. *Journal of the American Chemical Society*, 118(47), 11960–11961.

Suslick, K. S., and Grinstaff, M. W. (1990). Protein microencapsulation of nonaqueous liquids. *Journal of the American Chemical Society*, 112(21), 7807–7809.

Tho, P., Manasseh, R., and Ooi, A. (2007). Cavitation microstreaming patterns in single and multiple bubble systems. *Journal of Fluid Mechanics*, 576, 191–233.

Toublan, F. J.-J., Boppart, S., and Suslick, K. S. (2006). Tumor targeting by surface-modified protein microspheres. *Journal of the American Chemical Society*, 128(11), 3472–3473.

Webb, A. G., Wong, M., Kolbeck, K. J., Magin, R., and Suslick, K. S. (1996). Sonochemically produced fluorocarbon microspheres: A new class of magnetic resonance imaging agent. *Journal of Magnetic Resoning Imaging*, 6(4), 675–683.

Yasui, K. (2002). Influence of ultrasonic frequency on multibubble sonoluminescence. *Journal of the Acoustic Society of America*, 112(4), 1405–1413.

Young, F. R. (1989). *Cavitation*. London, McGraw-Hill.

Young, F. R. (2005). *Sonoluminescence*. Boca Raton, FL, CRC Press.

Zhang, X. H., Quinn, A., and Ducker, W. A. (2008). Nanobubbles at the interface between water and a hydrophobic solid. *Langmuir*, 24(9), 4756–4764.

Chapter 2
Acoustic Cavitation

Olivier Louisnard and José González-García

1 Introduction

The benefit of acoustic cavitation owes to its ability to concentrate acoustic energy in small volumes. This results in temperatures of thousands of kelvin, pressures of GPa, local accelerations 12 orders of magnitude higher than gravity, shock-waves, and photon emission. In a few words, it converts acoustics into extreme physics.

The counterpart is that it constitutes a complex multidisciplinary problem, involving a wide range of temporal and spatial scales, and is therefore difficult to measure. Furthermore, it is a diphasic problem in essence, with the peculiarity that the cavitation bubbles rise up "from nowhere" and self-arrange in a fascinating variety of structures. For all these reasons it is difficult to control, to predict, and to scale up. Several features of cavitation fields remain unexplained, although the progress in optic recording systems recently shed light on previously unreachable characteristics.

From a theoretical point of view, the physics of the single-bubble model has progressed considerably, thanks to single-bubble sonoluminescence experiments. Many features specific to multibubble fields, however, remain obscure and constitute an active research field. From an engineering point of view, the main unknown remains the bubble size distribution and spatial repartition, which in general constitute the main barrier to extrapolate the more or less known action of one bubble on a specific process, to macroscopically observed effects.

By this contribution, we would like to help the reader to assess the main physics involved when he switches on his sonotrode. This chapter is organized as follows. We first present general results for bubbles in a quiet liquid (Section 2). Then, in Section 3, the purely radial forced oscillations of a single bubble in an infinite liquid will be addressed, focusing on thermal effects, solvent evaporation in inertial

O. Louisnard (✉)
Centre RAPSODEE, FRE CNRS 3213, Université de Toulouse, Ecole des Mines d'Albi, 81013 Albi Cedex 09, France
e-mail: louisnar@enstimac.fr

H. Feng et al. (eds.), *Ultrasound Technologies for Food and Bioprocessing*, Food Engineering Series, DOI 10.1007/978-1-4419-7472-3_2,
© Springer Science+Business Media, LLC 2011

bubbles, and their relevance to sonochemistry. Bubbles' loss of sphericity and the resulting effects will be presented in Section 4. The last section addresses cavitation bubble fields and their interaction with the sound field, from both experimental and theoretical points of view.

2 The Quiet Bubble

Before entering in the complex field of acoustic cavitation, it is instructive to examine the behavior of a free spherical gas bubble in a quiet liquid, which can be intuitively apprehended from everyday life.

2.1 A Key Phenomenon: Surface Tension

Increasing the interface between two media requires energy in order to bring molecules from the bulk to the interface. Without a compensating force, an interface therefore has a natural tendency to decrease. In the case of the bubble, the compensating force is an overpressure in the bubble, known as Laplace tension:

$$p_\mathrm{b} = p_0 + \frac{2\sigma}{R} \tag{2.1}$$

where p_0 is the liquid pressure, R is the bubble radius, and σ is the surface tension. This overpressure is unimportant for large bubbles but increases when R approaches the value $2\sigma/p_0$ from above. For example, for an air bubble in water at atmospheric pressure ($\sigma = 0.072$ N^{-1}, $p_0 = 101$ kPa), $2\sigma/p_0$ is 1.45 μm so that the effect of surface tension becomes important in this range of radii. This is precisely the order of magnitude of the bubbles involved in cavitation, so that one can suspect that surface tension will play an important role.

2.2 Bubble Ambient Radius

We consider a bubble containing a given mass m_g of incondensable gas in a liquid at ambient pressure p_0, temperature T_0. The bubble also contains vapor of the liquid, in equilibrium with the latter at T_0, so that the partial pressure of vapor is the equilibrium saturation pressure $p_{\mathrm{v,eq}}(T_0)$. We seek the radius R_0 of such a bubble in mechanical equilibrium. Owing to surface tension, the pressure inside the bubble p_b is $p_0 + 2\sigma/R_0$. Using the law of perfect gases yields

$$p_{\mathrm{v,eq}}(T_0) + \frac{m_\mathrm{g}}{M_\mathrm{g}} \frac{\mathcal{R}T_0}{\frac{4}{3}\pi R_0^3} - \frac{2\sigma}{R_0} = p_0 \tag{2.2}$$

This cubic equation yields the bubble ambient radius R_0. The vapor pressure $p_{v,eq}(T_0)$ can be neglected for temperature well below the boiling point. For further use, we define the dimensionless Laplace tension for the bubble in ambient conditions

$$\alpha_S = \frac{2\sigma}{p_0 R_0} \tag{2.3}$$

2.3 Radial Mechanical Stability: The Blake Threshold

Equation (2.2) gives the radius of a bubble in mechanical equilibrium for a given liquid ambient pressure p_0. One might look for the evolution of the bubble radius from R_0 to R when the liquid pressure p_0 is decreased to $p = p_0 - p_a$. Assuming that this variation is slow enough to allow isothermal transformations of the gas, the evolution of R can be obtained implicitly by

$$p_{v,eq}(T_0) + \left(p_0 - p_{v,eq}(T_0) + \frac{2\sigma}{R_0}\right)\left(\frac{R_0}{R}\right)^3 - \frac{2\sigma}{R} = p_0 - p_a \tag{2.4}$$

Rather than seeking explicitly R from Equation (2.4), it is more instructive to look for a graphical solution. Figure 2.1 is obtained by using Equation (2.4), and it shows the variation of the equilibrium radius R as a function of the liquid pressure $p_0 - p_a$. It is seen that if the external pressure is lowered to a value smaller than $p_0 - p_a^{crit}$, there is no possible equilibrium radius R. Physically, at this point, the liquid starts to flow outward and the bubble undergoes an explosive expansion. This analysis is the key point of inertial cavitation.

This critical value p_a^{crit}, which depends on R_0 and thus on the quantity of gas m_g contained in the bubble, is called the "Blake threshold" (Akhatov et al., 1997a; Blake, 1949; Hilgenfeldt et al., 1998; Louisnard and Gomez, 2003) and can be calculated explicitly by seeking the minimal value of R from Equation (2.4). This yields

$$p_a^{crit} = p_0 - p_{v,eq} + p_0 \left(\frac{4}{27}\frac{\alpha_S^3}{1+\alpha_S}\right)^{1/2} \tag{2.5}$$

The values of p_a^{crit} are represented in Fig. 2.2 for an air bubble in water in ambient conditions ($\sigma = 0.0725\ \mathrm{N \cdot m^{-1}}, p_{v,eq} = 2,000\ \mathrm{Pa}, p_0 = 100\ \mathrm{kPa}$).

An important point to note from Equation (2.5) and Fig. 2.1 is that the corresponding external pressure $p_0 - p_a^{crit}$ can be lower than the vapor pressure of the liquid, and even negative for small values of R_0. It should be recalled that a liquid, owing to internal cohesion force, can effectively support negative pressures or "tensions" (see Section 5.2).

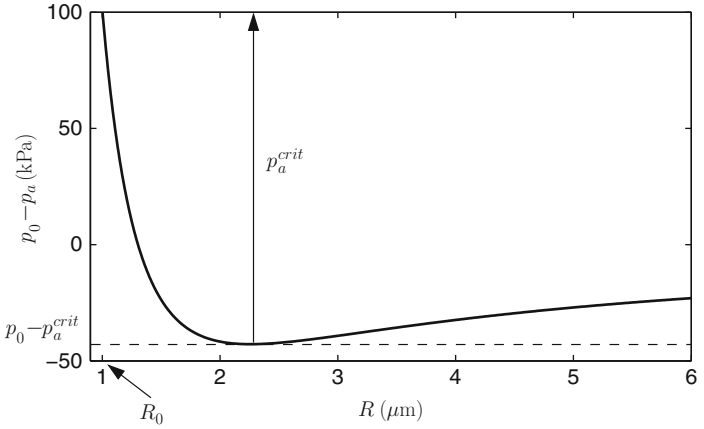

Fig. 2.1 Evolution of the bubble equilibrium radius R when the liquid pressure $p_0 - p_a$ is decreased, for a 1-μm bubble in ambient conditions

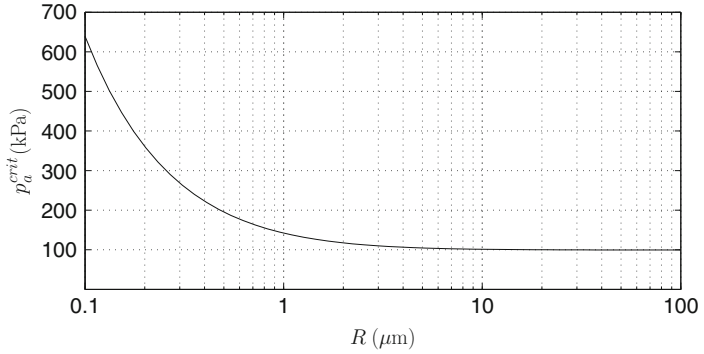

Fig. 2.2 Blake threshold for an air bubble in water in ambient conditions ($p_0 = 101325$ Pa, $\sigma = 0.0725\ \mathrm{N \cdot m^{-1}}$)

2.4 Perturbations of Radial Equilibrium: Free Frequency

The gas filling the bubble provides elasticity to the bubble/water mechanical system; the bubble will oppose a resistance to any compression or expansion imposed by the liquid motion. This force may in turn put the liquid into motion, so that the bubble/liquid constitutes a mass–spring system. Perturbing the bubble slightly from its equilibrium radius therefore results in free radial oscillations, whose frequency can be calculated from energy conservation consideration or from a bubble dynamics equation (see Section 3.2.3). If the oscillations are assumed isothermal, the angular frequency of the free oscillations reads

$$\omega_0 = \frac{1}{R_0}\left\{\frac{p_0}{\rho_1}\left[3(1+\alpha_S)-\alpha_S\right]\right\}^{1/2} \tag{2.6}$$

where ρ_1 is the liquid density.

Bubble-free oscillations are responsible for the noise emitted by running water. In the context of acoustic cavitation, one would expect that a bubble excited at its free frequency would undergo strong oscillations and would be the main factor for cavitation effects. Active bubbles in strong sound fields are in fact excited well below their resonant frequency, as will be discussed throughout further in the chapter.

2.5 Gas Exchange with the Liquid

In saturation condition, that is, if the liquid is saturated with gas at ambient pressure p_0, a gas bubble dissolves because of surface tension. This can be readily understood from Fick's law, as shown below.

Let us denote C_∞ as the concentration of dissolved gas in the solution, and let us consider a bubble of ambient radius R_0 in mechanical equilibrium in the liquid. Far from the bubble, the concentration is C_∞. At the bubble wall, the dissolved gas is in equilibrium with the gas inside the bubble, at pressure $p_{g_0} = p_0 + 2\sigma/R_0$ (let us neglect vapor to simplify the reasoning). Therefore, by virtue of Henry's law, the dissolved gas concentration at the bubble wall is $C_R = p_{g_0}/k_g$, where k_g is the Henry constant. We therefore express the difference in concentration between the bubble wall and at infinity as

$$C_R - C_\infty = C_0\left[\frac{p_{g_0}}{p_0} - \frac{C_\infty}{C_0}\right] = C_0\left[1+\alpha_S - \frac{C_\infty}{C_0}\right] \tag{2.7}$$

where $C_0 = p_0/k_g$ is the saturation concentration, that is the concentration of dissolved gas in the liquid in equilibrium with the gas at p_0. Thus if $C_\infty/C_0 < 1$ the liquid is under-saturated, if $C_\infty/C_0 > 1$ the liquid is supersaturated (as is the case in bubbly beverages that are saturated in CO_2 at a few bars)

For a saturated liquid, we have $C_\infty/C_0 = 1$, so that from Equation (2.7), $C_R - C_\infty > 0$. Fick's law thus predicts an outward gas diffusion flux, so that the bubble dissolves increasingly faster as its size decreases. The analytical solution of the problem has been given by Epstein and Plesset (1950). A practical implication of this phenomenon is that no stable gas bubble should exist in a quiet saturated liquid.

If the liquid is supersaturated in gas, that is $C_\infty/C_0 > 1$, Equation (2.7) shows that there exists a critical value of R_0 above which the bubble grows by gaining gas from the liquid, and below which it dissolves. The bubble growth can be easily observed in a glass of champagne, for example.

In a sound field, an oscillating bubble can grow even in a saturated or under-saturated liquid. The phenomenon is termed "rectified diffusion" and will be discussed in Section 3.4.

2.6 Translational Motion

Common observation tells us that a bubble rises. This is because the buoyancy force $\mathbf{F_A} = -4/3\pi R_0^3 \rho_l \mathbf{g}$ is greater in magnitude than the weight of the bubble $\mathbf{F_G} = 4/3\pi R_0^3 \rho_b \mathbf{g}$, where ρ_b is the bubble density. After some time, the bubble will reach a steady velocity, which can be obtained by balancing the buoyancy force $\mathbf{F}_\mathrm{A}$ with the viscous drag force $\mathbf{F_V} = -4\pi R_0 \mu_l \mathbf{v}$ (the weight being negligible since $\rho_\mathrm{b} \ll \rho_l$):

$$\mathbf{v} = -\frac{1}{3} R_0^2 \frac{\rho_l}{\mu_l} \mathbf{g}$$

where μ_l is the dynamic viscosity of the liquid.

In a sound field a bubble undergoes generalized buoyancy forces, termed Bjerknes forces, and can be either attracted or repelled by zones of high acoustic pressures. They also undergo mutual attraction or repulsion as they experience the field radiated by a neighboring bubble. This issue will be presented in Section 5.3.

2.7 Departure from Spherical Shape

Above some critical size, quiet bubbles depart from their spherical shape as they rise in the liquid, generally flattening their rear part. Radially oscillating bubbles exhibit various shape instabilities, leading to their destruction, and have a peculiar behavior near solid boundaries (Section 4).

3 The Forced Spherical Single Bubble

3.1 Introduction

This section recalls the main features of a radially oscillating spherical bubble in an infinite liquid. This ideal picture may sound unrealistic, and anyone having looked at a cavitation experiment may have doubts on its practical use. However, it leads to important fundamental results, whose usefulness in cavitation prediction has been proved. Moreover, levitation experiments of single bubbles, designed much earlier than their initial use by Gaitan et al. (1992) for single-bubble sonoluminescence (SBSL), produced numerous experimental confirmations of theory in a configuration relevant to the above hypothesis.

This section will refer frequently to recent theoretical and experimental work developed in the context of SBSL. This is because the latter issue has raised numerous papers presenting either new issues or theoretical and experimental refinements of known results. Most of these results are also relevant to multibubble fields.

In this section, after presenting the equations governing the forced oscillations of a spherical bubble and their reduction in the linear case, we will focus on the

case of inertial oscillations, which is responsible for most of the practical effects of acoustic cavitation. The thermal behavior of the bubble interior, along with vapor and gas transport at the interface will next be discussed. The chemistry in the bubble will only be briefly mentioned, and we refer the reader to the chapter of K.S. Suslick in this book. Finally, the rectified diffusion phenomenon, possibly leading to accumulation of gas in the bubble, will be presented.

3.2 Radial Oscillations

3.2.1 Rayleigh–Plesset Equations

Rayleigh (1917) studied the collapse of a spherical empty cavity, whatever its origin, in order to assess its possible responsibility for the erosion damage on ship propellers. He derived a differential equation, which is basically the principle of mechanical energy conservation in the absence of dissipative forces.

We assume a spherical bubble filled with incondensable gas and vapor, in a liquid of infinite extent, and we first neglect gas transport between the liquid and the bubble. A correct representation of the problem would require the resolution of conservation equations in both phases, but several levels of approximations have allowed us to obtain the equation of motion in the form of a second-order ordinary differential equation.

The most common assumption is the uniformity of the pressure inside the bubble, which, along with the liquid incompressibility hypothesis, yields the Rayleigh–Plesset family of equations (Noltingk and Neppiras, 1950; Plesset, 1949). The first assumption is questionable in view of the order of magnitude of the bubble wall velocities, which may attain several times the sound velocity in the gas. The validity of this assumption has been addressed recently by Lin et al. (2002a), and the Rayleigh–Plesset equation, almost one century after its first derivation, was finally found to be valid in a very wide range of parameters. In its most basic form, it reads

$$R\ddot{R} + \frac{3}{2}\dot{R}^2 = \frac{1}{\rho_\mathrm{l}}\left[p_\mathrm{b}(t) - \frac{2\sigma}{R} - 4\mu_\mathrm{l}\frac{\dot{R}}{R} - p(t)\right] \tag{2.8}$$

where over-dots denote time derivatives. $p(t)$ is the driving pressure, which can be understood as either the pressure infinitely far from the bubble, or the pressure that would be measured in the liquid at the bubble center, if the latter would be absent. For sinusoidal driving, $p(t)$ can be written as

$$p(t) = p_0 - p_\mathrm{a} sin(\omega t) \tag{2.9}$$

where p_a is the driving pressure amplitude, and ω is the angular frequency of the driving. In what follows, we note $f = \omega/2\pi$ the frequency, and $T = 1/f$ the period of the driving. It should be noted that a value of p_a greater than p_0 means that the liquid pressure becomes negative during some part of the expansion phase.

The pressure p_b in the bubble is the sum of the partial pressures of gas p_g and vapor p_v. We neglect vapor for now and will detail this issue in Section 3.3.5. Expression of the uniform pressure in the bubble $p_g(t)$ depends on the thermal behavior of the gas and the equation of state chosen. The gas may be considered as perfect, except at the end of the collapse, where it reaches high density so that van der Waals repulsion forces between atoms or molecules become important. Keeping the assumption of perfect gas, the gas pressure may be written as $p_{\mathrm{g}_0}(R_0/R)^3$ in the isothermal limit, and $p_{\mathrm{g}_0}(R_0/R)^{3\gamma}$, in the adiabatic limit, where γ is the ratio of the gas specific heats. A more detailed analysis of thermal effects shows that, in fact, none of these assumptions is uniformly valid, and we will detail this point in Section 3.3.

3.2.2 Effects of Liquid Compressibility

The compressibility of a medium can be neglected when the typical length of the system (the bubble radius R) is much lower than the wavelength. The latter is $c_\mathrm{l}\tau_\mathrm{dyn}$, where τ_dyn is the characteristic timescale of the bubble oscillation, and c_l the sound speed in the fluid.

For linear oscillations, τ_dyn is simply the acoustic period $1/f$ and $R \simeq R_0$, so that the conditions reads $R_0 \ll c_\mathrm{l}/f$. Compressibility can therefore be neglected for low frequency, and one may expect compressibility effects for high frequencies. This is indeed the case and is one of the reasons for damping of the oscillations (see Section 3.2.3).

For arbitrary oscillations, $\tau_\mathrm{dyn} \simeq R/\dot{R}$ so that compressibility can be neglected if $\dot{R} \ll c_\mathrm{l}$. This is not fulfilled for inertial cavitation, where the bubble wall can attain c_l or even more. Corrections to the Rayleigh equation thus involve corrective terms in $\dot{R}/c_\mathrm{l}$. Several compressible equations have been derived over the years (see Lezzi and Prosperetti, 1987; Prosperetti, 1999; Prosperetti and Lezzi, 1986, and references herein), and it has long been discussed to assess which form was the most appropriate, up to the work of Prosperetti and Lezzi (1986; Lezzi and Prosperetti, 1987) who rigorously derived classes of equations of first and second order. Their formulation recovers many earlier results, among which is the Keller equation (Keller and Miksis, 1980)

$$R\ddot{R}\left(1-\frac{\dot{R}}{c_\mathrm{l}}\right)+\frac{3}{2}\dot{R}^2\left(1-\frac{\dot{R}}{3c_\mathrm{l}}\right)= \frac{1}{\rho_\mathrm{l}}\left[\left(1+\frac{\dot{R}}{c_\mathrm{l}}+\frac{R}{c_\mathrm{l}}\frac{\mathrm{d}}{\mathrm{d}t}\right)\left(p_\mathrm{g}-p(t)\right)-\frac{2\sigma}{R}-4\mu_\mathrm{l}\frac{\dot{R}}{R}\right] \tag{2.10}$$

3.2.3 Linear Oscillations

The radial oscillations of a bubble are in essence non-linear. This can be seen mathematically from Equation (2.10), but can be more easily understood from a physical point of view (Lauterborn and Mettin, 1999): a bubble can be expanded to an

arbitrary size, but can be compressed only down to near zero radius. However, if one considers only low amplitude driving pressure, the bubble can respond with small oscillations around its ambient radius R_0. In this range, the bubble/water system can be considered as a linear forced oscillator, similar to a mass–spring system excited by a periodic force. Mathematically, this approximation can be easily obtained by setting

$$p(t) = p_0[1 + P\mathrm{e}^{\mathrm{i}\omega t}], \qquad R(t) = R_0\left[1 + X\mathrm{e}^{\mathrm{i}\omega t}\right] \tag{2.11}$$

in Equation (2.10) and neglecting terms of order greater than 1 in X or P. A linear relation is then obtained between the complex amplitudes of the bubble radius X and of the driving P:

$$X = \frac{1}{\rho_1 R_0^2}\,\frac{1}{\omega_0^2 - \omega^2 + 2\mathrm{i}b\omega}\,P \tag{2.12}$$

with

$$\omega_0 = \frac{1}{R_0}\left\{\frac{p_0}{\rho_1}\left[3\eta(1+\alpha_S) - \alpha_S\right]\right\}^{1/2} \tag{2.13}$$

$$2b = \frac{4\mu_1}{\rho_1 R_0^2} + \frac{\omega^2 R_0}{c_1} + \frac{p_0(1+\alpha_S)}{\rho_1 \omega R_0^2}\Im\Phi \tag{2.14}$$

where η is either 1 for isothermal, or γ for adiabatic behavior of the gas, respectively. More generally, η may take intermediate values, known as polytropic exponent, representing in an approximate way the diffusive heat transport between the bubble and the liquid (see Section 3.3). The damping factor b is the sum of three contributions: the first is due to viscous dissipation in the liquid, the second corresponds to energy loss by acoustic radiation in the compressible fluid, and the last owes to energy dissipation by heat diffusion in the gas ($\Im$ denotes the imaginary part of a complex number, and the value of Φ can be found in Prosperetti, 1977a).

From Equation (2.12), we can recover expected results for the bubble as a forced harmonic oscillator, which we think is important to review here:

- for $\omega < \omega_0$, the bubble radius is out of phase with the driving pressure (if we neglect the term $2\mathrm{i}b$). Thus, the bubble expands in the depression phase of the driving, which is the intuitively expected behavior.
- for $\omega > \omega_0$, the bubble radius is in phase with the driving pressure. This may sound intriguing since in that case, the bubble expands as the external pressure increases. This owes to the predominance of liquid inertia at high frequencies. It has practical consequences on the direction of the Bjerknes force (Section 5.3.1), or the acoustic opacity of bubbly liquids to waves of frequency larger than the bubble's resonance frequency (see Section 5.1.4).

- the bubble oscillations become increasingly large for frequencies near ω_0. It should be noted that such large amplitudes may invalidate the basic hypothesis on the weakness of the oscillations.

Acoustic cavitation is generally far from the linear regime, but the above remarks can help to understand some basic features. However, they predict wrong results at high drivings, especially for Bjerknes forces (Section 5.3.1).

Experimentally, the driving frequency $f = \omega/2\pi$ is a fixed parameter, while all bubbles ambient sizes may a priori exist in the liquid. It is therefore useful to define the resonance radius $R_{\rm res}$, which is the radius that a bubble should have to be resonant at ω. It can be obtained from Equation (2.13), replacing ω_0 by ω and R_0 by R_r. Neglecting surface tension terms ($\alpha_S \ll 1$), and assuming isothermal oscillations, we get

$$R_{\rm res} = \frac{1}{2\pi f}\left(\frac{3p_0}{\rho_{\rm l}}\right)^{1/2} \tag{2.15}$$

In the case of a bubble in water in ambient conditions, we may retain the approximate relation $R_{\rm res} f = 3\ {\rm m}\cdot{\rm s}^{-1}$. For $f = 20$ kHz, the resonant radius is 150 μm, while for $f = 1$ MHz, it drops down to 3 μm.

3.2.4 Non-linear Oscillations

When excited at larger amplitudes, the bubble oscillations can exhibit a rich collection of non-linear phenomena. To get a rapid insight into these behaviors, it is convenient to vary one or several parameters (among R_0, $p_{\rm a}$, and f) and to display only the maximum radius attained by the bubble over one cycle for this parameter. The curves obtained are termed "response curves." A large collection of such curves can be found in Lauterborn and Mettin (1999). We summarize these results below.

Non-linear resonances: When the ratio of the linear resonance frequency and the driving frequency f_0/f (or equivalently the ratio of the resonant radius to the ambient radius $R_{\rm r}/R_0$) approaches a rational number n/m, a non-linear resonance can occur and the amplitude of the bubble oscillations increases. This can be seen in the small peaks in the lower curve of Fig. 2.3. The 1/1 peak corresponds to the linear resonance frequency. Following the accepted terminology, the resonances $n/1$ are called harmonic resonance, the resonances $1/m$ are sub-harmonic resonances, while rational ratio n/m resonances are ultra-harmonic resonances (Lauterborn, 1976).

Period doubling and chaos: Period doubling denotes the destabilization of a non-linear oscillator, when varying one parameter (here R_0), to oscillations with a period twice as large as the driving. In this case two different maxima would be recorded, the first on even driving periods, the second on odd ones. This can be visualized by a separation of the response curve in two branches (see upper curve in Fig. 2.3 near $R_0 = 45$ μm). Changing the parameter yields further destabilizations toward period-4, period-8, and so on, ending in a chaotic regime. The latter is aperiodic and a different maximum is recorded at each driving period. This yields the clouds of

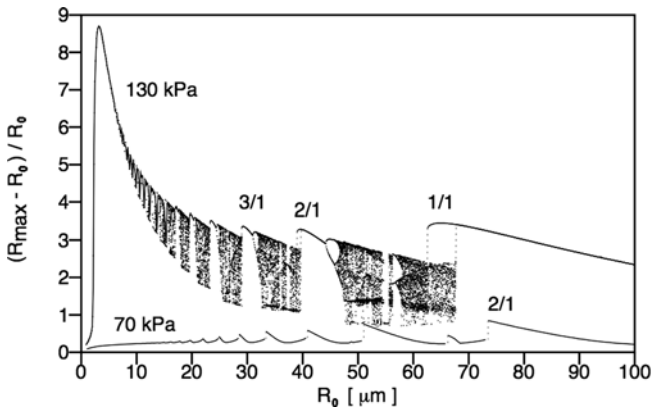

Fig. 2.3 Response curves for an air bubble driven at $f = 20$ kHz (the resonance radius is about 150 µm in this case), $p_a = 70$ kPa (*lower curve*), and $p_a = 130$ kPa (*upper curve*) as a function of the bubble ambient radius. The *fractional numbers* indicate the order of the resonances. Adapted from Sonochemistry and Sonoluminescence (1999, pp. 63–72), in the chapter "Nonlinear Bubble Dynamics: Response Curves and More" by Lauterborn and Mettin. With kind permission of Springer Science and Business Media

dots in the upper curve of Fig. 2.3 (period-4 and higher are scarcely visible because they occur in a narrow parameter range). These successive transitions are termed "sub-harmonic route to chaos."

The experimental consequence of period doubling is the appearance of a spectral component at *f*/2 in the emitted cavitation noise (Neppiras, 1969). The route to chaos has furthermore been demonstrated experimentally by Lauterborn and Cramer (1981a, b), who recorded *f*/2, *f*/4 spectral components, and finally broadband noise, as the driving was increased. The appearance of either a sub-harmonic spectral component *f*/2, or a broadband spectrum, is generally considered as a mark of strong cavitation, and has been correlated experimentally to erosive effects (Gaete-Garreton et al., 1997).

3.2.5 Dynamical Blake Threshold

A noticeable change can be observed between the two curves of Fig. 2.3 in the range [0, 10] µm. At 70 kPa, the response curve is monotonic, while at 130 kPa, the curve passes to a very marked maximum. This peak is termed "giant resonance" by Akhatov et al. (1997a), and is much larger than the main resonance 1/1. This feature has important implications for many cavitation phenomena, especially for diffusional stability of bubbles in levitation cells (Section 3.4.3), and inversion of Bjerknes forces (Section 5.3.1).

A zoom on the small range of R_0 can be seen in Fig. 2.4, for 130 kPa and higher drivings. It is seen that, starting from small radii, the response curves increase suddenly for a driving-dependent critical value of R_0. If conversely, p_a were increased

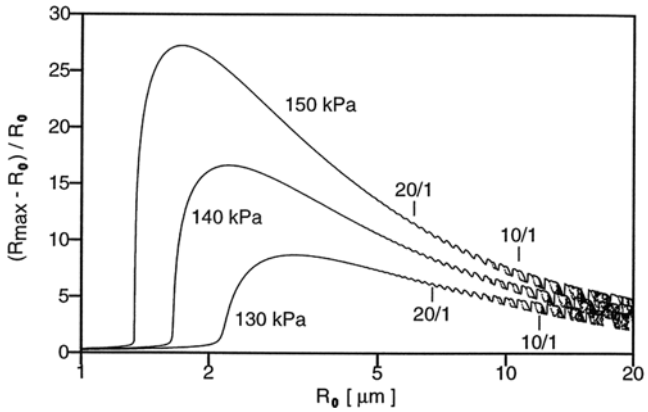

Fig. 2.4 Same as Fig. 2.3 in a range of smaller R_0 and large drivings. Adapted from Sonochemistry and Sonoluminescence (1999, pp. 63–72), in the chapter "Nonlinear Bubble Dynamics: Response Curves and More" by Lauterborn and Mettin. With kind permission of Springer Science and Business Media

for constant R_0, a similar brutal transition would be found (somewhere between the two curves of Fig. 2.3).

This is exemplified in Fig. 2.5, which represents one period of oscillation of a 1 µm bubble for three very close value of the driving p_a near 143 kPa, simulated

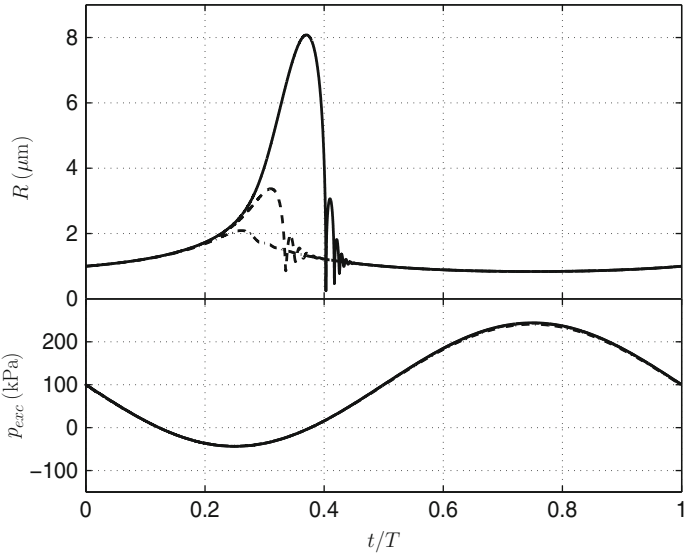

Fig. 2.5 *Upper graph*: dynamics of a 1-µm bubble driven at $f = 20$ kHz, driving amplitudes $p_a = 142$ kPa (*dash-dotted line*), 143.5 kPa (*dashed line*), and 144 kPa (*solid line*). The transition from stable to inertial oscillations can be clearly identified. *Lower graph*: corresponding driving pressures. The three curves are indistinguishable

from Equation (2.10). The bubble dynamics switches drastically from quasi-static oscillations (dash-dotted curve) to large amplitude ones. It is interesting to note that the three curves are indistinguishable at the beginning of the cycle, up to t slightly above $0.2T$.

In fact, this transition occurs at the Blake threshold, calculated from static arguments in Section 2.3. Its physical origin is a competition between the explosive motion caused by the liquid negative pressures and the stabilizing effect of surface tension (Akhatov et al., 1997a; Hilgenfeldt et al., 1998; Lauterborn and Mettin, 1999; Louisnard and Gomez, 2003). For the lowest driving, surface tension prevents the bubble to expand, while it can no longer do so for the largest. For a fixed p_a, Equation (2.5) can be inverted to yield a critical radius R_0^{crit}, which would coincide with the lift-off of the response curves in Fig. 2.4.

3.2.6 Inertial Oscillations

The upper curve in Fig. 2.5 displays an explosive growth, stopped by the recompression of the driving. The growth is then followed by a rapid collapse because the low internal pressure in the bubble at its maximum radius cannot retain the liquid to flow inward. This is the characteristic of "inertial oscillations." The term "inertial" refers to the large explosive expansion of the bubble ($0.25 < t/T < 0.35$ in the upper curve of Fig. 2.5), during which the motion is mainly governed by the liquid inertia. Inertial bubbles have been termed "transient bubbles" in the past, since at that time many experimental observations evidenced bubbles undergoing fragmentation after collapse (see Section 4). The SBSL experiments demonstrate that this is not necessarily the case, and SBSL bubbles are a typical example of inertial and stable bubbles.

Inertial oscillations appear in the parameter space just above the Blake threshold, and are in fact the only bubbles present in the high-pressure zone of strong sound fields (see Section 5.4.5). Inertial bubbles are the main contributors for most applications, owing to the extreme conditions mentioned hereafter.

3.2.7 The Bubble Collapse

We now turn to a brief description of the bubble collapse. The potential energy stored during expansion is then converted into kinetic energy of the liquid and the inward velocity increases drastically, possibly exceeding the sound velocity in the liquid. This is the original problem treated analytically by Rayleigh (1917), who derived scaling laws for the radius versus time (see also Hilgenfeldt et al., 1998; Löfstedt et al., 1993).

The collapse is stopped by the compression of incondensable gas in the bubble. The gas density increases and the van der Waals repulsion forces between molecules or atoms prevent further compression. The bubble rebounds on a timescale of the order of a few nanoseconds. The end of the collapse is almost adiabatic (see Section 3.3.4), and the gas is heated up to thousands of Kelvin, which can promote chemical reactions and sonoluminescence. The bubble internal pressure may

increase up to 1 GPa or more, and the outward acceleration as the bubble rebounds may reach 10^{12} g. The short timescale involved can reveal the effect of the compressibility of the liquid. A diverging spherical wave is emitted, which causes energy loss by radiation (Hilgenfeldt et al., 1998). This wave may steepen into a shock, whose characteristics have been calculated by Benjamin (1958), Tomita and Shima (1977), and Fujikawa and Akamatsu (1980) and demonstrated experimentally by Pecha and Gompf (2000). Shockwaves emitted from collapsing bubbles are held responsible for particle desagglomeration and emulsification (Li and Fogler, 2004).

After the rebound, the bubble expands again and undergoes secondary collapses, termed "afterbounces." The decay of these afterbounces is closely linked to the energy loss in the primary collapse, which in turn depends on several parameters: quantity of solvent in the bubble, thermal diffusion, and chemical reactions among others. The frequency of these rebounds is more or less the free frequency of the bubble. Indeed, the collapse acts mainly as an impulse excitation on a nearly free bubble, to which the latter responds with oscillations at its Eigen-frequency. These afterbounces play an important role in the spherical stability of bubbles (see Section 4).

Let us note that the energy restored in the collapse, in any form, is the potential energy stored during expansion. The latter decreases with frequency, since the bubble has less time to expand. One therefore expects less intense collapses as frequency increases, but this competes with the higher number of collapses per unit time. At the scale of a single bubble, some effects may therefore exhibit an optimum as frequency varies. A generalization for multibubble configuration is difficult because frequency also has effects on the acoustic field and the bubble size distribution. However, such effects have been observed in sonochemistry (see for example Pétrier and Francony, 1997).

3.3 Thermal Effects in the Bubble

3.3.1 The Physics

When the bubble is compressed, the gas in the bubble is heated. Because the surrounding liquid is colder, heat can escape by diffusion from the bubble toward the liquid. The center of the bubble is therefore hotter than the surface, and the opposite holds during the bubble expansion. Hence, the gas is not in thermal equilibrium and, rigorously, its behavior is neither isothermal nor adiabatic. Furthermore, the existence of temperature gradients implies an irreversible loss of energy over one oscillation cycle.

One may first wonder if temperature gradients also exist in the liquid. During bubble compression, for example, does this outward heat flux increase noticeably the temperature of the liquid near the bubble surface? This is an important issue for applications of cavitation, since the liquid may contain non-volatile species that may be altered by high temperatures (chemical reactions for sonochemistry or phase transition for sonocrystallization). A rough estimate of the liquid temperature increase

near the bubble surface can be obtained by using the continuity of the heat flux at the bubble (Prosperetti et al., 1988):

$$\frac{T_R - T_0}{T_C - T_R} = \left(\frac{K_g C_{p_g} \rho_g}{K_l C_{p_l} \rho_l} \right)^{1/2} \tag{2.16}$$

where T_R is the temperature of the liquid at the bubble surface, T_C is the temperature at the bubble center, and T_0 is the undisturbed liquid temperature far from the bubble. K, C_p, and ρ are the thermal conductivities, specific heats, and densities of the gas (subscript g), and of the liquid (subscript l), respectively. The right-hand side being typically of the order of 10^{-3} to 10^{-2}, the temperature variations of the liquid near the bubble surface are expected to be two or three orders of magnitude smaller than the ones at the bubble center.

The calculation of the gas pressure in the bubble (p_g in Equation (2.10)) requires the knowledge of the temperature field. The isothermal and adiabatic approximations avoid this difficulty, but should be considered as extreme ideal cases. The real behavior is governed by the equation of energy conservation in the gas phase (Prosperetti, 1991; Prosperetti et al., 1988), but it is instructive to draw a general picture from the comparison of the timescale of bubble dynamics τ_{dyn}, and the diffusive timescale τ_{diff}, whose ratio is the Peclet number Pe.

3.3.2 Linear Oscillations

For linear oscillations, $\tau_{dyn} = 1/f$ and $\tau_{diff} = R_0^2/\chi_g$, where $\chi_g = K_g/\rho_g C_{p_g}$ is the diffusivity of the gas, so that the thermal Peclet number is $\mathrm{Pe}_0 = \tau_{diff}/\tau_{dyn} = R_0^2 f/\chi_g$. A small value of Pe_0 (for a low frequency, or small bubbles) means that the diffusive timescale is very small, so that the gas will equilibrate immediately in response to a compressional heating and the bubble behaves isothermally. Conversely, for a large value (for high frequency, or large bubbles), heat cannot escape from the bubble, and the gas behaves adiabatically. For intermediate values, temperature gradients exist in the bubble interior, and part of the compressional heating can escape from the bubble.

The resolution of the problem within the linear approximation yields the gas pressure as a linearized form of

$$p_g = p_{g_0} \left(\frac{R_0}{R} \right)^{3\eta} \tag{2.17}$$

where η is called "polytropic exponent" (Devin, 1959; Prosperetti, 1977a) and can be expressed as a function of Pe_0. The limit cases η=1 for $\mathrm{Pe}_0 \to 0$, and η=γ for $\mathrm{Pe}_0 \to \infty$, are recovered in the isothermal and adiabatic limits, respectively. It should be noted that thermal diffusion also introduces a net energy loss over one period, contributing to the damping of the oscillations (see the third term in Equation (2.14)).

3.3.3 Non-linear Oscillations

The above simplified picture is satisfactory for linear or weakly non-linear oscillations, and far from resonances, and in agreement with experimental results (Crum, 1983; Crum and Prosperetti, 1983). It is known to fail, however, near resonances (see the discussion in Crum and Prosperetti, 1984).

For non-linear oscillations, a correct treatment of thermal diffusion in the bubble requires the resolution of the energy conservation equation in the gas. Approximate analytical solutions were proposed by Miksis and Ting (1984), Prosperetti (1991), and Kamath et al. (1992). Several numerical schemes have also been developed (Kamath and Prosperetti, 1989; Kamath et al., 1993; Prosperetti et al., 1988) and were shown to modify the response curves, especially near resonances, but were restricted to moderate drivings.

3.3.4 Inertial Bubbles

The maximum temperature obtained at the end of a perfect spherical collapse is a crucial issue for sonoluminescence and sonochemistry.

The main characteristic of inertial cavitation is the short timescale of the collapse, which may be much shorter than the diffusion timescale. Thus, during the final part of the collapse, the gas is expected to behave almost adiabatically. This idea was followed in the early paper of Noltingk and Neppiras (1950) in order to estimate the final collapse temperature:

$$T(R_{\min}) = T_0 \left(\frac{R_i}{R_{\min}} \right)^{3(\gamma-1)} \tag{2.18}$$

where R_i is the radius from which the behavior starts to be adiabatic. Noltingk and Neppiras (1950) considered the transition to occur at maximum radius. This result already indicated that in otherwise similar conditions, higher temperatures should be obtained for higher values of γ, so that a collapsing mono-atomic gas bubble is hotter than a polyatomic gas bubble (air for example). This is why sonochemical yields can be enhanced by bubbling the solution with argon or other noble gases. The decrease of multibubble sonoluminescence intensity when adding a small propane fraction in argon is a clear experimental demonstration of this effect (McNamara et al., 1999).

The timescale of the bubble expansion is three or four orders of magnitudes larger than that of the collapse, and can be much larger than the diffusive timescale, so that the bubble expansion and the initial stage of the collapse can be isothermal, the final stage being adiabatic. Hence, no two approximations are uniformly appropriate. In fact, the behavior of the gas in the different parts of the bubble oscillation now depends on the instantaneous value of the Peclet number $\mathrm{Pe}(t) = \tau_{\mathrm{diff}}/\tau_{\mathrm{dyn}}$, where $\tau_{\mathrm{diff}} = R(t)^2/\chi_{\mathrm{g}}$ and $\tau_{\mathrm{dyn}} = R(t)/|\dot{R}(t)|$. It is therefore tempting to extend the linear results by defining a dynamic polytropic exponent from $\mathrm{Pe}(t)$, so that the gas behavior automatically varies between isothermal and adiabatic. This approach

was used by Hilgenfeldt et al. (1999b) and independently by Storey and Szeri (2001), and were used successfully within a self-consistent theory of single-bubble sonoluminescence (Hilgenfeldt et al., 1999a, b).

A refined approach accounting for thermal (and also mass) diffusion, using a dynamic thermal diffusion length has been proposed by (Brenner et al., 2002; Toegel et al., 2000a), and found to be in good agreement with direct Navier–Stokes calculations of Storey and Szeri (2000). Yasui (1997) proposed a similar model independently. During compression, part of the compressional heat escapes toward the liquid by thermal diffusion, and therefore, the lower the thermal conductivity of the gas, the hotter the temperature reached in the bubble. This suggested that for noble gas bubbles, the collapse temperature should increase in the series He, Ne, Ar, Kr, Xe. This is indeed the case and is demonstrated unambiguously by the experimental results of Didenko et al. (2000) for multibubble cavitation.

3.3.5 Solvent Evaporation and Condensation

When the bubble expands, the internal pressure decreases, so that the volatile species must evaporate into the bubble to restore equilibrium. Conversely, when the bubble shrinks, condensation takes place. Therefore, if there is equilibrium at the bubble surface, accounting for the presence of vapor can be done easily by setting the partial vapor pressure p_v in the bubble to $p_{v,eq}$, the number of molecules of solvent adjusting to the bubble volume variations.

However, in view of the very short timescale of the bubble collapse, two processes limit this mass transport. First, evaporation and condensation have finite kinetics, so that the vapor in the bubble may not have enough time to condense during the collapse. Secondly, the vapor is not alone in the bubble and its diffusive transport through other species (typically air or any incondensable gas) can be limited. Storey and Szeri (2000) considered both phenomena in their model and found that the water transport in sonoluminescing bubbles was mainly diffusion-limited.

As seen above, the final temperature of the adiabatic collapse is very dependent on γ. Any solvent vapor present in the bubble lowers γ and therefore the final bubble temperature. It is therefore expected that the presence of a volatile species in the liquid will cool the bubble content. This is evidenced by experiments on SBSL intensity in water contaminated with various alcohols (Ashokkumar et al., 2000, 2002; Toegel et al., 2000b). Similarly, lowering the temperature decreases the vapor pressure, lowers the solvent evaporation into the bubble, and should thus increase the collapse temperature. This is confirmed by the experiments of McNamara et al. (1999) in octanol at various bulk temperatures. The higher brightness of SBSL in cold water (Barber et al., 1994; Hiller et al., 1992; Vazquez and Putterman, 2000) is also attributed to this effect (Storey and Szeri, 2000, 2002; Toegel et al., 2000a; Vazquez and Putterman, 2000; Yasui, 2001).

The effect of vapor pressure is exemplified in Fig. 2.6, obtained by using the model of Toegel et al. (2000a) for a 4 μm argon bubble in water at 25°C (solid lines) and 1°C (dashed lines), driven at 120 kPa, 26,500 Hz. The upper graph represents the radius-time curves. The bubble expands less in cold water because less vapor

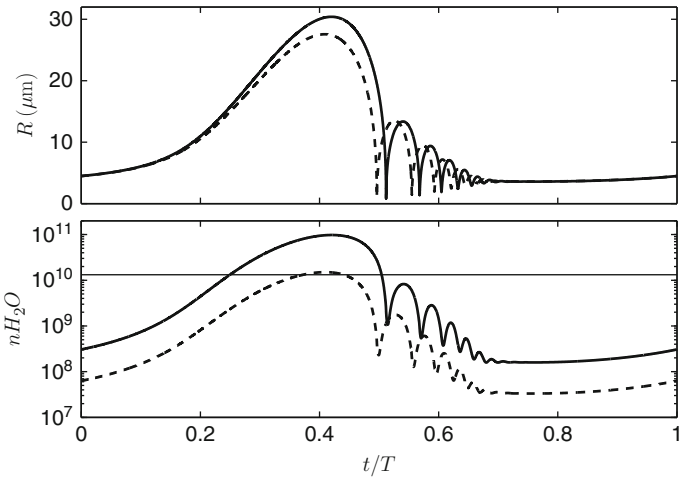

Fig. 2.6 Radius-time curves (*upper graph*) and number of water molecules in the bubble (*lower graph*) for a 4-μm Argon bubble in water at 25°C (*solid lines*) and 1°C (*dashed lines*), driven at 120 kPa, 26,500 Hz. The *horizontal thin solid line in the lower graph* is the number of Argon molecules in the bubble

evaporates, which leads to a shift between the two collapse times. The lower graph represents the number of water molecules in the bubble, and the horizontal line is the number of argon molecules. In hot water, it is seen that the number of water molecules at the end of the expansion is ten times higher than the number of gas molecules. It is seen that in both cases, some water remains trapped in the bubble after the first collapse, because water transport from the bubble center toward the surface is limited by diffusion through argon. Similar curves can be found in Storey and Szeri (2000). Finally, the collapse temperature for cold water is 9,600 K and drops down to 9,020 K for hot water. This difference would increase with higher drivings.

3.3.6 Relevance to Sonochemistry

Evaporation is fundamental in acoustic cavitation and constitutes the cornerstone of sonochemistry: the solvent contains the "fuel" for the reactions, which, once evaporated in the bubble, is heated by the nearly adiabatic compression, and can be dissociated into radicals, so that the bubble is filled with a mixture of polyatomic species. This process is termed "sonolysis." The endothermic reactions occurring in the bubble also consume a part of the collapse energy and therefore also influence the collapse temperature. Didenko et al. (2000) showed experimentally that by fixing the vapor pressures of octanol and dodecane to the same value, a noticeably hotter collapse was obtained in octanol, which suggests that the octanol expends less energy in its chemical reactions than dodecane.

A simple model in the form of a differential equations system is now available for bubble inertial oscillation accounting for heat and mass transport, and chemistry involving H, C, O, and N (Storey and Szeri, 2001, 2002; Yasui, 2001). This model yields interesting results and confirms some tendencies observed in sonochemistry (see, for example, Storey et al., 2001, for methane formation from water–methanol mixtures).

3.3.7 Measuring Cavitation Temperatures

Suslick and co-workers, in their early works, used reactions of known temperature-dependent kinetics to determine the temperature attained in cavitation bubbles (see Suslick et al., 1999, for a review). A more efficient and reliable method consists in recording the sonoluminescence spectra of species whose emission properties are known, used as thermal probes. The authors used molecular emission of diatomics (C_2) (Flint and Suslick, 1991), or emission from metal atoms (Fe, Cr, Mo) originating from volatile organometallics (McNamara et al., 1999). The comparison of recorded and calculated spectra yields an estimation of the collapse temperature with good accuracy. The order of magnitude of the temperatures attained reaches 5,000 K in some cases.

The temperature attained in SBSL experiments is more difficult to assess since the luminescence spectrum is continuous (although lines could be obtained in some cases) and the emission mechanism is controversial. On the basis of radiative collision processes in a weakly ionized gas, temperatures near 20,000 K have been proposed (Brenner et al., 2002; Hammer and Frommhold, 2000). Recent SBSL experiments in sulfuric acid yielded a 2,700-fold increase in light intensity, and following the authors, the bubble would contain a hot plasma core at 30,000 K (Flannigan and Suslick, 2005; Hopkins et al., 2005).

3.4 Rectified Diffusion

3.4.1 The Physics

As seen in Section 2.5, a quiet bubble in a saturated liquid dissolves, owing to surface tension. When the bubble undergoes radial oscillations, the situation may change. In the expansion phase, the gas pressure in the bubble decreases and so does the dissolved gas concentration at the bubble wall $C_R = p_g(t)/k_g$, by virtue of Henry's law. When the bubble shrinks, the concentration C_R increases. Hence, an oscillating concentration gradient appears in the liquid, resulting in an oscillating diffusion flux. During expansion gas enters in the bubble, and during contraction the bubble loses gas. The process has a non-zero average for the following reasons:

- during expansion, the area for gas exchange is higher, so that there is more gas entering the bubble than gas leaving it during contraction

- because of spherical symmetry and liquid mass conservation, the volume of liquid surrounding the bubble becomes thinner during expansion than during contraction; the outward concentration gradient is thus higher during expansion, and Fick's law predicts a larger inward flux during expansion

Both phenomena predict a net gas accumulation in the bubble over one oscillation cycle and can produce a noticeable bubble growth over many periods. This phenomenon is known as rectified diffusion (RD).

3.4.2 Rectified Diffusion Threshold

The above arguments would predict that an oscillating bubble always grows. In fact, surface tension still promotes dissolution, and a competition takes place between both phenomena. One therefore expects that above a certain oscillation level, the bubble grows, whereby it dissolves in the opposite case. Since the bubble oscillations increase with the driving, this analysis predicts a threshold for bubble growth, termed "rectified diffusion threshold," which defines a curve in the (R_0, p_a) plane. Above the threshold the bubble grows (R_0 increases), while below the threshold it dissolves (R_0 decreases). On the threshold, there is diffusive equilibrium on average, and the bubble keeps a constant R_0. A negative slope of the RD threshold in the (R_0, p_a) plane corresponds to an unstable equilibrium, while positive slope points are stable ones.

3.4.3 Bibliography

The first theoretical treatment dates back to Blake (1949), who did not account for liquid convection. Hsieh and Plesset (1961) proposed the first complete formulation of the problem, and derived an approximate solution for linear oscillations, in good agreement with the measurements of Strasberg (1961). A theoretical breakthrough was performed by Eller and Flynn (1965), who obtained a solution of the problem usable for any bubble dynamics $R(t)$ calculated separately, and opening the theory to non-linear and/or large amplitude oscillations. The mean outward flux across the bubble wall over one period was found to be proportional to the time-averaged concentration difference:

$$\langle C_R \rangle_4 - C_\infty = C_0 \left[\frac{\langle p_g \rangle_4}{p_0} - \frac{C_\infty}{C_0} \right] \tag{2.19}$$

where the notation $\langle . \rangle_4$ refers to the non-linear time average

$$\langle g \rangle_4 = \frac{\int_0^T g(t) R^4(t)\, \mathrm{d}t}{\int_0^T g(t)\, \mathrm{d}t}$$

This expression can be compared with the static case, Equation (2.7). The threshold is obtained for $\langle p_g \rangle_4 / p_0 = C_\infty / C_0$. The average gas pressure $\langle p_g \rangle_4$ decreases as

the bubble oscillation amplitude increases. One therefore expects that the threshold will be lower for any combination of parameters increasing the oscillation amplitude, for example, by increasing the driving, approaching a linear or non-linear resonance, or for inertial oscillations.

Further measurements were carried out by Eller (1972), showing good agreement with the theory of Eller and Flynn (1965) for the threshold. However, the measured growth rates were found to be much higher than predicted by the theory. This was confirmed by Gould (1974), who established a correlation between this abnormally high growth rate with the appearance of bubble shape instabilities. Crum (1980) repeated threshold and growth rate measurements, and also derived analytical expressions of both quantities for linear oscillations, taking into account the damping of the oscillations because of thermal effects in the bubble (see Section 3.3). He found excellent agreement for the threshold, and also for the growth rate for pure water, but noticed that the addition of a small amount of surfactant yielded a fivefold increase of the growth rate without any discernible bubble surface instability. This effect was attributed qualitatively to a layer of surfactant adsorbed at the bubble surface, and was later confirmed theoretically by Fyrillas and Szeri (1995). Crum and Hansen (1982) compared different expressions of the rectified threshold and proposed an interesting discussion on the case of pulsed driving.

The linear threshold of Crum (1980) and Crum and Hansen (1982) is presented in Fig. 2.7. As expected, a strong decrease is visible near the linear resonance. It is important to note that this threshold yields wrong results near non-linear resonances, and also for high drivings, typically near $p_a \simeq p_0$ (see Section 3.4.4).

Church (1988) calculated the rectified diffusion threshold in a wide parameter range, without relying on the hypothesis of linear oscillations. His results showed the existence of various positive slope branches, raising for the first time the possibility of small diffusively stable bubbles. Later, starting a series of papers on the possible effect of surfactants on rectified diffusion, Fyrillas and Szeri (1994) solved in an elegant manner the convection–diffusion problem by perturbation methods,

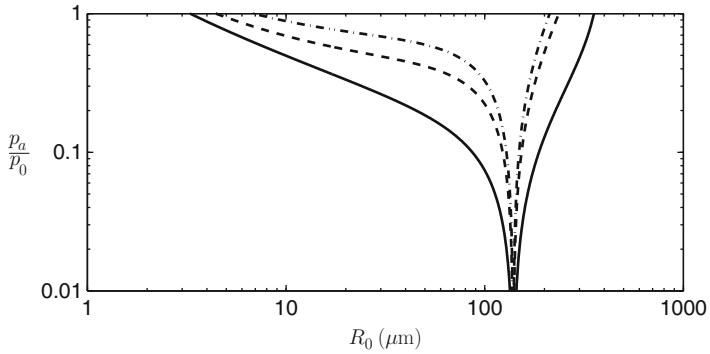

Fig. 2.7 Rectified diffusion threshold based on a hypothesis of linear oscillations. *Solid curve*: $C_1/C_0 = 1$ (saturation); *Dashed curve*: $C_1/C_0 = 0.9$; *Dash-dotted curve*: $C_1/C_0 = 0.8$

and were the first to obtain a consistent expression of the growth rate, valid either near the threshold or not. In a second paper (Fyrillas and Szeri, 1995), they examined the effect of surfactants, possibly resisting gas transport across the bubble interface, and found growth rates in agreement with earlier experiments, strengthening the early hypothesis of Crum (1980). They finally proposed a theoretical formulation for the oscillatory adsorption/desorption process of a surfactant at the surface of an oscillating bubble, and demonstrated that the average quantity of surfactant adsorbed over one period was higher than in the equilibrium case (Fyrillas and Szeri, 1996).

Meanwhile, the first experiments on SBSL revealed the actual existence of a diffusively stable cavitation bubble, neither growing, nor dissolving (Gaitan et al., 1992). This unusual feature in cavitation was investigated by several authors (Akhatov et al., 1997a; Hilgenfeldt et al., 1996; Löfstedt et al. 1995), who calculated that diffusively stable bubbles can be obtained in degassed conditions and that they correspond to the appearance of a positive slope of the rectified diffusion threshold. However, Barber et al. (1995) found that the ranges of dissolved gas concentrations for diffusive stability were lower by a factor 100 in pure argon than in air. The agreement with theory was found good for argon bubbles, but not for air bubbles, for which theory predicted growth instead of the stability observed experimentally. Löfstedt et al. (1995) and Barber et al. (1997) therefore postulated an "anomalous mass flow" necessary to reject more air in the compression phase than predicted by rectified diffusion theory. This key point of SBSL was solved by Lohse et al. (1997) and Lohse and Hilgenfeldt (1997), who proposed that the air in the bubble was heated enough to allow dissociation of O_2 and N_2, the product being easily expelled from the bubble. The air bubble in SBSL experiments were thus found to be in fact an argon bubble (present as 1% in air). This hypothesis is now accepted and has received experimental confirmation (Ketterling and Apfel, 1998; Matula and Crum, 1998). It is interesting to note that the theory of rectified diffusion, almost a half-century after its first theoretical treatment, indirectly supplied a clue to explain this singular chemical effect.

3.4.4 Merging of the Blake and Rectified Diffusion Thresholds for Small Bubbles

Very small bubbles are prevented from oscillating strongly by surface tension, and hence they need a strong driving to become inertial, which is evidenced by the increase of the Blake threshold toward small radii (see left part of Fig. 2.1). If their radial oscillation is so constrained, one may suspect that neither can they grow by rectified diffusion. This therefore suggests that the Blake and rectified diffusion thresholds would almost be the same for small ambient radii.

This is indeed the case, as demonstrated analytically and numerically by Louisnard and Gomez (2003) (this property was already apparent in the results of Church (1988), but remained unnoticed by the latter author). Figure 2.8 shows the RD threshold, computed from the Keller equation (2.10) (thick solid line) for saturated water ($C_\infty = 1$) in a 26.5 kHz acoustic field. Also shown is the threshold

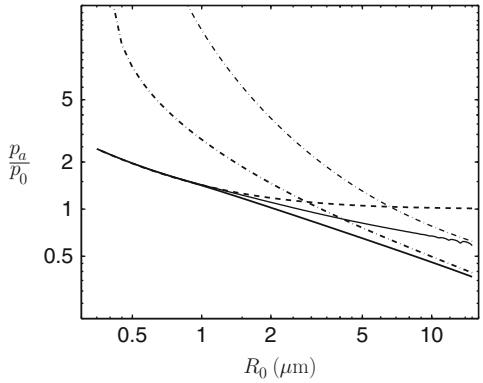

Fig. 2.8 Exact RD threshold for saturated water ($C_1 = 1$) calculated numerically from the Keller equation (*thick solid line*); Blake threshold from Equation (2.5) (*thick dashed line*); and linear theory RD threshold calculated from Crum and Hansen (1982) (*thick dot-dashed line*). The *thin lines* represent respectively the exact (*solid*) and linear (*dot-dashed*) RD thresholds calculated for slightly degassed water ($C_1 = 0.8$). Adapted from Louisnard and Gomez (2003)

calculated from the linear theory (Crum, 1980; Crum and Hansen, 1982, thick dot-dashed line); it is readily seen that for bubbles of small ambient radii, the linear theory fails to predict the pressure threshold value, but for larger bubbles the exact threshold merges with the linear one, at least in the range of radii considered here. The Blake threshold is also represented (thick dashed line), and it is seen that the two curves merge for acoustic pressure greater than, say 1.4 bar, for saturated water. Performing the same calculations for slightly degassed water ($C_\infty = 0.8$) yields the same conclusion, as attested by Fig. 2.8 (the numerical RD threshold is represented by a thin solid line and the linear one by thin dot-dashed line). The computation was also repeated for 50 and 100 kHz frequencies, leading to the same conclusion (not shown).

This feature casts some doubts on what is referred to as the "gaseous cavitation cycle" by Neppiras (1980), which states that small bubbles would grow by rectified diffusion by oscillating in a stable manner ("stable" should be understood in this context as non-inertial) up to the Blake threshold, where they oscillate inertially, break up, and seed new small bubbles. Indeed, for high drivings, the above result indicates that the region in the parameter space for growing non-inertial bubbles is negligible. This might suggest that other growth mechanisms, for example coalescence under secondary Bjerknes forces (Section 5.3.2), may initially participate in the development of the bubble fields (Louisnard, O. (2001). *Theoretical Study of Competition Between Dissolution and Coalescence of Small Bubbles in an Acoustic Field*, "Unpublished"; Louisnard and Gomez, 2003; Mettin, 2005).

Rectified diffusion however occurs in cavitation fields at moderate drivings (say below 100 kPa). In this case, bubbles can indeed grow by rectified diffusion toward large sizes, as attested by the experiments of Crum (1980), and this phenomenon can

be used for degassing applications (Kapustina, 1973). Even for strong drivings, there always exist lower pressure zones in the liquid, where some bubbles can undergo rectified diffusion.

4 Non-spherical Oscillations

4.1 Introduction

Two phenomena prevent the bubble from losing its sphericity: the first one is surface tension and the second is of dynamical origin (we refer the reader to an interesting discussion by Prosperetti, 1999). Conversely, various effects may induce loss of sphericity. First, the environment of the bubble may itself deviate from isotropy. One may think about the influence of a neighboring bubble or a solid boundary, the anisotropy of the acoustic field itself, the effect of gravity that introduces a translational motion, even in the case of levitation experiments, or steady liquid motion. Furthermore, a radially oscillating bubble can develop surface oscillation by an intrinsic shape instability mechanism.

4.2 Shape Instabilities

The dynamic stability of a purely radial motion has been investigated in the early work of Plesset (1949). The local bubble radius is expanded as the sum of spherical harmonics:

$$r(\theta,\phi,t) = R(t) + \sum_{n=1}^{\infty} a_n(t) Y_n(\theta,\phi) \tag{2.20}$$

Assuming potential flow, writing the continuity equations at the bubble interface and performing a linear stability analysis yields

$$\ddot{a}_n + \frac{3\dot{R}}{R}\dot{a}_n - (n-1)\left[\frac{\ddot{R}}{R} - (n+1)(n+2)\frac{\sigma}{\rho_l R^3}\right] a_n = 0 \tag{2.21}$$

The mode $n = 1$ corresponds to a translational motion of the spherical bubble with a velocity $v = \dot{a}_1$. For n>2, the second term in the square bracket shows that surface tension has a stabilizing role, increasing with the mode number. The first term has a destabilizing role when $\ddot{R} > 0$, that is, when the acceleration is oriented from the gas toward the liquid. This is the classical statement of the Rayleigh–Taylor instability, originally derived for a plane interface. Here, it can appear at the end of the collapse, as the bubble rebounds, where $\ddot{R}$ can reach huge values. Its occurrence is thought to limit the stability region of SBSL for increasing drivings p_a (see below). The second term in Equation (2.21) is seen to act as a negative damping

when $\dot{R} < 0$, that is, when the bubble is collapsing (Plesset and Mitchell, 1956), and therefore favors instability during the bubble collapse.

Another type of instability, termed "parametric" or "Faraday instability" (well known in the case of a plane interface), accumulates over time because of the periodic character of the square bracket in Equation (2.21). Figure 2.9 exhibits short exposure photographs of cavitation bubbles undergoing this type of instability (Kornfeld and Suvorov, 1944).

Fig. 2.9 Snapshots of shape instable bubbles. Reused with permission from Kornfeld and Suvorov (1944, p. 495). Copyright 1944, American Institute of Physics

Parametric instabilities have been correlated with an erratic translational motion of the bubble by Eller and Crum (1970) for drivings lower than 70 kPa, near 20 kHz. Their approximate calculations of thresholds for parametric instability compares reasonably with the measured thresholds for erratic drift.

The theory of Plesset has been extended by Prosperetti (1977b) to account for viscous effects, and simplified in the limit where viscous effects are concentrated in a diffusion layer near the bubble (Hilgenfeldt et al., 1996; Prosperetti and Seminara, 1978).

4.3 Stability Thresholds

In SBSL experiments, when p_a is increased, the sonoluminescing bubble suddenly disappears (near $p_a = 150$ kPa, Gaitan et al., 1992). This is attributed to the appearance of Rayleigh–Taylor instability as the bubble collapses. Besides, in the same experiments, if water is not degassed enough, bubbles may grow by rectified diffusion (emitting SL) up to a critical size (near 5 μm) where they break, pinch-off a microbubble, and start to grow again (this process is known as unstable SBSL). The upper critical size is found theoretically to correspond to parametric instabilities.

To explain these findings, Brenner et al. (1995), Hilgenfeldt et al. (1996), and Brenner et al. (2002) established the region in the parameter space where stable and unstable SBSL can be obtained. From this formulation, they sought the domain in the parameter space (R_0, p_a), where the bubble remains spherical against both parametric and Rayleigh–Taylor instability. The former was found to limit the stability domain toward increasing R_0, while the latter did so for increasing p_a.

The obtained results were then refined by several authors, taking into account the variations of the gas density during collapse (Lin et al., 2002b; Yuan et al., 2001), and/or using a more realistic model for the bubble radial oscillations. The latter

point is crucial especially for predicting the Rayleigh–Taylor instability threshold, which is very sensitive to the precise value of $\ddot{R}$ at the end of the collapse. Prosperetti and Hao (1999) showed that accounting for thermal effects in the gas reduced $\ddot{R}$ sufficiently to suppress the Rayleigh–Taylor instability in the SBSL range of parameters. The same conclusion was reached by Augsdorfer et al. (2000) and Yuan et al. (2001), while Lin et al. (2002b) recalculated the instability thresholds accounting for variations of gas density and for thermal effects and water transport at the bubble wall (Storey and Szeri, 2001). For the Rayleigh–Taylor threshold, they found a convincing agreement with the experiments of Ketterling and Apfel (2000).

Although initially relevant to SBSL, these thresholds are also of great importance for cavitation fields. Anisotropy is more important in multibubble fields than in single-bubble levitation experiments, so that, for the same drivings, the values of R_0 calculated or measured in the latter context may be considered as upper boundaries for bubble sizes in cavitation fields. In connection with this issue, we would like to mention the experimental work of Gaitan and Holt (1999), who measured the parametric instability threshold in a 20 kHz levitation cell for a wide range of driving p_a (Fig. 2.10). The points clearly define an upper bound for the ambient radius for a given driving. The resonant radius at 20 kHz is 150 μm, and it is clear from these measurements that no resonant bubble can survive even for relatively low drivings. Even for p_a as low as 30 kPa, it is seen that bubbles would undergo shape instability near 60 μm.

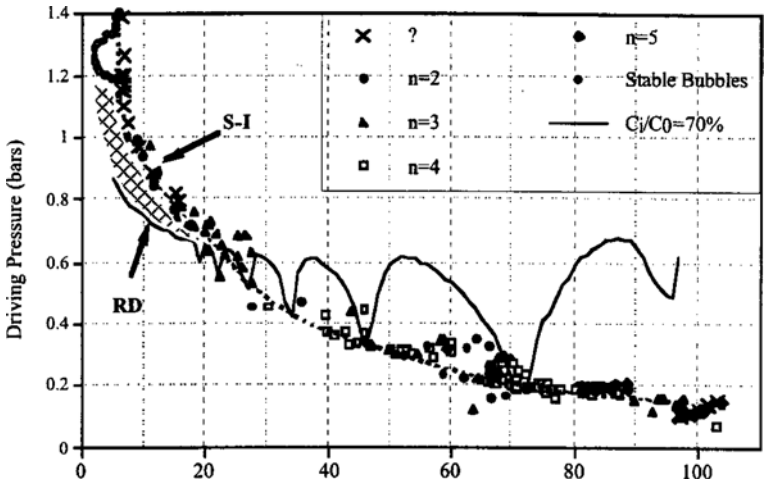

Fig. 2.10 Instability threshold measured in a 20 kHz levitation cell. The *different symbols* indicate the order of the unstable mode recorded by image processing. The *cross symbols* correspond to an instability whose order could not be determined. The *solid line* is the calculated rectified diffusion threshold for $C_1/C_0 = 0.7$. Reprinted Fig. 2.2 with permission from Gaitan and Holt (1999). Copyright (1999) by the American Physical Society

4.4 Self-Propulsion of Non-spherical Bubbles

Common observation of cavitation fields reveals bubbles undergoing erratic dancing motions. It was first suggested by Strasberg and Benjamin (1958) that this translation motion could originate from surface instabilities. As mentioned above, this has been confirmed experimentally by Eller and Crum (1970), who observed that the measured driving threshold for this behavior to occur coincided with the calculated threshold for parametric surface instabilities. The problem has been tackled theoretically by Benjamin and Ellis (1990) and Zardi and Seminara (1995), who showed that the translation motion could appear by a non-linear coupling between two adjacent instability modes. More recent treatment (Doinikov, 2004; Reddy and Szeri, 2002) generalized this result.

4.5 Non-spherical Collapses Near Boundaries and Erosion

A bubble collapsing near another bubble or near a solid surface undergoes a non-spherical collapse. The astonishing variety of shapes attained by these bubbles constitutes a scientific challenge, both theoretically and experimentally, owing to the short deformation timescales involved in the collapse. The main motivation for investigating non-spherical collapses dates back to the original issue of solids damaging by hydrodynamic cavitation bubbles. As noted by Lauterborn et al. (1999), no material has been found to resist their attack, a rather peculiar effect, if one intuitively thinks of bubbles as soft objects. The issue is of importance not only for erosion of propellers, blades, and hydraulic systems, but also for acoustic cavitation whose erosion effect is well known and generally damages the tip of the transducer.

The analysis of Rayleigh outlined that the high pressures, possibly as shockwaves, generated by a spherical implosion were the origin of erosion. Since then, it appeared that the impact of high-speed liquid jets, formed by the involution of collapsing cavities, could be a primary factor in cavitation damage. The important pioneering experimental and theoretical study of Benjamin and Ellis (1966) stated the problem in terms of the important concept of Kelvin impulse and presented images of spark-induced bubbles. Other results on spark-induced bubbles near boundaries can be found in the literature, but better reproducibility and precision in the location of the bubble can be obtained with laser-generated bubbles since the early experiments of Lauterborn and Bolle (1975).

The phenomenon can be seen in the photographic series in Fig. 2.11 from Lauterborn et al. (1999). The bubble involutes from the top, and the downward liquid jet develops, pushes the lower boundary of the bubble toward the solid surface, impinging on it violently, which creates a pit just below the bubble. On some occasions, the jet can pierce the bubble, which becomes a torus, and further disintegrates into a circle of small bubbles, whose implosion generates a circle of pits. The behavior is reproducible for a fixed ratio between the boundary-bubble separation and the maximum bubble radius. More experimental facts, including complex shockwaves

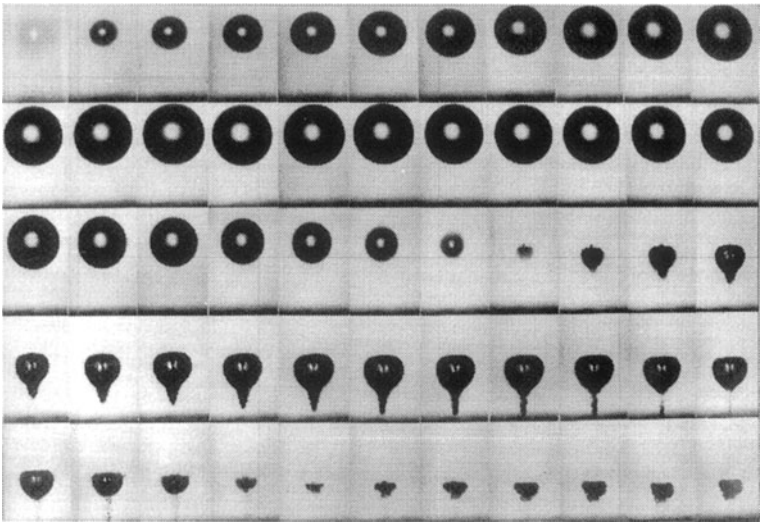

Fig. 2.11 Non-spherical collapse of a laser-induced bubble near a flat rigid boundary, recorded at 75,000 frames per second. The solid boundary is below the bubble. Adapted from Lauterborn et al. (1999), with kind permission of John Wiley and Sons Ltd

formation, can be found in Philipp and Lauterborn (1998), Lauterborn et al. (1999), and Lindau and Lauterborn (2003).

Erosion by acoustic cavitation is also well known, but is infinitely more difficult to control than laser bubbles. Recent experiments show that within the same experiment, the various bubble structures that emerge from the acoustic field (see Section 5.4) have different erosion effects (Krefting et al., 2004). Unlike laser experiments that allow the precise positioning of the bubble, acoustic cavitation bubbles can rise up from various places, and the solid boundaries themselves can act as bubble sources. Laser bubble experiments therefore constitute a perfect tool to assess the complex phenomena involved, and the precise mechanisms of damaging at the scale of a single bubble.

4.6 Non-spherical Collapses Far from Boundaries

Non-spherical collapses can also occur without the presence of a solid boundary. First by symmetry, a bubble collapsing at a distance s of a solid boundary problem is equivalent to the problem of two identical bubbles collapsing at a distance $2s$. This is confirmed by experiments of Lauterborn et al. (1999).

But a single bubble can also collapse non-spherically and form liquid jets because of its translational motion. This is supported by the experiments of spark-induced bubble with or without gravity (Benjamin and Ellis, 1966) and theoretically (Blake and Gibson, 1987; see also Prosperetti, 1999), on the basis of impulse conservation.

Even in levitation experiments, this is also the case because the bubble undergoes a small, but non-zero, translational motion, owing to gravity. It has been suggested that sonoluminescing bubbles could in fact collapse non-spherically, and that the corresponding liquid jet could be responsible for the light emission (Prosperetti, 1997). It was found, however, that under microgravity, where jets would be unexpected, even more light was emitted (Matula, 2000), and also that light emission decreases and even ceases with increasing asphericity (Ohl et al., 1998).

Whether or not aspherical collapses indeed occur in single bubble experiments remains an open question. In multibubble fields, it is generally accepted that the bubbles collapse aspherically, but this is difficult to assess experimentally. Another issue relevant to this discussion is the difference of light emission spectra between single- and multi-bubble sonoluminescence. Without entering into this complex problem, we would like to mention the experiments of Matula et al. (1995). The sonoluminescence spectrum of NaCl–water mixtures reveals that the sodium line emission is present in multi-bubble sonoluminescence (MBSL), and absent in SBSL. Since sodium cannot evaporate into the bubbles, this may suggest that droplets of solution could enter the bubble during a surface instability process or aspherical collapse with jetting. Therefore, one of the latter processes would necessarily occur in multi-bubble conditions. This is an important point, since it means that non-volatile species could also participate in this way to chemical reactions in the hot gaseous environment inside the bubble.

5 Cavitation Fields

5.1 Acoustics

5.1.1 Equation of Linear Acoustics

Linear acoustics refers to non-dissipative low amplitude sound propagation. Thus it may not be the relevant tool to study cavitation, since the latter converts acoustic energy into various forms of energy (thermal, interfacial or light). However, some basic concepts can be used profitably, on one hand to design sonoreactors, and on the other hand to characterize cavitation experiments.

The linear propagation of an acoustic wave results from the isotropic elastic properties of the liquid. When the liquid is expanded or compressed, an elastic force tends to restore equilibrium, and in doing so, accelerates the liquid. Non-dissipative acoustic waves can be described by linearized Euler equations, neglecting viscosity:

$$\frac{\partial p}{\partial t} + \rho_l c_l^2 \nabla . \mathbf{u} = 0 \tag{2.22}$$

$$\rho_l \frac{\partial \mathbf{u}}{\partial t} = -\nabla p \tag{2.23}$$

where $\mathbf{u}(\mathbf{x}, t)$ is the liquid velocity field associated to the acoustic wave, and $p(\mathbf{x}, t)$ the local acoustic pressure. This set of equations can be reduced to a propagation equation

$$\nabla^2 p - \frac{1}{c_l^2}\frac{\partial^2 p}{\partial t^2} = 0 \tag{2.24}$$

Various boundary conditions may be associated to this equation. Among the simplest, either the pressure or the velocity can be prescribed. An infinitely soft boundary is represented by p=0, and an infinitely rigid one by $\mathbf{u}.\mathbf{n} = \mathbf{0}$, where $\mathbf{n}$ is the outward unit vector normal to the boundary.

Assuming mono-harmonic waves at frequency ω, and using complex notation

$$p = \frac{1}{2}\left[p_\mathrm{a}(\mathbf{x})\mathrm{e}^{\mathrm{i}\omega t} + \mathrm{c.c.}\right], \qquad \mathbf{u} = \frac{1}{2}\left[\mathbf{u_a}(\mathbf{x})\mathrm{e}^{\mathrm{i}\omega t} + \mathrm{c.c.}\right] \tag{2.25}$$

where c.c. denotes the complex conjugate. Equation (2.24) reduces to the Helmholtz equation

$$\nabla^2 p_\mathrm{a} + k_\mathrm{l}^2 p_\mathrm{a} = 0 \tag{2.26}$$

where $k_\mathrm{l} = \omega/c_\mathrm{l}$ is the wavenumber.

5.1.2 Energy Conservation: Non-dissipative Acoustics

An energy conservation equation can be deduced from Eqs. (2.22) and (2.23):

$$\frac{\mathrm{d}}{\mathrm{d}t}\int\int_V\int\left(\frac{1}{2}\rho_\mathrm{l}u^2 + \frac{1}{2}\frac{p^2}{\rho_\mathrm{l}c_\mathrm{l}^2}\right)\mathrm{d}V = \int\int_S -p\mathbf{u}\mathbf{n}\,\mathrm{d}S \tag{2.27}$$

where V is an arbitrary volume of fluid and S its boundary. The parenthesis in the volume integral is the acoustic energy density (in W m^{-3}), which is the sum of the kinetic and potential compressional energy of the liquid, and $p\mathbf{u}$ is called acoustic intensity (in W m^{-2}). Both are local quantities. Equation (2.27) expresses that the variations of acoustic energy in a volume result from the difference between the fluxes of mechanical energy entering and leaving this volume, and result directly from the theorem of kinetic energy.

For mono-harmonic waves, it can be easily checked that the left side of Equation (2.27) is zero on average over one acoustic period. Besides, the average acoustic intensity $p\mathbf{u}$ can be shown to read $\Re(p_\mathrm{a}\mathbf{u_a})/2$, where $\Re$ denotes the real part of a complex number. Now, let us consider the case of a sonoreactor excited by the vibrating surface $S_\mathrm{sonotrode}$ of a sonotrode, and closed by boundaries $S_\mathrm{boundaries}$, of unspecified type for now. Equation (2.27) becomes

$$\underbrace{\int\int_{S_{\text{sonotrode}}} -\frac{1}{2}\Re(p_{\text{a}}\mathbf{u_a}).\mathbf{n}\ \mathrm{d}S}_{\substack{P_{\text{active}}=\text{ power}\\ (>0)\text{ emitted}\\ \text{into the liquid}}} = \underbrace{\int\int_{S_{\text{boundaries}}} \frac{1}{2}\Re(p_{\text{a}}\mathbf{u_a}).\mathbf{n}\ \mathrm{d}S}_{\substack{P_{\text{bound}}=\text{ power}\\ (>0)\text{ lost}\\ \text{through the}\\ \text{boundaries}}} \tag{2.28}$$

The left integral is the power transmitted from the sonotrode to the liquid, and is termed *active power*. The above relation states that all the mechanical energy entering the liquid is lost by boundaries. In the case of perfect rigid or soft boundaries, Equation (2.28) merely states that the acoustic power transmitted to the liquid by the sonotrode is zero. This a priori paradoxical result originates from the non-dissipative character of the medium, which is implicitly assumed in Eqs. (2.23) and (2.24).

5.1.3 Energy Conservation and Dissipation: Calorimetric Method

Various physical processes can yield attenuation of acoustic waves, including viscosity or finite thermal diffusion, among others. In the case of bubbly liquids, the main dissipation occurs at the bubble level (see Sections 3.2.3 and 5.1.4). Whatever its physical origin, attenuation of mono-harmonic linear waves (or their superposition) can be modeled by introducing a complex wavenumber

$$k = k_{\text{l}} - \mathrm{i}\alpha \tag{2.29}$$

in (2.26), where $\alpha > 0$ is the attenuation coefficient in m^{-1}. In this case, it can be shown that Equation (2.28) becomes

$$\underbrace{\int\int_{S_{\text{sonotrode}}} -\frac{1}{2}\Re(p_{\text{a}}\mathbf{u_a}).\mathbf{n}\ \mathrm{d}S}_{\substack{P_{\text{active}}=\text{ power}\\ (>0)\text{ emitted}\\ \text{into the liquid}}} = \underbrace{\int\int_{S_{\text{boundaries}}} \frac{1}{2}\Re(p_{\text{a}}\mathbf{u_a}).\mathbf{n}\ \mathrm{d}S}_{\substack{P_{\text{bound}}=\text{ power}\\ (>0)\text{ lost}\\ \text{through the}\\ \text{boundaries}}} + \underbrace{\int\int\int_{V} \alpha\frac{|p_{\text{a}}|^2}{\rho_{\text{l}}c_{\text{l}}}\ \mathrm{d}V}_{\substack{P_{\text{diss}}=\text{ power}\\ (>0)\text{ dissipated}\\ \text{in the liquid}}} \tag{2.30}$$

For perfectly reflecting boundaries, this equation now states that the period-averaged power sent through the sonotrode surface is the power dissipated in the liquid.

The integral P_{diss} represents the opposite of the power of internal dissipative forces (for example viscous friction). Combining the theorem of kinetic energy with the first principle of thermodynamics, it can be shown that

$$\int\int\int_V \rho_\mathrm{l} C_{v_\mathrm{l}} \frac{\mathrm{d}\langle T\rangle}{\mathrm{d}t} = P_\mathrm{diss} + \dot{Q} \tag{2.31}$$

where V is an arbitrary volume of insonified liquid, $\langle T\rangle$ is the local temperature of the liquid averaged over one or more acoustic periods, and $\dot{Q}$ is the (algebraic) heat gained or lost by volume V. This equation is the basis of the so-called calorimetric method. Taking V as the whole volume of insonified liquid, and stirring sufficiently to ensure uniform temperature, $\langle T\rangle$ is monitored in a given point of the sonoreactor by a temperature probe as soon as ultrasound is switched on. At $t = 0$ heat cannot escape owing to thermal inertia, so that $\rho_\mathrm{l} C_{v_\mathrm{l}} \langle \mathrm{d}T/\mathrm{d}t\rangle_{t=0}$ matches P_diss. Thus, the initial slope of the temperature curves yields an estimation of the power dissipated in the liquid, which, from Equation (2.30), is also the active power sent through the sonotrode area. This calorimetric method is easy to use and is commonly used to characterize cavitation experiments (Ratoarinoro et al., 1995). Finally, it should be noted that the quantity $|p_a|^2/(\rho_l c_l)$ is sometimes improperly termed "intensity." We emphasize that this is true only for plane traveling-wave, but is definitely not in other cases.

5.1.4 Acoustics of Bubbly Liquids

The presence of bubbles in a liquid increases the compressibility of the effective medium. Therefore, one expects the effective sound velocity to decrease. This is indeed the case for low-frequency waves or small bubbles. As the frequency or the bubble radius increases, the phase shift between the bubble response and the local driving pressure leads to a variation of the effective sound speed. The latter therefore varies with frequency, and waves in such a medium are called dispersive. Moreover, the non-linear behavior of the bubbles oscillation renders high-intensity waves non-linear.

Theory of bubbly liquids acoustics can be traced back to Foldy (1944) and Carstensen and Foldy (1947). Their result contains the main physics and is equivalent to the most recent theories in the linear case, and at low gas fractions. Linear experimental data were recorded by Fox et al. (1955) and Silberman (1957), the latter report still constituting a reference. Theory for non-linear waves has been derived independently by van Wijngaarden (1968) and Iordansky (1960), and a similar model, based on a rigorous averaging method, was derived by Caflish et al. (1985). Commander and Prosperetti (1989) developed a linear form of this model, extending it to polydisperse bubble populations and compared it to the experiments of Silberman.

The Caflish propagation equation reads

$$\frac{1}{c_\mathrm{l}^2}\frac{\partial p}{\partial t} - \nabla^2 p = \rho_\mathrm{l}\frac{\partial^2}{\partial t^2}\int_0^\infty N(\mathbf{x}, R_0)\frac{4\pi}{3}R^3[p(t), R_0]\,\mathrm{d}R_0 \tag{2.32}$$

where $N(\mathbf{x}, R_0)\mathrm{d}R_0$ is the number of bubbles per unit volume, in the range of sizes $[R_0, R_0 + \mathrm{d}R_0]$, located at $\mathbf{x}$, and $R[p(t), R_0]$ is the radial dynamics of a bubble of ambient radius R_0 excited with the local acoustic pressure $p(t)$, obtained from Equation (2.10) for example. The integral can be recognized as the instantaneous bubble volume fraction.

Equation (2.32) is intrinsically non-linear, but assuming mono-harmonic low-amplitude waves and using the linear theory of bubble oscillations exposed in Section 3.2.3, the Caflish model reduces to an Helmholtz equation $\nabla^2 p_\mathrm{a} + k^2 p_\mathrm{a} = 0$ with $k^2 = (\omega/c)^2$, and

$$\frac{1}{c^2} = \frac{1}{c_1^2} + 4\pi \int_0^{+\infty} \frac{R_0}{\omega_0^2(R_0) - \omega^2 + 2\mathrm{i}b(R_0)\omega} N(\mathbf{x}, R_0)\, \mathrm{d}R_0 \tag{2.33}$$

where ω_0 and b are given by Eqs. (2.13) and (2.14). It should be noted that k and c are now complex quantities, which implies a spatial wave attenuation (see Section 5.1.3). Moreover, both depend on frequency, traducing the dispersive character of the medium. From expression (2.33), the following conclusions can be drawn:

- For $\omega \ll \omega_0$, the sound speed in the bubbly liquid is lower than the sound speed in the pure liquid. This was expected owing to the larger compressibility of the medium.
- As ω approaches ω_0, the sound speed decreases drastically. Just above ω_0, c^2 becomes negative, so that the sound velocity has a large imaginary part, which produces strong attenuation of the waves. Physically, this peculiar result comes from the fact that above resonance, the bubble contracts in the expansion phase of the acoustic pressure (Section 3.2.3). Thus, all happens as if the bubbles had a negative compressibility.
- For increasingly large frequencies, the oscillation of the bubbles vanishes and the sound speed of the pure liquid is recovered.

It should be emphasized that the bubble size distribution N must be known if one wishes to calculate the effective sound speed c. Various studies solved the linear Caflish model in order to predict the sound field in sonoreactors (Dähnke et al., 1999; Servant et al., 2000, 2003), but used an arbitrary Gaussian distribution, involving bubbles much larger than experimentally observed (see Section 5.4.5), so that the validity of the predictions is difficult to assess. In fact, some of these results show negligible departure from linear acoustics, owing to the small bubble fractions introduced in the model.

5.2 Nucleation of Bubbles

As seen in Section 2.5, a spherical gas bubble is unstable in a saturated quiet liquid, and must dissolve. This questions the origin of the numerous cavitation bubbles observed shortly after switching on the sound field.

The theoretical tensile strength of pure water, which is the lowest negative pressure it can support without homogeneous nucleation of a cavity, is −100 MPa. The lowest measured tensile strength reaches −27 MPa (Briggs, 1950). This is still well below the negative acoustic pressures that can be reached with ultrasound. Thus, the bubbles originate necessarily from existing gas pockets, stabilized in the liquid in some way.

The first explanation is that free gas nuclei exist in the liquid, protected against dissolution by a shell of either hydrophobic ions or surface active species. The second explanation postulates that gas nuclei can remain trapped in the crevices of solid impurities or of the vessel wall. Both hypotheses are supported by experimental results. We refer the reader to the reviews of Crum (1982) and Apfel (1984).

It should be added that the size and location of such nuclei is an unknown data, and is one of the main limits to observation of acoustic cavitation. Single-bubble levitation experiments and laser bubbles may remedy this uncontrollable feature.

5.3 Forces Exerted on the Bubbles

5.3.1 Primary Bjerknes Force

Let us seek the force that would be exerted on the bubble if it were replaced by liquid, in otherwise equal conditions. Neglecting viscous effects, it reads

$$\mathbf{F} = \int\int_S -p\mathbf{n}\,\mathrm{d}S \tag{2.34}$$

where S is the bubble surface and p the local pressure on this surface. Using divergence theorem, one may also write

$$\mathbf{F} = \int\int\int_V -\nabla p\,\mathrm{d}V \tag{2.35}$$

where p should be understood as the pressure field that would exist *in the liquid replacing the bubble*. If the fluid is only submitted to the gravity field, $\nabla p = \rho_\mathrm{l}\mathbf{g}$, and we recover the buoyancy force $\mathbf{F_A} = -\rho_\mathrm{l} V\mathbf{g}$. If the pressure field now results from the acoustic wave, but varies little at the scale of the bubble (this implies $R/\lambda \ll 1$), ∇p can be considered as homogeneous in V and equal to its value at the bubble center, hence $\mathbf{F} = -V\nabla p$. This is the instantaneous primary Bjerknes force. For a radially oscillating bubble in an acoustic field, both V and ∇p are oscillating quantities, and the average of their product over one period may be different from zero, so that the bubble experiences an average force. The so-called primary Bjerknes force is this time average,

$$\mathbf{F_{B_1}} = -\langle V(t)\nabla p\rangle \tag{2.36}$$

and may be seen as a generalized buoyancy force in an accelerating liquid. Assuming a mono-harmonic standing wave, the acoustic field can be written as

$$p(\mathbf{x}, t) = p_{\mathrm{a}}(\mathbf{x})\, cos(\omega t) \tag{2.37}$$

so that the primary Bjerknes force becomes

$$\mathbf{F_{B_1}} = -\nabla p_{\mathrm{a}} \langle V(t) cos(\omega t) \rangle \tag{2.38}$$

It is seen that the force points toward pressure nodes (minima) or pressure antinodes (maxima), depending on the sign of the average. In the case of linear oscillations, the Bjerknes force can be easily evaluated from Equations (2.11) and (2.12), and the following conclusions can be drawn:

- for $R_0 < R_{\mathrm{res}}$, bubbles are attracted toward pressure antinodes
- for $R_0 > R_{\mathrm{res}}$, bubbles are attracted toward pressure nodes

Repulsion of bubbles larger than R_{res} has been reported by Goldman and Ringo (1949), and can be observed easily in most cavitation experiments, where large (and therefore visible) bubbles can be seen to escape and take refuge far from pressure antinodes, possibly coalesce, and then rise by buoyancy.

Attraction of bubbles smaller than resonance size by pressure antinodes is confirmed by the experiments of Crum and Eller (1970) for moderate drivings, and is used to levitate a bubble in SBSL experiments, the primary Bjerknes force compensating exactly the mean buoyancy force at a point slightly above the pressure antinode in the center of the cell (Barber et al., 1997; Gaitan et al., 1992).

However, it was shown by Akhatov et al. (1997b) that the primary Bjerknes force can also become repulsive for sub-resonant bubbles, above a threshold in the (p_{a}, R_0) plane. For example, bubbles of 10 μm are repelled by antinodes for drivings exceeding 170 kPa, in contradiction with linear theory. This has been confirmed by experiments (Parlitz et al., 1999) and is illustrated in Fig. 2.12. The inversion of primary Bjerknes force has also been invoked to explain the upper limit of the driving observed in SBSL experiments.

Finally, let us note that Bjerknes forces also exist in traveling waves, and may become important for large drivings. They could explain the conical bubble filaments observed under the transducer tip (Moussatov et al., 2003a), as mentioned recently by Koch et al. (2004b).

5.3.2 Secondary Bjerknes Force

The arguments leading to the expression of the primary Bjerknes force can be extended to the case where the bubble also experiences the acoustic field radiated by a second bubble. The resulting force averaged over one period reads

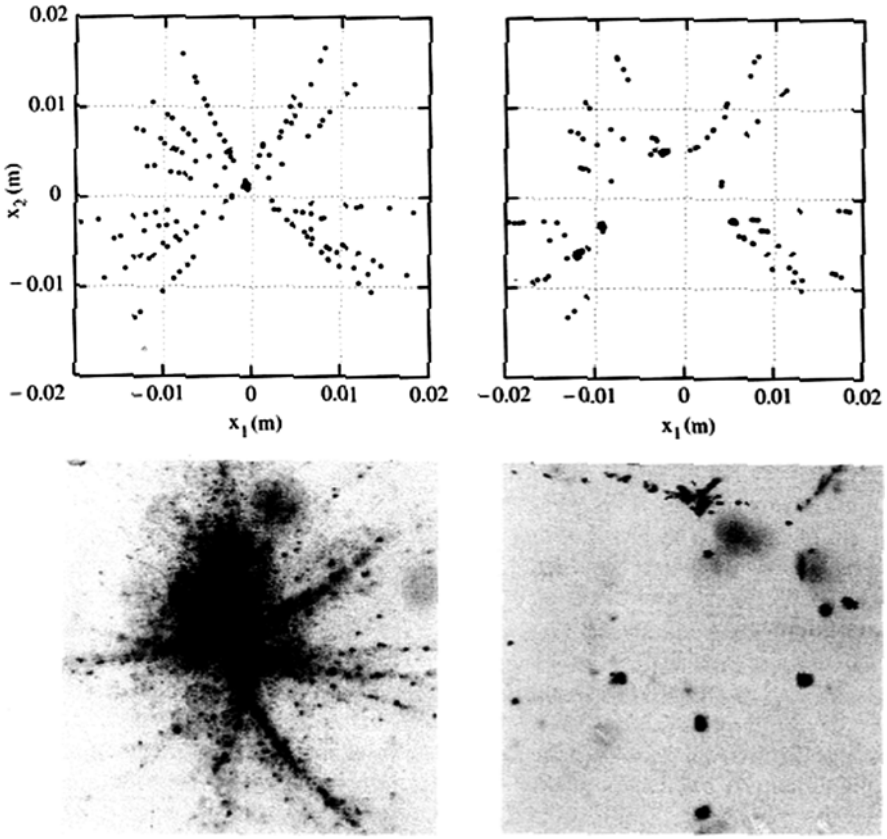

Fig. 2.12 Bubble filaments in a standing wave field. *Upper graphs*: simulations by a particle model. *Lower photos*: snapshots of experimental structures. The *left column* is obtained for a driving of 130 kPa, the *right one* for 190 kPa. The inversion of the Bjerknes force is apparent on the *right graphs*. Adapted from Lauterborn et al. (1999), with kind permission of John Wiley and Sons Ltd

$$\mathbf{F}_{\mathbf{B_2}} = -\frac{\rho_l}{4\pi}\langle \dot{V}_1 \dot{V}_2 \rangle \frac{\mathbf{x}_2 - \mathbf{x}_1}{|\mathbf{x}_2 - \mathbf{x}_1|} \tag{2.39}$$

where V_1, V_2 are the respective volumes of the bubbles, and $\mathbf{x}_1$ and $\mathbf{x}_2$ the spatial positions of their centers. Here again, a practical result is readily obtained in the case of linear oscillations:

- a bubble smaller than and a bubble larger than resonance size repels each other
- two bubbles smaller or two bubbles larger than resonance size experience an attracting force

The experiments of Crum (1975) confirm that the attraction of two sub-resonant bubbles for moderate drivings and quantitative agreement is obtained for the

bubble velocities. The effect of shape instabilities has been tackled by Pelekasis and Tsamopoulos (1993), and the effects of non-linearity have been studied by Oguz and Prosperetti (1990) and Mettin et al. (1997). The latter recalculated the secondary Bjerknes force for non-linear bubble dynamics, and predicted amplitudes orders of magnitude greater than with linear theory for bubbles ranging from 0.5 to 10 μm. An outstanding experimental confirmation of the theory, using laser-induced bubbles in a standing wave, can be found in Koch et al. (2004a)

Mettin et al. (1997) also found that possible mutual repulsion could occur, where linear theory predicts the opposite. Furthermore, the transition from attraction to repulsion can theoretically occur as the bubbles approach mutually, so that a stable separation distance could exist. The result is of importance in the context of bubble structures (see Section 5.4).

5.3.3 Added Mass and Viscous Drag Force

Bubble inertia is negligible, owing to the low density of the gas. However, as any body accelerating relatively to the liquid, a bubble must push the latter, and in reaction experiences a force from it. All happens as if the bubble had an added mass, which for a spherical body always amounts to half the mass of the displaced liquid (Magnaudet, 1997), so that

$$\mathbf{F_M} = -\frac{2}{3}\pi\, R(t)^3 \rho_l \frac{\mathrm{d}}{\mathrm{d}t}(\mathbf{v} - \mathbf{u}) \tag{2.40}$$

where $\mathbf{v}$ is the bubble velocity.

The bubble also experiences a viscous drag force from the liquid. The correct expression of the drag force on a bubble moving radially is a delicate issue. For high-Reynolds numbers, calculated either from the radial or the translational velocity, Magnaudet and Legendre (1998) showed that

$$\mathbf{F_V} = -12\pi\, R(t)\mu_l(\mathbf{v} - \mathbf{u}) \tag{2.41}$$

This completes the set of forces exerted on cavitation bubbles. Since the bubble inertia is negligible, the sum of these period-averaged forces must cancel. This yields a differential equation whose resolution allows a theoretical prediction of the bubble path. Good quantitative agreement with two bubbles experiments has recently been obtained by Koch et al. (2004a).

5.4 Bubble Structures

An immediate conclusion can be drawn from the naked-eye observation of acoustic cavitation: the bubble spatial repartition is neither homogeneous nor stationary. Bubbles self-organize in a variety of different patterns, evolving on a timescale much larger than the acoustic period.

Early observations report mainly two main classes of bubble structures: streamers (Neppiras, 1980; Nyborg and Hughes, 1967) and clusters (Rozenberg, 1971b; Sirotyuk, 1971), but these reports were penalized by a lack of sufficient imaging techniques. Since then, the group of Lauterborn has recorded an impressive collection of experimental data, using high-speed cameras and holographic systems, combined with digital image processing. An extensive review of these observations can be found in Mettin (2005) and references herein, establishing a "zoo" of bubble structures. We summarize in a few words the characteristics of some of these structures and their interpretation in terms of Bjerknes forces.

5.4.1 Streamers and Filaments

The basic streamer is a linear streak of bubbles traveling rapidly from one end to the other. The streamer seems to start from a specific point in the liquid. This structure appears in standing waves configurations at moderate drivings. The origin of the streamer corresponds to a pressure node and the bubbles travel toward pressure antinodes, under the influence of the primary Bjerknes force. Secondary Bjerknes forces act at various levels: they may help nuclei to coalesce near the streamer origin, and maintain an attraction between a bubble and its neighbors in the streamer. Bubbles are thought to break up as they reach the antinode, or form clusters.

Streamers can combine and form slowly evolving agglomerates of filaments, termed "Acoustic Lichtenberg Figures" by Lauterborn's group (Fig. 2.12). The main features of these structures have been explained theoretically by particle model simulations (Parlitz et al., 1999; see also Section 5.5).

5.4.2 Bubble Layers: The Jellyfish and the Starfish

This jellyfish structure consists of two flat parallel layers of bubbles, presenting filamentary structures when viewed from above. They appear in standing waves at high amplitudes, and the layers are located symmetrically on each side of a nodal plane. The layers are not located exactly at the antinodes; this confirms the repulsive character of primary Bjerknes force for high drivings. The estimated driving at the bubble locations is about 200 kPa, and the bubbles involved do not exceed a few micrometers. The starfish structure shares some similarities with the jellyfish, except that it is located near the liquid surface. Both structures are also predictable by particle models.

5.4.3 Clusters

Small clusters of a few (up to some dozens) bubbles appear for large drivings (between 190 and 300 kPa). They can form at the end of a filament. The bubbles constituting the cluster change their positions, can split or merge, and their separation is of the order of their maximum size. The cluster as an entity is a rather stable structure, and reacts to Bjerknes forces as if it were a single large bubble. Why the

bubbles constituting the cluster do not coalesce under secondary Bjerknes force is not completely understood.

Large clusters contain hundreds of bubbles of sizes and mutual distances comparable to small ones. They have a noticeable spherical shape, appear spontaneously in the liquid and travel rapidly. They are attracted by the surface to which they remain attached, taking a hemispherical form, and have a strong eroding action.

5.4.4 Sonotrode Cavitation and Conical Structures

Small diameter sonotrodes, commonly used in sonochemistry, produce a dense unstructured cloud of bubbles below the tip, increasing in size and density as the power is raised. Such transducers also generate strong acoustic currents, which may carry the bubbles far from the radiating surface. For larger diameter sonotrodes, the bubbles form conical structures (Moussatov et al., 2003a, b), which appear to be formed by filaments originating from the transducer when recorded with short-term exposures. The conical structure has been explained by the action of the primary Bjerknes force in a high-amplitude spatially attenuated traveling wave (Koch et al., 2004b). Other structures can be found in the report of Mettin (2005).

5.4.5 Bubble Sizes and Lifetimes

In all the above observation, the bubble sizes recorded (see Mettin et al., 1999a, for the method used) amount to a few micrometers or less, for driving amplitudes ranging from 100 to 300 kPa. This is consistent with the theory of shape instabilities, confirmed experimentally by single-bubble experiments (see Fig. 2.10). Other measurements by laser techniques (Burdin et al., 1999) lead to the same conclusion. This rules out the early picture of cavitation activity by resonant bubbles, and the bubble sizes are in fact confined in a range between sub-micronic nuclei and radii slightly above the Blake threshold radius. This reduction of the parameter space to explore is of fundamental importance for theoretical aspects.

This conclusion should, however, be tempered since, even in this narrow range, the behavior of bubbles can still vary noticeably. This is not only true for the response curves (see Fig. 2.4), but even more for quantities like maximum temperature or shockwave intensities, which explains qualitatively why different structures produce different chemical or mechanical effects. Recent calculations even show that the chemical composition of bubbles can drastically change for acoustic pressure changing from 180 kPa (jellyfishes) to 300 kPa (sonotrode cavitation) (Yasui et al., 2005).

Another conclusion drawn from the above observations is the relatively long lifetime of bubbles in streamers and filaments (up to hundreds of cycles). This owes probably to the relatively low driving to which they are submitted. Such bubbles are excited above the Blake threshold, so that they are inertial and collapse at each cycle. Theory even predicts that they should grow by rectified diffusion up to the instability threshold (Louisnard and Gomez, 2003). The term “transient” would be used

improperly in this case, and this observation therefore constitutes a breakthrough in cavitation research.

There remain some uncertainties about the conversion of nuclei to inertial bubbles. In high-pressure zones, the nuclei could directly be excited above the Blake threshold. But in low-pressure zones, for example, at the starting point of streamers, how do the nuclei grow to an observable size? Competing effects of dissolution, migration toward pressure antinodes, and coalescence may give an answer, and a simplified theoretical study seems feasible.

5.5 How to Simulate Cavitation Fields

5.5.1 The Unknowns

Admitting that one could quantify the effect on a specific process (a chemical yield for example), of a bubble of ambient radius R_0 driven at a given acoustic pressure p_a, predicting a macroscopic effect requires knowledge of the spatial bubble distribution $N(\mathbf{x}, R_0)$. Observation of cavitation structures indicate that this quantity also varies with time, but on a timescale τ much larger than the acoustic period. The second unknown is the acoustic field itself $p_a(\mathbf{x}, t)$, exciting the various bubbles present at point $\mathbf{x}$.

Both quantities N and p_a are coupled (Leighton, 1995); the bubbles can drift under primary Bjerknes force, grow or dissolve, coalesce under secondary Bjerknes forces, or break up under the influence of the acoustic field. Conversely, the evolution of the bubble distribution in the liquid modifies the local sound velocity (see Equation (2.32)) and therefore the acoustic field.

5.5.2 Continuum Approach

Assuming that the bubble distribution is a continuous function $N(\mathbf{x}, \tau, R_0)$, of space $\mathbf{x}$, time τ, and bubble size R_0, its evolution can be described by a bubble conservation equation, sometimes referred as a population balance equation. In generic form, this equation can be written as

$$\frac{\partial N}{\partial \tau} + \nabla.(N\mathbf{v}) + \frac{\partial}{\partial R_0}(Nw) = B - D \tag{2.42}$$

where $\mathbf{v}$ is the bubble velocity, w the growth or dissolution rate, B the birth rate and D the death rate. Such equations are commonly used in crystallization. It must be emphasized that all terms must be based on the relevant physics, part of which has been given in this chapter. With an optimistic point of view $\mathbf{v}$ could be obtained from a balance of forces, and w from rectified diffusion theory. The birth term B arises from bubble nucleation, coalescence, and fragmentation, while D originates from the two latter processes, which are poorly documented. Mathematical difficulty moreover arises because of coalescence, which renders Equation (2.42)

integro-differential. The most complete equation relevant to cavitation can be found in Alekseev and Yushin (1986), but no solution was sought.

Among the various early attempts to obtain practical results from this equation, we mention the work of Kobelev and Ostrovskii (1983, 1989), who considered coalescence under secondary Bjerknes forces and bubble drift under primary ones, to interpret the self-illumination effect of sound observed in bubbly liquids (Kobelev et al., 1979). However these studies are limited to moderate sound fields, well below the Blake threshold.

More recently, in order to explain why experimentally observed bubble fields are always spatially inhomogeneous, Akhatov et al. (1994, 1996) demonstrated the spontaneous emergence of a bubble spatial distribution instability. They used an equation similar to Equation (2.42), accounting for bubble drift under Bjerknes forces and heuristic birth and death terms, coupled with a linear propagation equation in bubbly liquids. Finally, in order to assess the importance of coalescence on the bubble field formation, attempts were made to study the competition between coalescence and dissolution of bubbles under the Blake threshold (Louisnard, O. (2001). *Theoretical Study of Competition Between Dissolution and Coalescence of Small Bubbles in an Acoustic Field*, "Unpublished").

5.5.3 Particle Models

The continuum approach is of limited practical interest, especially to explain the formation of bubble streamers and filaments. Moreover, the inversion of Bjerknes forces needs non-linear bubble dynamics. Lauterborn and co-workers treated the individual bubbles as particles moving under the action of the forces, as described in Section 5.3 (Lauterborn et al., 1999; Mettin et al., 1999b; Parlitz et al., 1999). The standing acoustic wave is assumed undisturbed by the bubble motion and a monodisperse bubble ambient radius is assumed. Structures obtained by simulation with up to thousands of bubbles show outstanding similarities with several experimental filamentary structures (see the comparison in Fig. 2.12).

The assumption of a fixed standing wave was recently released by Mettin et al. (2006) by coupling the particle model to the propagation equation in bubbly liquids. The results predict the intermittency of both the filamentary bubble structure and the acoustic field, as experimentally observed. As far as we know, this is the most sophisticated model of cavitation fields, trapping the essential physics involved.

6 Final Remarks

6.1 Topics Not Addressed

The recent experimental observations reported in this chapter have been obtained at low-frequency cavitation, say, below 100 kHz. High-frequency cavitation is less documented experimentally (we refer the reader to recent high-speed photography observations by Chen et al., 2006, 2007). First, SBSL is only possible at low

frequencies, so that the high-frequency range did not benefit from this precious opportunity to observe and measure a single bubble. The theoretical results presented above should, however, also be relevant for high frequency. Three major differences with low frequency should be mentioned. First, the resonance radius is much lower (3 μm at 1 MHz), and thus very near the Blake critical radius. This suggests that bubbles at high frequency might approach the resonance radius more closely than they do at low frequencies. Second, the wavelength is much smaller at high frequency (1.5 mm at 1 MHz in water), which necessarily has implications on the bubble structures. For example, streamers that build between nodes and antinodes would be much smaller. The third difference has already been mentioned: the expansion phase is shorter at high frequency, which reduces the collapse strength.

Chopped ultrasound also constitutes an interesting issue. From a fundamental point of view, their study would shed light on the mechanisms of bubble population build-up. For example, it has been observed that the delay for the bubble cloud establishment depends in a non-monotonic way on the chopping mode (Labouret et al., 2006). Besides, in view of industrial applications, chopped ultrasound could reduce energy consumption noticeably.

Finally, for information on principles, design, and available types of ultrasonic transducers, we refer the reader to the articles of Gallego-Juarez (1999) and Mason (1999).

6.2 Further Readings

There is abundant literature on acoustic cavitation. The first comprehensive report on the subject dates back to Flynn (1964), who influenced generations of researchers on the topic. The physics of high-intensity fields (not only cavitation, but also absorption, radiation pressure, and acoustic streaming) can be found in Rozenberg (1971a). A wide collection of ultrasound applications is compiled in Rozenberg (1973). Plesset and Prosperetti (1977) proposed a review of early results on bubble dynamics. Many interesting references to early experimental work can be found in the report of Neppiras (1980). Leighton (1994) presents a sound approach of cavitation physics and a wide collection of references. A large collection of results on cavitation and diphasic flows can be found in Brennen (1995). The proceedings of the 1997 NATO conference on sonochemistry and sonoluminescence include an interesting collection of articles on both topics (Crum et al., 1999). The comprehensive theoretical and experimental work of Lauterborn's group is reviewed in Lauterborn et al. (1999). More recent observations by the same group can be found in Mettin (2005) and references herein.

For an early review of MBSL, we refer the reader to Walton and Reynolds (1984). SBSL literature is interesting not only for the phenomenon itself, but also because its interpretation covers a large part of cavitation physics. The review of Brenner et al. (2002) presents a fascinating historical overview on sonoluminescence (including

MBSL), a comprehensive presentation of single-bubble physics and a wide collection of references. Other interesting reviews on SBSL have been written by Hammer and Frommhold (2001) and Putterman and Weninger (2000).

Notations

a_n	amplitude of the nth-order spherical harmonic
b	damping coefficient for linear oscillations
B	birth rate of bubbles
c_l	sound speed in the liquid
C_∞	dissolved gas concentration far from the bubble
C_0	dissolved gas concentration at saturation $= p_0/k_g$
C_{p_g}	specific heat of the gas
C_{p_l}	specific heat of the liquid
C_R	dissolved gas concentration at the bubble wall $= p_g/k_g$
c.c.	conjugated complex number
c	effective sound speed in a bubbly liquid
D	death rate of bubbles
f	acoustic frequency $= \omega/2\pi$
$\mathbf{F}_\mathrm{A}$	buoyancy force
$\mathbf{F}_\mathrm{G}$	bubble weight
$\mathbf{F}_\mathrm{v}$	viscous drag force
$\mathbf{F}_\mathrm{M}$	added mass force
$\mathbf{F}_{\mathbf{B_1}}$	primary Bjerknes force
$\mathbf{F}_{\mathbf{B_2}}$	secondary Bjerknes force
$\mathbf{g}$	gravity
k_g	Henry's constant
K_g	thermal conductivity of the gas
K_l	thermal conductivity of the liquid
k_l	wavenumber of acoustic waves in the liquid
k	wavenumber of acoustic waves in the bubbly liquid
m_g	mass of incondensable gas in the bubble
M_g	molar mass of the incondensable gas in the bubble
$\mathbf{n}$	outward unit vector
N	bubble-size-distribution function
P	complex amplitude of the driving pressure
p_0	ambient pressure
$p(t), p(\mathbf{x}, t)$	driving pressure
p_a	depression in the liquid (for the quiet bubble)
p_a	amplitude of the driving (for single oscillating bubble)
$p_\mathrm{a}(\mathbf{x})$	complex amplitude of acoustic pressure
p_b	pressure in the bubble $= p_\mathrm{g} + p_\mathrm{v}$
p_g	gas partial pressure in the bubble

p_{g_0}	gas partial pressure in the bubble in ambient conditions
p_v	vapor partial pressure in the bubble
p_a^{crit}	Blake threshold
$p_{v,eq}$	vapor equilibrium saturation pressure
Pe	thermal Peclet number $= \tau_{diff}/\tau_{dyn}$
Pe_0	thermal Peclet number for linear oscillations
P_{active}	active acoustic power
P_{bound}	active acoustic power lost through boundaries
$\dot{Q}$	heat lost by the sonoreactor
r	local radius of a deformed bubble
R_0	ambient radius of the bubble
R	instantaneous radius of the bubble
R_i	radius at which the bubble interior starts to behave adiabatically
R_{min}	minimum bubble radius
R_{max}	maximum bubble radius
R_{res}	resonance radius
$\mathcal{R}$	universal gas constant
S	surface delimiting volume V
t	time
T	acoustic period
T_0	ambient temperature
T_C	bubble center temperature
T_R	bubble surface temperature
$\mathbf{u}$, u	liquid velocity
$\mathbf{u_a}$, u_a	complex amplitude of liquid velocity, in linear acoustics
U	internal energy of a volume of liquid
$\mathbf{v}$, v	bubble velocity
V	volume of liquid
V_1, V_2	instantaneous volumes of bubbles 1 and 2
w	growth or dissolution rate of the bubble
$\mathbf{x}$	spatial position
$\mathbf{x}_1$, $\mathbf{x}_2$	spatial positions of the centers of bubbles 1 and 2
X	complex amplitude of the bubble radius
Y_n	spherical harmonics
α_S	dimensionless Laplace tension $2\sigma/p_0R_0$
α	attenuation coefficient of linear wave
η	polytropic exponent
γ	ratio of the gas-specific heats
λ	wavelength
μ_l	dynamic viscosity of the liquid
Φ	complex number for thermal effects in the linear theory
ρ_l	liquid density
ρ_g	gas density
ρ_b	bubble density
σ	surface tension

τ_{dyn}	characteristic time of bubble oscillations
τ_{diff}	characteristic time of thermal diffusion
χ_{g}	thermal diffusivity of the gas
ω	angular frequency of the driving
ω_0	free angular frequency of the bubble

Subscripts

b refers to the bubble interior
g refers to the gas
l refers to the liquid
v refers to vapor

References

Akhatov, I., Gumerov, N., Ohl, C. D., Parlitz, U., and Lauterborn, W. (1997a). The role of surface tension in stable single bubble sonoluminescence. *Physics Review Letters*, 78(2), 227–230.

Akhatov, I., Mettin, R., Ohl, C. D., Parlitz, U., and Lauterborn, W. (1997b). Bjerknes force threshold for stable single bubble sonoluminescence. *Physical Review E*, 55(3), 3747–3750.

Akhatov, I., Parlitz, U., and Lauterborn, W. (1994). Pattern formation in acoustic cavitation. *Journal of the Acoustical Society of America*, 96(6), 3627–3635.

Akhatov, I., Parlitz, U., and Lauterborn, W. (1996). Towards a theory of self-organization phenomena in bubble-liquid mixtures. *Physical Review E*, 54(5), 4990–5003.

Alekseev, V. N., and Yushin, V. P. (1986). Distribution of bubbles in acoustic cavitation. *Soviet Physics Acoustics*, 32(6), 469–472.

Apfel, R. E. (1984). Acoustic cavitation inception. *Ultrasonics*, 22, 167–173.

Ashokkumar, M., Crum, L. A., Frensley, C. A., Grieser, F., Matula, T. J., McNamara, W. B., and Suslick, K. (2000). Effects of solutes on single-bubble sonoluminescence. *Journal of Physical Chemistry A*, 104, 8462–8465.

Ashokkumar, M., Guan, J., Tronson, R., Matula, T. J., Nuske, J. W., and Grieser, F. (2002). Effects of surfactants, polymers, and alcohols on single bubble dynamics and sonoluminescence. *Physical Review E*, 65, 046310–1–046310–4.

Augsdorfer, U. H., Evans, A. K., and Oxley, D. P. (2000). Thermal noise and the stability of single sonoluminescing bubbles. *Physical Review E*, 61(5), 5278–5285.

Barber, B. P., Hiller, R. A., Löfstedt, R., Putterman, S. J., and Weninger, K. R. (1997). Defining the unknowns of sonoluminescence. *Physics Report*, 281, 65–143.

Barber, B. P., Weninger, K. R., Putterman, S. J., and Löfstedt, R. (1995). Observation of a new phase of sonoluminescence at low partial pressures. *Physics Review Letters*, 74, 5276–5279.

Barber, B. P., Wu, C. C., Löfstedt, R., Roberts, P. H., and Putterman, S. J. (1994). Sensitivity of sonoluminescence to experimental parameters. *Physics Review Letters*, 72(9), 1380–1383.

Benjamin, T. B. (1958). Pressure waves from collapsing cavities. *2nd Symposium on Naval Hydrodynamics*, pp. 207–229, Washington.

Benjamin, T. B., and Ellis, A. T. (1966). The collapse of cavitation bubbles and the pressures thereby produced against solid boundaries. *Philosophical Transactions of the Royal Society London A*, 260(110), 221–240.

Benjamin, T. B., and Ellis, A. T. (1990). Self-propulsion of asymmetrically vibrating bubbles. *Journal of Fluid Mechanics*, 212(2), 65–80.

Blake, F. G. (1949). *The onset of cavitation in liquids; Technical memo 12*. Acoustic Research Laboratory, Cambridge, MA, Harvard University.

Blake, J. R., and Gibson, D. C. (1987). Cavitation bubbles near boundaries. *Annual Review of Fluid Mechanics*, 19, 99–123.

Brennen, C. E. (1995). *Cavitation and bubble dynamics*. Oxford Engineering Science Series, no. 44. New York, Oxford, Oxford University Press.

Brenner, M. P., Hilgenfeldt, S., and Lohse, D. (2002). Single-bubble sonoluminescence. *Reviews of Modern Physics*, 74(2), 425–483.

Brenner, M. P., Lohse, D., and Dupont, T. F. (1995). Bubble shape oscillations and the onset of sonoluminescence. *Physics Review Letters*, 75(5), 954–957.

Briggs, L. J. (1950). Limiting negative pressure of water. *Journal of Applied Physics*, 21, 721–722.

Burdin, F., Tsochatzidis, N. A., Guiraud, P., Wilhelm, A. M., and Delmas, H. (1999). Characterisation of the acoustic cavitation cloud by two laser techniques. *Ultrasonics Sonochemistry*, 6, 43–51.

Caflish, R. E., Miksis, M. J., Papanicolaou, G. C., and Ting, L. (1985). Effective equations for wave propagation in bubbly liquids. *Journal of Fluid Mechanics*, 153, 259–273.

Carstensen, E. L., and Foldy, L. L. (1947). Propagation of sound through a liquid containing bubbles. *Journal of the Acoustical Society of America*, 19(3), 481–501.

Chen, H., Li, X., and Wan, M. (2006). Spatial-temporal dynamics of cavitation bubble clouds in 1.2 MHz focused ultrasound field. *Ultrasonics Sonochemistry*, 13, 480–486.

Chen, H., Li, X., Wan, M., and Wang, S. (2007). High-speed observation of cavitation bubble cloud structures in the focal region of a 1.2 MHz high-intensity focused ultrasound transducer. *Ultrasonics Sonochemistry*, 14, 291–297.

Church, C. C. (1988). Prediction of rectified diffusion during nonlinear bubble pulsations at biomedical frequencies. *Journal of the Acoustical Society of America*, 83(6), 2210–2217.

Commander, K. W., and Prosperetti, A. (1989). Linear pressure waves in bubbly liquids: comparison between theory and experiments. *Journal of the Acoustical Society of America*, 85(2), 732–746.

Crum, L. A. (1975). Bjerknes forces on bubbles in a stationary sound field. *Journal of the Acoustical Society of America*, 57(6), 1363–1370.

Crum, L. A. (1980). Measurements of the growth of air bubbles by rectified diffusion. *Journal of the Acoustical Society of America*, 68(1), 203–211.

Crum, L. A. (1982). Nucleation and stabilization of microbubbles in liquids. *Applied Science Research*, 38(3), 101–115.

Crum, L. A. (1983). The polytropic exponent of gas contained within air bubbles pulsating in a liquid. *Journal of the Acoustical Society of America*, 73(1), 116–120.

Crum, L. A., and Eller, A. I. (1970). Motion of bubbles in a stationary sound field. *Journal of the Acoustical Society of America*, 48(1), 181–189.

Crum, L. A., and Hansen, G. M. (1982). Generalized equations for rectified diffusion. *Journal of the Acoustical Society of America*, 72(5), 1586–1592.

Crum, L. A., Mason, T. J., Reisse, J. L., and Suslick, K. S. (eds.). (1999). *Sonochemistry and Sonoluminescence*. Dordrecht, Kluwer. *Proceedings of the NATO Advanced Study Institute on Sonoluminescence and Sonoluminescence*, Leavenworth, Washington, DC, 18–29 August 1997.

Crum, L. A., and Prosperetti, A. (1983). Nonlinear oscillations of gas bubbles in liquids: an interpretation of some experimental results. *Journal of the Acoustical Society of America*, 73(1), 121–127.

Crum, L. A., and Prosperetti, A. (1984). Erratum and comments on "Nonlinear oscillations of gas bubbles in liquids: An interpretation of some experimental results". *Journal of the Acoustical Society of America – Letters to the Editor*, 75(6), 1910–1912.

Dähnke, S., Swamy, K. M., and Keil, F. J. (1999). Modeling of three-dimensional pressure fields in sonochemical reactors with an inhomogeneous density distribution of cavitation bubbles. Comparison of theoretical and experimental results. *Ultrasonics Sonochemistry*, 6, 31–41.

Devin, C. Jr. (1959). Survey of thermal, radiation and viscous damping of pulsating air bubbles in water. *Journal of the Acoustical Society of America*, 31(12), 1654–1667.

Didenko, Y. T., McNamara, W. B., and Suslick, K. S. (2000). Effect of noble gases on sonoluminescence temperatures during multibubble cavitation. *Physics Review Letters*, 84(4), 777–780.

Doinikov, A. A. (2004). Translational motion of a bubble undergoing shape oscillations. *Journal of Fluid Mechanics*, 501, 1–24.

Eller, A. I. (1972). Bubble growth by rectified diffusion in an 11-kHz sound field. *Journal of the Acoustical Society of America*, 52, 1447–1449.

Eller, A. I., and Crum, L. A. (1970). Instability of the motion of a pulsating bubble in a sound field. *Journal of the Acoustical Society of America*, 47(3), 762–767.

Eller, A.I, and Flynn, H. G. (1965). Rectified diffusion during nonlinear pulsations of cavitation bubbles. *Journal of the Acoustical Society of America*, 37, 493–503.

Epstein, P. S., and Plesset, M. S. (1950). On the stability of gas bubbles in liquid-gas solutions. *Journal of Chemical Physics*, 18, 1505–1509.

Flannigan, D. J., and Suslick, K. S. (2005). Plasma formation and temperature measurement during single-bubble cavitation. *Nature*, 434, 52–55.

Flint, E. B., and Suslick, K. S. (1991). The temperature of cavitation. *Science*, 253, 1397–1399.

Flynn, H. G. (1964). Physics of acoustic cavitation in liquids. In: Mason, W. P. (ed.), *Physical Acoustics*, vol. 1B, pp. 57–172. New York, NY, Academic.

Foldy, L. L. (1944). The multiple scattering of waves. *Physical Review*, 67(3–4), 107–119.

Fox, F. E., Curley, S. R., and Larson, G. S. (1955). Phase velocity and absorption measurements in water containing air bubbles. *Journal of the Acoustical Society of America*, 27(3), 534–539.

Fujikawa, S., and Akamatsu, T. (1980). Effects of the nonequilibrium condensation of vapour on the pressure wave produced by the collapse of a bubble in a liquid. *Journal of Fluid Mechanics*, 97, 481–512.

Fyrillas, M. M., and Szeri, A. J. (1994). Dissolution or growth of soluble spherical oscillating bubbles. *Journal of Fluid Mechanics*, 277, 381–407.

Fyrillas, M. M., and Szeri, A. J. (1995). Dissolution or growth of soluble spherical oscillating bubbles: the effect of surfactants. *Journal of Fluid Mechanics*, 289, 295–314.

Fyrillas, M. M., and Szeri, A. J. (1996). Surfactant dynamics and rectified diffusion of microbubbles. *Journal of Fluid Mechanics*, 311, 361–378.

Gaete-Garreton, L., Vargas-Hernandez, Y., Vargas-Herrera, R., Gallego-Juarez, J. A., and Montoya-Vitini, F. (1997). On the onset of cavitation in gassy liquids. *Journal of the Acoustical Society of America*, 101(5), 2536–2540.

Gaitan, D. F., and Holt, R. G. (1999). Experimental observations of bubble response and light intensity near the threshold for single bubble sonoluminescence in an air-water system. *Physical Review E*, 59, 5495–5502.

Gaitan, D. F., Crum, L. A., Church, C. C., and Roy, R. A. (1992). Sonoluminescence and bubble dynamics for a single, stable, cavitation bubble. *Journal of the Acoustical Society of America*, 91(6), 3166–3183.

Gallego-Juarez, J. A. (1999). High power ultrasonic transducers. In Crum, L. A., Mason, T. J., Reisse, J. L., and Suslick, K. S. (eds.), *Sonochemistry and sonoluminescence*. Dordrecht, Kluwer, pp. 259–270. *Proceedings of the NATO Advanced Study Institute on Sonoluminescence and Sonoluminescence*, Leavenworth, Washington, DC, 18–29 August 1997.

Goldman, D. E., and Ringo, G. R. (1949). Determination of pressure nodes in liquids. *Journal of the Acoustical Society of America*, 21, 270.

Gould, R. K. (1974). Rectified diffusion in the presence of, and absence of, acoustic streaming. *Journal of the Acoustical Society of America*, 56, 1740–1746.

Hammer, D., and Frommhold, L. (2000). Spectra of sonoluminescent rare-gas bubbles. *Physics Review Letters*, 85(6), 1326–1329.

Hammer, D., and Frommhold, L. (2001). Sonoluminescence: how bubbles glow. *Journal of Modern Optics*, 48, 239–277.

Hilgenfeldt, S., Brenner, M. P., Grossman, S., and Lohse, D. (1998). Analysis of Rayleigh-Plesset dynamics for sonoluminescing bubbles. *Journal of Fluid Mechanics*, 365, 171–204.

Hilgenfeldt, S., Grossmann, S., and Lohse, D. (1999a). A simple explanation of light emission in sonoluminescence. *Nature*, 398, 402–405.

Hilgenfeldt, S., Grossmann, S., and Lohse, D. (1999b). Sonoluminescence light emission. *Physics of Fluids*, 11, 1318–1330.

Hilgenfeldt, S., Lohse, D., and Brenner, M. P. (1996). Phase diagrams for sonoluminescing bubbles. *Physics of Fluids*, 8(11), 2808–2826.

Hiller, R. A., Putterman, S. J., and Barber, B. P. (1992). Spectrum of synchronous picosecond sonoluminescence. *Physics Review Letters*, 69(8), 1182–1184.

Hopkins, S. D., Putterman, S. J., Kappus, B. A., Suslick, K. S., and Camara, C. G. (2005). Dynamics of a sonoluminescing bubble in sulfuric acid. *Physics Review Letters*, 95(254301), 1–4.

Hsieh, D. Y., and Plesset, M. S. (1961). Theory of rectified diffusion of mass into gas bubbles. *Journal of the Acoustical Society of America*, 33, 206–215.

Iordansky, S. (1960). On the equations of motion for liquids containing gas bubbles. *Journal of Applied Mechancis and Technical Physics*, 3, 102–110.

Kamath, V., Oguz, H. N., and Prosperetti, A. (1992). Bubble oscillations in the nearly adiabatic limit. *Journal of the Acoustical Society of America*, 92(4), 2016–2023.

Kamath, V., and Prosperetti, A. (1989). Numerical integration methods in gas-bubble dynamics. *Journal of the Acoustical Society of America*, 85(4), 1538–1548.

Kamath, V., Prosperetti, A., and Egolfopoulos, F. N. (1993). A theoretical study of sonoluminescence. *Journal of the Acoustical Society of America*, 94(1), 248–260.

Kapustina, O. A. (1973). Degassing of liquids. In: Rozenberg, L. D. (ed.), *Physical principles of ultrasonic TECHNOLOGY*. New York, NY, Plenum Press.

Keller, J. B., and Miksis, M. (1980). Bubble oscillations of large amplitude. *Journal of the Acoustical Society of America*, 68, 628–633.

Ketterling, J. A., and Apfel, R. E. (1998). Experimental validation of the dissociation hypothesis for single bubble sonoluminescence. *Physics Review Letters*, 81, 4991–4994.

Ketterling, J. A., and Apfel, R. E. (2000). Extensive experimental mapping of sonoluminescence parameter space. *Physical Review E*, 61(4), 3832–3837.

Kobelev, Yu. A., and Ostrovskii, L. A. (1983). Collective self-effect of sound in a liquid with gas bubbles. *Journal of Experimental and Theoretical Physics Letters*, 37(1), 4–7.

Kobelev, Yu. A., and Ostrovskii, L. A. (1989). Nonlinear acoustic phenomena due to bubble drift in a gas-liquid mixture. *Journal of the Acoustical Society of America*, 85(2), 621–629.

Kobelev, Yu. A., Ostrovskii, L. A., and Sutin, A. M. (1979). Self-illumination effect for acoustic waves in a liquid with gas bubbles. *JETP Letters*, 30(7), 395–398.

Koch, P., Krefting, D., Tervo, T., Mettin, R., and Lauterborn, W. (2004a). Bubble path simulations in standing and traveling acoustic waves. *Proceedings of ICA 2004, Kyoto (Japan)*, vol. Fr3.A.2, pp. V3571–V3572.

Koch, P., Mettin, R., and Lauterborn, W. (2004b). Simulation of cavitation bubbles in travelling acoustic waves. In: Casseraeu, D. (ed.), *Proceedings CFA/DAGA04 Strasbourg, DEGA Oldenburg*, pp. 919–920.

Kornfeld, M., and Suvorov, L. (1944). On the destructive action of cavitation. *Journal of Applied Physics*, 15, 495–506.

Krefting, D., Mettin, R., and Lauterborn, W. (2004). High-speed observation of acoustic cavitation erosion in multibubble systems. *Ultrasonics Sonochemistry*, 11, 119–123.

Labouret, S., Frohly, J., and Rivart, F. (2006). Evolution of an 1 MHz ultrasonic cavitation bubble field in a chopped irradiation mode. *Ultrasonics Sonochemistry*, 13(4), 287–294.

Lauterborn, W. (1976). Numerical investigation of nonlinear oscillations of gas bubbles in liquids. *Journal of the Acoustical Society of America*, 59(2), 283–296.

Lauterborn, W., and Bolle, H. (1975). Experimental investigations of cavitation-bubble collapse in the neighborhood of a solid boundary. *Journal of Fluid Mechanics*, 72, 391–399.

Lauterborn, W., and Cramer, E. (1981a). On the dynamics of acoustic cavitation noise spectra. *Acustica*, 49, 280–287.

Lauterborn, W., and Cramer, E. (1981b). Subharmonic route to chaos observed in acoustics. *Physics Review Letters*, 47(20), 1445–1448.

Lauterborn, W., Kurz, T., Mettin, R., and Ohl, C. D. (1999). Experimental and theoretical bubble dynamics. *Advanced in Chemical Physics*, 110, 295–380.

Lauterborn, W., and Mettin, R. (1999). Nonlinear bubble dynamics: response curves and more. In: Crum, L. A., Mason, T. J., Reisse, J. L., and Suslick, K. S. (eds.), *Sonochemistry and Sonoluminescence*, pp. 63–72. Dordrecht, Kluwer. *Proceedings of the NATO Advanced Study Institute on Sonoluminescence and Sonoluminescence*, Leavenworth, Washington, DC, 18–29 August 1997.

Leighton, T. G. (1994). *The acoustic bubble*. London, Academic.

Leighton, T. G. (1995). Bubble population phenomena in acoustic cavitation. *Ultrasonics Sonochemistry*, 2(2), S123–S136.

Lezzi, A., and Prosperetti, A. (1987). Bubble dynamics in a compressible liquid. Part 2. Second-order theory. *Journal of Fluid Mechanics*, 185, 289–321.

Li, M. K., and Fogler, H. S. (2004). Acoustic emulsification. Part 2. Breakup of the large primary oil droplets in a water medium. *Journal of Fluid Mechanics*, 88, 513–528.

Lin, H., Storey, B. D., and Szeri, A. J. (2002a). Inertially driven inhomogeneities in violently collapsing bubbles: the validity of the Rayleigh-Plesset equation. *Journal of Fluid Mechanics*, 452(10), 145–162.

Lin, H., Storey, B. D., and Szeri, A. J. (2002b). Rayleigh-Taylor instability of violently collapsing bubbles. *Physics of Fluids*, 14(8), 2925–2928.

Lindau, O., and Lauterborn, W. (2003). Cinematographic observation of the collapse and rebound of a laser-produced cavitation bubble near a wall. *Journal of Fluid Mechanics*, 479, 327–348.

Löfstedt, R., Barber, B. P., and Putterman, S. J. (1993). Toward a hydrodynamic theory of sonoluminescence. *Physics of Fluids*, A5(11), 2911–2928.

Löfstedt, R., Weninger, K., Putterman, S., and Barber, B. P. (1995). Sonoluminescing bubbles and mass diffusion. *Physical Review E*, 51(5), 4400–4410.

Lohse, D., and Hilgenfeldt, S. (1997). Inert gas accumulation in sonoluminescing bubbles. *Journal of Chemical Physics*, 107(17), 6986–6997.

Lohse, D., Brenner, M. P., Dupont, T. F., Hilgenfeldt, S., and Johnston, B. (1997). Sonoluminescing air bubbles rectify argon. *Physics Review Letters*, 78(7), 1359–1362.

Louisnard, O., and Gomez, F. (2003). Growth by rectified diffusion of strongly acoustically forced gas bubbles in nearly saturated liquids. *Physical Review E*, 67(036610), 1–12.

Magnaudet, J. (1997). The forces acting on bubbles and rigid particles. In: *ASME Fluids Engineering Division Summer Meeting*, Vancouver, Canada, paper 97–3522.

Magnaudet, J., and Legendre, D. (1998). The viscous drag force on a spherical bubble with a time-dependent radius. *Physics of Fluids*, 10, 550–554.

Mason, T. J. (1999). Laboratory equipment and usage considerations. In: Crum, L. A., Mason, T. J., Reisse, J. L., and Suslick, K. S. (eds.), *Sonochemistry and sonoluminescence*, pp. 245–258. Dordrecht, Kluwer. *Proceedings of the NATO Advanced Study Institute on Sonoluminescence and Sonoluminescence*, Leavenworth, Washington, DC, 18–29 August 1997.

Matula, T. J. (2000). Single-bubble sonoluminescence in microgravity. *Ultrasonics*, 357, 203–223.

Matula, T. J., and Crum, L. A. (1998). Evidence of gas exchange in single-bubble sonoluminescence. *Physics Review Letters*, 80(4), 865–868.

Matula, T. J., Roy, R. A., Mourad, P. D., McNamara, W. B., and Suslick, K. S. (1995). Comparison of multibubble and single-bubble sonoluminescence spectra. *Physics Review Letters*, 75(13), 2602–2605.

McNamara, W. B., Didenko, Y. T., and Suslick, K. S. (1999). Sonoluminescence temperatures during multi-bubble cavitation. *Nature*, 401, 772–775.

Mettin, R. (2005). Bubble structures in acoustic cavitation. In: Doinikov, A. A. (ed.), *Bubble and particle dynamics in acoustic fields: Modern trends and applications*, pp. 1–36. Kerala (India), Research Signpost.

Mettin, R., Akhatov, I., Parlitz, U., Ohl, C. D., and Lauterborn, W. (1997). Bjerknes force between small cavitation bubbles in a strong acoustic field. *Physical Review E*, 56(3), 2924–2931.

Mettin, R., Koch, P., Lauterborn, W., and Krefting, D. (11-15 September 2006). Modeling acoustic cavitation with bubble redistribution. *Sixth International Symposium on Cavitation – CAV2006 (Paper 75)*, Wageningen (The Netherlands), pp. 125–129.

Mettin, R., Luther, S., and Lauterborn, W. (1999a). Bubble size distribution and structures in acoustic cavitation. *Proceedings of 2nd conference on Applications of Power Ultrasound in Physical and Chemical Processing*, Toulouse, France, pp. 125–129.

Mettin, R., Luther, S., Ohl, C. D., and Lauterborn, W. (1999b). Acoustic cavitation structures and simulations by a particle model. *Ultrasonics Sonochemistry*, 6, 25–29.

Miksis, M. J., and Ting, L. (1984). Nonlinear radial oscillations of a gas bubble including thermal effects. *Journal of the Acoustical Society of America*, 76(3), 897–905.

Moussatov, A., Granger, C., and Dubus, B. (2003a). Cone-like bubble formation in ultrasonic cavitation field. *Ultrasonics Sonochemistry*, 10, 191–195.

Moussatov, A., Mettin, R., Granger, C., Tervo, T., Dubus, B., and Lauterborn, W. (2003b, 7-10 September). Evolution of acoustic cavitation structures near larger emitting surface. *Proceedings of the World Congress on Ultrasonics*, Paris (France), pp. 955–958.

Neppiras, E. A. (1969). Subharmonic and other low-frequency emission from bubbles in sound-irradiated liquids. *Journal of the Acoustical Society of America*, 46, 587–601.

Neppiras, E. A. (1980). Acoustic cavitation. *Physics Report*, 61, 159–251.

Noltingk, B. E., and Neppiras, E. A. (1950). Cavitation produced by ultrasonics. *Proceedings of the Physical Society*, B63, 674–685.

Nyborg, W. L., and Hughes, D. E. (1967). Bubble annihilation in cavitation streamers. *Journal of the Acoustical Society of America*, 42(4), 891–894.

Oguz, H. N., and Prosperetti, A. (1990). A generalization of the impulse and virial theorems with an application to bubble oscillations. *Journal of Fluid Mechanics*, 218, 143–162.

Ohl, C. D., Lindau, O., and Lauterborn, W. (1998). Luminescence from spherically and aspherically collapsing laser bubbles. *Physics Review Letters*, 80, 393–396.

Parlitz, U., Mettin, R., Luther, S., Akhatov, I., Voss, M., and Lauterborn, W. (1999). Spatio temporal dynamics of acoustic cavitation bubble clouds. *Philosophical Transactions of the Royal Society London A*, 357, 313–334.

Pecha, R., and Gompf, B. (2000). Microimplosions: cavitation collapse and shock wave emission on a nanosecond time scale. *Physics Review Letters*, 84(6), 1328–1330.

Pelekasis, N. A., and Tsamopoulos, J. A. (1993). Bjerknes forces between two bubbles. Part 2. Response to an oscillatory pressure field. *Journal of Fluid Mechanics*, 254, 501–527.

Pétrier, C., and Francony, A. (1997). Ultrasonic waste-water treatment: incidence of ultrasonic frequency on the rate of phenol and carbon tetrachloride degradation. *Ultrasonics Sonochemistry*, 4, 295–300.

Philipp, A., and Lauterborn, W. (1998). Cavitation erosion by single laser-produced bubbles. *Journal of Fluid Mechanics*, 361, 75–116.

Plesset, M. S. (1949). The dynamics of cavitation bubbles. *Journal of Applied Mechanics*, 16, 277–282.

Plesset, M. S., and Mitchell, T. P. (1956). On the stability of the spherical shape of a vapor cavity in a liquid. *Quarterly of Applied Mathematics*, 13(4), 419–430.

Plesset, M. S., and Prosperetti, A. (1977). Bubble dynamics and cavitation. *Annual Review of Fluid Mechanics*, 9, 145–185.

Prosperetti, A. (1977a). Thermal effects and damping mechanisms in the forced radial oscillations of gas bubbles in liquids. *Journal of the Acoustical Society of America*, 61(1), 17–27.

Prosperetti, A. (1977b). Viscous effects on perturbed spherical flows. *Quarterly of Applied Mathematics*, 34, 339–352.

Prosperetti, A. (1991). The thermal behaviour of oscillating gas bubbles. *Journal of Fluid Mechanics*, 222, 587–616.

Prosperetti, A. (1997). A new mechanism for sonoluminescence. *Journal of the Acoustical Society of America*, 101(4), 2003–2007.

Prosperetti, A. (1999). Old-fashioned bubble dynamics. In: Crum, L. A., Mason, T. J., Reisse, J. L., and Suslick, K. S. (eds.), *Sonochemistry and sonoluminescence*, pp. 39–62. Dordrecht, Kluwer. *Proceedings of the NATO Advanced Study Institute on Sonoluminescence and Sonoluminescence*, Leavenworth, Washington, DC, 18–29 August 1997.

Prosperetti, A., and Hao, Y. (1999). Modelling of spherical gas bubble oscillations and sonoluminescence. *Philosophical Transactions of the Royal Society London A*, 357, 203–223.

Prosperetti, A., and Lezzi, A. (1986). Bubble dynamics in a compressible liquid. Part 1. First-order theory. *Journal of Fluid Mechanics*, 168, 457–478.

Prosperetti, A., and Seminara, G. (1978). Linear stability of a growing or collapsing bubble in a slightly viscous liquid. *Physics of Fluids*, 21(9), 1465–1470.

Prosperetti, A., Crum, L. A., and Commander, K. W. (1988). Nonlinear bubble dynamics. *Journal of the Acoustical Society of America*, 83, 502–514.

Putterman, S. J., and Weninger, K. R. (2000). Sonoluminescence: How bubbles turn into light. *Annual Review of Fluid Mechanics*, 32, 445–476.

Ratoarinoro, Contamine, F., Wilhelm, A. M., Berlan, J., and Delmas, H. (1995). Power measurement in sonochemistry. *Ultrasonics Sonochemistry*, 2(1), S43–S47.

Rayleigh, Lord. (1917). On the pressure developed in a liquid during the collapse of a spherical cavity. *Philosophical Magazine*, 34, 94–98.

Reddy, A. J., and Szeri, A. J. (2002). Shape stability of unsteadily translating bubbles. *Physics of Fluids*, 14(7), 2216–2224.

Rozenberg, L. D. (ed.). (1971a). *High-intensity ultrasonic fields*. New York, NY, Plenum Press.

Rozenberg, L. D. (1971b). The cavitation zone. In: Rozenberg, L. D. (ed.), *High-intensity ultrasonic fields*. New-York, NY, Plenum Press.

Rozenberg, L. D. (ed.). (1973). *Physical principles of ultrasonic technology*. New York, NY, Plenum Press.

Servant, G., Caltagirone, J. P., Girard, A., Laborde, J. L., and Hita, A. (2000). Numerical simulation of cavitation bubble dynamics induced by ultrasound waves in a high frequency reactor. *Ultrasonics Sonochemistry*, 7, 217–227.

Servant, G., Laborde, J. L., Hita, A., Caltagirone, J. P., and Girard, A. (2003). On the interaction between ultrasound waves and bubble clouds in mono- and dual-frequency sonoreactors. *Ultrasonics Sonochemistry*, 10(6), 347–355.

Silberman, E. (1957). Sound velocity and attenuation in bubbly mixtures measured in standing wave tubes. *Journal of the Acoustical Society of America*, 29(8), 925–933.

Sirotyuk, M. G. (1971). Experimental investigations of ultrasonic cavitation. In: Rozenberg, L. D. (ed.), *High-intensity ultrasonic fields*. New-York, NY, Plenum Press.

Storey, B. D., and Szeri, A.J. (2000). Water vapour, sonoluminescence and sonochemistry. *Proceedings of the Royal Society of London, Series A*, 456, 1685–1709.

Storey, B. D., and Szeri, A.J. (2001). A reduced model of cavitation physics for use in sonochemistry. *Proceedings of the Royal Society of London, Series A*, 457, 1685–1700.

Storey, B. D., and Szeri, A. J. (2002). Argon rectification and the cause of light emission in single-bubble sonoluminescence. *Physics Review Letters*, 88(7), 074301-1–074301-3.

Storey, B. D., Lin, H., and Szeri, A. J. (2001). Physically realistic models of catastrophic bubble collapses. In: *Fourth International Symposium on Cavitation*. California Institute of Technology, Pasadena, CA, June 20–23.

Strasberg, A. (1961). Rectified diffusion: Comments on a paper of Hsieh and Plesset. *Journal of the Acoustical Society of America – Letters to the Editor*, 33, 359.

Strasberg, M., and Benjamin, T. B. (1958). Excitation of oscillations in the shape of pulsating gas bubbles. *Journal of the Acoustical Society of America (Abstract)*, 30, 697.

Suslick, K. S., McNamara, W. B., and Didenko, Y. (1999). Hot spot conditions during multi-bubble cavitation. In: Crum, L. A., Mason, T. J., Reisse, J. L., and Suslick, K. S. (eds.), *Sonochemistry and sonoluminescence*, pp. 191–204. Dordrecht, Kluwer. *Proceedings of the NATO Advanced Study Institute on Sonoluminescence and Sonoluminescence*, Leavenworth, Washington, DC, 18–29 August 1997.

Toegel, R., Gompf, B., Pecha, R., and Lohse, D. (2000a). Does water vapor prevent upscaling sonoluminescence? *Physics Review Letters*, 85(15), 3165–3168.

Toegel, R., Hilgenfeldt, S., and Lohse, D. (2000b). Squeezing alcohols into sonoluminescing bubbles: the universal role of surfactants. *Physics Review Letters*, 84(11), 2509–2512.

Tomita, Y., and Shima, A. (1977). On the behaviour of a spherical bubble and the impulse pressure in a viscous compressible liquid. *Bulletin of the JSME*, 20(149), 1453–1460.

Vazquez, G. E., and Putterman, S. J. (2000). Tempurature and pressure dependence of sonoluminescence. *Physics Review Letters*, 85(14), 3037–3040.

Walton, A. J., and Reynolds, G. T. (1984). Sonoluminescence. *Advances in Physics*, 33(6), 595–660.

Wijngaarden, V. L. (1968). On the equations of motion for mixtures of liquid and gas bubbles. *Journal of Fluid Mechanics*, 33(3), 465–474.

Yasui, K. (1997). Alternative model of single-bubble sonoluminescence. *Physical Review E*, 56, 6750–6760.

Yasui, K. (2001). Effect of liquid temperature on sonoluminescence. *Physical Review E*, 64(016310), 1–10.

Yasui, K., Tuziuti, T., and Iida, Y. (2005). Dependence of the characteristics of bubbles on types of sonochemical reactors. *Ultrasonics Sonochemistry*, 12, 43–51.

Yuan, L., Ho, C. Y., Chu, M. C., and Leung, P. T. (2001). Role of gas density in the stability of single-bubble sonoluminescence. *Physical Review E*, 64(016317), 1–6.

Zardi, D., and Seminara, G. (1995). Chaotic mode competition in the shape oscillations of pulsating bubbles. *Journal of Fluid Mechanics*, 286, 257–276.

Chapter 3
Ultrasound Applications in Food Processing

Daniela Bermúdez-Aguirre, Tamara Mobbs, and Gustavo V. Barbosa-Cánovas

1 Introduction

Food scientists today are focused on the development of not only microbiologically safe products with a long storage life, but, at the same time, products that have fresh-like characteristics and a high quality in taste, flavor, and texture. This focus is based on the needs of the consumer, which is one of the main reasons for constant research in the so-called area of emerging technologies. Traditionally, thermal treatments have been used to produce safe food products. Pasteurization of juice, milk, beer, and wine is a common process in which the final product has a storage life of some weeks (generally under refrigeration). However, vitamins, taste, color, and other sensorial characteristics are decreased with this treatment. High temperature is responsible for these effects and can be observed in the loss of nutritional components and changes in flavor, taste, and texture, often creating the need for additives to improve the product. Thus, one of the challenges in food science today is to develop new technologies that can simultaneously ensure high-quality properties and long storage life. In recent years, the most popular emerging technologies being tested in food science labs have been high pressure, electric pulsed fields, ultraviolet light, irradiation, light pulses, and ultrasound, and some are already being used in the food industry, while other emerging technologies are still in the lab testing stage. Ultrasound technology is applied in the food industry mostly as a processing aid and for the cleaning/disinfecting of factory surfaces, but many of its uses are still being researched.

The majority of literature on processing foods by ultrasound, including its use to enhance other food technologies, is application-specific and reports process parameters and results for one type of experiment only. This chapter examines the process parameters across many experiments, as well as many applications in ultrasonic

G.V. Barbosa-Cánovas (✉)
Biological Systems Engineering Department, Center for Nonthermal Processing of Food, Washington State University, Pullman, WA 99164-6120, USA
e-mail: barbosa@wsu.edu

H. Feng et al. (eds.), *Ultrasound Technologies for Food and Bioprocessing*, Food Engineering Series, DOI 10.1007/978-1-4419-7472-3_3,
© Springer Science+Business Media, LLC 2011

fields that have met with success. Discussion of the engineering principles behind the experimental results reported in literature is included. In order to show the differences between high- and low-frequency ultrasound, the parameters and applications of ultrasound will likewise be discussed. Special emphasis will be placed on food engineering applications as an update on microbial inactivation research, describing the types of experiments conducted, the basic theory about microbial inactivation, and the different processes involving the use of heat and pressure in combination with ultrasound. Uses in enzymatic inactivation will be addressed, although information is scarce, and applications of non-destructive ultrasound and high-frequency ultrasound will be reviewed in an attempt to show the broad applications of this technology in the field.

Thus, the overall goal of this chapter is to show the parameters, mechanisms, and results of different experiments around the world that have used low- and high-frequency ultrasound, so that readers can easily understand the fundamentals of this technology, which already has proven successful in many areas of food science and food processing technology.

2 General Principles

Ultrasound consists of a series of sound waves with high frequencies that begin at 16 kHz, which is near the upper limit of the human hearing range (Elmehdi et al., 2003; Hecht, 1996). When a given source radiates sound into a nearby medium that has mass (e.g., air, liquid, or solid), the sound propagates in sinusoidal waves. The medium responds to the propagation of these waves and also sustains them by vibrating elastically. The medium's elastic vibrations take two forms: condensation and rarefaction (Hecht, 1996; Knorr et al., 2004). During condensation, the medium particles are compressed (i.e., the spacing between particles is condensed), causing the medium's pressure and density to increase (Gallego-Juárez et al., 2003; Hecht, 1996). During rarefaction, the medium particles shift apart so that the medium's density and pressure decrease (American Heritage, 2002; Hecht, 1996).

McClements (1995) describes ultrasonic wave behavior insightfully by viewing the wave from two perspectives, time and distance. At a fixed position in the medium, the sound wave behaves sinusoidally with respect to time. As shown in Fig. 3.1, the time span from one peak amplitude to another is the time period τ of the sinusoidal wave. This physically means that each particle at some depth in the medium (along some line of equidistance) must wait for time period τ before experiencing another sound wave equal to the one just experienced. The sinusoid frequency f represents how often (frequently) the sinusoid completes an oscillation (cycling from peak to peak) in one second duration and is mathematically given by the inverse of the time period as shown in Equation (3.1) (McClements, 1995):

$$f = 1/\tau \tag{3.1}$$

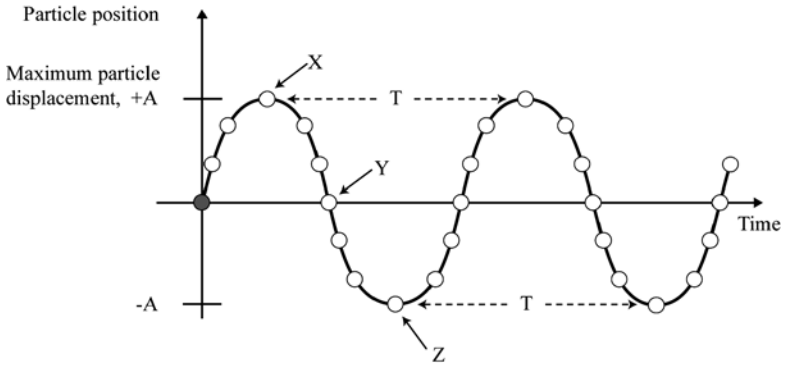

Fig. 3.1 Ultrasonic wave behavior (adapted from McClements, 1995)

The distance considers the effect of the sound wave at any fixed instant in time on particles that are successively deeper in the medium. At any time, the amplitude of the sound wave is felt strongly by particles near the sound wave source, but particles deeper in the medium experience the sound wave less strongly. This decrease in sound wave amplitude with distance is due to attenuation from the medium. The plot of sound amplitude versus distance is actually an exponentially decaying sinusoid, as shown in Fig. 3.2. The distance between successive amplitude peaks is the wavelength (λ). The wavelength relates to frequency through the velocity of the traveling wave c, as follows in Equation (3.2) (McClements, 1995):

$$\lambda = c/f \tag{3.2}$$

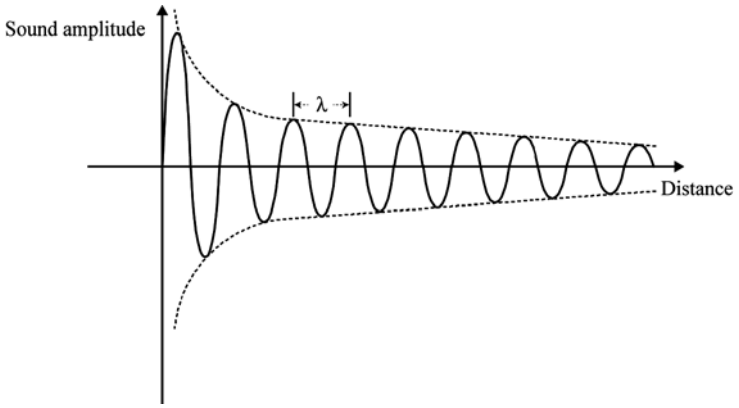

Fig. 3.2 Graph showing a sinusoidal ultrasound wave, distance versus sound amplitude

Thus, sound waves travel through the medium with a measurable velocity by acting on the medium particles. The waves oscillate the medium particles about their equilibrium positions. At any moment in time, the particles shift toward or away from each other. This shifting causes alternate increases and decreases in medium density and pressure. Consequently, the only type of energy imparted into the medium from the ultrasound is mechanical, which is associated with the oscillation of medium particles (Hecht, 1996).

With respect to imparted energy, treatments using ultrasound differ from treatments using waves from the electromagnetic (EM) spectrum, such as ultraviolet (UV) light waves, radio frequency (RF) waves, and microwaves (MW) (Kardos and Luche, 2001), as well as pulsed electric fields (PEF). EM waves and PEF introduce electric and magnetic energy into a medium, which are absorbed by the medium particles. For example, UV light from the sun can impart enough atomic energy (4 eV) to break a carbon–carbon bond. EM waves occur when subatomic particles, having positive and negative charges, move freely in non-uniform motion. Between positive and negative charges, electric and magnetic fields radiate. These electric and magnetic fields enter the medium and interact with the atoms, ions, or molecules in the medium. For example, microwaves interfere with polar molecules (those with one positive end, one negative end) in a medium by causing them to rotate and align with the electric fields associated with the microwaves. Inside microwave ovens, the water molecules in foods absorb much microwave radiation, and their subsequent rotations are converted to heat energy (Hecht, 1996). Hence, EM waves impart electric and magnetic energy into the medium, while sound waves impart only mechanical energy.

Also important to note in comparing sound waves with light is that only sound waves contain no particles of their own. Sound waves merely interrupt the stillness of the medium to oscillate the particles belonging to the medium. Unlike sound, physicists consider light to be an unsolved mystery, propagating as both streams of particle-like "energy concentrations" and massless waves simultaneously. This difference becomes apparent in a vacuum. As vacuums contain no medium particles, massless sound waves cannot propagate because they cannot create condensations and rarefactions of particles.

The pressure exerted on the human ear by loud sounds is very small (<10 Pa), but ultrasonic pressure in liquids can be high enough (several MPa) to help initiate a phenomenon called inertial cavitation, which can destroy the medium (Hecht, 1996; Povey and Mason, 1998). Inertial cavitation refers to bubble activity in a liquid and is produced by very high intensity ultrasonic waves, which can break apart the microstructures of a medium and generate free radicals. The cavitation ultimately leads to the destruction of microbiological cells and the production of free radicals and sonochemicals that react chemically with liquid media (Chemat et al., 2004; Knorr et al., 2004). Those ultrasonic applications concerned with detection of flaws, such as quality assurance in food processing, must be designed so that inertial cavitation cannot possibly occur. Other ultrasonic applications, however, rely directly on inertial cavitation to generate desired changes in foods. Changes produced by cavitation include the inactivation of microorganisms and the release of oils or

nutritional compounds through the erosion of a food's cellular structures (Knorr et al., 2004; Riera-Franco de Sarabia et al., 2000). Hence, cavitation is avoided in one branch of ultrasonic food processing and studied in the other branch as the mechanism responsible for all desired effects. In Table 3.1 there are some examples of the use of ultrasound in food applications, in both ranges, high and low frequencies.

2.1 Overview of Ultrasonic Equipment

No matter what industry or application involved, the same basic system components are needed to generate and transmit ultrasonic waves. Ultrasonic equipment consists of the electrical power generator, transducer(s), and emitter, which physically sends the ultrasonic waves into the medium (Povey and Mason, 1998). Exceptions include the "liquid whistle," which uses purely mechanical energy without an electrical generator to generate ultrasound (Mason et al., 1996), and airborne systems, which do not require an emitter (Gallego-Juárez et al., 2003; Povey and Mason, 1998).

Two types of ultrasound systems are reported to be used in food industry, one using a horn as the sound emitter and the other using a bath. The bath has been traditionally used in food processing due to its early availability (Povey and Mason, 1998). In recent research, horn-based systems appear to be cited as often as baths (Aleixo et al., 2004; Duckhouse et al., 2004; Mason et al., 1996; Neis and Blume, 2003; Patrick et al., 2004; Tian et al., 2004). The horn-based system is employed equally well in many applications, from ultrasonic food processing to cleaning of food process plant surfaces to ultrasonic welding of metals.

2.1.1 Electrical Generator

The electrical generator is the source of energy for the ultrasonic system, which must drive the transducer (Povey and Mason, 1998). Generally, an electrical generator produces electrical current with a specified power rating. Most generators allow the power to be set only indirectly through voltage (V) and current (I) settings. The voltage represents the potential energy stored in the electrons (measured in volts); the current represents the net charge of electrons traversing an area over some time interval (measured in amps); and the power is the product of these two represented in Equation (3.3) (Hecht, 1996):

$$P = IV\,[\mathrm{W}],\ [\mathrm{volt} \bullet \mathrm{amps}],\ [\mathrm{VA}] \tag{3.3}$$

Electrical generators that are designed specifically for ultrasound mostly focus on industrial cleaning, and therapeutic, welding, and disinfecting applications, and operate in the lower frequency range (10–40 kHz). Low frequencies are not used in non-destructive testing of foods, but power ultrasound has many potential applications in food processing as will be shown in this chapter.

Table 3.1 Summary of several ultrasound applications in food processing based on application

Type of application	Application	Processing parameters	Equipment used	References
Changes in food composition	Agglomeration for fine-particle separation	Power level: 400 W (each radiator); frequency: 10 and 20 kHz	Acoustic agglomerator with four stepped plate sound radiators	Riera-Franco de Sarabia et al. (2000)
	Crystallization (palm oil) and examination of sonochemicals (off-flavors from free radicals in sunflower oil)	Power level: 40 dB found to be most effective (cavitation threshold, 41 dB); frequency: depended on cell geometry and sample – cell resonant frequency determined by experimental calibrations	Proprietary ring-transducer cell: produces radial ultrasonic field (measured and calibrated by B&K Hydrophone) with cylindrical, batch-style reactor containing stirrers made of vertical blades moving up and down the walls	Patrick et al. (2004)
	Deagglomeration for improved microbial inactivation (bacterial clusters in water)	(a) Power density: 0.18 W/cm^3; Frequency: 38 kHz (b) Power density: 0.24 W/cm^3; Frequency: 20 kHz (c) Power density: 0.071 W/cm^3; Frequency: 512 kHz (d) Power density: 0.064 W/cm^3; Frequency: 850 kHz	(a) Langford Sonomatic US cleaning bath (b) Sonics & Materials probe system (c) Undatim Ultrasonics bath (d) Meinhart Ultrachalltechnik bath	Joyce et al. (2003)

Table 3.1 (continued)

Type of application	Application	Processing parameters	Equipment used	References
	Deagglomeration for improved microbial inactivation (bacteria in waste water)	Power level: 41–154 W Power intensity: 1.7–60.8 W/cm^2 Power density: 10–400 W/L with 30 W/L optimal; Frequency: 20 kHz	Branson W-450 Sonifier with horn having 1.3 cm tip diameter	Neis and Blume (2003)
	Deagglomeration for improved chlorination (*E. coli* in water)	(a) Power level: 22.34 W Power intensity: 16.92 W/cm^2 Frequency: 20 kHz (b) Power level: 1.22 W (40% amplitude) Power intensity: 0.029 W/cm^2 Frequency: 850 kHz (during pre-treatment)	a) Sonics & Materials VC-600 b) Meinhart Ultrachalltechnik K80–5	Duckhouse et al. (2004)
	Deliquoring for solid–liquid separation	Power level: 60 W Power intensity: 800 W/m^2 Frequency: 24.6 kHz	System with custom piezoelectric transducer, horn, and special coupling "radiator"	Gallego-Juárez et al. (2003)
	Denaturation of protein during emulsification (trypsin)	Power levels: 100–500 W Power intensities: 84.9–424.5 W/cm^2 Frequency: 20 kHz	Ultrasound processor with 2 cm horn, and tapered 0.2 cm microtip accessory	Tian et al. (2004)

Table 3.1 (continued)

Type of application	Application	Processing parameters	Equipment used	References
	Deterioration of oils and sonochemicals production (sunflower oil)	20 kHz (model 450), 47 kHz (model 5210)	Branson Sonifiers W-450 and 5210 with immersible horn and cylindrical jacket vessel	Chemat et al. (2004)
	Emulsification	20 kHz	Ultrasonic probe systems, with flow cell	Behrend and Schubert (2001)
	Erosion	Power level: 142 W Power intensity: 0.43 W/cm^2 Frequency: 40 kHz	Ultrasonic reactor	Krefting et al. (2004)
	Extraction (antioxidants from *Rosemary* herb)	20 kHz (probe), 40 kHz (bath)	Probe system, and bath with overhead stirring	Albu et al. (2004)
	Extraction (cadmium and lead in Brazilian vegetables and mussel)	Power level: 50 W (bath), 100 W (probe) Frequency: 20 kHz	(1) Ultrasonic bath model USC-SSS with piezoelectric transducers (2) Ultrasonic processor Vibracell VC 50–1 with titanium probe	Aleixo et al. (2004)
	Extraction (fat isolation)	Power level: 400 W; Frequency: 20 kHz	Branson 450 digital sonifier with probe in water bath	Ruis-Jiménez et al. (2004)
	Extraction (oil from soybeans)	Power intensity: 16.4–47.6 W/cm^2; Frequency: 20 kHz	Misonix S3000 generator with probe	Li et al. (2004)
	Extraction (proteins)	Power level: 550 W; Frequency: 20 kHz	Probe-based system	Mason et al. (1996)
	Fragmentation of DNA	Power level: 85 W; Frequency: 20 kHz	Vibra Cell processor with 5 mm microtip attachment	Mann and Krull (2004)

Table 3.1 (continued)

Type of application	Application	Processing parameters	Equipment used	References
Freezing/thawing	Enhancing freezing rate	Power level: 15.85 W; Frequency: 25 kHz	Bath with six transducers attached to tank	Sun and Li (2003)
	Enhancing thawing	Power intensity: 3 W/cm^2 (Therasonic), 0.5 W/cm^2 (custom transducers); Frequency: 3.3 and 1.1 MHz	Therasonic 1032, and custom transducers with RF amplifier and sine generator	Miles et al. (1999)
Inactivating enzymes and micro-organisms	Enzymatic inactivation (peroxidase in horseradish)	Power level: unspecified measurement from wattmeter rated 0–400 W; Frequency: unspecified, out of 20–100 kHz rating	Undatim Ultrasonics generator with horns and batch reactor	De Gennaro et al. (1999)
	Enzymatic inactivation (phospholipase, via mano-thermo-sonication)	Vibrational amplitude: 117 μm	TR-SC thermoresistometer in bath	Vercet et al. (2002)
	Microbial inactivation (cell killing and free radicals)	Power intensity: 0.3 and 0.5 W/cm^2; Frequency: 1 MHz	Giken Co. Sonicmaster with 5 cm diameter transducer	Feril and Kondo (2004)
	Microbial inactivation (*E. coli* in water)	Vibrational amplitude: 5 or 7 μm; Frequency: 27.5 MHz Power intensity: ≤42 W/ml	System with transducer and squeeze-film type horn	Furuta et al. (2004)
	Microbial inactivation (in liquid whole egg)	Power levels: 24.6, 34.6, and 42 W; Frequency: 20 kHz	Horn-based system	Lee et al. (2003)

Table 3.1 (continued)

Type of application	Application	Processing parameters	Equipment used	References
	Microbial inactivation (*L. monocytogenes*)	Vibrational amplitude: 117 μm; Frequency: 20 kHz		Pagán et al. (1999)
	Microbial inactivation (*S. cerevisiae* in water)	Power density: 42 Wm/L; Frequency: 27.5 kHz	Two squeeze-film type horn sonicators	Tsukamoto et al. (2004a)
	Review of applications for microbial inactivation and homogenization (milk)	Power levels: 100 or 160 W Power intensities: 1–3 W/cm^2 Vibrational wave amplitude: 117 μm; Frequency: 20–100 kHz	Primarily referred readers to text by Povey and Mason (1998)	Piyasena et al. (2003)

2.1.2 Transducer

All ultrasonic systems include a transducer as the central element, whose role is to generate the actual ultrasound. The transducer converts electrical energy (or mechanical energy, in the case of the liquid whistle) into sound energy by vibrating mechanically at ultrasonic frequencies (Povey and Mason, 1998). Lee et al. (2003) explain that a transducer attached to an electrical generator will transform, for instance, 20-kHz electrical energy from the generator into ultrasound energy of the same frequency by vibrating at 20,000 mechanical cycles per second.

Povey and Mason (1998) summarize three main types of transducers: liquid-driven, magnetostrictive, and piezoelectric (pzt). Liquid-driven transducers rely on purely mechanical energy to produce ultrasound, but magnetostrictive and piezoelectric transducers convert electrical and magnetic energy into mechanical, ultrasonic energy. While liquid whistles make excellent mixers and homogenizers, most power ultrasound equipment use piezoelectric or magnetostrictive transducers today (Knorr et al., 2004; Povey and Mason, 1998). The piezoelectric transducer (pzt) is the most common type and is used in most ultrasonic processors and reactors and cited often in literature (Aleixo et al., 2004; Gallego-Juárez et al., 2003; Povey and Mason, 1998). The pzt is also the most efficient, achieving better than 95% efficiency, and it is based on a crystalline ceramic material that responds to electrical energy.

2.1.3 Emitter (Baths, Horns, and Sonotrodes)

The purpose of the emitter, also called the reactor by some, and ultrasonic cell by others, is to radiate the ultrasonic wave from the transducer into the medium. Emitters may also fulfill the role of amplifying the ultrasonic vibrations while radiating them. The two main forms of emitters are baths and horns (i.e., probes); horns often require the attachment of a horn tip known as a sonotrode (Povey and Mason, 1998).

Baths usually consist of a tank to which one or more transducers have been attached. The tank holds a sample in solution and the transducers radiate ultrasound directly into the sample (Povey and Mason, 1998). In horn-based systems, a horn is attached to the transducer to amplify the signal and bring it to the sample. The tip of the horn, often a separate attachable device known as a sonotrode, radiates the ultrasonic wave into the sample. The shape of the horn determines the amount of amplification. Hence, the intensity of radiation can be controlled by selecting differently shaped horns. The main difference in equipment used in laboratories versus commercial processing plants is the type of emitter. More robust emitters that do not wear down after many hours of use are required in food manufacturing.

2.1.4 Examples of Ultrasound Systems in Food Processing

Many laboratory-scale and industrial food applications employ an integrated system called an ultrasonic processor. The ultrasonic processor is also called a reactor

(e.g., the "probe reactor" or "bath reactor") if the ultrasonic treatment is capable of producing chemical changes in the medium (Mason, 2003). Equipment manufacturers usually design the processor (or reactor) with the electrical generator and transducer contained in one housing (this is lightweight and portable) and offer several types of emitters as attachments, which are selected based on the application. Emitters are either horns (i.e., probes) or sonotrodes. A large number of companies in the world sell ultrasonic processors, among which are Hielscher, Branson, Undatim, Sonicmaster, Giken, Sonics & Materials, and Vibra Cell.

Food processing publications contain a number of examples of successfully custom-designed ultrasonic systems. For example, researchers Furuta et al. (2004), in a report on the inactivation of *Escherichia coli* cells, show a schematic of an apparatus containing a generator, transducer, and emitter. A function generator plus power amplifier is connected to an ultrasonic transducer, which uses a horn (i.e., probe) immersed in the sample. They also used a displacement meter for monitoring input/output vibrational amplitudes of the horn face to check the acoustic power introduced to the sample. Another custom system set up to inactivate *E. coli*, this time in liquid whole egg (LWE), is reported by Lee et al. (2003). Their laboratory-scale equipment included an electric generator (with adjustable power supply output), a transducer from Bandelin electronic, and a horn that both amplified the ultrasonic output and radiated it into the LWE.

Other researchers have successfully investigated ultrasonic thawing of meat and fish samples with transducers they constructed specially for their experiments (of diameters nearly equal to sample sizes). These custom transducers were powered by a sine-wave generator together with an RF power amplifier from ENI, Inc.; they also employed a Hewlett-Packard 5302A universal counter to monitor output frequency (Miles et al., 1999).

Gallego-Juárez et al. (2003) conducted airborne ultrasound experiments using a unique system in which an electrical generator was connected to a custom-designed stepped plate transducer. The ultrasound was emitted by an ultrasonic radiator and a flat plate parallel to it. The plate held the sample and acted as a reflector to help form a standing wave.

2.2 High-Versus Low-Intensity Ultrasound

Across the industry, engineering applications of ultrasound are separated into two distinct categories: low intensity (also called high frequency or "non-destructive" ultrasound) and high intensity (also called low frequency or "power" ultrasound) (Mason, 2003). These two categories differ in the goal to be achieved, the application, and the applied ultrasonic power and frequency. The goal of low-intensity ultrasound is usually to identify some unseen substance in a medium, while high-intensity ultrasound usually focuses on altering some part of a medium or promoting a chemical reaction. For instance, medical tomography applies low-intensity ultrasound to locate and outline (i.e., "image") objects suspended in various media

(Kennedy et al., 2004). Dolphins and bats likewise send out low-intensity ultrasonic waves to navigate by echoes; this phenomenon works similarly to SONAR (SOund NAvigation and Ranging) (Hecht, 1996). In contrast, high-intensity ultrasound is used to erode surface contaminations in welding and precision cutting of materials, and also to destroy tumors in therapeutic medical ultrasound (Kennedy et al., 2004; Krefting et al., 2004; Mason, 2003; Povey and Mason, 1998).

These differences are similar in food processing applications; while low-intensity ultrasound is applied non-invasively to locate flaws and foreign objects in foods during quality assurance testing, high-intensity ultrasound is applied for such manipulative purposes as damaging the cellular walls of microorganisms in foods, denaturing proteins, stimulating seed germination, and enhancing crystallization in foods (Knorr et al., 2004; Mason et al., 1996; Tian et al., 2004). The major process parameters differentiating the two types of ultrasound are ultrasonic energy and frequency. Low-intensity ultrasound is low energy, with power intensities below 1 W/cm^2 and high frequency of 1–10 MHz. Hence, low-intensity ultrasound is also termed high-frequency ultrasound. High-intensity ultrasound is high energy with power intensities above 10 W/cm^2 and low frequency of 10–100 kHz (Povey and Mason, 1998; McClements, 1995). High-intensity ultrasound likewise is referred to as low-frequency ultrasound.

2.2.1 Overview of Low-Intensity "Non-destructive" Ultrasound

Low-intensity (non-destructive, high-frequency) ultrasound is applied for detection purposes in general, and so it is utilized as a processing aid in the food industry to characterize food components, often on quality assurance lines. Aptly named non-destructive testing (NDT), this process sends ultrasonic waves through a medium without causing any permanent physical, chemical, or electrical change in the medium, because the ultrasonic intensity is too low (< 1 W/cm^2) to alter the material (Gestrelius et al., 1993; McClements, 1995). The medium particles oscillate in response to the low energy (purely mechanical) while exposed to the ultrasonic waves and simply return to their equilibrium position when the source of ultrasound is removed.

When acoustic waves pass through the medium, the waves are partially reflected or scattered wherever the medium changes from one material to another (Hecht, 1996). The distance to the reflection location can be calculated through measured ultrasonic properties like frequency (always higher than 1 MHz) and attenuation coefficient, to allow detection and location of the presence of foreign particles and compositional changes in foods (McClements, 1995).

Low-intensity ultrasound can invaluably aid quality control in food production, as well as monitor the changes that foods undergo as they are processed (freezing, emulsifying, drying, etc.). Food manufacturers use ultrasonic NDT to locate foreign bodies such as glass, organic residues, or bacterial infections in solids and liquids – even after foods are packaged (Gestrelius et al., 1993; Hæggström and Luukkala, 2001). Other examples include characterization of the cellular structure of pre-cooked dough to obtain predictions of cooked product quality (Elmehdi et al.,

2003), and monitoring the movement of the ice front in a solid food (as the food slowly freezes) to determine the energy efficiency of the freezing process (Sigfusson et al., 2004).

2.2.2 Overview of High-Intensity "Power" Ultrasound

High-intensity (low-frequency, power) ultrasound is used either to destroy cellular structures or to enhance or inhibit activities within foods (Mason et al., 1996), and is characterized by power intensities generally ranging between 10 and 1,000 W/cm^2. These intense acoustic waves can cause high pressures inside liquid foods, producing streams of fast-moving microbubbles and causing bubbles in liquids to collapse violently (Mann and Krull, 2004). These types of bubble activities in liquids, respectively termed non-inertial and inertial cavitation, are mechanisms that affect the physical and chemical properties of foods (Povey and Mason, 1998). The cavitation activities in liquids can be so intense that living cell walls are broken down, free radicals and sonochemicals are produced, and processes such as seed germination are enhanced whereas enzymatic activities are inhibited (Mason, 2003; McClements, 1995; Povey and Mason, 1998). Hence, Povey and Mason (1998) coin the term "material-altering" to describe high-power ultrasound, in parallel to the descriptor "non-destructive" for low-intensity ultrasound.

The material-altering applications of high-intensity ultrasound are numerous in the food processing arena. Major research schools working with power ultrasound in food processing mainly are studying extraction, emulsification, filtration, crystallization, producing of fine-particles, thawing, and freezing, while several research teams around the world are examining the inactivation of microorganisms and enzymes in foods (Mason, 2003).

When researchers analyze results from ultrasound experiments, they determine and use different process parameters for high-intensity applications than for low-intensity applications. The only parameters commonly used in both high- and low-intensity applications include frequency (f, or angular frequency $\omega = 2\pi f$) and power amplitude (denoted by A or P). These values are set or adjusted by the ultrasonic generation equipment and controlled by the experimenter based on the results desired. Parameters used extensively in low-intensity ultrasound include frequency, amplitude, velocity, time and distance of travel, attenuation coefficient, reflection coefficient, acoustic impedance, and density. High-intensity ultrasound parameters include power, frequency, treatment temperature, and treatment time.

3 Power and Energy

In general, power represents the strength of a treatment or, from another perspective, how much treatment a medium experiences. In ultrasound, the treatment is accomplished by passing an ultrasonic wave through the medium; therefore, the power of the treatment is determined by the power (or strength) of the ultrasonic wave.

Studies show that more power causes greater alterations in the material, at least up to some maximum power limit depending upon the properties of the medium in question (De Gennaro et al., 1999; Furuta et al., 2004; Joyce et al., 2003; Mason et al., 1996; Pagán et al., 1999; Povey and Mason, 1998; Riera-Franco de Sarabia et al., 2000; Sun and Li, 2003; Tian et al., 2004). Theoretically, high ultrasonic wave powers produce high pressures in the medium (Hecht, 1996). These high-acoustic pressures work to destroy microorganisms and enzymes in a food and break down microstructures, through cavitation (Povey and Mason, 1998). Of course, researchers aim to find the minimal power necessary to process the food as desired and yet preserve the vitamins, colors, textures, and flavors in foods (De Gennaro et al., 1999; McClements, 1995; Riera-Franco de Sarabia et al., 2000).

Power also relates to energy, and a few ultrasonic researchers prefer to measure the energy delivered to the medium rather than power. For example, researchers Duckhouse et al. (2004) measured the treatment time in seconds and multiplied these times by their power values to obtain the Joule-energy experienced by the medium. This method applies the basic physics relationship below in Equation (3.4) (Hecht, 1996):

$$1\ \mathrm{J} = 1\ \mathrm{W} \bullet \mathrm{s} \tag{3.4}$$

In a similar vein, other researchers have reported energy density in W•s/m in place of power density.

3.1 Vibrational Amplitude

A traditional way to represent the power or strength of ultrasonic waves is to measure the amplitude of the mechanical vibrations. The vibrational amplitude is measured as the maximum displacement in micrometers (μm) of the vibrating tip of the sonotrode (i.e., horn) as it sends the acoustic waves into the medium. Generally, vibrational amplitude is specified by the equipment manufacturers. Furuta et al. (2004) and Tsukamoto et al. (2004a, b) preferred to use vibrational amplitude, from 1 to 7 μm, to represent the actual acoustic power that their custom-made system introduced to their cell samples. They implied that their amplitude measurements provided a more exact and stable indication of ultrasonic cavitation than a power parameter would have provided; they were able to measure the vibrational amplitude during ultrasonic irradiation (Tsukamoto et al., 2004a).

Vibrational amplitude is also reported as the ultrasonic parameter in two other articles on microbial inactivation, those of Pagán et al. (1999) and Vercet et al. (2002). Additionally, Mason et al. (1996) mention vibrational amplitude in their overview of ultrasonic uses in food processing, although they also refer to many other ways that ultrasonic power can be represented. Other ways to represent ultrasonic wave strength do not relate to the vibrations of the transducer, but rather to the electrical generator powering the ultrasonic equipment.

3.2 Power Intensity

Power intensity is a way to measure power transmitted to the medium from the sonotrode tip surface, rather than from the ultrasonic generator. In general, power intensity P_i (also called power irradiance) represents power, P, distributed over surface area A as shown in Equation (3.5) (Hecht, 1996):

$$P_i = P/A \ [\mathrm{W/m^2}] \tag{3.5}$$

For ultrasonic systems, power intensity is calculated to obtain the power radiating from the sonotrode tip surface (Neis and Blume, 2003). This power intensity value is the actual power the medium experiences near the sonotrode surface, per unit area of the sonotrode tip. For a sonotrode that has a circular area, the power intensity becomes as shown in Equation (3.6):

$$P_i = P/\pi r^2 \ [\mathrm{W/m^2}] \tag{3.6}$$

Power intensity also enables relationships to be established between the dimensions of sonotrodes and the power. For example, if an ultrasonic generator has a power rating of 360 W and the sonotrode radius is 1 cm, then P_i equals 114.59 W/cm^2. For the same power of 360 W, if a smaller sonotrode of only half the radius (0.5 cm) is used, then P_i is much greater at 458.37 W/cm^2. This shows that the power is much more concentrated on the smaller sonotrode. Power intensity increases as sonotrode radius decreases.

Today so many different power and energy parameters are used in treating foods with ultrasound (parameters are too often unexplained in literature) that new researchers cannot always determine from reported data how much application of sonication is needed to build upon the published results. Hence, the use of one or two standard parameters, based on understood proven measurements and calculations of these parameters, could erase the current confusion.

3.3 Frequency

High-intensity ultrasound is accomplished with frequencies between 10 and 100 kHz. The frequency used mainly depends on process considerations related to equipment and the first consideration is the amount of power desired, for instance, transducers produce high-power radiations at low frequencies as the power changes inversely with the square of the frequency (Povey and Mason, 1998), as shown in Equation (3.7):

$$P \propto 1/f^2 \tag{3.7}$$

The second consideration is frequency dependence on emitter dimensions. Ultrasonic baths, which transmit ultrasound directly into the tank through bonded transducers, usually operate at 40 kHz. However, systems that attach a horn to the

transducer for power amplification are able to achieve lower frequencies of 20 kHz. The lower frequency is achieved by the length extension the horn provides to the transducer: frequency is reduced by half when the emitter length doubles.

The frequency selected for the application will have a strong effect on cavitation activity. The degree of cavitation occurring in a liquid depends on the relationship between frequency and bubble size. High pressures from acoustic vibrations cause the bubbles in liquids to increase rapidly in size and to pulsate even between expanded and reduced sizes (Povey and Mason, 1998). When the bubble pulsations take on too much amplitude, the bubbles collapse violently, a phenomenon termed inertial cavitation that can change the physicochemical properties of food. The ultrasonic frequency helps to promote bubble collapse by driving the bubble into resonance.

3.4 Temperature

Ultrasonic treatments raise the temperature of the sample, even if no external heat is applied in addition to the ultrasound. When the transducer or horn sends ultrasonic vibrations into the medium, the responding oscillations of the medium particles generate heat over time. Acoustic radiation forces move the liquid media in waves, generating heat from this motion (Povey and Mason, 1998). More heat is generated when the ultrasonic waves encounter bubbles in liquids; as the bubbles are set into motion this activity is converted into heat by thermal and viscous damping mechanisms. Also, when the high-intensity ultrasound causes inertial cavitation in liquids, very high temperatures (up to 5,000 K) are generated in small areas (called hotspots) in the sample due to the collapse of bubbles in the liquid. In contrast, more cavitation bubbles are produced as the temperature of the sample increases, leading to yet more heat-generating bubble movements and collapses. The net result of these ultrasonic effects is a steady increase in temperature in an ultrasonicated sample over time.

Additionally, food researchers may choose to introduce moderate heat to the system in order to enhance the effects of ultrasound; the combined treatment is termed thermo-sonication (Povey and Mason, 1998). Some food plants thermally processing foods, today, might be able to incorporate transducers into their heat exchangers and heating systems in the future, so that ultrasonic treatment can precede thermal treatments with lower process temperatures (Povey and Mason, 1998). Sometimes thermo-sonication can be accomplished without adding heat, by controlling the rise of heat in the sample during ultrasonic treatment to achieve a steady value of temperature over time.

3.5 Effects of High-Power Sonication

The effects ultrasound produces in a medium depend on the solid, liquid, and gas phases in the medium (Povey and Mason, 1998). Mostly, solid media will undergo

a "sponge" effect in response to the passage of sound waves, in which the condensations and rarefactions in the medium act upon the solid similar to the squeezing and releasing of a sponge (Riera-Franco de Sarabia et al., 2000). In liquid media, the condensations and rarefactions cause the liquid particles to accelerate in alternating (first forward, then reverse) directions, and any bubbles, i.e., gases entrapped in the liquid, accelerate as well (Povey and Mason, 1998). Ultimately, the pressures from the condensations/rarefactions can cause the bubbles in the liquid to collapse violently, a phenomenon called inertial cavitation (Piyasena et al., 2003).

3.6 Cavitation

Cavitation is the mechanism that enables the desired effects of high-intensity "power" ultrasound to occur in foods. The effects of cell killing, inhibition of enzyme activity, maturation of wines, cleaning of produce surfaces, extraction, filtration, emulsification, and crystallization all rely on the mechanism of cavitation (Mason et al., 1996; Povey and Mason, 1998).

The study of cavitation centers on the activity of bubbles in liquids (Povey and Mason, 1998). The activity of the bubbles determines which of the two types of cavitation occurs, inertial or non-inertial cavitation; both produce very different effects in the medium. When inertial cavitation occurs, the bubble dynamics are behind the activities produced in the food, for instance, whether free radicals are generated (or not) and to what degree erosion occurs in the food (Mason et al., 1996; Patrick et al., 2004). Yet, the bubbles cannot be controlled directly in experiments (Povey and Mason, 1998). Instead, the effects of other parameters on bubbles must be studied in depth if cavitation is to be optimized for the best effects. These parameters include the acoustic pressure amplitude (controlled by ultrasonic wave amplitude) and acoustic frequency.

3.6.1 Inertial Versus Non-inertial Cavitation

The two types of cavitation already mentioned, inertial (also called "transient") and non-inertial (also called "stable") (Povey and Mason, 1998), involve a sound field that drives the bubbles in a liquid into some kind of response. One response occurring in both cavitation cases is bubble growth; in a process called rectified diffusion, bubbles increase in size by drawing more gas from the surrounding liquid into the bubble. Bubbles also decrease in size by expelling the gas into the liquid. The pressure variations in the medium determine whether the gas will be drawn into the bubble (when the gas pressure inside the bubble happens to be less than the ambient liquid pressure) or released from the bubble into the liquid.

In non-inertial cavitation, the sound field causes bubbles either to increase in size and then dissolve or to pulsate between a smaller and larger size over many acoustic cycles. Because the bubbles never collapse or break into fragments, this form of cavitation was originally termed stable cavitation.

Inertial cavitation is characterized either by rapid growth followed by rapid collapse of the bubbles or by extremely high-amplitude pulsations in which bubbles greatly expand and greatly contract, continually and eventually collapsing (Povey and Mason, 1998). After a bubble collapses, it may fragment into much smaller bubbles or grow again to undergo more pulsations and/or collapses. Because first observations of inertial cavitation involved sonoluminescence from bubbles that fragmented after a few cycles, the phenomenon was termed transient cavitation.

The effects of cavitation can produce a number of desirable changes in foods, such as mechanical erosion and fracturing of food particles (for improved separation, mixing, and extractions), which are caused by the hydrodynamic shear stresses from high-amplitude pulsations, the rebound pressure pulse from a collapsed bubble; microstreaming; and jetting (Behrend and Schubert, 2001; Joyce et al., 2003; Li et al., 2004; Povey and Mason, 1998; Riera-Franco de Sarabia et al., 2000). Jetting in particular can dislodge dirt and bacteria from the surfaces of foods, such as eggs, and food processing plants (Povey and Mason, 1998). Other changes can be biological, such as stimulation of growth – seeds and hatching, for example; the hot spots created by bubble collapses can degrade hydrophobic pollutants in water (Mason, 2003). Changes also occur from chemical reactions, such as the decomposition of hydrophilic pollutants in water by hydroxyl radicals produced during inertial cavitation (Mason, 2003). The inactivation of microorganisms and enzymes in foods occurs from combinations of mechanical, chemical, and biological effects.

4 Microbial and Enzyme Inactivation in Food Using Ultrasound

As it was previously mentioned, depending on the frequency, ultrasound is used in two wide areas of food processing. In this section a more detailed view of some of its applications are described. First, high-intensity ultrasound is used for the degassing of liquid foods; the induction of oxidation/reduction reactions; the extraction of enzymes and proteins; the inactivation of enzymes and microorganisms; and the induction of crystallization processes. Sometimes ultrasound is combined with other types of treatments to enhance the effectiveness of the treatments. Inactivation of microorganisms by combining ultrasound treatments with antimicrobials, pressure, and heat is widely documented (Knorr et al., 2004). Low-intensity ultrasound is used in the stimulation of living cells and enzymes, surface cleaning of foods, ultrasonically assisted extraction, crystallization of fats and sugars, destruction of foams, extraction of flavorings, emulsification, filtration, drying, freezing and tenderization of meat (Chemat and Hoarau, 2004; Knorr et al., 2004), measurement of concentration of simple solutions and meat composition (Saggin and Coupland, 2001), mixing and homogenization, and precipitation of airborne powders (Mason, 1996).

Even so, applications of ultrasound in food processing are not limited to the process per se; in quality assurance, many applications of this novel technology are used

as mentioned throughout this chapter. Food manufacturers can use ultrasonic non-destructive technique (NDT) to locate foreign bodies such as glass, organic residues, or even bacterial infections in both solid and liquid foods, even after foods are packaged (Gestrelius et al., 1993; Hæggström and Luukkala, 2000). Other applications include characterization of the cellular structure of pre-cooked dough to obtain predictions of the quality of the cooked product (Elmehdi et al., 2003) and monitoring the movement of the ice front in a solid food as it is slowly frozen to determine the energy efficiency of the freezing process (Sigfusson et al., 2004).

Some of these applications are described in detail in the following paragraphs. The initial focus will be on power or low-frequency ultrasound, which has been used for disruption purposes such as the inactivation of microorganisms or enzymes. In the following, low-intensity or high-frequency ultrasound will be covered according to some food industry applications.

4.1 Microorganisms

The goal of emerging technologies in food processing is to inactivate the initial population of microorganisms to a safe level with minimal damage to the product's quality attributes. Nevertheless, with some emerging technologies, microorganisms become more resistant over time to the action of a specific factor such as pressure, electricity, or sound waves. In fact some microorganisms find that certain factors actually improve their growth during treatment. In the case of ultrasound, although it has been explored more deeply in recent years, some reports show that ultrasound exerts a positive effect, in combination with other preservation factors, on some microorganisms and enzymes.

Ultrasound treatments can have lethal effects on microorganisms when applied with sufficiently high intensity (e.g., frequencies above 18 kHz) (Rodríguez et al., 2003). Some reports in literature claim microbial inactivation with frequencies as low as 14 kHz, although the most common frequencies are 20 and 24 kHz. Nevertheless, it has been shown that ultrasound by itself is often not enough to reduce microbial populations. Sound waves should be applied with other preservation factors in order to increase the effectiveness of the treatment. The use of ultrasound in combination with heat, pressure, or both seems to be a good option. Raso and Barbosa-Cánovas (2003) reported that the use of ultrasound, pressure, and heat along with low water activity (a_w) was a good combination for reducing microbial populations in foods. The effect of pH, however, seems to be less important when combined with ultrasound, and only a few reports are focused on its effect. Jiménez-Fernández et al. (2001) studied the effect of pH in *Aspergillus flavus* during thermo-ultrasonic treatments and, depending on the other conditions of the medium such as a_w, the effect attributed to pH was found to be relevant in only some cases. When a_w was constant and the pH was decreased, the D values were lower, but when pH was constant, lower D values were achieved with the highest a_w (0.99). This is a logical result, considering some of the mechanisms of inactivation, and will be described in next sections. In another study the use of ultrasound to

inactivate *E. coli* in acidic media (model orange and apple juice systems; pH 3) showed that at low intensities (20 kHz; 0.4 and 7.5 μm) the inactivation rate was affected because of the strain of microorganisms and the prior acid adaptation of the bacteria in the media; however, at higher intensities these factors were not important (Patil et al., 2009). Higher water activity means the presence of free water in the medium, which increases the production of free radicals because of the destruction of water molecules generated by the sound waves, increasing the lethality of the microorganisms. In the same study, hurdle technology was used with antimicrobials such as potassium sorbate and vanillin in addition to ultrasound, heat, pH, and water activity, showing good results according to the *D* values reported. Guerrero et al. (2001) reported no change in the sensitivity of *Saccharomyces cerevisiae* when ultrasound and heat were applied in broth with different pH values. But in Sabouraud broth, at pH 5.6, the addition of chitosan enhanced the inactivation of yeast under thermo-sonication (Guerrero et al., 2005).

Other reports on the use of ultrasound and heat (thermo-sonication) show how certain combinations of factors affect different microorganisms in different ways. For instance, Knorr et al. (2004) reported that inactivation of *Bacillus stearothermophilus* and *E. coli* K12 DH5α was improved with the use of direct steam injected into the ultrasound treatment, leading to reduced temperature and process time. This method was ultrasound-assisted thermal (UST) treatment. Nevertheless, a different type of microorganism, *Lactobacillus acidophilus*, was more resistant to the UST combination process.

From previous research, using high pressure to inactivate microorganisms appears to be a good alternative to the use of heat. For this reason, high pressures have been used in combination with other preservation factors such as temperature and antimicrobials. In ultrasound technology, a new area called mano-sonication is currently being tested, in which the use of moderate and high pressures in combination with ultrasound effectively reduces the initial level of microbial populations. Some of the most studied microorganisms in non-thermal technology research are the so-called emergent pathogens, such as *E. coli*, *Salmonella*, and *Listeria monocytogenes*, because of their new importance in food microbiology and impact on food safety. Reports show improvements in *E. coli* inactivation through combined ultrasound and high-pressure treatments, as well as through the combined use of heat, sound, and pressure, achieving important reductions in the enzymatic activity of some very heat resistant pathogens. Other hurdles used in combination with MTS are antimicrobials exhibiting good results in microbial inactivation (Knorr et al., 2004). Mano-sonication and heat treatment have also been reported to have an additive effect in achieving inactivation of *L. monocytogenes*. When the microorganisms were subjected to ultrasound energy at 20 KHz and 117 μm at ambient conditions, no important reductions were achieved; however, when pressure was added as a hurdle the microbial inactivation was significant. Using 200 kPa under the same ultrasound conditions described above, the *D* value was 1.5 min, lowering to 1 min when pressure was increased to 400 kPa. The experiment was conducted at different temperatures up to 50°C but the effect of this parameter was not significant at the studied levels (Piyasena et al., 2003).

Mathematical models have been developed to describe the resistance of different bacteria to mano-sonication treatments (Raso and Barbosa-Cánovas, 2003) as well. Dr. Javier Raso and his research team at the Universidad of Zaragoza in Spain are some of the pioneers currently combining pressure, heat, and sound to achieve microbial inactivation. Beginning in the late 1990s and in the last 5 years, ultrasound research from this university has achieved important relevance in the food engineering field worldwide.

In Table 3.2, the inactivation of some microorganisms is shown for different treatment media and operating conditions. With the combination of heat and ultrasound, substantial reductions in *D* values are obtained for *Listeria innocua* and *Salmonella.* Apparently, studies with *Zygosaccharomyces bailii* have shown that thermo-sonication is independent of the treatment medium, at least in this case. Good reductions in *D* values are obtained with the combination of temperature and sonication. Furthermore, the combination of ultrasound with pressure clearly improves the inactivation of microorganisms as Pagán et al. (1999) showed for *L. innocua.* An additive effect has been shown with MTS in vegetative cells, while for *Enterococcus faecium* and *Bacillus subtilis* spores, the effect was shown to be synergistic (Raso and Barbosa-Cánovas, 2003). Research by Guerrero et al. (2001) with *S. cerevisiae* showed good results, indicating a synergistic effect between heat and ultrasound in the inactivation of the yeast. Furthermore, when temperature is constantly maintained below lethal values, the increase in the intensity of the ultrasound wave is the most important value in the inactivation of microorganisms, but results are not as clear as in the previous example. Raso et al. (1998b) also showed that the use of pressure in combination with thermo-sonication enhanced the inactivation of *B. subtilis* spores, compared to thermal treatment. Results of thermo-ultrasonic treatments tested on molds like *A. flavus* and *Penicillium digitatum* showed the effect of adding antimicrobials on enhancing the inactivation. The use of low-weight chitosan (1000 ppm) as a natural antimicrobial in the medium under ultrasound treatment and heat (45ºC) enhanced the inactivation compared to just thermo-ultrasonic treatment (Guerrero et al., 2005). Nevertheless, pressure, ultrasound, heat, and other preservation factors do not have an additive or synergistic effect in all cases. Each microorganism should be studied under different treatments to know its response. For example, the response of spores to different technologies is always different from other types of cells, because of their unique, intrinsic characteristics. Results of mano-thermo-sonication applied on *B. subtilis* spores showed that when pressure was increased in combination with heat and ultrasound, inactivation was enhanced. Yet over 500 kPa, pressure was no longer an important factor because no matter how much it was increased past 500 kPa, there was no further effect on spore inactivation observed under the conditions tested (70°C, 117 μm, and 20 kHz) (Raso et al., 1998b). An interesting study on the use of ultrasound is application of this energy to delay fruit decay and to maintain fruit quality. For example, ultrasound was used at different frequencies (maximum 59 kHz) and temperature 20°C to process strawberries immersed in water. Decay was delayed and the number of microorganisms reduced. The firmness of the fruit and the levels of total soluble solids, titratable acidity, and vitamin C were also retained after processing (Cao et al., 2010).

Table 3.2 Some examples of inactivation of microorganisms by ultrasound

Microorganism	Treatment	Medium	Reductions	References
Listeria monocytogenes	20 kHz, 117 μm, ambient temperature	Not specified	$D = 4.3$ min	Pagán et al. (1999)
Listeria monocytogenes	20 kHz, 117 μm, ambient temperature, 200 kPa or 400 kPa	Not specified	$D_{200} = 1.5$ min $D_{400} = 1.0$ min	Pagán et al. (1999)
Listeria monocytogenes	Heat @ 60ºC Heat @ 60ºC with sonication at 20 kHz	UHT milk	$D_{60} = 2.1$ min $D_{60\&S} = 0.3$ min	Earnshaw et al. (1995)
Listeria monocytogenes	Heat @ 60ºC Heat @ 60ºC with sonication at 800 kHz	Rice pudding	$D_{60} = 2.4$ min $D_{60\&S} = 4.5$ min	Earnshaw et al. (1995)
Salmonella spp.	160 kHz, 100 W by 10 min	Peptone water	4 log reductions	Lee et al. (1989)
Salmonella eastbourne	160 kHz, 100 W by 10 and 30 min	Chocolate	26% reduction with 10 min 74% reduction with 30 min	Lee et al. (1989)
Salmonella typhimurium	30 min at 40ºC and 20ºC	Brain Heart Infusion broth	3 log at highest temperature 1 log at lowest temperature	Wrigley and Llorca (1992)
Salmonella typhimurium	30 min at 50ºC and 40ºC	Skim milk	3 and 2.5 log reductions, respectively	Wrigley and Llorca (1992)
Escherichia coli	700 kHz, 32ºC, 10 and 30 min	Saline solution	0.83 and 0.2% survival	Utsunomiya and Kosaka (1979)
Escherichia coli K12 DH5 α<<DH5α throughout>>	Heat at 60ºC Ultrasound (110 μm) assisted with temperature (60ºC)	Phosphate buffer (pH 7)	$D_{60} = 84.6$ s $D_{60\&S} = 23.1$ s	Zenker et al. (2003)

Table 3.2 (continued)

Microorganism	Treatment	Medium	Reductions	References
Escherichia coli K12 DH5 α	Heat at 60ºC Ultrasound (110 μm) assisted with temperature (60ºC)	Carrot juice (pH 5.9)	$D_{60} = 84.3$ s $D_{60\&S} = 23.9$ s	Zenker et al. (2003)
Escherichia coli K12 DH5 α	Heat at 60ºC Ultrasound (110 μm) assisted with temperature (60ºC)	UHT milk (pH 6.7)	$D_{60} = 77$ s $D_{60\&S} = 23$ s	Zenker et al. (2003)
Bacillus subtilis	20 kHz and 150 W, 100ºC	Distilled water, milk, and glycerol	63 and 74% reduction in glycerol 79 and 40% reduction in milk 70 and 99.9% in distilled water (depending on the species of *Bacillus*)	García et al. (1989)
Yersinia enterocolitica	21–150 μm, 30ºC and 200 kPa		*D* from 4 to 0. 37 min depending on the amplitude	Raso et al. (1998a)
Staphylococcus aureus	24 kHz, 2–30 min, 3 W/cm^2		42–43% reduction depending on the treatment time	Scherba et al. (1991)
Zygosaccharomyces bailii	Heat @ 55ºC Heat @ 55ºC with sonication at 20 kHz	Orange juice	$D_{55} = 10.5$ min $D_{55\&S} = 3.9$ min	Earnshaw et al. (1995)

Table 3.2 (continued)

Microorganism	Treatment	Medium	Reductions	References
Zygosaccharomyces bailii	Heat @ 55ºC Heat @ 55ºC with sonication at 20 kHz	Rice pudding	$D_{55} = 11$ min $D_{55\&S} = 1$ min	Earnshaw et al. (1995)
Lactobacillus acidophilus	Heat at 60ºC Ultrasound (110 μm) assisted with temperature (60ºC)	Phosphate buffer (pH 7)	$D_{60} = 70.5$ s $D_{60\&S} = 43.2$ s	Zenker et al. (2003)
Lactobacillus acidophilus	Heat at 60ºC Ultrasound (110 μm) assisted with temperature (60ºC)	Orange juice (pH 3.7)	$D_{60} = 47.3$ s $D_{60\&S} = 31.1$ s	Zenker et al. (2003)

An additional factor that should be studied is the treatment medium. As a novel technology, ultrasound is being tested under many different conditions, and some results have shown that inactivation of cells can be either increased or decreased depending on the medium's composition. Comparison of the results of microorganisms under sonication treatment is difficult because of the non-uniform data of the operating conditions. As a novel technology, more homogeneity in some data is starting to be important because equipment is often different and some researchers do not report the full data. As authors of this chapter, and because literature is scarce, our aim is to summarize or draw general conclusions as to which microorganisms are more resistant (bacteria, yeasts, molds, or spores) and/or what are the best conditions for inactivation of specific organisms. Table 3.2 shows some of the relevant and most recent experiments that have been conducted with ultrasound. Target microorganisms under several conditions of sonication, temperature, pressure, and medium composition (among others) have been evaluated. Even so, more research and uniformity in experiment design and results could generate additional information to draw further conclusions. However, based on the information described above and in Table 3.2, ultrasound is clearly a potential technology for microbial inactivation.

4.1.1 Mode of Action of Ultrasound in Microorganisms

Ultrasound was studied as a microbial inactivation technique for the first time in the 1960s (Piyasena et al., 2003). The killing effect was first observed when ultrasonic waves were applied in a US army experiment to investigate their use in anti-submarine warfare, and fish died in large numbers. The effects of inactivation of cells by ultrasound have been attributed to shear disruption, heating, and free-radical production. In the 1970s, some cells showed a separation between the cytoplasmic membrane and cell wall after a short sonication (Earnshaw et al., 1995). However, the background of ultrasound technology reveals that development and research was temporarily halted due to a lack in the development of equipment (or specific parts) needed to generate good results, as well as greater interest in other emerging technologies by researchers, as in the case of ohmic heating. But gradually ultrasound is beginning to be explored by more researchers because of its effectiveness in inactivating bacteria. Due to this history, the main mechanisms of microbial inactivation are not totally understood, although there are several theories. Reports on ultrasound discussed previously were concerned with establishing how bacteria are inactivated with sound waves. The mode of action of ultrasonic inactivation is currently believed to be related to damage in the cell wall and cell wall structures, which is supported by the fact that some bacteria of specific species are more resistant to cavitation than to others under the same treatment conditions (Knorr et al., 2004). The thinning of cell membranes together with heating and free-radical production is essential in the inactivation. When ultrasonic waves pass through a liquid, some regions of compression and expansion are created. In these regions the physical phenomenon of cavitation starts and thousands of bubbles are formed. Bubbles are produced very rapidly and then hit each other inside the medium. Within the medium, very high localized temperatures (up to 5,500°C) and high pressures (50 MPa) are reached,

and extremely violent implosions eventually occur; these conditions kill some bacteria (Piyasena et al., 2003). With cavitation, either cell wall structures are disrupted or particles are removed from surfaces (Earnshaw et al., 1995). Cavitation is associated with shear disruption, heating, and free-radical formation, which are considered the primary effects. Thinning of cells is caused by the ultrasound and the cell wall is broken, releasing the cytoplasm content (Earnshaw et al., 1995). A schematic view of this is shown in Fig. 3.3. Some microscopy studies after thermo-sonication treatments enable some of these previously mentioned effects to be observed. In Fig. 3.4, the use of scanning electron microscopy (SEM) is shown for *L. innocua* after 30 min of treatment at 24 kHz, 400 W, 120 μm and 63°C in milk (Bermúdez-Aguirre, D., and Barbosa-Cánovas G. V. (2008) "Unpublished data"). First, disruption of the cell wall can be observed in the damaged cells. Here, the cytoplasm content has been released outside of the cell, causing the death of the microorganism. A common characteristic observed in a high proportion of these cells is the formation of pores in the outer layer of the bacteria. These pores, in some cases appearing as big holes, are generated in the cell because of the high pressures in the medium and the violent implosions and explosions of the bubbles. Some thermo-sonicated cells are fragmented into smaller pieces, which look like smaller cells cut into unnatural shapes. The cell wall is not defined by one or more sides because of the breakage during sonication. Additionally, the cell walls probably are weaker due to thermal treatment, making the cell more sensitive to the formation of pores.

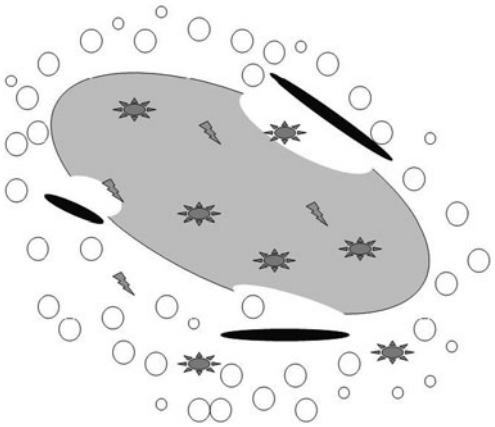

Fig. 3.3 Schematic view of a bacteria cell during cavitation, showing the lethal effects of ultrasound such as pore formation, cell membrane disruption, and cell breakage

4.2 Enzymes

Enzymatic inactivation using different technologies is a widely studied field and much research has been conducted in order to achieve low residual enzymatic activities in several products. From the point of view of quality, enzymatic reactions produce undesirable changes in many foods during processing and storage. For

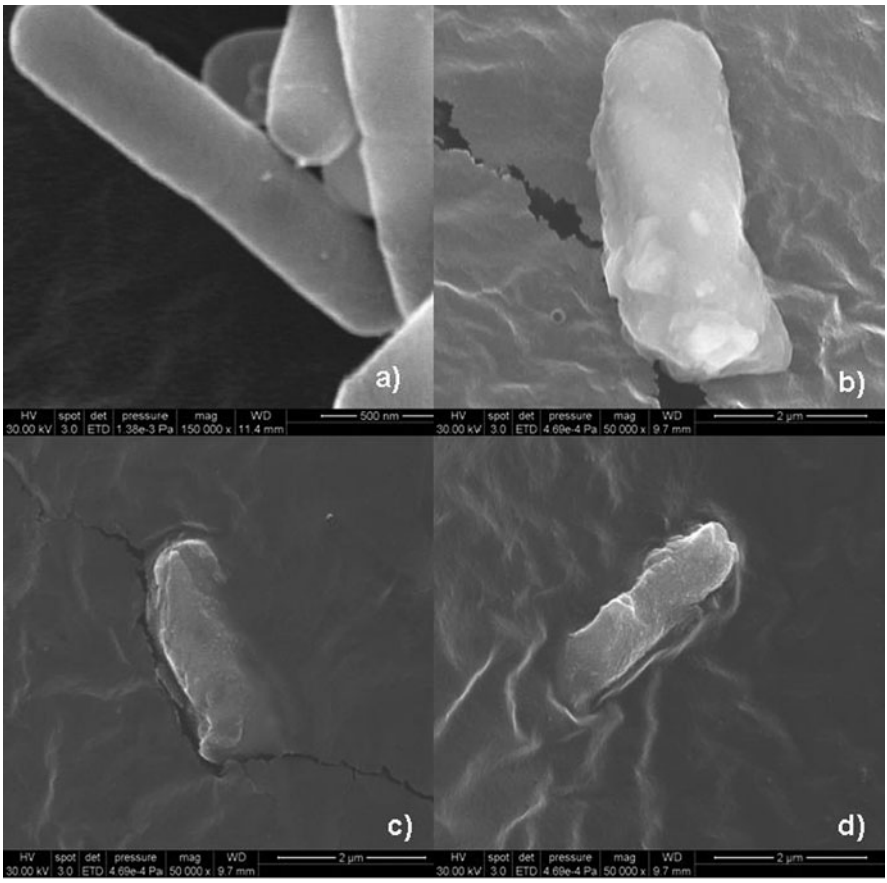

Fig. 3.4 High-vacuum scanning electron microscopy (SEM) pictures of control (*left top*) and thermo-sonicated *Listeria* cells, showing the lethal effects of cavitation in cells such as pore formation, cell membrane disruption, and cell breakage. Magnification: (**a**) 150,000×, (**b**) 50,000×, (**c**) 50,000×, and (**d**) 50,000×. (Photos: Courtesy of the authors)

this reason, non-thermal technologies are being tested as an option for reducing the enzymatic activities in foods.

The first studies in enzyme inactivation were conducted almost 60 years ago, in which pure pepsin was inactivated by ultrasound, probably due to cavitation. A more recent study shows that inhibition of sucrose inversion can also be achieved by cavitation. Since then the use of ultrasound in combination with heat and pressure has been proven effective in the inactivation of enzymes. Examples of these enzymes are soybean lipoxygenase, horseradish peroxidase, tomato pectic enzymes, orange pectin methylesterase (Vercet et al., 2002), watercress peroxidase (Cruz et al., 2006), PPO, lipase, and protease, among others (Raso and Barbosa-Cánovas, 2003). Some of these enzymes have been tested in a number of different food products, because,

as in the case of microorganisms, the medium is an important factor affecting the level of inactivation of enzymes. In this book, an entire chapter is devoted to inactivation of food enzymes using ultrasound and because of that this topic is not covered in depth in this chapter.

Encouraged by the results of microbial inactivation using ultrasound, some researchers are now focused on enzyme inactivation with this technology. However, one of the big challenges of using ultrasound is again the heterogeneity of the food matrix, as it needs to achieve enzyme inactivation not only after processing but during food storage as well.

4.2.1 Mode of Action of Ultrasound in Enzyme Inactivation

Ultrasound's mode of action in the inhibition of enzymes seems to be similar to its mode of action inactivating microorganisms. Mano-thermo-sonication is responsible for particle size reduction and molecular breakage. It has induced the breakage of pectin molecules in a purified pectin solution. It is also possible that ultrasound generates protein denaturation (Vercet et al., 2002). Changes in pressures generate stretching and compression in the cells and tissues. But as mentioned before free-radical production is promoted by ultrasound. Such free radicals as H^+ and OH^- could recombine with amino acid residues of the enzymes. These residues are associated with structure stability, substrate binding, and catalytic functions (Cruz et al., 2006). In the case of microorganisms, free-radical formation seems to be important to the main mechanism of inactivation, the disruption of the cell membrane. In the case of enzymes, the main mechanism is free-radical formation, which allows changing some characteristics of the enzymes. Disruption of tissue is mainly important because it generates better surface contact between the enzymes and free radicals. For example, oxidases are usually inactivated by sonication, while catalases are affected at low concentrations. Reductases and amylases are highly resistant to sonication (Mason, 1996). Mano-thermo-sonication has inactivated several enzymes at lower temperatures and/or in a shorter time than thermal treatments. Sensitivity of the enzymes to mano-thermo-sonication treatment is independent of the medium of treatment. In addition, the substrates, small co-solutes, and other proteins are unable to protect the enzymes during treatments (Vercet et al., 2001).

5 Other Applications of Ultrasound in Food Processing

In different areas of science, high-frequency ultrasound has many more applications than power ultrasound. In addition, low-intensity ultrasound has been used more in the food industry than power ultrasound due to its non-destructive, rapid, and convenient technique. It has been used to assess the quality of some foods such as meat, fish, beverages, oils, vegetables and fruits, and dairy products (Benedito et al., 2002). Yet ultrasound is a novel technology in many countries, and for this reason, Chemat and Hoarau (2004) suggest that ultrasound operations in food engineering require the establishment of a hazard analysis and critical control point (HACCP)

program in which the critical control points of food processing are identified, so that potential hazards in producing a quality safe product can be controlled.

5.1 Quality Assurance

Quality assurance is an area that concerns food technologists because of the consumer's desire for quality foods. Every food industry must have a quality assurance department for monitoring production, which requires testing of products. In some tests, long treatment times are required and destructive techniques are used. Ultrasound appears to be helpful in some of these tests, wherein low-intensity ultrasound has been used to assess the quality of avocados, mangos, and melons according to ripeness by evaluating ultrasonic parameters such as velocity and attenuation in relation to the physical characteristics of the medium. The quality of beef, chicken, cod, pork meat, milk, wine, sugar solutions, and oils has been evaluated with ultrasonic parameters (Benedito et al., 2002), by applying the theory of how wave behaviors (e.g., velocity and attenuation) relate to the physical composition of the medium. Textures of products like cheese and cooked vegetables and the ripeness of fruits have all been determined with the use of ultrasonic waves (Coupland, 2004).

5.1.1 Cheese and Tofu Manufacturing

In many countries cheese industry is one of the most important food industries as indicated in their sales reports of cheese products and high consumer demand. Depending on the place of manufacture and the type of cheese, cheese production can take several hours or several years to produce a final product. The specific characteristics desirable in cheese depend on the variety or type. Cheese manufacturing consists of various stages such as coagulation, drainage, salting, and ripening. Low-intensity ultrasound has been used to monitor different stages of the process, for example, in the evaluation of internal cracks due to bad fermentation and in the determination of the optimum rennet cut time; additionally, the compositions and textures of hundreds of cheeses around the world could be evaluated by this non-destructive technique to improve packaging and storage (Benedito et al., 2002). Along with monitoring the cheese as it is produced, ultrasound has been directly involved in the production of soft cheese by promoting the coagulation of proteins and oils (Mason, 1996).

High-frequency ultrasound has also been used to assess the quality of tofu during its manufacture. Tofu is a water-based gel composed mainly of soy protein; its quality is based a lot on the product's final texture. Ultrasound can be used to monitor the development of texture during the gelation process of tofu. The propagation of ultrasonic waves through the structure of the tofu gel provides information about the entire process (Ting et al. 2009), as in the case of cheese making, in relating the ultrasound variables to the enzyme activity in milk during the coagulation process.

5.1.2 Beverages

Power ultrasound has been able to achieve pasteurization standards for some beverages such as milk, fruit juices, and ciders; but low-intensity ultrasound can also be useful for quality assessment purposes. Ultrasound has been used to degass (removing oxygen) orange juice, proving that the final vitamin A content in product is higher during storage in ultrasonicated juice than in conventionally heat-treated juice. In another study, limonin content, brown pigments, and color were evaluated in orange juice after sonication (500 kHz; 240 W; low temperature, 5 and 14°C), finding only minor changes in these characteristics in the product (Valero et al., 2007). Ultrasound has been used successfully to process strawberry and blackberry juice and apple cider as well. Enzymes such as pectin methylesterase and polyphenol oxidase were inactivated along with pathogenic bacteria. Minor changes in ascorbic acid and anthocyanins were also detected in sonicated juice (Valdramidis et al., 2010). Beer yield is also improved with ultrasound applied at the beginning of the mashing process (Knorr et al., 2004). This improvement in yield does not only occur with beer, but in cheese production as well, with yield increasing after the milk is pasteurized with power ultrasound, which represents economic benefits for the dairy and beer industries. Additionally, ultrasound can improve several characteristics of products such as color, texture, and storage life, as well as maintain some of the same nutritional values found in fresh products. One example is the oxidation process widely used in the alcoholic beverage industry. The process is assisted by ultrasound as it enhances oxidation in fermented products leading to characteristic flavor and early maturation. Ultrasound of 1 MHz alters the alcohol/ester balance producing an apparent aging in the product. It has been used for wines, whiskey, and spirits (Mason, 1996).

5.1.3 Bread

Bread quality is always a topic and a factor that food scientists are trying to innovate and improve. Now that different options like frozen and freeze-dried breads are available in the market, the texture of the final product is an important parameter. Traditional techniques to evaluate the texture are very often destructive to the sample. Ultrasound offers the advantage of being a non-destructive technique that enables knowing the texture of breads through acoustic parameters. Physical structure of foods is hard to study because of the non-homogeneity of foods, as with breads, but sound waves can provide information about the structure of bread crumbs. Gas cells determine the structural integrity of bread crumbs, and through some ultrasonic parameters, the physical structure can be evaluated. Velocity and attenuation of ultrasonic waves (at 54 kHz) have been used to describe certain quality factors of bread. For example, changes in the microstructure of freeze-dried bread crumbs due to density changes (100–300 kg/m^3) have been evaluated, showing that size and shape of the gas cells in bread are sensitive to ultrasound measurements, whereas the signal amplitude was increased linearly with density (Elmehdi et al., 2003). This non-destructive technique is a very useful tool in the cereal industry

throughout the world allowing manufacturers to understand the structure of end products without modifications.

5.1.4 Product Identification

One area in food quality assurance refers to the detection of foreign bodies in the final product. In an attempt to ensure the safety of foods, all food industries have specific detectors for metals, glass, bones, and other materials that could potentially enter the food in the processing plant. Animal bones in meat products, fragments of glass in glass jars, and metal swarf are among the materials sometimes detected in products due to poor manufacturing practices (Hæggström and Luukkala, 2001). Various researchers have focused their work on this subject alone. Knorr et al. (2004) showed that foreign bodies like glass and plastic pieces, and raw materials, can be detected in yogurt, fruit juices, and tomato ketchup by ultrasonic signals in a time–frequency analysis. Strange bodies of material such as stone, glass, wood, plastic, bone<comma> and steel spheres were detected in cheese and marmalade by means of ultrasound, showing that this non-destructive and highly sensitive method is viable for use in a homogeneous product with 20–75 mm of probing depth (Hæggström and Luukkala, 2001). Ultrasonic pulse compression (UPC) is used to detect variations in the consistency of some liquids, liquid leveling in polymer-based soft drink bottles, and foreign objects in containers. This is possible as changes in the acoustic properties of the medium, mainly propagation velocity and acoustic impedance, can be related to changes in food product composition. Air-coupled ultrasonics is a new technique used to estimate the level of water within a polymer drink bottle (Gan et al., 2002). The volume fraction of some components in foods such as syrups, fruit juices, and alcoholic beverages can also be determined by ultrasonic waves, and measurements of the solid content of semicrystalline fats have also been tested successfully with ultrasound (Coupland, 2004). The thickness of some foods, including cheddar cheese, luncheon meat, and cranberry sauce, has been measured by ultrasonic techniques to measure the speed of sound in the product; this method produced results similar to the more difficult tests using calipers (Saggin and Coupland, 2001). In another example, demonstrating ultrasound's effect on product quality, the concentration of solids is an important parameter in slurries processing industry; in this industry, the parameters density and attenuation of ultrasonic waves have proven useful as tools for quality assurance and process control of the thick slurry suspensions; both parameters are related to concentration of the medium (Bamberger and Greenwood, 2004). One direct application of this kind of ultrasound is during fermentation, wherein the concentration of sugars changes accordingly with the production of ethanol because of the yeast activity. The concentration of ethanol and sugar can be estimated based on the sound wave velocity traveling through the medium (Schöck and Becker, 2010). Here it is important to remark that specific characteristics of the ultrasonic wave, such as frequency and intensity, or acoustic parameters related to the material – whether attenuation coefficient, velocity, acoustic impedance, or density – must be selected wisely for evaluation in order to determine the specific properties of foods for which the researchers are looking. Ultrasound also is being tested in microbial quality

control: some studies conducted on aseptically packaged milk show that the acoustic streaming induced by ultrasound in a liquid is affected by the microbial activity, and thus, those bacteria that alter physicochemical parameters can be detected (in quantity) through the use of ultrasonic waves (Gestrelius et al., 1993).

5.2 Thawing/Freezing/Crystallization

As in the case of high-pressure technology, ultrasound is not limited to the abovementioned examples; every day new applications are being used and tested in the food industry, while an important number are still under research. One such application would be its use in thawing processes, where high-power ultrasound is used to assist the thawing of beef, pork, and fish, with frequencies and intensities around 500 kHz and 0.5 W/cm^{-2}. With ultrasonic radiation, the common problem encountered in microwave thawing – surface heating – is minimized, in which samples have been thawed to a depth of 7.6 cm within about 2.5 h (Miles et al., 1999).

Power ultrasound, with frequencies in the range of 20–100 kHz, has proved useful in the formation of ice crystals during the freezing of water, since the rate is improved and cell damage reduced. The involved mechanism is acoustic cavitation, in which the acoustically generated bubbles act as nuclei for crystal growth (Sun and Li, 2003). Sonication is a highly useful tool in the control of crystallization processes because it enhances the nucleation rate and crystal growth rate, thus generating new and fresh nucleation sites. The freezing rate of potato assisted by ultrasound was very fast, with an output power of 15.85 W and a treatment time of 2 min; furthermore, a better microstructure was achieved under these freezing conditions due to the high rate of the process (Sun and Li, 2003). In some crystallization processes, as in the initial stage of freezing, ultrasound plays a very important role because it can accelerate the process. Thus the size of crystals is smaller than in conventional freezing, and for some products like strawberries, this fact results in important reductions in damage to the product's microstructure. Some studies using ultrasound have been made on ice lollipops, and although a better adherence of the lollipop to the wooden stick was observed, the lollipop became harder than the common product (Mason, 1996). Ultrasound has been used to monitor the cooling processes of gelatin, chicken, salmon, beef, and yogurt by measuring the ultrasonic pulse time-of-travel to the cool surface. In the same products, the movement of the ice front was measured by the time of flight of an ultrasonic pulse, by recording echoes as a function of time, which correlated with the percentage of frozen food (Sigfusson et al., 2004).

5.3 Extraction

The use of ultrasound in extraction processes delivers benefits that include greater penetration of the solvent into cellular materials, improvement in mass transfer, and improved release of contents due to the disruption of cell walls. Some examples of

ultrasound use are in the extraction of sugar from sugar beets, medicinal compounds (*helicid*, *berberine hydrochloride*, *bergenin*), and protein from defatted soybeans and tea. Through extraction of the enzyme rennin for cheese making, the use of ultrasound achieved a higher yield of the enzyme compared to normal extraction. The advantages of using ultrasound in extraction processes are the reduction of temperatures and the shortening of treatment times, resulting in a purer extract. Many of the ultrasonic extraction processes have been scaled up to industrial levels because of the above-cited advantages (Mason, 1996). An example of one specific advantage is in the extraction of tea solids from water, resulting in an increased yield of almost 20%. Another example is that reduction in maceration time was achieved with ultrasound in the extraction of alkaloid reserpine from *Rauwolfia serpentina*. Compounds from *Salvia officinalis* were also extracted faster, and the antioxidant carnosic acid extracted from the culinary herb *Rosmarinus officinalis* was increased even as extraction times were reduced. In the last example, ultrasound at 40 kHz was combined with temperature ranging from 47 to 53°C and evaluated for 15, 30, and 45 min; just 15 min was enough to extract most of the material, as the ultrasound enhanced the mass transfer, a result of cell breakage (Albu et al., 2004). In another example the use of power ultrasound in the extraction of sugar and protein from soy flakes showed excellent results after a few seconds (less than 120 s) of sonication, showing a total sugar and protein release of up to 50 and 46%, respectively, compared with untreated samples, enhancing the yield during extraction and reducing the cost of processing (Karki et al., 2010).

Other extraction processes reported in literature are the extraction of almond oils, herbal extracts (fennel, hops, marigold, mint), ginseng saponins, ginger, rutin, carnosic acid from rosemary, polyphenols, amino acid and caffeine from green tea, and pyrethrins from flowers. In general all of these processes have benefited from the use of ultrasound, showing higher extraction yields and rates, shorter processing times, and on the whole more efficient processing (Vilkhu et al., 2008).

Recently, study of the sonochemical reactions taking place during sonication showed that these reactions when successfully controlled could be an important tool for food extraction. The hydroxylation of some food chemicals plus some hydroxyl radicals generated during cavitation can enhance the functional properties of these chemicals; for example, the phenolic compounds can enhance their antioxidant properties under specified sonication conditions (Ashokkumar et al., 2008).

5.4 Cleaning

In addition to a myriad of other uses, ultrasound is a very efficient method for cleaning purposes. It can dislodge dirt and bacteria from surfaces and reach crevices that are difficult to access using conventional methods. Medical, surgical, dental, and food processing instruments and surfaces are cleaned with ultrasound. Recently,

ultrasound has been applied in combination with a bactericide to clean the surfaces of hatchery eggs. The activities of chemical biocides are also enhanced with ultrasound (Mason, 1996). Furthermore, a number of studies reveal that ultrasound (40 kHz) can be used to remove biofilm, which occasionally is the cause of fouling in some food industry equipment. In the dairy industry, for instance, fouling of tubes used to pasteurize and process certain products is often the reason for contamination of milk, because some microorganisms can be added to the walls of these tubes. Ultrasound was twice as effective in removing the biofilm from some of the evaluated surfaces compared to the common method of swabbing to clean the equipment (Oulahal-Lagsir et al., 2000); likewise, ultrasound is very useful for cleaning in dairy membrane processes during ultrafiltration activities when applied at a constant low frequency (i.e., 50 kHz), as compared to intermittent use (Muthukumaran et al., 2007).

Ultrasound also is being studied as an alternative to chlorination processes for disinfection of water. Due to the production of free radicals in aqueous solutions during the ultrasound treatment, some studies carried out in water have focused on the emergent pathogen *Cryptosporidium parvum*. With ultrasound as a disinfectant technique, some of the problems related to carcinogenic products formed in chlorination processes could be avoided. Studies were performed with *S. cerevisiae,* which, according to the author, has a structure similar to the pathogenic microorganisms. With a sodium hypochlorite solution, ultrasound treatment at 27.5 MHz for longer treatment times yielded a better effect against the cells (Tsukamoto et al., 2004a, b).

5.5 Other Applications

Changes in ultrasonic parameters are often associated with changes in the different food products during processing. Transmission of ultrasound in minced beef during simulated automated roasting showed good results as an alternative technique in temperature and process control. Temperatures ranged from 45 to 74°C, with ultrasonic equipment set at 300 kHz, and only small pieces of minced beef were used with thicknesses between 7.15 and 15 mm (Hæggström and Luukkala, 2000).

Ultrasound has also been used to study changes in flow behavior and thermophysical properties of whey protein isolate (WPI) and whey protein concentrate (WPC). Water solubility of both WPI and WPC was significantly increased after sonication compared to control samples. As for flow behavior, the apparent viscosity and flow behavior index and consistency coefficient of WPI and WPC were significantly changed after sonication. The thermophysical properties, such as initial freezing and initial thawing temperatures, were also changed compared to control samples (Krešić et al., 2008). In addition, the effects of ultrasound on the solubility and foaming properties of whey proteins were studied; important effects on these properties were observed when whey proteins were exposed at low frequency (20 kHz) compared to high frequency (40 kHz); even higher frequencies (i.e., 500 kHz) did

not have a significant effect. An important effect with temperature increase was also observed in sonicated samples after processing at low frequency (Jambrak et al., 2008).

Stable emulsions are generated with the use of ultrasound requiring little if any surfactant, some examples of which include tomato ketchup and mayonnaise (Mason, 1996). Ultrasonic velocity and attenuation spectra were also measured as a function of frequency in emulsions treated with ultrasound (1–5 MHz). The emulsions were made of corn oil in water and the velocity and attenuation increased with frequency in all emulsions having different particle sizes, as estimated from the ultrasonic spectra (Coupland and McClements, 2001).

Although ultrasound is being tested to inactivate microorganisms in combination with heat and pressure, ultrasound can also stimulate living cells. This application is very useful in the production of yogurt, in which up to 40% of production time is reduced by using ultrasound. Furthermore, milk is homogenized better using ultrasound than by conventional methods. Additional positive effects in yogurt due to ultrasound are improvements of consistency and texture, added sweetening effects, and reduced syneresis (Mason, 1996; Wu et al., 2001). Faster germination of agricultural crops has been observed as well when seeds are subjected to ultrasound treatment (Mason, 1996). Furthermore, ultrasound can be used in some wastewater treatment plants within the food industry. The use of sonic waves has assisted the bioprocess and an increased, improved biological activity has been observed. Still more research is needed in this area since specific parameters of ultrasound, such as the intensity of the treatment, can result in either a decrease or increase of biological activity (Schläfer et al., 2002).

Other applications being tested are the use of ultrasound in the filtration of industrial mixtures, fruit extracts, and drinks, and the drying processes of orange crystals, grated cheese, gelatin beads, and rice grains. In drying processes, the rate of drying was increased and the final moisture content reduced by ultrasonic treatments carried out at lower temperatures (Mason, 1996). Further studies have shown that ultrasound pre-treatment of vegetables for drying purposes not only decreases the drying time considerably, because of the enhanced water loss, but that the rehydration properties of some vegetables (e.g., mushrooms, sprouts, and cauliflower) are better than others (Jambrak et al. 2007). Similar results were achieved during the drying of bananas; a sonication treatment conducted prior to air drying showed important effects on the banana tissue; drying time was reduced by up to 11%, since sonication allowed removing larger amounts of water from the fruit (Fernandes and Rodrigues, 2007).

Ultrasound also has been shown to be effective during osmotic dehydration processes in speeding up and enhancing the diffusivity of water and solids. Cárcel et al. (2007) showed that sonication was able to increase the water diffusivity up to 117% and dry matter diffusivity up to 137% in apple–sucrose solution. This process is not a common drying phenomenon, involving only the loss of water; ultrasound application is effective not only in removing the water from the cell structure of the apple tissue, but also in taking in the solids from the sucrose solution.

6 Final Remarks

Ultrasound is applied today in high-frequency ranges in many industrial food processes. Taking advantage of the non-destructiveness of ultrasound at high frequencies, food processors are substituting some of the traditional methods with ultrasound technology to monitor the food quality in production chains. Basic scientific concepts that define wave behaviors allow such food industries to determine many properties of foods before, during, and after processing. More recently, however, and one of the most interesting areas for food scientists is high-intensity ultrasound at low frequencies. Microbial and enzymatic inactivation with sound waves in combination with temperature, pressure, and other preservation factors are all showing positive effects. Added advantages to products processed by ultrasound include positive changes in texture, yield, and color. Hence, ultrasound is now a promising option for the pasteurization of products like milk, fruit juices, and other liquid foods.

From an economical point of view, ultrasound equipment is not expensive compared to other technologies. Nevertheless, in order to calculate the cost of converting existing equipment in the adaptation of ultrasound, in addition to adapting cooling/heating baths on an industrial scale, more research is needed on low-frequency ultrasound, thereby testing target microorganisms in pasteurization and key enzymes for improved product stability. Other preservation factors (i.e., pressure, antimicrobials, pH) could be combined with ultrasound to enhance the bactericidal effect, but these other factors will depend on the target product. Future ultrasound research in the coming years for purposes of inactivating microorganisms and enzymes in processed foods will be decisive in defining the possibility of using this technology on a fuller industrial scale.

References

Albu, S., Joyce, E., Paniwnyk, L., Lorimer, J. P., and Mason, T. J. (2004). Potential for the use of ultrasound in the extraction of antioxidants from *Rosmarinus officinalis* for the food and pharmaceutical industry. *Ultrasonics Sonochemistry*, 11, 261–265.

Aleixo, P. C., Santos Junior, D., Tomazelli, A. C., Rufini, I. A., Berndt, H., and Krug, F. J. (2004). Cadmium and lead determination in foods by beam injection flame furnace atomic absorption spectrometry after ultrasound-assisted sample preparation. *Analytica Chimica Acta*, 512, 329–337.

American Heritage Stedman's Medical Dictionary. (2002). Boston, MA. Houghton Mifflin.

Ashokkumar, M., Sunartio, D., Kentish, S., Mawson, R., Simons, L., Vilkhu, K., and Versteeg, C. (2008). Modification of food ingredients by ultrasound to improve functionality: A preliminary study on a model system. *Innovative Food Science and Emerging Technologies*, 9, 155–160.

Bamberger, J. A., and Greenwood, M. S. (2004). Non-invasive characterization of fluid foodstuffs based on ultrasonic measurements. *Food Research International*, 37, 621–625.

Behrend, O., and Schubert, H. (2001). Influence of hydrostatic pressure and gas content on continuous ultrasound emulsification. *Ultrasonics Chemistry*, 8(3), 271–276.

Benedito, J., Carcel, J. A., Gonzalez, R., and Mulet, A. (2002). Application of low intensity ultrasonics to cheese manufacturing processes. *Ultrasonics*, 40, 19–23.

Cao, S., Hu, Z., Pang, B., Wang, H., Xie, H., and Wu, F. (2010). Effect of ultrasound treatment on fruit decay and quality maintenance in strawberry after harvest. *Food Control*. 21(4):529–532, doi:10.1016/j.foodcont.(2009).08.002.

Cárcel, J. A., Benedito, J., Rosselló, C., and Mulet, A. (2007). Influence of ultrasound intensity on mass transfer in apple immersed in a sucrose solution. *Journal of Food Engineering*, 78, 472–479.

Chemat, F., and Hoarau, N. (2004). Hazard analysis and critical control point (HACCP) for an ultrasound food processing operation. *Ultrasonics Sonochemistry*, 11, 257–260.

Chemat, F., Grondin, I., Cheong Sing, S., and Smadja, J. (2004). Deterioration of edible oils during food processing by ultrasound. *Ultrasonics Chemistry*, 11, 13–15.

Coupland, J. N. (2004). Low intensity ultrasound. *Food Research International*, 37, 537–543.

Coupland, J. N., and McClements, D. J. (2001). Droplet size determination in food emulsions: comparison of ultrasonic and light scattering methods. *Journal of Food Engineering*, 50, 117–120.

Cruz, R. M. S., Vieira, M. C., and Silva, C. L. M. (2006). Effect of heat and thermosonication treatments on peroxidase inactivation kinetics in watercress (*Nasturtium officinale*). *Journal of Food Engineering*, 72(1), 8–15.

De Gennaro, L., Cavella, S., Romano, R., and Masi, P. (1999). The use of ultrasound in food technology I: Inactivation of peroxidase by thermosonication. *Journal of Food Engineering*, 39, 401–407.

Duckhouse, H., Mason, T. J., Phull, S. S., and Lorimer, J. P. (2004). The effect of sonication on microbial disinfection using hypochlorite. *Ultrasonics Sonochemistry*, 11(3–4), 173–176.

Earnshaw, R. G., Appleyard, J., and Hurst, R. M. (1995). Understanding physical inactivation processes: combined preservation opportunities using heat, ultrasound and pressure. *International Journal of Applied Microbiology*, 28, 197–219.

Elmehdi, H. M., Page, J. H., and Scanlon, M. G. (2003). Using ultrasound to investigate the cellular structure of bread crumb. *Journal of Cereal Science*, 38, 33–42.

Feril, L. B., Jr., and Kondo, T. (2005). Major factors involved in the inhibition of ultrasound-induced free radical production and cell killing by pre-sonication incubation or by high cell density. *Ultrasonics Sonochemistry*, 12(5), 353–357.

Fernandes, F. A. N., and Rodrigues, S. (2007). Ultrasound as pre-treatment for drying of fruits: Dehydration of banana. *Journal of Food Engineering*, 82, 261–267.

Furuta, M., Yamaguchi, M., Tsukamoto, T., Yim, B., Stavarache, C. E., Hasiba, K., and Maeda, Y. (2004). Inactivation of *Escherichia coli* by ultrasonic irradiation. *Ultrasonics Sonochemistry*, 11(2), 57–60.

Gallego-Juárez, J. A., Elvira-Segura, L., and Rodríguez-Corral, G. (2003). A power ultrasonic technology for deliquoring. *Ultrasonics*, 41, 255–259.

Gan, T. H., Hutchins, D. A., and Billson, D. R. (2002). Preliminary studies of a novel air-coupled ultrasonic inspection system for food containers. *Journal of Food Engineering*, 53, 315–323.

García, M. L., Burgos, J., Sanz, B., and Ordoñez, J. A. (1989). Effect of heat and ultrasonic waves on the survival of two strains of *Bacillus subtilis. Journal of Applied Bacteriology*, 67(6), 619–628.

Gestrelius, H., Hertz, T. G., Nuamu, M., Persson, H. W., and Lindström, K. (1993). A Non-destructive ultrasound method for microbial quality control of aseptically packaged milk. *Lebensm.Wiss.u.-Tecnology*, 26, 334–339.

Guerrero, S., López-Malo, A., and Alzamora, S. M. (2001). Effect of ultrasound on the survival of *Saccharomyces cerevisiae*: Influence of temperature, pH and amplitude. *Innovative Food Science and Emerging Technologies*, 2, 31–39.

Guerrero, S., Tognon, M., and Alzamora, S. M. (2005). Response of *Saccharomyces cerevisiae* to the combined action of ultrasound and low weight chitosan. *Food Control*, 16, 131–139.

Hæggström, E., and Luukkala, M. (2000). Ultrasonic monitoring of beef temperature during roasting. *Lebensmittel-Wissenschaft und-Technologie*, 33(7), 465–470.

Hæggström, E., and Luukkala, M. (2001). Ultrasound detection and identification of foreign bodies in food products. *Food Control*, 12, 37–45.

Hecht, E. (1996). *Physics: Calculus*, pp. 445–450, 489–521. Pacific Grove, CA, Brooks/Cole.

Jambrak, A. R., Mason, T. J., Lelas, V., Herceg, Z., and Herceg, I. L. (2008). Effect of ultrasound treatment on solubility and foaming properties of whey protein suspensions. *Journal of Food Engineering*, 86, 281–287.

Jambrak, A. R., Mason, T. J., Paniwnyk, L., and Lelas, V. (2007). Accelerated drying of mushrooms, Brussels sprouts and cauliflower by applying power ultrasound and its rehydration properties. *Journal of Food Engineering*, 81, 88–97.

Jiménez-Fernández, M., Palou, E., and López-Malo, A. (2001). *Aspergillus flavus* inactivation by thermoultrasonication treatments. In: Welti-Chanes, J., Barbosa-Cánovas, G. V., and Aguilera, J. M. (eds.), *Proceedings of the Eight International Congress on Engineering and Food, ICEF 8*, Vol. II, pp. 1454–1458. Boca Ratón, FL, Technomic.

Joyce, E., Phull, S. S., Lorimer, J. P., and Mason, T. J. (2003). The development and evaluation of ultrasound for the treatment of bacterial suspensions. A study of frequency, power and sonication time on cultured *Bacillus* species. *Ultrasonics Sonochemistry*, 10, 315–318.

Kardos, N., and Luche, J. L. (2001). Sonochemistry of carbohydrate compounds. *Carbohydrate Research*, 332, 115–131.

Karki, B., Lamsal, B. P., Jung, S., van Leeuwen, J., Pometto A. L., III, Grewell, D., and Khanal, S. K. (2010). Enhancing protein and sugar release from defatted soy flakes using ultrasound technology. *Journal of Food Engineering*, 96, 270–278.

Kennedy, J. E., Wu, F., ter Harr, G. R., Gleeson, F. V., Phillips, R. R., Middleton, M. R., and Cranston, D. (2004). High-intensity focused ultrasound for the treatment of liver tumors. *Ultrasonics*, 42, 931–935.

Knorr, D., Zenker, M., Heinz, V., and Lee, D. (2004). Applications and potential of ultrasonics in food processing. *Trends in Food Science and Technology*, 15, 261–266.

Krefting, D., Mettin, R., and Lauterborn, W. (2004). High-speed observation of acoustic cavitation erosion in multibubble systems. *Ultrasonics Sonochemistry*, 11, 119–123.

Krešić, G., Lelas, V., Režek Jambrak, A., Herceg, Z., and Rimac Brnčić, S. (2008). Influence of novel food processing technologies on the rheological and thermophysical properties of whey proteins. *Journal of Food Engineering*, 87, 64–73.

Lee, D. U., Heinz, V., and Knorr, D. (2003). Effects of combination treatments of nisin and high intensity ultrasound with pressure on the microbial inactivation in liquid whole egg. *Innovative Food Science and Engineering Technologies*, 4, 387–393.

Li, H., Pordesimo, L., and Weiss, J. (2004). High intensity ultrasound-assisted extraction of oil from soybeans. *Food Research International*, 37, 731–738.

Mann, T., and Krull, U. J. (2004). The application of ultrasound as a rapid method to provide DNA fragments suitable for detection by DNA biosensors. *Biosensors and Bioelectronics*, 20(5), 945–955.

Mason, T. J. (1996). Power ultrasound in food processing – the way forward. In: Povey, M. J. W. and Mason, T. J. (eds.), *Ultrasound in Food Processing*, pp. 105–126. London, Blackie Academic and Professional.

Mason, T. J. (2003). Sonochemistry and sonoprocessing: the link, the trends and (probably) the future. *Ultrasonics Sonochemistry*, 10(4–5), 175–179.

Mason, T. J., Paniwnyk, L., and Lorimer, J. P. (1996). The uses of ultrasound in food technology. *Ultrasonics Sonochemistry*, 3, S253–S260.

McClements, J. D. (1995). Advances in the application of ultrasound in food analysis and processing. *Trends in Food Science and Technology*, 6, 293–299.

Miles, C. A., Morley, M. J., and Rendell, M. (1999). High power ultrasonic thawing of frozen foods. *Journal of Food Engineering*, 39, 151–159.

Muthukumaran, S., Kentish, S. E., Stevens, G. W., Ashokkumar, M., and Mawson, R. (2007). The application of ultrasound to dairy ultrafiltration: The influence of operating conditions. *Journal of Food Engineering*, 81, 364–373.

Neis, U., and Blume, T. (2003). Ultrasonic disinfection of wastewater effluents for high-quality reuse. *Water Science and Technology: Water Supply*, 3(4), 261–267.

Oulahal-Lagsir, N., Martial-Gros, A., Bonneau, M., and Blum, L. J. (2000). Ultrasonic methodology coupled to ATP bioluminescence for the non-invasive detection of fouling in food processing equipment – validation and application to a dairy factory. *Journal of Applied Microbiology*, 89, 433–441.

Pagán, R., Mañas, P., Alvarez, I., and Condón, S. (1999). Resistance of *Listeria monocytogenes* to ultrasonic waves under pressure at sublethal (manosonication) and lethal (manothermosonication) temperatures. *Food Microbiology*, 16, 139–148.

Patil, S., Bourke, P., Kelly, B., Frías, J. M., and Cullen, P. J. (2009). The effects of acid adaptation on *Escherichia coli* inactivation using power ultrasound. *Innovative Food Science and Emerging Technologies*, 10, 486–490.

Patrick, M., Blindt, R., and Janssen, J. (2004). The effect of ultrasonic intensity on the crystal structure of palm oil. *Ultrasonics Sonochemistry*, 11, 251–258.

Piyasena, P., Mohareb, E., and McKellar, R. C. (2003). Inactivation of microbes using ultrasound: a review. *International Journal of Food Microbiology*, 87, 207–216.

Povey, M., and Mason, T. (1998). *Ultrasound in food processing*. London, Blackie Academic and Professional.

Raso, J., and Barbosa-Cánovas, G. V. (2003). Nonthermal preservation of foods using combined processing techniques. *Critical Reviews in Food Science and Nutrition*, 43(3), 265–285.

Raso, J., Pagán, R., Condón, S., and Sala, F. J. (1998a). Influence of treatment and pressure on the lethality of ultrasound. *Applied and Environmental Microbiology*, 64(2), 465–471.

Raso, J., Palop, A., Pagán, J., and Condón, S. (1998b). Inactivation of *Bacillus subtilis* spores by combining ultrasonic waves under pressure and mild heat treatments. *Journal of Applied Microbiology*, 85, 849–854.

Riera-Franco de Sarabia, E., Gallego-Juárez, J. A., Rodríguez-Corral, G., Elvira-Segura, L., and González-Gómez, I. (2000). Application of high-power ultrasound to enhance fluid/solid particle separation processes. *Ultrasonics*, 38, 642–646.

Rodríguez, J. J., Barbosa-Cánovas, G. V., Gutiérrez-López, G. F., Dorantes-Álvarez, L., Yeom, H. W., and Zhang, Q. H. (2003). An update on some key alterative food processing technologies: Microwave, pulsed electric field, high hydrostatic pressure, irradiation and ultrasound. In: Gutiérrez-López, G. F., and Barbosa-Cánovas, G. V. (eds.), *Food science and food biotechnology*, pp. 279–312. Boca Ratón, FL, CRC Press.

Ruis-Jiménez, J., Priego-Capote, F., and Luque de Castro, M. D. (2004). Identification and quantification of *trans* fatty acids in bakery products by gas chromatography-mass spectrometry after dynamic ultrasound-assisted extraction. *Journal of Chromatography A*, 1045, 203–210.

Saggin, R., and Coupland, J. N. (2001). Non-contact ultrasonic measurements in food materials. *Food Research International*, 34, 865–870.

Scherba, G., Weigel, R. M., and O'Brien, W. D. (1991). Quantitative assessment of the germicidal efficacy of ultrasonic energy. *Applied and Environmental Microbiology*, 57(7), 2079–2084.

Schläfer, O., Onyeche, T., Bormann, H., Schröder, C., and Sievers, M. (2002). Ultrasound stimulation of micro-organisms for enhanced biodegradation. *Ultrasonics*, 40, 25–29.

Schöck, T., and Becker, T. (2010). Sensory array for the combined analysis of water-sugar-ethanol mixtures in yeast fermentations by ultrasound. *Food Control*. 21(4):362–369 doi:10.1016/j.foodcont.2009.06.017.

Sigfusson, H., Ziegler, G. R., and Coupland, J. N. (2004). Ultrasonic monitoring of food freezing. *Journal of Food Engineering*, 62, 263–269.

Sun, D. W., and Li, B. (2003). Microstructural change of potato tissues frozen by ultrasound-assisted immersion freezing. *Journal of Food Engineering*, 57, 337–345.

Tian, Z. M., Wan, M. X., Wang, S. P., and Kang, J. Q. (2004). Effects of ultrasound and additives on the function and structure of trypsin. *Ultrasonics Sonochemistry*, 11, 399–404.

Ting, C. H., Kuo, F. J., Lien, C. C., and Sheng, C. T. (2009). Use of ultrasound for characterizing the gelation process in heat induced $CaSO_4 \cdot 2H_2O$ tofu curd. *Journal of Food Engineering*, 93, 101–107.

Tsukamoto, I., Constantinoiu, E., Furuta, M., Nishimura, R., and Maeda, Y. (2004a). Inactivation of *Saccharomyces cerevisiae* by ultrasonic irradiation. *Ultrasonics Sonochemistry*, 11, 61–65.

Tsukamoto, I., Constantinoiu, E., Furuta, M., Nishimura, R., and Maeda, Y. (2004b). Inactivation effect of sonication and chlorination on *Saccharomyces cerevisiae*. Calorimetric analysis. *Ultrasonics Sonochemistry*, 11, 167–172.

Utsunomiya, Y., and Kosaka, Y. (1979). Application of supersonic waves to foods. *Journal of the faculty of Applied Biological Science, Hiroshima University*, 18(2), 225–231.

Valdramidis, V. P., Cullen, P. J., Tiwari, B. K., and O'Donnell, C. P. (2010). Quantitative modeling approaches for ascorbic acid degradation and non-enzymatic browning of orange juice during ultrasound processing. *Journal of Food Engineering*, 96, 449–454.

Valero, M., Recrosio, N., Saura, D., Muñoz, N., Martí, N., and Lizama, V. (2007). Effects of ultrasonic treatments in orange juice processing. *Journal of Food Engineering*, 80, 509–516.

Vercet, A., Sánchez, C., Burgos, J., Montañés, L., and Lopez Buesa, P. (2002). The effects of manothermosonication on tomato pectin enzymes and tomato paste rheological properties. *Journal of Food Engineering*, 53, 273–278.

Vercet, A., Burgos, J., Crelier, S., and Lopez-Buesa, P. (2001). Inactivation of proteases and lipases by ultrasound. *Innovative Food Science and Emerging Technologies*, 2, 139–150.

Vilkhu, K., Mawson, R., Simons, L., and Bates, D. (2008). Applications and opportunities for ultrasound assisted extraction in the food industry – A review. *Innovative Food Science and Emerging Technologies*, 9, 161–169.

Wrigley, D. M., and Llorca, H. G. (1992). Decrease of *Salmonella typhimurium* in skim milk and egg by heat and ultrasonic wave treatment. *Journal of Food Protection*, 55(9), 678–680.

Wu, H., Hulbert, G. J., and Mount, J. R. (2001). Effects of ultrasound on milk homogenization and fermentation with yogurt starter. *Innovative Food Science and Emerging Technologies*, 1, 211–218.

Zenker, M., Heinz, V., and Knorr, D. (2003). Application of ultrasound-assisted thermal processing for preservation and quality retention of liquid foods. *Journal of Food Protection*, 66(9), 1642–1649.

Chapter 4
The Thermodynamic and Kinetic Aspects of Power Ultrasound Processes

Hao Feng

1 Introduction

Most high intensity or power ultrasound applications involve a special transmission mode of sound waves in a medium that is composed of consecutive compressions and rarefactions. Since the propagation of such longitudinal waves is normally associated with a liquid medium, the use of power ultrasound is often termed as sonication. When the negative pressure in the rarefaction phase surpasses the tensile stress of the liquid, the liquid will be torn apart and cavities will be formed (Leighton, 1994). The inception of cavitation and the subsequent mechanical and chemical effects rising from the cavitation activity enable interactions between the acoustic energy and food and biological systems being processed. Such interactions take place at microscopic levels as the average diameters of cavitation bubbles are at 150–170 μm, for bubbles generated in water by 20 kHz ultrasound transducers (Awad, 1996; Vago, 1992). How to link the cavitation events at the micrometer scale to overall ultrasonic processing parameters is an important question that has not been touched upon in previous ultrasound research. In addition, the effect of changing system parameters, such as temperature and pressure, on microscale events during a sonication treatment also remains to be fully understood. If an ultrasonic process can be treated as a process of transmitting acoustic energy into a food or biological system to facilitate a target operation, the principles established in thermodynamics may be used to gain a better understanding of the process. In this chapter, a thermodynamic method will be used to shed light on an abnormality encountered in microbial inactivation when ultrasonic and thermal energies are combined, with the hope of triggering more investigations in the field.

Kinetics, which provide important information about reaction rate and kinetic data, have been used in the design of a number of food processing processes.

H. Feng (✉)
Department of Food Science and Human Nutrition, University of Illinois at Urbana-Champaign, 382F-AESB, 1304 W. Pennsylvania Ave, Urbana, IL 61801, USA
e-mail: haofeng@illinois.edu

H. Feng et al. (eds.), *Ultrasound Technologies for Food and Bioprocessing*, Food Engineering Series, DOI 10.1007/978-1-4419-7472-3_4,
© Springer Science+Business Media, LLC 2011

Pasteurization and sterilization are two typical processes where first-order microbial inactivation kinetics are used to obtain *D*- and *z*-values. With the *D*- and *z*-values, the treatment time of a thermal process can be determined to achieve a target microbial count reduction. Scientists working on power ultrasound have also attempted to provide similar *D*- and *z*-values to guide the design of, for instance, an ultrasound-assisted liquid food pasteurization process. Compared with traditional thermal processing and other non-thermal processing technologies, however, the kinetic data for ultrasound inactivation of bacteria and food enzymes are insufficient, especially for data in food systems. There are very limited reports about the reaction kinetics of food components during sonication. Moreover, the situation is compounded by the fact that most ultrasound treatments involve multiple parameters and most ultrasound applications employ the hurdle concept by employing a combination of ultrasound with other preservation methods. Nevertheless, a short summary about this important topic will be presented in this chapter based on currently available data.

2 Abnormality in Thermo-sonication Inactivation

Passing ultrasonic waves through a liquid was first reported to cause irreversible inactivation of bacteria in the 1920s (Harvey and Loomis, 1929). In the early years, to reach the five-log cycle reduction in the survival count of pathogenic cells as currently required by Food and Drug Administration (FDA) for food pasteurization (U.S. Food and Drug Administration, 2001), a relatively long process time and high acoustic power density (APD) were required when an ultrasonic treatment was performed at sublethal temperatures (or sonication). Because of the limitations of the hardware then in use, early sonication tests were conducted at relatively low APD and a low inactivation rate of microbial cells was reported, with one log reduction achieved between 3 to over 80 min, depending on the bacteria species and properties of the suspension medium (Jacobs and Thornley, 1954; Kinsloe et al., 1954). With the progress in the development of robust piezoelectric elements for power ultrasound generation, recent ultrasound inactivation studies have employed relatively high APD and, as a result, a five-log reduction was achieved in 12–22 min (Rodgers and Ryser, 2004; Ugarte-Romero et al., 2007). However, the time (12–22 min) needed to achieve a five-log reduction was still long for any practical pasteurization operations. Alternatively, a combination of sonication and heat was exploited in a process termed thermo-sonication (TS) to increase the microbial or enzyme inactivation rate (Earnshaw et al., 1995; López-Malo et al., 1999; Ordoñez et al., 1987). When treating the samples at TS mode, inactivation is a result of the combined action of heat and ultrasound, and usually additive or even synergistic effects can be observed. In a TS test at 61°C, for example, the *D*-value of *Escherichia coli* K12 in buffer was 0.13 min, which represents a sixfold increase in inactivation rate compared to a thermal-only treatment at the same temperature (Lee et al., 2009b). However, there is an upper temperature limit for TS inactivation of bacteria

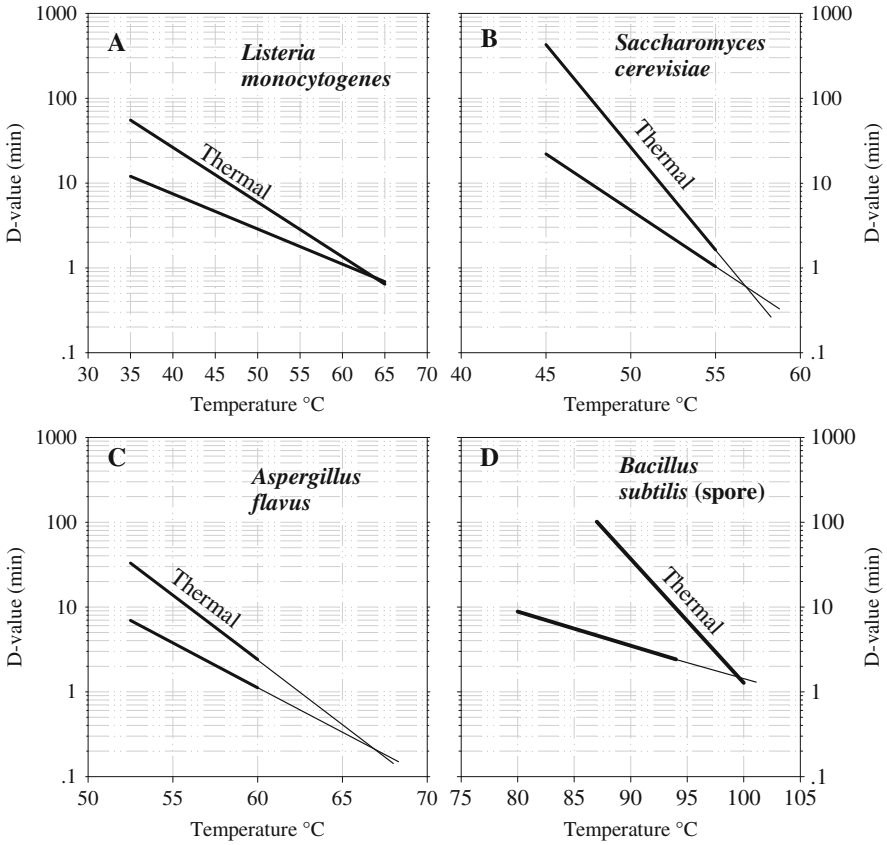

Fig. 4.1 Resistance of *L. monocytogenes* (**a**: Ugarte-Romero et al., 2007), *S. cerevisiae* (**b**: López-Malo et al., 1999), *Aspergillus flavus* (**c**: López-Malo et al., 2005), and *Bacillus subtilis* spores (**d**: Sala et al., 1999) to thermo-sonication treatment in comparison with thermal alone treatment. There are two lines for each microorganism, with the upper one denoting the thermal treatment and the lower one representing a thermo-sonication treatment. *Thick solid lines* represent the temperature range reported in the literature, while the *thin solid lines* are an extrapolation from the date reported

(Fig. 4.1). Due to a cushioning effect when vapor-filled bubbles implodes at a relatively high temperature, TS inactivation above this temperature do not result in any additional killing compared to a treatment using only heat at the same temperature (Ugarte-Romero et al., 2007). This temperature effect is found in the inactivation of yeast, spore formers, and Gram-positive and Gram-negative cells. Sometimes, inactivation beyond the threshold temperature exhibits some degree of uncertainty and is hard to explain with only the vapor-filled bubble cushioning effect theory. This phenomenon is therefore examined under the framework of thermodynamics in this chapter.

3 Non-equilibrium Thermodynamic Theory for Biological Systems

Classic thermodynamic theories apply only to equilibrium systems. Since no biological system is at equilibrium, non-equilibrium theories have been used to extend the useful domain of thermodynamics to biological applications (Singh, 1998). For microbial growth via biochemical reactions of catabolic nature, for instance, it is known that a Gibbs energy dissipation takes place, which is a combined process of entropy reduction through entropy exchange associated with heat ($Q/T < 0$) and by yielding products of higher entropy (von Stockar and Liu, 1999). Not much published information is available regarding the thermodynamic basis of microbial death or microbial inactivation, as the thermodynamic definition of biological death has been a challenge in biology (Nahle, 2009). One hypothesis proposed by Heinz and Knorr (2005) states that changes in the Gibbs energy correspond to either a recoverable or non-recoverable state of a bacterial spore, and hence $\Delta G = 0$ can be used to indicate pressure–temperature combinations for irreversible bacterial inactivation or killing. The conception of Heinz and Knorr is further developed in this work to take into account the energy input from the environment into a system, which hence can be used to provide a non-equilibrium thermodynamic explanation for microbial inactivation using acoustic energy.

To obtain Gibbs free energy changes in a microbial inactivation process, let us start with the definition of Gibbs free energy $G = H - TS$, where H is the enthalpy, T is the temperature, and S is the entropy. The enthalpy H is given by $H = U + pV$, where U is the internal energy, p the pressure, and V the volume. One C-mol of microbial cells is taken as a non-steady open thermodynamic system for the analysis. For an infinitesimal change, the general entropy balance is given by (von Stockar et al., 2006)

$$\mathrm{d}U = \mathrm{d}Q + \mathrm{d}W - pdV + \Sigma h_i \mathrm{d}n_i \tag{4.1}$$

where h_i and n_i are the partial molar enthalpy and number of moles of i-th species in the system, respectively. In the above equation, the dW refers to the work done on the system not accounted for by the pdV term.

With 1 C-mol of cellular mass as the system boundary, the balance of entropy is

$$\mathrm{d}S = \mathrm{d}Q/T + \Sigma s_i \cdot \mathrm{d}n_i \tag{4.2}$$

where s_i refers to the partial molar enthalpy of i-th species. From Equation (4.2), an expression for the infinitesimal change in heat imported can be obtained:

$$\mathrm{d}Q = T(\mathrm{d}S - \Sigma s_i \cdot \mathrm{d}n_i) \tag{4.3}$$

For an infinitesimal change in Gibbs energy, the following is available:

$$\mathrm{d}G = \mathrm{d}H - \mathrm{d}(TS) = \mathrm{d}H - T\mathrm{d}S - S\mathrm{d}T \tag{4.4}$$

On the other hand, the definition for enthalpy gives the following:

$$dH = dU + d(pV) = dU + pdV + Vdp \tag{4.5}$$

Substitute Equation (4.3) into Equation (4.1) and eliminate dQ resulting in the following:

$$dU = TdS + dW - pdV + \Sigma\mu_i \cdot dn_i \tag{4.6}$$

where $\mu_i = h_i - Ts_i$ is the chemical potential of the i-th species. Then, substitute Equation (4.6) into Equation (4.5) to eliminate dU, yielding

$$dH = TdS + dW + \Sigma\mu_i \cdot dn_i + Vdp \tag{4.7}$$

Finally, Equation (4.7) is substituted into Equation (4.4), eliminating dH to obtain the following expression:

$$dG = Vdp - SdT + dW + \Sigma\mu_i \cdot dn_i \tag{4.8}$$

In a similar fashion, when only changes in free energy ΔG are considered, Equation (4.8) becomes

$$d\Delta G = \Delta Vdp - \Delta SdT + d\Delta W + \Sigma\Delta\mu_i \cdot dn_i \tag{4.9}$$

Equation (4.9) applies to living microbial open systems. dn_i is the exchange rate of the chemical species. For a microbial inactivation process, species exchanges to the environment can be ignored, and hence $\sum \Delta\mu_i \cdot dn_i = 0$. Similar to Heinz and Knorr (2002), Equation (4.9) can be integrated using a Taylor series expansion up to the second-order term, which gives the following:

$$\begin{aligned}\Delta G = {} & \Delta G_0 + \Delta V_0(p - p_0) - \Delta S_0(T - T_0) + \tfrac{1}{2}\Delta\beta(p - p_0)^2 \\ & - \tfrac{1}{2}\Delta cp/T_0(T - T_0)^2 + \Delta\alpha(T - T_0)\,(p - p_0) + (\Delta W - \Delta W_0)\end{aligned} \tag{4.10}$$

In particular, the conditions where $\Delta G = 0$, corresponding to irreversible microbial inactivation, are of interest. In this case, Equation (4.10) reduces to the equation of a quadratic curve. To find the conditions that satisfy $\Delta G = 0$, let

$$\begin{gathered}A = -\tfrac{1}{2}\Delta c_p/T_0,\ 2b = \Delta\alpha,\ c = \tfrac{1}{2}\Delta\beta,\ 2d = -\Delta S_0,\ 2f = \Delta V_0, \\ g = \Delta G_0 + (\Delta W - \Delta W_0)\end{gathered} \tag{4.11}$$

where α is the thermal expansion coefficient of the microbial cells, β is the compressibility, and c_p is the heat capacity. The $\Delta G = 0$ conditions are then transformed to the standard form for the equation of a quadratic curve, as shown in Fig. 4.2.

$$ax^2 + 2bxy + cy^2 + 2dx + 2fy + g = 0, x = (T - T_0) \text{ and } y = (p - p_0) \tag{4.12}$$

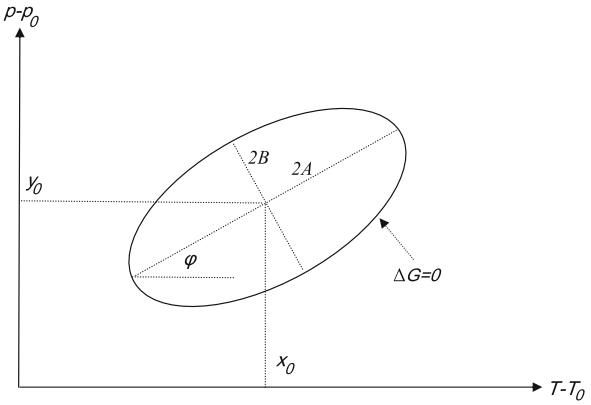

Fig. 4.2 The plane *P–T* corresponding to $\Delta G = 0$

Equation (4.12) would describe an ellipse when the following conditions are satisfied:

$$0 \neq \Delta = \begin{vmatrix} a & b & d \\ b & c & f \\ d & f & g \end{vmatrix}, 0 \neq \Delta = \begin{vmatrix} a & b \\ b & c \end{vmatrix} \tag{4.13}$$

$I = a + c$ with $\Delta / I < 0$

In this case, the center of the ellipse will be at the point (x_0, y_0) at an incline of

$$\begin{aligned} x_0 &= \frac{cd - bf}{b^2 - ac} \\ y_0 &= \frac{af - bd}{b^2 - ac} \\ \phi &= \frac{1}{2} \cot^{-1}\left(\frac{c - a}{2b}\right) \end{aligned} \tag{4.14}$$

The lengths of the major axes are given by

$$\begin{aligned} A &= \sqrt{\frac{2(af^2 + cd^2 + gb^2 - 2bdf - acg)}{(b^2 - ac)\left[(c - a)\sqrt{1 + \frac{4b^2}{(a-c)^2}} - (c + a)\right]}} \\ B &= \sqrt{\frac{2(af^2 + cd^2 + gb^2 - 2bdf - acg)}{(b^2 - ac)\left[(a - c)\sqrt{1 + \frac{4b^2}{(a-c)^2}} - (c + a)\right]}} \end{aligned} \tag{4.15}$$

Of particular interest is the value of g that will shrink the ellipse into a point; this is realized when $A = B = 0$, which implies the following:

$$af^2 + cd^2 + gb^2 - 2bdf - acg = 0 \quad g = \frac{af^2 + cd^2 - 2bd}{b^2 - ac} \tag{4.16}$$

In terms of the physical variables, this yields the following:

$$\Delta G_0 + \Delta W - \Delta W_0 = \frac{-\Delta c_p \Delta V_0^2 + T_0 \Delta\beta \Delta S_0^2 + 4T_0 \Delta\alpha \Delta S_0}{2T_0 \Delta\alpha^2 + 2T_0 \Delta c_p \Delta\beta} \tag{4.17}$$

In Equation (4.12), in order to achieve a maximum for the function z (and hence a minimum for $-\Delta G$), it requires the coefficients $a < 0$ and $c < 0$, since for either p or V being fixed, Equation (4.12) represents a parabola.

Furthermore, it is noted that for non-zero d and/or f, allow $X = ax - d/a$ and $Y = cy - f/c$, such that a non-zero d and/or f amounts only to a translation of the quadratic curve in the xy plane. Likewise, a non-zero g merely results in the translation of the quadratic curve in a direction parallel to the $z\,(-\Delta G)$ axis.

In Fig. 4.3, the effects of the coefficients a, b, and c on the shape of the ellipse as described by Equation (4.12) are presented, with the restriction that $a < 0$, $c < 0$ and $d = f = 0$, by plotting contour lines of the function as given by Equation (4.12), for various values of a, b, and c.

As can be seen from Fig. 4.3, the relative magnitude of the coefficients a and c determines the ratio of the lengths of the major axis A and B, while the coefficient b determines the direction of the major axis. In 3D, the plot of Equation (4.10) for $z\,(-\Delta G)$ as a function of $x = (T - T_0)$ and $y = (p - p_0)$ is given in Fig. 4.4.

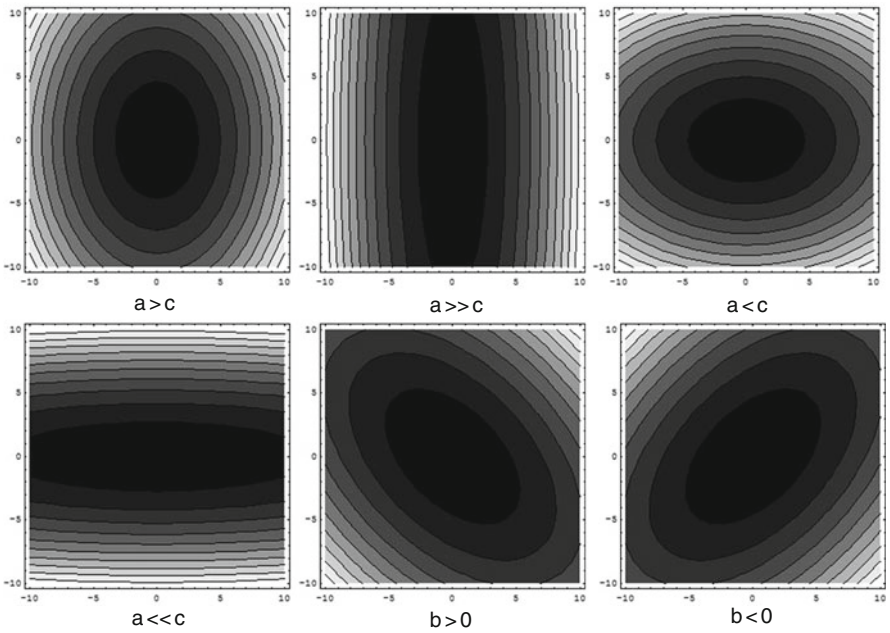

Fig. 4.3 The effect of **a**, **b**, and **c** on the shape and orientation of the ellipse defined by $\Delta G = 0$

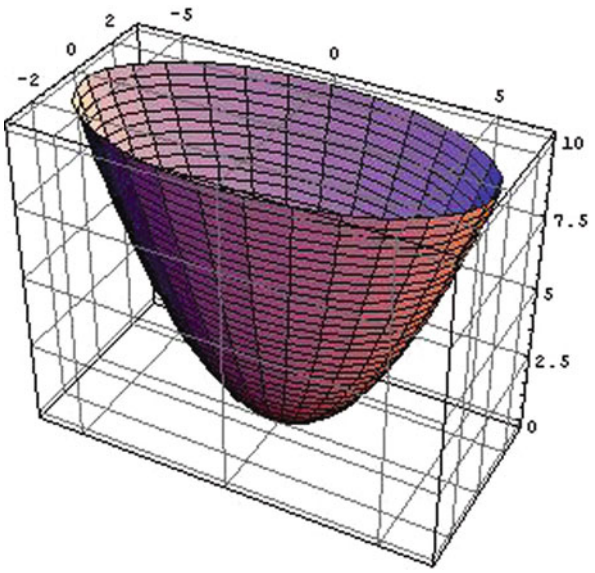

Fig. 4.4 Three-dimensional plot of the Gibbs free energy (G) function

4 Cut-Off Temperature for Thermo-sonication Inactivation

When the pressure of the system is fixed, as in the case for most ultrasound inactivation studies, a parabola in the $\Delta G - T$ plane can be obtained.

Consider now two different systems, one with ultrasound treatment and one without. The action of adding acoustic energy into the system corresponds to introducing a ΔW in Equation (4.10). Therefore, these two systems will have identical phase diagrams on the $\Delta G - T$ plane, except that the system with ultrasound treatment (termed as US+T) will be lying above the system without (denoted by T) by a difference of ΔW in z direction (Fig. 4.5).

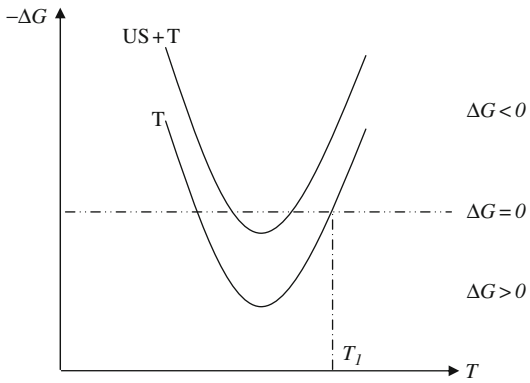

Fig. 4.5 The Gibbs free energy at the $\Delta G - T$ plane showing with (US + T) and without (T) ultra-sonication

When $T < T_1$, the application of ultrasound lowers the Gibbs energy of the system and allows $\Delta G < 0$ to be achieved over a wider temperature range on the $\Delta G - T$ plane. According to Heremans (2002), a certain constant free-energy difference (ΔG) region can be defined on the P−T plane where the T−P combinations can cause protein denaturation. If we allow the constant ΔG to be at a specific value of $\Delta G = 0$ and thus $\Delta G < 0$ corresponds to irreversible microbial inactivation, the conditions can also be extended to more complicated situations such as killing of bacteria. At $T > T_1$, however, the system without ultrasound treatment already has $\Delta G < 0$. As a result, any additional treatment by ultrasound will not cause the conditions to be more favorable than they are already. Consequently, no more additional killing in the US+T treatment will result from further temperature increase beyond T_1 as compared to a heat-only treatment at the same temperature. Therefore, $T = T_1$ defines a cut-off temperature whereby there will be no observable gain in killing efficiency above T_1.

Since the $\Delta G - T$ plane is built on information from non-steady open thermodynamic microbial systems, for different organisms, it is foreseeable that there exists a different T_1. Responses of bacteria to TS inactivation as shown in Fig. 4.1 thus can be attributed to the existence of T_1, which equals to approximately 64°C for *Listeria monocytogenes*, 53°C for *Saccharomyces cerevisiae*, 67°C for *Aspergillus flavus*, and 99°C for *Bacillus subtilis* spores (Ugarte-Romero et al., 2007).

5 A Note on Inactivation Kinetics

Similar to the thermal processing counterpart, most ultrasound inactivation studies have attempted to use first-order inactivation kinetics to describe the survival curves of microorganisms or activity reduction of enzymes. An advantage of using log-linear inactivation kinetic equations is that the well-established design procedure in thermal processing (pasteurization or sterilization) can be used in the design of an ultrasound-assisted treatment. When the first-order inactivation kinetics are valid, the survival count of a bacterium can be estimated by

$$-\frac{\mathrm{d}N}{\mathrm{d}t} = kN \quad \text{or} \quad \frac{N}{N_0} = \exp\left(-\frac{t}{D}\right) \quad \text{or} \quad \log N - \log N_0 = -\frac{t}{D} \tag{4.18}$$

where D is the decimal reduction time in min, k is a constant, N is survival count at time t, and N_0 is initial count. The survival count reduction in a treatment can be caused by a number of chemical or mechanical lethal factors, such as temperature, pressure, electric field intensity, acoustic energy intensity, ultraviolet light, irradiation, sanitizer concentration, etc. In ultrasound inactivation of microorganisms, the lethal factors could be a combination of different chemical and physical effects related to cavitation activity, which imparts ultrasound inactivation an inherent complexity compared to other non-thermal processing technologies. From a process operation point of view, the parameters that appear to affect the efficacy of an ultrasound treatment include the amplitude of the ultrasonic waves,

treatment time, frequency, reactor shape, shape and location of the ultrasound emitting element, temperature, static pressure, and properties of the liquid food, such as viscosity, surface tension, dissolved gas, solid concentration, pH, and water activity, as well as the type of organism, the growth phase, among others. When conducting an ultrasound kinetic study, it is critical to hold other factors constant when examining the effect of one parameter. It is also important to report the details about hardware set-up and the medium and treatment conditions. Unfortunately, not all of the above-mentioned information is provided in published reports on ultrasound applications, rendering a direct comparison of the data produced by different research groups difficult. Currently, there are two types of models for ultrasound inactivation kinetic studies: linear models and non-linear models.

5.1 First-Order Kinetic Models

Most ultrasonic inactivation studies have either employed first-order kinetic parameters (D-values and z-values) to describe microbial survival count reduction, or have simply reported the log-cycle reduction without using any kinetic parameters. To document the resistance of a microorganism to ultra-sonication, it is not a bad choice to only report the log reduction, since an ideal linear relation across the entire inactivation curve without a shoulder and a tail is rarely observed, especially when the microbial count reduction is over five log in the inactivation test. However, for process design purposes, kinetic parameters will be preferred, as long as the D-values are not giving an overestimate of the inactivation rate, which will result in an unsafe design. When processing the inactivation data with a first-order kinetic model, D values, which is the time used to cause 90% reduction in the number of microbial survival count or enzyme activity, are reported. From the published ultrasound inactivation results, the inactivation rate as indicated by the D values for a specific bacterium is influenced by a number of factors. Different bacteria and even different strains of the same organism exhibit different resistance to an ultrasonic treatment (Baumann et al., 2005). When temperature and pressure are fixed, the D-values are in the sequence of spores > fungi > yeasts > Gram-positive > Gram-negative cells, as can be seen in Fig. 4.6. As a result, the inactivation rate (log CFU/min) in ultra-sonication is in the sequence of Gram-negative cells > Gram-positive cells > yeasts > fungi > spores.

The temperature sensitivity of different bacteria is clearly shown in Fig. 4.6. An increase in temperature results in a fast decrease in D-values for all of the five types of organisms. The slope on a log D-value versus temperature curve is defined as z-value when a linear relation on a semi-log plot can be observed. Since the data in Fig. 4.6 were collected from inactivation data of different bacteria and treated under different conditions, the slope only functions as an indication of the changes in D-value as affected by sonication temperature. A few studies have reported z values for ultrasound inactivation of microorganisms. In a sonication test, in buffer with different acoustic power densities (APDs), Ugarte-Romero et al. (2007)

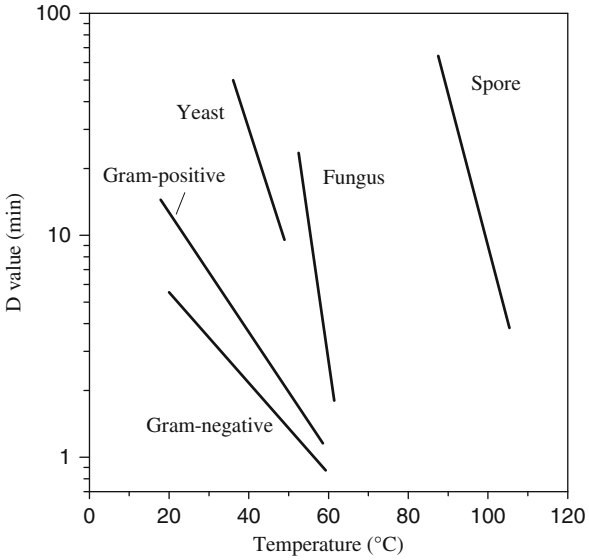

Fig. 4.6 *D*-values of bacteria with respect to temperature. Data for each bacterial group were collected from the literature. For spore formers, the data are from ultrasonic inactivation of *Bacillus cereus*, *Bacillus licheniformis*, *and Bacillus subtilis* (Burgos et al., 1972; Sala et al., 1999). The inactivation data for *Aspergillus flavus*, *Penicillium digitatium* and *Zygosaccharomyces bailii* are from López-Malo et al. (2005), and López-Malo and Palou (2005). The data for *Saccharomyces cerevisiae* are from López-Malo et al. (1999, 2005) and Guerrero et al. (2001). *Streptococcus faecium*, *Staphylococcus carnosus*, *Lactobacillus acidophilus*, and *Listeria monocytogenes* inactivation data were collected from the work of Pagán et al. (1999), Earnshaw et al. (1995), Zenker et al. (2003), Rodgers and Ryser (2004), Baumann et al. (2005), and D'Amico et al. (2006). The data of Gram-negative cells, i.e., *Yersinia*, *Flavobacterium* spp., *Salmonella enterica serovar enteritidis*, *Acinetobacter bauxmaii*, *Escherichia coli*, and *Shigella boydii* are from Ordóñez et al. (1987), Chamul and Silva (1999), Zenker et al. (2003), Cabeza et al. (2004), D'Amico et al. (2006), Rodríguez-Calleja et al. (2006), Ugarte-Romero et al. (2007), and Patila et al. (2009)

estimated that the *z*-value for *Shigella boydii* was 1.8 W/mL, while that for *Listeria monocytogenes* was 1.5 W/mL. At a given APD, the z value for thermo-sonication of *L. monocytogenes* was 23.4°C, while that for a thermal inactivation at the same temperature was 10.5°C. The higher *z*-value for the thermo-sonication corresponds to a less sensitive change in *D*-value when increasing temperature. As a result, when plotting the log *D*-values of the thermo-sonication and that for the thermal alone treatment on a *D*-value versus temperature chart, at a relatively high temperature, the curve for the thermo-sonication will traverse that for the thermal-only treatment. This is the root cause for the existence of the cut-off temperature, a phenomenon previously discussed in this chapter (see Fig. 4.6). The *z*-values corresponding to pressure changes during sonication have not been reported in the literature. This is partially because the treatment must be performed in a mano-thermo-sonication (MTS) mode with reliable temperature and pressure controls,

and only very few groups have developed the capacity to conduct MTS tests. Nevertheless, the limited data published until now seem to indicate that there exists an upper pressure in an MTS test (Lee et al., 2009b; Raso et al., 1998a). The effect of pressurization on ultrasonic microbial inactivation will diminish above the threshold pressure.

When examining the effect of temperature and pressure on sonication treatments, another method that utilizes linear inactivation kinetic models has been used (Raso et al., 1998a, b). This method assumes that the heat- and pressure-related lethal processes follow a log-linear relation and that the overall lethal effect is the addition of individual lethal effects. A detailed description of this method is given in Chapter 11 of this book. For inactivation curves with an obvious tail, a two-sectional linear inactivation model has also been used to describe the bacterial response to sonication treatments. An advantage of using two linear sections to fit the inactivation curve is that a *D*-value can be produced for each linear section, which may be used to compare with *D* values obtained from other inactivation tests. In addition, the inactivation in the first and fast reduction section is more efficient and of practical importance in real world applications. The inactivation in the second section is slow and ineffective, and should be avoided. This approach has been employed in the inactivation kinetic studies of *L. monocytogenes* in a thermo-sonication test in apple cider (Baumann et al., 2005) and *E. coli* K12 in an MTS test in a buffer (Lee et al., 2009b).

The inactivation of enzymes has been reported to mainly follow a log-linear relation for MTS inactivation of peroxidase (López and Burgos, 1995b) and lipoxygenase (López and Burgos, 1995a), thermo-sonication of peroxidase (De Gennaro et al., 1999), MTS of pectin methylesterase and polygalacturonase (López et al., 1998), and thermo-sonication of tomato pectin methylesterase (Raviyan et al., 2005). In contrast with most microbial inactivation data sets where an over five-log reduction in the survival count of a bacterium can often be seen, most enzyme inactivation tests have reported an enzyme activity reduction over a range of less than 2 log cycles (99% reduction). This may contribute to the dominant linearity observed on enzyme inactivation curves.

Reports on the reaction kinetics of nutrients and other quality attributes in foods during sonication treatment are especially limited. The few recent reports have documented the degradation of ascorbic acid in orange juice after sonication and during storage (Lee et al., 2005; Tiwaria et al., 2009), and a first-order degradation kinetics were observed during storage for the reduction of the ascorbic acid concentration (Tiwaria et al., 2009).

5.2 Non-linear Inactivation Models

There has been growing evidence that inactivation of microorganisms may not follow first-order kinetics, especially for inactivation with non-thermal processing methods, with more than one lethal factor, or with a log reduction of near or over

five-log cycles (Klotz et al., 2007; Peleg and Cole, 1998). Shoulders and/or tails have been observed on the inactivation curves for a combined treatment of ultrasound with chitasan (Guerrero et al., 2005), ultrasound with vanillin (Gastelum et al., 2010), ultrasound with lethal temperature (Baumann et al., 2005), and ultrasound with pressure (Lee et al., 2009a, b). For tested microorganisms, non-linear inactivation behavior has been observed for the inactivation of *L. monocytogenes* (Baumann et al., 2005; D'Amico et al., 2006), *E. coli* (Allison et al., 1996; D'Amico et al., 2006; Stanley et al., 2004; Ugarte-Romero et al., 2006), *Alicyclobacillus acidophilus*, and *A. acidoterrestris* (Wang et al., 2010), *Bacillus subtilis* spores (Raso et al., 1998b), natural flora in raw milk (D'Amico et al., 2006), and *Saccharomyces cerevisiae* (Guerrero et al., 2005). To describe non-linear inactivation kinetics, several models, including Weibull, modified Gompertz, biphasic linear, and log-logistic models have been used to fit non-linear inactivation data of several microorganisms for inactivation by heat, high pressure processing or pulsed electric field (Gómez et al., 2005; Lee et al., 2009a, b; Raso et al., 2000). Table 4.1 tabulates a few selected non-linear inactivation models. Non-linear regression methods are normally used to fit the inactivation data to the models for the estimation of parameters in the model equations. Statistical parameters and methods, such as mean square error of model (MSE), coefficient of determination (R^2), accuracy factor (A_f), F test, and Akaike information criterion (Akaike, 1973) can be employed to evaluate the goodness of fit of the models to the inactivation data. In the reports of Lee et al. (2009a, b), the biphasic linear, log-logistic, and modified Gompertz kinetic models produced better fitting of the inactivation data for MTS, thermo-sonication, and mano-sonication treatments of *E. coli* K12 than the first-order and Weibull models.

Table 4.1 Selected non-linear inactivation kinetic models

Model	Primary model equation	Reference
Weibull	$\log \frac{N}{N_0} = -\left(\frac{t}{\alpha}\right)^{\beta}$	Mafart et al. (2002)
Modified Gompertz	$\log \frac{N}{N_0} = a \cdot \exp[-\exp(b + c \cdot t)] - a \cdot \exp[-\exp(b)]$	Linton et al. (1995)
Biphasic linear	$\log \frac{N}{N_0} = \log_{10}\left[(1-f) \cdot 10^{\frac{t}{Dsens}} + f \cdot 10^{\frac{t}{Dres}}\right]$	Cerf (1977)
Log-logistic	$\log \frac{N}{N_0} = \frac{A}{1 + e^{4\sigma(\tau - \log t)/A}} - \frac{A}{1 + e^{4\sigma(\tau - \log t0)/A}}$	Chen and Hoover (2003)
Modified Baranyi	$\frac{dN}{dt} = -k_{max}\left(1 - \left(\frac{N_{min}}{N}\right)^m\right)N$	Koseki and Yamamoto (2007)
K-L-M	$\log \frac{N}{N_0} = -2\,k\,t^{0.5}$	Klotz et al. (2007)
Double Weibull	$\log \frac{N}{N_0} = \log_{10}\left[f \cdot 10^{-\left(\frac{t}{\delta 1}\right)^{p1}} + (1-f)\,10^{-\left(\frac{t}{\delta 2}\right)^{p2}}\right]$	Coroller et al. (2006)

In ultrasound inactivation, the non-linearity could be attributed to subpopulations of different resistance and physiological reactions of the cells to a lethal factor (Heldman and Newsome, 2003). The break-up of cell aggregates during sonication by cavitation has also been considered as a cause for shoulders in bacterial survival curves. The tails, in some cases, may be caused by a gradual change in the properties of the liquid medium during sonication. For instance, in a probe system open to air, air may be entrained into the liquid, which would induce a progressive decrease in the cavitation activity and hence a reduction in inactivation rate. For a treatment for a relatively long time, the output power of the generator would decrease over time, which will also result in a decrease in inactivation efficacy.

The potential use of non-linear kinetic models in process design has raised concerns (Heldman and Newsome, 2003). Since most non-linear models are either empirical or with assumption(s) about the resistance distribution of cells to certain lethal factor, the results cannot be used outside the range of inactivation conditions employed to obtain the model parameters. No extrapolation is recommended. Suggestions have been proposed to follow the conventions adopted by the industry for a log-linear model when applying non-linear models. A practice of only reporting the end-point log reduction has been recommended to control the delivery of an expected log reduction in a process, which can minimize the non-linear survivor issues and provide consistency with the log-linear kinetic model (Heldman and Newsome, 2003).

References

Akaike, H. (1973). Information theory and extension of the maximum likelihood principle. In: Petrov, B. N., and Cza'ki F. (eds.), *Proceedings of the 2nd international symposium of information theory*, pp. 267–281. Budapest, Hungary, Akademiai Kiado.

Allison, D. G., D′Emanuele, A., Eginton, P., and Williams, A. R. (1996). The effect of ultrasound on *Escherichia coli* viability. *Journal of Basic Microbiology*, 36, 3–11.

Awad, S. B. (1996). Ultrasonic cavitations and precision cleaning. *Precision Cleaning*, *November*, 12.

Baumann, A., Martin, S. E., and Feng, H. (2005). Power ultrasound treatment of *Listeria monocytogenes* in apple cider. *Journal of Food Protection*, 68, 2333–2340.

Burgos, J., Ordonez, J. A., and Sala, F. (1972). Effect of ultrasonic waves on the heat resistance of *bacillus cereus* and *bacillus licheniformis* spores. *Applied and Environmental Microbiology*, 24, 497–498.

Cabeza, M. C., Ordóñez, J. A., Cambero, I., De la Hoz, L., and García, M. L. (2004). Effect of thermoultrasonication on *Salmonella enterica serovar enteritidis* in distilled water and intact shell eggs. *Journal of Food Protection*, 67, 1886–1891.

Cerf, O. (1997). Tailing survival curves of bacterial spores. *Journal of Applied Bacteriology*, 42, 19.

Chamul, R. S., and Silva, J. L. (1999). High frequency ultrasound amplitude, column height and contact time on water disinfection. In: Barbosa-Canovas, G. V., and Lombardo, S. P. (eds.), *Proceedings of the 6th conference of food engineering*, AIChE, pp. 146–150. Dallas, TX.

Chen, H., and Hoover, D. G. (2003). Modeling the combined effect of high hydrostatic pressure and mild heat on the inactivation kinetics of *Listeria monocytogenes* Scott A in whole milk. *Innovative Food Science and Emerging Technology*, 4, 25–34.

Coroller, L., Leguerinel, I., Mettler, E., Savy, N., and Mafart, P. (2006). General model, based on two mixed Weibull distributions of bacterial resistance, for describing various shapes of inactivation curves. *Applied and Environmental Microbiology*, 72, 6493–6502.

D′Amico, D., Silk, T. M., Wu, J., and Guo, M. (2006). Inactivation of microorganisms in milk and apple cider treated with ultrasound. *Journal of Food Protection*, 69, 556–563.

De Gennaro, L., Cavella, S., Romano, R., and Masi, P. (1999). The use of ultrasound in food technology I: Inactivation of peroxidase by thermosonication. *Journal of Food Engineering*, 39, 401–407.

Earnshaw, R. G., Appleyard, J., and Hurst, R. M. (1995). Understanding physical inactivation processes: Combined preservation opportunities using heat, ultrasound and pressure. *International Journal of Food Microbiology*, 28, 197–219.

Gastelum, G. G., Avila-Sosa, R., López-Malo, A., and Palou, E. (2010). *Listeria innocua* multi-target inactivation by thermo-sonication and vanillin. *Food Bioprocess Technology*. doi:10.1007/s11947-010-0334-4.

Gómez, N., García, D., Álvarez, I., Condón, S., and Raso, J. (2005). Modeling inactivation of *Listeria monocytogenes* by pulsed electric fields in media of different pH. *International Journal of Food Microbiology*, 103, 199–206.

Guerrero, S., López-Malo, A., and Alzamora, S. M. (2001). Effect of ultrasound on the survival of *Saccharomyces cerevisiae*: Influence of temperature, pH and amplitude. *Innovative Food Science and Emerging Technologies*, 2, 31–39.

Guerrero, S., Tognon, M., and Alzamora, S. M. (2005). Response of *Saccharomyces cerevisiae* to the combined action of ultrasound and low weight chitosan. *Food Control*, 16, 131–139.

Harvey, E. N., and Loomis, A. L. (1929). The destruction of luminous bacteria by high frequency sound waves. *Journal of Bacteriology*, 17, 373–376.

Heinz, V., and Knorr, D. (2002). Effects of high pressure on spores. In: Hendrickx, M. E. G., and Knorr, D. (eds.), *Ultra high pressure treatments of foods*, pp. 77–113. New York, NY, Springer.

Heinz, V., and Knorr, D. (2005). High-pressure assisted heating as a method for sterilizing foods. In: Barbosa-Canovas, G. V. (eds.), *Novel Food processing technologies*, pp. 207–231. Boca Raton, FL, CRC Press.

Heldman, D. R., and Newsome, R. L. (2003). Kinetic models for microbial survival during processing. *Food Technology*, 57, 40–46, 100.

Heremans, K. (2002). The effects of high pressure on biomaterials. In: Hendrickx, M. E. G., and Knorr, D. (eds.), *Ultra high pressure treatments of foods*, pp. 23–51. New York, NY, Springer.

Jacobs, S. E., and Thornley, M. J. (1954). The lethal action of ultrasonic waves on bacteria suspended in milk and other liquids. *Journal of Applied Bacteriology*, 17, 38–56.

Kinsloe, H., Ackerman, E., and Reid, J. J. (1954). Exposure of microorganisms to measured sound fields. *Journal of Bacteriology*, 68, 373–380.

Klotz, B., Pyle, D. L., and Mackey, B. M. (2007). New mathematical modeling approach for predicting microbial inactivation by high hydrostatic pressure. *Applied and Environmental Microbiology*, 73, 2468–2478.

Koseki, S., and Yamamoto, K. (2007). A novel approach to predicting microbial inactivation kinetics during high pressure processing. *International Journal of Food Microbiology*, 116, 275–282.

Lee, H., Zhou, B., Feng, H., and Martin, S. E. (2009a). Effect of pH on inactivation of *Escherichia coli* K12 by sonication, manosonication, thermosonication, and manothermosonication. *Journal of Food Science*, 74, E191–E198.

Lee, H., Zhou, B., Liang, W., Feng, H., and Martin, S.E. (2009b). Inactivation of *Escherichia coli* cells with sonication, manosonication, thermosonication, and manothermosonication: Microbial responses and kinetics modeling. *Journal of Food Engineering*, 93, 354–364.

Lee, J. W., Feng, H., and Kushad, M. M. (2005). Effect of manothermosonication (MTS) on quality of orange juice. In *Proceedings of AIChE 2005 Annual Meeting*, Cincinnati, OH.

Leighton, T. G. (1994). *The acoustic bubbles*. London, UK, Academic.

Linton, R. H., Carter, W. H., Pierson, M. D., and Hackney, C. R. (1995). Use of a modified Gompertz equation to model nonlinear survival curves for *Listeria monocytogenes Scott A*. *Journal of Food Protection*, 58, 946–954.

López, P., and Burgos, J. (1995a). Lipoxygenase inactivation by manothermosonication: effects of sonication physical parameters, Ph, Kcl, sugars, glycerol, and enzyme concentration. *Journal of Agricultural and Food Chemistry*, 43, 620–625.

López, P., and Burgos, J. (1995b). Peroxidase stability and reactivation after heat-treatment and manothermosonication. *Journal of Food Science*, 60, 451–455.

López, P., Vercet, A., Sánchez, A. C., and Burgos, J. (1998). Inactivation of tomato pectic enzymes by manothermosonication. *Zeitschrift für Lebensmittel-Untersuchung und -Forschung*, 207, 249–252.

López-Malo, A., and Palou, E. (2005). *Zygosaccharomyces bailii Inactivation Kinetics During Thermo-Sonication Treatments at Selected Water Activities*. 2nd Mercosur Congress on Chemical Engineering, 2005.

López-Malo, A., Guerrero, S., and Alzamora, S. M. (1999). *Saccharomyces cerevisiae* thermal inactivation combined with ultrasound. *Journal of Food Protection*, 62, 1215–1217.

López-Malo, A., Palou, E., Jiménez-Fernández, M., Alzamora, S. M., and Guerrero, S. (2005). Multifactorial fungal inactivation combining thermosonication and antimicrobials. *Journal of Food Engineering*, 67, 87–93.

Mafart, P., Couvert, O., Gaillard, S., and Leguerinel, I. (2002). On calculating sterility in thermal preservation methods: Application of the Weibull frequency distribution model. *International Journal of Food Microbiology*, 72, 107–113.

Nahle, N. (2009). A thermodynamic description of life and death in biosystems. *Journal of Human Thermodynamics*, 5, 7–14.

Ordoñez, J. A., Aguilera, M. A., Garcia, M. L., and Sanz, B. (1987). Effect of combined ultrasonic and heat treatment (thermoultrasonication) on the survival of a strain of *Staphylococcus aureus*. *Journal of Dairy Research*, 54, 61–67.

Pagán, R., Mañas, P., Álvarez, I., and Condón, S. (1999). Resistance of *Listeria monocytogenes* to ultrasonic waves under pressure at sublethal (manosonication) and lethal (manothermosonication) temperatures. *Food Microbiology*, 16, 139–148.

Patila, S., Bourke, P., Kellya, B., Fríasa L. M., and Cullena, P. J. (2009). The effects of acid adaptation on *Escherichia coli* inactivation using power ultrasound. *Innovative Food Science and Emerging Technologies*, 10, 486–490.

Peleg, M., and Cole, M. B. (1998). Reinterpretation of microbial survival curves. *Critical Reviews in Food Science and Nutrition*, 38, 353–380.

Raso, J., Álvarez, I., Condón, S., and Trepat, F. J. S. (2000). Prediction inactivation of *Salmonella senftenberg* by pulsed electric fields. *Innovative Food Science and Emerging Technologies*, 1, 21–29.

Raso, J., Pagán, R., Condón, S., and Sala, F. J. (1998a). Influence of temperature and pressure on the lethality of ultrasound. *Applied and Environmental Microbiology*, 64, 465–471.

Raso, J., Palop, A., and Condón, S. (1998b). Inactivation of *Bacillus subtilis* spores by combining ultrasound waves under pressure and mild heat treatment. *Journal of Applied Microbiology*, 85, 849–854.

Raviyan, P., Zhang, Z., and Feng, H. (2005). Ultrasonication for tomato pectinmethylesterase inactivation: Effect of cavitation intensity and temperature on inactivation, *Journal of Food Engineering*, 70, 189–196.

Rodgers, S. L., and Ryser, E. T. (2004). Reduction of microbial pathogens during apple cider production using sodium hypochlorite, copper ion, and sonication. *Journal of Food Protection*, 67, 766–771.

Rodríguez-Calleja, J. M., Cebrian, G., Condón, S., and Mañas, P. (2006). Variation in resistance of natural isolates of *Staphylococcus aureus* to heat, pulsed electric field and ultrasound under pressure. *Journal of Applied Microbiology*, 100, 1054–1062.

Sala, F. J., Burgos, J., Condón, S., López, P., and Raso, J. (1999). Effect of heat and ultrasound on microorganisms and enzymes. In: Gould G. W. (ed.), *New methods of food preservation*, 2nd edn, pp. 176–204. Gaithersburg, Aspen.

Singh, D. V. (1998). Thermodynamics and biology. *Pure and Applied Chemistry*, 70, 579–582.

Stanley, K. D., Golden, D. A., Williams, R. C., and Weiss, J. (2004). Inactivation of *Escherichia coli* O157:H7 by high-intensity ultrasonication in the presence of salts. *Foodborne Pathogens Disease*, 1, 267–280.

Tiwaria, B. K., O′Donnell, C. P., Muthukumarappana, K., and Cullen, P. J. (2009). Ascorbic acid degradation kinetics of sonicated orange juice during storage and comparison with thermally pasteurised juice. *LWT – Food Science and Technology*, 42, 700–704.

Ugarte-Romero, E., Feng, H., and Martin, S. E. (2007). Inactivation of *Shigella boydii* 18 IDPH and *Listeria monocytogenes* Scott A with power ultrasound at different acoustic energy densities and temperatures, *Journal of Food Science*, 72, 103–107.

Ugarte-Romero, E., Feng, H., Martin, S. E., Cadwallader, K. R., and Robinson, S. J. (2006). Inactivation of *Escherichia coli* with power ultrasound in apple cider. *Journal of Food Science*, 71, E102–E108.

U.S. Food and Drug Administration. (2001). Hazard analysis and critical control (HACCP). Procedures for the safe and sanitary processing and importing of juice. *Federal Register*, 66, 6137–6202.

Vago, R. E. (1992). An ultrasonic cleaner′s prime mover. Finishing, March, http://findarticles.com/p/articles/mi_hb4307/is_n3_v16/ai_n28614608/. Accessed July 7, 2010.

von Stockar, U., and Liu, J. S., (1999). Does microbial life always feed on negative entropy? Thermodynamic analysis of microbial growth. *Biochimica et Biophysica Acta*, 1412, 191–211.

von Stockar, U., Maskow, T., Liu, J., Marison, I. M., and Patino, R. (2006). Thermodynamics of microbial growth and metabolism; An analysis of the current situation. *Journal of Biotechnology*, 121, 517–533.

Wang, J. Hu, X., and Wang, Z. (2010). Kinetics models for the inactivation of *Alicyclobacillus acidiphilus* DSM14558(T) and *Alicyclobacillus acidoterrestris* DSM 3922(T) in apple juice by ultrasound. *International journal of food microbiology*, 139, 177–181.

Zenker, M., Heinz, V., and Knorr, D. (2003). Application of ultrasound-assisted thermal processing for preservation and quality retention of liquid foods. *Journal of Food Protection*, 66, 1642–1649.

Chapter 5
Wideband Multi-Frequency, Multimode, and Modulated (MMM) Ultrasonic Technology

Miodrag Prokic

1 Introduction

Until recently, traditional high-intensity and fixed-frequency ultrasound has been applied in fields such as cleaning, plastic welding, mixing, and homogenization. However, new industrial ultrasound-related applications, such as sonochemistry, extractions, and waste water treatment, among others, are becoming increasingly important, where traditional fixed-frequency ultrasonic systems are showing certain limitations.

Current ultrasonic applications are based on fixed-frequency, well-tuned ultrasonic sources where a number of design and matching parameters must be respected. These basic requirements limit large-scale and practical applications of the findings in laboratory-scale testing.

Extensive field tests conducted by experts in ultrasonics have demonstrated that in order to achieve a high efficiency treatment, ultrasonic systems must be well tuned to the load. Since most ultrasound units work inherently in non-stationary conditions, they must, in theory, continuously adapt themselves to the load to maximize efficiency, which is difficult to achieve with fixed-frequency units. To meet this challenge, multi-frequency, multimode, modulated (MMM) signal-processing techniques have been developed by MP Interconsulting (Prokic, 2001; Prokic and Sandoz, 2005).

As a result of this effort, MMM technology has become the first to achieve "wideband-frequency high-power ultrasonic agitation" in existing ultrasonic equipment, regardless of its mass, load size or particular operating conditions. In addition, the application of the new signal-processing techniques in existing systems does not involve significant design modifications.

M. Prokic (✉)
MP Interconsulting, Marais 36, 2400 Le Locle, Switzerland
e-mail: mpi@bluewin.ch

H. Feng et al. (eds.), *Ultrasound Technologies for Food and Bioprocessing*,
Food Engineering Series, DOI 10.1007/978-1-4419-7472-3_5,
© Springer Science+Business Media, LLC 2011

2 Background and Relevant Theories

In recent years, efforts have been made to explore the use of multi-frequency techniques to improve the efficiency of ultrasound treatments. A high-frequency ultrasonic field coupled with low-frequency stimulation can enhance cavitation effects with a sharp rise in both sub-harmonic and sono-luminescence intensity (Iernettia et al., 1997). A dual-frequency sonic processor has been modeled to control the mode and spatial distribution of cavitation events (Moholkar et al., 2000). Furthermore, cavitation can be enhanced by a multi-frequency sonication field in which orthogonal continuous ultrasound is applied (Feng et al., 2002). The spatial-temporal dynamics of cavitation bubbles in mono- and dual-frequency sonoreactors has also been analyzed (Servant et al., 2003).

MMM technology, on the other hand, does not focus on application of multiple ultrasound sources with different but fixed frequencies in sonication system design. Rather, it utilizes concepts from control theory, digital signal processing, and power electronics to improve the performance of an ultrasonic system and to extend its operating frequency bandwidth. In the following section, we provide a concise introduction to some of the concepts and key technologies that are used in MMM.

2.1 Closed-Loop Control

Consider an automobile's cruise control, which is a device designed to maintain a constant vehicle speed. The output variable of the system is vehicle speed. The input variable is the engine's throttle position, which influences engine torque output. A simple way to implement cruise control is to lock the throttle position when the driver engages cruise control. However, on hilly terrain, the vehicle will slow down going uphill and accelerate going downhill. This type of controller is called an open-loop controller because there is no direct connection between the output of the system and its input. In a closed-loop control system, a feedback controller monitors the vehicle's speed and adjusts the throttle as necessary to maintain the desired speed. This feedback compensates for disturbances to the system, such as changes in slope of the ground or wind speed (Fig. 5.1).

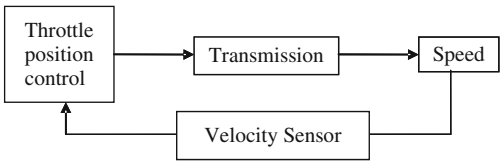

Fig. 5.1 Cruise control

Table 5.1 A summary of the traditional PLL concept (or ZPLL)

Input values, source CAUSE ⇒ (driving voltage)	Produced response CONSEQUENCE/s (output current)	Regulation method in order to obtain maximal active output power
Square (or sine) shaped driving-voltage on the output Power Bridge	Sinusoidal output current	To control the driving-voltage frequency in order to maintain stable phase difference between output load voltage and current signals.
Relatively stable driving frequency (or resonant frequency)	Load voltage and current have the same frequency	To control the current and/or voltage amplitude/s in order to get necessary Active Power Output (and to realize correct impedance matching)

Table 5.2 A summary of the new APT, multifrequency actuator concept (MMM technology) in relation to the average PLL or APLL concept

Input values, source CAUSE ⇒ (driving voltage)	Produced response CONSEQUENCE/s (output current)	Regulation method in order to obtain maximal active output power: The average phase difference between the output load current and voltage should be maintained stable (in a limited frequency interval).
Square-shaped voltage on the output Power Bridge: PWM + Band-Limited Frequency Modulation (+ limited phase modulation in some applications)	Multi-mode or single sinusoidal output current (or ringing decay current) with variable operating frequency + Harmonics	First PLL at resonant frequency: To control the central operating frequency (of a driving-voltage signal) in order to produce the Active Load Power to be much higher than its Reactive Power. To realize the maximal input (LF) power factor (Power Factor = cos $\theta = 1$).
Stable central operating, driving frequency + band-limited frequency modulation (+ limited phase modulation in some applications)	Stable mean operating (Load) frequency coupled with the driving-voltage central operating frequency, as well as with harmonics	To make that complete power inverter/converter look like resistive load to the principal Main Supply AC power input. To realize the maximal input (LF) power factor (Power Factor = cos $\theta = 1$).
Output transformer is "receiving" reflected harmonics (current and voltage components) from its load.	Particular frequency spectrum/s of a load voltage and current could sometimes cover different frequency ranges.	Second PLL at modulating (sub-harmonic) frequency: To control the modulating frequency in order to produce limited RMS output current, and maximal Active Power (on the load). To realize maximal input (LF) power factor (Power Factor = cos $\theta = 1$).

2.2 Phase-Locked Loop

A phase-lock or phase-locked loop (PLL) is an electronic control system that generates a signal that is locked to the phase of an input or "reference" signal. This circuit compares the phase of a controlled oscillator to the reference, automatically raising or lowering the frequency of the oscillator until its phase (and therefore frequency) is matched to that of the reference.

A phase-locked loop is an example of a control system using negative feedback. Phase-locked loops are widely used in radio, telecommunications, computers, and other electronic applications to generate stable frequencies, or to recover a signal from a noisy communication channel. Since a single integrated circuit can provide a complete phase-locked loop building block, the technique is widely used in modern electronic devices, with output frequencies from a fraction of a cycle per second up to many gigahertz (Fig. 5.2).

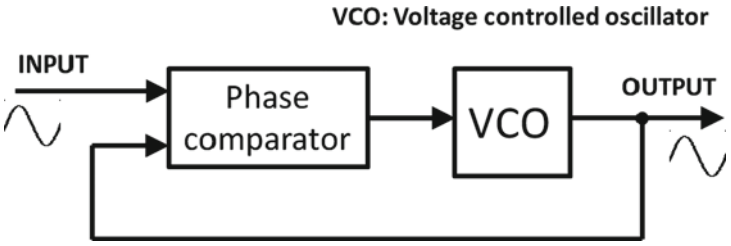

Fig. 5.2 A phase-locked loop (PLL) control

2.3 Pulse-Width Modulation (PWM) in Power Electronics

Pulse-width modulation (PWM) is one of the techniques used in power sources that involves modulation of its duty cycle to control the amount of power sent to a load. PWM uses a square wave with a duty cycle that is modulated, resulting in the variation of the average value of the waveform. If a square waveform $f(t)$ with a low value $y_{\min}$, a high value $y_{\max}$, and a duty cycle D is considered (see Fig. 5.3), the average value of the waveform is given by

$$\bar{y} = \frac{1}{T}\int_0^T f(t)dt \tag{5.1}$$

where $f(t)$ is a square wave, and its value is $y_{\max}$ for $0 < t < D \cdot T$ and $y_{\min}$ for $D \cdot T < t < T$. The above expression then becomes

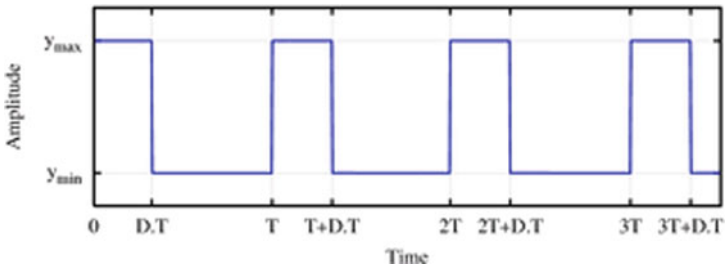

Fig. 5.3 Pulse-width modulation

$$\bar{y} = \frac{1}{T}\left(\int_0^{DT} y_{\max}\mathrm{d}t + \int_{DT}^{T} y_{\min}\mathrm{d}t\right) = \frac{D\cdot T\cdot y_{\max} + T\cdot(1-D)\cdot y_{\min}}{T} = D\cdot y_{\max} + (1-D)\cdot y_{\min} \tag{5.2}$$

This latter expression can be simplified in many cases where $y_{\min} = 0$ as $\bar{y} = D \cdot y_{\max}$. From this, it is obvious that the average value of the signal ($\bar{y}$) is directly dependent on the duty cycle D.

3 MMM System and How the MMM System Operates

3.1 System Components

An MMM system consists of (see Fig. 5.4a and b):

(A) A sweeping frequency, adaptively modulated waveform generated by an MMM ultrasonic power supply;
(B) High-power ultrasonic converter(s);
(C) Acoustical waveguide (metal bar), which connects the ultrasonic transducer to an acoustic load, an oscillating body, or a resonator;
(D) Acoustical load (mechanical resonating body, sonoreactor, radiating ultrasonic tool, sonotrode, test specimen, vibrating tube, solid or fluid medium, etc.); and
(E) Sensors of acoustical activity fixed on, in, or at the acoustical load (accelerometers, ultrasonic flux meters, laser vibrometer, etc.), which create regulation feedback between the acoustical load and ultrasonic power supply. In most cases *the piezoelectric converter can function as the feedback element*, thus avoiding the installation of other vibration sensors.

A mechanical coupling between the high-power ultrasonic converter (B) and the acoustical load (D) is realized with the metal bar as an acoustic waveguide (C). The

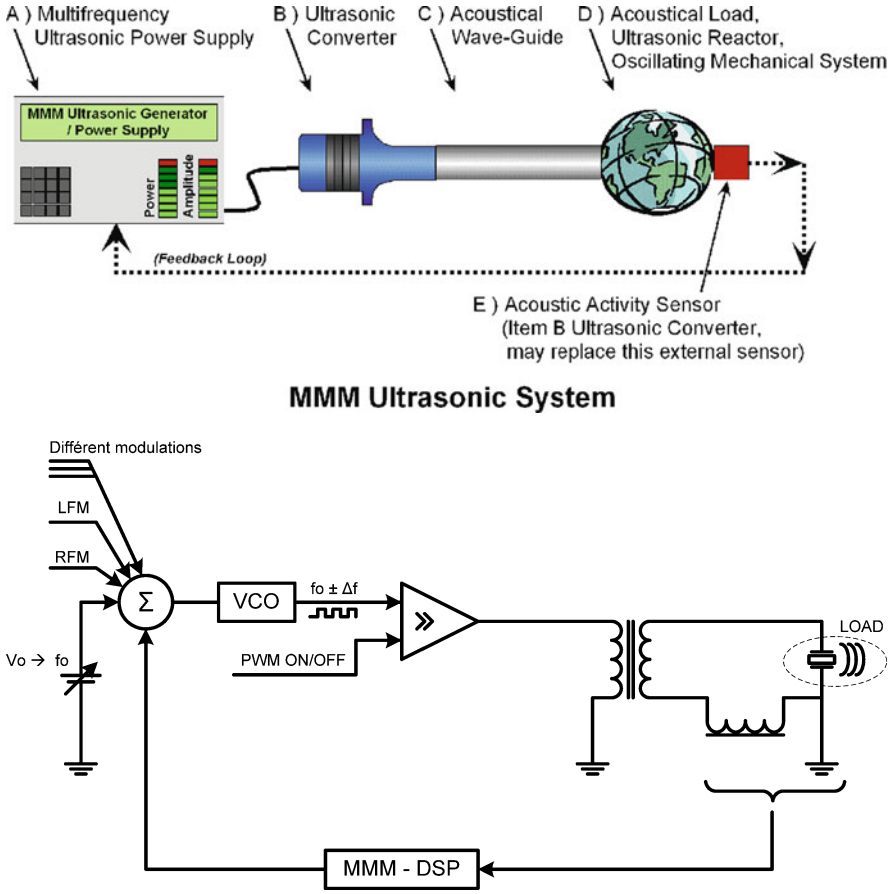

Fig. 5.4 (**a**) An MMM system. (**b**) MMM power supply block diagram. LFM – Low-frequency modulation, RFM – Randomized-frequency modulation; VCO – Voltage-controlled oscillator or DDS frequency source; and MMM–DSP – MMM digital signal processing

ultrasonic converter (B) is electrically connected to the ultrasonic multimode generator power supply (A). The acoustic activity sensor (E) relays physical feedback (for the purpose of process control) between the acoustical load (D) and the ultrasonic power supply (A).

3.2 Operation Mechanisms

As depicted in Fig. 5.4, the ultrasonic converter (B), driven by power supply (A), produces a sufficiently strong pulse-repetitive multifrequency train of mechanical oscillations or pulses. The acoustical load (D), driven by incoming frequency and amplitude-modulated pulse train starts to produce its own vibration and transient

response, oscillating in one or more of its natural vibration modes or harmonics. As the excitation changes, following the programmed pattern of the sweeping frequency pulse train, the amplitude in these modes will undergo exponential decay while other modes are excited. At the same time, the acoustic load will experience interference and superposition effects, which will generate new oscillatory products and dynamically modify its elastic and mechanical properties.

A simplified analogy is a single-pulsed excitation of a metal bell that will continue oscillating (ringing) on several resonant frequencies for a long period following the initial pulse. How long each resonant mode will continue to oscillate after a pulse depends on the mechanical quality factor for that mode.

3.2.1 Open-Loop Problems

Each mechanical system (in this case components B, C, and D) has many resonant modes (axial, radial, bending, and torsional) and all of these systems have higher frequency harmonics. Some of the resonant modes are well separated and mutually isolated, some of them are separated on a frequency scale but acoustically coupled, and some will overlap each other over a frequency range which tends to couple particularly well.

Since the acoustical load (D) is connected to an ultrasonic converter (B) by an acoustical waveguide (C), acoustical relaxing and ringing oscillations are traveling back and forth between the load (D) and ultrasonic converter (B), interfering mutually along the path of propagation. The best operating frequency of the ultrasonic converter (B) is normally found when the maximum traveling wave amplitude is reached and when a relatively stable oscillating regime is found, while the effects of thermal dissipation in all oscillating elements are minimal. The ultrasonic converter (B) is initially creating a sweeping frequency of repetitively pulsing mechanical excitation, resulting in generation of back-and-forth traveling waves, which can have much more complex frequency content because of the associated interference and superposition effects.

There is another important effect related to the ringing resonant system described above. An imminent and self-generated multifrequency Doppler effect (additional frequency shift, or frequency and phase modulation of traveling waves) can be created, since acoustical mirrors, (B) and (D), cannot be considered as stable infinite-mass solid plates. This self-generated and multifrequency Doppler effect is able to initiate different acoustic effects in the load (D), for instance, to excite several vibrating modes at the same time or to successively produce uniform amplitude distributions and phase shifts in the acoustic load (D).

3.2.2 Benefits of the Feedback Loop

It should be underlined that the oscillating system described here is different from the typical and traditional half-wave ultrasonic resonating system, where the total axial length of the ultrasonic system consists of an integer number of half-wavelengths. In MMM systems, the specific ultrasonic system geometry and

its axial (or any other) dimensions are not very important. Electronic multimode excitation continuously and automatically searches for the most convenient signal shapes in order to excite many vibration modes at the same time, and to make any mechanical system vibrate and resonate uniformly.

In addition to the effects described above, the ultrasonic power supply (A) is also able to produce variable frequency-sweeping oscillations around its central operating frequency, and has a phase and amplitude-modulated output signal, where the frequency of amplitude modulation follows sub-harmonic low-frequency vibrating modes. Thus, the ultrasonic power supply (A) is also contributing to the multi-mode ringing response or the self-generated multifrequency Doppler effect of an acoustical load (D). The ultrasonic system described here can drive an acoustic load (D) of almost any irregular shape and size. In operation, when the system oscillates, no stable nodal zones can be found because they are permanently moving as a result of the specific signal modulations coming from the MMM ultrasonic power supply (A).

It is important to note that by exciting the acoustical load (D), relatively stable and stationary oscillations and resonant effects at certain frequency intervals can be produced (Fig. 5.4a, b). However, a dangerous and self-destructive system response could be generated at other frequencies. The choice of the central operating frequency, sweeping frequency interval, and ultrasonic signal amplitudes from the ultrasonic power supply (A) are crucial to the operation of MMM systems. Because of the complex mechanical nature of different acoustic loads (D), the best operating regimes of the ultrasonic system must be carefully tested (B, C, D), starting with low driving signals (i.e., with low ultrasonic power). An initial test phase is thus required to select the best operating conditions, using a resistive attenuating dummy load in serial connection with the ultrasonic converter (A). This test phase minimizes the acoustic power produced by the ultrasonic converter and can also dissipate accidental resonant power. When the best driving regime is found, the dummy load can be disconnected and full electrical power can then be introduced into the ultrasonic converter.

3.2.3 Real-Time Load Parameter Estimation

In order to follow the evolving frequency of the load, certain real-time load parameter estimation mechanisms must be implemented in the power source to make proper adjustments. A quasi-instantaneous estimation of load parameters using band-limited Hilbert transformation was used in this study (Prokic and Sandoz, 2005). Figure 5.5 shows the basic block diagram that will be considered. The use of "Resonant Load" assumes that the global quality factor will be at least greater than or equal to 4.

Let $i(t)$ and $u(t)$ be expressed as follows:

$$i(t) = \hat{I}(t) \cos\left(2\pi fo\,(t)\, t + \phi_i\,(t)\right) \tag{5.3}$$

$$u(t) = \hat{U}(t) \cos\left(2\pi fo\,(t)\, t + \phi_u\,(t)\right) \tag{5.4}$$

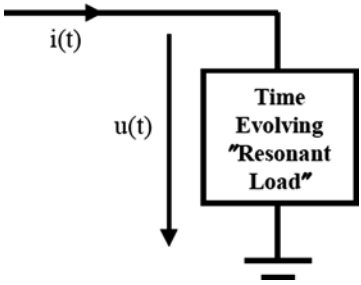

Fig. 5.5 Basic structure bloc diagram for time evolving resonant load

where $\hat{I}(t)$: instantaneous current envelope, $\phi_i(t)$: instantaneous current phase, $\hat{U}(t)$: instantaneous voltage envelope, $\phi_u(t)$: instantaneous voltage phase, and $fo(t)$: instantaneous driving signal frequency. It should be noted that all these instantaneous parameters are low-passed processes with cut-off frequencies well below $fo(t)$. Then, $i(t)$ and $u(t)$ can be represented in their respective analytical forms:

$$i(t) \Rightarrow i_{\text{analytic}}(t) = i(t) + j \cdot \tilde{i}(t) \tag{5.5}$$

$$u(t) \Rightarrow u_{\text{analytic}}(t) = u(t) + j \cdot \tilde{u}(t) \tag{5.6}$$

where

$$\tilde{i}(t) = \hat{I}(t) \sin(2\pi fo(t)\, t + \phi_i(t)) \tag{5.7}$$

$$\tilde{u}(t) = \hat{U}(t) \sin(2\pi fo(t)\, t + \phi_u(t)) \tag{5.8}$$

From trigonometric properties, the following relationships can be derived:

$$\sin(\phi_u(t) - \phi_i(t)) = \frac{i(t) \cdot \tilde{u}(t) - \tilde{i}(t) \cdot u(t)}{\sqrt{i(t)^2 + \tilde{i}(t)^2} \cdot \sqrt{u(t)^2 + \tilde{u}(t)^2}} \tag{5.9}$$

$$M_{stZ}(t) = \frac{\sqrt{u(t)^2 + \tilde{u}(t)^2}}{\sqrt{i(t)^2 + \tilde{i}(t)^2}} \tag{5.10}$$

The estimated load parameters are given by voltage and current phase difference $= \phi_{stZ}(t)$, i.e., "Short-Time" argument of the impedance, and ratio of voltage envelope to current envelope $= M_{stZ}(t)$, i.e., "Short-Time" magnitude of the impedance. Thus, $\phi_{stZ}(t)$ and $M_{stZ}(t)$ can be estimated in "Real-Time" with a minimum of basic arithmetic functions.

3.2.4 Band-Limited Hilbert Transformer

A band-limited Hilbert transformer (BL-HT) is realized with one second-order all-pass filters and two unit delay elements. This solution has the double advantage of simplicity and very low group delay. Figure 5.6 shows a structure in which

$$x\,(n) : \text{Input}, x_{\text{analytic}}\,(n) = x_{\text{Re}}\,(n) + j \cdot x_{Im}\,(n) \tag{5.11}$$

$$H\,(z) = \frac{-0.713 + z^{-2}}{1 - 0.713 \cdot z^{-2}} \tag{5.12}$$

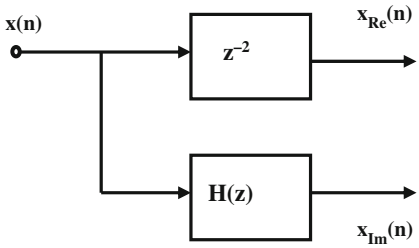

Fig. 5.6 Band-limited Hilbert transformation

An ideal HT has a 90° phase difference between its in-phase and quadrature outputs, i.e., between xRe(n) and xIm(n). Moreover, both output amplitude transfer functions are constant and independent of the frequency. This result is naturally the case with the structure shown in Fig. 5.6.

The BL-HT has the following parameters:

- sampling rate: 320 kHz
- frequency range: 16 kHz up to 25 kHz
- absolute phase error: less than 1 degree
- group delay: 6.25 μs (constant)

Even small changes in phase difference can be detected, which means that the "detectability" threshold is quite low with this method.

3.2.5 Maximum Active Power Tracking

The best operating ultrasonic regimes are those that produce very strong mechanical oscillations, or high and stable vibrating mechanical amplitudes, with moderate electric output power from the ultrasonic power supply. The second criterion is that thermal power dissipation on the total mechanical system continuously operating in air, with no additional system loading, is minimal. A low thermal dissipation in the mechanical system (B, C, D) indicates that the ultrasonic power supply (A) is driving the ultrasonic converter (B) with limited current and sufficiently high

voltage, delivering only the active or real power to a load. The multi-frequency ultrasonic concept described here is a Maximum Active Power Tracking System, which combines several PLL and PWM regulating loops.

In most traditional ultrasonic power supplies, the function of PLL is to keep the phase difference between electric current and voltage on ultrasonic converters close to zero, forcing the ultrasonic converter to maximize consumption of active or real power. Such resonant frequency control can be labeled as Zero-Phase-Locked Loop (ZPLL). Contrary to such traditional concepts, in MMM ultrasonic systems the average phase difference is kept stable and controllable inside certain frequency intervals, which can be called Average-Phase-Locked Loop (APLL). Averaged phase function or output voltage representing such frequency-modulated phase difference is frequency dependent, and if certain phase value is controlled to be inside certain frequency interval, control over average operating or driving frequency of the ultrasonic generator can be achieved at the same time. Since ultrasonic converter impedance is also frequency dependent, the converter or load current and voltage can also be controlled, and the control of the load power can be obtained by properly applying PWM power regulation concepts.

The actual size and geometry of the acoustical load are not directly or linearly proportional to the delivered ultrasonic driving power. It is possible that with a low-input ultrasonic power, a bulky mechanical system (B, C, D) can be strongly driven (in air, so there is no additional load), if the proper oscillating regime is found.

Traditionally, in high-power electronics, when driving complex impedance loads (like ultrasonic transducers) in resonance, a PLL (phase-locked loop) is related to a power control where the load voltage and current have the same frequency. In order to maximize the active load power, a zero-phase difference between time domain current and voltage signals is used to control the driving-voltage frequency. Switch-mode operating regimes are employed for driving half or full bridge or other output transistor configurations. The voltage on the output of the power bridge is square shaped (50% duty cycle), and current in the case of R-L-C resonant circuits as electrical loads, which have resistive, inductive, and capacitive elements, usually have a close to sinusoidal shape.

MMM technology uses active power tracking (APT) as the most general case for efficient transducer driving in the case of wide-frequency-band driving of complex R-L-C resonant circuits such as ultrasonic transducers, while maintaining stable average phase difference between the load current and load voltage.

The special MMM ultrasonic power supply in Fig. 5.4a and b delivers square-shaped PWM and modulated frequency output so that the output current presents multifrequency and multi-component signals. The objective in MMM regulation is to maximize the active load power, while not using the simple and traditional PLL concept in making the phase difference between the output voltage and current to be zero. The complex R-L-C oscillating circuits usually have coupled and mutually dependent sub-harmonics and higher frequency harmonics. They are also present at the load side, visible as load-current and load-voltage modulations. The discussions here deal with the time and frequency domains of real-time output-power

signals, as well as with time domains of corresponding load current and voltage signals and their harmonics. The APT effectively realizes closed-loop multiple PLLs and PWMs between output load signals and driving frequency modulating signal, combined with APLL or average phase PLL between the resonant frequency output load current and voltage. The second objective for APT is to force the power inverter/converter or MMM power supply to behave as a 100% resistive load (Power Factor $= \cos\theta = 1$) for a principal main AC power input.

4 Application of MMM Technology

Since MMM technology is based on different agitation mechanism and system designs, and does not depend on certain special system configurations, it is compatible with most existing applications with no major changes needed. MMM technology can be applied to virtually every area in which traditional ultrasonic technology is used. For instance, MMM technology has been applied to extrusion of composite plastic materials, cleaning processes using pressurized liquid carbon dioxide as a solvent, liquid waste material incineration assisted by an ultrasonic MMM atomizer, and continuous casting of molten metal for grain modifications. Small solid parts is successfully stress-relieved in MMM ultrasonic chambers, bringing in benefits such as increased fatigue limits, reduced cracking, artificial materials aging, increased dynamic load-bearing capacity, improved corrosion resistance, increased weld strength, and increased operating and service life. More information regarding the application of MMM in (a) ultrasonic cleaning, (b) treatment and testing, (c) powder sieving and screening, and (d) ultrasonic drawing, machining and extruding is given in the following sections.

4.1 Ultrasonic Cleaning with MMM Technology

Conventional ultrasonic generators drive the transducers at a fixed frequency without paying attention to the attached mechanical system including the steel tank, water, the parts loaded in the tank, and temperature. Each of these factors can significantly shift the resonant frequency of the transducers, and conventional ultrasonic generators are not equipped to adapt to the change. The problem is compounded because in industrial systems the load parameters continuously change. The result is inefficient transducer driving and reduced cavitation capabilities. Conventional fixed-frequency systems also create standing waves with areas of high acoustic activity and areas of low acoustic activity. When cleaning parts, the standing waves can over-treat or damage some areas while leaving other areas untreated. Some systems try to solve this problem with a small amount of generator frequency sweeping

around the fixed center frequency. This method helps, but does not normally correct the problem.

Unlike conventional systems, the flexibility of MMM generators starts with an adjustable primary frequency option. This feature allows us to consider shifts to the system resonance (e.g., 28 kHz shifting to 28.7 kHz) caused by the entire load factors. Such adjustment and fine tuning to the primary driving signal will greatly improve efficiency and system response.

Using a real-time feedback loop, the system creates an evolving and complex modulated multimode driving signal to stimulate coupled harmonics in the mechanical load (bath or chamber) to produce an effective wideband multi-frequency acoustic field from infrasonic up to the megahertz range. As a result, MMM systems using conventional transducers are capable of producing a very wide range of cavitation bubble sizes and a greater density of cavitation bubbles. This provides faster and better cleaning, faster sonochemical reactions, faster physical reactions, and faster liquid degassing. Furthermore, the unique modulation methods eliminate the standing waves typically seen in fixed-frequency systems. The strong and uniform acoustic field in an MMM cleaning unit will make it especially useful for food and food processing surface cleaning where microbial safety is the main concern (Fig. 5.7).

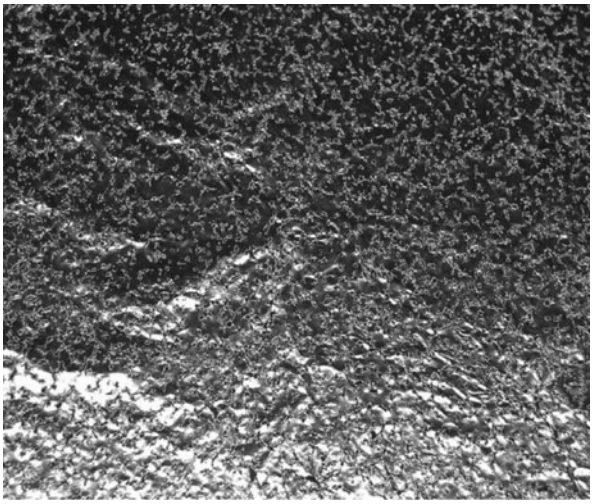

Fig. 5.7 MMM-treated aluminum foil for 5–10 s

4.2 Ultrasonic Treatments and Screening Using MMM Technology

MMM is used in a number of treatments and screening applications, which may find applications in the fabrication of food processing equipment. For instance,

an improved coating of metal parts under vibrations can be achieved by immersion in coating liquid and/or by dry ball peening in an MMM ultrasonic chamber. In coating applications, deeper coating and particle implementation can be realized. An accelerated stabilization of the coating layer is also observed. In treating welds by ultrasonically vibrating the parts, an extension of fatigue life of welds several times (3–5 times) can be obtained. Such treatment also causes a redistributing and minimizing of stress concentration caused by welding. A shot peening was used in applications where the effects of fatigue were caused by grinding, electrical discharge- and electrochemical-machining (EDM and ECM), electroplating, anodizing, thermal spraying, and welding. It also can help increase resistance to fretting, galling, cavitation erosion, stress-corrosion cracking, intergranular corrosion, and hydrogen embitterment.

4.3 Ultrasonic Powder Sieving and Seed Processing

Sieving is an important unit operation in flour processing. For traditional fixed-frequency ultrasonic sieving systems, the generators and the ring resonators must be tuned to operate at the system resonant frequency. In comparison, properly adjusted MMM ultrasonic generators can stimulate highly efficient wideband (sonic to megahertz) acoustic energy to nearly any sieve or screen shape. Wideband (sonic to megahertz) acoustic energy provides greater sieve/screen stimulation to improve process volumes (kg/h), beyond the limitations of standard fixed-frequency systems. MMM eliminates the standing waves seen in fixed-frequency systems, which reduces bending in low amplitude nodal points and damage to screens at high amplitude nodal points. Normal MMM factory options allow for system resonant frequency adjustment within a 12 kHz window (e.g., 25–37 kHz). Such agility allows fine tuning for optimum performance.

Ultrasound is an excellent method for agitating powders, seeds, and fluids. With MMM technology, it is easy to make large arbitrarily shaped (un-tuned) mechanical elements vibrate at ultrasonic frequencies. Normal ultrasonic generator systems cannot make the transition because they rely on carefully tuned mechanical elements of fixed size and shape that limit the scope of their use in large-scale applications.

4.4 Ultrasonic Drawing and Extruding

Application of ultrasonic extrusion and drawing include food extrusion, plastic extrusion, metal extrusion, glass extrusion, tube extrusion, wire drawing, glass drawing, and fiber-optic drawing. MMM ultrasonic generators have the unique ability to apply high-power ultrasonic energy to large mechanical systems like extruder heads and drawing dies, which will help to reduce friction between the tool and the extruded or drawn material, improve material flow, improve surface quality of extruded or drawn material, and reduce pressure. In the case of drawing, less

Fig. 5.8 Example plastic extruder head

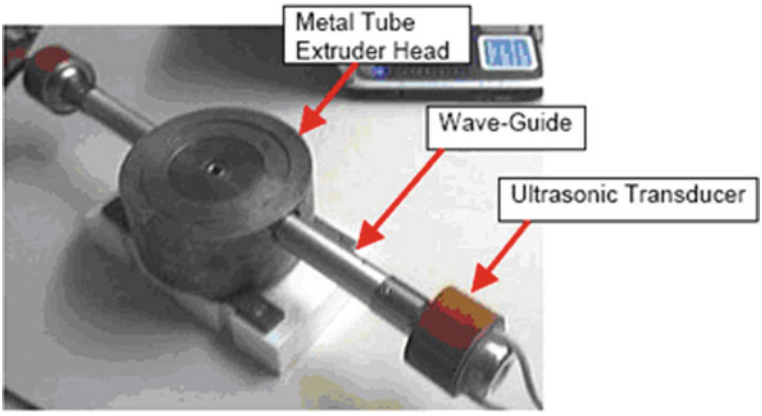

Fig. 5.9 Tube extruder die shown with dual driving transducers

breakage will improve production yield. In some processes the material structural characteristics may be improved (Figs. 5.8 and 5.9).

5 Conclusions

MMM technology, as a new method to continuously change ultrasound frequency in both time domain and frequency domain, provides numerous possibilities to fully utilize the potential of acoustic energy. It is foreseeable that MMM will find more applications in the food and bio-processing industries.

References

Feng, R., Zhao, Y., Zhu, C., and Mason, T. J. (2002). Enhancement of ultrasonic cavitation yield by multi-frequency sonication. *Ultrasonics Sonochemistry*, 9, 231–236.

Iernettia, G., Ciutia, P., Dezhkunovb, N. V., Realic, M., Francescuttod, A., and Johrie, G. K. (1997). Enhancement of high-frequency acoustic cavitation effects by a low-frequency stimulation. *Ultrasonics Sonochemistry*, 4, 263–268.

Moholkar, S., Rekveld, S., and Warmoeskerken, G. (2000). Modeling of acoustic pressure fields and the distribution of the cavitation phenomena in a dual frequency sonic processor. *Ultrasonics*, 38, 666–670.

Prokic, M. (2001). Multifrequency ultrasonic structural actuators. *European Patent Application* EP1238715. 2001.

Prokic, M., and Sandoz, J. P. (2005). *Innovative MMM technology for implementing power ultrasonic technique in food-processing industry*. New Orleans, LA, Institute of Food Technologists Annual Meeting, July 2005.

Servant, G., Laborde, J. L., Hita, A., Caltagirone, J. P., and Gerad, A. (2003). On the interaction between ultrasound waves and bubble clouds in mono- and dual-frequency sonoreactors. *Ultrasonics Sonochemistry*, 10, 347–355.

Chapter 6
Application of Hydrodynamic Cavitation for Food and Bioprocessing

Parag R. Gogate

1 Introduction

Cavitation is defined as the combined phenomena of formation, growth and subsequent collapse of microbubbles or cavities occurring over an extremely small interval of time (milliseconds), releasing large magnitudes of energy at the location of transformation. Very high energy densities (energy released per unit volume) are obtained locally, resulting in high pressures (of the order of 100–5,000 bars) and temperatures (in the range of 1,000–10,000 K), and these effects are observed at millions of locations in the reactor (Suslick, 1990). Cavitation also results in the formation of highly reactive free radicals, continuous cleaning, as well as an increase in the surface area of the solid catalysts and enhancement in mass transfer rates due to turbulence generated as a result of liquid circulation currents (Luche, 1999; Mason and Lorimer, 1988). Cavitation is generally classified into four types based on the mode of generation, viz. acoustic, hydrodynamic, optic, or particle, but only acoustic and hydrodynamic cavitation have been found to be efficient in bringing about the desired chemical/physical changes in processing applications, whereas optic and particle cavitation are typically used for single bubble cavitation, which fails to induce any physical or chemical change in the bulk solution. The spectacular effects of cavitation phenomena generated using ultrasound (acoustic cavitation) has been effectively harnessed in physical and chemical processing applications in food and bioprocessing industries (Mason and Lorimer, 2002; Povey and Mason, 1998). Similar cavitation phenomena can also be generated relatively easily in hydraulic systems. Engineers have generally been looking with caution at cavitation in hydraulic devices due to problems of mechanical erosion and initial efforts to understand it were aimed at the objective of suppressing it, in order to avoid the erosion of exposed surfaces (Chatterjee and Arakeri, 1997). However, a careful design of the system allows generation of cavity collapse conditions similar to acoustic

P.R. Gogate (✉)
Chemical Engineering Department, Institute of Chemical Technology,
Mumbai, Matunga 400 019, India
e-mail: pr.gogate@ictmumbai.edu.in

H. Feng et al. (eds.), *Ultrasound Technologies for Food and Bioprocessing*,
Food Engineering Series, DOI 10.1007/978-1-4419-7472-3_6,
© Springer Science+Business Media, LLC 2011

cavitation, thereby enabling different applications requiring different cavitational intensities, which have been successfully carried out using acoustic cavitation phenomena but at much lower energy inputs compared to sonochemical reactors. In the last decade, concentrated efforts have been made by a few researchers around the world to harness the spectacular effects of hydrodynamic cavitation for chemical/physical transformation (Gogate and Pandit, 2001). The current chapter aims at highlighting different aspects related to hydrodynamic cavitation, including the theoretical aspects for optimization of operating parameters, reactor designs, and overview of applications relevant to food and bioprocessing. Some case studies highlighting the comparison of hydrodynamic cavitation and acoustic cavitation reactors will also be discussed.

2 Generation of Hydrodynamic Cavitation

Hydrodynamic cavitation can be simply generated by the passage of liquid through a constriction such as orifice plate, venturi, or throttling valve. When the liquid passes through the constriction, the kinetic energy/velocity of the liquid increases at the expense of the local pressure at the constriction. If the throttling is sufficient to cause the pressure around the point of vena contracta to fall below the threshold pressure for cavitation (usually vapor pressure of the medium at the operating temperature), cavities are generated. Subsequently, as the liquid jet expands, the pressure recovers and this results in the collapse of the cavities. During the passage of the liquid through the constriction, boundary layer separation occurs and a substantial amount of energy is lost in the form of permanent pressure drop. Very high intensity fluid turbulence is also generated downstream of the constriction; its intensity depends on the magnitude of the pressure drop and the rate of pressure recovery, which, in turn, depends on the geometry of the constriction and the flow conditions of the liquid, i.e., the scale of turbulence. The intensity of turbulence has a profound effect on the cavitation intensity, as shown by Moholkar and Pandit (1997). Thus, by controlling the geometric and operating conditions of the reactor, one can produce the required intensity of the cavitation so as to bring about the desired physical or chemical change with maximum energy efficiency.

A dimensionless number known as the cavitation number (C_v) has generally been used to relate the flow conditions with the cavitation intensity (Save et al., 1997; Yan et al., 1988):

$$C_v = \frac{P_2 - P_\mathrm{v}}{\frac{1}{2}\rho v_\mathrm{o}^2}$$

where P_2 is the fully recovered downstream pressure, P_V is the vapor pressure of the liquid, and v_o is the velocity of the liquid at the constriction. The cavitation number at which the inception of cavitation occurs is known as the cavitation inception number C_vi. Ideally, cavitation inception occurs at $C_\mathrm{vi} = 1$ and there are significant

cavitational effects at C_v less than 1. However, cavitation has been found to occur at a higher cavitation number (in the range 2–4), also possibly due to the presence of dissolved gases or some impurities in the liquid medium. Yan and Thorpe (1990) have also shown that C_{vi} is a function of the flow geometry and usually increases with an increase in the size of the constriction. Moreover, comparison of experimental data of Yan and Thorpe (1990) for pipe diameter of 3.78 cm with the data of Tullis and Govindrajan (1973) for pipe diameters of 7.80 and 15.4 cm indicates that the cavitation inception number is a strong function of the pipe diameter also, and that it increases with an increase in the pipe diameter. This can be attributed to the fact that with an increase in the diameter of the pipe, the length scale of turbulence increases, thereby increasing the fluctuating velocity component (level of fluid turbulence downstream of the constriction) at same operating pressure drop. Though cavitation can be achieved even at higher cavitation numbers, for maximum benefit from the reactor, the flow conditions and the geometry should be adjusted in such a way that the cavitation number lies in the range of 0.1–1 as very low operating cavitation numbers can lead to super-cavitation resulting in vapor locking and no cavitational collapse (Yan and Thorpe, 1990).

3 Design of Hydrodynamic Cavitation Reactors

It is always important to choose an optimum design configuration of the hydrodynamic cavitation reactor so as to maximize the cavitational effects and result in cost-effective operation. In this section, we will discuss the available reactor configurations and give some guidelines, based on theoretical analysis coupled with experimental results, for selection of optimum design and operating parameters. A methodology will also be proposed for the development of design equations, which can be very useful in the scale-up of hydrodynamic cavitation reactors.

3.1 Hydrodynamic Cavitation Reactor Configurations

Hydrodynamic cavitation reactors are much simpler to design, and also the scale-up is quite easy as compared to their acoustic counterparts. The various laboratory scale/pilot plant scale reactors that have been used to study different applications of the cavitation process have been discussed with relative merits and demerits (Gogate and Pandit, 2001). Some advantages of hydrodynamic cavitation reactors, in general, as compared to sonochemical reactors, can be given, such as (a) cavitation is uniform throughout the reactor due to efficient mixing, and hence there is no problem of directional sensitivity; (b) cavitation is at the shear layer of the bulk liquid, and hence metal erosion problems are less severe; and (c) quantification and control over the design parameters is relatively easy, leading to optimization of the required cavitating conditions.

3.1.1 Liquid Whistle Reactors

The first reactor operation on the principle of hydrodynamic cavitation was conducted using a liquid whistle reactor, as depicted in Fig. 6.1. One of the primitive uses of this type of reactors was mixing and homogenization. Here, vibrations are generated in a steel plate as liquid passes over it at high velocity. The liquid couples itself with the vibrations to produce cavitation in the flow, which results in highly efficient mixing. The major feature of the operation of liquid whistle reactors is that the transfer of power is reversed, i.e., power is transferred from the medium to the device. However, these reactors suffer from shortcomings such as very low vibrational power, unavailability of an optimum irradiation frequency in the case of viscous materials, and high pumping costs as well as erosion of the vibrating blade in the presence of particulate matter. Also, the reactor configuration does not offer flexibility in terms of selecting different operating geometries for controlling the cavitational intensity in the hydrodynamic cavitation reactor.

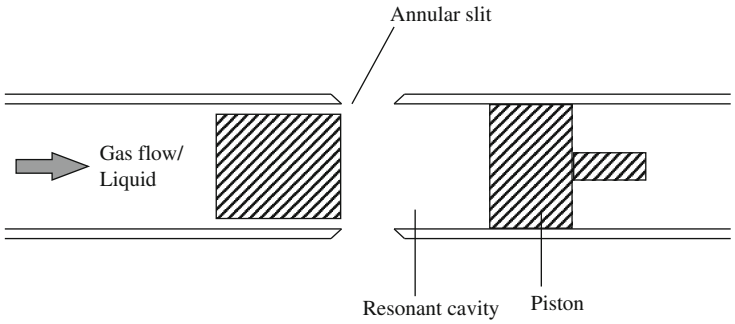

Fig. 6.1 Schematic representation of a liquid whistle reactor

3.1.2 High-Pressure Homogenizer (HPH)

The high-pressure homogenizer (HPH) is basically a high-pressure positive displacement pump with a throttling device that operates according to the principle of high-pressure relief technique. Typically, a high-pressure homogenizer reactor consists of a feed tank and two throttling valves designated as first stage and second stage (Fig. 6.2). The liquid from the feed tank is driven by a pump to the first stage valve. Pressure up to 1,000 psi can be attained by throttling this valve. Further increase in pressure is achieved by using the second stage valve. Upstream pressure up to 10,000 psi can be obtained in the second stage. From the second stage valve, the liquid is released into a low pressure region with the use of different types of pressure release valves and is then re-circulated back to the feed tank. With an increase in the throttling pressure, there is a rise in the temperature of the liquid. To maintain the temperature at ambient conditions, a coil immersed in the feed tank

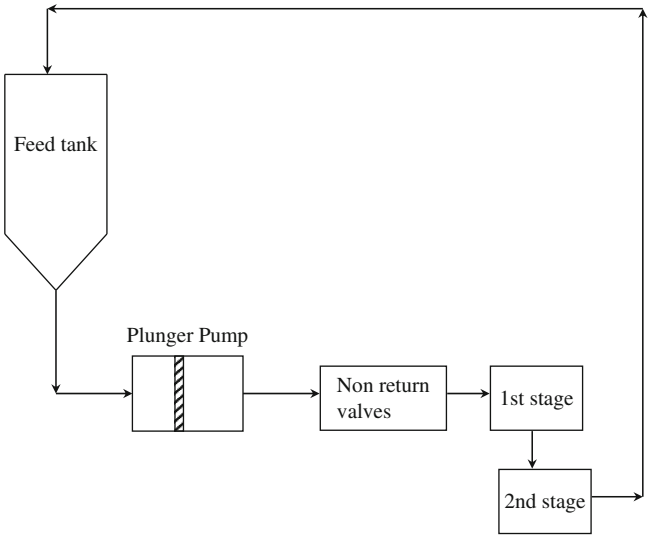

Fig. 6.2 Schematic representation of flow loop in a high-pressure homogenizer

can be used through which cooling water is circulated. There is a critical discharge pressure at which cavitation inception occurs and significant cavitational yields are obtained beyond this discharge pressure. It should also be noted that the value of critical discharge pressure leading to the desired cavitational effect is further dependent on the type of application and the geometry of the throttling valve. Shirgaonkar et al. (1998) have used these reactors for cell disruption purposes and reported that operating pressures up to 4,000 psi are not very effective either in disrupting yeast cells or in iodine liberation, whereas at a discharge pressure of 5,000 psi, substantial cell disruption and iodine liberation occur, which has been attributed to onset of cavitation phenomena.

HPH are especially suitable for the emulsification processes in the food, pharmaceutical, and bioprocess industries. Again, there is not enough control over the cavitationally active volume and the magnitude of the pressure pulses that will be generated at the end of the cavitation events (cavitational intensity).

3.1.3 High-Speed Homogenizer (HSH)

Cavitation can also be generated in rotating equipment. When the tip speed of the rotating device (impeller) reaches a critical speed, the local pressure near the periphery of the impeller falls and gets closer to the vapor pressure of the liquid. This results in the generation of vaporous cavities. Subsequently, as the liquid moves away from the impeller to the boundary of the tank, the liquid pressure recovers at the expense of the velocity head. This causes the cavities that have travelled with the liquid bulk to collapse. A high-speed homogenizer utilizes the above principle.

A high-speed homogenizer usually consists of a stator–rotor assembly preferably made of stainless steel, with flexibility of design of stators and rotors. A plate with holes attached to the stator can be provided for inserting baffles so as to avoid vortex formation and surface aeration in the bulk liquid. The speed of rotation of the homogenizer can be varied by changing the applied voltage on the power supplier.

Kumar and Pandit (1999) found that the critical speed for the inception of cavitation to occur is 8,500 rpm for the size and geometry of the stator–rotor used by them and it depends upon the dissolved gas content. Thus, the operation of the high-speed homogenizers should occur at speeds higher than the critical speeds, and at such high speeds the energy consumption is large. Kumar and Pandit (1999) successfully carried out degradation of potassium iodide to liberate iodine, which is a true indication of the fact that cavitation is occurring in the reactor under the given set of operating conditions. Shirgaonkar et al. (1998) used these reactors for cell disruption purposes and reported similar inception of cavitation phenomena at 8,500 rpm as indicated by significant release of the intracellular proteins beyond an operating speed of 8,500 rpm.

It should be noted that the energy consumption in these types of reactors is much higher and also flexibility over the design parameters is hardware dependent as compared to reactors based on the use of multiple plate orifice plates, which will be discussed later.

3.1.4 Microfluidizers

The advent of high-pressure jet fluidizers capable of pressure drops as high as 2 kbar and jet velocities approaching 200 m/s has led to numerous applications such as emulsification, cell disruption, etc. Suslick et al. (1997) used micro-jet fluidizers (air-driven model M-110Y from Microfluidics International Corp., 30, Ossipee Rd., Newton, MA 02164) for the decomposition of aqueous KI solutions to liberate iodine with conditions of 1.24 kbar liquid inlet pressure and velocities of 190 m/s. A portion of the reaction solution is pressurized by a large pneumatically driven pump into an interaction chamber, where two pulsed flows are redirected at each other through jewel orifices with velocities of 190 m/s controlled by a back pressure regulator. Cavitation occurs when there is sufficient turbulence upon the liquid jet impact or a sufficient pressure drop is created as the streams pass through the orifices. High-velocity pumping results in heating of the liquid medium; hence, the reactor along with the accessories is immersed in a thermally equilibrated bath. The cavitation inception was obtained at inlet pressure of 150 bar.

No quantitative data has been available until now on the energy efficiency of microfluidizers as compared to sonochemical reactors; and Suslick et al. (1997) showed that the rates of Weissler reaction are much lesser in these types of reactors as compared to acoustic cavitation. Also, the data regarding the flexibility of geometric conditions in terms of the orifices to generate cavitation of different intensities is lacking in the current literature.

3.1.5 Orifice Plates Setup

In this type of reactor, the flow through the main line passes through a constriction where the local velocities suddenly rise due to a reduction in the flow area resulting in lower pressures, which may even go below the vapor pressure of the liquid medium generating the cavities. The constriction can be a venturi (Kumar and Pandit, 1999), a single hole orifice (Yan et al., 1988), or multiple holes on an orifice plate (Senthilkumar et al., 2000). One such setup that has been designed and built with the help of local fabricators is described in detail below to provide an idea about the constructional features of the system.

Figure 6.3 gives the schematic representation of the experimental setup. The setup consists of a closed loop circuit comprised of a holding tank of 50 l volume, a centrifugal pump (2,900 rpm, 5.5 kW, Calama Industries Ltd., India), control valve, and flanges to accommodate the orifice plates. The suction side of the pump is connected to the bottom of the tank. The discharge from the pump branches into two lines that help to control the inlet pressure and the inlet flow rate into the main line with the help of valves V_2 and V_3. Care should be taken that the liquid lines must terminate well inside the tank, below the liquid level in order to avoid any induction of air into the liquid due to plunging liquid jets. The main line consists of a flange to accommodate the orifice plates, along with a hard glass tube next to these plates to make a visual observation easier. The holding tank is provided with a cooling jacket to control the temperature of the circulating liquid. The inlet pressure and the fully recovered downstream pressure can be measured with the pressure gauges P_1 and P_2, respectively.

Multiple hole orifice plates having different combinations of number and diameter of holes, varying free area offered for the flow, are represented in Fig. 6.4.

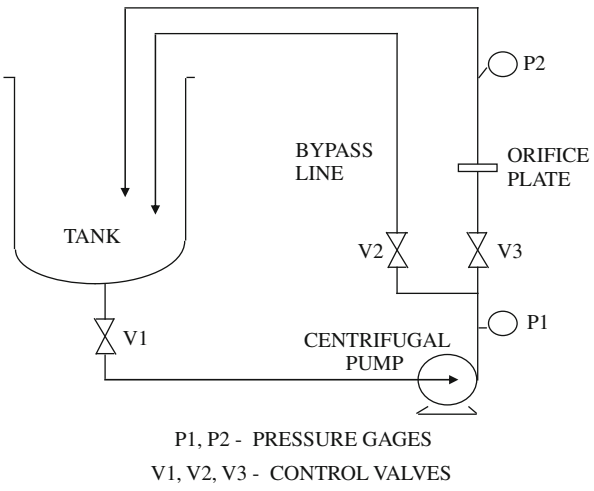

Fig. 6.3 Orifice plate hydrodynamic cavitation setup

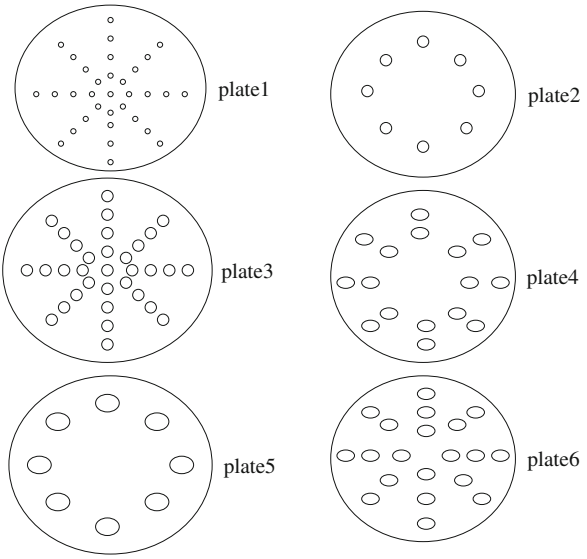

Fig. 6.4 Multiple hole orifice plates having different combinations of number and diameter of holes

Such an arrangement helps to achieve different intensities of cavitation, and also the number of cavitational events generated in the reactor is different. Thus, the setup described above presents tremendous flexibility in terms of the operating (control of inlet pressure, inlet flow rate, temperature) and geometric parameters (different arrangements of holes on the orifice plates). Thus, depending on the type of application and requirements, suitable geometry and operating conditions can be selected in the hydrodynamic cavitation reactor. For example, cell disruption requires milder cavitational intensity, whereas microbial disinfection of mixed culture microorganisms would require very high cavitation intensities. Some recommendations for selection of the operating parameters for achieving desired cavitational intensity are discussed later in this chapter. It should also be noted here that although this design has been reported to be efficient in different hydrodynamic cavitation applications, its commercialization is only in the initial stages in the area of ballast water treatment and elimination of biofouling of cooling towers, as reported by HyCa Technologies (www.hyca.co.in).

Sampathkumar and Moholkar (2007) recently put forth a conceptual design of a novel hydrodynamic cavitation reactor that uses a converging–diverging nozzle for creating pressure variation in the flow necessary for driving bubble motion instead of the orifice plates as discussed earlier. The cavitation bubbles or nuclei are introduced in the water flow externally, upstream of the nozzle, using a sparger. Different gases can be used for the introduction of bubbles. Also, the size of the gas distributor (usually a glass frit), flow rate of gas, and the pressure of gas in the reservoir (or source) from which gas is withdrawn can be suitably controlled to control the initial size of the cavitational nuclei, which significantly affects the resultant cavitational intensity. The aim should be to generate the smallest size of nuclei as possible to

maximize the intensity and hence the net cavitational effects. With numerical simulations, it has been shown that this design is able to produce a cavitation effect of moderate intensity sufficient for processes such as microbial cell disruption, water disinfection, etc. The results of the simulation show that a transient motion of the bubbles can be obtained with the converging–diverging nozzle, giving rise to radical formation in the bubble that induces the cavitational effect. The temperature peaks attained in the bubble in a nozzle flow are somewhat lower than those attained in an orifice flow, where temperatures on the order of ~5,000 K are seen. The maximum temperature peak that was seen among all parameter sets of simulations was 2,124 K. Thus, the cavitation intensity generated by bubbles in a nozzle flow is moderate, which is only suitable for conducting milder processes. Further, use in applications requiring varied cavitational intensity might be limited, as the length and diameter of the nozzle are the only geometric parameters that can be varied in this case, whereas the number, size, and shape of the holes in the case of the orifice plate can be varied for controlling the intensity of cavitation produced downstream of the orifice plate.

From the above discussion about various reactors, it can be easily concluded that the orifice plate setup offers maximum flexibility and can be used for a large range of applications ranging from cell disruption to microbial disinfection in water, as well as liquid foods, and can also be operated at relatively larger scales of operation. It should also be noted that the scale-up of such reactors is relatively easier as the efficiency of the pump increases with an increase in size (flow rate and discharge rate), which will necessarily result into higher energy efficiencies. In earlier work (Gogate et al., 2001), it has been clearly pointed out that the energy efficiency (indicating the transfer of the supplied electrical energy into the available energy for the cavitation phenomena) for the pilot plant scale orifice plate setup is 10 and 30% higher as compared to high-pressure and high-speed homogenizer, respectively. Gogate et al. (2001) have also shown that the net cavitational effects quantified in terms of the extent of iodine released are also higher in an orifice plate setup as compared to other two devices generating hydrodynamic cavitation.

3.2 Optimization of Hydrodynamic Cavitation Reactors Using Bubble Dynamics Studies

The bubble behavior and hence the pressure pulse generated at the collapse of the cavity in the case of hydrodynamic cavitation depends upon the operating conditions as well as the geometry of the mechanical constriction, which results in the generation of cavitating conditions downstream of the constriction. Thus, as a first step towards achieving efficient and optimum design of hydrodynamic cavitation reactors, it is important to understand the relationship between cavity behavior and the operating parameters and to attempt to quantify the intensity of cavitation and the net cavitational effects as a direct function of the operating parameters. The following sections deal with bubble dynamics analysis, starting from a basic single

cavity approach and extending to a more realistic cluster approach (details about the modeling aspects and the simulation strategies have not been mentioned here but can be obtained from the illustrated references).

3.2.1 Single Cavity Approach

Gogate and Pandit (2000) numerically investigated the effect of operating parameters such as inlet pressure through the system of orifice, initial cavity size, and the diameter of the hole on the orifice plate (which affects the frequency of turbulence in the vicinity of the orifice) on cavity behavior. The simulation of bubble dynamics has been conducted in two stages, first considering a Rayleigh-Plesset equation up to the point of bubble wall velocity = 1,500 m/s, and then the compressibility of medium has been considered in the form of the equation of Tomita and Shima (1986). The details of these equations, underlying assumptions, and solution strategies can be referenced in the work of Gogate and Pandit (2000). The trends obtained from the simulations have been compared with experiments using degradation of potassium iodide as a model reaction, and it has been seen that the numerical trends in the variation of the magnitude of collapse pressure with the variation in the operating parameters match the observed experimental results. Based on the results of these simulations and subsequent comparison with the experimental results, the following design considerations for achieving maximum benefits have been established:

(1) Inlet pressure into the system/rotor speed depending on the type of equipment: Use increased pressures or rotor speed, but avoid super-cavitation by operating below a certain optimum value. Some guidelines about the onset of super-cavitation phenomena and the dependency of the critical operating pressure on the system parameters can be obtained from the work of Yan and Thorpe (1990). It has been observed in the case of experiments with KI decomposition that the cavitational yield decreases when inlet pressure is increased beyond 40 psig (value is specific for the configuration and reaction, as described in the work of Vichare et al. (2000)).
(2) Physicochemical properties of the liquid and initial radius of the nuclei: It is important to have lower initial sizes of the cavitational nuclei in the reactor, and the liquid phase physicochemical properties can be suitably adjusted (use liquids with low vapor pressure, moderate viscosity, and higher surface tension so as to achieve violent collapse of the cavities). Table 6.1 gives some guidelines for selection of liquid physicochemical properties for optimum performance of hydrodynamic cavitation reactors.
(3) Geometry of the constriction: Free area available for the flow, i.e., the ratio of total cross-sectional area of holes on the orifice plate to the total cross-sectional area of the pipe, plays a crucial role in deciding the extent of cavitational intensity. Lower free areas must be used for producing high intensities as the rate and magnitude of pressure recovery affects the dynamics and the collapse of the cavities and hence the desired beneficial effects. Experiments with iodine liberation (Vichare et al., 2000) have indicated that an increase in the free area

Table 6.1 Effect of liquid phase properties on the performance of hydrodynamic cavitation reactors

Sr. No.	Liquid property	Effects	Favorable conditions
1.	Dissolved gas		
	A. Solubility	Gas content, nucleation, collapse phase	Low solubility
	B. Polytropic constant and thermal conductivity	Intensity of cavitation events	Gases with higher polytropic constant and lower thermal conductivity (monatomic gases)
2.	Liquid vapor pressure	Cavitation threshold, Intensity of cavitation, rate of chemical reaction	Liquids with low vapor pressure
3.	Viscosity	Transient threshold	Low viscosity
4.	Surface tension	Size of the nuclei (cavitation threshold)	Low surface tension
5.	Bulk liquid temperature	Intensity of collapse, rate of reaction, threshold/ nucleation, almost all physical properties	Optimum value exits, generally lower temperatures preferable
6.	Surfactants and electrolytes	Cavitation threshold, reaction kinetics	Case study of each system necessary to ascertain exact nature of the effect
7.	Solid constituents	Cavitation threshold/ nucleation, attenuation of sound intensity	Low concentrations
	Immiscible liquid phase	Interfacial cavitation, number of bubbles per unit volume, reaction kinetics	Depends on nature of the system

from 25 to 140 mm^2 decreases the cavitational yield by one order of magnitude. Also, for the same free area, the distribution of holes on the orifice plate, in the case of a multi-hole orifice plate, should be selected in such a way that large number of smaller diameter holes should be used in the system.

An empirical correlation developed by Gogate and Pandit (2000) for the prediction of the collapse pressure (P_C) as a function of the above-mentioned parameters is worth mentioning here as it forms the basic step toward the development of generalized design equations:

$$P_C = 7527\ (F)^{-2.55} \times \{(P_1)^{2.46}(R_o)^{-0.80}(d_o)^{2.37}\}$$

The above correlation uses the initial cavity size in units of millimeters, inlet pressure in units of atmospheres, the diameter of the hole in the orifice plate in units of millimeters, and free area as a percentage of the total cross-sectional area of the pipe, while the collapse pressure is given in terms of atmospheres and is developed over the following range of operating parameters.

Initial cavity size (R_o) = 0.01 to 0.1 mm (The initial cavity size formed (maximum) can be estimated from the critical Weber number concept at the operating orifice jet velocities).

Inlet pressure (P_I) = 1–8 atmospheres
Diameter of the orifice (d_o) = 1−3 mm
Percentage free area of the holes (F) = 1−20% of the pipe cross-sectional area

The proposed equation is by no means a generalized one, but it illustrates the dependency of the cavitational intensity on the operating parameters in a quantitative manner.

3.2.2 Improvement in the Bubble Dynamics Model Considering Bubble/Bubble and Bubble/Flow Interactions

The earlier model based on a single cavity does not consider the interactions of the cavitating bubble with the neighboring bubbles as well as the changing nature of the liquid flow. To attain a more realistic picture of the cavitating conditions, Moholkar and Pandit (2001b) modified the model to consider these interactions for a venturi type reactor, and the effect of operating parameters such as downstream pressure recovery, venturi to pipe area ratio, initial bubble void fraction in the liquid, and the initial bubble size in the flow on the dynamics of the flow has been studied. Based on the results obtained in the simulations, the following recommendations for the efficient design of hydrodynamic cavitation reactor (where mechanical constriction is venturi type) can be made:

1) A rise in the discharge pressure and hence the final recovery pressure results in reduced bubble cluster life and hence a decrease in the cavitationally active volume downstream of the throat of the venturi where the cavitational effects can be observed, though the cavitation intensity in this reduced volume represented by the magnitude of the collapse pressure pulse is higher. This phenomenon can be used for more stubborn chemical reactions.
2) Manipulation of the venturi to pipe area ratio offers good control over the cavitational activity. An increase in the venturi to pipe area ratio increases the active volume of the hydrodynamic cavitation reactor.
3) The contribution from the bubbles with smaller initial sizes to the overall cavitational effect is higher than the contribution from the bubbles with higher initial sizes. Although there is a wide variation in the initial size of the bubbles that are generated downstream of the throat of the venturi, partial control over the initial

bubble size to produce lower initial size of the bubbles can be obtained by the exposure of the flow at the throat of the venturi to ultrasonic irradiation.

3.2.3 Simulations on the Basis of a Liquid Continuum Mixture Model

It is also important to make some recommendations for the selection of a particular type of reactor desirable for a specific application. Moholkar and Pandit (2001a) have tried to address this situation and have investigated the comparative effect of several operating parameters on bubble motion in the cavitating flow in two different flow geometries: a venturi tube and an orifice plate. In the case of a venturi tube, a stable oscillatory radial bubble motion is obtained due to a linear pressure recovery gradient, whereas due to an additional oscillating pressure gradient due to turbulent velocity fluctuation, the radial bubble motion in the case of an orifice flow results in a combination of both stable and oscillatory cavity behavior. Thus, the intensity of cavitation will be higher in the case of an orifice system as compared to the classical venturi tube. Such simulations have enabled us to establish definite trends in the cavitation intensity produced in the hydrodynamic cavitation reactor with operating/design parameters, which can form a basis for the optimization of hydrodynamic cavitation reactors. The model also enables the quantification of magnitudes of temperature and pressure pulses for a given set of design parameters. The following important strategies for the design of hydrodynamic cavitation reactors have been established:

1) An orifice flow configuration is more suitable for applications requiring intense cavitational conditions, whereas for milder processes (requiring collapse pressure pulses typically between 15 and 20 bar) and for physical effects, a venturi configuration is more suitable and energy efficient.
2) In the case of a venturi flow, the most economical technique for increasing cavitation intensity would be to reduce the length of venturi, but for higher volumetric flow rates there could be a limitation due to the possibility of flow instability and super-cavitation. A similar argument can be given for the enhancement in the cavitation intensity by reducing the venturi throat to pipe diameter ratio.
3) In the case of an orifice flow configuration, the most convenient way of controlling the cavitation intensity is to control the orifice-to-pipe diameter ratio (basically throttling the discharge of a pump through a valve) and to control the cross-sectional flow area through the manipulation of the number and diameter of the hole on the orifice plate, although indiscriminate growth of bubbles downstream of the orifice can lead to splashing and vaporization (super-cavitation) of the flow.
4) Increasing pipe size downstream of the orifice (which offers a faster pressure recovery) is another option to intensify cavitation effects, but using pipes of larger size would mean handling higher volumetric flow rates (in order to carry out operation at the same cavitation number), and this could increase the fixed cost of processing.

3.2.4 Cluster Approach

Kumar and Pandit (1999) modeled the hydrodynamic cavitation phenomena in the venturi tube and high-speed homogenizer and observed that the modeling of the cavitation phenomena in hydraulic systems based on a single cavity dynamics equation is not a realistic picture, as visual observations indicated the presence of cavity clusters rather than individual cavities. The dynamics of the individual cavities are also affected by the neighboring cavities due to the generation of shock waves as a result of neighboring cavity collapse. The important assumptions in the approach of Kumar and Pandit (1999) are as follows:

1. A spherical cavity cluster is assumed to exist in isolation;
2. Liquid is inviscid and incompressible;
3. There is no relative motion between liquid and the cavity cluster;
4. Nucleation phase is neglected and a predetermined initial size of the cluster has been used.

The model has been reported to satisfactorily explain the effect of operating variables and equipment geometry on two different modes of cavitation generation qualitatively, and in some cases quantitatively. The important design-related information as obtained in this work can be summarized as follows:

1. Manipulation of the operating conditions aid in altering the intensity of cavitation suitable for various applications. The cluster approach satisfactorily explains the dependency of cavitational effects on the operating parameters.
2. High inlet pressure into the system and recovered downstream pressure of the liquid through the venturi/orifice can be used to generate cavitation of higher intensity, possibly useful for disinfection of water or liquid foods containing mixed cultures of microorganisms. On the other hand, lower inlet pressure and recovered downstream pressure generate cavitation of low intensity and are sufficient for carrying out applications, such as the disruption of yeast cells or possibly for emulsification purposes.

Kanthale et al. (2005) recently investigated the effect of various operating parameters on the cavitational intensity in an orifice plate type hydrodynamic cavitation reactor using the cluster approach. The trends of the variation in cavitational intensity with operating parameters such as cavitation number, inlet pressure, and initial size of nuclei were similar to that predicted on the basis of a single cavity approach, as discussed earlier. A new concept of active cavitational volume has been put forward, where the local pressure/temperature generated as a result of cavitation phenomena is greater than or equal to the threshold pressure capable of inducing a desired application. Based on the numerical simulations of the cluster model developed in their work, the following design correlations for cavitational intensity in terms of the collapse pressure (P_C) as well as for the active zone of cavitation

(V_W) has been given below for better quantitative understanding of the effect of the operating parameters:

$$P_C = 0.3023(P_2)^{0.972}(r_o)^{-0.714}(d_o)^{0.539}(\gamma)^{0.9316}(r/r_o)^{-2.604}$$

$$V_W = 2.0395\ P_s^{-1.2929}(P_2)^{1.2195}(r_o)^{2.2229}(d_o)^{0.5925}(\gamma^{0.1251})$$

where P_s is the starting pressure (threshold pressure) of the active volume of cavitation depending on the transformation to be carried out hydrodynamically. The above correlations are developed over the following range of parameters (observed generally in the literature):

Recovered pressure (P_2) = 1 − 5 atm
Initial cluster radius (r_o) = 0.001 − 0.02 m
Diameter of an orifice (d_o) = 0.015 − 0.03 m
Fraction of energy transfer (γ) = 0.25 − 0.50
Initial individual cavity size within the cluster (r) = 1 μm

The approach of cluster dynamics appears to be more logical as compared to the single cavity approach, although the exact quantitative comparison between the predictions of the cluster dynamics and single cavity approach (in this case, the total cavitational intensity will be number of cavities multiplied by the pressure pulse generated due to the collapse of a single cavity) needs to be explored so as to make firm recommendations. A drawback of the cluster approach, however, is that there is no information on the number of clusters generated in the system, which is needed to quantify the total cavitational intensity in the reactor.

It should be noted that the developed correlations are based on some simplistic assumptions and there is ample scope for further work, which may include establishing the validity of the equations over a wider range of operating parameters based on experiments in different reactors with varying power dissipation and/or frequency of fluid turbulence. Exact quantification of the number of free radicals generated during collapse (more importantly estimating the actual number taking part in the reaction, by considering the number of free radicals generated, time of collapse of the cavities, and the lifetime of the free radical, and also the relative rates of reaction of free radicals with the reactants and recombination reaction of free radicals) is also required. One more drawback of the developed equations is that it is based on the assumption of initial size, which is difficult to be quantified. Some techniques for estimating the size of the nuclei/cavity, which is dependent on the type of equipment used for the generation of cavitation, such as phase Doppler or theoretical approach based on the thermodynamic analysis considering the lattice structure and the intermolecular distance of the cavitating medium needs to be established for better accuracies. There is indeed a need for the development of these engineering equations for different systems, and the discussion presented here only proposes a methodology in that direction.

3.3 Development of Correlations for Cavitational Yield

A second step in the engineering design protocol is to develop design equations for the quantification of net cavitational effects. A simple methodology in terms of cavitational yield (quantification of chemical effects) for a model reaction has now been highlighted, as it is difficult to find illustrations from food or bioprocessing applications. The methodology, however, will remain equally applicable to these applications. Gogate et al. (2001) used Weissler reaction for the estimation of the cavitational yield in different hydrodynamic cavitation reactors (orifice plate setup with plates of different geometries, time of operation = 60 min, KI concentration = 1%, operating temperature of 30 ± 2°C, C_v in the range of 0.156–0.87 depending on the plate as well as for the high-speed homogenizer with operating speed of rotation = 12,000 rpm). These operating conditions were then used in simulations of bubble dynamics, and the magnitude of the collapse pressure pulse was predicted. A simple mathematical relationship between the cavitational yield and the predicted collapse pressure was developed and the developed equation for the prediction of cavitational yield can be given as:

$$\text{Cavitational yield} = 8.834 \times 10^{-11} \, (P_C)^{1.1633}$$

The above equation requires the collapse pressure values in terms of atmospheres, whereas the cavitational yield value is given in units of g/(J/ml). It should be noted here that the equation is only a starting point in establishing design strategies for hydrodynamic cavitation reactors and is valid for the specific reaction considered in the work. Similar equations need to be developed for different classes of applications based on the methodology depicted above. These engineering design equations (for cavitational yield as well as collapse pressure) will help in the selection of a set of operating parameters to achieve the desired objectives in a given hydrodynamic cavitation setup.

Overall, based on the theoretical bubble dynamics analysis as well as experimental analysis regarding the effect of different operating parameters as discussed in this section, the following useful guidelines/recommendations for the design of different hydrodynamic cavitation reactors, viz. orifice plate setup, venturi, high-speed and high-pressure homogenizers can be made:

1) An orifice flow configuration is necessary only for intense chemical reactions, whereas for milder processes (typically between 15 and 20 bar) and physical transformations, a venturi configuration is recommended.
2) Select higher operating inlet pressures upstream of the mechanical constriction, but just below the onset of super-cavitation.
3) Select optimum combination of liquid physical properties so as to enable easy generation of lower initial size nuclei, as discussed earlier.
4) For orifice plate setup, optimize the number and diameter of holes for the same free-flow area based on the type of applications; a smaller number of large

diameter holes for applications that require higher cavitation intensity, e.g., destruction of complex chemicals, and a higher number of smaller diameter holes for applications requiring relatively lower intensities, e.g., cell disruption.
5) Design the hydrodynamic cavitation reactor with lower free area for the flow.
6) Choose the speed of rotation in the case of high-speed homogenizers much above the critical speed for the cavitation inception and below the speed where air induction takes place.

4 Analogies and Comparison with Acoustic Cavitation

4.1 Analogy with Acoustic Cavitation

Acoustic cavitation is as a result of the passage of ultrasound through the medium, while hydrodynamic cavitation occurs as a result of the velocity variation in the flow due to the changing geometry of the path of fluid flow such as an orifice, venturi, or a throttling valve. In spite of this difference in the mechanisms of generation of these two types of cavitation, bubble behavior shows similar trends with the variation of parameters in both types of cavitation. The two main aspects of bubble behavior in cavitation phenomena are:

1) The amplitude of oscillation of cavity/bubble radius, which is reflected in the magnitude of the resultant pressure pulses of the cavity collapse; and
2) The lifetime of the bubble, which is reflected in the distance travelled and hence the extension of the zone of cavitational influence from point of its inception.

Moholkar et al. (1999) studied the effect of operating parameters, viz. recovery pressure, time of recovery, and its magnitude in the case of hydrodynamic cavitation reactors and the frequency and intensity of irradiation in the case of acoustic cavitation reactors, on the cavity behavior. From their study, it can be seen that the increase in the frequency of irradiation and reduction in the time of the pressure recovery result in an increment in the lifetime of the cavity, whereas amplitude of cavity oscillations increases with an increase in the intensity of ultrasonic irradiation and the recovery pressure and the rate of pressure recovery. Thus, it can be said that the intensity of ultrasound in the case of acoustic cavitation and the recovery pressure in the case of hydrodynamic cavitation are analogous to each other. Similarly, the frequency of the ultrasound and time or rate of pressure recovery are analogous to each other. Thus, it is clear that hydrodynamic cavitation can also be used for carrying out the so-called sonochemical transformations, and the desired cavitation intensities can be obtained using proper geometric and operating conditions as discussed above.

In hydrodynamic cavitation reactors, cavitation is produced at the fluid shear layer. The liquid vaporized at vena contracta, downstream of the orifice, is proportional to the area of this shear layer. This fact enables a designer to control bubble

population in the flow. By changing the shape of the orifice (e.g., by making it triangular or hexagonal), the area of shear layer can be varied (obviously it is lowest for a circular orifice), and hence the rate of vaporization and the bubble/cavity population can be controlled. Bubble behavior similar to acoustic cavitation can be obtained in the hydrodynamic cavitation reactor by simple modifications in the orifice design and subsequent pressure recovery. If a rotating valve is installed instead of a permanent orifice, bubbles formed in the shear layer will experience a sinusoidally varying pressure field rather than a constant or linearly increasing field. Also, if two or three orifices are installed one after the other at the downstream of the pump, then the bubbles that are generated experience a highly fluctuating pressure field, and collapse is more and more violent giving rise to high temperatures and pressure pulses of magnitudes comparable to those under acoustic cavitation. It is also possible that the cavities generated at the upstream of the orifice or their fragments can act as nuclei for orifices downstream of the first orifice. Moreover, air or steam bubbles of required sizes can be introduced in the flow, and the resultant pressure pulse magnitude can be manipulated.

4.2 Comparison with Acoustic Cavitation Reactors

Since cavitating conditions identical to acoustic cavitation can be generated in the hydrodynamic cavitation reactors and, these can serve as a replacement for sonochemical reactors, it is necessary to compare the hydrodynamic and acoustic cavitation reactors to come to firm conclusions. Suslick et al. (1997) reported that acoustic cavitation provides significantly higher rates for the Weissler reaction (a reaction generally used to assess the efficacy of the cavitational reactors) for the specific setup (microfluidizer) used in the experimentation, but no quantitative comparisons in terms of energy efficiencies were made. Moholkar et al. (1999) also indicated that cavitation generated using ultrasound is much more intense as compared to that generated by hydrodynamic means. In our earlier work (Gogate et al., 2001), the Weissler reaction was used for comparison of different cavitational reactors. It has been observed that hydrodynamic cavitation equipment is relatively far more energy efficient as compared to sonochemical reactors. Also, the efficiency increases from HPH (typically laboratory-scale equipment and energy efficiency of 54%) to orifice setup of 50 l capacity (typically pilot plant scale with observed energy efficiency of 60%). The values of cavitational yields (defined as iodine liberated per unit power density) have also been found to be higher (10–40 times) for hydrodynamic cavitation reactors as compared to acoustic cavitation reactors, at least for the model reaction considered in the work. Similar comparisons have also been found in the literature for cell disruption applications, as discussed in detail later.

Thus, it can be said from these results that hydrodynamic cavitation equipment gives better performance as compared to acoustic cavitation reactors. Also, hydrodynamic cavitation reactors are much more versatile, energy efficient, and also

amenable to an efficient scale-up to meet industrial scale demands. It should, however, be noted that the comparison made here is valid only for a model reaction, and the efficiency of the various equipment may be different for the variety of cavitation-based transformations. Laboratory-scale studies are recommended for the desired application under question unless specific data is available from the existing literature.

5 Overview of Applications of Hydrodynamic Cavitation

Hydrodynamic cavitation has been successfully used in a variety of applications ranging from wastewater treatment (Kalumuck and Chahine, 2000; Sivakumar and Pandit, 2002), polymer chemistry (Chivate and Pandit, 1993), synthesis of nanocrystalline materials (Moser et al., 1995, 1996; Sunstrom et al., 1996) to preparation of liquid dispersions (Kozyuk, 1998, 1999a, b). In the specific case of applications in food and bioprocessing industries, hydrodynamic cavitation can be effectively applied in cell disruption applications for the release of intracellular enzymes, water disinfection, and also in the effective disinfection of liquid food streams. We will next discuss the various literature illustrations to get a better insight into the efficacy and applicability of hydrodynamic cavitation.

5.1 Cell Disruption Using Hydrodynamic Cavitation

A key factor in economical production of industrially important intracellular enzymes is an efficient large-scale cell disruption process. The intracellular nature of many recombinant products and the potential use of the bacterial storage product, PHB, as a commodity thermoplastic, have developed interest in the improvement of this unit operation (Chisti and Moo-Young, 1986; Datar and Rosen, 1990). For the large-scale disruption of microorganisms, mechanical disintegrators such as high-speed agitator bead mills and high-pressure homogenizers (Harrison, 2002) are commonly employed, but the typical energy efficiencies of these methods are in the range of 5–10% and the rest of the energy is dissipated in the form of heat. Much of the research work has been reported in the literature using these methods (Engler, 1985; Geciova et al., 2002; Harrison, 2002); however, there is no integrated approach for cell disruption.

With an aim of improving the efficacy of the cell disruption process, keen interest has developed in the last decade in application of newer techniques including acoustic and hydrodynamic cavitation. Harrison and Pandit (1992) were the first to report the use of hydrodynamic cavitation for cell disruption process using a configuration where cavitation was generated using a throttling valve. Save et al. (1994) used a similar configuration of hydrodynamic cavitation reactor for disruption of Baker's yeast and brewer's yeast cells in a pressed yeast form and the extent of cell disruption was monitored in the form of increase in soluble protein content in the media

(water) used for the preparation of the cell suspension. A detailed study into effect of operating parameters such as initial cell concentration, time of treatment, and number of passes in the flow loop system on the extent of cell disruption has been reported. As expected, an increase in the time of treatment and number of passes resulted in a corresponding increase in the extent of cell disruption. The concentration of cells in the suspension influenced the disruption process significantly. An increase in concentration beyond 5% by weight was reported to reduce the energy advantage of the pump setup, though no quantification has been done. Optimization for operating pump discharge pressure (related to the strength of the cell wall) and the concentration of the yeast cells is recommended for obtaining energy-efficient disruption operation. The growth stage of the yeast cells is another parameter that affects energy efficiency. Preliminary experiments with fresh fermentation broth indicated that the cells in an exponential growth phase are far more susceptible to disruption compared with those which are either stored or frozen. Comparison of energy efficiencies for different operations, including hydrodynamic cavitation, mixer–blender, and ultrasonication, indicated that the energy requirement of hydrodynamic cavitation setup is lower than the other two methods by more than two orders of magnitude for equivalent protein release. Quantitatively speaking, energy utilization per milliliter of yeast suspension to observe the same level of protein release was 20.7 J/ml for hydrodynamic cavitation reactor, 1500 J/ml for ultrasonic irradiation, and 900 J/ml for the mixer–blender.

In a progression of the earlier work, Save et al. (1997) investigated the process of cell disruption using hydrodynamic cavitation operating at a capacity of 50 and 200 l. It has been established that to achieve a similar extent of protein release at higher cell concentration in the reactor, higher operating pressures are required. Comparison of the energy efficiency of the hydrodynamic cavitation reactor with a conventional mixer–blender system and acoustic cavitation induced using ultrasound confirmed the earlier findings of order of magnitude higher energy efficiencies for hydrodynamic cavitation, even at large-scale operation. Save et al. (1997) also established that even though cavitation is known to generate conditions of very high temperature and pressure locally along with the generation of free radicals, activity of the released enzymes from the cells remains unaltered. The activity of the glucosidase and invertase enzymes was not affected under normal circumstances, but prolonged exposure to severe conditions of cavitation (at severe operating conditions, as reported in the work) resulted in a marginal decrease in the activity of the enzymes. Thus, it is important to control the intensity of the cavitational phenomena by suitably adjusting the operating and geometric parameters in the system.

It should also be noted that the mechanism of the cell disruption process is also different depending on the equipment used (Balasundaram and Pandit, 2001a). Cell disruption process can proceed via complete breakage of the individual cells, releasing the intracellular enzymes in certain devices, or can be shear driven where only the cell wall breaks as a result of which only the enzymes present at the wall or periplasm will be released (leached slowly). In any case, cavitation phenomena mainly control the extent of cell disruption and release of enzymes.

Gopalkrishnan (1997) and Shirgaonkar et al. (1998) have conclusively established this fact. Shirgaonkar et al. (1998) reported that the rates of protein release at 10,000 rpm are much higher than at 5,000 rpm in a high-speed homogenizer. This can be explained on the basis of cavitation inception speed of 8,000 rpm, as reported by Kumar and Pandit (1999) for a high-speed homogenizer unit. At 10,000 rpm, the major contribution to cell disruption is by cavitation and mechanical forces, whereas at 5,000 rpm, only mechanical forces (shear) are contributing to the overall cell disruption. Thus, generating cavitating conditions in the system is important for maximizing the release of the intracellular enzymes for a given energy input.

Balasundaram and Pandit (2001a) investigated the release of invertase enzyme by disruption of *Saccharomyces cerevisiae* cells using sonication, high-pressure homogenization, and hydrodynamic cavitation. Invertase is an enzyme located in the periplasmic space of *S. cerevisiae* cells. The experimental setup was based on the use of an orifice plate instead of a throttling valve for the generation of cavitation. The plate consisted of 33 holes of 1 mm diameter. A total of 50 l of 1% yeast suspension in acetate buffer of pH 5 (100 mM) was disrupted at 75 psig pump discharge pressure for 50 min. The extent of release of the enzyme invertase was found to be higher than total soluble protein. This could be due to the periplasmic location of the enzyme. Based on the release pattern of enzyme and protein, a selective release of invertase (periplasmic) is expected in the early stages of disruption by hydrodynamic cavitation before complete mutilation of the cells releasing all the available proteins (cytoplasmic as well). For the case of ultrasonic-induced cavitation, the rate of release of invertase enzyme was comparable with proteins, which can be attributed to higher severity of the cavitational intensity in the case of acoustic cavitation as compared to hydrodynamic cavitation. Severe cavitation results in complete breakage of the cells, whereas mild cavitational intensity in the case of hydrodynamic cavitation reactor results in an impingement/grinding action on the cell due to the shear giving rise to breakage of the cell wall rather than of the complete cell. Comparison of hydrodynamic and acoustic cavitation modes for release of enzyme indicated that hydrodynamic cavitation results in 44 times more specific yield (mg of enzyme released per unit of energy supplied) than sonication when compared on the basis of overall energy consumption. The yields as obtained by different disruption techniques are illustrated in Fig. 6.5.

Balasundaram and Harrison (2006b) investigated the application of hydrodynamic cavitation for the partial disruption of *Escherichia coli* cells and selective release of specific proteins relative to the total soluble protein. The effects of the cavitation number, the number of passes, and the specific growth rate of *E. coli* on the release of periplasmic and cytoplasmic proteins have been studied. At the optimum cavitation number of 0.17 for this experimental configuration, 48% of the total soluble protein, 88% of acid phosphatase, and 67% of β-galactosidase were released by hydrodynamic cavitation in comparison to the maximum release attained using multiple passes through a French press. The higher release of the acid phosphatase over the total soluble protein suggested preferred release of periplasmic compounds. This was supported by SDS-PAGE analysis. *Escherichia coli* cells cultivated at a higher specific growth rate (0.36 h^{-1}) were more easily disrupted than slower

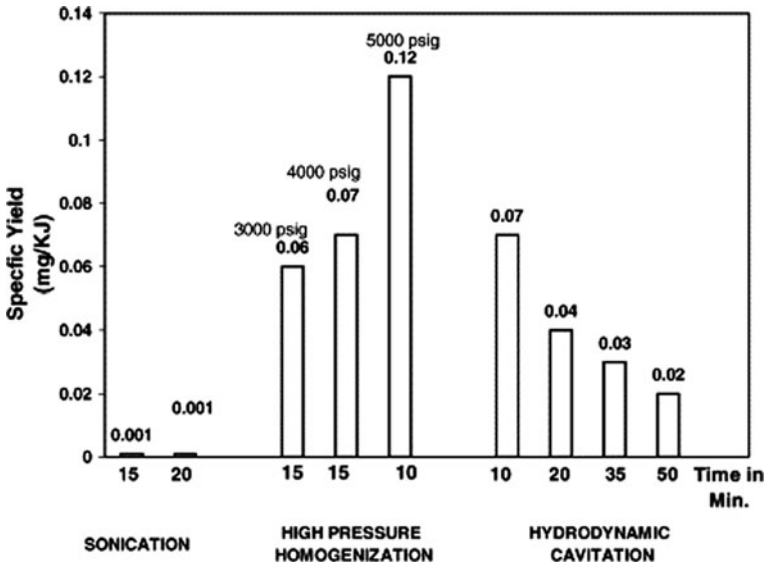

Fig. 6.5 Comparison of specific yield of invertase by different disruption techniques (Balasundaram and Pandit, 2001a)

growing cells (0.11 h^{-1}). The specific activity of the enzyme of interest released by hydrodynamic cavitation, defined as units of enzyme in solution per milligram of total soluble protein, was greater than that obtained on release by a French press, high-pressure homogenization, osmotic shock, and EDTA treatment. The selectivity offered indicates the potential of selective enzyme release by hydrodynamic cavitation to ease the subsequent purification in the downstream processing operation. These studies have clearly established the dependency of the extent of release of the enzymes on the location of the enzyme in the cell.

Balasundaram and Pandit (2001b) quantified the dependency of location of enzymes in the cell using a concept of location factor. Disruption of yeast cells for selective release of invertase, alcohol dehydrogenase (ADH) enzymes and disruption of *E. coli* cells for release of penicillin acylase was achieved using sonicator, hydrodynamic cavitation reactor, and high-pressure homogenizer. For the release of invertase and penicillin acylase, the location factor was observed to be greater than 1 for all the cavitation equipments, which confirms the periplasmic location of the two enzymes in the yeast and *E. coli* cells, respectively (Follows et al., 1971; Novella et al., 1994). Further, it was observed that the location factor is higher in the case of hydrodynamic cavitation reactor as compared to the other two, confirming that the mechanism of cell disruption in this case is by impingement/grinding action on the cell due to the shear, as discussed earlier. For the ADH enzyme, the location factor value was around 0.5, confirming that ADH is present mostly in the cytoplasm of the cell (Follows et al., 1971; Keshavarz et al., 1990). Heating the cell suspension as a pretreatment strategy for translocation of the enzyme was found to

be effective for the ADH enzyme (Umakoshi et al., 1998). Even the time of culture in the fermentation process was found to affect the location factor of the enzyme. For studies with *E. coli* cells, higher time of culturing resulted in periplasmic location of penicillin acylase, whereas lower time of culturing resulted in cytoplasmic location of the enzyme. The concept of location factor is very useful for identifying the suitability of the disruption equipment for differential product release.

Balasundaram and Harrison (2006a) investigated the effect of the process variables including cavitation number, initial cell concentration of the suspension, and the number of passes across the cavitation zone on the release of enzymes from various locations of the brewers' yeast. The release profile of the enzymes studied include β-glucosidase (periplasmic), invertase (cell-wall bound), alcohol dehydrogenase (ADH; cytoplasmic), and glucose-6-phosphate dehydrogenase (G6PDH; cytoplasmic). An optimum cavitation number C_v of 0.13 for maximum disruption was observed across the range of C_v from 0.09 to 0.99. The optimum cell concentration was found to be 0.5% (w/v, wet wt.) when varying over the range 0.1–5%. The sustained effect of cavitation on the yeast cell wall when re-circulating the suspension across the cavitation zone was found to release the cell-wall bound enzyme invertase (86%) to a greater extent than the enzymes from other locations of the cell (e.g., periplasmic β-glucosidase at 17%). Localized damage to the cell wall could be observed using transmission electron microscopy (TEM) of cells subjected to less intense cavitation conditions. Absence of the release of cytoplasmic enzymes to a significant extent, absence of micronization as observed by TEM, and the presence of a lower number of proteins bands in the culture supernatant on SDS-PAGE analysis following hydrodynamic cavitation compared to disruption by high-pressure homogenization confirmed the selective release offered by hydrodynamic cavitation. Thus, controlling the intensity of cavitation phenomena in the same reactor or using different reactor configurations can result in the selective release of enzymes from different locations in the cell. Some pretreatment strategies can be used for modification of the location of the enzyme in the cell before the cell suspension is subjected to the cell disruption. Translocation of enzymes due to the pretreatment step can be exploited to improve the efficacy of the cell disruption, because most of the target products are usually produced in the cytoplasm of the cells and cannot be obtained readily without spending a large amount of energy to completely mutilate the cell wall and the cytoplasm during disruption. More energy is required to recover cytoplasmic enzymes than periplasmic enzymes (Chisti and Moo-Young, 1986). Thus, translocation of enzymes from the cytoplasmic space to periplasmic space could result in a large saving in energy requirements. We will next discuss some of the pretreatment strategies that can be used for intensifying the release of the enzymes. The illustrated studies are with ultrasound-induced cavitation, though they should be equally applicable for hydrodynamic cavitation reactors.

Farkade et al. (2005) reported that heat stress was found to induce the translocation of the target enzyme (β-galactosidase) and also other proteins, though their translocation rates were found to be different. The location factor varied between 0.4 and 2 depending on the time of heat treatment and temperature of the treatment. Heat treatment also resulted in the formation of insoluble protein aggregates,

which could be removed by a centrifugation step, and thereby, reducing the total protein release in the suspension during the cell disruption by sonication and thereby increasing the specific enzyme activity. The translocation rate was found to be different at different treatment temperatures, increasing with an increase in time and the temperature of the treatment. However, treatment at temperatures above 50°C resulted in a substantial deactivation of the target enzyme. Therefore, heat treatment could be a good pretreatment step to improve the energy efficiency of the mechanical cell disintegration step, but it requires a rather heat stable target product, or an optimum pretreatment temperature needs to be established. The results of Farkade et al. (2005) clearly demonstrated that by using optimum heat treatment, cell disintegration can be considerably improved in terms of its energy efficiency.

Farkade et al. (2006) investigated the release of intracellular β-galactosidase by ultrasonic disruption of cells treated with aqueous solutions of different pH as a pretreatment step. Pretreatment of the cells at different pHs for various time intervals has been investigated with the aim of optimizing the pretreatment step for more efficient release of the target enzyme. The maximum yield (95 ± 3 U/ml) was obtained by pretreatment of the cells at pH 4.4 for 6 h and subsequent ultrasonic cell disruption for 40 min. The maximum yield on ultrasonic disruption without pretreatment was 7.2 ± 0.6 U/ml. The energy efficiency of the disruption process for releasing β-galactosidase using different pretreatments was calculated and compared. It was observed that the energy efficiency increased more than 19-fold for cells pretreated at pH 4.4 for 6 h as compared to the untreated cells.

Anand et al. (2007) reported that the combination of chemical treatment and high-pressure homogenization (HPH) can increase the release of intracellular components and decrease the exposure to mechanical disruption required for the breakage to attain maximum intracellular release. Through these processes, the energy requirement of microbial cell disruption can be decreased along with a reduction in the micronization of cell debris. Pretreatments to permeabilize or weaken the cell envelope were selected and the optimum conditions determined through a screening process. The permeabilization of *E. coli* with EDTA was successful in achieving maximum intracellular protein release at a lower pressure of 13.8 MPa on high-pressure homogenization, compared with 34.5 MPa in the absence of EDTA. Significant reduction in energy input required was observed with the use of this combination method. Pretreatment with guanidium hydrochloride (G-HCl) and Triton X-100 also resulted in increased intracellular release and decreased energy usage. Chemical pretreatment can be useful in enhancing mechanical disruption; however, careful selection of pretreatment conditions is required to avoid protein deactivation and chemical interference in the protein assay.

Overall, it can be said that use of hydrodynamic cavitation for cell disruption has been conclusively proven for large-scale applications and with much higher energy efficiencies as compared to acoustic cavitation reactors based on the use of ultrasound. A particular reactor configuration in terms of geometry of the cavitation chamber and operating parameters such as inlet pressure and circulation flow rate can be chosen based on the location of specific enzymes in the cells and cell concentration in the medium. Pretreatment strategies such as heat, pH, and chemical

treatment can aid in enhancing the selectivity of the target enzyme and at the same time significantly decrease the energy requirements.

5.2 Microbial Disinfection Using Hydrodynamic Cavitation

Over the years, disinfection of microorganisms in water has been achieved by various chemical and physical means (Bitton, 1994; Pontius, 1990; White, 1992). However, the drawbacks of all of these techniques outweigh their efficacy (Cheremissinoff et al., 1981; Minear and Amy, 1996; Simpson and Hayes, 1998). For example, chlorine, which is widely used as a disinfectant, results in the formation of mutagenic and carcinogenic agents (tri halo methane) in water. In addition to this formation of non-acceptable residual components, chemical methods are also limited by severe mass transfer limitations resulting into lower disinfection rates. Also, certain species of microorganisms produce colonies and spores that agglomerate into spherical or large clusters. Chemical treatment of such clusters may destroy microorganisms on the surface leaving the innermost organisms intact. Furthermore, the efficacy of any disinfection method is subject to a number of factors, including solution conditions (e.g., temperature, turbidity) and variable microorganism resistance to inactivation. The potency of certain physical techniques, such as ultraviolet light, is limited in solutions that result in scattering of the incident UV light (Parker and Darby, 1995) or in those solutions capable of absorbing the incident UV light (Harris et al., 1987), or when microorganisms are capable of photoreactivation (self-repair) (Harris et al., 1987). Fine particles such as clays are normally removed by flocculation using chemicals such as aluminum sulfate. The flocs can entrap bacteria and their spores, protecting them from chlorination. The vast majority of flocs are removed, but one or two may pass through the system unaffected by the final disinfection stage. Thus, there is a need for developing some alternate techniques for water disinfection. Cavitation, due to its spectacular effects in terms of generation of hot spots, highly reactive free radicals, and turbulence associated with liquid circulation, offers potential as an effective tool for water disinfection. Use of ultrasonic reactors for microbial disinfection has been substantially investigated and excellent reviews have been published by Phull et al. (1997), Mason et al., (2003) and Piyasena et al. (2003) on this subject. Though hydrodynamic cavitation has been found to be much more efficient as compared to acoustic cavitation-based reactors, its advent in the area of microbial disinfection has been only in the recent past. We next discuss the application of hydrodynamic cavitation reactors for microbial disinfection, which forms a very important step in food processing industries.

Jyoti and Pandit (2001) investigated the application of cavitation for disinfection of bore well water in different hydrodynamic cavitation reactors (high-speed homogenizer, high-pressure homogenizer, and orifice plate setup) and also compared its efficacy with the ultrasonic horn type of reactor (operating at 22 kHz and power rating of 240 W) that generates acoustic cavitation. In general, the extent of disinfection increased with an increase in the supplied energy into the system.

Increasing the operating pressure in the case of orifice plate setup operating at 75 l capacity resulted in a corresponding increase in the extent of disinfection. It has been reported that cavitation is equally effective in disinfection of bore well water samples and about 90% disinfection can be achieved in less than 30 min of treatment for the ultrasonic horn and the high-speed homogenizer. The extent of disinfection was somewhat lower in the orifice plate type setup, which was attributed to higher volumes of operation and generation of lower intensity cavitation. Comparison of all the equipment in terms of extent of disinfection per unit energy supplied, however, indicated that orifice plate setup at higher operating pressures was the most efficient among all cavitational reactors. Quantitatively speaking, the extent of disinfection in case of the orifice plate setup was 310 CFU/J as compared to only 45 CFU/J in the case of the ultrasonic horn and 55 CFU/J in the case of high-speed homogenizer. In the case of the high-pressure homogenizer, the rate of disinfection was substantially higher as compared to the other cavitating equipment, but the overall energy efficiency was extremely poor (5 CFU/J).

Apart from making contaminated water into potable water for drinking purposes, cavitational reactors can also find utility in a ship to treat ballast water that is being transported from one region to another. Shipping is the backbone of global economy and facilitates the transportation of 90% of commodities. It is estimated that 2–3 billion tons of ballast water are carried around the world each year. Translocation of organisms through ships (bio-invasion) is considered to be one of the important issues that threaten naturally evolved biodiversity, the consequences of which are being realized increasingly in recent years. Although many treatment technologies such as self-cleaning screen filtration systems, ozonation, de-oxygenation, electro-ionization, gas supersaturation, and chemical treatments have been adopted, they cannot limit the environmentally hazardous effects that may result from such practices. Pandit (Ballast water treatment technology: Challenges ahead, "Personal communication", 2007) reported on the application of cavitation for ballast water treatment and the design methodology for the incorporation of cavitational reactors in actual ships. Experimental investigations indicated that hydrodynamic cavitation (generated using multiple holes sharp-edge orifice plate of size 21.5 mm having circular hole of diameter 2 mm; fraction of open area= 0.75, flow rate= 1.3 lps and pressure= 3.2 kg/cm^2) resulted in 99% destruction of all bacteria and also resulted in 80% destruction of zooplanktons. An increase in recirculation time as well as operating pressure, which increases the intensity of generation cavitation, resulted in a decrease of treatment time. Use of multiple orifice plates arranged sequentially in the system also resulted in an increase in the extent of destruction. The aim of the designers in this type of application should be to make the process single pass, as it is practically impossible to have multiple passes in the ballast water treatment considering the volume of liquid to be treated and a typical piping network for the ballast water flow.

The above two studies with actual contaminated water (possibly containing a wide range of bacteria/microorganisms) confirms the suitability of the cavitation phenomena for microbial disinfection. Cost of the treatment is another important factor, which needs to be ascertained before cavitation can be recommended as a

replacement technique for conventional methods of disinfection. Jyoti and Pandit (2001) estimated the cost of treatment for different types of cavitational reactors compared to the costs associated with conventional methods of using ozone and chlorine. It has been reported that hydrodynamic cavitation induced using high-speed homogenizer or orifice plate setup is the most cost-effective treatment strategy (cost of treatment as 0.81 and 1.4 US $/m^3) as compared to sonochemical reactors or high-pressure homogenizer (cost of treatment as 14.88 and 6.55 US $/m^3). However, this cost of treatment is still higher as compared to chlorination (cost of treatment as 0.0071 US $/m^3) or ozonation (cost of treatment as 0.024 US $/m^3) estimated based on small-scale applications. Thus, applicability of cavitation is more suited when bulk treatment is required (e.g., ballast water treatment or large-scale municipal corporation water treatment plants) or when end use of treated water does not allow formation of hazardous by-products commonly associated with the conventional treatment schemes. Ways of improving the cavitational activity in the reactor and/or combining cavitation with conventional techniques would be another approach for reducing the cost of treatment. We will next look into these aspects of intensifying the cavitational activity in the reactor by way of using additives and also combining cavitation with conventional techniques for disinfection such as use of chlorine, ozone, hydrogen peroxide, hypochlorite etc.

Jyoti and Pandit (2003, 2004) studied different combinations of cavitation (acoustic and hydrodynamic cavitation) and chemical methods (hydrogen peroxide and ozone) for the treatment of bore well water. It has been reported that the efficacy of the ultrasonic horn as well as the ultrasonic bath for the destruction of HPC bacteria is increased when hydrogen peroxide or ozone is combined with ultra-sonication. The results are attributed to the increased permeability of hydrogen peroxide/ozone through the cell wall membrane, increased rates of mass transfer, and production of a higher number of free radicals. The extent of increase in the disinfection rates was higher for ozone as compared to hydrogen peroxide due to the disinfecting action of the molecular ozone in addition to the free radicals. In the case of hydrodynamic cavitation, the overall rate of disinfection is increased when hydrogen peroxide or ozone is added, leading to better efficacy for the disinfection of the HPC bacteria compared to only hydrodynamic cavitation. Similarly, when the ultrasonic flow cell is used along with hydrodynamic cavitation and hydrogen peroxide, the rate of disinfection is further enhanced as the intensity of cavitation in the hydrodynamic cavitation setup is increased by the presence of the ultrasonic flow cell, which in turn accelerates the decomposition of hydrogen peroxide or increases the probability of cell wall rupture, coupled with enhanced H_2O_2 penetration leading to an increase in the death rate of the microorganisms present in the bore well water. In addition to the generation of free radicals are the individual effects of hydrogen peroxide, ultrasonic cavitation, and hydrodynamic cavitation.

Chand et al. (2007) recently investigated the use of ozone treatment assisted by a liquid whistle reactor (LWR), which generates hydrodynamic cavitation, for water disinfection using a simulated effluent containing *E. coli.* A suspension having an *E. coli* concentration of approximately 10^8–10^9 CFU ml^{-1} was introduced into the LWR to examine the effect of hydrodynamic cavitation alone and in combination

with ozone. Hydrodynamic cavitation generated using a liquid whistle reactor alone results in only 22% disinfection, but ozone-assisted operation with a minimum time of ozone treatment produces 75% disinfection. The enhanced mass transfer rates achieved due to the re-circulatory flows in the liquid whistle reactor increase the effective utilization of ozone. The results indicate that an optimum operating treatment protocol is introduction of ozone in stages assisted by hydrodynamic cavitation at lower operating temperatures. If maintaining lower operating temperatures is not feasible, which can be the reality on an industrial scale, the same extent of disinfection can be achieved by using higher operating pressures in the liquid whistle reactor (increased contribution from the hydrodynamic cavitation). Higher pressures and similar conditions of ozone doses are particularly recommended for disinfecting wastewater with some organic loads and other contaminants. Optimization of ozone dose is essential in conjunction with hydrodynamic cavitation in order to develop a process that will consume less energy and at the same time be more cost effective. The combination has been found to be a cost-effective technique for achieving maximum disinfection compared to the individual operation of hydrodynamic cavitation (lower extent of disinfection) and ozonation (higher cost of treatment usually due to higher cost of ozone generation).

Physical stresses resulting from acoustic or hydrodynamic cavitation are understood to be the mechanisms responsible for cellular inactivation. Biological entities in the immediate area of the cavitation event endure stresses that induce severe damage to cell walls and ultimately inactivate the organism. It can be hypothesized on the basis of water disinfection results discussed earlier that hydrodynamic cavitation can effectively pasteurize and/or sterilize fluid foods at reduced temperatures by the combined thermal and cavitation effects. More studies are required to investigate the suitability of hydrodynamic cavitation in this area of food processing.

6 Recommendations for Future Work

Hydrodynamic cavitation reactors appear to be much more energy efficient as compared to their acoustic counterparts, at least for the different applications overviewed in this work. It can be said that the hydrodynamic cavitation reactors offer immediate and realistic potential for industrial-scale applications as compared to the sonochemical reactors, and the scale-up of these reactors is comparatively easier as a vast amount of information about the fluid dynamics downstream of the constriction is readily available and the operating efficiency of the circulating pumps which is the only energy dissipating device in the system is always higher at large scales of operation. The following studies are required to achieve this goal:

(1) Realistic modeling of the turbulence phenomena which then can be used to model the cavity/bubble dynamics either in isolation or in the form of cavity clusters in high-velocity flow. Modern and sophisticated CFD codes can be

employed to find the flow-field information, i.e., mean and fluctuating velocity components, Reynolds stresses, and turbulent pressure fluctuations, which can then be used to understand the role of these flow field parameters in altering cavity dynamics.

(2) Development of generalized design equations also providing a link between the bubble dynamics and net cavitational effects. The design correlations for cavitational yield and cavitational intensity should be made generalized and applicable for a variety of applications as well as reactors.

(3) It is necessary to develop user friendly computer codes (similar to modern CFD codes) for the use of engineers, which will allow them to change the geometrical and operating parameters of the hydrodynamic cavitation setup, and to define physico-chemical properties of the system under consideration. These codes, with the help of bubble/cavity dynamics and the equilibrium chemistry at cavity collapse conditions, will then predict the expected chemical effects, thus avoiding trial and error type of experimentation for the engineers.

(4) Design and fabrication of different types of hydrodynamic cavitation setup differing in flow field, turbulence characteristics, and geometry to study the effect of these on cavity/bubble/cluster dynamics. Sophisticated measuring techniques such as laser Doppler anemometry, hydrophones, and cavity luminescence spectral measurement need to be adapted for fast flowing cavities/clusters to be able to measure the magnitudes of cavity/cluster oscillations/collapse pressure pulse and temperature generated and the identification of the intermediate chemical species along with their concentrations.

(5) Experiments are needed on different scales of operation to understand and address scale-up issues, such as alteration in the flow field and turbulence characteristics due to the scale of operation.

7 Concluding Remarks

Hydrodynamic cavitation appears to be a novel technology and a suitable alternative for applications based on the use of ultrasound-induced cavitation in the food and bioprocessing applications. For various cell disruption and microbial disinfection applications illustrated in the present work, the energy efficiency is much higher in the hydrodynamic cavitation reactors as compared to their acoustic counterparts. The optimization strategies on the basis of theoretical analysis reported earlier should serve as a useful guideline to design engineers for the selection of an optimum set of operating parameters and design configurations to achieve maximum benefits. Amongst different hydrodynamic cavitation reactors, the orifice plate type configuration appears to be most suitable as it offers tremendous flexibility for controlling the intensity of cavitation for desired applications so that considerable energy savings are possible. It can be said that hydrodynamic cavitation reactors offer immediate and realistic potential for industrial-scale applications as compared to sonochemical reactors, and the scale-up of these reactors is comparatively easier

as vast amount of information about the fluid dynamics downstream of the constriction is readily available. Also the operating efficiency of circulating pumps, which are the only energy dissipating device in the case of the reactor assembly, is always higher at large scales of operation. Overall, it can be said that hydrodynamic cavitation is a well-established technology at both the laboratory and the pilot scale, and combined efforts of microbiologists, engineers, and physicists are required to effectively harness this technology on an industrial scale of operation.

References

Anand, H., Balasundaram, B., Pandit, A. B., and Harrison, S. T. L. (2007). The effect of chemical pretreatment combined with mechanical disruption on the extent of disruption and release of intracellular protein from *E. coli*. *Biochemical Engineering Journal*, 35(2), 166–173.

Balasundaram, B., and Harrison, S. T. L. (2006a). Disruption of Brewers' yeast by hydrodynamic cavitation: Process variables and their influence on selective release. *Biotechnology and Bioengineering*, 94(2), 303–311.

Balasundaram, B., and Harrison, S. T. L. (2006b). Study of physical and biological factors involved in the disruption of *E. coli* by hydrodynamic cavitation. *Biotechnology Progress*, 22(3), 907–913.

Balasundaram, B., and Pandit, A. B. (2001a). Selective release of invertase by hydrodynamic cavitation. *Biochemical Engineering Journal*, 8, 251–256.

Balasundaram, B., and Pandit, A. B. (2001b). Significance of location of enzymes on their release during microbial cell disruption. *Biotechnology and Bioengineering*, 75, 607–614

Bitton G. (1994). *Wastewater microbiology*. New York, NY, Wiley.

Chand, R., Bremner, D. H., Namkung, K. C., Collier, P. J., and Gogate, P. R. (2007). Water disinfection using a novel approach of ozone assisted liquid whistle reactor. *Biochemical Engineering Journal*, 35, 357–364.

Chatterjee, D., and Arakeri, V. H. (1997). Towards the concept of hydrodynamic cavitation control. *Journal of Fluid Mechanics*, 332, 377–394.

Cheremissinoff, N. P., Cheremissinoff, P. N., and Trattner, R. B. (1981). *Chemical and nonchemical disinfection*. Ann Arbor, MI, Ann Arbor Science.

Chisti, Y., and Moo-Young, M. (1986). Disruption of microbial cells for intracellular products. *Enzyme and Microbial Technology*, 8, 194–204.

Chivate, M. M., and Pandit, A. B. (1993). Effect of hydrodynamic and sonic cavitation on aqueous polymeric solutions. *Industrial and Chemical Engineering*, 35 (1–2), 52.

Datar R., and Rosen, C.-G. (1990). Downstream process economics. In: Asenjo, J. A. (eds.), *Separation processes in biotechnology*, pp. 741–793. New York, NY, Marcel Dekker.

Engler C. R. (1985). Disruption of microbial cells. In: Moo-Young, M. (ed.), *Comprehensive biotechnology*, Vol. 2, pp. 305–324. Oxford, Pergamon Press.

Farkade, V. D., Harrison, S. T. L., and Pandit, A. B. (2005). Heat induced translocation of proteins and enzymes within the cells: An effective way to optimize the microbial cell disruption process. *Biochemical Engineering Journal*, 23, 247–257.

Farkade, V. D., Harrison, S. T. L., and Pandit, A. B. (2006). Improved cavitational cell disruption following pH pretreatment for the extraction of β-galactosidase from Kluveromyces lactis. *Biochemical Engineering Journal*, 31(1), 25–30.

Follows, M., Heterington, P. J., Dunhill, P., and Lilly, M. D. (1971). Release of enzymes from bakers' yeast by disruption in an industrial homogenizer. *Biotechnology and Bioengineering*, 13(4), 549–560.

Geciova, J., Bury, D., and Jelen, P. (2002). Methods for disruption of microbial cells for potential use in the dairy industry: A review. *International Dairy Journal*, 12(6), 541–553.

Gogate, P. R., and Pandit, A. B. (2000). Engineering design methods for cavitation reactors II: Hydrodynamic cavitation reactors. *AIChE Journal*, 46(8), 1641–1649.

Gogate, P. R., and Pandit, A. B. (2001). Hydrodynamic cavitation reactors: A state of the art review. *Reviews in Chemical Engineering*, 17, 1–85.

Gogate, P. R., Shirgaonkar, I. Z., Sivakumar, M., Senthilkumar, P., Vichare, N. P., and Pandit, A. B. (2001). Cavitation reactors: Efficiency analysis using a model reaction. *AIChE Journal*, 47(11), 2326–2338.

Gopalkrishnan, J. (1997). Cell disruption and enzyme recovery. Masters Dissertation, University of Mumbai.

Harris, G. D., Adams, V. D., Sorensen, D. L., and Dupont, R. R. (1987). The influence of photoreactivation and water quality on ultraviolet disinfection of secondary municipal wastewater. *Journal of Water Pollution Control Federation*, 59, 781.

Harrison, S. T. L. (2002). Bacterial cell disruption: A key unit operation in the recovery of intracellular products. *Biotechnology Advances*, 9, 217–240.

Harrison, S. T. L., and Pandit, A. B. (1992). The disruption of microbial cells by hydrodynamic cavitation. *9th International Biotechnology Symposium*, Washington, DC.

Jyoti, K. K., and Pandit, A. B. (2001). Water disinfection by acoustic and hydrodynamic cavitation. *Biochemical Engineering Journal*, 7, 201–12.

Jyoti, K. K., and Pandit, A. B. (2003). Hybrid cavitation methods for water disinfection. *Biochemical Engineering Journal*, 14(1), 9–17.

Jyoti, K. K., and Pandit, A. B. (2004). Ozone and cavitation for water disinfection. *Biochemical Engineering Journal*, 18(1), 9–19.

Kalumuck, K. M., and Chahine, G. L., (2000). The use of cavitating jets to oxidize organic compounds in water. *Journal of Fluids Engineering*, 122, 465–470.

Kanthale, P. M., Gogate, P. R., Wilhelm, A. M., and Pandit, A. B. (2005). Dynamics of cavitational bubbles and design of a hydrodynamic cavitational reactor: Cluster approach. *Ultrasonics Sonochemistry*, 12, 441–452.

Keshavarz, E., Bonnerjea, J., Hoare, M., and Dunhill, P. (1990). Disruption of a fungal organism, rhizopus nigricans, in a high-pressure homogenizer. *Enzyme and Microbial Technology*, 12 (7), 494–498.

Kozyuk, O. V. (1998). Method of obtaining a free disperse system in liquid and device for effecting the same. *U. S. Patent, US 5810 052*, 22 Sep 1998.

Kozyuk, O. V. (1999a). Method and apparatus for producing ultra-thin emulsions and dispersions. *U. S. Patent, US 5931771 A*, 3 Aug 1999.

Kozyuk, O. V. (1999b). Use of hydrodynamic cavitation for emulsifying and homogenizing processes. *American Laboratory*, 31, 6–8.

Kumar, P. S., and Pandit, A. B. (1999). Modeling hydrodynamic cavitation. *Chemical Engineering and Technology*, 22, 1017–1027.

Luche, J. L. (1999). *Synthetic organic sonochemistry*. New York, NY, Plenum Press.

Mason, T. J., and Lorimer, J. P. (1988). *Sonochemistry: Theory, applications and uses of ultrasound in chemistry*. New York, NY, Wiley.

Mason, T. J., and Lorimer, J. P. (2002). *Applied sonochemistry: The uses of power ultrasound in chemistry and processing*. Weinheim, Wiley-VCH GmbH.

Mason, T. J., Joyce, E., Phull, S. S., and Lorimer, J. P. (2003). Potential uses of ultrasound in the biological decontamination of water. *Ultrasonics Sonochemistry*, 10(6), 319–323.

Minear R. A., and Amy G. L. (1996). *Disinfection by-products in water treatment*. Boca Raton, FL, CRC Press.

Moholkar, V. S., and Pandit, A. B. (1997). Bubble Behavior in Hydrodynamic Cavitation: Effect of Turbulence. *AIChE Journal*, 43, 1641–1648.

Moholkar, V. S., and Pandit, A. B. (2001a). Modeling of hydrodynamic cavitation reactors: A unified approach. *Chemical Engineering Science*, 56, 6295–6302.

Moholkar, V. S., and Pandit, A. B. (2001b). Numerical investigations in the behaviour of one-dimensional bubbly flow in hydrodynamic cavitation. *Chemical Engineering Science*, 56, 1411–1418.

Moholkar, V. S., Senthilkumar, P., and Pandit, A. B. (1999). Hydrodynamic cavitation for sonochemical effects. *Ultrasonics Sonochemistry*, 6, 53–65.

Moser, W. R., Marshik-Geurts, B. J., Kingsley, J., Lemberger, M., Willette, R., Chan, A., Sunstrom, J. E., and Boye, A. J. (1995). The synthesis and characterization of solid state materials produced by high shear hydrodynamic cavitation. *Journal of Materials Research*, 10, 2322.

Moser, W. R., Sunstrom, J. E., and Marshik-Guerts, B. (1996). The synthesis of nanostructured pure-phase catalysts by hydrodynamic cavitation. In: Moser, W. R. (ed.), *Advanced Catalysts and Nanostructured Materials*, Academic Press: New York, pp. 285–306.

Novella, I. S., Fargues, C., and Grevillot, G. (1994). Improvement of the extraction of penicillin acylase from *Escherichia coli* cells by a combined use of chemical methods. *Biotechnology and Bioengineering*, 44(3), 379–382.

Parker J. A., and Darby J. L. (1995). Particle-associated coliform in secondary effluents: Shielding from ultra-violet light disinfection. *Water Environment Research*, 67, 1065.

Phull, S. S., Newman, A. P., Lorimer, J. P., Pollet, B., and Mason, T. J. (1997). The development and evaluation of ultrasound in the biocidal treatment of water. *Ultrasonics Sonochemistry*, 4(2), 157–164.

Piyasena, P., Mohareb, E., and McKellar, R. C. (2003). Inactivation of microbes using ultrasound: A review. *International Journal of Food Microbiology*, 87(3), 207–216.

Pontius F. W. (1990). *American waterworks association: Water quality and treatment*. New York, NY, McGraw-Hill.

Povey, M. J. W., and Mason, T. J. (1998). *Ultrasound in food processing*. London, Blackie Academic and Professional.

Sampathkumar, K., and Moholkar, V. S. (2007). Conceptual design of a novel hydrodynamic cavitation reactor. *Chemical Engineering Science*, 62, 2698–2711.

Save, S. S., Pandit, A. B., and Joshi, J. B. (1994). Microbial cell disruption: Role of cavitation. *Chemical Engineering Journal*, 55, B67–B72.

Save, S. S., Pandit, A. B., and Joshi, J. B. (1997). Use of hydrodynamic cavitation for large scale cell disruption. *Chemical Engineering Research and Design*, 75(C), 41–49.

Senthilkumar, P., Sivakumar, M., and Pandit, A. B. (2000). Experimental quantification of chemical effects of hydrodynamic cavitation. *Chemical Engineering Science*, 55(9), 1633.

Shirgaonkar, I. Z., Lothe, R. R., and Pandit, A. B. (1998). Comments on the mechanism of microbial cell disruption in high pressure and high speed devices. *Biotechnology Progress*, 14(4), 657.

Simpson K. L., and Hayes K. P., (1998). Drinking water disinfection byproducts: An Australian perspective. *Water Research*, 32(5), 1522.

Sivakumar, M., and Pandit, A. B. (2002). Wastewater treatment: A novel energy efficient hydrodynamic cavitational technique. *Ultrasonics Sonochemistry*, 9, 123–131.

Sunstrom, J. E., Moser, W. R., and Marshik-Guerts, B. (1996). General route to nanocrystalline oxides by hydrodynamic cavitation. *Chemistry of Materials*, 8(8), 2061.

Suslick, K. S. (1990). The chemical effects of ultrasound. *Science*, 247, 1439.

Suslick, K. S., Mdleleni, M. M., and Reis, J. T. (1997). Chemistry induced by hydrodynamic cavitation. *Journal of the American Chemical Society*, 119(39), 9303.

Tomita, Y. and Shima, A. (1986). Mechanisms of impulsive pressure generation and damage pit formation by bubble collapse. *Journal of Fluid Mechanics*, 169, 535.

Tullis, J. P., and Govindrajan, R. (1973). Cavitation and size scale effect for orifices. *Journal of Hydraulics Division*, HY13, 417.

Umakoshi, H., Kuboi, R., Komasawa, I., Tsuchido, T., and Matsumura, Y. (1998). Heat-induced translocation of cytoplasmic β-galactosidase across inner membrane of Escherichia coli. *Biotechnology Progress*, 14(2), 210–217.

Vichare, N. P., Gogate, P. R., and Pandit, A. B. (2000). Optimization of hydrodynamic cavitation using a model reaction. *Chemical Engineering Technology*, 23, 683–690.

White G. C. (1992). *The handbook of chlorination and alternative disinfectants*. New York, NY, Van Nostrand.

Yan, Y., and Thorpe, R. B. (1990). Flow regime transitions due to cavitation in flow through an orifice. *International Journal of Multiphase flow*, 16(6), 1023.

Yan, Y., Thorpe, R. B., and Pandit, A. B. (1988). Cavitation noise and its suppression by air in orifice flow. *Proceedings of International Symposium Flow Induced Vibration and Noise*, pp. 25–40, Chicago, ASME.

Chapter 7
Contamination-Free Sonoreactor for the Food Industry

Jean-Luc Dion

1 Summary

A new sonoreactor technology is presented here, which should open vast development possibilities in various fields of chemical, pharmaceutical, and food industries. It should give a decisive impulse to sonochemistry in these various areas. These exclusive systems use high-power *converging* acoustic waves in a tube to produce a relatively large volume confined acoustic cavitation zone in flowing liquid reagents. It is well known that numerous chemical reactions are strongly accelerated when they take place inside such a zone. The new cylindrical sonoreactors do not contaminate the processed liquids with erosion products as other devices do. The processing conditions can be widely varied with pressure, power, temperature, and flow rate. The processing capacity of the largest models may be up to several tons per hour, using an electric power input of about 50 kW.

2 Introduction

Ever since the first reported chemical effects of acoustic or ultrasonic cavitation by Richards and Loomis in 1927 (Richards and Loomis, 1927), expectations have risen continuously in the chemical process industry in general without really being fulfilled, particularly during the last twenty years. During this last period, a considerable number of publications on experimental work have shown the advantages of ultrasonic activation for many chemical reactions and processes, mainly in the field of organic chemistry (Kelkar et al. 2006; Mason, 2003), crystallization (Li et al., 2006), food (Mason and Povey, 1995), and the pharmaceutical industry (Freitas et al., 2006). Some reaction rates have been shown to be increased by factors up to

J.-L. Dion (✉)
Département de Génie électrique et Génie informatique, Université du Québec à Trois-Rivières
3760, rue de Montpellier, Trois-Rivières, QC, G8Y 3P2, Canada
e-mail: jl.dion@cgocable.ca

H. Feng et al. (eds.), *Ultrasound Technologies for Food and Bioprocessing*,
Food Engineering Series, DOI 10.1007/978-1-4419-7472-3_7,
© Springer Science+Business Media, LLC 2011

100,000 due to ultrasonic cavitation (Suslick). The catalytic effect of ultrasonic cavitation in many processes is now well demonstrated (Suslick et al., 1999). Many other applications are also known, for example, extraction of valuable molecules from plants or animals (Albu et al., 2004), production of nanoparticles (Gedanken, 2004), sludge disruption (Tiehm and Neis, 1999), water decontamination (Ashokkumar et al., 2003).

One of the main reasons for the slow development of the industrial applications of *sonochemistry* is the fact that ultrasonic cavitation, a violent phenomenon, takes place on the metallic vibrating surfaces of most sonoreactors, and produces severe erosion of these surfaces as the driving power is increased. Even costly titanium alloy vibrators or *sonotrodes* are eroded. Consequently, the reagents are contaminated by erosion products, thus barring the application to most fine chemical and food processes. Until now, this has been the most serious barrier to the use of sonoreactors in industrial chemical processing besides low-volume treatment capacity. One of the unique features of the sonoreactor system that we present here is the absence of erosion and erosion products.

3 The Known Industrial Sonoreactors

Figure 7.1 was taken from the *Hielscher* company website (Hielscher) and shows the principle of their sonoreactors, which are similar to most others, except *CaviRex's*. This photograph represents a special unit where the outside casing is transparent. This casing surrounds the *sonotrode*, which is the concentric central cylinder. The piezoelectric elements to the left (not showing) are driven by an electric current at a frequency such that the sonotrode vibrates in an upper longitudinal mode. This figure illustrates the above-mentioned limitations.

As shown schematically in Fig. 7.2, it is observed that cavitation (clear zones) is induced at points where the acoustic displacement is high (region A) or maximum (region B). There is no cavitation where the vibration amplitude is weak or minimum (region C). We can see that the relative volume of the cavitation zones is rather low. Since the acoustic waves produced are *divergent*, their intensity drops

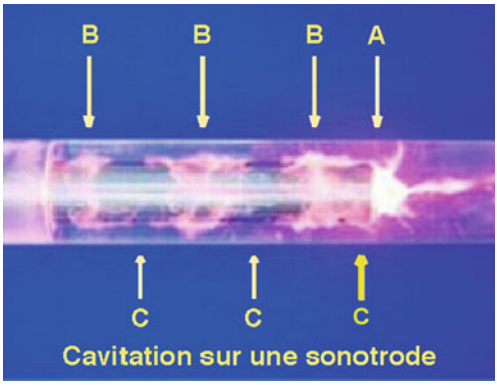

Fig. 7.1 Cavitation on a conventional sonotrode

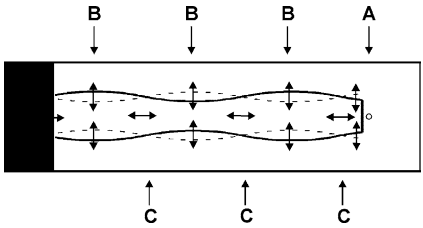

Fig. 7.2 Principle of a conventional sonotrode

quickly away from the sonotrode. It is then easily understood why acoustic cavitation is produced only in the immediate neighborhood of the surface, causing erosion, with a relatively small cavitation volume. It is also observed that cavitation appears mostly along broken lines, almost always at the same places, thus accelerating the erosion effects.

4 An Exclusive Sonoreactor System

We will describe here a new type of patented sonoreactor with its associated system, which is radically different from others in its operating principles (Dion and Agbossou, 2002). Two models presently exist: 5 kW (SR-31) and 50 kW (SR-42), as described below, with large volume processing capacity. These sonoreactors are particularly suited for chemical processing in general since they cannot contaminate reagents with erosion products extracted by acoustic cavitation from metallic surfaces as in other devices (Hielscher, Hydrodynamics.com). The reason for this advantage is that the powerful and efficient large and centered cylindrical cavitation zone produced under variable hydrostatic pressure is kept away from the walls of the tube made of PTFE (polytetrafluoroethylene, *Teflon*^{TM}) that transmits the acoustic energy into the freely flowing liquid (Fig. 7.3). In other sonoreactors,

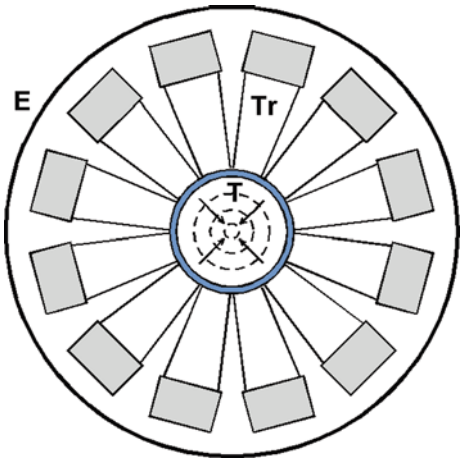

Fig. 7.3 Schematical cross-section of the cylindrical sonoreactor

the acoustic cavitation taking place on the vibrating metallic surfaces (*sonotrodes*), gradually destroys them, and they have to be replaced more or less frequently. Furthermore, in most configurations, the liquid is forced to change direction several times during transit, which is not ideal for thick liquids or sludges (Hielscher, Hydrodynamics.com).

However, due to the lack of appropriate sonoreactors, only a few limited applications to industrial chemical processing now exist on a small scale, mostly for crystallization, mixing, etc. (Hielscher 1000; Mason and Lorimer, 2002). The vast domain of *industrial sonochemical processing* is still open. However, the situation could be transformed by the new type of cylindrical sonoreactors presented here.

5 Using Cylindrical Converging Waves

One basic patented exclusive feature of the *CaviRex* sonoreactors is shown schematically in Fig. 7.3. Twelve special patented prismatic piezoelectric transducers Tr pressed around a PTFE tube T produce high-quality *converging*, and nearly *cylindrical*, ultrasonic waves in the pressurized liquid circulating in the tube. Consequently, the acoustic intensity is normally a maximum at the center of the tube where cavitation starts. This achievement is essentially the result of an initial concept that was extensively simulated with a special software called *Atila*, which is a finite element computation code applied to two- and three-dimensional electromechanical structures with piezoelectric or magnetostrictive elements (Claeyssen et al., 1989). Figure 7.4 shows one simulation result: the displacement of elements in a cross-section of the prismatic transducers of model SR-42, 50 kW, operating in an upper vibration mode at about 36 kHz. Dotted lines represent the rest positions. Each transducer bar is about 90 cm long in this model. Rectangular piezoelectric ceramic pairs are used in these transducers. Particular care has been taken to achieve close acoustic impedance matching between the transducers and the load, for high-power transmission, and low acoustic phase differences between adjacent transducer bases. This last point assures a nearly cylindrical acoustic field in the circulating liquid.

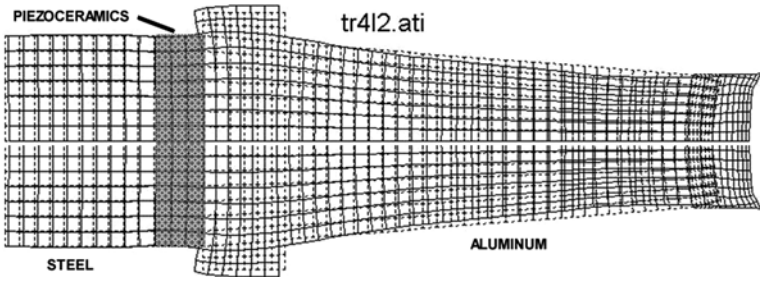

Fig. 7.4 Simulated displacement in the cross-section of the prismatic transducers

The cavitation zone is therefore centered in the tube, as shown in Fig. 7.5. This photograph is extracted from a video taken through a process window, end-on, with clear water flowing. We can see the cavitation zone produced at an input power of about 4 kW at 45 kHz, and medium pressure (4 bars = 400 kPa) in the 5-kW model SR-31. The diameter of the tube is 75 mm in this model. The photograph clearly shows that the cavitation zone is *confined* away from the wall of the tube, which is an exclusive feature of the *CaviRex* sonoreactors. The relative size of the zone should be compared with those in Fig. 7.1. The relative size of the cavitation zone depends mainly on power, frequency, and pressure in the flowing liquid. Cavitation intensity along the radius is a highly non-linear function of acoustic input power, frequency, tube radius, pressure, and other variables. For certain conditions, the intensity may even be lower at the center, since cavitation in a centered annular region strongly absorbs acoustic energy; a cavitation zone is a sort of "black hole" for acoustic energy. That is why, for a given chemical process, one has to determine the particular optimum conditions.

The zone in Fig. 7.5 looks black since the light from below is blocked by thousands of microscopic cavitation bubbles per cubic centimeter that appear, oscillate during a few periods, and implode violently. Imploding bubbles generate shockwaves with acoustic pressures well over 1,000 atmospheres (bars) and temperatures over 5,000 K due to adiabatic compression of the residual gases (Suslick, 2001). The design of the transducers with their supporting structure and the choice of building materials was quite an interesting challenge to achieve that type of cylindrical waves. It should be mentioned that the production of these waves requires the use of a large number of piezoelectric ceramics. So, even to produce very large power, each ceramic is driven at a small fraction of its maximum possible power and temperature. In fact, the temperature of the cooling oil flowing on the transducers is kept well below 60°C. This way, the useful life of these ceramics and that of the sonoreactors is considerably extended.

The bubbles are formed in violently agitated filaments radiating from the center, which look like electric corona discharges (Fig. 7.5), and a strong typical cavitation noise is heard through the massive steel and aluminum structure of the sonoreactor.

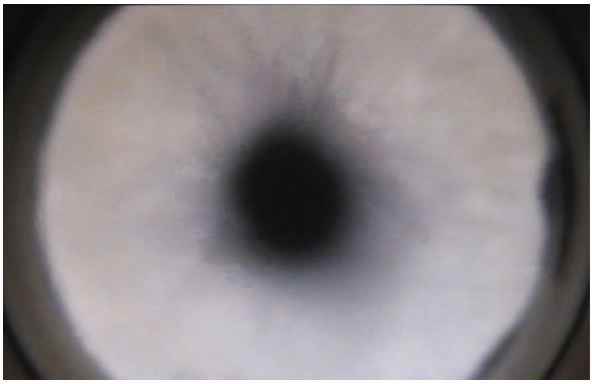

Fig. 7.5 Cavitation zone in the low-power SR-31 sonoreactor. Tube diameter: 75 mm

Varying the pressure and driving power allows a wide variety of processing conditions, where the relative volume of the cavitation zone is changed without destroying the wall of the tube or liberating contaminants. Of course, this zone is where interesting physical and chemical reactions take place. It is now well known that the extreme conditions produced by the implosion of cavitation bubbles can break any organic molecules, and generate very active free radicals, particularly in water. It has even been reported by Lahey et al. (2005) and Taleyarkhan et al. (2004) that *nuclear fusion* actually takes place in cavitation bubbles produced in a deuterated liquid at atmospheric pressure in a low-power sonoreactor.

One interesting feature of the new technology is the fact that the processed liquids flow freely through the tube, without any obstructions, as occurs in most other systems (Hielscher 6000). The flow rate can therefore be varied through a wide range. For example, a very high flow rate may be required for multiple passes through the sonoreactor in certain batch processes. This is so since (as in any other sonoreactor) not all the liquid passes through the cavitation zone in one pass. However, the relative volume of the concentric cylindrical zone is large as compared to that of the active volume in other sonoreactors (see Fig. 7.1).

6 Operating Under Pressure

Another exclusive feature of this new sonochemical sonoreactor is its capability of operating largely above atmospheric pressure in the circulating liquid, where the effective acoustic cavitation efficiency is radically increased with the same electric power input, without auto-destruction of the device. This increase of cavitation power with pressure was demonstrated in the former USSR in the early 1960s, particularly in the experimental work of Sirotyuk (1965). In the hemispherical device used to produce converging acoustic waves, it was demonstrated that cavitation intensity at 4 bars (400 kPa) was about 40 times larger than at atmospheric pressure for the same driving voltage, the ratio being still much larger for higher driving power. This is shown in Fig. 7.6, as taken from Sirotyuk's publication, where the cavitation efficiency was measured by the eroded mass from a small aluminum sphere placed at the focus of the device, as a function of the driving voltage on the transducers for different values of the hydrostatic pressure in the water.

More recently, Matula and Crum observed that an "*increase of up to two orders of magnitude may be achieved by simply increasing the static pressure over the cavitating solution*" in relation with sonoluminescence activity, but they apparently did not know about Sirotyuk's experiments (Matula and Crum, 2000).

The sonoreactors described here were designed with this phenomenon in view, and to operate normally above atmospheric pressure, where the cavitation activity is extremely efficient. In fact, the sonoreactors were operated up to 6 bars (600 kPa) with the present design. In future models, the operating pressure could easily be raised, if needed, to high limits such as 50 bars, where the active or destructive power of cavitation may be thousands of times larger than at atmospheric pressure (Fig. 7.6). This will be particularly useful for the decontamination of large volumes of water; for example, a considerable number of publications show that ultrasonic

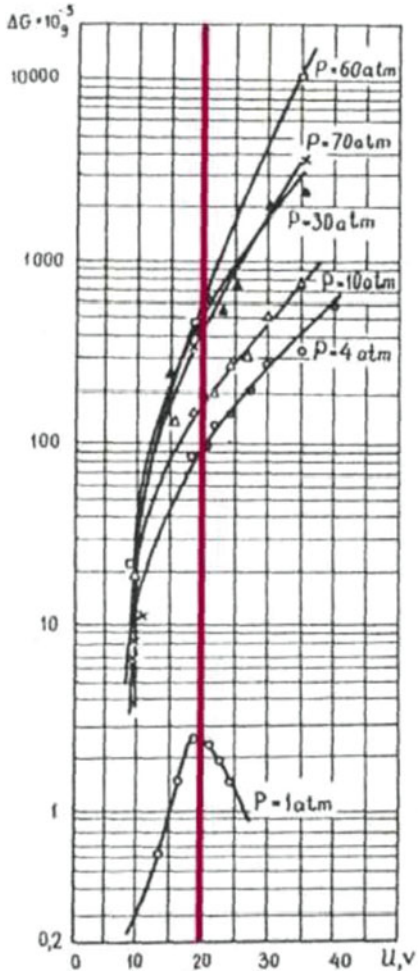

Fig. 7.6 Effect of pressure on the eroded mass of aluminum due to acoustic cavitation at the focus of converging spherical ultrasonic waves, as a function of the transducer driving voltage, for various values of hydrostatic pressure in water (Sirotyuk). It is to be noted that for the same driving voltage, 20 volts (*thick red line*), the cavitation efficiency is about 40 times higher at 4 atm (bars) than at 1 atm (bar), and 80 times higher at 10 bars. If the voltage is then doubled at 4 bars, this graph shows that the cavitation intensity is then about 250 times that at 20 V, 1 bar

cavitation can be efficiently used to reduce the concentrations of chlorinated and fluorinated pollutants to less than 1 ppm (Jiang et al., 2006; Rahuman et al., 2000). Strong cavitation is particularly useful in decontamination of highly polluted water.

However, for operation in food processing, it is desirable to use lower pressure and power, taking advantage of a larger cavitation zone in the free-flowing tube to process large quantities of material.

7 The Actual Systems

Two models of this type of sonoreactors have been designed, built, and operated. The smaller one is a 5 kW, 1 l treatment volume sonoreactor system (SR-31, 75 mm tube) that is well adapted for pilot plant and process development operations. Its control system is particularly suited for these operations, where a close control of

power, pressure, temperature, time, and flow volume is required in the batch or open circuit modes. The operation is entirely automatic after setup. One version is shown in Fig. 7.7, where we can see the cylindrical sonoreactor to the right, mounted on the cabinet containing the medium frequency 5 kW (45 kHz) power generator and the control system. The core of the sonoreactor is composed of 12 prismatic transducers, each of which can be driven with over 400 W of high-frequency power. The system can operate in closed circuit, with the tank to the left containing the liquid to be treated under pressure. In this particular model used for sludge treatment process development, a progressive volume pump forces the liquid through the central free-flowing tube in the sonoreactor, and an automatically adjusted pinch valve maintains its pressure. This unit does not have observation windows. The appropriate combination of power, pressure, and flow rate is maintained automatically, as required. The photograph of the cavitation zone in Fig. 7.5 was taken with a similar system equipped with observation process windows.

The other model is a 50 kW system for industrial applications (SR-42, 100 mm tube, about 900 kg). The sonoreactor core is composed of two groups of 12 concentric prismatic transducers, each being about 900 mm long, and each transducer is able to be driven with 2 kW of high-frequency current (shown rotated 90° in Fig. 7.8). Its operating frequency is normally about 39 kHz. One experimental unit can be seen in Fig. 7.9, as installed for testing in the Achères water treatment plant near Paris (France), the largest plant in Europe. This unit is being experimentally tested for sludge disruption in front of an anaerobic digester, to reduce the mass of residues, and to increase the biogas output. The sludge is fed into the 2 m high sonoreactor from below, and the pressure is maintained by a large pinch valve, partially visible to the right. To the left, we can see the automatic control system and the high-frequency current generator. This system can operate at any internal

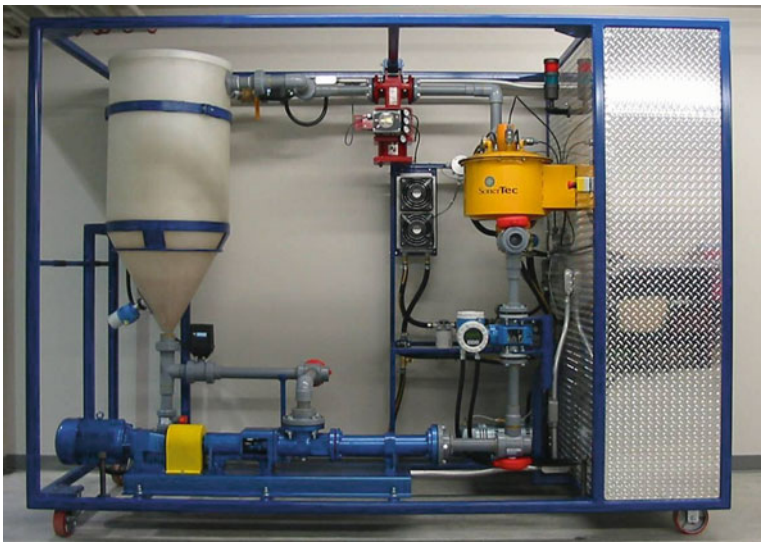

Fig. 7.7 The *SonerTec* SR-31 5 kW process development sonoreactor system

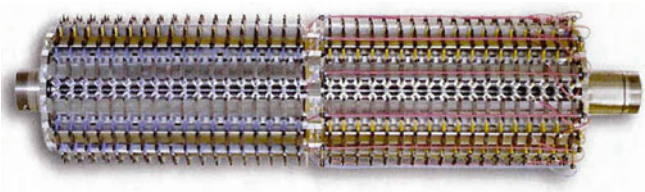

Fig. 7.8 The core of the 50 kW sonoreactor (rotated 90°)

Fig. 7.9 The "*DigestSonic*" SR-42 system installed in a sludge treatment plant in France

pressure from 1 to 6 bars (100–600 kPa). In this model, the pressure is also limited by the type of pipes used, in this case, CPVC. As with the smaller model, the operating pressure, power, flow rate, etc., and the type of associated systems (pumps, generator, etc.) can be varied widely to accommodate various processes.

8 The Powerful Effects of Confined Acoustic Cavitation

When a 0.6 mm thick hard aluminum alloy plate is inserted into the cavitation zone of Fig. 7.5, it can be observed that the center is pierced in less than 1 min. The photograph in Fig. 7.10 clearly shows the effect of a 3-min exposure in the smaller sonoreactor described above (SR-31). The total length of the eroded zone (narrow ends) is about 240 mm, the central strong erosion zone is about 100 mm long, while

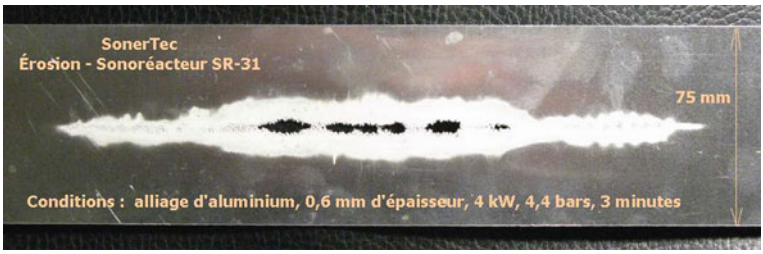

Fig. 7.10 Erosion of a 0.6 mm aluminium alloy plate during a 3-min exposure in model SR-31

the length of the surrounding prismatic transducers is 210 mm. This figure illustrates the end effects as predicted by the theory of diffraction of waves. If the same tube were much longer, the end effects would be more or less the same, while the relatively uniform intensity region would be much longer and more efficient. This has been well confirmed in the 50 kW model using a 1,800 mm long tube which is described above. A liquid can flow freely without any obstruction in this tube.

Figure 7.11 shows the effect of acoustic cavitation in the 1,800 mm long PTFE tube of the SR-42 sonoreactor operating at 39 kHz, 50 kW, 6 bar pressure. The hard aluminum alloy 1.5 mm thick plate was submitted to a 5-min exposure. These last two figures may be the best demonstrations of the unique possibilities of the new technology where industrial power and capacity are required.

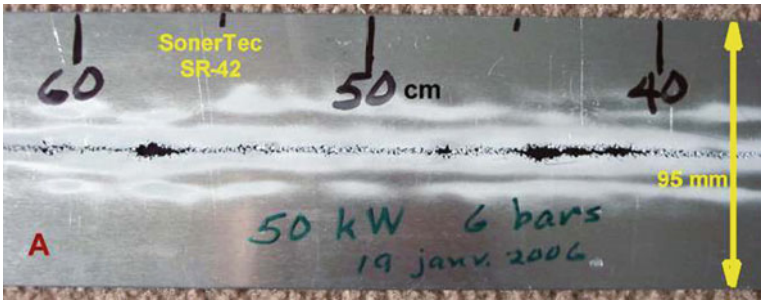

Fig. 7.11 Erosion of a 1.5 mm aluminum alloy plate during a 5-min exposure in model SR-42 (50 kW)

This result can be compared with the almost invisible erosion produced on an aluminum alloy plate at 12 mm under the sonotrode of a 500 W *Bransonics* system (Fig. 7.12a and b).

When secondary sludge from a water treatment plant is passed through this type of sonoreactor, it is fragmented into smaller particles, making it more efficiently degraded in an anaerobic digester. In Fig. 7.13, we can see the particle size distribution as measured by a laser instrument for different values of the specific electrical energy in kilojoules/liter consumed by the sonoreactor.

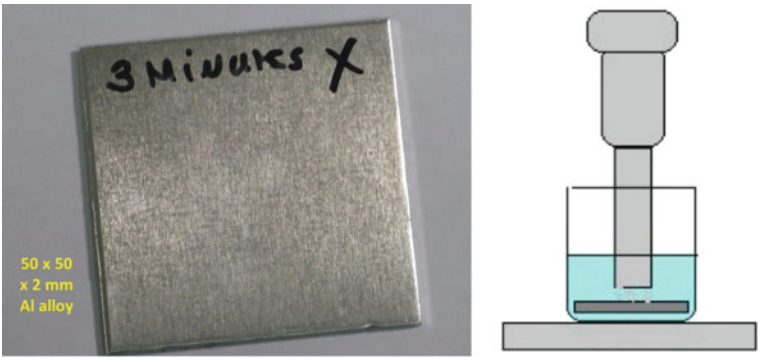

Fig. 7.12 Almost invisible erosion effect on an aluminum alloy plate (**a**), 12 mm under a 500 W Branson sonotrode irradiated for 3 min (**b**)

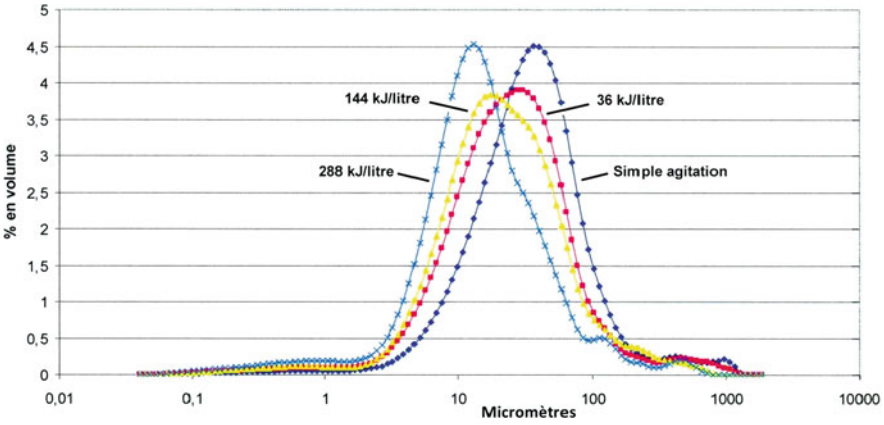

Fig. 7.13 Size distribution of sludge particles for various treatment energy

As a consequence of this fragmentation, there is an increase in the measured chemical oxygen demand (COD) in the sludge. This increase is in fact a clear indication of the extent of the sludge disruption, and is directly related to the increase of the volume of biogases to be produced in the digester, and the decrease of the mass of the residues. In Fig. 7.14, we can see that the COD increases linearly with the specific treatment energy.

9 Processing Conditions and Versatility

For each particular process, the operating conditions have to be determined with a laboratory unit before scale-up in most cases of chemical processing. Depending on the process, mild or strong cavitation may be required. For a given driving

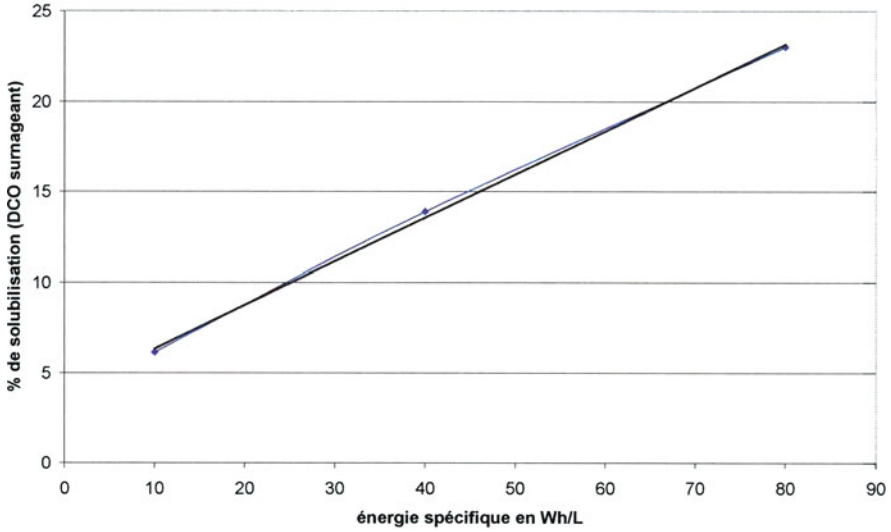

Fig. 7.14 Typical linear increase of COD with specific treatment energy (1 Wh/l = 3,600 J/l)

power and operating pressure above the cavitation threshold, each particular process requires a determined energy per unit volume, or specific cavitation energy (SCE). For example, we have experimented with sugar crystallization, and observed that the increased production of fine uniform crystals required low pressure, and low power above cavitation threshold. It is expected that strong cavitation destroys crystals as soon as they are formed.

Another practical feature of this type of sonoreactor is the fact that they can be used for almost any application with relatively minor modifications in the sonoreactor and outside tubing and pumps, with the same electronic systems. For example, if it is necessary to process corrosive liquids, the outside tubing would be made with appropriate stainless steel, or PTFE (*Teflon*™). Other practical models are also on the drawing board, with various improvements over the existing systems. New designs will also achieve larger relative volumes of the cavitation zone for increased efficiency. It should be noted that these sonoreactor systems can normally be simply inserted into an existing process with few changes. The floor space occupied by one SR-42 unit is typically only 2 × 3 m. Any number of units can be operated in series or parallel, or both, to process very large quantities.

10 Efficiency

The energy E (joules, J) used to raise the temperature of water in the sonoreactor is

$$E = m\,c\,\Delta T \tag{7.1}$$

where m is the mass of heated water in grams, c is the specific heat (4.18 J g^{-1} dgC^{-1}), and ΔT the rise of temperature in °C.

The "efficiency" ε of a sonoreactor is a characteristic, which is often not well defined in many publications. Most of the time, it is simply measured by this energy E divided by the electrical energy input E_e
and

$$\varepsilon = \frac{E}{E_e} \tag{7.2}$$

However, in most other configurations, much of the temperature rise is due to heat dissipated by the transducers, which are cooled by flowing processed liquid. Therefore, the result is an overestimation of the cavitation efficiency. In the *CaviRex* systems, the transducers, which are designed for the highest efficiency, are cooled separately by an oil flow. The quantity of heat energy propagating through the *Teflon*™ tube should only be a small unknown fraction of the total dissipation since PTFE is a good insulator. On the other hand, the PTFE tube absorbs a certain fraction of the acoustic energy propagating through its wall; it is a fairly high dissipative medium for acoustic waves at 40 kHz. That is why its thickness is kept below 5 mm.

Therefore, the major part of the temperature rise in the *CaviRex* sonoreactors is due to the effective acoustic and cavitation energy E_a. If we call the electrical energy input E_e, the *cavitation efficiency* ε_a is then defined approximately as

$$\varepsilon_a = \frac{E_a}{E_e} \tag{7.3}$$

where

$$E_a = m\,c\,\Delta T \tag{7.4}$$

m is the mass of the liquid, c is its specific heat, and ΔT the temperature rise.

Of course, such a definition should give lower efficiency values than those published for other sonoreactors. However, it should be more realistic. *CaviRex's* measurements gave values of ε_a up to nearly 50%. Various improvements in future models are expected to provide higher figures. For example, thinner tubes will be designed, and the transducers will be better optimized.

Finally, the real and effective efficiency of a sonoreactor system is essentially measured by the total cost of operation per processed ton of materials as an improvement in the higher cost of a regular process.

11 Processing Capacity

The volume of liquid that can be processed per hour essentially depends on the specific cavitation energy needed to achieve the required chemical or mechanical effect. Let us assume, for example, that a given process requires a reasonable SCE

(defined above), $S = 20$ J/cm^3 $= 20 \times 10^6$J/m^3, and that the SR-42 is operated at maximum power $P = 50$ kW. The total input energy E during 1 h is 50 kW-h, or

$$E = Pt = 50 \cdot 10^3\text{W} \times 3600\,\text{s} = 1.8 \cdot 10^8\ \text{J} \tag{7.5}$$

The possible processed volume D per hour is then easily computed:

$$D = \frac{E}{S} = \frac{1.8 \cdot 10^8\text{J}}{20 \cdot 10^6\text{J/m}^3} = 9\ \text{m}^3 = 9000\ \text{litres} \tag{7.6}$$

This flow rate is inversely proportional to the SCE. If larger flow rates are required, any number of these units can be easily installed in series or parallel.

12 Costs of Operation

At the moment, the known costs of operation of these two new sonoreactor systems are mainly those of the electric driving power. Let us suppose that the 50-kW system (SR-42) is operated at nominal power. Allowing an upper limit of 15 kW for peripheral systems (pumps, cooler, control system, etc.), the energy used in 1 h is then 65 kW-h. If the cost of energy is \$0.15 kW-h, the cost of operation is \$9.75 h.

With $S = 20$ J cm^{-3}, the cost of sonication per liter is therefore about \$0.001. This cost is directly proportional to the SCE. For an SCE of 100 J cm^{-3}, it is simply multiplied by 5 to give \$0.0055 l, meaning that the processing time is multiplied by 5 if the system is operated at full power. Or, put another way, for the same input power and same time, the processed volume is 5 times less for the same cost of operation if the SCE is 100 J cm^{-3}. The smaller SR-31 (5 kW) system has therefore a processing capacity, which is about ten times lower than the SR-42.

Currently, if the driving power is kept below the possible limit of 60 kW, the lifetime of the tube may be well over one year of continuous operation according to various observations. Let us also mention that the efficiency of the type of HF current generator used is over 90%, which reflects the ratio of HF power over the input low frequency power (50 or 60 Hz). If necessary, the tube can normally be replaced in less than a day, at a cost below \$5000.

13 Conclusion

It has been known for a long time that acoustic cavitation considerably accelerates many chemical processes, largely in organic chemistry, and produces energetic disruption effects on particles and molecules. Acoustic cavitation can also improve crystallization, extraction, mixing, emulsifying, etc. We presented a radically new sonoreactor technology which should open innovating and exciting perspectives for the modern food and chemical industry that is looking for significant and competitive process improvements with sonochemistry. This technology is based on

cylindrical converging ultrasonic waves producing a powerful concentric and confined chemically active cavitation zone in a *Teflon*™ tube, away from the wall, in such a way that there is no erosion or contaminating products. Processing conditions can vary widely depending on the particular process. The new *CaviRex* sonoreactors have industrial processing capabilities, measured in tons per hour for the larger model, depending on the cavitation energy per unit volume required to produce a given effect.

References

Albu, S., Joyce, E., Paniwnyk, L., Lorimer, J. P., and T. J. Mason (2004). Potential for the use of ultrasound in the extraction of antioxidants from *Rosmarinus officinalis* for the food and pharmaceutical industry. *Ultrasonics Sonochemistry*, 11, 261–265.

Ashokkumar, M., Vu, T., Grieser, F., Weerawardena, A., Anderson, N., Pilkington, N., and Dixon, D. R. (2003). Ultrasonic treatment of *Cryptosporidium oocysts*. *Waste Water Science and Technology*, 47(3), 173–177.

Claeyssen, F., Bouchen D., Anifrani K., Bossut R., and Decarpigny, J. N. (1989). Analysis of magnetostrictive transducers by the ATILA finite element code. *Journal of Acoustic Society of America*, 75(Suppl 1), LL4. The *Atila* code originates from *Institut Supérieur d'Électronique du Nord*, an engineering school in Lille, France.

Dion, J. L., and Agbossou, K. (2002). *US Patent 6,361,747*, Reactor with acoustic cavitation. Also patented in Canada, France, UK and Germany.

Freitas, S., Hielscher, G., Merkle, H. P., and Gander, B. (2006). Continuous contact- and contamination-free ultrasonic emulsification—a useful tool for pharmaceutical development and production. *Ultrasonics Sonochemistry*, 13, 76–85.

Gedanken, A. (2004). Using sonochemistry for the fabrication of nanomaterials, a review article. *Ultrasonics Sonochemistry*, 11(2), 47–55.

Hielscher. http://www.hielscher.com/ultrasonics/sonochem_01.htm. Accessed 2008.

Hielscher. http://www.hielscher.com/ultrasonics/i16000_p.htm. Accessed 2008.

Hielscher 1000. http://www.hielscher.com/ultrasonics/i1000_p.htm. Accessed 2008.

Hielscher. http://www.hielscher.com/ultrasonics/i2000_p.htm. Accessed 2008.

Hydrodynamics.com. http://www.hydrodynamics.com/about_us.htm. Accessed 2008.

Jiang, Y., Pétrier, C., and Waite, T. D. (2006). Sonolysis of 4-chlorophenol in aqueous solution: Effects of substrate concentration, aqueous temperature and ultrasonic frequency. *Ultrasonics Sonochemistry*, 13(5), 415–422.

Kelkar, M. A., Gogate, P. R., and Pandit, A. B. (2006). Process intensification using cavitation: Optimization of oxidation conditions for synthesis of sulfone. *Ultrasonics Sonochemistry*, 13(6), 523–528.

Lahey, R. T., Jr., Taleyarkhan, R. P., and Nigmatulin, R. I. (2005). Bubble power. *IEEE Spectrum*, May 2005.

Li, H., Li, H., Guo, Z., and Liu, Y. (2006). The application of power ultrasound to reaction crystallization. *Ultrasonics Sonochemistry*, 13(4), 359–363.

Mason, T. J. (2003). Sonochemistry and sonoprocessing: the link, the trends and (probably) the future. *Ultrasonics Sonochemistry*, 10(4–5), 175–179.

Mason, T. J., and Lorimer, J. P. (2002). *Applied Sonochemistry – the uses of power ultrasound in chemistry and processing*. Weinheim, Wiley. ISBN-10:3-527-30205-0.

Mason, T. J., and Povey, M. J. W. (1995). *Ultrasound in food processing*. New York, NY, Springer. ISBN-13: 978-0751404296.

Matula, T. J., and Crum, L. A. (2000). *The sonophysics and sonochemistry of liquid waste quantification and remediation*. U.S. Department of Energy, Office of Scientific and Technique

Information, http://www.osti.gov/em52/final_reports/54897.pdf. Accessed on 23 September, 2010.

Rahuman, M. S. M. M., Pistone, L., Trifirò, F., and Miertus, S. (2000). Destruction technologies for polychlorinated biphenyls (PCBs). *Proceedings of Expert Group Meetings on POPs and Pesticides Contamination: Remediation Technologies and on Clean Technologies for the Reduction and Elimination of POPs*. ICS-UNIDO publications. http://www.ics.trieste.it/core-programmes/biofuels/publications.aspx. Accessed on 23 September, 2010.

Richards, W. T., and Loomis, A. L. (1927). *Journal of American Chemistry Series* 49, 3086.

Sirotyuk, M. G. (1965). Ultrasonic cavitation processes at increased hydrostatic pressures. *5e Congrès International d'Acoustique,* Liège, 7–14 September 1965, paper #D46

Suslick, K. S. (2001). Sonoluminescence and sonochemistry. In: Meyers, R. A. (ed.), *Encyclopedia of physical science and technology*, 3rd edn. San Diego, CA, Academic.

Suslick, K. S., Didenko, Y., Fang, M. M., Hyeon, T., Kolbeck, K. J., McNamara W. B., III, Mdeleleni, M. M., and Wong, M. (1999). Acoustic cavitation and its chemical consequences. *Philosophical Transactions of the Royal Society A*, 357(1751), 335–353.

Suslick. http://www.scs.uiuc.edu/suslick/sonochemistry.html. Accessed on 23 September, 2010.

Taleyarkhan, R. P., Cho, J. S., West, C. D., Lahey, R. T., Jr., Nigmatulin, R. I., and Block, R. C. (2004). Additional evidence of nuclear emissions during acoustic cavitation. *Physical Review E, Statistical, Nonlinear, and Soft Matter Physics*, 69(32), art. no. 036109, 036109-1-036109-11.

Tiehm, A., and Neis, U. (1999). *Ultrasound in Environmental Engineering*, edited by Technical University Hamburg-Harburg, Reports on Sanitary Engineering 25 (ISSN 0724-0783, ISBN 3-930400-23-5), GFEU-Verlag, Hamburg.

Chapter 8
Controlled Cavitation for Scale-Free Heating, Gum Hydration and Emulsification in Food and Consumer Products

Douglas G. Mancosky and Paul Milly

Cavitation is defined as the sudden formation and collapse of bubbles in liquid by means of a mechanical force. As bubbles rapidly form and collapse, pressurized shock waves, localized heating events and tremendous shearing forces occur. As microscopic cavitation bubbles are produced and collapse, shockwaves are given off into the liquid, which can result in heating and/or mixing, similar to ultrasound. These shockwaves can provide breakthrough benefits for the heating of liquids without scale buildup and/or the mixing of liquids with other liquids, gases or solids at the microscopic level to increase the efficiency of the reaction.

One adverse effect of hydrodynamic cavitation has been the severe erosion of surfaces in contact with the fluid undergoing cavitation. This effect has been extensively documented, specifically on hydrofoils (Young, 1999). A unique design for equipment that induces fluid cavitation would allow the harnessing of destructive forces while eliminating equipment erosion and maximizing hydrodynamic cavitation in the product. The design of the ShockWave Power Reactor (SPR) system employed concentric cylinders with fluid in the annular space. The surface of the inner rotating cylinder contains multiple cavities where fluid was pressurized and depressurized many times, inducing hydrodynamic cavitation in the fluid. This type of cavitation was deemed "vortex" cavitation and occurs in the cavities of the rotor surface (Fig. 8.2). This novel design allows a continuous flow of fluid to replenish multiple cavities as the rotor spins, facilitating cavitation and product flow through the system. Centrifugal forces from the inner, rotating cylinder were countered with centripetal forces to avoid traveling cavitation, or cavitation that spills out of the cavity and travels through the system. Pressurizing the system during operation ensured continuous product contact with the inner rotor, resulting in the fluid undergoing controlled cavitation. As the product enters the SPR annular space with the rotor set at a specified operational speed (RPM), the mass rate of flow of the product dictats the frequency of cavitational events and, ultimately, the end exit temperature.

D.G. Mancosky (✉)
Application Development, Hydro Dynamics, Inc., Rome, GA, USA
e-mail: dmancosky@hydrodynamics.com

H. Feng et al. (eds.), *Ultrasound Technologies for Food and Bioprocessing*, Food Engineering Series, DOI 10.1007/978-1-4419-7472-3_8,
© Springer Science+Business Media, LLC 2011

In recent decades, acoustic cavitation has given rise to new disciplines in chemistry such as sonochemistry and sonoluminescence. Mechanically induced cavitation is referred to as hydrodynamic cavitation. Hydrodynamic cavitation is induced mechanically when fluids are pressurized and depressurized while flowing around or through an obstacle in the flow field. Innovative hydrodynamic cavitation reactors offer logical applications in the food industry such as degassing of fluids, releasing intracellular enzymes and metabolites, enhanced microbial inactivation, mixing, emulsification and homogenizing of fluid foods (Balasundaram and Pandit, 2001; Mason and Lorimer, 2002; Middelberg, 1995; Save et al., 1997; Young, 1999).

Cavitation is normally considered a very destructive force, known to damage pumps, boat impellers and water structures such as dams. Cavitation can destroy very durable substrates such as concrete and steel. Hydrodynamic cavitation is characterized for individual fluids by sanctioning a cavitation number, σ. The cavitation number, σ, is an index of the resistance of the flow to undergo cavitation and is denoted in Equation (8.1):

$$\sigma = \frac{P_0 - P_v}{0.5 \times \rho \times \mu^2} \tag{8.1}$$

where P_0 = ambient static pressure, P_v = vapor pressure, $(0.5) \times \rho \times \mu^2$ = dynamic pressure where ρ = density and μ = flow velocity. Cavitation is most likely to occur when the cavitation number is below a critical value characteristic of the fluid. The type of cavitation characterized by the cavitation number transpires in rotating cylinders, propellers, hydrofoils, fluid machinery and rapidly rotating rods (Young, 1999).

As fluid is forced through a configuration that induces formation of eddy currents such as flow around solid surfaces or small and large cross-sectional area in the flow stream, the fluid's kinetic energy is converted into elevated velocities at the expense of a drop in fluid pressure. Localized high and low velocities in a fluid bulk develops momentary gradients of reduced vapor pressures, causing dissolved or trapped gases and fluid vapors to accumulate and expand, forming a bubble. Small particulates, such as dust, debris, or biological entities provide a physical surface for bubble nuclei to attach, expand, and collapse. Bubbles traveling instantaneously from regions of low to high pressure will implode. The collapse of a vapor-filled cavity is accompanied by intense pressure waves, vigorous shearing forces, localized heating events and, in some cases, the formation of free radicals (Earnshaw, 1998; Leighton, 1998; Mason and Lorimer, 2002; Young, 1999). Cavitation can also cause damage to pipes, turbines and pumps. Such uncontrolled cavitation can quickly destroy stainless steel, often requiring costly maintenance and replacement.

The majority of research investigating cellular disruption via hydrodynamic cavitation has employed some variation of a Venturi configuration or multi-orifice plate, which permits sample collection after one pass or one cavitation event. These studies examined the efficacy of hydrodynamic cavitation when disinfecting wastewater (Gogate, 2002; Jyoti and Pandit, 2001, 2004; Sivakumar and Pandit, 2002). In addition to wastewater treatment, increasing focus is being placed on hydrodynamic

cavitation as a means of achieving cellular disruption or producing nano-sized suspended particles in large-scale operations with improved process control and reduced energy costs (Save et al. 1994, 1997).

One manufacturer of cavitation technology is Hydro Dynamics, Inc., who through the SPR has found a method to produce cavitation in a way that is not damaging to the equipment. Therefore, this powerful force can be used for mixing and heating applications in the food and consumer product industries.

1 How Cavitation Is Produced in the SPR

The SPR is a rotor–stator style device. The heart of the technology is a specialized rotor with cavities that spins. This novel design allows for a continuous flow of fluid to replenish multiple cavities as the rotor spins, facilitating cavitation and product flow through the system. Centrifugal forces from the inner rotating cylinder are countered with centripetal forces to avoid traveling cavitation, or cavitation that spills out of the cavity and travels through the system. Pressurizing the system during operation ensures continuous product contact with the inner rotor, resulting in the fluid undergoing controlled cavitation. As the product enters the SPR annular space with the rotor set at a specified operational speed (RPM), the mass rate of flow of the product dictates the frequency of cavitational events and, ultimately, the end exit temperature. As cavitation occurs, the fluid bulk receives energy dissipated by the bubbles in the vapor phase as the bubbles collapse; thus, the fluid in immediate contact with the bubbles before collapse will have instantaneous temperatures higher than the average temperature of fluid leaving the annular space. The exposure to temperatures exceeding that of the system's average temperature allows microbial inactivation to exceed that, which can be predicted by using microbial inactivation kinetics based on the fluid transient time–temperature history in the annular space and the residence time after leaving the SPR prior to sampling. The amount of energy required to do this is the tensile strength or the maximum stress that a material can withstand from stretching the load without tearing. Stretching creates a low-pressure zone in the bottom of the holes. A slight back pressure assures that the device always remains full and that the cavities do not run dry. Eventually, the low-pressure zones can no longer maintain themselves and they collapse, releasing all of the mechanical energy required to create them in the form of a shockwave. The spinning action generates hydrodynamic cavitation within the cavities away from the metal surfaces. This is depicted in Fig. 8.1.

Because the cavitation is collapsing in the bulk fluid, and not against a metal surface, it is rendered harmless to the device. The cavitation is controlled, and therefore there is no damage. Shockwaves do strike the metal surfaces, but they are a small fraction of the energy of a cavitation bubble and cause no damage. The cavitation also has an ultrasonic effect that helps to keep the unit clean.

Cavitation is an exponential function with RPM as it is based upon tip speed. As RPMs increase, cavitational energy increases. Heat output is the heat energy

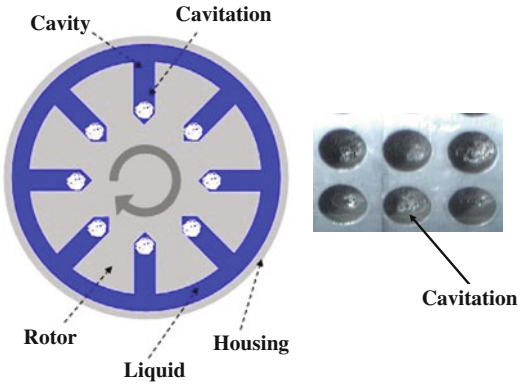

Fig. 8.1 Cross section of SPR and picture of cavitation

imparted to the liquid by the SPR. ΔT is the difference between the liquid temperature at the SPR inlet and SPR outlet and can be used as a proxy for cavitational energy.

At higher speeds, the SPR induces cavitation in the processed liquid, which results as an input of heat energy into the liquid. Operational parameters that influence the amount of heat energy input are as follows:

1. Rotor speed
2. Rotor diameter
3. Liquid flow rate
4. Liquid properties, e.g., tensile strength, specific weight.
5. Internal SPR geometry

A summary of the relationships between these parameters is noted below. With all other variables remaining constant:

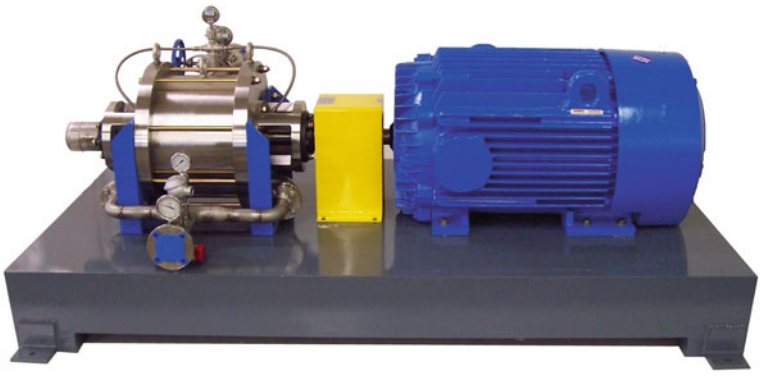

Fig. 8.2 SPR Skid system

↑ Rotor Speed =↑ Heat Output <>↓ Rotor Speed =↓ Heat Output
↑ Rotor Diameter =↑ Heat Output <>↓ Rotor Diameter =↓ Heat Output
↑ Fluid Flow Rate =↓ ΔT <>↓ Fluid Flow Rate =↑ ΔT (Total Heat Output)
↑ Tensile Strength =↑ Heat Output <>↓ Tensile Strength =↓ Heat Output
↑ Specific Weight =↑ Heat Output <>↓ Specific Weight =↓ Heat Output

The SPR is generally coupled with an electric motor on a skid, although it is possible to couple it with other spin sources such as a diesel motor. A depiction of an SPR skid system can be seen in Fig. 8.2.

2 Scale-Free Heating

Temperature increase from fractional degrees to hundreds of degrees can be obtained in a single pass using cavitation. Because the heat is created inside the liquid rather than transferred through high temperature metal surfaces, there is no scaling of equipment and no scorching of product. This is particularly important in high fat dairy products such as cheese and puddings. Equipment shutdowns and maintenance problems are greatly reduced, improving product yield and product quality and reducing overall costs associated with production. Product taste is also improved.

Hydrodynamic cavitation applied to products eliminates scaling and generates heat instantaneously within the processed product. Eliminating scaling during heating allows for uniform processing of the product while minimizing the surface fouling commonly associated with conventional heating equipment. Cavitation can heat liquids in seconds. As cavitation occurs, the bulk fluid receives the energy dissipated by the bubbles in the vapor phase as the bubbles collapse; thus, the fluid in immediate contact with the bubbles before collapse has instantaneous temperatures higher than the average temperature of fluid leaving the annular space. This heating can be done with pinpoint accuracy and consistency by varying the RPMs through a temperature controller and variable frequency drive. There is no temperature gradient or hot or cold spots, as can be seen in Fig. 8.3. There is also no heat transfer surface, so there is no scaling or fouling. The system is flameless and can be totally automated.

Cavitation can heat liquids with no degradation in the heat transfer coefficient. This was demonstrated in work conducted with a major university on a scaling liquid in a heating test cell meant to mimic conventional heat exchangers and comparing that to an SPR system. The results of this study can be seen in Fig. 8.4.

Cavitation is excellent for heating eggs, pudding, gels, cheeses, sauces and high protein food products without scorching and for the pasteurization of high fat milk products and fruit juices. All of these substances can be processed without scaling.

The food industry has always pursued novel processing technologies that allow for reduced energy consumption and minimized product exposure to thermal treatments. Excessive thermal treatment of food, although necessary to render the product safe for consumption and extend shelf-life, was also a primary reason for

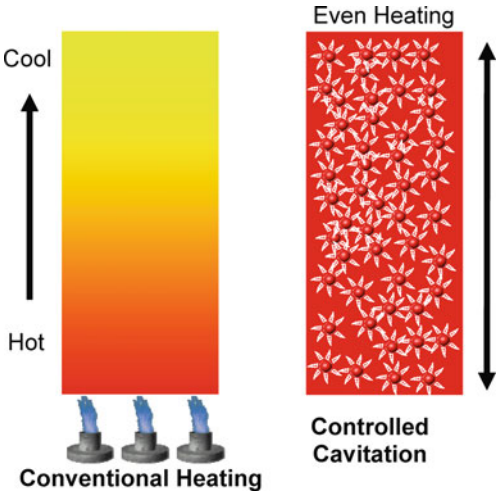

Fig. 8.3 Scale-free heating

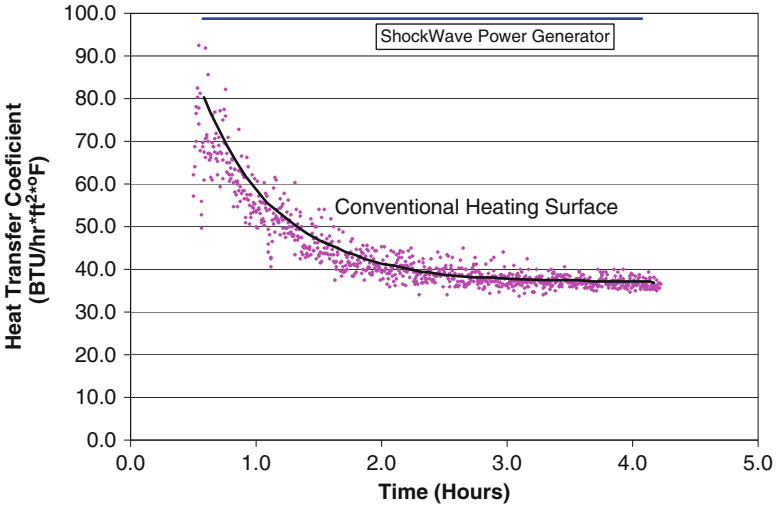

Fig. 8.4 Scaling comparison to conventional technology. Reproduced from Kazem et al. (2003)

reduced product quality and undesirable organoleptic properties. Table 8.1 depicts the energy consumption required for processing calcium-fortified apple juice using an SPR in comparison to conventional heating. Conventional pasteurization of apple juice required heating the product to 88C and holding for 15 s before cooling to eliminate spoilage and pathogenic microorganisms. Table 8.1 also portrays the amount of energy required to achieve a transient temperature change from 20°C to 65.6°C, 76.7°C and 88°C in order to achieve a 5-log reduction of *Saccharomyces cerevisiae*. Achieving target lethality at lower temperatures using an SPR resulted in a reduced energy requirement relative to that for conventional heat treatments to obtain a 5-log

Table 8.1 Energy comparisons of a 12 HP SPR unit during treatment of apple juice inoculated with *S. cerevisiae* at an initial temperature of 20°C using two SPR[1] settings (3,000 and 3,600 rpm) and two endpoint temperatures (65.6 and 76.7°C) to a conventional heat treatment (CHT) with an endpoint temperature of 88°C ($n = 6$)[2]

Process SPR vs. CHT	Setting (rpm)	$Temp_{out}$ (°C)	Mass flow rate (kg/s)	H_{input} (kJ/kg)	H_{loss} (kJ/kg)	$\%_{efficiency}$ (%)
SPR	3,000	65.6	0.026[c]	173[c]	118[b]	60[c]
	3,000	76.7	0.019[d]	215[b]	178[a]	55[d]
	3,600	65.6	0.044[a]	173[c]	32[d]	84[a]
	3,600	76.7	0.031[b]	215[b]	70[c]	75[b]
CHT	–	88.0	(0.019–0.44)	258[a]	–	–

[1]SPR = "Shockwave Power™ Reactor" or "controlled" cavitation system
[2]$n = 6$; Values calculated from three separate trials with two samples per treatment; means followed by same letter in column do not differ significantly ($\alpha = 0.05$) according to ANOVA and SNK analysis
– Data not applicable
(Data taken from Milly et al., 2008)

reduction of *S. cerevisiae*. The mean value of applied energy per unit weight of product to achieve 6.27 log cycles reduction of *S. cerevisiae* at SPR rotor speeds of 3,000 and 3,600 rpm at 65.6°C and 76.7°C were 173, 215, 173 and 215 kJ/kg, respectively. These values were considerably lower than the conventional heat treatment, which required the application of 258 kJ/kg to achieve the equivalent lethality of the SPR. Significant differences among mass flow rates and percentage energy efficiency at various SPR operating parameters suggested the use of SPR at rotor speeds of 3,600 rpm with an endpoint temperature of 65.6°C. These parameters required a mass flow rate of 0.044 kg/s and 173 kJ/kg of energy to induce a mean reduction of 6.27 log cycles with the lowest energy loss of 32 kJ/kg and highest energy efficiency of 84%. Operating the SPR at 3,600 rpm with an endpoint temperature of 76.7°C required a mass flow rate of 0.031 kg/s and 215 kJ/kg of energy to induce a mean reduction of 6.27 log cycles with an energy loss of 70 kJ/kg and an energy efficiency of 75%. SPR operation at 3,000 rpm with endpoint temperatures of 65.6 and 76.7°C required a mass flow rate of 0.026 and 0.019 kg/s and 173 and 215 kJ/kg of energy to induce a mean reduction of 6.27 log cycles with energy losses of 118 and 178 kJ/kg and energy efficiencies of 60 and 55%. These patterns suggested that the amount of energy lost to the system in the form of heat can be reduced by increasing the SPR rotational speed and product mass flow rates through the SPR system. Moreover, these data suggested a more efficient coupling of mechanical energy to the product when the SPR rotor speed was increased along with mass flow rate. As the specific heat of calcium-fortified apple juice was 3.792 (kJ/kg*K), excessive energy generated from hydrodynamic cavitation was lost as heat dissipated from the fluid to the SPR housing. Increasing the mass flow rate of the product through the system allowed energy to be coupled more efficiently to the product itself. These data supported the claim of utilizing an SPR to minimally heat treat apple juice, with benefits manifesting in the form of energy savings, superior organoleptic properties and increased retention of heat labile nutrients.

3 Mixing

Conventional batch mixing usually occurs in large tanks containing an impeller that constantly stirs the contents in order to achieve uniformity. Because the tanks are normally very large, long process times are required in order to achieve uniformity. In many cases, a completely homogeneous mixture cannot be achieved. Cavitation can often provide superior mixing because the powerful force of cavitation is applied to a limited volume of liquid.

When cavitation bubbles collapse and produce shockwaves, powerful forces are generated that cut the process material into microscopic sizes. This increases the surface contact area between the liquids, gases and/or solids being mixed and maximizes the efficiency of the procedure for processes such as hydration, emulsification and gas/liquid mixing. This procedure can be seen in Fig. 8.5.

Cavitation is a unique mixing mechanism and can often be used to effectively mix shear sensitive compounds. Cavitation can produce superior results when mixing liquids with gases, solids, or other liquids.

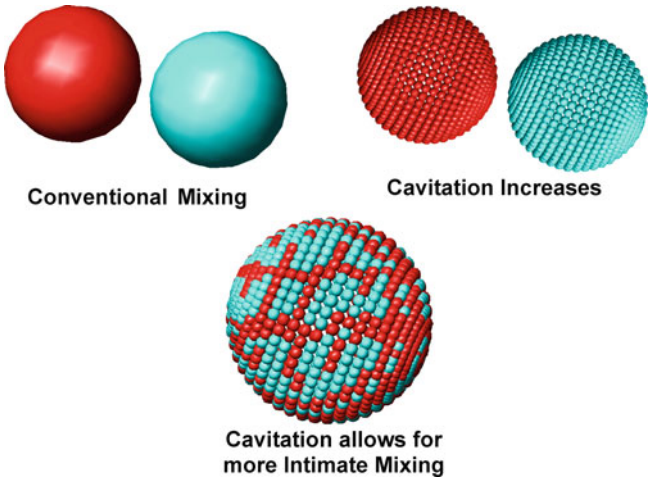

Fig. 8.5 Mixing comparison to conventional technology

4 Pasteurization

Cavitation has an added benefit when used for pasteurization in that it allows a higher "kill" than what would be possible at a given temperature. A similar phenomenon for ultrasound is often referred to as manothermosonification.

The term "mano" is added when moderate to high pressures are employed during the temperature/ultrasound process. The term manothermohydrodynamic cavitation is perhaps more descriptive of what occurs in the SPR.

The final FDA 1998 final rule (63 FR 37030) for processing fruit and/or vegetable juice requires processors to label products with a warning of potential illness upon consumption of the product unless the product was processed to inactivate the most likely pathogenic bacteria in the product by 5-log. This rule caused processors to employ conventional heat treatments for pasteurization to ensure that a 5-log reduction has been achieved to avoid the use of a warning label. Processors fear that the warning label may negatively impact a consumer's decision to purchase the product. More recently, the food processing industry has turned to non-thermal processing techniques to achieve the 5-log reduction of pathogens while minimizing heat exposure of the product (Morris, 2000). In essence, the product can be rendered microbially safe while maintaining the essential nutrients, the phytochemical-health-functional components and organoleptic properties of the original unprocessed juices (Rye and Mercer, 2003; Shomer et al., 1994). In light of these advantages of non-thermal processing technologies on quality, processors must acknowledge that today's consumers are better educated about minimally processed juices and that there is increased consumer demand for health-functional foods (Deliza et al., 2005). Utilizing non-thermal processing techniques such as hydrodynamic cavitation and ultraviolet irradiation would inactivate pathogens, and because of the low temperature exposure, the nutritional/nutraceutical components in the product are preserved. Certain fruit juices known to be rich in phytochemicals with health-functional properties can be processed with minimal damage to the overall nutritional/functional properties of the product (Konja and Lovric, 1993; McLellan and Acree, 1993; Shahidi and Naczk, 2004; Shahidi, and Weerasinghe, 2004). In addition to the preservation of health-promoting phytochemicals, research has shown that declaring the use of an alternative food processing technology in conjunction with a brief explanation of the technology elicits a positive response in consumers' decision to purchase a product (Deliza et al., 2005).

Innovative and novel equipment design for food applications must be validated for efficacy in producing safe and wholesome foods by microbial challenge tests using surrogates for pathogenic microorganisms. The Center for Food Safety and Applied Nutrition's (CFSAN, 2000) report on kinetics of microbial inactivation under the conditions applied in alternative food processing technologies clearly states the rising need for more research on the validation of innovative food processing technology. The following sections address fundamental scientific principles that govern the action of hydrodynamic cavitation by itself and in conjunction with ultraviolet light. Microbial challenge protocols and results are discussed in subsequent chapters. The overall intent of this research is to lay the groundwork for eventual commercialization of this technology for food processing.

Physical stresses resulting from acoustic or hydrodynamic cavitation are understood to be the mechanisms responsible for cellular inactivation. Biological entities in the immediate area of a cavitation event endure stresses that induce severe damage to cell walls and ultimately inactivate the organism (Earnshaw, 1998; Earnshaw et al., 1995; Frizzell, 1988; Geciova et al., 2002; Piyasena et al., 2003; Young, 1999). Earnshaw (1998) cites research suggesting that larger cells such as yeast (5–20 μm) are more susceptible to the effects of cavitation due to their larger surface area.

Gram-positive cells were once thought to be more resistant to cavitation than gram-negative bacteria due to additional layers of peptidoglycans in the former; however, more recent literature suggests no significant difference between gram-negative and gram-positive bacteria in their resistance to inactivation by cavitation. Spores of bacteria like *Bacillus* and *Clostridium* possess a higher tolerance to cavitational effects when compared to vegetative cells (Earnshaw, 1998). The SPR allows the inactivation of microorganisms through a combination of treatments, in this case cavitation in concert with temperature which exceeds that of temperature alone. This is demonstrated in Table 8.2.

Table 8.2 Enumeration[a] of high-acid fruit juice spoilage microorganisms processed in calcium-fortified apple juice (pH = 3.9) at two SPR[b] settings (3,000 and 3,600 rpm) at an initial temperature of 20°C and two exit temperatures of 65.6°C and 76.7°C, respectively (n = 6)[c]

Spoilage organism	Setting/exit temp (rpm/°C)	FR[d] (L/min)	ΔT_{avg} (°C/s)	LR[e]	TRTR[f]	SPR-L[g]	LT[h]
L. plantarum	3,000/65.6	1.48^{o}	0.39	7.48	1.62^{n}	5.87^{n}	0/6
	3,000/76.7	1.15^{p}	0.37	7.48	*	**	0/6
	3,600/65.6	2.55^{m}	0.67	7.48	0.96^{o}	6.52^{m}	0/6
	3,600/76.7	1.89^{n}	0.61	7.48	5.69^{m}	1.79^{o}	0/6
L. sakei	3,000/65.6	1.59^{o}	0.42	7.25	1.79^{m}	5.46^{n}	0/6
	3,000/76.7	1.10^{p}	0.36	7.25	*	**	0/6
	3,600/65.6	2.65^{m}	0.69	7.25	1.09^{n}	6.16^{m}	0/6
	3,600/76.7	2.00^{n}	0.65	7.25	*	**	0/6
Z. bailii	3,000/65.6	1.55^{o}	0.40	6.17	4.18^{m}	1.98^{n}	0/6
	3,000/76.7	1.15^{p}	0.37	6.17	*	**	0/6
	3,600/65.6	2.67^{m}	0.70	6.17	2.49^{n}	3.68^{m}	0/6
	3,600/76.6	1.96^{n}	0.63	6.17	*	**	0/6
Z. bailii (ascospores)	3,000/65.6	1.52^{o}	0.40	5.14	2.70^{m}	2.44^{n}	0/6
	3,000/76.7	1.13^{p}	0.37	5.14	*	**	0/6
	3,600/65.6	2.62^{m}	0.68	5.14	1.67^{n}	3.46^{m}	0/6
	3,600/76.7	1.92^{n}	0.62	5.14	*	**	0/6

[a]Average enumeration (means $\log_{10}$ CFU ± S.D.) data calculated from three separate trials with two samples per treatment (detection ≤1 CFU/mL)
[b]*SPR* "Shockwave Power^{TM} Reactor" or controlled cavitation system
[c]$n = 6$; means ± SD followed by same letter in column for each organism do not differ significantly ($\alpha = 0.05$) according to ANOVA and SNK analysis
[d]*FR* Flow Rate: rate of flow through SPR system and hold tube (L/min)
[e]*LR* Log Reduction: total mean log reduction for three separate trials (mean $\log_{10}$ CFU ± SD)
[f]*TRTR* Thermal Residence Time Reduction: mean log reduction due to integrated lethality during transient temperature change inside SPR plus lethality accumulated during hold time in exit piping of SPR (mean $\log_{10}$ CFU ± SD)
[g]SPR-L = Mean log reduction due to hydrodynamic cavitation treatment after TRTR effects have been removed (mean $\log_{10}$ CFU ± SD)
[h]LT = Lethality Test: incidence of growth after enrichment malt extract broth
*TRTR allowed for complete theoretical thermal inactivation; **SPR-L values do not reflect potential hydrodynamic cavitation inactivation due to TRTR.
(Data taken from Milly et al., 2007b)

5 Gum/Gel Hydration

Cavitation can be used to hydrate gums, gels and polymers in seconds. The process intensity helps to more completely hydrate the powders than with conventional mixers in a fraction of the time. The shockwaves can also break up dry powder agglomerates often referred to as "fish eyes." This can result in raw powder savings, higher viscosity or higher quality due to more efficient use of the gum and a more uniform product.

The images in Fig. 8.6 show a carrageenan gum mixture that has been stained with methylene blue. Areas of the gum that are not well hydrated appear a darker blue. Cavitation creates a much more even gel. These gels can be made with reduced raw material, in reduced time, and are more homogeneous than those made with conventional technology.

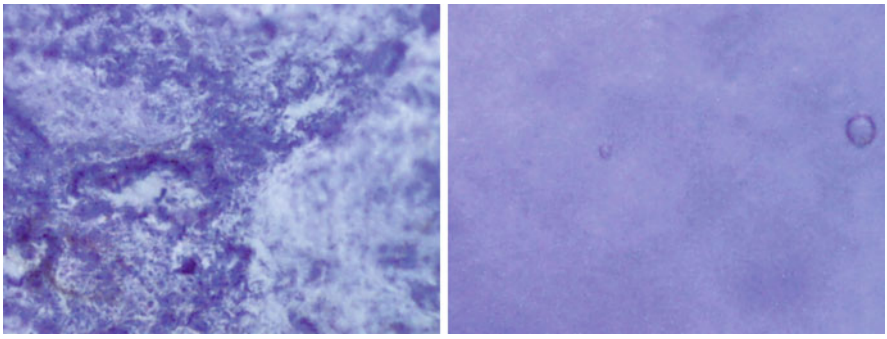

Conventional Cavitation Treated

Fig. 8.6 Gum hydration comparison

6 Emulsification

Cavitation can emulsify liquids in seconds, whether in batch or a continuous system. Emulsification levels can be changed continuously and instantly by varying cavitation intensity and this can be accomplished in a small footprint.

Emulsification studies were conducted with water and canola oil (no surfactant). Varying amounts of horsepower were used as designated by Hz under the jars. As horsepower was increased, the time during which the emulsion was stable increased. This can be directly related to the particle size achieved. Cavitation can be used to "tune" particle size. Images from this study can be seen in Fig. 8.7.

The image above, taken a day after the emulsions were made, shows how changing the cavitation level changes particle size in an emulsion and, thus, the stability. This can be especially useful in products such as salad dressings.

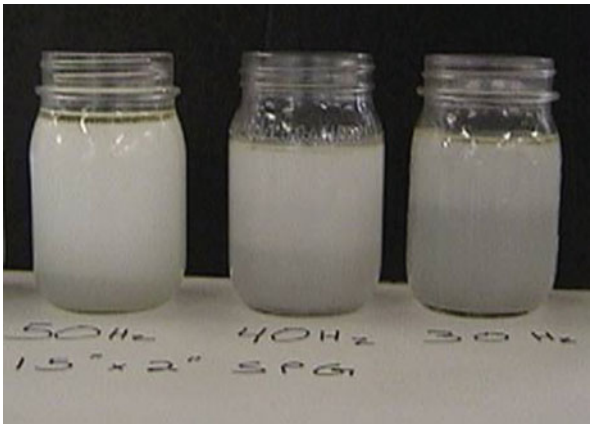

Fig. 8.7 Emulsification varying with cavitational intensity

7 Aeration

Gas/liquid mixing is one of the most widely used processes in the food industry. Since gases and liquids exist in two different phases, mixing them consistently and uniformly is not an easy task. Long retention times and excessive gas additions are often required and process inefficiencies are considered normal. The gas/liquid mixing ability of cavitation allows it to be used for aeration that is unperceivable by the consumer, which can directly increase profitability. A paste whipped with about 4% air can be seen in Fig. 8.8.

The gas–liquid mixing ability of the cavitation could also be used in other applications including hydrogenation, oxidation and ozonation. Gas–liquid ratios as high as 5:1 have been achieved in the SPR.

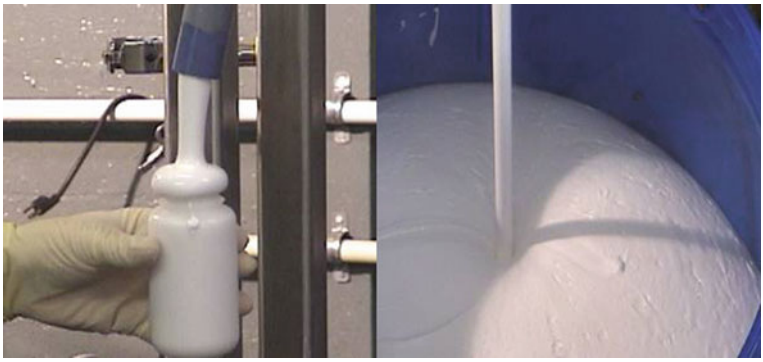

Fig. 8.8 A paste sample whipped with air

8 Mixing Thick Liquids

Cavitation is an excellent process for mixing thick and viscous liquids. The process intensity drives the mixing to be completely homogenous. The images in Fig. 8.9 show a paste mixed with a color. Cavitation creates a much more homogeneous gel as compared to a conventional technology such as a static mixer or homogenizer, which are often used to mix thick liquids.

Fig. 8.9 Thick liquid mixing comparison

9 Case Study of Cavitation Using the SPR

Several SPRs have been installed commercially for pasteurization and homogenization of egg products with excellent results. The main value of the SPR is heating without scaling while simultaneously homogenizing, because egg is a high scaling liquid.

Egg does not scale until it approaches its coagulation temperature, so it is possible to use a conventional heat exchanger to carry it to just before this level and then process it to completion with the SPR. For this pasteurization system, the SPR was used to add about 10°C in temperature after the conventional heating section.

The functionality of the product was tested by preparing a custard (% sag), a sponge cake (volume and consistency) and an omelet (color, aroma, taste and mouth feel). The first two products processed with the shock were a whole egg and a cholesterol-free egg white product. When compared with products processed under standard conditions, the products performed equally or better.

The second test studied replacing the high-pressure homogenizer. The product pasteurized with the SPR was compared with the same product that was pasteurized the previous day with the standard homogenizer. The product pasteurized without the SPR had an average aerobic plate count of 400–1,000 cfu/gr and a coliform count of 25–35. No aerobic bacteria or coliforms were detected in the product pasteurized with the SPR. The product was then tested by preparing a local cake that produced a cake 20% taller and with a better consistency than the cake prepared with standard

product. The plant was able to pasteurize whole eggs for 8 h, until they ran out of product, without the need for cleaning, when before they could only achieve this result for 4 h.

The use of SPR potentially allows for pasteurization at higher temperatures for extended periods of time, which can result in better shelf-life and longer run time with gentler handling of the egg products.

10 UV Light Using Cavitation in the SPR

Higher surface refreshing photon-related reactions can result in higher mass transfer. Any process, such as UV, that must occur on a surface could benefit from the SPR surface refreshing technology. The extreme mixing forces in the SPR increase the rate of surface refreshing on the inner surface of the housing. The result is a concentration gradient at the surface, which cycles the process chemicals for the treatment. This action increases the mass transfer of photons. At any fixed point on the inner housing surface, the refreshing rate may be as high as several thousand times per second.

The adoption of germicidal UV treatment in water and waste water processing facilities has generated a number of studies validating the efficacy of UV for processing transparent fluids (Liltved and Cripps, 1999; NACMCF, 2004; Sommer et al., 2000). Germicidal ultraviolet light (UVC) at 200 to 280 nm wavelength has proved to be successful for inactivating pathogenic microorganisms like *Escherichia coli* O157:H7 and *Cryptosporidium parvum* in processed fruit juices such as apple juice and cider (Vasavada 2003; Wright et al., 2000). Interest in UV treatment of fluid food as an alternative to conventional heat treatment continues to grow. Processors concerned with product flavor and nutrient changes brought on by conventional heat treatment continue to view UV processing as a favorable alternative. In addition, the equipment required for effective thermal pasteurization may be too high-priced for small operations.

Ultraviolet (UV) radiation is considered to be a physical treatment for achieving disinfection of certain foods. Primarily used in water disinfection and waste water processing, the intended use is to disinfect, not sterilize. Disinfection refers to the inactivation of vegetative cells and, in some cases, the inactivation of pathogenic bacterial spores. Radiation is the emission and proliferation of energy through space or a given substance. UV radiation is defined as part of the electromagnetic spectrum displaying wavelengths shorter than the visible region (380–800 nm), but longer than X-rays (0.1–13 nm). In general, UV radiation wavelengths can range from 1 to 400 nm with subdivisions consisting of long-wave UV (UVA: 315–400), medium wave UV (UVB: 280–315 nm) and short-wave UV (UVC: 200–280 nm) (Lopez-Malo and Palou, 2005). Figure 8.10 displays the electromagnetic spectrum in its entirety. Figure 8.11 allows one to see the subdivisions among the UV radiation range. Bactericidal effects are observed closest to the wavelength of 260 nm (Jay, 1998).

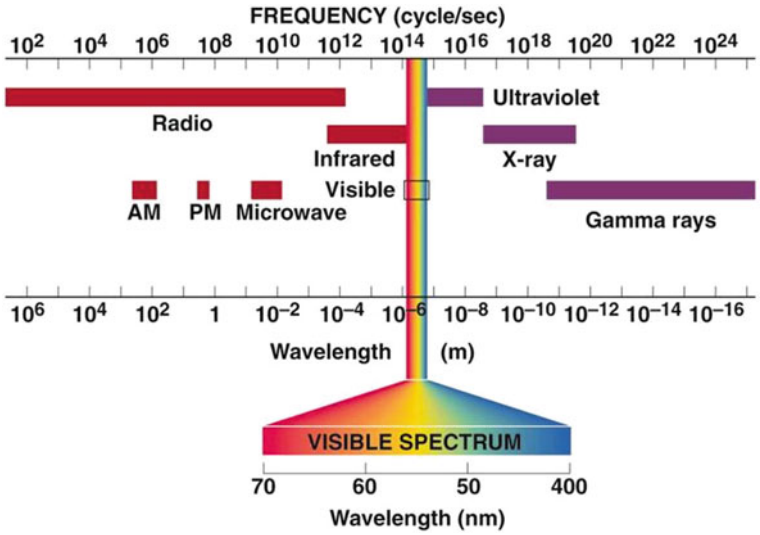

Fig. 8.10 Electromagnetic spectrum (taken from http://rst.gsfc.nasa.gov/Intro/emspec.jpg)

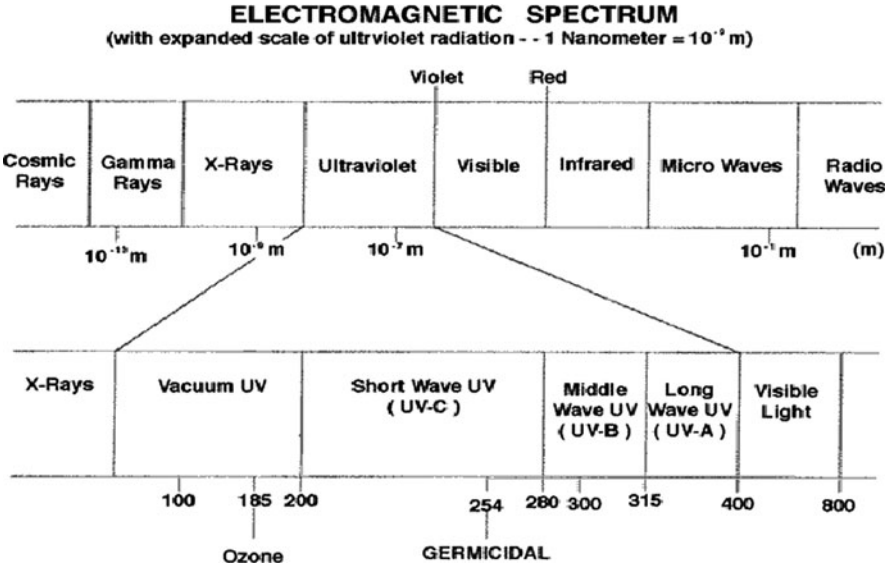

Fig. 8.11 Electromagnetic spectrum subdivisions of ultraviolet region (taken from www.uvlp.ca/images/electromagneticspectrum40x.gif)

The energy provided by UV radiation is non-ionizing and is readily absorbed by proteins and nucleic acids. The photochemical changes at the cellular level are responsible for the bactericidal effect observed in microorganisms exposed to UV radiation. The cell does not die immediately, but rather procreates into a mutated

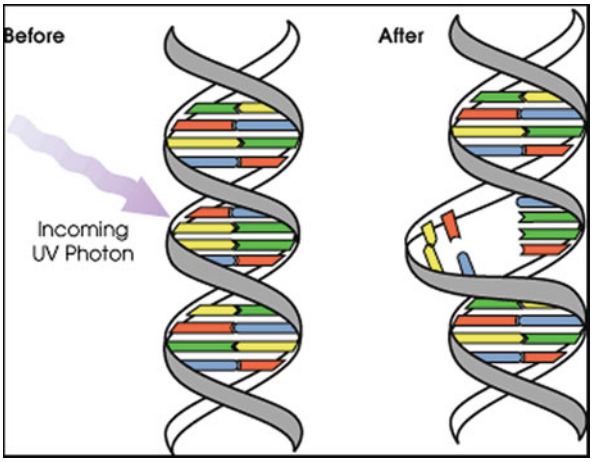

Fig. 8.12 Photochemical mutagenesis in DNA resulting in thymine dimer (taken from www.americanairandwater.com/images/DNA-UV.gif; accessed March 2007)

form and is less suited for survival of offspring. The exposure to UV radiation results in cross-linking of thymine dimers within the DNA of the exposed organism. Figure 8.12 illustrates this photochemical effect.

This photochemical reaction inhibits the microorganism's capacity to effectively repair injury or successfully reproduce (Vasavada, 2003). UV light has been documented to produce ozone, a known antimicrobial agent, when processing fruits and vegetables (Jay, 1998). However, due to the weak penetration capacity of UV radiation, use of UV technology is limited to surface decontamination and sterilization applications. In addition, opaque fluid foods and/or fluid foods containing particulates, such as citrus juices, provide "shading effects," which allow for microbial survival from UV radiation. Most UV applications can be found in waste water treatment plants, where the fluid is cleaned of any particulates before exposure to high-intensity UV radiation for decontamination and/or sterilization (CFSAN, 2000).

Currently available UV systems can effectively process only transparent fluids. Opaque fluids such as milk have been proven difficult to process with UVC because the depth of UVC penetration is small, and most microorganisms do not receive direct UVC exposure. In a well-mixed system, shadowing effects can be minimized and more of the target species would be exposed to UVC rays. Tables 8.3 and 8.4 illustrate the lethality effects of UV treatments in conjunction with SPR technology.

The UV-ShockWave Power Reactor (UV-SPR) is a non-immersive UV technology where the lamps do not come into contact with liquid. The bulbs are positioned outside a housing made of quartz to allow UV transmission. A depiction of the device can be seen in Fig. 8.13.

Table 8.3 Inactivation of *E. coli* ATCC 25922 in calcium fortified apple juice (pH = 3.9) processed in an Ultraviolet-Shockwave Power^{TM} Reactor at an initial temperature of 18 ± 1°C with varying rotational speeds ($n = 4$; mean values)[a]

Treatment reduction (rpm)	UV (253.7 nm)	T_{in}(°C)	T_{out}(°C)	Flow rate (L/min)	N_0 ($\log_{10}$)	N ($\log_{10}$)	Log ($\log_{10}$)
0–Control	No	18.6	18.6	1.5	7.17	7.17	0^{f}
0–Control	Yes	18.6	18.6	1.5	7.17	7.08	0.09^{e}
600	Yes	18.6	19.2	1.5	7.17	3.72	3.45^{d}
1200	Yes	18.6	19.2	1.5	7.17	2.97	4.20^{c}
1800	Yes	18.6	20.8	1.5	7.17	2.84	4.34^{c}
2400	Yes	18.6	24.7	1.5	7.17	2.56	4.71^{b}
3000	Yes	18.6	33.1	1.5	7.17	2.21	4.96^{b}
3600	Yes	18.6	44.2	1.5	7.17	2.45	4.72^{b}
3600	No	18.6	44.2	1.5	7.17	7.03	0.14^{e}

[a]$n = 4$; means followed by same letter in column do not differ significantly ($\alpha = 0.05$) according to ANOVA and SNK analysis (detection ≥ 10 CFU/mL)
(Data taken from Milly et al., 2007a)

Table 8.4 Inactivation of *E. coli* ATCC 25922 in skim milk (pH = 6.0) processed in an Ultraviolet-Shockwave Power^{TM} Reactor at an initial temperature of 15 ± 1°C with varying rotational speeds ($n = 4$; mean values)[a]

Treatment reduction (rpm)	UV (253.7 nm)	T_{in}(°C)	T_{out}(°C)	Flow rate (L/min)	N_0 ($\log_{10}$)	N ($\log_{10}$)	Log ($\log_{10}$)
0–Control	No	15.8	15.8	1.5	7.11	7.11	0^{f}
0–Control	Yes	15.8	15.8	1.5	7.11	7.03	0.08^{e}
600	Yes	15.8	15.8	1.5	7.11	6.79	0.33^{d}
1200	Yes	15.8	16.4	1.5	7.11	6.57	0.54^{d}
1800	Yes	15.8	18.6	1.5	7.11	5.78	1.33^{c}
2400	Yes	15.8	23.1	1.5	7.11	3.86	3.25^{b}
3000	Yes	15.8	29.7	1.5	7.11	3.84	3.24^{b}
3600	Yes	15.8	40.8	1.5	7.11	3.88	3.24^{b}
3600	No	15.8	44.4	1.5	7.11	6.97	0.15^{e}

[a]$n = 4$; means followed by same letter in column do not differ significantly ($\alpha = 0.05$) according to ANOVA and SNK analysis (detection ≥10 CFU/mL)
(Data taken from: Milly et al., 2007a)

The reactor itself utilizes UV and cavitation for applications such as water disinfection, cold pasteurization and decolorization. Conventional UV technologies have attempted to find a way to improve the efficiency of existing systems by increasing UV lamp intensity. However, high-intensity lamps are not effective in opaque solutions; they are only effective in clear solutions. Conversely, the UV-SPR system utilizes a surface refreshing technique that brings microbials close to the lamp for improved exposure instead of using higher intensity bulbs to disinfect opaque solutions.

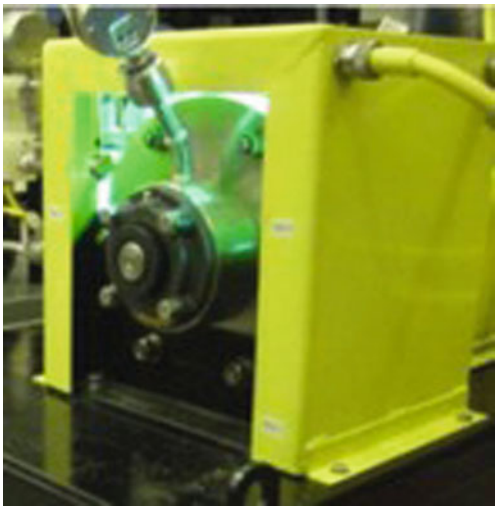

Fig. 8.13 UV-SPR

11 Conclusions

Cavitation can have many benefits over conventional technology. It can be used for heating and intense mixing. Cavitation could provide a paradigm shift for many applications in the food industry.

References

Balasundaram, B., and Pandit, A. B. (2001). Selective release of invertase by hydrodynamic cavitation. *Biochemical Engineering Journal*, 8, 251–256.

Center for Food Safety and Applied Nutrition. (2000). Kinetics of microbial inactivation for alternative food processing technologies. Retrieved July 1, 2004 from vm.cfsan.fda.gov on the World Wide Web: http://vm.cfsan.fda.gov/~comm/ift-toc.htm

Deliza, R., Rosenthal, A., Abadio, F. B. D., Silva, C. H. O., and Castillo, C. (2005). Application of high pressure technology in the fruit juice processing: Benefits perceived by consumers. *Journal of Food Engineering*, 67, 241–246.

Earnshaw, R. G. (1998). Ultrasound: A new opportunity for food preservation. In: Povey, M. J. W., and Mason, T. J. (eds.), *Ultrasound in food processing*, pp. 183–192. London SE1 8HN, UK, Blackie Academic and Professional.

Earnshaw, R. G. Appleyard, J., and Hurst, R. M. (1995). Understanding physical inactivation processes: combined preservation opportunities using heat, ultrasound and pressure. *International Journal of Food Microbiology*, 28, 197–219.

Frizzell, L. A. (1988). Biological effects of acoustic cavitation. In: Suslick, K. S. (ed.), *Ultrasound: Its chemical, physical, and biological effects*, pp. 287–304. New York, NY, VCH.

Geciova, J., Bury, D., and Jelen, P. (2002). Methods for disruption of microbial cells for potential use in the dairy industry-a review. *International Dairy Journal*, 12, 541–553.

Gogate, P. R. (2002). Cavitation: an auxiliary technique in wastewater treatment schemes. *Advances in Environmental Research*, 6, 335–358.

Jay, J. (1998). *Modern food microbiology*, 5th edn, 661pp. Maryland, Aspen.

Jyoti, K. K., and Pandit, A. B. (2001). Water disnfection by acoustic and hydrodynamic cavitation. *Biochemical Engineering Journal*, 7, 201–212.

Jyoti, K. K., and Pandit, A. B. (2004). Ozone and cavitation for waster disinfection. *Biochemical Engineering Journal*, 18, 9–19.

Kazem, B., Armstead, D. A., Mancosky, D. G., Lien, S. J., and Verrill, C. J. (2003). *Heating Black Liquor by partial oxidation with controlled cavitation as a means to reduce evaporator fouling*. Chicago, IL, TAPPI Pulping Conference.

Konja, G., and Lovric, T. (1993). Berry fruit juices. In: Nagy, S, Chen, C. S., and Shaw, P. E. (eds.), *Fruit juice processing technology*, pp. 436–514. Auburndale, FL, Agscience.

Leighton, T. G. (1998). The principles of cavitation. In: Povey, M. J. W., and Mason, T. J. (eds.), *Ultrasound in food processing*, pp. 151–182. London SE1 8HN, UK, Blackie Academic and Professional.

Liltved, H., and Cripps, S. J. (1999). Removal of particle-associated bacteria by prefiltration and ultraviolet irradiation. *Aquaculture Research*, 30, 445–450.

Lopez-Malo, A., and Palou, E. (2005). Ultraviolet light and food preservation. In: Barbosa-Canovas, G. V., Tapia, M. S., and Cano, M. P. (eds.), *Novel food processing technologies*, pp. 405–422. Boca Raton, FL, CRC Press LLC.

Mason, T. J., and Lorimer, J. P. (2002). *Applied sonochemistry: The uses of power ultrasound in chemistry and processing*, 303 pp. Weinheim, Germany, Wiley-VCH Verlag GmbH.

McLellan, M. R., and Acree, T. (1993). Grape juice. In: Nagy, S., Chen, C. S., and Shaw, P. E. (eds.), *Fruit juice processing technology*, pp. 318–333. Auburndale, FL, Agscience.

Middelberg, A. P. J. (1995). Process-scale disruption of microorganisms. *Biotechnology Advances*, 13(3), 491–551.

Milly, P. J., Toledo, R. T., Chen, J., and Kazem, B. (2007a). Hydrodynamic cavitation to improve bulk fluid to surface mass transfer in a nonimmersed ultraviolet system for minimal processing of opaque and transparent fluid foods. *Journal of Food Science*, 72(9), M407–M413.

Milly, P. J., Toledo, R. T., Harrison, M. A., and Armstead, D. (2007b). Inactivation of food spoilage microorganisms by hydrodynamic cavitation to achieve pasteurization and sterilization of fluid foods. *Journal of Food Science*, 72(9), M414–M422.

Milly, P. J., Toledo, R. T., Kerr, W. L., and Armstead, D. (2008). Hydrodynamic cavitation: characterization of a novel design with energy considerations for the inactivation of *Saccharomyces cerevisiae* in apple juice. *Journal of Food Science*, 73(6), M298–M303.

Morris, C. E. (2000). US developments in non-thermal juice processing. *Food Engineering and Ingredients*, 25(6), 26–28.

National Advisory Committee on Microbiological Criteria for Foods. (2004). *Requisite scientific parameters for establishing the equivalence of alternative methods of pasteurization: UV radiation*, 66pp.

Piyasena, P., Mohareb, E., and McKellar, R. C. (2003). Inactivation of microbes using ultrasound: A review. *International Journal of Food Microbiology*, 87, 207–216.

Rye, G. G., and Mercer, D. G. (2003). Changes in headspace volatile attributes of apple cider resulting from thermal processing and storage. *Food Research International*, 36(2), 167–174.

Save, S. S., Pandit, A. B., and Joshi, J. B. (1994). Microbial cell disruption: Role of cavitation. *Chemical Engineering Journal*, 55, B67–B72.

Save, S. S., Pandit, A. B., and Joshi, J. B. (1997). Use of hydrodynamic cavitation for large scale microbial cell disruption. *Trans IChemE*, 75(C), 41–49.

Shahidi, F., and Naczk, M. (2004). *Phenolics in food and nutraceuticals*, 558pp. Boca Raton, FL, CRC Press.

Shahidi, F., and Weerasinghe, D. K. (2004). Nutraceutical beverages: An overview. In: Shahidi, F., and Weerasinghe, D. K. (eds.), *Nutraceutical beverages: Chemistry, nutrition, and health effects*, pp. 1–5. Washington, DC, American Chemical Society.

Shomer, R., Manheim, C. H., and Cogan, U. (1994). Thermal death parameters of orange juice and effect of minimal heat treatment and carbon dioxide on shelf-life. *Journal of Food Processing and Preservation*, 18(4), 305–315.

Sivakumar, M., and Pandit, A. B. (2002). Wastewater treatment: a novel energy efficient hydrodynamic cavitational technique. *Ultrasonic Sonochemistry*, 9, 123–131.

Sommer, R., Lhotsky, M., Haider, T., and Cabaj, A. (2000). UV inactivation, liquid-holding recovery and photoreactivation of *Escherichia coli* O157 and other pathogenic *Escherichia coli* strains in water. *Journal of Food Protection*, 63, 1015–1020.

Vasavada, P. C. (2003). Alternative processing technologies for the control of spoilage bacteria in fruit juices and beverages. In: Foster, T., and Vasavada, P. C. (eds.), *Beverage quality and safety*, pp. 73–93. Boca Raton, FL, CRC Press LLC.

Wright, J. R., Sumner, S. S., Hackney, C. R., Pierson, M. D., and Zoecklein, B. W. (2000). Efficacy of ultraviolet light for reducing *Escherichia coli* O157:H7 in unpasteurized apple cider. *Journal of Food Protection*, 63, 563–567.

www.americanairandwater.com/images/DNA-UV.gif. Accessed March 2007.

http://rst.gsfc.nasa.gov/Intro/Part2_2a.html

Young, F. R. (1999). *Cavitation*, 418 pp. London WC2H 9HE, Imperial College.

Chapter 9
Ultrasonic Cutting of Foods

Yvonne Schneider, Susann Zahn, and Harald Rohm

1 Introduction

In the field of food engineering, cutting is usually classified within a group of mechanical unit operations dealing with size reduction which, more clearly, means to reduce the average size of solid materials by applying external forces. Apart from fulfilling particular requirements concerning particle size itself (for example, an appropriate fineness of sugar or cocoa particles in chocolate is important for the sensory perception of smoothness), size reduction causes an increase in the surface area per unit volume which, in many cases, leads to more efficient processing (increase in drying or heating rate, accelerated extraction etc.). When individual pieces of a material are separated into more or less smaller pieces of certain or random shape, the width of the particle size distributions largely depends on both the principle and method of size reduction and may require additional screening procedures. Saravacos and Kostaropoulos (2002) suggested to classify size reduction operations with respect to (a) the final size and/or shape of the products; (b) the type of force applied during size reduction and (c) the characteristics of the size reduction equipment.

Apart from emulsification or homogenization (restricted to immiscible liquid systems, which are not considered here), the comminution of solids results in a wide range of product size distributions, covering large to medium products, medium to small products, and small to granular or pulverized products. Depending on feed particle size and the applied separation principle, one may distinguish between methods such as crushing, grinding, slicing or dicing (Fellows, 2000). Though a combination of forces is always present in comminution equipment, the main acting forces may be categorized under compressive forces, shearing forces and impact forces. Regarding their application, Saravacos and Kostaropoulos (2002) considered forces that are either attributable to pressure and/or friction exerted on a material

H. Rohm (✉)
Institute of Food Technology and Bioprocess Engineering, Technische Universität Dresden, 01069 Dresden, Germany
e-mail: harald.rohm@tu-dresden.de

H. Feng et al. (eds.), *Ultrasound Technologies for Food and Bioprocessing*, Food Engineering Series, DOI 10.1007/978-1-4419-7472-3_9,
© Springer Science+Business Media, LLC 2011

placed between tool surfaces, then shearing forces acting on a material, forces that are exerted by shock collisions between particles or by the impact of tools on particles and, finally, forces generated through friction as a result of contact with a surrounding medium. Using fracture or yielding stress as a criterion, Loncin and Merson (1979) classified food materials, which are usually subjected to cutting, either as hard/strong or soft/weak and, with respect to yielding, further differentiated between brittle and ductile materials (Fig. 9.1). It is then obvious that the properties of the material significantly affect the method of and the equipment used in comminution (Brennan, 2006; Brennan et al., 1990). Based on the number and type of working tools, size reduction may be achieved by using two tools and the application of compression forces, compression and shearing forces, impact and shearing forces, and almost pure shearing forces as it appears during cutting. With only one tool, the forces acting on the particular pieces are either of the impact or shearing type (Saravacos and Kostaropoulos, 2002), and size reduction without a mechanical tool is achieved by impact forces and shear forces between particles accelerated in an air stream (for example, jet mills).

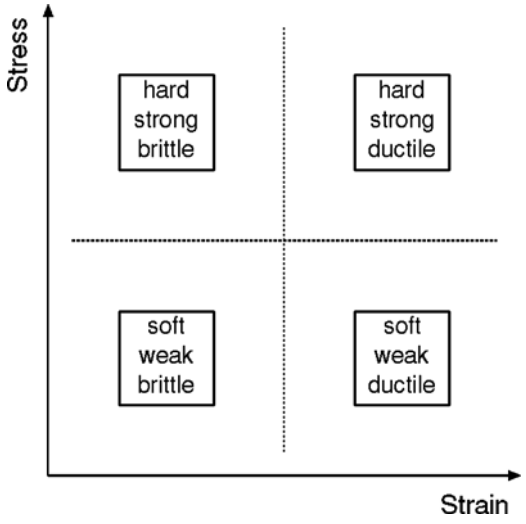

Fig. 9.1 Classification of materials with respect to rupture

2 Cutting in Food Processing

Cutting is utilized to separate semi-solid or soft solid materials. With the exception of jet cutting or laser cutting, separation force is generated by the relative motion between a mechanical tool, usually a knife or a blade of a particular shape, and the product. The separating tool continuously penetrates the material with a predefined velocity, with or without removing material, and produces two cut faces. A common feature, which distinguishes cutting from other separation methods involving

knives or blades (for example, cleaving or carving), is that the product is in almost permanent contact with both sides of the tool. In contrast to the performance of cutting mills or mincers, which is also based on the action of blades, cutting usually results in product sections of predefined size and geometry. However, size and shape of the products may vary considerably, starting with large pieces when separating meat or cheese wheels; more sophisticated assemblies of blades or knife systems with different moving directions may be used for generating slices or dices. Apart from the geometrical properties of the tool (wedge angle, blade thickness, displacement volume, and edge sharpness), the cutting velocity, along with the direction of the applied force, the efficiency of a cutting system as well as the magnitude of the resulting cutting force depend on the mechanical properties of the product to be cut (Atkins et al., 2004). Hence, conventional knives or blades may be replaced by saws or wire systems when appropriate (Goh et al., 2005; Kamyab et al., 1998).

2.1 The Principle of Conventional Cutting

The main aim of the cutting process is to break internal bonds in a material by stressing structural elements; this is achieved by the progressive motion of a mechanical tool. The stress within the material to be cut is directly proportional to the applied force, and inversely proportional to the contact area. Cutting starts when the total stress exceeds the internal strength of the cutting material. Food products are predominantly characterized by viscoelastic deformation properties that are associated with the ability toward stress relaxation and creep deformation. These time-dependent effects are responsible for the scattering of deformation energy in the zone where the cutting edge contacts the product, and for the expanding deformation. Therefore, the cutting velocity must exceed the stress relaxation velocity to reach the fracture limit; otherwise, the product will not be cut, but rather squeezed. In addition to the desired separation, there is some displacement of the cutting material while the cutting tool penetrates. This displacement is responsible for the special features and characteristics as regards the cutting of foods.

When a knife with a defined wedge angle α and a blade thickness d cuts into a semi-solid material, three zones with different deformation characteristics can be distinguished: a separation zone in the immediate vicinity of the cutting edge, a deformation zone along the wedge, and a compression zone along the flank of the blade. In these deformation zones (Fig. 9.2a) the individual force components acting on the blade play different roles (Raeuber, 2004):

- Upon contact with the edge of the knife, the product will be pushed down. The stress in the separation zone propagates and increases because of the resistance of the material until the fracture stress is exceeded. The characteristic force component at this stage is the cutting resistance F_R which, apart from cohesive forces in the material, is heavily influenced by the sharpness of the tool (Kluge and Linke, 1993).

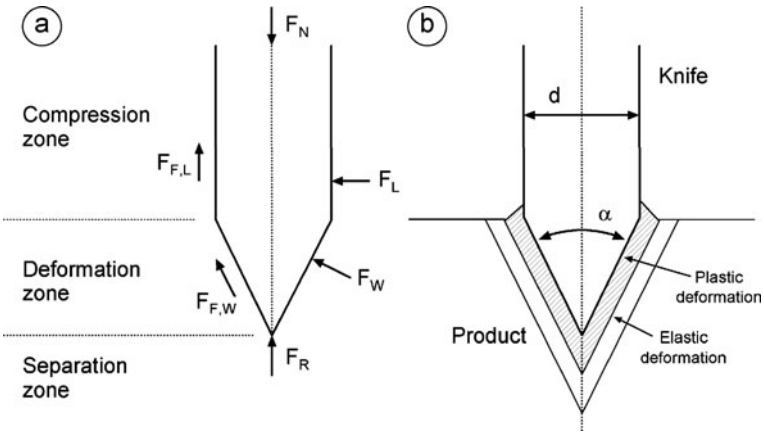

Fig. 9.2 (**a**) Force distribution during cutting. F_N, normal force; F_R, product resistance; F_W, side force; F_L, lateral compression force; $F_{F,W}$, friction force along the cutting wedge; $F_{F,L}$, flank friction force. (**b**) Deformation during cutting. d, blade thickness; α, wedge angle. For further explanation, see text

- In the deformation zone, the action of the wedge leads to biaxial (horizontal and vertical) deformation, the magnitude of which depends on wedge angle and blade thickness. When referring to the deformed or distorted fraction of the material, it is necessary to distinguish between a zone of plastic deformation, located in the close vicinity of the cutting edge, and a zone of elastic deformation, which follows the zone of plastic deformation (Fig. 9.2b). Lateral displacement leads to the deformation force F_W (Fig. 9.2a), which is also responsible for the formation of frictional forces $F_{F,W}$ along the wedge surface (Linke and Kluge, 1993).
- Further displacement of the material causes the generation of lateral compression forces F_L in the compression zone, which becomes important since the relative motion accounts for the development of frictional forces along the tool flanks. F_L increases with blade thickness and is of high relevance when cutting products with high friction coefficients.

The properties of the material from which the blade is constructed are, along with lateral forces, responsible for the friction that occurs between the product and the knife along the wedge and the flank, which is significantly involved in the formation of the plastic deformation zone. For efficient cutting, it is especially the plastic deformation that must be efficiently controlled to protect cutting segments from irreversible damage. It is, therefore, extremely important to keep the wedge angle, the thickness of the blade, and the flank area that is in direct contact with the food as small as possible. Otherwise, the cutting tool must show a sufficient firmness to resist the cutting forces.

The efficiency of cutting additionally depends on the cutting angle λ between the edge axis and the axis that is perpendicular to the cutting direction. In a simple guillotine cutting configuration (λ = 0), the normal cutting force F_N corresponds to the sum of F_R and the normal component of F_W. Additionally, the normal component of the frictional force along the cutting wedge $F_{F,W}$ and along the cutting flank $F_{F,L}$ must be taken into account:

$$F_N = F_R + 2 \cdot F_W \cdot \sin\frac{\alpha}{2} + 2 \cdot F_{F,W} \cdot \cos\frac{\alpha}{2} + 2 \cdot F_{F,L} \tag{9.1}$$

As acceleration effects are not considered here, this equation only holds for low cutting velocities. The particular force components depend largely on the properties of the material and on the properties of the cutting unit so that the cutting forces can only be determined experimentally (Linke and Kluge, 1993).

Integration of the cutting force F_C along cutting depth s finally yields the cutting work W_C:

$$W_C = \int_{s=0}^{s_S} F_C(s)\mathrm{d}s \tag{9.2}$$

W_C represents the entire energy in a cutting process and comprises the stored fraction related to elastic deformation W_{elast}, the dissipative fraction W_{diss}, which is not accompanied with fracture (viscous flow, friction, relaxation, matrix bonding, and debonding), and the work W_{fract}, which originates from the fracture strength of the material (Atkins and Mai, 1985):

$$W_C = W_{elast} + W_{diss} + W_{fract} \tag{9.3}$$

2.2 Ultrasonic Cutting

Ultrasonic cutting can be distinguished from conventional cutting by the specific motion characteristics of the cutting tool, as the conventional movement of the device is superpositioned by ultrasonic vibration. Generally, ultrasonic cutting systems consist of a chain of elements that generate and propagate the ultrasonic vibration to the separation zone (Fig. 9.3). The generator provides an alternating current (AC) voltage with the desired ultrasonic frequency, usually in the 20–50 kHz range. This electric oscillation is converted into an alternating mechanical displacement of corresponding frequency by means of a piezo-electric transducer (converter). A coupling unit (amplifier) transfers the mechanical vibration as a solid-borne sound wave to the sonotrode, either as it is or after amplification or attenuation of the amplitude. The sonotrode acts as a mechanical resonator, which vibrates mainly longitudinally along the vibration axis. The sonotrode may even act as the cutting tool which, however, requires maximum amplitudes at the cutting

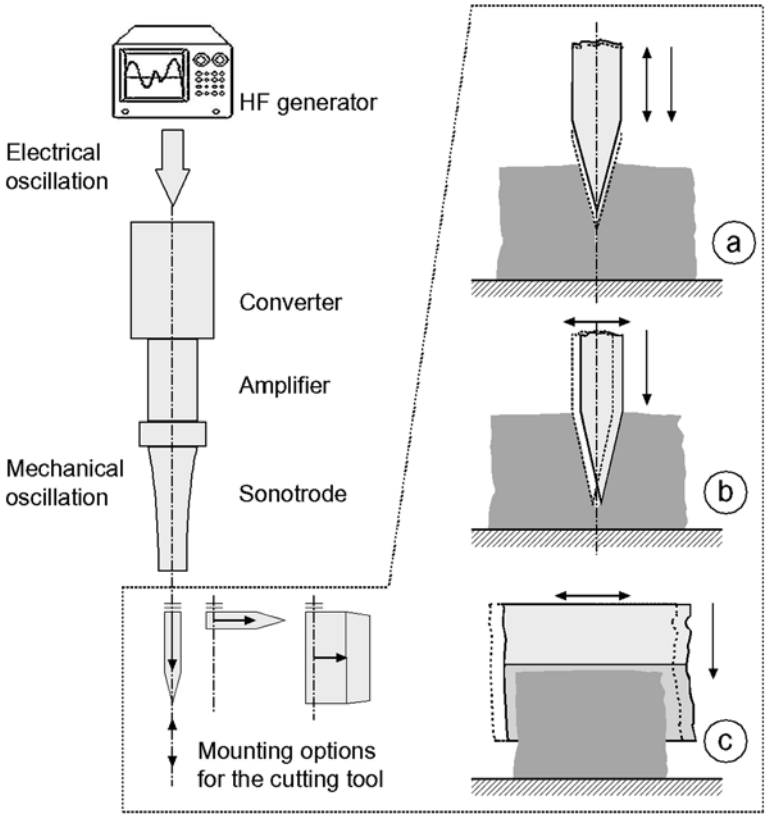

Fig. 9.3 Principle of ultrasonic cutting systems and main configurations for interaction between cutting material and the cutting tool. Detailed description for a, b and c, see text. ||, excitation point. *Simple arrows*, moving axis; *double-headed arrows*, vibration axis

edge, or may act as a coupling unit for an independent cutting blade. To ensure stable performance, the entire vibrating system is tuned to a constant operating frequency.

Depending on the mounting of the cutting tool to the sonotrode and on the orientation of the cutting edge relative to the vibration axis, three main configurations may be distinguished:

- The main vibration axis and the moving axis of the cutting tool are identical, but the main vibration axis is perpendicular to the cutting edge (Fig. 9.3a). This is, for example, true in a guillotine-type cut where the stress and strain acting on the material due to the macroscopic feed motion is intensified or diminished by a periodical stress with a high frequency (that is, 20–50 kHz) and a low amplitude (in the micrometer range). Stress and strain are mainly exerted in the separation zone where the edge is in contact with the crack tip in the product.

- A vibration direction perpendicular to both moving axis and edge axis (Fig. 9.3b) supports product separation as the gap expands due to a vibration direction orthogonal to the gap itself. This expansion causes very high stresses at the crack tip in the separation zone, thus enforcing crack propagation. Additionally, contact mechanisms as well as frictional forces at the tool flanks are significantly affected.
- When the vibration direction is perpendicular to the moving axis but parallel to the edge (Fig. 9.3c), the macroscopic normal component is superpositioned by a microscopic tangential movement, causing bidirectional saw movement.

It is typical for longitudinally operating systems that the tool material is subjected to periodic compression and expansion. However, surface effects result in a complex combination of longitudinal, transversal and bending oscillation. Changes in the vibration mode are frequently associated with a frequency shift, resulting in corresponding loss of energy (Cardoni et al., 2004; Lucas et al., 2001).

2.3 Ultrasound-Induced Modifications of the Cutting Process

Ultrasonic cutting is an application of power ultrasound where product behavior and processing properties are directly affected by the supplied energy. The excitation of the cutting device results in a complex vibration that determines tool–product interactions at the edge and the flank of the tool but, on the other hand, is itself affected by these interactions. Product separation is triggered by applying a load at the edge of the cutting tool, the motion of which consists of a macroscopic feed and a microscopic vibration component, thus determining a periodical fluctuation of contact and detachment (Lucas et al., 1996; Rawson, 1998). Stress peaks associated with very high deformation velocities finally lead to a modification of fracturing. Longitudinal and transversal movements influence the contact mechanisms along the wedge and the flanks of the tool: The vibration amplitude of the longitudinal oscillation decreases with an increase in the distance from the edge until a wave node is reached ($y_0 = 0$), while transversal contractions and bend vibrations consequently induce movements that are both parallel and orthogonal to the tool flank and which, in turn, significantly affect frictional forces. By direct coupling, an energy transfer into the material takes place at the tool wedge and at the tool flanks, finally inducing ultrasonic effects such as cavitation and sound absorption.

2.3.1 Fracture Modification

When using a tool where the cutting direction corresponds to the vibration direction (see Fig. 9.3a), the effective cutting velocity v_C is the sum of the linear velocity v_L and the vibration speed v_{US} at the tool wedge which, in turn, is influenced by the vibration amplitude y_0, angular velocity ω and time t:

$$v_C = v_L + v_{US} = v_L + y_0 \cdot \omega \cdot \cos(\omega \cdot t) \tag{9.4}$$

When the feed and vibration directions are opposing, the tool separates from the product, although the feed motion continues; in the following extension period of the tool the actual cutting velocity approaches its maximum (see Equation (9.4)). As deformations per loading cycle remain very small, cohesive bonds in the material are subjected to enormous stresses on a microscopic scale. Time-dependent stress relaxation does not occur because of the high-frequency cyclic loading, which also inhibits the generation of a spacious zone of plastic deformation and energy dissipation, because sliding only occurs to a limited extent (Blumenauer and Pusch, 1993). On the microscopic scale, the high deformation velocities virtually increase the stiffness of the product, thus inducing local cleavage and a conversion from ductile to brittle fracture. On a macroscopic scale, this fact finally results in reduced deformation and damage of the product and the cut face, respectively. Consequently, both the cutting force and the energy (especially the stored and the dissipative fraction) necessary for separation are significantly reduced (Schneider, 2007).

An indicator for a fundamental change in the loading conditions is the critical linear velocity $v_{L,c}$. If $v_{L,c}$ reaches the same magnitude as v_{US} (Fig. 9.4)

$$v_{L,c} = v_{US} = y_0 \cdot \omega = y_0 \cdot 2\pi \cdot f \tag{9.5}$$

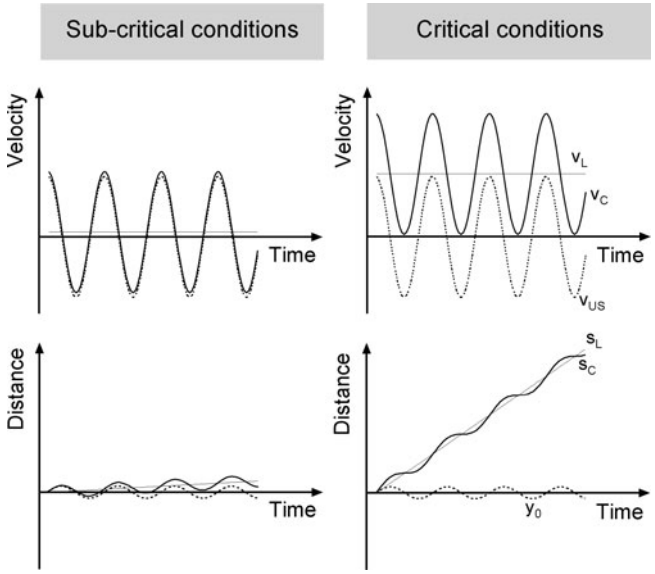

Fig. 9.4 Superposition of cutting movement and vibration movement. Velocity indicators: v_L, linear cutting velocity (*thin line*); v_{US}, vibration speed (*thick dotted line*); v_C, effective cutting velocity (*thick solid line*). Distance indicators: s_L, linear cutting depth (*thin line*); y_0, ultrasonic amplitude (*thick dotted line*); s_C, effective cutting depth (*thick solid line*). Right hand graphs refer to a value of v_L, where the critical point ($v_{L,c}$) is reached (see text)

or, if the ratio of v_L to v_{US} exceeds 1, there is no more separation of the cutting wedge from the product and the supporting influence of ultrasound due to the modification of relative motion characteristics becomes negligible (Kim and Choi, 1997; Littmann et al., 2001; Mracek and Wallaschek, 2005).

2.3.2 Modification of Friction

During penetration of the product by the cutting device, the tool flanks and the separating surfaces are in permanent contact, and a relative motion occurs. Friction is defined as the force F_F which acts against the relative motion of two contacting materials. Apart from the properties of the contacting materials, the friction force is determined by the force normal to the contact surface F_N and the type of relative motion (for example, rolling, or sliding). Whether normal force or relative motion are influenced by ultrasonic excitation mainly depends on the orientation of the vibration axis toward the contact area of interest.

- A vibration axis perpendicular to both contact area and sliding direction (Fig. 9.5a) results in alternating loading conditions of the material. Assuming that a particular displacement y of the contact area causes a normal force F_N which, in relation to its magnitude, follows the excitation of the surface and achieves its maximum at y_0. Further assuming that the coefficient of friction, that is the ratio of friction force to normal force, is constant, any fluctuation in F_N affects F_F. Inertia and a delayed retardation of the compressed material is then responsible for a temporary ablation of the contacting surfaces, which finally causes a macroscopic reduction of the frictional force.

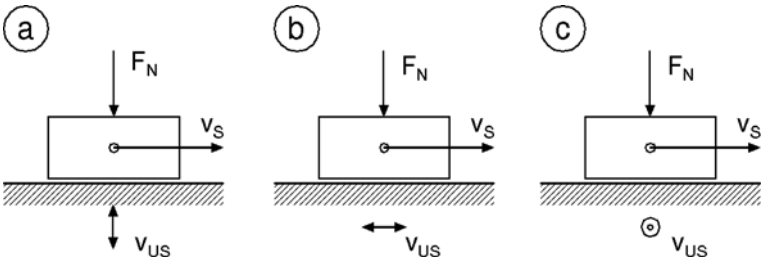

Fig. 9.5 Superposition of sliding movement and ultrasonic vibration. (**a**) Vibration axis is parallel to normal force but perpendicular to sliding direction and contact area. (**b**) Vibration axis is perpendicular to normal force but parallel to sliding direction and contact area. (**c**) Vibration axis is perpendicular to normal force and sliding direction but parallel to contact area. F_N, normal force; v_S, sliding velocity; v_{US}, vibration speed

- An alternating excitation perpendicular to the normal force but parallel to the contact area and the sliding direction (Fig. 9.5b) directly affects the relative velocity between the contacting materials. Hence, the sliding velocity is superpositioned by the vibration velocity (see also Equation (9.4)). Despite a continuous

movement, an alternating moving direction on a microscopic scale must also be considered; hence, in addition to elements of sliding friction, the frictional force also comprises elements of ultrasonic friction. When the sliding motion is in the opposite direction to the motion induced by the vibrating cycle, sliding is supported which, on a macroscopic level, leads to a reduction of friction. This reduction diminishes when the sliding velocity increases (Littmann et al., 2001; Mracek and Wallaschek, 2005).

- Finally, a vibration axis parallel to the contact area but perpendicular to the sliding motion (Fig. 9.5c) results in a periodic fluctuation of the direction of the movement. Frictional forces are reduced, even when the sliding motion becomes larger than the maximum vibration speed (Littmann et al., 2001; Mracek and Wallaschek, 2005; Storck et al., 2002).

Phenomenological studies concerning the influence of periodic excitations have revealed certain effects on friction. Chandiramani et al. (2006) showed that an increase of the excitation frequency in the 20–40 kHz range caused a transition from stick-slipping to pure sliding. Astashev and Babitsky (1998) pointed out the dynamic fluidization of dry friction, resulting in a reduction of the friction coefficient under conditions of ultrasonic excitation.

Because sliding velocity can be interpreted as an analog of linear cutting velocity, friction interactions along longitudinally oscillating cutting devices are affected as depicted in Fig. 9.5a and b, whereas the conditions depicted in Fig. 9.5c become additionally important for a cutting angle $\lambda > 0$. The above-mentioned interrelations also imply that the properties of the contacting surfaces are independent from the friction process itself. However, especially in the case of food materials, a change in mechanical properties in the immediate vicinity of the contact layer is expected due to deformations at the contact points and because of the transformation of mechanical into thermal energy (Myshkin et al., 2005). In particular foods, a temperature increase might result in a liquefaction of the interface and in a transition to fluid friction. The increase in the distance of solids and viscous shear of the fluid layer finally leads to reduced frictional forces.

2.3.3 Secondary Effects

Apart from the desired mechanical effects of ultrasonic excitation on the cutting process, a number of side effects must be considered, mainly absorption and cavitation, which might exert a particular influence on the product; these are usually addressed as secondary effects and result from the propagation of the sound field in the product.

Because of the non-ideal elastic behavior of real materials, acoustic waves do not propagate indefinitely, but the energy of the wave declines by, for example, a conversion of mechanical energy into thermal energy as it occurs in absorption. Depending on residence time and the amount of the converted energy, absorption causes an increase in product temperature. Interfacial friction as an absorption mechanism is

particularly important in products with large inhomogeneities or in the presence of a large amount of macromolecules and, therefore, varies to a large extent. For example, a temperature increase up to 65 K was observed when using ultrasonic scalpels for the cutting of flesh tissue; similar temperature changes were evident while cutting bones or wood (Cardoni et al., 2006; Kinoshita et al., 1999; Koch, 2001; Koch et al., 2004; Lucas et al., 2005). As foods do rarely represent homogeneous materials with pure elastic properties, the importance of absorption as a contributor to sound attenuation is considerably high. Large attenuation also means a limited penetration of ultrasound into the material, and thermal effects are therefore restricted to thin layers in the vicinity of the excited tool. Consequences are cut faces covered with films of liquefied components, but also agglutinations or thermally induced effects (for example, protein denaturation).

Products containing large amounts of free fluids are especially susceptible to cavitation, which results in pronounced turbulences and, after the collapse of the cavitation bubbles, in microjets exerting extreme stresses toward solid components of the product or toward the cutting tool surfaces. Cavitation bubbles magnify product inhomogeneities, generate structural impurities and intensify absorption. The intensity of cavitation in the fluid phase mainly depends on physical properties such as vapor pressure or surface tension (Jiménez-Fernández and Crespo, 2005; Li et al., 2004; Wenge et al., 2006). Chemical changes induced by cavitation were observed in a number of materials subjected to ultrasonic excitation, including certain foods (Chemat et al., 2004a, b; Lifka et al., 2002; Mason, 2003; Petrier et al., 1994; Schneider et al., 2006; Suslick et al., 1999; Xia et al., 2006). Secondary effects are generally undesirable, but can be minimized by adjusting the operating parameters to properties of the material.

3 Practical Aspects of Ultrasonic Cutting of Foods

Stimulated by the omnipresent concentration in the food industry, there are increasing demands toward a higher capacity and throughput for a number of cutting applications, and it is necessary to gain knowledge on cutting forces for several food types and how they vary to have a sound basis for developing optimum cutting and slicing systems (Brown et al., 2005). Besides performance characteristics, however, a number of quality issues should also be considered. These issues are related to, for example, the accuracy and precision of the cut, the physical stability of the cut product as well as the structural stability and smoothness of the cut face, the attrition, the separability of the product from the tool and the persistence of both tool and the surrounding equipment to contamination (Linke and Liebers, 1992). Adherence to these prerequisites is particularly difficult when the products exhibit problematic material properties, for example, extreme hardness or brittleness, but also stickiness, or an extended compressibility with low cohesiveness and/or high adhesiveness. The difficulties multiply when the products are inhomogeneous and show largely differing mechanical properties along the separation plane.

Because most of the problems with conventional cutting arise from the occurrence of excessive total cutting forces associated with large product deformation and high friction forces, a more sensitive separation with a decreased stressing of the product can be expected from the application of ultrasound. The results of cutting experiments presented in this chapter were taken from experiments performed under laboratory conditions: a constant linear cutting velocity was realized by using a universal testing machine, force–distance-profiles were acquired by the electronic measurement unit of the testing machine, power–time data were recorded from the output of the ultrasonic generator and vibration speeds were varied via amplitude selection by generator adjustment (Schneider et al., 2002; Zahn et al., 2005, 2006). In line with theoretical aspects of fracture and friction modification discussed previously, some basic information can be extracted from the cutting force profiles schematically depicted in Fig. 9.6. When cutting with a straight edge, the force versus cutting depth profile may be divided into four phases. Generally, the cutting process starts with the feeding phase (phase 1), where the cutting edge is brought into contact with the product. In the subsequent deformation phase (phase 2), the

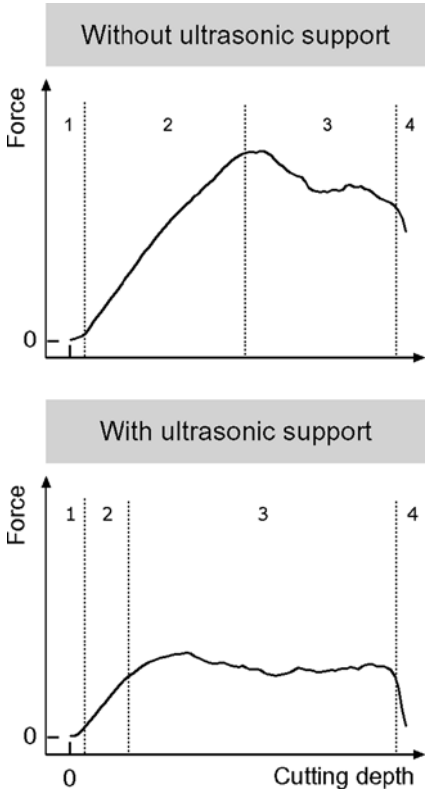

Fig. 9.6 Evolution of cutting force versus cutting depth in a guillotine cut of the crumb of malted bread. Experimental conditions: linear cutting velocity, 1,000 mm/min; excitation frequency, 40 kHz; excitation amplitude, 12 μm

cutting force increases significantly, although no separation occurs since the supplied energy is utilized for elastic and plastic deformation, but the fracture limit is not yet reached. This stage is clearly truncated when using excited cutting tools: the separation starts at lower cutting forces and at smaller cutting depths. The consecutive penetration phase (phase 3) is characterized by a proceeding separation of the product, an increasing contact area between the tool and the product and an increasing displacement of the product by the cutting wedge. The final lag phase (phase 4) is an indicator for adhesion forces when the separation is completed; generally, the ablation of the product from the tool is forced by ultrasonic excitation (Schneider et al., 2002). As a first approximation, it becomes evident that ultrasonic excitation affects the initial and the final cutting phase, but also the corresponding force level. In this chapter, some details will be discussed with respect to the properties of products cut by an ultrasonic device.

The decrease of the cutting force as induced by ultrasonic excitation of the tool obviously implies that the cutting work (see Equation (9.2)) is also reduced. In order to quantify the ultrasonic effect, the relative cutting work coefficient k_W introduced by Schneider et al. (2002) relates the cutting work with ultrasonic support $W_{C,US}$ to the cutting work of a reference cut without ultrasonic excitation $W_{C,0}$ (Fig. 9.7):

$$k_W = \frac{W_{C,US}}{W_{C,0}} \tag{9.6}$$

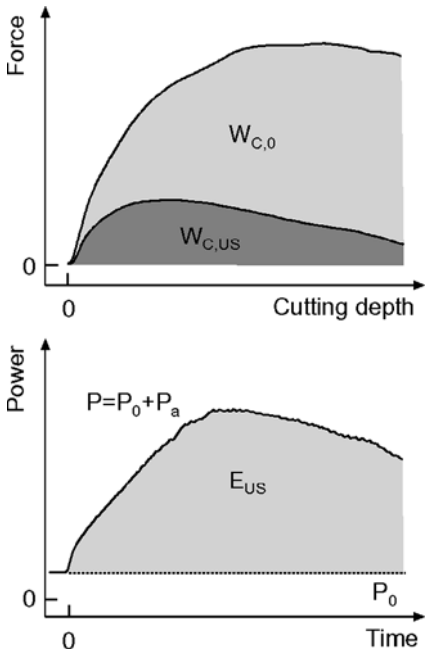

Fig. 9.7 Determination of characteristic parameters for the cutting performance by calculation of cutting work without ($W_{C,0}$) or with ultrasonic support ($W_{C,US}$), and additional ultrasonic energy E_{US}. P_0, power necessary to maintain vibration of the blade in air; P_a, additional power to maintain vibration when cutting the material

Hence, for $k_W = 1$, there is no influence of the ultrasonic excitation on the cutting process at all; a priori, a very small cutting work coefficient is desirable. The ultrasonic cutting process can also be characterized by the amount of electric power P that is supplied by the generator to keep the vibrating unit in a defined vibration state. This electric power refers to the sum of the fraction P_0, which is necessary for maintaining the vibration of the tool in air, and of an additional fraction P_a, which severely increases under operation, that is, when the tool is in contact with the product to be cut (Schneider et al., 2007). The additional ultrasonic energy E_{US} (see Fig. 9.7), which corresponds to the power demand of the sonotrode to maintain vibration when contacting the food, provides further insight into cutting performance:

$$E_{US} = \int_{t=0}^{t=t_C} P_a \mathrm{d}t = \int_{t=0}^{t=t_C} (P - P_0)\,\mathrm{d}t \tag{9.7}$$

3.1 Impact of Material Properties

3.1.1 Material Properties and Cutting Performance

Although an ultrasound-induced reduction of cutting force (and cutting work) can be achieved for most food products, a strong dependency of the cutting performance on the properties of the cutting material must be considered. Generally, the relative cutting work coefficients range between 0.1 and 1.0 (Zahn et al., 2005, 2006). To classify foods with respect to their response to ultrasonic cutting, their macroscopic structure, their mechanical properties or the dominant cutting force components might be considered as most important. In this context, three main categories of foods can be identified (Schneider et al., 2002):

- Homogenous and compact materials, for example, fats, gels, cheese, filling masses and so on, are characterized by a closed, non-porous structure. Hence, in conventional cutting, the cutting forces are mainly generated by increasing friction as separation proceeds. In turn, the magnitude of friction is correlated with the adhesiveness of the product. Ultrasonic excitation diminishes these interactions, and interrelated consequences such as friction grooves and lamellar or squamous surface rupture and, additionally, plastic deformation of the cut sections are avoided (Fig. 9.8). On the other hand, power consumption during cutting of non-porous materials, especially if they show a considerably high fat content (for example, short pastry dough and Gouda cheese; Fig. 9.9) is very pronounced. Most of the non-porous materials contain liquids (that is, oil or water) or solid ingredients (for example, fat), which may fluidize upon absorption heating. Therefore, an excellent coupling of the vibrating tool to the cutting material by

Fig. 9.8 Impact of ultrasonic excitation of the cutting tool on the appearance of cutting surfaces of a compact product (short pastry dough) and a porous food (hamburger bun). Experimental conditions: cutting velocity, 1,000 mm/min; excitation frequency, 40 kHz; ultrasonic amplitude, 12 μm

wetting and fluid layers may be expected, equivalent to optimum conditions for the transportation of energy into the material. Consequently, the power demand increases continuously with increased cutting depth.

- Porous products, for example, bread crumb, cakes, marshmallows, or similar products, are characterized by a spongy or a foamy structure with open surfaces and pores, and appear either brittle or highly compressible. Highly compressible systems are deformed pronouncedly before the cutting tool starts to penetrate into the material as a consequence of local fracture. With proceeding separation, crumbling, frazzling and squeezing occurs. When using a vibrating tool, the initial deformation (prior to any local fracture; see stage 2 in Figs. 9.6, 9.9 and 9.10) is much lower due to the rapid initiation of fracture. The cutting force is reduced because of the modified separation mechanisms in such materials: elastic and plastic compression is avoided, and smooth cut surfaces without abrasion can be achieved (see Fig. 9.8). If the food matrix adheres to the cutting tool, ultrasonic excitation is also responsible for the reduction of friction effects. However, and generally speaking, friction forces are less important during cutting of porous products, mainly because the real contact area between food and tool is, due to the presence of pores, much lower than that of the geometric contact area. As compared to non-porous materials, the power demand increases until the tool penetrates, and then remains constant during continuing separation. Even for porous products with relatively high cutting forces, the amount of power consumption is lower than for non-porous products because of the poor coupling (see

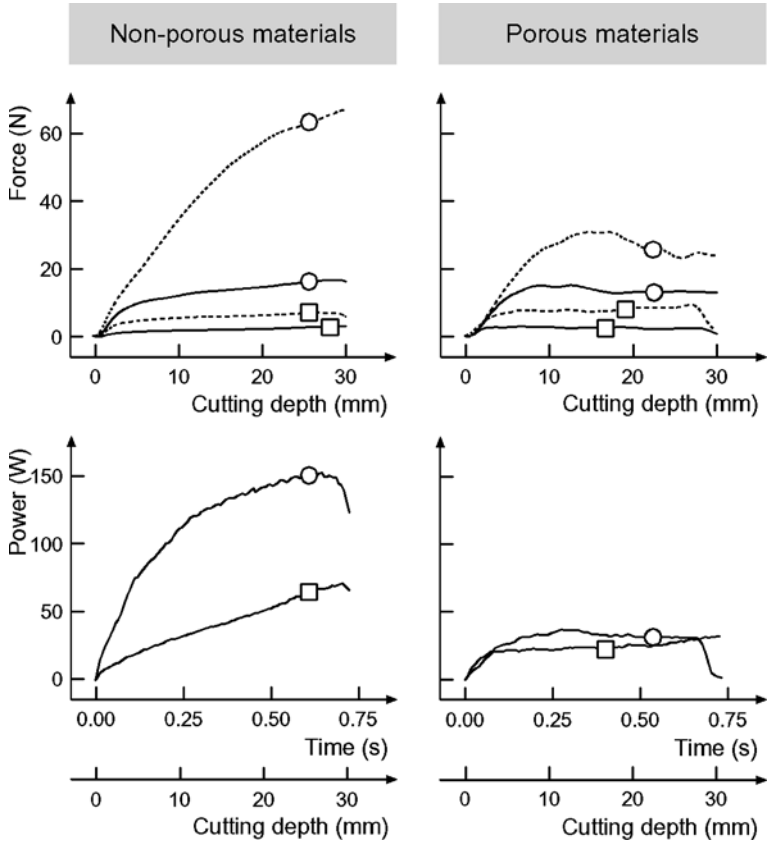

Fig. 9.9 Resistance force and power consumption during ultrasonic cutting of non-porous and porous foods as a function of cutting depth and cutting time. *Dotted lines*, cutting force without ultrasonic excitation; *full lines*, cutting force and generator power with ultrasonic excitation. Experimental conditions: cutting velocity, 2,500 mm/min; excitation frequency, 40 kHz; ultrasonic amplitude, 12 μm. Non-porous samples: ◯, Gouda cheese; □, short pastry dough. Porous samples: ◯, malted bread crumb; □, pound cake

Fig. 9.9). In porous brittle products (for example wafers, crisp bread, meringue), a reduction of separation forces can be achieved. However, displacement by the cutting wedge increases with increasing cutting depth and leads to a cleavage of the material.

- Plant and animal tissues are cellular structures, which vary largely with respect to, for example, size or composition. Because of their high moisture content and the formation of lubricating liquid films from the sectioned matrix, friction forces during cutting are less important. Material stiffness dominates the cutting forces which, by using ultrasonic excitation, can be significantly reduced for most plant tissues. Problems may occur in the case of ductile filamentous structures (for

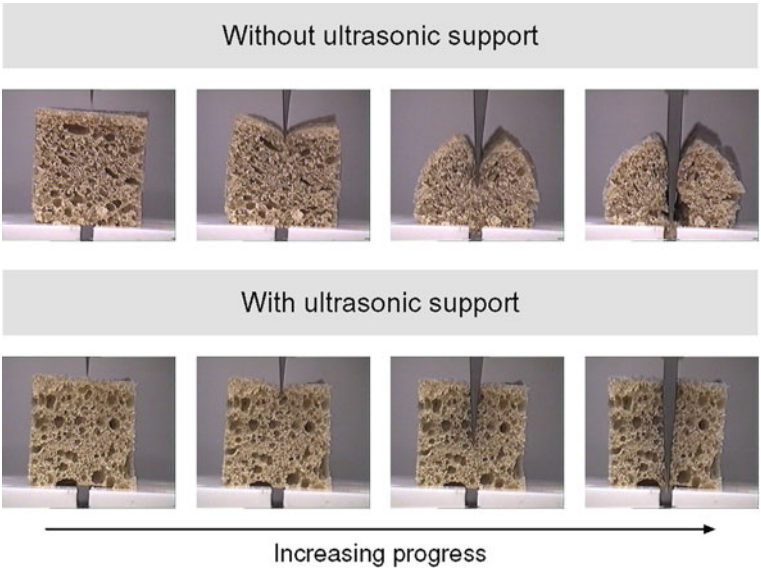

Fig. 9.10 Appearance of malted bread crumb during conventional and ultrasonic cutting. Experimental conditions: cutting velocity, 1,000 mm/min; excitation frequency, 40 kHz; ultrasonic amplitude, 12 μm. Sample cross-section is 30 × 30 mm

example, flesh tissue), as these need a proper fixation of the structural elements by pre-tensioning, frosting or cooking. If such preparations are considered, a reduction of separation forces can be achieved.

Besides experimental evaluation of the cutting performance, the interaction between vibrating cutting tools and cutting materials has also been subject of simulations. Establishing finite element models for ultrasonic cutting of cheese, toffee and some non-food materials presents new approaches for adjusting cutting parameters, such as frequency and blade tip amplitude, and for predicting the excitation force or cutting speed required to cut effectively through different material layers. Nevertheless, model validation heavily depends on the accuracy of the underlying data (material properties) and on the definition of the friction and boundary conditions (temperature) at the contact area between the cutting tool and the material (Lucas et al., 2006; McCulloch et al., 2006).

Many real food products are macroscopically inhomogeneous, especially when materials as mentioned above are combined in layers (for example, filled cakes, multi-layered sweets) or mixtures (e.g., pieces of fruits, nuts, kernels in a crumb matrix or creams and gels). Therefore, the cutting performance of each component affects the stability and the resistance of the others. For example, by decreasing the cutting force for an elastic cover, a viscous filling is preserved from displacement; or, by reducing separation forces for fruit pieces, the surrounding matrix is prevented

Fig. 9.11 Appearance of multiple-layer bakery products after conventional and ultrasonic cutting. Experimental conditions: cutting velocity, 1,000 mm/min; excitation frequency, 40 kHz; ultrasonic amplitude, 12 μm. Sample width is approx. 30 mm

from damage (Fig. 9.11). However, varying product properties in a multilayered material may cause considerable fluctuations in the power demand of the generator.

Generally, for establishing energy balances, it must be considered that ultrasonic cutting systems need additional energy supply to raise and maintain the vibration unit in the predefined operation mode, even though analyses of cutting force and cutting work have revealed a decreasing demand of energy for ultrasonic cutting (Schneider et al., 2007).

3.1.2 Material Properties and Secondary Effects

Secondary effects relevant for food cutting are sound absorption and cavitation. Whether and in which intensity one or both of these effects become important largely depends on the material properties which, in turn, are responsible for the coupling with the excited tool as well as for sound propagation and sound attenuation. In general, a high level of power consumption necessary for specific materials leads to an enhanced risk of quality losses (Schneider, 2007).

The fraction of the cutting material that is affected by sound absorption is located at the contact area and the bordering layer in its immediate vicinity. The effective temperature increase due to sound absorption depends on the chemical composition and the structural constitution of the sonicated food. In porous materials, temperature compensation takes place by conductive transport of heat into the material via matrix bridges. Especially in the crumb of bakery products, no related quality losses

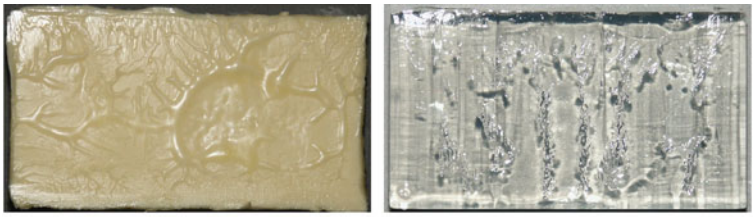

Fig. 9.12 Damage of the cutting surface due to secondary effects caused by ultrasonic excitation of the cutting tool. Absorption heating is responsible for the occurrence of a melted layer on margarine, and a cavitation erosion pattern becomes visible on the surface of gelatin gels

might be suspected. On the other hand, a more intense heating must be expected in products with a high fat content, showing a good coupling to the tool. Such materials enforce energy dissipation associated with increasing power consumption of the generator. Quality losses arise from the generation of droplets and films of melted fat (Fig. 9.12).

The presence of free liquids is a prerequisite for the occurrence of ultrasonic cavitation. In several food systems, hydrophilic or lipophilic liquids or liquefiable phases are free or entrapped in matrices (cellular liquids in plant tissues, fat globuli as filler in protein matrices, hydrocolloid gels) or appear as crystals (solid fat, ice). Dissolved or dispersed components may contribute to a decrease of the cavitation threshold. Cavitation occurs in the contact layer, but also up to a couple of millimeters inside the cutting material and this phenomenon is associated with the generation of bubbles and noise, surface erosion, macroscopic structural damages (Fig. 9.12) and the atomization of liquids (Chiu et al., 2005; Suslick et al., 1999; Wenge et al., 2006). Cavitation around titanium alloy-cutting sonotrodes has recently been shown by Schneider et al. (2006).

3.2 Impact of Cutting Parameters

3.2.1 Ultrasonic Parameters

While a particular tool operates at a predefined frequency, one can choose between assemblies built for different frequencies. Usually, systems operating at 20, 30 and 40 kHz are offered. Because of the dynamic strength of the sonotrode material, systems with lower operating frequencies allow the application of higher amplitudes (up to approximately 30 μm). In ultrasonic cutting devices as described above, the vibration amplitude might be adjusted within a particular limit by tuning the generator. The generator delivers a particular power to the sonotrode which, in the no-load status, ensures a stable operation at constant amplitude and frequency. A load on the sonotrode throttles the amplitude, leading to a detuning of the voltage signal at the generator. The energy delivered to the sonotrode is then regulated by a control loop

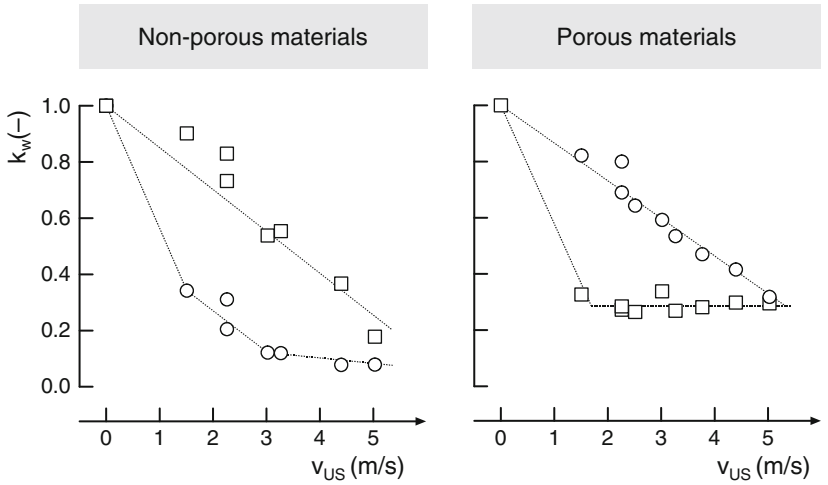

Fig. 9.13 Impact of maximum vibration speed v_{US} on the relative cutting work coefficient k_W. Linear cutting velocity, 1,000 mm/min. v_{US} was calculated according to Equation (9.5). Non-porous samples: ◯, Gouda cheese; □, gelatin gel. Porous materials: ◯, malted bread crumb; □, pound cake. Data of porous materials are from Zahn et al. (2005)

to maintain the preset values (Cardoni and Lucas, 2002; Lim et al., 2004; Lucas et al., 1996).

Generally, a gradual reduction of cutting force and cutting work can be achieved by increasing vibration amplitudes or by increasing frequencies (Zahn et al., 2005, 2006). Both ultrasonic amplitude and ultrasonic frequency determine the vibration speed of the cutting edge (see Equation (9.4)), which can be regarded as the most important factor affecting the magnitude of this reduction. Therefore, an increasing vibration speed causes a decrease of the relative cutting work coefficient and, as can be deduced from the cutting performance, this interrelation strongly depends on the material properties. For compact homogenous systems, as well as for porous materials, k_W may decline either linearly or with a declining decrease when vibration speed increases (Fig. 9.13). Especially for materials with a pronounced ductility (for example, malted bread crumb or gelatin), the interrelation follows a steady trend. For products with a very low ductility (for example, pound cake), the relative cutting work coefficient evidently drops at low vibration speed and then remains on a particular level even if vibration speed further increases. For other types of products, the reduction of cutting resistance, which is similar to a reduction of the separation force, is as important as the reduction of friction. The strong influence of even low vibration speeds on the magnitude of friction forces is evident from the Gouda cheese profile in Fig. 9.13; for this product, the moderate decrease of k_W with further increasing v_{US} is mainly related to reduction of the cutting resistance.

Unfortunately, secondary ultrasonic effects become more pronounced with increasing amplitude and increasing frequency, which is also equivalent to an increase in the vibration speed. For small vibration amplitudes, a temperature increase in the product due to sound absorption can be neglected. At specific

constellations (for example, good coupling between tool and product, high absorption coefficients, liquefiable components), heating effects become rapidly perceptible with increasing amplitudes or frequencies, and the visual quality of the cut face can be detracted from droplets or films arising from fat or ice melting, or gel liquefaction. The intensity of cavitation in liquids or in components liquefied by absorption heating also increases with vibration speed (Schneider et al., 2006), and structural damages are enforced.

Besides quality losses, a higher intensity of secondary effects is reflected by an increased power consumption of the generator. This amount corresponds to the energy leakage from the excited tool, which is enforced by good coupling conditions, sound propagation in the product, scattering of the sound wave, and the transformation of the mechanical energy of the sound wave into thermal energy and deformation energy. Consequently, the ultrasonic energy E_{US} increases with increasing vibration speeds.

3.2.2 Cutting Movement

As in conventional cutting, the relative velocity of the vibrating tool is an important parameter that determines cutting quality and the operational capacity of a particular cutting unit (Zahn et al., 2006). Generally, the cutting force increases with increasing cutting velocity, both in conventional and in ultrasonic cutting. A decrease in the cutting work reduction is the consequence of increasing cutting velocities: the decline of the ultrasonic impact is expressed by the increase of k_W, as depicted in Fig. 9.14. Depending on the properties of the material under action, the slope of the k_W/v_L interrelation varies.

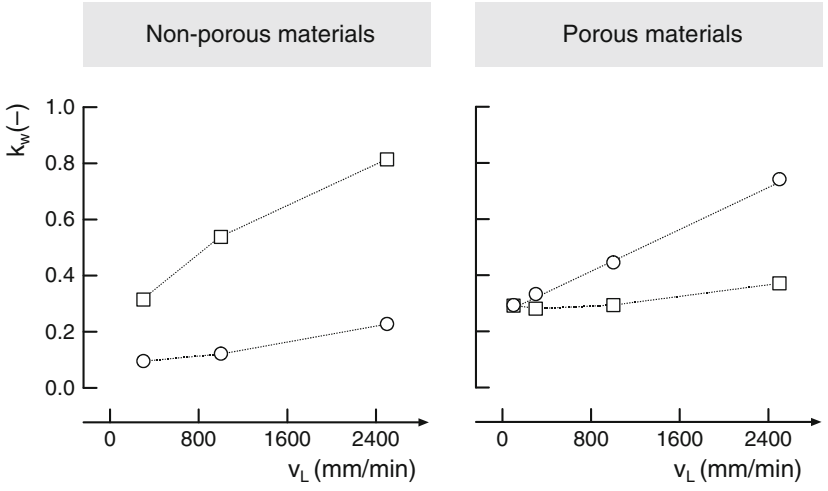

Fig. 9.14 Impact of linear cutting velocity v_L on the relative cutting work coefficient k_W. Excitation frequency, 40 kHz; ultrasonic amplitude, 12 µm. Non-porous samples: ◯, Gouda cheese; □, gelatin gel. Porous materials: ◯, malted bread crumb; □, pound cake

Although existing applications are beyond approaching the above-mentioned critical point (see Equation (9.4), Fig. 9.4), a neutralization of the mechanical ultrasonic effect must be expected for several materials when further increasing cutting velocity. However, the unequivocal benefit of ultrasonic cutting lies in the high quality of the cut, and the performance is not the main issue; currently, ultrasonic cutting does not meet the requirements of high-capacity processing.

The application of higher cutting velocities is accompanied by a simultaneous truncation of the cutting period, which is equivalent to a reduction of the sonication time. The amount of energy supplied to the product is definitely diminished, and secondary effects might be limited by applying high cutting velocities (Zahn et al., 2006). In accordance with conventional cutting, the cutting movement needs to be adapted to the properties of the material. Therefore, guillotine cuts with special speed profiles or with superposition of normal and tangential motion are applied.

3.3 Impact of Design Parameters

Basic requirements for sonication tools are a proper mechanical stiffness, the stability toward corrosion, and the suitability for being used for foods. The most commonly used sonotrode materials are titanium alloys, which are naturally protected against corrosion by an oxide layer and show excellent mechanical properties (Althof et al., 1973; Neville and McDougall, 2001). However, some abrasion of the tools may be induced by cavitation erosion, cavitation corrosion and fatigue. Therefore, the use of several coatings or surface modifications have been the subject of recent investigations to improve tool stability (Chiu et al., 2005; Rech et al., 2005; Wenge et al., 2006). Especially in the food industry, a critical issue is that titanium materials are non-magnetic and, therefore, eroded particles cannot be detected by magnetic separators.

Flexibility and endurance are crucial parameters for establishing preferences for ultrasonic cutting systems. Shape and dimensions of the longitudinally oscillating sonotrodes for guillotine cuts are restricted by the acoustic properties of the tool material and require a robust design. Nevertheless, a great variety of especially adapted geometries is available in the market (Fig. 9.15). At present, an efficient and stable performance, and a limitation of secondary effects (for example, noise, heating) are the main targets for designing and optimizing ultrasonic cutting tools (Cardoni and Lucas, 2002, 2005; Cardoni et al., 2004, 2006; Lucas et al., 2001, 2005). Initial costs for titanium sonotrodes are considerably high, but they offer good durability and performance at high ultrasonic amplitudes. However, resharpening, which might become necessary because of abrasion or operational damage, is problematic, as it might detune the entire vibration system. Such systems are very well suited for periodic cuts, e.g., for portioning of cheese wheels or flat bulky goods such as cakes, cereal bars, etc.

The coupling of independent cutting tools to the sonotrode allows a rapid replacement of worn or damaged components, but also the application of various

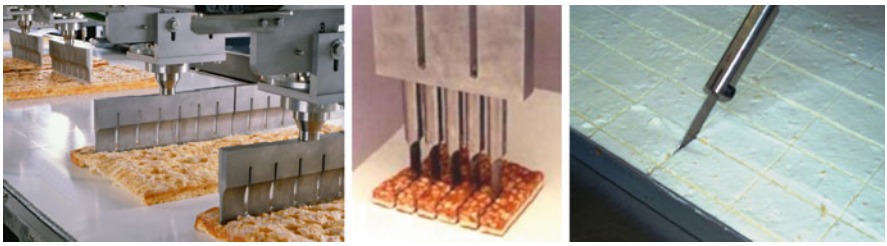

Fig. 9.15 Application of ultrasonic cutting tools: An assembly of cutting sonotrodes excited perpendicular to the cutting edge (*left*; courtesy of Döinghaus GmbH, Delbrück-Hagen, Germany); A sonotrode with slitter elements (*middle*; http://www.dukcorp.com/us/products/food/food.htm, accessed: 08/08/2007) and an ultrasonic assembly with an independent blade excitation is parallel to the cutting edge (*right*; courtesy of Dr. Wolf and Partner, Halle/Saale, Germany)

geometries, including those of a slim shape. These blades are relatively cheap, but a reproducible clamping to the sonotrode and a re-tuning of the entire vibrating system is necessary for stable performance. The coupling point is susceptible to fatigue and energy losses. Especially, knife-shaped tools are well suited for continuous cutting of plane products (for example, cakes on baking trays).

4 Synopsis

Ultrasonic cutting is realized by superpositioning the macroscopic feed motion of the cutting device (or of the product) with a microscopic vibration of the cutting tool. The interactions between excited tool and product generate various effects, which may be distinguished into primary and secondary effects.

Primary effects mainly arise from the cyclic loading and lead to energy concentration in the separation zone and contact friction modification along the tool flanks. General benefits for the ultrasound-induced cutting of food are:

- reduction of cutting forces
- exact cutting path and a smooth cut surface
- marginal product deformation
- reduced crumbling, squeezing and debris and
- reduction of smearing contamination and self-cleaning effects

Although the magnitude of possible force reduction strongly depends on product properties, the relative effects increase with increasing vibration speed (or increasing vibration amplitude) of the cutting edge and with decreasing cutting velocities.

Secondary effects result from the propagation of the sound field in the product and are closely related to chemical and physical properties of the cutting material. Sound absorption leading to heating effects, and cavitation, are most important and

cause quality losses when these effects become dominating. The magnitude of secondary effects increases with increasing vibration speed and with decreasing cutting velocities.

When applying ultrasonic cutting in the field of food materials, the optimization of the process, that is, the maximization of mechanical effects associated with an appropriate reduction of separation and friction forces and a simultaneous minimization of secondary effects displays the real challenge. Considering all of these aspects, ultrasonic cutting is especially suited for segmenting and scoring of cheese and bean curd, cakes, confectionary products and sweets, dough, pastry, meat or fish pies, frozen products, and convenience food and snacks.

Notation

Symbol	Unit	Description
E_{US}	J	Additional ultrasonic energy
F_C	N	Cutting force
F_F	N	Friction force
$F_{F,L}$	N	Friction force (lateral flank zone)
$F_{F,W}$	N	Friction force (wedge zone)
F_L	N	Lateral compression force
F_N	N	Normal force
F_R	N	Resistance force
F_W	N	Deformation force (wedge zone)
P	W	Power demand of the sonotrode
P_0	W	Power demand of the sonotrode in air
P_a	W	Product-specific power demand of the sonotrode for cutting
W_C	J	Cutting work
$W_{C,0}$	J	Cutting work without ultrasonic support
$W_{C,US}$	J	Cutting work with ultrasonic support
W_{diss}	J	Dissipated fraction of the cutting work
W_{elast}	J	Fraction of the cutting work stored for elastic deformation
W_{frakt}	J	Cutting work fraction for fracture
d	m	Blade thickness
f	Hz	Frequency
k_W	–	Relative cutting work coefficient
s	m	Cutting depth
s_C	m	Effective cutting depth
s_L	m	Linear cutting depth
t	s	Time
y_0	m	Vibration amplitude
v_C	m/s	Effective cutting velocity
v_L	m/s	Linear velocity

$v_{L,c}$	m/s	Critical linear velocity
v_S	m/s	Sliding velocity
v_{US}	m/s	Vibration speed
α	°	Wedge angle
λ	°	Cutting angle
ω	rad/s	Angular velocity

References

Althof, F. C., Buhl, H., and Voigt, H. (1973). Zum Potenzialverhalten der Oberfläche metallischer Werkstoffe bei milder und starker Schwingungskavitation. III. Titanwerkstoffe. *Werkstoffe und Korrosion*, 24, 1019–1027.

Astashev, V. K., and Babitsky, V. I. (1998). Ultrasonic cutting as a nonlinear (vibro-impact) process. *Ultrasonics*, 36, 89–96.

Atkins, A. G., and Mai, Y. M. (1985). *Elastic and plastic fracture: Metals, polymers, ceramics, composites, biological materials*. Chichester, Ellis Horwood.

Atkins, A. G., Xu, X., and Jeronimidis, G. (2004). Cutting, by 'pressing and slicing', of thin floppy slices of materials illustrated by experiments on cheddar cheese and salami. *Journal of Materials Science*, 39, 2761–2766.

Blumenauer, H., and Pusch, G. (1993). *Technische Bruchmechanik*. Leipzig, Deutscher Verlag für Grundstoffindustrie.

Brennan, J. G. (2006). Mixing, emulsification and size reduction. In: Brennan, J. G. (ed.), *Food processing handbook*, pp. 513–558. Weinheim, Wiley-VCH.

Brennan, J. G., Butters, J. R., Cowell, N. D., and Lilley, A. E. V. (1990). *Food engineering operations*. London, Elsevier.

Brown, T., James, S. J., and Purnell, G. L. (2005). Cutting forces in foods: Experimental measurements. *Journal of Food Engineering*, 70, 165–170.

Cardoni, A., and Lucas, M. (2002). Enhanced vibration performance of ultrasonic block horns. *Ultrasonics*, 40, 365–369.

Cardoni, A., and Lucas, M. (2005). Strategies for reducing stress in ultrasonic cutting systems. *Strain*, 41, 11–18.

Cardoni, A., Lucas, M., Cartmell, M., and Lim, F. (2004). A novel multiple blade ultrasonic cutting device. *Ultrasonics*, 42, 69–74.

Cardoni, A., MacBeath, A., and Lucas, M. (2006). Methods for reducing cutting temperature in ultrasonic cutting of bone. *Ultrasonics*, 44(Suppl 1), E37–E42.

Chandiramani, N. K., Srinivasan, K., and Nagendra, J. (2006). Experimental study of stick-slip dynamics in a friction wedge damper. *Journal of Sound and Vibration*, 291, 1–18.

Chemat, F., Grondin, I., Costes, P., Moutoussamy, L., Sing, A. S. C., and Smadja, J. (2004a). High power ultrasound effects on lipid oxidation of refined sunflower oil. *Ultrasonics Sonochemistry*, 11, 281–285.

Chemat, F., Grondin, I., Shum Cheong Sing, A., and Smadja, J. (2004b). Deterioration of edible oils during food processing by ultrasound. *Ultrasonics Sonochemistry*, 11, 13–15.

Chiu, K. Y., Chenga, F. T., and Man, H. C. (2005). Evolution of surface roughness of some metallic materials in cavitation erosion. *Ultrasonics*, 43, 713–716.

Fellows, J. P. (2000). *Food processing technology: Principles and practice*. Cambridge, Woodhead.

Goh, S. M., Charalambides, M. N., and Williams, J. G. (2005). On the mechanics of wire cutting of cheese. *Engineering Fracture Mechanics*, 72, 931–946.

Jiménez-Fernández, J., and Crespo, A. (2005). Bubble oscillation and inertial cavitation in viscoelastic fluids. *Ultrasonics*, 43, 643–651.

Kamyab, I., Chakrabarti, S., and Williams, J. G. (1998). Cutting cheese with wire. *Journal of Materials Science*, 33, 2763–2770.

Kim, J. D., and Choi, I.-H. (1997). Micro surface phenomenon of ductile cutting in the ultrasonic vibration cutting of optical plastics. *Journal of Materials Processing Technology*, 68, 89–98.

Kinoshita, T., Kanehira, E., Omura, K., Kawakami, K., and Watanabe, Y. (1999). Experimental study on heat production by a 23.5-kHz ultrasonically activated device for endoscopic surgery. *Surgical Endoscopy*, 13, 621–625.

Kluge, C., and Linke, L. (1993). Schneiden von Obst und Gemüse: Ursache – Wirkung – Zusammenhänge. *Zeitschrift für Lebensmitteltechnik*, 44, 26–30.

Koch, C. (2001). Thermische Wirkungen von Ultraschall. *Ultraschall in der Medizin*, 22, 146–152.

Koch, C., Nürnberger, H., and Reimann, H. P. (2004). Measurement of temperature elevation in tissue for the optimum and safe use of scalpel-type ultrasonic surgery devices. *Journal of Physics: Conference Series*, 1, 122–127.

Li, H., Pordesimo, L., and Weiss, J. (2004). High intensity ultrasound-assisted extraction of oil from soybeans. *Food Research International*, 37, 731–738.

Lifka, J., Ondruschka, B., and Hofmann, J. (2002). Einsatz von Ultraschall zum Schadstoffabbau in Wasser: Aquasonolyse – Eine Übersicht. *Chemie Ingenieur Technik*, 74, 403–413.

Lim, F. C. N., Cartmell, M. P., Cardoni, A., and Lucas, M. (2004). A preliminary investigation into optimising the response of vibrating systems used for ultrasonic cutting. *Journal of Sound and Vibration*, 272, 1047–1069.

Linke, L., and Kluge, C. (1993). Schneiden von Lebensmitteln. *Lebensmitteltechnik*, 25, 12–16.

Linke, L., and Liebers, H. (1992). Qualitätsanforderungen beim Schneiden von Obst und Gemüse. *Lebensmitteltechnik*, 24, 24–29.

Littmann, W., Storck, H., and Wallaschek, J. (2001). Sliding friction in the presence of ultrasonic oscillations: Superposition of longitudinal oscillations. *Archive of Applied Mechanics*, 71, 549–554.

Loncin, M., and Merson, R. L. (1979). *Food engineering: Principles and selected applications*. New York, NY, Academic.

Lucas, M., Cardoni, A., and MacBeath, A. (2005). Temperature effects in ultrasonic cutting. *CIRP Annals*, 54, 195–198.

Lucas, M., Graham, G., and Smith, A. C. (1996). Enhanced vibration control of an ultrasonic cutting process. *Ultrasonics*, 34, 205–211.

Lucas, M., MacBeath, A., McCulloch, E. M., and Cardoni, A. (2006). A finite element model for ultrasonic cutting. *Ultrasonics*, 44(Suppl 1), E503–E509.

Lucas, M., Petzing, A., and Smith, L. J. (2001). Design and characterization of ultrasonic cutting tools. *CIRP Annals*, 50, 149–152.

Mason, T. J. (2003). Sonochemistry and sonoprocessing: The link, the trends and (probably) the future. *Ultrasonics Sonochemistry*, 10, 175–179.

McCulloch, E., A. MacBeath, A., and Lucas, M. (2006). A finite element model for ultrasonic cutting of toffee. *Applied Mechanics and Materials*, 5–6, 519–526.

Mracek, M., and Wallaschek, J. (2005). A system for powder transport based on piezoelectrically excited ultrasonic progressive waves. *Materials Chemistry and Physics*, 90, 378–380.

Myshkin, N. K., Petrokovets, M. I., and Kovalev, A. V. (2005). Tribology of polymers: Adhesion, friction, wear, and mass-transfer. *Tribology International*, 38, 910–921.

Neville, A., and McDougall, B. A. B. (2001). Erosion- and cavitation-corrosion of titanium and its alloys. *Wear*, 250, 726–735.

Petrier, C., Lamy, M. F., Francony, A., Benahcene, A., Renaudin, V., and Gondrexon, N. (1994). Sonochemical degradation of phenol in dilute aqueous solutions: Comparison of the reaction rates at 20 and 487 kHz. *Journal of Physical Chemistry*, 98, 10514–10520.

Raeuber, H. J. (2004). Zerteilen nichtspröder Stoffe. In: Tscheuschner H. D. (ed.), *Lebensmitteltechnik*, pp. 248–270. Hamburg, Behr's.

Rawson, F. F. (1998). An introduction to ultrasonic food cutting. In: Povey, M. J. W., and Mason T. J. (eds.), *Ultrasound in food processing*, pp. 254–269. London, Blackie Academic.

Rech, J., Battaglia, J. L., and Moisan, A. (2005). Thermal influence of cutting tool coatings. *Journal of Material Processing Technology*, 159, 119–124.

Saravacos, G. D., and Kostaropoulos, A. E. (2002). *Handbook of food processing equipment*. New York, NY, Kluwer.

Schneider, Y. (2007) *Einsatz von Ultraschall zur Modifikation lebensmitteltechnischer Grundoperationen am Beispiel des Schneidens*. Dresden, Technische Universität Dresden, Faculty Mechanical Engineering, PhD thesis.

Schneider, Y., Zahn, S., Hofmann, J., Wecks, M, and Rohm, H. (2006). Acoustic cavitation induced by ultrasonic cutting devices: A preliminary study. *Ultrasonics Sonochemistry*, 13, 117–120.

Schneider, Y., Zahn, S., and Linke, L. (2002). Qualitative process evaluation for ultrasonic cutting of food. *Engineering in Life Sciences*, 2, 153–157.

Schneider, Y., Zahn, S., and Rohm, H. (2007). Power requirements of the high-frequency generator in ultrasonic cutting of foods. *Journal of Food Engineering*, 86, 61–67.

Storck, H., Littmann, W., Wallaschek, J., and Mracek, M. (2002). The effect of friction reduction in presence of ultrasonic vibrations and its relevance to travelling wave ultrasonic motors. *Ultrasonics*, 40, 379–383.

Suslick, K. S., Didenko, Y., Fang, M. M., Hyeon, T., Kolbeck, K. J., Mc Namara, W. B., III, Mdleleni, M. M., and Wong, M. (1999). Acoustic cavitation and its chemical consequences. *Philosophical Transactions of the Royal Society A*, 357, 335–353.

Wenge, C., Chenqing, G., Kang, Z., and Fusan, S. (2006) Correlation of cavitation erosion resistance and mechanical properties of some engineering steels. *Journal of Materials Science*, 41, 2151–2153.

Xia, T., Shi, S., and Wan, X. (2006). Impact of ultrasonic-assisted extraction on the chemical and sensory quality of tea infusion. *Journal of Food Engineering*, 74, 557–560.

Zahn, S., Schneider, Y., and Rohm, H. (2006). Ultrasonic cutting of foods: Effects of excitation magnitude and cutting velocity on the reduction of cutting work. *Innovative Food Science and Emerging Technologies*, 7, 288–293.

Zahn, S., Schneider, Y., Zücker, G., and Rohm, H. (2005). Impact of excitation and material parameters on the efficiency of ultrasonic cutting of bakery products. *Journal of Food Science*, 70, E510–E513.

Chapter 10
Engineering Food Ingredients with High-Intensity Ultrasound

Jochen Weiss, Kristberg Kristbergsson, and Gunnar Thor Kjartansson

1 Introduction

The use of ultrasound in the food industry has increased in the last decades. Ultrasound has been used both to analyze food structure and composition at low ultrasonic intensities and high frequencies and to modify ingredients at high ultrasonic intensities and low frequencies. Application of the latter is referred to as high-intensity (power) ultrasonication and is generally carried out at frequencies of ≤ 0.1 MHz and ultrasonic intensities of 10–100 W cm^{-2}. In the food industry, power ultrasonication has proved to be a highly effective food processing and preservation technology, and use of high-intensity ultrasound with or without heat may be used, for example, to denature enzymes, aid in the extraction of valuable compounds from plants and seeds, tenderize meat, and homogenize or disperse two-phase systems such as emulsions or suspensions (Mason et al., 1996). The processing-related effects of ultrasound are related to induced cavitation, heating, dynamic agitation, shear stress, and turbulence, a subject that was discussed in depth earlier in this book (Floros and Liang, 1994; Fukase et al., 1996; Mason et al., 1996).

Application of power ultrasound, at frequencies between 20 and 100 kHz, may cause chemical and physical changes in a viscous medium by cyclic generation and collapse of cavities. The increased pressure and temperature in the vicinity of these cavities is the basis for the observed chemical and mechanical effects of power ultrasonication. Cavitation bubbles generate localized hot spots at temperatures in excess of 4,000 K and pressures of more than 100 MPa. The lifetime of a cavitational bubble may be as short as 0.1 m s^{-1}. The cooling rate of a bubble can be above 10^{10} K s^{-1} (Floros and Liang, 1994). Rapid bubble collapse produces shear forces in the surrounding bulk liquid and these shear forces are strong enough to break covalent bonds in polymeric materials that are present in the bulk phase. In addition, cleavage of small molecular weight compounds located inside the cavities may lead to

J. Weiss (✉)
Department of Food Structure and Functionality, Institute of Food Science and Biotechnology, Universität Hohenheim, Garbenstraße 21/25, 70599, Stuttgart, Germany
e-mail: j.weiss@uni-hohenheim.de

H. Feng et al. (eds.), *Ultrasound Technologies for Food and Bioprocessing*, Food Engineering Series, DOI 10.1007/978-1-4419-7472-3_10,
© Springer Science+Business Media, LLC 2011

generation of radical species which can drive a large number of chemical reactions that are of interest to the food industry. Finally, the collapse of cavitation bubbles in heterogeneous solid–liquid systems leads to the generation of localized highly turbulent fluid flow comparable to the flow situation encountered in a liquid jet with speeds as high as 110 m s^{-1}, which in turn may accelerate the kinetics of a variety of chemical reactions (Mason, 1992). Sonochemistry is thus clearly a unique process with respect to its effects due to the nature of the underlying process of cavitation where bubbles pulsate and oscillate, merge and collapse, deform and break up into fragments.

In this chapter we will highlight the use of high-intensity ultrasound to alter the structure of food ingredients (proteins, carbohydrates, and lipids) and thereby their functional behavior. We will begin by reviewing the general sonochemical principles that drive potential reactions that may be encountered when applying high-intensity ultrasound to solutions containing organic molecules. While most of the potential reactions utilized by the food industry are likely to be carried out in aqueous solutions, we will briefly highlight some reactions that are carried out in organic solvents. We will then focus on reviewing studies that have been reported in the literature or have been conducted in our laboratories which describe the effects of high-intensity ultrasound on the functionality and structure of food ingredients, namely proteins, carbohydrates, and lipids. The objective is to give the reader an overview over the current and potential application of high-intensity ultrasound to tailor in particular protein and carbohydrate functionality.

For the food industry, this new technology could be of significant interest, as it allows "green" chemistry to be conducted, i.e., conducting chemical reactions using environmentally benign solvents and reactants. Moreover, since the generation of ultrasonic waves is simply a matter of applying a current to the ultrasonic transducer, the reaction can be turned on or off by the push of a button (Jambrak et al., 2009; Kresic et al., 2008; Vilkhu et al., 2008). Issues of scale up and equipment design are increasingly being solved and the technology is thus quickly becoming a viable additional tool in the arsenal of food scientists who are interested in creating new food structures and ingredients.

2 Fundamental Sonochemistry with a Focus on Aqueous Systems Containing Organic Compounds

2.1 Cavitation Drives Chemical Reactions

The biological and chemical effects of ultrasound were first reported by Richards and Loomis in 1927 in their paper "The Chemical Effects of High Frequency Sound Waves" (Richards and Loomis, 1927). In this groundbreaking article the authors described for the first time that they observed a number of chemical reactions under the influence of power ultrasound. Subsequent investigations quickly revealed that the chemical effects of ultrasound are diverse and may include substantial

improvements in both stoichiometric and catalytic chemical reactions. Other investigators found that ultrasonic irradiation can in general substantially increase the reactivity of reactants (Lintner and Hanesian, 1976). This fact immediately raised the interest level of the chemical industries in the new technology, resulting in an increased pursuit of research in this area (Shoh, 1988; Heusinger, 1990; Leighton, 1997).

Ultrasonic irradiation is different from any other source of energy with respect to duration, pressure, and energy per molecule. As previously mentioned, and as explained in detail earlier in this book, the chemical effects of ultrasound are not the result of direct molecular interactions of the acoustic waves with the sonicated matter, but are rather a byproduct of cavitation, i.e., the formation, growth, and collapse of cavitation bubbles in the sonicated medium. As with any sound wave, ultrasound propagates through a medium via a series of compressional and rarefactional waves. At sufficiently high wave amplitudes, the rarefaction cycle may exceed the attractive forces between solvent molecules and, consequently, cavities are formed (Mason and Lorimer, 1989). As the amplitude of the waves increases, a threshold value for cavity nucleation is eventually reached. Subsequently, cavities begin to grow in number and size and collapse becomes increasingly violent. This increasing cavitational activity is directly related to an increase in the sonochemical reaction rate (Leighton, 1997). The formation and collapse of cavities occur over extremely short periods of time, typically a few microseconds (Hardcastle et al., 2000). Upon the collapse of cavities, very high local temperatures and pressure fluctuations result and a significant amount of energy in the form of thermal excitation is introduced into the system. Interestingly, at sufficiently high intensities and near radiating surfaces a self-quenching effect can sometimes be observed; that is, the cavitation of the liquid becomes so intense that the shroud of cavities formed near the solid surface quenches the energy input into the liquid, thus decreasing the sonochemical reaction rates.

A number of theoretical models have been proposed to describe the observed cavitation events under the influence of high-intensity ultrasound. For example, Blake considered the situation of a small cavity in solution where the pressure in the liquid suddenly increases or decreases. The analysis revealed that a critical cavity size R_{crit} must exist, at which a pressure balance across the phase boundary can no longer be maintained and explosive growth must follow. Blake calculated this critical size as

$$R_{\text{crit}} = \left(\frac{3R_0^3}{2\sigma} \left(p_0 + \frac{2\sigma}{R_0} - p_{\text{v}} \right) \right)^{\frac{1}{2}} \tag{10.1}$$

where R_0 is the size of the bubble nuclei, p_0 is the hydrostatic pressure, p_{v} is the vapor pressure of the liquid, and σ is the surface tension. In other words, explosive growth can be initiated if $p_L \geq p_{\text{v}} - 4\sigma/3R_{\text{crit}}$. Minneart, in a different approach, established a relationship between the radius of the cavities and the applied frequency of the applied sound wave (Suslick and Price, 1999; Suslick et al., 1987):

$$f_0 = \frac{1}{2\pi R_o}\sqrt{\frac{3\gamma p_o}{\rho}} \tag{10.2}$$

where R_0 is the resonant cavity size, f_0 is the wave frequency, γ is the specific heat ratio of the gas, p_0 is the total external pressure, and ρ is the density of the media. Equation (10.2) explains why high-intensity ultrasound equipment usually operates at low frequencies (20–100 kHz) since cavities grow larger as the frequency of the ultrasonic wave decreases (Povey, 1998; Povey and Mason, 1998). A widely accepted theory known as the hot-spot theory predicts local temperatures to be approximately 2,000–5,000 K and pressures to range from 10 to 100 MPa. However, since the collapse of the cavities occurs within a few microseconds, there is insufficient time to allow for heat conduction to occur, and temperatures of the solvent phase therefore increase slowly. Theoretically calculated cooling rates within the cavities are in the order of 10^{10} K s^{-1}. If one assumes nearly adiabatic conditions within the bubble, the temperature inside the bubble at the end of the collapse can be estimated as

$$T_{max} = T_0\left(\frac{V_0}{V_{max}}\right)^{\frac{C_p}{C_v}-1} \tag{10.3}$$

where c_p/c_v is the heat capacity ratio and V_0/V_{max} is the change in the bubble volume. Considering the frequency dependence of the bubble size (equation (10.2)), the temperature should therefore decrease as the frequency increases since the size of the bubble decreases. In reality, thermal conductivity effects begin to play a role for smaller bubbles and the collapse is no longer adiabatic at higher frequencies. The chemical effects of high-intensity ultrasound, which are the focus of this chapter, are closely related to the conditions inside the bubble and if the goal is to predominantly utilize the chemical effects of high-intensity ultrasound, the use of higher frequency transducers is preferable. At higher frequencies, mechanical effects are more subdued and sonochemical reactions are instead promoted (Margulis, 1983).

2.2 Basic Sonochemical Reactions

Sonochemical reactions are ultrasound-initiated or -mediated reactions that can occur in three different systems: homogeneous liquids, heterogeneous liquid–liquid mixtures or dispersions, and heterogeneous liquid–solid dispersions (Suslick, 1997). These reactions may lead to the breakdown of existing compounds or to the creation of combination products, depending on the components present, environmental conditions such as pressure, temperature, pH, ionic strength, and ultrasonication conditions including intensity, frequency, sonication length. In homogeneous one-phase systems such as pure water or other solute–solvent systems, the application of ultrasound readily induces single electron transfers resulting in a ligand metal

bond cleavage of transition metal complexes which then leads to the generation of a large variety of reactive species (Luche, 1992). A large number of radicals ($OH^{\bullet}$, $H^{\bullet}$, $X^{\bullet}$, etc.) may be formed inside the cavities during the collapse cycle. These radicals may react with other molecules in the liquid phase to create additional reactive species or they may cross-react inside the collapsing cavity to form a variety of intermediate compounds that subsequently serve as reactants to other reactions. While primary products include H_2 and H_2O_2, there is strong evidence that various other high-energy intermediates are also generated, e.g., HO_2, H, OH, and possibly $e^-_{(aq)}$ (Kotronarou et al., 1991).

A byproduct of homogeneous sonochemical reactions may be the induction of sonoluminescence, which is defined as a reoccurring short-lived light emission from inside the cavitation bubble with peak intensities of the order of 1–10 mW and emission times ranging from several tens to hundreds of picoseconds. Sonoluminescence is an extremely complex phenomenon that is still under intense investigation. In the context of this chapter, we will not discuss sonoluminescence because it does not play a significant role in the modification of food ingredients, and interested readers are instead referred to a number of excellent review articles that have been published on this subject (Flannigan et al., 2005; Margulis, 1985; Margulis and Margulis, 2002; Ostrovskii et al., 1999).

In contrast to sonochemical reactions in homogeneous systems, sonochemistry in heterogeneous systems, i.e., systems that are composed of multiple phases such as liquid–liquid and liquid–solid dispersions, is even more complex than in homogeneous systems because not only radical reactions but also ionic reactions may be promoted (Flannigan et al., 2005; Mason and Lorimer, 1989). Ionic reactions may also be stimulated by the mechanical effects of high-intensity ultrasound, which can lead to improvements in rate and yield of a wide variety of reactions. The degree to which this stimulation occurs is governed by the physical properties of the dispersed phases including interfacial tension, densities, viscosities, elastic moduli, and others. Moreover, since heterogeneous sonochemistry occurs in multiphase systems, interfacial chemical phenomena play an important role. Reactions thus also depend on the characteristics of the dispersion, that is, the size and concentration of dispersed liquid or solid particles.

In this section, we will highlight a few fundamental sonochemical reactions that are the basis of the subsequent modification of food ingredients under the influence of ultrasound. To this purpose, we will focus on organic rather than inorganic compounds. For more information on inorganic sonochemistry, the reader is directed to the most recent work in the production of nanostructures using ultrasound, which utilizes mainly inorganic compounds, e.g., nanocrystals, nanodisks, and spherical nanoparticles composed of ZnO, mercury chalcogenides HgE (E = S, Se, Te), and TiO_2 which have been successfully produced using power ultrasound (Arami et al., 2007; Bhattacharyya and Gedanken, 2008; Drofenik et al., 2008; Hibino et al., 2005; Kristl and Drofenik, 2008; Park et al., 2005; Wang et al., 2008; Zolfaghari et al., 2007). The reader is also directed to a chapter in this book that focuses on the production of nanostructures using high-intensity ultrasound.

2.2.1 Sonochemistry in Homogeneous Systems

Thermolytic cleavage of water. A key reaction in sonochemistry is the thermolytic cleavage of water since water is one of the most commonly used solvents in many reactions. This reaction is also of key importance in explaining some of the reactions described later in this chapter that focus on the sonication of food ingredients. In general, ultrasound-induced pyrolysis (or thermolytic cleavage) is the predominant degradation pathway, not only for water, but for many compounds that are subjected to high-intensity ultrasound (Drijvers et al., 1996). In the course of this reaction, both strong oxidants and reductants capable of causing secondary oxidation and reduction reactions are formed (Margulis, 1985). For food systems, these reactions may be beneficial if the functionality of ingredients is enhanced, or on the other hand detrimental if the quality and functionality of ingredients decrease. The thermolytic cleavage of water is caused by exposure of water molecules to the high temperatures and pressures that occur during the collapse cycle of the cavities, resulting in the formation of hydrogen and hydroxyl radicals ($H^{\bullet}$, $OH^{\bullet}$):

$$H_2O \rightarrow H^{\bullet} + OH^{\bullet} \tag{10.4}$$

These radicals may recombine to form, among other compounds, hydrogen and hydrogen peroxide (Anbar and Pecht, 1964):

$$H^{\bullet} + H^{\bullet} \rightarrow H_2 \tag{10.5}$$

$$OH^{\bullet} + OH^{\bullet} \rightarrow H_2O_2 \tag{10.6}$$

In a study by Riesz and coworkers that focused on investigating ultrasonically initiated free radical polymerization and polymer degradation by electron paramagnetic resonance with chemical spin traps, a definite generation of hydrogen and hydroxyl radicals ($H^{\bullet}$ and $OH^{\bullet}$) under high-intensity ultrasound was confirmed (Riesz et al., 1985). However, Hart and Henglein noted that in addition to the hydrogen and hydroxyl radicals, $HO_2^{\bullet}$ radicals may be formed if oxygen is present in the gas phase (Hart and Henglein, 1985):

$$H^{\bullet} + O_2 \rightarrow HO_2^{\bullet} \tag{10.7}$$

A subsequent cross-reaction of these radicals could then also lead to the production of H_2O_2:

$$HO_2^{\bullet} + HO_2^{\bullet} \rightarrow H_2O_2 + O_2 \tag{10.8}$$

Indeed, Kotronarou and coauthors reported a high sonolytic production rate of hydrogen peroxide, H_2O_2, in air-saturated water of $2.40 - 2.52 \times 10^{-3}$ mmol L^{-1} min^{-1} at an ultrasonic frequency of 24 kHz and a volumetric energy input of 3,360 W L^{-1} (Hung et al., 1998; Kotronarou et al., 1991). On the other hand, hydrogen peroxide production rates at higher ultrasonic frequencies (205 kHz) at a

volumetric energy input of 244 W L^{-1} under either an argon or an oxygen atmosphere were found to be similar and not influenced by the dissolved gas type, i.e., 3.5×10^{-4} mmol L^{-1} min^{-1} (Kang et al., 1999). However, since the reaction of two $HO_2^{\bullet}$ produces O_2 as a byproduct only small initial concentrations of oxygen may be required to get the reaction started, which may explain these seemingly contradictory results.

The hydrogen peroxide formation reaction has been shown to follow a simple zero-order kinetics, that is, the concentration of hydrogen peroxide at a specific ultrasonic intensity increases linearly with time (Barbier and Petrier, 1996). This may be because mass transport processes limit how much hydrogen peroxide can be transported across the cavitational bubble interface. The concentration of hydroxyl radicals at the interface of the cavity has been estimated to be approximately 4 mmol L^{-1} (Gutierrez et al., 1991). Thus, at low concentrations of hydrogen peroxide in the aqueous phase, the diffusion-driven rate of transport of hydrogen peroxide would remain approximately constant if the number and size of cavitational bubbles are constant, giving rise to the observed zero-order kinetics.

While the production of these radical species appears not to be significantly influenced by the type of atmosphere under which the sonication is carried out, the reaction may be influenced by the presence of solutes in the aqueous phase. For example, dissolved salts may act as a catalyst to increase the concentration of hydrogen peroxide or, alternatively, may increase the subsequent reaction of hydrogen peroxide with susceptible components (Strukul, 1992). In systems where sonoluminescence may occur, the presence of salts in an ultrasonicated aqueous system has been shown to increase the sonoluminescence intensity (Finch, 1963; Gunther et al., 1956; Sehgal et al., 1980), which is an indication of increased production of transient radical species. For example, while the addition of 1 M NaCl did not noticeably affect sonoluminescence activity, an increase to 2 M NaCl increased sonoluminescence activity by a factor of 7 (Harvey and Loomis, 1929; Jarmon and Taylor, 1970; Negishi, 1961). The outcome of this increased production of hydrogen peroxide has been utilized in the ultrasonically driven inactivation of microorganisms, where the presence of salts was found to lead to a significant improvement in loss of cell homeostasis. The increased concentration of hydrogen peroxide apparently caused stronger oxidation of lipid membranes, disruption of enzymatic activity of protein complexes responsible for ATP production, and maintenance of solute concentration in the cell interior, as well as damage to the genetic material required for reproduction of cells (Stanley et al., 2004).

Sonochemistry in aqueous solutions. The homogeneous sonochemistry of compounds dissolved in water has been widely studied and a variety of unusual reactivity patterns have been observed during ultrasonic irradiation of aqueous solutions, including multiple ligand dissociation, novel metal cluster formation, and the initiation of homogeneous catalysis at low ambient temperature (De Visscher and Van Langenhove, 1998; Disselkamp et al., 2005; Drijvers et al., 1998; Gutierrez et al., 1991; Ince et al., 2001; Riesz et al., 1985; Snell, 1965; Yim et al., 2003). It should be noted that for homogeneous sonochemical reactions to occur, all compounds must be dissolved in the aqueous phase. If the concentration of compounds is above the

aqueous solubility limit, reactions will proceed via a heterogeneous sonochemical pathway (see below). For example, if an organic compound is dispersed in water above its solubility, the subsequent sonication will induce formation of a dispersed two-phase system, i.e., oil-in-water or water-in-oil emulsions, depending on the concentration of compounds and the presence of interfacially active compounds. We will now look at just a few reactions that have been carried out in aqueous systems to highlight the versatility and application potential of high-intensity ultrasound to modify organic (and thus eventually food) compounds.

A classical homogeneous sonochemical reaction that has been the focus of a number of studies is the degradation of chlorobenzene in water. Chlorobenzene has received much attention because it is a very useful model for noxious compounds that pollute wastewater. The ability of high-intensity ultrasound to remove organic compounds from water is based on the fact that hydroxyl radicals produced from the sonolysis of water are essentially able to attack all organic compounds (including halocarbons, pesticides, and nitroaromatics) and through a series of reactions to oxidize them fully. Sonolysis has thus garnered substantial interest in this field of application due to its low maintenance requirements and high energy efficiency compared to alternative methods (e.g., ozonolysis or UV photolysis) (Adewuyi, 2001).

The sonolytical degradation of chlorobenzene present in water may lead to the production of a large variety of volatile compounds such as CO, CO_2, CH_4, and C_2H_2 in the gas phase, while phenols, polyphenols, chlorophenols, and benzene have been identified and quantified in the liquid phase of the reaction mixture (Stavarache et al., 2004). Interestingly, the reaction could also be carried out in the presence of a radical scavenger (*n*-butanol), and similar products were observed when the reaction was carried out pyrolytically rather than sonolytically (Drijvers et al., 1998). Spurlock and his coworkers reported that the irradiation of aqueous suspensions of thioethers yielded mostly sulfoxides and sulfonic acids, while aldehydes yielded mostly carboxylic acids (Reifsneider and Spurlock, 1973; Spurlock and Reifsneider, 1970).

Another interesting reaction that, to some degree, shows the uniqueness of conducting reaction chemistry via ultrasound is the degradation of chloroform (CCl_4). When high-intensity ultrasound was applied to a potassium iodine solution with a large excess of CCl_4, C–Cl bonds were shown to be broken and chlorine was released. Typically, chlorine cannot be liberated from CCl_4 by activated O_2, but under the influence of high-intensity ultrasound it appears that CCl_4 yields chlorine radicals that may recombine in a termination reaction (Weissler et al., 1950) to form Cl_2:

$$CCl_4 \rightarrow Cl_3C^{\bullet} + Cl^{\bullet} \tag{10.9}$$

$$Cl_3C^{\bullet} + Cl_3C^{\bullet} \rightarrow Cl_3CCCl_3 \tag{10.10}$$

$$Cl^{\bullet} + Cl^{\bullet} \rightarrow Cl_2 \tag{10.11}$$

Another example that demonstrates the potential of sonochemistry is the ultrasonically induced oxidation of acetic acid. Acetic acid is one of the most resistant chemicals to oxidation because of the difficulty of oxidizing the methyl group in the alpha position of the carboxylic group. For example, when oxidizing phenol, the reaction leading to acetic acid is a dead end. Nevertheless, acetic acid could be oxidized under the influence of ultrasound, with the yield being influenced by the ultrasonic frequency and the applied power (FindIk et al., 2006).

There are many other examples of remarkable sonochemical reactions that can be carried out in ultrasound-treated aqueous solutions, including isomerization of malic acid, decomposition of alkyl bromide, alkylphenols, dichlorocyclopropanation, and epoxidation of 1,7octadiene, which illustrates why sonochemistry has attracted the interest of many chemists (Troia et al., 2006; Wang and Rajendran, 2007a, b; Yim et al., 2003). Clearly, for food scientists, reactions in water could be of significant interest to produce and modify a variety of ingredients, and more information on aqueous sonochemistry can be found in a number of reviews that have been published on the subject (De Visscher and Van Langenhove, 1998; Ince et al., 2001).

Sonochemistry in organic solvents. While sonochemical reactions in water and the thermolytic cleavage of water constitute some of the most important reactions in sonochemistry, sonochemical reactions may also occur in organic solvents. Suslick et al. established that virtually all organic liquids will generate free radicals upon ultrasonic irradiation, as long as the total vapor pressure is low enough to allow for an effective bubble collapse (Suslick et al., 1999). The production of radicals from solutions of organic compounds can generate the same types of products that are typically associated with very high temperature pyrolysis. Most of these products develop via a well-understood radical chain mechanism (Henglein, 1987) and these reactions have been used to produce a variety of useful industrial products. For example, the dechlorination of trichlorobenzenes in solution in hexane at 60°C or room temperature was facilitated by ultrasonication (Rodriguez and Lafuente, 2002). In addition, direct halogenation of alkanes, which was previously thought to be difficult and impractical to functionalize alkanes, was achieved by high-intensity ultrasound using iodoform (CHI_3) and sodium hydroxide (NaOH) (Kimura et al., 2002).

It is important to note though that sonochemical reactions occur to a much lesser degree or not at all if volatile organic solvents are irradiated. This is because many organic liquids have a high vapor pressure, which greatly diminishes the intensity of the cavitational collapse. The vapors that diffuse from the organic solvent into the cavitation bubble effectively dampen the collapse. Consequently, single-bubble sonoluminescence (SBSL), that is, the emission of a pulse of light with each compression of a single cavity trapped in an acoustic standing wave, when emitted from organic liquids such as alcohols were much weaker than the sonoluminescence emitted from water. For example, sonication of *n*-butanol resulted in a very weak sonoluminescence emission that was approximately 200 times less intense than that of water (Weninger et al., 1995). A reduction in solution temperature can to some degree help overcome limitations encountered in working with volatile

organic solvents. Theoretically, as long as the liquid temperature is low enough to sufficiently decrease the vapor pressure, cavitation may again become sufficiently intense to induce bond homolysis (Henglein, 1987).

2.2.2 Heterogeneous Sonochemistry

Heterogeneous sonochemistry occurs in systems that consist of two or more phases. For food scientists, this is probably the most common scenario (in addition to the ultrasound-induced cleavage of water), as most food components (e.g., proteins, carbohydrates, lipids) cannot be dissolved but only dispersed in water. In addition, foods and raw materials of food products are typically composed of many different components that form complex multiphase structures. In heterogeneous sonochemistry, mechanical effects of cavitation contribute to the observed effects. An erosive action of micro jets may occur during the asymmetric collapse of bubbles in the vicinity of solid or liquid interfaces that can accelerate reactions by influencing mass transport rates and increase surface areas (Peters, 1996; Sáeza et al., 2005). The intense microstreaming caused by the presence of an obstacle in the acoustic field allows an enhanced degree of mixing or surface modification of solid reagents (Elder, 1959). Microstreaming is not related to spatial attenuation, but arises from frictional forces between a boundary and a medium carrying vibration. Heterogeneous sonochemistry has been used to tailor the molecular weight of polymers, to initiate polymerization and to improve the activity of solid catalysts in the reaction mix.

Polymer degradation. Effects of high-intensity ultrasound are particularly noticeable for large macromolecules such as polymeric materials. As we will see later, this can have dramatic impacts on the functional properties of both carbohydrates and proteins, both of which are considered "food biopolymers." While ultrasound waves do not directly interact with the polymers, the collapse of cavitational bubbles results in the generation of high shear gradients. This shear force can be sufficiently high in magnitude to break chemical bonds in large macromolecules and thus reduce the molecular weight of these polymers (Peacocke and Pritchard, 1968; Pritchard et al., 1965). Of great importance in the degradation of polymers is the nature of the solvent. The influence of the solvent type on the degradation of dextran, polyethylene glycol, hydroxypropyl cellulose, and polystyrene has been described by a variety of researchers (Basedow and Ebert, 1975; Basedow et al., 1978; Malhotra, 1982a; Price and Smith, 1993; Thomas and Alexander, 1957). For example, in the presence of acids, many polymers are much more readily degraded by high-intensity ultrasound than under alkaline conditions.

To date, there is still ongoing discussion as to the precise mechanism of polymer degradation. Some researchers have suggested that polymer degradation occurs via a non-random process that produces fragmentation at the mid-point (Price and Smith, 1991), while others have suggested a random chain cleavage. Chakraborty et al. (2004), studying the ultrasonic degradation of both isotactic polypropylene and polybutadiene, developed a theoretical model based on a mid-point splitting

of polymers (Chakraborty et al., 2004). They suggested that the sonication-driven breakdown produces two fragments of equal size:

$$P(x) \xrightarrow{k(x)} 2P\left(\frac{x}{2}\right) \tag{10.12}$$

where $P(x)$ presents polymer species of molecular weight x. The population balance equation for the above reaction then yields an expression for $p(x, t)$, the molecular weight distribution that is generated from the starting polymers as a function of time:

$$\frac{\delta p(x,t)}{\delta t} = -k(x)p(x,t) + 2\int_x^\infty k(x)\, p(x',t)\, \delta\left(x - \frac{x'}{2}\right) \mathrm{d}x' \tag{10.13}$$

The degradation rate $k(x)$ is assumed to take the form of $k(x) = k(x - x_1)$, where x_1 represents the limiting molecular weight. This ensures that the rate coefficient k is independent of x and becomes zero when $x = x_1$ and no further degradation can thus take place (Chattopadhyay and Madras, 2003). Applying the moment operation $\int_0^\infty x^{(n)}\ [\,]\,\mathrm{d}x$ to equation (10.13) and solving for initial conditions, i.e., a polymer distribution $p(x, t = 0)$ and defining the average molecular weight as $p(1)/p(0)$, a simple description for the molecular weight decrease with time emerges:

$$\ln H = kx_1 t \tag{10.14}$$

where

$$H = \left[\frac{(x_1 - M_{n_0}^{-1})}{(x_1 - M_n^{-1})}\right] \tag{10.15}$$

and M the average molecular weight. While this model has been shown to fit the degradation of polypropylene and polybutadiene well, an earlier degradation model developed by Schmid (1940) has been shown to fit the degradation of biopolymers better (Baxter et al., 2005). This model instead assumes a random cleavage yielding a number of fragments. Schmid described the molar disruption rate as

$$\frac{1}{N_L}\frac{\mathrm{d}x}{\mathrm{d}t} = k\,(P - P_e) \tag{10.16}$$

where $1/N_L\ \mathrm{d}x/\mathrm{d}t$ is the molar disruption velocity or the number of new moles generated per liter per minute and $P = M/M_{\text{monomer}}$ is the degree of polymerization. The number of molecules present in the solution at time t is thus determined by the initial number of molecules n_0 and the number of newly generated molecules n_n:

$$n_t = n_0 + n_n \tag{10.17}$$

At a known polymer concentration c, n_t can then be expressed as

$$n_t = \frac{N_L c}{P} \tag{10.18}$$

Combining equations (10.16), (10.17), and (10.18) followed by integration from t=0 with M_0 to t with M_t yields

$$-\frac{M_e}{M_t} - \ln\left(1 - \frac{M_e}{M_t}\right) = \frac{k}{c} P_e^2 t + C \tag{10.19}$$

Where P_e is the final degree of polymerization given by $P_e = M_e/M_{\text{monomer}}$. Equation (10.19) should thus yield a straight line if the so-called Schmid declination factor (left-hand side of the equation) is plotted versus time. The rate constant k can then be calculated from the slope of the Schmid declination factor plot as

$$k = \frac{c}{P_e^2} m \tag{10.20}$$

Polymer synthesis. Ultrasound has also been applied to facilitate polymer synthesis by initiating both radical polymerization and organometallic reactions. For example, application of ultrasound as a radical polymerization initiator has been described for methyl methacrylate and styrene (Kruus et al., 1990; Price et al., 1992). Methyl methacrylate irradiated by ultrasound at 25°C produced radicals which initiated polymerization with a total monomer conversion in excess of 13% over a 3- to 4-h period. The molecular mass reached a maximum at 2.5×10^5 Da after 30 min and then decreased gradually to 1.7×10^5 Da after 3 h (Price et al., 1992). Radical trapping measurements using 1,1-diphenyl-2-picrylhydrazyl,DPPH, in methyl butyrate indicated that radical initiation rates were comparable to reactions rates of the chemical initiator azobis (isobutyronitrile) at 70°C. The decrease in the molecular mass with prolonged sonication has been attributed to shear effects from the collapsing cavitation bubbles that subsequently yield narrower molecular weight distributions in ultrasound initiated polymerization reactions. For styrene, 0.7% of the monomer polymerized after 1 h of sonication at 60°C yielded a very high-molecular weight polymer of 5×10^5 Da. Radical trapping measurements with 1,1-diphenyl-2-picrylhydrazyl, DPPH, suggested a radical initiation rate of 3×10^{-9} mol L^{-1} s^{-1}, which is significantly higher than rates obtained by thermal initiation using traditional methods (Kruus et al., 1990).

Ultrasound has also been used to prepare block co-polymers. One of the most difficult tasks in production is to control the block size. High-intensity ultrasound has been proved to be beneficial in this respect due to the fact that ultrasound may lead to some polymer degradation in solution and production of terminal radicals. These radicals can form co-polymers either by reacting with a second monomer or by combining with a second macromolecular radical. These block co-polymers can be used in production of compatible blends of immiscible polymers

such as polystyrene with *cis*-polybutadiene (Lebovitz et al., 2003; Price and West, 1996).

Heterogeneous catalysis. An important application of ultrasound, that is, emerging now is the acceleration of reactions that are catalyzed by the presence of solid or liquid-dispersed catalysts in the reaction mix. The effects of ultrasound on catalysis may be felt during various stages of the catalytic reaction, for example, during the formation of supported catalysts, during the activation of pre-formed catalysts, or during the actual catalytic conversion of compounds. It appears that the predominant cause of the improvements seen under ultrasound-assisted heterogeneous catalysis is the increase in effective surface area, which is of particular importance in the case of catalysts that are supported on brittle solids (Suslick, 1997). Examples of reactions that have been mediated and accelerated by ultrasound are extremely diverse and demonstrate the range of applications of high-intensity ultrasound, including palladium-catalyzed carbonyl allylation by allylic alcohols such as diethyl ether, diisopropyl ether, and toluene (Masuyama et al., 1994), selective oxidation of CO in the presence of air over gold-based catalysts (George et al., 2008), synthesis of thioether from alkyl bromides and sodium sulfide by quaternary ammonium salts in liquid–liquid two-phase dispersions (Wang and Rajendran, 2006), and hydrogenation of cinnamaldehyde using Pd-black and Raney Ni catalysts (Disselkamp et al., 2005). Finally, an excellent overview of the topic of ultrasound-mediated heterogeneous catalysis has been published by Bonrath, and readers may find additional information there (Bonrath, 2005).

2.2.3 Summary

As shown in this section, high-intensity ultrasound has been extensively exploited in the field of chemistry to produce reactive species that can initiate reactions, increase reaction rates, alter reaction paths by promoting radical-driven reactions, modify macromolecules, and accelerate catalysis. The potential use of ultrasound is thus extremely diverse and ranges from predominantly radical-driven reactions in homogeneous systems to both radical and ionic reactions in heterogeneous systems. It is important to note, though, that it currently remains very difficult to predict how the specific application of ultrasound will alter the standard reaction chemistry. This is because the physical basis of the chemical changes – the generation and collapse of cavities – has been difficult to model. In fact, a substantial amount of research is ongoing to better describe what is happening during cavitation in both homogeneous and heterogeneous systems. For the food industry this means not only that utilization of high-intensity ultrasound to conduct food chemistry has an extremely high potential to yield an unexpected number of new products and modified ingredients, but also that a clear understanding of the involved reaction chemistry is required to fully predict the outcome of the ultrasonically mediated reactions. Throughout the remainder of this chapter, we will attempt to provide an overview of some of the progress that has recently been made in sonochemistry with respect to food components and ingredients and to highlight some of the further research needs in this area.

3 Effect of Ultrasound on the Functional Properties of Food Ingredients

3.1 Engineering Protein Functionality by High-Intensity Ultrasound

3.1.1 Introduction

Proteins, an essential part of the human diet, are polymers of amino acids (Damodaran et al., 2005; Lehninger et al., 1993). With respect to foods, they are key functional ingredients that contribute to the stabilization of foams and emulsions, produce gels or increase the viscosity of food products, and modify the appearance and flavor of foods. As such, they are a key part of the toolbox of components used by food scientists to create foods with desirable sensory characteristics. The most important functional properties of proteins include solubility, surface activity, viscosity increase, and gelation and these are governed by their molecular characteristics such as molecular weight, chain flexibility conformation, amino acid polarity, and hydrophobicity. In proteins, these functional properties are thus a direct result of the type, number, and sequence of monomers of which the protein is comprised (Kinsella et al., 1989). These base amino acids have varying polarities (ionic, polar, non-polar, or amphiphilic), physical dimensions, and cross-molecular interactions, and they contain a number of reactive groups (Darby and Creighton, 1995). Based on the sequence of amino acids on the backbone, a so-called primary structure, secondary structure (alpha-helix, beta-sheet, random coil), tertiary structure (overall fold of the protein with loops and turns), or quaternary structure (complexes of several polypeptide subunit) may develop.

High-intensity ultrasound can lead to a modification of the structure of proteins via heterogeneous sonochemical pathways, and changes in protein functionality can thus be expected to occur after application of high-intensity ultrasound. Key functional properties affected by high-intensity ultrasound are discussed below.

3.1.2 Protein Solubility

The solubility of proteins is a function of the distribution of hydrophilic and hydrophobic amino acids present at the surface of the folded protein. While most hydrophobic patches can be found at the inside of the folded proteins, some are present at the surface of proteins. The higher the content of hydrophobic amino acids in a protein, the lower their solubility. In addition, amino acids present at the surface may carry a charge that contributes to the dissolution of the protein by preventing aggregation between protein molecules and subsequent precipitation. Ultrasound may interact with the protein macromolecule and alter the primary, secondary, tertiary, or quaternary structures of proteins, which could either increase or decrease protein solubility.

When the effects of high-intensity ultrasound (20 kHz, 15 min) on the thermophysical properties of whey protein isolate (WPI) and whey protein concentrate

(WPC) were investigated, researchers have found that treatment with ultrasound caused significant ($p < 0.05$) water solubility increases in WPC and WPI compared to control samples and that the effect was more pronounced in WPI (98.9/100 g) than in WPC (96.2/100 g) (Kresic et al., 2008). The authors suggested that protein solubility was improved due to a change in protein conformation and structure that allowed hydrophilic parts of amino acids previously buried inside the globular proteins to be exposed to the water phase (Morel et al., 2000). The authors further found that ultrasound treatment decreased protein molecular weight, and they concluded that a larger area of protein would thus be covered by water molecules. On the other hand, the decrease in molecular weight could be because peptide bonds were broken; the resulting peptide fragments may then have an improved solubility compared with the parent protein. Similarly, in a study by Jambrak and coauthors (Jambrak et al., 2008), solubility increased significantly for whey protein isolate (WPI) and whey protein hydrolysate (WPH) sonicated at 20, 40, and 500 kHz, but did not significantly increase for whey protein concentrate powder. The highest increase was found with a treatment with 20 and 40 kHz high-intensity ultrasound for 15 min, with WPI solubility increasing from 66.8 to 85% and 84% and WPH solubility increasing from 72.1 to 82% for 20 and 40 kHz, respectively. In this case, the authors suggested that changes in the three-dimensional structures of globular protein resulted in an increased number of charged groups (NH_4^+, COO^-), which was confirmed by the higher electrical conductivity of treated proteins compared to that of control samples.

Theoretically, ultrasound could also result in protein precipitation rather than in improved solubility if precipitating agents such as salts were present. In the presence of a precipitant such as salts, mass transport processes play an important role. Protein aggregates are formed if a precipitant (salt) and proteins are mixed, a process that may be affected by application of high-intensity ultrasound as the precipitant–protein target collision frequencies may be increased. Unfortunately, to date, the solubility of proteins after ultrasonication in the presence of salts has not yet been investigated.

3.1.3 Protein Interfacial Activity

The surface activity of proteins is one of the key functionalities that make them an excellent emulsifier. This essential functionality is derived from the amphiphilicity of proteins, i.e., the presence of both hydrophilic and hydrophobic amino acids. The major driving force for adsorption of proteins to oil–water interfaces is the hydrophobic effect. Hydrophobic patches on the protein preferentially interact with the dispersed oil phase, while hydrophilic amino acids prefer to interact with the solvent phase. When proteins are dispersed in an aqueous system containing dispersed oil phases, proteins will thus adsorb at the oil–water interface, then unfold and rearrange to optimize oil–hydrophobic amino acid interactions and water–hydrophilic amino acid interactions. Adsorption also reduces the contact area between the oil and water molecules at the oil–water interface, which reduces the interfacial tension. Ultrasound could potentially alter the number of hydrophilic and hydrophilic

amino acid patches that are present at the surface of folded proteins, thus altering the driving force for the adsorption process. Moreover, if tertiary or quaternary structures are lost due to application of high-intensity ultrasound, the protein may more rapidly assume new configurations at the interface, thus potentially accelerating the adsorption process.

Indeed, in a number of studies, it has been reported that the ultrasonic treatment of purified protein solutions may increase the surface activity of proteins at the solution–air interface under a range of experimental conditions (Gülseren et al., 2006; Güzey, 2002; Guzey et al., 2004, 2006; Weiss and Seshadri, 2001). For example, with increasing sonication time, the surface activity of bovine serum albumin (BSA) solutions was found to increase, whereas the operational mode (i.e., pulsed or continuous sonication) did not have a significant effect. While thermal processing is known to enhance surface activity, thermosonication increased the surface activity beyond that of a comparable thermal treatment, suggesting the formation of a non-native, molten-globular state that is profoundly different from a thermally denatured state. It was reported that both mobility and α-helix content of proteins increased (Güzey et al., 2006), which is contrary to the loss of structure that is generally reported when proteins are heat denatured. Sonication treatments increased both short- and long-term surface activities, as well as equilibrium surface pressures and diffusion coefficients of BSA (Fig. 10.1) (Güzey et al., 2006).

Similarly, the enhancement of surface activity by sonication was found to be independent of pH solution. The highest surface activity was observed around the pI of both native and sonicated BSA samples, i.e., pH 5 (Gülseren, 2004). Previously published studies similarly described that the surface excess concentration of BSA at the air–water interface increased (Lu and Su, 1999), the initial adsorption rate at a solid–solution interface (Elgersma et al., 1992) accelerated, and foaming activity (i.e., surface coverage at the air–water interface) (Yu and Damodaran, 1991) was maximal around the pH of the investigated proteins. For the short-term adsorption kinetics, samples adjusted to an acidic pH of 3 adsorbed to the interface and reduced the surface tension very rapidly, reaching an equilibrium shortly thereafter. Basic solutions had slightly higher diffusion coefficients calculated from the long-term adsorption kinetics solution, but were accompanied by higher equilibrium surface tension values (Gülseren, 2004).

3.1.4 Emulsion Stabilization

A great number of studies have been published on the ultrasonic preparation of protein and surfactant stabilized emulsions, including multiple-layered emulsions, o/w and w/o emulsions, and polymerized emulsions. In high-intensity ultrasound treatment of milk in combination with or without heat, the particle size of fat globules was reduced (Villamiel and de Jong, 2000). Production of proteinaceous microcapsules was achieved by high-intensity ultrasound and the oxidative environment generated by sonication (Suslick and Grinstaff, 1990). Ultrasound also reduced the particle diameters of primary and secondary emulsions and stabilized the system against creaming (Güzey, 2002). Thus, production of emulsions

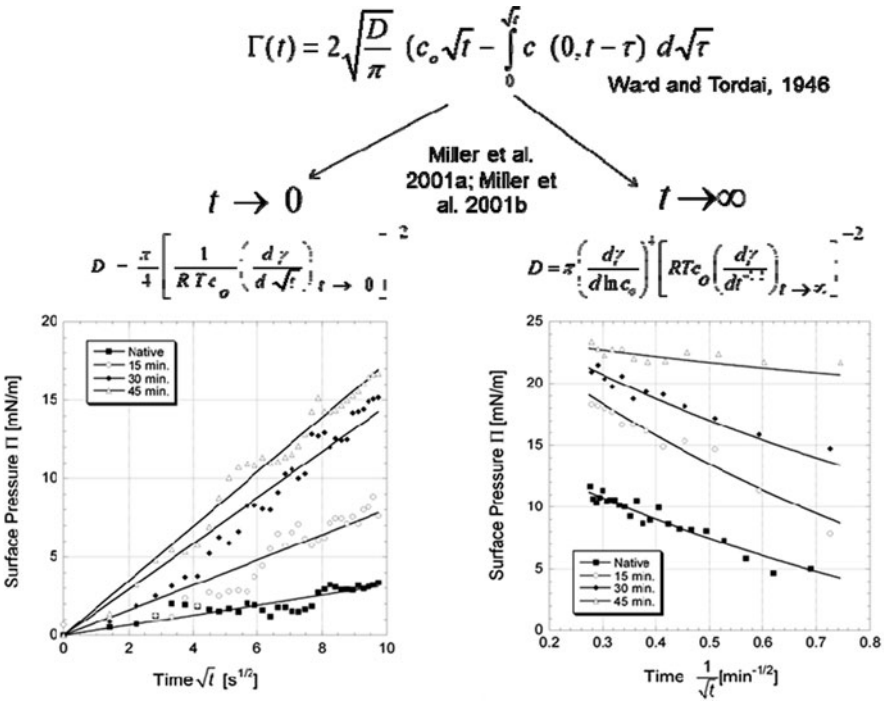

Fig. 10.1 Effect of ultrasonication on the surface activity of bovine serum albumin. This figure illustrates the recently derived solution by Miller and coauthors to solve Ward and Tordai's theoretical approach that models the adsorption kinetics of surface active species by considering only the initial adsorption process ($t \rightarrow 0$) and the completion of the adsorption process ($t \rightarrow \infty$), also known as the short-term and long-term adsorption behavior of surfactants. Both the long-term (*bottom right*) and short-term (*bottom left*) adsorption kinetics of proteins were significantly accelerated by the application of high-intensity ultrasound (Güzey et al., 2006)

by use of high-intensity ultrasound is well understood and is increasingly being used in the industry to design high-efficiency flow-through emulsification systems. Moreover, ultrasound has been shown to have a beneficial effect even after primary production of emulsions. For example, high-intensity ultrasound treatment reduced the degree of droplet flocculation in palm oil-in-water emulsions stabilized by 0.45 wt% β-lactoglobulin (β-Lg, 5 mM phosphate buffer) containing sodium alginate (< 0.5 wt%), thereby increasing creaming stability (Pongsawatmanit et al., 2006).

However, relatively little is known about the actual effect of high-intensity ultrasound on the ability of proteins to stabilize emulsions. Currently, most studies use ultrasound to produce the actual emulsion, and the observed beneficial effects may thus be predominantly derived from the mechanical and not the sonochemical action of high-intensity ultrasound. Unfortunately, information available on the structural changes of protein molecules in solution or adsorbed to the surface of emulsion

droplets during sonication is limited. In one study, the ability of native and sonicated WPI to stabilize a corn oil-in-water emulsion was investigated (Gülseren, 2004). The emulsification activity of the samples was assessed via determination of their ability to decrease the particle size of the emulsion during homogenization. Instead of applying high-intensity ultrasound to homogenize the emulsion, proteins were pretreated by high-intensity ultrasound and then used as emulsifiers with emulsions being produced by high-pressure homogenization. In this case, no significant changes in the particle-size distribution of emulsion droplets stabilized by sonicated WPI solutions compared to those stabilized by native WPI solutions were observed, leading to the conclusion that high-intensity ultrasound did not improve the emulsification ability of WPI (Gülseren, 2004). This finding was attributed to the fluid dynamic processes occurring during homogenization. The timescale for the droplet surface disruption in a high-pressure homogenizer is within the range of a few milliseconds. Thus, the increase in short-term surface activity previously described may not be high enough to cause any significant difference in the emulsification capacity. Moreover, according to Krause et al. (2000), under certain circumstances, resistance of proteins to denaturation can become at least as important as surface hydrophobicity in the emulsification capacity of proteins. In addition, as previously discussed, ultrasonication may lead to an increased solubility of proteins which may in turn have a beneficial influence of emulsion production and stability, as more protein may be solubilized in the solution and thus be available to stabilize the dispersed emulsion droplets.

3.1.5 Foam Stabilization

Recent investigations on the ultrasonic treatment of purified protein solutions have reported increased surface activity at the solution–air interface (Gülseren, 2004; Gülseren et al., 2006; Güzey, 2002; Guzey et al., 2004, 2006; Weiss and Seshadri, 2001). Potentially, the increased flexibility and surface activity might yield proteins that are better able to stabilize foams. A research group in the UK demonstrated that foam stability and bubble uniformity increased and bubble diameter decreased in whey protein concentrate (WPC) foams upon sonication (Lim and Barigou, 2005a, b). This finding suggests that high-intensity ultrasound might be used to improve the performance and quality of food foams. The group also reported that an increase in protein concentration allowed for production of foams with a better texture, but that the increased strength of protein films at the interface required use of higher ultrasonic wave amplitudes.

Interestingly, other researchers have used high-intensity ultrasound not to produce but to destroy foams. In these studies, non-proteinaceous materials such as polymeric liquids and surfactants in combination with high-intensity ultrasound were used to destabilize foams (Lim and Barigou, 2005a; Morey et al., 1999; Sandor and Stein, 1993). Similarly, in an investigation on the destruction of static foam composed of sodium lauryl sulfate (SLS) and water, Dedhia and coauthors reported that the ultrasonic vibrations generated by an ultrasonic horn produced surface waves leading to very high local drainage rates at the foam surface, thus

causing subsequent bubble collapse and the destruction of the foam (Dedhia et al., 2004).

3.1.6 Protein Thickening

Proteins may increase the viscosity of a solution, thereby modifying the texture and mouthfeel of food products, as well as reducing the rate by which particles in a multiphase dispersion sediment or cream, resulting in a more stable dispersion. An increase in the viscosity upon addition of proteins to a solution using high-intensity ultrasound could thus be of significant interest to the food industry. In the previously mentioned study by Kresic focusing on the investigation of the thermophysical properties of ultrasonicated whey protein solutions, changes in apparent viscosity were also measured (Kresic et al., 2008). When flow curves of sonicated whey protein concentrates and whey protein isolates were measured, significant increases in apparent viscosity (8.0 mPas) ($p < 0.05$) and significant changes in flow behavior indices and increases in consistency coefficients (0.152 for WPC and 0.186 for WPI) ($p < 0.05$) were found compared to controls. It has been suggested that flow behavior after ultrasound treatment is a consequence of changes in the binding capacity of water (Phillips and Williams, 1995), but changes in the viscosity may also be derived from alterations in the three-dimensional structure of proteins. In general, the effectiveness of protein in increasing the viscosity of a solution depends on its effective volume (Damodaran et al., 2005). In solution, the effective volume of proteins is much greater than simply the volume occupied by the atoms that make up the biopolymer chain, because it sweeps out a large volume of solvent as it rapidly rotates due to Brownian motion. Generally, the effective volume of a protein depends on its three-dimensional structure. Proteins that have a compact globular structure have an effective volume that is actually quite close to the actual volume of the molecule. However, as the protein unfolds and becomes less compact, the effective volume increases and, as a consequence, the viscosity increases (McClements, 2006).

3.1.7 Protein Gelation

Proteins are one of the major agents used in many foods to cause the aqueous phase to gel to form a wide class of soft solid foods such as yogurts, cheeses, desserts, eggs, and meat products (Damodaran, 1997; Kinsella et al., 1989; Mine et al., 2010; Sikorski, 2001; Whitaker et al., 1977). Protein gels are formed when individual protein molecules aggregate to form a three-dimensional network that contains a large volume of entrapped water. The aggregation can be driven by a number of different methods such as change in environmental conditions (pH, temperature, ionic strength, solvent composition) or by adding cross-linking agents such as enzymes or denaturants. Ultimately, the aggregation behavior of proteins, which is the foundation of gel formation, is governed by the underlying molecular structure of the proteins, which determines their interaction with the solvent and with other proteins. For example, proteins that contain a large number of hydrophobic amino

acids tend to associate via hydrophobic interactions, e.g., caseins or denatured whey proteins. On the other hand, proteins may also be gelled upon changes in the electrostatic interactions between proteins. For example, at pH values sufficiently far away from their isoelectric point, proteins may be prevented from gelling because of the strong electrostatic repulsion between the molecules; however, if the pH is adjusted to near the isoelectric point, or if salt is added, the proteins tend to aggregate and form a gel. Also, the addition of multivalent ions, such as Ca^{2+}, can promote gelation of charged biopolymer molecules by forming salt bridges between anionic groups on molecules or by forming salt bridges between negatively charged helical regions.

High-intensity ultrasonication may thus have the potential to alter the gelation behavior of proteins, since heterogeneous sonochemical modifications can lead to changes in the structure of proteins. For example, when the gelation behavior of ultrasonically pretreated whey protein isolates (WPI) was investigated (Weiss et al., 2000), ultrasonically pretreated proteins formed stronger acid-induced gels than untreated proteins (Fig. 10.2). The strength of the acid-induced protein gels was also influenced by the thermal pretreatment temperature. With higher pretreatment temperatures gel strength increased, but an additional increase in gel strength of thermosonicated proteins compared to only thermally treated proteins was observed. The ability of proteins to form a strong gel increased with increasing amplitude of the ultrasonic wave and duration of the sonication treatment (Weiss et al., 2000). In another study, fermentation of manothermosonicated milk formed firmer yoghurt samples with high viscosity and consistency (Vercet et al., 2002). Similar results were presented by Wu et al. (2001), but unlike Vercet et al. a shorter fermentation time was suggested for sonicated samples. On the other hand, in a more recent study by Sánchez-Gimeno and coauthors, the use of manothermosonication, which is a combination process of pressure, heat, and sonication, the gelation of ovalbumin was studied (Sánchez-Gimeno et al., 2006). Here, surprisingly, the manothermosonication treatment reduced G' values of the obtained ovalbumin gels by about 50% when measured immediately after the gelation was induced. When the gel strength was again measured after 24 h of storage, the elastic moduli of heat treated and thermosonicated gels were not significantly different, indicating that gels over 24 h had set to about the same gel strength, albeit that the manothermosonicated gels appeared to take longer to reach final gel strength. The authors hypothesize that manothermosonication may have led to a partial unfolding of the protein rather than a full denaturation.

3.1.8 Enzyme Activity

A number of proteins display strong catalytic activities that play an important role in food processing and food systems. These enzymes may either be used to catalyze reactions relevant to the food industry, in which case their presence is highly beneficial, or catalyze reactions that can result in a loss of quality in food products, in which case their presence is harmful. Ultrasound has been used both to improve and to degrade the catalytic activity of enzymes. While this seems initially like a

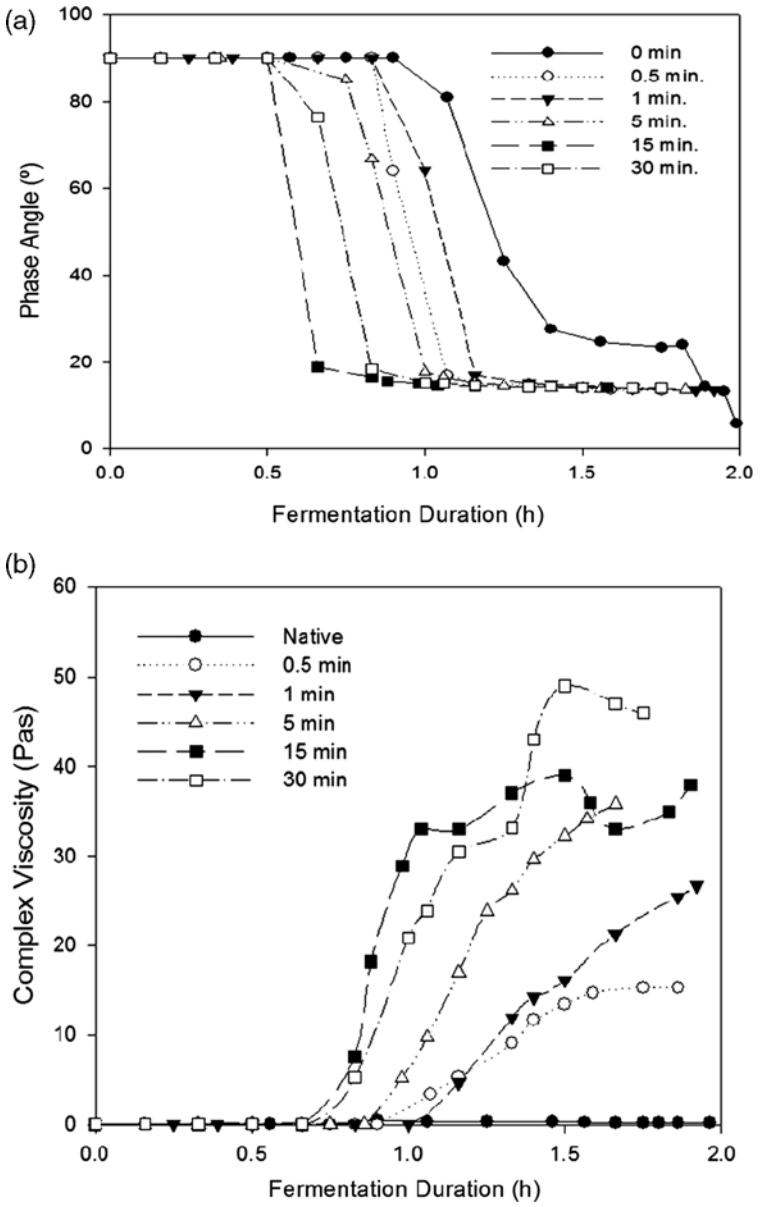

Fig. 10.2 Effect of ultrasonication on the acid-induced gelation of whey protein isolate (WPI). (**a**) The decrease in the phase angle from 90 to <10° is indicative of a transition from a liquid to a solid (sol–gel transition) and is accelerated by the pretreatment of proteins by high-intensity ultrasound. (**b**) The complex viscosity suggests an overall increase in the strength of the developing gel with increasing sonication time (Weiss et al., 2000)

contradiction, it highlights the complexity of the processes involved in the treatment of functional food ingredients with ultrasound. These two distinctly different results may be obtained by varying the ultrasonic intensity, duration of the treatment, treatment temperature, and ultrasonic frequencies. Since many studies vary in their processing conditions, it is thus not surprising that the reported effect of high-intensity ultrasound on the activity of enzymes varies.

For example, at low ultrasonic energy levels (0.27–0.85 W cm^{-2}), the activity of invertase increased with sonication intensity regardless of whether pH orsubstrate inhibition was suppressed (Sakakiabra et al., 1996). Both the release and activity of invertase from *Aspergillus niger* were shown to increase under ultrasonication using moderate intensities (Vargas et al., 2004). More recently, low-intensity ultrasound was found to stimulate the efficiency of biological phosphorus removal. When phosphorus content and dehydrogenase activity were measured as indicators of the efficiency of the reaction, low-intensity ultrasound stimulation was found to increase release of phosphorus by more than 70% in comparison with the control under anaerobic condition and to reduce TP concentration in the effluent to less than 50% of the control (Xie et al., 2008). Ultrasonication was also found to enhance the degree of lipase-catalyzed soy oil hydrolysis in a solvent-free system, and under optimum conditions the overall hydrolysis reaction rate in the ultrasonic bath was about twice as high as that in a shaking bath (Liu et al., 2008). The authors reported that sonication appeared to cause no essential damage to lipase activity. Mason et al. (Mason and Cordmas, 1996; Mason et al., 1996) briefly reviewed the increased activity of immobilized enzymes, namely chymotrypsin and amylase, during sonication. Immobilization of enzymes is a natural phenomenon observed in soil. Sonication was shown to be useful in mobilizing and dispersing acid phosphatase in soil samples, which increases the reproducibility of enzyme assays in soil samples (De Cesare et al., 2000). Finally, for a variety of glycosidases, ultrasound accelerated starch hydrolysis (Barton et al., 1996). The authors suggested that the disruption of molecular clusters and the homogeneity generated by ultrasonic mixing were at the cause of the improved hydrolysis.

Conversely, manothermosonication of pectic materials decreased the activity of pectin methylesterase (PME), whereas polygalacturonase (PG) remained fully active. The authors were able to conclude that the observed decreases in activity were attributed to the effects of sonication (thermal, chemical, and mechanical effects of cavitation) rather than the application of pressure. Ultrasonically treated tomato products were found to be more stable due to inactivation of enzymes, thereby improving the rheological properties of the tomato products (Vercet et al., 2002).

In another study, increasing treatment time and cavitation intensity also resulted in loss of pectin methylesterase (PME) activity. A synergism with temperature was reported as higher thermosonication temperatures led to significantly decreased enzyme activities compared to thermally or ultrasonically treated enzymes (Raviyan et al., 2005). Among a variety of purified and buffered enzyme solutions, only alkaline phosphatase remained fully stable and active upon ultrasonication, whereas all other microbial and mammalian enzymes underwent some inactivation depending

on the ultrasonic processing conditions (Özbek and Ü.K.Ö., 2000). During manothermosonication of peroxidases, heat and sonication were found to act synergistically toward the inactivation of the enzymes almost independent of pH (Lopez and Burgos, 1995). The authors hypothesized that the inactivation mechanism could be due to the splitting of the heme group from the apoenzyme.

3.1.9 Structural Basis of Observed Modifications of Protein Functionalities

The above effects of high-intensity ultrasound on the functional properties of proteins suggest that the underlying mechanisms are quite complex. In an effort to elucidate the possible nature of a distinct ultrasonically induced structural state of proteins, a series of structural investigations on BSA were carried out (Gülseren et al., 2006). To this purpose, BSA was subjected to high-intensity ultrasound and characterized by a variety of physicochemical techniques. For example, the thermal denaturation temperature of BSA was not affected by application of high-intensity ultrasound, but a slight reduction in thermal denaturation enthalpy was observed; the results were quite different from those obtained from proteins that were thermally treated. Minimal changes were observed in the global structure of BSA, but surface charge increased, particularly at basic pH values (e.g., pH > 9). Surface charge of proteins increased on both sides of the BSA isoelectric point, but the extent of the increase in sonicated proteins was higher compared to that in native proteins. Dynamic light scattering measurements indicated that the particle size of BSA increased up to 3.4 times after 90 min of sonication, but no change in the oligomeric state of BSA was observed when analyzed by blue native PAGE analysis. In addition, the amount of free sulfhydryl groups in BSA decreased after sonication where the extent of the reduction was proportional to the sonication time (Fig. 10.3). The increased particle size and decreased number of free sulfhydryl groups suggest that protein aggregates may have been formed, possibly due to an increased exposure of functional groups previously buried in the core of the globular protein. Circular dichroism (CD) spectroscopy and FTIR analysis indicated changes in the secondary structure of BSA. In addition, surface hydrophobicity and surface charges increased, while free sulfhydryl content decreased (Gülseren, 2004).

Taken together, these measurements suggest that structural changes lie at the basis of the observed functional alterations. In the case of BSA, the various physicochemical property changes suggest a molten-globular state where some of the structure of the native protein is lost, but not to the degree that would be typically encountered had the protein been completely denatured (Gülseren et al., 2006). Clearly, the degree of structural changes in proteins upon sonication depends on the nature of the protein, the ultrasonic wave amplitude, sonication time, and environmental conditions such as pH, temperature, and ionic strength, as well as solvent type. For example, when the effect of ultrasound on the surface activity and structure of a variety of proteins was determined (Güzey, 2002), very different results were obtained for the different proteins. Ultrasound increased the rate of adsorption for all investigated proteins including BSA, fatty acid-free BSA, β-lactoglobulin, and lysozyme, but the degree of the susceptibility of proteins varied substantially.

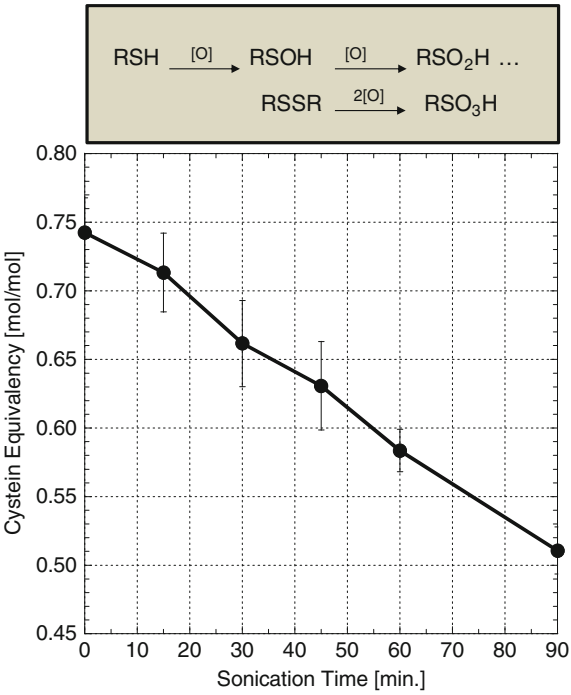

Fig. 10.3 Loss of free sulfhydryl groups in bovine serum albumin with increasing sonication time, which may be indicative of an oxidation of the thiol group, leading to the production of a number of new reactive species (Gülseren, 2004)

Lysozyme, a relatively compact and rigid protein, was interestingly the protein most sensitive to ultrasound, followed by BSA, fatty acid-free BSA, and β-lactoglobulin (Güzey, 2002).

Finally it should be noted that while much progress has been made regarding the functional changes that occur in proteins upon ultrasonication, there is still a lack of information as to the underlying reaction mechanism. It has been assumed that most of the effects are due to the mechanical rather than the sonochemical effects of high-intensity ultrasound. However, the above-described studies suggest that sonochemistry may play a more important role than previously thought (Fig. 10.4). The loss of free sulfhydryl groups could be an indication that radicals that are generated due to the cavitation may react with functional amino acids, effectively oxidizing the proteins. Proteins that are high in thiols may thus show some quite complex sulfur chemistry that should warrant closer investigation. In general, an increased focus on chemical and not only structural modifications of proteins under the influence of high-intensity ultrasound may be required. A breakage of the peptide bond in proteins is difficult, but not impossible, depending on the volume-specific ultrasonic energy that is introduced into the system. Oxidation of proteins is clearly a possibility and may have dramatic effects, not only on the functional properties described above, but also on the flavor of ultrasonicated protein-containing foods.

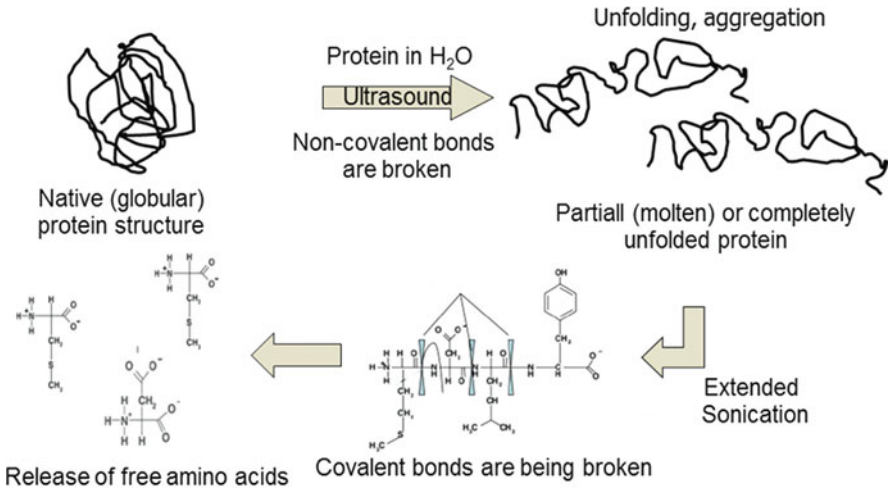

Fig. 10.4 Schematic illustration of the effect of high intensity on the chemical integrity of proteins. At low ultrasonic intensities, changes to secondary and tertiary structures may occur, leading to partial unfolding and formation of aggregates. At larger ultrasonic intensities, peptide bonds may be broken and free amino acids released

3.2 Engineering Polysaccharide Functionality by High-Intensity Ultrasound

3.2.1 Introduction

Polysaccharides are another class of important functional ingredients that are used to modify the appearance, texture, and flavor of foods. Polysaccharides, extracted predominantly from plants, albeit they are also present in animal tissues, typically vary in their molecular weight and structure even within a single type and class of polysaccharides. Their structure is generally linear, although random coil structures or ordered helices can be found under certain solvent conditions. Compared to proteins, polysaccharides are stiffer and more rigid, which have important implications for their functional properties such as ability to form gels or thicken solutions. They sweep out more volume than proteins of comparable molecular weight and thus increase their viscosity more dramatically than proteins. This explains why polysaccharides are probably some of the most commonly used texture modifiers in the food industry.

The differences in the mechanical and structural properties of polysaccharides also lead to distinctly different effects of ultrasonication on their functionalities. Most of the available literature has focused on the use of high-intensity ultrasound to improve the extraction of polysaccharides from plant or animal tissues. However, ultrasound may have significant potential to alter the functionality of polysaccharides via heterogeneous sonochemical pathways. For example, polysaccharides subjected to high-intensity ultrasound can undergo a large number of sonochemical

reactions including glycosylation, acetalyzation, oxidation, C–D, C-heteroatom, and C–C bond formations (Kardos and Luche, 2001). We have previously discussed that one of the most important results of application of high-intensity ultrasound in heterogeneous systems containing macromolecules can be the chain splitting of polymers, and similar effects may be observed when sonicating polysaccharide solutions with dramatic impacts on their functionalities (Figs. 10.5 and 10.6). These observed changes may be beneficial or detrimental with respect to a particular functionality. For example, the digestibility of a polysaccharide could be improved, while the ability of the same polysaccharide to thicken a solution could be decreased. On the other hand, many linear carbohydrates in the absence of branching have the ability to form crystalline structures that are difficult to dissolve, and the development of new technologies that can bring these compounds into solution remains a high priority. In this section, we will provide an overview of the current state of the knowledge with respect to alterations in the functional properties of polysaccharides upon ultrasonication. Additional information may be found in an excellent review article on the subject of sonochemistry of carbohydrate compounds (Kardos and Luche, 2001). Readers interested in the effect of ultrasonication on the extraction of polysaccharides may find more information in other chapters in this or other books that are dedicated to discussing the use of ultrasound during extraction (Weiss et al., 2011).

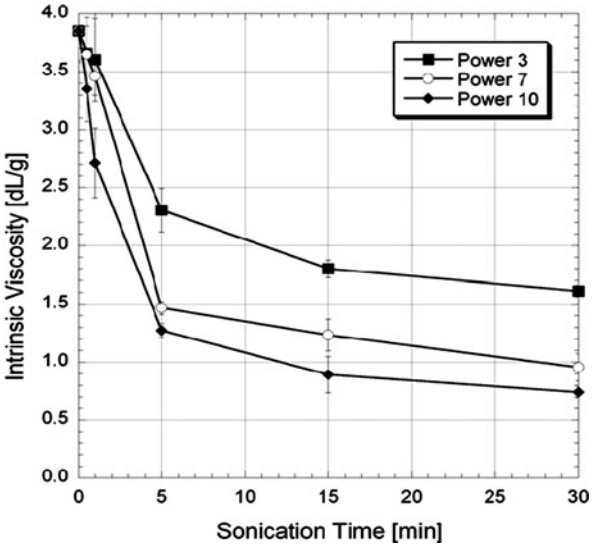

Fig. 10.5 Decrease in intrinsic viscosity of chitosan solutions upon continued ultrasonication at three different ultrasonic intensities. Results illustrate that molecular weights tend to approach a limiting intrinsic viscosity value, which may correspond to a molecular weight below which the application of high-intensity ultrasound does not lead to further scission of the backbone (Baxter et al., 2005)

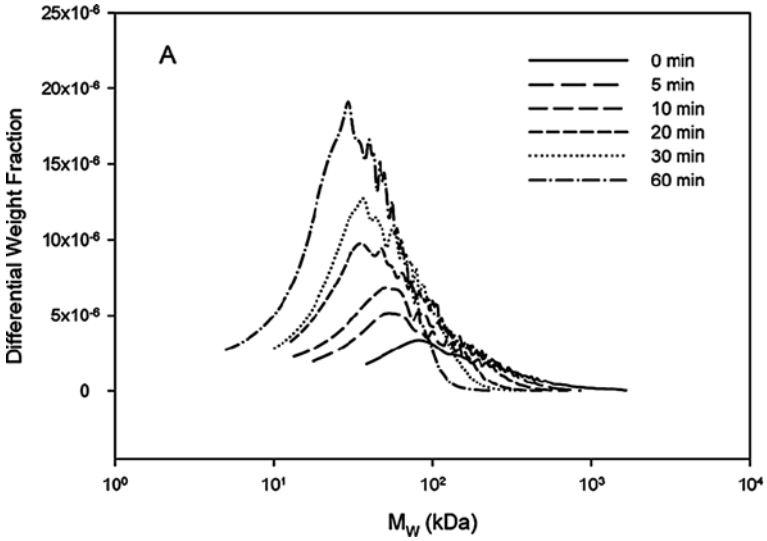

Fig. 10.6 Changes in molecular weight distribution of ultrasonicated chitosan solutions. The results demonstrate that not only does the average molecular weight decrease, but also the width of the distribution decreases, yielding a more uniform chitosan preparation in terms of distribution of their molecular weights (Wu et al., 2008)

3.2.2 Solubility

Many polysaccharides are insoluble in water and need to be digested by hydrolysis to produce water-soluble smaller fragments. Other polysaccharides may form molecular dispersions upon addition to an aqueous phase. As such, the interaction of water with polysaccharides and vice versa is complex, and a description of the ongoing processes is even more complex if other compounds are added that can compete with polysaccharides for hydrogen-bonding sites (e.g., salts). Ultrasound may alter the solubility of polysaccharides either by aiding in the dispersion of the polysaccharides by improving fluid dynamics and disrupting crystalline structures or by improving the hydrolysis of polysaccharides in the presence of acids or in the presence of catalyzing enzymes. As previously discussed, high-intensity ultrasound can directly result in reduction of molecular weight of polysaccharides even in the absence of a hydrolyzing agent such as acid.

For example, hydrolysis of pectin from plant cell walls and their solubilization at a low pH and high temperature was greatly improved upon sonication (El-Nawawi and Shehata, 1987; Kertesz, 1951). Low-molecular weight dextrans, of great importance in the medical industry for applications such as blood plasma extenders and as a starting material for dextran sulfate (Alsop, 1993; DeBelder, 1993; Goto et al., 2004), can be generated not only by partial acid hydrolysis (Alsop, 1993) and enzymolysis (Corman and Tsuchiya, 1957) but also by ultrasonication (Lorimer et al., 1995). Sonication of starch led to formation of shorter chain molecules and reducing sugars (Tomasik and Zaranyika, 1995) with higher solubilities. Similar results have

been observed for rayon and hydroxyalkyl cellulose derivatives (Malhotra, 1982b). A variety of other reactions that involve production of carbohydrate oligomers from sonolytically produced fragments have been reported (Fuchs and Heusinger, 1994; Heusinger, 1990). Depolymerization of xyloglucan by ultrasound at a frequency of 20 kHz yielded products with average molecular weights of about 13,100 Da after 120 min without significant alteration of their primary structure (Vodenicarová et al., 2006).

3.2.3 Polysaccharide Reactivity

Polysaccharide reactivity is governed by the distribution and number of functional groups attached to the polymerized sugar units that form the backbone of the polysaccharide. Modification of these side groups may thus influence the reactivity of the polymers. We previously mentioned that conditions in the cavitational bubbles may lead to production of $H^{\bullet}$, $OH^{\bullet}$, and nitrogen oxides (NO_x) (Lohse and Hilgenfeldt, 1997). $OH^{\bullet}$ can react readily with organic compounds or recombine to H_2O_2, while NO_x will react with water yielding nitrate and nitrate ions (Mead et al., 1976). $H^{\bullet}$ and $OH^{\bullet}$ radicals in aqueous solution react with carbohydrates by abstracting a H-atom from their carbon (Heusinger, 1990). In small saccharides such as monosaccarides (e.g., D-glucose) and disaccharides, the attack occurs almost at random at various positions, although a slight preference for attack at the C_1–H and the C_6–H has been noted (Heusinger, 1991). Interestingly and conversely to the degradation of larger macromolecules by high intensity, in presence of oxygen, polymers in the molecular weight range of 4,000 Da could be produced from ultrasonication of smaller saccharides (Snell, 1965).

In a series of studies, we recently investigated the ability of high-intensity ultrasound to modify side groups of polysaccharides to improve both their solubility and their reactivity. As a model polysaccharide, chitin, one of the most abundant polysaccharides on earth, was chosen. While chitin is water and acid insoluble, it can be converted into acid-soluble chitosan or water-soluble glucosamine by alkaline-catalyzed deacetylation, a process that typically requires long processing times and high solvent concentrations (e.g., 50% NaOH). Moreover, while chitin is an uncharged polymer, chitosan is positively charged, which is the basis of its high antimicrobial activities and its ability to bind free fatty acids. Under alkaline conditions, chitosan may also bind heavy metals. As such, chitosan has become of great interest to a variety of industries, including the pharmaceutical, cosmetics, and food industries. In our studies, we used high-intensity ultrasound to accelerate the conversion of chitin to chitosan (Fig. 10.7). For samples sonicated at 25, 44, and 65 W cm^{-2}, filter yield decreased significantly, i.e., at an ultrasonic intensity of 65 W cm^{-2}, filterable solids decreased from 81.9 wt% to 67.6 wt% (based on initial mass) for untreated samples after 160 min of deacetylation in 45 wt% NaOH, which was attributed to increased solubility of ultrasonically deacetylated chitosan and additional loss of protein. Chitin yield upon subsequent suspension of ultrasonically treated crustacean flakes in 45% NaOH for 160 min decreased from 73.2 to 70.7% and from 74.9 to 60.2% after 15 and 30 min sonication at 90°C,

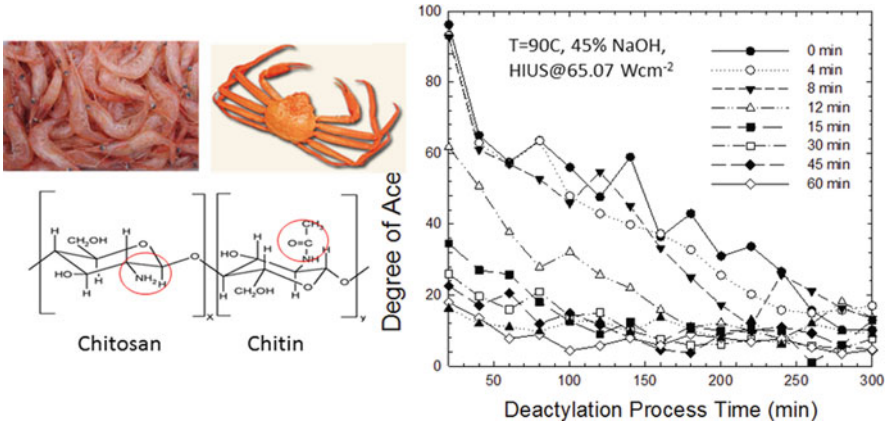

Fig. 10.7 Deacetylation of chitin by pretreatment of high-intensity ultrasound in 0.25 M NaOH. The results demonstrate the dramatic acceleration of the subsequent deacetylation on 45% NaOH, with chitin pretreated for 60 min reaching a final degree of acetylation of <10% in less than 100 min

respectively. At 28°C, yield decreased from 81.2 to 69.2% and 74.9 to 60.2% for 15 and 30 min sonication, respectively. DDA of samples increased after pretreatment with ultrasound in 0.25 M NaOH; i.e., DDA of samples sonicated at 60°C increased from 8.8 to 9.3, 19.7 and 26.1% for 0, 5, 15 and 30 min of sonication, respectively. Suspension in 45% NaOH led to further deacetylation at increased rates. For example, DDA of non-sonicated samples increased from 7.8 to 42.5% and 63.6% after suspension in NaOH for 60 and 160 min, respectively, but increased from 17.3 to 83.7% and 87.7% after 15 min of sonication at 28°C. The amount of proteins liberated increased from 0.17 to 7.18 and 43.79 mg/g after sonication with 25, 44, and 65 W cm^{-2} for 30 min, respectively, suggesting additional removal of contaminating proteins after sonication. FTIR scans showed only slight increases in chitin DDA after HIU pretreatment. However, during the subsequent deacetylation treatment, HIU accelerated removal of acetyl groups, e.g., after 60 min of deacetylation following the application of ultrasound for 15 min at 44 and 64 W cm^{-2}, the DDA increased to 63.6 and 84.1%. Efficiency of HIU to accelerate the reaction decreased with increasing temperature and few improvements in the reaction kinetics were found at 90°C. These results indicate significant reductions in time of deacetylation upon application of high-intensity ultrasound, but reaction temperatures need to be carefully controlled since decreases in efficiency and increases in yield losses at higher temperatures were observed. A brief pretreatment with HIU, however, was able to dramatically reduce the time required for chitin to chitosan conversion.

The above-described study represents just one example of the promising use of high-intensity ultrasound to modify the side groups of polysaccharides to alter the reactivity and functionality of the molecule. Another reaction modification by high-intensity ultrasound such as glycosylation, which is a particular case of acetalization, has been demonstrated for O-unprotected aldoses (D-glucose, D-galactose,

and D-mannose) and D-fructose in THF or 1,4-dioxane using anhydrous $FeCl_3$ as a promoter (Ferrières et al., 1995).

3.2.4 Thickening

Many polysaccharides are excellent thickeners. This is because they are linear molecules that sweep out large volumes of water due to their Brownian motion. In a first approximation, the viscosity of a suspension of hydrated biopolymer molecules rotating in solution can be described using a modification of a semi-empirical equation developed initially by Lui and Masliya (McClements, 2000)

$$\frac{\eta}{\eta_1} \approx \left(1 - \frac{\phi_{\text{eff}}}{P}\right)^{-[\eta]P} \approx \left(1 - \frac{R_V c}{P\rho}\right)^{-[\eta]P} \tag{10.21}$$

where ϕ_{eff} is the effective volume fraction of the biopolymer molecules in solution ($= \phi R_V$), ϕ is the actual volume fraction occupied by the biopolymer chains ($= c/\rho$), c is the polysaccharide concentration, ρ is the density of the polysaccharide chains, which is approximately 1,600 kg m^{-3}, and P is a packing parameter which has been determined experimentally as $P = 0.57$ at low shear stresses and $P = 0.68$ at high shear stresses (Rahman, 1995). The volume ratio R_V describes the ratio between the actual volume of the biopolymer in solution and the volume that is swept out (the effective volume), e.g.,

$$R_V = \frac{V_E}{V_A} \approx \frac{4\pi r_g^3 \rho N_A}{3M} \tag{10.22}$$

where V_E is the "effective" volume of the biopolymer molecule in solution, V_A is the actual volume occupied by the biopolymer chain, r_g is the radius of gyration of the molecule, ρ is the density of the biopolymer chain, N_A is Avagadro's number, and M is the molecular weight of the biopolymer. For rigid molecules, R_v can be approximated as

$$R_V \approx \frac{\pi n^3 l^3 \rho N_A}{6M} \tag{10.23}$$

where M_0 is the molecular weight of a monomer segment and $n = M/M_0$ while for random coil biopolymers, R_v can be described as

$$R_V \approx \frac{\pi n^{3/2} l^3 \rho N_A}{6M} \tag{10.24}$$

As can be seen from equations (10.22), (10.23), and (10.24), the viscosity of the solution thus increases with increasing effective volume of the polysaccharide chains, which increases with increasing molecular weight of the polysaccharide. This explains why application of high-intensity ultrasound can decrease the viscosity of many polysaccharide solutions, since cleavage of the backbone may readily

result in a decrease in the molecular weight of ultrasonically treated polysaccharides. For example, measurements of the apparent viscosity of sonicated chitosan solutions as a function of ultrasonic power level and treatment time showed significant decreases in viscosity with treatment time until a constant viscosity was reached (Baxter et al., 2005), which was directly attributed to a reduction in the average molecular weight of the treated chitosan (Figs. 10.5 and 10.6).

During cavitation, the exerted shear stresses in the vicinity of the collapsing bubbles are large enough to cause uncoiling and stretching of polymer molecules. Not surprisingly, larger carbohydrates are more susceptible to high-intensity ultrasound, and below a minimal molecular weight polysaccharides are no longer susceptible to the chain scission process. Moreover, there are differences with respect to the influence of the molecular weight reduction on solution viscosity depending on whether the polysaccharides have a stiff linear or random coil configuration. More importantly though, the nature of the carbohydrates, that is their molecular structure and flexibility, has shown to be the primary factor that influences their susceptibility to ultrasonic degradation processes (Ram and Kadim, 1970). Flexible chain polysaccharides are not only subject to smaller decreases in viscosity upon reductions in molecular weight, but the chains themselves are less susceptible to decreases in molecular weight upon ultrasonication. For example, carbohydrates are more readily degraded as the shear rate (a function of the extent of cavitation) increases (Moore and Parts, 1968). Thus, increasing ultrasonic power levels decreases the average molecular weights of carbohydrates. Similarly, degradation efficiency decreases with increasing frequency since cavities collapse less violently.

In addition to changes in viscosity, the flow behavior of polysaccharide solutions may be altered. Dispersions of polysaccharides can be characterized by a power law viscosity relationship

$$\tau = K\gamma^n \tag{10.25}$$

where τ is the shear stress (Pa), γ is the shear rate (s^{-1}), n is the flow behavior index, and K is the consistency index (Pas^n). A value of $n = 1$ indicates Newtonian flow behavior. Generally, polysaccharide dispersions have a value of $n<1$ indicating a shear thinning behavior that is the apparent viscosity decreases with increasing shear rate. In contrast, shear thickening, that is, the increase in apparent viscosity with shear rate, is only observed at very high and within certain polysaccharide concentration regimes. The shear thinning behavior of many polysaccharide solutions is due to overlap and entanglement of the polymers which is governed by the molecular characteristics of the polysaccharides, i.e., molecular conformation and weight. Upon application of shear, the polymers are increasingly disentangled and orient themselves in the flow field to become less resistant to the superimposed flow. For example, when the flow index n of sonicated solutions of chitosan in acetic acid was determined from measurements of the flow curve, n was found to increase from 0.75 for untreated solutions to 0.99 for ultrasonically treated solutions (Baxter et al., 2005). Ultrasonication may influence the flow behavior of polysaccharide solutions by reducing the molecular weight of the polysaccharides, altering their molecular

conformation and/or disrupting entangled structures. In chemical processes where polysaccharides are used as reactants, entanglement can be a major hurdle to the reaction, and application of ultrasound during the reaction has consequently been found to improve the reaction (Bestul, 1954).

3.2.5 Gelation

High-intensity ultrasound typically has a negative effect on the ability of polysaccharides to form a gel. This is because molecular weight is a key parameter in the formation of gels and polysaccharides, with high-molecular weight carbohydrates forming stronger gels at lower polysaccharide concentration. As previously discussed, ultrasound may at sufficiently high wave amplitudes result in a cleavage of polysaccharide chains, thus reducing their average molecular weight and weakening gels. For example, Seshadri and coauthors (Seshadri et al., 2002) reported that ultrasonication of high methoxyl pectin dispersions prior to addition of acid and sugar to induce gelation leads to weaker gels in proportion with increased sonication power and time. When a power law model was fitted to the viscosities of the treated pectin solutions in the absence of added gelling agents such as sugar or acid, the flow index of the dispersion increased from approximately 0.7–1.0, indicating that dispersions become increasingly Newtonian in their flow behavior (Seshadri et al., 2002). Interestingly, at intermediate sonication intensities, pectin gels could still be formed, although it took more than 24 h for the setting of the gel to complete. The ultrasonically treated gel, however, was much less turbid, which may be of interest to food manufacturers trying to optimize the appearance of pectin gels. In a study by Cote and Willet (1999), the influence of ultrasonication (at 20 kHz and 1.5 MHz), jet cooking with high-pressure steam, and twin screw extrusion under various condition was measured by size exclusion chromatography and rheology. Although all methods reduced the molecular weight and viscosity of dextran, the greatest degree of depolymerization was achieved when dispersions were treated with 20 kHz ultrasound.

On the other hand, the ability of polysaccharides to form gels may not be impacted by high-intensity ultrasound if ultrasound is used as part of the extraction procedure rather than as a post-extraction treatment. For example, Hromadkova showed that polysaccharides extracted from insoluble residues of sage via a combination of hot NaOH extraction combined with high-intensity ultrasound were able to form strong gels. (Hromadkova et al., 1999). Similarly, Panchev and coauthors reported that intermittent sonication of apple pomace at 1–1.2 W cm^{-2} increased the yield of pectin samples by 28% when compared to the standard extraction procedure (Panchev et al., 1994), but did not affect the strength of their gels.

3.2.6 Digestibility

The reduction in molecular weight and subsequent viscosity decrease may, however, be an advantage in the case of indigestible fibers. Here, increases in viscosity may be undesirable in food formulations where high fiber concentrations are desirable

while maintaining a low viscosity. Depolymerization of fibers by high-intensity ultrasound could thus maintain the non-digestibility of the fiber while improving functional behavior in food products. On the other hand, in the presence of appropriate reactants, conversion of a non-digestible product to a more digestible product may be feasible. For example, Choi reported that sulfuric acid-catalyzed hydrolysis of ultrasonically treated starch at a moderate temperatures range (90–100°C) and in dilute sulfuric acid was significantly faster than in untreated starch (Choi and Kim, 1994). Here, depolymerization may improve subsequent acid-catalyzed or enzyme-catalyzed degradation of the polymers.

3.2.7 Immunology

Polysaccharide fractions of plant cells of herbal origin have been extensively used by the pharmaceutical industry due to their pharmacological activity, and application of high-intensity ultrasound has been reported to influence this activity (Rice, 1995). For example, Ebringerova and coauthors, when studying the structure/function relationship of two acidic heteroxylan types, 4-*O*-methylglucuronoxylans (GXs) from beech wood and arabino-(glucurono) xylan from corn cobs, found that ultrasonication resulted in a decrease of GX immunomodulatory activity (Ebringerova et al., 2002). Clearly, more investigation is needed to further investigate the effect of sonochemical modifications on the pharmacological activity of bioactive polysaccharides.

3.3 Lipids

3.3.1 Introduction

The last functional ingredients discussed in this chapter are food lipids. Lipids have been defined as compounds that are "...generally soluble in organic solvents and largely insoluble in water" (Akoh and Min, 2002). Lipids constitute a relatively large class of compounds that vary in their molecular structures and include compounds such as fatty acyls (including fatty acids), glycerolipids, glycerophospholipids, sphingolipids, sterol and prenol lipids, and saccharolipids. Of these, triacylglycerols (TAG) are probably the most commonly used lipids in food systems. Depending on whether lipids are liquid or solid at room temperature, they are by convention referred to as oil or fat, respectively, although these terms are often used interchangeably (Damodaran et al., 2005).

Dietary fats and oils influence the nutritional, organoleptic, and physicochemical properties of foods in a variety of ways. First, they are a major source of energy and are essential nutrients in the human diet. While essential components, overconsumption of certain types of lipid (cholesterol, saturated fat, trans fatty acids) has been linked to a number of chronic diseases such as obesity, cardiovascular disease, diabetes, and cancer (Smolin and Grosvenor, 1994). On the other hand, many bioactive compounds of which consumption appears to promote good health

are lipids, e.g., ω-3 fatty acids, conjugated linolenic acid, phytosterols, carotenoids, and others. Second, lipids serve as major texture and flavor modifiers. Addition of lipids in the form of emulsion droplets increases the creaminess and smoothness of foods. Lipids also serve as carriers to lipid soluble flavors in many food products. Finally, the presence of lipids on the form of emulsion droplets may influence the appearance and rheology of a food product. If the oil droplet concentrations are increased to above 75–80 v/v/%, the food product becomes viscoelastic and attains weak gel-like properties. Addition of lipids in the form of oil droplets with mean droplet diameters above 100 nm also contributes to increased scattering of light, which gives the food a turbid, milky white appearance.

To date, surprisingly little attention has been paid to the influence of ultrasonication on the functionality of lipids, but theoretically, based on the susceptibility of lipids to radical-driven degradations that could influence all of the above-mentioned functional properties, the sonochemical effects of high-intensity ultrasound could lead to dramatic changes in both functionality and chemical integrity of lipids. The absence of more research studies is in particular stunning since high-intensity ultrasound is often used to disperse lipids and to produce emulsions. Reviewed below are a few key functionalities of lipids that may be influenced by ultrasonication.

3.3.2 Lipid Crystallization

The transition from a crystallized solid to a liquid and vice versa is one of the most important functionalities of lipids (Garti, 1982). Lipid crystallization occurs when conditions change so that the free energy of the solid phase of the lipids is lower than the free energy of the corresponding existing liquid lipid. In systems where no initial seeds are present crystallization proceeds homogeneously, requiring larger degrees of supercooling, while in systems where initial seeds are present, e.g., due to impurities or localized mechanical disturbances, crystallization proceeds heterogeneously. In almost all liquid bulk lipids some impurities in the melt will act as the starting point for nucleation before a degree of supercooling can be reached where new nuclei would be formed by homogeneous nucleation. Therefore, crystallization of food lipids occurs mostly by heterogeneous nucleation.

High-intensity ultrasound may influence lipid crystallization in a number of ways. First, it may improve the process of nucleation, that is, the step where crystal nuclei are formed, which requires molecules later forming the nuclei to gather into clusters that become stable under the given environmental system conditions. If the clusters are not stable, i.e., if their size has not increased to a critical minimum size, they may redissolve rather than forming stable nuclei. The induction of fluid flow, localized turbulences, and cavitation via ultrasound may lead to a reduction in the degree of supercooling, that is, required to induce the formation of crystals, which subsequently may accelerate the kinetics of the crystallization process. The ability of high-intensity ultrasound to enhanced crystallization (sonocrystallization) was reported as early as 1927, when ultrasound was applied to induce crystallization in a supersaturated thiosulfate solution (Abramov, 1998). Crystallization of palm oil upon cooling was greatly accelerated when high-intensity ultrasound above a critical threshold intensity level was used (Patrick et al., 2004).

Second, high-intensity ultrasound may affect the process of crystal growth which is the subsequent growth of stable nuclei, e.g., nuclei that have exceeded the critical cluster size and are growing into larger crystals. Lipid crystal morphology, which in contrast to crystal structure (the relative arrangement of the molecules), is the macroscopic crystal size and shape, may thus be altered by the application of high-intensity ultrasound (Fig. 10.8). For example, when palm oil was cooled during the application of high-intensity ultrasound, a great variety of different crystal morphologies were observed that depended on the wave amplitude. The lipid crystals changed progressively from large spherulitic crystals to needle-like structures, smaller more uniform crystals, and very small crystals as the ultrasonic wave intensity increased. As a result, the crystallized palm oil had textures that ranged from clotted cream to a smooth cream.

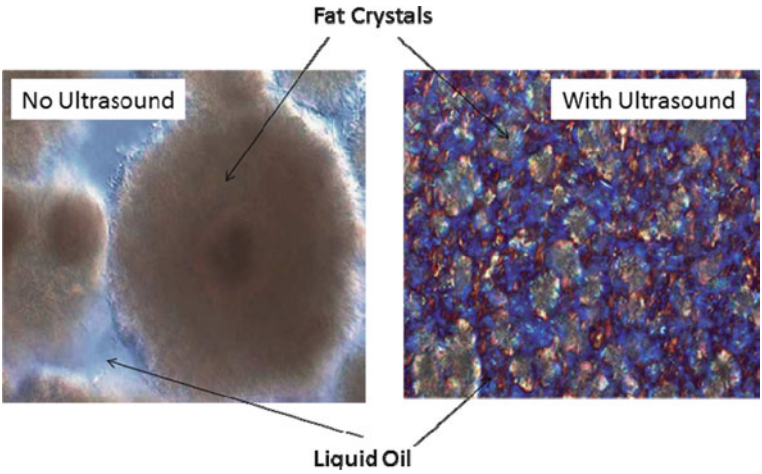

Fig. 10.8 Modification of palm oil crystallization by application of high-intensity ultrasound. (*Left*) In the absence of ultrasound, a mixture of large and smaller spherulitic palm fat crystals was obtained. (*Right*) With application of ultrasound (30 dB), the sample contained much smaller dispersed fat crystals which led to the sample becoming highly viscous with a clotted cream type texture. Magnification 40× (Patrick et al., 2004)

Finally, high-intensity ultrasound may alter the crystallization behavior of lipids in two-phase systems indirectly by simply dispersing the lipids in the system more finely. As mentioned, high-intensity ultrasonication is an effective homogenization technique that can yield oil droplets with very small average particle diameters (Freitas et al., 2005, 2006; Jafari et al., 2007). Crystallization in emulsions depends on the droplet size since with decreasing droplet size, the number of droplets may exceed the number of impurities and the bulk of the mass of the lipid droplets may be impurity free and crystallize by an apparently homogeneous mechanism. Moreover, high-intensity ultrasound may yield emulsions that are highly polydispersable and, since crystallization rates may increase with polydispersity, ultrasonically homogenized emulsions may thus crystallize more rapidly.

3.3.3 Oxidative Stability and Rancidity Development

Lipid oxidation and development of off-flavors may greatly decrease the acceptability of lipid-containing products. Lipid oxidation occurs by a complex sequence of chemical reactions that are due to interaction of lipids with oxygen and depends on the presence and generation of radical species. Lipid oxidation occurs in three steps: (1) initiation, i.e., the abstraction of hydrogen from a fatty acid to form a fatty acid radical (alkyl radical); (2) propagation, i.e., the addition of oxygen to the alkyl radical to form a peroxyl radical, which may rapidly abstract another hydrogen from another lipid and (3) termination, i.e., the cross-reaction of two radicals yielding a nonradical species. Formation of these primary and intermediate radical species may be accelerated by the presence of metal catalysts in the reactant solution, high temperature, or exposure to light irradiation. The sonochemical effects of high-intensity ultrasound greatly promote radical reactions and high reactive species are generated during the collapse of cavities. Consequently, ultrasound may have a detrimental effect on lipid functionality and integrity by promoting radical-driven oxidation processes consequently limiting the application of power ultrasound to lipids.

Indeed, when the effects of high-power ultrasonication (20 kHz; 150 W; 2 min) on sunflower oil were studied, peroxide values increased from 5.38 to 6.33 meq O_2/kg oil for untreated oil (Chemat et al., 2004). In addition, off-flavor compounds such as hexanal and limonene were identified by gas chromatography coupled to mass spectrometry upon treatment of the oil with high-intensity ultrasound. Similarly, when liposomes were used as models for polar lipids and subjected to ultrasonication, a dose-dependent linear increase in lipid peroxidation as determined by the concentrations of conjugated dienes, lipid hydroperoxides, and malondialdehydes were found (Jana et al., 1990). In direct sonication processes using a sonicator probe, metal fragments may be released into the solution due to microstreaming, causing surface erosion of the probe. Therefore, in addition to generating radicals, ultrasound may indirectly promote lipid oxidation by increasing the presence of metal catalysts that can lead to stabilization of transient, reactive radical species.

3.3.4 Fatty Acid Composition

The type of lipids that are present in foods is becoming of great importance to food manufacturers due to concern about “good” (health-promoting) and “bad” (health-degrading) lipids. In triacylglycerides, the fatty acid composition is a major factor that distinguishes “ more healthy” oils from “less healthy” oils. Most vegetable oils, with the notable exception of palm oil and cocoa butter, are highly unsaturated and contain fatty acids with carbon lengths above 16. In contrast, lipids from non-marine animal sources are significantly higher in saturated fatty acids, with palmitic and stearic acid being the two dominant fatty acids. To alter the fatty acid composition of a lipid, a number of reactions are employed in the food industry including hydrogenation and interesterification. Hydrogenation involves elimination of the double bonds in unsaturated fatty acids by addition of hydrogen to yield less unsaturated

or completely saturated fatty acids and triacylglyerols. This procedure is used to modify the crystallization behavior of lipids, to improve their chemical stability, and to bleach lipid pigments such as carotenoids. The reaction is conducted in the presence of a catalyst such as, for example, nickel. Depending on the hydrogenation conditions (e.g., temperature, hydrogen pressure, agitation), fatty acids may not be fully saturated and yield trans isomers of the initial fatty acids, a fact that has been recognized to contribute to an increased risk for cardiovascular diseases. Interesterification, on the other hand, involves the rearrangement of the individual fatty acid groups in triacylglycerides, which again is used to modify the crystallization behavior of the lipids. The reaction may involve transfer of acyl groups within a single triacylglyceride (intraesterification) or transfer of acyl groups between different lipids (interesterification). In food lipids, this reaction is catalyzed by the carbonyl anion of the diacylglycerol.

Based on the fact that ultrasound excels at improving catalytic reactions in heterogeneous systems, it is surprising to see that power ultrasound has not been more intensively investigated to alter the reaction pathways and products obtained during these two key food lipid reactions. Clearly, extensive ultrasonication could lead to a degradation of lipids as described previously, but ultrasonication at higher frequencies and intermittent intensities may prove to increase reaction rates and allow for a better control over the obtained products. While not directly focusing on food lipids, Disselkamp studied the hydrogenation of *cis*-2-buten-1-ol (C4 olefin) and *cis*-2-penten-1-ol (C5 olefin) on Pd-black under application of high-intensity ultrasound. They found that the ultrasound-assisted reaction had an altered selectivity compared to the control (untreated) reaction systems, that is, approximately 50% less *trans*-olefin was produced compared to the control reaction system (Disselkamp et al., 2005). Based on the reported results, it would be interesting to test whether such a reduction in trans-species generation may be possible when food oils are hydrogenated. With respect to the potential use of high-intensity to modify the interesterification of lipids, Stavarache and coauthors reported positive results for the transesterification of vegetable oils combined with alcohol to produce biodiesel based on the ability of ultrasound to improve the critical reagent blending step (Stavarache et al., 2007a, b). This could bode well for the application of high-intensity ultrasound to the interesterification of food lipids, since the mechanical mixing step is of similar importance. Finally, lipids may indirectly be modified by application of high-intensity ultrasound by influencing the activity of lipases that may be used to alter lipids (Fig. 10.9).

4 Conclusions

High-intensity ultrasound is able to modify the chemical structure and hence the functionality of all major food ingredients. For example, depending on the ultrasonic intensity and the environmental conditions (temperature, pressure, solvent pH, and ionic strength), the functionality of proteins can be affected by high-intensity

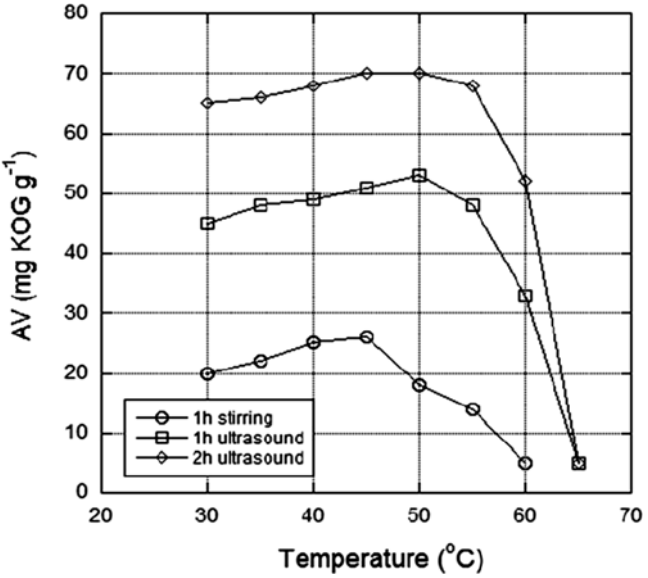

Fig. 10.9 Influence of high-intensity ultrasonication (1.64 W cm^{-2}) on enzyme-catalyzed hydrolysis of soy bean oil in water (0.675:1 w/w) at various temperatures (30–65°C). The extent of hydrolysis is shown as the acid value (AV) which was measured by titration with KOH. The AV is indicative of the amount of free fatty acids generated. Adapted from Liu et al. (2008)

ultrasound. The observed changes are due to more or less intense modifications of the fundamental protein structure, including possible backbone breakage as well as difference in self-assembly and folding of the proteins (secondary and tertiary structures). If used correctly, these changes may be highly beneficial, such as in the case of the treatment of enzymes, the de-bittering of some proteins, and the treatment of surface active proteins to improve their adsorption kinetics and gelation kinetics and their ability to stabilize foams.

In the case of polysaccharides, treatment by high-intensity ultrasound in appropriate solvents can lead to significant changes in the structure and functionality of carbohydrates, either due to scission of the backbone or via modification of the functional side groups of polysaccharides. Finally, in the case of lipids, ultrasound has the potential to modify the crystallization process of lipids, which is critical in a large number of food products such as butter, margarine, and ice cream, and to influence the hydrogenation and interesterification of lipids. However, in the case of lipids, the ultrasonic energy input and the applied frequency are of critical importance, as excessive sonication can lead to oxidation, thus degrading the quality and acceptability of food lipids.

The potential to exploit high-intensity ultrasound to chemically modify a wide variety of food ingredients has barely begun to be exploited. It is known that high-intensity ultrasound, especially at higher frequencies, can accelerate chemical reactions, a fact that should similarly be applied to modification reactions that

could be used to tailor and improve the functionality of many food ingredients. Nevertheless, a clear understanding of the involved reaction pathways and the mechanism by which ultrasound influences the reaction is of critical importance, and more research is clearly needed to further exploit this emerging use of high-intensity ultrasound.

References

Abramov, O. V. (1998). *High Intensity Ultrasonics: Theory and Industrial Applications*. Hawthorn, Australia, Gordon and Breach Science Publishers.

Adewuyi, Y. G. (2001). Sonochemistry: Environmental science and engineering applications. *Industrial and Engineering Chemistry Research*, 40, 4681–4715.

Akoh, C. C., and Min, D. B. (2002). *Food Lipids: Chemistry, Nutrition, and Biotechnology*. Boca Raton, FL, CRC.

Alsop, R. M. (1993). *Industrial Production of Dextrans*. Amsterdam, Elsevier.

Anbar, M., and Pecht, I. (1964). On sonochemical formation of hydrogen peroxide in water. *Journal of Physical Chemistry*, 68, 352–355.

Arami, H., Mazloumi, M., Khalifehzadeh, R., and Sadrnezhaad, S. K. (2007). Sonochemical preparation of TiO_2 nanoparticles. *Materials Letters*, 61(23–24), 4559–4561.

Barbier, P., and Petrier, C. (1996). Study at 20 kHz and 500 kHz of the ultrasound-ozone advanced oxidation system: 4-nitrophenol degradation. *Journal of Advanced Oxidation Technologies*, 1, 154–159.

Barton, S., Bullock C., and Weir D. (1996). The effects of ultrasound on the activities of some glycosidase enzymes of industrial importance. *Enzyme and Microbial Technology*, 18, 190–194.

Basedow, A. M., and Ebert, K. H. (1975). Zum Mechanismus des Abbaus von Polymeren in Lösung durch Ultraschall. *Die Makromolekulare Chemie*, 176(3), 745–757.

Basedow, A. M., Ebert, K. H., and Fosshag, E. (1978). Ultrasonic degradation of polymers in mixed solvents. *Die Makromolekulare Chemie*, 179(10), 2565–2568.

Baxter, S. R., Zivanovic, S., and Weiss, J. (2005). Molecular weight and degree of acetylation of high-intensity ultrasonicated chitosan. *Food Hydrocolloids*, 19, 821–830.

Bestul, A. B. (1954). Composition of apparent shearing forces during shear degradation of polymers. *Journal of Applied Physics*, 25(9), 1069–1074.

Bhattacharyya, S., and Gedanken, A. (2008). A template-free, sonochemical route to porous ZnO nano-disks. *Microporous and Mesoporous Materials*, 110(2–3), 553–559.

Bonrath, W. (2005). Ultrasound supported catalysis. *Ultrasonics Sonochemistry*, 12(1–2), 103–106.

Chakraborty, J., Sarkar, J., Kumar, R., and Madras, G. (2004). Ultrasonic degradation of polybutadiene and isotactic polypropylene. *Polymer Degradation and Stability*, 85(1), 555–558.

Chattopadhyay, S., and Madras, G. (2003). Influence of temperature on the ultrasonic degradation of poly(vinyl acetate) and poly(vinyl chloride). *Journal of Applied Polymer Science*, 88(12), 2818–2822.

Chemat, F., Grondin, I., Costes, P., Moutoussamy, L., Sing, A. S. C., and Smadja, J. (2004). High power ultrasound effects on lipid oxidation of refined sunflower oil. *Ultrasonics Sonochemistry*, 11(5), 281–285.

Choi, J. H., and Kim, S. B. (1994). Effect of ultrasound on sulfuric acid catalysed hydrolysis of starch. *Koren Journal of Chemical Engineering*, 11(3), 178–184.

Corman, J., and Tsuchiya, H. M. (1957). Enzymatic production of dextrans of intermediate molecular weights. US Patent, 2776925.

Cote, G. L., and Willet, J. L. (1999). Thermomechanical depolymerization of dextran. *Carbohydrate Polymers*, 39, 119–126.

Damodaran, S. (1997). *Food Proteins and Lipids*. New York, NY, Plenum.
Damodaran, S., Parkin, K. L., and Fennema, O. R. (2005). *Food Chemistry*. Boca Raton, FL, CRC.
Darby, N., and Creighton, T. E. (1995). Disulfide bonds in protein folding and stability. Methods in Molecular Biology, 40, 219–252.
De Cesare, F., Garzillo, A. M. V., Buonocore, V., and Badalucco, L. (2000). Use of sonication for measuring acid phosphatase activity in soil. *Soil Biology and Biochemistry*, 32, 825–832.
De Visscher, A., and Van Langenhove, H. (1998). Sonochemistry of organic compounds in homogeneous aqueous oxidising systems. *Ultrasonics Sonochemistry*, 5(3), 87–92.
DeBelder, A. N. (1993). *Dextran*. San Diego, Academic.
Dedhia, A. C., Ambulgekar, P. V., and Pandit, A. B. (2004). Static foam destruction: role of ultrasound. *Ultrasonics Sonochemistry*, 11(2), 67–75.
Disselkamp, R. S., Denslow, K. M., Hart, T. R., White, J. F., and Peden, C. H. F. (2005). The effect of cavitating ultrasound on the aqueous phase hydrogenation of cis-2-buten-1-ol and cis-2-penten-1-ol on Pd-black. *Applied Catalysis A: General*, 288(1–2), 62–66.
Disselkamp, R. S., Hart, T. R., Williams, A. M., White, J. F., and Peden, C. H. F. (2005). Ultrasound-assisted hydrogenation of cinnamaldehyde. *Ultrasonics Sonochemistry*, 12(4), 319–324.
Drijvers, D., DeBaets, R., DeVisscher, A., and Langenhove, H. (1996). Sonolysis of trichloroethylene in aqueous solution: Volatile organic intermediates. *Ultrasonic Sonochemistry*, 3, S83–S90.
Drijvers, D., Van Langenhove, H., and Vervaet, K. (1998). Sonolysis of chlorobenzene in aqueous solution: Organic intermediates. *Ultrasonic Sonochemistry*, 5, 13–19.
Drofenik, M., Kristl, M., Makovec, D., Jaglicic, Z., and Hanzel, D. (2008). Sonochemically assisted synthesis of zinc-doped maghemite. *Ultrasonics Sonochemistry*, 15(5), 791–798.
Ebringerova, A., Kardosova, A., Hromadkova, Z., Malovikova, A., and Hribalova, V. (2002). Immunomodulatory activity of acidic xylans in relation to their structural and molecular properties. *International Journal of Bilogical Macromolecules*, 30, 1–6.
El-Nawawi, S. A., and Shehata, F. R. (1987). Extraction of pectin from egyptian orange peel. Factors affecting the extraction. *Biological Wastes*, 20, 281–290.
Elder, S. A. (1959). Cavitation microstreaming. *Journal of the Acoustical Society of America*, 31, 54–65.
Elgersma, A. V., Zsom, R. L. J., Lyklema, J., and Norde, W. (1992). Kinetics of single and competitive protein adsorption studied by reflectometry and streaming potential measurements. *Colloids and Surfaces*, 65(1), 17–28.
Ferrières, V., Bertho, J.-N., and Plusquellec, D. (1995). A new synthesis of O-glycosides from totally O-unprotected glycosyl donors. *Tetrahedron Letters*, 36(16), 2749–2752.
Finch, R. D. (1963). Sonoluminescence. *Ultrasonics*, 1, 87–88.
FindIk, S., Gündüz, G., and Gündüz, E. (2006). Direct sonication of acetic acid in aqueous solutions. *Ultrasonics Sonochemistry*, 13(3), 203–207.
Flannigan, D. J., Hopkins, S. D., and Suslick, K. S. (2005). Sonochemistry and sonoluminescence in ionic liquids, molten salts, and concentrated electrolyte solutions. *Journal of Organometallic Chemistry*, 690(15), 3513–3517.
Floros, J. D., and Liang, H. (1994). Acoustically assisted diffusion through membranes and biomaterials. *Food Technology*, 48(12), 79–84.
Freitas, S., Hielscher, G., Merkle, H. P., and Gander, B. (2006). Continuous contact- and contamination-free ultrasonic emulsification – a useful tool for pharmaceutical development and production. *Ultrasonics Sonochemistry*, 13(1), 76–85.
Freitas, S., Rudolf, B., Merkle, H. P., and Gander, B. (2005). Flow-through ultrasonic emulsification combined with static micromixing for aseptic production of microspheres by solvent extraction. *European Journal of Pharmaceutics and Biopharmaceutics*, 61(3), 181–187.
Fuchs, E., and Heusinger, H. (1994). Ultrasound-induced scission of the glycosidic bond in disaccharides. *Zeitschrift für Lebensmittel-Untersuchung und-Forschung*, 198, 486–490.

Fukase, K., Kinoshita, I., Kanoh, T., Nakai, Y., Hasuoka, A., and Kusumoto, S. (1996). A novel method for stereoselective glycosidation with thioglycosides: promotion by hypervalent iodine reagents prepared from PhIO and various acids. *Tetrahedron*, 52, 3897–3904.

Garti, N. (1982). *Crystallization and Polymorphism of Fats and Fatty Acids*. Baco Raton, FL, CRC.

George, P. P., Gedanken, A., Perkas, N., and Zhong, Z. (2008). Selective oxidation of CO in the presence of air over gold-based catalysts Au/TiO_2/C (sonochemistry) and Au/TiO_2/C (microwave). *Ultrasonics Sonochemistry*, 15(4), 539–547.

Goto, M., Johanssona, H., Maedac, A., Elguea, G., Korsgrena, O., and Nilsson, B. (2004). Low–molecular weight dextran sulfate abrogates the instant blood-mediated inflammatory reaction induced by adult porcine islets both in vitro and in vivo. *Transplantation Proceedings*, 36(4), 1186–1187.

Gülseren, İ. (2004). *High-Intensity Ultrasound Mediated Structure-Function Changes of BSA as Affected by pH*. Department of Food Science and Technology, Knoxville, University of Tennessee, MS.

Gülseren, İ., Güzey, D., Bruce, B. D., and Weiss, J. (2007). Structural and functional changes in ultrasonicate bovine serum albumin. *Ultrasonics Sonochemistry*, 14(2), 173–183.

Gunther, P., Zeil, U., Grisar, U., Langmann, W., and Heim, E. (1956). Über Sonoluminsecence. *Naturforschung*, 11, 882–883.

Gutierrez, M., Henglein, A., and Ibanez, F. (1991). Radical scavenging in the sonolysis of aqueous-solutions of I-, Br-, and N3. *Journal of Physical Chemistry*, 95, 6044–6047.

Güzey, D. (2002). *Modification of Protein Structure and Functionality Using High-Intensity Ultrasound*. Department of Food Science and Technology, Knoxville, University of Tennessee, MS.

Güzey, D., Gülseren, İ., Bruce, B., and Weiss, J. (2006). Interfacial properties and structural conformation of thermosonicated bovine serum albumin. *Food Hydrocolloids*, 20(5), 669–677.

Guzey, D., Kim, H. J., and McClements, D. J. (2004). Factors influencing the production of o/w emulsions stabilized by β-lactoglobulin-pectin membranes. *Food Hydrocolloids*, 18, 967–975.

Hardcastle, J. L., Ball, J. C., Hong, Q., Marken, F., Compton, R. G., Bull, S. D., and Davies, S. G. (2000). Sonoelectrochemical and sonochemical effects of cavitation: correlation with interfacial cavitation induced by 20 kHz ultrasound. *Ultrasonics Sonochemistry*, 7(1), 7–14.

Hart, E. J., and Henglein, A. (1985). Free-radical and free atom reactions in the sonolysis of aqueous iodide and formate solutions. *Journal of Physical Chemistry*, 89, 4342–4347.

Harvey, E. N., and Loomis, A. (1929). The destruction of luminous bacteria by high frequency sound waves. *Journal of Bacteriology*, 17, 373–379.

Henglein, A. (1987). Sonochemistry:historical developments and modern aspects. *Ultrasonics*, 25, 6–15.

Heusinger, H. (1990). Comparison of the reactions induced by ultrasound and gamma rays in aqueous lactose solutions. *Ultrasonics*, 28(January), 30–36.

Heusinger, H. (1991). Gel-permeation chromatography of solutions of D-glucose after irradiation by ultrasound and g-rays. *Carbohydrate Research*, 209, 109–118.

Hibino, M., Zhou, H., and Honma, I. (2005). Electrode properties of manganese oxide synthesized by sonochemical method in non-aqueous system. *Journal of Power Sources*, 146(1–2), 304–309.

Hromadkova, Z., Ebringerova, A., and Valachovic, P. (1999). Comparison of classical and ultrasound-assisted extraction of polysaccharides from *Salvia officinalis* L. *Ultrasonics Sonochemistry*, 5, 163–168.

Hung, H. M., Ling, F. H., and Hoffmann, M. R. (1998). Kinetics and mechanism of the enhanced reductive degradation of nitrobenzene by elemental iron in the presence of ultrasound. *Environmental Science and Technology*, 34, 1758–1763.

Ince, N. H., Tezcanli, G., Belen, R. K., and Apikyan, I. G. (2001). Ultrasound as a catalyzer of aqueous reaction systems: the state of the art and environmental applications. *Applied Catalysis B: Environmental*, 29(3), 167–176.

Jafari, S. M., He, Y., and Bhandari, B. (2007). Production of sub-micron emulsions by ultrasound and microfluidization techniques. *Journal of Food Engineering*, 82(4), 478–488.

Jambrak, A. R., Lelas, V., Mason, T. J., Kresic, G., and Badanjak, M. (2009). Physical properties of ultrasound treated soy proteins. *Journal of Food Engineering*, 93(4), 386–393.

Jambrak, A. R., Mason, T. J., Lelas, V., Herceg, Z., and Herceg, I. L. (2008). Effect of ultrasound treatment on solubility and foaming properties of whey protein suspensions. *Journal of Food Engineering*, 86(2), 281–287.

Jana, A. K., Agarwal, S., and Chatterjee, S. N. (1990). The induction of lipid peroxidation in liposomal membrane by ultrasound and the role of hydroxyl radicals. *Radiation Research*, 124(1), 7–14.

Jarmon, P. D., and Taylor, K. J. (1970). The spectra of sonoluminescence. *Australian Journal of Physics*, 23, 319–323.

Kang, J. W., Hung, H. M., Lin, A., and Hoffmann, M. R. (1999). Sonolytic destruction of methyl tertbutyl ether by ultrasonic irradiation: The role of O_3, H_2O_2, frequency, and power density. *Environmental Science and Technology*, 33, 3199–3205.

Kardos, N., and Luche, J. (2001). Sonochemistry of carbohydrate compounds. *Carbohydrate Research*, 332, 115–131.

Kertesz, K. (1951). *The Pectin Substances*. New York, Interscience.

Kimura, T., Fujita, M., Sohmiya, H., and Ando, T. (2002). Ultrasonic acceleration of iodination of unactivated aliphatic hydrocarbons. *Ultrasonics Sonochemistry*, 9(4), 205–207.

Kinsella, J. E., Soucie, W. G., and American Oil Chemists' Society. Protein and Co-products Division. (1989). *Food Proteins*. Champaign, IL, American Oil Chemists' Society.

Kotronarou, A., Mills, G., and Hoffmann, M. R. (1991). Ultrasonic irradiation of para-nitrophenol in aqueous-solution. *Jounal of Physical Chemistry*, 95, 3630–3638.

Krause, J. P., Dudek, S., and Schwenke, K. D. (2000). Changes in interfacial behaviour, emulsifying and foaming properties of faba bean legumin after modification with dimethylsuberimidate. *Die Nahrung*, 44(6), 403–406.

Kresic, G., Lelas, V., Jambrak, A. R., Herceg, Z., and Brncic, S. R. (2008). Influence of novel food processing technologies on the rheological and thermophysical properties of whey proteins. *Journal of Food Engineering*, 87(1), 64–73.

Kristl, M., and Drofenik, M. (2008). Sonochemical synthesis of nanocrystalline mercury sulfide, selenide and telluride in aqueous solutions. *Ultrasonics Sonochemistry*, 15(5), 695–699.

Kruus, P., O'Neill, M., and Robertson, D. (1990). Ultrasonic initiation of polymerization. *Ultrasonics*, 28(5), 304–309.

Lebovitz, A. H., Gray, M. K., Chen, A. C., and Torkelson, J. M. (2003). Interpolymer radical coupling reactions during sonication of polymer solutions. *Polymer*, 44(10), 2823–2828.

Lehninger, A., Cox, M., and Nelson, D. L. (1993). *Principles of Biochemistry*. New York, W.H. Freeman and Company.

Leighton, T. G. (1997). *The Acoustic Bubble*. London, Academic.

Lim, K. S., and Barigou, M. (2005a). Pneumatic foam generation in the presence of a high intensity ultrasound field. *Ultrasonics Sonochemistry*, 12(5), 385–393.

Lim, K. S., and Barigou, M. (2005b). Ultrasound-assisted generation of foam. *Industrial and Engineering Chemistry Research*, 44, 3312–3320.

Lintner, W., and Hanesian, D. (1976). The effect of ultrasonic vibrations on heterogeneous catalysis. *Ultrasonics*, 15(1), 21–26.

Liu, Y., Jin, Q., Shan, L., Liu, Y., Shen, W., and Wang, X. (2008). The effect of ultrasound on lipase-catalyzed hydrolysis of soy oil in solvent-free system. *Ultrasonics Sonochemistry*, 15(4), 402–407.

Lohse, D., and Hilgenfeldt, S. (1997). Inert gas accumulation in sonoluminescing bubbles. *Journal of Chemical Physics*, 107, 6986–6997.

Lopez, P., and Burgos, J. (1995). Peroxidase stability and reactivation after heat treatment and manothermosonication. *Journal of Food Science*, 60(3), 451–455, 482.

Lorimer, J. P., Mason, T. J., Cuthbert, T. C., and Brookfield, E. A. (1995). Effect of ultrasound on the degradation of aqueous native dextran. *Ultrasonics Sonochemistry*, 2(1), s55–s57.

Lu, J. R., and Su, T. J. (1999). Adsorption of serum albumins at the air/water interface. *Langmuir*, 15(20), 6975–6983.

Luche, J. L. (1992). New orientation in sonochemsitry. *Current Trends in Sonochemistry*. G. J. Price. Cambridge, The Royal Society of Chemistry.

Malhotra, S. L. (October 1982a). Ultrasonic modification of polymers. II. Degradation of polystyrene, substituted polystyrene, and Poly(n-vinyl Carbazole) in the presence of flexible chain polymers. *Journal of Macromolecular Science*, *Part A*, 18(7 & 8), 1055–1085.

Malhotra, S. L. (1982b). Ultrasonic degradation of hydroxypropyl cellulose solutions in water, ethanol, and tetrahydrofuran. *Journal of Macromolecular Science Part A: Pured and Applied Chemistry*, 17(4), 601–636.

Margulis, M. A. (1985). Sonoluminescence and sonochemical reactions in cavitation fields. A review. *Ultrasonics*, 23(4), 157–169.

Margulis, M. A., and Grundel, LM (1983). Chemical effect of low-frequency acoustic vibrations. *Doklady Akademii Nauk SSSR*, 265, 914–917.

Margulis, M. A., and Margulis, I. M. (2002). Contemporary review on nature of sonoluminescence and sonochemical reactions. *Ultrasonics Sonochemistry*, 9(1), 1–10.

Mason, T. J. (1992). Industrial sonochemistry: potential and practicality. *Ultrasonics*, 30(3), 192–196.

Mason, T. J., and Cordmas, E. D. (1996). Ultrasonic intensification of chemical processing and related operations – a review. *Transactions of the Institute of Chemical Engineers*, 74(A), 511–516.

Mason, T. J., and Lorimer, J. P. (1989). *Sonochemistry, Theory, Applications and Uses of Ultrasound in Chemistry*. London, Wiley-VCH.

Mason, T. J., Paniwnyk, L., and Lorimer, J. P. (1996). The uses of ultrasound in food technology. *Ultrasonics Sonochemistry*, 3, S253–S260.

Masuyama, Y., Hayakawa, A., Kishida, M., and Kurusu, Y. (1994). Ultrasound-promoted palladium-catalyzed carbonyl allylation by allylic alcohols with tin(II) chloride in non-polar solvents. *Inorganica Chimica Acta*, 220(1–2), 155–159.

McClements, D. J. (2000). Comments on viscosity enhancement and depletion flocculation by polysaccharides. *Food Hydrocolloids*, 14(2), 173–177.

McClements, D. J. (2006). *Food Emulsions: Principles, Practice, and Techniques*. Boca Raton, FL, CRC.

Mead, E. L., Sutherland, R. G., and Verrall, R. E. (1976). The effect of ultrasound on water in presence of dissolved gases. *Journal of Physical Chemistry*, 54, 1114–1120.

Mine, Y., Li-Chan, E., and Jiang, B. (2010). *Bioactive Proteins and Peptides as Functional Foods and Nutraceuticals*. Ames, IA, Wiley-Blackwell.

Moore, D. E., and Parts, A. G. (1968). Mechanical degradation of polystyrene in solution. *Polymer*, 9(1), 52–54.

Morel, M.-H., Dehlon, P., Autran, J. C., Leygue, J. P., and Bar-L'Helgouac'h, C. (2000). Effects of temperature, sonication time, and power settings on size distribution and extractability of total wheat flour proteins as determined by size-exclusion high-performance liquid chromatography. *Cereal Chemistry*, 77, 685–691.

Morey, M. D., Deshpande, N. S., and Barigou, M. (1999). Foam destabilization by mechanical and ultrasonic vibrations. *Journal of Colloid and Interface Science*, 219, 90–98.

Negishi, K. (1961). Experimental studies on sonoluminescence and ultrasonic cavitation. *Journal of the Physical Society of Japan*, 16(7), 1450–1465.

Ostrovskii, I. V., Korotchenkov, O. A., Goto, T., and Grimmeiss, H. G. (1999). Sonoluminescence and acoustically driven optical phenomena in solids and solid-gas interfaces. *Physics Reports*, 311(1), 1–46.

Özbek, B., and Ü.K.Ö. (2000). The stability of enzymes after sonication. *Process Biochemistry*, 35, 1037–1043.

Panchev, I. N., Kirtchev, N.A., and Kratchanov, C. G. (1994). On the production of low esterfied pectins by acid maceration of pectic raw materials with ultrasound treatment. *Food Hydrocolloids*, 8(1), 9–17.

Park, J.-E., Atobe, M., and Fuchigami, T. (2005). Sonochemical synthesis of conducting polymer-metal nanoparticles nanocomposite. *Electrochimica Acta*, 51(5), 849–854.

Patrick, M., Blindt, R., and Janssen, J. (2004). The effect of ultrasonic intensity on the crystal structure of palm oil. *Ultrasonics Sonochemistry*, 11, 251–255.

Peacocke, A. R., and Pritchard, N. J. (1968). The ultrasonic degradation of biological macromolecules under conditions of stable cavitation. II. Degradation of deoxyribonucleic acid. *Biopolymers*, 6(4), 605–623.

Peters, D. (1996). Ultrasound in materials chemistry. *Journal of materials chemistry*, 6, 1605–1618.

Phillips, G. O., and Williams, P. A. (1995). Interaction of hydrocolloids in food systems. In: Gaonkar, A. G. (ed.), *Ingredient Interactions*, pp. 131–169. New York, NY, Marcel Dekker.

Pongsawatmanit, R., Harnsilawat, T., and McClements, D. J. (2006). Influence of alginate, pH and ultrasound treatment on palm oil-in-water emulsions stabilized by [beta]-lactoglobulin. *Colloids and Surfaces A: Physicochemical and Engineering Aspects*, 287(1–3): 59–67.

Povey, M. J. W. (1998). Ultrasonics of food. *Contemporary Physics*, 39(6), 467–478.

Povey, M. J. W., and Mason, T. J. (eds.). (1998). *Ultrasound in Food Processing*. London, Blackie Academic and Professional.

Price, G. J., Norris, D. J., and West, P. J. (1992). Polymerization of methyl methacrylate initiated by ultrasound. *Macromolecules*, 25(24), 6447–6454.

Price, G. J., and Smith, P. F. (1991). Ultrasonic degradation of polymer solutions. 1. Polystyrene revisited. *Polymer International*, 24(3), 159–164.

Price, G. J., and Smith, P. F. (1993). Ultrasonic degradation of polymer solutions—III. The effect of changing solvent and solution concentration. *European Polymer Journal*, 29(2–3), 419–424.

Price, G. J., and West, P. J. (1996). Ultrasonic production of block copolymers as in situ compatibilizers for polymer mixtures. *Polymer*, 37(17), 3975–3978.

Pritchard, N. J., Hughes, D. E., and Peacocke, A. R. (1965). The ultrasonic degradation of biological macromolecules under conditions of stable cavitation. I. Theory, methods, and application to deoxyribonucleic acid. *Biopolymers*, 4(3), 259–273.

Rahman, S. (1995). *Food Properties Handbook*. Boca Raton, FL, CRC.

Ram, A., and Kadim, A. (1970). Shear degradation of polymer solutions. *Journal of Applied Polymer Science*, 14(8), 2145–2156.

Raviyan, P., Zhang, Z., and Feng, H. (2005). Ultrasonication for tomato pectinmethylesterase inactivation: effect of cavitation intensity and temperature on inactivation. *Journal of Food Engineering*, 70, 189–196.

Reifsneider, S. B., and Spurlock, L. A. (1973). Chemistry of ultrasound: 2. Irradiative behavior of aliphatic aldehydes and carboxylic-acids in an aqueous-medium. *Journal of American Chemical Society*, 95, 299–305.

Rice, E. L. (1995). *Biological Control of Weeds and Plant Diseases*. Norman, University of Oklahoma Press.

Richards, W., and Loomis, A. (1927). The chemical effects of high frequency sound waves. *Journal of the American Chemical Society*, 49, 3086–3089.

Riesz, P., Berdahl, D., and Christman, C. L. (1985). Free radical generation by ultrasound in aqueous and nonaqueous solutions. *Environmental Health Perspectives*, 64, 233–252.

Rodriguez, J. G., and Lafuente, A. (2002). A new advanced method for heterogeneous catalysed dechlorination of 1,2,3-, 1,2,4-, and 1,3,5-trichlorobenzenes in hydrocarbon solvent. *Tetrahedron Letters*, 43(52), 9645–9647.

Sáeza, V., Frías-Ferrera, A., Iniestaa, J., González-García, J., Aldaza, A., and Rierab, E. (2005). Characterization of a 20 kHz sonoreactor. Part II: analysis of chemical effects by classical and electrochemical methods. *Ultrasonics Sonochemistry*, 12(1–2): 67–72.

Sakakiabra, M., Wang, D., Takahashi, R., and Mori, S. (1996). Influence of ultrasound irradiation on hydrolysis of sucrose catalyzed by invertase. *Enzyme and Microbial Technology*, 18, 444–448.

Sánchez-Gimeno, A. C., Vercet, A., and López-Buesa, P. (2006). Studies of ovalbumin gelation in the presence of carrageenans and after manothermosonication treatments. *Innovative Food Science and Emerging Technologies*, 7(4), 270–274.

Sandor, N., and Stein, H. N. (1993). Foam destruction and ultrasonic vibrations. *Journal of Colloid and Interface Science*, 161(1), 265–267.

Schmid, G. (1940). Zur Kinetik der Ultraschalldepolymerisation. *Zeitschrift für physikalische Chemie*, 186(3), 113–128.

Sehgal, C., Sutherland, R. G., and Verrall, R. E. (1980). Selective quenching of species that produce sonoluminescence. *Journal of Chemical Physics*, 84, 529–530.

Seshadri, R., Weiss, J., Hulbert, G. J., and Mount, J. (2002). Ultrasonic processing influences rheological and optical properties of high-methoxyl pectin dispersion. *Food Hydrocolloids*, 17, 191–197.

Shoh, A. (1988). Industrial applications of ultrasound. In: Suslick, K. S. (ed.), *Ultrasound: Its Chemical, Physical and Biological Effects*. New York, NY, VCH.

Sikorski, Z. E. (2001). *Chemical and Functional Properties of Food Proteins*. Lancaster, PA, Technomic.

Smolin, L. A., and Grosvenor, M. B. (1994). *Nutrition: Science and Applications*. Fort Worth, TX, Saunders College.

Snell, J. B. (1965). Polymer production from aqueous solutions of D-glucose by high energy radiation. *Journal of Polymer Science*, 3A, 2591–2607.

Spurlock, L. A., and Reifsneider, S. B. (1970). Chemistry of ultrasound. 1. A reconsideration of first principles and applications to a dialkyl sulfide. *Journal of American Chemical Society,* 92, 6112–6117.

Stanley, K. D., Golden, D. A., Williams, R. C., and Weiss, J. (2004). Inactivation of *Escherichia coli* O157:H7 by high-intensity ultrasonication in the presence of salts. *Foodborne Pathogens and Disease*, 1(1), 267–273.

Stavarache, C., Vinatoru, M., and Maeda, Y. (2007a). Aspects of ultrasonically assisted transesterification of various vegetable oils with methanol. *Ultrasonics Sonochemistry*, 14(3), 380–386.

Stavarache, C., Vinatoru, M., Maeda, Y., and Bandow, H. (2007b). Ultrasonically driven continuous process for vegetable oil transesterification. *Ultrasonics Sonochemistry*, 14(4), 413–417.

Stavarache, C., Vinatoru, M., Nishimura, R., and Maeda, Y. (2004). Short-time sonolysis of chlorobenzene in the presence of Pd(II) salts and Pd(0). *Ultrasonics Sonochemistry*, 11(6), 429–434.

Strukul, G. (1992). *Catalytic Oxidations with Hydrogen Peroxide as Oxidant*. Dordrecht, Kluwer Academic.

Suslick, K. S. (1997). Sonocatalysis. In: Ertl, G., Knozinger, H., Weitkamp, J. (eds.), *Handbook of Hetereogenous Catalysis*. Weinheim, Wiley-VCH.

Suslick, K. S., Casadonte, D. J., Green, M. L. H., and Thompson, M. E. (1987). Effects of high intensity ultrasound on inorganic solids. *Ultrasonics*, 25(Jan), 56–59.

Suslick, K. S., Didenko, Y., Fang, M. M., Hyeon, T., Kolbeck, K. J., McNamara, W. B., Mdleleni, M. M., and Wong, M. (1999). Acoustic cavitation and its chemical consequences. *Philosophical Transactions of The Royal Society A*, 357, 335–353.

Suslick, K. S., and Grinstaff, M. W. (1990). Protein microencapsulation of nonaqueous liquids. *Journal of American Chemical Society*, 11, 7807–7809.

Suslick, K. S., and Price, G. J. (1999). Applications of ultrasound to materials chemistry. *Annual Review of Materials Science*, 29, 295–326.

Thomas, B. B., and Alexander, W. J. (1957). Ultrasonic degradation of cellulose nitrate. II. Effects of temperature, solvent, and other process variables. *Journal of Polymer Science*, 25(110), 285–303.

Tomasik, P., and Zaranyika, M. F. (1995). Nonconventional methods of modification of starch. *Advances in Carbohydrate Chemistry*, 51, 302–307.

Troia, A., Ripa, D. M., Spagnolo, R., and Maurino, V. (2006). Single bubble sonochemistry: Decomposition of alkyl bromide and the isomerization reaction of maleic acid. *Ultrasonics Sonochemistry*, 13(5), 429–432.

Vargas, L. H. M., Pião, A. C. S., Domingos, R. N., and Carmona, E. C. (2004). Ultrasound effects on invertase from *Aspergillus niger*. *World Journal of Microbiology and Biotechnology*, 20, 137–142.

Vercet, A., Burgos, J., and Lopez-Buesa, P. (2002). Manothermosonication of heat-resistant lipase and protease from *Pseudomonas fluorescens*: Effect of pH and sonication parameters. *Journal of Dairy Research*, 69, 243–254.

Vercet, A., Sánchez, C., Burgos, J., Montañés, L., and Buesa, P. L. (2002). The effects of manothermosonication on tomato pectic enzymes and tomato paste rheological properties. *Journal of Food Engineering*, 53, 273–278.

Vilkhu, K., Mawson, R., Simons, L., and Bates, D. (2008). Applications and opportunities for ultrasound assisted extraction in the food industry – A review. *Innovative Food Science and Emerging Technologies*, 9(2), 161–169.

Villamiel, M. and de Jong, P. (2000). Influence of high-intensity ultrasound and heat treatment in continuous flow on fat, proteins, and native enzymes of milk. *Journal of Agricultural and Food Chemistry*, 48, 472–478.

Vodenicarová, M., Drímalová, G., Hromádková, Z., Malovíková, A., and Ebringerová, A. (2006). Xyloglucan degradation using different radiation sources: A comparative study. *Ultrasonics Sonochemistry*, 13(2), 157–164.

Wang, M.-L., and Rajendran, V. (2006). A kinetic study of thioether synthesis under influence of ultrasound assisted phase-transfer catalysis conditions. *Journal of Molecular Catalysis A: Chemical*, 244(1–2), 237–243.

Wang, M.-L., and Rajendran, V. (2007a). Kinetics for dichlorocyclopropanation of 1,7-octadiene under the influence of ultrasound assisted phase-transfer catalysis conditions. *Journal of Molecular Catalysis A: Chemical*, 273(1–2), 5–13.

Wang, M.-L., and Rajendran, V. (2007b). Ultrasound assisted phase-transfer catalytic epoxidation of 1,7-octadiene – A kinetic study. *Ultrasonics Sonochemistry*, 14(1), 46–54.

Wang, X., Yao, Z., Wang, J., Guo, W., and Li, G. (2008). Degradation of reactive brilliant red in aqueous solution by ultrasonic cavitation. *Ultrasonics Sonochemistry*, 15(1), 43–48.

Weiss, J., Farriols, G., and Liao, W. (2000). *Rheological Study of Fermentation of Ultrasonically-Homogenized Whey Protein Emulsions*. 5th International Food Hydrocolloids Conference, Raleigh, NC.

Weiss, J., Gülseren, I., and Kjartansson, G. (2011). Physicochemical effects of high-intensity ultrasonication on food proteins and carbohydrates. In: Barbosa-Canovas, G. V., and Bermundez-Aguirre, D. (eds.), *Nonthermal Processing Technologies for Food.* Blackwell Publishing Ltd and Institute of Food Technologists.

Weiss, J., and Seshadri, R. (2001). *Modifying Interfacial and Colloidal Properties of Proteins Using Thermosonication*. Abstracts of Papers of the Annual Meeting of the ACS, Chicago, IL.

Weissler, A., Cooper, H. W., and Snyder, S. (1950). Chemical effect of ultrasonic waves – oxidation of potassium iodide solution by carbon tetrachloride. *Journal of American Chemical Society*, 72, 1769–1775.

Weninger, K., Hiller, R., Barber, B. P., Lacoste, D., and Putterman, S. J. (1995). Sonoluminescence from single bubbles in nonaqueous liquids – new parameter space for sonochemistry. *Journal of Physical Chemistry*, 99, 14195–14197.

Whitaker, J. R., Tannenbaum, S. R., Institute of Food Technologists, and International Union of Food Science and Technology. (1977). *Food Proteins*. Westport, CT, Avi.

Wu, H., Hulbert, G. J., and Mount, J. R. (2001). Effects of ultrasound on milk homogenization and fermentation with yogurt starter. *Innovative Food Science and Emerging Technologies*, 1, 211–218.

Wu, T., Zivanovic, S., Hayes, D. G., and Weiss, J. (2008). Efficient reduction of chitosan molecular weight by high-intensity ultrasound: Underlying mechanism and effect of processing parameters. *Journal of Agricultural and Food Chemistry*, 56(13), 5112–5119.

Xie, B., Wang, L., and Liu, H. (2008). Using low intensity ultrasound to improve the efficiency of biological phosphorus removal. *Ultrasonics Sonochemistry*, 15(5), 775–781.

Yim, B., Yoo, Y., and Maeda, Y. (2003). Sonolysis of alkylphenols in aqueous solution with Fe(II) and Fe(III). *Chemosphere*, 50(8), 1015–1023.

Yu, M., and Damodaran, S. (1991). Kinetics of protein foam destabilization: evaluation of a method using bovine serum albumin. *Journal of Agricultural and Food Chemistry*, 39(9), 1555–1562.

Zolfaghari, A., Ataherian, F., Ghaemi, M., and Gholami, A. (2007). Capacitive behavior of nanostructured MnO_2 prepared by sonochemistry method. *Electrochimica Acta*, 52(8), 2806–2814.

Chapter 11
Manothermosonication for Microbial Inactivation

Santiago Condón, Pilar Mañas, and Guillermo Cebrián

1 Introduction

Most traditional technologies of food preservation, such as freezing, dehydration, acidification, are based on the inhibition or slowing of bacterial growth, which extends the shelf life of the product. However, the sanitary quality of the products manufactured according to the above processes can only be guaranteed if the raw materials used for their manufacture show a contamination by pathogenic microbial species lower than the infective dose. Even when starting from quality raw materials, it must be assumed that there could be low concentrations of pathogens that, though slowly, can multiply during subsequent storage, thereby jeopardizing the sanitary security of the product, which can obviously change over the course of time. Therefore, on many occasions, not only is it necessary to inhibit the microbial growth in the product to extend its shelf life, but the pathogenic species contained in it must be inactivated as well. In other words, it must be pasteurized.

Up to very recent times, heat has been practically the only method of preservation/pasteurization of food to guarantee the sanitary quality of the product, even if manufactured from raw materials of uncertain microbiological quality. The major problem of heat is its non-specificity, since heat treatments at the same time that they inactivate microorganisms can modify the nutritional value and sensorial properties of foods, thereby damaging their quality. Therefore, food technology is currently looking for alternatives and more specific methods of pasteurization and preservation, which besides guaranteeing the stability and safety of foods will not greatly modify their quality.

Ultrasound (US) is one of the new technologies of microbial inactivation that has been suggested as an alternative to current heat treatments. As a matter of fact, the bactericidal effect of ultrasound has been known since the beginning of the past century (Harvey and Loomis, 1929). Nevertheless, the first apparatus only

S. Condón (✉)
Departamento de Producción Animal y Ciencia de los Alimentos, Tecnología de los Alimentos, Facultad de Veterinaria, Universidad de Zaragoza, C/Miguel Servet, 177, 50013, Zaragoza, Spain
e-mail: scondon@unizar.es

H. Feng et al. (eds.), *Ultrasound Technologies for Food and Bioprocessing*, Food Engineering Series, DOI 10.1007/978-1-4419-7472-3_11,
© Springer Science+Business Media, LLC 2011

allowed generation of low-intensity ultrasound (10 W/cm^2), which had low lethal efficacy, preventing their use as a food pasteurization method. The development of high-power ultrasound generators opened new ways to this technology, and this has roused a new interest to study its microbial inactivating effects.

Despite the patent improvement of current ultrasound generators, most published data indicate that the germ-killing efficacy of the process is still relatively low under room conditions, and only under special situations could ultrasound become an actual alternative to the current heat treatments. Therefore, most investigators have tried to improve the efficacy of the process, either by increasing cavitation intensity or by designing combined processes to enhance their effect (Arce-García et al., 2002; Guerrero et al., 2005; Lee et al., 2003; López-Malo et al., 2005; Ordóñez et al., 1984, 1986; Raso et al., 1998a; Sala et al., 1992).

In 1992, our research team assumed that the lethal efficacy of ultrasound was due to cavitation and that the loss of bactericidal effect with increasing temperature was due to decreased water vapour tension. Therefore, increasing the hydrostatic pressure of the system should also increase the cavitation intensity (which could be maintained even at temperatures over 100°C) and, therefore, the lethal efficacy of ultrasound. In order to check the above hypothesis, we constructed an instrument, the manothermoresistometer (Raso et al., 1998a), which allowed the application of heat, ultrasound and combined heat/ultrasound treatments under pressure, at different temperatures (up to 140°C), different pressures (up to 1,000 kPa) and different intensities of ultrasonication (up to 340 W, 170 μm of amplitude at a constant frequency of 20 kHz). In this new combined method of food preservation was called manothermosonication (MTS, Spanish Patent No. 9200686), and the first results concerning its lethal effect on microorganisms were published in the mid-1990s (Raso et al., 1994; Sala et al., 1995). In this section we review the accumulated knowledge in the last 15 years concerning the microbial lethal efficacy of manothermosonication.

2 Lethal Effect of Ultrasonic Waves Under Pressure

One of the major problems when assessing the efficacy of a new method of microbial inactivation concerns the quantification of the lethal effect on cells. In other words, the inactivation kinetics must be determined, and a mathematical equation to describe the survivor's behaviour must be found. By comparing the equation parameters, we will be able to quantify the differences of resistance between species, as well as the effect of various environmental factors. Furthermore, these parameters could be the basis for the development of secondary and tertiary models that would allow the adjustment of the treatment intensity in order to guarantee the achievement of a given inactivation level.

Once the inactivation kinetics has been established, it is important to quantify the efficacy of the new technology in regard to microbial species of reference, which must include both pathogenic and spoilage species. The study of the efficacy

on bacterial spores will allow establishment of the actual possibility of the new technology as a food sterilization method.

2.1 MS/MTS Microbial Inactivation Kinetics

In general, when the kinetics of microbial inactivation by a new technology is first approached, it is intended to adjust the equations of first-order reaction kinetics by using the models already developed for heat. Works carried out by Bigelow (1921) led him to conclude that the number of survivors following heat treatment was an exponential function of time. Therefore, by representing the logarithm of the number of survivors against time, a straight line should be obtained, the so-called survival curve.

The negative inverse of the survival line slope is called D_t, and it is defined as the treatment time at a constant temperature "t" that must be applied to the population in order to reduce the count to a tenth. By representing the logarithm of the D_t value against the corresponding treatment temperatures, a straight line is again obtained. In our research group we denominate this curve the decimal reduction time curve (DRTC), in order to distinguish it from the so-called thermal death time curve (TDT), which was obtained by representing the logarithm of time necessary to achieve a fixed number of logarithmic cycles of inactivation (F value) at each temperature. In any case, if the inactivation follows a strictly exponential course, the DRTC and TDT lines are parallel and the negative inverse of their slope corresponds to the z value. The z value is indicative of the thermodependence of the reactions leading to microbial inactivation and quality loss, and it allows calculation of treatments of similar lethal efficacy at different temperatures.

If one assumes that the microbial inactivation rate follows a first-order kinetics, one must admit that the inactivation is due to the alteration of a unique key molecule that, in the case of heat, has been traditionally associated with DNA denaturizing (Gould, 1989). In this case, the exponential course of the inactivation may be due either to a normal distribution of the resistance of the key molecule against the inactivating agent or to the existence of a distribution of energies in the treatment medium. Thus, in the latter case the quantity of heat received by each molecule would be different. If we assume that the heat resistance of the key molecule is similar in all cells, and that the number of molecules with enough energy to produce the inactivation is kept constant, under this circumstances microbial death would be a probabilistic phenomenon, which explains the fact that a constant percentage of the population becomes inactivated at similar time intervals.

Although the exponential model has been used for years for the calculation of heat treatments, and D_t values are widely used to compare microbial heat resistance, nowadays a number of experimental data showing the existence of linearity deviations of the survival curves have accumulated. The occurrence of such deviations, which are known as shoulder and tail phenomena, does not necessarily mean that the inactivation course does not follow an exponential kinetics, but they may reflect the addition of different events, such as the activation of spores, their simultaneous

inactivation or even their adaptation to heat (Palop et al., 1997). The reader will find further information about survival curve deviations in the classical works by Rahn (1945), Shull et al. (1963), Moats et al. (1971) and Cerf (1977). In the last 20 years, considerable efforts have been made to find alternative mathematical approaches to describe these non-linear kinetics, even to predict the effect of anisothermal heating (Hassani et al., 2005, 2006; Mafart et al., 2002; Peleg, 1999; Peleg and Cole, 1998), but it is difficult to find an unique and final model, since the causes of the deviations largely depend on the microbial species and, above all, on the physiological state of the cells (vegetative cells vs. bacterial spores). No matter the cause of the occurrence of these deviations, their practical consequences are evident: the use of the equations of survival curves and DRTC for the calculation of survival probability of the microbial population will lead to an overestimation of the lethal efficacy of the treatment, with subsequent increased risks for public health. Furthermore, the direct comparison of D_t and z values will not be sufficient to predict which microbial species will limit the intensity of the heat treatment. For similar reasons, it is essential to precisely establish the inactivation kinetics of any food preservation technology.

Our investigations with this technology in the last 15 years allow us to state that the microbial inactivation by MS/MTS fits a first-order kinetics more closely than that of heat, at least for 99.9% of the cell population. Figure 11.1 exemplifies some survival curves obtained with bacterial spores and vegetative cells of gram-positive and gram-negative species. Linearity deviations are very rare and, in general, both the shoulders and the tails shown in the diagrams of survival to heat are minimized when ultrasound under pressure is applied. This effect is well illustrated in works by Sala et al. (1995) and Pagán et al. (1999b). These results are logical if, as discussed

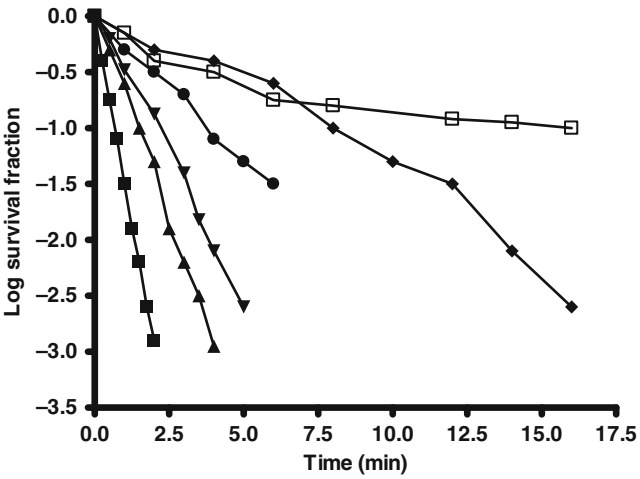

Fig. 11.1 Survival curves for ultrasonic under pressure treatments (40°C, 200 kPa, 117 μm) of *B. subtilis* (□), *B. circulans* (♦), *E. faecium* (●), *S. aureus* (▼), *L. monocytogenes* (▲) and *A. hydrophila* (■)

below, we consider that inactivation by manosonication meets the two necessary requirements so that the inactivation may follow an exponential order: the microbial inactivation by ultrasound under pressure is an "all or nothing" event, with the cell envelopes as the key target; and, the inactivation is due to transitory cavitation, which occurs in specific points of the media and whose intensity is kept nearly constant throughout the treatment, at least in our experimental conditions. Under these circumstances, it is reasonable to think that the percentage of living cells affected by the treatment remain constant throughout time. However, recent investigations have shown that tailing effects may appear when higher levels of inactivation are reached (Lee et al., 2009).

We have found small but frequent shoulders in the survival curves to manosonication with some strains of *Staphylococcus aureus*. In this case, shoulders occur as a result of the initial disintegration of the naturally present cell aggregates, as produced by the shock waves generated by cavitation. Sonication at atmospheric pressure under sublethal conditions provokes an increase in the microbiological count of the suspension, up to the expected N_0 value estimated with the equation of the straight stretch of the survival curve. The appearance of tails is also quite rare, at least when 99.9% of cells of the initial population are inactivated. Under our usual experimental conditions, the counts for less than the 0.1% of the initial cell population have little statistical reliability (usually less than 300 ufc/ml). Occasionally, we have found a tailing phenomenon corresponding to a suspension of *Bacillus cereus*, which cannot be assigned to a methodological device (Sala et al., 1995). Perhaps this suspension contained two sub-populations of the same strain with different resistance to ultrasound, as we have demonstrated with spores of other microbial species against heat (Palop et al., 1997).

In short, microbial inactivation by MS/MTS is an exponential function of the treatment time. Therefore, the $D_{MS/MTS}$ parameter can be defined as the treatment time necessary so that the survival line goes through a logarithm cycle. Similar to heat treatments, the time of an industrial treatment can be calculated by multiplying the $D_{MS/MTS}$ value by the number of inactivation cycles we intend to achieve.

As described below, D_{MS} values are influenced by a number of physical parameters of the treatment, whereas heat resistance depends only on temperature. Therefore, up to now, we had not tried to develop a DRTC for manosonication. The data by Raso et al. (1999) prove the existing relationship between the amplitude of ultrasonic waves, the hydrostatic pressure of the system and the energy transmitted to the medium by ultrasound. The data by Mañas et al. (2000a) demonstrate that the lethal efficacy of ultrasound is related to the energy transmitted to the medium. Figure 11.2 shows the relationship existing between the logarithm of D_{MS} values of *Listeria monocytogenes* and the energy transmitted to the medium by the ultrasonic waves at different amplitudes (62, 90 and 117 μm) and pressures (0, 100, 200 and 300 kPa). As shown in the figure, the decimal reduction time to the MS treatment is an exponential function of the energy transmitted to the medium by ultrasound and, therefore, similar to heat treatments, a Z_{MS} value can be defined. In the example $Z_{MS} = 56.2$, which means that an increase in 56.2 W in the energy transferred to the medium by the ultrasound, the inactivation rate of *L. monocytogenes* will be

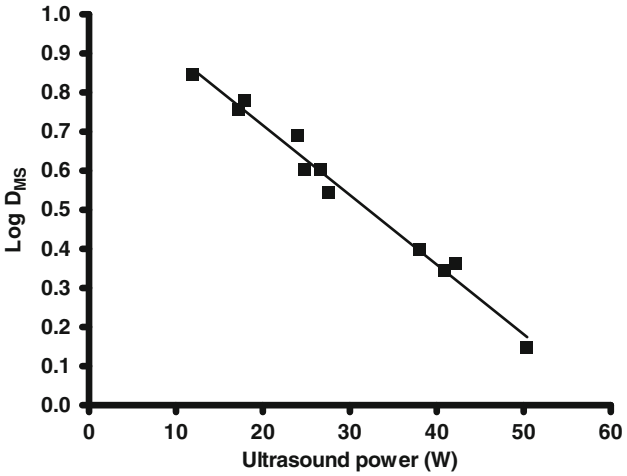

Fig. 11.2 Decimal reduction time curve of *L. monocytogenes* to manosonication

increased by 10 times. Later, we will discuss the effect of pressure and amplitude on the energy transferred to the medium by the ultrasound, as well as on the lethal efficacy.

2.2 Microbial MS/MTS Resistance

As mentioned in the corresponding sections, cavitation intensity is influenced by a multitude of physical parameters (wave frequency and amplitude, pressure, viscosity and temperature of the medium, etc.), but the geometry of the chamber and that of the sonication horn is also important. Since cavitation is limited to an area close to the transducer (the intensity of ultrasonic waves being inversely proportional to the square of the distance to the sonication tip), the effect of ultrasound depends on the shape and volume of the treatment chamber. Furthermore, cavitation should not take place too close to the horn's tip, as the bubbles generated could attenuate the effect by dispersing sonic waves (Berlan and Mason, 1992). The geometry and size of the horn also determine the energy transmitted to the medium (Berliner, 1984). The characteristics of the treatment medium can also affect the intrinsic resistance of the microorganism against MS/MTS. Because of all the above, it is very difficult to compare the values of resistance to ultrasound obtained by different investigators with different methodologies. In this chapter, we will use mainly those data obtained by our research group with the same equipment, previously described by Raso et al. (1998a). All data included in tables and figures in this section were obtained in a McIlvaine buffer of pH 7; therefore, the D_{MS} values in Table 11.1 are directly comparable.

Table 11.1 D_t(62°C) and D_{MS}(40°C, 200 kPa, 117 μm) values of different bacterial species

Bacterial species	$D_{62°C}$(min)	D_{MS}(min)
Bacterial spores		
B. subtilis	Insensitive	10
B. circulans	Insensitive	6.5
B. coagulans	Insensitive	9
Gram-positive vegetative cells		
L. monocytogenes	0.62	1.5
E. faecium	15.3	4.0
S. aureus	0.5	2.5
Gram-negative vegetative cells		
Y. enterocolitica	0.39	1.2
P. aeruginosa	0.18	0.92
E. coli	0.012	0.87
S. enteritidis	0.068	0.73
S. typhimurium	0.12	0.80
S. senftenberg	1.1	0.84
A. hydrophila	0.024	0.86

Table 11.1 shows the D_{MS} values of different bacterial spores and vegetative species, both gram positive and gram negative. Their resistance to heat is also included as a reference. The data in the table indicate that it is possible to inactivate bacterial spores at sublethal temperatures; therefore, MS treatments could be used as a food sterilization method, although the D_{MS} values for spores are relatively high in the experimental conditions tested. We should also highlight the small difference concerning resistance to ultrasound under pressure between the three species of spore formers investigated, as compared to their heat resistance. Whereas the D_{100} values of *Bacillus circulans* differ practically 10 times in regard to those of *Bacillus coagulans* ($D_{100} = 0.47$ and 5.0, respectively) (Mañas, 1999; Raso, 1995), the D_{MS} values barely differ by about 30%. Finally, it is worth highlighting that resistance against ultrasound is about 10 times higher in spores than in vegetative cells, a negligible difference in regard to the 10^7 times that their resistance to heat changes.

As far as vegetative cells are concerned, it can be concluded that gram-positive species are more resistant to manosonication, as well as against heat, than gram-negative species. As in the previous case, the differences between the D values of both groups are much lower against manosonication than against heat. Within the gram-positive group, whereas the heat resistance of *S. aureus* is lower than that of *L. monocytogenes*, the opposite occurs in regard to manosonication. This could indicate that spherical cellular shapes are more resistant to MS than bacillary cells, as previously suggested for ultrasound at ambient pressure (Alliger, 1975; Jacobs and Thornley, 1954). The gram-negative group is the most sensitive against heat and manosonication. However, as in the above-mentioned groups, differences in resistance to MS among genera and strains are lower than to heat. It is also worth mentioning that whereas the heat resistance of *Salmonella senftenberg* 775 W is

10–100 times higher than that of the rest of species, its resistance against MS is about in the middle of the range. A similar phenomenon has been observed when studying the resistance of *Salmonella* against irradiation (Álvarez et al., 2006b) and high pressure (Sherry et al., 2004).

The above results imply that the mechanisms of inactivation by heat and manosonication are different, although the target molecule might not be different. In any case this behaviour may have remarkable practical consequences. Current pasteurization treatments are calculated by establishing a determined survival risk for the most heat-resistant pathogenic species that can usually be expected to contaminate the food. Under these circumstances, if the raw material is contaminated by other pathogenic species that are less frequent but more heat resistant, the increased safety risk may be enormous. On the contrary, considering the scarce differences in resistance to MS, a change in the pathogenic species that usually contaminate the food would have a much smaller effect on the safety of the product pasteurized by MS. For example, according to the data included in Table 11.1, we can conclude that current pasteurization treatment of liquid whole eggs in the USA (3.5 min at 60°C, which would be equal to 1.81 min at 62°C) would allow the reduction of the population of our strain of *Salmonella typhimurium* by 15 logarithmic cycles, which exceeds by far the usually recommended 7–8 logarithmic cycles. However, if liquid whole egg is contaminated by the strain of *S. senftenberg* 775 W (data included in Table 11.1), the treatment would allow reduction of the microbial population by 1.64 cycles only. In other words, the safety risk would increase by $10^{13.36}$. On the contrary, an MS treatment designed to inactivate, as in the previous case, the population of *S. typhimurium* by 15 cycles (12 min, 40°C, 200 kPa, 117 μm) would also reduce the population of *S. senftenberg* by 14.28 cycles, i.e. the safety risk would not increase more than five times, although the serotype of the *Salmonella* contaminating the liquid egg would change. An additional advantage of MS in the above-mentioned example would be its effect on the spores of *B. circulans*, which is a usual spoilage agent of ultrapasteurized liquid whole egg. Whereas the above-mentioned treatment of heat pasteurization would not affect its viability at all, the corresponding MS treatment would allow a reduction of the population of *B. circulans* by 70 times, which would probably contribute to the extension of its shelf life. Obviously, there are not only advantages; whereas the heat treatment of the example would be 1.8 min at 62°C, the manosonication should be extended for 12 min. However, this MS treatment would still be more efficient to inactivate *S. senftenberg* and *B. circulans* than pasteurization at 62°C for 12 min.

3 Effect of Physical Parameters on the MS/MTS Lethal Effect

The lethal efficacy of MS/MTS depends on the cavitation intensity, which is highly influenced by a multitude of physical parameters. Among these, ultrasonic wave amplitude, pressure of the medium and temperature are the most significant, from a practical point of view. Other parameters, including viscosity, are also very

important, but they cannot be easily modified in an industrial process. Therefore, their relevance, for our purposes, is lower. Further information concerning the influence of these variables on the energy transmitted to the medium by the ultrasound in our equipment can be found in Raso et al. (1999) and Condón et al. (2005).

3.1 Effect of the Amplitude of Ultrasonic Waves

The amplitude of ultrasonic waves influences cavitation intensity by determining the number of bubbles that implode by time unit (Suslick, 1988). Therefore, this parameter should be carefully controlled and maintained during sonication (Berliner, 1984). The data published by Raso et al. (1999) and Mañas et al. (2000a) demonstrate that, in our equipment, the energy transmitted to the medium by MS/MTS is an exponential function of the amplitude of the sonic waves. Furthermore, we have demonstrated that the lethal efficacy of MS at constant pressure and temperature is also an exponential function of the amplitude, i.e. the logarithm of the D_{MS} values decreases linearly with the ultrasonic wave amplitude, both in bacterial spores (Raso et al., 1998b) and vegetative cells of gram-positive species, e.g. *L. monocytogenes* (Pagán et al., 1999a) and *Enterococcus faecium* (Pagán et al., 1999c), and in gram-negative species, e.g. *Yersinia enterocolitica* (Raso et al., 1998a), *Aeromonas hydrophila* (Pagán et al., 1999c), *Salmonella enteritidis*, *S. typhimurium* and *S. senftenberg* (Mañas et al., 2000b).

Since it seemed that the effect of ultrasonic waves on D_{MS} values was the same for all vegetative cells investigated, we developed the following general equation:

$$\log D_{MS} = \log D_0 - 0.0091 \times (A - 62)$$

where D_{MS} is the decimal reduction time to MS, D_0 is the decimal reduction time to MS at an amplitude of 62 μm and A is the amplitude of ultrasonic waves.

The above equation fits all data obtained in our investigations (Álvarez, 2000; Mañas, 1999; Pagán, 1997) between 62 and 150 μm of amplitude, for the different species, with a correlation higher than 0.98. The good fit of the above equation has been well demonstrated by the works of Pagán et al. (1999c), Mañas et al. (2000b) and Condón et al. (2005). The equation parameters imply that the inactivation rate of vegetative cells by ultrasound will increase by 10 times when increasing the amplitude of ultrasonic waves by 110 μm. At present, there are no sufficient experimental data available that allow demonstration of the utility of the above equation to predict the inactivation of bacterial spores by MS.

The good fit of this unique equation to the experimental data obtained with different microbial species, whose resistance to manosonication varies about 10 times (Table 11.1), indicates that the effect of the amplitude is not related to a change in the intrinsic resistance of each species, but, most likely, to its physical effects. The existence of an exponential relationship between the energy transmitted to the medium by ultrasound and the amplitude of the ultrasonic waves (Mañas et al.,

2000b; Raso et al., 1999) seems to confirm this hypothesis. Bacterial inactivation by ultrasound seems to be due to very high pressure and temperature (Frizzell, 1988; Harvey and Loomis, 1929) and/or to the release of free radicals in the medium (Jacobs and Thornley, 1954; Riesz and Kondo, 1992) by transient cavitation. The higher inactivation rate at greater amplitudes could be due to an increase of the number of bubbles liable to implode per unit of time in a given volume and/or to an increase of the volume of liquid in which transient cavitation is liable to occur (Suslick, 1990).

3.2 Effect of Hydrostatic Pressure

When the hydrostatic pressure of a system increases, the intramolecular cohesion forces are strengthened, which reduces the tension of the vapour of the solvent and increases its viscosity. Both circumstances hinder the transient cavitation phenomenon. However, if the generator's power is sufficient to maintain the amplitude of the ultrasonic waves and cavitation occurs, its physicochemical and biological effects are higher (Berliner, 1984). We have demonstrated (Mañas et al., 2000a; Raso et al., 1999) that, in our equipment, the energy released to the medium by ultrasound increases exponentially with the hydrostatic pressure, until reaching a threshold value that depends on the temperature. Above this threshold, the effect of pressure progressively decreases, until it vanishes. A similar relationship has been found when correlating the D_{MS} values and the hydrostatic pressure of the medium (Fig. 11.3), both in bacterial spores (Raso et al. 1998b) and in vegetative cells (Mañas et al., 2000b; Pagán et al., 1999a; Raso et al. 1998a).

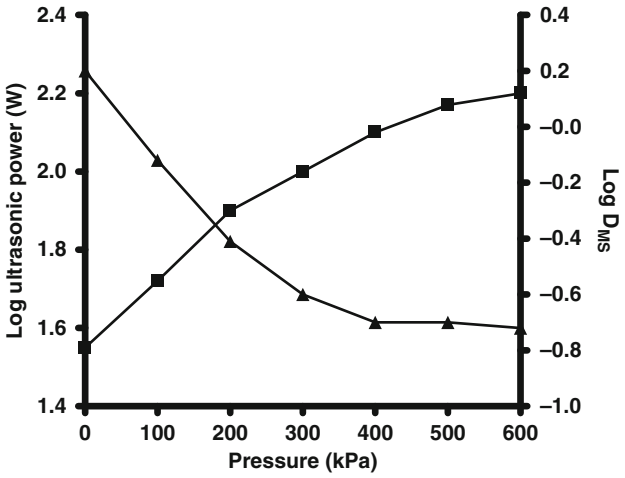

Fig. 11.3 Effect of pressure on ultrasonic output power (■) and on lethality of ultrasound (▲) (40°C, 20 kHz, 150 μm)

In 1999c Pagán et al. developed the following polynomial equation:

$$\log D_{MS} = \log D_0 - 0.0026 \times P + 2.2 \times 10^{-6} \times P^2$$

where D_{MS} is the decimal reduction time corresponding to an MS treatment at an amplitude of 117 μm and 40°C, D_0 is the D value corresponding to ultrasonic treatment of the same amplitude and temperature but at room pressure and P is the static relative pressure.

This general equation allows the adjustment of all D_{MS} values of vegetative cells obtained in our equipment, at sublethal temperatures (up to 40°C) and at different pressures (up to 400 kPa) (Mañas et al., 2000b; Pagán et al., 1999a; Raso et al., 1998a), with a correlation that is always higher than 0.98. The good fit of the experimental data to this general equation is supported by the works of Mañas et al. (2000b) and Condón et al. (2005). According to this equation, an increase of the pressure of the system from 0 to 400 kPa of relative pressure reduces the D_{MS} values by approximately five times. At present, there are not enough available data allowing demonstrating the adequacy of this equation to predict the effects of the pressure of the system on the lethal efficacy of manosonication on bacterial spores. The only available data (Raso et al., 1998b) seem to indicate that the percentage of survivors of a spore population of *Bacillus subtilis* subjected to MS treatment (250 kHz, 117 μm, 70°C) during a fixed time exponentially decrease with pressure up to 500 kPa. Above this threshold value, the lethal efficacy of the process decreases. The difference between the threshold values above which the increase of pressure barely affects the efficacy of MS on vegetative cells (300–400 kPa) and spores (500 kPa) is most probably due to the different treatment temperatures used (40 and 70°C, respectively). Raso et al. (1999) demonstrated that if the temperature of the manosonication medium is increased, the pressure of the system must be increased as well in order to achieve a constant power output. They also proved that the curve correlating both variables shows a profile similar to the water vapour pressure curve.

As with the amplitude, a good fit of a unique equation to the experimental data obtained at different pressures with different species showing a different resistance to MS would indicate that the differences in cell structure do not affect the effect of pressure, which will most likely be related to changes in cavitation intensity. Increased pressure will affect the occurrence of cavitation, but if cavitation takes place, the intensity of the implosion will be increased (Whillock and Harvey, 1997) and, therefore, its lethal effects. When a particular pressure threshold is reached, the ultrasonic field will be incapable of overcoming the combined forces of overpressure and the cohesive force of the liquid molecules, and the number of bubbles undergoing cavitation will decrease (Suslick, 1988), as well as the microbial inactivating effects of the treatment. This is a significant aspect that should be taken into account when trying to establish the optimum pressure of treatment in an eventual industrial process, where an increased pressure not always will lead to increased lethal efficacy.

3.3 Effect of Temperature

The earliest bibliographic references about the effect of temperature on the bactericidal efficacy of ultrasound date back to the 1970s. At that time it was demonstrated that prior ultrasonic treatment sensitizes bacterial spores to subsequent heat treatment (Burgos et al., 1972). Some years later, it could be proven that the application of ultrasound at high temperatures synergistically increased the efficacy of the combination on spores (García, 1985). In the 1980s, Ordóñez et al. (1986) proposed the name "thermoultrasonication" to designate this combined process. Thermoultrasonication has proven to be efficient in inactivation of vegetative cells of different species (Earnshaw et al., 1995; Hurst et al., 1995; Ordóñez et al., 1984) and, in some temperature ranges, on bacterial spores (García et al., 1989). However, in the latter, the sensitizing effect of heat decreased with temperature, until it practically vanished at temperatures close to the boiling point (García, 1985).

Changes in the lethal efficacy of ultrasound at different temperatures may be attributed to direct and indirect mechanisms. As discussed below, the increased temperature of the medium may determine some structural changes in the envelopes of vegetative cells, which would lose a part of their mechanical resistance. Nevertheless temperature can also act by modifying cavitation intensity, although this effect can be misleading. Bubbles form and grow more quickly as the temperature of the liquid becomes higher, because vapour pressure increases and tensile strength decreases (Suslick, 1988). However, the violence of these collapses is lower, because high vapour tension inside the bubble acts as a cushion (Alliger, 1975). The final biological effect of the combination of heat and ultrasound will depend on the balance between these opposite phenomena, whose relative significance will also depend on the range of temperatures under study. Since the slope of the vapour tension line progressively increases with temperature, the undesirable effects on cavitation intensity will increase as well, especially at temperatures higher than 70–80°C (Raso et al., 1999). This physical phenomenon can easily explain the loss of efficacy of thermoultrasonication on bacterial spores, as described by García (1985).

Sala et al. (1992) developed an instrument that allowed application of ultrasonic treatments at different pressures and temperatures. We demonstrated that it was possible to maintain the bactericidal efficacy of ultrasound even at temperatures higher than 100°C, just by increasing the hydrostatic pressure of the system. We named this new combined process "manothermosonication". From a theoretical point of view, if the cavitation intensity depended only on changes of the vapour tension of the solvent, such intensity could be maintained by keeping constant the difference between the hydrostatic pressure of the system and the vapour pressure of the solvent at treatment temperature. Actually, there are small deviations (Raso, 1995), as heating produces other changes, including decreased viscosity, which also influences cavitation.

On the other hand, in order to study the influence of temperature on the microbial lethal efficacy of ultrasound at constant cavitation intensities, the hydrostatic pressure of the system should be constantly corrected. However, in practice, values sufficiently close to constant pressure can be obtained, provided that the differential

pressure is very high with regard to changes of vapour pressure of the solvent within the range of temperatures under study. These conditions occur between room temperature and 70°C, a range where the slope of the vapour tension line is very low. Raso et al. (1999) demonstrated that at 200 kPa a change of temperature from 20 to 70°C barely modifies the energy transmitted to the medium by ultrasound by 10%.

Figure 11.4 shows the relationship existing between the $D_{MS/MTS}$ values (20 kHz, 117 μm, 200 kPa) and the treatment temperature for two species (i.e. *L. monocytogenes* and *A. hydrophila*) with high and low resistance to manosonication. The corresponding decimal reduction time curves (DRTC) against heat, as well as a theoretical curve obtained through a predictive model developed by our group (which will be discussed below), are also included for reference purposes. As shown in the figure, resistance to ultrasonic treatments under pressure is kept practically independent from temperature until reaching a threshold value, above which the $D_{MS/MTS}$ values decrease rapidly until becoming equal to D_t values. This behaviour implies that inactivation by ultrasonic waves under pressure and inactivation by heat are two independent processes. At low treatment temperatures (sublethal temperatures), the lethal effect of the treatment would only be due to the action of ultrasonic waves under pressure. When lethal temperatures are reached, the independent inactivating effects of ultrasonic waves under pressure and heat would be added. Thus, the total lethal effect achieved would be equal to the addition of the lethal effects produced by each technology, i.e. an additive effect. From this point, whereas the lethal efficacy of ultrasonic waves under pressure would remain constant when increasing the temperature, the lethal effects of heat would increase exponentially, and the contribution of the ultrasonic waves under pressure to the total lethal effect would obviously decrease, until it would practically disappear and the $D_{MS/MTS}$ values

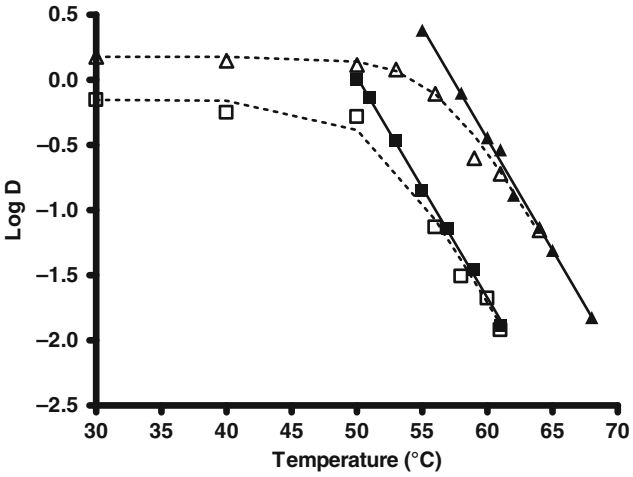

Fig. 11.4 Theoretical (*dotted line*) and experimental (*symbols*) D_{MS} values (200 kPa, 117 μm) of *L. monocytogenes* (▲) and *A. hydrophila* (■). *Straight lines* represent the corresponding decimal reduction time curves to heat treatments

would equal the D_t values. The above results encouraged us to distinguish two processes, which we called manosonication (MS) and manothermosonication (MTS). Manosonication is the process in which heat has no lethal effect and depends on cavitation intensity only. Manothermosonication is a similar process, in which the lethal effects of ultrasound under pressure and those of heat would be added. Obviously, the temperature at which the MS process becomes MTS will depend on the microbial species under study and, more specifically, on its resistance to heat. The data in Fig. 11.4 imply that MS would become MTS at 50 and 55°C approximately, for *A. hydrophila* and *L. monocytogenes*, respectively.

In order to check the above hypothesis indirectly, we developed a predictive model that allowed us to compare experimental values and theoretical values estimated by assuming that microbial death by ultrasound under pressure and by heat is caused through different and independent mechanisms of action, and that, in both cases, the inactivation follows an exponential kinetics. Under these conditions, the course of microbial inactivation by heat, MS and MTS would meet the following equations:

$$\begin{aligned} \log N_t &= \log N_0 - (1/D_t) \times t \quad \text{for heat} \\ \log N_t &= \log N_0 - (1/D_{\mathrm{MS}}) \times t \quad \text{for manosonication} \\ \log N_t &= \log N_0 - (1/D_{\mathrm{MTS}}) \times t \quad \text{for manothermosonication} \end{aligned}$$

where N_t is the number of cells surviving after a treatment time "t", N_0 is the number of living cells in the time t=0 and D_t, D_{MS} and D_{MTS} are the corresponding decimal reduction times.

If heat and ultrasound under pressure act in an independent manner, the inactivation rate by MTS can be estimated from the individual inactivation rates by MS and heat. This will allow deduction of the relationship existing between the decimal reduction times against each technology through the following equation:

$$D_{\mathrm{MTS}} = (D_{\mathrm{MS}} \times D_t)/(D_{\mathrm{MS}} + D_t)$$

The dotted lines in Fig. 11.4 represent the estimations of $D_{\mathrm{MS/MTS}}$ values for *A. hydrophila* and *L. monocytogenes* at different temperatures, as obtained with the above equation. The good fit of the experimental data to theoretical estimations seems to confirm the starting hypothesis. This equation allowed us to estimate the D_{MTS} values at different temperatures of most vegetative cells investigated, both gram positive (*L. monocytogenes,* Pagán et al., 1999a) and gram negative (*Y. enterocolitica*, Raso et al., 1998a; *A. hydrophila*, Pagán et al., 1999c; *S. enteritidis, S. typhimurium* and *S. senftenberg*, Mañas et al., 2000b). These results indicate that microbial inactivation by ultrasonic waves under pressure is independent of temperature when the cavitation intensity is kept constant. However, in the past few years, we have found some cases in which the lethal effect of MTS is synergistic, i.e. the total lethal effect of the treatment is higher than the mere addition of the lethal effect of ultrasound under pressure plus heat. This topic will be further discussed in Section 5.

3.4 Interactions

As mentioned in the above sections, the rate of microbial inactivation by ultrasonic waves exponentially increases with hydrostatic pressure, but only up to a definite threshold value, above which it may even decrease. Moreover, in narrow temperature ranges and below 70°C, the lethal effect of ultrasound barely depends on temperature when the pressure is kept above 200 kPa. Investigations supporting these conclusions were designed, keeping constant two of the three parameters and

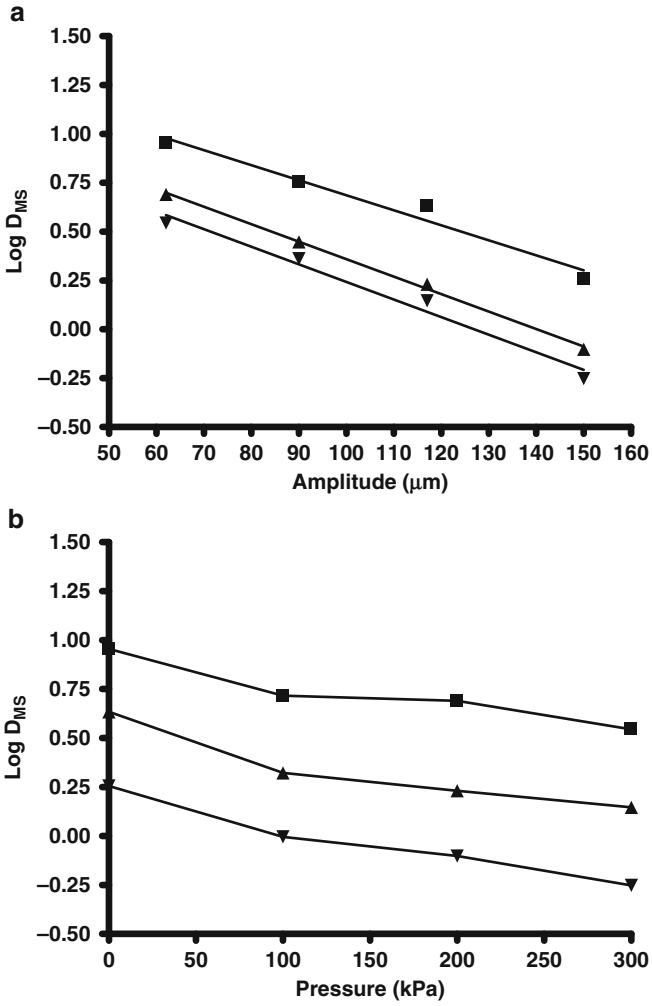

Fig. 11.5 (**a**) Effect of amplitude on D_{MS} values of *L. monocytogenes*: 0 kPa (●), 200 kPa (▲) and 300 kPa (■). (**b**) Effect of pressure on D_{MS} values of *L. monocytogenes*: 62 μm (●), 117 μm (▲) and 150 μm (■)

modifying only the third one, which raises a doubt about their eventual interactions. This is an interesting aspect about which, as far as we know, there are no data available except those by Pagán (1997).

Figure 11.5a,b shows the relationship between amplitude of ultrasonic waves and D_{MS} values for *L. monocytogenes* at various treatment pressures and the relationship between D_{MS} values of the same species and hydrostatic pressure at various amplitudes, respectively. These results indicate that the effect of amplitude is independent of pressure and vice versa. Raso et al. (1999) demonstrated that the increase of energy transmitted to the medium by increased amplitude was independent of the pressure of the system at constant temperature, which seems to indicate that the lethal efficacy of MS depends only on cavitation intensity, no matter if the changes of intensity occur by modifying the pressure, the amplitude or both variables.

4 Environmental Factors Affecting Bacterial MS/MTS Resistance

It is a well-known fact that microbial resistance against any inactivation agent has a genetic component, but it is also influenced by a multitude of environmental factors such as growth conditions and treatment media. Actually, in regard to some technologies such as heat, these environmental factors may even mask those differences that are genetically defined (Pagán et al., 1999c, d; Stumbo, 1965; Tomlins and Ordal, 1976). Therefore, it is important to determine the effect of these environmental factors on the resistance against the inactivating agent under study for every species of reference, since the species limiting the treatment may change in each specific situation.

The factors that may modify the microbial resistance vary greatly, and these factors have been traditionally classified, according to the moment in which they act, as either previous or simultaneous to treatment. Among the former, temperature of growth and stress factors are the most relevant; among the latter, pH, water activity and chemical composition of the medium are the most investigated. Sometimes, a third group of factors, which act "after the treatment", is also included, but these are actually related to the phenomena of cell damage and recovery, and they will be discussed in Section 5.

Table 11.2 summarizes the data currently available on this topic, under conditions of reference. These data were obtained by different researchers in our group (Álvarez, 2000; Álvarez et al., 2003b, 2006a; Mañas, 1999; Mañas et al., 2000a; Pagán, 1997; Pagán et al., 1999a, c; Raso, 1995) over the course of 15 years, but using the same equipment and with a similar methodology, which allows their direct comparison.

4.1 Factors Prior to Treatment

It is well known that changes in growth temperature induce some changes in cell envelopes, which can largely modify their resistance to different lethal agents. This

Table 11.2 Effect of some environmental factors on the D_{MS} (40°C, 200 kPa, 117 μm) values of different bacterial species

	Growth temperature (°C)			Treatment medium pH		Water activity			Medium Composition			Heat shock	
	37	20	4	7.0	4.0	>0.99	0.96	0.93	Buffer	Milk	Egg	Non-HS	HS
L. monocytogenes	1.5	–	1.5	1.5	0.96	1.6	–	3.1	1.5	1.8	–	1.7	1.6
Y. enterocolitica	0.31	0.59	0.81	0.89	1	–	–	–	0.81	0.82	–	–	–
A. hydrophila	0.69	0.23	–	–	–	–	–	–	–	–	–	–	–
S. typhimurium	0.80	0.81	–	–	–	–	–	–	0.80	–	0.84	–	–
S. enteritidis	–	–	–	0.73	0.56	0.89	1.3	–	0.73	–	0.76	–	–
S. senftenberg	–	–	–	0.84	0.96	1.7	2.1	1.8	0.84	–	1.4	0.85	0.78

is especially significant when the inactivating agent specifically acts on these structures, as in the case of MS (see Section 5). Amazingly, growth temperature barely affects the MS resistance of any of the species investigated, as compared with changes in their resistance to heat. For example, an increase of growth temperature from 4 to 37°C in *L. monocytogenes* increases its heat resistance by 2.1 times (Pagán et al. 1999a), but it does not affect its resistance to MS.

From a scientific point of view, the influence of this factor on the MS resistance of *Y. enterocolitica* is particularly interesting. Pagán et al. (1999d) demonstrated that the heat resistance of this microorganism was independent of culture temperature between 4 and 20°C, but in cells grown at 37°C, the D_{62} values increased by a factor of 4. These results may be explained by the increase in the ratio of saturated to unsaturated fatty acids of the cell membrane. Tsuchiya et al. (1987) found that an increase of the culture temperature from 5 to 25°C barely changed the composition of the cell membrane of *Y. enterocolitica*, but a further raise to 37°C increased that ratio drastically. On the contrary, as results in Table 11.2 show, the MS resistance of *Y. enterocolitica* exponentially decreases with increased growth temperature, which would indicate that the mechanisms through which ultrasound and heat treatments affect the cell membrane are different and that the composition in fatty acids does not affect its MS resistance.

Heat shocks develop a degree of protection against subsequent heat treatments in microorganisms (Lindquist, 1986; Mackey and Derrick 1986). Heat shocks trigger a physiological response that leads to the synthesis of a specific set of proteins known as heat shock proteins (HSPs) (Lindquist, 1986; Schlesinger 1986). The action mechanism of HSPs is not fully understood. Parsell and Lindquist (1993) suggested that, among others, the role of HSPs could be to prevent the accumulation of aberrant proteins generated by stress and also to protect the original structure and metabolic activity of other important proteins by avoiding their aggregation and by restoring heat damage. Pagán et al. (1999b) carefully studied the effect of time and temperature of heat shocks on the heat resistance of the strain *of L. monocytogenes* included in Table 11.2. Their work indicated that the probability of survival to heat of a population of this strain increased by thousands of times after being subjected to a sublethal heat shock. On the other hand, the heat shocks changed the profile of the survival curves, which showed prolonged shoulders in the case of heat-shocked cells. Furthermore, their results proved that the higher heat resistance of the shocked cells was partly due to a higher thermal stability of their cell structures and partly due to a higher capacity of damage repair. As shown in Table 11.2, sublethal heat shocks do not protect *L. monocytogenes* and *S. senftenberg* against manosonication. These results imply that heat shocks do not stabilize the cell structures against ultrasound. Moreover, they indicate that either sublethal damages previous to the inactivation by MS do not occur or the shocks do not increase the capacity of repairing the damages caused by ultrasound.

As mentioned above, the lethal effect of manothermosonication was additive on most species investigated. However, the only work existing on this topic (Pagán et al., 1999b) implies that when MTS (62°C, 200 kPa, 117 μm) is applied to heat-shocked cells (180 min at 45°C) of *L. monocytogenes*, the combination shows a

synergistic effect, as it reduces the population 10 times more than expected after 1.5 min treatment. This synergistic effect on heat-shocked cells when heat and ultrasonic waves under pressure (MS) act simultaneously (MTS) could be due to a lower resistance to MS of the cells damaged by heat during the MTS treatment. In order to check this hypothesis, the authors compared the lethal efficacy of MTS and that of a treatment in which the heat treatment (1.5 min at 62°C) and the MS treatment (1.5 min, 200 kPa, 117 μm) were applied successively and not simultaneously. The authors demonstrated that the previous heat treatment makes the cells more sensitive against manosonication, but its lethal effect does not equal that of the corresponding MTS. They concluded that, most likely, ultrasound interferes with the phenomena of recovery of the damages inflicted by heat, and that heat alters the physical characteristics of the cell envelopes by sensitizing them against ultrasound.

4.2 Factors Simultaneous to Treatment

The pH is one environmental factor with high influence on microbial resistance to different technologies, such as heat (Jay, 1992; Pagán, 1997; Tomlins and Ordal, 1976), high pressure (Alpas et al., 2000; Koseki and Yamamoto, 2006; Mackey et al., 1995; Stewart et al., 1997; Wouters et al., 1998) and pulsed electric fields (Álvarez et al., 2000, 2002; Aronsson and Rönner, 2001; Aronsson et al., 2004; García et al., 2003, 2005; Geveke and Kozempel, 2003). Acidification, besides its remarkable depressing effect on resistance, is easily modifiable in foods. Therefore, it is frequently applied in the food industry. Contrary to most other technologies, the pH of the treatment medium barely affects microbial resistance to MS. As Table 11.2 shows, a reduction of pH from 7.0 to 4.0, which reduces the D_t values of *L. monocytogenes* by four times (Condón et al., 2005), only reduces its D_{MS} value by 1.6 times. The effect on other studied species is even lower. At present, the mechanism of sensitization to heating in media of low pH is not known with accuracy. It has been suggested that acidification of the medium could facilitate the denaturation of cellular proteins by physical agents (Bender and Marquis, 1985) and/or produce lixiviation of divalent cations from cell envelopes, thereby reducing their resistance (Alderton et al., 1964; Ando and Tsuzuki, 1983). The lethal effect of MTS on *L. monocytogenes* cells treated in acid media has, as in neutral media, an additive effect (Pagán, 1997).

According to published data, water activity is the parameter most influential on microbial resistance to different physical agents of inactivation. For example, it has been demonstrated that the reduction of water activity of the treatment medium may increase bacterial resistance to heat by hundreds of times (Kwast and Verrips, 1982; Sumner et al., 1991). There are only two works (Álvarez et al., 2003b, 2006a) dealing in detail with the influence of water activity on the resistance *of S. enteritidis* and *S. senftenberg* to MS/MTS and only one brief reference to its effect on *L. monocytogenes* (Pagán et al., 1999a). A reduction of water activity from 0.99 to 0.96 increases the D_t values of *S. enteritidis* by 30 times, but it barely increases its D_{MS} value twofold (Álvarez et al., 2003b). Similarly, the reduction of water activity from

0.99 to 0.93, which increases the D_t values of *S. senftenberg* by four times, does not increase its resistance to MS (Álvarez et al., 2006a). The addition of 57% (w/v) of sucrose to the treatment medium increases the D_{61} value from 0.22 to 5.7 min and the D_{MS} from 1.5 to 3.1 min. These results indicate that the hypothetical advantages of a pasteurization treatment by MS in regard to heat pasteurization will be higher in foods with low water activity.

Contrary to what happens in media with water activity close to 1, at low water activities the lethal efficacy of MTS is the result of a synergistic effect. Figure 11.6 shows that the influence of treatment temperature on the $D_{MS/MTS}$ values of *S. enteritidis* treated in media of water activity = 0.96. The figure includes, as a reference, a theoretical curve calculated by assuming that the total lethal effect is the addition of the independent effects of ultrasound under pressure and heat. As the figure demonstrates, the D_{MS} values are remarkably lower than expected between 50 and 65°C. For example, at 50°C, the lethal efficacy of manosonication is four times higher than expected. Álvarez et al. (2006a) demonstrated that the lower the water activity of the treatment medium, the higher the synergistic effect. They developed a tertiary mathematical model able to predict the survival of *S. senftenberg* to MTS in media of different water activity.

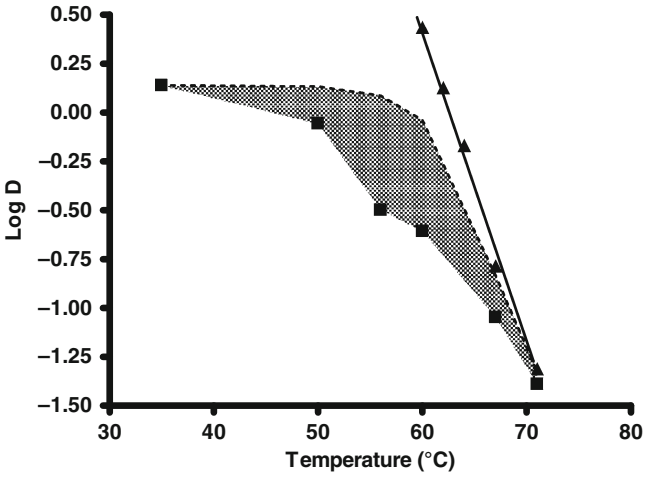

Fig. 11.6 Resistance of *S. enteritidis* to ultrasound (117 μm) under pressure (175 kPa) at different temperatures in medium with a_w = 0.96. Decimal reduction time values to ultrasonic waves under pressure (■) and to heat (▲) are shown. The *dotted line* represents the theoretical DRTC to ultrasonic waves under pressure calculated with the equation $D_{MTS} = (D_t \times D_{MS})/(D_t + D_{MS})$

It has been demonstrated that increased heat resistance in media of low water activity is partly due to a stabilization of the cell structures against heat and partly due to a higher capacity of repairing the damages inflicted by heat (Álvarez et al., 2003d). Microbial inactivation by MS at low water activities is, as in high water

activities, an "all or nothing" event, which could partly explain the small influence of this factor on resistance to MS.

It is well known that bacterial thermal tolerance changes with heating media (Doyle and Mazzotta, 2000; Mañas et al., 2001; Murphy et al., 2000; Tomlins and Ordal, 1976). It has been suggested (Hansen and Riemann, 1963; Mañas et al., 2001) that these changes in resistance could be due to pH and/or to water activity differences. However, some authors (Condón and Sala, 1992; Mañas et al., 2001) have demonstrated that microorganisms can show different heat resistance in several media with the same pH. It has also been demonstrated that microorganisms suspended in media of the same water activity, through the addition of different solutes, can show different thermal sensitivities (Baird-Parker et al., 1970; Corry, 1974; Mañas et al., 2001). Therefore, it could be concluded that chemical components, regardless of pH and water activity, could protect bacterial cells against heat treatments. Similar results have been obtained when comparing resistance to high hydrostatic pressure (Hauben et al., 1998; Patterson et al., 1995; Simpson and Gilmour, 1997) and to pulsed electric fields (Grahl and Märkl, 1996; Hülsheger et al., 1981) both in laboratory media and food. Table 11.2 shows that MS resistance barely changes in laboratory media and liquid foods, such as milk or liquid whole egg. At present, all of the mechanisms involved in the increased heat tolerance are not accurately known. Mañas et al. (2001) demonstrated that, at least in milk and liquid whole egg, the entire heat protective effect of foods on microbial resistance was not the result of the addition of the protective effect of each component, but the result of a synergistic effect of the interaction of some of the components. We demonstrated that low-molecular weight milk components protected *S. senftenberg* envelopes against heat by a mechanism involving divalent cations (Mañas et al., 2001). According to the data included in Table 11.2, this increased thermostability of cell envelopes is not accompanied by an increased mechanical resistance to shock waves generated by cavitation.

4.3 Summary

From the results discussed in the above sections it can be deduced that, contrary to what happens with other preservation technologies, environmental factors have very little effect on MS resistance. Figure 11.7 summarizes and exemplifies the effect of each factor investigated on the resistance of *L. monocytogenes* to heat and to MS. As shown in the figure, whereas the D_t values may vary about 100 times depending on the growth conditions and the kind of treatment medium, the D_{MS} values change barely by twofold.

The above observations imply significant practical conclusions. As compared to heat, MS will probably not be a choice technology when intending to sanitize acid foods, such as juices. On the other hand, whereas acidification is applied as a hurdle in a combined process based on a heat treatment, it will be of little interest for those based on the application of ultrasound under pressure. Manothermosonication will be especially useful when cells are subjected to different stresses during industrial

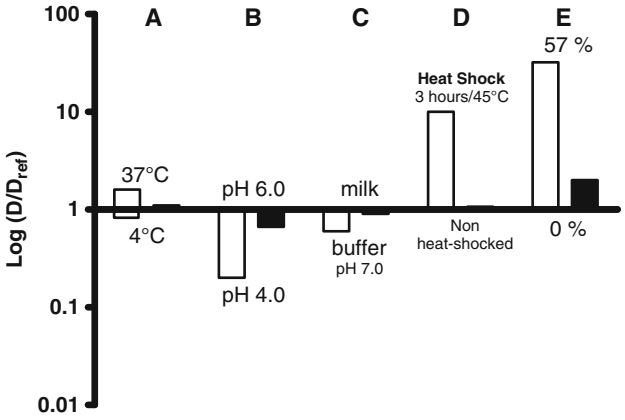

Fig. 11.7 Effect of different environmental factors on heat (*white bars*) and MS (*black bars*) resistance of *L. monocytogenes*. Effect of growth temperature (**a**), pH (**b**), medium composition (**c**), previous heat shock (**d**) and sucrose concentration (**e**). Values represented were calculated by dividing the *D* values obtained for each condition by the D_{ref} values of each technology (D_{ref} values are the D_t and D_{MS} values obtained for cells grown at 20°C and treated skim milk)

processing, allowing them to develop resistance against subsequent technological treatment, as in the case of heat shocks. MS/MTS is also a process especially interesting when intending to pasteurize foods with low water activity, in which the heat resistance of the microorganisms may increase by hundreds of times. In these foods, the bactericidal efficacy of ultrasound under pressure is practically the same as in media of high water activity and, furthermore, they exert a synergistic lethal effect when heat is applied simultaneously.

5 MS/MTS Bacterial Inactivation Mechanisms

The study of the mechanisms of action of ultrasonic waves, as well as any other agents intended for use for microbial inactivation in foods, is essential. An adequate design of new food preservation processes, especially in the case of combined processes, has to be based on the biological mode of action of the various hurdles used.

The lethal effect of low-power ultrasound is small, and most authors agree that the microbial lethal effect produced by high-power ultrasound is related to the cavitation phenomenon (Davies, 1959; Kinsloe et al., 1954; Pagán, 1997; Raso et al., 1998a), more specifically to its mechanical and chemical effects. When bubbles collapse under an ultrasonic field, high temperatures and pressures are generated at the implosion point. Therefore, heat, pressure shock waves or both could be responsible for the lethal effect of ultrasound. On the other hand, these extreme conditions lead to the dissociation of water into hydroxyl radicals and hydrogen atoms

(Suslick, 1990). These reactive radicals could also be involved in the inactivation of microorganisms through oxidative damage (Shin et al., 1994); however, this last effect seems to be negligible compared with the mechanical damage. Current available data may indirectly lead to a sound hypothesis about the mode of action of ultrasound and will be reviewed next.

The role of reactive radicals on the lethal effect of ultrasonic waves under pressure has been studied by the addition of the free radical scavenger cysteamine. Results have shown that the lethality of the treatment on bacterial spores (Raso, 1995) and vegetative cells (Allison et al., 1996; Pagán, 1997; Raso et al., 1998a) was the same when cysteamine was added to the treatment media. Moreover, oxidative agents generally provoke injuries in cell envelopes before inactivation begins. These injuries are commonly detected by the addition of sodium chloride to the recovery media, which constitutes the most frequently used technique to prevent bacterial damage recovery. MS survival curves of various vegetative cells were the same when cells were recovered in media with and without sodium chloride (Mañas, 1999; Pagán, 1997; Pagán et al., 1999a), which indicates that the mechanisms of inactivation by ultrasound and oxidative compounds are different. Therefore, any important contribution of the sonolysis to the inactivating effect of ultrasound on microorganisms has been discarded.

When a bubble generated by ultrasound implodes, heat is generated in the liquid around the cavity. The quantity of heated liquid is very small and heat dissipates quickly, but the temperature of this region remains very high (5,000°C) for a very short time, just a few microseconds (Flint and Suslick, 1991; Suslick, 1988). The occurrence of these hot spots could explain, following the Arrhenius equation, the exponential rate of death by ultrasound through a mechanism involving thermal inactivation. As has been discussed above, decimal reduction time values to MS/MTS treatments fit the theoretical curve calculated by assuming that heat and ultrasonic microbial inactivation are independent processes, which clearly points to different inactivation mechanisms for each agent. Furthermore, whereas bacterial heat resistance varies widely with the strain and the experimental conditions, resistance to MS is close in all vegetative cells studied under various environmental factors. Finally, the percentage of damaged cells of a bacterial population treated by heat increase throughout the treatment time, but damaged cells have not been detected after MS treatments (Pagán, 1997; Raso, 1995). This would also demonstrate different mechanisms of inactivation for heat and ultrasonic treatments. Therefore, all of these factors indicate that, in most occasions, heat would not contribute to the lethal effect of ultrasound.

Most authors have suggested that the mechanical effects of ultrasonic waves are probably the reason for its inactivating effect, in such a way that pressure waves passing through the liquid media would provoke the mechanical disruption of cell envelopes (Davies, 1959; Kinsloe et al., 1954; Lee et al., 2009; Pagán, 1997; Raso et al., 1998a). There are, however, only a few data supporting this idea. Raso et al. (1998a) studied the integrity of cells of *Y. enterocolitica* through a microscopic approach following various heat, MS and MTS treatments with equivalent lethality levels (more than 99% of bacterial inactivation). The

percentage of inactivated cells were calculated by the difference between plate counts before and after each treatment, and the percentage of disrupted cells were estimated through phase contrast microscopy. We observed that no disrupted cells were obtained after heat treatment. On the contrary, after an MS treatment of the same lethality, no undisrupted cells could be observed. After the corresponding MTS treatment, approximately 80% of cells remained undisrupted. Pagán (1997) found similar results with *L. monocytogenes*. These results confirmed that MS inactivates microorganisms through cell envelope breakdown.

In fact, the mechanical disruption of cell envelopes as the key event leading to cell death by ultrasound explains most of the physiological observations described. This hypothesis would also explain that the effect of pressure and amplitude of ultrasonic waves is the same in all of the bacterial species investigated, the additive lethal effect of manothermosonication treatments (inactivating effect of heat added to that of ultrasonic waves under pressure) and the profile of the corresponding DRTC. On the other hand, the absence of damaged vegetative cells indicates that mechanical cell disruption by ultrasound is an "all or nothing" event. This mode of action will complicate the inclusion of ultrasound in combined processes with a synergistic effect, which would only be expected if the additional hurdle added to the ultrasonic treatment modifies the mechanical resistance of the cell envelopes. Finally, it is also noticeable that from data obtained it would be concluded the possible differences in mechanical resilience among envelopes of the various vegetative cells would have a minor effect on bacterial inactivation by ultrasound.

Occasionally, as discussed above, a synergistic effect of ultrasound plus heat has been observed. However, this observation is not in disagreement with the general hypothesis. The synergistic lethal effect of manothermosonication has been reported on bacterial spores (Raso et al., 1994, 1998b), heat-shocked cells of *L. monocytogenes* (Pagán et al., 1999b), particularly heat-resistant vegetative cells (Pagán et al., 1999c), and several strains of *Salmonella* treated in low water activity media (Álvarez, 2000). Bacterial spores have a very complex structure and mechanically resistant envelopes, which isolate the protoplast from the environment. It has been reported that ultrasonic treatments are able to disrupt the spore exosporium (Berger and Marr, 1960). It has also been observed that ultrasound provokes the release of dipicolinic acid and low-molecular weight polypeptides from the cortex of some bacterial spores (Palacios et al., 1991). Furthermore, Raso et al. (1998b) found that manosonication treatment sensitized the spores of *B. subtilis* to lysozyme action. Some strains of spore formers are known to have naturally leaky coats and are therefore lysozyme sensitive, but, in most cases, lysozyme is only capable of hydrolyzing the peptidoglycan of the spore cortex if the overlying coat is first made leaky. These results suggest that the mechanism of action of ultrasonic waves on bacterial spores is also based on the mechanical disruption of the most external envelopes. The external damage would lead to the rehydration of the protoplast, which would result in a loss of heat tolerance (Sala et al., 1995). This would explain the observed synergistic effect of manothermosonication on bacterial spores. Ultrasonic waves under pressure would act, in this case, by sensitizing bacterial spores to heat.

Pagán et al. (1999a) reported the synergistic effect of manothermosonication on heat-shocked cells of *L. monocytogenes*, but not on native non-shocked cells (Pagán et al., 1999b). The authors reported that if a heat treatment was applied prior to an MS treatment, cells were slightly sensitized to ultrasound under pressure. However, this sensitizing effect did not explain the entire lethal effect of MTS. They concluded that, contrary to what was observed with bacterial spores, heat sensitized the cells to ultrasonic waves under pressure. Several authors have reported the occurrence of various changes induced by heat in cell envelopes (Helander et al., 1997; Stevens et al., 1992). Some of these changes modify cell membrane rigidity. It has been observed that heat may cause the release of some divalent cations from the cell envelope and melt cell membrane fatty acids (Helander et al., 1997; Stevens et al., 1992). Therefore, some temperature-induced changes occurring in the cell envelopes could weaken them against mechanical stress. The disruption of envelopes seems to be the mechanism of action of ultrasonic waves, even when a synergistic effect is observed. The synergistic effect reported in the highly heat-resistant *Streptococcus faecium* (Pagán et al., 1999c) and in *Salmonella* serotypes treated at low water activity (Álvarez, 2000) could be explained in a similar way. When heat-sensitive bacteria are treated by manothermosonication, the lethal effect of heat begins at low temperatures and the weakening effect of heat on the mechanical resistance of cell envelopes cannot be observed. As a consequence, an additive effect is expected. On the contrary, when heat-resistant bacteria or cells whose thermal resistance is increased by the particular characteristics of the treatment medium are treated by MTS, the lethal effect of heat only appears at higher temperatures. These higher temperatures may exert changes in cell envelopes and a synergistic effect should be expected. Specific investigations have not been carried out in this matter and new data would be very useful.

6 Control of MS/MTS Industrial Processes

Since it is impossible to ensure a "zero" risk when implementing an industrial process, it is convenient (if not necessary) to establish a kinetic model of inactivation. This model will allow selection of treatment conditions to achieve a definite objective, i.e. performance criteria. It is also important to determine those physical parameters on which the final efficacy depends, as well as to establish the relevant equations allowing to a forecast of the consequences from an error in the treatment conditions, in regard to the stability and safety of the manufactured product. Concerning the above questions, the MS/MTS process shows some advantages when compared to other technologies for the preservation and hygienization of foods.

For example, kinetics of inactivation by high hydrostatic pressure and pulsed electric fields does not follow an exponential pattern, which makes calculation and adjustment of industrial treatments very difficult. The survival curves obtained with these technologies often show tailing phenomena, whose importance, i.e. level of

surviving population, also varies with the treatment intensity. Therefore, it is difficult to even find primary models able to predict the lethal efficacy of a treatment at constant intensity of different durations. The current trend is to use models based on a Weibull-like distribution on the basis of their robustness and simplicity (Álvarez et al., 2003a, d; Chen and Hoover, 2003; Fernández et al., 2002; Heinz and Knorr, 1996; Mafart et al., 2002). However, at present, consensus has not been reached in regard to the convenience of their use, and there have been only two or three sporadic trials to develop secondary and tertiary models (Álvarez et al., 2007; Chen and Hoover, 2004; Gómez et al., 2005a, b), which are in fact the models that can really interest the industrial sector. As mentioned above, inactivation kinetics by MS/MTS fits an exponential primary model, very simple and robust, which has been widely used by the canning industry to adjust the intensity of heat treatment. Furthermore, as indicated in Section 2.1, it is possible to easily develop secondary models that are also based on first-order kinetics. In summary, simple, robust tertiary models, similar to those developed for the adjustment of heat treatments and of direct application to the industrial sector, can be developed.

On the other hand, since the efficacy of manosonication depends both on amplitude and pressure, it could be expected that the simultaneous control of both variables within an industrial process would be difficult, as well as quantification of the effect of any possible processing mistake. However, as has been described in previous sections, the effects of amplitude and pressure are independent of each other. Furthermore, the biological effects of each of them are directly related to the energy transmitted to the medium by ultrasound under any experimental conditions. Therefore, the energy transferred to the treatment medium is an appropriate parameter to measure in order to control the process. Mañas et al. (2000a) developed a very simple linear equation that allowed calculation of the lethal efficacy of MS treatments from the measurement of energy transferred to the medium. Following the same procedure, it would be very easy to develop some specific equations for particular industrial equipment, which would allow us to quantify the efficacy of the process by measuring just one parameter: the energy transferred. This simplification, for instance, could not be used to control pulsed electric fields processes, as the application of a given quantity of energy has different biological effects depending on the strength of the electric field applied (Álvarez et al., 2003c).

An additional aspect of relevance for the industry is the possibility of forecasting the consequences from an eventual processing error. In this regard, MS also shows some particular advantages. For example, in a heat treatment, the factor to be controlled is temperature, and there is the theoretical possibility of predicting the consequences from an error in treatment temperature through the use of z values. However, these calculations are very risky, as each microbial species has a different z value, and the raw materials are usually contaminated with heterogeneous bacterial flora. On the contrary, as we have discussed before, the effects of pressure and amplitude of the ultrasonic waves are the same for all species investigated. Therefore, the consequences of any eventual processing error could be easily estimated in a reliable manner.

Lastly, besides the actual practical utility of this technology for food processing, the MS/MTS processes could already be transferred to the industrial sector with the mathematical tools necessary for optimization of treatments and control of the process.

7 Concluding Remarks

As a consequence of consumer's increasing requirements, the food industry has been challenged to improve the safety, stability and convenience of foods and a great effort has been made to develop more appropriate methods of preservation/hygienization. At present, it can be foreseen that none of the new technologies under study will replace traditional preserving procedures for a wide range of products. However, each one shows some particular advantages that may make it the choice technology for given products or processes.

The major advantage of MS/MTS in regard to other new preservation technologies is their capacity to inactivate bacterial spores at sublethal temperatures, although the treatment times for the sterilization of foods with this technology would probably be long. Concerning the inactivation of vegetative cells, the major advantages are based on the exponential course of inactivation and on the fact that microbial resistance barely changes with species and the environmental factors. It seems that there are no mechanisms of development of cross resistance and occurrence of cell damage/recovery either, which represents an additional safety guarantee.

As far as the development of combined processes is concerned, current knowledge indicates that, with the exception of the combination with heat, the application of traditional hurdles will barely allow development of any processes of synergistic lethal effects, unless the hurdle is selected to lower the mechanical resistance of cell envelopes. In this regard, it is worth highlighting that bacterial spores represent an exception, since MS treatment sensitizes these spores against lysozyme. This is a most interesting aspect that should be further investigated.

The combination of ultrasound under pressure and heat (manothermosonication) could be especially advantageous. Although an additive effect has been generally observed, on some occasions when heat treatments are less effective, a synergistic effect can be achieved. Moreover, the application of manothermosonication would be highly energetically profitable, since almost all of the ultrasonic energy applied to the medium is finally converted into heat, which could be reused in the process. An additional advantage is that various different individual operations, such as mixture, emulsification, degasification, could be carried out in just one step.

The major limitation of manothermosonication could be its effects on the physicochemical and nutritional properties of foods. Unfortunately, there are not enough data available in this regard, and general conclusions cannot be drawn. Appropriate specific equipment to apply this technology to foods at a pilot-plant

level has not been developed either. Since knowledge about the biological effects of manothermosonication is enough and food characteristics may vary widely, probably the next step is to apply this technology to some particular product whose preservation/pasteurization is especially difficult at present. In this way, an overall assessment of its effects on the quality, in its different aspects, will be possible.

References

Alderton, G., Thompson, P. A., and Snell, N. (1964). Heat adaptation and ion exchange in *Bacillus megatherium* spores. *Science*, 143, 141–143.

Alliger, H. (1975). Ultrasonic disruption. *American Laboratory*, 10, 75–85.

Allison, D. G., D'Emanuele, A., Egington, P., and Williams, A. R. (1996). The effect of ultrasound on *Escherichia coli* viability. *Journal of Basic Microbiology*, 36, 3–11.

Alpas, H., Kalchayanand, N., Bozoglu, F., and Ray, B. (2000). Interactions of high hydrostatic pressure, pressurization temperature and pH on death and injury of pressure-resistant and pressure-sensitive strains of foodborne pathogens. *International Journal of Food Microbiology*, 60, 33–42.

Álvarez, I. (2000). Resistencia al calor y a los ultrasonidos bajo presión de *S. enteritidis* y *S. senftenberg* en medios de distinta actividad de agua. Master's thesis, University of Zaragoza.

Álvarez, I., Raso, J., Palop, A., and Sala, F. J. (2000). Influence of different factors on the inactivation of *Salmonella senftenberg* by pulsed electric fields. *International Journal of Food Microbiology*, 55, 143–146.

Álvarez, I., Condón, S., and Raso, J. (2007). Microbial inactivation by pulsed electric fields. In: Raso, J., and Heinz, V. (eds.), *Pulsed Electric Field Technology for the Food Industry*, pp. 95–128. New York, NY, Springer Applied Science.

Álvarez, I., Mañas, P., Condón, S., and Raso, J. (2003a). Resistance variation of *Salmonella enterica* serovars to pulsed electric fields treatments. *Journal of Food Science*, 68, 2316–2320.

Álvarez, I., Mañas, P., Sala, F. J., and Condón, S. (2003b). Inactivation of *Salmonella enteritidis* by ultrasonic waves under pressure at different water activities. *Applied and Environmental Microbiology*, 69(1), 668–672.

Álvarez, I., Mañas, P., Virto, R., and Condón, S. (2006a). Inactivation of *Salmonella senftenberg* 775 W by ultrasonic waves under pressure at different water activities *International Journal of Food Microbiology*, 108, 218–225.

Álvarez, I., Niemira, B. A., Fan, X. T., and Sommers, C. H. (2006b). Inactivation of *Salmonella* serovars in liquid whole egg by heat following irradiation treatment. *Journal of Food Protection*, 69(9), 2066–2074.

Álvarez, I., Pagán, R., Condón, S., and Raso, J. (2003c). The influence of process parameters for the inactivation of *Listeria monocytogenes* by pulsed electric fields, *International Journal of Food Microbiology*, 87, 87–95.

Álvarez, I., Pagán, R., Raso, J., and Condón, S. (2002). Environmental factors influencing the inactivation of *Listeria monocytogenes* by pulsed electric fields. *Letters in Applied Microbiology*, 35, 489–493.

Álvarez, I., Virto, R., Raso, J., and Condón, S. (2003d). Comparing predicting models for the *Escherichia coli* inactivation by pulsed electric fields. *Innovative Food Science and Emerging Technologies,* 4, 195–202.

Ando, Y., and Tsuzuki, T. (1983). Mechanism of chemical manipulation of the heat resistance of *Clostridium perfringens* spores. *Journal of Applied Bacteriology*, 54, 197–202.

Arce-García, M. R., Jiménez-Murguía, M. T., Palou, E., and López-Malo, A. (2002). Ultrasound treatments and antimicrobial agents effects on *Zygosaccharomyces rouxii*. IFT Annual Meeting Book of Abstracts, 2002, Session 91E-18.

Aronsson, K., Borch, E., Stenlöf, B., and Rönner, U. (2004). Growth of pulsed electric field exposed *Escherichia coli* in relation to inactivation and environmental factors. *International Journal of Food Microbiology*, 93, 1–10.

Aronsson, K., and Rönner, U. (2001). Influence of pH, water activity and temperature on the inactivation of *Escherichia coli* and *Saccharomyces cerevisiae* by pulsed electric fields. *Innovative Food Science and Emerging Technologies*, 2, 105–112.

Baird-Parker, A. C., Boothroyd, M., and Jones, E. (1970). The effect of water activity on the heat resistance of heat sensitive and heat resistant strains of *Salmonellae*. *Journal of Applied Bacteriology*, 33, 515–522.

Bender, G. R., and Marquis, R. E. (1985). Spore heat resistance and specific mineralization. *Applied and Environmental Microbiology*, 50(6), 1414–1421.

Berger, J. A., and Marr, G. G. (1960). Sonic disruption of spores of *Bacillus cereus*. *Journal of General Microbiology*, 22, 1–64.

Berlan, J., and Mason, T. J. (1992). Sonochemistry: From research laboratories to industrial plant. *Ultrasonics*, 30, 203–212.

Berliner, S. (1984). Application of ultrasonic processors. *International Biotechnology Laboratory*, 2, 42–49.

Bigelow, W. D. (1921). The logarithmic nature of thermal death-time curves. *Journal of Infectious Diseases*, 28, 528–532.

Burgos, J., Ordóñez, J. A., and Sala F. J. (1972). Effect of ultrasonic waves on the heat resistance of *Bacillus cereus* and *Bacillus licheniformis* spores. *Applied Microbiology*, 24, 497–498.

Cerf, O. (1977). Tailing of survival curves of bacterial spores. *Journal of Applied Bacteriology*, 42, 1–19.

Chen, H., and Hoover, D. G. (2003). Pressure inactivation kinetics of *Yersinia enterocolitica* ATCC 35669. *International Journal of Food Microbiology*, 87, 161–171.

Chen, H., and Hoover, D. G. (2004). Use of Weibull model to describe and predict pressure inactivation of *Listeria monocytogenes* Scott A in whole milk. *Innovative Food Science and Emerging Technologies*, 5, 269– 276.

Condón, S., Raso, J., and Pagán, R. (2005). Microbial inactivation by ultrasound. In Barbosa-Cánovas, G. V., Tapia M. S., Cano, M. P. (eds.), *Novel Food Processing Technologies*, pp. 423–442. Boca Ratón, FL, CRC.

Condón, S., and Sala, F. J. (1992). Heat resistance of *Bacillus subtilis* in buffer and foods of different pH. *Journal of Food Protection*, 55, 605–608.

Corry, J. (1974). The effect of sugars and polyols on the heat resistance of salmonellae. *Journal of Applied Bacteriology*, 37, 31–43.

Davies, R. (1959). Observations of the use of ultrasound waves for the disruption of microorganisms. *Biochemica Biophysica Acta*, 33, 481–493.

Doyle, M. E., and Mazzotta, A. S. (2000). Review of studies on the thermal resistance of salmonellae. *Journal of Food Protection*, 63, 779–795.

Earnshaw, R. G., Appleyard, J., and Hurst, R. M. (1995). Understanding physical inactivation processes: combining preservation opportunities using heat, ultrasound and pressure. *International Journal of Food Microbiology*, 28, 197–219.

Fernández, A., Collado, J., Cunha, L. M., Ocio, M. J., and Martinez, A. (2002). Empirical model building based on Weibull distribution to describe the joint effect of pH and temperature on the thermal resistance of *Bacillus cereus* in vegetable substrate. *International Journal of Food Microbiology*, 77, 147–153.

Flint, E. B., and Suslick, K. S. (1991). The temperature of cavitation. *Science*, 253, 1397–1398.

Frizzell, L. A. (1988). Biological effects of acoustic cavitation. In: Suslick, K. (ed.), *Ultrasound: Its Chemical, Physical, and Biological Effects*, pp. 287–306. New York, NY, VCH.

García, D., Gómez, N., Condón, S., Raso, J., and Pagán, R. (2003). Pulsed electric fields cause sublethal injury in *Escherichia coli*. *Letters in Applied Microbiology*, 36, 140–144.

García, D., Gómez, N., Raso, J., and Pagán, R. (2005). Bacterial resistance after pulsed electric fields depending on the treatment medium pH. *Innovative Food Science and Emerging Technologies*, 6, 388–395.

García, M. L. (1985). Acción de los tratamientos ultrasónicos y térmicos en los esporos de *B. subtilis*. Ph.D. Thesis. University of Complutense, Madrid.

García, M. L., Burgos, J., Sanz, B., and Ordónez, J. A. (1989). Effect of heat and ultrasonic waves on the survial of two strains of *Bacillus subtilis*. *Journal of Applied Bacteriology*, 67, 619–628.

Geveke, D. J., and Kozempel, M. F. (2003). Pulsed electric field effects on bacteria and yeast cells. *Journal of Food Processing and Preservation*, 27, 65–72.

Gómez, N., García, D., Álvarez, I., Condón, S., and Raso, J. (2005a). Modeling inactivation of *Listeria monocytogenes* by pulsed electric fields. *International Journal of Food Microbiology*, 103, 199–206.

Gómez, N., García, D., Álvarez, I., Raso, J., and Condón, S. (2005b). A model describing the kinetics of inactivation of *Lactobacillus plantarum* in a buffer system of different pH and in orange and apple juice. *Journal of Food Engeeniering*, 70, 7–14.

Gould, G. W. (1989). Heat induced injury and inactvation. In: Gould, G. W. (ed.), *Mechanisms of Action of Food Preservation Procedures*, pp. 11–42. London, Elsevier Applied Science.

Grahl, T., and Märkl, H. (1996). Killing of microorganisms by pulsed electric fields. *Applied Microbiology and Biotechnology*, 45, 148–157.

Guerrero, S., Tognon, M., and Alzadora, S. M. (2005). Response of *Saccharomyces cerevisiae* to the combined action of ultrasound and low weight chitosan. *Food Control*, 16, 131–139.

Hansen, N. J., and Riemann, H. (1963). Factors affecting the heat resistance of nonsporing organisms. *Journal of Applied Bacteriology*, 20, 314–318.

Harvey, E., and Loomis, A. (1929). The destruction of luminuous bacteria by high frequency sound waves. *Journal of Bacteriology*, 17, 373–379.

Hassani, M., Álvarez, I., Raso, J., Condón, S., and Pagán, R. (2005). Comparing predicting models for heat inactivation of *Listeria monocytogenes* and *Pseudomonas aeruginosa* at different pHs. *International Journal of Food Microbiology*, 100, 213–222.

Hassani, M., Mañas, P., Condón S., and Pagán, R. (2006). Predicting heat inactivation of *Staphylococcus aureus* under nonisothermal treatments at different pH. *Molecular Nutrition and Food Research*, 50, 572–580.

Hauben, K. J. A., Bernaerts, K., and Michiels, C. W. (1998). Protective effect of calcium on inactivation of *Escherichia coli* by high hydrostatic pressure. *Journal of Applied Microbiology*, 85, 678–684.

Heinz, V., and Knorr, D. (1996). High pressure inactivation kinetics of *Bacillus subtilis* cells by a three-state model considering distributed resistance mechanisms. *Food Biotechnology*, 10, 149–161.

Helander, I. M., von Wright, A., and Mattila-Sandholm, T. M. (1997). Potential of lactic acid bacteria and novel antimicrobials against Gram-negative bacteria. *Trends in Food Science and Technology*, 8, 146–150.

Hülsheger, H., Potel, J., and Niemann, E. G. (1981). Killing of bacteria with electric pulses of high field strength. *Radiation and Environmental Biophysics*, 20, 53–65.

Hurst, R. M., Betts, G. D., and Earnshaw, R. G. (1995). The antimicrobial effect of power ultrasound. RandD Report No.4; Glos, Chipping Campden.

Jacobs, S. E., and Thornley, M. J. (1954). The lethal action of ultrasonic waves on bacteria suspended in milk and other liquids. *Journal of Applied Bacteriology*, 17, 38–56.

Jay, J. M. (1992). High temperature food preservation and characteristics of thermophilic microorganisms. In: Jay, J. M. (ed.), *Modern Food Microbiology*, pp. 335–355. New York, NY, Chapman and Hall.

Kinsloe, H., Ackerman, E., and Reid, J. J. (1954). Exposure of microorganisms to measured sound fields. *Journal Bacteriology*, 68, 373–380.

Koseki, S., and Yamamoto, K. (2006). pH and solute concentration of suspension media affect the outcome of high hydrostatic pressure treatment of *Listeria monocytogenes*. *International Journal of Food Microbiology*, 11, 175–179.

Kwast, R. H., and Verrips, C. T. (1982). Heat resistance of *Salmonella senftenberg* 775 W at various sucrose concentrations in distilled water. *European Journal of Applied Microbiology and Biotechnology*, 14, 193–201.

Lee, D. U., Heinz, V., and Knorr, D. (2003). Effects of combination treatments of nisin and high-intensity ultrasound with high pressure on the microbial inactivation of liquid whole egg. *Innovative Food Science and Emerging Technologies*, 4, 387–393.

Lee, H., Zhou, B., Liang, W., Feng, H. and Martin, S. E. (2009). Inactivation of *Escherichia coli* with sonication, manosonication and manothermosonication: Microbial responses and kinetics modelling. *Journal of Food Engineering*, 93, 354–364.

Lindquist, S. (1986) The heat-shock response. *Annual Reviews in Biochemistry*, 55, 1151–1191.

López-Malo, A., Enrique Palou, E., Maribel Jiménez-Fernández, M., Alzamora, S. M., and Guerrero, S. (2005). Multifactorial fungal inactivation combining thermosonication and Antimicrobials. *Journal of Food Engineering*, 67, 87–93.

Mackey, B. M., and Derrick, C. M. (1986) Elevation of the heat resistance of *Salmonella typhimurium* by sub-lethal heat shock. *Journal of Applied Bacteriology*, 61, 389–393.

Mackey, B. M., Forestiere, K., and Isaacs, N. (1995). Factors affecting the resistance of *Listeria monocytogenes* to high hydrostatic-pressure. *Food Biotechnology*, 9, 1–11.

Mafart, P., Couvert, O., Gaillard, S., and Leguerinel, I. (2002). On calculating sterility in thermal preservation methods: Application of the Weibull frequency distribution model, *International Journal of Food Microbiology*, 72, 107–113.

Mañas, P. (1999). Higienización del huevo liquido por ultrasonidos y calor. Ph.D. Thesis, University of Zaragoza.

Mañas, P., Pagán, R., and Raso, J. (2000a). Predicting lethal effect of ultrasonic waves under pressure treatments on *Listeria monocytogenes* ATCC 15313 by power measurements. *Journal of Food Science*, 65(4), 663–667.

Mañas, P., Pagán, R., Raso, J., Sala F. J., and Condón S. (2000b). Inactivation of *S. typhimurium, S. enteritidis* and *S. senftenberg* by ultrasonic waves under pressure. *Journal of Food Protection*, 63, 451–456.

Mañas, P., Pagán, R., Sala, F. J., and Condón, S. (2001). Low molecular weight milk whey components protect *Salmonella senftenberg* 775 W against heat by mechanism involving divalent cations. *Journal of Applied Microbiology*, 91, 871–877.

Moats, W. A., Dabbah, R., and Edwards, V. M. (1971). Interpretation of nonlogarithmic survivor curves of heated bacteria. *Journal of Food Science*, 36, 523–526.

Murphy, R. Y., Marks, B. P., Johnson, E. R., and Johnson, M. J. (2000). Thermal inactivation kinetics of *Salmonella* and *Listeria* in ground chicken breast meat and liquid medium. *Journal of Food Science*, 65, 706–710.

Ordóñez, J. A., Aguilera, M. A., García M. L., and Sanz, B. (1986). Effect of combined ultrasonic and heat treatment (thermoultrasonication) on the survival of a strain of *Staplylococcus aureus*. *Journal of Dairy Research*, 54, 61–67.

Ordóñez, J. A., Sanz, B., Hernández, P. E., and López-Lorenzo, P. A. (1984). Note on the effect of combined ultrasonic and heat treatments on the survival of thermoduric streptococci. *Journal of Applied Bacteriology*, 56, 175–177.

Pagán, R. (1997). Resistencia frente al calor y los ultrasonidos bajo presión de *Aeromonas hydrophila*, *Yersinia enterocolitica* y *Listeria monocytogenes*. Ph.D. Thesis, University of Zaragoza.

Pagán, R., Mañas, P., Álvarez, I., and Condón, S. (1999a). Resistance of *Listeria monocytogenes* to ultrasonic waves under pressure at sublethal (manosonication) and lethal (manothermosonication) temperatures. *Food Microbiology*, 16, 139–148.

Pagán, R., Mañas, P., Palop, A., and Sala, F. J. (1999b). Resistance of heat-shocked cells of *Listeria monocytogenes* to manosonication and to manothermosonication. *Letters in Applied Microbiology*, 28, 71–75.

Pagán, R., Mañas, P., Raso, J., and Condón, S. (1999c). Bacterial resistance to ultrasonic waves under pressure at non lethal (manosonication) and lethal (manothermosonication) temperatures. *Applied and Environmental Microbiology*, 65, 297–300.

Pagán, R., Mañas, P., Raso, J., and Sala-Trepat, F. J. (1999d). Heat resistance of *Yersinia enterocolitica* grown at different temperatures and heated in different media. *International Journal of Food Microbiology*, 47, 59–66.

Palacios, P., Burgos, J., Hoz, L., Sanz, B., and Ordóñez, J. A. (1991). Study of the substances released to ultrasonic treatment form *Bacillus stearothermophilus* spores. *Journal of Applied Bacteriology*, 71, 445–451.

Palop, A., Sala, F. J., and Condón, S. (1997). Occurrence of a highly heat-sensitive spore subpopulation of *Bacillus coagulans* STCC 4522 and its conversion to a more heat-stable form. *Applied and Environmental Microbiology*, 63(6), 2246–2251.

Parsell, D. A., and Lindquist, S. (1993). The function of heat-shock proteins in stress tolerance: Degradation and reactivation of damaged proteins. *Annual Reviews in Genetics*, 27, 437–496.

Patterson, M. F., Quinn, M., Simpson, R., and Gilmour, A. (1995). Sensitivity of vegetative pathogens to high hydrostatic pressure treatment in phosphate-buffered saline and foods. *Journal of Food Protection*, 58, 524–529.

Peleg, M. (1999). On calculating sterility in thermal and nonthermal preservation methods. *Food Research International*, 32, 271–278.

Peleg, M., and Cole, M. B. (1998). Reinterpretation of microbial survival curves. *Critical Reviews in Food Science and Nutrition*, 38, 353–380.

Rahn, O. (1945). Physical methods of sterilization of microorganisms. *Bacteriological Reviews*, 9, 1–45.

Raso, J. (1995). Resistencia microbiana a un tratamiento combinado de ultrasonidos y calor bajo presión. Manotermosonicación. Ph.D. Thesis, University of de Zaragoza.

Raso, J., Condón, J., and Sala-Trepat F. J. (1994). Mano-thermo-sonication: A new method of food preservation? Food Preservation by Combined Processes. Final Report FLAIR Concerted Action No. 7, Subgroup B. Lesitner, L. and Gorris, L. G. M. Food linked agro-industrial research. Directorate-General XII, Science, Research and Development.

Raso, J., Mañas, P., Pagán, R., and Sala, F. J. (1999). Influence of different factors on the output power transferred into medium by ultrasound. *Ultrasonics Sonochemistry*, 5, 157–162.

Raso, J., Pagán, R., Condón, S., and Sala, F. J. (1998a). Influence of temperature and pressure on the lethality of ultrasound. *Applied and Environmental Microbiology*, 64, 465–471.

Raso, J., Palop, A., Pagán, R., and Condón, S. (1998b). Inactivation of *Bacillus subtilis* spores by combining ultrasonic waves under pressure and mild heat treatment. *Journal of Applied Microbiology*, 85, 849–854.

Riesz, P. and Kondo, T. (1992). Free radical formation induced by ultrasoundand its biological implications. *Free Radical Biology and Medicine*, 13, 247–270.

Sala, F. J., Burgos, J., Condón, S., López, P., and Raso, J. (1992). Procedimiento para la destrucción de microorganismos y enzimas: proceso MTS. Spanish Patent 93/00021.

Sala, F. J., Burgos, J., Condón, S., López, P., and Raso J. (1995). Effect of heat and ultrasound on micro-organisms and enzymes. In: Gould, G. W. (ed.), *New Methods of Food Preservation*, pp. 176–204. London, Blackie Academic and Professional.

Schlesinger, M. J. (1986) Heat shock proteins: The search for functions. *Journal of Cell Biology*, 103, 321–325.

Sherry, A. E., Patterson, M. F., and Madden, R. H. (2004). Comparison of 40 *Salmonella enterica* serovars injured by thermal, high-pressure and irradiation stress. *Journal of Applied Microbiology*, 96, 887–893.

Shin, S. Y., Calvisi, E. G., Beaman, T. C., Pankratz, H. S., Gerhardt, P., and Marquis, R. E. (1994). Microscopic and thermal characterisation of hydrogen peroxide killing and lysis of spores and protection by transition metal ions, chelators and antioxidants. *Applied and Environmental Microbiology*, 60, 3192–3197.

Shull, J. J., Cargo, G. T., and Ernst, R. R. (1963). Kinetics of heat activation and thermal death of bacterial spores. *Applied Microbiology*, 11, 485–487.

Simpson, R. K., and Gilmour, A. (1997). The effect of high hydrostatic pressure on the activity of intracellular enzymes of *Listeria monocytogenes*. *Letters in Applied Microbiology*, 25, 48–53.

Stevens, K. A., Sheldon, B. W., and Klaenhammer, N. A. (1992). Effect of treatment conditions on nisin inactivation of Gram negative Bacteria. *Journal of Food Protection*, 55, 763–766.

Stewart, C. M., Jewett, F. F., Dunne, C. P., and Hoover, D. G. (1997). Effect of concurrent high hydrostatic pressure, acidity and heat on the injury and destruction of *Listeria monocytogenes*. *Journal Food Safety*, 17, 23–36.

Stumbo, C. R. (1965). *Thermobacteriology in Food Processing*. London, Academic.

Sumner, S. S., Sandros, T. M., Harmon, M. C., Scott, V. N., and Bernard, D. T. (1991). Heat resistance of *Salmonella typhimurium* and *Listeria monocytogenes* in sucrose solutions of various water activities. *Journal of Food Science*, 56(6), 1741–1743.

Suslick, K. S. (1988). Homogeneous sonochemistry. In: Suslick, K. S. (ed.), *Ultrasound. Its Chemical, Physical and Biological Effects*, pp. 123–163. New York, NY, VCH.

Suslick, K. S. (1990). Sonochemistry. *Science,* 247, 1439–1445.

Tomlins, R. I., and Ordal, Z. J. (1976). Thermal injury and inactivation in vegetative bacteria. In: Skinner, F. A., and Hugo, W. B. (eds.), *Inhibition and Inactivation of Vegetative Microbes*, pp. 153–191. London, Academic.

Tsuchiya, H., Sato, M., Kanematsu, N., Kato, M., Hoshino, Y., Takagi, N., and Namikawa, I. (1987). Temperature-dependent changes in phospholipid and fatty acid composition and membrane lipid fluidity of *Yersinia enterocolitica*. *Letters in Applied Microbiology*, 5, 15–18.

Whillock, G. O. H., and Harvey, B. F. (1997). Ultrasonically enhanced corrosion of 304L stainless steel: I. The effect of temperature and hydrostatic pressure. *Ultrasound sonochemistry*, 4, 23–31.

Wouters, P. C., Glaasker, E., and Smelt, J. P. P. M. (1998). Effects of high pressure on inactivation kinetics and events related to proton efflux in *Lactobacillus plantarum*. *Applied and Environmental Microbiology*, 64, 509–514.

Chapter 12
Inactivation of Microorganisms

Stella Maris Alzamora, Sandra N. Guerrero, Marcela Schenk, Silvia Raffellini, and Aurelio López-Malo

1 Introduction

Minimal processing techniques for food preservation allow better retention of product flavor, texture, color, and nutrient content than comparable conventional treatments. A wide range of novel alternative physical factors have been intensely investigated in the last two decades. These physical factors can cause inactivation of microorganisms at ambient or sublethal temperatures (e.g., high hydrostatic pressure, pulsed electric fields, ultrasound, pulsed light, and ultraviolet light). These technologies have been reported to reduce microorganism population in foods while avoiding the deleterious effects of severe heating on quality. Among technologies, high-energy ultrasound (i.e., intensities higher than 1 W/cm^2, frequencies between 18 and 100 kHz) has attracted considerable interest for food preservation applications (Mason et al., 1996; Povey and Mason, 1998).

Several reports have indicated that sonication applied alone (at room temperature and atmospheric pressure) is not very effective for inactivating microorganisms. However, the combination of ultrasound with other preservation factors and/or the selection of operative conditions that enhance per se the effect of high-power sonication shows considerable promise (Knorr et al., 2004; Piyasena et al., 2003). Combining emerging factors with conventional preservation factors or with other novel techniques to impede the homeostatic mechanisms of microorganisms has been successfully explored in recent years (Alzamora et al., 2003; Lado and Yousef, 2002; Raso and Barbosa-Cánovas, 2003; Ross et al., 2003). If ultrasound is combined with another preservation technique that sensitizes the organism's structure to the action of ultrasonic waves, microbial disruption and, consequently, inactivation will be probably enhanced. On the other hand, ultrasound application will induce the uptake of antimicrobials by disturbing or stressing the membrane, thus reducing the viability of microorganisms.

S.M. Alzamora (✉)
Departamento de Industrias, Universidad de Buenos Aires, Ciudad Universitaria, 1428 Buenos Aires, Argentina
e-mail: smalzamora@gmail.com

H. Feng et al. (eds.), *Ultrasound Technologies for Food and Bioprocessing*, Food Engineering Series, DOI 10.1007/978-1-4419-7472-3_12,
© Springer Science+Business Media, LLC 2011

This chapter will focus on the mode of action of ultrasound on microorganisms and the use of ultrasound in conjunction with other preservation factors to enhance microbial inactivation.

2 Mechanisms of Action of Ultrasound

Ultrasound has long been considered to be the simplest and most versatile method for breaking cells, preparing extracts, and releasing enzymes and proteins. Injury to or disruption of microorganisms by ultrasound is widely attributed to acoustic cavitation, that is, the rupture of liquids when applying high-intensity ultrasound and the effects produced by the motion of the cavities thus generated (Lauterborn and Ohl, 1997).

Cavitation bubbles appear by tearing a liquid with brute force. The generation of cavitation bubbles may essentially occur by two physical mechanisms: by setting up tension in the liquid (with sound or fluid flow) or by depositing energy (with light waves, heat, or particles) (Lauterborn et al., 1999). Sound waves consist of pressure and tension phases, and strong sound waves are able to rupture a liquid in the under-pressure phase, giving rise to the phenomenon of acoustic cavitation. The inception of cavitation is a threshold process, because a specific intensity is necessary for cavitation bubbles to form. Depending on acoustic pressure, amplitude, and frequency; initial bubble size; and other ambient conditions, microbubbles (containing vapor and/or gas) can grow, oscillate extremely rapidly, and may even collapse violently (Perkins, 1990). Thus, different types of cavitation can be distinguished, many of which may occur simultaneously and interact in the power ultrasound field (Leighton, 1998):

In the so-called stable or non-inertial cavitation, the bubbles can undergo relatively stable, low-energy oscillations, often nonlinear, around some equilibrium size, provoking acoustic, optical, and electrical effects. The bubble begins as a nucleus and grows by rectified diffusion, with gas moving into the bubble from liquid solution. At a particular size, depending on the frequency of the sound field, the bubble exhibits resonance, with vibration amplitude several orders of magnitude greater than that of the liquid particles in the absence of the bubble (Clarke and Hill, 1970). The bubbles are relatively permanent and may oscillate for many cycles of acoustic pressure (Perkins, 1990). Because of these oscillations, the liquid in the vicinity of the bubbles flows or streams (microstreaming effect). This eddying or microstreaming could shear and disrupt cellular membranes or break cells (Hughes and Nyborg, 1962).

In "*transient*" or " *inertial cavitation*," small bubbles expand rapidly, often to many times their original size and, on the positive pressure half-cycle, collapse violently, breaking up into many smaller bubbles. During the expansion of the bubble, work is done against the ambient pressure which stops the expansion at some maximum radius and from there, as the bubble content is compressed, the bubble starts to collapse (Lauterborn and Ohl, 1997). On collapse, the energy that is dissipated into the system by the passage of ultrasound and then taken up and concentrated by the

cavities during their isothermal growth is released back into the liquid as a pressure pulse, resulting in shock waves with very high energy density and short flashes of light (Lauterborn et al., 1999; Vichare et al., 2000). The gas and vapor within the bubble may be heated to high temperatures. Thus, hot spots of high temperature (up to 5,000 K) and pressure (up to 100 MPa) may occur in very short events (on the order of microseconds) at highly localized spots of the sonicated medium (Scherba et al., 1991). Shock waves radiated by collapsing bubbles could be strong enough to shear and break cell walls and membrane structures (Earnshaw et al., 1995). In addition to these mechanical effects, electric discharges and production of free radicals and electronically excited species associated with the collapse of cavities could also cause chemical and biological effects. However, it has been reported that cell breakage is not dependent on free radical formation (Hughes and Nyborg, 1962).

Processes in the bubble cloud are very complex due to the influence of attracting and repelling forces and to the thousands of interacting bubbles (Lauterborn and Ohl, 1997). Bubbles exhibit large distortions associated with non-radial motion and fragmentation into small cavities (Lepoint and Mullie, 1994). The dynamics of bubble clouds has been analyzed with high-speed photography, holography, and cinematography observations (Lauterborn et al., 1999). A homogeneous cloud of bubbles has never been observed in previous studies, but the bubbles always organized themselves into dendritic branches of filaments. Although inertial cavitation has been considered to be of primary concern regarding killing of cells, non-inertial cavitation critically influences the sound field and the bubble size distribution. Moreover, experiments performed by Hughes and Nyborg (1962) showed that cell rupture can occur in the absence of the collapse phenomenon and at surprisingly low power. The streaming produced near trapped gas bubbles vibrating at 20 kHz is of sufficient magnitude to cause cell disruption. In addition, the amount of inertial cavitation activity depends on both the energetics of each collapse and the number of collapses (Leighton, 1998). These considerations make it difficult to assess the mode of action of inertial and stable cavitation and to discriminate mechanical, chemical, and biological effects. Also, the significant spatial variations in the sound field point out the lack of uniformity of the treatment undergone by a microbial population.

The cavitation threshold of a medium and the fate of a bubble in a sinusoidal sound field are influenced by a number of parameters (Alliger, 1975; Earnshaw et al., 1995; Ince and Belen, 2001; Lorimer, 1990; Muthukumaran et al., 2006; Patist and Bates, 2008; U.S. FDA, 2000) including

– *amplitude of the ultrasonic waves*. The acoustic pressure (P_a) produced by sound waves is time (t) and frequency (f) dependent:

$$P_a = P_A \sin(2\pi f t) \tag{12.1}$$

where P_A is the maximum acoustic pressure amplitude of the wave. P_A is related to the intensity of the source (I, energy flowing per unit area per unit time) according to

$$I = P_A^2 / 2\,\rho\,c \tag{12.2}$$

where ρ is the density of the medium and c is the velocity of sound in the medium. The larger the intensity, the greater the value of P_A, the displacement of the molecules, and the collapse pressure. Hence, the faster and more violent is collapse.

- *frequency of the ultrasonic waves*. The bubble size is inversely proportional to the frequency. At lower frequencies, the bubbles generated are bigger in size, and when collapse occurs, higher energies are liberated. As the frequency increases, bubble formation becomes increasingly difficult and at frequencies above 2.5 MHz, cavitation is no longer observed and the main mechanism is acoustic streaming.
- *external pressure*. Increasing external pressure increases the cavitation threshold; thus, the number of cavitation bubbles is reduced. However, increasing the external pressure will increase the pressure in the bubble at the moment of collapse, resulting in a more rapid but violent collapse.
- *temperature*. Temperature affects vapor pressure, surface tension, and viscosity of the medium. More cavitation bubbles are produced at higher temperatures because vapor pressure is increased and tensile strength decreases. Also, increased temperature reduces viscosity, resulting in a decrease in the amount of energy needed to separate the liquid. Thus, cavitation bubbles form more easily. On the other hand, collapse is cushioned by higher vapor pressure. There is thus an optimum temperature at which the viscosity is low enough to allow violent cavitation bubbles to form, yet low enough to avoid the dampening effect caused by a high vapor pressure.
- *presence of impurities*. Impurities such as soluble gases and/or solid particles reduce the cavitational threshold through formation of excess cavitational nuclei leading to a larger number and variety of collapse events.

It is clear that many process and food parameters affect ultrasound output and the effect on microorganisms. This complexity and the sometimes poor control of process variables in inactivation experiments might explain the contradictory results found in the literature in relation to the mode of action and efficacy of high-power ultrasound and the sensitivity of different organisms. Kinetic data reported in the literature are usually not directly comparable because of the very dissimilar experimental conditions used in the studies.

Resistance of different species to ultrasound differs widely. Sporulated microorganisms are much more resistant than vegetative microorganisms, and fungi are more resistant in general than vegetative bacteria (Alliger, 1975). Previous research about the relative germicidal efficacy of ultrasound versus gram-negative and gram-positive bacteria is not in agreement (Piyasena et al., 2003). Alliger (1975) and Ahmed and Russel (1975) reported that gram-negative rod-shaped bacteria were more sensitive than gram-positive coccus-shaped bacteria, concluding that the smaller and rounder the cell, the more difficult it was to disrupt. In the same way,

a greater resistance was exhibited by the gram-positive *Streptococcus thermophilus* as compared to the gram-negative *Pseudomonas fluorescens* during continuous flow ultrasonication of Trypticase Soy Broth (Villamiel, and de Jong, 2000). In contrast, Scherba et al. (1991) did not find any difference in the killing rate of gram-negative (*Pseudomonas aeruginosa* and *Escherichia coli*) and gram-positive (*Staphylococcus aureus* and *Bacillus subtilis*) bacteria by ultrasonic treatment. As gram-positive bacteria have a thicker and a more tightly adherent layer of peptidoglycans than gram-negative bacteria, the authors argued that this morphological difference did not seem to affect the percent killed by ultrasound. They concluded that the target of ultrasonic damage may be the cytoplasmic membrane, which consists of a lipoprotein bilayer.

In spite of the substantial work conducted since the 1960s to understand the mechanism of ultrasound interaction with microorganisms, there is still no complete agreement about the specific effect(s) of cavitation which results in the death of cells. Clarke and Hill (1969) stated that ultrasound killing appears to be an "all or nothing effect," since survivors appeared to be unaffected with respect to growth rate and microscopic appearance. In a study carried out by Alliger (1975), cell walls of sonicated bacteria often appeared thinner than non-sonicated cell walls. The cytoplasmic layers were released from the cell wall, although these layers were difficult to separate. Mitochondria were disrupted with fine membrane fragmentation and changes in sedimentation pattern, but organized structure was retained, since these subcellular particles were able to conduct oxidative phosphorylation.

Ultrasound has also been proved to depolymerize large molecules. The chain breaking reaction can be produced by pulsation of bubbles as well as bubble collapse. The greater the molecular weight, the more pronounced is the effect (Alliger, 1975). Doty et al., in a study published in 1958 (Hughes and Nyborg, 1962), demonstrated that a DNA molecule was broken across the phosphate sugar backbone by liquid shear. In contrast, free radical attack breaks the hydrogen bonding between bases. The breakdown of DNA occurred more rapidly at the higher amplitudes. These chemical effects resulting from shear due to eddying of the liquid around bubbles were thus clearly separated from the chemical effects of free radical formation.

Structural studies were performed by Guerrero et al. (2001a) in *Saccharomyces cerevisiae* cells sonicated at 45°C and 95.2 μm of wave amplitude (20 kHz, 600 W, 95 ml sample) in Sabouraud broth (pH 5.6) for 20 min. The treatment caused puncturing of cell walls with leakage of content as well as damage at the inner cellular level. Micrographs in Fig. 12.1 illustrate some structural changes observed: cytological disruption of organelles, puncturing of cell wall, wall rupture or fragmentation, and breakage of plasma membrane. In some cells, the contents emptied until the cells appeared as a ghost. These observations lead to two important conclusions. In the first place, pitting and erosion of the cell surface was not the only mechanism responsible for *S. cerevisiae* damage, since the inner structure of the cell seemed to be strikingly affected. Second, the cells appeared damaged in different ways, as seen in Fig. 12.1. Some cells showed discomposed inner structure, but the cell wall and cytoplasmic membrane were not broken; in other cells, disorganization of inner content as well as rupture of wall and plasma membrane was observed. The treatment

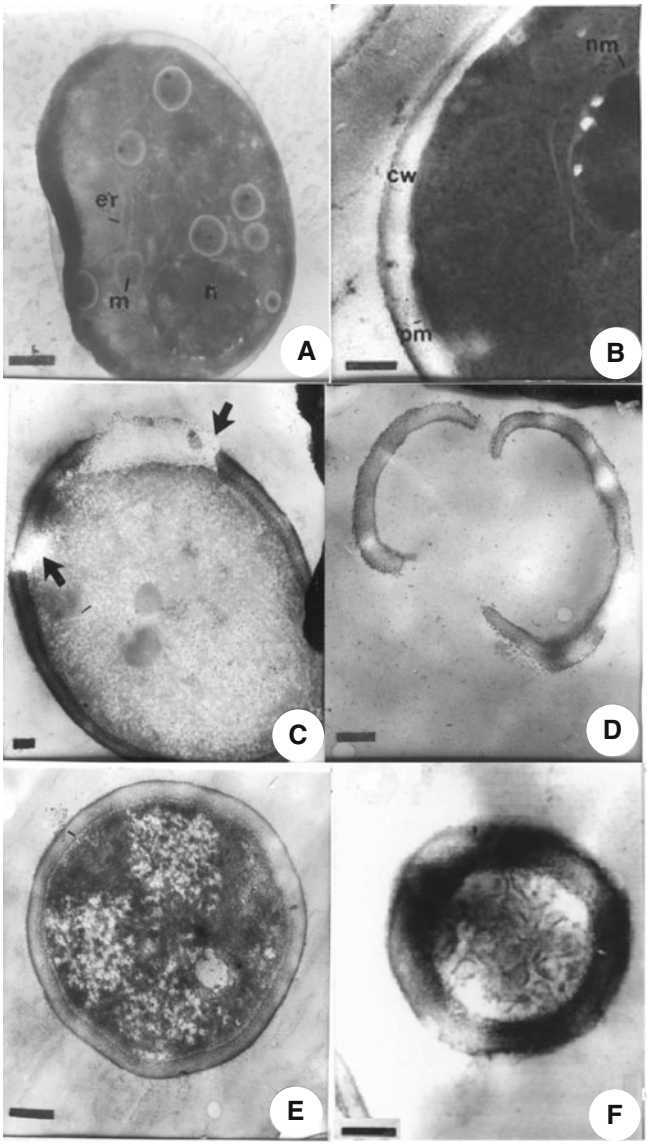

Fig. 12.1 TEM images of *S. cerevisiae*. (**A**, **B**) Control. (**C**–**F**) sonicated cells (20 kHz, 95.2 μm of wave amplitude, T=45°C, 20 min). (**A**) Very well differentiated organelles; (**B**) detail of electronically dense cell wall and a continuous plasma membrane; (**C**) inner material radiating from the cell wall (*arrow*); (**D**) rests of cell wall and plasma membrane; (**E**) disturbed inner structure, cell wall, and cytoplasmic membrane not broken; (**F**) swollen damaged cell wall, shrinkage of inner material, complete disruption of organelles. Scale: a, c, f: 200 nm; b: 100 nm; d, e: 500 nm. cw: cell wall, pm: plasma membrane; er: endoplasmic reticulum; m: mitochondrium, n: nucleolus (adapted from Guerrero et al., 2001a)

provoked a 1.7 log reduction and the inactivation appeared to follow a first-order kinetics throughout the assayed sonication time (20 min).

Cameron et al. (2008) evaluated the effect of power ultrasound (20 kHz, 750 W, 124 μm wave amplitude, 25°C, 40 ml sample) on the survival of *E. coli*, *Lactobacillus acidophilus*, and *S. cerevisiae* suspended in sterile saline solution and UHT milk and used TEM to assess structural damage inflicted ultrasonically. Ultrasonication provoked damage to the outer cell wall and inner cell membranes on all three microbes. This damage was not uniform in the population. In the three cases, after 2 min ultrasound treatment, intact cells were seen, as well as cells without cytosol and intracellular content. In the case of yeast, internal damage to the cell organelles was also observed. In *E. coli*, the dissociation of the three layers of the gram-negative cell boundary and associated formation of vesicles were visualized. These minute vesicles were seen within and external to the cells. The formation of these liposome-like vesicles was attributed to an emulsification process of membrane lipids and air bubbles associated with cavitation.

Multiparameter flow cytometry analysis was applied by Ananta et al. (2005) and by Schenk et al. (Schenk, M., Raffellini, S., Guerrero, S., and Alzamora, S. M. (2008), "unpublished results") to obtain a more precise explanation regarding ultrasound-induced cell death. This technique allows determination of physiological characteristics of microorganisms on a single-cell basis as well as identification of heterogeneities within populations with regard to structure and function (Ueckert et al., 1995). Overall population susceptibility after ultrasound is dependent on the physiological state distributions of subpopulations, which can be determined by flow cytometry. Different fluorescent probes have been shown to be good indicators for determination of relevant cellular characteristics in flow cytometry studies. In particular, non-fluorescent, membrane-permeant carboxy-fluorescein diacetate (cFDA) or fluorescein diacetate (FDA) cross intact or damaged cell membranes and, once inside the cell, are hydrolyzed by non-specific intracellular esterases to form green fluorescent, impermeant (or slowly permeant) products (cF and F, respectively). The fluorescent products are retained in cells with intact membranes and are quickly lost from non-viable cells with damaged membranes. Thus, these fluorescein derivates are employed as indicators of metabolic activity (enzyme activity) and membrane integrity. Propidium iodure (PI), used to determine damage in membranes, is a membrane impermeable dye that can enter cells mainly via damaged membranes of stressed, injured, or dead cells and intercalate into DNA and RNA, *giving* red fluorescence . Failure of a cell to be stained with PI is taken as a viability indicator, although transient permeability to this dye can be induced by certain chemical and physical treatments, with subsequent recovery of membrane integrity and viability (Shapiro, 2000).

The effect of exposure to ultrasound (20 kHz, 160 μm wave amplitude, ≈16°C), up to 20 min on gram-negative *E. coli* and gram-positive *Lactobacillus rhamnosus*, was evaluated by applying a double-staining strategy using cFDA and PI (Ananta et al., 2005). The majority (77%) of *L. rhamnosus* 20 min treated cells were still able to retain cF and were not stained by PI, showing that the integrity of cytoplasmic membrane was not seriously affected in this subpopulation. Only 7% of the cell population was labeled with PI and was considered as dead. In contrast,

only 8% of the initial population could resume growth when plating sonicated cells on MRS agar. When *E. coli* was exposed to high-power ultrasound, the population accumulating cF increased progressively (up to ≈83%) within the first 10 min and afterward no considerable changes in the percentage of cF-stained *E. coli* cells were observed. It is well known that the outer membrane of intact gram-negative bacteria excludes the viability marker cFDA. Apparently, the penetration of cFDA, and consequently its conversion by intracellular esterase, resulted from the destabilizing impact of ultrasound on the outer membrane of the gram-negative *E. coli*. The *E. coli* cells solely labeled with PI were not detectable, suggesting that the cytoplasmic membrane was not drastically ruptured. A small percentage (16%) of cells were double stained with cF and PI, indicating an intermediate state of membrane damage. When flow cytometry data were compared with plate count results, the percentage of survival cells decreased as the proportion of cF-labeled cells increased as the treatment progressed. Thus, disruption of the outer membrane was shown to be accompanied with the loss of viability, despite the metabolic activity still present in the *E. coli* cells, which emitted green fluorescence. The authors concluded that the major action site of ultrasound on inducing lethal effects on gram-positive and gram-negative bacteria was not necessarily the cytoplasmic membrane, as it was observed that the majority of ultrasound-treated population was still able to accumulate cF and did not allow PI penetration.

Cellular injuries occurring in cells of *S. cerevisiae* in response to high-power ultrasound (20 kHz, 600 W, 45°C, 95.2 μm wave amplitude; 95 ml sample) were also evaluated using classical plate count technique and flow cytometry with FDA–PI staining (Schenk, M., Raffellini, S., Guerrero, S., and Alzamora, S. M. (2008), "unpublished results"). To differentiate bacterial population based on their fluorescence properties as well as to assess treatment effect, the dual-parameter density plot of the green fluorescence (*x*-axis) and the red fluorescence (*y*-axis) was used (Figs. 12.2 and 12.3). Each dot, which constitutes the cell cloud, represents one

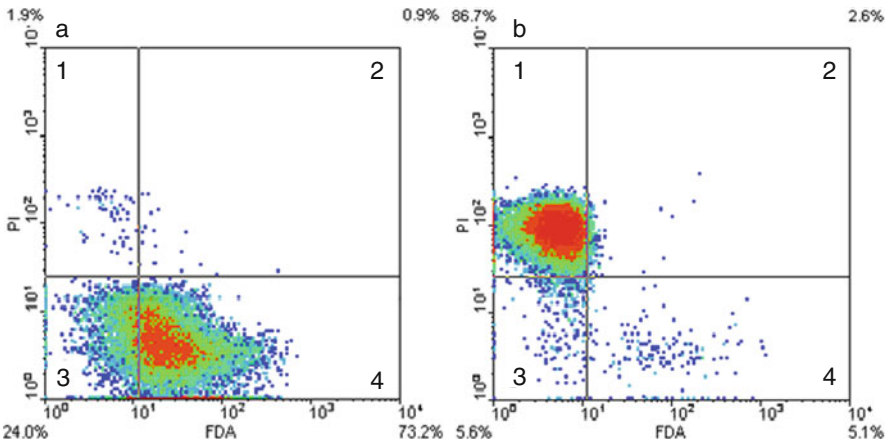

Fig 12.2 Fluorescence density plot of intact (**a**) and heat-treated *S. cerevisiae* cells (80°C, 15 min) after FDA and PI staining (**b**)

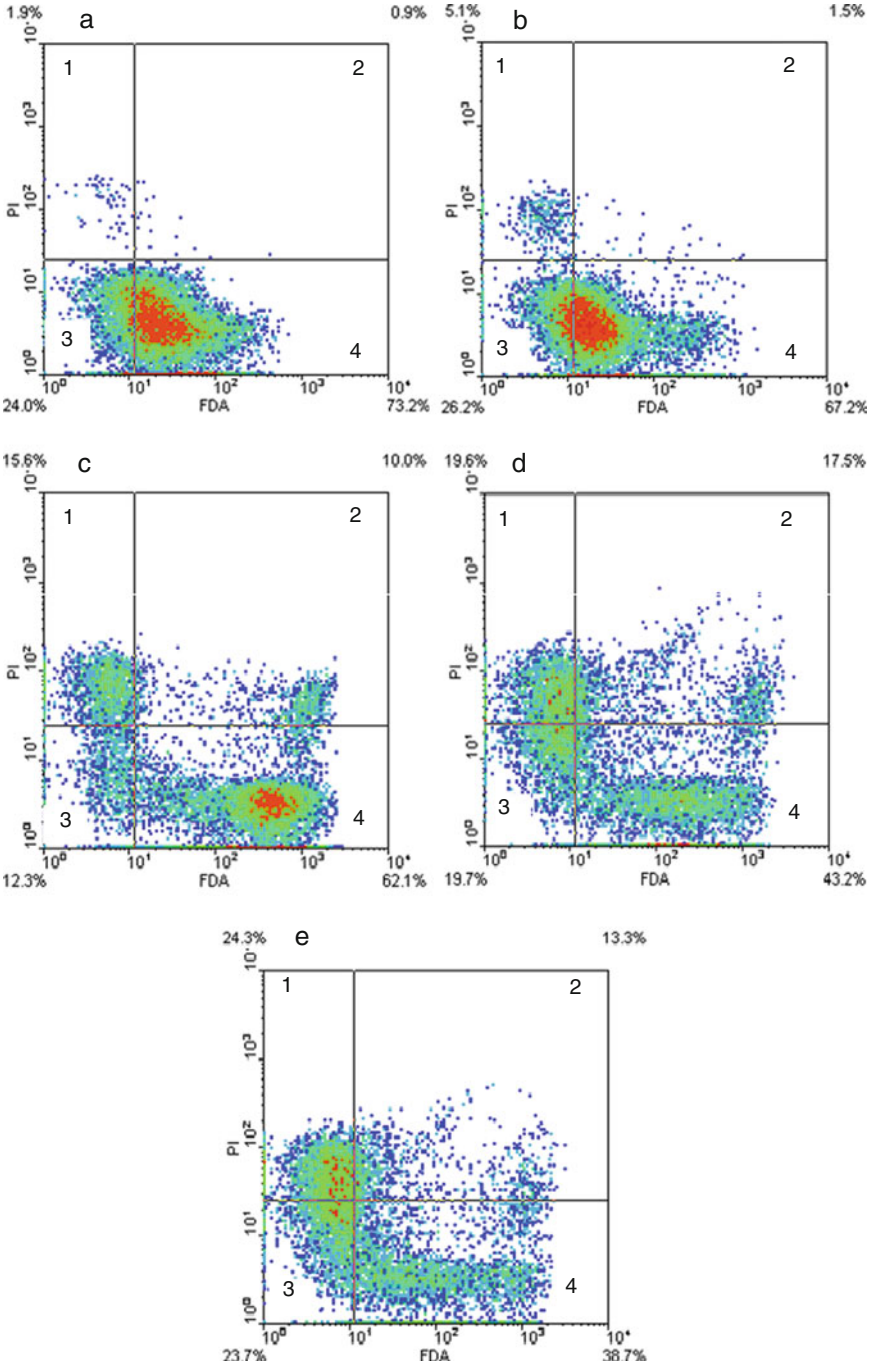

Fig. 12.3 Fluorescence density plots of *S. cerevisiae* cells in response to staining with FDA and PI after ultrasound treatment (20 kHz, 600 W, 45°C, 95.2 μm wave amplitude) in Sabouraud broth (pH 5.6) at different exposure times: (**a**) 0 min, (**b**) 5 min, (**c**) 10 min, (**d**) 15 min, and (**e**) 20 min

single cell, which is plotted as a coordinate of its green and red fluorescence value. The response of untreated and heat-damaged cells (80°C, 15 min) toward FDA–PI staining was used to set the quadrants' arrangement (Fig. 12.2). Events on the density plots were grouped in four distinct populations according to their fluorescence status. Cells with active esterase and intact membrane were detected in quadrant 4 (cF positive/PI negative), whereas dead cells (esterase activity not detectable, membrane compromised) were detected in quadrant 1 (cF negative/PI positive). Unstained cells (esterase activity not detectable or F extruded out of the cells, intact membrane) appeared in quadrant 3 (cF negative/PI negative). Cells in quadrant 2 (cF positive/PI positive) represented cells with permeabilized cytoplasmic membrane and esterase activity.

Prior to treatment, 73% of *S. cerevisiae* cells actively accumulated F (high green fluorescence) and excluded PI (low red fluorescence) as they were encountered in quadrant 4 (Fig. 12.2a). However, 24% of the yeast population did not yield green fluorescence and was thus gated in quarter 3. This deviating behavior could be attributed to an F-active efflux from yeast cells in the presence of glucose contained in the reaction medium (Breeuwer et al., 1994). This F efflux is most likely mediated by an ATP-driven transport system and could also be used as an additional indicator of metabolic performance of the cell (Ananta et al., 2004). Some cells (2.8%) in the presumed totally healthy population were already in "injured" or even permeabilized state. Upon heat-induced rupture of the cell membrane, yeasts were not capable of excluding PI and did not exhibit metabolic activity (low green fluorescence). These cells were thus framed in quadrant 1 (Fig. 12.2b).

When *S. cerevisiae* cells were exposed to ultrasound up to 20 min (Fig. 12.3a–e), yeast membrane integrity was gradually lost, increasing the percentage of cells in quadrant 1 (low green fluorescence and high red fluorescence) up to 24.3%. Metabolic activity (quadrant 2+4) also decreased slowly during US treatment. However, a great number of cells (38.7%) were still able to retain F and were not stained by PI remaining in quadrant 4 (Fig. 12.3e). In this subpopulation, and also in cells included in quadrant 3 (percentage values ranging between 12 and 26% during treatment), the integrity of the cytoplasmic membrane was not seriously affected by ultrasound. Thus, different subpopulations could be identified based on their differential uptakes of the probes, representing intact membrane cells, permeabilized/dead cells, and potentially injured/non-culturable cells.

The flow cytometry results tended to overestimate the viability of *S. cerevisiae* compared to plate counts (Fig. 12.4). According to culture results, viability loss was at least 1 log cycle after 20 min of ultrasound. On the other hand, the cells with cytoplasmic membrane damage (labeled by PI and gated in quadrant 1 and 2) constituted only 37.6% of the population. In agreement with the findings of Ananta et al. (2005), this fact suggests that the loss of the ability of *S. cerevisiae* to reproduce induced by sonication was not only due to cytoplasmic membrane damage. Microphotographs shown in Fig. 12.1 for *S. cerevisiae* sonicated in similar conditions confirm the findings of the flow cytometry test.

These more recent transmission electron microscopy (TEM) and flow cytometry studies constitute a step toward better understanding of the inactivation mechanism

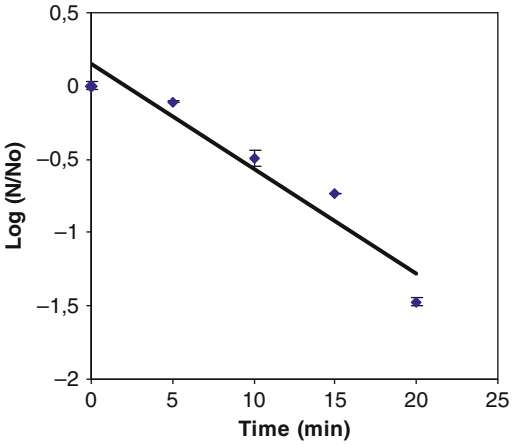

Fig. 12.4 Survival curve of *S. cerevisiae* during ultrasound treatment (20 kHz, 600 W, 45°C, 95.2 μm wave amplitude) in Sabouraud broth (pH 5.6). Error bar: S.D. Predicted values using first-order kinetic model (No: initial number of yeast cells and N: survival yeast count, CFU/ml)

by power ultrasound. These studies have demonstrated that (a) cells contain several targets for the disruptive action of ultrasound (cell wall, cytoplasmic membrane, DNA, internal cell structure, outer membrane); (b) membranes do not appear to be the primary target of ultrasound; and (c) the primary target depends on the specific microorganism (for instance, the outer membrane in *E. coli*).

3 Combinations with Other Hurdles

Because of the long contact times and large ultrasound power required to achieve high levels of microorganism reduction, current research to enhance microbial inactivation by ultrasound is focused on two approaches (Earnshaw, 1998; Ince and Belen, 2001; Ordoñez et al., 1984; Piyasena et al., 2003; Sala et al., 1995):

(a) The combination of ultrasound with other gentle hurdles to disturb the active homeostasis of vegetative microorganisms and the passive refractory homeostasis of spores at a number of sites or in a cooperative manner;
(b) The selection of ultrasound process variables to increase cavitation phenomenon and bubble collapse energy.

The efficiency of ultrasound has been demonstrated to be improved when applied in combination by heat and/or pressure, chemicals often used for sanitation and disinfection (synthetic or natural antimicrobials), and other physical preservation factors (ultraviolet-C light, pulsed electric fields, etc.). Microbial lethal efficacy of manothermosonication has been highly revised and updated in this book in Chapter 11. Selected recently published studies mainly based on the first approach are considered next.

3.1 Ultrasound and Mild Heating

The aim of the simultaneous application of ultrasound and temperature on microorganism inactivation has been to reduce the temperature and/or the process time of the sterilization processes. Ultrasound processing in combination with sublethal temperatures or with lethal temperatures (ultrasound-assisted thermal processing) has many advantages and has proven to be of potential interest in food preservation. It can lead to better quality products than conventional heat-treated products, with improvements in taste, texture, and appearance. It also could result in reduced energy requirements and therefore reduced cost.

In addition to the effect on the cavitation phenomenon per se, temperature can be a factor in the ultrasound sensitivity of an organism. If pressure changes that occur during cavitation are responsible for the inactivation effect of ultrasound, then raising the temperature and, hence, membrane fluidity (i.e., weakening the intermolecular forces) would enhance the disruption (Russell, 2002). As first introduced by García et al. (1989), bacterial cells become more sensitive to heat treatment if they have undergone ultrasound treatment. Increased cell death has been demonstrated in cells that are subjected to ultrasound and heat treatment in combination compared with cells subjected to only sonication.

Table 12.1 summarizes the resistances to heating and thermoultrasound for different microorganisms at varied temperatures and media reported in the literature. Differences in cell sensitivity against thermoultrasonic treatment are evident. These differences may result from the specific impact of ultrasound on the cell wall and differences in the cell wall structures, cell shape, and volume of species or ultrasonic processing conditions. In general, thermoultrasonic treatment caused a higher killing effect than heat treatment. This effect was more notorious in real food than in culture media. However, as temperature increased toward lethal values, the benefits of ultrasound application were reduced (Table 12.1), probably as a result of an increased thermal effect and a reduced intensity of cavitation (Guerrero et al., 2001a; López-Malo et al., 1999, 2005).

The use of thermoultrasonication could represent benefits as a potential technology for selective inactivation of microorganisms, promising pasteurization of fermented products while retaining the viability of probiotic cultures (Knorr et al., 2004). In particular, Zenker et al. (2003) studied the combined effects of ultrasound-assisted temperature (20 kHz, 50–160 μm; T 48–60°C; sample volume =10 ml) and heat treatment versus conventional heating (56–68°C) on the inactivation of *E. coli* K12 DH 5α and *L. acidophilus* in phosphate buffer (pH 7.0) using a batch-type reactor. Their research clearly indicated improved inactivation of *E. coli* K12 DH by the treatment in combination, achieving, for example, at 60°C, nearly 6 log reductions in 2 min compared with 2 log reductions obtained with ultrasound (20 kHz, 110 μm, 28°C) or thermal treatment (60°C). When comparing the improved effectiveness regarding microbial inactivation by the thermoultrasonic process in comparison to thermal processing, *L. acidophilus* proved more resistant to the combined process than *E. coli* (see Table 12.1), in spite of an almost identical heat resistance.

Table 12.1 *D* parameter[a] (min) for thermal and thermoultrasonic inactivation of microorganisms in batch-type reactors

References	Microorganism	Media	T (°C)	D_T	D_{TUS}
García et al. (1989)[b]	*B. subtilis* spores	Whole milk	100	2.6	1.6
		Glycerol	100	40.5	9.1
	L. monocytogenes	UHT milk	60	2.1	0.3
Earnshaw et al. (1995)	*Zygosaccharomyces bailii*	Rice pudding	55	11.0	1.0
	Z. bailii	Orange juice	55	10.5	3.9
Guerrero et al. (2001a)[c]	*S. cerevisiae*	Sabouraud broth (pH 5.6)	55	1.2	1.3
			45	98.0	14.4
			35	NLV	21.4
Zenker et al. (2003)[d]	*E. coli*	Phosphate buffer (pH 7.0)	60	1.4	0.4
		UHT milk (pH 6.7)	60	1.3	0.4
	L. acidophilus	Phosphate buffer (pH 7.0)	60	1.2	0.7
		Orange juice	60	0.8	0.5
		Distilled water	57	0.89	0.38
Cabeza et al. (2004)[e]	*S. enteritidis*	Eggs (60 g) immersed in water	57.8		0.25
			52		1.8
López-Malo et al. (2005)[f]	*Aspergillus flavus*	Sabouraud broth (a_w: 0.99 – pH 5.5)	60	2.6	1.2
	Penicillium digitatum	Sabouraud broth (a_w: 0.99 – pH 3.0)	60	1.6	0.8
		Sabouraud broth (a_w: 0.95 – pH 5.5)	60	2.5	1.2
		Sabouraud broth (a_w: 0.99 – pH 5.5)	52.5	13.3	5.3
		Sabouraud broth (a_w: 0.95 – pH 5.5)	52.5	34.4	11.5

[a] *D* values were obtained by fitting a first-order kinetics. *NLV*: the microorganism did not lose viability during the assayed time; D_T: *D*-value for thermal treatment; D_{TUS}: *D*-value for thermoultrasonic treatment at the same temperature

[b] US: 20 kHz, 150 W, *V*=30 ml; [c] US: 20 kHz, 107 μm, *V*:100 ml; [d] US: 20 kHz, 110 μm,10 ml; [e] US:24 kHz, 60 μm; *V*: 200 ml; [f] US: 20 kHz, 120 μm, *V*:100 ml

Inactivation studies with *Listeria monocytogenes* 10403S, an ultrasound-resistant strain, were conducted at sublethal (20–40°C) and lethal (50–60°C) temperatures in saline solution (pH 7.0), acidified saline solution (pH 3.4), and apple cider (pH 3.4) with and without application of ultrasound (20 kHz, 750 W, sample volume = 99 ml) (Baumann et al., 2005). Application of ultrasound increased the inactivation rate at both lethal and sublethal temperatures. The reduction in the *L. monocytogenes* population followed first-order kinetics at sublethal temperatures, but at lethal temperatures semilogarithmic survival curves were clearly nonlinear, showing a fast inactivation section and a tailing. The effects of pH on inactivation were negligible at sublethal temperatures, but were significant at lethal temperatures. The bactericidal effect of the combined process was additive in apple cider. After 5 min of thermoultrasonic treatment at 60°C, cells of *L. monocytogenes* 10403S died during a 6 h period at room temperature. These treatment conditions could provide a solution for apple cider industries to achieve the required 5 log reduction in pathogenic populations.

3.2 Ultrasound and Chemicals

The addition of naturally occurring and/or synthetic antimicrobials has proven to be an effective hurdle when combined with non-thermal processing techniques (Lado and Yousef, 2002) (Table 12.2). The overall inactivation effect observed when ultrasound treatment was combined with addition of antimicrobials has been reported to depend on several factors, such as the considered antimicrobial agent and its concentration, the medium, and the studied microorganism, making it difficult to draw a general conclusion (Alzamora et al., 2003).

Phenolic compounds have lipophilic nature and could accumulate in the lipid bilayer of the cell, disturbing and sensitizing the membrane to ultrasound (Brul and Coote, 1999). In addition, ultrasonic waves improve antimicrobial action by weakening the cell wall. Improved inactivation was obtained when *S. cerevisiae* was exposed to the combined action of ultrasound and cinnamon at non-growth inhibitory concentrations (less than 50 ppm) in laboratory media (Guerrero et al., 2001c). The effect depended on the type of cinnamon and specific process conditions. Addition of 50 ppm cinnamon-type China was significantly more effective than addition of 100 ppm cinnamon-type Ceylon, reaching more than 2.5 log reductions in 20 min exposure to ultrasound (600 W, 20 kHz, 95 μm; 45°C; sample volume = 100 ml). The preincubation of the yeast in the presence of 100 ppm cinnamon-type Ceylon during 35 h and subsequent ultrasonic treatment yielded more inactivation than the direct exposure to cinnamon and ultrasound (Guerrero et al., 2001c). In the same way, the addition of vanillin (800 ppm) did not significantly improve the inactivation effect of thermoultrasonic treatment against *S. cerevisiae* cells at pH 5.6 in laboratory media. But when a lower amount of vanillin (500 ppm) was combined with the addition of citric acid to reduce pH value to 3.0, the effect was greater. This synergy was even greater when the medium was supplemented in equal proportions (500 ppm) with EDTA (Guerrero et al.,

Table 12.2 Summary of combined antimicrobial ultrasound research

References	Media	Microorganism	Ultrasound conditions	Antimicrobial	Log reductions
Guerrero et al. (2001a, b, c)	SB (pH 5.6)	*S. cerevisiae*	600 W; 95.2 μm; 20 min; 45°C	w/antimicrobial	1.13
Guerrero et al. (2001b)	SB (pH 5.6)	*S. cerevisiae*	600 W; 92.5 μm; 20 min; 45°C	1,000 ppm EDTA	1.54
				500 ppm EDTA + 500 ppm vanillin	1.42
				100 ppm KS/500 ppm KS	1.34/1.76
	SB (pH 3.0)	*S. cerevisiae*	600 W; 95.2 μm; 20 min; 45°C	50 ppm Ch. cinnamon	2.74
Guerrero et al. (2001c)	SB (pH 5.6)	*S. cerevisiae*	600 W; 95.2 μm; 20 min; 45°C	100 ppm Cy. cinnamon	1.30
				100 ppm Cy. cinnamon (35 h preinc)	1.88
López-Malo et al. (2005)	SB (pH 5.6)	*A. flavus*	400 W; 90 μm; 9 min; 52.5°C	w/antimicrobial	0.55
				500 ppm vanillin	1.31
				500 ppm KS	2.27
				1,000 ppm LW chitosan	1.97
Guerrero et al. (2005)	SB (pH 5.6)	*S. cerevisiae*	600 W; 95.2 μm; 30 min; 45°C	1,000 ppm LW chitosan (30 min preinc)	2.98
				1,000/1,500 ppm vanillin	1.80/3.45
				75/100 ppm citral	2.28/2.00
Ferrante et al. (2007)	Orange juice (pH 3.7)	*L. monocytogenes*	600 W; 95.2 μm; 15 min; 45°C	w/antimicrobial	2.60
				75/100 ppm citral + 1,000/1,500 ppm vanillin	3.18/5.89

KS: potassium sorbate; *Ch. cinnamon*: Chinese cinnamon; *Cy. cinnamon*: Ceylon cinnamon; *LW chitosan*: low-weight chitosan; *w/antimicrobial*: without antimicrobial; *SB*: Sabouraud broth; *preinc*: preincubation

2001c). As previously stated, EDTA and vanillin would share at least one common mechanism of action altering microbial cell permeability, permitting the loss of macromolecules from the interior and facilitating the penetration of the phenolic compound into the cell and its interaction with enzymes and proteins (Conner and Beuchat, 1984). Both antimicrobials would cooperate with ultrasound action on the yeast.

Guerrero et al. (2005) investigated the use of low-weight chitosan (1,000 ppm) in combination with high-intensity ultrasound (600 W; 20 kHz, 95.2 μm wave amplitude, 45°C; V:100 ml) against *S. cerevisiae* in Sabouraud broth (pH 5.6). Incubation of yeast with 1,000 ppm low-weight chitosan for 30 min at room temperature reduced the viable cells by approximately 1 log cycle prior to sonication. This pretreatment led to the greatest yeast inactivation throughout the ultrasonic treatment (3 log cycles after 25 min sonication) (Fig. 12.5a). Transmission electron microphotographs of the cells revealed, for the majority of cells in the population, that ultrasonic treatment in the presence of chitosan (without preincubation) resulted in swollen and loose walls (Fig. 12.5b). When the yeast was preincubated with chitosan for 30 min and then sonicated, cell walls appeared less swollen and more densely stained than those without preincubation. Cells seemed deformed and with an unnatural shape. The efflux of intracellular material could be visualized to originate from puncture sites at the cell surface. Disrupted cytoplasm appeared separated from the wall to the inner part of the cell. The plasma membrane was not visible. The increase of the chitosan (a flexible polymer) content of the cell wall would result in a less rigid and more easily deformed cell wall. Interaction of chitosan with anionic groups of the yeast cell wall could prevent transport of essential constituents, destabilizing the cell and cooperating with the ultrasonic treatment to provoke cell leakage.

The addition of the different antimicrobials to the sonication media also changed the inactivation kinetics. Yeast inactivation in systems treated by ultrasound alone generally followed a first-order kinetics during the greater part of the process, while combination with cinnamon, vanillin, or chitosan addition (with or without preincubation) showed nonlinear survival curves (Guerrero et al., 2001b).

Additional efficiency achieved by the combination of vanillin, citral, and ultrasound was demonstrated by Ferrante et al. (2007). The combination of high-intensity ultrasound (600 W, 20 kHz, 95 μm, 45°C; V:100 ml) with vanillin (500–1,500 ppm) and citral (25–100 ppm) significantly increased *L. monocytogenes* inactivation in fresh squeezed orange juice (pH 3.5) with respect to individual treatments. The addition of 1,000 ppm vanillin followed by sonication slightly improved *L. monocytogenes* inactivation observed when single treatments were applied, achieving only 1.8 log cycle reductions after 15 min exposure. In contrast, 3.5 log reductions were obtained with an increase in vanillin concentration from 1,000 to 1,500 ppm followed by 15 min ultrasonic treatment. The addition of a small proportion of citral (25–100 ppm) significantly increased the efficacy of *L. monocytogenes* inactivation due to the ultrasound/vanillin combined treatments in orange juice. Vanillin and citral both would alter microbial membrane permeability, facilitating the loss of specific ions from the interior, affecting proton motive force,

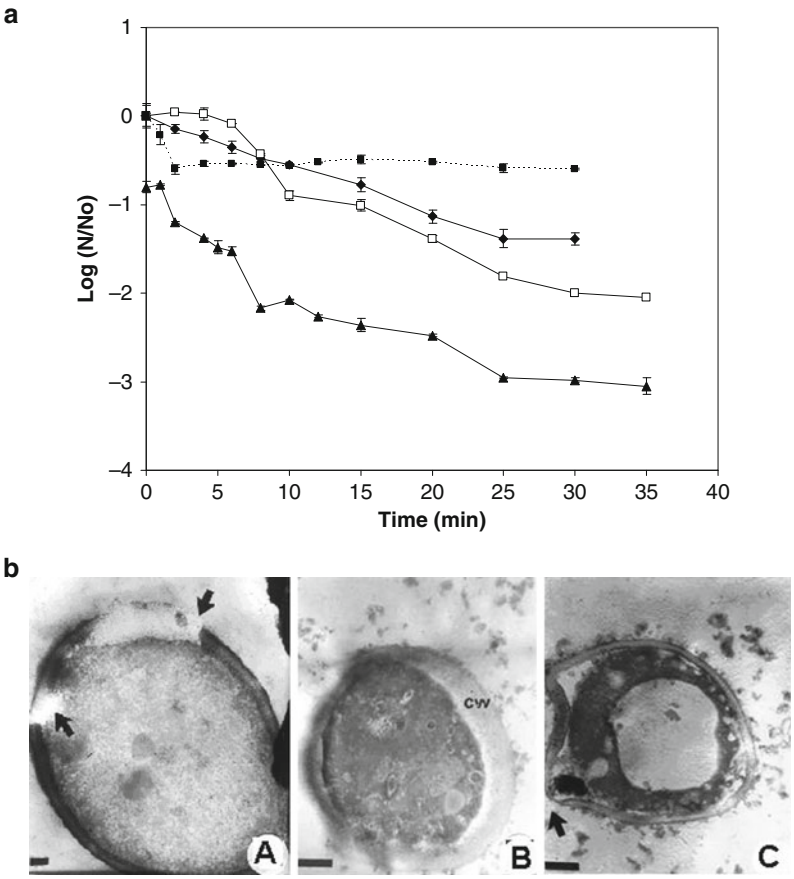

Fig. 12.5 (**a**) Semilogarithmic survival curves of *S. cerevisiae* during ultrasonic treatments in Sabouraud broth: ultrasonic treatment (-♦-); 1,000 ppm chitosan without sonication (- -■- -); 1,000 ppm chitosan and sonication (-□-); 1,000 ppm chitosan, incubation 30 min and sonication (-▲-); standard deviation (I); initial number of yeast cells (No: CFU/ml) and yeast survivor count (N: CFU/ml) (**b**) TEM images of *S. cerevisiae. A*: sonicated cell (20 min; 20 kHz; 95.2 μm of amplitude; *T*: 45°C). *B* cell sonicated 20 min in presence of chitosan. *C* cell incubated during 30 min in presence of chitosan and then sonicated 20 min (adapted from Guerrero et al., 2005)

and reducing the intracellular ATP content and the overall activity of microbial cells (Conner and Beuchat, 1984). Semilogarithmic survival curves of *L. monocytogenes* exposed to the combined action of ultrasound and antimicrobials were clearly non-linear. The different survival patterns could be well described in terms of Weibull distributions, considering that there was a spectrum of resistances to the treatments in the population (Peleg and Cole, 1998). Figure 12.6a illustrates some experimental survival data corresponding to US vanillin, citral, US/vanillin, US/citral, and US/vanillin/citral treatments fitted using the cumulative Weibull distribution function. The correspondent frequency distributions are shown in Fig. 12.6b. The

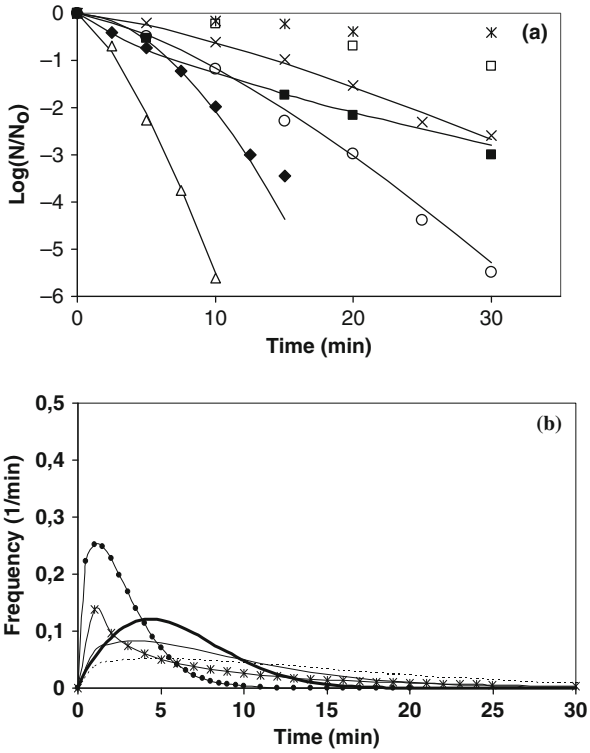

Fig. 12.6 Effect of ultrasound (US); 1,500 ppm vanillin and/or 75 ppm citral on survival of *L. monocytogenes* in orange juice (pH 3.5; 20 kHz; 95.2 μm; 45°C). (**a**) Experimental survival curves (*points*) and fitted values with the Weibullian model (*lines*): (⁎) control; (x) US; (□) citral; (■) vanillin; (◯) US/citral; (♦) US/ vanillin; (△) US/ vanillin/citral. (**b**) Frequency distribution of resistances: (- - -) US; (—⁎—) vanillin; (—) US/vanillin; (—) US/citral; (—•—) US/vanillin/citral (adapted from Ferrante et al., 2007)

presence of vanillin and/or citral not only greatly increased the bactericidal effect of thermosonication, but also changed the distribution of inactivation times. When both antimicrobials were added together and ultrasound was applied, narrowest frequency shapes, skewed to the right, with low dead time means and a very substantial decrease in its overall spread, were obtained. Ternary combinations (citral plus vanillin plus sonication) at moderate temperature highly reduced times of exposure to ultrasound in order to reach a determined inactivation.

Other authors have investigated ultrasound as a potential facilitator of the delivery and absorption of drugs. Rediske et al. (1999) reported that ultrasound (70 kHz, 2.2 W/cm^2) in combination with erythromycin reduced the viability of *P. aeruginosa* by 1–2 orders of magnitude compared with antibiotic alone, even at concentrations below the minimum inhibitory concentration. Electron spin resonance studies have suggested that physical disruption or stress of the outer membrane by ultrasound

may decrease the stability of the tightly packaged lipopolysaccharide molecules, thereby allowing a greater sorption or diffusion of the hydrophobic molecules of erythromycin.

3.3 Ultrasound and "Non-thermal" Physical Factors

Very few studies have attempted to apply non-thermal physical treatments (high hydrostatic pressure, pulsed electric field, or ultraviolet light) in combination with ultrasound.

Lee et al. (2003) investigated the application of ultrasound prior to high hydrostatic pressure (HHP) to pasteurize liquid whole egg. High-intensity ultrasound treatments were carried out using a lab-scale ultrasound equipment (20 kHz; 34.6 W; ΔT: 25°C; sample volume = 10 ml; 150 s). Pressure treatments were conducted at 5°C at 250 MPa for 886 s or at 300 MPa for 200 s. A consecutive combination of ultrasound and HHP resulted in no significant effects on *E. coli* and *Listeria seeligeri* in liquid whole egg within the experimental conditions. *E. coli* was more susceptible to both ultrasound and HHP than *L. seeligeri*, and the combined treatments of ultrasound and HHP caused a slightly increased extent of *E. coli* inactivation (∼0.8 log cycle reduction) due to the additional effect of ultrasound. The authors attributed the lack of combination effect on microbial inactivation to the low temperature used in the study (Lee et al., 2003).

Huang et al. (2006) studied the inactivation of *Salmonella enteritidis* in liquid whole egg using pulsed electric fields (PEF), high hydrostatic pressure (HHP), and ultrasound, alone and in combinations (PEF–ultrasound, ultrasound–PEF, HHP–PEF, PEF–HHP, ultrasound–HHP, and HHP–ultrasound). The conditions that yielded the maximum log reductions of *S. enteritidis* for each single treatment were applied in the combination treatments. The PEF conditions applied were 30 pulses with field strength of 5.67 kV/mm and 55°C, while the ultrasound conditions were 40 W at 55°C for 5 min with 25 ml sample volume. The optimal conditions for HHP were 2–2–4 min cyclic treatment at 138 MPa and 20°C. Combinations of PEF–ultrasound and ultrasound–PEF produced similar results to the sum of the two treatments alone (2.30 versus 2.40 log cycles), with no significant difference between the two treatments. Thus, combinations involving PEF and ultrasound were essentially a preheat treatment followed by an ultrasound treatment, and vice versa. The consecutive combination treatments involving ultrasound and HHP resulted in significant reductions of *S. enteritidis*. Although no synergy was observed, up to a 3 log reduction was achieved.

López-Malo et al. (2006) analyzed the response of *L. monocytogenes* and *S. cerevisiae* to the single and combined effects of high-intensity ultrasound (20 kHz, 400 W, 95.2 μm, T: 35°C, sample volume = 500 ml) and UV-C light (continuous flow system; 90 cm long glass tube with a 100 W xenon lamp, 1,100 $\mu W/cm^2$) in buffer model solution and in clarified apple juice. The inactivation pattern of individual and combined treatments was highly dependent on the medium of treatment and on the type of microorganism. Accordingly, survival curves exhibited

first-order inactivation kinetics, a marked upward concavity, or a marked downward concavity. In general, treatments involving UV-C light were slightly more effective applied in buffer solution than in apple juice. This effect could be explained by the presence of organic compounds and colored compounds, which reduced the efficiency in UV-C disinfection (Bintsis et al., 2000). The effect of the US/UV-C combination was additive and led to a large inactivation (≈4–5 log cycles reduction after 5 min treatment), with the majority of the population dead in the first minutes of treatment

The effect of thermosonication (TS) followed by pulsed electric fields (PEF) on inactivation of *S. aureus* and selected quality aspects in orange juice was investigated by Walkling-Ribeiro et al. (2009). Maximum bacterial inactivation was observed under the most severe conditions (TS for 10 min at 55°C with PEF at 40 kV/cm for 150 μs), resulting in an overall bacterial reduction of 6.8 log cycles, similar to the cycle reduction obtained by conventional thermal pasteurization (HTST, 94°C for 26 s). An additive effect on microbial inactivation between TS (1.8 log) and PEF (5.5) was detected. TS/PEF did not affect the pH, conductivity, or Brix and had a milder impact on juice color than thermal treatment. Thermal treatment caused an overall darkening of orange juice. By contrast, TS showed a significant increase in L^*, a minor decrease in a^*, and increase in b^*. But, when TS was followed by PEF, a gradual compensating effect was observed with increasing PEF duration. Thus, the TS/PEF-treated product was more similar to untreated juice than that obtained using PEF alone or the HTST process. In conclusion, the TS/PEF hurdle approach showed great potential for improving the quality and the safety of orange juice.

4 Future Prospects

The future of ultrasound in the food industry for fungicidal and bactericidal purposes lies in multifactorial processes. Although the results of multitarget inactivation presented in this study did not reveal spectacular microbial reduction, further studies can lead to the design of new combination processes with specific applications. A considerable amount of systematic work in controlled ultrasound operative conditions is still necessary. In addition, FTIR spectroscopy analysis, multiparameter cytometry, LM, SEM, and TEM images, as well as biochemical assays, molecular biological techniques, and analysis of DNA repair mechanisms could help to assess the contribution of primary and secondary damages due to ultrasound.

An in-depth understanding of the targets of ultrasound alone and combined with other stress factors as well as an examination of influencing parameters can open numerous opportunities in the commercial development of novel combined preservation systems.

Acknowledgments We acknowledge financial support from Universidad de Buenos Aires, CONICET and ANPCyT of Argentina, as well as from BID and Universidad de las Américas, Puebla and CONACyT (Projects 62275 and 84859) of Mexico.

References

Ahmed, F. I. K., and Russel, C. (1975). Synergism between ultrasonic waves and hydrogen peroxide in the killing of microorganisms. *Journal of Applied Bacteriology*, 39, 31–40.

Alliger, H. (1975). Ultrasonic disruption. *American Laboratory*, 10, 75–85.

Alzamora, S. M., Guerrero, S., López-Malo, A., and Palou, E. (2003). Plant antimicrobials combined with conventional preservatives for fruit products. In: Roller, S. (ed.), *Natural Antimicrobials for the Minimal Processing of Foods*, pp. 235–249. England, Woodhead.

Ananta, E., Heinz, V., and Knorr, D. (2004). Assessment of high pressure induced damage on *Lactobacillus rhamnosus* GG by flow cytrometry. *Food Microbiology*, 21, 567–577.

Ananta, E., Voigt, D., Zenker, M., Heinz, V., and Knorr, D. (2005). Cellular injuries upon exposure of *Escherichia coli* and *Lactobacillus rhamnosus* to high-intensity ultrasound. *Journal of Applied Microbiology*, 99, 271–278.

Baumann, A. R., Martín, S. E., and Feng, H. (2005). Power ultrasound treatment of *Listeria monocytogenes* in apple cider. *Journal of Food Protection*, 68, 2333–2340.

Bintsis, T., Litopoulou-Tzanetaki, E., and Robinson, R. (2000). Existing and potential applications of ultraviolet light in the food industry. A critical review. *Journal of the Science of Food and Agriculture*, 80, 637.

Breeuwer, P., Drocourt, J. L., Rombouts, F. M., and Abee, T. (1994). Energy-dependent, carrier-mediated extrusion of carboxyfluorescein from *Saccharomyces cerevisiae* allows rapid assessment of cell viability by flow cytrometry. *Applied and Environmental Microbiology*, 60, 1467–1472.

Brul, S., and Coote, P. (1999). Preservative agents in foods. Mode of action and microbial resistance mechanisms. *International Journal of Food Microbioligy*, 50, 1–17.

Cabeza, M. C., Ordoñez, J., Cambero, I., De la Hoz, L., and García M. L. (2004). Effect of thermoultrasonication on *Salmonella enterica* Serovar Enteritidis in distilled water and intact shell eggs. *Journal of Food Protection*, 67, 1886–1891.

Cameron, M., McMaster, L. D., and Britz, T. J. (2008). Electron microscopic analysis of dairy microbes inactivated by ultrasound. *Ultrasonics Sonochemistry*, 15, 960–964.

Clarke, P. R., and Hill, C. R. (1969). Biological action of ultrasound in relation to the cell cycle. *Experimenta .Cell Research*, 58, 443–444.

Clarke, P. R., and Hill, C. R. (1970). Physical and chemical aspects of ultrasonic disruption of cells. *The Journal of the Acoustical Society of America*, 47, 649–653.

Conner, D., and Beuchat, L. R. (1984). Effects of essential oils from plants on growth of food spoilage yeasts. *Journal of Food Science*, 49, 429–434.

Doty, P., McGill, B. B., and Rice, S. A. (1958). The properties of sonic fragments of deoxyribose nucleic acid. *Proceedings of the National Academy of Sciences* USA, 44, 432–438.

Earnshaw, R. G. (1998). Ultrasound: a new opportunity for food preservation. In: Povey, M. J. W., and Mason, T. J. (eds.), *Ultrasound in Food Processing*, pp. 183–192. London, New York, Blackie Academic and Professional.

Earnshaw, R. G., Appleyard, J., and Hurst, R. M. (1995). Understanding physical inactivation processes: Combined preservation opportunities using heat, ultrasound and pressure. *Food Microbiology*, 28, 197–219.

Ferrante, S., Guerrero, S., and Alzamora S. M. (2007). Combined use of ultrasound and natural antimicrobials to inactivate *Listeria monocytogenes* in orange juice. *Journal of Food Protection*, 70, 1850–1857.

García, M. L., Burgos, J., Sanz, B., and Ordóñez, J. (1989). Effect of heat and ultrasonic waves on the survival of two strains of *Bacillus subtilis*. *Journal of Applied Bacteriology*, 67, 619–628.

Guerrero, S., López-Malo, A., and Alzamora, S. M. (2001a). Effect of ultrasound on the survival of *Saccharomyces cerevisiae*: Influence of temperature, pH and amplitude. *Innovative Food Science and Emerging Technologies*, 2, 31–39.

Guerrero, S., Tognon, M., and Alzamora, S. M. (2001b). Utilización de la Ecuación de Gompertz modificada para predecir el efecto combinado de ultrasonido, pH y algunos aditivos en la inactivación de *Saccharomyces cerevisiae*. III Congreso Iberoamericano de Ingeniería de Alimentos. I Congreso Español de Ingeniería de Alimentos. Valencia, Spain.

Guerrero, S., Tognon, M., and Alzamora, S. M. (2001c). *Ultrasound and Natural Antimicrobials: Inactivation of Saccharomyces cerevisiae by the Combined Treatment*. New Orleans, LA, Institute of Food Technologists Annual Meeting.

Guerrero, S., Tognon, M., and Alzamora, S. M. (2005). Modeling the response of *Saccharomyces cerevisiae* to the combined action of ultrasound and low weight chitosan. *Food Control*, 16, 131–139.

Huang, E., Mittal, G. S., and Griffith, M. W. (2006). Inactivation of *Salmonella enteritidis* in liquid whole egg using combination treatments of pulsed electric field, high pressure and ultrasound. *Biosystems Engineering*, 94, 403–413.

Hughes, D. E., and Nyborg, W. L. (1962). Cell disruption by ultrasound. *Science*, 138, 108–114.

Ince, N. H., and Belen, R. (2001). Aqueous phase disinfection with power ultrasound: Process kinetics and effect of solid catalysts. *Environmental Science Technology*, 35, 1885–1888.

Knorr, D., Zenker, M., Heinz, V., and Lee, D. U. (2004). Applications and potential of ultrasonics in food processing. *Trends in Food Science and Technology*, 15, 261–266.

Lado, B. H., and Yousef, A. E. (2002). Alternative food-preservation technologies: Efficacy and mechanisms. *Microbes and Infection*, 4, 433–440.

Lauterborn, W., Kurz, T., Mettin, R., and Ohl, C. D. (1999). Experimental and theoretical bubble dynamics. In: Prigogine, I., and Rice, S. A. (eds.), *Advances in Chemical Physics*, pp. 295–380. New York, NY, Wiley.

Lauterborn, W., and Ohl, C. D. (1997). Cavitation bubble dynamics. *Ultrasonics sonochemistry*, 4, 65–75.

Lee, D.U., Heinz, V., and Knorr, D. (2003). Effects of combination treatments of nisin and high-intensity ultrasound with high pressure on the microbial inactivation in liquid whole egg. *Innovative Food Science and Emerging Technologies*, 4, 387–393.

Leighton, T. G. (1998). The principles of cavitation. In: Povey, M. J. W., and Mason, T. J. (eds.), *Ultrasound in Food Processing*, pp. 151–182. London, New York, Blackie Academic and Professional.

Lepoint, T., and Mullie, F. (1994). What exactly is cavitation chemistry? *Ultrasonics Sonochemistry*, 1, S13–S22.

López-Malo, A., Guerrero, S., and Alzamora, S. M. (1999). *Saccharomyces cerevisiae* thermal inactivation kinetics combined with ultrasound. *Journal of Food Protection*, 62, 10–13.

López-Malo, A., Guerrero, S., Santiesteban, A., and Alzamora, S. M. (2006). Inactivation kinetics of *Saccharomyces cerevisiae* and *Listeria monocytogenes* in apple juice processed by novel technologies. *ENPROMER 2005*. Rio das Pedras, Brasil, August 14–18.

López-Malo, A., Palou, E., Jiménez-Fernández, M., Alzamora, S. M., and Guerrero, S. (2005). Multifactorial fungal inactivation combining thermosonication and antimicrobials. *Journal of Food Engineering*, 67, 87–93.

Lorimer, J. P. (1990). Ultrasound in polymer chemistry. In: Mason, T. J. (ed.), *Sonochemistry: The Uses of Ultrasound in* Chemistry, pp. 112–131. England, The Royal Society of Chemistry.

Mason, T. J., Paniwnyk, J. P., and Lorimer, J. P. (1996). The uses of ultrasound in food technology. *Ultrasonics Sonochemistry*, 3, S253–S260.

Muthukumaran, S., Kentisch, S. E., Stevens, G. W., and Ashokkumar, M. (2006). Application of ultrasound in membrane separation processes: A review. *Reviews in Chemical Engineering*, 22, 155–194.

Ordoñez, J. A., Sann, B., Hernández, P. E., and López-Lorenzo, P. (1984). A note on the effect of combined ultrasonic and heat treatments on the survival of a strain of *Staphylococcus aureus*. *Journal of Dairy Research*, 54, 61–67.

Patist, A., and Bates, D. (2008). Ultrasonic innovation in the food industry: from the laboratory to commercial product. *Innovative Food Science and Emerging Technologies*, 9, 147–154.

Peleg, M., and Cole, M. B. (1998). Reinterpretation of microbial survival curves. *Critical Reviews in Food Science*, 38, 353–380.

Perkins, J. P. (1990). Power ultrasound. In: Mason, T. J. (ed.), *Sonochemistry: The Uses of Ultrasound in Chemistry*, pp. 47–59. England, The Royal Society of Chemistry.

Piyasena, P., Mohareb, E., and McKellar, R. C. (2003). Inactivation of microbes using ultrasound: a review. *International Journal of Food Microbiology*, 87, 207–216.

Povey, M. J. W., and Mason, T. J. (eds.). (1998). *Ultrasound in Food Processing*. London, New York, Blackie Academic and Professional.

Raso, J., and Barbosa-Cánovas, G. V. (2003). Nonthermal preservation of foods using combined processing techniques. *Critical Reviews in Food Science and Nutrition*, 43, 265–285.

Rediske, A. M., Rapoport, N., and Pitt, W. G. (1999). Reducing bacterial resistance to antibiotics with ultrasound. *Letters in Applied Microbiology*, 28, 81–84.

Ross, A. I. V., Griffiths, M. W., Mittal, G. S., and Deeth, H. C. (2003). Combining nonthermal technologies to control foodborne microorganisms. *International Journal of Food Microbiology*, 89, 125–138.

Russell, N. J. (2002). Bacterial membranes: the effect of chill storage and food processing. An overview. *International Journal of Food Microbiology*, 79, 27–34.

Sala, F. J., Burgos, J., Condon, S., López, P., and Raso, J. (1995). Manothermosonication. In: Gould, G. W. (ed.), *New Methods of Food Preservation*. London, Blackie.

Scherba, G., Weigel, R. M., and O'Brien, W. D., Jr. (1991). Quantitative assessment of the germicidal efficacy of ultrasonic energy. *Applied and Environmental Microbiology*, 57, 2079–2084.

Shapiro, H. M. (2000). Microbial analysis at the single-cell level: tasks and techniques. *Journal of Microbiological Methods*, 42, 3–16.

Ueckert, J., Breeuwer, P., Abee, T., Stephens, P., Nebe von Caron, G., and ter Steeg, P. F. (1995). Flow cytrometry applications in physiological study and detection of foodborne microorganisms. *International Journal of Food Microbiology*, 28, 317–326.

U.S. FDA (2000). *Kinetics of Microbial Inactivation for Alternative Food Processing Technologies – Ultrasound*. U.S. Food and Drug Administration, Center for Food Safety and Applied Nutrition, June 2.

Vichare, N. P., Senthikumar, P., Moholkar, V. S., Gogate, P. R., and Pandit, A. B. (2000). Energy analysis in acoustic cavitation. *Industrial and Engineering Chemical Research*, 39, 1480–1486.

Villamiel, M., and de Jong, P. (2000). Inactivation of *Pseudomonas fluorescens* and *Streptococcus thermophilus* in Trypticase® Soy Broth and total bacteria in milk by continuous-flow ultrasonic treatment and conventional heating. *Journal of Food Engineering*, 45, 171–179.

Walkling-Ribeiro, M., Noci, F., Riener, J., Cronin, D. A., Lyng, J. G., and Morgan, D. J. (2009). The impact of thermosonication and pulsed electric fields on *Staphylococcus aureus* inactivation and selected quality parameters in orange juice. *Food Bioprocess and Technology*, 2, 422–430.

Zenker, M., Heinz, V., and Knorr, D. (2003). Application of ultrasound assisted thermal processing for preservation and quality retention of liquid foods. *Journal of Food Protection*, 66, 1642–1649.

Chapter 13
Ultrasonic Recovery and Modification of Food Ingredients

Kamaljit Vilkhu, Richard Manasseh, Raymond Mawson, and Muthupandian Ashokkumar

1 Basic Mechanisms

1.1 Physical Effects of Sound on Fluids

There are two general classes of effects that sound, and ultrasound in particular, can have on a fluid. First, very significant modifications to the nature of food and food ingredients can be due to the phenomena of *bubble acoustics and cavitation*. The applied sound oscillates bubbles in the fluid, creating intense forces at microscopic scales thus driving chemical changes. Second, the sound itself can cause the fluid to flow vigorously, both on a large scale and on a microscopic scale; furthermore, the sound can cause particles in the fluid to move relative to the fluid. These *streaming phenomena* can redistribute materials within food and food ingredients at both microscopic and macroscopic scales.

1.2 Bubble Acoustics and Cavitation

1.2.1 Fundamentals of Bubble Acoustics

A bubble in the context of ultrasound and food processing is a gas surrounded by a liquid. For bubble-acoustic phenomena to occur the substance, surrounding the bubble should allow the gas in the bubble to easily expand and contract; a liquid around the bubble permits easy expansion and contraction because it can flow. The liquid surrounding the bubble might be extremely viscous or contain solid particles, but as long as it can flow, bubble-acoustic phenomena can occur.

Gases are compressible, and they are much more compressible than liquids. Bulk modulus is a property representing the resistance of a substance to volumetric compression. The bulk modulus of air is only about 1/10,000 that of water, so while

R. Mawson (✉)
CSIRO Food and Nutritional Sciences, 671 Sneydes Road, Werribee VIC 3030, Australia
e-mail: raymond.mawson@csiro.au

H. Feng et al. (eds.), *Ultrasound Technologies for Food and Bioprocessing*, Food Engineering Series, DOI 10.1007/978-1-4419-7472-3_13,
© Springer Science+Business Media, LLC 2011

an air bubble is easily compressed, the surrounding liquid is comparatively incompressible. On the other hand, liquids have much higher densities than gases; the density of water is about 800 times that of air. Thus, a gas bubble in liquid is effectively a spring attached to a mass. The "spring" is a spherical spring owing to the compressibility of the gas, and the mass is a spherical shell of liquid, but the same phenomenon occurs for any mass attached to a spring. There is a natural frequency with which the mass bounces on the spring in response to a disturbance.

The physics of bubble acoustics was first mathematically formulated nearly a century ago (Rayleigh, 1917). For the special case in which the amplitude with which the bubble's radius oscillates is a small fraction of its radius, the natural frequency, f_0, was simply derived by Minnaert (1933) as

$$f_0 = \frac{1}{2\pi}\sqrt{\frac{3\Gamma P_0}{\rho_0}} \times \frac{1}{R_0} \tag{13.1}$$

where f_0 is in hertz, Γ is the polytropic index of the gas, P_0 is the total ambient pressure that includes atmospheric pressure plus any additional constant pressure imposed on the bubble, ρ_0 is the density of the liquid, and R_0 is the equilibrium radius of the bubble. Since Γ and ρ_0 are properties of the gas and liquid, respectively, for a given applied pressure the natural frequency of the bubble is inversely proportional to the radius. For the case of an air bubble in water, $f_0 \approx 3.3/R_0$ in SI units. For example, a bubble with 1 mm in radius has a natural frequency of roughly 3 kHz while a bubble with 1 μm in radius has a natural frequency of roughly 3 MHz. Since the great majority of bubbles of practical relevance in the food industry are millimeters in size or smaller, their natural frequencies are vibrations measured in kilohertz or megahertz, in other words, vibrations that are classified as sound or ultrasound.

As with any naturally vibrating system, if the system is forced to vibrate near its natural frequency, resonance will occur. Resonance in a bubble-acoustic system would occur if the bubble is forced to vibrate by applied sound. Resonance can lead to large-amplitude vibrations in the fluid over the immediate vicinity of the bubble and extreme conditions in the gas, which could ultimately drive some physical and chemical modifications of interest to food technologists.

It is important to note that Minnaert's equation (13.1) neglects many factors that are significant in a food processing context. For example, chemical reactions and phase transformations as the bubble expands and contracts, the viscosity of the liquid, the gas–liquid surface tension, the speed of sound in the liquid, and influence of other bubbles and the containing walls have all been ignored in equation (13.1). A good review of many of these effects is given in Leighton (1994) and detailed analyses of other effects have been made elsewhere, for example, by Prosperetti (1977) on viscous and thermal effects, Vokurka (1986) on sound speed in liquid, and Manasseh et al. (2004) on the effect of other bubbles. Nevertheless, for practical applications, the fact that in Minnaert's equation f_0 is proportional to $1/R_0$ provides an excellent rule of thumb that food technologists can use to estimate the size of bubbles that

would be affected by sound or the sound frequency needed to drive a process at a particular scale.

It is possible for the bubble to be encapsulated in a thin, solid shell, and as long as the shell has some elasticity, bubble-acoustic phenomena can still occur (de Jong et al., 2002).

1.2.2 Cavitation

Many foods ingredients do not naturally contain significant quantities of gas bubbles. Rather, as ultrasound is applied, gas bubbles are created and then go on to modify the substance. Cavitation is the phenomenon by which bubbles can be created by ultrasound. Leighton (1994) and Brennen (1995) provide a good general introduction to all types of cavitation.

Liquids can be turned into gases (vaporized) if the temperature is raised sufficiently – simply boiling water is the classic illustration of this. However, vaporization is also possible if the pressure is dropped sufficiently. Many engineering systems can vaporize liquids by pressure drops, particularly systems with blades such as pumps and propellers or venturi nozzles. If the pressure in the wake of a pump blade is low enough, the liquid in the low-pressure zone will effectively "boil," forming bubbles on the blade analogous to the bubbles formed on the hot plate of a heated saucepan. This is called *cavitation* and has been studied extensively from the mid-twentieth century owing to its importance for turbomachinery and submarine noise (for reviews, see Blake and Gibson, 1987; Brennen, 1995, 2005; Leighton, 1994).

Sound propagation through a fluid is a wave with high pressure in the crests and low pressure in the troughs. In practical fluids, a few tiny bubbles, in the order of a micron in size or less, are always present and are referred to as *cavitation nuclei* (Brennen, 1995). During the low-pressure trough, liquid evaporates into the nuclei, enlarging them. The crest of each wave reverses this process, condensing the vapor in the bubbles back to liquid, and one might think that there would be no net effect. However, during the low-pressure trough, the bubble is expanded, so its surface area is larger than during the high-pressure crest when it is compressed. The process of evaporation thus benefits from a larger surface area than that of the competing process of condensation, and therefore, with the bubble grows slightly with each passing sound wave. This is called *rectified diffusion* (Brennen, 1995; Leighton, 1994).

Moreover, as the bubble grows, its radius gets closer to the Minnaert radius R_0 corresponding to the applied frequency f_0. As this happens, the bubble begins to resonate; the amplitude with which it expands and contracts gets larger, pumping vapor into the bubble at an accelerating rate until R_0 is passed. In general, the bubble population will eventually stabilize.

However, if the ultrasound power is high enough, the bubbles grow explosively. The amplitude of oscillation becomes extreme and unstable and usually the bubble collapses violently, fragmenting into a number of smaller bubbles. This is the analogue of the situation behind a cavitating pump blade, which is called *ultrasonic*

cavitation (Brennen, 1995; Leighton, 1994). It can happen with the passage of only a single ultrasonic cycle of the appropriate frequency. Thresholds at which cavitation occurs have been measured and calculated for many conditions, but mostly for water and seawater rather than food ingredients. For example, 2 μm cavitation nuclei driven at 1 MHz will cavitate if the peak negative pressure is greater than 0.3 MPa, but at 5 MHz a peak pressure of 1 MPa would be required (Apfel and Holland, 1991).

1.2.3 Nonlinearity and Collapse

During cavitation the bubble expands and contracts through a spectacular amplitude; experimental imaging typically shows that cavitation bubbles can shrink to a diameter of only 1/10 of their maximum radius (see, e.g., Brenner et al., 2002; Brujan et al., 2001; Putterman and Weniger, 2000). Under these conditions, the assumption of small amplitude oscillation made by Minnaert (1933) is invalid and the behavior of the bubble is extremely nonlinear. The forces generated in the liquid are so high that they can make holes in metal surfaces nearby, which was one of the original engineering motivations for studying cavitation. As detailed in Section 3.2, the bubble collapse can create an intense micro-jet that can puncture plant cell walls, leading to food ingredient extraction.

Moreover, even a cursory attempt at calculating conditions inside the bubble quickly leads to the conclusion that conditions during cavitation collapse are so extreme that the ideal gas law is invalid. Clearly, if the bubble volume is being reduced by two to three orders of magnitude, temperatures during this extreme compression can potentially reach thousands of degrees. The gas breaks down, forming free radicals that diffuse into the liquid and form the basis of many of the chemical modifications to be discussed in Section 3.

1.3 Streaming Phenomena

1.3.1 General Streaming Phenomena

It is well known that a class of net fluid motions, both with and without particles, can be driven by oscillatory fluid waves (Riley, 2001). As any wave passes through a fluid it causes the fluid and any particles suspended in it to oscillate to and fro; after the passage of each wave, there is no net displacement of the fluid or particles according to linear theory. This is, of course, an exact model for experimental reality if the wave power is extremely low. In general, however, a rectification of the oscillatory motion is possible owing to nonlinear effects, giving a net drift of the fluid or particles within it.

The most general explanation for a net drift in fluid dynamics is that there is nonlinearity in the equations of fluid motion, and that this nonlinearity is quadratic (Batchelor, 1967). Hence, all such streaming motions will be proportional to the

square of the wave amplitude and thus proportional to the wave power. Thus, the higher the power, the greater the net fluid motions, increasing in general linearly with power. The net motions are second-order effects. This means that although they vary with the square of the wave amplitude, their velocity is much weaker than the velocity with which the fluid oscillates as the waves pass. Furthermore, the quadratic nonlinearity is actually a velocity multiplied by the gradient in velocity with distance. Thus, in order for the net motion to be possible, there should be a gradient in the wave velocity with distance. The larger the gradient, the larger the local net motion.

The simplest example of a net motion relevant to ultrasound in the food industry is acoustic streaming. Acoustic streaming could be used to mix or stir food ingredients without any mechanical moving parts. It is induced by the dissipation that leads to a gradient in sound power with distance. It has often been termed the "quartz wind" (Eckart, 1948); another term is Eckart streaming.

Rayleigh (1883) analyzed the acoustic streaming induced by sound waves propagating between parallel plates. This is usually called Rayleigh streaming. An illustration of Eckart and Rayleigh streaming effects is given in Fig. 13.1. It can be seen that Rayleigh streaming forms flow cells with their boundaries aligned with the nodes and antinodes of a standing wave pattern, while Eckart streaming does not require boundaries or a standing wave. Appropriate design of food ingredient vessels could lead to one or the other type of streaming, depending on what kind of flow patterns are needed.

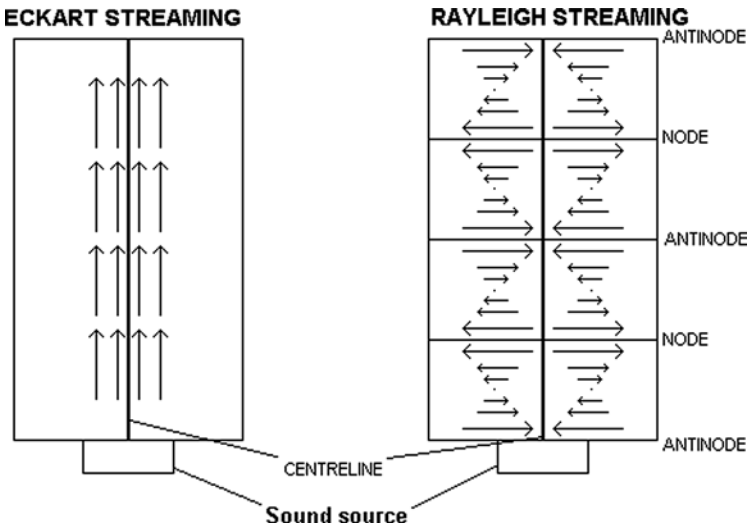

Fig. 13.1 Eckart and Rayleigh acoustic streaming. Eckart streaming – the classical "quartz wind" – would occur without any containment at all, but Rayleigh streaming requires a standing wave pattern

A particular type of streaming arises in the fluid-dynamical boundary layer very close to the boundary, causing a vortex in the boundary layer. This is called Schlichting streaming.

1.3.2 Sound Radiation Pressure on a Sphere

There is also a type of net motion where particles, droplets, or bubbles (a *dispersed phase*) dispersed in a fluid are made to move relative to the fluid (the *continuous phase*). This could be particularly useful in the food industry to separate a dispersed phase from a continuous phase. The existence of a velocity field with a non-zero gradient near the object makes a net motion possible. For simplicity the word "particle" will be used below to cover any possible dispersed-phase object: solid particles, droplets, or bubbles. The first analysis of this phenomenon was made by King (1934). King noted that particles could be made to migrate in either traveling or standing waves, but he calculated that the radiation force on a rigid sphere much smaller than the sound wavelength was an order of magnitude greater if the sphere was in a standing wave field rather than a traveling wave field. This finding means that practical ultrasonic separation equipment must be designed with the wavelength of the ultrasound in mind. Under these circumstances, the "radiation pressure" acting on an incompressible sphere, F_r, was given by King (1934) as

$$F_r = \pi \rho_0 A^2 \sin(2\kappa h)\,(\kappa a)^3 D \tag{13.2}$$

where a is the particle radius, ρ_0 is the liquid density as before, κ is the wave number given by $2\pi f/c$ where f is the frequency in hertz and c is the speed of sound, h is the distance of the particle from a node, A is the sound wave amplitude (the velocity potential amplitude in m^2/s), and a relative-density factor D is given by

$$D = [1 + 2/3(1 - \rho_0/\rho_1)]/(2 + \rho_0/\rho_1) \tag{13.3}$$

where ρ_1 is the particle density.

King's "radiation pressure" F_r is in fact a force since it has the dimensions of force and is usually called the direct radiation force (DRF). It can be seen straight away that the DRF is proportional to the square of the sound amplitude and hence proportional to the power. As noted in Section 1.3.1, this is a fundamental feature of all such net-motion phenomena. The factor D changes sign when $\rho_0/\rho_1 = 2.5$, i.e., when the specific gravity of the particle $\rho_1/\rho_0 = 0.4$. A particle with a specific gravity denser than 0.4 will be pushed from the nodes toward the antinodes, while a particle less dense than 0.4 will be pushed from the antinodes toward the nodes. In most practical situations of interest to the food industry, only bubbles would have a specific gravity less than 0.4, so the majority of particles or droplets would move toward the antinodes.

Yoshikawa and Kawashima (1955) extended King's analysis to include compressible spheres; the result is similar to King's, with the factor D being modified by a term that incorporates the compressibility. Gupta et al. (1995) proposed using

the differences in DRF due to compressibility to segregate particles with different compressibility.

King (1934) analytically calculated the paths taken by particles as they moved to their target antinodes; Townsend et al. (2004) give a more recent example of a computation of particle paths.

1.3.3 Separation of Particles Much Smaller than the Wavelength and Larger than About a 100 μm

The time a particle takes to move toward the antinodes or nodes is relevant to many practical food industry applications, since this clearly affects whether ultrasonic separation will be feasible or not. Since the DRF changes sign on either side of the particle's target antinode, it is a restoring force – like gravity acting on a pendulum bob. The period of this natural oscillation gives a convenient estimate of the time a particle would take to be separated, in the absence of viscosity. King (1934) showed that the inviscid migration time T_i taken by a particle much smaller than the sound wavelength ($\kappa a << 1$) to reach its nearest antinode is estimated by

$$T_i = {}^1\!/_4 f/(cu)\, d\, 2/\pi K(\cos(2\pi\, h_0 f/c)) \tag{13.4}$$

where h_0 is the particle's initial distance from a node, $K(\cos(2\pi h_0 f/c))$ is the complete elliptic integral with argument $\cos(2\pi h_0 f/c)$ and $u = \kappa A$, a relative-density factor d is given by

$$d^2 = (2 + \rho_0/\rho_1)^2/((\rho_0/\rho_1)(5 - 2\rho_0/\rho_1)) \tag{13.5}$$

It is important to note that this estimate T_i for an inviscid continuous phase is independent of particle size. For most typical applications, it predicts that particles initially uniformly distributed would arrive at the antinode, creating clear bands, in the order of a second. Numerous experiments since the 1920s have shown such estimates to be good.

However, as particles become smaller than roughly 100 μm, the drag force due to the continuous-phase viscosity begins to dominate. Viscous friction damps any tendency for the particle to overshoot its target. An alternative estimate of the migration time is necessary. Although King did not estimate it, a crude estimate is possible, by equating an average of the DRF with the Stokes drag (Batchelor, 1967) given by

$$F_d = 6\,\pi\mu a u \tag{13.6}$$

where u is the speed the particle moves through the fluid and calculating the time T_v taken to travel a quarter wavelength. This gives

$$T_v = 3(\,c/f)\,\mu/(\rho_0 A^2 D\kappa^3 a^2) \tag{13.7}$$

Unlike in the inviscid relation, particle size a clearly matters in a viscous fluid, and virtually all food industry fluids will have significant viscosity.

The cubic relation between particle size a and the DRF means that for a given sound frequency and power, the DRF becomes dramatically weaker for smaller particles. This is significant for smaller particles where viscosity dominates. The cubic relation between frequency and DRF means the DRF becomes dramatically stronger with frequency and the separation speed faster. However, the attendant reduction in wavelength means the separation would occur over shorter lengths which would be of less practical use.

Finally, in practical devices there is also a lateral radiation force, which is due to variations in the acoustic field at right angles to the traveling wave (Spengler et al., 2003). This is two orders of magnitude weaker than the DRF but will tend to make particles clump within their target planes.

1.4 Acoustic Microstreaming

In Section 1.3.1 it was noted that steady streaming motions are possible if there is a gradient in the acoustic field, and that the larger the gradient, the larger the streaming velocity. In the vicinity of an acoustically oscillating microbubble, there is a significant change in the sound field over a very small distance, and hence the large gradient necessary for steady streaming is present in the small region around the microbubble. The resulting flows and shear forces, though often only a 100 μm in extent, can be very intense. This type of streaming flow, called *acoustic microstreaming*, was first experimentally noticed by Kolb and Nyborg (1956) and a convenient experimental review is given by Tho et al. (2007). Acoustic microstreaming can also be created around any small particle with a different acoustic impedance to the surrounding liquid, such as a solid grain in a liquid matrix, and indeed the separation effects noted in Section 1.3.2 could be considered as a manifestation of acoustic microstreaming. Nonetheless, the most powerful and varied microstreaming phenomena are those around cavitation bubbles, where they are called *cavitation microstreaming*. These intense small-scale flows could locally transport ingredients as well as breaking down food ingredient cells (Rooney, 1989; Ugarte-Romero et al., 2006).

2 Practical Ultrasonic Separation

Ultrasonic separation of food ingredients has obvious advantages over conventional methods like filtration and natural settling:

- The acoustic forces are non-contact, in principle eliminating the need to clean and replace filters;
- Acoustic separation is in principle quite rapid, apparently separating particles down to sub-micron size in seconds;

- The acoustic forces are "gentle": they do not involve large shearing forces that may damage delicate materials;
- Removing the need for physical devices in the stream would further reduce shearing forces on the mixture, reduce the pressure head needed to pump liquid, and minimize clogging and consequent maintenance costs;
- Acoustic separation could offer means of further segregating particles on the basis of their density and compressibility.

The first patent on acoustic separation of particles from liquid was filed by C.R. Holden in 1937, claiming mining industry applications. There have been a number of other patents, including Muralidhara et al. (1988) on the concurrent use of electric and acoustic fields and Gallego-Juarez et al. (1998) on the use of orthogonal ultrasonic fields of different frequencies in a gas.

Commercial devices using ultrasound for separation have been on the market for a few years. An example, used for the separation of live cells from a culture medium, is shown in Fig. 13.2.

This class of devices can only handle up to about 200 l/day, generally separating 95% of cells but falling sharply in efficiency if flow rates are pushed higher (Gorenflo et al., 2002). This is certainly suitable for biotechnology applications where there is high value in a small quantity of the product, usually pharmaceutical,

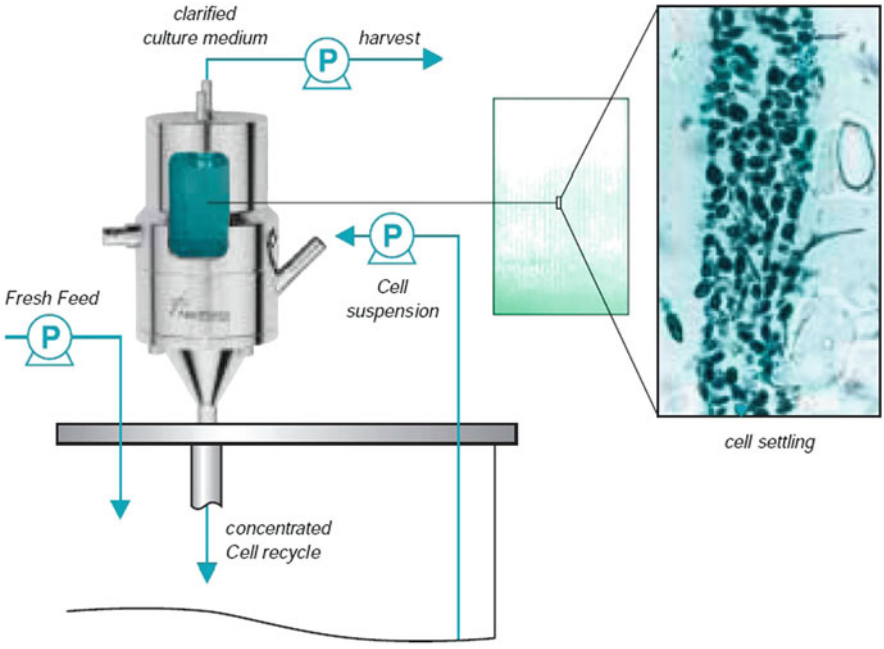

Fig. 13.2 An ultrasonic separator product (BioSep, made by Applikon Biotechnology in the Netherlands) used for separation of live cells. Its operating frequency is 2.1 MHz and the maximum power drawn is 100 W for the model that handles 200 l/day

and where conventional methods of filtration would kill or damage the delicate mammalian cells being cultured. However, such low flow rates would seem impractical for all but the most specialized food industry applications. Nonetheless, the Canadian/US/Austrian company SonoSep, founded in 1997, claims food processing as an application area. It licenses ultrasonic separation for bioengineering to the Netherlands company Applikon Biotechnology.

Ultrasonic separators have also been used in the photographic film industry for many years (Barbee and Brown, 1978). Although they are not commercial products, they are part of the plant equipment and were custom-made for fine bubble removal. In these industries, the need is to remove bubbles that have become entrained in film emulsion during its manufacture and would seriously affect the quality of photographic media were they not removed. As with the biotechnology application, the volume flow rates are quite small so that the use of ultrasonic separation is feasible at low power.

Attempts to develop laboratory precursors to industrial prototypes have also been made (e.g., Spengler and Jekel, 2000). Etrema Products in the USA developed an ultrasonic oil–water separator (Fig. 13.3) in 2000.

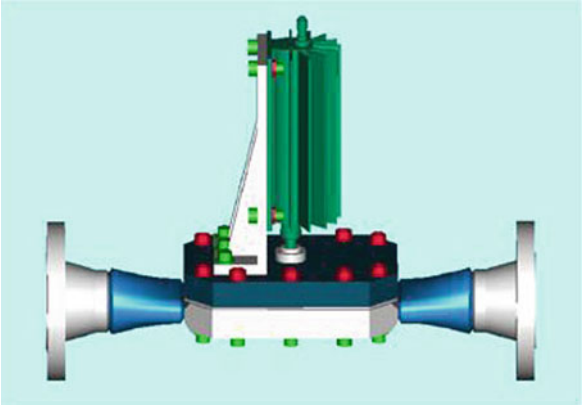

Fig. 13.3 An ultrasonic oil–water separator produced by Etrema Products, Inc., USA, in 2000

However, large-scale industrial applications of ultrasonic separation have been absent. The major stumbling block appears to be the bulk streaming phenomenon (Eckart and Rayleigh streaming) that tends to destroy the separation if power is ramped up, limiting the speed and scale of the application (Spengler et al., 2003). Complex baffle systems (e.g., Spengler and Jekel, 2000) have been proposed to overcome bulk streaming, but would clearly tend to eliminate some of the advantages noted above. A similar proposal is to limit the device size to a single quarter wavelength (e.g., Hawkes et al., 2002), with similar consequences.

An important new application is in microfluidics, where the separation of cells or large molecules like proteins may be achieved (Manasseh et al., 2006). Ultrasonic separation of cells in microdevices has been achieved (Nilsson et al., 2005) and clearly the flow rates in these applications are extremely small, making low power

feasible. In principle, the bulk streaming problems of ultrasound should be absent at microscale, but the extremely large acoustic field gradients in microdevices can also lead to bulk streaming motions (Tho et al., 2006, 2007; Manasseh et al., 2005, 2006; see also Section 1.3.1).

3 Ultrasonic Extraction

3.1 Background Introduction

Ultrasonically assisted extraction of different vegetational materials has been studied since the 1950s. There were studies on extraction of chymosin from abomasa and aroma compounds from grape musts using ultrasound. It was reported that an ultrasonic extraction method could increase the recovery and purity of chymosin extracted from abomasum tissues (Kim and Zayas, 1991) and gave high extraction efficiency for aroma compounds in must and wine (Cocito et al., 1995). The use of ultrasound has been studied in assisting extraction of bioactive principles from herbs at laboratory and large scale (Vinatoru, 2001). The mechanism of ultrasonic extraction is based on the effect of sonication breaking vegetal cells and improving diffusion and osmotic processes (Vinatoru, 2001). This may result in an increase in the extraction efficiency as well as extraction rate. In addition, ultrasound has an effect on increasing the swelling of vegetal tissue; facilitating cell wall rupture and releasing intracellular components into water during sonication.

Horticultural production releases a large amount of waste that is found to contain a significant amount of nutritional components and dietary fiber, which are valuable substances. Extraction of substances/materials from horticultural products and waste could provide an additional income for producers and possibly reduce the cost of waste treatment. Conventional extraction is associated with many problems including high solvent consumption, long operating time, and low yield. A new extraction method using ultrasound could overcome these problems and also allow collection of functional ingredients in natural forms, which have more value in term of health benefits.

3.2 Extraction Mechanisms and Process Development

Extraction enhancement by ultrasound has been attributed to the propagation of ultrasound pressure waves and resulting cavitation phenomena as outlined in Section 1. High shear forces cause increased mass transfer of extractable materials (Jian-Bing et al., 2006). The implosion of cavitation bubbles generates macro-turbulence, high-velocity inter-particle collisions, and perturbation in micro-porous particles of the biomass which accelerates eddy and internal diffusion. Cavitation near liquid–solid interfaces directs a fast moving stream of liquid through the cavity

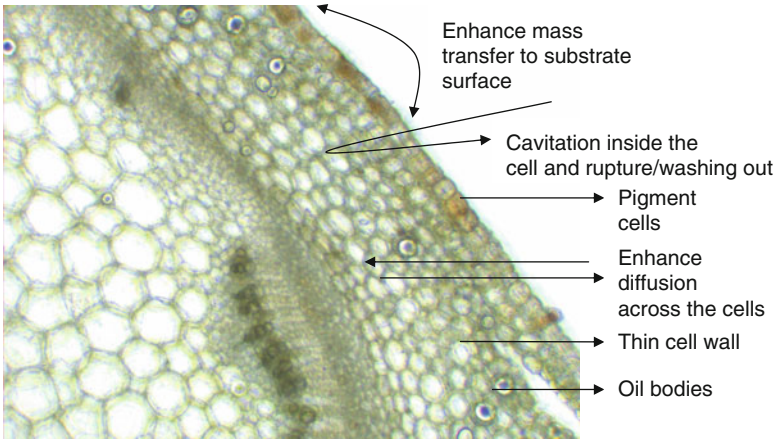

Fig. 13.4 Microscopic transverse section (TS) of apical stem of mint (*Mentha piperita*) showing mechanism of actions during ultrasonic extraction from cells (magnification 2000×)

at the surface (Blake and Gibson, 1987). Impingement by these micro-jets results in surface peeling, erosion, and particle breakdown. This effect provides exposure of new surfaces further increasing mass transfer (Fig. 13.4).

This phenomenon was confirmed by scanning electron microscopy of peppermint leaves and trichomes (leaf glands). After the leaves were ultrasonically treated for menthol extraction, microscopy found that there were two mechanisms involved in extraction: (a) the diffusion of product through the cuticle of peppermint glandular trichomes and (b) the exudation of the product from broken and damaged trichomes (Shotipruk et al., 2001).

Acceleration in solvent extraction kinetics and improved extraction yield of pyrethrine from pyrethrum was largely attributed to ultrasonics increasing the intra-particular diffusion of the solute, which is considered the rate-limiting step (Romdhane and Gourdon, 2002). If the substrate is dry, in aqueous extraction ultrasound may be used to facilitate swelling and hydration and cause enlargement of the cell wall pores (Vinatoru, 2001). Improved extraction performance was also attributed to diffusion through the plant cell walls, disruption, and washing out of the cell contents. Reduction in the size of vegetal material particles by ultrasonic disintegration will increase the number of cells directly exposed to extraction by solvent and ultrasonic cavitation (Vinatoru, 2001). Intensive ultra-sonication can also serve to reduce particle size in tomato juice (Food Science Australia, unpublished data).

Acoustic cavitation bubble collapse occurring at or in close vicinity to the surface of the plant membranes may cause microfractures (Vinatoru, 2001). The occurrence of microfracture by ultrasound was demonstrated in soybean flakes (Li et al., 2004). Cavitation at cell surfaces has the ability to punch holes through the cell wall as has been recently demonstrated with studies of bacterial cell sonication (Ugarte-Romero et al., 2006).

Variation in the extraction yield from different plant materials may result from structure, plasticity, or the compositional differences resulting in varying degrees of susceptibility to ultrasound shock waves and the likelihood that cavitation bubbles will contact with the plant surface causing micro-jetting (Li et al., 2004). Factors such as plant tissue turgor and the mobility of particles such as starch granules within the cell cytoplasm can be expected to influence ultrasound energy dispersion and extraction effectiveness (Zhang et al., 2005).

In their study on supercritical fluid extraction enhancement by ultrasound, Balachandran et al. (2006) were able to demonstrate that the effectiveness of ultrasound was gained by increasing superficial mass transfer and that effectiveness declined sharply after the readily accessible surface solute had been removed. However, by reducing the substrate particle size major gains in extraction efficiency and extraction time reduction could be achieved. Even in the supercritical environment ultrasound was demonstrated to inflict significant surface cell damage.

Solvent selection is usually based on achieving high molecular affinity between the solvent and solute. When ultrasound is also applied the cavitation will be affected by the physical properties of the solvent. Cavitation intensity decreases as vapor pressure and surface tension are increased. Li et al. (2004) demonstrated this phenomenon in soybean oil extraction where greater ultrasonic extraction was achieved by isopropanol compared with hexane, the latter having approximately fivefold higher vapor pressure.

3.3 Extraction Process for Functional Compounds

Ultrasonic extraction of industrial waste resulting from processing vegetable and plant material can be used to recover valuable components. Aqueous and combined aqueous/organic solvents are used for extraction. Ultrasound can be used to benefit both low-temperature and high-temperature extraction systems, regardless of solvent pH, ionic environment, surface tension, or surfactant processing aids.

Low-frequency ultrasound (16–100 kHz) can be used for the extraction of components/substances such as hydrophilic flavonoids (anthocyanins, tannins) and hydrophobic carotenoids (lycopene, beta-carotene, capsaicin, and lutein) from horticultural products such as carrot, ginger, tomato, grapes, olives, olive pomace, and capsicum and from their processing waste.

Preliminary study of ultrasonic extraction of carotenes in carrot waste showed that ultrasound enhanced the extraction yield in both organic solvent and water as shown in Table 13.1. The number of repeated extractions with fresh solvent or water provided additional benefit enhancing the yield of extracted material.

Extraction efficiency can be improved by using ultrasonic horn (sonotrodes) designed for the specific application. The type of sonotrode can increase solvent penetration, cavitation at surfaces, and thus removal of components and extraction efficiency. The organic load and nature of the material being processed will determine the type of sonotrode design. The design of a specific sonotrode will allow for greater penetration of the ultrasonic wave/cavitational energy, better coupling of

Table 13.1 Comparison between ultrasonic and conventional extraction methods

Methods	Solvent system	Percent extraction	Number of repeated extractions with fresh solvent or water
Ultrasonic	Organic	55.82	1
Ultrasonic	Water	33.88	1
Conventional	Organic	40.33	1
Conventional	Water	7.12	1
Ultrasonic	Organic	99.9	5
Ultrasonic	Water	44.19	2
Conventional	Organic	72.88	5

energy to the product and improved energy efficiency resulting in greater extraction of components, solvent penetration, and removal of components from plant tissues. Focused sonotrodes with a frequency of 20–24 kHz gave better extraction yields than other frequencies in ultrasonic extraction of carotenes, whereas increasing power levels of sonication tended to increase the extraction yield (Tables 13.2 and 13.3).

Table 13.2 Comparison of the effect of ultrasonic frequencies on extraction yield

Frequencies	Solvent system	Percent extraction
24 kHz (focused)	Organic	55.82
24 kHz (radial)	Organic	52.78
40 kHz (bath)	Organic	40.26
1 MHz (bath)	Organic	32.42

Table 13.3 Comparison of the effect of ultrasonic power levels on extraction yield

Power levels	Solvent system	Percent extraction
50 W	Organic	55.2
100 W	Organic	56.83
200 W	Organic	58.8
400 W	Organic	58.37

3.4 Opportunities for Food Industry

A limited number of publications have included continuous ultrasonic process development and pilot-scale applications. The range of published extraction applications includes herbal, oil, protein, and bioactives from plant materials (e.g., flavones, polyphenolics), as summarized in Table 13.4.

Table 13.4 List of ultrasound extraction studies from the literature on various food components (Vilkhu et al. 2008)

Product	Ultrasound process	Solvent	Performance	Authors
Almond oils	Batch, 20 kHz	Supercritical carbon dioxide	30% increased yield or extraction time reduction	Riera et al. (2004)
Herbal extracts (fennel, hops, marigold, mint)	Stirred batch, 20–2,400 kHz	Water and ethanol	Up to 34% increased yield over stirred	Vinatoru (2001)
Ginseng saponins	Batch, 38.5 kHz	Water, methanol, and *n*-butanol	Threefold increase of extraction rate	Wu et al. (2001)
Ginger	Batch, 20 kHz	Supercritical carbon dioxide	30% increased yield or extraction time reduction	Balachandran et al. (2006)
Soy protein	Continuous, 20 kHz 3 W/g	Water and alkali (Sodium hydroxide)	53 and 23% yield increase Over equivalent ultrasonic batch conditions	Moulton and Wang (1982)
Soy isoflavones	Batch, 24 kHz	Water and solvent	Up to 15% increase in extraction efficiency	Rostagno et al. (2003)
Rutin from Chinese Scholar Trees	Batch, 20 kHz	Water and methanol	Up to 20% increase in 30 min.	Paniwynk et al. (2001)
Carnosic acid from rosemary	Batch, 20 and 40 kHz	Butanone and ethyl acetate	Reduction in extraction time	Albu et al. (2004)
Polyphenols , amino acid, and caffeine from green tea	Batch, 40 kHz	Water	Increased yield at 65°C, compared with 85°C	Xia et al. (2006)
Pyrethrines from flowers	Batch, 20 and 40 kHz	Hexane	Increased yield at 40°C, compared with 66°C	Romdhane and Gourdan (2002)
Olive oil from olives	Batch, 24 and 25 kHz	Water	8% increased yield at optimal temperature conditions	Jiménez et al. (2007)

Ultrasound has a unique capacity to both enhance extraction from substrates while simultaneously encapsulating the extracted substance with an encapsulant material in the extraction fluid by hydroxyl radical-initiated covalent bonding and microsphere formation. To successfully accomplish this, the encapsulating material should have a higher reductive potential than the material being extracted and be relatively more hydrophobic. Preferably, a mixed frequency ultrasound field is used, a relatively low frequency to facilitate extraction and a higher frequency under independent amplitude control to facilitate hydroxyl radical production for cross linking and microsphere formation. Proteins are suggested encapsulants as the sonochemistry and conditions favoring sphere development have previously been established. For scale up to industrial application treatment vessel geometries, frequency combinations, and frequency modulation to achieve the desired outcomes on a large scale need to be explored and optimized.

Potential exists for applying UAE for enhancing of aqueous extraction as an alternative to organic solvents. The presence of cavitation bubbles effectively renders the water more hydrophobic than its natural conditions. UAE can also enhance extraction of heat-sensitive bioactive and food components by enabling lower processing temperatures.

Sonochemical modification of bioactive compounds during the extraction process is possible which can be used to facilitate the extraction process or modify the extracted material in desirable ways, for example, either elimination or reduced use of enzyme in the commercial extraction processes for vegetable oils and grape juices (Ashokkumar et al., 2008; Jiménez et al., 2007).

There is a more detailed discussion of simultaneous extraction and component modification in Section 4.

State of the art in UAE can achieve improvements in extraction efficiency and extraction rate, which if realized on the industrial scale can achieve economic gains. Ultrasonic equipment engineering has developed to the extent that ultrasonic technology is sufficiently scalable to consider industrial-scale ultrasonic-aided extraction as a commercially viable option.

3.5 Separation of Extracted Components

Dispersed phases can in principle be separated in standing wave fields at Food Science Australia, the separation of emulsions and colloidal suspensions by ultrasound has been demonstrated (unpublished data). However, as the separation of the dispersed phase by ultrasound is dependent on the establishment of stable wave fields which necessitates different vessel geometries to those required for efficient extraction, it is unrealistic to expect separation to occur in the same processing chamber as the extraction process. Although the technologies for large scale acoustic separation are not as well developed as for extraction, it is nevertheless feasible that a practical acoustic separation technology could be developed to follow the extraction process. Acoustic separation technologies were discussed in more detail in Section 2 and were explained theoretically in Sections 1.3.2 and 1.3.3.

3.6 Industrial Extraction Application and Design

The use of ultrasound in food processing has been reviewed by Mason et al. (1996). Recently, the design of ultrasound processing equipment has advanced to provide industrially robust processing capability. Enabling design and operational features have included (a) automated frequency scanning to enable maximum power delivery during fluctuation of processing conditions; (b) non-vibrational flanges on sonotrodes for construction of high-intensity inline flow cells; and (c) construction of radial and hybrid sonotrodes to provide greater range in application design and product opportunities. Presently, 16 kW is the largest available single ultrasound flow cell, which can be configured in series or in parallel modules. Industrial ultrasound manufacturers within the last 2 years have promoted industrial processing capability for food extraction applications (Hielscher, 2007).

Several ultrasound reactor designs have been described by Chisti (2003) and Vinatoru (2001), the latter specifically for industrial extraction of plant tissue. These included (a) an ultrasonic horn (sonotrode) directly immersed into stirred bath or reactor; (b) a stirred reactor with ultrasound coupled to the vessel wall; and (c) recycling of product from the stirred reactor through an external ultrasonic flow cell. These configurations may provide both intermittent and continuous ultrasound exposure, from low intensity in a large volume reactor (0.01–0.1 W/cm^3) to high intensity (1–10 W/cm^3) in an external flow cell. Mixed frequency reactors have been shown to offer advantages with respect to process efficiency and energy distribution (Delgadino et al., 2002; Feng et al., 2002; Moholkar et al., 2000; Swamy and Narayana, 2001; Tatake and Pandit, 2002). Reactor geometries that are asymmetrical and polygons preferably with odd-numbered sides using swept frequencies are also reported to be more effective (Gogate et al., 2004; Puskas, W. (2008) retired RandD director for Branson Ultrasonics Inc. USA and Ney Ultrasonics Inc. USA, "personal communication").

Modern ultrasonic systems include automated frequency scanning which adjusts operation of the system to the optimal frequency to ensure that maximum power is transmitted to the extraction vessel. The benefit of automated frequency scanning as opposed to a fixed frequency was demonstrated by Romdhane and Gourdan (2002), where the former achieved a 32% increase in pyrethrine extraction and a 30% increase in power delivered to the product.

Where it is not a disadvantage to extract oily materials as stable emulsions, ultrasound can be used to carry out aqueous extraction of oily materials into water with yields in the order of 50% (Food Science Australia, unpublished results). The presence of a dispersed phase contributes to the ultrasound wave attenuation. The active sonication region in a reactor is restricted to a zone located at the surface of the probe which favors treatment in flow-through reactor configurations.

The application of ultrasound at Food Science Australia has focused on the use of high-powered systems for extraction of bioactives. Principal targets have been polyphenols and carotenoids in both aqueous and solvent extraction systems. The ultrasound extraction trials have demonstrated improvements in extraction yield ranging from 6 to 35%, as summarized in Table 13.5. Results of ultrasonically

Table 13.5 Examples of bioactive ultrasound-assisted extraction work completed at Food Science Australia

Extract target	Product	Solvent	Process	Processing conditions	Improvement range (%)
Beta-carotene	Carrot	Aqueous ethyl acetate	Laboratory; 24 kHz, 20–75 W .s/ml Laboratory; 24 kHz, 20–75 W s/ml	Ambient Ambient	15–25 8–20
Polyphenols	Red grape marc	Aqueous	Laboratory; 24 kHz, 20–75 W .s/ml	Ambient	11–35
Polyphenols	Black tea	Aqueous	Laboratory; 24 kHz, 8–10 W .s/ml	Hot processing 90°C	6–18
Polyphenols	Apple	Aqueous	Laboratory; 40 kHz, 20–75 W .s/ml	Hot processing 80°C	6
Gingerol	Ginger	Supercritical carbon dioxide	Laboratory; 20 kHz	Pressure 160 bar	30

treated Shiraz and Sangiovese grape marc showed 17 and 35% increase in phenolic compounds, respectively, higher recovery of these compounds was obtained from their respective seeds.

To improve extraction effectiveness the material to be extracted should be reduced to as smaller particle size as practical without denaturing the material to be extracted and commensurate with separation from the solvent post-extraction. If this is done very high yields and extraction rates are possible with ultrasonic augmentation of the extraction process (Balachandran et al., 2006).

The benefits of UAE for the food industry include (a) overall enhancement of extraction yield or rate; (b) enhancement of aqueous extraction processes which is of particular benefit where solvents cannot be used (juice concentrate processing); (c) providing the opportunity to use alternative (GRAS) solvents by improvement of their extraction performance; (d) enabling sourcing/substitution of cheaper raw product sources (variety) while maintaining bioactive levels; and (e) enhancing extraction of heat-sensitive components under conditions which would otherwise have low or unacceptable yields.

4 Simultaneous Extraction and Modification

4.1 Extraction and Molecular Weight Reduction of Polymeric Materials

The extraction of high-molecular weight biopolymers such as amylose from starch granules, pectin from cell wall materials, and chitin from seafood wastes and fungal sources can be facilitated by the application of ultrasound. However, experience suggests that there is a simultaneous reduction of molecular weight during this process.

While this has been seen as a problem it can also be an opportunity for novel applications of the extracted materials where high molecular weight is not desirable.

The challenge is how to achieve extraction and controllable molecular weight reduction. The mechanics of molecular weight reduction are likely to involve different mechanics to molecular weight reduction of polymers in solution where intense hydrodynamic flows between the synchronous expansion and contraction of cavitation bubbles stretch the polymers to the breaking point. In extraction one end of the polymer molecule is anchored in the substrate surface it is being extracted from and the other is in "solution." Following the mechanism proposed for polymers in free solution it could be expected that cleavage at the surface will occur when the free length is long enough for the hydrodynamic flows to cavitation bubbles close to the surface generate sufficient force to snap the polymer from the surface. If this is the dominant mechanism, then for a given extraction and set of extraction conditions the molecular weight of the cleaved biopolymer would be expected to be in a relatively narrow size range. In our work with amylose extraction from rice starch granules it appears that this is the case. Other mechanisms for cleavage at the

surface could be the impact of micro-jetting from cavitation bubbles at the surface at the point of attachment of the polymer to the surface. In this instance the cleaved polymer would be expected to have random molecular size, which has not been observed in our laboratory.

Chitin is the second most abundant biopolymer after cellulose, being the structural polymer found in crustacean, mollusc, and insect exoskeletons and fungal cell walls. It is built up from an acetylated amino glucan and is associated with magnesium and calcium phosphates and proteins. Extraction involves demineralization with hydrochloric acid followed by protein removal with sodium hydroxide. The functional value of the extracted chitosan is related to the polymer molecular weight and the degree of acetification. Ultrasound application during the acid demineralization of ground shrimp shell can reduce the process time but less mineral is extracted, more protein is extracted, and there is significant chitin loss from the shell particles into solution (Kjartansson et al. 2006) as low-molecular weight polymer fragments by a similar mechanism noted for the extraction of amylose from granular starch. In a process not dissimilar to ultrasonic cleaning the softer biopolymer material is removed from the hard mineral structure rather than vice versa until eventually everything ends up in solution or colloidal suspension.

However, sonication during the subsequent alkaline treatment following demineralization without ultrasound facilitates the removal of protein enabling lower residual protein contents and structurally transforms the chitin for more efficient subsequent processing. Sonication of extracted chitosan in solution results in molecular weight and solution viscosity reduction but does not reduce acetylation.

Ultrasonic molecular weight reduction of biopolymers in solution is related to the composition and structural configuration of the polymer. In homopolymers with a linear structure such as esterified cellulose, chitosan, or the starch polymer amylose the molecular weight is reduced by successive cleavages at the mid-point of the polymer molecule by the action of intense hydrodynamic flows between the synchronous expansion and contraction of cavitation bubbles stretching the polymers to breaking point. By contrast the other starch polymer amylopectin, while still a homopolymer, is highly branched and the cavitation-induced microstreaming cleaves the molecule in an apparently random manner. Other carbohydrate gum biopolymers such as pectin, alginate, carrageenan, guar, and locust bean are typically block copolymers built up from two or more different sugar monomers having varying degrees of esterification and branching and may be bound into a complex structure by ionic, hydrophobic, and hydrogen bonding and are cleaved in an unpredictable manner. Similarly proteins cleave unpredictably, being built from approximately 22 amino acid monomers; they are typically linear polymers but are folded into complex structures involving one or more polymer chains that are often stabilized by covalent, ionic, hydrophobic, and hydrogen bonds. Amino acids with sulfhydryl and phenolic residues can be modified by hydroxyl radicals generated by cavitation bubbles to form new covalent bonds between protein polymer chains. Radicals formed by the cleavage of biopolymers also have the potential to recombine into novel polymer structures.

4.2 Extraction and Modification of Antioxidant Capacity and/or Color

As noted elsewhere in this chapter anthocyanins are readily extracted by ultrasound but they are subject to modification by overprocessing, typically resulting in loss of color and antioxidative capacity. This can be countered by strategies managing the ultrasonic treatment intensity, reduction in particle size treated, and reducing the treatment exposure time. There is also the potential to regulate the amount of ultrasonic exposure to enhance the antioxidative capacity through the addition of –OH residues to the ring structures in the anthocyanin molecules.

In a recent study, Ashokkumar et al. (2008) have shown the potential use of high-frequency ultrasound for enhancing the antioxidant properties of phenolic compounds. While this work did not involve any extraction, the experimental results reported in this study clearly indicate that modification of the functionality of food ingredients is possible during the extraction process. Phenol was taken as a model compound. The reaction between phenol and hydroxyl radicals generated during acoustic cavitation resulted in the formation of hydroxylated phenols. The antioxidant activity of the sonicated phenol solution showed a significant antioxidant property (phenol alone did not shown any antioxidant activity). The results shown in Fig. 13.5 demonstrate that the antioxidant activity of hydroxylated phenols is higher than that of cyaniding 3-glucoside.

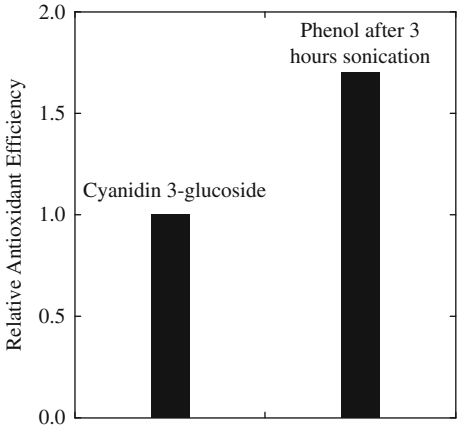

Fig. 13.5 Relative antioxidant efficiency of hydroxylated phenols (phenol after sonication) compared to cyaniding 3-glucoside (a well-known antioxidant)

4.3 Extraction and Encapsulation

Lipophilic materials can be extracted into aqueous media by virtue of the increased hydrophobicity of the water induced by the presence of cavitation bubbles. When the material to be extracted is lipophilic and labile to oxidation, for example, a carotenoid pigment, it is desirable to protect the material against oxidation from

either the oxidative radicals generated by cavitation or during subsequent handling. One strategy for protecting such materials is by encapsulation. Simultaneous extraction and encapsulation of lipophilic materials is possible with low-frequency ultrasound provided there is an appropriate protein, carbohydrate polymer, or surfactant present in the extraction solvent. Potentially the protein, carbohydrate polymer, or surfactant could originate in the substrate being extracted. Typically in this event the extracted lipophilic material unexpectedly forms a very stable emulsion.

Acknowledgments The authors thank Yonggang Zhu at CSIRO, who investigated aspects of ultrasonic separation and Jenny Zho at CSIRO who investigated the sonication of swollen starch granules.

References

Apfel, R. E., and Holland, C. K. (1991). Gauging the likelihood of cavitation from short-pulse, low-duty cycle ultrasound. *Ultrasound in Medicine and Biology*, 17, 179–185.

Ashokkumar, M., Sunartio, D., Kentish, S., Mawson, R., Simons, L., Vilkhu, K., and Versteeg, C. (2008). Modification of food ingredients by ultrasound to improve functionality: A preliminary study on a model system. *Innovative Food Science and Emerging Technologies*, 9, 155–160.

Balachandran, S., Kentish, E., Mawson, R., and Ashokkumar, M. (2006). Ultrasonic enhancement of the supercritical extraction from ginger. *Ultrasonics Sonochemistry*, 13, 471–479.

Batchelor, G. K. (1967). *An introduction to fluid dynamics*. Cambridge, MA, Cambridge University Press.

Barbee, E. H., and Brown, R. C. (1978). Sonic apparatus for removing gas from photographic emulsions. *United States Patent 4,070,167*.

Blake, J. R. and Gibson, D. C. (1987) Cavitation bubbles near boundaries. Annual Review of Fluid Mechanics, 19, 99–123.

Brenner, M. P., Hilgenfeldt, S., and Lohse, D. (2002). Single-bubble sonoluminescence. *Review of Modern Physics*, 74, 425–484.

Brennen, C. E. (1995). Cavitation and Bubble Dynamics. Oxford University Press, 245pp.

Brennen, C. E. (2005). Fundamentals of Multiphase Flow. Cambridge University Press, 407pp.

Brujan, E.-A., Nahen, K., Schmidt, P., and Vogel, A. (2001). Dynamics of laser-induced cavitation bubbles near an elastic boundary. *Journal of Fluid Mechanics*, 433, 283–314.

Chisti, Y. (2003). Sonobioreactors: Using ultrasound to enhance microbial productivity. *Trends in Biotechnology*, 21, 89–93.

Cocito, C., Gaetano, G., and Delfini, C. (1995). Rapid extraction of aroma compounds in must and wine by means of ultrasound. *Food Chemistry*, 52, 311–320.

de Jong, N., Bouakaz, A., and Frinking, P. (2002). Basic acoustic properties of microbubbles. *Echocardiography*, 19(3), 229–240.

Delgadino, A., Bonetto, J., and Lahey, T., Jr. (2002). The relationship between the method of acoustic excitation and the stability of single bubble sonoluminescence for various noble gasses. *Chemical Engineering Communications*, 189, 786–802.

Eckart, C. (1948). Vortices and streams caused by sound waves. *Physical Review*, 73(1), 68–76.

Feng, R., Zhao, Y., Zhu, C., and Mason, J. (2002). Enhancement of ultrasonic cavitation yield by multi-frequency sonication. *Ultrasonics Sonochemistry*, 9, 231–236.

Gogate, R., Mujumdar, S., Thampi, J., Wilhelm, M., and Pandit, B. (2004). Destruction of phenol using sonochemical reactors: Scale up aspects and comparison with conventional reactors. *Separation and Purification Technology*, 34, 25–34.

Gorenflo, V. M., Smith, L., Dedinsky, B., Persson, B., and Piret, J. L. (2002). Scale-up and optimizaton of an acoustic filter for 200 L/day perfusion of a CHO cell culture. *Biotechnology and Bioengineering*, 80(4), 438–444.

Gupta, S., Feke, D. L., and Manas-Zloczower, I. (1995). Fractionation of mixed particulate solids according to compressibility using ultrasonic standing wave fields. *Chemical Engineering Science*, 50(20), 3275–3284.

Hawkes, J. J., Coakley, W. T., Groschi, M., Benes, E., Armstrong, S. and Tasker, J. (2002). Single-half, wavelength ultrasonic particle filter; Predictions of the transfer matrix multilayer resonator model and experimental filtration results. Journal of the Acoustics Society of America, 111, 1259–1266.

Hielscher Gmhb, Berlin, Germany (2007). Ultrasound in the food industry. http://www.hielscher.com/ultrasonics/food_01.htm. Accessed 23 June, 2007.

Holden, C. R. (1937). Apparatus for the separation of solids in liquid suspension. *United States Patent 2,071,260*.

Jian-Bing, J., Xiang-hong, L., Mei-qiang, C., and Zhi-chao, X. (2006). Improvement of leaching process of Geniposide with ultrasound. *Ultrasonics Sonochemistry*, 13, 455–462.

Jiménez, A., Beltrán, G., and Uceda, M. (2007). High-power ultrasound in olive paste pretreatment. Effect on process yield and virgin olive oil characteristics. *Ultrasonics Sonochemistry*, 14, 725–731.

Gallego-Juarez, J. A., Riera- Franco de Sarabia, E., Rodriguez-Corral, G. Juarez, J. A. G., de Sarabia, E. R. F., and Corral, G. R. (1998). Multifrequency acoustic chamber for the agglomeration and separation of particles suspended in gaseous effluents. *United States Patent 5,769,913*.

Kim, S. M., and Zayas, J. F. (1991). Comparative quality characteristics of chymosin extracts obtained by ultrasound treatment. *Journal of Food Science*, 56(2), 406–410.

King, K. V. (1934). On the acoustic radiation pressure on spheres. Proceedings of the Royal Society of London, A., 147, 212–240

Kjartansson, G., Zivanovic, S., Kristbergsson, K., and Weiss, J. (2006). Sonication-assisted extraction of chitin from North Atlantic shrimps (Pandalus Borealis). *Journal of Agricultural and food Chemistry*, 54, 5894–5902.

Kolb, J., and Nyborg, W. (1956). Small-scale acoustic streaming in liquids. *Journal of the Acoustical Society of America*, 28, 1237–1242.

Leighton, T. G. (1994). *The acoustic bubble*. London, Academic.

Li, H., Pordesimo, L., and Weiss, J. (2004). High intensity ultrasound-assisted extraction of oil from soybeans. *Food Research International*, 37, 731–738.

Manasseh, R., Nikolovska, A., Ooi, A., and Yoshida, S. (2004). Anisotropy in the sound field generated by a bubble chain. *Journal of Sound and Vibration*, 278(4–5), 807–823.

Manasseh, R., Petkovic-Durana, K., Tho, P., Zhu, Y., and Ooi, A. (2005). Acoustic microstreaming applied to batch micromixing. *SPIE International Symposium on Microelectronics, MEMS, and Nanotechnology*, 11–15 December 2005, Brisbane, Australia.

Manasseh, R., Petkovic-Duran, K., Zhu, Y., and Ooi, A. (2006). Chaotic mixing using acoustic microstreaming for pathology screening diagnostics. *10th International Conference on Miniaturized Systems for Chemistry and Life Sciences*, 5–9 November 2006, Tokyo, Japan.

Mason, J., Paniwynyk, L., and Lorimer, P. (1996). The use of ultrasound in food technology. *Ultrasonics Sonochemistry,* 3, S253–S260.

Minnaert, M. (1933). On musical air bubbles and the sound of running water. *Philosophical Magazine*, 16, 235–248.

Moholkar, S., Rekveld, S., and Warmoeskerken, G. (2000). Modeling of acoustic pressure fields and the distribution of the cavitation phenomena in a dual frequency sonic processor. *Ultrasonics*, 38, 666–670

Muralidhara, H. S., Parekh, B. K., and Nagabhusan, S. (1988). Solid-liquid separation process for fine particle suspensions by an electric and ultrasonic field. *United States Patent 4,747,920*.

Nilsson, M., Johansson, L., Lilliehorn, T., Lindvall, M., Piškur, J., Almqvist, M., Johansson, S., Laurell, T., and Nilsson, J (2005). Acoustic trapping of cells in a microfluidic format. *9th International Conference on Miniaturized Systems for Chemistry and Life Sciences*, 9–13 October 2005, Boston, USA.

Prosperetti, A (1977) Thermal effects and damping mechanism in the forced radial oscillations of gas bubbles in liquids. *Journal of the Acoustical Society of America*, 61(1).

Putterman, S. J. and Weniger, K. R. (2000). Sonoluminescence how bubbles turn sound into light. Annual Review of Fluid Mechanics, 32, 445–476.

Rayleigh (Lord) (1883). On the circulation of air observed in Kundt's tubes and some allied acoustical problems. *Philosophical Transactions of the Royal Society London Series A*, 175, 1–21.

Rayleigh (Lord) (1917). On the pressure developed in a liquid during the collapse of a spherical cavity. *Philosophical Magazine*, 34, 94–98.

Riley, N. (2001). Steady streaming. *Annual Review of Fluid Mechanics*, 33, 43–65.

Romdhane, M., and Gourdan, C. (2002). Investigation in solid-liquid extraction – influence of ultrasound. *Chemical Engineering Journal*, 87, 11–19.

Rooney, J. A. (1989). Shear as a mechanism for sonically induced biological effects. *Journal of the Acoustical Society of America,* 52, 1718–1724.

Shotipruk, A., Kaufman, B., and Wang, Y. (2001). Feasibility study of repeated harvesting of menthol from biologically viable *Mentha piperata* using ultrasonic extraction. *Biotechnology Progress*, 17, 924–928.

Spengler, J., Coakley, W. T., and Christensen, K. T. (2003). Microstreaming effects on particle concentration in an ultrasonic standing wave. *AIChE Journal*, 49(11), 2773–2782.

Spengler, J., and Jekel, M. (2000). Ultrasound conditioning of suspensions – studies of streaming influence on particle aggregation on a lab- and pilot-plant scale. *Ultrasonics*, 38, 624–628.

Swamy, M., and Narayana, L. (2001). Intensification of leaching process by dual-frequency ultrasound. *Ultrasonics Sonochemistry*, 8, 341–346.

Tatake, A., and Pandit, B (2002). Modelling and investigation into cavitation dynamics and cavitational yield: Influence of dual-frequency ultrasound sources. *Chemical Engineering Science*, 57, 4987–4995.

Tho, P., Manasseh, R., Zhu, Y., Metcalfe, G., and Ooi, A (2006) Method for microfluidic mixing and mixing device. *Australian Patent Application* 2005901760.

Tho, P., Manasseh, R., and Ooi, A. (2007) Cavitation microstreaming patterns in single and multiple bubble systems. *Journal of the Fluid Mechanics,* 576, 191–233.

Townsend, R. J., Hill, M., Harris, N. R., White, N. M. (2004). Modelling of particle paths passing through an ultrasonic standing wave. *Ultrasonics*, 42, 319–324.

Ugarte-Romero, E., Feng, H., Martin, E., Cadwallader, R., and Robinson, J. (2006). Innactivation of *Echerichia coli* in apple cider with power ultrasound. *Journal of Food Science*, 71, 102–109.

Vinatoru, M. (2001) An overview of the ultrasonically assisted extraction of bioactive principles from herbs. *Ultrasonics Sonochemistry*, 8, 303–313.

Vokurka, K. (1986) Comparison of Rayleigh's, Herring's and Gilmore's models of gas bubbles. *Acustica*, 59, 214–219.

Yoshikawa, K., and Kawashima, Y (1955). Acoustic radiation pressure on a compressible sphere. *Acustica*, 5, 167–173.

Zhang, T., Niu, X., Eckhoff, R., and Feng, H. (2005). Sonication enhanced cornstarch separation. *Starch-Starke*, 57, 240–245.

Chapter 14
Ultrasound in Enzyme Activation and Inactivation

Raymond Mawson, Mala Gamage, Netsanet Shiferaw Terefe, and Kai Knoerzer

1 Basic Principles

As discussed in previous chapters, most effects due to ultrasound arise from cavitation events, in particular, collapsing cavitation bubbles. These collapsing bubbles generate very high localized temperatures and pressure shockwaves along with micro-streaming that is associated with high shear forces. These effects can be used to accelerate the transport of substrates and reaction products to and from enzymes, and to enhance mass transfer in enzyme reactor systems, and thus improve efficiency. However, the high velocity streaming, together with the formation of hydroxy radicals and heat generation during collapsing of bubbles, may also potentially affect the biocatalyst stability, and this can be a limiting factor in combined ultrasound/enzymatic applications. Typically, enzymes can be readily denatured by slight changes in environmental conditions, including temperature, pressure, shear stress, pH and ionic strength.

Ultrasound can cause inactivation of many enzymes. Inactivation of enzymes by ultrasound is mainly attributed to the mechanical and chemical effects of cavitation. Collapse of bubbles is accompanied by extreme local increase in pressure (1,000 MPa) and temperature (5,000°K). In addition, ultrasound makes stable cavitating bubbles vibrate, creating shock waves that cause strong shear, and microstreaming in the adjacent liquid. Under these extreme conditions, sonication could cause the breakdown of hydrogen bonding and van der Waals interactions in the polypeptide chains, leading to the modification of the secondary and tertiary structure of the protein. With such changes in the protein secondary and tertiary structure, the biological activity of the enzyme is usually lost. The extreme localized increase in pressure and temperature also leads to homolytic water molecule cleavage generating high energy intermediates such as hydroxyl and hydrogen-free radicals. The free radicals formed may react with some amino acid residues that participate in

R. Mawson (✉)
CSIRO Food and Nutritional Sciences, 671 Sneydes Road, Werribee, VIC 3030, Australia
e-mail: raymond.mawson@csiro.au

H. Feng et al. (eds.), *Ultrasound Technologies for Food and Bioprocessing*, Food Engineering Series, DOI 10.1007/978-1-4419-7472-3_14,
© Springer Science+Business Media, LLC 2011

enzyme stability, substrate binding or in the catalytic function with a consequent change in biological activity.

The inactivation of trypsin by ultrasound has been partly attributed to the large interfacial area between air and water created by ultrasound, which disturb the hydrogen bonds and hydrophobic interactions in the molecule. This was indirectly confirmed by the fact that Tween 80, which provides a hydrophilic environment and decreased exposure to air, protected trypsin against inactivation by ultrasound and the increased inactivation with aeration (Zhong et al., 2004). Prolonged (2–4 h) sonication treatment of subtilisin in organic media resulted in change in the shape of the enzyme particles and irreversible inactivation, probably due to the mechanical effects of cavitation (Bracey et al., 1998). The inactivation of human butyrylcholinesterase (BChE) by ultrasound exposure (20 kHz, 46–138 W) was explained to be due to cavitation-induced high shear stress and pressure causing partial dissociation of the tetrameric enzyme (Froment et al., 1998a).

Several studies suggest that free radicals generated during sonication play a major role in enzyme inactivation. Barteri et al. (2004) studied the inactivation of fumarase by ultrasound. They observed progressive oxidation of cysteine by hydroxyl-free radicals and aggregation of the enzyme. They concluded from this observation that the inactivation of the enzyme was due to the formation of disulfide-linked aggregates formed during sonication (Barteri et al., 2004). The involvement of free radicals in the inactivation of trypsin has also been observed indirectly through the strong protective effect of mannitol against ultrasound inactivation, which is a free radical scavenger, as well as the presence of polypeptide fragments following sonication (Zhong et al., 2004). Aggregation of laccase was observed following sonication at different frequencies (20, 50, 500 kHz). The addition of polyethylene glycol (PEG) and polyvinyl alcohol (PVA), which are free radical scavengers, to laccase solution increased the stability of the enzyme against inactivation showing that free radicals are involved in the inactivation of the enzyme (Basto et al., 2007a). The role of free radicals on the ultrasound inactivation of enzymes has also been indirectly confirmed through the effect of free radical scavenging solutes in horseradish peroxidase (Grintsevich et al., 2001), catalase (Potapovich et al., 2003b), glucose-6-phosphate dehydrogenase (G6PDH) (Karaseva and Metelitza, 2006; Rachinskaya et al., 2004), and urease (Tarun et al., 2003). Sonication-induced aggregation was observed in α-amylase, while no such aggregation was observed in β-amylase, which showed that free-radical-induced oxidation of amino acid residues is dependent on the structure of the protein (Liu et al., 2003a).

Ultrasound does not inactivate all enzymes at mild temperature conditions. Villamiel and de Jong (2000a) reported that ultrasound treatment (20 kHz, 120 μm) at temperature less than 55°C did not inactivate alkaline phosphatase in milk, while only 22 and 14% inactivation, respectively, was observed in γ-glutamyltranspeptidase and lactoperoxidase (Villamiel and de Jong, 2000a). Similar results were obtained for the sonication (20 kHz, 7–40 W) of alkaline phosphatase in buffer (Ozbek et al., 2000). Ultrasonication (26 kHz, 4 W/cm^2, 10 W/cm^2) did not cause conformational or catalytic activity changes or catalytic activity in chymotrypsin (Ovsianko et al., 2005b). The study by Liu et al. (2003a)

showed that free radicals generated during cavitation do not affect the structure of all enzymes, with the effect being dependent on the chemical structure of the protein. In addition, it is known that not all proteins are denatured by ultrasound (Guzey et al., 2006; Villamiel and de Jong, 2000a). These observations may explain why not all enzymes are inactivated by ultrasound.

There have been several studies on the ultrasound inactivation of enzymes. These studies can be broadly classified into two categories: (1) studies dealing with the effect of ultrasound on enzymes and proteins that can be used as therapeutic agents to see how ultrasound encapsulation as a delivery technique affects their bioactivity and (2) studies dealing with food quality-related enzymes with the aim of using sonication (mainly in combination with other inactivating agents such as heat and pressure) as an alternative food preservation technology. Several studies have also been conducted on enzymes that are used in enzyme catalyzed reactions in the chemical industries with the view of using ultrasound to enhance such reactions.

2 Denaturation of Proteins by Applied Force

Only within the past decade, since the advent of atomic force microscopy, and the related single molecular force spectroscopy, has it been possible to study the effects of force on the denaturing of individual protein molecules (Rief et al., 1997). Coinciding with the capability of using high-powered computer molecular modeling techniques, it is now possible to make inferences about the mechanisms that are involved in denaturing proteins by force (Sotomayor and Schulten, 2007). Cytoskeletal proteins have been an obvious focus for this work, as their function is to maintain cellular structure against applied forces, particularly in animal tissues. In fact, there are examples within the cytoskeletal proteins of how force can modulate enzymatic activity associated with these proteins. The sarcomeric protein titin, for example, which is found in muscle tissue, is responsible for maintaining the structural integrity of these sarcomeres. Upon stretching of this enzyme under applied force, an active kinase site is exposed, thus providing a biofeedback link to the contractile proteins of muscle. In another example, the ubiquitous cytoskeletal protein ankyrin is readily distorted by mechanical force. It is believed that it may act as a gatekeeper for the passage of hormones through membrane channels, and in this way, force can regulate the metabolic function of the cell. In terms of applied force, these are relatively subtle effects and forces of the order of piconewtons are all that is required to modify the structure of these proteins at the single molecular level. Excessive force can modify the equilibrium conformation of these proteins (Johnson et al., 2007), which could have implications for their function. Transferring these studies to a whole cell context, it has been possible to confirm that the observations made in single molecule studies are valid in cells (Johnson et al., 2007). The applied forces in this instance are relatively mild: whole red blood cells are mixed mechanically in an aqueous medium at speeds sufficiently low to prevent gross mechanical damage to the cell wall structures.

This work on cytoskeletal proteins suggests that force has the potential for denaturing enzymes in general and could have a major influence on their biochemical function as a result. Studies at the broader molecular level have yet to confirm this result, either on isolated enzyme molecules or within their cellular context.

3 Physical Effects

In the context of the relatively mild forces described in the discussion above, the application of ultrasound, with its generation of extremely high localized temperatures and shockwaves, may seem like applying a very large hammer to crack a very small nut. This appears to be confirmed by observations on the use of ultrasonics in enzyme activity studies. High-intensity low-frequency ultrasound usually results in the permanent denaturing of enzymes, while high-frequency ultrasound, with more stable cavitation, micro-streaming, and fewer implosion events often results in stimulating enzyme activity.

At low frequencies, ultrasound can be used to either activate or inactivate enzymes, and the effect is strongly intensity and system dependent, as has been observed in reports by a number of researchers (Bracey et al., 1998; Sakakibara et al., 1996; Wood et al., 1997). Where clumping, aggregation, or flocculation occurs, masking the enzyme from the substrate during processing, pulses of low-frequency ultrasound are effective in breaking up the flocks and thus exposing both the enzyme and substrate for further reaction activity. Substrate inhibition of enzymes can occur when inappropriate parts of the substrate molecules are presented to the active enzyme site, thus occluding the site and preventing reaction. It is believed that ultrasound may also be effective in preventing or minimizing this effect (Sakakibara et al., 1996).

In some systems, it is more appropriate to focus on substrate pre-treatment rather than using ultrasound to increase the activity of enzymes. The approach typically used to date is to hit the substrate hard with high-intensity low-frequency ultrasound in order to make the substrate more available to enzyme reaction processes (Aliyu and Hepher, 2000; Gama et al., 1997; Imai et al., 2004; Mahinpour and Sarbolouki, 1998; vanWyk, 1997).

At surfaces, microbubbles flatten and collapse with a very high velocity streaming jet directed through the center of the flattened shape at the surface. This micro-jet potentially accelerates transportation of biocatalysts from the liquor to the surface and, subsequently, through the surface into the underlying structure. The same phenomenon also facilitates the removal of products from enzymic processes at surfaces, although it has been suggested that the transport of substrate to the enzyme is more important than the removal of products (Antonenko and Pohl, 1995; Sinisterra, 1992). However, within solids such as hydrogels and tissues further mechanisms can also be involved in enhancing mass transfer through micro-channels (1–10 μm) in the gel or tissue, particularly when the tissue is exposed to high frequency (2–6 MHz) ultrasound. Raleigh micro-vortices overcome the laminar flow, which

would normally be evident in such confined spaces (Bengtsson and Laurell, 2004; Francis et al., 1995; Nikolaev et al., 2001) and actively transport materials through micro-channels.

Enzymes at surfaces are typically immobilized and surrounded by boundary layers. From modeling studies it appears that the boundary layers form in two zones. The thinner stable zone immediately adjacent to the enzyme surface is probably not greatly disturbed by ultrasonic effects and diffusion remains the predominant transport mechanism. In the outer boundary layer the phenomena such as cavitation-induced micro-jets and micro-streaming probably accelerate the transport of substrates to the enzyme and product removal from the enzyme (Antonenko and Pohl, 1995).

In studying a whole tissue system (krill), it was found that it was difficult to differentiate between ultrasound as an enhancer of mass transfer through the cellular structure, as opposed to a direct effect on accelerating the action of the intracellular enzymes on the substrate. However, the dominant effect was believed to be associated with mass transfer, but a direct effect on enzymes could not be excluded (Siwek et al., 2006).

Ultrasonic standing waves can be applied at top exits from bioreactors so that the substrate, cells, or immobilized enzymes can be flocculated and allowed to settle back into the reactor without being swept out of the reactor along with the products, thus maintaining the activity of the reactor for longer duty cycles (Durrschmid et al., 2003).

Most of the energy from cavitation events is dispersed as heat, and a minor amount of energy as audible and other ultrasonic frequencies. As in all studies relating to the application of ultrasound, when considering impacts on enzyme denaturation and biological systems, it is important when considering physical effects to differentiate the mechanisms of ultrasound per se from simple thermal effects (Rosenthal et al., 2004). This is particularly important when the sonication is carried out at temperatures near to the denaturation temperature of the enzyme or in batch applications where sonication is carried out for a long time.

4 Sonochemical Effects

Mechanisms involved in sonochemistry are described in detail elsewhere in this book. Sonochemistry and its implications for biological materials are reviewed by Riesz and Kondo (1992). Three zones for sonochemistry are identified within the cavitation bubble at the cavitation bubble surface and within the bulk liquid surrounding the bubble. The concentration of hydroxyl radicals are greatest at the interface between the bubble and the surrounding liquid, so surface active materials that accumulate at this interface are most prone to sonochemical attack. When surface active materials are present, few free radicals from the cavitation bubble escape the surface region of the bubble. Radical propagation beyond the surface results from subsequent radical reaction chains initiated in the surface active material. Enzymes by virtue of their proteinaceous nature, if in free solution, have the

potential to act as surface active agents and associate with the cavitation bubble surface. In this circumstance, enzymes are directly prone to sonochemically induced radical attack. Enzymes immobilized at surfaces or within cells are much less likely to be attacked directly by hydroxyl radicals produced by cavitation events.

In the sonication of living biological material and in the absence of intracellular cavitation it has been determined that intracellular superoxide radical formation is generated by enzymic processes within stressed mitochondria, rather than directly from the extracellular sonication cavitation bubbles (Kagiya et al., 2006). In contrast to ionizing radiation, there is no clear evidence of the genotoxic potential of ultrasound, most probably because of the site of production of the hydroxyl and hydrogen radicals. In ultrasonic treatments, production of these short-lived radicals is most likely to occur extracellularly, whereas during irradiation hydroxyl radical generation can occur wherever the radiation penetrates to. There is no conclusive evidence to date that cavitation can occur intracellularly, but should such an event occur, it would lead to immediate cell destruction because the resonance size of cavitation bubbles, even in the low megahertz range, is comparable to the size of the cells (Rosenthal et al., 2004). With the aid of modeling studies it has been determined that at 1 or 2 MHz (intensity 0.1 MPa) microstreaming surrounding cavitation bubbles may be sufficient to generate sonoporation of cell membranes (Wu, 2007). At a lower sonication frequency of 20 kHz, the threshold stress for sonoporation was 12 $\pm$4 Pa for ultrasonic exposure times of 7 min. Sonoporation permits the passage of larger molecules than would otherwise pass through the cell membrane, potentially leading to unexpected cell responses.

5 Kinetic Considerations

The diversity of mechanisms through which ultrasonics acts to modify the kinetics of enzymic processes has, by analogy, led to a diversity of approaches to study the kinetics of enzyme inactivation and activation. Enzyme kinetics modification by ultrasound in food systems is summarized in Tables 14.1 and 14.2. There is no agreed upon measure of ultrasonic treatment, as is evident in the tables, which makes direct comparison of the effects of ultrasound with respect to enzymes unachievable. To facilitate interpretation of the tables, the following measures are used:

- where power is given in W, this is usually the ultrasonic generator input power (sometimes the transducer input power); generators typically have energy conversions of 60–80%;
- where power is given in W/cm^2, this is usually the generator (sometimes transducer input) input power divided by the area of the tip of the ultrasonic horn;
- where the power is given in Pa, it is likely to have been measured with a hydrophone;

Table 14.1 Inactivation of enzymes; enzyme kinetics modification by ultrasound in food related systems

Enzyme	Medium	Treatment	Effect on activity	References
Horseradish peroxidase type VI	In water suspension	20, 40, and 60 kHz, 0–120 W, 80°C	D_{80}, reduces from 65 to 10 min with ultrasonic application	De Gennaro et al. (1999)
Native milk enzymes alkaline phosphatase, γ-glutamyl transpeptidase, and lactoperoxidase	Milk	20 kHz, 120 μm amplitude, 15–0 W	Synergistic effects of heat and ultrasound at 61, 70, and 75.5°C was observed on the inactivation of alkaline phosphatase, γ-glutamyl transpeptidase, and lactoperoxidase, respectively	Villamiel and de Jong (2000b)
Milk enzyme adenosine deaminase (ADA)	Milk	37 and 65°C	Ultrasonic treatment decreased ADA activity compared to heat treatment	Martin and Schlimme (2002)
Glucose-6-phosphate dehydrogenase from Leuconostoc sp5	In 0.1 M phosphate buffer – pH 7.4	LF 27 kHz, 60 W/cm^2, HF 880 kHz, 1.0 W/cm^2 36–50°C	Thermo-sonication was more effective than thermal inactivation of the enzyme under all conditions	Rachinskaya et al. (2004)
PME of tomato	0.5% (w/v) solution of citrus pectin, prepared in 0.15 M NaCl	20 kHz, 20 μm, 100 W, 61 and 72°C cavitation intensity over the range of 0.004–0.020 mg/L/min. hydrogen peroxide yield	Compared to thermal inactivation thermo-sonication, increased inactivation by 39- to 374-fold at 61°C, while at 72°C increase was 3.6- to 84-fold	Raviyan et al. (2005)
Peroxidase in watercress (Nasturtium officinale)	3 g/100 ml water suspension of watercress leaves	Cole Palmer sonicator, 20 kHz, 13 mm horn, 50% power, 40–92.5°C	TS showed increase in activity of peroxidase at 40–80°C; thermo-sonication at ≥85°C led to higher enzyme inactivation compared to thermal treatment	Cruz et al. (2006)

Table 14.1 (continued)

Enzyme	Medium	Treatment	Effect on activity	References
Tomato pectic enzymes PME and PG	Phosphate buffer	20 kHz Temperature 52–86°C Pressure 1.2–4.5 kg/cm^2 Amplitude 0–104 μm	*D* values PME @ 62.5°C heat – 45 min, MTS – 0.85 min *D*-values for PG I – @ 86°C heat – 20.6 min MTS – 0.24 min *D*-values for PG II – @ 52.5°C Heat – 38.4 min MTS – 1.46 min	Lopez et al. (1998)
Egg white lysozyme	pH 6.2 100 mM phosphate buffer	20 kHz, Amplitude 117 μm Pressure 200 kPa; Temperature 50–80°C	Application of external pressure and temperatures increased the inactivating effect of ultrasound	Manas et al. (2006)
Tomato paste Pectin methyl esterase (PME) and polygalacturonase (PG)	Tomato puree, approx 5.5% solids	20 kHz, Pressure 200 kPa Amplitude 117 μm Temperature 70°C	100% inactivation of PME, 62% inactivation of PG	Vercet et al. (2002b)
Orange juice Pectin methyl esterase heat-resistant fraction (PME)	in citrate buffer, 38 and 72°C in orange juice	20 kHz Amplitude 117 μm Pressure 200 kPa Temperature 33 and 72°C	MTS increased the inactivation by 25 times in citrate buffer and >400 times in orange juice Synergistic effect of heat and ultrasonics on thermostable PME fraction is reported	Vercet et al. (1999)
Lipase milk whey @ selected pH (*Pseudomonas fluorescens*) and protease	0.1 M phosphate buffer @ selected pHs 5.5–8.0	20 kHz Amplitude 60–150 μm Pressure 350–600 kPa Temperature 110–140°C	Decreased activity in both enzymes Effect of amplitude was different depending on temperature Lipase inactivation by MTS depends on pH	Vercet et al. (2002a)

Table 14.1 (continued)

Enzyme	Medium	Treatment	Effect on activity	References
Extracellular lipase and protease from *P. fluorescens*	Milk	20 kHz Amplitude 60–150 μm Pressure 350–650 kPa Temperature 110–140°C	Mano-thermo-sonication inactivates both enzymes more efficiently than heat treatment	Vercet et al. (1997)
Soyabean lipoxygenase	buffer	Pressure 392 kPa, temperature 67–77°C, 20 kHz, amplitude 76 μm	Synergistic inactivation effect between heat and ultrasound	Lopez et al. (1994)
Mushroom polyphenoloxidase	buffer	Pressure 392 kPa, temperature 70.7°C, 20 kHz, amplitude 35 μm	Synergistic inactivation effect between heat and ultrasound	Lopez et al. (1994)
Soyabean lipoxygenase	buffer	Pressure 117–441 kPa, temperature 67–72.5°C, 20 kHz, amplitude 0–104 μm	Synergistic inactivation effect increasing with amplitude	Lopez and Burgos (1995b)
Milk lactoperoxidase and alkaline phosphatase	buffer	Ultrasound different power level, 90–360 W, time up to 120 s temperature, 20 and 40°C, 20 kHz	Inactivation dependent on time, temperature, and amplitude, synergistic inactivation effect with heat	Ertugay et al. (2003)
Bovine liver catalase, Horseradish peroxidize type IV A Bovine lactoperoxidase	10 mM phosphate buffer, pH 7.0	22 kHz, 15 W/cm^3, temperature approx. 5°C	Catalase showed no inactivation; activity of both peroxidases decreased with increased sonication time	Gebicka and Gebicki (1997b)
Trypsin	Water	20 kHz, 100–500 W, 1–20 min, 84.9–424.5 W/cm^2	Decreased activity with increase in ultrasound power; addition of Tween 80 completely protective with increase in activity; Mannitol partially protective, sucrose not protective	Tian et al. (2004)

Table 14.1 (continued)

Enzyme	Medium	Treatment	Effect on activity	References
Serine protease and precursors	pH 7.4 0.01 M Potassium phosphate buffer	26.4 kHz, 26 W/cm^2	Decrease	Ovsianko et al. (2005a)
Soya lipoxygenase	Soy flour suspended in distilled water, pH adjustment with 0.1 M NaOH and HCl	20 kHz, pH 5–4, temperature 22°C	By reducing pH of the suspension to 5 and 4, 70–85% inactivation was observed, at this pH range enzyme activity decreased with the increase of US frequency	Thakur and Nelson (1997)
P. fluorescens lipase and protease	Milk	Ultrasonic homogenization 150 W for 1 min at 7°C	Growth of *Pseudomonas* fluorescence in the homogenized milk at 7°C studied, lipase activity completely inhibited, and the production of protease inhibited by 88%	Jaspe and Sanjose (1999)
Horseradish peroxidase	0.01 M phosphate citrate buffer at various pH	Ultrasonication 2.64 MHz, 1 W/cm^2, 1–2 h at 35.5–55°C	Inactivation stopped in the presence of polyphenolic antioxidants, indicating that free radicals play a significant role in inactivation	Grintsevich and Metelitsa (2002)
Laccase from *T. villosa*	0.1 M Acetate buffer, pH 5.0	Ultrasonication; 50 W at 20 kHz, 72 W at 150 kHz and 47 W at 500 kHz and mixed 150 and 500 kHz at 72 and 47 W, respectively. All at 50°C. Treatments 0–6 h	Increased inactivation kinetics for all treatments as compared to heat (50°C), half-life decreased by 80–82%; inactivation due to protein aggregation	Basto et al. (2007a)

Table 14.1 (continued)

Enzyme	Medium	Treatment	Effect on activity	References
Glucose-6-phosphate dehydrogenase	Distilled water (pH=5.6)	Ultrasound (27 kHz, 60 W/cm^2) and (880 kHz, 1 W/cm^2), 36–47°C	Caused higher inactivation as compared to thermal treatment, dependent on enzyme concentration, higher activation energy at lower frequency, and substantial effect of free radical scavengers; substrate and co-factor of the enzyme had a protective effect against ultrasound inactivation	Karaseva and Metelitza (2006)
Catalase (bovine liver)	Buffer (pH 4.15–7.90)	Ultrasound (20.8 kHz, 48–62 W/cm^2) and (2.64 MHz, 0.05–1.0 W/cm^2)	Inactivation rate increased with power, decreased with enzyme concentration, and varied with pH; higher inactivation by ultrasound was obtained at higher frequency; free radicals assumed to play a role in inactivation	Potapovich et al. (2003a)

Table 14.1 (continued)

Enzyme	Medium	Treatment	Effect on activity	References
Catalase (bovine liver)	Buffer (pH 4.0–11.0)	Ultrasound (20.8 kHz, 48–62 W/cm^2 36–55°C)	Higher inactivation rate as compared to thermal inactivation at the same condition (2.25-fold increase in the inactivation rate at 45°C); value of inactivation rate increased with the ultrasound power (range, 48–62 W/cm^2), and exhibited strong dependence on the pH of the medium; inactivation attributed to radicals is determined by the degree of association between the enzyme molecules and the composition of the reaction medium	Potapovich et al. (2003b)
Catalases from yeast *Pichia pastoris* and fungus *Penicillium piceum*	Phosphate buffer (pH7.4 or 5.5)	Ultrasound (27 kHz, 60 W/cm^2, 45 and 50°C)	Purpose was to compare stability of catalases; enzymes exhibited the following rank order of resistance to ultrasonic inactivation: fungal catalase > bovine > yeast	Potapovich et al. (2001)
Human butyrylcholinesterase resistance to denaturation	Buffer, enzyme concentration of 0.01 mg/ml in 20 mM phosphate or 10 mM Tris-HCl, containing 1 mM EDTA, pH 7.4	20 kHz power input of 60 or 85 W, 3 mm tipped horn. Pulsed 50% on–off, temperature 20 or 27°C. Delivered power 0.13 mmol I_2/l/min and 0.37 mmol I_2/l/min for input power of 60 and 85 W, respectively	Partial inactivation due to dissociation of tetramer structure related to enzyme microheterogeneity, i.e., nicked (C-terminal segment depleted) tetramers were less stable than native tetramers	Froment et al. (1998a)

Table 14.1 (continued)

Enzyme	Medium	Treatment	Effect on activity	References
Chitin degradation and stability during sonication	Solutions of 2.0, 1.4, 0.8 and 0.2% (w/v) chitosan 0.2 M acetic acid/0.1 M sodium acetate were prepared	20 kHz, 0.5 in horn tip at 420 W power output for 0.5, 1.0, 1.5, 2.0, and 2.5 h	Molecular weights of chitosan solutions, which underwent concurrent removal of smaller degraded molecules during sonolysis, were lower than those without the concurrent removal of degraded molecules; degradation rate remained relatively constant during sonolysis; however, it increased with decreasing solution concentration	Tsaih et al. (2004)

Table 14.2 Activation of enzymes; enzyme kinetics modification by ultrasound in food systems

Enzyme	Medium	Treatment	Effect on activity	References
Tomato pectin methylesterase	Extracting buffer	Thermo-sonication (50–72°C, 20 kHz, 20 μm, 100 W), *d/t* cavitation intensity	39- to 374-fold increase in inactivation at 61°C and 36- to 84-fold at 72°C	Raviyan et al. (2005)
Regulated delivery of drugs – bioactivities	Designed bio-compatible/degradable polymeric structures	Focused ultrasound in vivo	Enhanced polymeric structure erosion and released kinetics under focused ultrasound	Kost (1993)
Dosimetry study of mammalian cell lysis	Low count cell suspensions with inhibitors of peroxide consuming enzymes	10 ms pulsed 2.17 MHz ultrasound at 0.8 MPa peak negative pressure amplitude	Hydrogen peroxide analysis gave a reliable measure of ultrasonic treatment and cell lysis	Miller and Thomas (1994)
Fibrinolysis/ thrombolysis	Blood plasma	1 MHz ultrasound at 4 W/cm^2	Doubling of uptake of plasminogen-activating factor enzymes by the application of ultrasound and subsequent clot lysis	Francis et al. (1995)
Modeling aqueous-phase oxidation sonochemistry	Aqueous buffer	Air-saturated aqueous solutions sonicated at 20 kHz and 75 W/cm^2 at pH greater than or equal to 10	The use of simplified approaches for modeling the liquid-phase sonochemistry of a well-mixed solution may be justified when (OH)-O-. radical reactions predominate	Kotronarou and Hoffmann (1995)

Table 14.2 (continued)

Enzyme	Medium	Treatment	Effect on activity	References
B-galacosidase release from *E. Coli*	Buffer (50 mM Tris-HCl, 10 mM $MgCl_2$, 100 mM NaCl, and 10 mM b-mercaptoethanol, pH 7.2)	20 kHz, 4 mm tip horn, 35–95 W, Temperature <10°C. Pulsed 0.5 s on 0.5 s off to minimize radical generation. Volume 5–50 ml, Time 3–21 min	Ionic strength and cell concentration have the least influence on the rate of enzyme recovery, whereas sample volume (fourfold decrease) and acoustic power (threefold increase) dramatically affect the final yield of soluble protein	Feliu et al. (1998)
Human butyryl-cholinesterase resistance to denaturation	Buffer, enzyme concentration of 0.01 mg/ml in 20 mM phosphate or 10 mM Tris-HCl, containing 1 mM EDTA, pH 7.4	20 kHz at varying intensity input: 46, 92 and 138 W/cm^2, pulsed 50% on–off. Delivered power was 0.1 1 mmol I_2/l/min, 0.29 mmol I_2/l/min and 0.40 mmol I_2/l/min	Short ultrasound irradiation induced a faint transient enzyme activation, but prolonged irradiation caused partial dissociation of the tetrameric enzyme and irreversible inactivation	Froment et al. (1998a)
Mixed *Trichoderma viride* and *Aspergillus nigercellulases* and substrate pre-sonication	Pre-hydrolysis sonication Carboxymethylcellulose powder was suspended in 0.2 M acetate buffer, pH 4.8. Hydrolysis; hydrolysis reaction was carried out in 0.2 M acetate buffer solution, pH 4.8, at 50°C	20 kHz, power 72–135 W, temperature 50°C, time 10–60 min	Reaction time needed for effective degradation could be markedly reduced (to a third) by increasing ultrasonication time and intensity	Imai et al. (2004)

Table 14.2 (continued)

Enzyme	Medium	Treatment	Effect on activity	References
T. viride cellulose hydrolysis of paper wastes	0.001 M acetate buffer solution of pH 4.8	20 kHz, 30 W (delivered, measured calorimetrically) in 0.8 l of 7.5–25 g/l paper slurry in buffer for up to 48 h	Waste papers, except newspaper, were more efficiently hydrolyzed with increasing specific ultrasonic intensities the adverse effect on the hydrolysis of newspaper was considered to be that some impurities such as lignin were activated by the ultrasonic treatment to form a rigid and closed network, which inhibited the access and adsorption of cellulase to the substrate, leading to retarded hydrolysis	Li et al. (2005)
Lipases from *Candida rugosa* and *Mucor miehei*	Oil (bleached palm oil), the aqueous phase and gum arabic added as an emulsifying agent in the ratio of 0.005 g/g of oil were first dispersed either by ultrasonication or by mechanical agitation	20 kHz, 175 W (input), 19 mm tipped horn, time 1 min, temperature 40°C	Hydrolysis rate of lipids was significantly enhanced (two- to fourfold) by ultrasonic emulsification; the interfacial area saturation with enzyme was also not observed due to the large interfacial area generated	Ramachandran et al. (2006)

Table 14.2 (continued)

Enzyme	Medium	Treatment	Effect on activity	References
B-Galactosidase from *Kluyveromyces marxianus*	Milk	20 kHz, 12.7 mm tip horn, 20 and 100 W, 250 ml milk, temperature 37°C; ultrasonic energy was pulsed using the duty cycle control from 10 to 90%, in order to reduce the formation of free radicals	Ultrasonic treatment resulted in 90% lactose hydrolysis and residual enzyme activity of 75% at the optimum operational conditions; acoustic power of 20 W, duty cycle rate of 10% and enzyme concentration of 1 ml/l	Sener et al. (2006)
Alpha-amylases produced from mixed *Bacillus* species and from *Bacillus licheniformins*	0.2 g of soluble starch was dissolved in 100 mL boiling 50 mM sodium acetate buffer (pH 5.9)	20 kHz, 20 and 100 W, pulsed 10–80% on, 250 ml, temperature 40 and 50°C	Compared to non-sonicated controls, no apparent impact of sonication at any operating condition or either temperature	Apar et al. (2006)
Sonoporation of living Jurkat lymphocytes	Tissue culture medium	21.4 kHz, 400 μm tipped horn at varying amplitude 0–26 μm, temperature 37°C	Threshold shear stress for cell sonoporation was 12 ± 4 Pa for ultrasound exposure time up to 7 min; numerical calculations have shown that shear stress associated with micro-streaming surrounding encapsulated bubbles may be large enough to generate sonoporation at 0.1 MPa of 1 or 2 MHz ultrasound	Wu (2007)

Table 14.2 (continued)

Enzyme	Medium	Treatment	Effect on activity	References
Mechanical effects on cytoskeletal proteins	Steered molecular dynamics stimulations, in which external forces are used to explore the response and function of macromolecules		Protein mechanics simulations: elasticity of muscle protein titin and extracellular matrix protein fibronectin; linker-mediated elasticity of the cytoskeleton proteins spectrin, and elasticity of ankyrin repeats, a protein module found ubiquitously in cells	Sotomayor and Schulten (2007)

- where the power is given as W/cm^3, it is likely, but not necessarily, to have been derived calorimetrically, taking into account that the amount of material sonicated, its specific heat and the temperature rise. Alternatively some workers use the volume sonicated and the input power to the generator or the transducer to derive this value;
- where the power is given as mmol I^2/I/l, it is a measure of the hydroxyl radicals generated by cavitation.

There is clearly no single approach to kinetic modeling that is universally applicable to ultrasonic processing, and each processing case will have a unique modeling approach, based on a comprehensive understanding of the mechanisms involved.

5.1 Activation

Using ultrasound treatments at appropriate frequencies and intensity levels can lead to an increase of enzyme activity due to several different effects. These effects can be subdivided into physical and (bio-)chemical effects: physical effects such as an enhancement of mass transfer due to (micro)-mixing, resulting in an increase of substrate availability and enzyme release due to cell break-up; and stimulation of biochemical reactions within cell tissues to enhance the production of specific enzymes.

Applications can be further distinguished into enzyme activity enhancements through pre-treatment procedures and/or combined enzyme and ultrasound treatment.

The following will elaborate on these effects and explain them on the basis of examples found in literature.

1. *Physical effects*: As mentioned before, there are a number of effects enhancing enzyme activity based on pure physical effects elaborated in the following part of this contribution.

    a. *Mass transfer and micro-mixing*: Enzymatic reactions are often limited by a lack of substrate due to structural configuration of the substrate (Cadoret et al., 2002; Sakakibara et al., 1996) or restricted diffusion of substrate to enzymes or vice versa (Francis et al., 1995). Ultrasound waves at different frequencies can overcome this limitation by inducing fluid motions to increase this mass transfer, ensuring substrate availability at the enzyme and removal of products from the enzyme (Sinisterra, 1992). This increase in mass transfer is either obtained at lower frequencies by the generation of cavitation or at higher frequencies through the generation of turbulent microstreams and the induction of a turbulent channel flow in narrow porous structures (Bengtsson and Laurell, 2004; Francis et al., 1995; Sinisterra, 1992). Starting in the early 1990s, a number of workgroups investigated this effect of synergistically enhancing enzyme activities across a variety of applications. Typically, systems that involved solid–liquid or liquid–liquid

interfaces were investigated. Applications that were investigated include: enzyme scouring of cotton (Basto et al., 2007b; Yachmenev et al., 1998, 1999, 2002, 2004); paper recycling (Xie et al., 2002); cellulose hydrolysis (Aliyu and Hepher, 2000; Barton et al., 1996; Li et al., 2005); sucrose hydrolysis (Sakakibara et al., 1996); esterifications (Vulfson et al., 1991; Xiao et al., 2005); hydrolysis of esters (Jie and Syedrahmatullah, 1995); hydrolysis of phenolic compounds in wastes and bleaching (Basto et al., 2007b; Entezari and Petrier, 2004; Entezari et al., 2006; Tauber et al., 2005); and biofilm removal (Oulahal-Lagsir et al., 2003).

b. *Enzyme release*: The spatial constraint of enzymes within cells also leads to limitations of enzyme activity or hinders their extraction. Ultrasound waves at low frequencies and high intensities can induce cell break-up leading to a discharge of the cell content including enzymes (Agrawal and Pandit, 2003; Farkade et al., 2006; Persike et al., 2002; Vargas et al., 2004). However, using ultrasound at lower intensities can also release enzymes from cells while causing little damage to cell membranes (Roncales et al., 1993). These applications allow for an enhancement of enzyme activity by overcoming the limitation of inter-membrane transport or to an improved enzyme extraction from cellular material. Compared to the effect of enhancing enzyme activity through increasing mass transfer by means of ultrasonic "agitation," the number of groups investigating the enhancement by means of enzyme release is significantly smaller, most likely due to the fact that the energy intensity necessary for overcoming the spatial constraint of enzymes in cells is much higher, and thus the likelihood of denaturing the enzyme itself is greater as well. Issues relating to extraction are discussed in Chapter 13.

c. *Immobilized enzymes*: Besides using enzymes randomly distributed within solutions, a further approach to allow for better control of enzymatic reactions is the immobilization of enzymes on and inside carrier material (e.g., gels, polymers, etc). The effects of increasing enzyme activities of immobilized enzymes by using ultrasound are described by mass transfer and micromixing (see above), and increasing substrate availability by enhanced mass transfer to and through the carrier material (Nikolaev et al., 2001; Schmidt et al., 1987). To date, few papers describe the combined use of immobilized enzymes and sonication to enhance enzyme activity. The frequencies used were in the range of 1 MHz and greater, allowing turbulent micro-streams to be generated.

d. *Pretreatment procedures leading to enhanced enzyme activity*: Not only can the combined process of enzymatic reaction and ultrasonication lead to improvement in enzyme activity, but also a substrate or immobilization carrier pretreatment with ultrasound irradiation can significantly enhance substrate conversion. This enhancement occurs through an increase of available substrate surface, e.g., degradation of substrate masking substances such as lignin on cellulose (Aliyu and Hepher, 2000; Entezari and Petrier, 2005; Li et al., 2005; Wood et al., 1997), grafting of a polymeric surface on which enzymes are immobilized (Jiang and Xiang, 1992; Popa et al., 1994), or the

size reduction of oil droplets by means of ultrasonic emulsification (Lin et al., 1995; Ramachandran et al., 2006).

2. *Biochemical effects:* As opposed to the applications where physical effects enhance enzyme activity, ultrasound waves can also induce biochemical effects in living cells, leading to an increase of the production of certain enzymes (Lin and Wu, 2002; Liu et al., 2003b; Wu and Ge, 2004; Wu and Lin, 2002, 2003). Given the nature of ultrasound waves, the triggering of this production enhancement is also a physical effect; however, a biochemical stress response, similar to the one occurring after cell treatment with high hydrostatic pressure, is the cause for the production and thus the enhancement in activity. The modified metabolic activity is clearly the tissue's stress response; the tissue reverts to normal metabolism if there is no further ultrasonic stimulation (Wu and Lin, 2002).

5.2 Inactivation

Enzyme inactivation by ultrasound is widely reported in literature. The collapse of ultrasonically generated cavitation bubbles (cavitation phenomenon) during the compression phase produces thermal, chemical, and mechanical effects, which may account for the irreversible breakdown and inactivation of the enzyme. It has been reported that aromatic/aromatic interactions are stabilized by pressure, whereas ion pairs and hydrophobic aliphatic interactions are disrupted by pressure (Froment et al., 1998a). Ultrasonic inactivation of enzymes depends on ultrasonic-related parameters such as frequency and US power and enzyme-related factors such as enzyme type, concentration, pH of the medium, and temperature (Tarun et al., 2006).

The ultrasonic inactivation of different types of enzymes such as monomeric, dimeric, tetrameric, and homohexameric enzymes are reported in the literature. The mechanism of inactivation shows a difference based on the type of enzyme. The general trends of inactivation for monomeric enzymes are either to form aggregates or for the enzyme molecule to break down into fragments. According to the literature, the polymeric enzymes generally fragment into monomeric forms during ultrasonic inactivation.

6 Formation of Aggregates

High temperature and mechanical stresses have been identified as the main causes of enzyme inactivation in industrial systems (Liu et al., 2003a).The formation of aggregates has been observed under mechanical stress such as simple stirring, in particular in the case of the effects of mechanical stirring on aggregation and inactivation of lysozyme (Colombie et al., 2001). Collision of enzyme molecules during stirring in a reactor (72°C and 700 rpm) has been considered to be responsible for the aggregate formation and reduction in enzyme activity under simple mechanical stirring.

The formation of protein microspheres due to sonication of protein in solution has been reported by many research groups. The effect of ultrasound on some proteins (e.g., bovine serum albumin and hemoglobin), where microspheres were formed due to the chemical cross-linking of oxidized cysteine has been described (Suslick and Grinstaff, 1990; Wong and Suslick, 1995). The formation of stable proteinaceous microspheres, based on sonochemical treatment, was also reported by Avivi and Gedanken (2002, 2005). Basto et al. (2007a) reported that the sonication of laccase from *Trametes villosa* and bovine serum albumin promotes the formation of protein aggregates with high molecular weight. Aggregation of porcine fumarase and a loss of its enzymatic activity due to ultrasound (38 kHz) generating hydroxyl-free radicals have also been reported (Barteri et al., 2004).

According to these authors, the formation of aggregates leads to the deactivation of the enzyme upon ultrasound treatment. This inactivation was mainly caused by the radicals formed by the cavitation phenomenon (Basto et al., 2007a). The ultrasonic aggregation of porcine fumarase enzyme has been reported due to the formation of intermolecular disulfide bridges, originating from the oxidation of cysteine residues, together with a diffuse increase in h-turn in the protein's secondary structure. These conformational changes have led to a fibrous, amyloid-like aggregation that appears ordered and regular under TEM microscopy (Barteri et al., 2004). Studies conducted with sonication effects on α-amylase from *Bacillus subtilis* and soyabean β-amylase enzyme solutions have revealed that the average aggregate size was largest at the iso-electric point of the enzymes. It has also been reported that some enzymes are less prone to aggregation due to the electrostatic repulsion and steric hindrance (Liu et al., 2003a). The aggregates are made up of dimers and trimers that are linked with disulfide bridges. The thiol group in the amino acid cystine undergoes oxidation at neutral and alkaline pH to form disulfide bonds, and this leads to aggregate formation. Although sulfur containing amino acids are reported to form disulfide bonds, the presence of a higher number of cystine amino acid residues does not cause protein to form disulfide bond-induced aggregates (Liu et al., 2003a). Similar changes have been reported in enzymes irreversibly inactivated by heat.

7 Breakdown of Oligomers

Some proteins exist in solution as oligomers. When oligomeric enzymes are subjected to ultrasonic energy oligomers disassociate, leading to the inactivation of enzymes. Disassociation of components could happen rapidly or in stages, depending on the attributes of the enzyme.

7.1 Dimeric Enzymes

Formate dehydrogenase from *Arabidopsis thaliana* was isolated as a mixed monomer and dimer using ultrasound (Li et al., 2000). While the relative activities of the two enzyme species were not determined, it is likely that the monomer is an artifact generated by the ultrasonic treatment. By contrast, ribonucleotide reductase isolated from *Streptomyces aureofaciens* using ultrasound was determined to be

a dimer, but it was demonstrated that the concurrent removal of calcium ions rather than the action of ultrasound per se caused the dissociation of the dimer (Racay and Kollarova, 1996).

7.2 Tetrameric Enzymes

Glucose-6-phosphate dehydrogenase (G6PDH) is a tetramer of four subunits, which is a "dimer of an ordinary dimer." The loss of activity in GPDH due to low-frequency ultrasonication (27 kHz; 60 W/cm^2; amplitude 57 μM; 36–47°C) has been linked with the gradual disassociation of tetramer into dimers and then into monomers. Under normal conditions, the dimers are mainly stabilized by ionic interactions, while hydrogen bonds and hydrophobic interactions predominantly maintain subunits in the dimers. The ultrasonic disassociation of tetramers into monomers has been observed as a lag phase in the inactivation curves of the enzyme (Karaseva and Metelitza, 2006).

The associative–disassociate pathway of the inactivation of subunit G6DPH has been described (Rachinskaya et al., 2004). The inactivation of G6PDH was characterized by the effective first-order rate constants (min^{-1}): k(in), $k*$(in), and k(in)(us) for the total, thermal, and ultrasound (US) inactivation, respectively. The temperature dependence of the total rate k(in) and k^*(in) shows a point of inflection at 44°C in the Arrhenius coordinates. This feature was attributed to the existence of two phases of inactivation.

The effects of ultrasound (20 kHz; 60 and 80 W) on catalytic activity and structure of the tetramer of wild-type human butyrylcholinesterase (BChE) from plasma and recombinant D70G mutant enzyme has been reported at constant temperatures (Froment et al., 1998b). Native BChE was found to be resistant to ultrasound inactivation. Short ultrasound exposure induced a weak transient enzyme activation (60 W), but by contrast, prolonged exposure caused partial dissociation of the tetrameric enzyme and irreversible inactivation. Inactivation kinetics was found to be multiphasic and buffer dependent. Partial dissociation was related to enzyme microheterogeneity, i.e., nicked (C-terminal segment depleted) tetramers were less stable than native tetramers.

Infiltration of water molecules inside the protein structure is considered to be responsible for the denaturation of BChE (Froment et al., 1998a). The stability of the native tetrameric structure (G4) to ultrasound has been explained by the stability of aromatic–aromatic interactions that are stabilized by localized pressure generated by the propagation of ultrasound in a medium and which is accompanied by a periodic variation of pressure during the positive half-period. It is stated that aromatic interconnections stabilize the quaternary structure of BChE.

7.3 Homohexameric Enzymes

High-frequency ultrasonication (2.64 MHz, 1.0 W/cm^2) of soybean urease in aqueous solution at pH 5.4 and 36°C has been reported (Tarun et al., 2006). The absence of lag-periods on the kinetic curves of the urease ultrasonic inactivation indicates the rapid dissociation of homohexamer.

8 Changes in Secondary Structure

The secondary structure of catalase enzyme in phosphate buffer (pH 5.5 or 7.4) is changed when subjected to thermal treatment (45 and 50°C) or low-frequency ultrasound (27 kHz, 60 W/cm^2) (Potapovich et al., 2005). A decrease in alpha helices and an increase in anti-parallel beta structures and irregular regions were observed in the inactivated enzyme fraction (Potapovich et al., 2005).

In another study, a two-stage inactivation of lysozyme by thermo-sonication and mano-thermo-sonication (MTS) has been reported (Manas et al., 2006). It has been speculated that during the first step of the inactivation process, the protein unfolds along the interfacial area of the microbubbles generated by the ultrasonic radiation. The conformational change in protein is reported to have a small effect on enzyme activity, but possibly modifies the physical resistance of the molecule, favoring the action of a second denaturing agent such as heat. The inactivation curves showed an initial lag phase (shoulder) with a slow loss of enzymatic activity, followed by a second phase characterized by a sudden increase of the inactivation rate.

9 Changes in Primary Structure

Trypsin breaks down into polypeptide fragments when subjected to ultrasonication (20 kHz; 300 W for 10 min) (Tian et al., 2004). It has been concluded that free radicals are responsible for the damage or modification of trypsin structure. Tian et al. also suggested that exposure of protein molecules to water–air interphase could be responsible for the attenuation of hydrophobic interactions and the denaturation of proteins (Tian et al., 2004).

10 Mode of Action

As discussed above, several hypotheses have been proposed to explain the mechanism of ultrasonic modification of enzyme activity (Floros and Liang, 1994; Manas et al., 2006). The biological effects of ultrasound have been largely attributed to cavitation phenomena through two main mechanisms: the chemical reactions due to the free radicals formed by water and the mechanical damage generated by the high pressures attaining strong shear forces and micro-streaming (Suslick, 1988).

10.1 Free Radicals-Related Effects on Enzymes

Sonochemical effects of sonication are discussed in detail in Chapter 13. The specific free radical effects reported on enzymes are summarized here. Sonolysis of water produces free radicals (Riesz and Kondo, 1992). These free radicals can promote enzyme denaturation, and the relative importance depends on the structure of the protein (Barteri et al., 2004; Manas et al., 2006).

Sonication also promotes chemical reactions due to the formation of $H^{\bullet}$ and $OH^{\bullet}$ free radicals from water decomposition inside the oscillating bubbles (Thakur and

Nelson, 1997). Some amino acid residues participating in the stability, substrate binding, or catalytic activity of the enzyme can react with these free radicals, thus affecting the enzyme activity. Proline, leucine, isoleucine, lysine, and glutamic acid have all been reported to readily form peroxides with $OH^{\bullet}$ radicals. The $OH^{\bullet}$ radicals can also undergo combination to form hydrogen peroxide, which is known to be an effective lipoxygenase inhibitor even at very low concentration and at room temperature. Decomposition of hydrogen peroxide by reaction with the Fe^{2+} site on lipoxygenase generates new $OH^{\bullet}$ radicals.

It has been shown that the ultrasonic aggregation of the porcine fumarase enzyme is caused by hydrogen peroxide and/or $HO^{\bullet}$ free radicals, which are responsible for a complex aggregation mechanism, driven by intermolecular disulfide bonds and stabilized by amyloid-like hydrophobic interactions (Barteri et al., 2004). Cysteine residues are particularly sensitive to oxidation by free radicals and, even under mild conditions, are converted to disulfide by preferential oxidation. The inactivation processes are initiated by free radicals that are formed due to cavitation. In ultrasonic inactivation of G6PDH, free radicals are reported to attack amino acid residues that are responsible for ionic interactions in the dimers and hydrogen bonding and hydrophobic interactions between the monomer pairs (Karaseva and Metelitza, 2006).

The formation of free radicals formed by ultrasonically generated cavitation has been reported to play a major role in the inactivation of urease (Tarun et al., 2003) and catalase (Potapovich et al., 2003b) by ultrasound. Surfactants, including sodium *n*-dodecyl sulfate and the reducing agent beta-mercaptoethanol, dramatically reduce aggregate size, especially for α-amylase, by destroying the intermolecular disulfide linkages (Liu et al., 2003a). Ultrasonic inactivation rate constants in the presence of low concentrations of HO- free radical scavengers, including dimethylformamide, ethanol, and mannitol, are reduced (Rachinskaya et al., 2004). Ethanol at very low concentrations (0.72 M) decreased the ultrasonic enzyme inactivation by half. It has been verified that the addition of polyvinyl alcohol to laccase had a protecting effect against enzyme inactivation (Basto et al., 2007a).

By the addition of mannitol, a strong free radical scavenger, the inactivation of trypsin by ultrasonication can be minimized (Tian et al., 2004). It is concluded that this inactivation is partially due to free radical-related reactions.

The effect of cavitation intensity on the PME inactivation by thermo-sonication has been described in the literature (Raviyan et al., 2005). Depending upon cavitation intensity over a range of 0.004–0.020 mg/l min hydrogen peroxide yield, inactivation at 61°C was increased 39- to 374-fold by thermo-sonication (20 kHz, 20 μm, 100 W), while at 72°C the increase was 3.6- to 84-fold.

10.2 Physical Effects of Sonication on Enzymes

The physical effects of ultrasonics could be due to sonocapillary effects and mechano-acoustic interactions (Grintsevich and Metelitsa, 2002). Non-thermal and non-cavitational mechanisms include effects due to radiation pressure, force, radiation torque, and acoustic streaming (Tarun et al., 2006).

Based on enzyme inactivation profiles in the presence and absence of free radical scavengers and conformational changes of the enzymes, it was concluded that horseradish peroxidase and lactoperoxidase are partially inactivated due to the mechanical effects of ultrasound (Gebicka and Gebicki, 1997a).

Inactivation of enzymes by long-time exposure to ultrasound at low temperature has been reported to be due to the splitting of low molecular weight polypeptides or individual amino acids, or due to the oxidative mechanisms (Thakur and Nelson, 1997). Ultrasonically generated shear stress can degrade polymers of high molecular mass (Price et al., 1990). Shear stresses also promote enzyme and protein denaturation (Thakur and Nelson, 1997; Vercet et al., 1997).

Under stable cavitation the oscillating resonant bubbles result in shear stress due to micro-streaming (Tarun et al., 2006). In contrast to stable cavitation, transient cavitation induces shockwaves and free radical formation as a result of the implosive collapse of cavitation bubbles.

During thermo-sonication, the substrate protection effect of pectin on thermo-resistant fraction of the orange PME is decreased (Vercet et al., 1999). The shear stress produced due to bubble implosion is believed to be responsible for the overcoming of co-solute effect and making the enzyme more vulnerable to heat. Similar effects have been reported during ultrafiltration of orange juice by Snir et al. (1995).

11 Medium-Related Factors Affecting Ultrasonic Inactivation of Enzymes

The differences in enzyme inactivation response to sonication is related to the presence of cavitation, presence of air in the medium, generation of free radicals, free radical scavengers (Grintsevich et al., 2001; Vercet et al., 2002a), differences in energy input (Basto et al., 2007b), other ultrasonics-related parameters, enzyme-related factors such as enzyme concentration, pH of the medium, and presence of co-solutes (Vercet et al., 2002a). According to the literature, only some enzymes are fully inactivated by the application of high-intensity ultrasound alone (Basto et al., 2007b; Guzey et al., 2006).

11.1 Ultrasound Application

Decimal reduction time (at 0°C) of peroxidase type VI from horseradish suspended in water, varied with ultrasonic power, sonotrode geometry, and volume of suspensions submitted to the treatment. It has been demonstrated that the influence of these variables on the decimal reduction time can be grouped by considering the ultrasound power density, i.e., the ultrasound power per unit area of tip of the probe together with the unit volume of suspension (De Gennaro et al., 1999).

Vercet et al. (1998) studied the factors affecting $OH^{\bullet}$ free radical production in aqueous solution under manothermosonication (20 kHz). They reported that free radical production increased with an increase of amplitude from 20 to 145 μm at both 70°C/200 kPa and 130°C/500 kPa. Increase in hydrostatic pressure was reported to result in an increase in free radical production at 70°C/117 μm.

The effect of increasing pressure at 130°C/117 μm was minimal on free radical production.

It has been also shown that the value of total inactivation rate constant of US inactivation of G6DPH (Rachinskaya et al., 2004) increased with the increase in ultrasonic specific power from 53 to 65 W/cm^2.

The application of external pressure (2 MPa) and temperature (60–80°C) can increase the inactivation effects of ultrasound (117 μm) on lysozyme (Manas et al., 2006). It has been reported that application of external pressure could amplify the propagation, growth, and implosion of microbubbles (Suslick, 1988). Bubble formation is also influenced by temperature.

11.2 Temperature

To improve the efficiency of ultrasonic inactivation of enzymes, heat and pressure application have been used by many research groups. Heat and ultrasonic application is known as thermo-sonication, while heat, pressure, and ultrasonic application are referred to as mano-thermo-sonication. The production of hydroxyl radicals by ultrasound is favored at low temperatures, while the ultrasonic energy input is higher (Raso et al., 1999).

It has been reported that increasing the temperature from 30° to 140°C at 117 μm amplitude showed a decrease in free radical production. Since enzyme inactivation is linked with free radical production parameters, including temperature, pressure, and ultrasound amplitude, all of these parameters could affect the inactivation of enzymes under different conditions (Vercet et al., 1998).

With an increase of temperature, the cavitation intensity decreases, and at the boiling point cavitation disappears. Mano-thermo-sonication techniques allow cavitation at or above boiling temperature under moderate pressure. This has been reported to increase the implosion intensity due to the difference between static pressure and vapor pressure inside the bubble. However, it has also been reported that the efficiency of MTS decreases with the increase in temperature. This is attributed to the decrease in the bubble collapse intensity, which is related to the increase in water vapor pressure inside the bubbles due to temperature increase (Vercet et al., 1999).

All rate constants of US inactivation of G6DPH increased with the increase of temperature (36–50°C) and pH (6.0–9.1) (Rachinskaya et al., 2004). It was also observed that the activation energy of US inactivation of G6DPH was lower than that of the thermal inactivation at enzyme concentrations between 3 and 20 nM (Rachinskaya et al., 2004).

11.3 Air

The presence of air or oxygen in the solution has been claimed to be important for ultrasonic inactivation of enzymes (Grintsevich et al., 2001). In the absence of air or in the presence of inert gases, many proteins were resistant to ultrasonic treatment.

11.4 Enzyme Concentration

Several workers have observed that enzyme inactivation can be, but are not necessarily, related to the initial enzyme concentration. The extent of enzyme inactivation of horseradish peroxidase and bovine lactose peroxidase depends upon the initial enzyme concentration (Gebicka and Gebicki, 1997a). When lower enzyme concentrations were used, higher enzyme inactivation was observed. However, in the same study, dilution of bovine liver catalase did not lead to greater inactivation by sonication at 26 kHz (15 W/cm^2; 10 mM phosphate buffer at pH 7.0).

Ultrasonic inactivation of peroxidase by high-frequency ultrasound at 2.64 MHz (1 W/cm^2; 0.1 M phosphate citrate buffer at pH 5.4; 45°C) is independent of the enzyme concentration in solution (Grintsevich and Metelitsa, 2002). However, it has been shown that inactivation increases with dilution of the solution when peroxidase was treated with low-frequency ultrasound at 27 kHz (60 W/cm2; 0.01 M acetate buffer at pH 5.2; 36°C) and under thermal inactivation (0.1 M phosphate citrate buffer at pH 5.4; 45°C). The discrepancy in behavior under these two conditions was explained by the level of disassociation in enzyme associates. Under thermal inactivation and low-frequency ultrasound at 27 kHz, the enzyme associates are assumed to be completely or partially preserved; hence, the inactivation is dependent on concentration of the enzyme.

Ultrasonic (27 kHz, 10–60 W/cm^2, 37–60°C or 2.64 MHz, 1 W/cm^2, 35–56°C) inactivation of urease also strongly depends on the urease concentration (25.4–200 nM) and pH of the aqueous solution (maximum inactivation was observed at pH 4.55). The presence of antioxidants (propyl gallate or poly(gallic acid disulfide)) reduced the amount of inactivation, preventing inactivation completely at the higher frequency (Tarun et al., 2003).

The efficiency of catalase inactivation by ultrasonically generated free radicals has been reported to be dependent on the degree of free radical association between the enzyme and the composition of the enzyme (Potapovich et al., 2003b).

11.5 pH

A pH dependency has been noted in the resistance of lipoxygenase against heat, and mano-thermo-sonification was pH dependent (Lopez and Burgos, 1995a). The synergistic effect of heat and ultrasound waves was higher at acidic pH than at neutral or alkaline pH.

The inactivation of soyabean lipoxygenase is influenced by pH (4–10), the time of exposure (0–3 h), and the frequency (0–50 KHz) of ultrasound (Thakur and Nelson, 1997). Exposure to 20 kHz of ultrasound for 3 h at pH > 5.0 had no effect on the activity of the enzyme. However, under similar conditions, the activity decreased by 70–85% when pH was lowered to 5.0 and 4.0, respectively. Lipoxygenase activity also decreased with increase in frequency of the ultrasound waves when pH was less than or equal to 5.0. Above pH 5.0, increase in frequency did not affect the enzyme activity after exposure of 1 h.

The higher inactivation of lipoxygenase at lower pH was ascribed to the formation of hydroperoxy radicals, $HO^{\bullet}$. Since pK of $HO^{\bullet}$ is about 4.7, the concentration of $HO^{\bullet}$ is expected to be higher at low pH values. The $HO^{\bullet}$ radicals undergo H^{+}-dependent reactions to form H_2O_2, thus promoting increased H_2O_2 concentration at acidic pH. H_2O_2 was considered as a very efficient inhibitor of lipoxygenase and the inactivation was higher at lower pH. The increased stability of lipoxygenase at optimum pH of about 9.0 was explained by the stability of enzymes near their optimum pH (Thakur and Nelson, 1997).

The inactivation of peroxidase is also dependent at 40°C (Grintsevich and Metelitsa, 2002). The maximum inactivation was observed at pH 4.1. The inactivation rate constant decreased with the increase of pH. It has been concluded that $HO^{\bullet}$ free radicals formed in ultrasonic cavitation fields react rapidly with functionally important amino acid residues at the active sites of this enzyme at pH values less than 5. At pH < 5 the amino acid residues of histidine, asparagine, cystine, and phenylalanine are believed to be partly protonated based on their pK_a values. Similarly, the ultrasonic inactivation of urease strongly depends on the pH of the aqueous solution and maximum inactivation is observed at pH 4.55 (Tarun et al., 2003).

11.6 Co-Solutes

Co-solutes have been reported as both promoting and inhibitory toward inactivation of enzymes in combined heat and ultrasonic treatments.

Substrate-mediated protection of enzymes against inactivation methods is ascribed to the impairment of protein unfolding due to the binding of enzymes to the substrate. The presence of pectin at 0.01%, orange juice, ascorbic acid, sucrose, glucose, or fructose in citrate buffer increased the resistance of pectin methylesterase toward inactivation by heat. However the introduction of sonication in combination with heat markedly reduced the protective effects, increasing inactivation by 25 times in the absence of a protective agent and more than 400 times in the presence of orange juice (Vercet et al., 1999).

By contrast, the presence of bovine and human serum albumin inhibited the sonication-induced inactivation of catalase. Similarly, 10% dimethyl formaldehyde, a scavenger of hydroxyl-free radicals, prevented inactivation of catalase by sonication (Potapovich et al., 2003b). Also, the inhibitory action of a natural compound with anti-radical activity (flavanolic glycoside astragalin) on ultrasonic inactivation of catalase has been reported (Kovganko et al., 2004). Tomato polygalacturonase is resistant to combined heat and sonication, which has been ascribed to the presence of co-solutes and binding of the enzyme to its substrate in tomato paste (Vercet et al., 2002b).

In skim milk the ultrasonic inactivation of alkaline phosphatase γ-glutamyltranspeptidase and lactoperoxidase was lower than that in whole milk (Villamiel and de Jong, 2000a). This difference in the effect of ultrasonics on milk enzyme inactivation was attributed to the compositional differences of

skim and whole milk. It has been demonstrated that the effect of ultrasonic waves increases with the increase in solid concentration (Berliner, 1984; Sala et al., 1995; Santamaria et al., 1952) and the decrease of enzyme concentration in the treatment medium.

11.7 Antioxidants/Free Radical Scavengers

The generation of hydroxyl radicals in aqueous systems by ultrasound is strongly frequency dependent. Generation is minimal at low frequencies, reaching a maximum at 3–400 kHz, and then reducing at higher frequencies. Temperature has less impact, but generally decreases as temperature increases. The propagation of hydroxyl radicals and consequent oxidation reactions in biological systems can be inhibited in three ways aside from frequency selection and applied sonication intensity: water soluble antioxidants inhibit free radicals in bulk solution; soluble polar antioxidants (typically phenol derivatives) inhibit free radicals at the cavitation bubble solution interface; and polar solvents, such as low molecular weight alcohols that evaporate into the body of the cavitation bubbles, reduce the temperature sufficiently to extinguish radical generation (Ashokkumar et al., 2008).

A low molecular weight antioxidant alcohol has been investigated for its capacity to reduce the inactivation of horseradish peroxidase and lactoperoxidase by ultrasonic treatments (Gebicka and Gebicki, 1997a). There was no change in the activity loss profile when the two enzymes were sonicated with *t*-butanol (0.1 M), which could scavenge all hydroxyl radicals in the bulk solution. Hence, it was concluded that hydroxyl radicals produced under experimental conditions did not contribute to the inactivation of these two enzymes. While the conclusion is substantially correct, at the ultrasonic treatment frequency employed (22 kHz), the generation of hydroxyl radicals would have been minimal (Ashokkumar et al., 2008).

A number of phenol derivative antioxidants have been investigated for their potential to scavenge free radicals in sonication systems in an investigation of the mechanism of ultrasonic inhibition of horseradish peroxidase. The use of antioxidants (polysulfides of substituted phenols) with horseradish peroxidase solutions prevented inactivation by low-frequency ultrasound (27 kHz, 60 W/cm^2 for 1 h) (Grintsevich et al., 2001). At high frequency (2.64 MHz, 1 W/cm^2) two polymer antioxidants poly(2-aminodisulfide-4-nitrophenol) and poly(gallic acid disulfide) totally inhibited ultrasonic inactivation of horseradish peroxidase in phosphate citrate buffer at pH 5.4 (Grintsevich and Metelitsa, 2002). Urease inactivation by high frequency (2.64 MHz, 1 W/cm^2, 35–56°C) sonication is also diminished by the presence of antioxidants (propyl gallate and gallic acid disulfide) (Tarun et al., 2003).

References

Agrawal, P. B., and Pandit, A. B. (2003). Isolation of alpha-glucosidase from *Saccharomyces cerevisiae*: Cell disruption and adsorption. *Biochemical Engineering Journal*, 15, 37–45.

Aliyu, M., and Hepher, M. J. (2000). Effects of ultrasound energy on degradation of cellulose material. *Ultrasonics Sonochemistry*, 7, 265–268.

Antonenko, Y. N., and Pohl, P. (1995). Steady-state nonmonotonic concentration profiles in the unstirred layers of bilayer-lipid membranes. *Biochimica et Biophysica Acta-Biomembranes*, 1235, 57–61.

Apar, D. K., Turhan, M., and Ozbek, B. (2006). Enzymatic hydrolysis of starch by using a sonifier. *Chemical Engineering Communications*, 193, 1117–1126.

Ashokkumar, M., Sunartio, D., Kentish, S., Mawson, R., Simons, L., Vilkhu, K., and Versteeg, C. (2008). Modification of food ingredients by ultrasound to improve functionality: A preliminary study on a model system. *Innovative Food Science and Emerging Technologies*, 9, 155–160.

Avivi, S., and Gedanken, A. (2002). S-S bonds are not required for the sonochemical formation proteinaceous microspheres: The case of streptavidin. *Biochemical Journal*, 366, 705–707.

Avivi, S., and Gedanken, A. (2005). The preparation of avidin microspheres using the sonochemical method and the interaction of the microspheres with biotin. *Ultrasonics Sonochemistry*, 12, 405–409.

Barteri, M., Diociaiuti, M., Pala, A., and Rotella, S. (2004). Low frequency ultrasound induces aggregation of porcine furnarase by free radicals production. *Biophysical Chemistry*, 111, 35–42.

Barton, S., Bullock, C., and Weir, D. (1996). The effects of ultrasound on the activities of some glycosidase enzymes of industrial importance. *Enzyme and Microbial Technology*, 18, 190–194.

Basto, C., Silva, C. J., Gubitz, G., and Cavaco-Paulo, A. (2007a). Stability and decolourization ability of *Trametes villosa laccase* in liquid ultrasonic fields. *Ultrasonics Sonochemistry*, 14, 355–362.

Basto, C., Tzanov, T., and Cavaco-Paulo, A. (2007b). Combined ultrasound-laccase assisted bleaching of cotton. *Ultrasonics Sonochemistry*, 14, 350–354.

Bengtsson, M., and Laurell, T. (2004). Ultrasonic agitation in microchannels. *Analytical and Bioanalytical Chemistry*, 378, 1716–1721.

Berliner, S. (1984). Application of ultrasonic processors. *International Biotechnology Laboratory*, 2, 42–49.

Bracey, E., Stenning, R. A., and Brooker, B. E. (1998). Relating the microstructure of enzyme dispersions in organic solvents to their kinetic behavior. *Enzyme and Microbial Technology*, 22, 147–151.

Cadoret, A., Conrad, A., and Block, J. C. (2002). Availability of low and high molecular weight substrates to extracellular enzymes in whole and dispersed activated sludges. *Enzyme and Microbial Technology*, 31, 179–186.

Colombie, S., Gaunand, A., and Lindet, B. (2001). Lysozyme inactivation under mechanical stirring: Effect of physical and molecular interfaces. *Enzyme and Microbial Technology*, 28, 820–826.

Cruz, R. M. S., Vieira, M. C., and Silva, C. L. M. (2006). Effect of heat and thermosonication treatments on peroxidase inactivation kinetics in watercress (*Nasturtium officinale*). *Journal of Food Engineering*, 72, 8–15.

De Gennaro, L., Cavella, S., Romano, R., and Masi, P. (1999). The use of ultrasound in food technology I: Inactivation of peroxidase by thermosonication. *Journal of Food Engineering*, 39, 401–407.

Durrschmid, M. P., Landauer, K., Simic, G., Klug, H., Keijzer, T., Trampler, F., Oudshoorn, A., Groschl, M., Muller, D., and Doblhoff-Dier, O. (2003). Comparison of fluidized bed and ultrasonic cell-retention systems for high cell density mammalian cell culture. *Biotechnology Progress*, 19, 1045–1048.

Entezari, M. H., and Petrier, C. (2004). A combination of ultrasound and oxidative enzyme: Sonobiodegradation of phenol. *Applied Catalysis B-Environmental*, 53, 257–263.

Entezari, M. H., and Petrier, C. (2005). A combination of ultrasound and oxidative enzyme: Sonoenzyme degradation of phenols in a mixture. *Ultrasonics Sonochemistry*, 12, 283–288.

Entezari, M. H., Mostafai, M., and Sarafraz-yazdi, A. (2006). A combination of ultrasound and a bio-catalyst: Removal of 2-chlorophenol from aqueous solution. *Ultrasonics Sonochemistry*, 13, 37–41.

Ertugay, M. F., Yuksel, Y., and Sengul, M. (2003). The effect of ultrasound on lactoperoxidase and alkaline phosphatase enzymes from milk. *Milchwissenschaft-Milk Science International*, 58, 593–595.

Farkade, V. D., Harrison, S. T. L., and Pandit, A. B. (2006). Improved cavitational cell disruption following pH pretreatment for the extraction of beta-galactosidase from *Kluveromyces lactis*. *Biochemical Engineering Journal*, 31, 25–30.

Feliu, J. X., Cubarsi, R., and Villaverde, A. (1998). Optimized release of recombinant proteins by ultrasonication of *E. coli* cells. *Biotechnology and Bioengineering*, 58, 536–540.

Floros, J. D., and Liang, H. H. (1994). Acoustically assisted diffusion through membranes and biomaterials. *Food Technology*, 48, 79–84.

Francis, C. W., Blinc, A., Lee, S., and Cox, C. (1995). Ultrasound accelerates transport of recombinant tissue-plasminogen activator into clots. *Ultrasound in Medicine and Biology*, 21, 419–424.

Froment, M. T., Lockridge, O., and Masson, P. (1998a). Resistance of butyrylcholinesterase to inactivation by ultrasound: Effects of ultrasound on catalytic activity and subunit association. *Biochimica et Biophysica Acta-Protein Structure and Molecular Enzymology*, 1387, 53–64.

Froment, M. T., Lockridge, O., and Masson, P. (1998b). Resistance of butyrylcholinesterase to inactivation by ultrasound: Effects of ultrasound on catalytic activity and subunit association 143. *Biochimica et Biophysica Acta-Protein Structure and Molecular Enzymology*, 1387, 53–64.

Gama, F. M., Carvalho, M. G., Figueiredo, M. M., and Mota, M. (1997). Comparative study of cellulose fragmentation by enzymes and ultrasound. *Enzyme and Microbial Technology*, 20, 12–17.

Gebicka, L., and Gebicki, J. L. (1997a). The effect of ultrasound on heme enzymes in aqueous solution. *Journal of Enzyme Inhibition*, 12, 133–141.

Gebicka, L., and Gebicki, J. L. (1997b). The effect of ultrasound on heme enzymes in aqueous solution 152. *Journal of Enzyme Inhibition*, 12, 133–141.

Grintsevich, E. E., and Metelitsa, D. I. (2002). Kinetics of ultrasonic inactivation of peroxidase in aqueous solutions. *Russian Journal of Physical Chemistry*, 76, 1368–(1373).

Grintsevich, E. E., Adzerikho, I. E., Mrochek, A. G., and Metelitza, D. I. (2001). Polydisulfides of substituted phenols as effective protectors of peroxidase against inactivation by ultrasonic cavitation. *Biochemistry-Moscow*, 66, 740–746.

Guzey, D., Gulseren, I., Bruce, B., and Weiss, J. (2006). Interfacial properties and structural conformation of thermosonicated bovine serum albumin. *Food Hydrocolloids*, 20, 669–677.

Imai, M., Ikari, K., and Suzuki, I. (2004). High-performance hydrolysis of cellulose using mixed cellulase species and ultrasonication pretreatment. *Biochemical Engineering Journal*, 17, 79–83.

Jaspe, A., and Sanjose, C. (1999). Extracellular enzyme production by *Pseudomonas fluorescens* in homogenized cold milk. *Milchwissenschaft-Milk Science International*, 54, 493–495.

Jiang, B., and Xiang, M. (1992). Immobilization of enzymes on polymers modified by ultrasonic irradiation. *European Polymer Journal*, 28, 827–830.

Jie, M. S. F. L., and Syedrahmatullah, M. S. K. (1995). Enzymatic-hydrolysis of long-chain N-heterocyclic fatty esters. *Lipids*, 30, 995–999.

Johnson C. P., Tang, H.-Y., Carag, C., Speicher, D. W., and Discher, D. E. (2007). Forced unfolding of proteins within cells. *Science*, 317, 663–666.

Kagiya, G., Ogawa, R., Tabuchi, Y., Feril, L. B., Nozaki, T., Fukuda, S., Yamamoto, K., and Kondo, T. (2006). Expression of heme oxygenase-1 due to intracellular reactive oxygen species induced by ultrasound. *Ultrasonics Sonochemistry*, 13, 388–396.

Karaseva, E., and Metelitza, D. I. (2006). Stabilization of glucoso-6-phosphate dehydrogenase by its substrate and cofactor in an ultrasonic field. *Russian Journal of Bioorganic Chemistry*, 32, 436–443.

Kost, J. (1993). Ultrasound induced delivery of peptides. *Journal of Controlled Release*, 24, 247–255.

Kotronarou, A., and Hoffmann, M. R. (1995). The chemical effects of collapsing cavitation bubbles – mathematical-modeling. *Aquatic Chemistry*, 244, 233–251.

Kovganko, N. V., Kashkan, Z. N., Krivenok, S. N., Potapovich, M. V., Eremin, A. N., and Metelitsa, D. I. (2004). Bioactive compounds in the Flora of Belarus. 2. Astragalin, an effective protector of catalase from ultrasonic inactivation in aqueous solutions. *Chemistry of Natural Compounds*, 40, 71–74.

Li, C. Z., Yoshimoto, M., Ogata, H., Tsukuda, N., Fukunaga, K., and Nakao, K. (2005). Effects of ultrasonic intensity and reactor scale on kinetics of enzymatic saccharification of various waste papers in continuously irradiated stirred tanks. *Ultrasonics Sonochemistry*, 12, 373–384.

Li, R., Ziola, B., and King, J. (2000). Purification and characterization of formate dehydrogenase from *Arabidopsis thaliana*. *Journal of Plant Physiology*, 157, 161–167.

Lin, L. D., and Wu, J. Y. (2002). Enhancement of shikonin production in single- and two-phase suspension cultures of *Lithospermum erythrorhizon* cells using low-energy ultrasound. *Biotechnology and Bioengineering*, 78, 81–88.

Lin, G. L., Liu, H. C., and Liu, S. H. (1995). Azeotropic distillation- and ultrasound-promoted lipase-catalyzed reactions. *Journal of the Chinese Chemical Society*, 42, 957–961.

Liu, H. L., Chen, W. J., and Chou, S. N. (2003a). Mechanisms of aggregation of alpha- and beta-amylases in aqueous dispersions. *Colloids and Surfaces B-Biointerfaces*, 28, 215–225.

Liu, Y. Y., Yoshikoshi, A., Wang, B. C., and Sakanishi, A. (2003b). Influence of ultrasonic stimulation on the growth and proliferation of *Oryza sativa Nipponbare callus* cells. *Colloids and Surfaces B-Biointerfaces*, 27, 287–293.

Lopez, P., and Burgos, J. (1995a). Peroxidase stability and reactivation after heat-treatment and manothermosonication. *Journal of Food Science*, 60, 451–455.

Lopez, P., and Burgos, J. (1995b). Lipoxygenase inactivation by manothermosonication – effects of sonication physical parameters, Ph, Kcl, sugars, glycerol, and enzyme concentration. *Journal of Agricultural and Food Chemistry*, 43, 620–625.

Lopez, P., Vercet, A., Sanchez, A. C., and Burgos, J. (1998). Inactivation of tomato pectic enzymes by manothermosonication. *Zeitschrift fur Lebensmittel-Untersuchung Und-Forschung A-Food Research and Technology*, 207, 249–252.

Lopez, P., Sala, F. J., Delafuente, J. L., Condon, S., Raso, J., and Burgos, J. (1994). Inactivation of peroxidase, lipoxygenase, and polyphenol oxidase by manothermosonication. *Journal of Agricultural and Food Chemistry*, 42, 252–256.

Mahinpour, R., and Sarbolouki, M. N. (1998). Enhancing enzymatic hydrolysis of cellulose by ultrasonic pretreatment. *Iranian Journal of Chemistry and Chemical Engineering-International English Edition*, 17, 8–13.

Manas, P., Munoz, B., Sanz, D., and Condon, S. (2006). Inactivation of lysozyme by ultrasonic waves under pressure at different temperatures. *Enzyme and Microbial Technology*, 39, 1177–1182.

Martin, D., and Schlimme, E. (2002). Influence of technological measures on the activity behaviour of the milk enzyme adenosine deaminase (ADA, EC 3.5.4.4). *Kieler Milchwirtschaftliche Forschungsberichte*, 54, 305–315.

Miller, D. L., and Thomas, R. M. (1994). Cavitation dosimetry – estimates for single bubbles in a rotating-tube exposure system. *Ultrasound in Medicine and Biology*, 20, 187–193.

Nikolaev, A. L., Chicherin, D. S., Sinani, V. A., Noa, O. V., Melikhov, I. V., and Plate, N. A. (2001). Catalytic activity of trypsin immobilized into a polymeric thermosensitive hydrogel. *Polymer Science Series A*, 43, 21–25.

Oulahal-Lagsir, O., Martial-Gros, A., Bonneau, M., and Blum, L. J. (2003). "Escherichia coli-milk" biofilm removal from stainless steel surfaces: Synergism between ultrasonic waves and enzymes. *Biofouling*, 19, 159–168.

Ovsianko, S. L., Chernyavsky, E. A., Minchenya, V. T., Adzerikho, I. E., and Shkumatov, V. M. (2005a). Effect of ultrasound on activation of serine proteases precursors. *Ultrasonics Sonochemistry*, 12, 219–223.

Ovsianko, S. L., Chernyavsky, E. A., Minchenya, V. T., Adzerikho, I. E., and Shumatov, V. M. (2005b). Effect of ultrasound on activation of serine proteases precursors. *Ultrasonics Sonochemistry*, 12, 219–223.

Ozbek, B., Kutlu, O., and Ulgen (2000). The stability of enzymes after sonication. *Process Biochemistry*, 35, 1037–1043.

Persike, D. S., Bonfim, T. M. B., Santos, M. H. R., Lyng, S. M. O., Chiarello, M. D., and Fontana, J. D. (2002). Invertase and urease activities in the carotenogenic yeast *Xanthophyllomyces dendrorhous* (formerly *Phaffia rhodozyma*). *Bioresource Technology*, 82, 79–85.

Popa, M., Ionescu, P. C., and Vasiliuoprea, C. (1994). Mechanochemical Complexation of Micronized cellulose with Co(3+) ions by ultrasonic treatment in order to obtain macromolecular carriers for invertase immobilization. *Cellulose Chemistry and Technology*, 28, 129–141.

Potapovich, M. V., Adzerikho, I. E., Eremin, A. N., and Metelitsa, D. I. (2003a). Kinetics of inactivation of catalase in solutions under high- and low-frequency ultrasound. *Russian Journal of Physical Chemistry*, 77, 299–306.

Potapovich, M. V., Eremin, A. N., and Metelitza, D. I. (2003b). Kinetics of catalase inactivation induced by ultrasonic cavitation. *Applied Biochemistry and Microbiology*, 39, 140–146.

Potapovich, M. V., Eryomin, A. N., Artzukevich, I. M., Chernikevich, I. P., and Metelitza, D. I. (2001). Isolation, purification, and characterization of catalase from the methylotrophic yeast *Pichia pastoris*. *Biochemistry-Moscow*, 66, 646–657.

Potapovich, M. V., Eryomin, A. N., and Metelitza, D. I. (2005). Ultrasonic and thermal inactivation of catalases from bovine liver, the methylotrophic yeast *Pichia pastoris*, and the fungus *Penicillium piceum*. *Applied Biochemistry and Microbiology*, 41, 529–537.

Price, G. J., Daw, M. R., Newcombe, N. J., and Smith, P. F. (1990). Polymerization and copolymerization using high-intensity ultrasound. *British Polymer Journal*, 23, 63–66.

Racay, P., and Kollarova, M. (1996). Purification and partial characterization of Ca2+-dependent ribonucleotide reductase from *Streptomyces aureofaciens*. *Biochemistry and Molecular Biology International*, 38, 493–500.

Rachinskaya, Z. V., Karasyova, E. I., and Metelitza, D. I. (2004). Inactivation of glucose-6-phosphate dehydrogenase in solution by low- and high-frequency ultrasound. *Applied Biochemistry and Microbiology*, 40, 120–128.

Ramachandran, K., Al-Zuhair, S., Fong, C. S., and Gak, C. (2006). Kinetic study on hydrolysis of oils by lipase with ultrasonic emulsification. *Biochemical Engineering Journal*, 32, 19–24.

Raso, J., Manas, P., Pagan, R., and Sala, F. J. (1999). Influence of different factors on the output power transferred into medium by ultrasound. *Ultrasonics Sonochemistry*, 5, 157–162.

Raviyan, P., Zhang, Z., and Feng, H. (2005). Ultrasonication for tomato pectinmethylesterase inactivation: Effect of cavitation intensity and temperature on inactivation. *Journal of Food Engineering*, 70, 189–196.

Rief, M., Gautel, F., Oesterhelt, F., Fernandez, J. M., and Gaub, H. E. (1997). Reversible unfolding of individual titin immunoglobulin domains by atomic force microscopy. *Science*, 276, 1109–1112.

Riesz, P., and Kondo, T. (1992). Free-radical formation induced by ultrasound and its biological implications. *Free Radical Biology and Medicine*, 13, 247–270.

Roncales, P., Cena, P., Beltran, J. A., and Jaime, I. (1993). Ultrasonication of lamb skeletal-muscle fibers enhances postmortem proteolysis. *Zeitschrift fur Lebensmittel-Untersuchung Und-Forschung*, 196, 339–342.

Rosenthal, I., Sostaric, J. Z., and Riesz, P. (2004). Sonodynamic therapy – a review of the synergistic effects of drugs and ultrasound. *Ultrasonics Sonochemistry*, 11, 349–363.

Sakakibara, M., Wang, D., Takahashi, R., Takahashi, K., and Mori, S. (1996). Influence of ultrasound irradiation on hydrolysis of sucrose catalyzed by invertase. *Enzyme and Microbial Technology*, 18, 444–448.

Sala, F. J., Burgos, J., Condon, S., Lopez-Buesa, P., and Raso, J. (1995). Effect of heat and ultrasound on microorganisms and enzymes. In: Gold, G. (ed.), *New methods of food preservation*, pp. 167–204. Glascow, Blackie.

Santamaria, L., Castelani, A., and Levi, F. A. (1952). Haluronidase inactivation by ultrasonic waves and its mechanism. *Enzymologia*, 15, 285–294.

Schmidt, P., Rosenfeld, E., Millner, R., Czerner, R., and Schellenberger, A. (1987). Theoretical and experimental studies on the influence of ultrasound on immobilized enzymes. *Biotechnology and Bioengineering*, 30, 928–935.

Sener, N., Apar, D. K., and Ozbek, B. (2006). A modelling study on milk lactose hydrolysis and beta-galactosidase stability under sonication. *Process Biochemistry*, 41, 1493–(1500).

Sinisterra, J. V. (1992). Application of ultrasound to biotechnology – An overview. *Ultrasonics*, 30, 180–185.

Siwek, M., Noubar, A. B., Bergmann, J., Niemeyer, B., and Galunsky, B. (2006). Enhancement of enzymatic digestion of Antarctic krill and successive extraction of selenium organic compounds by ultrasound treatment. *Analytical and Bioanalytical Chemistry*, 384, 244–249.

Snir, R., Koehler, P. E., Sims, K. A., and Wicker, L. (1995). Ph and cations influence permeability of marsh grapefruit pectinesterase on polysulfone ultrafiltration membrane. *Journal of Agricultural and Food Chemistry*, 43, 1157–1162.

Sotomayor, M., and Schulten, K. (2007). A single-molecule experiments in vitro and silico. *Science*, 316, 1144–1148.

Suslick, K. S. (1988). Only the smile is left. *Nature*, 334, 375–376.

Suslick, K. S., and Grinstaff, M. W. (1990). Protein microencapsulation of nonaqueous liquids. *Journal of the American Chemical Society*, 112, 7807–7809.

Tarun, E. I., Adzerikho, I. E., and Metelitsa, D. I. (2003). Inactivation of urease under the action of ultrasonically induced cavitation. *Russian Journal of Physical Chemistry*, 77, 468–476.

Tarun, E. I., Kurchenko, V. P., and Metelitza, D. I. (2006). Flavonoids as effective protectors of urease from ultrasonic inactivation in solutions. *Russian Journal of Bioorganic Chemistry*, 32, 352–359.

Tauber, M. M., Guebitz, G. M., and Rehorek, A. (2005). Degradation of azo dyes by laccase and ultrasound treatment. *Applied and Environmental Microbiology*, 71, 2600–2607.

Thakur, B. R., and Nelson, P. E. (1997). Inactivation of lipoxygenase in whole soy flour suspension by ultrasonic cavitation. *Nahrung-Food*, 41, 299–301.

Tian, Z. M., Kang, J. Q., Wang, S. P., and Wan, M. X. (2004). Effect of ultrasound and additives on the function and structure of trypsin. *Ultrasonics Sonochemistry*, 11, 399–404.

Tsaih, M. L., Tseng, L. Z., and Chen, R. H. (2004). Effects of removing small fragments with ultrafiltration treatment and ultrasonic conditions on the degradation kinetics of chitosan. *Polymer Degradation and Stability*, 86, 25–32.

vanWyk, J. P. H. (1997). Cellulose hydrolysis and cellulase adsorption after pretreatment of cellulose materials. *Biotechnology Techniques*, 11, 443–445.

Vargas, L. H. M., Piao, A. C. S., Domingos, R. N., and Carmona, E. C. (2004). Ultrasound effects on invertase from *Aspergillus niger*. *World Journal of Microbiology and Biotechnology*, 20, 137–142.

Vercet, A., Burgos, J., and Lopez-Buesa, P. (2002a). Manothermosonication of heat-resistant lipase and protease from *Pseudomonas fluorescens*: Effect of pH and sonication parameters. *Journal of Dairy Research*, 69, 243–254.

Vercet, A., Lopez, P., and Burgos, J. (1999). Inactivation of heat-resistant pectinmethylesterase from orange by manothermosonication. *Journal of Agricultural and Food Chemistry*, 47, 432–437.

Vercet, A., Lopez, P., and Burgos, J. (1998). Free radical production by manothermosonication. *Ultrasonics*, 36, 615–618.

Vercet, A., Lopez, P., and Burgos, J. (1997). Inactivation of heat-resistant lipase and protease from Pseudomonas fluorescens by manothermosonication. *Journal of Dairy Science*, 80, 29–36.

Vercet, A., Sanchez, C., Burgos, J., Montanes, L., and Buesa, P. L. (2002b). The effects of manothermosonication on tomato pectic enzymes and tomato paste rheological properties. *Journal of Food Engineering*, 53, 273–278.

Villamiel, M., and de Jong, P. (2000a). Influence of high-intensity ultrasound and heat treatment in continuous flow on fat, proteins, and native enzymes of milk. *Journal of Agricultural and Food Chemistry*, 48, 472–478.

Villamiel, M., and de Jong, P. (2000b). Influence of high-intensity ultrasound and heat treatment in continuous flow on fat, proteins, and native enzymes of milk 132. *Journal of Agricultural and Food Chemistry*, 48, 472–478.

Vulfson, E. N., Sarney, D. B., and Law, B. A. (1991). Enhancement of subtilisin-catalyzed interesterification in organic-solvents by ultrasound irradiation. *Enzyme and Microbial Technology*, 13, 123–126.

Wong, M., and Suslick, K. S. (1995). Hemoglobin microbubbles. *Abstracts of Papers of the American Chemical Society*, 210, 587-INOR.

Wood, B. E., Aldrich, H. C., and Ingram, L. O. (1997). Ultrasound stimulates ethanol production during the simultaneous saccharification and fermentation of mixed waste office paper. *Biotechnology Progress*, 13, 232–237.

Wu, J. (2007). Shear stress in cells generated by ultrasound. *Progress in Biophysics and Molecular Biology*, 93, 363–373.

Wu, J., and Lin, L. (2003). Enhancement of taxol production and release in *Taxus chinensis* cell cultures by ultrasound, methyl jasmonate and in situ solvent extraction. *Applied Microbiology and Biotechnology*, 62, 151–155.

Wu, J. Y., and Lin, L. D. (2002). Ultrasound-induced stress responses of Panax ginseng cells: Enzymatic browning and phenolics production. *Biotechnology Progress*, 18, 862–866.

Wu, J. Y., and Ge, X. C. (2004). Oxidative burst, jasmonic acid biosynthesis, and taxol production induced by low-energy ultrasound in *Taxus chinensis* cell suspension cultures. *Biotechnology and Bioengineering*, 85, 714–721.

Xiao, Y. M., Wu, Q., Cai, Y., and Lin, X. F. (2005). Ultrasound-accelerated enzymatic synthesis of sugar esters in nonaqueous solvents. *Carbohydrate Research*, 340, 2097–2103.

Xie, Y. M., Wu, H., and Lai, Y. M. (2002). Deinking of colored offset newsprint with enzyme treatment in cooperation with ultrasonic wave. *Cellulose Chemistry and Technology*, 36, 285–293.

Yachmenev, V. G., Bertoniere, N. R., and Blanchard, E. J. (2002). Intensification of the bioprocessing of cotton textiles by combined enzyme/ultrasound treatment. *Journal of Chemical Technology and Biotechnology*, 77, 559–567.

Yachmenev, V. G., Blanchard, E. J., and Lambert, A. H. (1998). Use of ultrasonic energy in the enzymatic treatment of cotton fabric. *Industrial and Engineering Chemistry Research*, 37, 3919–3923.

Yachmenev, V. G., Blanchard, E. J., and Lambert, A. H. (1999). Study of the influence of ultrasound on enzymatic treatment of cotton fabric. *Textile Chemist and Colorist and American Dyestuff Reporter*, 1, 47–51.

Yachmenev, V. G., Blanchard, E. J., and Lambert, A. H. (2004). Use of ultrasonic energy for intensification of the bio-preparation of greige cotton. *Ultrasonics*, 42, 87–91.

Zhong, M. T., Ming, X. W., Su, P. W., and Ju, Q. K. (2004). Effects of ultrasound and additives on the function and structure of trypsin. *Ultrasonics Sonochemistry*, 11, 399–404.

Chapter 15
Production of Nanomaterials Using Ultrasonic Cavitation – A Simple, Energy Efficient and Technological Approach

Sivakumar Manickam and Rohit Kumar Rana

1 Introduction

Much effort is currently being devoted to the study of nanomaterials including metallic, inorganic, and polymeric material, due to their wide variety of applications. Nanomaterial science is defined as the creation of functional materials through control of matter on the nanometer length scale, which is normally 1–100 nm and which then exploits novel properties such as physical, chemical, biological, optical, or electronical that can be observed at that length scale. In short, nanoparticles have generated a large research effort because of their properties, which differ markedly from those of their bulk counterpart. It is well known that the properties or behavior of materials are size dependent and so with a change in size, totally different behavior of materials may be obtained. Such nanomaterials hold technological potential in various applications, which include magnetic data storage, ferrofluids, medical imaging, drug targeting, and catalysis, and thus their development is essential in this nanotechnological world.

The growing interest in nanostructured materials calls for development of processing techniques that allow for the tailoring of specific features of nanometer size. Conventionally, a wide variety of techniques are followed for fabrication of these nanomaterials, including ball milling, hydrothermal synthesis and co-precipitation. In order to address and overcome the constraints inherent in these methods, new and prominent methods have been developed such as sol–gel, microwave plasma, co-precipitation in reverse and normal micelles. Recently, with the advent of ultrasonic cavitation as an alternative processing method using reactants in the liquid state, novel processing strategies and therefore materials have emerged. Although cavitation and its effects have been studied for more than 100 years, the interest in utilization of this technique in nanomaterials was born very recently, and this has resulted in a dramatic increase in the depth and breadth of research. The importance

S. Manickam (✉)
Department of Chemical and Environmental Engineering, Faculty of Engineering, University of Nottingham (Malaysia Campus), Semenyih, Selangor, Malaysia
e-mail: sivakumar.manickam@nottingham.edu.my

H. Feng et al. (eds.), *Ultrasound Technologies for Food and Bioprocessing*, Food Engineering Series, DOI 10.1007/978-1-4419-7472-3_15,
© Springer Science+Business Media, LLC 2011

of cavitation has been demonstrated not only for synthesis, but also to control shapes and morphologies of nanomaterials and processing techniques such as encapsulation, coating, and nanocomposites. Due to various advantages, cavitation is widely used in nanomaterial generation. Some inherent advantages are the following:

1. results in a rapid reaction rate,
2. reactions can be carried out under milder conditions,
3. promotion of heterogeneous reactions involving multicomponents, mainly through increased mass transport and thermal effects,
4. avoidance of the use of toxic reagents and complicated organometallic precursors,
5. generation of stable colloidal dispersion of nanoparticles,
6. produced nanoparticles sometimes have unusual shape and interesting properties,
7. nanomaterials that are difficult if not impossible to produce by other conventional ways can be prepared, and
8. technique is highly energy efficient.

Cavitation as an approach for synthesizing a variety of compounds under milder conditions is already widespread in materials technology. The major advantage of this new method is that it affords a reliable and facile route for the control of both the synthetic process and nanostructure for producing advanced materials. Also, this process provides chemical homogeneity and reactivity through atomic-level mixing within the precursor system, and phase pure crystalline materials can be prepared by annealing at reduced temperatures. Of the four cavitational techniques, ultrasonic cavitation and hydrodynamic processes are useful as far as chemical processing is concerned. The other two cavitational techniques, particle cavitation and optic cavitation, are less used. Over the last few years, the ultrasonic cavitation technique has started to catch on in the materials science community as a way to prepare new materials with interesting properties. Nanostructured metals, alloys, oxides, carbides, and sulfides, nanometer colloids, or nanostructure-supported catalysts can all be prepared by using high-intensity ultrasound (Suslick and Price, 1999). In this chapter, various advanced nanomaterials obtained using this novel technology are discussed, along with how this technology is effectively utilized in a way that allows to produce particles with characteristics such as uniform particle size, crystalline structure, and desired morphologies. The ability to achieve the formation of nanomaterials utilizing the cavitation approach by avoiding the usage of otherwise necessarily difficult conditions not only provides a simple route, but also opens a new avenue to design and engineer original and novel nanomaterials. We summarize such sonochemical strategies that have been successfully used to engineer various nanostructured materials. Many of the contributions related to ultrasonic cavitation for the synthesis of nanomaterials are from the research groups of Prof. Gedanken (Israel), Prof. Suslick (USA), Prof. Maeda (Japan), and Prof. Grieser (Australia). Schematically, the ultrasound-mediated synthesis of various nanomaterials and involved processes is illustrated in Fig. 15.1. Practically, each of these processes can be influenced by ultrasound.

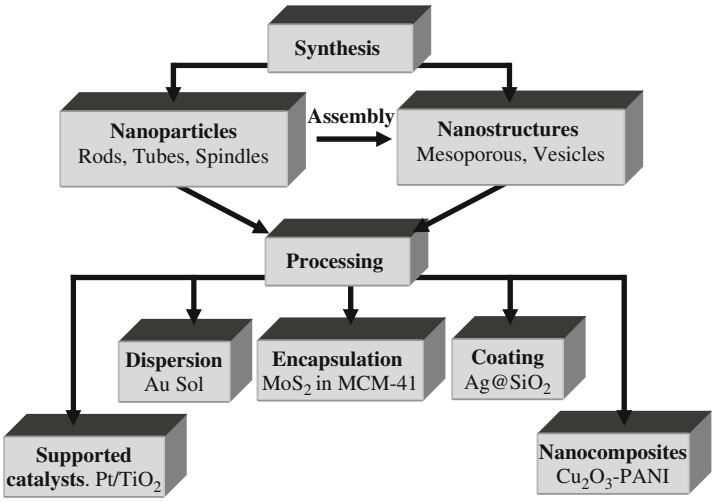

Fig. 15.1 Use of ultrasound in nanomaterials synthesis and processing. Each *arrow* represents a step where ultrasound can have a role

2 Ultrasonic Cavitation

2.1 Generation

There are two types of ultrasonic or sonochemical reactors used for generating nanomaterials. The first type is the frequently used ultrasound horn and the second one is the standing wave sonochemical reactor, as shown in Fig. 15.2a and b, respectively.

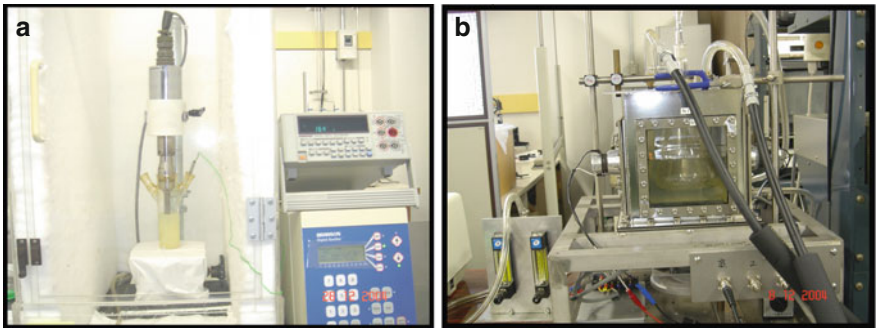

Fig. 15.2 (**a**) Ultrasonic horn (Branson Digital Sonifier, 20 kHz) and (**b**) standing wave sonochemical reactor (164 kHz)

2.2 Driving Force Responsible for Nanoparticle Formation

Although ultrasonic cavitation results in the generation of nanomaterials, the main question concerns the force that is responsible for the formation of nanoparticles

when ultrasound is passed inside the solution having the reactants. Bubbles are formed in the liquid due to the passage of ultrasound waves and with the formation of bubbles there are three possible sonochemical reaction regions; The first region is the inner environment or core of the bubble where elevated temperature and pressure conditions are generated due to bubble collapse. The second region is the interfacial region, which is between the core of the bubble and the surrounding liquid. Here, the conditions are lower than that of the core of the bubble and the temperature of this region is about 1,900 K, but this is still high enough to induce a chemical reaction. The third region is the bulk liquid which is at ambient conditions. These three regions are shown schematically in Fig. 15.3.

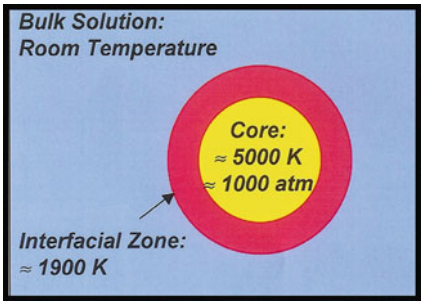

Fig. 15.3 Sonochemical reaction regions

Considering the first case, i.e., when the solute or the precursor is highly volatile, then it will be able to enter into the bubble. Once it enters, it will be exposed to the intense conditions of the bubble when it collapses. It has been found that the bubble collapse occurs in less than a nanosecond and thus the generated heat conditions accompany very high cooling rates which are in excess of 10^{11} K/s. These very high cooling rates hinder the organization as well as the crystallization of the formed products and thereby result in the formation of amorphous products. While the explanation for the formation of amorphous nature of the products is well understood, the reason for the formation of nanostructured products is not clear. One possible explanation is that the fast kinetics due to fast intense collapse conditions of the bubble restricts the growth of the nuclei, which may result in the nanostructured form. Considering the second case, when the precursor is non-volatile or when it is not able to enter into the bubble, then the reaction occurs in the interfacial region. In this case, the products are either nanoamorphous or nanocrystalline, depending upon the temperature of this region. Formation of nanoparticles is also possible in the third region, but the formation rate is low (Gedanken, 2004).

3 Preparation of Nanomaterials

Ultrasonic cavitation is highly versatile in the preparation of various inorganic nanomaterials. Most of the initial works used volatile organometallic precursors, which are generally known to undergo thermal decomposition such as in chemical

vapor deposition processes to generate fine particles (Suslick, 1998). When irradiated with high-intensity ultrasound in low-volatility solvents under argon, these volatile organometallic precursors decompose sonochemically and produce high surface area solids consisting of amorphous or agglomerates of nanometer clusters. For example, if the iron or cobalt carbonyls are subjected to ultrasound in high-boiling hydrocarbons or alkane solvents, respective nanostructured metal powders are obtained, whereas in case of Mo and W containing carbonyls, metal carbides are produced. So, selection of a proper precursor to achieve a desired material is very important in sonochemistry. If the precursors are subjected to ultrasound in the presence of stabilizer, e.g., polyvinylpyrrolidone, stable nanophase colloids could be obtained. In presence of oxide supports such as silica and alumina, supported metal catalysts could be formed (Suslick et al., 1995, 1996).

3.1 Metal Nanoparticles

Metal nanoparticles are of considerable interest in industrial powder technology, metallurgy, and catalysis. Moreover, ultrafine particles of noble metals have attracted particular interest because of their increased number of edges, corners, and faces, which gives them a high surface/volume ratio and therefore they are useful in various fields of chemistry. Suslick et al. (1996) first reported the sonochemical preparation of a variety of metallic nanoparticles. Following are some of the important metal nanoparticles prepared by this technique.

3.1.1 Fe Colloids

Suslick et al. (1996) found that ultrasonic cavitation in the presence of a suitable stabilizer could prevent agglomeration and permitting the isolation of stable nanocolloids. For example, iron nanoparticles dispersed in polyvinylpyrrolidone (PVP) matrix or stabilized by the adsorption of oleic acid have been synthesized by the sonochemical decomposition of $Fe(CO)_5$. By using PVP, it has been observed that the formed Fe nanoparticles have a relatively narrow size distribution from 3 to 8 nm, whereas even more uniform distribution of Fe particles has been obtained by using oleic acid (Fig. 15.4). This work has also been extended to colloids of other metals and to alloys of two or more metals, simply by using multiple volatile precursors. For example, nanostructured Fe/Co alloys have been prepared. In addition, controlled reaction with oxygen or other oxidants also permitted the formation of transition metal oxide colloids.

3.1.2 Co Nanoparticles

Erasmus and van Steen (2007) obtained cobalt nanoparticles of 5 nm using a solution of $Co(CO)_3(NO)$ in *n*-decane. Addition of silica powder or oleic acid to the solution in order to stabilize the particles resulted in a decrease in the size of the cobalt particles. Changing the concentration of the precursor in the solution had

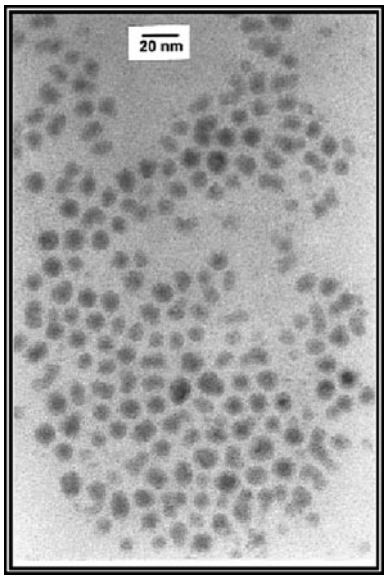

Fig. 15.4 Transmission electron micrograph of sonochemically prepared iron colloid particles (with average particle size of 8 nm) stabilized by oleic acid

no observable effect on the particle size distribution, indicating that particle size is not determined by the amount of the precursor vapor present within the bubble. Instead, it was thought that a single cavitation event results in the formation of many particles.

3.1.3 Noble Metal Nanoparticles

Okitsu et al. (1996) sonochemically prepared metal particles such as Ag, Pd, Au, Pt, and Rh in nanometer size with a fairly narrow distribution. For example, Pd particles of about 5 nm were obtained using 1.0 mM Pd(II) in polyethylene glycol monostearate solution. The formation of nanoparticles due to ultrasound has been accounted for through three different reduction pathways: (i) reduction by H atoms; (ii) reduction by secondary reducing radicals formed by hydrogen abstraction from organic additives with OH radicals and H atoms; (iii) reduction by radicals formed from pyrolysis of the additives at the interfacial region between cavitation bubbles and the bulk solution. The reduction of Ag(I) and Pt(II) mainly proceeds through the reaction pathway (ii). In the cases of Pd(II) and Au(III), the reaction pathway (iii) is predominant. However, the reduction of Rh(III) was not achieved under the same conditions, but, with the addition of sodium formate, reduction occurred resulting in the formation of Rh nanoparticles.

Mizukoshi et al. (1999) used SDS (sodium dodecyl sulfate) as an additive for the synthesis of platinum nanoparticles. The particles formed were stable and relatively monodispersed with an average size of 2.6 nm.

Further, Mizukoshi et al. (2001) extended the study in investigating the effect of various other surfactants such as sodium dodecylbenzenesulfonate (DBS) as

anionic, polyethylene glycol monostearate (PEG-MS) as non-ionic, and dodecyltrimethylammonium chloride (DTAC) and bromide (DTAB) as cationic surfactants on the formation of Pt nanoparticles. The average diameter (1.0 nm) of platinum particles prepared from the system of PEG-MS is smaller than those from the aqueous solution of anionic surfactant SDS (3.0 nm) and DBS (3.0 nm). It was concluded that the surfactants scarcely influenced acoustic cavitation, but they had a definite role in the reduction process producing Pt nanoparticles.

Pd and Pt nanoparticles have also been prepared by the sonochemical reduction of aqueous solutions containing metal salts of H_2PtCl_6 or K_2PdCl_4 by Fujimoto et al. (2001). They investigated in detail the effect of different gases on formed particle size distribution. For example, average diameters of the Pd particles prepared under Ar (Pd/Ar) and N_2 (Pd/N_2) were found to be 3.6 ± 0.7 nm and 2.0 ± 0.3 nm, respectively. Thus, smaller and narrower distribution of particle size was observed for Pd particles prepared under a N_2 atmosphere, whereas for Pt, a Xe atmosphere was good. The results suggested that the particle formation rates for Pd and Pt are different and are controlled by the hot-spot temperature depending on the dissolved gases (Ar or N_2).

Nemamcha et al. (2006) prepared stable palladium nanoparticles (3–6 nm) using palladium (II) nitrate solution with ethylene glycol and PVP as reducing and stabilizing agents, respectively. The following reaction mechanism has been proposed by the authors for the sonochemical reduction of Pd (II) to yield Pd nanoparticles.

$$H_2O \xrightarrow{\text{Ultrasonic irradiation}} {}^{\bullet}OH + {}^{\bullet}H \tag{15.1}$$

$$HOCH_2CH_2OH + {}^{\bullet}OH\,({}^{\bullet}H) \longrightarrow HOCH_2C^{\bullet}\,HOH + H_2O(H_2) \tag{15.2}$$

$$n\text{Pd(II)} + 2n\text{HOCH}_2\text{C}\bullet\,\text{HOH} \longrightarrow n\text{Pd(0)} + 2n\text{HOCH}_2\text{CHO} + 2n\text{H}^+ \tag{15.3}$$

The authors observed that at the lowest Pd(II)/PVP molar ratio, the colloid was formed by a high number of stabilized nanoparticles with small diameter, whereas for higher Pd(II)/PVP molar ratios, the number of stabilized nanoparticles decreases and the mean particle diameter increases slightly, but with an increase in global particle surface.

Significant enhancement in the rate of formation of Pt nanoparticles in the presence of aliphatic alcohols as additives has been observed by Caruso et al. (2000). With increasing alkyl chain length, and hence hydrophobicity of the alcohol, the reduction was more efficient. This was explained by assuming that alcohol molecules adsorbed at the bubble surface scavenge the primary radicals produced within the bubble, forming secondary radicals which then go on to react with Pt(IV) in bulk solution. Since the surface active nature of alcohols depends on their hydrophobicity, longer chain lengths would allow more of them to adsorb at the bubble/solution interface, leading to the formation of more secondary radicals to reduce Pt(IV) ions.

Interestingly, the sonochemical reduction of tetrachloropalladate (II) in the presence of alcohols as organic additives resulted in the formation of Pd nanoparticles

with interstitial carbon (PdC*x*) (Okitsu et al., 1997). The organic radicals formed during sonication were suggested to be catalytically dissociated on the Pd surface, forming interstitial carbon atoms. In this technique the number of interstitial carbon atoms in the Pd lattice could be controlled by changing the concentration of tetrachloropalladate (II) precursor as well as the type of organic additives.

3.1.4 Au Nanoparticles

Nagata et al. (1996) reduced aqueous solutions of $NaAuCl_4$ to form gold nanoparticles. They also studied the rate of formation of gold nanoparticles in the presence of certain organic additives such as surfactants, water-soluble polymers, and aliphatic alcohols and ketones. The rates of formation of gold nanoparticles from 1 mM Au(III) ions in pure water were 3 μM/min under argon atmosphere and approximately zero under air, and in solutions containing additives the rates were 9–133 pM/min under argon and 8–40 μM/min under air. Usage of surfactants stabilized the particles in the colloidal state for more than several months. The rates of formation of both hydrogen atoms and hydroxyl radicals were estimated to be equal to 25 μM/min in the sonolysis of pure water under argon. Three reaction pathways leading to the reduction of metal ions were proposed, which is similar to the case of Pt reduction. The average size of gold particles formed in surfactant solutions under argon atmosphere was about 10 nm, with a fairly narrow size distribution.

Okitsu et al. (2001, 2002) investigated the effect of gas atmosphere, temperature of the bulk solution, intensity of the ultrasound, ultrasound frequency, and the distance of the reaction vessel from the oscillator on the rates of gold(III) reduction. They found that there is a strong dependence on gas atmosphere and the rate of reduction under several atmospheres, which were in the order of $CH_4 = CO_2 < N_2 < Ne < He < Ar < Kr$, where no reduction proceeded under the CH_4 and CO_2 atmospheres. It was clearly found that the rates of reduction were influenced by the cavitation phenomenon. The average size of the formed gold particles changed from 30 to 120 nm by selecting the irradiation parameters. Also, the size of the gold particles was closely correlated to the initial rate of gold(III) reduction; the higher the rate of reduction, the smaller the particles. This relationship suggests that the rate of reduction would affect the initial gold nucleation processes. For this study the authors used a 200 kHz standing wave system. Also, the results of Okitsu et al. (2005) clearly suggest that the rate of Au(III) reduction, as well as the size distribution of Au particles, is governed by the chemical effects of cavitation and is not significantly affected by the physical effects accompanying ultrasound-induced cavitation.

Mori et al. (2005) also investigated the effect of type of alcohol as additives and hydrogen ion concentration on the formation rate of Au nanoparticles. It was found that the formation rate was controllable by varying the type of alcohol and the hydrogen ion concentration. Thus, when lower alcohol such as methanol or ethanol was used, the formation rate of gold nanoparticles at the neutral pH was rapid as compared to that in the acidic or alkaline range. At pH below 8, the formation rate in

the presence of higher alcohol such as pentanol or hexanol was higher than that with lower alcohol. When the formation rate was higher, the particle size became smaller under this pH condition. The formation rate at pHs higher than 9.5 using butanol, pentanol, or hexanol as an additive, however, was extremely low and the size of gold nanoparticles prepared was very small. Similar results were also obtained by Yeung et al. (1993) for the formation of colloidal gold particles.

Caruso et al. (2002) studied the reduction of $AuCl_4^-$ to colloidal gold in the presence of aliphatic alcohols and sodium dodecyl sulfate. For a particular alcohol concentration, smaller particles were obtained when the hydrophobicity of the alcohol was greater. According to the authors, alcohol adsorbed onto gold in aqueous solutions stabilized the particles at a smaller size and prevented further growth of the colloid. With more hydrophobic alcohols being adsorbed more readily, the growth is prevented, resulting in smaller particle formation.

3.1.5 Metallic Cu Nanoparticles

Nanoscale particles of metallic copper clusters were prepared by Dhas et al. (1998). For this purpose, they adopted two methods, namely the thermal reduction and sonochemical reduction of copper(II) hydrazine carboxylate Cu-$(N_2H_3COO)_2 \cdot 2H_2O$ complex in an aqueous medium under an argon atmosphere over a period of 2–3 h. Their thermally derived products showed the formation of pure metallic copper, while the sonochemical method yielded a mixture of metallic copper and copper oxide (Cu_2O). The formation of Cu_2O along with the copper nanoparticles in the sonochemical process was attributed to the partial oxidation of copper by the in situ generated H_2O_2 under sonochemical conditions. However, the authors observed that the presence of a mixture of an argon/hydrogen (95:5) atmosphere yielded pure copper metallic nanoparticles, due to the scavenging action of the hydrogen toward $OH^{\bullet}$ radicals that were produced in solution during ultrasonic irradiation. Thermally derived copper showed the presence of irregularly shaped particles (200–250 nm) having sharp edges and facets. On the other hand, the sonochemically derived copper powder showed the presence of porous aggregates (50–70 nm) that contained an irregular network of small nanoparticles. Moreover, the copper nanoparticles prepared by the sonochemical method were catalytically active toward an "Ullmann reaction" – that is, the condensation of aryl halides to an extent of 80–90% conversion.

3.1.6 Ru Nanoparticles

He et al. (2006) prepared ruthenium nanoparticles using different ultrasound frequencies in the range of 20–1,056 kHz. According to the authors, the reduction proceeded sequentially from Ru(III) to Ru(II) to Ru(0), and this reaction took almost 13 h and the diameters of the formed Ru particles were between 10 and 20 nm.

3.2 Bimetallic Nanoparticles

In addition to the preparation of single metal nanoparticles, studies of bimetallic nanoparticles (NPs) have received great attention from both scientific and technological communities. The ability to control composition and size in the synthesis of bimetallic nanoparticles is important for the exploitation of their electronic, magnetic, and catalytic properties. Following are some of the bimetallic nanoparticles obtained by the sonochemical method.

3.2.1 Au/Pd

Colloidal dispersions of bimetallic spherical nanoparticles with core–shell structure composed of gold (core) and palladium (shell) with 8 nm were prepared by Mizukoshi et al. (1997). In this method, Au (III) and Pd (II) ions in an aqueous solution of sodium tetrachloroaurate (III) dihydrate and sodium tetrachloropalladate (II) were reduced by ultrasound irradiation in the presence of sodium dodecyl sulfate (SDS). In addition to the stabilizing effect, it has also been observed that SDS remarkably enhanced the reduction rate of Au(III) and Pd(II) ions, probably due to the thermal decomposition that occurs at the interfacial region between cavitation bubbles and bulk solution and provides the reducing radicals required for the reduction of the above ions. Interestingly, the authors have also found out through UV-Vis monitoring that Au(III) ions were first reduced and after their consumption, reduction of Pd(II) ions sets in, which leads to the formation of core–shell structure rather than a simple physical mixture of these two nanoparticles.

3.2.2 Pt/Pd

Pt/Pd bimetallic nanoparticles with an average diameter of 2.8 nm were prepared by Fujimoto et al. (1998) by the application of ultrasonic irradiation of aqueous solutions containing salts of both metal ions. Interestingly, the size was similar to Pt monometallic particles, and the shape was similar to Pd monometallic particles, both prepared by ultrasound in the same way.

3.3 Metal Oxide Nanoparticles

Metal oxides are particularly attractive with respect to applications in catalysis, sensing, energy storage and conversion, optics, and electronics. For decades metal oxides have been extensively investigated by solid-state chemists. To obtain metal oxides as nanoscale materials with well-defined shape, size, and composition, traditional solid-state synthesis based on the reaction of powder precursors is unsuitable and is now being replaced by soft-chemistry routes. Particularly appealing are the advantages of the sonochemical approach, such as the possibility of

obtaining metastable materials, achieving superior purity and compositional homogeneity of the products, and influencing particle morphology during the chemical transformation of the molecular precursor to the final oxidic network.

3.3.1 Nanosized γ-MnO_2

Using $KMnO_4$ and $MnSO_4$ as raw materials, nanosized γ-MnO_2 was prepared by a new precipitation method under ultrasonic radiation by Li et al. (2005). The effects of reaction concentration, titration rate, ultrasonic time, and power on the formed nanometer γ-MnO_2 were also discussed and the optimum conditions were derived. The ultrasonic radiation had great impact on the reaction system, which resulted in γ-MnO_2 paticles having an average diameter of 10 nm with a spherical shape and good dispersity, whereas the precipitation product obtained from normal oxidation–reduction reaction was bar-shaped KMn_8O_{16} and the average sizes were ca. 250 × 25 nm.

3.3.2 MnO_2 Nanorods

Highly dispersed and non-agglomerated α-MnO_2 nanoneedles of dimensions 20–30 nm were synthesized by Kumar and Kim (2006) with the application of ultrasound radiation on an aqueous solution consisting of manganese (III) acetate at near neutral pH, followed by mild drying. With a similar reaction system, hot hydrolysis (non-sonochemical process) produced β-MnO_2 nanorods of length 100–200 nm with a high degree of agglomeration. In this case also, sonochemical cavitation phenomenon was suggested to have a pronounced effect for the formation of special phase and morphology, and the effect is proved by the differences in the intermediate products with respect to crystallinity and phase purity. The intermediate phases were identified to be single-phase γ-MnOOH for the non-sonochemical reaction and mixture of γ-MnOOH, α-MnO_2, and β-MnO_2 for the sonochemical products.

3.3.3 Nanosized Hollow Hematite (α-Fe_2O_3)

Nanosized hollow iron oxide was synthesized using high-intensity ultrasound with carbon nanoparticles as a removable template by Bang and Suslick (2007) (Fig. 15.5). According to the authors, the amorphous iron nanoparticles produced from sonochemical decomposition of $Fe(CO)_5$ formed shells around the pre-existing carbon nanoparticles. Upon exposure to oxygen, the heat released from rapid oxidation of iron to oxide ignited the carbon particles. Then the combustion of the carbon particles generated enough heat to crystallize the iron oxide shells with hollow cores. Magnetization measurements showed that the hollow nanospheres of hematite were weakly ferromagnetic. Upon annealing, the hollow hematite became more crystalline, but still maintained a hollow structure. The authors also confirmed that without the use of the carbon template, only agglomerated amorphous iron oxide was obtained.

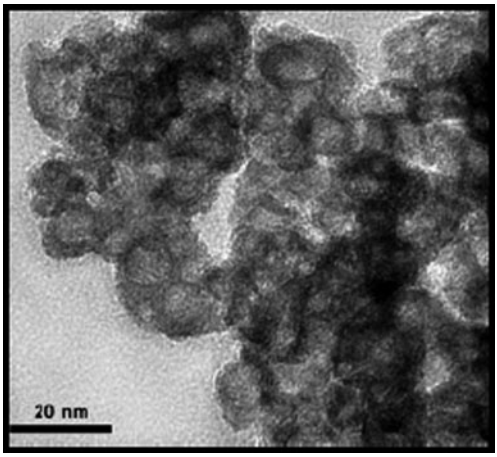

Fig. 15.5 Bright-field TEM image of nanosized hollow iron oxide

3.3.4 Molybdenum Oxide

Whiskers of molybdenum oxides with high aspect ratios were synthesized from peroxomolybdate precursor solutions irradiated with ultrasound (40 kHz) in the presence of small amounts of poly(ethylene glycol) at temperatures of 25–70°C (Krishnan et al., 2006). The application of ultrasound reduced the time needed for growth of micrometer sized whiskers from weeks to a few hours when compared to hydrothermal procedures. The presence of PEG was suggested to control the growth rates of various crystal faces by binding to peroxomolybdate ions and subsequent growth of the whiskers.

Hollow spheres of MoS_2 and MoO_3 were obtained by Dhas and Suslick (2005) by the sonochemical synthesis of MoS_2 and MoO_3 in the presence of silica nanoparticles as templates (diameters 50–500 nm), followed by acid etching to remove the silica core. Ultrasonic irradiation of a slurry containing $Mo(CO)_6$, sulfur (S_8), and nanometer silica spheres in isodurene under Ar flow yielded a MoS_2-coated silica composite. After removal of the silica followed by thermal annealing, the obtained MoS_2 hollow spheres showed very good catalytic activity for the hydrodesulfurization of thiophene. Following the same methodology, hollow spheres of MoO_3 were also prepared. However, upon heating those samples, hollow crystals of MoO_3 with sharp-edged truncated cubes containing inner voids were formed from the initial spheres.

Chen et al. (2007) reported the formation of spherical-like MoO_3 nanoparticles under ultrasonic irradiation, while only mechanical agitation led to the formation of bulk-like MoO_3 particles. These observed changes have been explained on the basis of interparticle collisions driven by ultrasound irradiation. The obtained MoO_3 nanoparticles under ultrasonic condition were also found to show improved photochromism effect as compared to the particles prepared by other conventional methods.

3.3.5 Sb_2O_3 Nanobelts

Fabrication of nanobelts of Sb_2O_3 using low-power ultrasound agitation and with the assistance of surfactant has been reported (Li et al., 2007). To achieve the nanobelts, a Sb_2O_3 precursor prepared by base hydrolysis of antimony trichloride in ethanol was redispersed in a sodium oleate solution and then treated in an ultrasonic cleaning bath for 20 min. The microjet and shock wave created due to cavitaion was thought to activate the assembly of surfactant to form the rod-like micelles, which then acted as a structure-directing agent for the formation of Sb_2O_3 nanobelts.

3.3.6 Zinc Oxide Nanostructures

Zinc oxide in the size range of 200–250 nm has been synthesized by Sivakumar et al. (2006b) using a novel ultrasonic emulsification approach. Figure 15.6 shows the TEM, SEM, and FE-SEM images of the ultrasonically formed zinc oxide, and it can be observed that the ultrasonic cavitation approach generates uniform-sized zinc oxide particles.

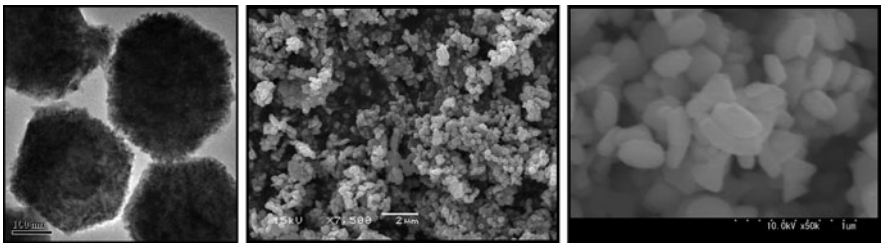

Fig. 15.6 TEM, SEM, and FE-SEM images of zinc oxide obtained by ultrasonic cavitation approach

Controlling the shape of the ZnO material is also possible using this sonochemical approach. Zhang et al. (2005) prepared nanorods and trigonal-shaped ZnO ultrafine particles through the decomposition of zinc acetate in the presence of stearic acid in paraffin oil, and the optical experiments clearly confirm that prepared ultrafine particles have a perfect crystal form. The temperatures used for the preparation were above 280°C, and at these temperatures zinc acetate decomposes to form ZnO nuclei. As a surface agent, stearic acid absorbed on the nuclei surface defines the growth of certain facets, resulting in the generation of rod-like morphology. With a further increase in reaction time, the growth of ZnO crystals with certain facets continues to form bigger and more stable triangular-shaped structure.

3.3.7 Nanocrystalline ZrO_2, TiO_2, $NiFe_2O_4$, and $Ni_{0.5}Zn_{0.5}Fe_2O_4$ Powders (Ultrasound-Assisted Hydrothermal Treatment)

Meskin et al. (2006) investigated the ultrasonic–hydrothermal and hydrothermal treatment for the synthesis of nanocrystalline zirconia, titania, nickel ferrite, and

nickel–zinc ferrite powders from precipitated amorphous zirconyl, titanyl, binary nickel–iron, and ternary nickel–zinc–iron hydroxides, respectively. It was observed by the authors that the ultrasonically assisted hydrothermal treatment of amorphous zirconyl and titanyl gels results in significant rise of the rate of ZrO_2 and TiO_2 crystallization and promotes formation of thermodynamically stable monoclinic zirconia, but does not affect the microstructure and mean particle size of resulting nanopowders. Also, it has been observed that the ultrasonic–hydrothermal processing of co-precipitated amorphous nickel, zinc, and iron hydroxides favors the formation of nanocrystalline ferrite powders with narrower particle size distribution.

3.3.8 Nanocrystalline TiO_2

A sonochemical method has also been established by Guo et al. (2003) to directly prepare columnar-shaped anatase nanocrystalline TiO_2 (3×7 nm) by the hydrolysis of tetraisopropyl titanate (TPT) in the presence of water and ethanol. The TiO_2 structure and the particle sizes were dependent upon the reaction temperature, the acidity of the medium, and the reaction time. The authors attributed this formation to rapid polycondensation of Ti-OH or Ti-OR species. Moreover, nanocrystalline products were obtained only when the system temperature was above 70°C; otherwise, the products were amorphous.

3.3.9 TiO_2 Nanoarrays

Pure single crystal rutile TiO_2 nanoarrays (20–300 nm) were successfully synthesized by Xia et al. (2007) using $TiCl_4$/HCl solution. Each of the arrays consisted of small nanorods of about 8 nm in diameter and 200 nm in length. The photocatalytic activity of the nanoarrays for photodegradation of brilliant red X-3B in aqueous solution was better than TiO_2 nanorods and Degussa P25.

3.3.10 TiO_2 Nanotubes and Whiskers

Zhu et al. (2001) produced both titania whiskers and nanotubes by sonicating titania particles in NaOH aqueous solution, followed by washing with deionized water and dilute HNO_3 aqueous solution. The mixture was sonicated by the direct immersion of a 560 W titanium horn for 80 min and the resulted precipitate was then washed with 0.1 M HNO_3 aqueous solution and deionized water to prepare the titania whiskers (Fig. 15.7). To prepare the titania tubes, the mixture was sonicated at 280 W for 60 min. This process was claimed to be more convenient than template methods in which special templates are required. The role of sonication is to accelerate the reaction between the precursor and the NaOH, leading to the oriented growth of titanates due to the extreme conditions generated. Further, these titanates undergo ion exchange and dehydration in the presence of HNO_3, forming titania. It was found that no titanate whiskers could be obtained without sonication.

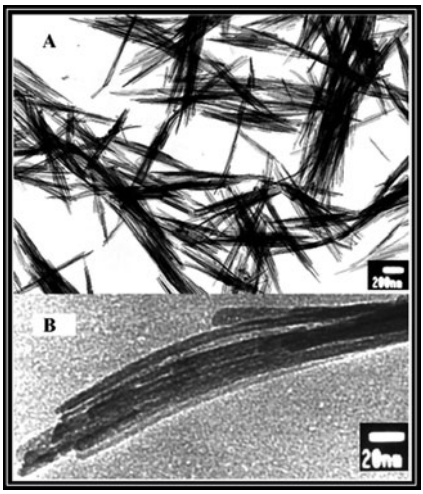

Fig. 15.7 TEM images of the as-prepared whiskers

3.3.11 V_2O_5 Nanowire Bundles

Mao et al. (2006) synthesized self-assembled V_2O_5 bundles with highly ordered superstructures and spindle-like morphology by sonochemical method. The spindle-like V_2O_5 bundles were composed of several tens of homogeneous nanowires with diameters of 30–50 nm and lengths of 3–7 μm. The suggested mechanism involved three steps in sequence: (1) ultrasound-induced dissolution of V_2O_5 and formation of nuclei and primary nanoparticles; (2) ultrasound-induced fusion of these primary nanoparticles accompanying oriented attachment to form the nanowires; and (3) the individual nanowires were further attached side by side to assemble into bundles, accompanying an Ostwald ripening process.

3.4 Mixed Oxides

3.4.1 Gd_2O_3-Doped CeO_2 Nanoparticles

Yao and Xie (2007) prepared 10 mol% Gd_2O_3-doped CeO_2 (20 GDC) nanoparticles via carbonate co-precipitation using ammonium carbonate as the precipitant. In order to alleviate the agglomeration of the nanoparticles during synthesis, ultrasonic and surfactants including sodium oleate and polyethylene glycol 400 were applied to disperse the precursor suspensions. It was found that the deagglomeration treatment to the precursor by ultrasonic and surfactants was effective in improving the size distribution and sinterability of the final 20 GDC nanoparticles. The 20 GDC nanoparticles resulted from the combined deagglomeration treatment reached to a relative density of above 99.5% after being sintered at 1,100°C for 4 h.

3.4.2 CuO–ZrO_2 Catalysts

Nanosized CuO–ZrO_2 catalysts have also been prepared by Sivakumar and Gedanken (2006) using a simple precipitation technique that was assisted by ultrasonic cavitation. To understand the effect of ultrasound intensity on the formed products, two intensities, 20 and 70%, were employed by the authors using the same reactants as in the conventional precipitation reaction. The calculated surface area of the catalysts obtained with 70% intensity was 2.7 times higher than that obtained with 20% intensity. Also, the ultrasonically assisted reaction was almost five orders of magnitude higher in rate than the conventional precipitation reaction. Figure 15.8 shows the TEM image of the catalysts obtained with 70% intensity indicating a large number of pores of 4–6 nm average diameter. Even in the case of catalysts obtained with 20% intensity, a similar size of pores was formed, but with fewer pores. Consequently, the catalyst prepared with 70% intensity showed higher activity for the decomposition of N_2O within temperatures in the range of 350–620°C.

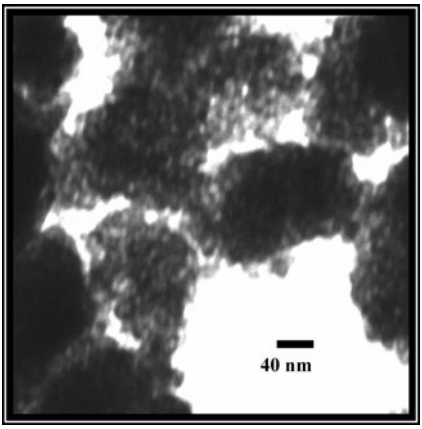

Fig. 15.8 Transmission electron micrograph of the calcined CuO–ZrO_2 obtained with 70% ultrasonic intensity

An increase in ultrasonic intensity increases the turbulent flow and shock waves produced by cavitation, which locally increases molecular mobility, and hence aids in their collisions at sufficiently high velocity. This has been attributed to a marked increase in the hydrolysis rate of precursors to yield the respective hydroxides. For the same reason, a greater amount of copper hydroxides was also deposited on the ZrO_2 support.

3.4.3 Nanomagnetic Oxide (Ferrites) Materials: Role of Ultrasonic Cavitation

The successful preparation of nanosized ferrites with precise stoichiometry poses a synthetic challenge, particularly in the case of complex materials having two or more elements. Recently, a simple sonochemical approach to prepare a variety of nanomagnetic rare earth ferrites has been reported by a number of researchers,

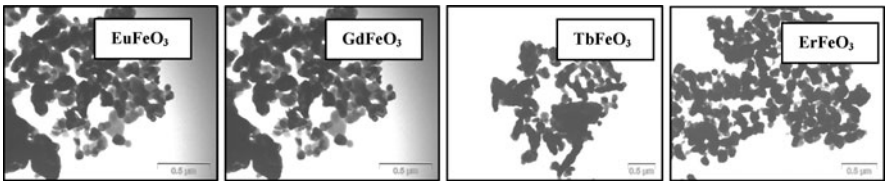

Fig. 15.9 TEM images of the rare earth nanomagnetic ferrites

Sivakumar et al. (2004a, b, c) and Sivakumar and Gedanken (2004), using a highly volatile organometallic precursor, $Fe(CO)_5$. Figure 15.9 shows TEM images of the four ferrites obtained using this approach representing the nanosizes of the ferrite particles (40–60 nm). The advantage of this sonochemical process is that it enables ferrite formation at a substantially lower calcination temperature. It is particularly noteworthy that the cogeneration of the garnet phase has not been observed in this process, as is usual with conventional methods. It has been proposed by the authors that the drastic reduction in the calcination temperature could be due to the ultrasonic generation of amorphous iron oxide from $Fe(CO)_5$. Nanosized strontium ferrite has also been derived using the same sonochemical approach.

Another technologically important material is zinc ferrite, which is used as a gas sensor as well as in semiconductor photocatalysis. This ferrite was obtained using the ultrasonic approach of several researchers including Sivakumar et al. (2006a, c), using simple precursors. The approach followed is shown schematically in Fig. 15.10.

The above approach was based on two stages of sonication. The first stage involved ultrasonically dispersing an aqueous solution consisting of zinc and iron acetates into rapeseed oil in a sonoreactor in order to form well-dispersed W/O emulsion droplets. Sonication was carried out for 20 min in air atmosphere and temperature was maintained between 25 and 30°C using a cooling bath. With the application of ultrasound, the two distinct layers formed were changed into a uniformly turbid emulsion. It is to be noted that the emulsion droplets were formed without using a surfactant. In the second stage, sonication was applied without any cooling. In the absence of cooling, temperature increased rapidly with the continuous dissipation of ultrasound energy. In this way, at the end of 30 min of sonication, temperature reached 125°C so that all the water present in the internal aqueous droplets evaporated, leaving behind the solid particles dispersed in the oil phase. So, in this stage, hydrolysis of zinc and iron acetates occurred by applying ultrasound without using any precipitants. In addition, the authors predicted that ultrasonic cavitation events provide high-temperature conditions or in situ calcination environment that result in the formation of zinc ferrite nanocrystals. Following is the proposed reaction steps that occur due to ultrasound to obtain the ferrite.

$$H_2O \longrightarrow H^{\cdot} + OH\cdot \tag{15.4}$$

$$H\cdot + H\cdot \longrightarrow H_2 \tag{15.5}$$

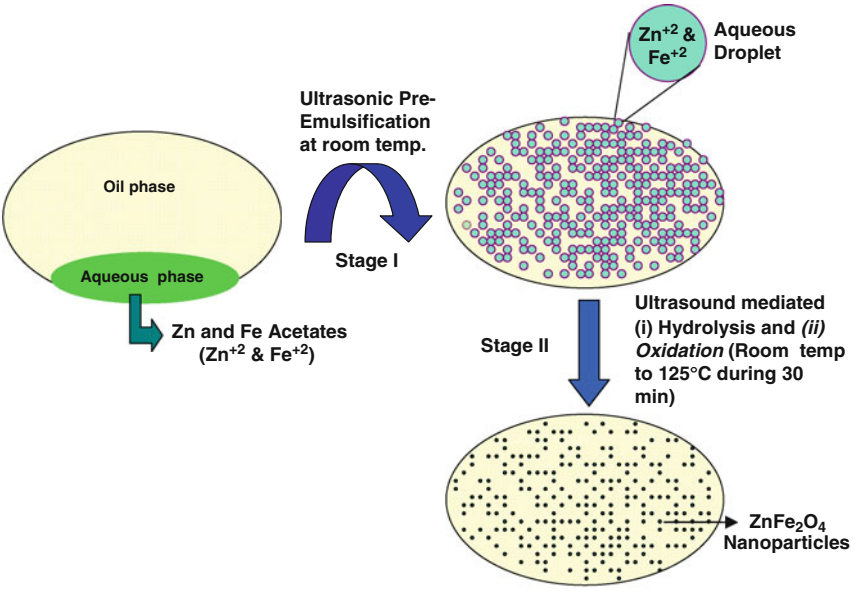

Fig. 15.10 Schematic representation of two-stage ultrasonication approach for the synthesis of zinc ferrite

$$OH\cdot + OH\cdot \longrightarrow H_2O_2 \tag{15.6}$$

$$Fe(CH_3COO)_2 + 2\ H_2O \longrightarrow Fe(OH)_2 + 2\ CH_3COOH \tag{15.7}$$

$$3\ Fe(OH)_2 + H_2O_2 \longrightarrow Fe_3O_4 + 4\ H_2O \tag{15.8}$$

$$Zn(CH_3COO)_2{\cdot}H_2O + H_2O \longrightarrow ZnO + 2\ CH_3COOH + 2\ H_2O \tag{15.9}$$

$$2\ Fe_3O_4 + 3\ ZnO \xrightarrow[\text{Due to u/s cavitations}]{(O)} 3\ ZnFe_2O_4 \tag{15.10}$$

The morphology of the zinc ferrite particles obtained by this approach is shown in Fig. 15.11. The size of the as-prepared material is 4 nm, whereas the heat-treated material is about 12 nm. Heat treatment was necessary in order to remove the small amount of oil present on the surface of the ferrite.

The authors also explained that the uniform-sized ferrite particles obtained in this process should be due to the generation of efficient droplet size induced by ultrasound because ultrasound generates sufficient and strong mechanical forces that can easily and evenly disperse an aqueous solution containing zinc and iron acetates in the oil phase. It was also reported that emulsification is critical for tailoring the size distribution of the particles. The formed droplets act as a template for the formation of zinc ferrite nanoparticles. In addition, the viscosity of the oil phase was

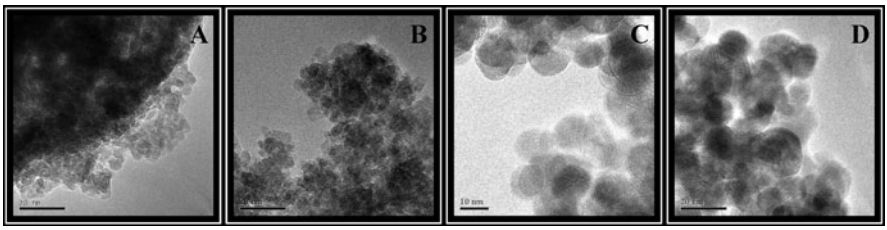

Fig. 15.11 Transmission electron micrographs of as-prepared (**a**, **b**) and heat-treated (**c**, **d**) zinc ferrite nanocrystals

suggested to likely restrict the oil droplets from higher mobility, thereby preventing it from coalescence. This phenomenon avoids the agglomeration of the resultant particles to a greater extent.

3.5 Porous Materials

Synthesis of porous inorganic materials with interesting morphologies has been the subject of many investigations owing to their potential applications in catalysis, sorption, and separation. Practical applications require synthesis of porous structures with well-defined structural, interfacial, compositional, and morphological properties.

3.5.1 Mesoporous TiO_2: Wormhole-Like Framework Structures

Wang et al. (2000) synthesized mesoporous TiO_2 with wormhole-like framework structures using a long-chain organic amine as structure-directing agent under ultrasound irradiation. High surface areas were obtained after extraction or calcination to remove the organic amine. This work suggests that the sonochemical technique can serve as a general method for the synthesis of other mesoporous oxides.

3.5.2 Mesoporous Silica Vesicles

Rana et al. (2002) reported a direct and efficient synthesis route to form vesicles of mesoporous silica by the sonochemical method in a very short reaction time (Fig. 15.12). The importance of this approach is that it does not require any specialized structure-directing reagents other than the normally used cetyltrimethylammonium bromide (CTAB) as the surfactant, similar to the original work to prepare mesoporous silicates. The authors have proposed that the surfactant enrichment at the liquid–vapor interface of the cavitating bubbles can induce the process of silica-surfactant self-assembling into micelles and further organization into micellar rods. These micellar rods then rearrange themselves on the surface of the bubbles, producing the liquid-crystalline mesophase with a vesicular morphology. Because of very high cooling rates due to ultrasonic cavitation, silicate species condense at

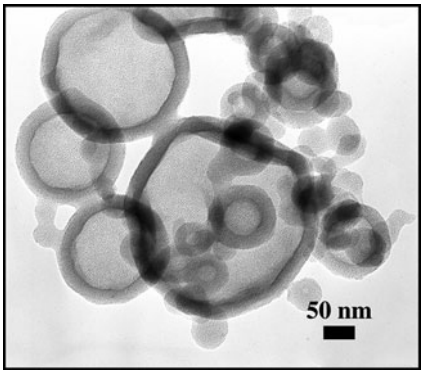

Fig. 15.12 Mesoporous silica vesicles prepared via ultrasonication

a faster rate so that the silica-surfactant micellar rods cannot arrange themselves properly in a hexagonal pattern, thereby yielding a wormhole-like feature.

3.5.3 ZnS Nanoparticle-Assembled Mesoporous Structure

A stable mesoporous network formed by nanoparticles of ZnS was achieved by an ultrasound-mediated fabrication method by Rana et al. (2003). The ZnS nanoparticles were generated in situ during the sonication, and dodecylamine was used as the structure-directing agent. After the template extraction, authors observed a mesoporous ZnS with a high surface area of 210 m^2/g and with an average pore diameter of 28 Å. High-resolution transmission electron microscopic (HRTEM) analysis of the prepared material revealed a mesostructure consisting of closely spaced ZnS nanocrystallites of 3 nm size. Also, the existence of ZnS particles in a compact structure resulted in a dramatic increase in the thermal stability of the cubic phase. It has been reported that the sonochemically generated ZnS nanoclusters electrostatically interact with the dodecylamine (DDA) surfactants. Once the nanocrystallites are bound to the DDA molecules, they rearrange themselves in an ordered fashion to form the mesostructured pattern at the air–water interface region of the cavitating bubbles.

3.5.4 Fe-Doped Mesoporous TiO_2 Powder

Highly photoactive nanocrystalline mesoporous Fe-doped TiO_2 powders were prepared by the ultrasonic-induced hydrolysis reaction of tetrabutyl titanate ($Ti(OC_4H_9)_4$) in a ferric nitrate aqueous solution (Zhou et al., 2006). Notably, the mesoporous TiO_2 structure with average pore diameter of 7–8 nm was formed without using any templates or surfactants. The photocatalytic activity of Fe-doped TiO_2 powders prepared by this method and calcined at 400°C exceeded that of Degussa P25 (P25) by a factor of more than two times at an optimal atomic ratio of Fe to Ti of 0.25. The high activities of the Fe-doped TiO_2 powders have been attributed to the results of the synergetic effects of Fe doping, large BET-specific surface area, and small crystallite size.

3.6 Nanocomposites

Inorganic/organic nanocomposite systems, in which inorganic particles are encapsulated into the polymer matrix, are new classes of polymeric materials. These materials combine the properties of both components. This means that polymer component with excellent optical property, flexibility, and toughness could improve the brittleness of inorganic particles and also that inorganic particles could increase the strength and modulus of polymers. Mixing of the nanoparticles with the polymer is the most critical issue. Better mixing between these two can provide higher strength and stiffness. Ultrasonic cavitation is widely exploited for polymerization in the presence of inorganic nanoparticles, producing a wide variety of nanocomposites. The inorganic nanoparticles in the aqueous solution can redisperse more effectively by ultrasonic irradiation than by conventional stirring; this is the basis for the preparation of polymer/inorganic nanoparticles composites. Following are some of the nanocomposites prepared by this technique. A review by Gedanken (2007) on the use of ultrasound in synthesizing various nanocomposites was recently published.

3.6.1 PMMA/Montmorillonite Clay Nanocomposite

Jothi Rajan et al. (2006) synthesized poly(methyl methacrylate) (PMMA)–Montmorillonite (MMT) clay nanocomposites by ultrasonic mixing. For comparison purposes, authors also carried out synthesis by magnetic stirring. From TG, DTG studies they found that thermal stability increased by nearly 30% for the nanocomposites obtained by ultrasonic mixing than by magnetic stirring.

3.6.2 PP/Clay Nanocomposite

A continuous ultrasound-assisted process was developed by Lapshin and Isayev (2005) to prepare PP/clay composite with varying clay concentrations. Their obtained results clearly indicate a possibility of the rapid intercalation and partial exfoliation of PP/clay nanocomposite without the matrix being chemically modified.

3.6.3 Polyurethane Foam/Clay Nanocomposite

PU foam/clay nanocomposite was prepared by Seo et al. (2006). They observed that with the application of ultrasound, the flexural and tensile strength of the nanocomposite were increased. This was mainly due to the uniform distribution of the clay particles under sonication. Notably, fire resistance properties also increased.

3.6.4 Polystyrene/Fe_3O_4 Nanocomposite

Ultrasonically initiated miniemulsion polymerization of styrene in the presence of Fe_3O_4 nanoparticles was successfully employed by Qiu et al. (2006, 2007) to prepare polystyrene (PS)/Fe_3O_4 magnetic emulsion and nanocomposite. The authors

observed that an increase in Fe_3O_4 nanoparticles drastically increased the polymerization rate. When compared with neat PS, the thermal stability of PS/Fe_3O_4 nanocomposite was better.

3.6.5 Polystyrene/Amorphous Fe Nanocomposite

Wizel et al. (2000) prepared polystyrene–iron (PS–Fe) nanocomposite by ultrasound-mediated polymerization of styrene in the presence of amorphous iron nanoparticles. Amorphous iron was first prepared by sonication of iron pentacarbonyl and was then mixed with styrene in dry hexadecane. The suspension was sonicated for 3 h under an argon flow in a 20°C cooling bath to get the composite material. In this case, the PS–Fe composite exhibited thermal stability comparable to that of commercially available polystyrenes.

3.6.6 Polystyrene/Ni Nanocomposite

Kumar et al. (2002) obtained well-dispersed Ni nanoparticles of 5 nm in polystyrene by sonicating a solution of nickel formate and polystyrene in *N,N*-dimethylformamide (DMF) under 1.5 atm of Ar/H_2 at room temperature for 3 h. It was proposed that the CH_3 and $N(CH_3)CHO$ radicals formed from the sonolysis of DMF along with the generation of high temperature and pressure reduce nickel formate to form metallic nickel nanoparticles. In contrast, without ultrasound under similar conditions no nickel nanoparticles were formed in polystyrene.

3.6.7 SiO_2/Poly(3-Aminophenylboronic Acid) (PAPBA) Nanocomposite

Zhang et al. (2007) synthesized SiO_2/poly(3-aminophenylboronic acid) (PAPBA) composites under ultrasonic irradiation. Polymerization was carried out in the presence of sodium fluoride and D-fructose to anchor 3-aminophenylboronic acid groups onto SiO_2 surface. The SiO_2/PAPBA nanocomposite prepared in this way showed different morphology, electrical properties, and thermal behavior in comparison to the nanocomposites prepared under other conventional methods. Application of ultrasonic irradiation in this case minimizes the aggregation of nanosilica and promotes anchoring of PAPBA units over SiO_2 surface. In addition, the conductivity of the composite prepared via ultrasonication shows around 0.2 S/cm.

3.6.8 Conducting Polymeric Nanomaterials and Composites

There have been reports on sonochemical methods for the synthesis of conducting polymers and their nanocomposites (Sivakumar and Gedanken, 2005). In general, the intense bubble collapse due to cavitation enhances the polymerization process and, due to these effects, polymer sonochemistry has become an active area of research. Improved properties have also been observed in most cases. For example,

Osawa et al. (1987) observed considerably improved electrical and mechanical properties of polythiophene film by ultrasonic irradiation of the electrolytic solution during polymerization. Following are some of the important polymeric nanomaterials and nanocomposites obtained using this technique.

Polyaniline (PANI)

High-intensity ultrasound can not only accelerate heterogeneous liquid–liquid chemical reactions, but also break the aggregation and reduce particle size due to its dispersion, crushing, emulsifying, and activation effect and thus has a better control on the morphology of particles, especially on hard solid particles such as PANI. Attempts have been made to ultrasonically prepare conducting PANI nanoparticles in the range of 10–50 nm by Xia and Wang (2001) through ultrasonic-assisted inverse microemulsion polymerization method. In this process, polymerization of aniline was confined to a nanoreactor called a "water pool" surrounded by surfactant molecules in the apolar continuous phase. Here, ultrasound not only enhances the polymerization rate of aniline that is usually very slow under conventional stirring in inverse microemulsion, but also has a better control on the morphology of PANI compared to conventional stirring. In addition, ultrasound irradiation promotes the diffusion of HCl molecules and improves the degree of doping. Atobe et al. (2003) reported an ultrasonic preparation of polyaniline colloids using polyethylene oxide as a stabilizer and potassium iodate as an oxidant, and the reaction was carried out for 12 h.

It has been very well recognized that water, due to the action of ultrasound, leads to the formation of H_2O_2. Thus, it will be highly advantageous to exploit the in situ ultrasonically generated H_2O_2 for reactions, which can potentially be utilized. Motivated by this, Sivakumar and Gedanken (2005) applied ultrasound to a dispersion of aniline in water for its polymerization to give PANI, without using any surfactant and/or stabilizer. However, no formation of PANI was observed in a 3 h sonochemical reaction. Following this result, a reaction was carried out, but with the external addition of H_2O_2 to the same reaction mixture and ultrasound irradiation for the same 3 h period. After 20 min, the authors observed a green color, followed by a material precipitation. Thus, it has been confirmed that the external addition of H_2O_2 to the reaction medium provides a different oxidative atmosphere that enhances the reaction rate. In contrast, without ultrasound, a very small amount of PANI was formed only after 18 h of reaction. The yield of the stirred reaction was very low even after 6 days. These results clearly show the significant effect of ultrasonic irradiation on increasing the polymerization of aniline to provide PANI. In addition, the same approach has been followed in successfully preparing an Au–PANI composite, where H_2O_2 acted as a reducing agent in the generation of Au nanoparticles from chloroauric acid. Improvements in reducing the reaction time (1/48 times) combined with unusual reaction yield ($\sim$20 times) were observed due to ultrasound usage. An enhancement in the conductivity of the Au–PANI composite with even a small amount of incorporated Au has been reported.

PANI/Nano-SiO_2

Polyaniline/nano-SiO_2 particle composites were also prepared through ultrasonic irradiation by Xia and Wang (2003). Polymerization of aniline was conducted under ultrasonic irradiation in the presence of two types of nano-SiO_2: porous nanosilica and spherical nanosilica. It was found that the aggregation of nano-SiO_2 could be reduced under ultrasonic irradiation and that nanoparticles were redispersed in the aqueous solution. The formed polyaniline deposited on the surface of the nanoparticle, which led to the core–shell structure. The conductivity of the polyaniline/porous nanosilica (23.1 wt% polyaniline) and polyaniline/spherical nanosilica (20.6 wt% polyaniline) composites was 2.9 and 0.2 s/cm, respectively.

Polypyrrole/Au-NPs and Polypyrrole/Pt-NPs

Colloidal dispersions of hybrid nanocomposite composed of polypyrrole (PPy) and gold nanoparticles (Au-NPs) or platinum nanoparticles (Pt-NPs) were prepared by Park et al. (2005). In this method, Au ion and pyrrole monomer in an aqueous solution were reduced and oxidized, respectively, by ultrasonic irradiation in the presence of sodium dodecyl sulfate (SDS).

3.6.9 Carbon Nanofibers/Polyurethane Foam (CNFs/PU) Composite

Effects of different process parameters of sonication technique for the doping of carbon nanofibers (CNFs) into rigid polyurethane (PU) foam were investigated by Kabir et al. (2007). They found that higher sonication time was required for higher weight percentage of nanoparticle loading, but an optimum sonication time was necessary to achieve maximum dispersion.

3.6.10 Polymer-Encapsulated Carbon Nanotubes by Ultrasound Initiated In Situ Emulsion Polymerization

Xia et al. (2003) investigated an ultrasound-initiated in situ emulsion polymerization approach for the surface modification of multi-walled carbon nanotubes (MWCNTs) and also the dispersion behavior of MWCNTs in an aqueous solution. From their results it can be observed that by employing ultrasound, the aggregation and entanglement of carbon nanotubes in an aqueous solution can be broken down, while in situ polymerization of monomer *n*-butyl acrylate (BA) and methyl methacrylate (MMA) on the surface of MWCNTs proceeds without any added chemical initiator; consequently, the MWCNTs are coated by the formed polymer. Further, the polymer-encapsulated carbon nanotubes can be well dispersed in nylon 6 matrix, and this result showed improved yield, strength and Young's modulus.

Poly(ethylene terephthalate) (PET)-based nanocomposites were prepared with single-walled carbon nanotubes (SWNTs) through an ultrasound-assisted dissolution–evaporation method (Anand et al., 2007). Comparison of crystallization, conductivity, and transmission electron microscopy studies revealed that

ultrasound-assisted dissolution–evaporation method enables more effective dispersion of SWNTs in the PET matrix as compared to the melt compounding method.

3.7 Supported/Immobilized Metallic Nanoparticles

Supported nanoparticles have attracted a great deal of interest, and their unique properties are directly related to the specific particle morphology (size and shape), metal dispersion, concentration, and the electronic properties of the metal within their host environment. Nanoparticles supported on different support materials having high surface area are currently used extensively as catalysts for chemical transformations. The surface atoms are chemically more active compared to the bulk atoms because they usually have fewer adjacent coordinate atoms and unsaturated sites or more dangling bonds. To deposit metal nanoparticles onto the surfaces of structured or porous solid supports, the ultrasound-mediated synthesis has been found promising as it provides control over particle dimensions, distribution, and metal concentration on the support.

3.7.1 Pd Nanoparticles Immobilized on Alumina Surface

Preparation of Pd nanoparticles immobilized on alumina at room temperature by ultrasonic irradiation of an aqueous solution of tetrachloropalladate (II) was reported by Okitsu et al. (1999). It was observed that the size of Pd particles could be controlled by changing the type of alcohol. Here, alcohol acts as an effective accelerator for Pd(II) reduction. The dispersion of metallic Pd particles on the Al_2O_3 surface was appreciably enhanced by increasing the rate of reduction. The major pathway in the formation of Pd nanoparticles on Al_2O_3 was speculated to proceed via the following three steps: (1) the reduction of Pd(II) ions by the reducing radicals formed from the sonolysis of water and alcohol, resulting in the formation of Pd nuclei; (2) the growth and/or the agglomeration of the Pd nuclei to form Pd nanoparticles; and (3) the simultaneous adsorption of Pd particles onto the Al_2O_3 surface. The catalytic activities of the supported Pd nanoparticles for the hydrogenation of olefins at room temperature showed higher reaction rates than those over a conventionally prepared Pd/Al_2O_3 catalyst and a commercially available Pd black (Okitsu et al., 2000).

3.7.2 Pt on Rutile TiO_2

Fine particles of rutile TiO_2 supporting nanosized particles of Pt were prepared by simultaneous in situ sonochemical deposition method using a standing wave sonochemical reactor method by Sivakumar et al. (2010). Using this technique, different weight percentage of Pt on TiO_2 was also deposited. Figure 15.13 shows the TEM images of the Pt deposited on TiO_2. Larger particles with a size between 20 and

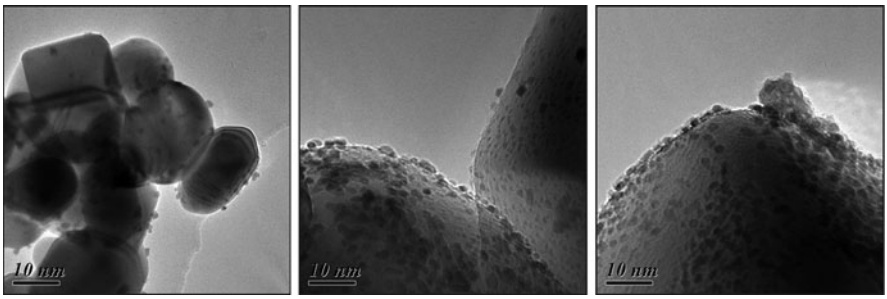

Fig. 15.13 TEM images of Pt on TiO_2

30 nm correspond to TiO_2 and smaller Pt particles of about few nanometers are distributed all over the TiO_2. Also, it has been observed that the size of the Pt particles formed is independent of the amount of loading.

All supported catalysts showed catalytic activity for CO oxidation between 100 and 180°C. Using the present ultrasonic cavitation approach, the prepared 0.8 wt% Pt on TiO_2 was sufficient for complete CO conversion in comparison with 90% conversion for conventionally prepared 1.44 wt% Pt on TiO_2 using the same reaction temperature of 125°C. An increased conversion of CO, even with small amounts of deposition of Pt, was attributed to the uniform distribution of Pt species on TiO_2 obtained by the sonochemical approach. In addition, the smaller particle size obtained by this approach was suggested to increase the surface active sites for increased reaction rates. The hydrogen and propanol radicals generated due to ultrasonic cavitation reduce Pt(IV) to Pt(II) and then to Pt(0). Further, the cavitational collapse forces Pt particles to be deposited on TiO_2 (Sivakumar et al. 2010).

3.7.3 Au/γ-Fe_2O_3 Composite Nanoparticles

Mizukoshi et al. (2005) prepared Au/γ-Fe_2O_3 composite nanoparticles by sonochemical means of reducing Au(III) ions without using any stabilizer in an aqueous solution to form stable Au nanoparticles and allowing them to attach onto the surface of γ-Fe_2O_3 particles. The number of Au nanoparticles supported on each γ-Fe_2O_3 particle was controlled by changing the relative amounts of Au(III) ions and γ-Fe_2O_3 particles. The composite nanoparticles were further successfully used for magnetic separation of biomolecules having affinity to bind onto the Au nanoparticles.

3.7.4 SBA-15-Supported Ru Nanoparticles

Li et al. (2004) reported the incorporation of metallic Ru nanoparticles into the pores of SBA-15 employing a simple ultrasound-assisted polyol method. Ultrasound usage provided both the energy for the reduction of the Ru(III) ion and the driving

force for the loading of the Ru^0 nanoparticles into the SBA-15 pores. An ultrasound-assisted insertion mechanism was also proposed based on the microjets and shock wave effect of the collapsed bubbles. The catalytic properties of the SBA-15-supported Ru nanoparticles were tested by the partial oxidation of methane, which showed very high activity and high CO selectivity.

3.7.5 Pt–Ru Nanoparticles Supported on Carbon

Carbon-supported Pt–Ru nanoparticles were obtained by Nagao et al. (2007). Under sonochemical conditions, the nanoparticles were formed through the reduction of Pt and Ru ions with sodium borohydride and were impregnated on carbon powder. The ultrasonic irradiation resulted in single nanometer-sized Pt–Ru particles supported on the carbon, while aggregated Pt–Ru particles were observed in the non-irradiated sample. Consequently, the sonochemically prepared catalyst showed higher catalytic activity in the electrochemical oxidation of methanol.

3.7.6 Immobilization of Metal Nanoparticles (Pt, Pd, and Au) on TiO_2 Surface

A general sonochemical method to prepare noble metal nanoparticle-supported TiO_2 photocatalysts was reported by Mizukoshi et al. (2007). First, the Pt, Au, and Pd nanoparticles were prepared by sonochemically reducing the respective ions in presence of polyethyleneglycol monostearate. Then, TiO_2 powder was added to the sample solution and prolonged sonication was carried out for 5–60 min under an air atmosphere to form the supported catalysts. Because of the smaller sizes of the metallic particles, the sonochemically prepared catalysts showed higher photocatalytic activities than did the conventional ones.

3.7.7 Nano-Fe into the Pores of Mesoporous Titania

Ultrasound irradiation was also used by Perkas et al. (2001) for depositing nanosized iron oxide catalyst into the pores of mesoporous titania. The irradiation of titania with a solution of iron pentacarbonyl in decalin under an atmospheric pressure of air was carried out at 0°C for 3 h. The sonochemical decomposition of iron pentacarbonyl formed amorphous nanoparticles deposited into the pores of mesoporous titania. The resulting material was also used for the oxidation of cyclohexane under mild conditions.

3.7.8 Gold Nanoparticles in Mesoporous Silica

Gold nanoparticles dispersed inside the pores of monolithic mesoporous silica were prepared by Fu et al. (2003) by soaking the silica in gold(III) ion solution and subsequent ultrasound irradiation. Acoustic cavitation cannot occur in nanosized pores and thus it was thought that the gold nanoparticles in silica were not formed in situ

within the pores, but should have been produced mainly by the diffusion of the gold clusters formed in the solution. This hypothesis was supported by the fact that the ultrasound-mediated radicals formed in solution were exhausted before entering the pores of silica.

3.7.9 Ceria–Zirconia-Supported Ruthenium

Bedrane et al. (2002) reported the preparation of ruthenium nanoparticles supported on ceria and ceria–zirconia under sonochemical conditions. When the impregnation of ruthenium on the support was carried out with ultrasound assistance, the resulting catalysts exhibited optimal metal dispersion. In addition, a large increase in the metal accessibility for H_2 chemisorption was also observed.

3.8 Ultrasound-Assisted Coating

Ultrasound has been used extensively to coat or deposit nanoparticles on various materials, e.g., silver nanoparticles on nylon 6,6 and silica submicrospheres. This deposition method can provide materials with structural control at nanometer-scale level. Moreover, it can produce uniform, nanostructured, and functional coating with well-controlled dimension and unique structure. In addition, it is a non-destructive technique to deposit desired materials under mild conditions.

3.8.1 Silver Nanoparticles on Nylon 6,6

Silver/nylon 6,6 nanocomposite containing 1 wt% metallic silver was produced from an aqueous solution of silver nitrate in the presence of ammonia and ethylene glycol by an ultrasound-assisted reduction method by Perkas et al. (2007). It was observed that the nanocrystals of pure silver, 50–100 nm in size, were finely dispersed on the polymer surface without damaging the nylon 6,6 structure. Also, the authors observed that the silver–nylon nanocomposite was stable through many washing cycles and thus predicted that this could be used as a master batch for the production of nylon yarn by melting and spinning processes. Notably, the fabric knitted from this yarn also showed excellent antimicrobial properties.

3.8.2 Silver Nanoparticles on Wool Fibers

Silver nanoparticles were also deposited on the surface of natural wool with the aid of power ultrasound by Hadad et al. (2007). The average particle size of silver was 5–10 nm, but large aggregates were also observed. From this study, the authors confirmed that the strong adhesion of the silver to the wool was a result of the adsorption and interaction of silver with sulfur moieties of the cysteine group present in the fiber.

3.8.3 Nano-Ni Coating

Nanophasic amorphous clusters of elemental nickel in the size range of 10–15 nm were deposited on submicrospheres of silica by the sonication of a suspension containing nickel tetracarbonyl and silica submicrospheres in decalin by high-intensity ultrasound irradiation (Ramesh et al., 1997). The authors proposed that ultrasound-driven cavitation desorbed the adsorbed water on silica, making the free silanols available for reaction with nickel species. According to the authors, ultrasound irradiation resulted in the dehydrative condensation of hydrogen-bonded silanols to form siloxane links followed by the formation of a bond between nickel and the bridging oxygen of the siloxane links.

Following the same method, preparation and coating of Ni on amorphous and crystalline alumina were carried out by Zhong et al. (1999). The interaction between the nickel as well as its oxide and the alumina core was well studied by various measurements. Magnetization measurements showed that the as-prepared sonication products were superparamagnetic due to the ultrafine nature of the nickel particles.

3.8.4 Ag Nanoparticles on Silica Submicrospheres

Silver-decorated sub-micrometer-sized silica spheres with a core–shell structure were obtained based on a seed-mediated growth process by Ye et al. (2007). In this process, silver nanoparticles were first formed by reducing Ag^{+} to Ag^{0} in *N*,*N*-dimethylformamide (DMF) as reducer and poly(vinylpyrrolidone) (PVP) as protective agent under ultrasound irradiation, followed by the deposition of the particles on silica. By repeating the cycles of silver deposition process, the deposited silver particles act as seeds and mediate the growth of silver shell on the core silica.

3.8.5 Au Nanoparticles on Silica Submicrospheres

Gold nanoparticles with an average size of 5 nm were deposited on the surface of preformed silica submicrospheres with the aid of power ultrasound. Optimization of the amount of gold precursor was required for the uniform deposition of gold nanoparticles on various sizes of silica surfaces. The advantage of the process is that it is a simple, efficient, one-step synthesis that produces a uniform coating of gold nanoparticles (Pol et al., 2003). The same method was further used to achieve deposition of silver nanoparticles with an average size of ∼5 nm on the surface of silica submicrospheres with the aid of power ultrasound (Pol et al., 2002).

3.8.6 Chalcogenide Nanoparticles on Silica Microspheres

Preparation of PbS nanoparticles of 30 nm size coated on sub-micrometer silica spheres was described by Xie et al. (2007). In this sonochemical process, triethanolamine acts as a complex agent that plays an important role for the homogeneous coating of PbS nanoparticles on silica spheres. In addition, by dissolving

the silica cores with diluted HF solution, stable PbS hollow structures could be obtained.

ZnS of 1–5 nm coated on silica were prepared by Arul Dhas et al. (1999) by subjecting a slurry of amorphous silica microspheres, zinc acetate, and thioacetamide in an aqueous medium to ultrasonic treatment for 3 h under ambient air. It was proposed that the coating process takes place via ultrasonic cavitation-induced initial grafting of zinc acetate onto the silica surface, followed by the displacement of acetate ion by an in situ generated S^{2-} species from thioacetamide decomposition. Following a similar sonochemical approach, CdS nanoparticles were also homogeneously coated on silica particles (Arul Dhas and Gedanken, 1998).

Zinc sulfide-coated polystyrene core–shell particles for use in photonic crystals were prepared by Breen et al. (2001). The deposition process was the same as above, except that carboxyl-modified polystyrene microspheres were employed instead of silica. The resulting particles were "optically hollow," due to a large refractive index contrast between the core and shell materials. Continuous, uniform films were also obtained after 3–4 h and reached a maximum thickness of 70–80 nm after 13 h of growth.

3.8.7 Fe–FeC Nanocrystalline Particles

Nikitenko et al. (2001) reported an in situ method for the coating of iron carbide and carbon on Fe nanoparticles to confer air stability. The coated samples were prepared by the sonolysis of $[Fe(CO)_5]$ in diphenylmethane (DPhM) followed by annealing of the as-prepared material. The sonolysis of DPhM formed a polymer-like solid product, which then coated the surface of iron nanoparticles. After annealing, the polymer-like solid formed carbon or iron carbide on the surface. The nanocrystalline particles exhibited strong resistance to oxidation with oxygen and the saturation magnetization of the prepared material was almost as high as that of bulk bcc iron.

3.9 Chalcogenides

Semiconductor selenides and sulfides have found application as sensors, laser materials, optical filters, and solar cells. Therefore, the synthesis of metal chalcogenide semiconductors has received intense attention. For implementation of these semiconductor nanomaterials in functional devices, preparation of metal chalcogenide particles with desired size and morphology is essential. Following are the examples mainly focused on the preparation of nanosized metal chalcogenides using sonochemistry.

3.9.1 Pb Chalcogenides

Ag_2Se, CuSe, and PbSe were prepared by irradiating the mixtures of $AgNO_3$, CuI, or $PbCl_2$ with selenium in ethylenediamine (en) with ultrasound (Li et al., 1999).

The authors observed that the formed products were orthorhombic Ag_2Se, hexagonal CuSe, and cubic PbSe, respectively, and all were well crystallized in nanometers. A similar procedure further led to the synthesis of nanocrystalline lead chalcogenides PbE (E = S, Se, Te) by the reaction of $Pb(CH_3COO)_2{\cdot}3H_2O$ and elemental chalcogens in ethylenediamine (en) under ultrasonic irradiation by Li et al. (2003). The solubility of chalcogen in en was found to be the key factor of the reaction. Ultrasonic irradiation favors the dissolution of chalcogens and the formation of E^{2-} and hence accelerates the formation of PbE.

3.9.2 ZnSe Nanoparticles

A general procedure for the synthesis of metal sulfides and selenides was reported by Zhu et al. (2000). According to this method, the sonochemical decomposition of selenourea or thiourea in water generates H_2Se or H_2S, which then reacts with the metal ions, forming the respective chalcogenides. It is believed that the sonochemical reaction occurs within the interfacial region of the bubbles, yielding nanoparticles because of the very high cooling rate experienced by the products. For example, in this study, ZnSe nanoparticles of about 3 nm in size were prepared by the sonochemical irradiation of an aqueous solution of selenourea and zinc acetate under argon.

3.9.3 Copper Chalcogenide Nanoparticles

Applying ultrasound irradiation (23 kHz, 200 W cm^{-2}) into sulfur powder and copper nitrate in ethylenediamine solvent mixed with a complexing agent of 1-decanethiol results in the formation of non-stoichiometric Cu_7S_4 nanocrystallites of 20 nm in size (Behboudnia and Khanbabaee, 2007). Ethylenediamine is easily decomposed by ultrasonic waves and with sulfur it forms H_2S. The complex formed by 1-decanthiol with copper nitrate then reacts with H_2S to produce Cu_7S_4 nanoparticles under ultrasound.

3.9.4 HgS and PbS Nanoparticles

HgS and PbS nanoparticles of about 15 and 20 nm in size were prepared by Zhu et al. (2000). The sonochemical method is similar to the above method, except that the ultrasonic irradiation was accomplished with a lower frequency ultrasonic probe (20 Hz, 60 W/cm^2). It has been reported that different concentrations of 1-decanethiol can affect particle size. For example, in the case of PbS, higher concentrations of thiol have led to smaller particles.

3.9.5 CdS Nanoparticles

Cadmium sulfide (CdS) nanoparticles of about 3 nm in diameter were prepared by the sonochemical reduction of a mixed solution of cadmium chloride ($CDCl_2$),

sodium thiosulfate ($Na_2S_2O_3$), and isopropyl alcohol ($(CH_3)_2CHOH$) in Ar atmosphere at room temperature (Wang et al., 2001). The alcohol generated a highly reducing radical ($(CH_3)_2(OH)C^{\cdot}$), which rapidly reacted with $S_2O_3^{2-}$ ions to form S^{2-} ions and S^{2-} ions combined with Cd^{2+} to yield CdS nanoparticles.

Jiana and Gao (2006) followed an ultrasound activation liquid–liquid (water and cyclohexane) two-phase approach for the preparation of CdS nanocrystals. According to the proposed mechanism, the sodium borohydride present in water reacts with Cd(II) source to achieve active Cd(0) at the water–cyclohexane interface under ultrasound activation. The simultaneous activation of sulfur source in the cyclohexane solvent allows it to react with the active Cd(0), resulting in the formation of a large amount of nuclei at the water–cyclohexane interface. The nuclei further develop to form CdS nanocrystals wrapped by the organic amine surfactants. Scale-up synthesis could also be achieved through simply enlarging the reaction vessels and multiplying the reaction sources. In addition, preparation of Au/CdS nanocomposites was also realized by the same method.

3.9.6 Metal Chalcogenides with Hollow Spherical Assembly

A hollow spherical assembly composed of CdSe nanoparticles was synthesized via a sonochemical route by Zhu et al. (2003). In this study, $Cd(OH)_2$ acted as the in situ template that directed the final formation of the structure. Following the above procedure the same group (Xu et al., 2004) fabricated a series of nanoscale metal chalcogenides in the form of well-defined hollow spherical assemblies with well-controlled dimensions. The authors proposed that initially metal hydroxide particles generated in situ self-assemble into spherical templates, and the subsequent surface crystal growth leads to hollow spherical structures. Ultrasound irradiation plays a critical role both in the formation of the intermediate templates and in the crystal-growth process. This approach provides a convenient and efficient one-step pathway to the large-scale fabrication of hollow spherical nanostructures.

The use of bacterium as a sacrificial template with the assistance of sonochemistry for the one-step in situ synthesis of hollow nanostructures of ZnS was carried out by Zhou et al. (2007) at room temperature. Sonochemically produced ZnS nanoparticles first deposit onto cell surfaces based on the interaction between functional groups of cell surfaces and the precursors under sonochemical conditions. The surface ZnS further act as a nucleating site for the adhesion of ZnS formed in the bulk solution. In the last step, cell disruption under sonication or cell division takes place and the fragments are released from the porous ZnS shells, leaving the ZnS shells as hollow spheres.

PbS hollow nanospheres with diameters of 80–250 nm were also synthesized by a surfactant-assisted sonochemical route by Wang et al. (2006). According to the authors, the effect of ultrasound leads to self-aggregation of sodium dodecylbenzenesulfonate (DBS) surfactant molecules to form vesicle structures followed by the growth of PbS nanoparticles on the vesicle surface. The wall of the hollow spheres is composed of PbS nanoparticles with diameters of about 12 nm.

3.10 Other Nanomaterials

3.10.1 Metal Phosphides

A novel sonochemical method for the preparation of MP (M = Ga, In) nanocrystalline materials was developed by Li and Casadonte (2007). The procedure consists of an in situ synthesis of sodium phosphide and its subsequent reaction with the appropriate metal chloride using ultrasound. The phosphides are produced as an agglomerate of nanoparticles with an average size of 6–10 nm. The authors found that the choice of solvent and the use of high-power ultrasound are both important in the formation of the products.

3.10.2 Hydroxyapatite (HAP)

Stable hydroxyapatite (HAP) nanoparticles were synthesized from $Ca(H_2PO_4)_2$ aqueous solution and saturated $Ca(OH)_2$ aqueous solution by an improved precipitation method under ultrasound. Glycosaminoglycans (GAGs), which are known to have strong interaction with HAP, were used as an additive. The GAGs concentration influenced the particle size, the size distribution, and the zeta potential of nanoparticles by inhibiting the crystal growth and thereby stabilizing HAP nanoparticles. With an increase in irradiation time, better crystallinity of nanoparticles was achieved (Han et al., 2007).

3.10.3 Nanotubes

A sonochemical method of producing carbon nanotubes was reported by Katoh et al. (1999). This method was achieved by applying ultrasound to liquid chlorobenzene with $ZnCl_2$ particles or to *o*-dichlorobenzene with $ZnCl_2$ and Zn particles. It has been considered that the polymer and the disordered carbon, which are formed from the organic liquid by cavitational collapse, are annealed by the interparticle collision of the solids ($ZnCl_2$ and Zn) induced by the turbulent flow and shock waves.

Jeong et al. (2004) proposed another sonochemical route to prepare single-walled carbon nanotubes (SWNTs). Sonication of silica powder immersed in a mixture of ferrocene and *p*-xylene at atmospheric pressure and room temperature, resulted in high-purity SWCNTs. Although details of SWCNT growth mechanism are still under investigation, it was thought that the sonochemical treatment could both facilitate decomposition of ferrocene and *p*-xylene and provide the required energy to synthesize SWCNTs from these decomposed products. The process could be further utilized to synthesize other forms of carbon-based materials, such as fullerenes, multi-walled nanotubes, carbon onions, and diamond, in liquid solution under ambient conditions.

3.10.4 Nanowires

A sonochemical route was exploited by Gates et al. (2002) for the large-scale synthesis of uniform nanowires made up of trigonal selenium (t-Se). It has been proposed

that the hot spots generated due to ultrasonic cavitation cause local fluctuation in the solubility of selenium and thus induce the formation of nanometer-sized seeds of t-Se in an alcohol suspension containing amorphous selenium (a-Se) colloids. A complete solid–solution–solid transformation from amorphous to trigonal phase was achieved with 100% yield within several hours. Moreover, the nanowires could be prepared as either suspensions in alcohols or interwoven 2D arrays supported on solid substrates. Figure 15.14 shows the TEM image of the sonochemically synthesized t-Se.

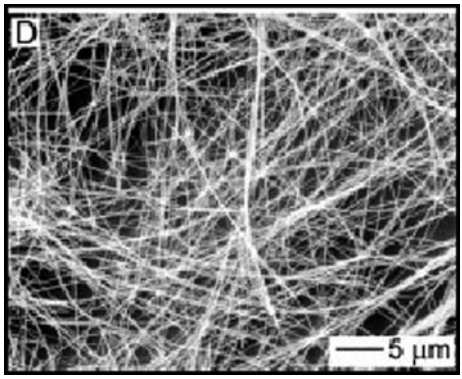

Fig. 15.14 t-Se with uniform diameter (40 ± 7 nm) (SEM image)

4 Conclusions

There is increasing interest in the sonochemical methodology to prepare nanomaterials, and this interest has led to new developments made by many researchers currently experimenting in this exciting field. Given the space constraint, in this chapter we have tried to cover the most relevant contributions. Using the ultrasonic cavitation approach, synthesis of a variety of nanosized particles has been possible with flexibility for controlling the size, shape, and structure of the nanocrystals. In the ultrasonic cavitational preparation of nanoparticles, the following parameters are very important: (a) frequency; (b) power intensity; (c) power density; (d) gas atmosphere; (e) additives; (f) reaction temperature; (g) concentration of the reactants; and (h) reaction time, and all of these parameters should be considered with intense care. This sonochemical protocol confers distinct advantages and opens up many possibilities for conducting rapid synthesis in an efficient and eco-friendly manner. The only problem that exists at present with this technique is "scale-up." One of the reasons for this problem is that the ultrasonic field generated is not uniform in large-scale reactors. It is also not possible to transmit an intense cavitation field more than 2–5 cm beyond the end of the probe due to geometric losses and acoustic decoupling problems. But, with the advent of collaborative research between chemical, mechanical, and electrical engineers with physicists and chemists it is expected to bring about modifications for the production scale-up. There are now reports on multiperturbation techniques in sonochemistry which include the use of

simultaneous microwave and ultrasound irradiation. The emergence of sonoelectrochemistry has also been crucial for efficient production of nanomaterials. Thus, looking at the variety of possibilities for improvement and the potential diverse nanomaterials obtained, there is no doubt that ultrasonic cavitation will be recognized as a key enabling synthesis technique, and it is expected to see a tremendous growth in the near future.

Acknowledgments We would like to thank Prof. Aharon Gedanken, Bar-Ilan University, Israel; Dr. Iida, Dr. Yasui, Dr. Tuziuti, Dr. Towata, and Dr. Kozuka, Ultrasonic Processing Group of National Institute of Advanced Industrial Science and Technology (AIST), Nagoya, Japan; Prof. Pandit and Dr. Gogate, Department of Chemical Engineering, University Institute of Chemical Technology (UICT), India; Prof. Ethirajulu, Director of BIT, Tiruchirappalli; Prof. Ruckmani and other faculty colleagues at Anna University, Tiruchirappalli, India; the nanomaterials group at Indian Institute of Chemical Technology, Hyderabad, India and the faculty colleagues of Department of Chemical and Environmental Engineering at University of Nottingham for all their support in completing this chapter.

References

Anand, K. A., Agarwal, U. S., Nisal, A., and Joseph, R. (2007). PET-SWNT nanocomposites through ultrasound assisted dissolution-evaporation. *European Polymer Journal*, 43(6), 2279–2285.

Arul Dhas, N., and Gedanken, A. (1998). A sonochemical approach to the surface synthesis of cadmium sulfide nanoparticles on submicron silica. *Applied Physics Letters*, 72(20), 2514–2516.

Arul Dhas, N., Zaban, A., and Gedanken, A. (1999). Surface synthesis of zinc sulfide nanoparticles on silica microspheres: Sonochemical preparation, characterization, and optical properties. *Chemistry of Materials*, 11(3), 806–813.

Atobe, M., Chowdhury, A.-N., Fuchigami, T., and Nonaka, T. (2003). Preparation of polyaniline colloids under ultrasonication. *Ultrasonics Sonochemistry*, 10(2), 77–80.

Bang, J. H., and Suslick, K. S. (2007). Sonochemical synthesis of nanosized hollow hematite. *Journal of the American Chemical Society*, 129(8), 2242–2243.

Bedrane, S., Descorme, C., and Duprez, D. (2002). An optimized route for the preparation of well dispersed supported ruthenium catalysts. *Journal of Materials Chemistry*, 12, 1563–1567.

Behboudnia, M., and Khanbabaee, B. (2007). Investigation of nanocrystalline copper sulfide Cu_7S_4 fabricated by ultrasonic radiation technique. *Journal of Crystal Growth*, 304(1), 158–162.

Breen, M. L., Dinsmore, A. D., Pink, R. H., Qadri, S. B., and Ratna, B. R. (2001). Sonochemically produced ZnS-coated polystyrene core-shell particles for use in photonic crystals. *Langmuir*, 17(3), 903–907.

Caruso, R. A., Ashokkumar, M., and Grieser, F. (2000). Sonochemical formation of colloidal platinum. *Colloids and Surfaces A: Physicochemical and Engineering Aspects*, 169(1–3), 219–225.

Caruso, R. A., Ashokkumar, M., and Grieser, F. (2002). Sonochemical formation of gold sols. *Langmuir*, 18(21), 7831–7836.

Chen, J.-J., Yang, H.-B., Chang, L.-X., Fu, W.-Y., Zeng, Y., Zhu, H.-Y., and Zou, G.-T. (2007). Sonochemical preparation and characterization of photochromic MoO_3 nanoparticles. *Frontiers of Physics in China*, 2(1), 92–95.

Dhas, N. A., and Suslick, K. S. (2005). Sonochemical preparation of hollow nanospheres and hollow nanocrystals. *Journal of the American Chemical Society*, 127(8), 2368–2369.

Dhas, N. A., Raj, C. P., and Gedanken, A. (1998). Synthesis, characterization, and properties of metallic copper nanoparticles. *Chemistry of Materials*, 10(5), 1446–1452.

Erasmus, W. J., and van Steen, E. (2007). Some insights in the sonochemical preparation of cobalt nano-particles. *Ultrasonics Sonochemistry*, 14(6), 732–738.

Fu, G., Cai, W., Kan, C., Li, C., and Fang, Q. (2003). Optical study of the ultrasonic formation process of noble metal nanoparticles dispersed inside the pores of monolithic mesoporous silica. *Journal of Physics D: Applied Physics*, 36(12), 1382–1387.

Fujimoto, T., Terauchi, S., Umehara, H., Kojima, I., and Henderson, W. (1998). Formation of platinum and palladium bimetallic superfine particles by ultrasonic irradiation. *Materials Research Society Symposium – Proceedings*, 497, 129–134.

Fujimoto, T., Terauchi, S.-Y., Umehara, H., Kojima, I., and Henderson, W. (2001). Sonochemical preparation of single-dispersion metal nanoparticles from metal salts. *Chemistry of Materials*, 13(3), 1057–1060.

Gates, B., Mayers, B., Grossman, A., and Xia, Y. (2002). A sonochemical approach to the synthesis of crystalline selenium nanowires in solutions and on solid supports. *Advanced Materials*, 14(23), 1749–52.

Gedanken, A. (2004). Using sonochemistry for the fabrication of nanomaterials, *Ultrasonics Sonochemistry*, 11(2), 47–55.

Gedanken, A. (2007). Doping nanoparticles into polymers and ceramics using ultrasound radiation. *Ultrasonics Sonochemistry*, 14(4), 418–430.

Guo, W., Lin, Z., Wang, X., and Song, G. (2003). Sonochemical synthesis of nanocrystalline TiO_2 by hydrolysis of titanium alkoxides. *Microelectronic Engineering*, 66(1–4), 95–101.

Hadad, L., Perkas, N., Gofer, Y., Calderon-Moreno, J., Ghule, A., and Gedanken, A. (2007). Sonochemical deposition of silver nanoparticles on wool fibers. *Journal of Applied Polymer Science*, 104(3), 1732–1737.

Han, Y., Li, S., Wang, X., Bauer, I., and Yin, M. (2007). Sonochemical preparation of hydroxyapatite nanoparticles stabilized by glycosaminoglycans. *Ultrasonics Sonochemistry*, 14(3), 286–290.

He, Y., Vinodgopal, K., Ashokkumar, M., and Grieser, F. (2006). Sonochemical synthesis of ruthenium nanoparticles. *Research on Chemical Intermediates*, 32(8), 709–715.

Jeong, S.-H., Ko, J.-H., Park, J.-B., and Park, W. (2004). A sonochemical route to single-walled carbon nanotubes under ambient conditions. *Journal of the American Chemical Society*, 126(49), 15982–15983.

Jiana, D., and Gao, Q. (2006). Synthesis of CdS nanocrystals and Au/CdS nanocomposites through ultrasound activation liquid–liquid two-phase approach at room temperature. *Chemical Engineering Journal*, 121(1), 9–16.

Jothi Rajan, M. A., Mathavan, T., Ramasubbu, A., Thaddeus, A., Fragrance Latha, V., Vivekanandam, T. S., and Umapathy, S. (2006). Thermal properties of PMMA/Montmorillonite clay nanocomposites. *Journal of Nanoscience and Nanotechnology*, 6(12), 3993–3996.

Kabir, Md. E., Saha, M. C., and Jeelani, S. C. (2007). Effect of ultrasound sonication in carbon nanofibers/polyurethane foam composite. *Materials Science and Engineering A*, 459(1–2), 111–116.

Katoh, R., Tasaka, Y., Sekreta, E., Yumura, M., Ikazaki, F., Kakudate, Y., and Fujiwara, S. (1999). Sonochemical production of a carbon nanotube. *Ultrasonics Sonochemistry*, 6(4), 185–187.

Krishnan, C. V., Chen, J., Burger, C., and Chu, B. (2006). Polymer-assisted growth of molybdenum oxide whiskers via a sonochemical process. *Journal of Physical Chemistry B*, 110(41), 20182–20188.

Kumar, R. V., Koltypin, Yu., Palchik, O., and Gedanken, A. (2002). Preparation and characterization of nickel-polystyrene nanocomposite by ultrasound irradiation. *Journal of Applied Polymer Science*, 86(1, 3), 160–165.

Kumar, V. G., and Kim, K. B. (2006). Organized and highly dispersed growth of MnO_2 nano-rods by sonochemical hydrolysis of Mn(3)acetate. *Ultrasonics Sonochemistry*, 13(6), 549–556.

Lapshin, S., and Isayev, A. I. (2005). Continuous process for melt intercalation of PP-clay nanocomposites with aid of power ultrasound. *Annual Technical Conference – ANTEC* (Conference Proceedings), 5, 239–243.

Li, B., Xie, Y., Huang, J., and Qian, Y. (1999). Sonochemical synthesis of silver, copper and lead selenides. *Ultrasonics Sonochemistry*, 6(4), 217–220.

Li, B., Zhao, Y., Xu, X., Zhou, H., He, B., Wu, Z., and Zhang, Z. (2007). A simple method for the preparation of containing Sb nano- and microcrystallines via an ultrasound agitation, *Ultrasonics Sonochemistry*, 14(5), 557–562.

Li, D.-S., Wang, Y.-Y., Liu, P., Wang, W.-L., and Shi, Q.-Z. (2005). Preparation of nanosized γ-MnO_2 by precipitation under ultrasound radiation. *Chinese Journal of Inorganic Chemistry*, 21(2), 202–206.

Li, H., Wang, R., Hong, Q., Chen, L., Zhong, Z., Koltypin, Y., Calderon-Moreno, J., and Gedanken, A. (2004). Ultrasound-assisted polyol method for the preparation of SBA-15-supported ruthenium nanoparticles and the study of their catalytic activity on the partial oxidation of methane. *Langmuir*, 20(19), 8352–8356.

Li, Q., Ding, Y., Shao, M., Wu, J., Yu, G., and Qian, Y. (2003). Sonochemical synthesis of nanocrystalline lead chalcogenides: PbE (E = S, Se, Te). *Materials Research Bulletin*, 38(3), 539–543.

Li, Z., and Casadonte, D. J., Jr. (2007). Facile sonochemical synthesis of nanosized InP and GaP. *Ultrasonics Sonochemistry*, 14(6), 757–760.

Mao, C.-J., Pan, H.-C., Wu, X.-C., Zhu, J.-J., and Chen, H.-Y. (2006). Sonochemical route for self-assembled V_2O_5 bundles with spindle-like morphology and their novel application in serum albumin sensing. *Journal of Physical Chemistry B*, 110 (30), 14709–14713.

Meskin, P. E., Ivanov, V. K., Barantchikov, A. E., Churagulov, B. R., and Tretyakov, Y. D. (2006). Ultrasonically assisted hydrothermal synthesis of nanocrystalline ZrO_2, TiO_2, $NiFe_2O_4$ and $Ni_{0.5}Zn_{0.5}Fe_2O_4$ powders. *Ultrasonics Sonochemistry*, 13(1), 47–53.

Mizukoshi, Y., Okitsu, K., Maeda, Y., Yamamoto, T. A.., Oshima, R., and Nagata, Y. (1997). Sonochemical preparation of bimetallic nanoparticles of gold/palladium in aqueous solution. *Journal of Physical Chemistry B*, 101(36), 7033–7037.

Mizukoshi, Y., Oshima, R., Maeda, Y., and Nagata, Y. (1999). Preparation of platinum nanoparticles by sonochemical reduction of the Pt(II) ion. *Langmuir*, 15(8), 2733–2737.

Mizukoshi, Y., Takagi, E., Okuno, H., Oshima, R., Maeda, Y., and Nagata, Y. (2001). Preparation of platinum nanoparticles by sonochemical reduction of the Pt(IV) ions: Role of surfactants. *Ultrasonics Sonochemistry*, 8(1), 1–6.

Mizukoshi, Y., Seino, S., Okitsu, K., Kinoshita, T., Otome, Y., Nakagawa, T., and Yamamoto, T. A. (2005). Sonochemical preparation of composite nanoparticles of Au/γ-Fe_2O_3 and magnetic separation of glutathione. *Ultrasonics Sonochemistry*, 12(3), 191–195.

Mizukoshi, Y., Makise, Y., Shuto, T., Hu, J., Tominaga, A., Shironita, S., and Tanabe, S. (2007). Immobilization of noble metal nanoparticles on the surface of TiO_2 by the sonochemical method: Photocatalytic production of hydrogen from an aqueous solution of ethanol. *Ultrasonics Sonochemistry*, 14(3), 387–392.

Mori, Y., Kitamoto, N., and Tsuchiya, K. (2005). Effect of kind of alcohols as additives on preparation of gold nanoparticles by sonochemistry. *Journal of Chemical Engineering of Japan*, 38(4), 283–288.

Nagao, D., Shimazaki, Y., Saeki, S., Kobayashi, Y., and Konno, M. (2007). Effect of ultrasonic irradiation on carbon-supported Pt-Ru nanoparticles prepared at high metal concentration. *Colloids and Surfaces A: Physicochemical and Engineering Aspects*, 302(1–3), 623–627.

Nagata, Y., Mizukoshi, Y., Okitsu, K., and Maeda, Y. (1996). Sonochemical formation of gold particles in aqueous solution. *Radiation Research*, 146(3), 333–338.

Nemamcha, A., Rehspringer, J.-L., and Khatmi, D. (2006). Synthesis of palladium nanoparticles by sonochemical reduction of palladium(II) nitrate in aqueous solution. *Journal of Physical Chemistry B*, 110(1), 383–387.

Nikitenko, S. I., Koltypin, Y., Palchik, O., Felner, I., Xu, X. N., and Gedanken, A. (2001). Synthesis of highly magnetic, air-stable iron-iron carbide nanocrystalline particles by using power ultrasound. *Angewandte Chemie*, 40(23), 4447–4449.

Okitsu, K., Ashokkumar, M., and Grieser, F. (2005). Sonochemical synthesis of gold nanoparticles: Effects of ultrasound frequency. *Journal of Physical Chemistry B*, 109(44), 20673–20675.

Okitsu, K., Mizukoshi, Y., Bandow, H., Maeda, Y., Yamamoto, T., and Nagata, Y. (1996). Formation of noble metal particles by ultrasonic irradiation. *Ultrasonics Sonochemistry*, 3(3), S249-S251.

Okitsu, K., Mizukoshi, Y., Bandow, H., Yamamoto, T. A., Nagata, Y., and Maeda, Y. (1997). Synthesis of palladium nanoparticles with interstitial carbon by sonochemical reduction of tetrachloropalladate(II) in aqueous solution. *Journal of Physical Chemistry B*, 101(28), 5470–5472.

Okitsu, K., Nagaoka, S., Tanabe, S., Matsumoto, H., Mizukoshi, Y., and Nagata, Y. (1999). Sonochemical preparation of size-controlled palladium nanoparticles on alumina surface. *Chemistry Letters*, 3 271–272.

Okitsu, K., Yue, A., Tanabe, S., and Matsumoto, H. (2000). Sonochemical preparation and catalytic behavior of highly dispersed palladium nanoparticles on alumina. *Chemistry of Materials*, 12(10), 3006–3011.

Okitsu, K., Yue, A., Tanabe, S., Matsumoto, H., and Yobiko, Y. (2001). Formation of colloidal gold nanoparticles in an ultrasonic field: Control of rate of gold(III) reduction and size of formed gold particles. *Langmuir*, 17(25), 7717–7720.

Okitsu, K., Yue, A., Tanabe, S., Matsumoto, H., Yobiko, Y., and Yoo, Y. (2002). Sonolytic control of rate of gold(III) reduction and size of formed gold nanoparticles: Relation between reduction rates and sizes of formed nanoparticles. *Bulletin of the Chemical Society of Japan*, 75(10), 2289–2296.

Osawa, S., Ito, M., Tanaka, K., and Kuwano, J. (1987). Electrochemical polymerization of thiophene under ultrasonic field. *Synthetic Metals*, 18, 145–150.

Park, J.-E., Atobe, M., and Fuchigami, T. (2005). Sonochemical synthesis of conducting polymer-metal nanoparticles nanocomposite. *Electrochimica Acta*, 51(5), 849–854.

Perkas, N., Wang, Y., Koltypin, Y., Gedanken, A., and Chandrasekaran, S. (2001). Mesoporous iron-titania catalyst for cyclohexane oxidation. *Chemical Communications*, 11, 988–989.

Perkas, N., Amirian, G., Dubinsky, S., Gazit, S., and Gedanken, A. (2007). Ultrasound-assisted coating of nylon 6,6 with silver nanoparticles and its antibacterial activity. *Journal of Applied Polymer Science*, 104(3), 1423–1430.

Pol, V. G., Gedanken, A., and Calderon-Moreno, J. (2003). Deposition of gold nanoparticles on silica spheres: A sonochemical approach. *Chemistry of Materials*, 15(5), 1111–1118.

Pol, V. G., Srivastava, D. N., Palchik, O., Palchik, V., Slifkin, M. A., Weiss, A. M., and Gedanken, A. (2002). Sonochemical deposition of silver nanoparticles on silica spheres. *Langmuir*, 18(8), 3352–3357.

Qiu, G., Wang, Q., Wang, C., Lau, W., and Guo, Y. (2006). Ultrasonically initiated miniemulsion polymerization of styrene in the presence of Fe_3O_4 nanoparticles. *Polymer International*, 55(3), 265–272.

Qiu, G., Wang, Q., Wang, C., Lau, W., and Guo, Y. (2007). Polystyrene/Fe_3O_4 magnetic emulsion and nanocomposite prepared by ultrasonically initiated miniemulsion polymerization. *Ultrasonics Sonochemistry*, 14(1), 55–61.

Ramesh, S., Koltypin, Y., Prozorov, R., and Gedanken, A. (1997). , Sonochemical deposition and characterization of nanophasic amorphous nickel on silica microspheres. *Chemistry of Materials*, 9(2), 546–551.

Rana, R. K., Mastai, Y., and Gedanken, A. (2002). Acoustic cavitation leading to the morphosynthesis of mesoporous silica vesicles. *Advanced Materials*, 14(19) 1414–1418.

Rana, R. K., Zhang, L., Yu, J. C., Mastai, Y., and Gedanken, A. (2003). Mesoporous structures from supramolecular assembly of in situ generated ZnS nanoparticles. *Langmuir*, 19(14), 5904–5911.

Seo, W. J., Sung, Y. T., Kim, S. B., Lee, Y. B., Choe, K. H., Choe, S. H., Sung, J. Y., and Kim, W. N. (2006). Effects of ultrasound on the synthesis and properties of polyurethane foam/clay nanocomposites. *Journal of Applied Polymer Science*, 102(4), 3764–3773.

Sivakumar, M., and Gedanken, A. (2004). Insights into the sonochemical decomposition of $Fe(CO)_5$: Theoretical and experimental understanding of the role of molar concentration and power density on the reaction yield. *Ultrasonics Sonochemistry*, 11(6), 373–378.

Sivakumar, M., Gedanken, A., Bhattacharya, D., Brukental, I., Yeshurun, Y., Zhong, W., Du, Y. W., Felner, I., and Nowik, I. (2004a). Distinctive and multiadvantageous sonochemical method for the synthesis of nanocrystalline rare earth ferrites using a novel $Fe(CO)_5$ precursor. *Chemistry of Materials*, 16, 3623–32.

Sivakumar, M., Gedanken, A., Zhong, W., Du, Y. W., Bhattacharya, D., Yeshurun, Y., and Felner, I. (2004b). Nanophase formation of strontium hexaferrite fine powder by the sonochemical method using $Fe(CO)_5$. *Journal of Magnetism and Magnetic Materials*, 268(1–2), 95–104.

Sivakumar, M., Gedanken, A., Zhong, W., Jiang, Y. H., Du, Y. W., Brukental, I., Bhattacharya, D., Yeshurun, Y., and Nowik, I. (2004c). Sonochemical synthesis of nanocrystalline $LaFeO_3$. *Journal of Materials Chemistry*, 14(4), 764–769.

Sivakumar, M., and Gedanken, A. (2005). A sonochemical method for the synthesis of polyaniline and Au-polyaniline composites using H_2O_2 for enhancing rate and yield. *Synthetic Metals*, 148, 301–306.

Sivakumar, M., and Gedanken, A. (2006). Acoustic cavitation – An efficient tool to synthesize nanosized CuO-ZrO_2 catalysts with mesoporous distribution. *New Journal of Chemistry*, 30(1), 102–107.

Sivakumar, M., Takami, T., Ikuta, H., Bhattacharya, D., Yasui, K., Towata, A., Tuziuti, T., and Iida, Y. (2006a). Fabrication of zinc ferrite nanocrystals by sonochemical activation – Observation of magnetization and its relaxation at low temperature. *Journal of Physical Chemistry B*, 110(31), 15234–15243.

Sivakumar, M., Towata, A., Yasui, K., Tuziuti, T., and Iida, Y. (2006b). Ultrasonic cavitational activation: A simple and feasible route for the direct conversion of zinc acetate to highly monodispersed ZnO. *Chemistry Letters*, 35 (1), 60–61.

Sivakumar, M., Yasui, K., Towata, A., Tuziuti, T., and Iida, Y. (2006c). A new ultrasonic cavitation approach for the synthesis of zinc ferrite nanocrystals. *Current Applied Physics*, 6(3), 591–593.

Sivakumar, M., Towata, A., Yasui, K., Tuziuti, T., Kozuka, T., Tsujimoto, M., Zhong, Z., and Iida, Y. (2010). Fabrication of Nanosized Pt on rutile TiO_2 using a standing wave sonochemical reactor (SWSR) – Observation of an enhanced catalytic oxidation of CO. *Ultrasonics Sonochemistry,* 17, 213–218.

Suslick, K. S. (1998). *Sonochemistry – in Kirk-Othmer encyclopedia of chemical technology*, Vol. 26, 4th edn, pp. 517–541. New York, NY, Wiley.

Suslick, K. S., and Price, G. J. (1999). Applications of ultrasound to materials chemistry. *Annual Review of Materials Science*, 29, 295–326.

Suslick, K. S., Fang, M., and Hyeon, T. (1996). Sonochemical synthesis of iron colloids. *Journal of the American Chemical Society*, 118(47), 11960–11961.

Suslick, K. S., Hyeon, T., and Fang, M. (1996). Nanostructured materials generated by high-intensity ultrasound: Sonochemical synthesis and catalytic studies. *Chemistry of Materials*, 8(8), 2172–2179.

Suslick, K. S., Hyeon, T., Fang, M., and Cichowlas, A. A. (1995). Sonochemical synthesis of nanostructured catalysts. *Materials Science and Engineering A*, A204(1–2), 186–192.

Wang, S. F., Gu, F., and Lu, M. K. (2006). Sonochemical synthesis of hollow PbS nanospheres. *Langmuir*, 22(1), 398–401.

Wang, G. Z., Chen, W., Liang, C. H., Wang, Y. W., Meng, G. W., and Zhang, L. D. (2001). Preparation and characterization of CdS nanoparticles by ultrasonic irradiation. *Inorganic Chemistry Communications*, 4(4), 208–210.

Wang, Y., Tang, X., Yin, L., Huang, W., Hacohen, Y. R., and Gedanken, A. (2000). Sonochemical synthesis of mesoporous titanium oxide with wormhole-like framework structures. *Advanced Materials*, 12(16), 1183–1186.

Wizel, S., Margel, S., and Gedanken, A. (2000). The preparation of a polystyrene-iron composite by using ultrasound radiation. *Polymer International*, 49(5), 445–448.

Xia, H., and Wang, Q. (2001). Synthesis and characterization of conductive polyaniline nanoparticles through ultrasonic assisted inverse microemulsion polymerization, *Journal of Nanoparticle Research*, 3, 401–411.

Xia, H., and Wang, Q. (2003). Preparation of conductive polyaniline/nanosilica particle composites through ultrasonic irradiation. *Journal of Applied Polymer Science*, 87(11), 1811–1817.

Xia, H., Wang, Q., and Qiu, G. (2003). Polymer-encapsulated carbon nanotubes prepared through ultrasonically initiated in situ emulsion polymerization. *Chemistry of Materials*, 15(20), 3879–3886.

Xia, X. H., Luo, Y. S., Wang, Z., Liang, Y., Fan, J., Jia, Z. J., and Chen, Z. H. (2007). Ultrasonic synthesis and photocatalytic activity investigation of TiO_2 nanoarrays. *Materials Letters*, 61(11–13), 2571–2574.

Xie, R., Li, D., Yang, D., and Jiang, M. (2007). Surface synthesis of PbS nanoparticles on silica spheres by a sonochemical approach. *Journal of Materials Science*, 42(4), 1376–1380.

Xu, S., Wang, H., Zhu, J.-J., Xin, X.-Q., and Chen, H.-Y. (2004). An in situ template route for fabricating metal chalcogenide hollow spherical assemblies sonochemically. *Journal of Inorganic Chemistry*, 23, 4653–4659.

Yao, S.-Y., and Xie, Z.-H. (2007). Deagglomeration treatment in the synthesis of doped-ceria nanoparticles via coprecipitation route. *Journal of Materials Processing Technology*, 186(1–3), 54–59.

Ye, X., Zhou, Y., Chen, J., and Sun, Y. (2007). Deposition of silver nanoparticles on silica spheres via ultrasound irradiation. *Applied Surface Science*, 253(14), 6264–6267.

Yeung, S. Au., Hobson, R. A., Biggs, S., and Grieser, F. (1993). Formation of gold sols using ultrasound. *Journal of the Chemical Society Chemical Communications*, 4, 378–379.

Zhang, X., Zhao, H., Tao, X., Zhao, Y., and Zhang, Z. (2005). Sonochemical method for the preparation of ZnO nanorods and trigonal-shaped ultrafine particles. *Materials Letters*, 59, 1745–1747.

Zhang, Y.-P., Lee, S.-H., Reddy, K. R., Gopalan, A. I., and Lee, K.-P. (2007). Synthesis and characterization of core-shell SiO_2 nanoparticles/poly(3-aminophenylboronic acid) composites. *Journal of Applied Polymer Science*, 104(4), 2743–2750.

Zhong, Z., Mastai, Y., Koltypin, Y., Zhao, Y., and Gedanken, A. (1999). Sonochemical coating of nanosized nickel on alumina submicrospheres and the interaction between the nickel and nickel oxide with the substrate. *Chemistry of Materials*, 11(9), 2350–2359.

Zhou, H., Fan, T., Zhang, D., Guo, Q., and Ogawa, H. (2007). Novel bacteria-templated sonochemical route for the in situ one-step synthesis of ZnS hollow nanostructures. *Chemistry of Materials*, 19(9), 2144–2146.

Zhou, M., Yu, J., and Cheng, B. (2006). Effects of Fe-doping on the photocatalytic activity of mesoporous TiO_2 powders prepared by an ultrasonic method. *Journal of Hazardous Materials*, 137(3), 1838–1847.

Zhu, J., Koltypin, Y., and Gedanken, A. (2000). General sonochemical method for the preparation of nanophasic selenides: Synthesis of ZnSe nanoparticles. *Chemistry of Materials*, 12(1), 73–78.

Zhu, J., Liu, S., Palchik, O., Koltypin, Y., and Gedanken, A. (2000). A novel sonochemical method for the preparation of nanophasic sulfides: Synthesis of HgS and PbS nanoparticles. *Journal of Solid State Chemistry*, 153(2), 342–348.

Zhu, J.-J., Xu, S., Wang, H., Zhu, J.-M., and Chen, H.-Y. (2003). Sonochemical synthesis of CdSe hollow spherical assemblies via an in-situ template route. *Advanced Materials*, 15(2), 156–159.

Zhu, Y., Li, H., Koltypin, Y., Hacohen, Y. R., and Gedanken, A. (2001). Sonochemical synthesis of titania whiskers and nanotubes. *Chemical Communications*, 24, 2616–2617.

Chapter 16
Power Ultrasound to Process Dairy Products

Daniela Bermúdez-Aguirre and Gustavo V. Barbosa-Cánovas

1 Introduction

Conventional methods of pasteurizing milk involve the use of heat regardless of treatment (batch, high temperature short time – HTST or ultra high temperature – UHT sterilization), and the quality of the milk is affected because of the use of high temperatures. Consequences of thermal treatment are a decrease in nutritional properties through the destruction of vitamins or denaturation of proteins, and sometimes the flavor of milk is undesirably changed. These changes are produced at the same time that the goal of the pasteurization process is achieved, which is to have a microbiological safe product, free of pathogenic bacteria, and to reduce the load of deteriorative microorganisms and enzymes, resulting in a product with a longer storage life.

During the processing of dairy products, milk must be pasteurized under specific conditions in order to achieve the ideal characteristics of flavor, color, or texture for the final product such as yogurt, cheese, or ice cream, while at the same time maintaining the microbiological limits established for these products.

Currently, we have available new alternatives to process food to retain fresh-like characteristics, reducing the loss of quality attributes, but at the same time producing a safe and stable product, with low cost and availability for consumers. One of these emerging technologies is ultrasound (the use of sound waves applied to the food as an alternative to heat) in order to inactivate microorganisms and enzymes while producing minimal changes in the product. Ultrasound technology is not new in food processing; this technology has been widely used, for example, in quality control where high-frequency ultrasound is used as a non-destructive technique. However, the use of ultrasound at low frequencies to promote cell disruption and chemical reactions is now under study, with many favorable results.

G.V. Barbosa-Cánovas (✉)
Biological Systems Engineering Department, Center for Nonthermal Processing of Food, Washington State University, Pullman, WA 99164-6120, USA
e-mail: barbosa@wsu.edu

H. Feng et al. (eds.), *Ultrasound Technologies for Food and Bioprocessing*, Food Engineering Series, DOI 10.1007/978-1-4419-7472-3_16,
© Springer Science+Business Media, LLC 2011

This chapter will focus on the use of ultrasound at low frequency (also called power ultrasound) applied to pasteurize and homogenize milk. A brief review of the current progress in the processing of some dairy products such as sonicated cheese and sonicated yogurt will also be included, remarking on the advantages and potential of this technology in the dairy industry.

2 Basic Concepts of Ultrasound Technology

Ultrasound is an emerging technology under research in the food engineering field. There are two broad ranges of application of ultrasound according to the frequency: high frequency uses from 2 to 10 MHz and low-frequency or power ultrasound uses frequencies from 20 to around 100 kHz. The main difference between these technologies is the effect generated in the medium. When ultrasound at high frequency is applied to a food, a non-destructive effect is generated and the different parameters of this technology, such as the attenuation coefficient, relate important information, e.g., the structure or internal properties of the product. However, when the ultrasound is supplied at low frequency, the passage of sound waves through a liquid medium causes the vibration of molecules, generating physical effects into the food. Ultrasound at low frequency is the technique that is used for disruptive purposes.

3 Power Ultrasound

Power ultrasound is responsible for physical disruption in some materials, such as cells, and also for promoting chemical reactions in liquid media. This kind of ultrasound is used in processes in which the breakage of cells or material is required for different goals, such as inactivation of microorganisms, extraction of components from cells or tissues, but also when a chemical reaction must be sped up or stopped, for example, to accelerate or inactivate the enzymatic activity into a food.

Power ultrasound is characterized by the use of low frequencies but high power levels; between 10 and 10,000 W/cm^2 (Carcel et al., 1998). The main effect of power ultrasound is called cavitation, which means the generation of thousands of bubbles during the passage of sound waves through the medium. These bubbles have cycles of implosion and explosion that generate micro-currents; each time bubbles are collapsing important increases in temperature and pressure are produced in the medium. The intensity of the cavitation will depend on the temperature, pressure, amplitude of the ultrasound wave, and media composition, etc.

Specific details of how ultrasound technology works have already been discussed in other chapters; this chapter will focus on how this technology can be applied to the dairy industry and its advantages and disadvantages.

4 Pasteurization of Milk with Power Ultrasound

Pasteurization is used in milk with the main goal of inactivating pathogenic bacteria, reducing the number of deteriorative microorganisms and reducing the enzymatic activity in milk. This food contains a rich medium for bacterial growth; proteins, fat, carbohydrates, minerals, vitamins, and a high percentage of water make it an excellent substrate for growing of bacteria, not only the natural flora but also the pathogenic bacteria that can be in the environment, and a prosperous medium for enzymatic activity (Pelczar and Reid, 1972). However, through time, the concept of pasteurization has changed accordingly with new technologies and the presence of more resistant microorganisms. The original concept of pasteurization was based on the time–temperature relation to inactivate the most heat-resistant pathogen in milk, *Mycobacterium tuberculosis*. However, more than 30 years ago, the relationship of time–temperature changed because of the discovery of a new bacteria that was transmitted to humans via milk ingestion, generating Q fever: *Coxiella burnetii* (Pelczar and Reid, 1972).

Nowadays, pasteurization of milk is also based on some microorganisms that have shown to be more heat resistant and that have been found in the recent infamous outbreaks in the dairy industry. These outbreaks are related not only to the contamination of food after processing and during handling and transportation, but also to inadequate and insufficient thermal treatment conditions during processing. The new emerging pathogens are under study by several techniques, some of them specifically designed to address the microorganisms under consideration. Motarjemi and Adams (2006) briefly define the emerging pathogens, such as the microorganisms that have recently appeared and those that are increasing in incidence. Many foodborne outbreaks have been reported in the food industry (Klima and Montville, 1995; Ko and Grant, 2003; Kozak et al., 1996; Mohan Nair et al., 2005) related to the presence of pathogenic bacteria due to under processing or post-pasteurization contamination. *Listeria monocytogenes* is one of the leading foodborne pathogenic microorganisms generating problems in the food industry, followed by *Salmonella*, *Escherichia coli* 0157:H7, *Clostridium botulinum, Campylobacter*, and *Staphylococcus aureus* (Banasiak, 2005). *L. monocytogenes* was discovered in the early part of the last century, but in the 1980s there was a large increase in the incidence of this microorganism in food, making it now one of the most important food pathogens found in raw and processed meat, dairy products, vegetables, and seafood (McLauchlin, 2006). However, the facilities of the dairy industry are often a good source for *Listeria* contamination; soil, water, and even the cows themselves can transmit the bacteria to unprocessed and processed products.

Several studies have been conducted with ultrasound for the inactivation of bacteria such as *Saccharomyces cerevisiae* (Guerrero et al., 2005; Tsukamoto et al., 2004a, b), *E. coli* (Ananta et al., 2005; Furuta et al., 2004; Ugarte-Romero et al., 2006), *L. monocytogenes* (Mañas et al., 2000; Ugarte-Romero et al., 2007), *Salmonella* (Cabeza et al., 2004), and *Shigella* (Ugarte-Romero et al., 2007) in different media, but only a few have been carried out on milk. Microorganisms such as

S. aureus, *Bacillus subtilis* (Carcel et al., 1998), *Salmonella typhimurium* (Wrigley and Llorca, 1992), *E. coli* (Zenker et al., 2003), *L. monocytogenes* (Earnshaw et al., 1995; Pagán et al., 1999), *Listeria innocua* (Bermúdez-Aguirre and Barbosa-Cánovas, 2008), and total count plate and coliforms (Villamiel et al., 1999) have been tested in sonicated milk.

Results of inactivation studies under sonication are favorable, showing a positive effect of the use of sound waves to inactivate cells. For example, in studies performed with *L. monocytogenes* in skim milk, the decimal reduction value was reduced from 2.1 min ($D_{60°C}$) from thermal treatment to 0.3 min when ultrasound was applied in combination with heat ($D_{60°C\&US}$) (Earnshaw et al., 1995); this treatment is called thermo-sonication. When pressure is used in combination with ultrasound (mano-sonication), important reductions are achieved in the inactivation of *L. monocytogenes* in skim milk. Using ambient pressure and temperature, the decimal reduction value at the processing conditions of ultrasound in this study was 4.3 min; increasing the pressure up to 200 kPa, the *D* value was reduced to 1.5 min; and using twice the previous pressure (400 kPa), the value was 1.0 min. When the temperature was increased above 50ºC, the lethality of ultrasound on *Listeria* cells was enhanced (Pagán et al., 1999).

Zenker et al. (2003) studied the inactivation of *E. coli* K12DH5α in UHT milk using thermal treatment at 60°C and combining the same thermal treatment with ultrasound, reducing the *D* value from 77 to 23 s. These results are examples of the additive effect of the combination between ultrasound and heat, leading to microbial inactivation.

Studies conducted in UHT milk with a surrogate of *L. monocytogenes*, such as *L. innocua* ATCC 51742, showed that the inactivation of cells is possible using thermo-sonication treatments. After 30 min of treatment, almost 5 log reduction is achieved when fat-free milk is used, whereas up to 2.5 log reduction is achieved in whole milk, having intermediate inactivation levels in milk with 1 and 2% butter fat contents (Bermúdez-Aguirre and Barbosa-Cánovas, 2008).

Thermo-sonication has also been useful in extending the shelf life of raw whole milk (Bermúdez-Aguirre et al., 2009) and UHT milk (Bermúdez-Aguirre and Barbosa-Cánovas, 2008) retarding the growth of mesophilic bacteria. In the first case, after pasteurizing raw and whole milk at 63°C using 120 μm of ultrasound (24 kHz) for 30 min, mesophilic growth was lower than 2 log after 16 days at 4°C. Meanwhile, in the second case, after treating UHT milk with thermo-sonication under the same processing conditions mentioned above, the growth of mesophilic bacteria was retarded compared with the control samples regardless of storage temperature (ambient or refrigeration), but with butter fat content being an important factor favoring the growth of bacteria.

It is important to highlight that ultrasound has the capability to pasteurize milk, but not to sterilize it. According to the HHS/PHS/FDA (2001), a pasteurization process is one that inactivates the entire population of pathogenic microorganisms in the milk, whereas sterilization is a process that achieves the inactivation of pathogenic, deteriorative, and spores of microorganisms, using in both cases different time–temperature parameters. Ultrasound, at this moment, regardless of the use

of different temperatures, amplitudes, or pressures, has been shown to be a viable process only to pasteurize some liquid foods.

4.1 Enzymes

Few experiments have been reported in enzyme inactivation with ultrasound on milk. Ultrasound has the ability to accelerate reactions because of an increase in mass transfer (Wang et al., 1996) or to denaturize proteins, stopping or decreasing the enzymatic activity. The main chemical reactions associated with power ultrasound can be classified as generation of free radicals, single electron transfer, and electron transfer catalysis. The generation of free radicals is the mechanism related with denaturation of proteins because of the effect on disulfur bonds (Sinisterra, 1992).

The main studies conducted in enzyme inactivation in milk with ultrasound have been related to its curdling properties. Previous research was conducted to study the activity of clotting enzymes of milk under sonication. Chymosin, pepsin, and fungal enzymes (proteases) were sonicated in milk and buffer solutions, with enzymes from fungi microorganisms showing the highest resistance. As the sonication time was increased, the curdling activity of chymosin decreased and the buffered media showed a protective effect for the enzymatic denaturation. The presence of H_2O_2 was reported in the solutions after sonication because of the action of ultrasound to generate free radicals (Raharintsoa et al., 1977). When raw and reconstituted milk were used as media to test clotting enzymes after sonication, reconstituted milk showed less curdling capacity (Raharintsoa et al., 1978). These were some of the first studies in enzymatic inactivation with ultrasound using 27 kHz; non-pressure or temperature values were reported at this time. However, as ultrasound technology has developed, new variables have been combined to enhance the effect of cavitation. Other studies report the use of ultrasound at 20 kHz, using 25°C for 80 min, finding an increase in the yield and activity of chymosin extraction, reducing the time considerably, and offering an alternative to the high demand of chymosin for the cheese-making industry (Kim and Zayas, 1989). Another example of ultrasound is manothermosonication, which has been applied to study lipoxygenase, peroxidase, polyphenol oxidase, lipase, and protease. Chymosin and pepsin have been studied under sonication with an apparent decrease of the activity in model systems, but when chymosin was mixed with milk, the inactivation was almost null and the change in coagulation time was minimal (Raharintsoa et al., 1978; Villamiel and de Jong, 2000). In general, the proteolytic activity of some enzymes such as chymosin, pepsin, and fungal enzymes decreases with sonication, as reported by Villamiel et al. (1999).

Protease and lipase, which are enzymes related to quality problems during the storage of milk even under refrigerated conditions, have also been studied under manothermosonication. Both enzymes were released from *Pseudomonas fluorescens*, and when ultrasound was applied in combination with temperature

(110–140°C) and pressure (650 kPa), enzyme inactivation was more favorable than when using only heat (Carcel et al., 1998).

4.2 Nutritional Properties

4.2.1 Proteins

Emerging technologies are now a new option to process food, in the specific case of ultrasound it is an option for milk pasteurization. However, in addition to the microbial and enzyme inactivation some aspects related with overall quality should be considered, for example, the possible loss of protein. There are just few reports about the nutritional or physicochemical changes of milk after sonication because it is a new technology.

For example, in skim milk there is an increase of antioxidant activity when the product is subjected to sonication, and this effect is probably because of the action of cavitation in the disruption of the quaternary and tertiary structure of the proteins (Villamiel and de Jong, 2000). Disruption of the casein micelles in milk during sonication increases the real concentration of casein in milk and has an important antioxidant effect. Furthermore, when fat globules are sonicated, their size is reduced revealing a higher surface area and reducing considerably the concentration of phospholipids and copper, giving the milk good oxidative stability (Taylor and Richardson, 1980).

Some studies performed with raw whole milk under thermo-sonication showed that there is a significant difference ($p<0.05$) between the crude protein of thermal-treated (63°C) samples and thermo-sonicated (63°C plus ultrasound) samples compared with untreated milk. The decrease of protein content between the raw milk and the thermo-sonicated samples with cavitation at different intensities was around 0.26% (Bermúdez-Aguirre et al., 2009). One possible reason for this decrease is the use of high temperature in combination with ultrasound, generating a probable denaturation of proteins. In another study a synergistic effect was reported in milk when heat plus ultrasound were used together in the inactivation of enzymes and the study of the potential denaturation of proteins, i.e., alkaline phosphatase, γ-glutamyltranspeptidase and lactoperoxidase, α-lactalbumin, β-lactoglobulin at temperatures of 61, 70, and 75.5°C; however, under these processing conditions, casein content did not show any important change (Villamiel and de Jong, 2000). It appears that the use of higher temperatures (above 60°C) in combination with ultrasound is responsible for the denaturating effect in proteins, because in a contrasting study using skim milk, when the food was thermo-sonicated at temperatures below 50°C, the soluble protein content of milk was not different from the control sample (Wrigley and Llorca, 1992).

In a more recent study ultrasound was used to process whey proteins, and results showed that a possible change in protein conformation and structure led to changes in water solubility of the proteins. Because of the sonication, the structure of the protein was modified, exposing it to the medium and allowing the hydrophilic part

of amino acids to be in contact with water molecules, binding most of the proteins and therefore increasing their water solubility (Krešić et al., 2008).

One of the keys to processing milk under thermo-sonication is to find the ideal conditions for microbial inactivation, while at the same time generating the minimal denaturation of protein content. At this moment most of the studies related with inactivation of microorganisms and enzymes are showing encourage results and the loss of nutrients is minimal; however, as in any new technology more studies must be performed to evaluate the overall quality and make sure to offer to consumers a safe and high-quality food.

4.2.2 Vitamins and Minerals

Scarce information exists related to the vitamin or mineral content of milk after sonication. Indeed, one of the most important parameters after milk treatment with ultrasound is protein content because of its caloric and nutritional importance in the human diet. However, milk also contains important vitamins such as riboflavin and niacin and minerals such Ca, P, Na, K, or Cl (Walstra et al., 2006).

One of the few studies related to milk after sonication concerned the calcium content after treatment at 27 kHz. The soluble Ca ultra-filterable value changed from 0.420 g/l in raw milk to 0.460 g/l in processed milk regardless the time of sonication, whereas the non-sedimentable Ca changed from 0.482 (untreated milk) up to 0.504 g/l after 60 min of sonication. According to the authors, this change of Ca in milk is not significant (Raharintsoa et al., 1978).

4.3 Physical–Chemical Characteristics

Although many of the studies with ultrasound in milk have been conducted to study the microbial inactivation of target bacteria, there are some data related to physical–chemical properties such as viscosity, density, pH, and color. Table 16.1 presents a comparison between fresh and raw milk, pasteurized milk with conventional thermal treatment and sonicated milk, skim and whole milks.

4.3.1 Viscosity

Viscosity can be defined as the resistance of a liquid to flow related to the attraction forces between the molecules of a liquid. The viscosity reported for fresh milk is 1.9 mPa s (Walstra et al., 2006), as can be seen in Table 16.1. However, as can be observed in the same table, skim milk (low pasteurized) shows a lower value because of the absence of the fat content. Regarding sonicated milk, there is a difference between the viscosity of the fresh milk and the treated milks; from 1.9 mPa s, the viscosity decreased up to 1.76 and 1.77 mPa s regardless of the butter fat content (Raharintsoa et al., 1978). One possible explanation for this decrease could be the effect of homogenization that the ultrasound generates in the fat content, making the

Table 16.1 Physical–chemical properties of different kinds of milk

Physical–chemical properties	Fresh milk	Beverage milk (low pasteurized)	Skim milk (low pasteurized)	Sonicated skim milk	Sonicated whole milk
pH	6.7	6.7	6.7	6.5[a]	6.6[c]
Viscosity (mPa s)	1.9	1.8	1.65	1.76[b]	1.77[d]
Density (kg/m^3)	1,029	1,030	1,035	1,033[a]	1,025[c]
Fat globule size (μm)	3.4	0.5	0.4	–	<0.5[c]
References	Walstra et al. (2006)	Walstra et al. (2006)	Walstra et al. (2006)	Bermúdez-Aguirre and Barbosa-Cánovas (2008)[a]; Raharintsoa et al. (1978)[b]	Bermúdez-Aguirre et al. (2009)[c]; Raharintsoa et al. (1978)[d]

[a]Skim milk previously UHT pasteurized after 30 min of sonication at 63°C
[b]Skim milk after 60 min of sonication, viscosity at 20°C
[c]Whole and raw milk after 30 min of sonication at 63°C
[d]Whole milk after 60 min of sonication, viscosity at 20°C
–Data not available

milk more fluid because of the reduction in size of the fat globules. However, the viscosity for both sonicated milks is in the range for beverage milk.

In another reported study (Krešić et al., 2008) investigating whey proteins, after sonication significant ($p < 0.05$) changes were observed in the flow behavior of the whey protein isolate (WPI) and whey protein concentrate (WPC). The apparent viscosity was increased from 7 to 8 mPa s in both cases and the consistency coefficient was also increased; the flow behavior index showed some changes as well after sonication.

4.3.2 Density

According to Table 16.1, the density of whole milks, both fresh and sonicated (Bermúdez-Aguirre et al., 2009; Walstra et al., 2006), is very similar (1,029 and 1,025 kg/m^3, respectively), whereas skim milks, low pasteurized, and sonicated (Bermúdez-Aguirre and Barbosa-Cánovas, 2008; Walstra et al., 2006) are also in the same range (1,035 and 1,033 kg/m^3, respectively). In summary, density is a property of milk that does not change in an important way during sonication, regardless of the butter fat content.

4.3.3 pH

The pH of milk is a useful parameter to express the degree of acidity of milk. Although it is not a routinely measured parameter in milk, this value provides information about the degree of lactic acid that milk contains at specific times. The reported pH of fresh milk is 6.7, as seen in Table 16.1, although this value can change because of many situations related to the milk source, for example, the kind of mammal, season, feeding, but the values are always close to 6.7.

Sonicated milk showed lower values of pH after treatment, 6.5 and 6.6 for skim and whole milk, respectively. However, these values do not represent a significant change in the pH of milk. There are some possible explanations as to why pH decreases in milk after sonication. These explanations are proposed for water; at this moment there are no available data for these explanations in milk, but considering that milk has a high percentage of water, these theories could be extrapolated to milk.

One of the former theories related to chemical changes in a sonicated medium was related to formation of free radicals from water molecules (Tsukamoto et al., 2004a, b). Water molecules are divided into free radicals such as OH^- and H^+, and some authors (Sochard et al., 1997) even mention the presence of radicals O^- between the most abundant components of the sonolysis of water after treatment. Sonolysis is the breakage of water molecules in free radicals because of the violent cavitation generated by the sound waves in a liquid medium. These free radicals are responsible for lowering the pH of the medium, but are not necessarily the only factor to increase the acidity of the solution. The presence of hydroxyl radicals after sonication is also responsible for increasing the conductivity of the medium

(Jambrak et al., 2008). Studies reported by Supeno (2000) showed how the sonication of aqueous solutions in the range of ultrasound frequency from 41 to 3,217 kHz generated the highest production of nitrite and hydrogen peroxide as primary products in the liquid at 360 kHz, with the successive generation of nitrate as a product of the oxidation of nitrite.

Walstra et al. (2006) mention that the decrease of pH in milk could be due to the hydrolysis of phosphoric esters because of enzymatic action. As previously observed, ultrasound is responsible for promoting the activity of some enzymes, and cavitation can accelerate some chemical reactions, lowering the pH. In some studies using whey proteins suspensions, no significant changes ($p > 0.05$) were observed between the pH of the control sample and sonicated samples at 20 kHz (Jambrak et al., 2008). However, at this moment, there are no available data to determine the exact reason for low pH in milk after sonication.

4.3.4 Color

One of the main characteristics of milk is color; consumers look for the conventional white color, and some studies show that the whiter the milk is, the higher the consumer preference. So, it is of interest to know if after sonication cavitation modifies the color of milk, because it will also affect the final color of other dairy products such as cheese or yogurt.

Sonicated milk showed a significant change in luminosity after treatment in comparison with raw and thermal-treated milk. Depending on the extent of cavitation, milk was whiter as the intensity was increased. In addition to *L* value, *a* value changed significantly in thermo-sonicated milk, having an important contribution to the blue region, whereas *b* value did not change significantly between the raw, thermal, and thermo-sonicated milk samples (Bermúdez-Aguirre et al., 2009). The reason for this is the reduction of fat globule size (Ertugay et al., 2004). The color of milk is due to the fat globules that scatter the light, making it a white fluid; however, when cavitation acts over these globules, their size is reduced and the agglomerate of these globules becomes more homogeneous, modifying the light reflection and showing whiter milk. In Fig. 16.1, the variation in color parameters (*L, a, b*) between raw milk, thermal-treated milk, and sonicated milk at different intensities is shown. *L* and *a* are the parameters that changed significantly with respect to the control sample, whereas *b* did not change in any important way.

The whiter color and homogenization of sonicated milk are maintained during the storage life of the milk. Some studies showed that even after 16 days under refrigerated conditions, the whiter color remained and no problems related with gelation or syneresis were observed (Bermúdez-Aguirre et al., 2009).

Indeed, sonication offers many advantages at the time that milk is being pasteurized; white color is enhanced and homogenization allows milk to have a better appearance through the storage life. All of these positive effects are generated during the one-step sonication process.

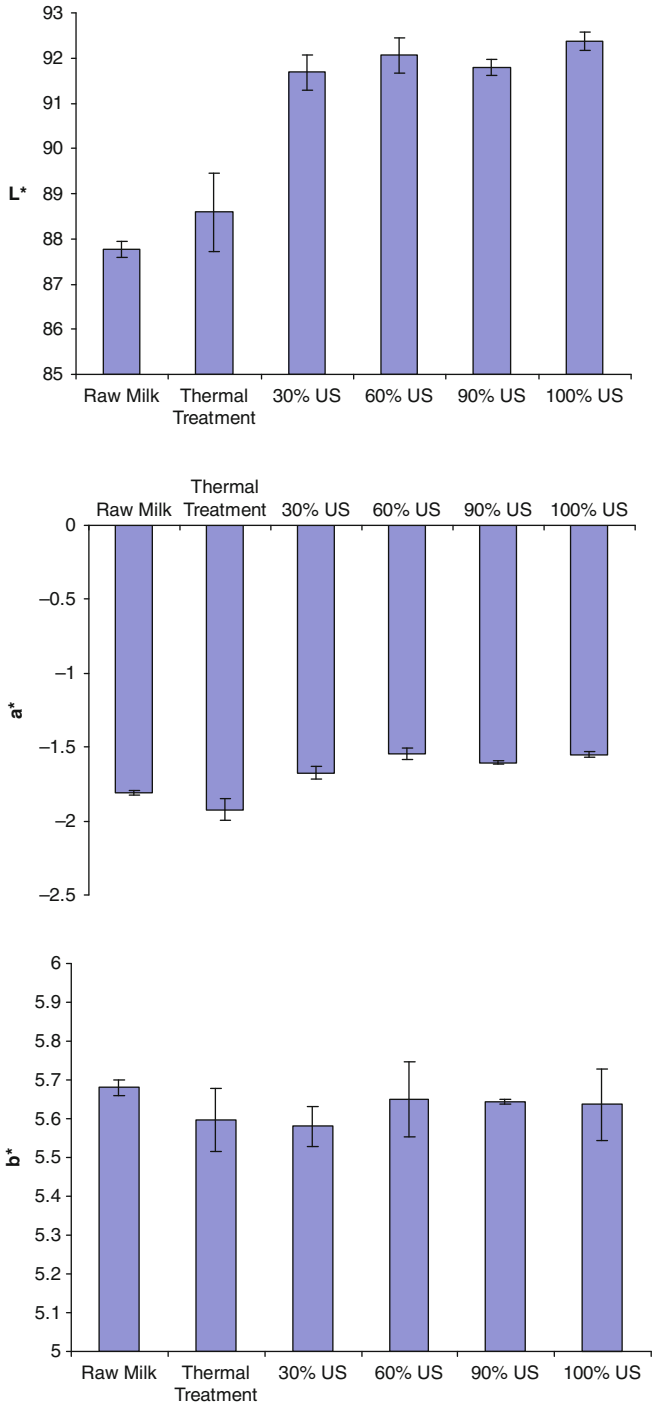

Fig. 16.1 Changes in color parameters (L^*, a^*, b^*) in raw, thermal-treated, and sonicated milk samples at different intensities. L^* and a^* were significantly different from each other; b^* was not significantly different

5 Microstructure of Milk After Sonication

One of the main changes in milk after sonication is observable at first sight: the color and the homogeneity of the product is quite different from the thermal-treated or untreated milk. Objective measurements of color show a higher luminosity, whiter samples, and a better color that lasts even during storage. The reasons for these changes can be better explained from the microstructure point of view.

Milk, by itself, is an interesting food, not only for its rich variety of components, enzymes, and microorganisms, but also for its peculiar microstructure. At the microscopic level, milk is loaded with fat globules, casein structures, and soluble solids such as lactose; even more interesting is the study of the dairy products when the matrix of proteins, fats, carbohydrates, and other components interacts.

When milk is processed under thermo-sonication, its microstructure changes in an important way that is reflected directly in its color, homogeneity, and general appearance. The main effect of ultrasound in milk is cavitation. This physical phenomenon is generated because of the passage of sound waves through the liquid; thousands of bubbles are produced inside the product with a considerable number of explosions and implosions, increasing the pressure in high degree. This raise in pressure causes the physical disruption of cells; in the case of milk, this disruption is seen in the disturbance of fat globules, breaking down the big globules and producing smaller ones.

Commonly, the fat globules are surrounded by a milk fat globule membrane (MFGM). One of the main functions of the MFGM, in addition to containing fatty acids, is to provide certain protection against lipid oxidation. The core of the fat globules is composed mainly of triacylglycerols (lauric, myristic, oleic, stearic, and linoleic acids) (Michalski et al., 2005). The surface of the globules contains cholesterol and phospholipids, such as sphingomyelin and phosphoglycerides of choline, ethanolamine, inositol, and serine (Keenan and Patton, 1995). When milk is processed under ultrasound, and sometimes under heat conditions, the important increase in pressure in the medium disrupts the MFGM, breaking down the globules and releasing the triacylglycerol content to the medium. As cavitation continues in the medium, the fat content is further homogenized and the size of fat globules is considerably reduced.

An important reduction in the size of fat globules (81.5%) was found in milk after performing sonication for some seconds, and higher reduction was achieved when heat was used in combination with ultrasound (Villamiel and de Jong, 2000). In addition to smaller globule size, the surface of the globules changed from the smooth surface of a native globule to a new roughened structure. Some microscopy studies were performed on milk structure after sonication, using heat plus ultrasound, and the general aspect of butter fat content, and specifically the globules, was observed. In Fig. 16.2, the effect of cavitation on fat globules is shown. First Fig. 16.2a shows a native fat globule in raw milk, its surface is smooth and the size is within the highest range reported for native fat globules. Figure 16.2b shows a thermal-treated fat globule with minor changes; but Fig. 16.2c is a good example of the new structure of fat globules after sonication, the surface now is totally roughened. Figure 16.2d

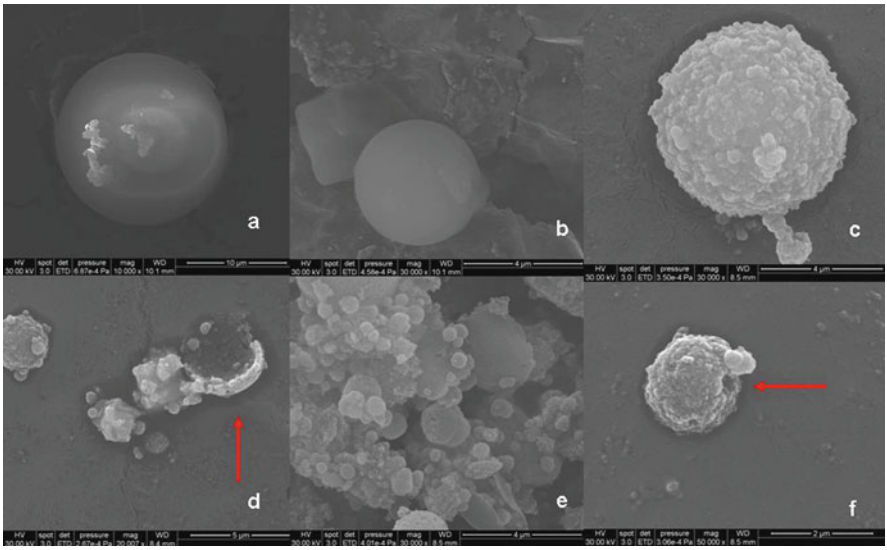

Fig. 16.2 Scanning electron microscopy of milk fat globules. Images show (**a**) the integrity of a non-disrupted fat globule (large globule) in raw and unprocessed milk (10,000× magnification); (**b**) the structure of a thermal-treated fat globule (30,000× magnification); (**c**) smaller and disrupted fat globule with roughened surface because of sonication action (30,000× magnification); (**d**) part of the fat globule membrane after sonication (20,000× magnification); (**e**) the new structure of fat globules–casein micelles complex in sonicated milk (30,000× magnification); (**f**) the presence of orifices in disrupted fat globules membrane because of sonication (50,000× magnification) (Photos: Courtesy of the authors)

shows how the cavitation destroys the fat globules; in this image the presence of half of a fat globule membrane is shown. In Fig. 16.2e the new structure of fat globules and casein micelles in sonicated milk is shown, the remaining fat globules have been disrupted because of cavitation and their sizes are smaller (less than 0.5 μm), and their surfaces present a roughened texture. Finally in the Fig. 16.2f a sonicated fat globule is shown with an orifice in the membrane, a roughened surface and smaller size.

Wu et al. (2001) studied the effect of ultrasound in the homogenization of milk to process yogurt and they found that longer times of exposure to sound radiation (10 min) achieved a better homogenization because the size of the fat globules was smaller and more uniform. The globules were disrupted and finely dispersed in the milk; after 6 min of sonication the average diameter size of fat globules was smaller than 2 μm. In raw milk the diameter size of fat globules ranged from 0.2 to 10 μm, the average diameter being 4 μm (Keenan and Patton, 1995; Michalski et al., 2005).

Indeed, the structure of milk after sonication is an important tool for the dairy industry. Most current dairy products such as yogurt, cream, or milk shakes have quality problems during storage such as syneresis. Hence, the new structure conferred to milk after processing with sound waves could be an important key to

improve the quality of some of these products, having a better homogenization, while at the same time being a good starting point to develop new dairy products.

6 Processing of Dairy Products with Ultrasound Technology

6.1 Milk

6.1.1 Milk as Beverage

At this time, ultrasonicated milk is not commercially available yet; because of all the new technologies, series of experiments must be conducted to show the efficacy of the technology and to achieve the sanitary, microbiological, and governmental regulations in each country. However, sonicated milk could be a potential product that offers many advantages to the consumer as a beverage or to the dairy industry as an ingredient of other products.

Milk as a beverage after sonication has many advantages compared with heat-treated milk or conventional pasteurized product; color, homogenization, and appearance are better; for milk processors, homogenization and pasteurization can take place in one step instead of two (homogenization and further pasteurization), ensuring better stability throughout storage.

Although only a few experiments have been carried out in milk stability during storage, quality problems such as syneresis, "sweet-curdling" because of the enzymatic action (protease and lipase from *Bacillus* spores), oxidation could be minimized or avoided with ultrasound. The storage life of sonicated milk under refrigerated conditions (4°C) has been shown to be extended longer than that of conventional milk (Bermúdez-Aguirre et al., 2009), with butter fat content being a decisive parameter in the bacterial growth.

6.1.2 Lactose-Free Milk

A common health problem is the intolerance of lactose by a large part of the population. Lactase, the enzyme responsible for metabolizing lactose in milk, is present only in low levels in some people, depending mainly on ethnicity. Lactose-free milk has been successfully commercialized in many countries for lactose-intolerant consumers. This milk without lactose can be produced by fermentation of lactose-hydrolyzed milk or by the simultaneous addition of β-galactosidase and lactic acid bacteria (Carcel et al., 1998; Wang et al., 1996). These bacteria produce β-galactosidase which hydrolyzes the lactose in fermented milk (Villamiel et al., 1999).

Ultrasound has the capability of raising the reaction activity of cells or to stimulate a new action into the cells, for example, in sterol synthesis with baker's yeasts or in lactose-hydrolyzed fermented milk. Using ultrasound in the processing of lactose-free milk, the lactose hydrolysis was around 55%; using traditional methods to produce lactose-free milk (fermentation), hydrolysis was around 36% (Wang

et al., 1996). In general, studies have shown that hydrolysis of lactose by ultrasound can be enhanced up to 20% compared with conventional methods (Toba et al., 1990; Villamiel et al., 1999). β-Galactosidase is released from *Lactobacillus*, shortening the fermentation time considerably and hydrolyzing the lactose (Carcel et al., 1998).

6.1.3 Human Milk

Sometimes newborns need to be fed by a different source of milk other than human milk directly from their own mothers, because of illness problems or early childbirth. In such special cases, newborns are fed using a feeding tube (gavage or ostomy tube) with stored human milk that has been previously pasteurized, homogenized, and frozen or lyophilized. However, almost 47% of the fat content separates from the milk during the storage process and thus does not reach the child (Carcel et al., 1998; Dhar et al., 1995), so fat can be added to the feed tube. Not only is the fat lost in milk, but also liposoluble vitamins, proteins, and minerals, leading to a high degree of nutritional losses. When sonication is used to homogenize the milk, the final product is much more stable because of the reduction of fat globule size and the longer maintenance of the emulsion, which considerably reduces the nutrient losses in the milk (Martínez et al., 1992).

Some current experiments in human milk homogenization have shown that using sonication at temperatures below 45°C reduces fat losses during feeding because of an increase in lipolytic activity which at the same time protects immunoprotective substances such as immunoglobulin A (IgA) and immunoglobulin G (IgG) and lactoferrin. Temperatures higher than 55°C not only totally inhibited the lipolytic activity and the bacteria load, but also decreased the IgA and IgG (Martínez et al., 1992), which is not convenient for newborns.

Thus, one of the many alternatives that ultrasound offers is the homogenization of human milk at low temperatures, providing a better consistency and avoiding the loss of vitamins, minerals, proteins, and fat, an important component in the caloric diet for newborns.

6.2 Yogurt

Regular yogurt is a very common and demanded dairy product. Although in some underdeveloped countries yogurt is processed at home, nowadays there are many varieties of yogurt available commercially in many other countries. Addition of special flavors, fruits, cereals, or specific bacteria are some examples of the current products. However, one of the biggest issues in yogurt production is the presence of lactose in the milk that is used to process it; the segment of the population that is intolerant to lactose needs to find a better option for yogurt consumption. Hydrolyzed lactose yogurt is a product focused on people who have zero tolerance to lactose, providing at the same time a sweetener effect without calories. As in the case of lactose-free milk, fermented milk to process yogurt can be prepared by ultrasound releasing the β-galactosidase from the starter bacteria and hydrolyzing

the lactose (Carcel et al., 1998; Toba et al., 1990). The conventional processing of yogurt requires a long time; in order to allow the fermentation to take place, a starter culture is added to milk and lactic acid production begins dropping the pH of the product. After some hours, when lactic acid reaches the desirable value for yogurt (0.65–0.70%) fermentation is stopped by immediately cooling the product. Fermentation times are also reduced in sonicated yogurt because of faster acid production enhanced by the use of ultrasound. Cavitation stimulates acid production because of the release of intracellular enzymes from microorganisms. Lactose is inside the cells of the starter culture for yogurt and the enzyme β-galactosidase increases its activity because the ultrasound hydrolyzes this sugar and accelerates the acid production (Wu et al., 2001).

Some common quality problems of yogurt are related to the separation of the serum from the main matrix containing the protein and fat; this phenomenon is known as syneresis. This problem occurs during the transportation and/or storage of the product and is a non-desirable characteristic of yogurt. Some studies have been performed using manothermosonication of milk (12 s, 20 kHz, 2 kg pressure, and 40°C) to process yogurt, and the final characteristics of the product were improved. For example, viscosity was much better in sonicated yogurt and fermentation time was reduced when milk was previously homogenized with ultrasound. The final structure of manothermosonicated yogurt was stronger than the control because of a better interaction of the components of the network. Casein micelles captured serum and fat globules, showing a significant difference ($p < 0.05$) in the water-holding capacity between the control and the manothermosonicated samples, releasing 18.8 and 14.8% of serum, respectively. Rheological parameters of sonicated yogurt such as penetration and relaxation forces, texture profile analysis parameters, consistency, flow behavior, yield stress, storage modulus (G′), and loss modulus (G″), among others, were improved in the product after the use of ultrasound in milk and prior to the fermentation process (Vercet et al., 2002). Similar studies were conducted in milk used to process yogurt, only with ultrasound without pressure, and final results also showed very good homogenization of the yogurt, reduction in fermentation time, and important and general improvements in water-holding capacity, viscosity, and reduction of syneresis (Wu et al., 2001).

The result of having better water-holding capacity and minimum syneresis could be explained from the microstructure and physical chemistry point of views. Cavitation is responsible for the disruption of fat globules and decreases the size of fat globules while at the same time conferring a new surface. All these globules together represent a bigger surface area than the original one and in this new area there will be new attached casein micelles (Wu et al., 2001) because of the action of the cavitation regrouping the milk components. These micelles are hydrophilic, which will bind water molecules in the new structure having a more compact network of proteins, fat globules, and water (serum), presenting better water-holding capacity, better structure, and low degree of syneresis. In Fig. 16.3, an example of thermo-sonicated yogurt is shown. The milk was sonicated at 120 μm, 85°C for 30 min, and after that it was cooled at 4°C in order to store the milk until the yogurt processing. Yogurt processing followed the conventional

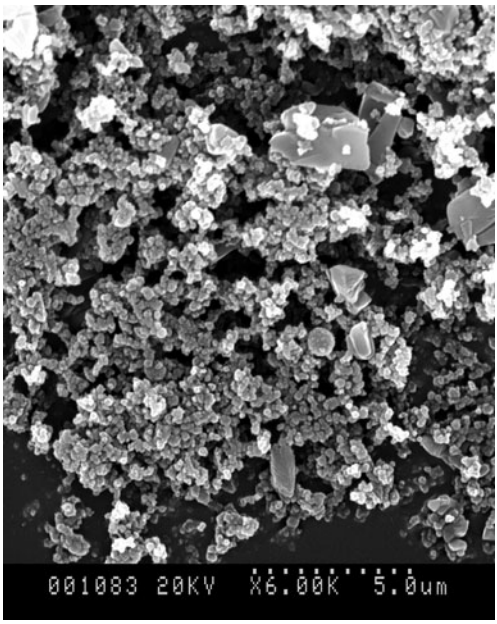

Fig. 16.3 Scanning electron microscopy of thermo-sonicated yogurt. Image shows the interaction between the yogurt components such as protein structures and fat globules. Better homogenization and color was achieved in yogurt microstructure after sonication. Ultrasound equipment has a frequency of 24 kHz, 400 W, and 120 μm (6,000× magnification) (Photo: Courtesy of the authors)

procedure used for the commercial product, heating the milk at 45°C, inoculation with starter cultures, and determination of acidity content until reaching 0.65–0.70%. The microstructure of yogurt showed a better homogenization and interaction between all the components and that is probably the reason for a better product, with better characteristics.

Indeed, ultrasound technology offers many advantages in yogurt processing: some of the common quality defects such as syneresis could be reduced considerably and better rheological properties for the consumer are achieved after the use of ultrasound.

6.3 Cheese

Cheese is one of the most demanded products around the world. Each year, the cheese industry reports considerable sale increases; in 2003 cheese production in the United States was more than 8,600 pounds of cheese. Varieties of this dairy product with the highest demand include cheddar, colby, monterey jack, mozzarella, ricotta. (Miller et al., 2007). The main processing steps of cheese making include the clotting or curdling of the milk, removal of whey, acid production, salting, shaping, and ripening (Walstra et al., 2006). The essential step during cheese processing is the formation of the curd that occurs by enzymatic and microbial activity. Many environmental conditions such as temperature, enzyme concentration, or microbial load are very important during the process to generate a firm curd in a specific time. One

of the desirable aspects in cheese making is to reduce the curdling time and increase the yield, because the final yield of cheese is around 10%. New technologies are being tested in cheese making in order to improve these aspects while at the same time improving the overall quality of cheese.

When sonication was applied to milk to study the proteolytic activity of the enzymes related to curdling, the main observable effect was that ultrasound speeds up the hardening of the curd and the final product showed a better firmness because of the activity on the chymosin, pepsin, and other related enzymes (Villamiel et al., 1999). Chymosin is the main enzyme related to the curdling formation in the cheese-making industry. This enzyme is produced naturally in the stomach of bull calves, and the conventional extraction of the enzyme with salt and acid solution takes a long time and the quality and yield are not favorable. Chymosin has a proteolytic activity in liquid milk, coagulating the protein and conferring a solid-like coagulated gel (Kim and Zayas, 1991). When ultrasound (20 kHz) was used to enhance the extraction not only the yield and enzyme activity were increased considerably, but also extraction times were much shorter than without sonication. The reason for that could be attributed to the destruction of cellular structure because of the action of ultrasound, increasing the activity of the substances contained in the cells and the migration of proteins and minerals from the cells to the solution (Carcel et al., 1998). The activity of the chymosin increased with sonication and the nitrogen content of the extract decreased at the same time (Kim and Zayas, 1991).

Other uses of power ultrasound in the cheese-making industry are in the flavor arena. Proteolysis is the main process that takes place during cheese ripening, and it can be divided into two main phases: the primary phase in which the residues of chymosin interact with the casein in the curd and the secondary phase in which proteins and polypeptides are broken into amino acids by enzymatic action released from bacteria (Engels and Visser, 1996). When *Lactococcus lactis* subsp. *cremoris* was sonicated, a "cell-free extract" was obtained by cell disruption (Engels and Visser, 1996) and the extraction of peptides and amino acids was easier and these components were used in the development of flavor of the cheese (Villamiel et al., 1999).

In addition to all of these benefits of the ultrasound technology, the process of "queso fresco," a typical product from Hispanic countries, made with sonicated milk showed better characteristics, such as whiter color, better texture (hardness), higher water-holding capacity, higher yield, and in general better acceptance by consumers (Bermúdez-Aguirre, D., and Barbosa-Cánovas, G. V. 2009 unpublished data). This is one of the areas that deserve further research in ultrasound technology.

7 Other Uses of Power Ultrasound in the Dairy Industry

Ultrasound offers a great variety of uses in industry; the specific case of applications for the dairy industry is wide enough to satisfy different requirements in processing and preservation. Some other examples of the use of ultrasound in the dairy industry are described below.

Edible films is an interesting topic for many researchers in food preservation worldwide; however, some specific characteristics of the films are required in order to be used in food, as well as their mechanical properties. Sodium caseinate and whey proteins can be used for manufacturing edible films and their mechanical properties are improved using sonication (Carcel et al., 1998).

Other uses of power ultrasound reported in literature are related to cleaning operations. Power ultrasound has been used to disperse cumulus of bacteria in raw milk and to clean cheese moulds in cheese-making industry (Villamiel et al., 1999).

8 Final Remarks

Certainly, ultrasound offers many advantages in dairy processing. Although this is a new technology that is still being tested at the lab and pilot plant scale, sonication has the potential to be scaled up to the industry level in order to take advantage of all its properties. Inactivation of bacteria and enzymes is possible with ultrasound, achieving pasteurization standards and conferring better quality attributes to the milk. Beverage milk, yogurt, and cheese have been processed successfully under ultrasound activity, and other dairy products such as cream or ice cream could make use of the beneficial effects of sonication on texture and rheological characteristics to improve their quality as well.

References

Ananta, E., Voigt, D., Zenker, M., Heinz, V., and Knorr, D. (2005). Cellular injuries upon exposure of *Escherichia coli* and *Lactobacillus rhamnosus* to high-intensity ultrasound. *Journal of Applied Microbiology*, 99, 271–278.

Banasiak, K. (2005). News. *Food Technology*, 59(11), 13–14.

Bermúdez-Aguirre, D., and Barbosa-Cánovas, G. V. (2008). Study of butter fat content in milk on the inactivation of *Listeria innocua* ATCC 51742 by thermo-sonication. *Innovative Food Science and Emerging Technologies*, 9(2), 176–185.

Bermúdez-Aguirre, D., Mawson, R., Versteeg, K., and Barbosa-Cánovas, G. V. (2009). Composition parameters, physical-chemical characteristics and shelf-life of whole milk after thermal and thermo-sonication treatments. *Journal of Food Quality*. 32, 283–302.

Cabeza, M. C., Ordóñez, J. A., Cambero, I., De la Hoz, L., and García, M. L. (2004). Effect of thermoultrasonication on *Salmonella* enterica Serovar Enteridits in distilled water and intact shell eggs. *Journal of Food Protection*, 67(9), 1886–1891.

Carcel, J. A., Benedito, J., SanJuan, N., and Sánchez, E. (1998). Aplicación de los ultrasonidos en las industrias de productos lácteos y derivados. *Alimentación, Equipos y Tecnología*, 135–141.

Dhar, J., Davidson, A. G. F., Martinez, F. E., Barr, S., Desai, I. D., and Nakai, S. (1995). Ultrasonication, lyophilization, freezing and storage effects on fat loss during mechanical infusion of expressed human milk. *Journal of Food Science*, 60(2), 375–377, 394.

Earnshaw, R. G., Appleyard, J., and Hurst, R.M. (1995). Understanding physical inactivation processes: Combined preservation opportunities using heat, ultrasound and pressure. *International Journal of Applied Microbiology*, 28, 197–219.

Engels, W. J. M., and Visser, S. (1996). Development of cheese flavor from peptides and amino acids by cell-free extracts of *Lactococcus lactis* subsp. *cremoris* B78 in a model system. *Netherlands Milk and Dairy Journal*, 50, 3–17.

Ertugay, M. F., Şengül, M., and Şengül, M. (2004). Effect of ultrasound treatment on milk homogenization and particle size distribution of fat. *Turkish Journal of Veterinary and Animal Sciences*, 28, 303–308.

Furuta, M., Yamaguchi, M., Tsukamoto, T., Yim, B., Stavarache, C. E., Hasiba, K., and Maeda, Y. (2004). Inactivation of *Escherichia coli* by ultrasonic irradiation. *Ultrasonics Sonochemistry*, 11(2), 57–60.

Guerrero, S., Tognon, M., and Alzamora, S. M. (2005). Response of *Saccharomyces cerevisiae* to the combined action of ultrasound and low weight chitosan. *Food Control*, 16, 131–139.

HHS/PHS/FDA. (2001). Grade A pasteurized milk ordinance. US Department of Health and Human Services/Public Health Services/Food and Drug Administration, 60, 19.

Jambrak, A. R., Mason, T. J., Lelas V., Herceg, Z., and Herceg I. L. (2008). Effect of ultrasound treatment on solubility and foaming properties of whey protein suspensions. *Journal of Food Engineering*, 86, 281–287.

Keenan, T. W., and Patton, S. (1995). The structure of milk: Implications for sampling and storage. In: Jensen, R. G. (ed.), *Handbook of Milk Composition*, pp. 5–50. San Diego, CA, Academic.

Kim, S. M., and Zayas, J. F. (1989). Processing parameters of chymosin extraction by ultrasound. *Journal of Food Science*, 54(3), 700–703.

Kim, S. M., and Zayas, J. F. (1991). Comparative quality characteristics of chymosin extracts obtained by ultrasound treatment. *Journal of Food Science*, 56(2), 406–410.

Klima, R. A., and Montville, T. J. (1995). The regulatory and industrial responses to listeriosis in the USA: A paradigm for dealing with emerging foodborne pathogens. *Trends in Food Science and Technology*, 6, 87–93.

Ko, S., and Grant, S. A. (2003). Development of a novel FRET method for detection of *Listeria* or *Salmonella*. *Sensors and Actuators*, B96, 372–378.

Kozak, J., Balmer, T., Byrne, R., and Fisher, K. (1996). Prevalence of *Listeria monocytogenes* in foods: Incidence in dairy products. *Food Control*, 7(4–5), 215–221.

Krešić, G., Lelas, V., Jambrak, A. R., Herceg, Z., and Brnčić, S.R. (2008). Influence of novel food processing technologies on the rheological and thermophysical properties of whey proteins. *Journal of Food Engineering*, 87, 64–73.

Mañas, P., Pagán, R., and Raso, J. (2000). Predicting lethal effect of ultrasonic waves under pressure treatments on *Listeria monocytogenes* ATCC 15313 by power measurements. *Journal of Food Science*, 65(4), 663–667.

Martínez, F. E., Davidson, A. G. F., Anderson, J. D., Nakai, S., Desai, I. D., and Radcliffe, A. (1992). Effects of ultrasonic homogenization of human milk on lipolysis, IgA, IgG, lactoferrin and bacterial content. *Nutrition Research*, 12, 561–568.

McLauchlin, J. (2006). Listeria. In: Motarjemo, Y., and Adams, M. (eds.), *Emerging Foodborne Pathogens*, pp. 406–428. Boca Ratón, FL, CRC.

Michalski, M. C., Briard, V., and Juaneda, P. (2005). CLA profile in native fat globules of different sizes selected from raw milk. *International Dairy Journal*, 15, 1089–1094.

Miller, G. D., Jarvis, J. K., and McBean, L. D. (2007). *Handbook of Dairy Foods and Nutrition*. Boca Ratón, FL, CRC.

Mohan Nair, M. K., Vasudevan, P., and Venkitanarayanan, K. (2005). Antibacterial effect of black seed oil on *Listeria monocytogenes. Food Control*, 16, 395–398.

Motarjemi, Y., and Adams, M. (2006). Introduction. In: Motarjemo, Y., and Adams, M. (eds.), *Emerging Foodborne Pathogens*, pp. xvii–xxii Boca Ratón, FL, CRC.

Pagán, R., Mañas, P., Alvarez, I., and Condón, S. (1999). Resistance of *Listeria monocytogenes* to ultrasonic waves under pressure at sublethal (manosonication) and lethal (manothermosonication) temperatures. *Food Microbiology*, 16, 139–148.

Pelczar, M. J., and Reid, R. D. (1972). *Microbiology*, pp. 783–807. New York, McGraw-Hill.

Raharintsoa, C., Gaulard, M. L., and Alais, C. (1977). Étude de l'action des ultrasons cavitants sur quelques enzymes coagulants. *Le lait*, 57, 569–570.

Raharintsoa, C., Gaulard, M. L., and Alais, C. (1978). Effet des ultrasons cavitants sur la coagulation du lait par les enzymes. *Le lait*, 58, 579–580.

Sinisterra, J. V. (1992). Application of ultrasound to biotechnology: An overview. *Ultrasonics*, 30(3), 180–185.

Sochard, S., Wilhelm, A. M., and Delmas H. (1997). Modeling of free radicals production in a collapsing gas-vapor bubble. *Ultrasonics Sonochemistry*, 4, 77–84.

Supeno, P. K. (2000). Sonochemical formation of nitrate and nitrite in water. *Ultrasonics Sonochemistry*, 7, 109–113.

Taylor, M. J., and Richardson, T. (1980). Antioxidant activity of skim milk: Effect of sonication. *Journal of Dairy Science*, 63, 1938–1942.

Toba, T., Hayasaka, I., Taguchi, S., and Adachi, S. (1990). A new method for manufacture of lactose-hydrolysed fermented milk. *Journal of the Science of Food and Agriculture*, 52, 403–407.

Tsukamoto, I., Constantinoiu, E., Furuta, M., Nishimura, R., and Maeda, Y. (2004a). Inactivation effect of sonication and chlorination on *Saccharomyces cerevisiae*. Calorimetric analysis. *Ultrasonics Sonochemistry*, 11, 167–172.

Tsukamoto, I., Yim, B., Stavarache, C.E., Furuta, M., Hashiba, K., and Maeda, Y. (2004b). Inactivation of *Saccharomyces cerevisiae* by ultrasonic irradiation. *Ultrasonics Sonochemistry*, 11, 61–65.

Ugarte-Romero, E., Feng, H., and Martin, S.E. (2007). Inactivation of *Shigella boydii* 18 IDPH and *Listeria monocytogenes* Scott A with power ultrasound at different acoustic energy densities and temperatures. *Journal of Food Science*, 72(4), M103–M107.

Ugarte-Romero, E., Feng, H., Martin, S. E., Cadwallader, K. R., and Robinson, S. J. (2006). Inactivation of *Escherichia coli* with power ultrasound in apple cider. *Journal of Food Science*, 71(2), E102–E108.

Vercet, A., Oria, R., Marquina, P., Crelier, S., and Lopez-Buesa, P. (2002). Rheological properties of yogurt made with milk submitted to manothermosonication. *Journal of Agricultural and Food Chemistry*, 50, 6165–6171.

Villamiel, M., and de Jong, P. (2000). Influence of high-intensity ultrasound and heat treatment in continuous flow on fat, proteins, and native enzymes of milk. *Journal of Agricultural and Food Chemistry*, 48, 472–478.

Villamiel, M., van Hamersveld, E. H., and de Jong, P. (1999). Review: Effect of ultrasound processing on the quality of dairy products. *Milchwissenschaft*, 54(2):69–73.

Walstra, P., Wouters, J. T. M., and Geurts, T. J. (2006). *Dairy Science and Technology*, 2nd edn. Boca Ratón, FL, CRC, Taylor and Francis.

Wang, D., Sakakibara, M., Kondoh, N., and Suzuki, K. (1996). Ultrasound-enhanced lactose hydrolysis in milk fermentation with *Lactobacillus bulgaricus*. *Journal of Chemical Technology and Biotechnology*, 65, 86–92.

Wrigley, D. M., and Llorca, H. G. (1992). Decrease of *Salmonella typhimurium* in skim milk and egg by heat and ultrasonic wave treatment. *Journal of Food Protection*, 55(9), 678–680.

Wu, H., Hulbert, G. J., and Mount, J. R. (2001). Effects of ultrasound on milk homogenization and fermentation with yogurt starter. *Innovative Food Science and Emerging Technologies*, 1, 211–218.

Zenker, M., Heinz, V., and Knorr, D. (2003). Application of ultrasound-assisted thermal processing for preservation and quality retention of liquid foods. *Journal of Food Protection*, 66(9), 1642–1649.

Chapter 17
Sonocrystallization and Its Application in Food and Bioprocessing

Parag R. Gogate and Aniruddha B. Pandit

1 Introduction

The use of ultrasound within the food industry has been a subject of research and development for many years (Demirdöven and Baysal, 2009; Mason et al., 1996; Prakash and Ramana, 2003), and, as is the case in other areas, the sound ranges employed can be divided basically into high-frequency, low-energy, and diagnostic ultrasound operating in the megahertz range and low-frequency, high-energy, power ultrasound in the kilohertz range. Till a few years ago the majority of applications and developments involved non-invasive analysis with particular reference to food quality assessment, e.g., by monitoring the attenuation of an ultrasound pulse or by measurement of the ultrasonic velocity, it has been possible to determine the degree of homogenization of fat within milk, the degree of emulsification in such materials, and the degree of 'creaming' (or 'settling') of a sample, i.e., the movement of solid particles/fat droplets to the surface (or to the base). Ultrasound can also be used in analysis of edible fats and oils, and for the determination of the extent of crystallization and melting in dispersed-phase droplets in emulsion. The application of power ultrasound (20–100 kHz, but can be as high as 2 MHz) to chemical processing is a process intensification approach that has undergone much development over the past 15 years or so. The most widely reported facet of this has been in the research area of sonochemistry: the use of ultrasound to promote or modify chemical reactions (Thompson and Doraiswamy, 1999). Power ultrasound has been also used for wastewater treatment, in particular, anaerobic digestion (Khanal et al., 2007; Palmowski et al., 2006), and applied to a range of other activities in the food processing industry, e.g., emulsification, crystallization, microbial fermentation, cell disintegration, homogenizing (Mason et al., 1996; Prakash and Ramana, 2003). However, while the concept of ultrasonic processing is not new, the ability to use it on an industrial scale has indeed been a major problem. Recent advances in these

P.R. Gogate (✉)
Chemical Engineering Department, Institute of Chemical Technology,
Mumbai, Matunga 400 019, India
e-mail: pr.gogate@ictmumbai.edu.in

H. Feng et al. (eds.), *Ultrasound Technologies for Food and Bioprocessing*,
Food Engineering Series, DOI 10.1007/978-1-4419-7472-3_17,
© Springer Science+Business Media, LLC 2011

equipments have made its implementation at industrial scale feasible, particularly in the area of biomass sludge disintegration and crystallization. This chapter aims at understanding in detail the application of ultrasound for intensification of crystallization operation. The first application of ultrasound to crystallization, described commonly as sonocrystallization, in 1927 predates by decades any serious application to chemistry. In addition, there is considerable literature from the former Soviet Union in the 1950s to the 1970s, albeit dealing with small-scale applications. Interest in the application of ultrasound to crystallization, particularly in the pharmaceutical and fine chemical sectors of industry, has received further impetus in recent years with the increased focus on specificity of effect and the corresponding requirement to prepare and purify complex chemical entities to very exacting standards. The use of ultrasound provides a non-invasive way of improving crystal properties and process controllability, chiefly by controlling the size distribution and the habit and morphology of the crystals. The following benefits accrue (Kordylla et al., 2008; Krishna et al., 2007; Luque de Castro and Priego-Capote, 2007; McCausland and Cains, 2004; Prakash and Ramana, 2003):

- improved product and process consistency;
- improved crystal purity;
- improved secondary physical properties (flowability, packing density, etc.) of the product;
- shorter crystallization cycle times and less frequent rework;
- shorter and more reliable downstream processes.

Additionally, ultrasound can be used to replace seeding as a nucleator in difficult-to-nucleate systems. By varying the power and duration of insonation the crystal size distribution can be tailored to optimize downstream processing. Insonation to nucleate shows a marked increase in the mean crystal size, whereas continuous insonation dramatically reduces the mean crystal size. Manipulating the size and habit of the product crystals can be made to achieve the following benefits:

- Crystals of a more uniform size and compact habit can be filtered much more rapidly.
- Similarly, better access to the intercrystal voids greatly improves the speed of washing and drying, as well as the achievable decontamination level.
- The milling of crystals is a messy process which risks contamination of product and environment. By sonically tailoring crystal size distribution, the milling step may be eliminated altogether.
- Powder filling operations can be made much more reliable and trouble free because sonically nucleated crystals usually flow much better than those produced conventionally. The bulk density of the product may also be improved; doubling of bulk density has also been reported.

We now discuss the various aspects of sonocrystallization starting with mechanism of intensification or betterment in the crystallization operation followed by an

overview of the available reactor designs and applications with specific reference to the food industry.

2 Mechanism of Sonocrystallization

Ultrasound may influence crystallization through the mechanisms of cavitation and acoustic streaming. Cavitation appears to be particularly effective as a means of inducing nucleation, and there is evidence of dramatic improvements in reproducibility obtained through such sononucleation (Luque de Castro and Priego-Capote, 2007). Furthermore, using ultrasound to generate nuclei in a controlled and reproducible way provides a well-defined starting point for the crystallization process. This allows focus on controlling the crystal growth via the residence time in the crystallizer. The combined approach can be effectively used to influence crystal size distribution, assist in morphological control, eliminate impurities in the crystal, and improve solid–liquid separation behavior. Sononucleation can also eliminate the requirement to add seed crystals, and this can be particularly advantageous in contained crystallizations.

It is quite normal to consider crystallization in terms of the fundamental processes of nucleation and crystal growth; while such events will occur sequentially in any crystallization process, they can be very difficult to decouple for fundamental investigations and individual control. Ultrasound can induce primary nucleation in nominally particle-free solutions and, noteworthy, at much lower supersaturation levels as compared to the conventional mechanical agitation-based crystallization operation (Ruecroft, 2007; Ruecroft et al., 2005). The passage of ultrasound through a liquid medium induces the phenomenon of cavitation if the amplitudes are sufficiently high. Indeed, most sonochemical and sonoluminescence effects of ultrasound have been attributed to transient cavitation (Luche, 1998). This cavitation effect creates bubbles during successive cycles of compression and rarefaction to a point of transient bubble collapse, generally within one acoustic cycle but depending on the operating ultrasonic parameters, two or more cycles can also exist. This bubble collapse produces highly spatially resolved regions of extreme excitation, temperature (5,000–10,000 K), and pressure (100–5,000 atm), as well as concomitant release of shock waves (Luche, 1998). The reasons why such local and transient energy concentrations correlate with nucleation events have not yet been fully explained. In one sense, the effect is counterintuitive, in that a local temperature increase will reduce or eliminate the supersaturation in the immediate vicinity, effectively removing the driving force to nucleation. However, the shock waves may contribute to nucleation in the regions of the supersaturated solution somewhat remote from the cavitation event. Other postulates (McCausland et al., 2001; Ruecroft et al., 2005) suggest that (i) subsequent rapid local cooling rates, calculated at 10^7–10^{10} K/s especially during the rapid growth of cavitation bubble, play a significant part in increasing supersaturation; (ii) localized high-pressure pulse due to the cavitation phenomena reduces the crystallization temperature, and (iii) the

cavitation events allow the excitation energy barriers associated with nucleation to be surmounted, in which case it should be possible to correlate the numbers of cavitation and nucleation events in a quantitative way. There is clearly a need for further research for exactly identifying the relationship between cavitation and nucleation.

In many respects, the ease or difficulty of carrying out a crystallization process can be linked to an understanding of the metastable zone (MZ) of the temperature solubility curve. For a cooling crystallization, the width of this zone (MZW) can be described as the temperature drop below the solubility curve at which the solid starts to separate spontaneously for a given supersaturation level and cooling rate (supersolubilty limit). Use of ultrasound can aid in narrowing MZW and result in appearance of crystals much earlier as compared to the conventional nucleation approach (Fig. 17.1).

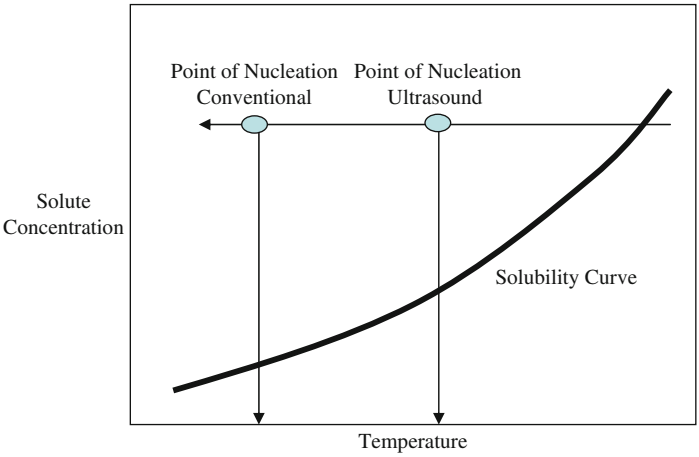

Fig. 17.1 Schematic representation of reduction in the metastable zone using ultrasound

It is possible to 'tailor' a crystal size distribution between the extreme cases of a short burst of ultrasound to nucleate at lower levels of supersaturation and allow growth to large crystals and the production of small crystals via continuous (or perhaps a longer single burst) insonation throughout the duration of the crystallization process, which can facilitate prolific nucleation at higher levels of supersaturation at the expense of some crystal growth. Pulsed or intermittent application of ultrasound can give intermediate effects. In any event, the optimum needs to be determined by experimental investigations. It is also possible that ultrasound may induce secondary nucleation by mechanically disrupting crystals or loosely bound agglomerates that have already formed. The acoustic streaming, described as the microscopic flow generated as a result of the cavity motion or the pressure gradients created due to the passage of ultrasound, also facilitates the bulk fluid mixing process, supplementing the diffusion of the solute to the already present nuclei. This enhances the solid–liquid mass transfer coefficient, promoting the crystal growth. Thus, these two processes are opposing in their effects and hence the duration and intensity

of ultrasound bursts need to be manipulated for desired betterment of the overall crystallization operation.

Polymorphism is very common among organic materials, and given that small-molecule drugs can be flexible and exhibit significant internal freedom, it is no surprise that such entities can exist as two or more crystalline phases with different packing in the crystal lattice. Indeed, isolation of the 'wrong' polymorph brings substantial problems especially in the case of pharmaceutical applications. Judicious application of ultrasound to a polymorphic system at the right level of supersaturation can assist in isolating the ground-state polymorph (the most thermodynamically favored and least soluble) or the one nearest to the ground state. Conversely, without ultrasound (or careful seeding) one may expect to generate a kinetically favored and more soluble metastable polymorph. Narrowing of the MZW for the more stable polymorph can lead to nucleation at lower levels of supersaturation than would otherwise be the case and, ideally, undersaturated with respect to the less stable polymorph. Supersaturation can then be managed over the process cycle, such as with slow or exponential cooling coupled with sonic energy, so as to avoid indiscriminate nucleation.

In crystallization processes induced by the addition of an anti-solvent (Guo et al., 2005), where high supersaturation levels (locally at the point of addition of the anti-solvent) may be produced very rapidly, it has been shown that the application of ultrasound reduces not only the induction times of nucleation but also the spread of variability in the induction times at a given level of supersaturation. Typically, in anti-solvent-based crystallizations, the anti-solvent is added to the point of precipitation, which can lead to high supersaturation levels. For a number of molecules it has been shown that significantly less anti-solvent can be used in conjunction with ultrasound to induce crystallization in a controlled manner.

Reactive crystallization (Li et al., 2006), i.e., controlled reaction precipitation, is another application where use of ultrasound can be of significant advantage. Reactive crystallization is often regarded as an irreversible process where the precipitate is a virtually insoluble substance produced by a chemical reaction. This is distinct from reversible crystallization processes such as cooling and vapor crystallization. During the reaction, which is usually initiated by a change in pH rather than temperature or concentration as in reversible crystallization, the solution becomes progressively more saturated and eventually supersaturated with respect to the reactant. Nucleation and crystal growth then occur in the supersaturated state. A common method to produce the precipitate is to mix the reactant and precursor solutions together as quickly as possible while avoiding any sharp temperature gradients. In such a rapid mixing, it is essential to create a reasonable uniformity of temperature and concentration gradients throughout the solution to ensure good product quality. Alternatively the reactant can be fed into the precursor slowly and continuously, but again the extent of supersaturation becomes much higher at the point of precipitant addition as compared to that prevailing in the rest of the solution leading to non-uniformity. In the extreme case, if the reactant is added at too slow a rate, supersaturation of the solution will increase to an unstable level and solute will rapidly precipitate/crystallize as a result of high nucleation rates with

uncontrollable formation of fines. Conventional crystallizers attempt to overcome these problems with the use of agitators to improve the mixing of the liquid phase. Agitators, however, only promote the motion of macroscopic layers and effective mixing occurs mostly at the interfaces between these layers. Mixing inside the layers depends mainly on the slow self-diffusion of reactant molecules. Since the speed of the reaction is generally very fast, such non-uniform mixing can result in local pockets of reactant in non-stoichiometric ratio and undesirable pH level and lead to excessive supersaturation and high nucleation rates. Therefore, it is necessary to find an effective method to control reactive crystallization, which can mix reactants more uniformly on a micro-level and enhance mass transfer in the reacting solution, more rapidly than conventional agitation. Sonication presents such a source of efficient mixing. The shock wave and microjets from local high pressure of the cavitation collapse can accelerate the motion of the liquid molecules and increase molecular impacts so as to prompt reaction and nucleation. Because the thickness of the stagnant film and the adsorption layer adjacent to the growing crystal surface depends on the relative solid–liquid slip velocity, ultrasonically mediated solute transfer will help promote crystal growth in the solution. The cavitation collapse may also act as a crystal nucleation center in the solution supersaturated with solute. A recent study has also suggested that the ultrasound produces a thin film surface layer on the crystal in which the crystallizing molecules can better align themselves for incorporation in the unit cell (Li et al., 2006). Ultrasound can also cause macrostreaming by incident and reflective waves. These ultrasonic effects are believed to be superior to conventional agitation in controlling reaction rate, level of supersaturation, nucleation, and crystal growth, mainly due to the length scales over which they are effective.

3 Reactor Designs

One of the most important barriers to the adoption of power ultrasound technology in manufacturing has been the lack of suitable equipment for use in industrial environments at the required operational scale. Most discoveries in sonochemistry and sonoprocessing have been carried out in laboratories on the milligram to gram scale using either high-intensity horn or bath systems.

Ultrasonic horns are the most commonly used reactor designs among the sonochemical reactors, although the cavitational effects are only observed close to the vibrating surface. The cavitational intensity decreases exponentially on moving away from the horn and vanishes at a distance of as low as 2–5 cm, depending on the supplied energy to the equipment and the operating frequency (Gogate et al., 2002). Thus, the efficacy of the horn-type system with larger scales of operation is poor compared to systems based on multiple transducers due to the fact that ultrasonic horns cannot effectively transmit the acoustic energy throughout a large process fluid volume. Additionally, ultrasonic horn-type reactors suffer from erosion and particle shedding at the delivery tip surface due to high surface energy

intensity. Also, cavitational blocking (acoustic decoupling) and large transducer displacement (amplitude) increases stress on the material of construction, resulting in the possibility of stress-induced fatigue failure. Typically, these reactors are recommended for laboratory-scale characterization studies or for larger scale operations where lower residence times are sufficient to bring about the desired change.

Reactors based on the use of multiple transducers irradiating identical or different frequencies seems to be a logical approach. The use of multiple transducers also results in lower operating intensities at similar levels of power dissipation, and hence, problems of cavitational blocking, erosion, and particle shedding at the delivery surface are reduced. The position of the transducers can also be easily modified in order for the wave patterns generated by the individual transducers to overlap, resulting in an acoustic pattern that is spatially uniform and noncoherent above the cavitational threshold throughout the reactor working volume. Arrangements (Fig. 17.2) such as transducers arranged at the bottom in triangular pitch in the case of ultrasonic bath (Dahlem et al., 1999; Soudagar and Samant, 1995), tubular reactors with two ends either irradiated with transducers or one end with transducer and the other with a reflector (Gonze et al.,

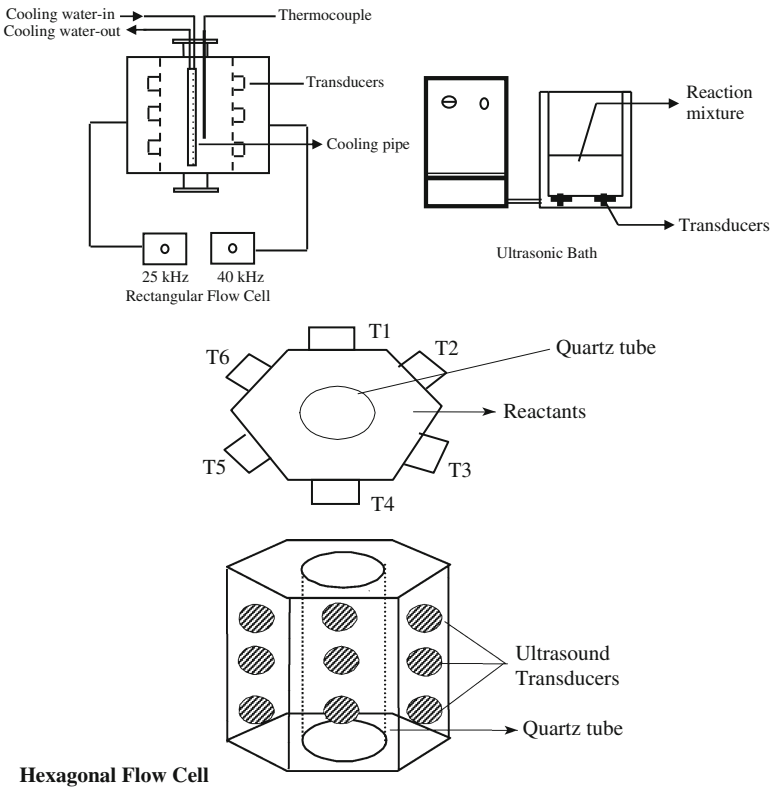

Fig. 17.2 Multiple transducer-based sonochemical reactors

1998), parallel plate reactors with each plate irradiated with either same or different frequencies (Gogate et al., 2001; Thoma et al., 1997), and transducers each on sides of hexagon (Gogate et al., 2003; Romdhane et al., 1995) can be constructed. It is of utmost importance to have uniform distribution of the ultrasonic activity in order to get increased cavitational effects, and using multiple transducers is the only possible way of an effective scale-up for large-scale operation. Kumar et al. (2007) have clearly shown that it is indeed possible to get good distribution of cavitational activity by using multiple transducers in a hexagonal configuration. It should also be noted here that these reactor configurations are usually based on the direct bonding of the transducer to the surface of the vessel. It is possible to increase the number of transducers attached to the vessel depending on the required power input and size of the vessel (Fig. 17.3) or arrange these vessels or modules in sequence to generate a full-scale operating system (Fig. 17.4). Improvements in the bonding method, and a move to transducers with lower individual outputs, have enabled the design of systems with large numbers of transducers to give an acoustic pattern that is uniform and noncoherent above the cavitational threshold throughout the reactor working volume. The use of low-output transducers gives the additional advantage of avoiding the phenomenon of cavitational blocking (acoustic decoupling), which arises where power densities close to the delivery point are very high. In addition, these multi-transducer units very effectively concentrate ultrasonic intensity toward the central axis of the cylinder and away from the vessel walls, thus reducing problems of wall erosion and particle shedding. The vessel can be operated in batch mode

Fig. 17.3 A 20 L Prosonitron multiple 20 kHz bonded transducer flow cell (WO 00/35579). Photograph courtesy of Prosonix Ltd, UK, www.prosonix.co.uk

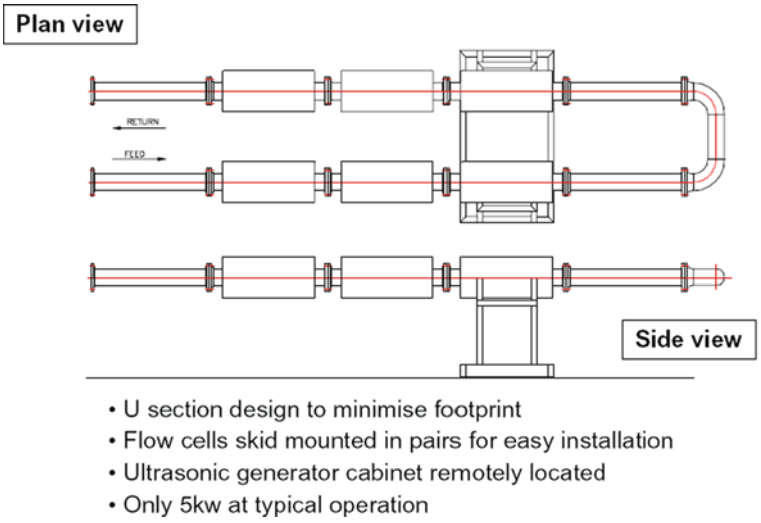

Fig. 17.4 Schematic view of a continuous sonocrystallization unit of 6 × 20L Prosonitron multiple 20 kHz bonded transducer flow cells (WO 00/35579) as used in the minerals (alumina) processing industries. Photograph courtesy of Prosonix Ltd, UK, www.prosonix.co.uk

or, for larger scale work, in continuous mode whereby units can be combined in a modular fashion for 'scale-out' and increased residence time. In summary, a plurality of low electrical and acoustic power (1–3 W/cm^2) transducers produces 25–150 W/l, but ideally 40–80 W/l. The power can be applied continuously or in a pulsed mode.

The magnitudes of collapse pressures and temperatures, as well as the number of free radicals generated at the end of cavitation events, are strongly dependent on the operating parameters of the sonochemical reactors. Intensity and frequency of irradiation along with the geometrical arrangement of the transducers and the liquid-phase physicochemical properties affect the initial size of the nuclei and the nucleation process. Proper selection of the operating, geometric parameters and physicochemical properties of the liquid phase decides the efficacy of the cavitational reactors in the desired application. Based on the careful bubble dynamics analysis (Sutkar and Gogate, 2009) obtained from the existing literature, some qualitative recommendations can be made in the optimization of these operating parameters, as given below:

1. Select an optimum intensity of irradiation based on the specific application; use of multiple transducers results in higher active cavitational volume.
2. It is better to use an optimum frequency of irradiation; applying excessive frequencies usually requires higher power for inception and leads to erosion problems.
3. Liquids with low vapor pressure, low surface tension, and low viscosity are preferred as the reaction medium for conducting cavitational reactions.

4. Presence of additives such as gases and/or solid particles eases the generation of cavitation events and generally results in overall higher cavitational effects.
5. Theoretical analysis of the cavitational activity distribution and energy dissipation patterns in the sonochemical reactors can aid in optimum designing of the reactors as well as in selection of the optimum operating parameters for maximizing the beneficial effects. It should be also noted here that a detailed analysis for cavitational activity distribution can be used to identify the regions with maximum pressures in a large-scale reactor and then may be small reactors containing the reaction mixtures can be placed strategically at these locations in order to get maximum benefits.

4 Case Study of Lactose Recovery from Whey

With an aim of better understanding the effect of ultrasound on the crystallization operation and approach to be used for optimization of the operating parameters, we now discuss a specific case study dealing with lactose recovery from the whey samples. Whey, viz., cheese whey, paneer (resembles cottage cheese) whey, skimmed milk whey, is commonly used as source for lactose recovery. Many factors such as temperature, pH, and impurities, which influence the mutarotation and solubility of lactose in solution, affect lactose concentration in the supernatant and in turn the gross yield of lactose during crystallization. Whey proteins and the minerals present in the solution affect the yield and purity of final lactose. The key to make lactose recovery an economical process lies in developing a speedy recovery process from low lactose concentration whey, i.e., less evaporation cost (lactose content of 19–20% w/v) and with high purity in the first step of crystallization itself. The conventional lactose recovery process from cheese whey or permeate involves concentration of whey to 55–65% of total solids (high evaporation costs) followed by cooling to yield yellow colored separated lactose. The process is tedious with variation in crystallization time from 12 to 72 h (Kapil et al., 1991). The raw lactose is re-dissolved, charcoal treated, and recrystallized to yield various grades of the lactose, with a maximum yield of around 50–60% (Elvers et al., 1990; Kapil et al., 1991). We now discuss in details a case study (Bund and Pandit, 2007a) related to the recovery of lactose from whey in the form crystals, where effect of sonication has been compared with the conventional approach. In the study, the reconstituted lactose solution was insonated in the presence of pre-optimized concentration of anti-solvent 'ethanol' to study the effect of sonication on the rate of the lactose recovery and crystal habit. Effect of different operating parameters such as concentration, pH, and protein content on the crystal size and lactose recovery has been examined.

4.1 Experimental Methodology

The experiments were performed using the ultrasonic bath assembly (Supersonics; frequency 22 kHz) as shown in Fig. 17.5. The ultrasonic bath has a rated power

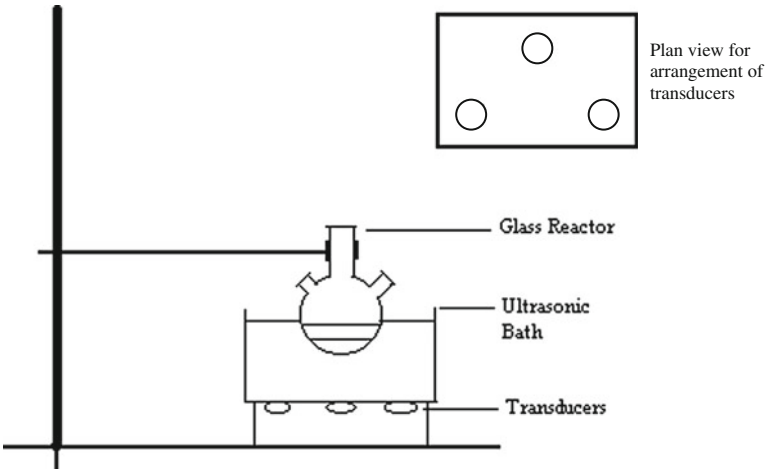

Fig. 17.5 Schematic representation of ultrasonic bath used for lactose recovery

output as 120 W (the net power dissipation was 42 W yielding an operating power density of 13.33 W/l) and operating frequency of 22 kHz. The dimensions of the bath were 15 ×15 × 15 cm and the surface area of ultrasound irradiated face was 225 cm^2. The flask was kept immersed in the ultrasonic bath assembly filled with water at a fixed height (3.5 cm from the bottom of ultrasonic bath assembly) where maximum cavitational activity was observed using mapping studies (Gogate et al., 2002). It is important to keep the micro-reactors (especially used when laboratory scale characterization studies are to be performed for a specific application under question) at a location where maximum cavitational activity is observed so that maximum beneficial effects can be obtained. During sonication experiments, irradiation was started followed by immediate addition of ethanol (95% v/v) to achieve an effective ethanol concentration of 85% v/v in the flask. The sonication was continued for the desired time intervals (1–15 min).

4.2 Effect of Operating Parameters on Lactose Recovery and Crystal Habit

Figure 17.6 shows the difference in the lactose recovery with an increase in time in the presence and absence of sonication from reconstituted lactose solution (17.5% w/v, pH 4.2). It can be clearly seen that the lactose recovery was much higher (91.48%) in the case of sonicated samples when compared with non-sonicated (14.63%) ones at the end of 5 min. In the case of sonicated samples the process of crystallization is rapidly completed. The ultrasound travels throughout the crystallization vessel to mix the anti-solvent uniformly in the concentrated lactose solution. The cavitational events are also likely to be increased due to the lowering of the

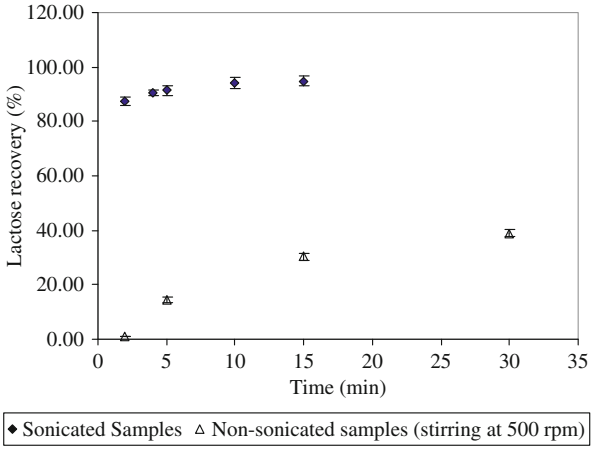

Fig. 17.6 Sonocrystallization of lactose solutions: comparison with conventional stirring approach

vapor pressure of the solution as a result of addition of ethanol. This causes sharp decrease in the solubility of lactose (locally) in the solvent (ethanol and water). The solution reaches supersaturation causing nucleation and rapid lactose recovery. In sonocrystallization, the insonation provides microscopic mixing by cavity oscillations, and cavitation induced acoustic streaming, which could be responsible for higher lactose recovery observed in the sonicated samples.

It is also worthwhile to compare the rates of lactose recovery in other conventional crystallization approaches. During an earlier study of anti-solvent crystallization (ethanol, 85% v/v) with a combination of seed at a concentration of 3% w/w at a temperature of 7 ± 2°C, lactose recovery of 92.6% was obtained from paneer whey (which resembles cottage cheese whey) in 60 min of crystallization time. Kapil et al. (1991) have reported that 64% lactose recovery from heat-induced deproteinated paneer whey (concentrated to 55% of total initial solids) is obtained over a period of 12 h in an evaporative and cooling type of crystallization process (conventional process). Another crystallization study (Hartel, 2001) have reported a lactose recovery of 44 and 47% at the end of 5 and 8 h of time, when crystallization was carried out at 40°C, with initial lactose content of 44%, in a batch crystallizer with 2.5 g of seed crystals. Thus, sonocrystallization is much faster (recovery time is few minutes as against few hours) as against conventional approaches such as evaporative and cooling type of crystallization and anti-solvent-based crystallization. Not only the overall process of crystallization is quicker with higher yields but the average crystal size was also lower and crystals were uniform in shape. Figure 17.7 shows the images of the lactose crystals recovered from reconstituted lactose solution (lactose content 17.5% w/v, protein content 0%), in the presence and absence of sonication. It can be easily seen that the crystals obtained using sonication are small, uniform in shape, and showed no aggregation as compared to those obtained in the absence of sonication (stirring) at the end of 5 min of crystallization time. Some lactose

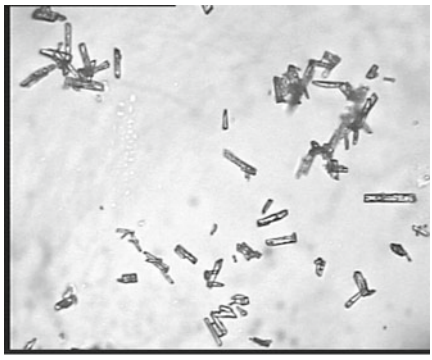

A. L17.5%, 5 min Sonication

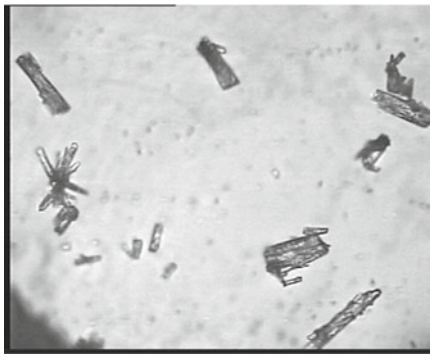

B. L17.5%, 5 min Only Stirring

Fig. 17.7 Comparison of shape and size of the crystals obtained using sonocrystallization as against conventional crystallization

crystals recovered without sonication showed broken corners and dendritic forms of crystals.

As discussed earlier, it is proposed that sometimes the effect of sonication is only on the nucleation process and hence it may be advisable to use sonication for a short duration followed by the conventional process. To investigate the role of sonication in the case of lactose recovery, different approaches of sonocrystallization were undertaken. When the reconstituted solution (17.5% w/v lactose content) was sonicated for only 1 min (for nucleation), followed by standing time (slow crystallization process), different shape characteristics were obtained as shown in Fig. 17.8. The lactose crystals were found to be larger in size with shape closer to tomahawk in comparison to needle-shaped crystals obtained at the end of sonication of 5 min and without the standing time. The size of crystals after a standing time of 12 h was found to be larger than those observed after 30 min of standing time. The crystal size was lowest with no agglomeration when continuous sonication was used for 5 min. Thus, this clearly indicates that sonication is required during the entire operation; first it contributes to nucleation and later it prevents crystal agglomeration leading to a uniform crystal shape and resultant lower size.

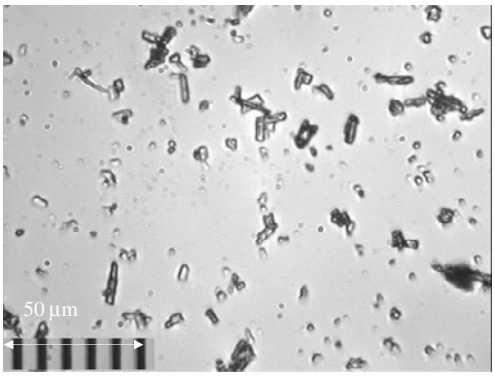

A. L17.5%, 5 min Sonication

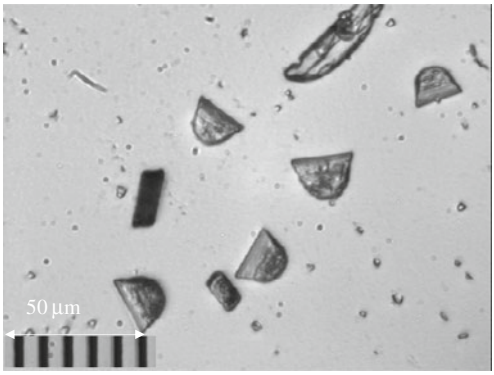

B. L17.5%, 1 min Sonication followed by 30 min standing

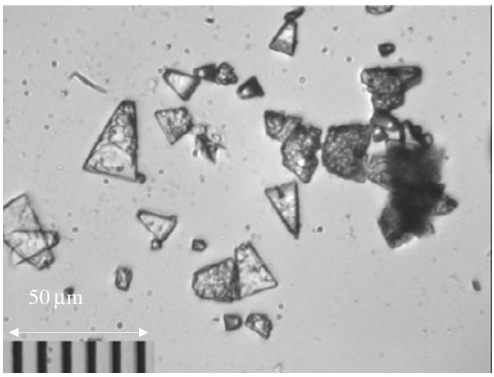

C. L17.5%, 1 min Sonication followed by 12 h standing

Fig. 17.8 Comparison of shape and size of the crystals obtained using different approaches of sonocrystallization

The dependency of the crystal size and the recovery time on the lactose concentration and the protein content in the solution was also investigated (Bund and Pandit, 2007a). The lactose recovery increased with an increase in the initial lactose concentration of the reconstituted solution. The lactose recovery was strongly

dependent on the initial lactose content of the reconstituted solution, even for the sonocrystallization approach. Higher the lactose content of the parent solution, faster would be the supersaturation achieved, resulting in even higher nucleation rate and subsequent higher lactose recoveries. Not only the extent of recovery was higher, the crystal size distribution was also very narrow.

Irrespective of the lactose concentration of the parent reconstituted lactose solution, the lactose recovery in insonated samples decreased with an increase in the protein concentration. The average diameter of the crystals also increased with an increase in the protein content (0–0.4% w/v) irrespective of the lactose concentration of reconstituted solution at pH 2.8. The increase in the average diameter of the crystals with an increase in the protein content clearly indicate that fewer nuclei are formed in the presence of the protein, which grew faster in the presence of sonication. Thus, the main influence of the protein is in delaying the nucleation phenomena.

The crystals recovered at pH 2.8 (8.08 μm) showed larger average diameter compared to those recovered at pH 4.2 (4.55 μm) irrespective of protein and lactose content. Also, the extent of lactose recovery was also higher at an operating pH of 4.2 as compared to an operating pH of 2.8.

The study has clearly indicated that sonication can be used with beneficial effects for improving the crystallization operation. The pH, protein, and lactose concentration of the reconstituted lactose solution play a crucial role in the process of lactose recovery by sonocrystallization. By controlling the insonation time, standing time, lactose concentration, pH, and protein content, the lactose crystals of desired crystal shape, size, and crystal size distribution (CSD) could be obtained. Sonocrystallization not only enables rapid crystallization but also guarantees a relative uniformity of CSD and prevention of agglomeration in comparison to non-sonicated samples. The lactose recovery reduced marginally but delayed drastically at pH of 2.8, even in the presence of only 0.4% w/v of protein. It was found that 87.45% of lactose recovery could be obtained in just 2 min of sonication time compared to the conventional lactose recovery process which takes anywhere between 12 and 72 h for only 55–60% recovery.

4.3 Process Optimization Using Statistical Approach

To maximize the synergistic effects it is always important to optimize the operating parameters in any process. Process optimization by one-parameter-at-time method (full factorial design) results in a large number of experiments, which usually is time consuming and also is economically not viable. Taguchi constructed a special set of general design guidelines for factorial experiments that cover many applications (Peace, 1993). The method uses a special set of arrays called orthogonal arrays, which stipulate the way of conducting the minimal number of experiments and gives full information of all the parameters that affect the performance. The additive assumption of the Taguchi design implies that the individual or main effects of the independent variables on performance parameter are separable. Taguchi

designs are balanced, that is, no parameter is weighted 'more or less' in an experiment, thus allowing parameters to be analyzed independent of each other. The statistical design approach (Taguchi orthogonal array method) has been used for the process optimization of rapid lactose recovery using sonocrystallization from deproteinated paneer whey (Bund and Pandit, 2007b). The important parameters to be considered for optimization with typical operating range can be given as deproteination (with/without $CaCl_2$), crystallization time (10 and 20 min), sonocrystallization temperature (7 and 30 ± 2°C), initial pH (i.e., pH of processed whey adjusted just before the crystallization, 2.8 and 4.2 ± 0.2), end pH (i.e., pH of slurry adjusted at the end of sonication time, 2.8 and 4.2 ± 0.2), 'mechanical stirring' in addition to insonation, using glass impeller and overhead stirrer (Remi equipments, Mumbai, India) (without stirring and stirring at 250–300 rpm), and seeding which was carried out immediately after the addition of ethanol (without seeding and seeding of 1% w/w). A detailed analysis of the responses (Bund and Pandit, 2007b) obtained in terms of percentage lactose recovery and other characteristics of the recovered lactose can then be performed using mean values obtained using MINITAB analytical software. A higher mean value indicates an optimum level for the respective parameter when responses were analyzed using option 'higher is better' and vice versa when the option chosen is 'smaller is better.' The difference between the mean values at two different levels for respective parameter is termed as 'delta' and it represents the degree of influence of that parameter on the desired response. Higher the delta value, higher is the influence of that parameter on the desired response. Based on the delta value the parameters are ranked. 'Rank' arranges the parameters in order of the greatest influence to the least influence on the response. The typical expected response table for mean values obtained with L_{12} orthogonal array for lactose recovery is given in Table 17.1 (the option

Table 17.1 Response table for ranking of the operating parameters for maximizing the lactose recovery

	Parameters						
Level	A	B	C	D	E	F	G
1	26.5	32.5	43.77	32.15	38.78	29.75	20.89
2	50.2	44.2	32.93	44.55	37.92	46.95	55.82
Delta	23.7	11.7	10.84	12.40	0.86	17.20	34.93
Rank	2	5	6	4	7	3	1

A – deproteination step (W/O – without $CaCl_2$, W – with $CaCl_2$ effective concentration of 2 mM)
B – sonication time (min)
C – temperature of reactants and crystallization temperature (°C)
D – initial pH (i.e., pH of processed whey before starting of sonocrystallization)
E – end pH (i.e., pH of processed whey adjusted just before end of crystallization (sonication) time)
F – stirring (N – no stirring (i.e., only sonication), Y – stirring on before starting the insonation and throughout the rest of crystallization time at 250–300 rpm)
G – seeding (% w/w of the lactose present in processed whey sample used for crystallization)

chosen for the analysis of responses was 'higher is better,' as experiments were aimed for higher lactose recovery). The table shows the mean value for each parameter level. For higher lactose recovery, deproteination at level 2 (deproteination in presence of $CaCl_2$), crystallization time at level 2 (20 min), crystallization temperature at level 1 (7 ± 2°C), initial pH at level 2 (pH 4.2 ± 0.2), end pH at level 2 (pH 4.2 ± 0.2), stirring at level 2 (250–300 rpm), and seeding at level 2 (1% w/w) were found to be at optimum levels. The last two rows in the tables document the delta values and ranks for the system. The individual components (parameters) selected in the present study can be ranked in terms of their influence toward the lactose recovery in the order as seeding > deproteination step > stirring > initial pH > sonication time > crystallization temperature > end pH suggesting that seeding had a major influence and end pH had the least effect on the lactose recovery. In the similar way the analysis can be done for the purity of lactose recovered in terms of lactose content, protein content, and the ash content (Bund and Pandit, 2007b).

It can be said that use of statistical analysis results in effective determination of the set of optimum parameters and also in establishing the controlling factor for the crystallization process. The work discussed here serves as a guideline for the methodology to be followed for process optimization of the sonocrystallization operation.

5 Overview of Recent Literature on Sonocrystallization

This section aims at analyzing different literature illustrations for use of sonication for improvement of the crystallization operation with an objective of understanding the effects of operating and geometric parameters. Mostly, the applications related to food technology and biotechnology, have been considered so as to maintain the focus of this chapter.

Chow et al. (2003a, 2005) reported the use of ultrasound for improvement in the crystallization of ice from sucrose solutions in the concentration range of 0–45 wt % of sucrose. It has been observed that the primary nucleation of ice in sucrose solutions can be achieved at higher nucleation temperatures in the presence of ultrasound. The nucleation temperatures can be reproduced with a lower standard deviation and a greater precision than under the control conditions (without ultrasound). The results have shown that increasing both the ultrasonic output level and the duty cycle increases the nucleation temperature, possibly due to the higher cavitational activity under these conditions. An increase in the power dissipation level or increase in the duty cycle means that the number of cavitational events or bubbles generated in the reactor increases. The greater number of bubbles could simply act as templates for new nuclei, increasing the probability of nucleation. Snapshot images of the bubble clouds obtained from the ultrasonic horn (Chow et al., 2005) have confirmed the hypothesis of possible increase in the number of bubbles with an increase in the ultrasonic output. It has been also reported that using a novel microscope system allowed the observation of actual nucleation of ice in sucrose

solutions. However, cavitational pitting of the surfaces in contact with the sample has prevented a full study of primary nucleation using this system due to the templating effects of the surface; however, a study of the secondary nucleation of ice in sucrose solutions was possible. The use of sucrose solutions has made possible the study of fine dendritic structures and crystal breakup to form new smaller crystal nucleating sites (i.e., secondary nucleation). Images taken using a microscope system show that the pre-existing ice dendrite crystals can be broken up into smaller fragments by an ultrasonic field. Cavitation bubbles appear to be important during the fragmentation process, possibly melting any ice crystals in their path. Flow patterns around cavitation bubbles have also been observed, and these may be responsible for the fragmentation of ice crystals. Chow et al. (2003b, 2005) have also reported a fundamental investigation into the effect of a single cavitation bubble in an ultrasonic standing wave (at approximately 27 kHz) on the sonocrystallization of ice. High-speed movies (1,120 fps) have shown that the crystallization appears to occur in the immediate vicinity of the single bubble. In most cases, many crystals are observed and it is not known whether a single ice crystal is being fragmented by the bubble or whether many crystals are being initiated. The bubble appears to undergo a dancing regime, frequently splitting and rejoining, and also emitting some small microbubbles.

Improvement in the crystal structure of ice due to the use of ultrasound dictates the application of ultrasound to freezing operations (Li and Sun, 2002). The quality of the frozen foods depends on the size of the ice crystals formed during the freezing. Presence of large ice crystals within the frozen food tissue could result in mechanical damage, drip loss, and thus reduction in product quality. Sun and Li (2003) investigated the role of ultrasound in improvement of the immersion freezing of the potato tissues. The reactor used was an ultrasonic bath operating at 25 kHz frequency and with variable power dissipation in the range of 0–300 W. The results showed that the freezing rate of potato sample was improved with the application of ultrasound, compared to that without ultrasound. The beneficial effects were observed only above a critical power dissipation level and beyond this power, higher output power and longer exposure time to ultrasound would help to enhance the freezing rate. However, the heat produced when ultrasound passes through the medium limited the power applied and the exposure time. In this work, the freezing rate was fastest with an output power of 15.85 W and a treatment time of 2 min. The analyses conducted on the microstructure of potato tissue using cryo-scanning electron microscopy technique showed that the plant tissue exhibited a better cellular structure under ultrasonic power of 15.85 W. Much less intercellular void and cell disruption was observed. This was attributed to high freezing rate obtained under high ultrasonic level and thus the domination of intracellular small ice crystals. Thus, it can be said that the application of power ultrasound is effective in improving the structure of frozen-then-thawed potato tissue.

Patrick et al. (2004) investigated the effect of the ultrasonic field on the crystal structure of palm oil in an ultrasonic ring cell generating ultrasound at intensities in the range of 30–45 dB. It has been reported that the absence of ultrasonic field (conventional crystallization approach) resulted in a mixture of large and smaller

spherulitic crystals. Applying ultrasound to the sample had a dramatic effect, even at the lowest level of 30 dB. The crystals were of a more uniform size than the control. The results obtained also show that at a level just below the cavitational threshold, crystallization occurs in the minimum time implying that the system is working at its most efficient level at this point. The crystal structure appears to be highly dependent on the intensity of the ultrasound with the resultant samples having different properties dependent upon the intensity of ultrasound applied. The same material (in this case palm oil) can be used to yield a variety of textures from something that resembles clotted cream to a smooth cream, similar to a face cream simply by altering the intensity at which the ultrasound is applied, provided it is below the cavitational threshold. When the ultrasound was applied at the 30 dB level, there was very little effect on the kinetics but it appeared as if the ultrasound had prevented the large spherulitic crystals, observed in the control, from forming. Also, the network surrounding the crystals appeared to be made up of needle-like structures and it has been hypothesized that the ultrasound has caused an increase in the number of nucleation sites limiting the size to which the crystals can grow. The matrix of long needle-like structures is thought to be due to lack of space for either the crystals to grow or needles that have been knocked off from larger crystals during the crystallization process. Increasing the ultrasonic intensity to 35 dB produced smaller and more uniform crystals that tend to clump together and fall to the bottom of cell. A further increase in intensity to 40 dB, below the cavitational threshold, produced a uniform product of very small crystals suggesting that there were numerous nucleation sites that produced crystals simultaneously. The increase in the applied ultrasound to above the cavitational threshold gave areas where no clear crystal structure could be seen and it is hypothesized that these are areas where cavitation has its maximum effect. The work has clearly demonstrated the fact that by controlling the ultrasonic intensity, it is possible to generate required crystal size distribution and hence the required texture, at the same time not producing the adverse sonochemical reactions that typically occur with very high-power probes. This gives us the ability to structure materials simply by choosing the correct power levels for ultrasonic treatment.

Lyczko et al. (2002) have investigated the effect of ultrasound on the induction time and metastable zone width considering potassium sulfate as a model compound using an immersion transducer-type (ultrasonic horn) sonochemical reactor. It has been reported that ultrasound reduces the induction time especially for low absolute supersaturation. Quantitatively speaking, the induction time without ultrasound is about 9,000 s whereas with ultrasound, it is about 1,000 s. For experiments with ultrasound, the predominant effect has been identified as a specific effect of ultrasound and not an effect of the lower wall temperature, which was applied to remove the heat generated due to ultrasonic power dissipation. The metastable zone width can also be reduced by the application of ultrasound. Results indicate that it would be sufficient to apply a low ultrasonic power (50 W/l as against 120 W/l) to decrease the metastable zone width. Thus, the use of ultrasound has clearly shown to decrease the apparent order of the primary nucleation rate and increase the rate of appearance of the solid. Guo et al. (2005) have reported similar effect of reduction

in the induction time with the application of ultrasound for roxithromycin as the model compound. It has been reported that after applying ultrasound to the system, the change in the apparent nucleation order is small; however, the nucleation rate constant increases significantly (4.25-fold). The diffusion constant also increased significantly (3.82-fold by using 400 W ultrasound). This suggests that diffusion intensification is the main reason for the reduction in the induction time. These studies conclusively establish the fact that ultrasound permits to set off nucleation at supersaturation lower than that without ultrasound. Thus, in industrial crystallization processes, ultrasound can induce nucleation in conditions where spontaneous primary nucleation cannot occur without ultrasound.

Amara et al. (2001) investigated the effect of ultrasonic power dissipation on the crystallization of potash alum in an ultrasonic reactor operating at 20 kHz frequency and variable power dissipation in the range of 10–300 W. Homogenization of the solution was also ensured by external agitation using a propeller rotating at a speed of 1,000 rpm. It has been reported that ultrasound decreases the limit of supersaturation as the nucleation temperature increases due to the presence of ultrasound. Also there was a significant increase in the extent of recovery but the extent of recovery remains independent of the power dissipation similar to the variation of the nucleation temperature with the power dissipation levels. However, the crystal size was found to be dependent on the power dissipation levels. In general, the crystal size distribution was narrower when ultrasound was used as compared to the conventional stirring operation. At enhanced power dissipation levels, mean crystal size was reported to be smaller. However, high-power ultrasound also leads to the abrasion of the potash crystals as indicated by the electron scanning microscope measurements. Thus it is important to optimize the ultrasonic power dissipation levels as any additional power input does not necessarily add to any more beneficial effects.

In continuation of the earlier work, Amara et al. (2004) investigated the effect of addition of crystals (as seed) on the sonocrystallization operation. It has been reported that with ultrasound the solubility is approached more rapidly than in silent conditions. Ultrasonic power therefore increases the rate of desupersaturation and hence the mass growth rate of the crystals. Estimation of the values of the kinetic parameters (k is the overall growth rate coefficient and g is the order of the growth mass rate) of the growth rate law indicated that these are lower for a growth with ultrasound as compared to that without the use of ultrasound. The growth rate of the crystals was also independent of the initial crystal size (total added surface area was maintained constant by varying the size and the total mass) unlike the conventional operation which showed a decrease in the supersaturation with an increase in the initial crystal size.

Li et al. (2003) investigated the application of ultrasound for ‘salting-out crystallization’ operation. In the conventional salting-out crystallization, the entire process from solution with a suitable concentration to supersaturation, nucleation of solution, and growth of crystals needs generally several hours with addition of precipitant dosage and blend of mechanical agitation. Mechanical agitation provides mainly macroscopic mixing, a layer of liquid moving to another layer. In

this manner of mixing, the precipitant molecules are not aptly distributed among the solution molecules rapidly and uniformly. Therefore, if a large amount of precipitant is added too rapidly, local excessive supersaturations will be caused so as to produce amorphous and agglomerated crystals of uncontrollable size. For the rapid sonocrystallization, insonation provides microscopic mixing by vibration, cavitation, and the travel of ultrasound wave creating fluctuating pressure fields. Satisfactory mixing, especially at micro-level, is achieved much more rapidly than in the conventional mixing. This promotes nucleation and crystal growth, i.e., promote the mass transfer. Furthermore, the physical nature of crystals can be controlled to some extent by varying the ultrasonic parameters and the size of crystallization vessel. The sonochemical reactor used by Li et al. (2003) was capable of operating at variable frequency of irradiation (15–30 kHz) and power dissipation (0–1,200 W). Application of ultrasound for different irradiation periods indicated that the crystal size distribution was strongly dependent on the irradiation time and lowest mean crystal size was obtained at highest treatment time. The scanning electron micrographs of the crystal product indicated that, with the same duration of ultrasound and volume of mixture, the crystals become shorter and thicker as the ultrasound power increases. The crystals insonated with the power of 1,000 W are thicker and shorter and the crystals insonated with 100 W are longer and thinner. The observed effect was attributed to the fact that large ultrasonic energy (power) accelerates effectively the mass transfer in the mixture and thus enhances the hydrodynamic driving force for crystallization. With large kinetic energy and speed, the solute molecules will have an increased opportunity to collide with each other, penetrate the stagnant film, and hence insert into the crystal lattice more uniformly and easily (enhancement in the mass transfer coefficient). It is known that the shape of the crystal depends on the growth rate at each face of a crystal. The speed of insonated molecules is fast enough for them to approach each side of the crystal to compensate partly for differences in the growth rate of each side in the conventional crystallization, where diffusion limitations may be present. Thus, it is reasonable that the shape of the crystal insonated with larger energy appears shorter and thicker. Ultrasound waves of different frequency; 15, 20, 25, and 30 kHz were also used in the rapid sonocrystallization. Using these frequencies, there are no obvious differences in the shape, the mean size, and the size distribution of resulting crystals. This means that these different frequencies, i.e., different wavelengths in the sonoprocess, have similar influence on nucleation and growth of crystal and these effects appear to be frequency independent. A possible cause is that these wavelengths are much larger than the size of the nuclei and crystals and hence the effects of the insonation are similar.

Li et al. (2006) have investigated the action of power ultrasound in controlling the supersaturation, nucleation, and crystal growth during the acid–base reaction crystallization of 7-amino-3-desacetoxy cephalosporanic acid (7-ACDA). The sonochemical reactor used operated at 25 kHz and maximum power dissipation was 1,000 W, though generally power dissipation used was only 100 W. The induction period was observed to be substantially lower for the insonated sample as compared to the conventional mixing operation. Also nucleation is promoted due to the

cavitational effects, namely generation of cavities in the medium and generation of local high temperatures and pressure, which alters the local levels of supersaturation. It has been also reported that the added reactant is rapidly distributed in the reaction mixture under ultrasonic field as compared to mechanical agitation due to the enhanced turbulence and acoustic streaming. When the NH_4OH reactant solution was added rapidly to the precursor 7-ADCA solution and an agitator with rotation rate of 800 rpm was used, the resulting product was poorly crystalline with irregular shapes and many small broken pieces. This indicates that conventional agitation cannot cope with the fast feeding in such crystallization. Without sufficient nucleation and mass transfer, high supersaturation in some region leads to the very fast aggregation of solute. When aggregation predominates over the orientation arrangement during crystal growth, the end product will be poorly crystalline. Poor bonding in the crystalline structure leads to the breakage of crystals during agitation leading to blunt edges and corners where the molecules would be less firmly held than in the middle of a surface. Sonication increases the relative movement of crystals and provides the benefits of rapid crystal growth to a product with a regular outline, sharp edges, and corners. Sonication also prevents agglomeration of the crystal particles not only by maintaining turbulent conditions continuously but also by preventing accumulation of the reactant leading to very high levels of supersaturation locally. The main controlling parameters in the case of reaction crystallization have been reported to be the concentration of the reactant and the ultrasonic time as well as power dissipation. Proper optimization of these parameters is recommended for getting the desired crystal size distribution.

Dhumal et al. (2008) have investigated the role of using ultrasound as a seeding and compared the results with the conventional crystallization process. Lactose crystals were obtained from solution by ultrasound-assisted in situ seeding, followed by growth in viscous glycerin solution. The crystals were characterized for physical properties and 63–90 μm size fractions of different batches were mixed with salbutamol sulfate (SS) and compared for in vitro deposition. It has been reported that cooling crystallization with stirring for 10–20 h resulted in crystals with wide particle size distribution (PSD) and varied shape; however, application of ultrasound resulted in rapid and complete crystallization in 5 min with rod-shaped fine crystals (15–30 μm) and narrow PSD. Seeding followed by growth in glycerin showed desirable size, high elongation ratio, smooth surface, and narrow PSD, while growth under stirring showed high elongation ratio with rough surface. Crystals grown in glycerin showed highest dispersibility and fine particle fraction (FPF) of SS. These results have clearly established the role of ultrasound in the process of in situ seeding and use of ultrasound followed by ordered growth in glycerin offers rapid technique for separation of nuclei induction from crystal growth yielding desirable characteristics for better dispersion and possible application of in vitro deposition.

Patel and Murthy (2009) have recently investigated the process of lactose crystallization for the recovery of lactose from reconstituted lactose solutions with the aid of ultrasound, in the presence of ‘acetone,’ as an anti-solvent. It has been reported that use of ultrasound offers spontaneous supersaturation resulting in early

nucleation. With cavitation and acoustic streaming, ultrasound shows a great ability in rapid and uniform blending of the anti-solvent with the lactose solution resulting in rapid lactose recovery from sonicated samples as compared to non-sonicated samples. The lactose recovery was found to be directly proportional to the acetone concentration. Acetone has been found to be effective as an anti-solvent and its usage can give high yield of lactose recovery. The sonication time, pH, and initial lactose concentration of reconstituted lactose solution were observed to be most influencing parameters for the recovery of lactose. The recovery of lactose is found to be in the range of 80–92% within 4 min of sonication, while the conventional techniques are time consuming and not effective enough. Spontaneous nucleation and growth of seeds accelerate the growth of length rather than the width and thickness resulting in rod-shaped seed crystals.

Based on the overview of the literature illustrations, in general it can be said that the positive influence of ultrasound (US) on crystallization processes is shown by the dramatic reduction of the induction period, supersaturation conditions, and metastable zone width. Manipulation of this influence can be achieved by changing US-related variables such as frequency, intensity, power, and even geometrical characteristics of the ultrasonic device (e.g., horn type, size, transducer arrangement changing the ultrasonic pressure field). The volume of the sonicated solution and irradiation time are also variables to be optimized in a case-by-case basis as the mechanisms of US action on crystallization remain to be established. Nevertheless, the results obtained so far make foreseeable that crystal size distribution, and even crystal shape, can be 'tailored' by appropriate selection of the sonication conditions. We now give some recommendations for effective utilization of the ultrasound effects in crystallization operation:

1. Ultrasound aids in significantly reducing the induction time required for the onset of crystallization process mainly by providing additional nuclei sites due to cavities/bubbles generated in the medium. The effect is more predominant at lower supersaturation levels and should be optimized on a case-to-case basis.
2. Ultrasound can induce nucleation under conditions where spontaneous primary nucleation cannot occur in its absence, thus avoiding seeding and hence the introduction of foreign particles into the solution.
3. The metastable zone width (MZW) can also be reduced by application of ultrasound mainly by influencing the nucleation and local supersaturation levels. It has been generally observed that ultrasound application at low-power dissipation levels is also sufficient for these effects and application at higher power dissipation might not be useful or sometimes even lead to detrimental effects due to enhanced heat dissipation by ultrasound. The solvent properties such as vapor pressure and surface tension usually do not significantly affect the nucleation process including the MZW.
4. The ultrasound typically used in common crystallization media (mainly aqueous media) falls in the low-frequency range. It has been also shown that low-frequency US waves of variable frequency (15–50 kHz) result in no substantial differences in shape, mean size, or size distribution in the resulting crystals. It

is also possible that optimum frequency might exist beyond which detrimental effects are observed rather than improving the yields and crystal size distribution.
5. The crystal size distribution is also affected by the ultrasonic power dissipation and the dimensions of the ultrasonic transducers which mainly affect the magnitude of the acoustic streaming and turbulence existing in the reactor. These parameters need to be optimized by weighing the beneficial effects as against the cost of operation.
6. It is possible to 'tailor' a crystal size distribution between the extreme cases of a short burst of US to nucleate at lower levels of supersaturation and allow growth to large crystal and the production of small crystal via continuous (or perhaps a longer single burst) US application throughout the duration of the process, which can facilitate prolific nucleation at higher levels of supersaturation at the expense of some crystal growth. Pulsed or intermittent application of US can give an intermediate effect. In any event, the optimum needs to be determined by experimental investigation at least at this state of the knowledge base.
7. Judicious application of US to a polymorphic system at the right level of supersaturation can assist in isolating the ground-state polymorph (the most thermodynamically favored and less soluble) or the one very near the ground state. This availability to induce the formation of a given polymorph under US action is of paramount importance particularly in the pharmaceutical industry.
8. In crystallization processes induced by the addition of an anti-solvent or reactive crystallization, where high supersaturation levels may be produced very rapidly, it has been shown that the application of US reduces not only the induction times of nucleation but also the spread of variability in induction time at a given level of supersaturation in the vicinity of the crystal surface. Under these conditions, bulk-phase mass transfer becomes rate limiting in supplying growth units to the crystal surface, and its ultrasonic enhancement will enhance the growth rate.
9. Sonocrystallization also avoids the problems involved in intentional seeding, very common in industrial crystallization process. The effects of intentional seeding include narrowing of the MZW, shortening of induction times, and control of particle size distribution, which can be effectively, achieved using ultrasonic field under optimized levels of power dissipation and treatment times.

6 Concluding Remarks and Scope for Future Work

Overall it appears that use of ultrasound can significantly improve the crystallization operation by significant reduction in the processing time and also generating better quality of crystals. An efficient optimization protocol for operating and geometric parameters of the sonocrystallization operation as per the guidelines discussed earlier is required for maximizing the effects of the use of ultrasound. It also appears that the present trend from users to apply ultrasound to initiate and control crystallization processes will attract more attention than sonochemistry in the near future as ultrasound allows a new dimension of control over the nucleation regime and

may allow the nucleation and crystal growth balance to be regulated in order to optimize the product and particle properties. Developments in equipment in recent years, in particular the availability of large-scale sonochemical reactors operating on the principle of multiple transducer irradiations (with or without multiple frequency operation), has increased the possibilities of using ultrasound in larger scale processes. Use of large number of transducers also helps in achieving near-uniform dissipation of incident energy and hence the cavitational effects, which is essentially required in the crystallization operation.

With an aim of obtaining fundamental information related to efficient design and operation of sonocrystallization equipments, it is recommended that experimental analysis for different systems should be carried out to establish the correspondence between the cavitational activity and the improvements in the crystallization parameters. On a theoretical front, it is recommended to develop generalized models incorporating population balance, cavity–crystal interaction parameters, and local energy dissipation due to cavitational oscillatory collapse and integrating molecular modeling with polymorph.

References

Amara, N., Ratsimba, B., Wilhelm, A. M., and Delmas, H. (2001). Crystallization of potash alum: effect of power ultrasound. *Ultrasonics Sonochemistry*, 8, 265.

Amara, N., Ratsimba, B., Wilhelm, A. M., and Delmas, H. (2004). Growth rate of potash alum crystals: comparison of silent and ultrasonic conditions. *Ultrasonics Sonochemistry*, 11, 17.

Bund, R. K., & Pandit, A.B. (2007a). Rapid lactose recovery from buffalo whey by use of 'anti-solvent, ethanol. *Journal of Food Engineering*, 82, 333.

Bund, R. K., and Pandit, A. B. (2007b). Rapid lactose recovery from paneer whey using sonocrystallization: A process optimization. *Chemical Engineering and Processing*, 46, 846.

Chow, R., Blindt, R., Chivers, R., and Povey, M., (2003a). The sonocrystallization of ice in sucrose solutions: primary and secondary nucleation, *Ultrasonics*, 41, 595.

Chow, R., Mettin, R., Lindinger, B., Kurz, T., and Lauterborn, W. (2003b). The importance of acoustic cavitation in the sonocrystallisation of ice - high speed observations of a single acoustic bubble. *IEEE International Ultrasonics Symposium Proceedings*, USA, pp 1447.

Chow, R., Blindt, R., Chivers, R., and Povey, M. (2005). A study on the primary and secondary nucleation of ice by power ultrasound. *Ultrasonics*, 43, 227.

Dahlem, O., Reisse, J., and Halloin, V. (1999). The radially vibrating horn: A scaling up possibility for sonochemical reactions. *Chemical Engineering Science*, 54, 2829.

Demirdöven, A., and Baysal, T. (2009). The use of ultrasound and combined technologies in food preservation. *Food Reviews International*, 25(1), 1.

Dhumal, R. S., Biradar, S. V., Paradkar, A. R., and York, P. (2008) Ultrasound assisted engineering of lactose crystals. *Pharmaceutical Research*, 25(12), 2835.

Elvers, B., Hawkins, S., and Schulz, G. (1990) *Ullmann's encyclopedia of industrial CHEMISTRY*, 5th edn. Germany, VCH.

Gogate, P. R., Mujumdar, S., and Pandit, A.B. (2003). Large scale sonochemical reactors for process intensification: Design and experimental validation, *Journal of Chemical Technology and Biotechnology*, 78, 685.

Gogate, P. R., Shirgaonkar, I. Z., Sivakumar, M., Senthilkumar, P., Vichare, N. P., and Pandit, A. B. (2001). Cavitation reactors: Efficiency analysis using a model reaction *American Institute of Chemical Engineer's Journal*, 47, 2326.

Gogate, P. R., Tatake, P.A., Kanthale, P. M., and Pandit, A. B. (2002) Mapping of sonochemical reactors: Review, analysis and experimental verification. *American Institute of Chemical Engineer's Journal*, 48, 1542.

Gonze, E., Gonthier, Y., Boldo, P., and Bernis, A. (1998). Standing waves in a high frequency sonoreactor: Visualisation and effects. *Chemical Engineering Science*, 53, 523.

Guo, Z., Zhang, M., Li, H., Wang, J., and Kougoulos, E. (2005). Effect of ultrasound on anti-solvent crystallization process. *Journal of Crystal Growth*, 273, 555.

Hartel, R. W. (2001). *Crystallization in foods*. Gaithersburg, USA, Aspen.

Kapil, V., Dodeja, A. K., and Sarma, S.C. (1991). Manufacture of lactose – effect of processing parameters on yield and purity. *Journal of Food Science and Technology*, 28, 167.

Khanal, S. K., Grewell, D., Sung, S., and Van Leeuwen, J. (2007). Ultrasound applications in wastewater sludge pretreatment: A review. *Critical Reviews in Environmental Science and Technology*, 37, 277.

Kordylla, A., Koch, S., Tumakaka, F., and Schembecker, G. (2008) Towards an optimized crystallization with ultrasound: Effect of solvent properties and ultrasonic process parameters. *Journal of Crystal Growth*, 310(18), 4177

Krishna, M. V., Babu, J. R., Latha, P. V. M., and Sankar, D. G. (2007) Sonocrystallization: For better pharmaceutical crystals. *Asian Journal of Chemistry*, 19, 1369.

Kumar, A., Gogate, P. R., and Pandit, A.B. (2007). Mapping the efficacy of new designs for large scale sonochemical reactors. *Ultrasonics Sonochemistry*, 14, 538.

Li, B., and Sun, D.-W. (2002). Effect of power ultrasound on freezing rate during immersion freezing. *Journal of Food Engineering*, 55, 85.

Li, H., Wang, J., Bao, Y., Guo, Z., and Zhang, M. (2003). Rapid sonocrystallization in the salting-out process. *Journal of Crystal Growth*, 247, 192.

Li., H., Li, H., Guo, Z., and Liu, Y. (2006). The application of power ultrasound to reaction crystallization. *Ultrasonics Sonochemistry*, 13, 359.

Luche, J. L. (1998). *Synthetic organic sonochemistry*. New York, NY, Plenum Press.

Luque de Castro, M. D., and Priego-Capote, F. (2007) Ultrasound-assisted crystallization (sonocrystallization). *Ultrasonics Sonochemistry*, 14, 717.

Lyczko, N., Espitalier, F., Louisnard, O., and Schwartzentruber, J. (2002). Effect of ultrasound on the induction time and the metastable zone widths of potassium sulphate. *Chemical Engineering Journal*, 86, 233.

Mason, T. J., Paniwnyk, L., and Lorimer, J.P. (1996). The uses of ultrasound in food technology. *Ultrasonics Sonochemistry*, 3, S253.

McCausland, L. J., and Cains, P. W. (2004). Power ultrasound – A means to promote and control crystallization in biotechnology. *Biotechnology and Genetic Engineering Reviews*, 21, 3.

McCausland, L. J., Cains, P. W., and Martin, P. D. (2001) Use the power of sonocrystallization for improved properties. *Chemical Engineering Progress*, 97, 56.

Palmowski, L., Simons, L., and Brook, R. (2006) Ultrasonic treatment to improve anaerobic digestibility of dairy waste streams. *Water Science and Technology*, 53, 281.

Patel, S. R., and Murthy, Z. V. P. (2009) Ultrasound assisted crystallization for the recovery of lactose in an anti-solvent acetone. *Crystal Research and Technology*, 44, 889

Patrick, M., Blindt, R., and Janssen, J. (2004). The effect of ultrasonic intensity on the crystal structure of palm oil. *Ultrasonics Sonochemistry*, 11, 251.

Peace, G. S. (1993). *Taguchi methods*. Reading, MA, Addison-Wesley.

Prakash, M. N. K., and Ramana, K. V. R. (2003). Ultrasound and its application in the food industry. *Journal of Food Science and Technology*, 40, 563.

Romdhane, M., Gourdon, C., and Casamatta, G. (1995). Local investigation of some ultrasonic devices by means of a thermal sensor, *Ultrasonics*, 33, 221.

Ruecroft, G. (2007). Power ultrasound and particle engineering crystals for drug delivery and formulation. *Chimica Oggi*, 25, 12.

Ruecroft, G., Hipkiss, D., Ly, T., Maxted, N., and Cains, P. W. (2005) Sonocrystallization: The use of ultrasound for improved industrial crystallization. *Organic Process Research and Development*, 9, 923.

Soudagar, S. R., and Samant, S. D. (1995). Semiquantitative characterization of ultrasonic cleaner using a novel piezoelectric pressure intensity measurement probe. *Ultrasonics Sonochemistry*, 2, S49.

Sun, D.-W., and Li, B. (2003). Microstructural change of potato tissues frozen by ultrasound-assisted immersion freezing. *Journal of Food Engineering*, 57, 337.

Sutkar, V. S., and Gogate, P.R. (2009) Design aspects of sonochemical reactors: Techniques for understanding cavitational activity distribution and effect of operating parameters, *Chemical Engineering Journal*, 155, 26

Thoma, G., Swofford, J., Popov, V., and Som, M. (1997). Sonochemical destruction of dichloromethane and o-dichlorobenzene in aqueous solution using a near field acoustic processor. *Advances in Environmental Research*, 1, 178.

Thompson, L. H., and Doraiswamy, L. K. (1999). Sonochemistry: Science and engineering. *Industrial and Engineering Chemistry Research*, 38, 1215.

Chapter 18
Ultrasound-Assisted Freezing

A.E. Delgado and Da-Wen Sun

1 Summary

Freezing is a well-known preservation method widely used in the food industry. The advantages of freezing are to a certain degree counterbalanced by the risk of damage caused by the formation and size of ice crystals. Over recent years new approaches have been developed to improve and control the crystallization process, and among these approaches sonocrystallization has proved to be very useful, since it can enhance both the nucleation rate and the crystal growth rate. Although ultrasound has been successfully used for many years in the evaluation of various aspects of foods and in medical applications, the use of power ultrasound to directly improve processes and products is less popular in food manufacturing. Foodstuffs are very complex materials, and research is needed in order to define the specific sound parameters that aid the freezing process and that can later be used for the scale-up and production of commercial frozen food products. In this chapter we present the experimental results of our research on the effects of ultrasound application on apple and melon fruits and discuss its influence on the freezing rate, nucleation temperature, and physical structure.

2 Introduction

Freezing is a well-established preservation method widely used in the food industry, which involves lowering product temperature generally to −18°C or below. At temperatures lower than −10°C few microorganisms can develop, chemical reactions rates are greatly reduced, and cellular metabolic reactions are also delayed (Delgado and Sun, 2001). One of the key issues in maintaining the shelf life and other quality attributes of frozen food is ice crystallization (Kennedy, 2003). On the

A.E. Delgado (✉)
Food Refrigeration and Computerised Food Technology, Agriculture and Food Science Centre, University College Dublin, Belfield, Dublin 4, Ireland
e-mail: adriana.delgado@ucd.ie

H. Feng et al. (eds.), *Ultrasound Technologies for Food and Bioprocessing*, Food Engineering Series, DOI 10.1007/978-1-4419-7472-3_18,
© Springer Science+Business Media, LLC 2011

one hand, the conversion of water into ice has the advantage of fixing the tissue structure and separating the water fraction in the form of ice crystals in such a way that it is not available as a solvent or to take part in deterioration reactions; but on the other hand, the size and location of the ice crystals can cause damage to cell membranes and break down the physical structure with disappointing consequences in terms of texture. As is well known, the rate of freezing largely affects the size and distribution of ice crystals; high freezing rates lead to the production of small crystals evenly distributed throughout the tissue, while slow freezing rates generally cause large ice crystals to form exclusively in extracellular areas. Therefore, extensive research has been carried out to control crystal size and to minimize the time of water–ice transition, since this can contribute to better preserving product quality (Brennan et al., 1990). Air blast, plate contact, immersion freezing, cryogenic freezing, and their combinations are the most common methods used for food freezing (Sun, 2001). Within the last few years, new methods are being analyzed in order to accelerate and/or improve the freezing process. These innovations include high-pressure shift freezing, dehydrofreezing, applications of antifreeze protein and ice nucleation protein, and ultrasound-assisted freezing (Sun and Zheng, 2006).

Ultrasound has attracted considerable interest in food science and technology due to its promising effects in food processing and preservation (Knorr et al., 2004). The sound ranges employed can be broadly divided into high-frequency, low-energy, diagnostic ultrasound in the megahertz range and low-frequency, high-energy, power ultrasound in the kilohertz range (Mason and Chemat, 2003). Power ultrasound, in particular, has proved to be extremely useful in crystallization processes (Mason, 1998). Controlled crystallization of sugar solutions, hardening of fats, and the manufacture of chocolate and margarine are examples of food processes that can be improved by the application of power ultrasound (Leadley and Williams, 2006). Although the potential of power ultrasound to assist food freezing is promising, it has not yet been sufficiently exploited (Zheng and Sun, 2006). Because the fundamentals and theoretical considerations of ultrasound in food processing are being considered in other chapters of this book, in this chapter we will discuss the experimental results from research carried out by our group related to the use of ultrasound to assist freezing, focusing on the effect of ultrasound on freezing efficiency, nucleation temperature, and food tissue orientation.

3 Ultrasound and Freezing Efficiency

3.1 Influence of Ultrasound on Freezing Rate

The advantages of food preservation by freezing are to a certain degree counterbalanced by the risk of damage caused by the formation of ice within the tissue, since it can mechanically affect cell membranes and distort tissue structure (Martino et al., 1998; Sanz et al., 1999). However, minimizing the time to cross the zone of

maximum ice crystal formation or "thermal arrest time" helps to better maintain the quality of the product. Under the influence of ultrasound, food materials such as soft fruits can be frozen with a reduced freezing time through the zone of ice crystal formation (Leadley and Williams, 2006). Li and Sun (2002) reported a significant improvement of the freezing rate when ultrasound at 15.85 W was applied on immersion-frozen potatoes for 2 min during the phase change period. It is considered that the formation and behavior of bubble of cavitation upon the propagation of acoustic waves constitute the essential events that induce the majority of acoustic effects (Knorr et al., 2004; Leighton, 1998).

The potential of ultrasonic energy as a heat transfer enhancing agent has been demonstrated to be efficient during sterilization and other heat treatments where the fluid-to-particle heat transfer coefficient was significantly enhanced (Sastry et al., 1989). Furthermore, ultrasound was also used to supply all energy requirements for thawing frozen meat and fish, i.e., sonic and ultrasonic vibrations were used in a different approach than that to only assist heat transfer into the material (Miles et al., 1999). In addition, acoustic streaming, which describes a steady flow field superimposed upon the oscillatory motion of a sound wave, has been cited by many authors as a mechanism for enhancing mass transfer processes in membranes, porous materials, and foods (Cárcel et al., 2007; Floros and Liang, 1994; García-Pérez et al., 2006; Haydock and Yeomans, 2003; Mulet et al., 2003). Since freezing is a simultaneous heat and mass transfer process, it can well benefit from the effects generated by the application of power ultrasound.

The experimental results of the research presented here were undertaken on cylindrical samples (length 2.5 cm, diameter 1.8 cm) of apples and melons immersed in an ultrasonic bath system filled with a mixture of ethylene glycol and water at the proportion of 50%:50% in volume. Fresh apples (*Malus pumila*) of the Granny Smith variety (86.9% w/w average moisture content, wet basis, soluble solids content $\cong$ 12 °Bx) and melons (*Cucumis melo*) commonly known as "Honeydew" (89.9% w/w average moisture content, wet basis, soluble solids content $\cong$ 9.4 °Bx) were purchased in a local market and stored at 4 $\pm$ 1°C until use. An ultrasonic bath system (Elma MC 300 LC, Elma GmbH & Co KG, Germany), which operates at 40 kHz frequency and dissipated powers from 130.6 to 201.2 W (0.23 to 0.36 W/cm^2 acoustic intensity, respectively), was used. Because the application of ultrasound produces heat, which is adverse to the freezing process, ultrasound was applied intermittently at 15 or 30 s intervals. Table 18.1 summarizes the ultrasound treatments applied for different exposure times and from different initial temperatures. The ultrasonic exposure time was referred to as the sum of every treatment time (Li and Sun, 2002). The freezing rate represented by the characteristic freezing time and considered as the time for the center to traverse the temperature range from -1 to -7°C is also indicated in Table 18.1 for the sonicated and control samples (without ultrasound application). Figure 18.1 shows the orientation of the cylinders cut from the apple and melon flesh. At least four replications were carried out for each test in order to minimize the natural and inevitable variability from fruit to fruit. Particular attention was also paid to keep the experimental setup constant since the intensity of ultrasound might vary with the position in the tank. Samples

Table 18.1 Ultrasound treatments and characteristic times for apple (tangential orientation) and melon samples at 131.3 W ultrasonic power level and coolant temperature of –25°C

Treatment	Exposure time (min)	Ultrasound application/ interval (s)	Initial temperature for ultrasound application (°C)	Characteristic time (min)
Apple				
Control				4.85 (±0.19)[a]
1	2	30/30	–1	4.56 (±0.24)
2	1.5	30/30	–1	4.84 (±0.17)
3	2	30/30	–2	4.88 (±0.19)
4	1.5	30/30	–2	4.88 (±0.18)
5	2	30/30	0	4.54 (±0.24)
6	1.33	20/30	–1	4.82 (±0.21)
Melon				
Control				3.76 (±0.24)
7	2	30/30	–1	4.17 (±0.16)
8	1	15/30	–1	4.01 (±0.08)
9	2	30/30	0	4.08 (±0.11)
10	1	15/30	0	4.04 (±0.05)
11	1.5	15/15	–1	4.02 (±0.03)
12	1.5	15/15	0	3.88 (±0.22)
13	1	15/15	–1	3.62 (±0.16)
14	1	15/15	0	3.83 (±0.05)

[a]Standard deviations in brackets

were placed in a cage consisting of a thin wire and then positioned to stand on the bottom of the ultrasonic unit, i.e., there was no free space between the sample and the bottom of the ultrasonic vessel except for that of the wire of the cage, the sample being well below the air–liquid interface.

In a previous work, Li and Sun (2002) found that the freezing rate was significantly improved when ultrasound was applied to the phase change period, while there was no effect when it was applied to the pre-cooling or tempering phases, and freezing rates were almost equal to those without ultrasound. Thus, the initial temperature from which ultrasound was applied was selected to be close to the initial freezing point. This temperature, sometimes referred to as the transition temperature (Miles et al., 1999), was experimentally determined from the time–temperature curves and was found to be around −2 and −1.4°C for apple and melon fruits, respectively. Figure 18.2 shows typical freezing curves obtained for apple and melon samples frozen with and without the application of ultrasound. Analysis of the characteristic time (ANOVA followed by Tukey's comparison of means) showed that for apples the freezing rates were significantly improved ($P<0.05$) when ultrasound was applied for 2 min in total, with 30 s intervals, from −1 to 0°C (Treatments 1 and 5). Although there was a reduction of about 4% in the characteristic time for Treatment 13 for melon, this reduction was not significant ($P>0.05$) at the acoustic power level of 131.3 W.

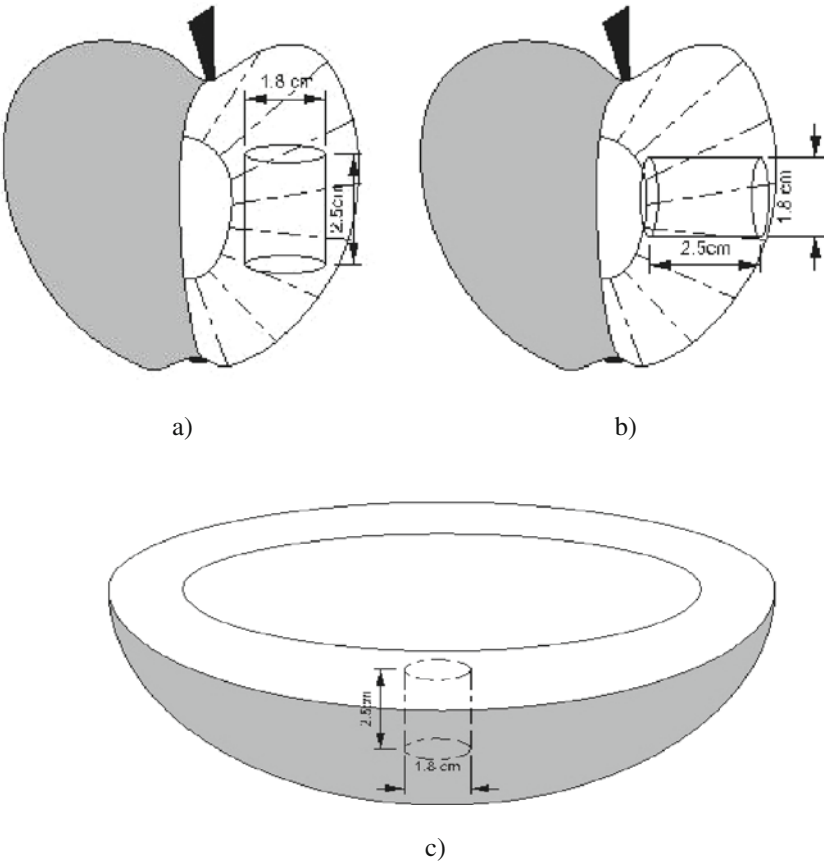

Fig. 18.1 Cut orientations of the fruit tissue: (**a**) apple tangential orientation; (**b**) apple radial orientation; (**c**) melon

It should be noted that ultrasound is extremely sensitive to the presence of gas bubbles; fruits and vegetables in particular are non-homogenous materials, with the flesh of some of them, such as apples, containing 20–25% air (Khan and Vincent, 1993; McClements, 1997; Mizrach et al., 1994). This explains why many fruits and vegetables have very large attenuation coefficients and why their ultrasonic velocities are often lower than that of air (McClements, 1997). Table 18.2 shows the mean compression wave velocity for some fresh fruits and vegetable specimens. It can be observed that the velocity of sound in apples is relatively low, probably due to the lack of a clear fibrous structure and large intercellular air spaces, while potato, on the other hand, allows a higher sound velocity even though it does not present a clear fibrous structure, but has only 2% of intercellular spaces (Mizrach et al., 1989). In the study of Li and Sun (2002) an acoustic intensity of 0.053 W/cm^2 (15.85 W) delivered at 25 kHz frequency was sufficient to cause a significant reduction in the freezing rate of potatoes. Mizrach et al. (1994) observed different attenuation coefficients for melon flesh, depending on the location from which samples were taken:

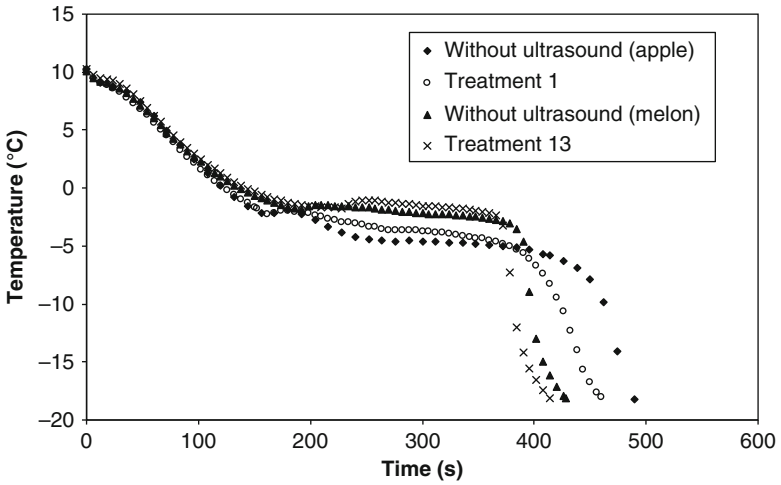

Fig. 18.2 Comparison of freezing curves for apple and melon samples frozen without ultrasound and under ultrasound treatments 1 and 13

Table 18.2 Compression wave velocity for some fresh fruits and vegetables using a 50 kHz transmitter and 50 kHz receiver

Material	Mean velocity (m/s)	Standard deviation
Air	331.00	
Potato	380.04	±6.59
Melon	242.81	±13.17
Apple	184.55	±24.21

Adapted from Mizrach et al. (1989)

next to the peel, at the center of the flesh, or next to the seed cavity. Melon samples were taken in the present work so as to try to include the inner, middle, and outer flesh of the fruit (Fig. 18.1), and probably due to the differences in attenuation coefficients, very little effect of ultrasound was observed when an acoustic intensity of 0.23 W/cm^2 (40 kHz) was used. Thus, it is sometimes difficult to transmit ultrasound through fruits and vegetables, higher ultrasonic intensities and lower frequencies (<100 kHz) (McClements, 1997; Mizrach et al., 1989), that is, appropriate and specific ultrasound variables, might be needed. Therefore, much higher levels of ultrasound power than in previous work (Li and Sun, 2002) were experimented upon in the current study.

3.2 Influence of Acoustic Power on Freezing Process

An ultrasonic wave is characterized by its amplitude and frequency and its wavelength and attenuation coefficient, which are (frequency-dependent) characteristics

of a material (McClements, 1997). As mentioned before, fruit tissue is a highly attenuated material for high-frequency ultrasonic signals normally used in the ultrasonic testing of foods (0.1–100 MHz) (McClements, 1997; Mizrach et al., 1994). In order to overcome this problem, many researchers have tried to use higher acoustic powers despite certain disadvantages. Since higher frequencies are more attenuated than lower ones, high-intensity ultrasound is applied at low frequencies (<100 kHz) to obtain high power levels (McClements, 1997; Mulet et al., 2002). The experimental results presented here were obtained by using an ultrasonic unit that operates at a fixed frequency of 40 kHz. Variable ultrasonic power could be delivered to the liquid medium, from 131.3 to 201.2 W, which were determined by the calorimetric method. Table 18.3 shows the effects of increasing the ultrasonic power level on the characteristic freezing time when ultrasound was applied from −1°C and for 1 min exposure time. It can be observed that when apple samples (tangential orientation) were exposed to increasing power levels, the freezing rates were enhanced except for Treatment C. Analysis of the characteristic time revealed that this enhancement was significant only for Treatment B (0.26 W/cm^2). Therefore, the freezing rate of immersed frozen apple samples represented by the characteristic freezing time can be significantly improved ($P < 0.05$) as compared to that of immersion freezing without ultrasound when ultrasound is applied from 0°C (Treatment 5, Table 18.1) or −1°C (Treatment 1, Table 18.1) for 2 min in total, with 30 s intervals at 0.23 W/cm^2, or from −1°C for 1 min with 30 s intervals at 0.26 W/cm^2.

Melon samples showed a similar trend of reduced characteristic times as ultrasound irradiation increased. The increased freezing rates were significant (P<0.05) for all melon treatments except for Treatment E (131.3 W). It can also be noted that for the operating conditions used, a significant increase (P<0.05) in the freezing

Table 18.3 Ultrasound treatments and characteristic times under different power ultrasound levels. Ultrasound application from −1°C for 1 min exposure time and coolant temperature of −25°C

Treatment	Ultrasonic power level (W)	Ultrasound application/ interval (s)	Characteristic time (min)
Apple			
Control			4.85 (±0.19)[a]
A	131.3	30/30	4.73 (±0.04)
B	145.8	30/30	4.59 (±0.12)
C	159.0	30/30	4.86 (±0.17)
Melon			
Control			3.76 (±0.24)
D	131.3	15/15	3.62 (±0.16)
E	159.0	15/30	3.42 (±0.12)
F	159.0	15/15	3.34 (±0.11)
G	201.2	15/30	3.43 (±0.11)
H	201.2	15/15	3.41 (±0.07)

[a]Standard deviations in brackets

efficiency of 11% was achieved for Treatment F, i.e., when melon samples were sonicated at 159.0 W (0.28 W/cm^2) for 1 min in total (15 s four times) intermittently at 15 s. Heat, cavitation, and turbulence are among the sound effects that high-intensity acoustic radiation causes as it propagates through a medium (Floros and Liang, 1994), which are in accordance with the results observed. At liquid/solid interfaces, acoustic waves cause extreme turbulence, "acoustic streaming" or "microstreaming," which in conjunction with the formation, growth, and collapse of small bubbles or cavitation produces mixing and/or agitation that enhances heat and mass transfer processes; hence, reduced freezing rates are obtained when increasing output levels are applied. On the other hand, when an ultrasonic wave propagates through a material it causes periodic fluctuations in the local temperature and pressure (McClements, 1997). Thus, there is a heating or thermal effect as a result of specific absorption of acoustic energy which will increase refrigerant and sample temperatures. This heat generation might be particularly adverse to the freezing process unless means are implemented to compensate for this negative effect, for example, in this case, by increasing the fluid flow rate so as to help maintain the refrigerant temperature constant (Zheng and Sun, 2005). The thermal effect can be noticed when comparing the effective freezing times of apple samples for Treatments 1 and 5, which were sonicated for 2 min, and Treatment B, which was irradiated for 1 min and at a higher acoustic intensity, 0.26 W/cm^2 instead of 0.23 W/cm^2. The effective freezing time was calculated by considering the total time required to reach −18°C from an initial temperature of 10°C and was equal to 7.77 (±0.24), 7.63 (±0.27), 7.54 (±0.16), and 7.91 (±0.25) for Treatments 1, 5, B, and control, respectively. Although the characteristic freezing times for all these treatments were significantly lower than that for the control treatment (without ultrasound), the difference in effective freezing time was significant (P<0.05) only when a power ultrasound level of 145.8 W was applied for 1 min (Treatment B) as compared to that of immersion freezing without ultrasound. Longer exposure times of Treatments 1 and 5, even though at lower ultrasound power level, caused higher heat generation that could not be easily removed in this case by the cooling capabilities of the temperature bath system. In the practical point of view, ultrasonic power level applied should be chosen under the consideration of combining the thermal effect of ultrasound and its enhancing effect on heat transfer (Li and Sun, 2002).

4 Ultrasound and Ice Nucleation Temperature

The crystallization process is an important unit operation used in the chemical, pharmaceutical, and food industries and is usually divided into two essential stages: nucleation and crystal growth. In this process a crystalline phase is created as a result of molecular aggregation in a solution, leading to the formation of nuclei and, later, crystal growth. Supersaturation, nucleation, and crystal growth are the predominant physical phenomena associated with crystallization (Banga et al.,

2004). In recent years new approaches have been developed to enhance the crystallization process such as supercritical, capillary, laser-induced crystallization, and sonocrystallization, and all of these strategies target the nucleation stage because nucleation is more energetically demanding than crystal growth and, hence, can have a remarkable influence on the crystallization rate (Banga et al., 2004; Price, 1997). Sonocrystallization is an appropriate descriptor for using ultrasound to influence both nucleation and crystal growth behavior (Price, 1997). A number of papers and patents have been published relating ultrasound to improved crystallization of organic compounds, including substances such as carbohydrates and proteins, which under conventional conditions can be troublesome due to the difficulties of crystallizing and the large supersaturation driving forces involved (Ruecroft et al., 2005). Studies carried out on cavitation-induced nucleation suggest that the collapse of a cavitation bubble increases the equilibrium freezing temperature of water and then triggers the nucleation of ice, although the exact mechanism is unclear and it is still not known whether or not cavitation, either stable or transient, is a pre-requisite for the sonocrystallization of ice in water (Chow et al., 2003, 2005; Zhang et al., 2003). Most of the literature on the experimental effects of ultrasound has paid attention to the increase of primary nucleation temperature, and few works have been reported on the effect of an ultrasonic field on the growth of an ice crystal (Chow et al., 2003). In general, sonocrystallization exhibits a number of characteristics specific to the ultrasonic wave, which for most materials include (i) faster primary nucleation (formation of a nucleus in a previously crystal-free solution); (ii) the initiation of secondary nucleation (nucleation induced by the presence of pre-existing crystals); and (iii) the production of smaller crystals with greater size uniformity (Chow et al., 2005).

Evidence of the stimulation of primary nucleation of ice has been observed by Chow et al. (2003) for sucrose solutions in the concentration range of 0–45%. The authors (Chow et al., 2003) reported that for increasing concentration of sucrose solutions under fixed ultrasonic conditions and for increased ultrasonic power output level, the nucleation temperature consistently occurred at a higher nucleation temperature in the presence of ultrasound; however, no definitive conclusions were drawn about the significance of any differences between both ultrasonically irradiated and control samples. The nucleation temperature or initiation of primary nucleation of ice was recorded in our research as the temperature at which the center temperature of apple and melon samples rapidly increased caused by the latent heat of crystallization (Chow et al., 2003, 2005). The experimental results are shown in Fig. 18.3, where supercooling, i.e., the number of degrees below 0°C, is plotted for the control and ultrasound treatments. Although there were no significant differences among the nucleation temperature of the different treatments of apple (tangential orientation) and melon samples as compared to the control without ultrasound, it can be noted that at 131.3 W, apple samples of Treatments 2, 4, 6, and A, which were irradiated for shorter periods of time, from 1 to 1.5 min, exhibited a slight increase in nucleation temperature (lower supercooling). This effect was not observed for Treatments 1, 3, and 5 and Treatments B and C, probably due to the heating effects caused by longer exposure times (2 min) and/or higher

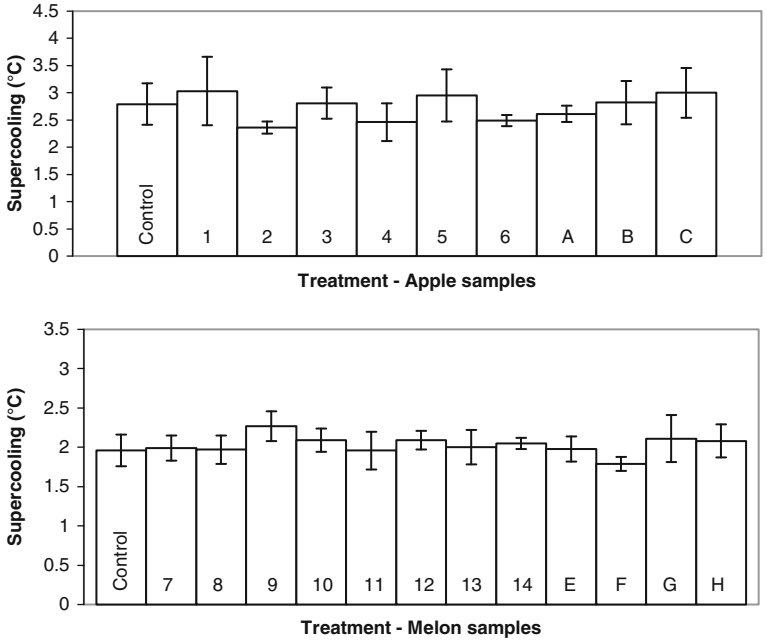

Fig. 18.3 Effect of ultrasound on the nucleation temperature of ice in apple (tangential orientation) and melon samples (error bars indicate standard deviations)

acoustic intensities (0.26–0.28 W/cm^2), respectively, which resulted in an increase in the temperature of the refrigerant fluid; thus, sufficient supercooling for ice nucleation was not achievable.

The supercooling range determined for melon samples was narrower (up to 2.3°C) than that for apple samples (up to 3.6°C), which together with the operating conditions used might have made it difficult for the effects of ultrasound on crystal nucleation to manifest. Only when melon samples were sonicated at 159 W for 1 min from −1°C (Treatment F), a small increase in the nucleation temperature (−1.79°C) was observed, though the difference was not significant (P>0.05) when compared to the ice nucleation temperature of samples frozen in the absence of ultrasound (−1.96°C). There is reliable evidence that applying ultrasound not only induces nucleation but also increases reproducibility (Luque de Castro and Priego-Capote, 2007). This effect of ultrasound is consistent with the nucleation temperatures determined for Treatment F, which had lower standard deviation (0.09) than the control samples (0.20). It was also observed for melon samples that when comparing treatments that had the same acoustic level, time duration and application of ultrasound, and different initial temperature from which ultrasound was applied (e.g., Treatments 7 and 9, 8 and 10, and 11 and 12), the samples that were irradiated from 0°C exhibited slightly higher supercooling or lower nucleation temperature than when they were sonicated from −1°C where the nucleation

temperature was almost the same or slightly higher (Treatment F) than the control sample. As reported in the literature, extremely small seed crystals generated by insonation offer all the advantages of intentional seeding, a common practice in industrial crystallization (Luque de Castro and Priego-Capote, 2007; Ruecroft et al., 2005). In a batch process, seeds must be added at precisely the correct time, that is, during the development of the supersaturation profile; addition too soon to a solution that is undersaturated will result in the seed dissolving, while seeding too late will also be ineffective because the solute material may already have crystallized (Luque de Castro and Priego-Capote, 2007; Ruecroft et al., 2005). In the particular case of melon samples, it seems that the application of ultrasound from 0°C is rather earlier and before the appropriate level of supersaturation is achieved. It is important to note here that many of the reports in the literature relating ultrasound with the increase in the primary nucleation of ice were carried out in pure water systems or in sucrose solutions, while the results shown in Fig. 18.3 correspond to a more complex system as it is a fruit, even though some evidence of ultrasonic induction of crystal nucleation could be observed.

5 Ultrasound and Tissue Orientation

The structure or physical arrangement of foods (e.g., voids, non-homogeneities, fiber orientation) can affect ultrasound transmission. In meat products, as is well known, heat can transfer differently depending on the fiber orientation, i.e., parallel or perpendicular to the muscle fibers. In a similar way, Shore et al. (1986) found that the amplitude attenuation coefficient for muscle tissue is approximately proportional to frequency and varies with the orientation of the muscle fibers relative to the direction of ultrasound transmission (Miles et al., 1999). Thus, foods can display different values in their properties depending on the direction in which they are tested and then they can be isotropic or anisotropic. Potato parenchyma, for example, is isotropic, with small cells tightly packed with less than 2% intercellular spaces, showing no cellular orientation, while apple parenchyma is highly anisotropic (Khan and Vincent, 1993). An apple fruit is mainly composed of the flesh made of parenchyma tissue permeated with vasculature and intercellular air spaces that amount to about 21% of the fruit volume (Dražeta et al., 2004; Sterling, 1968). Because the apple parenchyma is mechanically anisotropic, the influence of applying ultrasound on radial or tangential orientated samples was examined in our work; radial samples were cut radially from the surface to the core of the fruit, while in tangential samples, the cut was parallel to the fruit core, as indicated in Fig. 18.1. Experiments were carried out at 131.3 W ultrasound power level using the operating conditions of Treatments 1 and 5 (Table 18.1), since the freezing rates corresponding to these treatments were significantly improved ($P<0.05$) under ultrasound irradiation. Table 18.4 shows the average characteristic times, the nucleation temperatures, and the standard deviations obtained at an average refrigerant fluid of −25.2°C. The large standard deviation values in the nucleation temperatures of

Table 18.4 Characteristic times and nucleation temperatures for radial and tangential apple samples

Treatment	Characteristic time (min)	Nucleation temperature (°C)
Control – radial	4.75 (±0.23)[a]	–2.76 (±0.21)[a]
Control – tangential	4.85 (±0.19)	–2.79 (±0.38)
1 – radial	4.46 (±0.11)	–2.50 (±0.24)
1 – tangential	4.56 (±0.24)	–3.03 (±0.63)
5 – radial	4.54 (±0.05)	–3.63 (±0.82)
5 – tangential	4.54 (±0.24)	–2.95 (±0.48)

[a]Standard deviation in brackets

Treatments 1 – tangential (0.63) and 5 – radial (0.82) are due to some unusual and high supercooling values that were also included when averaging the data. For the control treatment (without the application of ultrasound), radial and tangential orientated samples were also analyzed, although there was no significant difference between them. Statistical analysis of the characteristic time indicated that samples of Treatments 1 and 5 cut in radial or tangential orientation were not significantly different ($P>0.05$). It was also observed that a slightly lower characteristic time was obtained when samples cut in radial orientation were sonicated for 2 min from −1°C (Treatment 1). Analysis of the nucleation temperature showed that Treatment 5 – radial was different ($P<0.05$) from Treatment 1 – radial and from both radial and tangential control samples. Thus, nucleation occurred at a higher temperature (lower supercooling) for apple samples of Treatment 1 radially orientated, while radial samples of Treatment 5 showed higher supercooling. Although there was no difference from the freezing rate efficiency point of view for Treatments 1 and 5 for both radial and tangential samples, some effect of ultrasound on the nucleation temperature was noticeable for apple samples cut in radial orientation, which might suggest a relation between the direction of orientation of cell columns and intercellular spaces (dashed lines in Fig. 18.1) and ultrasound transmission. Dražeta et al. (2004) studied the radial disposition of air in the flesh of Braeburn apples and found that there is a gradient of declining air content from just beneath the skin to the center of the fruit with a sharp discontinuity at the core line. Granny Smith variety might exhibit a similar behavior, and since ultrasound is sensitive to the presence of intercellular air spaces, it seems possible that radial samples could be more affected by ultrasound than tangential ones.

Among other factors, the rate of nucleation is influenced by the degree of supercooling (or supersaturation); greater supercooling (lower nucleation temperature) causes the formation of a large number of nuclei, while a lower degree of supercooling favors crystal growth (Fennema, 1973; Zheng and Sun, 2006). Knowledge of the effect of ultrasound on the nucleation temperature is useful when selecting an ultrasound treatment in relation to a particular process. For example, during immersion freezing of fruits and vegetables by direct contact with salt or sugar solutions, the control of solid uptake by the food is very important since it can have

an adverse effect on product flavor caused by residual refrigerant. It is known that high-intensity ultrasound can produce an increase in mass transport kinetics, thus being a way of accelerating these kinds of processes (Floros and Liang, 1994, Mulet et al., 2003). Studies on apple cylinders dipped into a sodium chloride solution showed that as long as the product remains unfrozen, including freezing conditions when supercooling persists, mass transfer is relatively high (Lucas et al., 1998), so the level of salt impregnation reached could be inconveniently high, and then Treatment 1 appears to be more adequate for this situation. Treatment 5 can be a better choice if, for example, a higher gain of sugars is desirable; Cárcel et al. (2007) recently reported an increase in the diffusion coefficient of water and solids of apples immersed in a sucrose solution at 30°C once an ultrasound intensity threshold was achieved. Therefore, a lower or higher degree of supercooling may be a positive or negative effect and will depend on the particular product and process. Analysis on the relation size/distribution of ice crystals to microstructure and freezing conditions should also be taken into account.

6 Conclusions

The use of ultrasound to assist the immersion freezing process was investigated and experimental results obtained on apple and melon samples were presented. Ultrasound power, its intensity, pulsed or intermittent application, and time duration all influenced freezing rates. Results showed that when ultrasound was applied on apple samples from 0°C or −1°C for 2 min in total, with 30 s intervals at 0.23 W/cm^2, or from −1°C for 1 min at 0.26 W/cm^2, the freezing rate represented by the characteristic freezing time was significantly improved for up to 8% ($P < 0.05$) as compared to that of immersion freezing without ultrasound. For melon samples, the positive effect of ultrasound as an enhancing heat transfer agent was observed at ultrasonic intensities higher than 0.26 W/cm^2, and the improvement of the freezing rate efficiency was significant ($P<0.05$) when melon samples were irradiated at 159.0 W–0.28 W/cm^2 for 1 min from −1°C. Under the studied conditions no significant differences were observed between irradiated radial and tangential apple samples, though the freezing rates were enhanced and different ($P < 0.05$) from the control treatment (without ultrasound). Under specific ultrasound treatments, evidence of the influence of ultrasound to stimulate primary nucleation was observed on apple and melon samples. As fruits are complex and non-homogenous materials with soft tissues in general, their texture can be greatly affected by the freezing process. The use of ultrasound as a means to control the crystallization process offers promising application in this field. More research is necessary in order to establish appropriate and specific sound parameters since fruits and vegetables are very highly attenuated materials. Nowadays, great advertising efforts are being conducted to draw consumers to frozen foods, since they unfortunately have a cheap or inferior image compared to their chilled product counterparts. In this context, ultrasound can play an important and promising role by providing higher quality ranges of frozen foods.

References

Banga, S., Chawla, G., and Bansal, A.K. (2004). New trends in the crystallization of active pharmaceutical ingredients. *Business Briefing: Pharmagenerics*, 6, 70–74.

Brennan, J. G., Butters, J. R., Cowell, N. D., and Lilly, A. E. V. (1990). *Food engineering operations*, 3rd edn. Amsterdam, Elsevier.

Cárcel, J. A., Benedito, J., Rosselló, C., and Mulent, A. (2007). Influence of ultrasound intensity on mass transfer in apple immersed in a sucrose solution. *Journal of Food Engineering*, 78(2), 472–479.

Chow, R., Blindt, R., Chivers, R., and Povey, M. (2003). The sonocrystallisation of ice in sucrose solutions: Primary and secondary nucleation. *Ultrasonics*, 41(8), 595–604.

Chow, R., Blindt, R., Chivers, R., and Povey, M. (2005). A study on the primary and secondary nucleation of ice by power ultrasound. *Ultrasonics*, 43(4), 227–230.

Delgado, A. E. and Sun, D.-W. (2001). Heat and mass transfer models for predicting freezing process – A review. *Journal of Food Engineering*, 47(3), 157–174.

Dražeta, L., Lang, A., Hall, A. J., Volz, R. K., and Jameson, P.E. (2004). Air volume measurement of "Braeburn" apple fruit. *Journal of Experimental Botany*, 55(399), 1061–1069.

Fennema, O. (1973). Nature of the freezing process. In: Fennema, O. R., Powrie, W. D., and Marth, E. H. (eds.), *Low-temperature preservation of foods and living matter*, pp. 150–239. New York, NY, Marcel Dekker.

Floros, J. D., and Liang, H. (1994). Acoustically assisted diffusion through membranes and biomaterials. *Food Technology*, December, 79–84.

García-Pérez, J. V., Cárcel, J. A., de la Fuente-Blanco, S., and Riera-Franco de Sarabia, E. (2006). Ultrasonic drying of foodstuff in a fluidized bed: Parametric study. *Ultrasonics*, 44(Suppl 1), e539–e543.

Haydock, D., and Yeomans, J. M. (2003). Acoustic enhancement of diffusion in a porous material. *Ultrasonics*, 41(7), 531–538.

Kennedy, C. (2003). Developments in freezing. In: Zeuthen, P., and Bøgh-Sørensen, L. (eds.), *Food preservation techniques*, pp. 228–240. Cambridge, CRC Press.

Khan, A. A., and Vincent, J. F. V. (1993). Compressive stiffness and fracture properties of apple and potato parenchyma. *Journal of Texture Studies*, 24(4), 423–435.

Knorr, D., Zenker, M., Heinz, V., and Lee, D.-U. (2004). Applications and potential of ultrasonics in food processing. *Trends in Food Science and Technology*, 15(5), 261–266.

Leadley, C. E., and Williams, A. (2006). Pulsed electric field processing, power ultrasound and other emerging technologies. In: Brennan, J. G. (ed.), *Food processing handbook*, pp. 201–236. Weinheim, Wiley-VCH GmbH and Co.kGaA.

Leighton, T. G. (1998). The principles of cavitation. In: Povey, M. J. W., and Mason, T. J. (eds.), *Ultrasound in food processing*, pp. 151–182. London, Blackie Academic and Professional.

Li, B. and Sun, D.-W. (2002). Effect of power ultrasound on freezing rate during immersion freezing of potatoes. *Journal of Food Engineering*, 55(3), 277–282.

Lucas, T., François, J. and Raoult-Wack, A.-L. (1998). Transport phenomena in immersion-cooled apples. *International Journal of Food Science and Technology*, 33(5), 489–499.

Luque de Castro, M. D. and Priego-Capote, F. (2007). Ultrasound-assisted crystallization (sonocrystallization). *Ultrasonics Sonochemistry*, 14(6), 717–724.

Martino, M. N., Otero, L., Sanz, P. D., and Zaritzky, N. E. (1998). Size and location of ice crystals in pork frozen by high-pressure-assisted freezing as compared to classical methods. *Meat Science*, 50(3), 303–313.

Mason, T. J. (1998). Power ultrasound in food processing – The way forward. In: Povey, J. W., and Mason, T. J. (eds.), *Ultrasound in food processing*, pp. 105–126. London, Blackie Academic and Professional.

Mason, T. J., and Chemat, F. (2003). Ultrasound as a preservation technology. In: Zeuthen, P., and Bøgh-Sørensen, L. (eds.), *Food preservation techniques*, pp. 303–337. Cambridge, CRC Press.

McClements, D. J. (1997). Ultrasonic characterization of foods and drinks: Principles, methods, and applications. *Critical Reviews in Food Science and Nutrition*, 37(1), 1–46.

Miles, C. A., Morley, M. J., and Rendell, M. (1999). High power ultrasonic thawing of frozen foods. *Journal of Food Engineering*, 39(2), 151–159.

Mizrach, A., Galili, N., and Rosenhouse, G. (1989). Determination of fruit and vegetable properties by ultrasonic excitation. *Transactions of the American Society of Agricultural Engineers*, 32(6), 2053–2058.

Mizrach, A., Galili, N., and Rosenhouse, G. (1994). Determining quality of fresh products by ultrasonic excitation. *Food Technology*, 48(12), 68–71.

Mulet, A., Cárcel, J. A., Benedito, J., and Sanjuan, N. (2002). Applications of low-intensity ultrasonics in the dairy industry. In: Welti-Chanes, J., Barbosa-Cánovas, G. V., and Aguilera, J. M. (eds.), *Engineering and food for the 21st century*, pp. 763–783. Boca Raton, FL, CRC Press.

Mulet, A., Cárcel, J. A., Sanjuán, N., and Bon, J. (2003). New food drying technologies – Use of ultrasound. *Food Science and Technology International*, 9(3), 215–221.

Price, C. J. (1997). Take some solid steps to improve crystallization. *Chemical Engineering Progress*, 93(9), 34–43.

Ruecroft, G, Hipkiss, D., Ly, T., Maxted, N., and Cains, P.W. (2005). Sonocrystallization: The use of ultrasound for improved industrial crystallization. *Organic Process Research and Development*, 9(6), 923–932.

Sanz, P. D., de Elvira, C., Martino, M., Zaritzky, N., Otero, L. and Carrasco, J. A. (1999). Freezing rate simulation as an aid to reducing crystallization damage in foods. *Meat Science*, 52(3), 275–278.

Sastry, S. K., Shen, G. Q., and Blaisdell, J. L. (1989). Effect of ultrasonic vibration on fluid-to-particle convective heat transfer coefficients. *Journal of Food Science*, 54(1), 229–230.

Shore, D., Woods, M. O., and Miles, C. A. (1986). Attenuation of ultrasound in post rigor bovine skeletal muscle. *Ultrasonics*, 24(2), 81–87.

Sterling, C. (1968). Effect of low temperature on structure and firmness of apple tissue. *Journal of Food Science*, 33, 577–580.

Sun, D.-W. (ed.). (2001). *Advances in food refrigeration*. Surrey, Leatherhead Publishing, LFRA.

Sun, D.-W., and Zheng, L. (2006). Innovations in freezing process. In: Sun, D.-W. (ed.), *Handbook of frozen food processing and packaging*, pp. 175–195. Boca Raton, FL, CRC Press, Taylor and Francis Group.

Zhang, X., Inada, T., and Tezuka, A. (2003). Ultrasonic-induced nucleation of ice in water containing air bubbles. *Ultrasonics Sonochemistry*, 10(2), 71–76.

Zheng, L. and Sun, D.-W. (2005). Ultrasonic assistance of food freezing. In: Sun, D.-W. (ed.), *Emerging technologies for food processing*, pp. 603–626. San Diego, CA, Elsevier.

Zheng, L., and Sun, D.-W. (2006). Innovative applications of power ultrasound during food freezing process – a review. *Trends in Food Science and Technology*, 17(1), 16–23.

Chapter 19
Ultrasound-Assisted Hot Air Drying of Foods

Antonio Mulet, Juan Andrés Cárcel, José Vicente García-Pérez, and Enrique Riera

1 Introduction

This chapter deals with the application of power ultrasound, also named high-intensity ultrasound, in the hot air drying of foods. The aim of ultrasound-assisted drying is to overcome some of the limitations of traditional convective drying systems, especially by increasing drying rate without reducing quality attributes. The effects of ultrasound on drying rate are responsible for some of the phenomena produced in the internal and/or external resistance to mass transfer.

Ultrasonic energy transfer in gas media is more difficult than in liquid media, due to the poor impedance match between the radiating element systems and the air and between the air and the particle being dried. This chapter will show the different alternatives available for improving acoustic energy transfer in the gas media during drying. Stepped plate ultrasonic systems have shown high transfer efficiency working at direct contact between the samples and the radiating element. Despite their high efficiency, applying stepped plate ultrasonic devices to conventional drying systems is quite difficult. A vibrating cylinder constituting not only the drying chamber but also the acoustic radiating element represents an interesting alternative to stepped plate systems.

Using the vibrating cylinder ultrasonic application system, the influence of the main process variables which affect hot air drying has been addressed. This chapter shows the main results of the influence of the velocity and temperature of the air flow used during drying assisted by power ultrasound. It also addresses the influence of the acoustic energy level in the medium and the importance of the structure of the material being dried.

A. Mulet (✉)
Grupo de Análisis y Simulación de Procesos Agroalimentarios, Departamento de Tecnología de Alimentos, Universidad Politécnica de Valencia, Camí de Vera, s/n, 46022, Valencia, Spain
e-mail: amulet@tal.upv.es

H. Feng et al. (eds.), *Ultrasound Technologies for Food and Bioprocessing*, Food Engineering Series, DOI 10.1007/978-1-4419-7472-3_19,
© Springer Science+Business Media, LLC 2011

2 The Food Drying Process

Although the preservation of food based on the partial removal of its water content dates back a long time, it is still one of the most relevant and challenging unit operations in food processing. The drive toward improved drying technologies is spurred by the need to produce better quality products (Chou and Chua, 2001) and to save energy. Because dehydration operations, in general, are very costly in terms of energy consumption, there is still a lot of room for improvement (Vega-Mercado et al., 2001). Drying is a notoriously energy-intensive operation that easily accounts for up to 15% of all industrial energy usage, often with relatively low thermal efficiency in the range of 25–50%. Thus, in order to reduce energy consumption per unit of product moisture, it is necessary to examine different methodologies to improve the energy efficiency of the drying equipment (Chua et al., 2001). The slowness of moisture transport is usually one of the main factors responsible for a long drying process that affects both the quality of the product and the energy consumption.

During the drying process, two types of resistance control water transport: internal resistance to the water movement inside the material and external resistance between the solid surface and the air (Rosselló et al., 1997; Simal et al., 2001). Internal resistance is a characteristic of the material, while external resistance depends on the thickness of the diffusion boundary layer.

Nowadays, several methods are applied to accelerate the loss of moisture and to minimize quality degradation in the final dried product. It is also very important to point out that the selection of the best drying technique is still determined by the type of product, its composition, and its physical properties (Vega-Mercado et al., 2001).

An increase in air velocity results in an increase of turbulence around the solid surface that reduces the thickness of the diffusion layer, thus attaining a higher drying rate (Cárcel et al., 2007a). An air velocity threshold is usually observed, above which an increase in the drying rate is no longer significant (Mulet et al., 1999). In this sense, fluidized bed drying is applied to reduce the external resistance of mass transfer in the drying of granular solid food. Infrared drying helps to reduce the drying time by providing additional sensible heat to expedite the drying process (Chou and Chua, 2001). For the drying of liquids, slurries, or purees, external resistance is overcome using spray driers (Vega-Mercado et al., 2001). In microwave drying techniques, the microwaves applied produce internal heating and a vapor pressure within the product that gently "pumps" the moisture to the surface (Turner and Jolly, 1991), thereby reducing the internal resistance of food to moisture transport. Another attempt to deal with the heat transport in conventional hot air drying combines radio frequency heating with conventional convective drying. The high processing costs of the superior quality products achieved by freeze drying are partially compensated by heat pump drying techniques (Strommen and Kramer, 1994). Other techniques to save energy and to improve the quality of products are based on the use of several air temperatures in stepwise drying (Chua et al., 2001).

The dehydration of food products can take place not only in gas–solid (or liquid) systems but also in liquid–solid systems such as osmotic dehydration (Mavroudis et al., 1998). This kind of process consists of immersing the solid in a hypertonic solution to dehydrate. Two main fluxes of matter take place, but moving in opposite directions: a moisture flux from the solid to the liquid and a solute flux from the solution to the solid. As a consequence, the changes in solid composition produce a decrease in the amount of water available for degradation reactions by enzymes and microorganisms (Cárcel et al., 2007b).

The use of high-intensity ultrasound may constitute a technique to accelerate the mass transfer in both liquid–solid systems (Cárcel et al., 2007c) and gas–solid systems (García-Pérez et al., 2006a).

3 Influence of Ultrasound on Mass Transfer

When ultrasound is applied in a solid–fluid system, it produces a series of effects that can affect both internal and external resistance to mass transfer between solid and fluid (Mulet et al., 2003). In liquid systems, the main mechanical effects of ultrasound are provided by cavitation. Cavitation consists of the appearance, growth, and collapse of bubbles inside the liquid which, for example, in water, generates temperature of about 40,000 K and pressure in excess of 1,000 atm in many localized points called "hot spots" (Mason et al., 2005). This bubble collapse, distributed through the medium, has a variety of effects. Thus, the collapse of bubbles is asymmetric near to the interfaces and produces a microjet that hits the solid surface (Mason, 1998). This is the main effect observed when using high-intensity ultrasound in cleaning operations. The microjets hitting the solid food surface may produce an injection of fluid inside the solid (Mason and Lorimer, 2002) and affect the mass transfer between the solid and the fluid. If cavitation is produced in the inner liquid phase of foods, it can facilitate moisture transport from the solid to the surrounding medium. Depending on the system characteristics, bubbles sometimes do not collapse and continue vibrating at the same frequency as the applied ultrasound (Leighton, 1998). This vibration also contributes to liquid agitation.

High-intensity ultrasound can generate a sound wind in the fluid produced by plane ultrasonic waves. This kind of agitation can reduce external resistance to mass transfer by increasing the bulk transport within the fluid (Mulet et al., 2003). The interaction of ultrasound in solid–fluid interfaces can produce a microstirring (Pugin and Turner, 1990). This microagitation is very important because it is formed in the immediate vicinity of the solid surface (Borisov and Gynkina, 1973) and exerts an important influence on the reduction of diffusion boundary layer thickness. All these effects influence external resistance and should affect mass transfer in the same way as mechanical stirring.

In the solid, ultrasonic waves produce a series of rapid compressions and expansions of the material that can be compared to a sponge squeezed and released repeatedly (Floros and Liang, 1994). This effect, known as the "sponge

effect," helps the liquid to flow out of the samples (Gallego-Juárez et al., 1999). On the other hand, the compressions and expansions of the material can create microchannels which are suitable for fluid movement (Muralidhara et al., 1985).

The effects described can affect both internal and external resistances to mass or heat transport and are the reason why high-intensity ultrasounds are applied to improve some transport operations. In heat transfer processes, high-intensity ultrasound can be used to improve the convective heat transfer coefficient (Cárcel et al., 2002; Lima and Sastry, 1990; Sastry et al., 1989) in a similar way to mechanical agitation. The advantage of "ultrasonic agitation" is that it may increase the turbulence and the heat transfer in places where it is not possible to introduce a mechanical agitation device (for example, inside a hermetically closed recipient) (Riera et al., 2004). The cavitation and the microstirring generated by high-intensity ultrasound in freezing processes can not only accelerate heat transfer (Li and Sun, 2002) but can also promote ice nucleation and control crystal size distribution in the frozen product (Zheng and Sun, 2006).

In mass transfer processes, the use of high-intensity ultrasound has been considered because it enhances mass transfer in solid–liquid extraction processes (Li et al., 2007; Romdhane and Gourdon, 2002; Vinatoru et al., 1997). The yield and the quality of the extracts obtained with ultrasound are, in general, better than non-ultrasonic extracts (Jiménez et al., 2007; Xia et al., 2006). High-intensity ultrasound has also been used in solid–liquid systems to affect the mass transfer in processes such as the osmotic dehydration of apples (Cárcel et al., 2007c; Liang, 1993; Simal et al., 1998), the brining of meat (Cárcel et al., 2007b; Sajas and Gorbatow, 1978), cheese (Sánchez et al., 1999), and peppers (Gabaldón-Leiva et al., 2007). Fernández and Rodrigues (2007) applied high-intensity ultrasound in solid–liquid systems as a pre-treatment for air drying bananas. They observed an increase in moisture diffusion after the application of ultrasound and a decrease in the total process time, pre-treatment, and air drying, compared to pre-treatment in a hypertonic solution followed by air drying.

The application of high-intensity ultrasound in air drying processes has been known for more than five decades. However, its development has been very slow due to the technical problems of designing an efficient and powerful air-borne acoustic generator (Mason et al., 2005). Many of these problems have been solved in the last few years, and this has allowed research of the influence of ultrasound in air drying of some food products. Thus, acoustic drying has been applied in the drying of cereals (Muralidhara et al., 1985), vegetables (Da Mota and Palau, 1999; Gallego-Juárez et al., 1999; García-Pérez et al., 2006b; Riera et al., 2002), and fruits (Cárcel et al., 2007a; García-Pérez et al., 2006a).

It is interesting to be aware of the difficulties when applying high-intensity ultrasound in air drying processes and how some of these problems have been solved. The influence of the main process variables, such as air velocity, air temperature, and applied acoustic energy in the kinetic of dehydration, will be described below.

4 Main Systems for Ultrasonic Application in Hot Air Drying

A system for producing ultrasonic waves consists of three different main components: the generator, the transducer, and the application system. All of the methods used for producing ultrasonic fields convert another kind of energy (electric, magnetic, kinetic, etc.) into acoustic energy. The generator supplies the energy to the system, and the transducer is responsible for carrying out the conversion of the energy supplied by the generator into acoustic energy. A good transducer must achieve a good rate of energy conversion. Usually, the losses of energy are converted into heat that produces a temperature increase in the system. Finally, the application system must transmit the generated acoustic signal to the product.

The application system represents one of the main handicaps in the application of ultrasound. The transfer of acoustic energy generated from a transducer to a food material is relatively inefficient due to the mismatch between the acoustic impedances of the application system, the propagation medium, and the food (Mason et al., 2005).

In solid–liquid applications, there are lower differences in the acoustic impedances of media than in solid–gas applications. As a consequence, applications in solid–liquid systems are much more developed than in solid–gas media. For applications in solid–liquid systems, two main types of ultrasonic equipment are used for laboratory and the large-scale applications, i.e., bath and probe (sonotrode) systems. Bath systems consist of a metallic vessel with piezoelectric transducers attached to the bottom. When the transducers vibrate, they transmit their vibration to the whole vessel, and then the vessel transmits the vibration to the liquid medium contained in the tank. In the probe system, a horn is attached to the transducer. The horn transmits the ultrasonic signal to the medium. Its shape defines whether the signal is transmitted or amplified.

In solid–gas systems, the application of high-intensity ultrasound is more difficult than in solid–liquid systems due to the poor match between ultrasonic application systems and air. There are reflections in the interface with air of a high proportion of the acoustic signal generated, heating the transducer and not reaching the food. However, the efficiency of the energy transformation depends not only on the equipment itself but also on ultrasonication conditions (Raso et al., 1999). In this sense, air produces a greater attenuation (power loss) in the transmission of sound than liquids (Gallego-Juárez, 1998). Significant attempts have been made to alleviate these problems by developing a very powerful source of air-borne ultrasound that can achieve a more efficient energy transmission to the material.

4.1 Siren and Whistle Systems

Air-borne ultrasound systems convert the kinetic energy of a fluid into an acoustic wave. For that purpose, two main kinds of setups can be used: sirens and whistles. In sirens the fluid is forced to pass across a hole, thus generating turbulence that

constitutes a mechanical wave. In whistles, the fluid is forced across a thin blade which causes the blade to vibrate. For each vibrational movement, the leading face of the blade produces a pressure wave (Mason, 1998). In liquid applications, the whistle constitutes a powerful tool for mixing and homogenization (Mason and Lorimer, 2002). The air applications is generally within human audible range, and this could be an obstacle to its use. Da Mota and Palau (1999) used a siren system to apply ultrasound during the drying process of onions. The results obtained showed that drying rates were increased by the acoustic vibration and that this increase depended on the sound frequency.

4.2 Stepped Plates

As previously mentioned, gas media present low specific acoustic impedance and high acoustic absorption. Therefore, in order to obtain an efficient transmission of energy, it is necessary to achieve the following requirements: a good impedance match between the transducer and the medium, large amplitude of vibration, and high-directional or focused beams for energy concentration. In addition, for large-scale industrial applications, a high power capacity and an extensive radiating area would be required in the transducers. Gallego-Juárez et al. (1999) developed a transducer with a flexural-vibrating plate radiator and an electronic unit for driving the transducer (Fig. 19.1). The extensive vibrating plate has a stepped profile driven by a piezoelectrically activated vibrator. The extensive surface of the plate increases radiation resistance, offering a better impedance match with air, thus increasing the power capacity of the system. The stepped surface avoids the phase cancellations produced in flat plate radiators. The system achieves high electroacoustic efficiency (75–80%) and produces a maximum intensity level of 175 dB working in the frequency range of 10–50 kHz .

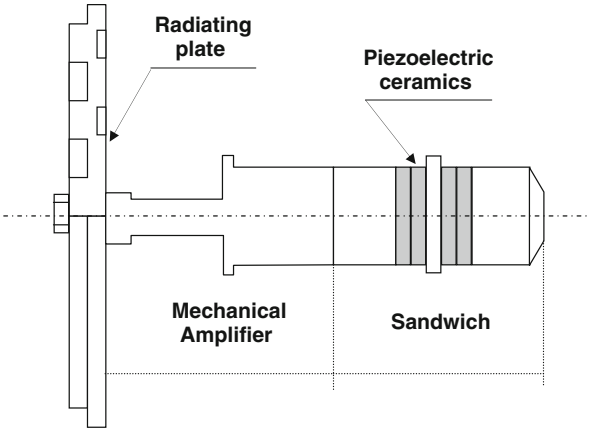

Fig. 19.1 Structure of the stepped plate transducer (Gallego-Juárez, 1998)

The stepped plate system has been used to apply air-borne power ultrasound in the drying of several vegetables (carrots, apples, and mushrooms), subsequently observing an increase in drying kinetics (Gallego-Juárez, 1998; Gallego-Juárez et al., 1999; Riera et al., 2002). If the stepped plate transducer is in direct contact with the samples, the dehydration rate is greater than in air-borne ultrasound drying. Riera et al. (2002) attributed this fact to the low penetration of ultrasonic energy in the vegetable material produced by the high mismatch between the acoustic impedance of media, the air, and the vegetables.

4.3 Vibrating Cylinders

The main disadvantage of the stepped plate transducer is its industrial scale application of conventional hot air drying, mainly the contact technique. A promising alternative technique, more adaptable to traditional hot air driers, has been developed (de la Fuente et al., 2005; García-Pérez et al., 2006a), allowing for the efficient application of high-intensity ultrasound during drying. This new ultrasonic application system was installed in a pilot-scale conventional hot air drier (Fig. 19.2), which was modified to install the new device. In the drying apparatus, two PID control algorithms allowed the temperature and the velocity of the air to be computer controlled. The drier is equipped with a pneumatic device, allowing samples to be weighed automatically at preset drying times (Sanjuán et al., 2003). The novelty concerns the drying chamber. The conventional container was replaced by an aluminum vibrating cylinder (internal diameter 100 mm, height 310 mm, and thickness 10 mm) driven by a piezoelectric composite transducer generating a high-intensity ultrasonic field inside the cylinder. The driving transducer consists of an extensional piezoelectric sandwich element together with a mechanical amplifier (Fig. 19.3). The ensemble has to be resonant at the frequency of the selected vibration mode

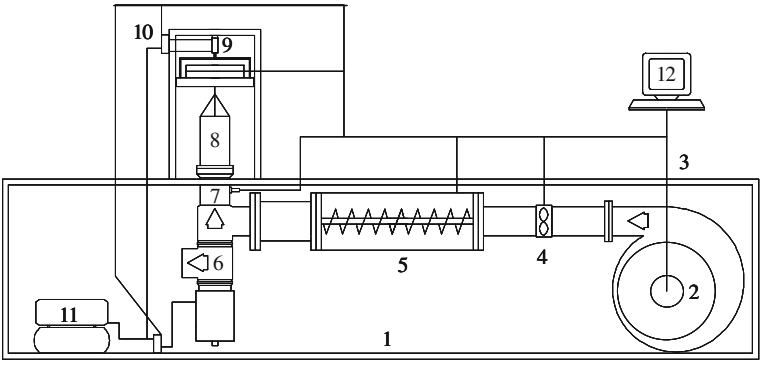

Fig. 19.2 Laboratory convective drier: 1 – metallic frame; 2 – fan; 3 – flux control; 4 – anemometer; 5 – heater element; 6 – pneumatic valve; 7 – measurement and control of temperature; 8 – drying chamber; 9 – balance; 11 – air compressor (Sanjuán et al., 2003)

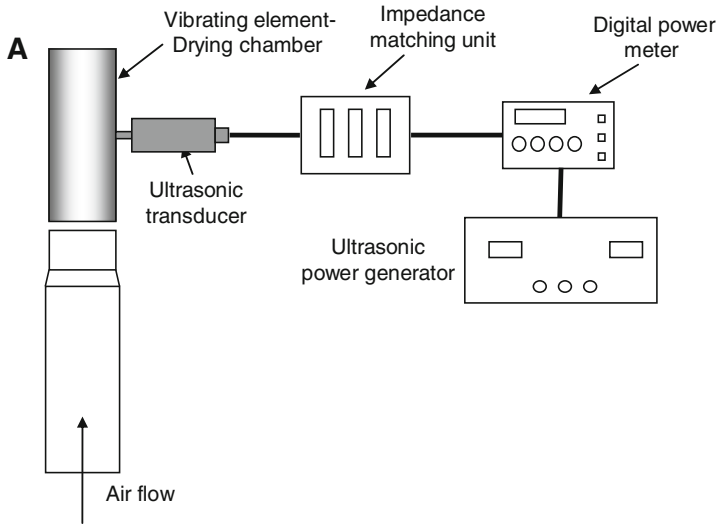

Fig. 19.3 Experimental setup for hot air ultrasound combined drier (Cárcel et al., 2007a)

of the chamber. For that purpose, the vibration modes of the cylindrical chamber were analyzed using finite element methods (FEM). The resonant frequency of the chamber at 21.8 kHz corresponds to a flexural mode of the tube with 12 nodal lines (Fig. 19.4). The acoustic field inside the chamber was calculated by FEM and it was found that for a displacement of 5 μm at the edge of the tube, an average sound pressure level of about 156 dB was obtained. The extensional transducer was screwed to the central part of the cylindrical chamber which corresponds to a point of maximum displacement. The vibration amplitudes along the tube were measured with a Polytec Scanning Vibrometer and fitted with numerical predictions calculated by FEM. The electrical characteristics of the transducer were measured ($IZI = 365\ \Omega$) by an impedance analyzer HP-4192 A in order to properly match the output impedance of the electronic generator. The acoustic field inside the chamber was measured, and raster scans were carried out with a 1/8″ GRAS microphone parallel to the tube axis (y-axis) and perpendicular to the radial distance to the walls (x-axis) to measure the sound pressure levels (SPL) in a plane of symmetry. An average SPL of about 154.3 dB was measured in the tube for an electrical power applied to the transducer of 75 W. Therefore, a high-intensity acoustic field inside the tube was obtained with relatively low applied power. Such a result confirms the FEM predictions for the acoustic field and the feasibility of using this type of system to ultrasonically assist a hot air drier. These measurements were carried out without air flow.

The vibrating cylinder setup described was used to study the effect of high-intensity ultrasound on hot air drying of food. This setup allowed the influence of high-intensity ultrasound on the effects of the main process variables during hot air drying to be addressed.

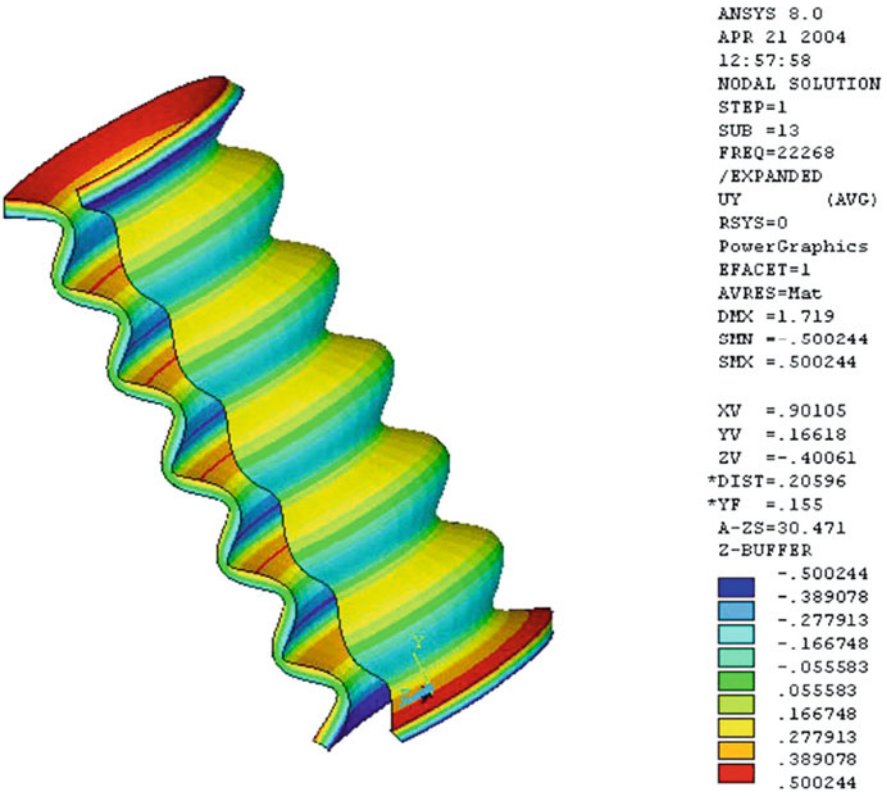

Fig. 19.4 Flexural mode of the ultrasonic drying chamber simulated by FEM (21.8 kHz) (García-Pérez et al., 2006a)

5 Influence of Some Process Variables on Hot Air Drying of Foods Assisted by High-Intensity Ultrasound

Although the literature provides scarce results, some preliminary conclusions can be reached. These conclusions about how the application of high-intensity ultrasound affects convective drying were obtained by analyzing experimental drying kinetics of several products (carrot, persimmon, apricot, and lemon peel) and quantified by using diffusion models to consider external resistance (ER model) or neglect it (NER model), which were developed for the different geometries being considered (cubes, cylinders, and slabs). It needs to be pointed out that a larger research effort is needed to apply ultrasound-assisted drying on a large scale. Although several systems have been used, there are two that seem particularly promising: stepped plates and vibrating cylinders. The most relevant results using vibrating cylinder ultrasonic systems will be noted in the next sections. The variables studied include variables related with air (temperature and velocity), with the raw matter being treated (some

vegetables and fruits), and also with the characteristics of the applied acoustic field (applied energy).

5.1 Effect of Air Velocity

Using a vibrating cylinder, hot air drying experiments using eight portions of apricots were carried out under fluidized bed conditions (air velocity between 10 and 14 m/s) and different air temperatures (30, 35, 40, 45, 50, 55, and 60°C) without (AIR) and with power ultrasound application (US, 21.7 kHz, 75 W). A close fit of experimental drying data was obtained using an NER model for slabs (L=10 mm), which provided percentages of explained variance of greater than 99%. The effective moisture diffusivities (D_e) identified showed an Arrhenius-type relationship with temperature (Fig. 19.5), which was not affected by power ultrasound application. No effect of ultrasound was found under these experimental conditions characterized by a high air flow. This discovery pointed to the fact that high air velocity may affect the intensity of ultrasound, since previous results showed the influence of ultrasound on drying rate increase (Gallego-Juárez et al., 1999).

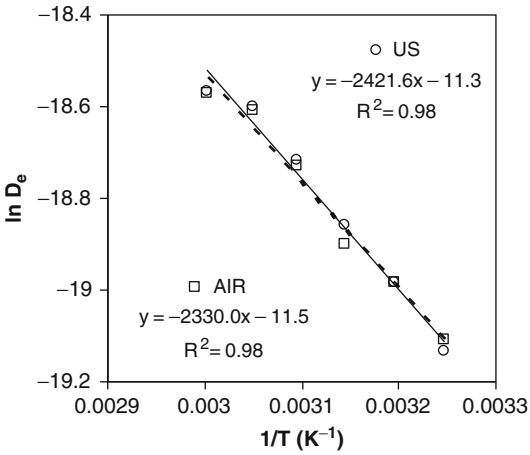

Fig. 19.5 Influence of air temperature (°C) on effective moisture diffusivity. AIR and US (21.7 kHz, 75 W) drying of apricots on fluidized bed

For that reason, new experiments without ultrasound (AIR) and with ultrasound (US) were considered. AIR and US (21.7 kHz, 75 W) drying kinetics of persimmon cylinders (diameter 13 mm and height 30 mm) were carried out at 50°C and at several air velocities: 0.5, 1, 2, 4, 6, 8, 10, and 12 m/s (Cárcel et al., 2007a). A different effect of power ultrasound was found at low and high air velocities (Fig. 19.6). In experiments carried out at 0.5 m/s, applying power ultrasound reduced the drying time required to reach a moisture content of 1 kg/kg of dry matter by 28%; however, no effect was found at 12 m/s. As can be observed in Fig. 19.7, the influence of power ultrasound on D_e values identified using an NER model was only found at air velocities lower than 6 m/s. For that reason, no effects of power ultrasound

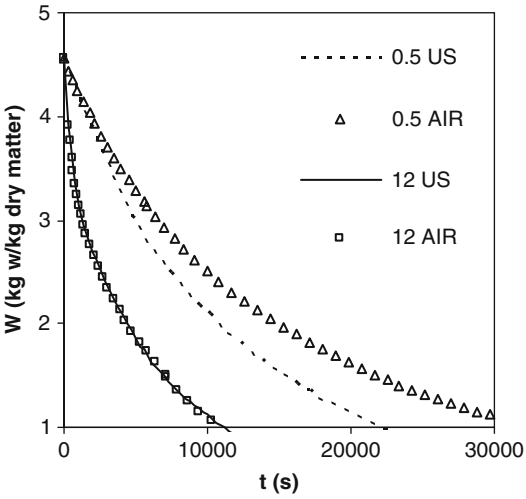

Fig. 19.6 AIR and US (21.7 kHz, 75 W) drying kinetics of persimmon cylinders at low (0.5 m/s) and high air velocities (12 m/s) (García-Pérez et al., 2007)

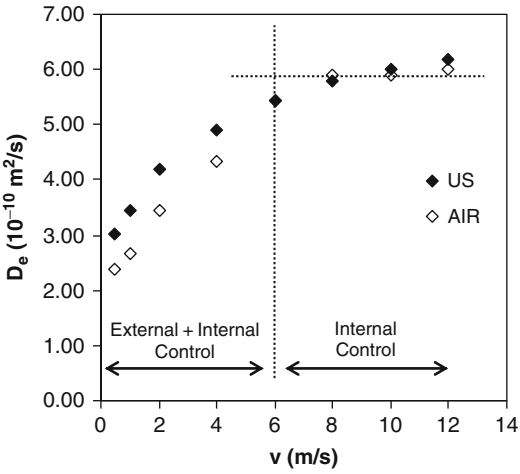

Fig. 19.7 Influence of air velocity (m/s) on effective moisture diffusivity. AIR and US (21.7 kHz, 75 W) drying experiments of persimmon cylinders (50°C) (García-Pérez et al., 2007)

application were found in previously reported fluidized bed drying experiments of apricots (air velocity range: 10–14 m/s).

There has been very little work conducted on the influence of air velocity on airborne acoustic drying. The effects of power ultrasound application on carrot drying, using a stepped plate ultrasonic system, decreased when the air velocity changed from 1 to 3 m/s (Gallego-Juárez et al., 1999). The drying rate of surimi slices increased under power ultrasound application, using a probe-type ultrasonic system, in experiments carried out at air velocities between 1.6 and 2.8 m/s (Nakagawa et al., 1996). These experiments agree closely with the results obtained on persimmon drying, since the low air velocities used in these experiments (<6 m/s) may

explain the effects observed when applying power ultrasound. However, no previous references have been found to confirm the results obtained at air velocities of over 6 m/s.

Below 6 m/s, D_e values were not only affected by power ultrasound but also by air velocity (Fig. 19.7), which showed that the external resistance to mass transfer cannot be neglected. Above this threshold, mass transfer seems to be controlled by internal resistance; consequently D_e is independent of air velocity. Furthermore, it is important to note that the NER model did not fit drying kinetics below 6 m/s adequately, since the behavior of the systems under these conditions, characterized by a significant external resistance, departs from boundary conditions assumed in the NER model (external resistance neglected).

The use of the ER model for cylinders allowed for an adequate fitting of the drying kinetics of persimmon samples carried out at below 6 m/s (Table 19.1). D_e values remained almost constant with the air velocity, and the overall effect of this variable was found on mass transfer coefficient (k). The ER model also permitted the influence of applying power ultrasound on D_e and k to be split (Table 19.1). Power ultrasound application significantly increased the identified D_e and k values when low air velocities were used (<6 m/s), which involves a significant reduction of internal and external resistance to mass transfer. The microstreaming and oscillating velocities produced by the ultrasound on interfaces are responsible for the effects on external resistance (Gallego-Juárez et al., 1999), while alternative expansions and compressions (sponge effect) in the material being dried reduced internal resistance (Arkhangel'skii and Stanikov, 1973; Borisov and Gynkina, 1973; Muralidhara et al., 1985).

Table 19.1 Effective moisture diffusivities (D_e, 10^{-10} m^2/s) and mass transfer coefficients (k, 10^{-3} kg $w/m^2/s$) identified using the ER model from experimental drying kinetics of persimmon cylinders carried out at low air velocities (v, m/s) (Cárcel et al., 2007a)

	AIR			US		
V	D_e	k	VAR	D_e	k	VAR
0.5	5.25±0.35	0.54±0.08	99.6	6.75±0.35	0.61±0.04	99.8
1	5.70±0.42	0.58±0.02	99.5	6.93±1.05	0.78±0.06	99.9
2	5.49±0.54	0.96±0.06	99.9	6.67±1.56	1.09±0.04	99.9
4	6.02±0.48	1.45±0.08	99.9	6.09±1.08	1.59±0.21	99.8

For a close examination of these effects, the sound pressure level generated by the vibrating cylinder inside the drying chamber was measured at different air velocities. The measurement was carried out using a microphone (1/8″, GRAS, Holte, Denmark) and followed a preset pathway; thus, the average sound pressure level was calculated integrating the values measured in the different points of the whole volume (García-Pérez et al., 2006a). It was found that the measurement was disturbed by the noise produced by the air flow on the protective hood of the microphone (Fig. 19.8). In fact, the sound pressure obtained without filtering increased as the

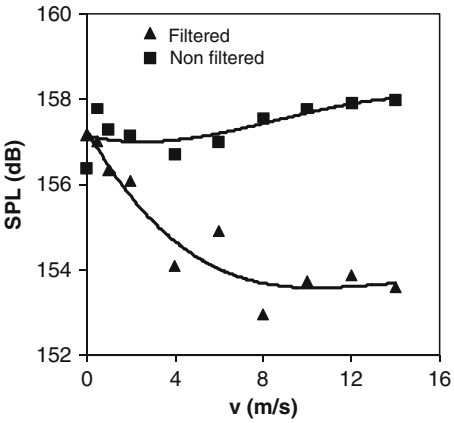

Fig. 19.8 Average sound pressure level measured in the drying chamber at different air velocities (m/s)

air velocity got higher, which is explained by the increase in noise intensity produced by the air. For that reason, it was necessary to filter the electric signal using a Heterodyne (Brüel & Kjær, Naerum, Denmark) around the resonance frequency of the transducer (21.7 kHz, widthband 100 kHz). In that case, the real average sound pressure (filtered) in the drying chamber decreased as the air velocity got higher, remaining almost constant at above 8 m/s (Fig. 19.8). This means that there was a reduction of the acoustic energy in the medium at high air flow rates. The effect of turbulence on the acoustic field has also been addressed in a liquid medium; thus, the acoustic energy produced by a probe system (20 kHz) decreased when a mechanical agitator was used, when compared with those found without agitation (Cárcel, 2003).

It may be concluded that the air flow produced a disruption of the acoustic field generated inside the drying chamber, which explains the lack of any effects caused by power ultrasound application in experiments carried out on persimmon at high air velocities and also those found on fluidized bed drying of apricots.

5.2 Air Temperature Effect

Vibrating cylinder AIR and US (75 W, 21.7 kHz) drying experiments on carrot cubes (8.5 mm side) were carried out at air temperatures ranging between 30 and 70°C (García-Pérez et al., 2006b). In order to ensure high acoustic energy levels in the medium, a low air velocity (1 m/s) was used. Different effects of power ultrasound were found at low and high air drying temperatures (Fig. 19.9). At low temperatures the drying time needed to reach a moisture content of 1 kg/kg of dry matter was reduced (28% at 30°C) by ultrasound application. Nevertheless, the effect of power ultrasound application disappeared at the highest air temperature tested (70°C). By modeling, the influence of power ultrasound at the different air velocities tested may be quantified.

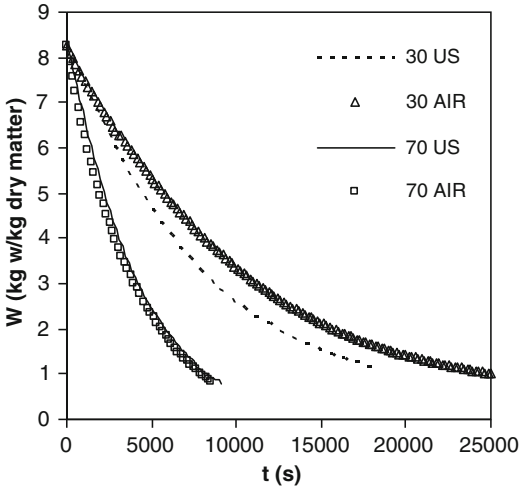

Fig. 19.9 AIR and US (21.7 kHz, 75 W) drying kinetics of carrot cubes at low (30°C) and high air temperatures (70°C) (García-Pérez et al., 2006b)

The ER model was used to fit the experimental drying kinetics due to the low air velocity used. As expected, the ER model contributed to fit the drying kinetics adequately (percentages of explained variance > 99%), showing the importance of external resistance at low air velocities (Table 19.2). Power ultrasound application significantly increased the mass transfer coefficients in the air temperature range tested. This finding points to significant effects of power ultrasound on the gas–solid interfaces reducing boundary layer thickness and thus diminishing external resistance to mass transfer (Gallego-Juárez et al., 1999).

Table 19.2 Effective moisture diffusivities (D_e, 10^{-10} m^2/s) and mass transfer coefficients (k, 10^{-4} kg $w/m^2/s$) identified using the ER model from experimental drying kinetics of carrot cubes carried out at different air temperatures (T, °C) (García-Pérez et al., 2006b)

	AIR			US		
T	D_e	k	VAR	D_e	k	VAR
30	1.38±0.25	2.87±0.40	99.9	2.14±0.60	3.06±0.36	99.9
40	1.93±0.22	4.13±0.21	99.9	2.71±0.51	5.86±0.48	99.9
50	2.87±0.70	6.17±0.86	99.9	3.91±0.33	8.80±0.50	99.9
60	3.83±0.61	6.77±0.23	99.9	4.69±0.40	9.07±1.27	99.9
70	4.57±0.07	8.83±0.38	99.9	4.88±0.41	9.40±0.70	99.9

A significant (p<0.05) influence of power ultrasound application on effective moisture diffusivity was only found at air temperatures of less than 60°C. The D_e value identified at 30°C increased by 53% when power ultrasound was applied (Table 19.2). However, the effects were almost negligible at 70°C (Table 19.2). This could be explained by assuming that ultrasound introduces a given amount of energy into the solid producing alternative expansions and contractions, thus improving

water mobility (Muralidhara et al., 1985). As the temperature increases, water movement is faster and the relative importance of the acoustic energy effect on internal resistance diminishes. Nevertheless, more experimentation is needed to verify this assumption.

In AIR experiments, D_e values followed the Arrhenius-type relationship with temperature quite well (Fig. 19.10). An activation energy figure of 26.7 ± 5.3 kJ/mol was identified, which is similar to others reported in literature for convective drying of carrots (Reyes et al., 2002; Srikiatden and Roberts, 2006). However, this relationship could not be established in US experiments, since the D_e values identified at high air temperatures departed from the linearity found at low temperatures. The linear relationship found for D_e values identified at low temperatures in US experiments presented a similar slope to those found in AIR experiments; the effect of power ultrasound was only observed on the *y*-axis intercept.

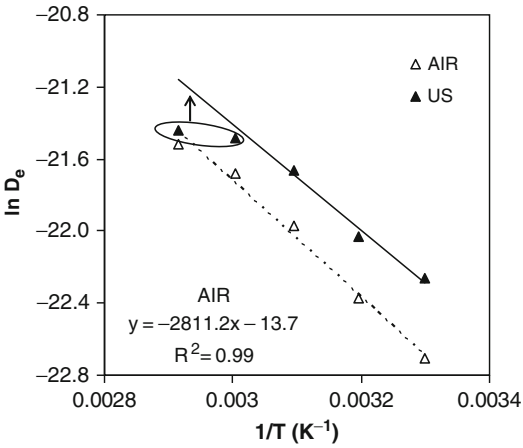

Fig. 19.10 Influence of air temperature (°C) on effective moisture diffusivity. AIR and US (21.7 kHz, 75 W) drying experiments of carrot cubes (1 m/s) (García-Pérez et al., 2006b)

The literature reports agree with these results on the influence of air temperature. Gallego-Juárez et al. (1999) found that the effects of high-intensity ultrasound application on carrot drying, using a stepped plate ultrasonic system, decreased from experiments carried out at 60°C to those found at 90°C and disappeared completely at 115°C.

Those authors also reported a similar temperature-related tendency of high-intensity ultrasound effects to those shown in Fig. 19.10, since the influence decreased as the air velocity got higher. Nevertheless, the effects were still significant at temperatures of over 60°C, which may be explained by the different ultrasonic application systems used. High-intensity ultrasound application, or using a probe-type system increased the drying rate at 20, 30, 40, and 50°C during the drying of surimi slices (Nakagawa et al., 1996), which confirms the effectiveness of ultrasound in a moderate temperature range (<60°C).

5.3 Applied Acoustic Energy

Carrot cube drying experiments (side 8.5 mm) were carried out in a vibrating cylinder ultrasonic system by applying several acoustic energy levels, which were set by applying different electric powers to the ultrasonic transducer: 0, 10, 20, 30, 40, 50, 60, 70, 80, and 90 W (García-Pérez et al., 2008, 2009). According to previously reported results, a low air velocity (1 m/s) and a moderate temperature (40°C) were used (García-Pérez et al., 2007) to highlight the effect of acoustic energy.

The level of acoustic energy applied was found to have a significant ($p < 0.05$) influence on drying kinetics; thus, the drying time needed to reach a moisture content of 1.5 kg/kg of dry matter was reduced by 32% when the electric power applied increased from 10 to 90 W (Fig. 19.11). Similar results about the influence of the amount of acoustic energy have been reported related to the convective drying of carrots, mushrooms, apples, and potatoes, assisted by power ultrasound (Riera et al., 2002; de la Fuente et al., 2004) using a stepped plate system.

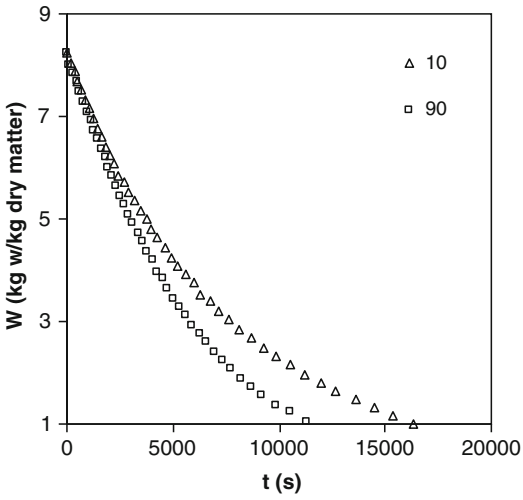

Fig. 19.11 US drying kinetics of carrot cubes (40°C, 1 m/s) applying low and high electric power (W) to the ultrasonic transducer (García-Pérez et al., 2009)

The literature has not pointed to results that quantify the effects produced by power ultrasound at different acoustic energy levels. For that reason, in order to quantify the influence of acoustic energy level on drying kinetics, the ER model was fitted to the drying kinetics of carrot cubes. The ER model fitted the experimental drying data well (Table 19.3), reaching percentages of explained variance (VAR) higher than 99% in all cases. Both effective moisture diffusivity and mass transfer coefficients values increased significantly as the electric power was raised, which means there were more intense effects of power ultrasound on internal and external resistance to mass transfer. Nevertheless, the effects were only observed when the acoustic energy level in the medium exceeded a minimum value, which, under these

Table 19.3 Effective moisture diffusivities (D_e, 10^{-10} m^2/s) and mass transfer coefficients (k, 10^{-4} kg $w/m^2/s$) identified using the ER model from experimental drying kinetics of carrot cubes carried out at different levels of electric power applied to the ultrasonic transducer (P, W) (García-Pérez et al., 2008)

P	D_e	k	VAR
0	2.03±0.04	4.60±0.09	99.9
10	2.05±0.33	4.66±0.41	99.9
20	2.01±0.36	4.58±0.15	99.9
30	2.24±0.22	4.40±0.54	99.9
40	2.33±0.17	4.98±0.32	99.9
50	2.48±0.20	5.55±0.01	99.8
60	2.53±0.01	5.45±0.49	99.9
70	2.63±0.03	5.60±0.25	99.9
80	2.57±0.31	6.03±0.66	99.9
90	2.82±0.27	6.60±0.48	99.9

experimental conditions, corresponded to applying an electric power of 30 W to the transducer (Table 19.3, Fig. 19.12). Below this threshold, no significant influence of the acoustic energy level was found (Fig. 19.12). Above 30 W, the influence the level of electric power applied had on the mass transfer coefficient was fitted well by a linear correlation. That means that the effects of power ultrasound application on the gas–solid interface were proportional to the acoustic energy level in the medium. A similar influence of acoustic energy level was found on the effective moisture diffusivities.

No reports have been found in the literature about the ultrasound intensity threshold necessary to affect air drying.

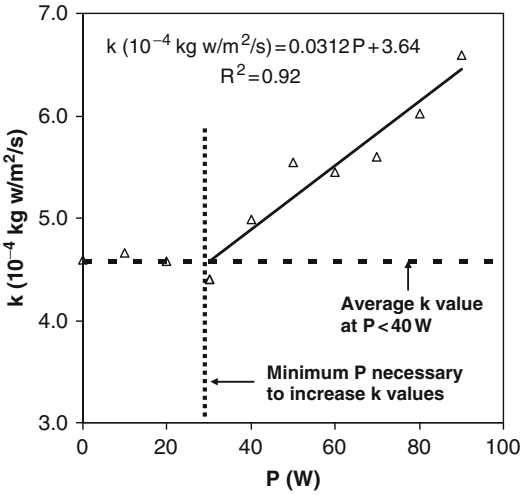

Fig. 19.12 Influence of electric power applied (W) on mass transfer coefficients. US (21.7 kHz) drying experiments of carrot cubes (40°C, 1 m/s) (García-Pérez et al., 2008)

5.4 Material Structure

Experiments with different products under the same experimental conditions were carried out to test the influence of the material being treated on hot air drying assisted by power ultrasound. For that reason, vibrating cylinder AIR and US (21.7 kHz, 75 W) drying experiments at air velocities of between 0.5 and 9 m/s and at constant temperature (40°C) were carried out on carrot cubes (8.5 mm side) and lemon peel slabs (thickness 10 mm) (García-Pérez, 2007; García-Pérez et al., 2007). According to previously shown results, the increase in air velocity reduces acoustic energy in the medium. Therefore, the planned US experiments permitted us not only to illustrate the behavior of both materials but also to compare with AIR experiments.

Although power ultrasound application reduced the drying rate of both lemon peel and carrots at low air velocity, the ultrasound effects were more intense in lemon peel (Fig. 19.13). However, whereas power ultrasound was found to have

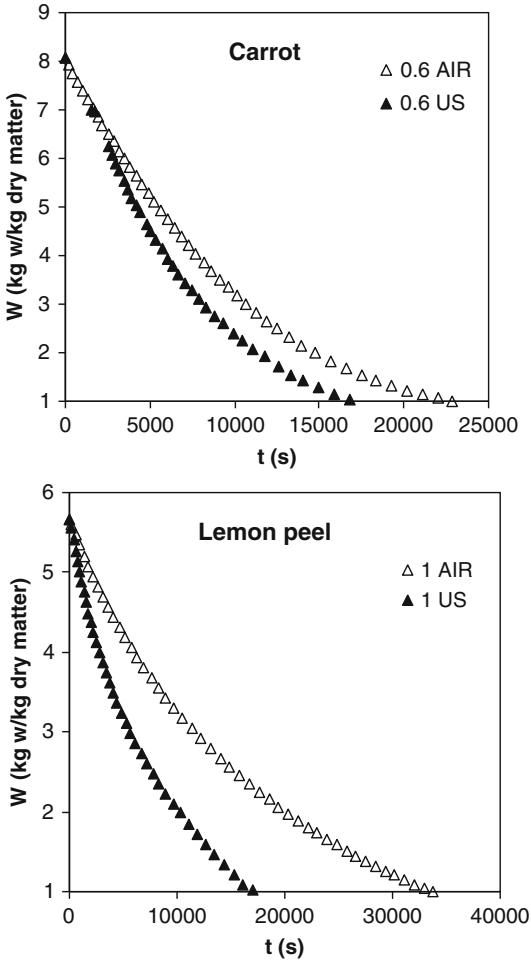

Fig. 19.13 AIR and US (21.7 kHz, 75 W) drying kinetics of carrot cubes and lemon peel slabs at low air velocities (García-Pérez et al., 2007)

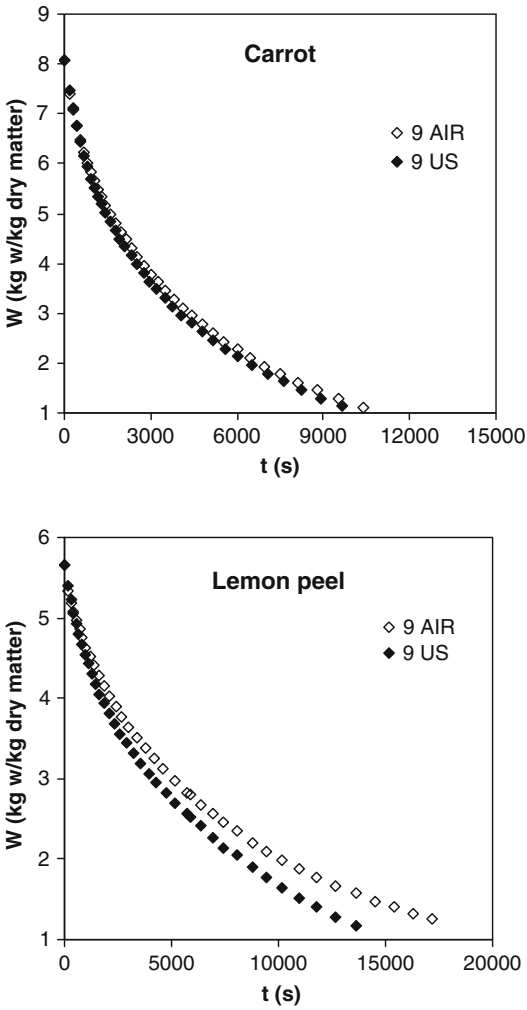

Fig. 19.14 AIR and US (21.7 kHz, 75 W) drying kinetics of carrot cubes and lemon peel slabs at high air velocities (García-Pérez et al., 2007)

no effect on carrot drying at high air velocities (Fig. 19.14), in the case of lemon peel, the drying rate was also reduced by ultrasound application at high air velocities. Through drying kinetics modeling, the influence of power ultrasound may be quantified and, furthermore, the different behavior of the materials may be clarified.

An NER model was used to identify the effective moisture diffusivities at different air velocities on carrot and lemon peel drying, as shown in Fig. 19.15. The influence of power ultrasound application on carrot drying was very similar to the results found for persimmon drying (Cárcel et al., 2007a). Effective moisture diffusivities were only improved by ultrasound at low air velocities, as the effect was negligible at air velocities higher than 5 m/s. At high air velocities, the amount of

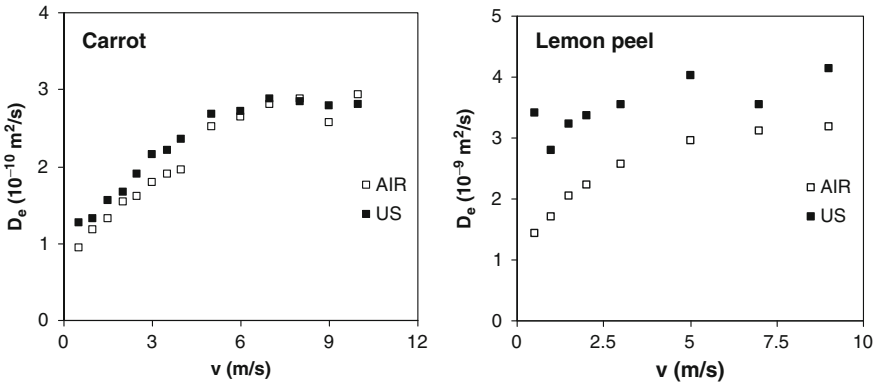

Fig. 19.15 Influence of the air velocity (m/s) on the effective moisture diffusivity. AIR and US (21.7 kHz, 75 W) drying experiments of carrot cubes and lemon peel slabs (García-Pérez et al., 2007)

acoustic energy remaining due to acoustic field disruption was not enough to affect the mass transfer process in carrot drying.

The behavior found in lemon peel drying was quite different than in carrot or persimmon drying, since a power ultrasound effect was found for the whole range of air velocity tested (Fig. 19.15). Despite reducing acoustic energy by increasing air velocity, the acoustic energy in the medium was able to effect a more sensitive product like lemon peel; consequently, acoustic effects on lemon peel were stronger.

An explanation for the fact that lemon peel behaves differently when compared to carrot and persimmon could be linked to its structure (García-Pérez et al., 2009). In fact, lemon peel is considered to be a more porous product than carrot or persimmon (Boukouvalas et al., 2006). Porosity may be considered as one of the most important structural variables for determining the acoustic effectiveness in foodstuffs. High porosity products may be considered to be more prone to alternating compression and expansion cycles produced by ultrasonic waves (sponge effect) (Gallego-Juárez, 1998), improving the water transfer rate in its large intercellular spaces. Small intercellular spaces are also found in low porosity products, which means a high internal resistance to water transfer. Thus, high acoustic energy levels are required to affect mass transfer in low porosity products (persimmon and carrot) (García-Pérez et al., 2007).

The influence of porosity may also be explained by taking the greater acoustic energy absorption of high porosity products into account. As a consequence, the internal energy available in the particles would increase, leading to more intense compressions and expansions (sponge effect), which could improve water removal and therefore reduce internal resistance. Furthermore, the acoustic effects on the solid–gas interfaces of intercellular spaces could increase in high porosity products due to a larger porous net. Indeed, this phenomenon also contributes to reduce internal resistance to mass transfer.

Raw material may be considered as one of the most important variables to be evaluated when considering the application of power ultrasound during the convective drying of foodstuffs. A sound knowledge of the material structure would contribute to determine its response to acoustic energy during hot air drying assisted by power ultrasound, since structure is important to determine how difficult it is for water molecules to leave the solid matrix.

6 Final Remarks

The use of high-intensity ultrasound in hot air drying seems to be a promising technology to improve quality and energy savings. As it appears to be more effective at low temperatures, the related quality effects of high temperatures can be avoided without compromising the kinetics of the process. Decreasing the drying air temperature also produces energy savings.

High-intensity ultrasound also appears to be more effective at low air velocities, which is very interesting to accelerate the drying kinetics of products with a tendency to suffer case hardening during drying. Drying at low air velocities also results in energy savings.

The existence of an intensity threshold for ultrasound affecting the process is an important point to be considered when planning experiments on either the laboratory or the industrial scale.

Acknowledgments The authors would like to acknowledge the support of MICINN projects: Ref. PSE-060000-2009-003 (CEE, European Regional Development Fund) and Ref. DPI2009-14549-C04-04, and Generalitat Valenciana project Ref. PROMETEO/2010/062.

References

Arkhangel'skii, M. E., and Stanikov, Y. G. (1973). Diffusion in heterogeneous systems. In: Rozenberg, L. D. (ed.), *Physical principles of ultrasonic technology*. New York, NY, Plenum Press.

Borisov, Y. Y., and Gynkina, N. M. (1973). Acoustic drying. In: Rosenger, L. D. (ed.), *Physical principles of ultrasonic technology*, Vol. 2, pp. 381–474. New York, NY, Plenum Press.

Boukouvalas, C. J., Krokida, M. K., Maroulis, Z. B., and Marinos-Kouris, D. (2006). Density and porosity: Literature data compilation for foodstuffs. *International Journal of Food Properties*, 9, 715–746.

Cárcel, J. A. (2003). Influencia de los ultrasonidos de potencia en procesos de transferencia de materia. Doctoral dissertation, Politechnic University of Valencia.

Cárcel, J. A., Benedito, J., Bon, J., and Mulet, A. (2007b). High intensity ultrasound effects on meat brining. *Meat Science*, 76, 611–619.

Cárcel, J. A., Benedito, J., Rosselló, C., and Mulet, A. (2007c). Influence of ultrasound intensity on mass transfer in apple immersed in a sucrose solution. *Journal of Food Engineering*, 78, 472–479.

Cárcel, J. A., Cortés, I., Clemente, G., and Mulet, A. (2002). Influencia de los ultrasonidos de potencia en la transferencia de calor por convección. *Symposium on Emerging Technologies for the Food Industry*, pp. 11–13, March, Madrid, Spain.

Cárcel, J. A., García-Pérez, J. V., Riera, E., and Mulet, A. (2007a). Influence of high-intensity ultrasound on drying kinetics of persimmon. *Drying Technology*, 25, 185–193.

Chou, S. K., and Chua, K. J. (2001). New hybrid drying technologies for heat sensitive foodstuffs. *Trends in Food Science and Technology*, 12, 359–369.

Chua, K. J., Mujumdar, A. S., Hawlader, M. N. A., Chou, S. K., and Ho, J. C. (2001). Convective drying of agricultural products. Effect of continuous and stepwise change in drying air temperature. *Drying Technology*, 19, 1949–1960.

Da Mota, V. M., and Palau, E. (1999). Acoustic drying of onion. *Drying Technology*, 17, 855–867.

de la Fuente, S., Riera, E., and Gallego-Juárez, J. A. (2004). Estudio de los parámetros involucrados en el proceso de deshidratación ultrasónica de vegetales, *Revista de Acústica*, 35, 25–30.

de la Fuente, S., Rodríguez, G., Riera, E. Gallego, J. A., and Mulet. A. (2005). Desarrollo de un sistema de secado mediante lecho fluido asistido por ultrasonidos de potencia. *Revista de Acústica*, 36, 19–25.

Fernández, F. A. N., and Rodrigues, S. (2007). Ultrasound as pre-treatment for drying of fruits: Dehydration of banana. *Journal of Food Engineering*, 82, 261–267.

Floros, J. D., and Liang, H. (1994). Acoustically assisted diffusion through membranes and biomaterials. *Food Technology*, December, 79–84.

Gabaldón-Leiva, C. A., Quintero-Ramos, A., Barnard, J., Balandrán-Quintana, R. R., Talamás-Abbud, R., and Jiménez-Castro, J. (2007). Effect of ultrasound on the mass transfer and physical changes in brine bell pepper at different temperatures. *Journal of Food Engineering*, 81, 374–379.

Gallego-Juárez, J. A. (1998). Some applications of air-borne power ultrasound to food processing. In: Povey, M. J. W., and Mason, T. J. (eds.), *Ultrasound in food processing*, pp. 127–143. London, Chapman and Hall.

Gallego-Juárez, J. A., Rodríguez-Corral, G., Gálvez-Moraleda, J. C., and Yang, T. S. (1999). A new high intensity ultrasonic technology for food dehydration. *Drying Technology*, 17, 597–608.

García-Pérez, J. V. (2007). Contribution to the knowledge on the use of power ultrasound in convective drying of foods. Doctoral dissertation, Polytechnic University of Valencia.

García-Pérez, J. V., Cárcel, J. A., Benedito, J., and Mulet, A. (2007). Power ultrasound mass transfer enhancement in food drying. *Food and Bioproducts Processing*, 85, 247–254.

García-Pérez, J. V., Cárcel, J. A., Benedito, J., Riera, E., and Mulet, A. (2008). Drying of a low porosity product (carrot) as affected by power ultrasound. *Defect and Diffusion Forum*, 273–276, 764–769.

García-Pérez, J. V., Cárcel, J. A., de la Fuente-Blanco, S., Riera-Franco de Sarabia, E. (2006a). Ultrasonic drying of foodstuff in a fluidized bed: Parametric study. *Ultrasonics*, 44, 539–543.

García-Pérez, J. V., Cárcel, J. A., Riera, E., and Mulet, A. (2009). Influence of the applied acoustic energy on the drying of carrots and lemon peel. *Drying Technology*, 27, 281–287.

García-Pérez, J. V., Rosselló, C., Cárcel, J. A., de la Fuente, S. and Mulet, A. (2006b). Effect of air temperature on convective drying assisted by high power ultrasound. *Defect and Diffusion Forum*, 258–260, 563–574.

Jiménez, A., Beltrán, G., and Uceda, M. (2007). High-power ultrasound in olive paste pretreatment. Effect on process yield and virgin olive oil characteristics. *Ultrasonics Sonochemistry*, 14, 725–731.

Leighton, T. G. (1998). The principles of cavitation. In: Povey, M. J. W., and Mason, T. J. (eds.), *Ultrasound in food processing*, pp. 155–182. London, Chapman and Hall.

Li, B. and Sun, D. W. (2002). Effect of power ultrasound on freezing rate during immersion freezing of potatoes. *Journal of Food* Engineering, 55, 277–282.

Li, J. W., Ding, S. D., and Ding, X. L. (2007). Optimization of the ultrasonically assisted extraction of polysaccharides from *Zizyphys jujuba* cv. Jinsixiaozao. *Journal of Food Engineering*, 80, 176–183.

Liang, H. (1993). Modelling of ultrasound assisted and osmotically induced diffusion in plant tissue. Doctoral dissertation, Perdue University.

Lima, M., and Sastry, S. K. (1990). Influence of fluid rheological properties and particle location on ultrasound-assisted heat transfer between liquid and particles. *Journal of food Science*, 55, 1112–1115.

Mason, T. J. (1998). Power ultrasound in food processing. The way forward. In: Povey, M. J. W., and Mason, T. J. (eds.), *Ultrasound in food processing*, pp. 105–126. London, Chapman and Hall.

Mason, T. J., and Lorimer, J. P. (2002). *Applied sonochemistry. The uses of power ultrasound in chemistry and processing*. Weinheim, Wiley-VCH.

Mason, T. J., Riera, E., Vercet, A., and Lopez-Buesa, P. (2005). Applications of ultrasound. In: Sun, D. (ed.), *Emerging technologies for food processing*, pp. 323–351. Amsterdam, Elsevier.

Mavroudis, N. E., Gekas, V., and Sjöjolm, I. (1998). Osmotic dehydration of apples – Effects of agitation and raw material characteristics. *Journal of Food Engineering*, 57, 367–374.

Mulet, A., Cárcel, J. A., Sanjuán, N., and Bon, J. (2003). New food drying technologies – use of ultrasound. *Food Science and Technology International*, 9, 215–221.

Mulet, A., Sanjuán, N., Bon, J., and Simal, S., (1999). Drying model of highly porous hemispherical bodies. *European Food Research and Technology*, 210, 80–83.

Muralidhara, H. S., Ensminger, D. and Putnam, A. (1985). Acoustic dewatering and drying (low and high frequency): State of the art review. *Drying Technology*, 3, 529–566.

Nakagawa, S., Yamashita, T., and Miura, H. (1996). Ultrasonic drying of walleye Pollack surimi. *Nipon Shokutin Kagaku Kagaku Kaishi*, 43, 388–394.

Pugin, B., and Turner, A. T. (1990). Influence of ultrasound on reaction with metals. In: Mason, T. J. (ed.), *Advances in sonochemistry*, pp. 81–118. London, JAI Press.

Raso, J., Mañas, P., Pagán, R., and Sala, F. J. (1999). Influence of different factor son the output power transferred into medium by ultrasound. *Ultrasonics Sonochemistry*, 5, 157–162.

Reyes, A., Alvarez, P. I., and Maquardt, F. H. (2002). Drying of carrots in a fluidized bed. Effects of drying conditions and modelling. *Drying Technology*, 20, 1463–1483.

Riera, E., Gallego-Juárez, J. A., Rodríguez, G., Acosta, V. M., and Andrés, E. (2002). Applications of high-power ultrasound for drying vegetables. *Revista de Acústica*, 33, 1–6.

Riera, E., Golas, Y., Blanco, A., Gallego, J. A., Blasco, M., and Mulet, A. (2004). Mass transfer enhancement in supercritical fluids extraction by means of power ultrasound. *Ultrasonics Sonochemistry*, 11, 241–244.

Romdhane, M., and Gourdon, C. (2002). Investigation in solid-liquid extraction: Influence of ultrasound. *Chemical Engineering Journal*, 87, 11–19.

Rosselló, C., Simal, S., Sanjuán, N., and Mulet, A. (1997). Nonisotropic mass transfer model for green bean drying. *Journal of Agriculture and Food Chemistry*, 45, 337–342.

Sajas, J. F., and Gorbatow, W. M. (1978). Use of ultrasound in meat technology. *Fleischwirtschaft*, 58, 1009–1021.

Sánchez, E. S., Simal, S., Femenia, A., Benedito, J. and Rosselló, C. (1999). Influence of ultrasound on mass transport during cheese brining. *European Food Research Technology*, 209, 215–219.

Sanjuán, N., Lozano, M., García-Pascual, P., and Mulet, A. (2003). Dehydration kinetics of red pepper (*Capsicum annuum* L var Jaranda). *Journal of the Science of Food and Agriculture*, 83, 697–701.

Sastry, S. K., Shen, G. Q., and Baisdell, J. L. (1989). Effect of ultrasonic vibration on fluid-to-particle convective heat transfer coefficients. *Journal of Food Science*, 54, 229–230.

Simal, S., Benedito, J., Sánchez, E. S., and Rosselló, C. (1998). Use of ultrasound to increase mass transport rates during osmotic dehydration. *Journal of Food Engineering*, 36, 323–336.

Simal, S., Sánchez, E., Bon, J., Femenia, A., and Rosselló, C. (2001). Water and salt diffusion during cheese ripening: Effect of external and internal resistance to mass transfer. *Journal of Food Engineering*, 48, 269–275.

Srikiatden, J., and Roberts, S.S. (2006). Measuring moisture diffusivity of potato and carrots (core and cortex) during convective hot air and isothermal drying. *Journal of Food Engineering*, 74, 143–152.

Strommen, I., and Kramer, K. (1994). New applications of heat pumps in drying processes. *Drying Technology*, 12, 889–901.

Turner, I. W., and Jolly, P. (1991). Combined microwave and convective drying of a porous material. *Drying Technology*, 9, 1209–1270.

Vega-Mercado, H., Góngora-Nieto, M. M., and Barbosa-Cánovas, G. V. (2001). Advances in dehydration of foods. *Journal of Food Engineering*, 49, 271–289.

Vinatoru, M., Toma, M., Radu, O., Filip, P. I., Lazurca, D., and Mason T.J. (1997). The use of ultrasound for the extraction of bioactive principles from plant materials. *Ultrasonics Sonochemistry*, 4, 135–139.

Xia, T., Shi, S., and Wan, X. (2006). Impact of ultrasonic-assisted extraction on the chemical and sensory quality of tea infusion. *Journal of Food Engineering*, 74, 557–560.

Zheng, L., and Sun, D. W. (2006). Innovative applications of power ultrasound during food freezing processes – a review. *Trends in Food Science and Technology*, 17, 16–23.

Chapter 20
Novel Applications of Power Ultrasonic Spray

Ke-ming Quan

1 Introduction

Atomization is a process where a liquid is dispersed into droplets in a gas. Ultrasonic atomization was discovered in the 1920s (Loomis and Woods, 1927). Since then, atomization has seen diversified applications in devices such as drug nebulizers, room humidifiers, and air refreshers, as well as in industrial processes such as combustion, prilling, and web coating. In contrast to conventional liquid atomizers, ultrasound atomizers generally handle lower flow rates, and atomization of the liquid is achieved not by pressure, but by the vibration of ultrasonic waves (Morgan, 1993). This latter feature decouples the requirement of orifice geometry and pressure from the flow rate, allowing the flow to be controlled independently. Typically, ultrasonic atomizers excel in accurately processing low flow rates and slurry without clogging issues.

2 Snack Food Seasoning Coating

In food processing, it is common to deposit a coating on a food substrate. The coating material may be solid, liquid, or slurry. If the coating material is a fluid or slurry, it is often applied to the food substrate with conventional spray nozzles. These nozzles dispense the fluid in a spray pattern, using only hydrostatic pressure. Solid coating may be accomplished by dropping the slurry directly onto the substrate or through tumbling in a rotating drum. The coating materials may consist of seasoning, flavor additives, nutrients, and other elements, and generally make up a small portion of the whole compared to the weight of the food substrate.

In practice, there are a number of limitations in applying the conventional spray nozzle. One of the difficulties involves the ability of applying low flow rates, especially below 500 ml/min, while maintaining a steady spray pattern. Another problem

K. Quan (✉)
Procter and Gamble Company, 8256 Union Centre Boulevard, West Chester, OH 45069, USA
e-mail: quan.k@pg.com

H. Feng et al. (eds.), *Ultrasound Technologies for Food and Bioprocessing*,
Food Engineering Series, DOI 10.1007/978-1-4419-7472-3_20,
© Springer Science+Business Media, LLC 2011

resides in the momentum of spray, which, if closely coupled with the food product, can be destructive to the shape and texture of the product. The momentum may also disorient the packing arrangement of the product on the process line. Yet another disadvantage involves the difficulty of spraying a slurry of large particles. This problem is due to the fact that the orifice of a conventional nozzle can be smaller than 500 μm in diameter. Nozzle clogging is known to be a major drawback, especially for slurry applications. Since most processing lines are generally continuous, the cost of downtime due to build-up and clogging can be significant. The drawbacks of the conventional nozzle technologies limit the usage of the nozzle spray in the food industry.

Among the different sectors in the food industry, snack foods have annual sales of more than $25 billion (Enggalhardjo and Narsimhan, 2005), of which potato chip sales in the United States exceed $6 billions (Berry, 2003). Seasoning is an important part of the snack food experience, influencing the acceptability of the snacks (Kunt, 1996). In order to gain consumer loyalty in this competitive market, companies need to be able to consistently produce well-coated products. In particular, even distribution of seasoning topping is highly desired as it is essential to providing uniform appearance and taste of the product. From the processing point of view, this represents a challenge in at least two areas: (1) consistent rate of dispensing of the coating materials onto each food substrate and (2) consistent rate of adhesion of the coating materials onto each food substrate.

Many snack foods are fried and powder coated. The two most common ways to apply seasoning are by tumble drum and conveyor belt. In the case of conveyor belt, the powder is usually dispensed directly onto the moving chips. Over-dispensing in order to compensate for poor adhesion increases material and line cleaning cost. Potato chips contain about 35% oil (Pedreschi, and Moyano, 2005). Oil on the surface of the chip contributes to the adhesion of the seasoning, so most manufacturers coat the chips immediately after frying or applying the oil and seasoning simultaneously (Berry, 2003). In addition, Buck and Barringer (2007) report that solid size, shape, and chip temperature also have an impact on the rate of adhesion. Other deposition processes, such as electrostatic coating (Abu-ali and Barringer, 2005), have been tested to improve both adhesion and uniformity.

3 Ultrasonic Atomization Fundamentals

The most widely used ultrasonic atomizers are capillary wave-type atomizers. In this case, atomization occurs predominately from the effects of the surface capillary waves produced in a thin film of liquid as it wets an oscillating surface. The leading commercial suppliers for this type of atomizers are Sono-Tek Corporation (http://www.sono-tek.com/) and Sonics and Materials Inc. (http://www.sonics.biz/), both of which provide a range of nozzles that have the liquid atomized at the nozzle tip. Figure 20.1 shows a typical design of an atomizer by Sono-Tek Corporation, where the ultrasonic transducer and the nozzle are integrated as one piece. The

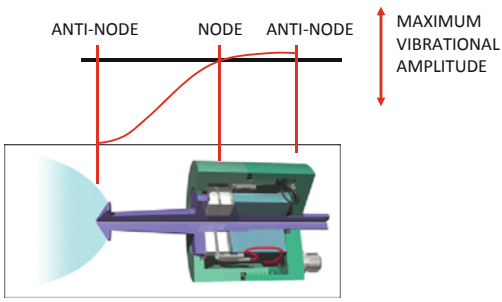

Fig. 20.1 Ultrasonic atomizer by Sono-Tek Corp.

source of vibration is provided by a stack of piezeoelectric transducers located at the pressure node plane where the vibration amplitude is at the minimum. The tip of the nozzle is located at the pressure anti-node where the amplitude is at the maximum. The fluid is supplied through the center tube to the nozzle tip, where it forms a thin film as it wets the tip. Typically, the nozzles provided by Sonics and Materials, Inc. are designed as a separate part, which can be screwed onto an ultrasound transducer (Fig. 20.2). A side port is made at the node plane as the liquid inlet.

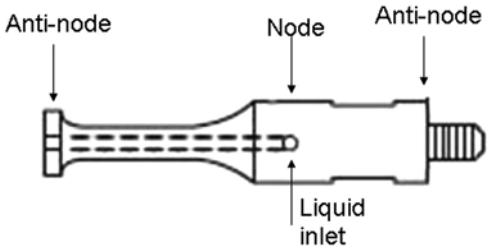

Fig. 20.2 Ultrasonic atomizer by Sonics and Materials, Inc.

These atomizers operate at low ultrasonic frequency up to 120 kHz and generally operate with power less than 20 W. The mean droplet size at a given frequency is predicted by the Lang equation (Lang, 1962):

$$D = 3.4 \times 10^{-3} \left(\frac{8\pi\sigma}{\rho f^2} \right)^{1/3} \tag{20.1}$$

where σ is the surface tension (liquid/gas) (N/m), ρ is the liquid density (kg/m^3), f is the ultrasound frequency (Hz), and D is the droplet diameter (m). The distribution of water droplet size at different frequencies has been reported by Berger (1998). If, however, the amplitude is operated beyond the cavitation threshold, the disturbances caused by cavitation will broaden the droplet size distribution (Topp and Eisenklam, 1972).

At high liquid flow rates the empirically derived equation of Mochida (1979) applies:

$$D = 2.21 \times 10^{-2} \, (\sigma/\rho)^{0.354} \, \eta^{0.303} q^{0.139} \tag{20.2}$$

where η is the liquid viscosity (Pa s) and q is the volumetric flow rate (l/s).

The flow of the liquid can be supplied by a positive displacement pump. Since atomization does not depend on hydrostatic pressure, the nozzle diameter can be enlarged (typically on the order of several millimeters), making the ultrasonic nozzle attractive to spraying slurry without clogging issues.

4 Ultrasonic Atomizers for Seasoning Applications

To be useful for seasoning applications, the atomizer must be versatile over a wide range of operating conditions. The table below lists the range of conditions likely to be encountered by a single nozzle.

Some combinations of high-end requirements demand an ultrasonic nozzle capable of ultra-high amplitude. At 20 kHz, it was found that the amplitude requirement for these conditions ranges from 20 to 200 μm. None of the commercial units were capable of the full range of the conditions listed in Table 20.1. Specialty nozzles were therefore developed in collaboration with Sonics and Materials, Inc. (Fig. 20.3).

Table 20.1 Operating conditions for an ultrasonic nozzle

Operating parameters	Low	High
Flow rate (ml/min)	0.1	1,000
Viscosity (cp)	1	500
Solid content (%w/w)	0	50
Solid particle size (μm)	0	500

Fig. 20.3 One of the specialty nozzles used for seasoning application

4.1 Continuous Atomization

A design of continuous atomization process is schematically illustrated in Fig. 20.4. A fluid or slurry was prepared in a mixing tank. The flow rate to the nozzle was controlled by a positive displacement pump, with optional feedback control through a flow meter. The feed temperature can be controlled with a heating element, preferably just before the nozzle. This feature is particularly useful for slurry applications, where slurry viscosity is kept high for solid suspension, and only lowered for a very short time period before atomization.

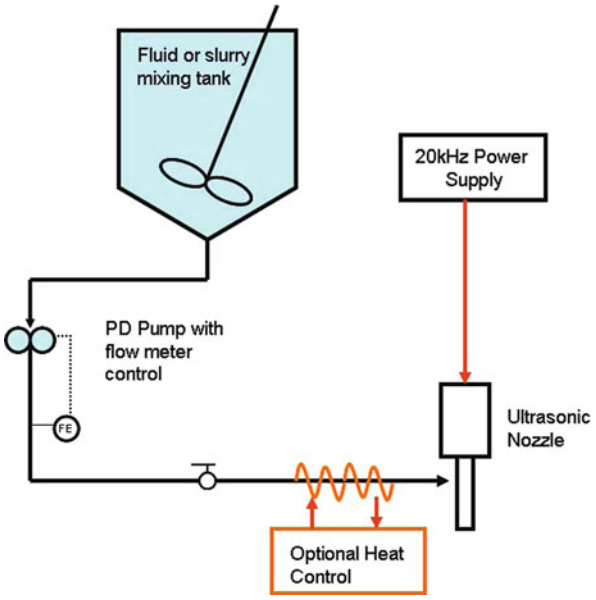

Fig. 20.4 One of the specialty nozzles used for seasoning application

In one application, the system was tested to spray salt/vegetable oil slurry on potato chips on a moving conveyer. The operating condition is presented in Table 20.2. The result of salt adhesion measurement is compared to a process where the salt was applied directly onto the chips as dry particles (Table 20.3). Note that two adhesion rates are shown. One is calculated by mass balance, i.e., the total salt

Table 20.2 Conditions for salt/vegetable oil slurry spray

Flow rate	50–500 ml/min
Salt load	15–25%w/w
Mean solid particle size	130 μm
Ultrasonic vibration amplitude	60 μm
Ultrasonic frequency	20 kHz

Table 20.3 Salt distribution

	% salt	SD	% adhesion (mass balance)	% adhesion (actual)
Baseline	1.29	0.24	50	66.7
Ultrasonic	1.31	0.08	74	98.6

deposited on the chips vs. the total salt applied. The actual percentage of adhesion was calculated by taking into account the spacing between chips. The ultrasonic slurry application significantly improved salt adhesion and reduced the variation of seasoning coating.

4.2 Registered Pulsed Spray

Registered pulsed spray refers to targeting of the atomization at the individual chips on a moving conveyor. This capability is desired, as it eliminates overspray in the gap between chips. If multiple nozzles are used, each with a different additive/flavor, they can be programmed to produce a variety of products with unmatched process flexibility. However, to be useful on the production scale, the nozzle must be able to pulse the spray accurately at a rate, in pulses per minute, that matches the number of chips per minute to be coated, which could be higher than 500. The target pulse must be focused on each chip so that flavor contamination across chips is kept at the minimum.

A block diagram (Fig. 20.5) shows the control of the registered pulsed ultrasonic spray. A seasoning/flavor liquid or slurry is supplied by a positive displacement pump at a constant flow rate. An optional heating element may be applied just before the ultrasonic nozzle. The nozzle is powered on at all times. However, the amplitude of the nozzle is switched between a “resting” mode, which is below the threshold of atomization, and an “active” mode, which is above the threshold of atomization. In the resting mode, the seasoning liquid wets the atomizer surface. In the active mode, the accumulated liquid is sprayed onto the substrate. The position of the chip on a moving conveyor can be detected by an optical sensor. Given the moving speed of the conveyor, the control sets a delay time for the amplitude to switch from resting to active, so that a pulsed spray targets the desired position on a chip. The ratio of the chip length over the conveyor speed is used to set the active duration so that the length of the pulsed spray can either fully or partially cover the entire chip. This amplitude modulation approach is the key to ensure that the pulse can respond at the production rate. Since the flow rate is unchanged, the setup is ideal for a conveyor where the chips are spaced equally.

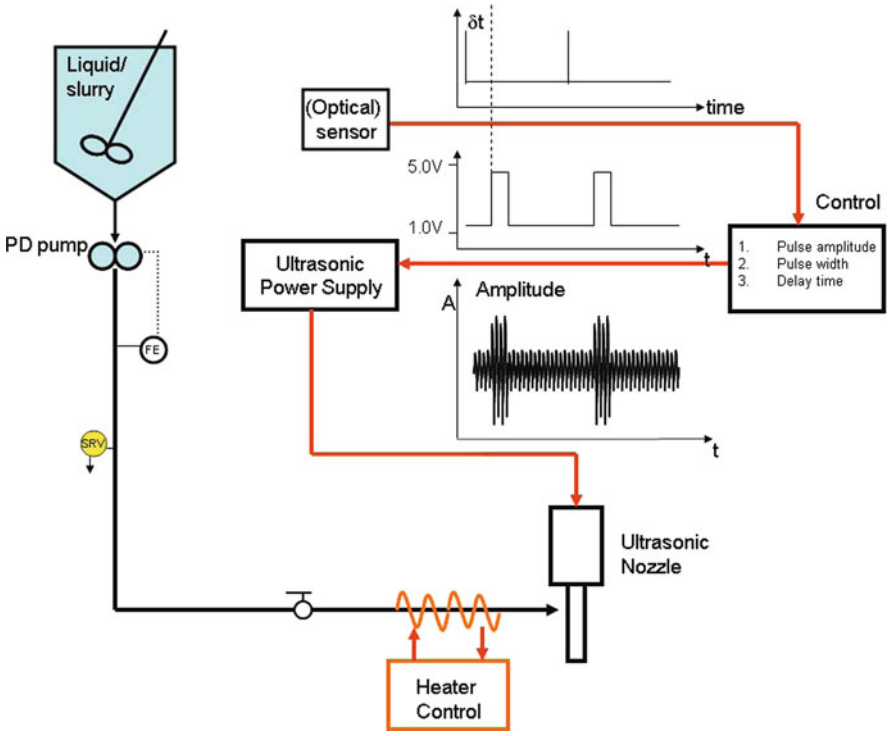

Fig. 20.5 Block diagram of registered pulsed ultrasonic spray

Operation of a single nozzle is illustrated by images captured with a high-speed video camera (Fig. 20.6). In this case, a row of equally spaced chips was moved at a constant speed under a nozzle. The sequence of seasoning spray over a single chip is illustrated.

An ultrasonic seasoning unit consisting of multiple nozzles to cover the width of a conveyor is shown in Fig. 20.7. This arrangement allows the seasoning of multiple rows of chips on the conveyor, with each nozzle targeted at a single row of chips. Because of the accuracy of the spray, an individual nozzle can have different flavors without concern of cross-contamination between the rows. Since the seasoning is fed to each of the nozzles individually, each row can have a different seasoning if desired, so that different flavored products can be made on the same conveyor at the same time. Further, if using two nozzles along the same row of chips and each having a different flavor, a variety of flavored chips may be created. For example, the first nozzle can be timed to spray every other chip and the second nozzle to spray on the chip in between. It is also feasible to time the two nozzles so that each can spray on multiple chips before activating the other nozzle.

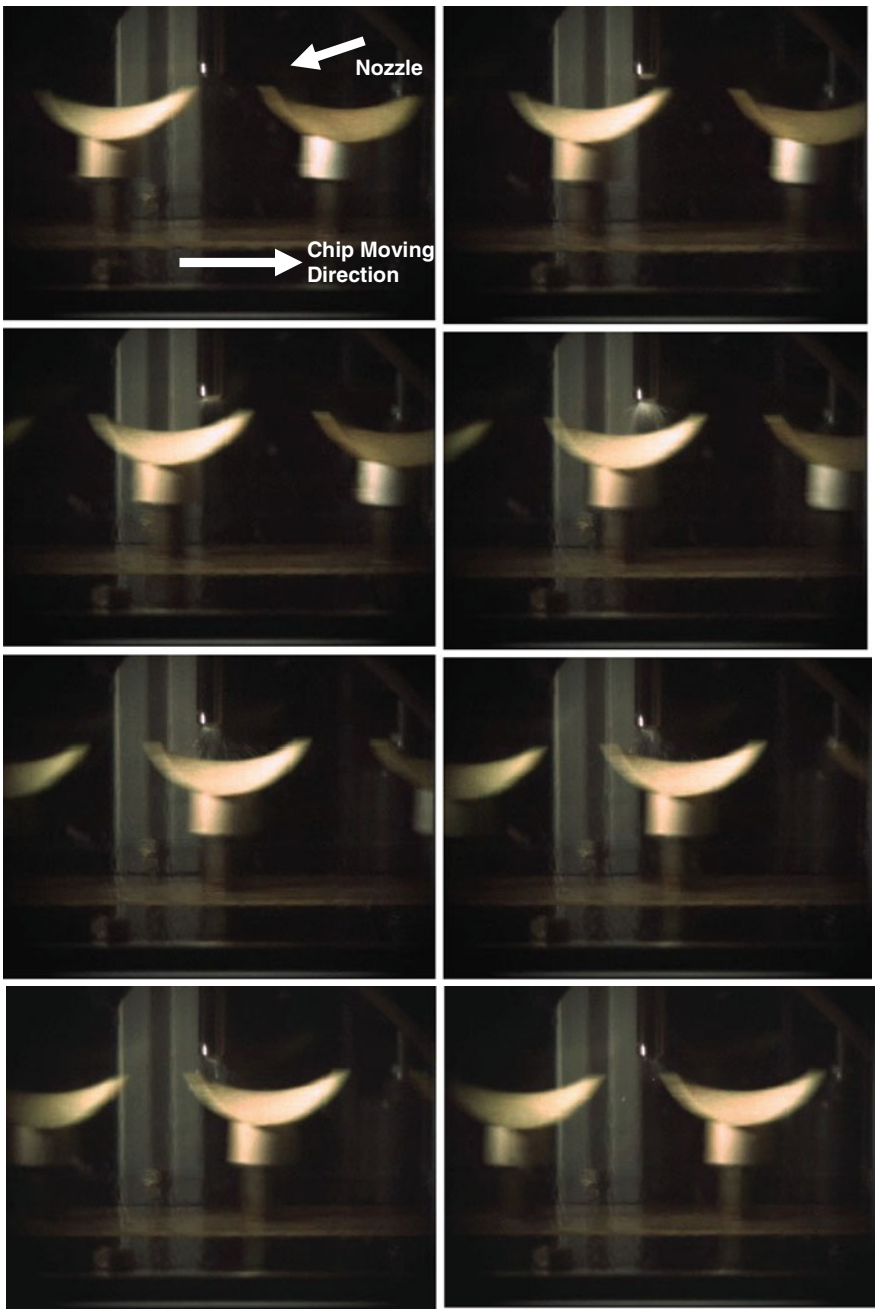

Fig. 20.6 High-speed video images showing registered pulsed spray over a row of chips

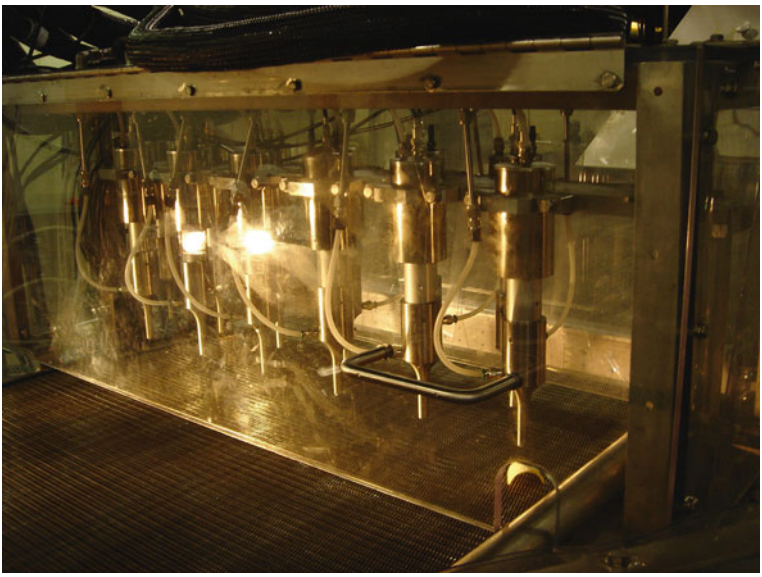

Fig. 20.7 An ultrasonic seasoning unit on a conveyor, consisting of an array of nozzles

5 Conclusions

High-power ultrasonic spray has been explored within Procter and Gamble Company for food seasoning applications. This method provides an alternative to the conventional spray nozzle in a rotating drum. The main advantages of ultrasonic sprays are as follows:

- Accurate metering of flow rate
- Clogging resistance enabling slurry applications
- Gentler spray minimally impacting the substrate

The ability to spray large particles without clogging opens the possibility of spraying solid seasoning in slurry, which improves solid adhesion and reduces variability in seasoning coating. With appropriate control, ultrasonic spray can be pulsed to target individual chips. This new process capability offers not only superior seasoning accuracy, but also unmatched flexibility in product innovation.

Handling the range of flow rates and the variety of liquid properties appropriate to seasoning applications stretches the limit of ultrasonic nozzle design, in particular vibration amplitude. Design changes create challenges in control, power supply, and connector interface to the nozzle. More research is needed in high-power ultrasonic nozzle development in order to ensure the robustness of this technology in industrial applications.

References

Abu-ali, J., and Barringer, S. A. (2005). Method for electrostatic atomization of emulsions in an EHD system. *Journal of Electrostatics*, 63, 361–369.

Berger, H. L. (1998). *Ultrasonic liquid atomization – Theory and applications*. Sono-Tek Milton, New York.

Berry, D. (2003). Chip celebration. *Food Product Design*, 12(5), 33–34, 37, 49–50, 54.

Buck, V. E., and Barringer, S. A. (2007). Factors dominating adhesion of NaCl onto potato chips. *Journal of Food Science*, 72(8), E435–E441.

Enggalhardjo, M., and Narsimhan, G. (2005). Adhesion of dry seasoning particles onto Tortilla chip. *Journal of Food Science*, 70(3), E215–E222.

Kuntz, L. A. (1996). Seasoning Secrets for Salty Snacks, Food Product Design, Available from http://www.foodproductdesign.com/articles/1996/01/seasoning-secrets-for-salty-snacks.aspx. Accessed on September 24, 2010.

Lang, R. J. (1962). Ultrasonic atomization of liquids. *Journal of Acoustic Society of America*, 34, 6–8.

Loomis, W. R., and Woods, A. L. (1927). The Physical and Biological Effects of High Frequency Sound Waves of Great Intensity. *Philosophical Magazine Letters*, 4, 417.

Mochida, T. (1979). *Proceedings of ICLASS-79*, *International Conference on Liquid Atomization and Spray Systems*, Tokyo, 193.

Morgan, A. (1993). Ultrasonic atomization. In: Mason, T. J. (ed.), *Advances in sonochemistry*, vol. 3, pp. 145–164. London, JAI Press.

Pedreschi, F., and Moyano, P. (2005). Effect of predrying on texture and oil uptake of potato chips. *Lebensmittel-Wissenschaft and Technologie*, 38(6), 599–604.

Topp, M. N., and Eisenklam, P. (1972). Industrial and medical uses of ultrasonic atomizers. *Ultrasonics*, 10, 127–133.

Chapter 21
High-Power Ultrasound in Surface Cleaning and Decontamination

Sami B. Awad

High-power ultrasound is being widely utilized for decontamination in different industrial applications. The same technology is also being investigated as an effective tool for cleaning of components in the decontamination of produce. An understanding of the basic technology and how it works in cleaning various industrial parts should help in applying it on a large scale in the food industry. The technology has evolved throughout the past four decades. Different frequencies were developed and are now industrially available. The frequency range is from 20 kHz to 1 MHz. Current sound technology provides a uniform ultrasonic activity throughout the cleaning vessel, which was a major disadvantage in the earlier technology. The two main driving forces that affect cleaning of surfaces are cavitation and acoustic streaming. Both are generated as a result of the direct interaction of high-frequency sound waves with fluids. The intensity of each force varies with the frequency used. In addition to cleaning of industrial components, other known applications of high-power ultrasound are in the areas of spray drying, emulsification, degassing, flavor extraction, homogenization, meat tenderization, and removal of bio-contaminants. Very high-frequency ultrasound with moderate to very low power is being used in sonar, therapeutic, and medical diagnostics.

1 High-Power Ultrasound

A minimum level of ultrasound energy is needed to generate cavitation in a liquid. The threshold was found to be about 0.3 and 0.5 W/cm^2 at the radiating surface when the frequencies of the ultrasound waves are 20 and 40 kHz, respectively.

Currently available high-power ultrasound frequency range is from 20 kHz to 1 MHz. A frequency that is good for one application may be not good for another. The basic reason for this is that every application is unique in its nature with respect to material of construction, contaminants, and required cleanliness level. For

S.B. Awad (✉)
VP Technology, Crest Ultrasonics Corp., Trenton, NJ 08628, USA
e-mail: sawad@rcn.com

H. Feng et al. (eds.), *Ultrasound Technologies for Food and Bioprocessing*, Food Engineering Series, DOI 10.1007/978-1-4419-7472-3_21,
© Springer Science+Business Media, LLC 2011

example, cleaning of very thin fragile wafers requires higher frequencies, while cleaning of automotive components requires lower frequency.

At the low end of 20–60 kHz, cavitation implosion energy is the main scrubbing force, while at the high end of 1 MHz, micro-streaming of the fluid molecules is the main force in fine cleaning. It is important to note that both types of forces exist at every frequency. Cavitation implosion energy is good for the removal of heavy contaminants, while micro-streaming is good for the removal of nano-size particulates. There is a linear relationship between the applied frequency and the generation of cavitation and micro-streaming in fluids.

2 Ultrasonic Cleaning Mechanism

2.1 Cavitation and Micro-streaming

A unique phenomenon takes place when high-energy ultrasonic waves [20 kHz to about 500 kHz (at about 0.3–1 W/cm^2)] travel in a liquid or in a solution. The waves interact with the liquid medium to generate a highly dynamic agitated solution. In the process, high-intensity ultrasonic waves create micro-vapor/vacuum bubbles in the liquid medium, which grow to a maximum size proportional to the applied ultrasonic frequency and then implode, releasing their energies. This phenomenon is known as cavitation implosion. The higher the frequency, the smaller the cavity size, with lower implosion energy. The high-intensity ultrasonics can grow cavities to a maximum in the course of a single cycle. At 20 kHz, the bubble size is roughly 170 μm in diameter (Fig. 21.1). At a higher frequency of 68 kHz, the total time from nucleation to implosion is estimated to be about one-third of that at 25 kHz. The vacuum bubble size becomes smaller at higher frequencies as a function of the wavelength. For example, at 132 kHz the bubble size is estimated to be about half of that generated at 68 kHz, and the size will be even much smaller at 200 kHz.

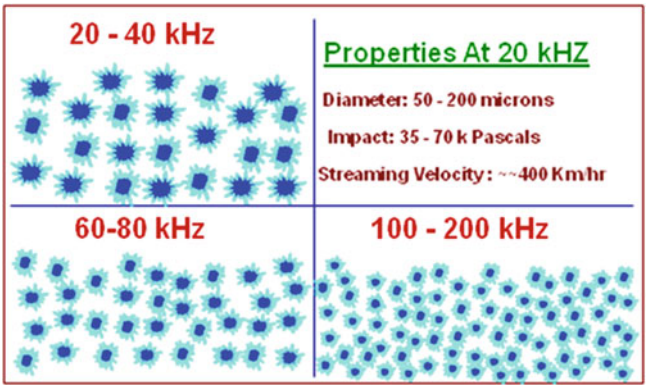

Fig. 21.1 Ultrasound frequency and cavitation size and population

Meanwhile, at higher frequencies, the minimum amount of energy required to produce ultrasonic cavities is higher and must be above the cavitation threshold. In other words, the ultrasonic waves must have enough pressure amplitude to overcome the natural molecular bonding forces and the natural elasticity of the liquid medium in order to grow the cavities. For water, at ambient temperature, the minimum amount of energy needed to be above the threshold was found to be about 0.3 and 0.5 W/cm^2 per tank radiating surface for 20 and 40 kHz, respectively. The energy released from implosions is expressed in new forces, namely shock wave, micro-streaming, shear forces, and miniature eddy currents.

2.2 Ultrasonic Generation

The transducers most commonly used for generating ultrasonic vibrations are piezoelectric, magnetostrictive, electromagnetic, pneumatic, and other mechanical devices. The piezoelectric transducer (PZT) assembly (Fig. 21.2) is the most widely used configuration in cleaning and plastic welding applications. Lead zirconate titanate is used interchangeably for PZT (but is not discussed in this chapter). The PZT assembly can generate a wide range of frequencies from about 20 kHz to the megasonic range.

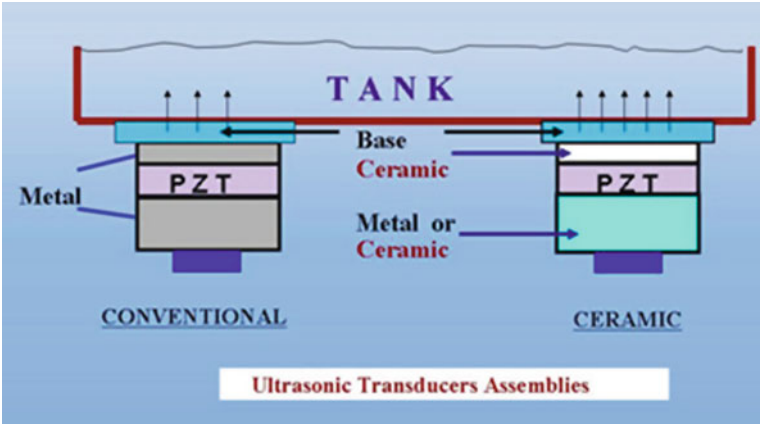

Fig. 21.2 Ultrasonic PZT transducer assembly bonded to the bottom of a tank

Typical piezoelectric (PZT) transducers are normally mounted on the bottom and/or sides of the cleaning tanks. The transducers can be mounted onto various designs and sizes that are sealed in stainless steel containers or immersed in the cleaning fluid (immersibles).

Another design for immersibles (manufactured by Martin Walter Co., a Crest Tech company) is known as the push–pull transducer. It is an immersible transducer. The push–pull is made of two PZT transducers mounted on the ends of a titanium rod with different lengths and diameters. The ultrasonic waves generated along the

rod axis propagate perpendicularly to the resonating surface. The waves interact with the fluid medium to generate cavitation implosions.

2.3 Cavitation Formation Mechanism

The ultrasonic cleaning illustration (Fig. 21.3) shows the generating cavitation through at least three steps: nucleation, growth and violent collapse, or implosion. The transient cavities (or vacuum bubbles or vapor voids), ranging from 50 to 150 μm in diameter at 25 kHz, are produced during the sound waves' half cycles. During the rarefaction phase of the sound wave, the liquid molecules are extended outward against and beyond the liquid's natural physical elasticity/bonding/attraction forces, generating vacuum nuclei that continue to grow to a maximum. Then, violent collapse occurs during the compression phase of the wave. It is believed that the latter phase is augmented by the enthalpy of the medium and the degree of mobility of the molecules, as well as the hydrostatic pressure of the medium.

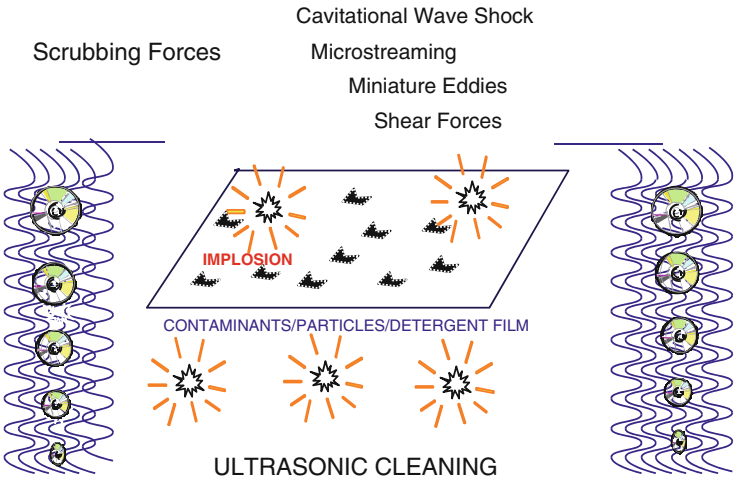

Fig. 21.3 Micro-vacuum bubble formation and scrubbing forces released on implosion

Cavitations are generated in the order of microseconds. At 20 kHz frequency, it is estimated that the pressure is about 35–70 kPa and the transient localized temperatures are about 5,000°C, with the velocity of micro-streaming around 400 km/h (Table 21.1). Several factors have great influence on the cavitation intensity and abundance in a given medium. Among these factors are the ultrasonic wave form, its frequency, and the power amplitude. Other determining factors are the physical properties of the liquid medium including viscosity, surface tension, density, and vapor pressure; the medium temperature and the liquid flow, whether laminar or turbulent; and dissolved gases.

Table 21.1 High-Power ultrasound in water

Frequency (kHz)	Cavitation size (μm) and intensity	Microstreaming velocity (m/s)	Boundary layer (μm)
20 – 30	~ 125 High	~ 50	4.4
40	75 Medium	>100	2.82
68	42		
72, 80	Medium		
104			
132	23 Mild		
172			
192			1.6
400	Very mild		0.594
0.8 – 1 M Hz	Extremely mild		

2.4 Frequency and Cavitation Abundance

At low frequencies of 20–30 kHz, a smaller number of cavitations with larger sizes and higher energy are generated. Much denser cavitations with moderate or lower energies are formed as frequency increases. Frequencies of 20–35 kHz are more appropriate for cleaning heavy and large size components, while a frequency of 60–80 kHz is recommended for cleaning delicate surfaces such as optics. Frequencies of 132 and 192 kHz are recommended for cleaning ultra-delicate materials such as thin films and tiny components. The latter two ranges are appropriate for use during rinsing steps with all applications. For example, at 60–80 kHz, the cavitation abundance is high enough and mild enough to remove detergent films and to remove submicron particles in the rinsing steps without inflicting damage on surfaces. The 35–45 kHz frequency range was found to be appropriate for a wide range of industrial heavy components such as automotive engines and steel molds.

Estimates of cavitation abundance at various ultrasonic frequencies have shown that cavitations are more abundant at higher frequencies. For example, about 60–70% more cavitation sites per unit volume of liquid are generated at 68 Hz

than at 40 kHz because the size of the micro-cavities decreases at higher frequencies (Awad, 1996). Therefore, one would expect that at the higher frequency, at a given energy level, the scrubbing intensity would be milder, particularly on soft and thin or delicate surfaces. In general, selecting the proper frequency for a particular application is critical and must be carefully investigated.

3 Precision Cleaning

Precision or critical cleaning of components or substrates is the complete removal of undesirable contaminants to a desired preset level, without introducing new contaminants in the process (Awad, 1996). The preset level is normally the minimum level at which no adverse effects take place in a subsequent operation. To achieve the desired cleanliness level, it is critical not to introduce new contaminant(s) into the cleaning process. For example, in an aqueous cleaning process, it is important to have high-quality rinse water and a minimum of two rinse steps. Otherwise, residual detergent and/or salts from the rinsing water will become new contaminants. Recontamination of cleaned parts with out-gassed residues produced from packaging or storing materials is another source (Awad, 1996).

To meet production and quality demands, one must keep in mind that one essential element is choosing the appropriate cleaning chemistry/process. Moreover, rejected parts are the curse of the assembly line and improper cleaning methods are often to blame. Even beyond the factory floor, improper or inadequate cleaning of a component could directly affect warranty claims (Bhatt, 1998; Durkee, 1994).

3.1 Ultrasonic Cavitations and Surface Cleaning

The energy released from an implosion in close vicinity to the surface collides with and fragments or disintegrates the contaminants, allowing the detergent or the cleaning solvent to displace it at a very fast rate. The implosion also produces dynamic pressure waves, which carry the fragments away from the surface. The implosion is also accompanied by high-speed micro-streaming currents of the liquid molecules. The cumulative effect of millions of continuous tiny implosions in a liquid medium provides the necessary mechanical energy to break physically bonded contaminants, speeds up the hydrolysis of chemically bonded contaminants, and enhances the solubilization of ionic contaminants. The chemical composition of the medium is an important factor in speeding the removal rate of various contaminants.

Cleaning with ultrasonics offers several advantages over other conventional methods. Ultrasonic waves generate and evenly distribute cavitation implosions in a liquid medium. The released energies reach and penetrate deep into crevices, blind holes, and areas that are inaccessible to other cleaning methods (Fuchs, 1997; O'Donoghue, 1984). The removal of contaminants is consistent and uniform, regardless of the complexity and the geometry of the substrates.

3.2 Power Requirements

The general ultrasonic power requirements for almost all cleaning applications, expressed in terms of electrical-input wattage to the transducers, is in the range of 7.15–9.15 W/cm^2 of transducer radiating surface.

4 Ultrasonic Cleaning Equipment

Ultrasonic aqueous batch cleaning equipment consists of at least four steps: ultrasonic wash tank, minimum of two ultrasonic separate (or reverse cascading) water rinse tanks, and heated recirculated clean air for drying. The last drying step is not included if the post-cleaning operation includes an aqueous bath, as in electro- or electroless plating. Ultrasonic transducers are bonded to the outside bottom surface (Fig. 21.2) or to the outside of the sidewalls or provided as immersibles inside the tanks. The latter is usually the preferred method when large size tanks are under consideration. Two types of immersibles (Fig. 21.4) are commercially available in various sizes and frequencies. The traditional sealed metal box contains a multi-transducer system and a cylindrical immersible, which is powered by two main transducers at both ends, known as push–pull immersibles (Weber and Walter, 1993).

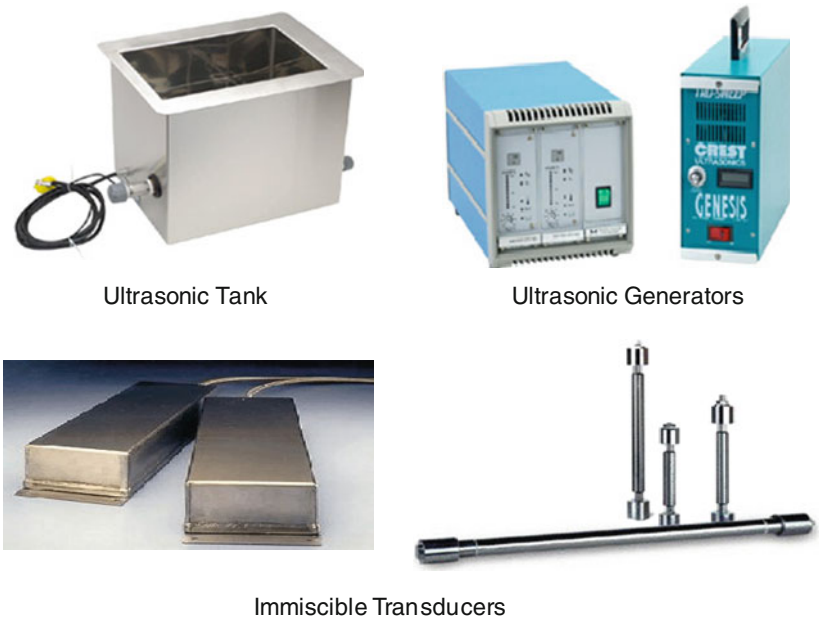

Fig. 21.4 Ultrasound units (courtesy of Crest Ultrasonics)

Prior to selecting equipment, it is imperative that an effective cleaning process first be developed, and then the number and size of the stations are subsequently determined based on the required yield, total process time, and space limitation.

The automation of ultrasonic cleaning systems is well established. Automation includes a computerized transport system able to run different processes for various parts simultaneously, along with data monitoring and acquisition. The advantages of automation are numerous, including consistency, achieving desired throughputs, and full control of process parameters (Awad, 2000).

Typical tank size ranges from 10 to 2,500 l, based on the size of the parts, production throughput, and required drying time. The entire machine can be enclosed to provide a clean room environment meeting class 10,000 down to class 100 clean room specifications. Process control and monitoring equipment consists of flow controls, chemical feed pumps, in-line particle count, TOC measurement, pH, turbidity, conductivity, refractive index, etc. The tanks are typically made of corrosion-resistant stainless steel or electro-polished stainless steel. Titanium nitride or a similar coating such as hard chrome or zirconium is used to extend the lifetime of the radiating surface in the tanks or the immersible transducers.

The number and the size of the stations are determined based on the required process time. A semi-aqueous cleaning system, for example, includes an extra station for solvent displacement, connected to a phase separation/recovery system. The entire machine can be enclosed to provide a clean room environment meeting class 10,000 down to class 100 clean room specifications.

5 Cleaning Chemistry

It is important to realize that the use of ultrasonics does not eliminate the need for proper cleaning chemicals and implementation and maintenance of the proper process parameters (Seelig, 1995).

Furthermore, the chemical composition of the cleaning medium (for aqueous cleaning or organic solvent cleaning) is a critical factor in achieving the complete removal of various contaminants without inflicting any damage to the components.

Cleaning with ultrasonics using only plain water is workable, but only for short time. The question, then, is how long ultrasonic cleaning is going to work before failing to clean. In fact, cleaning is more complex in nature than just extracting contaminants away from the surface. Soil loading and encapsulation/dispersion of contaminants are determining factors for both the effective lifetime of the cleaning medium and the cleaning results.

Reproducibility and consistency of the cleaning results are essential requirements for all successful cleaning processes. Cleaning chemistry, as part of the overall cleaning process, is a very crucial element in achieving such consistency (Kaneegsburg, 1999). Requirements for the selected chemistry are many. It must cavitate well with ultrasonics and be compatible with the components to be cleaned. Other properties such as wettability, stability, soil loading, oil separation, effectiveness, dispersion or encapsulation of solid residues, ability to rinse freely, and disposal are all important factors that must be addressed when deciding on the

appropriate chemistry. Clearly, an expert in the field is the best individual to make this decision.

Both aqueous and organic solvent cleaning methods have advantages and disadvantages. Aqueous cleaning is universal and achieves better cleaning results. Organic solvents are effective in removing organic contaminants, but short on removing inorganic salts. Drying and protection of steel components are valid concerns. However, the current available technologies offer effective ways to alleviate these concerns.

Power ultrasound enhances the effect of cleaning or decontaminating chemicals, in part due to the dislodging of general and bio-contaminants such as oils, protein, or bacterial clumps from surfaces, thus making them available to the chemicals (Mason, 1998).

The role of aqueous chemistry is to displace oil, to solubilize it or emulsify organic and bio-contaminants, to encapsulate particles, and to disperse and prevent redeposition of contaminants after cleaning. Special aqueous formulations assisted with ultrasonics are being used to decontaminate post-operation surgical instruments, dental and medical devices, and in food processing (Boucher, 1980). Decontamination of hatchery eggs was recently reported using a bactericide and ultrasound (Slapp, 1995). Some additives in cleaning chemicals are used to assist in the process of breaking chemical bonding, removal of oxides, preventing corrosion, or enhancing the physical properties of the surfactants or to enhance the surface finish. Post-cleaning, it is important to use deionized water (RO water) for rinsing off the aqueous chemical(s) to achieve spot-free surfaces. A minimum of two rinse steps is recommended.

5.1 Selection of Cleaning Fluids

Effective cleaning fluids are essentially selected on the basis of (1) the chemical and physical nature of the contaminants to be removed; (2) compatibility with the substrate material(s); (3) environmental considerations; and (4) required cleanliness specifications. Therefore, in precision or fine cleaning there is no one specific chemistry for all applications. Every case must be examined individually to determine the most effective and safe chemical.

6 Contaminants

Three general classes of common contaminants are organic, inorganic, and particulate matter. Particles do not necessarily belong to a certain class and can be from any one class or a mixture thereof. Insoluble particulate contaminants can, for example, be divided into two groups: (1) water-wettable or hydrophilic particles, including metal particles, metal oxides, minerals, and inorganic dusts; and (2) nonwater-wettable or hydrophobic substances, including plastic particles, smoke and carbon particles, graphite dust, and organic chemical dusts. Substrate surfaces, too, can be divided into hydrophilic and hydrophobic groups.

Contaminants of any class can be water soluble or water insoluble. Organic contaminants in most cases will be hydrophobic in nature, such as oils, greases, waxes, polymers, paints, print, adhesives, or coatings.

Except in a very few cases, inorganic materials or salts are insoluble in solvents that are nonwater miscible. Water is the best universal solvent for organic or inorganic ionic materials. However, water-insoluble inorganics, such as polishing compounds made of oxides of aluminum, cerium, or zirconium, require a more elaborate cleaning process.

Organic contaminants can be classified into three general classes: long-chain, medium-chain, and short-chain molecules. The physical and chemical characteristics are related to their structure and geometry.

7 Mechanism of Cleaning

Two main steps take place in surface cleaning. The first step is contaminant removal and the second step is to keep those contaminants from re-adhering to the surface. The removal of various contaminants involves different mechanisms, based on the nature and/or the class of the contaminant.

Organic contaminants are removed by two main mechanisms. The first is by solubilization in an organic solvent. Degree of solubilization in various solvents is directly related to their molecular structure. The second mechanism is by displacement with a surfactant film followed by encapsulation and dispersion.

In aqueous cleaning, the detergent contains a single or mixture of surfactants. Surfactants are long-chain organic molecules with polar and non-polar sections in their chains. Surfactants can be ionic or nonionic in nature, based on the type of functional groups attached to or part of their chains. When diluted with water, surfactants form aggregates, called micelles, at a level above their critical micelle concentration (CMC). The micelles are composed of aggregates of hydrophilic moiety and hydrophobic portion of the surfactant molecules. They act as a solvent and encapsulate similar contaminants, thus preventing redeposition.

The mechanism of removal of organic contaminants by detergent involves wetting of the contaminant as well as the substrate. According to Young's equation, this will result in increasing the contact angle (θ) between the contaminant and the surface, thus decreasing the surface area wetted with the hydrophobe and reducing the scrubbing energy needed for removal:

$$\cos\,\theta \;=\; \frac{\gamma_{SB} - \lambda_{SO}}{\gamma_{OB}}$$

where γ_{SB} is substrate bath interfacial energy, γ_{OB} is soil bath interfacial energy, and γ_{SO} is substrate soil interfacial energy.

Ultrasonic cavitation plays an important role in initiating and completing the removal of hydrophobic contaminants (e.g., oils, soils). The shock wave (and the

micro-streaming currents) greatly speed up the breaking up of the hanging contaminants, thus enhancing displacement with the detergent film. The removed contaminants are then encapsulated in the micellic aggregates, thus preventing their redeposition. The net result is that ultrasonic cavitations accelerate the displacement of contaminants from the surface of the substrate and also facilitate their dispersion throughout the cleaning medium.

7.1 Particle Removal

Particles, in general, have irregular shapes. All the adhesion forces, i.e., van der Waals, electrical double layer, capillary, and electrostatic, are in theory directly proportional in magnitude to the size of the particle. One would expect that the energy of detachment would decrease with the size of particle. However, smaller particles are always more difficult to detach. This is mainly due to the lodging effect. Smaller particles tend to get trapped in the valleys of a rough surface.

7.2 Particle Removal Mechanism

The mechanism of particle removal involves shifting the free energy of detachment to be near or smaller than zero, according to Gibbs adsorption equation. Surfactants play a very important role in decreasing interfacial tension by adsorption at particle and substrate interface with the bath. The interfacial tension γ_{OB} and γ_{SB} will decrease and, accordingly, the force needed to detach the particles will decrease, when ΔG is greater than zero or a positive value:

$$\Delta G = \gamma_{SB} + \gamma_{OB} - \gamma_{SO}$$

where γ_{SB} is substrate bath interfacial energy, γ_{OB} is soil bath interfacial energy, γ_{SO} is substrate soil interfacial energy.

The wettability of the surface plays an important role in achieving this step. The ultrasonic cavitation role is to provide the necessary energy for the detachment (i.e., the removal force). At high-frequency (60–70 kHz) ultrasonics, the detachment or the removal efficiency of very small size particles of 1 ?m, measured in deionized water, was found to be 95% versus 88% at 40 kHz. This is to be expected in light of the fact that cavitation size is smaller at higher frequencies and can reach deeper into the surface valleys. One would then anticipate that by using a combination of high-frequency ultrasonics at 65–68 kHz and the appropriate chemistry, the removal efficiency of various particles could be further optimized (Busnaina et al., 1994).

7.3 Prevention of Redeposition

Redeposition of contaminants is inhibited by another mechanism that forms a barrier between the removed contaminant and the cleaned surface. In solvent cleaning, the adsorbed solvent layers on the surface provide a film barrier. In aqueous cleaning, a good surfactant system is capable of encapsulating contaminants inside their micellar structure, as depicted in (Fig. 21.5). Thus, redeposition of the encapsulated contaminants (soils) onto an adsorbed surfactant film on the surface is prevented via steric hindrance for nonionic surfactants, while anionic surfactants prevent redeposition via an electrical repulsive barrier (Fig. 21.6).

Encapsulation can be permanent or transient, based on the nature of the used surfactants. Transient encapsulation is superior to emulsification, as it allows better

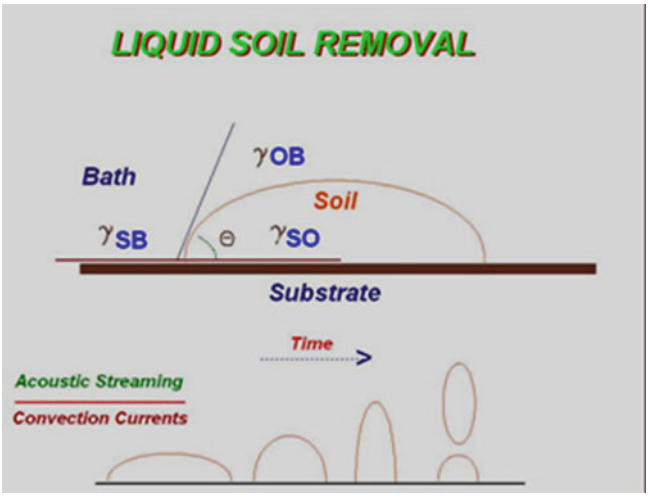

Fig. 21.5 Soil removal

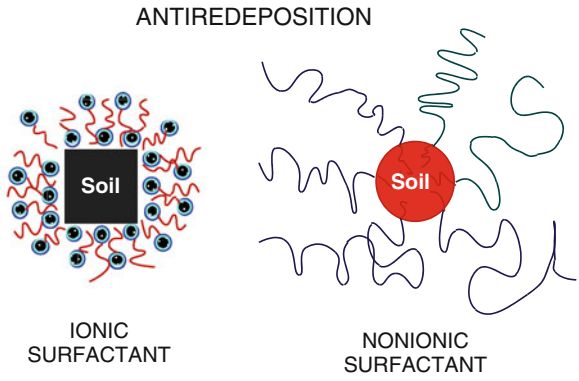

Fig. 21.6 Soil encapsulation

filtration and/or phase separation of contaminants. The potential of reversing the redeposition step by the application of sonic shock waves on loaded micelles results in partial re-adhesion. Therefore, allowing an increase in the soil load in a cleaning solution to reach saturation point, without good filtration, will result in a significant decrease in the detergent cleaning efficiency, at which point the cleaning action may cease. To ensure steady cleaning efficiency, the dispersed contaminants must be removed by means of continuous filtration or separation of contaminants, along with maintaining the recommended concentration of the cleaning chemical.

7.4 Cleaning Chemistry and Particles

A crucial element in small particle removal is prevention of redeposition. Cleaning chemistry plays this crucial role. The cleaning fluid should be capable of encapsulating the removed particles and thus preventing their redeposition on surfaces. Also, the cleaning fluid, whether aqueous or solvent, must displace the insoluble contaminants and form an insulating boundary film on the surface. The physical nature of the substrate and the degree of its surface finish are important factors in submicron particle removal (Awad, 1999; Mittal, 1995). For example, a silicon wafer surface is different from that of an aluminum disk, regarding their physical makeup, topography, and finish. Plastics are another challenge when dealing with submicron particles because of the inherent static electricity charges.

8 Conclusion

Cleaning with the assistance of ultrasonic cavitation has numerous advantages, most importantly a high level of decontamination and cleanliness and consistency in results. For the best cleaning results, selection of ultrasonic frequency and the cleaning chemistry (organic solvent or aqueous) is specific per application.

References

Awad, S. B. (1996). Ultrasonic cavitations and precision cleaning. *Precision Cleaning*, 4, 12.
Awad, S. B. (1999). Ultrasonic aqueous cleaning and particle removal of disk drive components. *Datatech*, 59.
Awad, S. B. (2000). Ultrasonic cleaning of medical and pharmaceutical devices and equipment. *A2C2 Magazine*, February, 7.
Bhatt, H. A. (1998). How now. *Parts Cleaning*, May, 17.
Boucher, R. M. G. (1980). *US patent 4,211,744*.
Busnaina, A. A., Gale, G. W., and Kashkoush, I. I. (1994). Ultrasonic and megasonic theory and experimentation. *Precision Cleaning*, 2, 13–19.
Durkee, J. B. (1994). *The parts cleaning handbook without Cfcs: How to manage the change*. Cincinnati, Hanser Gardner.
Fuchs, F. J. (1997). Ultrasonic cleaning principles for parts cleaning potential. *Parts Cleaning Magazine*, December, 14.

Kaneegsburg, B. (1999). Aqueous cleaning for high-value processes. *A2C2 Magazine*, September 1999, 25.
Mason, T. J. (1998). Power ultrasound in food processing – the way forward. In: Povey, M. J. W., and Mason, T. J. (eds.), *Ultrasound in food processing*, pp. 114–126. London, Blackie Academic and Professional.
Mittal, K. L. (1995). Surface contamination concepts and concerns. *Precision Cleaning*, 3, 17.
O'Donoghue, M. (1984). The ultrasonic cleaning process. *Microcontamination*, 2, 14.
Seelig, S. S. (1995). The chemical aspects of cleaning. *Precision Cleaning*, 3, 33.
Slapp, P. (1995). *BP 95 00587 2*.
Weber, D., and Walter, M. (1993). *Ultrasonic transducer*. US Patent 05,200,666.

Chapter 22
Effect of Power Ultrasound on Food Quality

Hyoungill Lee and Hao Feng

1 Introduction

Recent food processing technology innovations have been centered around producing foods with fresh-like attributes through minimal processing or nonthermal processing technologies. Instead of using thermal energy to secure food safety that is often accompanied by quality degradation in processed foods, the newly developed processing modalities utilize other types of physical energy such as high pressure, pulsed electric field or magnetic field, ultraviolet light, or acoustic energy to process foods. An improvement in food quality by the new processing methods has been widely reported. In comparison with its low-energy (high-frequency) counterpart which finds applications in food quality inspection, the use of high-intensity ultrasound, also called power ultrasound, in food processing is a relatively new endeavor. To understand the effect of high-intensity ultrasound treatment on food quality, it is important to understand the interactions between acoustic energy and food ingredients, which is covered in Chapter 10. In this chapter, the focus will be on changes in overall food quality attributes that are caused by ultrasound, such as texture, color, flavor, and nutrients.

The interaction of acoustic energy with a food is mainly substantiated through a liquid medium because cavitation and cavitation-induced physical and chemical actions play an important role in food quality alterations in an ultrasound-processed food. The chemical effects of cavitation include free radical generation, production of hydrogen peroxide, among others. The physical effects of cavitation include localized high temperature and pressure, shock waves, and microstreaming. At a solid and liquid interface, the water jet formed by an imploding transient cavitation is also a factor that may contribute to changes in the overall properties of a food product. It is noteworthy that all these chemical and physical effects of ultrasound are microscopic. The interplay of these cavitation-induced chemical and physical

H. Feng (✉)
Department of Food Science and Human Nutrition, University of Illinois at Urbana-Champaign, 1304 W. Pennsylvania Ave., Urbana, IL 61801, USA
e-mail: haofeng@illinois.edu

H. Feng et al. (eds.), *Ultrasound Technologies for Food and Bioprocessing*, Food Engineering Series, DOI 10.1007/978-1-4419-7472-3_22,
© Springer Science+Business Media, LLC 2011

activities with a food, however, is manifested through macroscopic changes that can be perceived by consumers and may be expressed with terms such as texture, color, and flavor. Nevertheless, it is not the intention of this chapter to translate microscopic activities into changes in overall quality attributes of foods since there are no sufficient data from systematic studies on the changes in a selected food quality attribute as affected by ultrasonic process parameters. Until now, there has been no reliable measure to quantify cavitation and cavitation-induced activities in a food system. No reports have documented an attempt to correlate cavitation activity to process conditions that can be used to predict quality changes. Therefore, wherever appropriate, a descriptive approach is employed to provide an argument for quality alterations in a food product caused by ultrasound. As a result, the conclusion that might be drawn is strictly limited to the specific food and ultrasound parameters used in the studies, which might still be far away from optimal process conditions.

2 Texture

Texture is a physical characteristic describing the flow behavior or responses to deformation of a liquid or solid food product. As a key food quality attribute, texture is mainly determined by the microstructure of the product. The presence of texturizing ingredients, such as proteins, as well as the interactions between food components during processing or storage, also plays an important role in food texture. The texture of ultrasound-treated foods can thus be determined by the structure or property changes of proteins and enzymes during sonication. For instance, it has been reported that ultrasound produced structural changes followed by functional changes in bovine serum albumin (BSA) (Gülseren et al., 2007). Such changes in a protein may be attributed to the mechanical, thermal, and/or chemical effect of sonication. Ultrasound also alters the activity of food enzymes. In some studies, an increased enzymatic activity, such as the activity of proteolytic enzyme, was reported after ultrasonication (Ronscale et al., 1992), while other reports have documented the use of ultrasound to inactivate food enzymes (Raviyan et al., 2005). In addition, high-intensity ultrasound is known to reduce particle sizes in a liquid food. Banerjee et al. (1996) ascribed the improved mechanical properties in protein-based films to fat globule size reduction by ultrasound. In solid foods, ultrasound may damage the cell wall structure of vegetables, thereby inducing changes in the texture (Gabaldón-Leyva et al., 2007). In this section, the effect of ultrasound treatment on the texture of food products, such as tomato juice, bell peppers, yogurt, edible films, and meat, will be discussed. The texture changes under different sonication conditions are summarized in Table 22.1.

There are a number of studies about changes in proteins and enzymes by an ultrasound treatment and their effects on food texture. Yogurt produced with ultrasound-treated milk showed a stronger and firmer structure than that with untreated milk (Fig. 22.1, Vercet et al., 2002a). An improvement in rheological properties of tomato juice was reported after inactivation of detrimental enzymes,

Table 22.1 Effect of ultrasound on texture of food products

Food product	Treatment conditions					Effect of ultrasound	References
	Frequency (kHz)	Acoustic energy	Temperature (°C)	Pressure	Treatment time (s)		
Yogurt	20	NA	40	2 kg/cm^2	12	Firmer structure of yogurt made with manothermosonicated milk than that prepared by a standard method	Vercet et al. (2002a)
Yogurt	20	0.6–3 W/ml	15	Ambient pressure	360 and 480	Higher viscosity of yogurt prepared with sonicated milk than that prepared by a standard method	Wu et al. (2001)
Tomato juice	20	NA	70	200 kPa	60	Higher apparent viscosity, yield stress value and consistency of manothermosonicated tomato juice than those of thermally treated juice	Vercet et al. (2002b)
Beef *pectoralis* and *longissimus* muscles	20	22 W/cm^2	Up to 62 and 70ºC (internal temperature)	Ambient pressure	Around 480 and 540 for *Pectoralis*, 480 and 600 for *Longissimus*	Significantly lower peak force work and higher myofibrillar tenderness of ultrasound-cooked meat than traditionally cooked meat	Pohlman et al. (1996)
Semitendinosus muscle	25.9	NA	10	Ambient pressure	Up to 600	Significant decrease in shear force of cooked ultrasound-treated meat	Smith et al. (1991)

Table 22.1 (continued)

Food product	Treatment conditions					Effect of ultrasound	References
	Frequency (kHz)	Acoustic energy	Temperature (°C)	Pressure	Treatment time (s)		
Broiler breast muscle	40	NA	26	Ambient pressure	900	Lower shear values of cooked breast meats from ultrasound-treated carcass than without ultrasound treatment	Dickens et al. (1991)
Beef *pectoralis* muscle	20	22 W/cm^2	4	Ambient pressure	300 and 600	Reduced peak force and total work in ultrasound-treated muscle	Pohlman et al. (1997a)
Bovine *semimembranosus* muscle	25	2 W/cm^2	NA	Ambient pressure	60 and 120	After cooking at 50°C, significantly lower hardness of ultrasound-treated samples than in untreated samples, whereas after cooking at 70°C, significantly higher hardness of ultrasound-treated samples than in untreated samples	Dolatowski et al. (2000)
Bovine *semitendinosus* and *longissimus* muscles	24	12 W/cm^2	Room temperature	Ambient pressure	0, 30, 60, 120, and 240	Significantly decreased in Warner–Bratzler shear force and hardness of ultrasound-treated meat	Jayasooriya et al. (2007)
Beef *semitendinosus* muscle	20	1.55 W/cm^2	4	Ambient pressure	Up to 14,400	No effect on meat tenderness	Pohlman et al. (1997b)

Table 22.1 (continued)

Food product	Treatment conditions					Effect of ultrasound	References
	Frequency (kHz)	Acoustic energy	Temperature (°C)	Pressure	Treatment time (s)		
Beef *longissimus thoracis and lumborum*, *semitendinosus*, and *biceps femoris*	30–47	0.29–0.62 W/cm^2	1–2	Ambient pressure	Up to 1,800	No effect on meat tenderness	Lyng et al. (1997)
Beef *longissimus thoracis and lumborum* and *semitendinosus*,	20	62 W/cm^2	15	Ambient pressure	Treated by ultrasound probe tip for 15-s periods	No effect on meat tenderness	Lyng et al. (1998)
Milk protein-based edible films	168, 520, and 860	1.90, 3.00, 3.35, and 5.22 W	NA	Ambient pressure	1,800 and 3,600	Higher tensile strength of edible films prepared with sonicated milk protein than that of control film	Banerjee et al. (1996)
Red bell pepper	47	NA	25, 35, 45, and 55	Ambient pressure	0–10,800	Rapid softening with ultrasound-assisted brining	Gabaldón-Leyva et al. (2007)

NA, not available

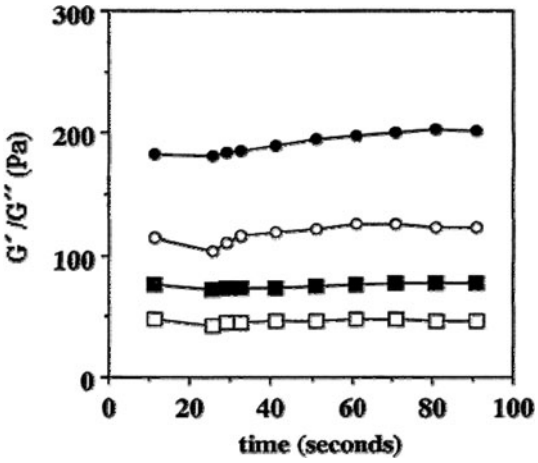

Fig. 22.1 Oscillation tests of MTS-treated (*filled symbols*) and control (*empty symbols*) yoghurts. Storage modulus, G' (*circles*). Loss modulus, G'' (*squares*). *Source*: Vercet et al. (2002a)

i.e., endopolygalacturonases and pectinmethylesterase, with manothermosonication (MTS) (Vercet et al., 2002b). Gülseren et al. (2007) noticed that ultrasound-treated BSA became more susceptible to heat denaturation. Sonication also increased the surface hydrophobicity and reduced the particle sizes of BSA. Denaturation of serum proteins, such as α-lactalbumin and β-lactoglobulin, was observed in milk treated by continuous thermosonication (Villamiel and De Jong, 2000). Some researchers have postulated that hydrophobic amino acid groups, which were originally located inside a protein, might have been exposed by a high level of denaturation or unfolding of the protein in ultrasound-treated samples (Iametti et al., 1996; Qi et al., 1997). The exposed hydrophobic amino acid groups might have induced aggregation of proteins, which finally yielded a stronger and firmer structure in yogurt made with the sonicated milk than in the control (Totosaus et al., 2002).

Tenderness is one of the most important quality aspects in cooked meat. Two primary muscle components that contribute to meat tenderness are myofibrillar protein and connective tissues such as collagen (Tarrant, 1998). Improved meat tenderness in ultrasound-assisted cooking was reported by Pohlman et al. (1996). Meat tenderness can also be improved by ultrasound before postmortem or aging processes (Dickens et al., 1991; Dolatowski et al., 2000; Jayasooriya et al., 2007; Pohlman et al., 1997a; Smith et al., 1991). Jayasooriya et al. (2004) proposed that proteolysis of myofibrillar protein was the major mechanism of meat tenderization. The enzymes responsible for the proteolysis of myofibrillar protein include calpains (calcium-activated proteinase) present in sarcoplasm and cathepsins (lysosomal cystein proteinase). Stangi and Bernard (1968) observed that an ultrasound treatment on rat and beef skeletal muscles caused a release of cathepsin and thus an increase in calpain activity in treated muscles. An enhanced postmortem proteolysis of ultrasound-treated lamb skeletal muscles was reported with a release of lysosomal enzymes found in treated lamb liver samples (Ronscale et al., 1992). Ultrasound treatment could also increase the activity of calpains by an increase of calcium

released from sarcoplasmic reticulum and/or cathepsins released from lysosomes (Ronscale et al., 1992). Got et al. (1999) treated beef *semimembranosus* muscles before the aging process with ultrasound and observed an immediate increase of calcium in the cytosol. The improved tenderness by an ultrasound treatment before postmortem or aging may thus be attributed to the release of calcium and cathepsin. During aging, a high degradation of myofibrillar protein in ultrasound-treated meat may also be accompanied by a high activity of calpains caused by released calcium and cathepsin. In the case of meat treated by ultrasound after postmortem or aging, and before cooking, disruption of muscle structures may play an important role in increased meat tenderness.

In contrast to the reports on improved tenderness of ultrasound-treated meats, several studies found that ultrasound has no effect on meat tenderness (Lyng et al., 1997, 1998; Pohlman et al., 1997b). The authors suggested that the low ultrasound intensity (UI) (0.29–1.55 W/cm^2) used in their studies might have been responsible for that result. It was noted that for those studies where improved meat tenderness was reported, the UIs were in the range of 22 and 2,400 W/cm^2 (Dickens et al., 1991; Pohlman et al., 1996, 1997a). The low acoustic energy input during a treatment could be insufficient to disrupt muscle structure and/or to release calcium and cathepsin. The different experimental conditions in ultrasound treatments may also play a role. For instance, Lyng et al. (1998) applied ultrasound to one side of the steak which had a thickness of 2.5 cm, but Jayasooriya et al. (2007) exposed both sides of their meat samples (0.2 cm thickness) to ultrasound by turning it over at half of the total treatment time. The thicker sample and one-side treatment may have prevented ultrasound from reaching the inside of the meat, rendering the treatment less effective.

In addition to traditional ultrasound treatments, hydrodynamic shock waves have also been used to tenderize meat. Hydrodynamic shock waves are generated by the explosion of a small amount of an explosive in a liquid medium (water). If an object submerged in water has an acoustic match with the water, the shock waves can pass through the object (Kolsky, 1980). Since meat compositionally contains approximately 75% water, it is easy to achieve a close acoustic match (Price and Schweigert, 1978). It has been reported that such shock waves cause disruption of myofibrillar structure and direct alteration of muscle proteins, resulting in meat tenderization (Zuckerman and Solomon, 1998). The hydrodynamic shock wave method has been proven effective in improving the tenderness of beef and other meat products (Callahan et al., 2006; Liu et al., 2006; Schilling et al., 2002; Solomon et al., 1997; Spanier and Romanowski, 2000).

Improved mechanical properties in edible films prepared using ultrasound-treated whey protein concentrate (WPC) and sodium caseinate (SC) were reported by Banerjee et al. (1996). The tensile strength of ultrasound-treated WPC and SC films was increased by up to 224%. A longer exposure time yielded a higher tensile strength at all acoustic energy levels. Transmission electron micrographs (TEMs) of ultrasound-treated WPC films showed a more orderly and condensed knit matrix of proteins, fat, and other components than that in the control. With the TEM observations, the authors also confirmed that the ultrasound treatment reduced the

particle size of milk components in the film solution. Increased molecular interactions may be induced due to smaller particle sizes, leading to a high level of molecular order (Banerjee et al., 1996). High chain order polymers can be related to the high cohesion in edible films (Gontard and Guilbert, 1994), which may contribute to the high film strength of ultrasound-treated WPC films.

In an ultrasound-assisted brine process, ultrasound showed a negative effect on the firmness of bell peppers (Gabaldón-Leyva et al., 2007). A rapid softening in ultrasound-treated samples occurred in 30 min, while the softening was not observed until 120 min for peppers from a brine process without ultrasound. It was reported that a thermal or physical treatment can cause losses in cell wall rigidity and intracellular adhesion, which could enhance water movement from tissue to brine (Heredia-Léon et al., 2004; Lazarides and Mavroudis, 1995). The combined action of ultrasound and thermal treatment thus would induce changes in bell pepper cells, causing a decrease in the firmness of the processed peppers.

3 Flavor

A limited number of reports have been published on flavor changes in ultrasound-treated food products, which include flavor improvement in Mahon cheese, generation of off-flavor in edible oil, and loss of active aroma compound in apple juice. The effect of ultrasound on flavor is directly related to the physical and chemical effects of cavitation. Until now, almost all the reports on flavor/aroma alterations caused by sonication have been experimental, with an emphasis on reporting findings rather than elucidating the mechanisms. Nevertheless, an effort is made in this section to summarize studies conducted on the impact of ultrasound on flavor changes in selected food products (Table 22.2).

An ultrasound-assisted brining process was used to prepare Mahon cheese, a noncooked pressed cheese salted in brine. During ripening, the acoustically brined cheese showed a higher concentration of free fatty acid (FFA), and more intense aroma and flavor than the conventionally brined counterpart (Sánchez et al., 2001a). In addition, the acoustically brined cheese had a higher level of total free amino acids (TFAAs) in all the stages of ripening than the conventionally brined counterpart (Sánchez et al., 2001b). It was proposed that the reduced fat globule sizes and sonication-induced protein denaturation might be responsible for the high FFA and TFAA in the cheese (Sánchez et al., 2001a, b). Villamiel and De Jong (2000) reported reduced fat globule sizes in milk after sonication at 20 kHz and 8 W/ml. Good homogenization was also observed in ultrasound-treated milk at 20 kHz and 3 W/ml (Wu et al., 2001). On the other hand, ultrasound treatment can denature whey protein in milk (Villamiel and De Jong, 2000), and the resulting denatured whey protein might be less resistant to proteolysis than the native whey protein during cheese ripening (Sánchez et al., 2001b). Mahon cheese is classified as a semisoft cheese, which is surface ripened with microflora (Scott, 1998). Normally, the surface-ripened soft cheese shows a high level of proteolysis and lipolysis on the external area or surface of the cheese (Gripon, 1997). Consequently, the Mahon

Table 22.2 Effect of ultrasound on flavor in food products

Sample	Treatment conditions					Effect of ultrasound	References
	Frequency (kHz)	Acoustic energy	Temperature (°C)	Pressure	Treatment time (s)		
Mahon cheese	30	NA	NA	Ambient pressure	NA	Higher level of total free fatty acids and aroma intensity in acoustically brined cheese than those in cheese brined by a conventional method	Sánchez et al. (2001a)
Mahon cheese	30	NA	NA	Ambient pressure	NA	Higher level of total free amino acids in acoustically brined cheese than that in a conventionally brined one	Sánchez et al. (2001b)
Emulsion	20, 47	NA	NA	Ambient pressure	NA	Metallic and rancid off-flavors in ultrasound-treated emulsion and sunflower oil	Chemat et al. (2004a)
Sunflower oil	20	1.5 W/ml	20	Ambient pressure	30–1,800	Rapid rate of primary oxidation, polymer formation, and off-flavor compounds in ultrasound-treated sunflower oil	Chemat et al. (2004b)

Table 22.2 (continued)

Sample	Treatment conditions					Effect of ultrasound	References
	Frequency (kHz)	Acoustic energy	Temperature (°C)	Pressure	Treatment time (s)		
Sunflower oil treated by ultrasonic cutting device	40	NA	NA	Ambient pressure	10	Fishy, rancid, and tallowy odors in sunflower oil treated by ultrasonic cutting device	Schneider et al. (2006)
Liposome	20	NA	In ice-salt bath	Ambient pressure	30–120	Lipid peroxidation in liposome prepared with phospholipids Hydroxyl radical (•OH) generated by ultrasound may initiate lipid peroxidation in liposome	Jana et al. (1986, 1990a, b)
Geosmin in purified water	200	NA	NA	Ambient pressure	0–3,600	Degradation of geosmin may be attributed to radical reaction with •OH	Yoo et al. (1995)
Volatile fatty acids in purified water	200	NA	NA	Ambient pressure	0–3,600	Degradation of volatile fatty acids may be attributed to radical reaction with OH	Yoo et al. (1997)

Table 22.2 (continued)

Sample	Treatment conditions					Effect of ultrasound	References
	Frequency (kHz)	Acoustic energy	Temperature (°C)	Pressure	Treatment time (s)		
Commercial apple juice	20	0.6 W/ml	60	Ambient pressure	252	99% reduction of 1-butanol-3-methyl acetate	Unpublished data
Rice wine	20	NA	20	Ambient pressure Closed system	NA	Decrease in off-flavors (acetaldehyde and polyols) and increase in pleasant flavor (ethyl acetate) in ultrasound-assisted aged rice wine	Chang and Chen (2002)
Maize wine	20	NA	20	Ambient pressure Closed system	NA	An increase in off-flavors (acetaldehyde and polyols) and a decrease in pleasant flavor (ethyl acetate) in ultrasound-assisted aged maize wine	Chang and Chen (2002) and Chang (2004)

NA, not available

cheese with small-sized fat globules and denatured surface proteins would have a high lipolytic and proteolytic activity during surface ripening and thus high levels of FFAs, TFFAs, and aroma intensity.

Free radicals produced by ultrasound in the aqueous phase may catalyze the degradation of flavor compounds (geosmin and volatile fatty acids) and the oxidation of sunflower oil to generate off-flavors (Chemat et al., 2004b; Yoo et al., 1995, 1997). It is known that sonolysis of water due to cavitation forms hydrogen ($H^{\bullet}$) and hydroxyl ($^{\bullet}OH$) radicals (Stanley et al., 2004). Yoo et al. (1995, 1997) proposed that the $H^{\bullet}$ and $^{\bullet}OH$ radicals generated by water sonolysis were mainly responsible for the degradation of geosmin and volatile fatty acids. A deterioration of sunflower oil was also found during emulsification by ultrasound, with oxidized volatile compounds produced from the oil (Chemat et al., 2004b). Hydroxyl radicals ($^{\bullet}OH$) were believed to initiate lipid peroxidation in liposome (Jana et al., 1986, 1990a, b). Since hydroperoxide can be produced by lipid peroxidation (Jana et al., 1986, 1990a, b), the homolysis of hydroperoxide would finally lead to the formation of off-flavors (Grosh, 1987). Sunflower oil directly treated by ultrasound also shows quality degradation as indicated by high peroxide values (Chemat et al., 2004a). Similar off-flavors were detected in sunflower oil treated by an ultrasonic cutting device (Schneider et al., 2006). The authors suggested that the off-flavors might be a result of oxidation of the sunflower oil catalyzed by the metallic part of the ultrasound horn (Chemat et al., 2004b). Additionally, metal ions, such as copper, that occur naturally in edible oil might be involved in cavitation-related reactions, which may also contribute to the formation of oxy radical species, thus inducing generation of volatile off-flavors (Chemat et al., 2004b).

In a study to treat commercial apple juice in an open system by thermosonication to achieve a 5-log reduction of *E. coli* K12 population, the concentration of 1-butanol-3-methyl acetate, a major active aroma compound in apple juice, was 6,071 ppb in untreated juice and was 502 and 40 ppb in thermal- and thermosonication-treated juice, respectively (unpublished data). The loss of 1-butanol-3-methyl acetate during sonication might have been caused by the degassing effect of ultrasound or by the physical (localized high temperature and pressure) or chemical (radical) reactions associated with cavitation. More studies are needed to ascertain the mechanism for the reduction of 1-butanol-3-methyl acetate in sonicated apple juice.

Ultrasound-assisted aging was applied to process rice and maize wines (Chang, 2004; Chang and Chen, 2002). The hypothesis was that localized high temperature and pressure generated by ultrasound might accelerate the aging process of wines and produce more flavor and taste. The wine was circulated through a 10 mm orifice atomizer where ultrasound treatment was applied up to 16 times. After treatment the concentration of acetaldehyde (unpleasant stingy flavor) decreased, and ethyl acetate (apple and/or fruit flavor) increased in the ultrasound-treated rice wine. Polyols in rice wine, causing a sense of greasy aftertaste in the mouth, were decreased by the ultrasound treatment (Chang and Chen, 2002). In contrast, the content of acetaldehyde in an aged maize wine following ultrasound treatment was higher than that of the conventionally aged maize wine. The polyols content in a maize wine aged with ultrasound was higher, whereas the concentration of ethyl acetate, a pleasant flavor

compound, in the ultrasound-aged maize wine was lower (Chang and Chen, 2002). It appears that ultrasound-assisted aging is appropriate only for certain wines and hence further research must be conducted to determine if ultrasound-assisted aging is appropriate for a specific wine.

4 Color

Color changes in a food product may affect the overall acceptability of the product for consumers. Several researchers have documented the effect of ultrasound on the color of liquid and solid food products, including milk, orange juice, apple cider, dehydrated rabbiteye blueberry, blanched watercress, and meat. Table 22.3 summarizes the reports on color changes of ultrasound-treated foods and experimental conditions used in the studies.

Nonenzymatic browning in milk model (0.1 M phosphate buffer, pH 6.6, 3% (w/v) sodium caseinate, and 2% (w/v) glucose) and fruit juice model (0.1 M citrate buffer, pH 3.5, and 12% (w/v) glucose) systems was studied with a continuous MTS system (Vercet et al., 2001). Brown pigments in MTS-treated milk model system increased with treatment time compared to heat-treated milk, which was probably caused by the Maillard reaction. Browning was also observed in MTS-treated artificial fruit juice. Due to the absence of amine groups in the juice, the authors suggested that a mechanism other than Maillard reaction may have played a role (Vercet et al., 2001). The ultrasound treatment of glucose in an aqueous phase could yield glucosyl radical and polymers in the presence of oxygen, which could contribute to the formation of browning pigments (Portenlänger and Heusinger, 1994; Vercet et al., 2001). In a nitrogen-protected MTS system, the browning index of MTS-treated orange juice was significantly lower than that treated by a commercial thermal method, but was significantly higher than that of raw juice (Lee et al., 2005). In a report by Valero et al. (2007), orange juice was sonicated by both batch and continuous systems. An increase in brown pigments in ultrasound-treated orange juice was observed only in the continuous system. Valero et al. (2007) attributed this result to greater exposure of the orange juice to oxygen in the continuous system.

In another color parameter, lightness was found to increase in ultrasound-treated liquid foods. For instance, orange juice sonicated with a continuous system showed an increase in lightness with treatment time (Zenker et al., 2003). The authors postulated that partial precipitation of suspended, insoluble particles in the juice probably contributed to the increase in lightness. In ultrasound-treated apple cider, the turbidity was significantly ($p < 0.05$) lower than that of untreated or thermally treated samples. Particle separation and reduction in particle sizes by ultrasound were suggested as the possible cause of the low turbidity (Ugarte-Romero et al., 2006). Less darkness was also observed in ultrasound-treated apple cider compared to the untreated counterpart. Since polyphenol oxidase (PPO) is known to promote browning or darkening in apple cider (Zárate-Rodríguez et al., 2000), the PPO inactivation plus removal of particulates by ultrasound may thus help to produce less dark colors in ultrasound-treated samples (Ugarte-Romero et al., 2006).

Table 22.3 Effect of ultrasound on color in food products

Food product	Treatment conditions					Effect of ultrasound	References
	Frequency (kHz)	Acoustic energy	Temperature (°C)	Pressure	Treatment time (s)		
Milk model (0.1 M phosphate buffer, pH 6.6, 3% (w/v) sodium caseinate, and 2% (w/v) glucose) and fruit juice model (0.1 M citrate buffer, pH 3.5, and 12% (w/v) glucose) systems	20	NA	69–111	200 kPa	300	Nonenzymatic browning in manothermosonicated milk model and fruit juice model systems	Vercet et al. (2001)
Orange juice	23 and 50	NA	NA	Ambient pressure	900 with batch system 10,800 with continuous system	Increase in brown pigments in ultrasound-treated orange juice with continuous system Increase in lightness of ultrasound-treated orange juice	Valero et al. (2007)
Orange juice	20	7.2, 15.4, and 17.6 W	75	Ambient pressure	1–30	Increase in lightness of ultrasound-treated orange juice	Zenker et al. (2003)

Table 22.3 (continued)

Food product	Treatment conditions					Effect of ultrasound	References
	Frequency (kHz)	Acoustic energy	Temperature (°C)	Pressure	Treatment time (s)		
Orange juice	20	NA	70	400 kPa	30	Higher browning index in continuous MTS-treated orange juice than in untreated juice	Lee et al. (2005)
Orange juice	20	NA	70	200 kPa	30	Higher browning index in orange juice treated by continuous MTS than in thermal-pasteurized orange juice or raw orange juice	Feng (2005)
Apple cider	20	0.46 W/ml	40 and 60	Ambient pressure	1,062 at 40°C 216 at 60°C	Less darkness and lower turbidity in ultrasound-treated apple cider than in untreated sample	Ugarte-Romero et al. (2006)
Rabbiteye blueberry	850	NA	21	Ambient pressure	3 h	Lighter, more reddish, and yellowish colors in dried blueberries 3 h pre-osmotic concentrated with ultrasound than in those 12 h-pre-osmotic concentrated without ultrasound	Stojanovic and Silva (2007)

Table 22.3 (continued)

Food product	Treatment conditions					Effect of ultrasound	References
	Frequency (kHz)	Acoustic energy	Temperature (°C)	Pressure	Treatment time (s)		
Watercress	20	1.25 W/ml	82.5, 85, 87.5, 90, and 92.5°C	Ambient pressure	0 up to 120	Darker and less yellow color in conventional and thermosonication blanched watercress Greener color in thermosonication blanched watercress than conventional blanched watercress	Cruz et al. (2007)
Beef *pectoralis* muscle	20	22 W/cm^2	4	Ambient pressure	300, 600	Lighter, less red, and more yellow color in ultrasound-treated meat than in untreated meat	Pohlman et al. (1997a)
Beef *semitendinosus* muscle	20	1.55 W/cm^2	4	Ambient pressure	1,800	No effect on meat color	Pohlman et al. (1997b)
Bovine *semitendinosus* and *longissimus* muscles	24	12 W/cm^2	Room temperature	Ambient pressure	0, 30, 60, 120, and 240	No effect on meat color	Jayasooriya et al. (2007)

NA, not available

Other ultrasound-assisted processes, such as osmotic dehydration and blanching, could also indirectly affect the color of processed fruits and vegetables. Dried rabbiteye blueberries processed by ultrasound-assisted osmotic dehydration exhibited more reddish and yellowish colors than those processed without ultrasound treatment (Stojanovic and Silva, 2007). Thermosonication used in the blanching of watercress resulted in darker and less yellowish colors than in raw watercress (Cruz et al., 2007). There was no significant ($p < 0.05$) difference in lightness and yellowish colors between conventional and thermosonication blanching. However, the thermosonication-blanched watercress showed a greener color than the conventionally blanched one. Compared to conventional blanching, the thermosonication blanching also developed green color at a higher rate. Ultrasonication may help to expel gases inside the intercellular space and enhance blanching medium transfer into the product due to enhanced mass transfer induced by ultrasound. As a result, the light refraction from the cell surface and hence the color perception of the product will be changed (Bower, 1992).

Ultrasound treatment has been reported to alter meat colors. One observation was that ultrasound-treated meat showed lighter, less red, and more yellow colors than untreated meat (Pohlman et al., 1997a). Since high-intensity ultrasound was reported to generate heat on meat surfaces (Dickens et al., 1991; Eggleton et al., 1965; Gersten, 1965), the color changes during sonication might be caused by thermal denaturation of myoglobin and hemoglobin pigments on product surfaces (Marten et al., 1982). In other reports, however, no color changes were found in ultrasound-treated meat products (Jayasooriya et al., 2007; Pohlman et al., 1997b). The low ultrasound intensity (UI) and short treatment times used in those studies might not allow any measurable changes in meat proteins and pigments. For example, in the study of Pohlman et al. (1997b), the UI was 1.55 W/cm^2, while that used by Pohlman et al. (1997a) was 22 W/cm^2. Jayasooriya et al. (2007) also used a relatively low UI (12 W/cm^2) and shorter treatment time (up to 240 s) than Pohlman et al. (1997a).

5 Nutrients

Interactions between ultrasound and chemical compounds in a food that provides nutritional values are complicated. Unfortunately, not much research has been conducted and reported to elucidate the underlying mechanisms for the observed reduction or enhancement in nutritional values after an ultrasound treatment and during storage. Therefore, this section is not aimed at drawing any conclusions about the effect of ultrasound on food nutrients. Instead, it only serves to report the limited findings documented in current publications. A summary of the studies dealing with the effect of ultrasound on nutrients is given in Table 22.4.

The release of anthocyanin and phenolics was reported for rabbiteye blueberries processed by ultrasound-assisted osmotic dehydration (Stojanovic and Silva, 2007). Anthocyanin and phenolics loss was higher after 3-h ultrasound-assisted osmotic dehydration than when treated by osmotic dehydration only. It was proposed that

Table 22.4 Effect of ultrasound on nutrients in food products

Food product	Treatment conditions					Effect of ultrasound	References
	Frequency (kHz)	Acoustic Energy	Temperature (°C)	Pressure	Treatment time (s)		
Anthocyanin and phenolics in rabbiteye blueberry	850	NA	21	Ambient pressure	3 h	Decrease in anthocyanin and phenolics in 3 h pre-osmotic concentrated with ultrasound treatment	Stojanovic and Silva (2007)
L-Ascorbic acid in distilled water	800	2 W/cm^2	NA	Ambient pressure	NA	Degradation of L-ascorbic acid initiated by H$^\bullet$ and $^\bullet$OH·generated by ultrasound	Portenlänger and Heusinger (1992)
(All-*E*)-astaxanthin in ethanol	25	20, 40, 60, 80, 100, and 120 W/ml	In ice bath	Ambient pressure	60, 120, 180, 240, 300, and 360 min	Decrease in concentration of (all-*E*)-astaxanthin with an increase in treatment time from 1 to 6 min At 2-min treatment, a linear decrease in the concentration of (all-*E*)-astaxanthin with an increase in power density	Zhao et al. (2006)

Table 22.4 (continued)

Food product	Treatment conditions					Effect of ultrasound	References
	Frequency (kHz)	Acoustic Energy	Temperature (°C)	Pressure	Treatment time (s)		
Milk and orange juice	20	NA[a]	62	200 kPa	15 and 30	No effect of MTS on contents of thiamin and riboflavin in milk Around 10% loss of ascorbic acid and carotenoids in MTS orange juice	Vercet et al. (2001)
Orange juice	20	7.2, 15.4, and 17.6 W	75	Ambient pressure	1–30	After 35-day storage, lower degradation of ascorbic acid in thermosonicated orange juice than in thermally treated juice	Zenker et al. (2002)
Orange juice	20	NA	70	400 kPa	30	After storage at 4ºC for 45 days, higher retention of ascorbic acid in continuous MTS-treated orange juice than in thermal-pasteurized juice	Lee et al. (2005)
Orange juice	20	NA	70	200 kPa	30	In two of six storage tests at 4ºC for 90 days, higher retention of ascorbic acid in continuous MTS-treated orange juice than in thermal-pasteurized juice	Feng (2005)

NA, not available

the surface cell rupture caused by cavitation might contribute to the release of anthocyanin and phenolics in berry samples (Stojanovic and Silva, 2007). In addition, the final product, dried blueberries, was found to retain higher anthocyanin and phenolics in ultrasound-treated samples compared to those dried with conventional osmotic dehydration.

It was reported that L-ascorbic acid in distilled water was degraded by ultrasound treatment, possibly due to the generation of $H^{\bullet}$ and $^{\bullet}OH$ radicals (Portenlänger and Heusinger, 1992). Degradation of (all-*E*)-astaxanthin, a carotenoid, in ethanol by ultrasound treatment was also reported (Zhao et al., 2006). Degradation of oxidation-sensitive nutrients, such as thiamin and riboflavin in milk, as well as ascorbic acid and carotenoids in orange juice, was analyzed after a continuous MTS treatment (Vercet et al., 2001). The MTS treatment showed no effect on the concentration of thiamin and riboflavin in milk. In contrast, the contents of ascorbic acid and carotenoids in orange juice decreased by around 10% after the MTS treatment.

Zenker et al. (2003) observed that ascorbic acid concentration in thermally treated orange juice was slightly higher than in thermosonication-treated juice immediately after the treatment. Similar results were reported by Lee et al. (2005) in which the ascorbic acid concentration in MTS-treated orange juice was lower than that in thermally pasteurized juice (Lee et al., 2005). Interestingly, during storage, ascorbic acid retention in ultrasound-treated orange juice could be better than that in a thermally processed juice. In Zenker et al.'s report (2003), the loss of ascorbic acid in thermal-treated orange juice was faster than that in ultrasound-treated juice, ultimately resulting in higher ascorbic acid content in ultrasound-treated orange juice after 35-day storage. Lee et al. (2005) also found a higher retention of ascorbic acid in MTS-treated orange juice than in thermally processed juice after 63-day storage

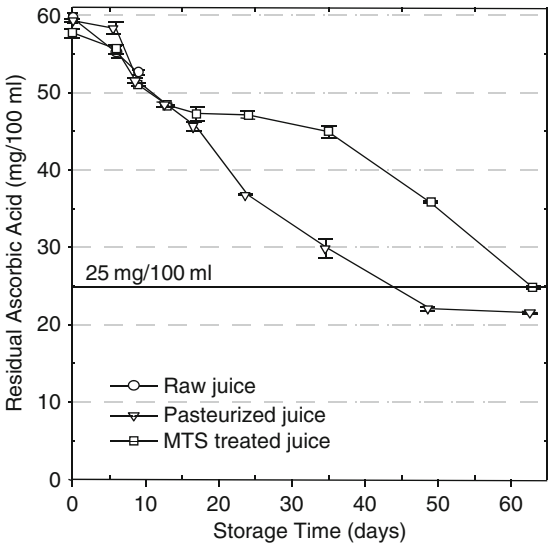

Fig. 22.2 Changes in ascorbic acid concentration in orange juice for samples treated with different methods during storage at 4°C. *Source*: Lee et al. (2005)

(Fig. 22.2). The lower degradation of ascorbic acid in thermosonicated orange juice was attributed to degassing of juice by ultrasound (Zenker et al., 2003). Dissolved gases, including oxygen, can act as nuclei to form bubbles, which could float to the surface and be removed from the juice. This degassing effect could lower the dissolved oxygen level in the juice and hence reduce oxidative degradation of ascorbic acid during storage. In another study (Feng, 2005), improvement in ascorbic acid retention of MTS-treated juice was observed in two out of six storage tests. The dissolved oxygen levels in MTS- and thermal-pasteurized orange juice were about same during storage, and oxygen levels became negligible after 50 days. There might be factors other than dissolved oxygen that contribute to degradation reactions in juice. It has been found that during MTS treatment, due to strong cavitation activities, some metal ions, including iron, manganese, and nickel, were released from the metal container wall. These metal ions may function as catalysts to speed up some degradation reactions. More studies are needed to better understand the degradation reactions in ultrasound treatment of juice products.

References

Banerjee, R., Chen, H., and Wu, J. (1996). Milk protein-based edible film mechanical strength changes due to ultrasound process. *Journal of Food Science*, 61, 824–828.

Bower, J. (1992). *Food theory and application*. New York, NY, Macmillan.

Callahan, J. A., Berry, B. W., Solomon, M. B., and Liu, M. N. (2006). Hydrodynamic pressure-processed beef *semitendinosus* muscle using a steel reflector bowl. *Journal of Muscle Foods*, 17, 105–113.

Chang, A. C. (2004). The effects of different accelerating techniques on maize wine maturation. *Food Chemistry*, 86, 61–68.

Chang, A. C., and Chen, F. C. (2002). The application of 20 kHz ultrasonic wave to accelerate the aging of difference wines. *Food Chemistry*, 79, 501–506.

Chemat, F., Grondin, I., Costes, P., Moutoussamy, A., Shum Cheong Sing, A., and Smadja, J. (2004a). High power ultrasound effects on lipid oxidation of refined sunflower oil. *Ultrasonics Sonochemistry*, 11, 281–285.

Chemat, F., Grondin, I., Shum Cheong Sing, A., and Smadja, J. (2004b). Deterioration of edible oils during food processing by ultrasound. *Ultrasonic Sonochemistry*, 11, 13–15.

Cruz, R. M. S., Vieira, M. C., and Silvia, C. L. M. (2007). Modelling kinetics of watercress (*Nasturtium officinale*) color changes due to heat and thermosonication treatments. *Innovative Food Science and Emerging Technologies*, 8, 244–252.

Dickens, J. A., Lyon, C. E., and Wilson, R. L. (1991). Effect of ultrasonic radiation and some physical characteristics of broiler breast muscle and cooked meat. *Poultry Science*, 70, 389–396.

Dolatowski, Z., Stasiak, D. M., and Latoch, A. (2000). Effect of ultrasound processing of meat before freezing on its texture after thawing. *Electronic Journal of Polish Agricultural Universities. Agricultural Engineering*, 3(2). Available online http://www.ejpau.media.pl/series/volume3/issue2/engineering/art-02.html. Accessed on April 9, 2007.

Eggleton, R. C., Kelly, E., Fry, F. J., Chalmer, R., and Fry, W. J. (1965). In: Kelly, E. (ed.), *Ultrasonic energy*, pp. 117–136. Urbana, IL, University of Illinois Press.

Feng, H. (2005). *Manothermosonication for Dual-Inactivation of Thermoresistant Pectin-Methyl-Esterase and Acid Tolerant Foodborne Pathogens in Orange Juice*. CAPPS Project Final Report.

Gabaldón-Leyva, C. A., Quintero-Ramos, A., Barnard, J., Balandrán-Quintana, R. R., Talamás-Abbud, R. T., and Jiménez-Castro, J. (2007). Effect of ultrasound on the mass transfer and physical changes in brine bell pepper at different temperature. *Journal of Food Engineering*, 81, 374–379.

Gersten, J. W., and Kelly E. (ed.). (1965). *Ultrasonic energy*. Urbana, IL, University of Illinois Press.

Gontard, N., and Guilbert, S. (1994). Bio-packaging: Technology and properties of edible and/or biodegradable material of agricultural origin. In: Mathlouthi, M. (ed.), *Food packaging and preservation*, pp. 159–181. Glasgow, UK, Blackie Academic and Professional.

Got, F., Culioli, J., Berge, P., Vignon, X., Astruc, T., Quideau, J. M., and Lethiecq, M. (1999). Effects of high-intensity ultrasound on ageing rate, ultrastructural and some physico-chemical properties of beef. *Meat Science*, 51, 35–42.

Gripon, J.-C. (1997). Flavor and texture in soft cheese. In: Law, B. A. (ed.), *Microbiology and biochemistry of cheese and fermented milk*, pp. 193–206. London, UK, Blackie Academic and Professional.

Grosh, W. (1987). Reactions of hydroperoxide-products of low molecules. In: Chan, H. W. S. (ed.), *Autoxidation of unsaturated lipids*, pp. 95–139. Orlando FL, Academic.

Gülseren, İ., Güzey, D., Bruce, B. D., and Weiss, J. (2007). Structural and functional changes in ultrasonicated bovine serum albumin solutions. *Ultrasonics Sonochemistry*, 14, 173–183.

Heredia-Léon, J. C., Talamás-Abbud, R., Mendoza-Guzmán, V., Solís-Martínez, F., Jimenez-Castro, J., and Barnard, J. (2004). Structural and physical properties of dried Ananheim chilli peppers modified by low-temperature blanching. *Journal of the Science of Food and Agriculture*, 84, 59–65.

Iametti, S., De Gregori, B., Vecchio, G., and Bonomi, F. (1996). Modifications occur at different structural levels during heat denaturation of β-lactoglobulin. *European Journal of Biochemistry*, 237, 106–112.

Jana, A. K., Agarwal, S., and Chatterjee, S. N. (1986). Ultrasonic radiation induced lipid peroxidation in liposomal membrane. *Radiation and Environmental Biophysics*, 25, 309–314.

Jana, A. K., Agarwal, S., and Chatterjee, S. N. (1990a). The induction of lipid peroxidation in liposomal membrane by ultrasound and the role of hydroxyl radicals. *Radiation Research*, 124, 7–14.

Jana, A. K., Agarwal, S., and Chatterjee, S. N. (1990b). Membrane lipid peroxidation by ultrasound: Mechanism and implication. *Journal of Biophysics*, 15, 211–215.

Jayasooriya, S. D., Bhandari, B. R., Torley, P. J., and D'Arcy, B. R. (2004). Effect of high power ultrasound wave on properties of meat: A review. *International Journal of Food Properties*, 7, 301–319.

Jayasooriya, S. D., Torley, P. J., D'Arcy, B. R., and Bhandari, B. R. (2007). Effect of high power ultrasound and ageing on the physical properties of bovine *Semitendinosus* and *Longissimus* muscles. *Meat Science*, 75, 628–639.

Kolsky, K. (1980). *Stress wave in solids*. New York, NY, Dover.

Lazarides, H. N., and Mavroudis, N. E. (1995). Mass transfer kinetics during osmotic preconcentration aiming at minimal solid uptake. *Journal of Food Engineering*, 25, 151–166.

Lee, J. W., Feng, H., and Kushad, M. M. (2005). *Effect of manothermosonication on quality of orange juice*. Cincinnati, OH, AIChE 2005 Annual Meeting.

Liu, M. N., Solomon, M. B., Vinyard, B., Callahan, J. A., Patel, J. R., West, R. L., and Chase, C. C., Jr. (2006). Use of hydrodynamic pressure processing and blade tenderization to tenderize top rounds from Brahman cattle. *Journal of Muscle Foods*, 17, 79–91.

Lyng, J. G., Allen, P., and McKenna, B. M. (1997). The influence of high intensity ultrasound baths on aspects of beef tenderness. *Journal of Meat Science*, 8, 237–249.

Lyng, J. G., Allen, P., and McKenna, B. M. (1998). The effect on aspects of beef tenderness of pre- and post-rigor exposure to a high intensity ultrasound probe. *Journal of the Science of Food and Agriculture*, 78, 308–314.

Marten, H., Stabursvik, E., and Marten, M. (1982). Texture and color changes in meat during cooking related thermal denaturation of muscle proteins. *Journal of Texture Studies*, 13, 291–309.

Pohlman, F. W., Dickeman, M. E., and Kropf, D. H. (1997a). Effects of high intensity ultrasound treatment, storage, time and cooking method on shear, sensory, instrumental color and cooking properties of packaged and unpackaged beef *Pectoralis* muscle. *Meat Science*, 46, 89–100.

Pohlman, F. W., Dickeman, M. E., Zayas, J. F., and Unruh, J. A. (1996). Effects of ultrasound and convection cooking to different end point temperatures on cooking characteristics, shear force and sensory properties, composition, and microscopic morphology of beef *Longissimus* and *Pectoralis* muscle. *Journal of Animal Science*, 75, 386–401.

Pohlman, F. W., Dickeman, M. E., and Zayas, J. F. (1997b). The effect of low-intensity ultrasound treatment on shear properties, color stability and shelf-life of vacuum-packed beef *Semitendinosus* and *bicep femoris* muscle. *Meat Science*, 45, 329–337.

Portenlänger, G., and Heusinger, H. (1992). Chemical reactions induced by ultrasound and γ-rays in aqueous solutions of L-ascorbic acid. *Carbohydrate Research*, 232, 291–301.

Portenlänger, G., and Heusinger, H. (1994). Polymer formation from aqueous solutions of α-D-glucose by ultrasound and γ-rays. *Ultrasonic Sonochemistry*, 1, 125–129.

Price, J. F., and Schweigert, B. S. (1978). *The science of meat and meat products*. Westport, CT, Food and Nutrition.

Qi, X. L., Holt, C., McNulty, D., Clarke, D. T., Brownlow, S., and Jones, G. R. (1997). Effect of temperature on the secondary structure of β-lactoglobulin at pH 6.7, as determined by CD and IR spectroscopy: A test of the molten globule hypothesis. *Biochemical Journal*, 324, 341–346.

Raviyan, P., Zhang, Z., and Feng, H. (2005). Ultrasonication for tomato pectinmethylesterase inactivation: Effect of cavitation intensity and temperature on inactivation, *Journal of Food Engineering*, 70, 189–196.

Ronscale, P., Ceña, P., Beltran, J. A., and Jaime, I. (1992). Ultrasonication of lamb skeletal muscle fibers enhances post-mortem proteolysis. In *Proceedings 38th International Congress of Meat Science and Technology*, pp. 411–414. Clermont, France.

Sánchez, E. S., Simal, S., Femenia, A., Benedito, J., and Rosselló, C. (2001a). Effect of acoustic brining on lipolysis and on sensory characteristics of Mahon cheese. *Journal of Food Science*, 66, 892–896.

Sánchez, E. S., Simal, S., Femenia, A., Llull, P., and Rosselló, C. (2001b). Proteolysis of Mahon cheese as affected by acoustic-assisted brining. *European Food Research Technology*, 212, 147–152.

Schilling, M. W., Claus, J. R., Marriott, N. G., Solomon, M. B., Eigel, W. N., and Wang, H. (2002). No effect of hydrodynamic shock wave on protein functionality of beef muscle. *Journal of Food Science*, 67, 335–340.

Schneider, Y., Zahn, S., Hofmann, J., Wecks, M., and Rohm, H. (2006). Acoustic cavitation by ultrasonic cutting device: A preliminary study. *Ultrasonic Sonochemistry*, 13, 117–120.

Scott, R. (1998). *Cheesemaking Practice*. Maryland, Aspen.

Smith, N. B., Cannon, J. E., Novakofski, J. E., McKeith, F. K., and O'Brien, W. D., Jr. (1991). Tenderization of *Semitendinosus* muscle using high intensity ultrasound. *IEEE Ultrasonics Symposium*, 1371–1374.

Solomon, M. B., Long, J. B., and Eastridge, J. S. (1997). The hydrodyne: A new process to improve beef tenderness. *Journal of Animal Science*, 75, 1534–1537.

Spanier, A. M., and Romanowski, R. D. (2000). A potential index for assessing the tenderness of hydrodynamic pressure (HDP)-treated beef strip loins. *Meat Science*, 56, 193–202.

Stangi, N., and Bernard, B. (1968). Lysosomal enzyme activity in rat and beef skeletal muscle. *Biochimica Et Biophysica Acta*, 170, 129–139.

Stanley, K. D., Golden, D. A., Williams, R. C., and Weiss, J. (2004). Inactivation of *Escherichia coli* O157:H7 by high-intensity ultrasonication in the presence of salts. *Foodborne Pathogens and Disease*, 1, 267–280.

Stojanovic, J., and Silva, J. L. (2007). Influence of osmotic concentration, continuous high frequency ultrasound and dehydration on antioxidants, color and chemical properties of rabbiteye blueberries. *Food Chemistry*, 101, 898–906.

Tarrant, P. V. (1998). Some recent advances and future properties in research for the meat industry. *Meat Science*, 49, S1–S16.

Totosaus, A., Montejan, J. G., Salazar, J. A., and Guerrero, I. (2002). A review of physical and chemical protein-gel induction. *International Journal of Food Science and Technology*, 37, 589–601.

Ugarte-Romero, E., Feng, H., Martin, S. E., Cadwallader, K. R., and Robinson, S. J. (2006). Inactivation of Escherichia coli with power ultrasound in apple cider. *Journal of Food Science*, 71, E102–E108.

Valero, M., Recrosio, N., Saura, D., Muñoz, N., Martí, N., and Lizama, V. (2007). Effects of ultrasonic treatments in orange juice processing. *Journal of Food Engineering*, 80, 509–516.

Vercet, A., Burgos, J., and Lopez-Buesa, P. (2001). Manothermosonication of foods and food-resembling system: Effect on nutrient content and nonenzymatic browning. *Journal of Agricultural and Food Chemistry*, 49, 483–489.

Vercet, A., Oria, R., Marquina, P., Crelier, S., and Lopez-Buesa, P. (2002a). Rheological properties of yogurt made with milk submitted to manothermosonication. *Journal of Agricultural and Food Chemistry*, 50, 6165–6171.

Vercet, A., Sánchez, C., Burgos, J., Montañés, L., and Buesa, P. L. (2002b). The effects of manothermosonication on tomato pectic enzymes and tomato paste rheological properties. *Journal of Food Engineering*, 53, 273–278.

Villamiel, M., and De Jong, P. (2000). Influence of high-intensity ultrasound and heat treatment in continuous flow on fat, proteins, and native enzyme of milk. *Journal of Agricultural and Food Chemistry*, 48, 472–478.

Wu, H., Hulbert, G. J., and Mount, J. R. (2001). Effects of ultrasound on milk homogenization and fermentation with yogurt starter. *Innovative Food Science and Emerging Technologies*, 1, 211–218.

Yoo, Y., Takenaka, N., Bandow, H., Nagata, Y., and Maeda, Y. (1995). Decomposition of geosimin in aqueous solution by sonication. *Chemistry Letter*, 24, 961–962.

Yoo, Y., Takenaka, N., Bandow, H., Nagata, Y., and Maeda, Y. (1997). Characteristics of volatile fatty acids degradation in aqueous solution by the action of ultrasound. *Water Research*, 31, 1532–1535.

Zárate-Rodríguez, E., Ortega-Rivas, E., and Barbosa-Cánovas, G. V. (2000). Quality changes in apple cider as related to nonthermal processing. *Journal of Food Quality*, 23, 337–349.

Zenker, M., Heinz, V., and Knorr, D. (2003). Application of ultrasound-assisted thermal processing for preservative and quality retention of liquid foods. *Journal of Food Protection*, 66, 1642–1649.

Zhao, L., Zhao, G., Chen, F., Wang, Z., Wu, J., and Hu, X. (2006). Different effects of microwave and ultrasound on the stability of (all-E)-astaxanthin. *Journal of Agricultural and Food Chemistry*, 54, 8346–8351.

Zuckerman, H., and Solomon, M. B. (1998). Ultrastructural changes in bovine *longissimus* muscle caused by the hydrodyne process. *Journal of Muscle Foods*, 9, 419–426.

Chapter 23
Ultrasonic Membrane Processing

Sandra Kentish and Muthupandian Ashokkumar

1 Introduction

A membrane is a semipermeable material that permits the passage of some molecules while retaining others. The membrane can discriminate between species based on their size, concentration, or electrical charge.

Membranes are widely used throughout the food and bioprocessing industries for both separation and concentration purposes. Specific applications include

- microfiltration of milk to concentrate caseins (Le Berre and Daufin, 1994, 1996, 1998),
- microfiltration of fermentation broths and milk products to retain bacteria and spores (Krstic et al. 2001),
- ultrafiltration of dairy whey and skim milk to concentrate solids prior to spray drying (De Boer and Hiddink, 1980; De Boer et al., 1977; Renner, 1984),
- membrane bioreactors for cell culture (Drioli and De Bartolo, 2006) and enzymatic fermentation (Prazeres and Cabral, 1994; Rios et al., 2004),
- concentration of flavors and colors (Babu et al., 2006; Rodrigues et al., 2004),
- membrane affinity methods for protein separation (Charcosset, 1998; Klein, 2000; Zou et al., 2001),
- reverse osmosis to produce purified water for specialized bioprocesses and for steam generation (Noble and Stern, 1995),
- emulsification (Joscelyne and Tragardh, 2000), and
- clarification of beers and fruit juices (Cassano et al., 2003; Gan et al., 1999; Vaillant et al., 2005).

Ceramic membranes are generally provided as tubes or flat discs. Conversely, polymeric membranes may be supplied in a spiral wound format or as hollow

S. Kentish (✉)
Department of Chemical and Biomolecular Engineering, Particulate Fluids Processing Centre, University of Melbourne, Melbourne, VIC 3010, Australia
e-mail: sandraek@unimelb.edu.au

H. Feng et al. (eds.), *Ultrasound Technologies for Food and Bioprocessing*, Food Engineering Series, DOI 10.1007/978-1-4419-7472-3_23,
© Springer Science+Business Media, LLC 2011

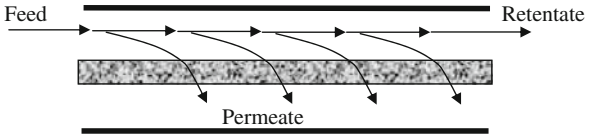

Fig. 23.1 Basic overview of membrane operation

fibers. In all cases, the processing fluid flows tangentially to the membrane surface (Fig. 23.1).

1.1 Concentration Polarization and Membrane Fouling

It is a natural outcome of membrane operation that retained solutes will tend to accumulate near the surface of the membrane, while permeating species are depleted. This is known as *concentration polarization* (Fig. 23.2). The reduced concentration of the permeating species at the membrane surface leads to a reduction in flow through the membrane and thus ultimately restricts membrane performance.

In some cases, the concentration of retained solutes increases to a point where precipitation occurs. Alternatively, the feed solution may contain suspended solids that precipitate continuously. These solids accumulate at the membrane surface. Initially, they will act to partially cover the membrane pores and may also enter the pore structure. This is known as *pore blockage*. Further precipitation leads to *cake formation.* This is a buildup of a layer of precipitated or suspended solids at the membrane surface, which further restricts flow through the membrane and thus further reduces the ability of the membrane to operate.

If the driving force for flow through a membrane is a pressure difference (ΔP), then this flow is described by the following expression:

$$J = \frac{\Delta P - \Delta \pi}{\mu R} \tag{23.1}$$

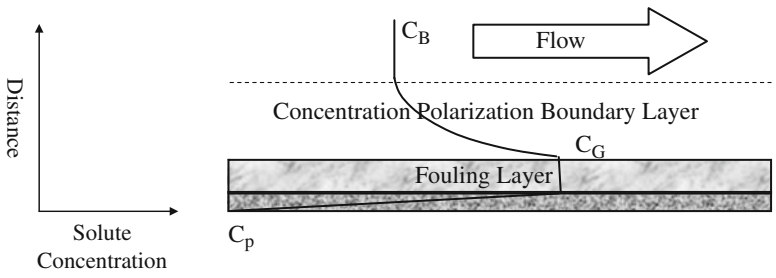

Fig. 23.2 Schematic of membrane fouling. The concentration of the retained species varies from a bulk value in the feed (C_B) to a permeate concentration (C_P). The concentration at the surface of the fouling layer is known as the gel concentration (C_G)

where J is the flow of permeate per unit area, usually referred to as the membrane flux and with units of l/m^2/h; μ is the viscosity of the fluid; and R is the resistance to flow. $\Delta\pi$ represents the difference in osmotic pressure between the two sides of the membrane. Comparable expression can be developed for membrane operations where concentration or electrical potential drives the separation (Noble and Stern, 1995).

The resistance to flow (R) is composed of several parts, i.e., the resistance provided by the membrane itself (R_m), the resistance provided by the cake layer (R_p), and the resistance provided by concentration polarization (R_c) so that

$$R = R_m + R_\mathrm{p} + R_c \tag{23.2}$$

The resistance provided by concentration polarization is often expressed in terms of a mass transfer coefficient, k. In this case, a more appropriate expression for the flux is

$$J = k \ln \frac{C_\mathrm{G}}{C_\mathrm{B}} \tag{23.3}$$

where C_G is the concentration at the surface of the cake layer and C_B is the concentration in the bulk feed solution.

2 Ultrasonic Flux Enhancement

The principle application of ultrasound to membrane processing is to enhance the membrane flux (J) by reducing the impact of the various resistance terms (R) as described above. Flux enhancements between 40 and 800% have been reported (Ahner et al., 1993; Narayan et al., 2002; Teng et al., 2006a, b; Zhu and Liu, 2000).

There are several specific effects of ultrasonic irradiation that can be implicated in this flux enhancement:

(a) The asymmetric collapse of cavitating bubbles can scour the surfaces and this leads to removal or control of the fouling cake layer (Chen et al., 2006a, b, c; Duriyabunleng et al., 2001; Kobayashi and Hosaka, 2003; Latt et al., 2004; Matsumoto et al., 1996). This surface action can also dislodge particles attached to the surface and break down large aggregates into smaller particles (Hagenson and Doraiswamy, 1997; Kost and Langer, 1988; Zhu and Liu, 2000).

(b) Acoustic streaming and/or cavitation causes turbulence, which results in bulk water movement near the membrane surface. This reduces the effects of concentration polarization and thus increases the mass transfer coefficient at the membrane surface (Ahner et al., 1993; Chai et al., 1998; Kobayashi et al., 1999; Kokugan et al., 1995; Muthukumaran et al., 2005a; Simon et al., 2000). Muthukumaran et al. (2005a) found that the mass transfer coefficient (k) increased from 9 to 16 $\times$ 10^{-7} m/s when ultrasound was applied. Similarly,

Simon et al. (2000) found that ultrasound was effective in disrupting the concentration polarized layer.

(c) The added turbulence can lead to a looser, more porous fouling cake layer (Kokugan et al., 1995; Muthukumaran et al., 2005a). The use of ultrasound acts to lower the compressibility of both the initial fouling deposit and the growing cake. In a similar manner, the turbulence associated with ultrasound separates physical aggregates by disrupting the intermolecular forces (Kost and Langer, 1988).

(d) There is evidence that sonication can cause agglomeration of fine particles and thus could potentially reduce pore blockage and cake compaction (Matsumoto et al., 1996). However, both Kokugan et al. (1995) and Muthukumaran et al. (2005a) show that ultrasound is not effective in reducing pore blockage by such mechanisms.

Kobayashi et al. (1999) found that the highest permeate flux in an ultrafiltration application was obtained when the sonication was directed to the retentate side of the membrane. Conversely, Kylloenen et al. (2006) obtained a higher flux when irradiating from the permeate side in a microfiltration experiment. These authors (Kylloenen et al., 2005) argue that when pore sizes are relatively small, sonication is most effective on the retentate side as cake formation is reduced, whereas for larger pore sizes, permeate side irradiation acts as a backflushing mechanism, reversing flow through the pores.

2.1 The Effects of Ultrasonic Intensity

Ultrasonic intensity can be increased by either increasing the applied power or reducing the frequency. Power densities between 0.05 (Muthukumaran et al., 2007) and 83 W/cm^2 have been reported (Li et al., 2002), with frequencies between 1 MHz (Lamminen et al., 2004) and 20 kHz (Chen et al., 2006a). Most workers note that the flux enhancement improves as ultrasonic intensity increases (Kylloenen et al., 2006; Muthukumaran et al., 2007).

At low ultrasonic intensities, that is, at either low power densities or high frequencies, the flux enhancement principally arises through acoustic streaming effects. Thus, Muthukumaran et al. (2005a), working at about 0.05 W/cm^2 and 50 kHz, found that the main mechanisms involved in flux enhancement were due to acoustic streaming. However, as the acoustic intensity increases, either through a lowering of ultrasonic frequency or through an increase in power, bubbles begin to form through the process known as acoustic cavitation. Thus, Lamminen et al. (2004) found that at 0.2–0.5 W/cm^2 and 205–620 kHz, particles were loosened from the membrane surface by cavitational mechanisms (microstreaming and microjets), although acoustic streaming assisted in the movement of particles away from the surface (see Fig. 23.3). Latt et al. (2004), working at 28 kHz and comparable power

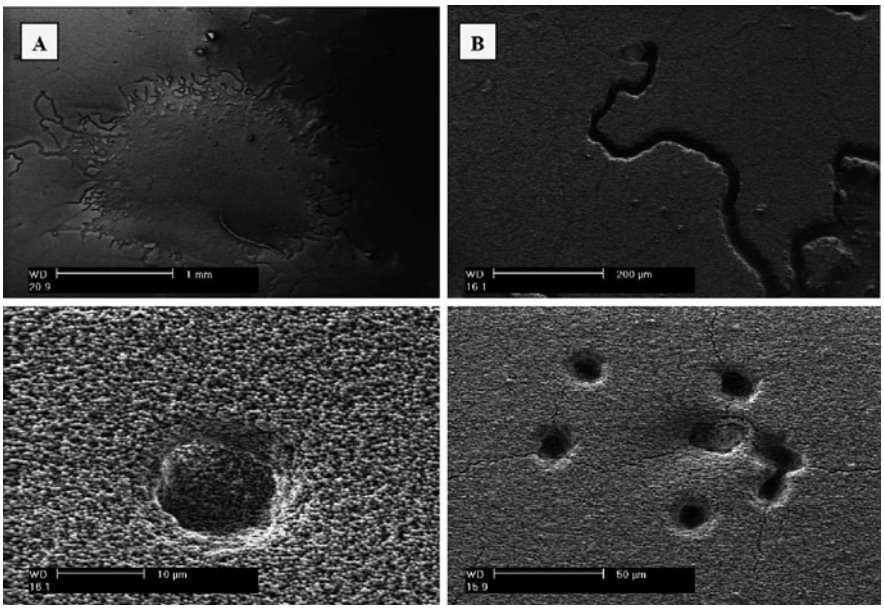

Fig. 23.3 Scanning electron microscope (SEM) images of circular patches of cake layer removal and channel-like formations along the edges of the circular patches attributed to microstreaming/microstreamers: (**a**) 620 kHz for 5 s, 0.21 W/cm^2; (**b**) 620 kHz for 5 s, 0.12 W/cm^2, SEM images showing evidence of microjet impacts on the surface of the cake layer; (**c**) 1062 kHz for 5 s, 0.21 W/cm^2; (**d**) 620 kHz for 5 s, 0.12 W/cm^2 (reproduced from Lamminen et al., 2004)

densities, concluded that violent collapse of cavity bubbles was the source of enhanced permeability.

In general, increases in acoustic intensity result in an increase in the number of bubbles formed (Sivakumar and Pandit, 2001) and increase the size of the cavitation zone (Suslick, 1988). However, cavitation efficiency increases with increasing power only up to a critical power level. Further increase beyond this critical power level can result in a decrease in cavitational activity (Thompson and Doraiswamy, 1999). A possible explanation for the observed decrease at high power is the formation of a cluster of bubbles due to Bjerknes forces (Leighton, 1994). This clustering shields the inner bubbles from the transmission of acoustic energy.

The optimization of ultrasonic intensity is important for a number of other reasons. The use of high ultrasonic intensities has the potential to lead to changes in the feed solution itself. Chai et al. (1998) reported that there was a slight change in the gel permeation chromatograms of dextran molecular size before and after sonication, when the solution was directly exposed to ultrasonic irradiation of 248 W for 30 min. However, they found no changes in the dextran molecular size when the dextran solution was exposed through a crossflow ultrafiltration cell and suggested that this may be due to the shielding of ultrasonic power by the ultrafiltration module. Residence times would also be much shorter in a crossflow unit. Villamiel and

De Jong (2000) found some evidence for the denaturation of whey proteins when sonication was performed at temperatures in excess of 60°C.

Some researchers have also found that if membranes are used at higher power levels, membrane damage may occur (Juang and Lin, 2004). In the study of Wang et al. (2005) polymeric membranes were immersed in an ultrasonic bath at 40 kHz and 1–4 W/cm^2. They reported the formation of large cracks resulting from the interconnection of neighboring large pores. Similarly, Masselin et al. (2001) indicated that polyethersulfone membranes could be damaged after as few as 5-min exposure at 47 kHz. The ultrasonic power intensity in this work is not reported. While working at 3.8 W/cm^2 and 20 kHz Chen et al. (2006a) observed pitting and cracking of ceramic membrane material if the acoustic irradiation was within the cavitation region. Other researchers have found no evidence of membrane damage, but those researchers typically work at lower ultrasonic intensity levels (Chai et al., 1998; Lamminen et al., 2004; Muthukumaran et al., 2004).

Membrane damage will lead to a reduction in membrane life and this is likely to have a significant impact on the economic viability of the process. Similarly, the capital costs of transducers and the operating costs arising from operating at higher power levels can make such an operation economically unfeasible. A careful balance is required between the positive effects of ultrasound on system performance and the negative effects of capital and electricity expenses.

Many researchers have considered the use of intermittent or pulsed ultrasound to mitigate the potentially high energy consumption (Chen et al., 2006a; Matsumoto et al., 1996; Muthukumaran et al., 2007; Simon et al., 2000; Yuk and Youm, 2003). Yuk and Youm (2003) observed that intermittent ultrasound was very effective in maintaining the high flux and high permeability of BSA during crossflow ultrafiltration. Similarly, Matsumoto et al. (1996) found that alternate operation of an ultrasonic generator and the feed pump was effective in removing BSA fouling layers from a membrane during crossflow microfiltration. However, Chen et al. (2006a) argued that the relative permeate flux improvement decreased with long pulse intervals of ultrasound and only approached that of continuous sonication when the pulse interval was short (1.0 s on/0.1 s off). This is consistent with our own results (Muthukumaran et al., 2007) and those of Simon et al. (2000), which show very little flux enhancement when the pulse interval was of the order of minutes.

It is common in the food industry to operate a sequence of membrane modules in series, with the concentration of solids increasing across the system. In this instance, it may also be optimal to provide ultrasonic enhancement only to the final module, where fouling is the greatest. Use in this mode could significantly enhance productivity for minimum energy expense.

2.2 Operating Pressure Effects

In the absence of ultrasound, membrane permeate flux usually increases as the feed side pressure increases and then plateaus, as the effects of a greater driving force

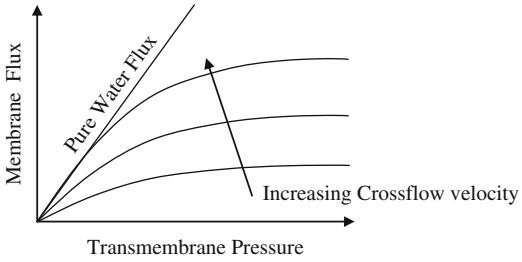

Fig. 23.4 A schematic of how membrane flux changes in the absence of ultrasound, as both transmembrane pressure and crossflow velocity are increased

are balanced by compaction of the fouling cake (see Fig. 23.4). Conversely, increasing the fluid pressure under ultrasound will increase the cavitation threshold and thus fewer bubbles will form (Henglein, 1987; Leighton, 1994). While this may reduce the number of cavitational collapse events, the pressure in the cavitating bubble will also be greater at the moment of collapse, and this can lead to more rapid and violent collapse events (Lorimer and Mason, 1987). These effects can also lead to unevenness of the ultrasonic field (Kylloenen et al., 2005). Conversely, a reduced number of bubbles can lead to greater penetration of the sound field, and this may increase the extent of cavitation at the membrane surface itself (Chen et al., 2006a).

There is thus likely to be an optimum operating pressure at which the membrane performance is maximized under ultrasound. Both Duriyabunleng et al. (2001) and Matsumoto et al. (1996) report such an optimum transmembrane pressure difference (Fig. 23.5). Chen et al. (2006a) found that at higher operating pressure, the cavitational intensity at the membrane surface increased, but that the ultrasonic enhancement declined. They argued that in this case, the fouling cake compaction caused by the higher transmembrane pressure was more significant than the turbulence due to ultrasound. Other researchers note only that increasing operating

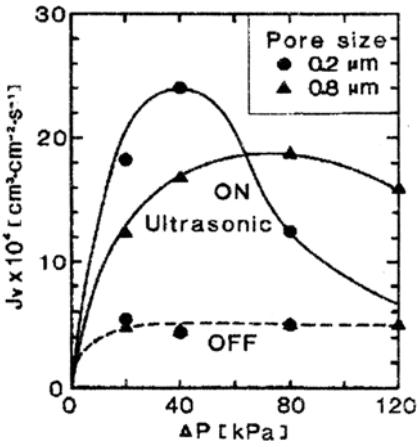

Fig. 23.5 Relationship between steady-state permeate flux (J_v) and transmembrane pressure (ΔP) for microfiltration of a yeast solution of 10 g/l (crossflow velocity 0.46 m/s, nominal ultrasonic power of 240 W) (reproduced from Matsumoto et al., 1996)

pressures leads to improved performance (Kobayashi et al., 1999; Yuk and Youm, 2003). Our own work showed that the effect of pressure was minimal when continuous low-frequency ultrasound was used (50 kHz), but that performance declined at high pressures when intermittent high-frequency ultrasound (1 MHz) was used (Muthukumaran et al., 2007). Indeed, in this work the permeate flux in the presence of ultrasound dropped below that without ultrasound at the highest operating pressure used.

2.3 The Influence of Crossflow Velocity

As shown in Fig. 23.4, in the absence of ultrasound, permeate flux generally increases as the flow velocity across the membrane increases. High fluid velocities reduce the thickness of the fouling cake by increasing the shear forces across the cake surface. Greater turbulence also reduces concentration polarization and thus increases mass transfer in the boundary layer. Some researchers have found that ultrasound has a proportionately greater effect at lower crossflow velocities when these effects are minimized (Duriyabunleng et al., 2001). However, our results (Muthukumaran et al., 2005a) showed that the effects of ultrasound were independent of crossflow velocity. This work also found that ultrasound remained effective even when hydrodynamic turbulence across the membrane was enhanced by the use of spacers. Hacias et al. (1997) suggest that the physical effects of cavitation can be more pronounced in fluid flow conditions. A moving fluid can assist the free flow of particles dislodged from the membrane, away from the membrane area.

High crossflow velocities will also assist in the movement of cavitation bubbles. In all cases where polymeric membrane damage due to sonication has been observed, there has been no crossflow across the membrane. In a stagnant environment it is possible for a cavitation bubble to become trapped at a point on the membrane surface and physically erode the surface by repeated oscillations at this point. Such a failure mechanism fits with the discussion of membrane damage reported in these papers.

2.4 Solids Concentration

A high concentration of particulate solids in the solution will attenuate the sound waves through acoustic impedance (Duriyabunleng et al., 2001; Wakeman and Tarleton, 1991). The degree of attenuation varies with the type of solids and experimental conditions. Furthermore, increasing feed concentrations can lead to higher viscosities and this is well known to dampen the effects of cavitation. Several studies report the effects of feed concentration (Duriyabunleng et al., 2001; Muthukumaran et al., 2005a; Wakeman and Tarleton, 1991; Yuk and Youm, 2003), but results of those studies conflict, with some research showing greater flux enhancement at high feed concentrations (Yuk and Youm, 2003), others showing no effects

(Muthukumaran et al., 2005a), and still others showing a loss of performance at high feed concentrations (Tarleton and Wakeman, 1992; Wakeman and Tarleton, 1991).

3 Membrane Cleaning

In all membrane operations, the processing operation must be halted regularly and the membranes cleaned for sanitation purposes and to remove the fouling cake. A typical cleaning cycle might include rinsing with an alkaline surfactant solution to remove protein or other organic deposits and/or an acid solution to remove inorganic contaminants, as well as a series of water flushes. Chlorine-derived cleaning agents may also be used to sanitize the membrane, and enzyme cleaning agents for protein removal are also gaining in popularity.

There has been considerable work on the use of ultrasound to supplement or replace some of these cleaning cycles (Chai et al., 1999; Feng et al., 2006; Kahler, 2004; Kawai et al., 2006; Kobayashi et al., 2003; Lamminen et al., 2004, 2006a, b; Muthukumaran et al., 2004, 2005b). There is particular interest in using this approach for membrane bioreactors, as ultrasonic cleaning can be completed in situ (Hoehn, 1998; Huang et al., 2005).

Our work shows that the use of ultrasound can increase the effectiveness of the alkaline cleaning step for removing protein deposits (Muthukumaran et al., 2005b). However, Fig. 23.6 shows that this step should still be conducted at a comparable pH, as a sharp optimum in cleaning effectiveness is apparent at this hydroxide concentration.

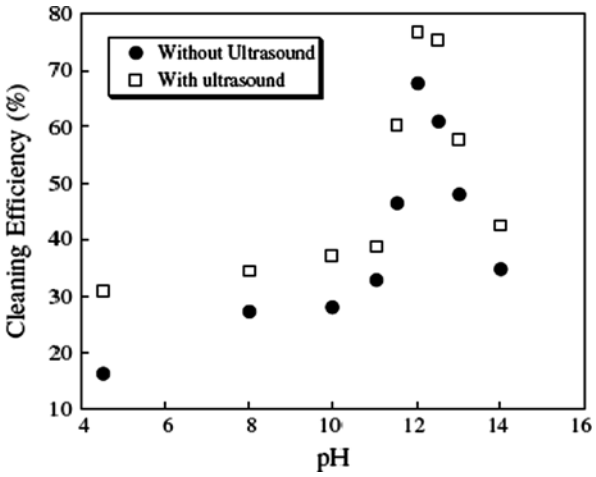

Fig. 23.6 Effect of solution pH on cleaning efficiency at 25°C of an ultrafiltration membrane fouled with a dairy whey solution in the presence and in the absence of ultrasound (50 kHz, nominal power 300 W) (reproduced from Muthukumaran et al., 2005b)

Alkaline cleaning is most effective at elevated temperatures where protein solubility is increased. However, high temperatures lead to high vapor pressures inside cavitation bubbles, which results in a dampening in collapse events. As a result, ultrasound has only a marginal impact when used to supplement a hot alkaline cleaning cycle for protein removal (Muthukumaran et al., 2005b).

Membrane cleaning is ideally conducted at low transmembrane pressures and high crossflow velocities so as to loosen the fouling cake. Several researchers (Li et al., 2002; Muthukumaran et al., 2005b) have found that the cleaning effect of ultrasound is not decreased by a higher crossflow velocity. As low pressures are generally associated with maximum cavitational activity, these conditions are also conducive to ultrasonic cleaning. Indeed, Bayevsky (2004) suggests that a vacuum pressure should be applied during cleaning to further reduce the cavitation threshold. This allows cavitational activity at lower acoustic pressures, which reduces the energy demand and the potential damage to sensitive filter membranes.

Many authors also indicate that lower frequencies (between 20 and 50 kHz) produce better membrane cleaning effectiveness than higher frequencies (between 100 and 200 kHz) (Kobayashi et al., 2003; Lamminen et al., 2004; Wakeman and Tarleton, 1991).

It is sometimes argued that it is environmentally attractive to use ultrasound to reduce the high chemical and water usage of classical membrane cleaning. However, a true environmental analysis must also include the greenhouse gas release associated with the power requirements of ultrasound. Caution must also be applied to ensure that the use of ultrasound for cleaning is economically viable. Our current calculations suggest that membrane cleaning applications may not provide sufficient return on investment unless deployed in conjunction with flux enhancement, as discussed in Section 2.

4 Industrial Scale Module Design

While most laboratory studies of membrane processing utilize baths or horns to supply ultrasonic power, such devices are not practically scalable to industrial operation. The only documented study of the large-scale use of ultrasonics in the food industry is a pilot scale study where a 94 × 10 cm spiral wound plastic microfiltration membrane was installed in a working wine plant (Bjorno and Bjorno, 2001). In this case, the membrane module was assembled with 24 standard transducers placed evenly around the unit (four rows of six transducers each). The 25–27 kHz transducers drew a total power of 3.6 kW. These authors observed no damage to the filter structure as determined by optical microscopy. The flux rate was observed to increase by between 3.5 and 10%, and the time between filter cleans was increased by 100%. The mining industry also uses ceramic microfilters at a commercial scale which are cleaned by ultrasound in an off-line process (Heikkinen et al., 2000).

Similarly, pilot scale studies have been completed on a range of pulp and paper mill waste streams, where ceramic microfiltration membranes were used with in situ ultrasonic cleaning. In this case, the tubular membranes were placed within a large feed vessel and ultrasound was provided by a bank of transducers along one wall of the vessel. The tubular membranes could be rotated within the acoustic field to both increase the crossflow velocity and provide an even exposure to the ultrasonic field (Kylloenen et al., 2005).

One of the greatest challenges facing this technology is the generation of a uniform acoustic field across the entire membrane surface in a full-scale module. An uneven application of the acoustic field is likely to result in membrane damage and will also cause inefficient energy consumption. Weavers et al. (2006) propose a number of novel configurations that might meet this objective (see Fig. 23.7). In one example, a cylindrical transducer is mounted around the outside of a membrane module, forming a shell that radiates ultrasonic energy inward. In a second example, a ring-shaped transducer is mounted externally or internally around the membrane element in a way that it can be moved longitudinally along the length of

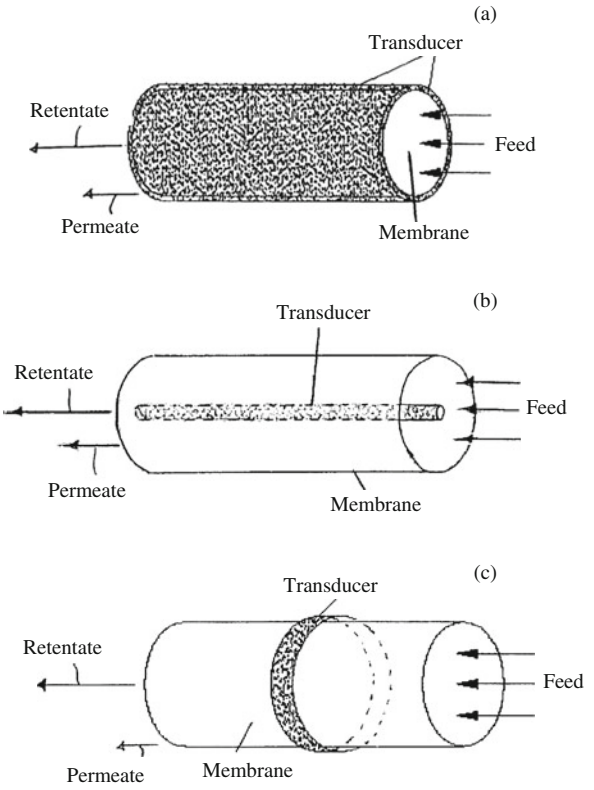

Fig. 23.7 Possible transducer configurations of a spiral wound or hollow fiber membrane module. Adapted from Weavers et al. (2006)

the membrane to provide a sweeping mode of operation. In yet a further example, a smaller diameter cylindrical transducer is mounted at the center of the membrane unit, providing a radial ultrasonic field that extends outward.

5 Related Technologies

There are a number of technologies that have been proposed for membrane flux enhancement that share common features with the use of ultrasonics. Most notable is the use of lower frequency vibration (around 50–60 Hz) in a direction tangent to the face of the membrane (New Logic International, 2001; Choi, 2003; Petala and Zouboulis, 2006). Vibratory shear-enhanced filtration (VSEP) is a commercialized technology that uses a sequence of parallel disc membranes located above a torsion spring that moves the stack back and forth between 1.9 and 3.2 cm (New Logic Research, 2007). Flux enhancements of 300–400% have been observed in these systems relative to a standard spiral wound membrane (Akoum et al., 2003, 2004). The disadvantage of this system is that the use of disc membranes limits the membrane area that can be provided (up to 151 m^2) (Akoum et al., 2005) and leads to a relatively large processing volume per unit of membrane area. The membrane unit must be placed vertically to accommodate the drive arrangement underneath. Rotating disc units produce similar effects (Bouzerar et al., 2003; Frappart et al., 2006; Jaffrin et al., 2004).

Researchers have also considered the injection of gas bubbles concurrently with the feed solution (Cui and Wright, 1994) and pulsatile flow (Finnigan and Howell, 1989). For membranes and/or foulants that are charged, the use of a pulsed electric field can also be used to create similar effects (Bowen and Sabuni, 1992; Tarleton and Wakeman, 1990, 1992; Wakeman and Tarleton, 1991).

6 Conclusions

Ultrasonic technology is now well established at a laboratory scale for membrane flux enhancement. However, the technology uptake to a commercial scale has been slow, and it is this area where future research must be focused. The particular issues that must be addressed in this respect are ensuring that a larger scale process is economical and provides an even ultrasonic intensity across the entire breadth of the membrane unit.

References

Ahner, N., Gottschlich, D., Narang, S., Roberts, D., Sharma, S., and Ventura, S. (1993). Piezoelectrically assisted ultrafiltration. *Separation Science and Technology*, 28(1–3), 895–908.

Akoum, O., Ding, L. H., Frappart, M., and Jaffrin, M. Y. (2004). COD reduction in nanofiltration of dairy process water using a vibratory dynamic filtration system. *Proceedings – World Filtration Congress, 9th,* New Orleans, LA, April 18–24, 2004, pp. 1733–1741.

Akoum, O., Jaffrin, M. Y., and Ding, L. (2003). Skim milk ultrafiltration using a rotating disk and VSEP vibrating system. *Recents Progres en Genie des Procedes 90* (9e Congres de la SFGP, 2003), 16–23.

Akoum, O., Jaffrin, M. Y., and Ding, L.-H. (2005). Concentration of total milk proteins by high shear ultrafiltration in a vibrating membrane module. *Journal of Membrane Science*, 247(1–2), 211–220.

Babu, B. R., Rastogi, N. K., and Raghavarao, K. (2006). Mass transfer in osmotic membrane distillation of phycocyanin colorant and sweet-lime juice. *Journal of Membrane Science*, 272(1–2), 58–69.

Bayevsky, M. (2004). Systems and methods for ultrasonic cleaning of cross-flow membrane filters. *US Patent No. 2004016699*.

Bjorno, I., and Bjorno, L. (2001). An approach to ultrasound cleaning of wine filtering plants. *17th International Congress on Acoustics*, Rome.

Bouzerar, R., Paullier, P., and Jaffrin, M. Y. (2003). Concentration of mineral suspensions and industrial effluents using a rotating disk dynamic filtration module. *Desalination*, 158(1–3), 79–85.

Bowen, W. R., and Sabuni, H. A. M. (1992). Pulsed electrokinetic cleaning of cellulose nitrate microfiltration membranes. *Industrial and Engineering Chemistry Research*, 31(2), 515–523.

Cassano, A., Drioli, E., Galaverna, G., Marchelli, R., Di Silvestro, G., and Cagnasso, P. (2003). Clarification and concentration of citrus and carrot juices by integrated membrane processes. *Journal of Food Engineering*, 57(2), 153–163.

Chai, X., Kobayashi, T., and Fujii, N. (1998). Ultrasound effect on cross-flow filtration of polyacrylonitrile ultrafiltration membranes. *Journal of Membrane Science*, 148(1), 129–135.

Chai, X., Kobayashi, T., and Fujii, N. (1999). Ultrasound-associated cleaning of polymeric membranes for water treatment. *Separation and Purification Technology*, 15(2), 139–146.

Charcosset, C. (1998). Purification of proteins by membrane chromatography. *Journal of Chemical Technology and Biotechnology*, 71(2), 95–110.

Chen, D., Weavers, L. K., and Walker, H. W. (2006a). Ultrasonic control of ceramic membrane fouling by particles: Effect of ultrasonic factors. *Ultrasonics Sonochemistry*, 13(5), 379–387.

Chen, D., Weavers, L. K., and Walker, H. W. (2006b). Ultrasonic control of ceramic membrane fouling: Effect of particle characteristics. *Water Research*, 40(4), 840–850.

Chen, D., Weavers, L. K., Walker, H. W., and Lenhart, J. J. (2006c). Ultrasonic control of ceramic membrane fouling caused by natural organic matter and silica particles. *Journal of Membrane Science*, 276(1–2), 135–144.

Choi, H. B. (2003). Process for treatment of livestock wastewater using Gas Stripper Disintegrator (GSD), Bio-Ceramic System SBR (BCS/SBR) and Vibratory Shear Enhanced Processing (VSEP) Membrane Filters. *Korean Patent No. 2003016721*.

Cui, Z. F., and Wright, K. I. T. (1994). Gas-liquid two-phase cross-flow ultrafiltration of BSA and dextran solutions. *Journal of Membrane Science*, 90(1–2), 183–189.

De Boer, R., De Wit, J. N., and Hiddink, J. (1977). Processing of whey by means of membranes and some applications of whey protein concentrate. *Journal of the Society of Dairy Technology*, 30(2), 112–120.

De Boer, R., and Hiddink, J. (1980). Membrane processes in the dairy industry: State of the art. *Desalination*, 35, 169–192.

Drioli, E., and De Bartolo, L. (2006). Membrane bioreactor for cell tissues and organoids. *Artificial Organs*, 30(10), 793–802.

Duriyabunleng, H., Petmunee, J., and Muangnapoh, C. (2001). Effects of the ultrasonic waves on microfiltration in plate and frame module. *Journal of Chemical Engineering of Japan*, 34(8), 985–989.

Feng, D., van Deventer, J. S. J., and Aldrich, C. (2006). Ultrasonic defouling of reverse osmosis membranes used to treat wastewater effluents. *Separation and Purification Technology*, 50(3), 318–323.

Finnigan, S. M., and Howell, J. A. (1989). The effect of pulsatile flow on ultrafiltration fluxes in a baffled tubular membrane system. *Chemical Engineering Research and Design*, 67(3), 278–282.

Frappart, M., Akoum, O., Ding, L. H., and Jaffrin, M. Y. (2006). Treatment of dairy process waters modelled by diluted milk using dynamic nanofiltration with a rotating disk module. *Journal of Membrane Science*, 282(1+2), 465–472.

Gan, Q., Howell, J. A., Field, R. W., England, R., Bird, M. R., and McKechinie, M. T. (1999). Synergetic cleaning procedure for a ceramic membrane fouled by beer microfiltration. *Journal of Membrane Science*, 155(2), 277–289.

Hacias, K. J., Cormier, G. J., Nourie, S. M., and Kubel, E. J. (1997). *Guide to Acid, Alkaline, Emulsion, and Ultrasonic Cleaning*. ASM International, Ohio, USA.

Hagenson, L. C., and Doraiswamy, L. K. (1997). Comparison of the effects of ultrasound and mechanical agitation on a reacting solid-liquid system. *Chemical Engineering Science*, 53(1), 131–148.

Heikkinen, J., Tuori, T., Wakeman, R. J., Juarez, J. A., Elvira, L., Rodriguez, G., Kaess, G., James, A., and Ekberg, B. (2000). *Proceedings of the 8th World Filtration Congress*, Brighton, UK, 767–770.

Henglein, A. (1987). Sonochemistry: Historical developments and modern aspects. *Ultrasonics*, 25(1), 6–16.

Hoehn, K. (1998). Method and device for cleaning a filter membrane in a bioreactor. Hoehn, Kai, Germany. *DE Patent No. 97–19703877, Germany*.

Huang, X., Chen, F., and Wen, X. (2005). Method and apparatus for on-line ultrasonic cavitation cleaning of membrane bioreactor. *Patent Application: CN 1621359*, Tsinghua University, People's Republic of China.

New Logic International. Is membrane fouling a thing of the past? (2001). *Filtration and Separation*, 38(1), 20–21.

Jaffrin, M. Y., Ding, L. -H., Akoum, O., and Brou, A. (2004). A hydrodynamic comparison between rotating disk and vibratory dynamic filtration systems. *Journal of Membrane Science*, 242(1–2), 155–167.

Joscelyne, S. M., and Tragardh, G. (2000). Membrane emulsification – a literature review. *Journal of Membrane Science*, 169(1), 107–117.

Juang, R. -S., and Lin, K. -H. (2004). Flux recovery in the ultrafiltration of suspended solutions with ultrasound. *Journal of Membrane Science*, 243(1–2), 115–124.

Kahler, B. (2004). Procedure and plant for wastewater disinfection by ultrasound. *Patent No. DE 10252544*, Kahler, Papst and Schmidt Patentverwertungs GESBR, Austria.

Kawai, Y., Yasunaga, N., and Furukawa, S. (2006). Membrane filtration apparatus. *Patent No. JP 2006007179*, Mitsubishi Electric Corporation, Japan.

Klein, E. (2000). Affinity membranes: A 10-year review. *Journal of Membrane Science*, 179(1–2), 1–27.

Kobayashi, T., Chai, X., and Fujii, N. (1999). Ultrasound enhanced cross-flow membrane filtration. *Separation and Purification Technology*, 17(1), 31–40.

Kobayashi, T., and Hosaka, Y. (2003). Enhanced membrane treatment for hollow-fiber microfiltration in ultrasonic reflection field. *Japanese Journal of Applied Physics, Part 1: Regular Papers, Short Notes and Review Papers*, 42(5B), 2954–2955.

Kobayashi, T., Kobayashi, T., Hosaka, Y., and Fujii, N. (2003). Ultrasound-enhanced membrane-cleaning processes applied water treatments: Influence of sonic frequency on filtration treatments. *Ultrasonics*, 41(3), 185–190.

Kokugan, T., Kaseno, Fujiwara, S., and Shimizu, M. (1995). Ultrasonic effect on ultrafiltration properties of ceramic membrane. *Maku*, 20(3), 213–23.

Kost, J., and Langer, R. S. (1988). Ultrasound enhancement of membrane permeability. *U.S. Patent No. 4780212*, Massachusetts Institute of Technology, USA, 7.

Krstic, D. M., Markov, S. L., and Tekic, M. N. (2001). Membrane fouling during cross-flow microfiltration of *Polyporus squamosus* fermentation broth. *Biochemical Engineering Journal*, 9(2), 103–109.

Kylloenen, H., Pirkonen, P., Nystroem, M., Nuortila-Jokinen, J., and Groenroos, A. (2006). Experimental aspects of ultrasonically enhanced cross-flow membrane filtration of industrial wastewater. *Ultrasonics Sonochemistry*, 13(4), 295–302.

Kylloenen, H. M., Pirkonen, P., and Nystrom, M. (2005). Membrane filtration enhanced by ultrasound: A review. *Desalination*, 181(1–3), 319–335.

Lamminen, M. O., Walker, H. W., and Weavers, L. K. (2004). Mechanisms and factors influencing the ultrasonic cleaning of particle-fouled ceramic membranes. *Journal of Membrane Science*, 237(1–2), 213–223.

Lamminen, M. O., Walker, H. W., and Weavers, L. K. (2006a). Effect of fouling conditions and cake layer structure on the ultrasonic cleaning of ceramic membranes. *Separation Science and Technology*, 41(16), 3569–3584.

Lamminen, M. O., Walker, H. W., and Weavers, L. K. (2006b). Cleaning of particle-fouled membranes during cross-flow filtration using an embedded ultrasonic transducer system. *Journal of Membrane Science*, 283(1+2), 225–232.

Latt, K. K., Kobayashi, T., and Kobayashi, T. (2004). Effect of ultrasound on membrane cleaning processes for enhancement of its permeability. *Transactions of the Materials Research Society of Japan*, 29(7), 3303–3306.

Le Berre, O., and Daufin, G. (1994). Fouling and Selectivity of Membranes during Separation of β-casein. *Journal of Membrane Science*, 88, 263–270.

Le Berre, O., and Daufin, G. (1996). Skim milk crossflow microfiltration performance versus permeation flux to wall shear stress ratio. *Journal of Membrane Science*, 117(1–2), 261–270.

Le Berre, O., and Daufin, G (1998). Microfiltration (0.1 μm) of milk: Effect of protein size and charge. *Journal of Dairy Research*, 65(3), 443–455.

Leighton, T. G. (1994). *The acoustic bubble*. San Diego, CA, Academic.

Li, J., Sanderson, R. D., and Jacobs, E. P. (2002). Ultrasonic cleaning of nylon microfiltration membranes fouled by Kraft paper mill effluent. *Journal of Membrane Science*, 205(1–2), 247–257.

Lorimer, J. P., and Mason, T. J. (1987). Sonochemistry Part 1. The physical aspects. *Chemical Society Reviews*, 16(2), 239–274.

Masselin, I., Chasseray, X., Durand-Bourlier, L., Laine, J. M., Syzaret, P. Y., and Lemordant, D. (2001). Effect of sonication on polymeric membranes. *Journal of Membrane Science*, 181(2), 213–220.

Matsumoto, Y., Miwa, T., Nakao, S. -I., and Kimura, S. (1996). Improvement of membrane permeation performance by ultrasonic microfiltration. *Journal of Chemical Engineering of Japan*, 29(4), 561–567.

Muthukumaran, S., Kentish, S. E., Ashokkumar, M., and Stevens, G. W. (2005a). Mechanisms for the ultrasonic enhancement of dairy whey ultrafiltration. *Journal of Membrane Science*, 258(1–2), 106–114.

Muthukumaran, S., Kentish, S., Lalchandani, S., Ashokkumar, M., Mawson, R., Stevens, G. W. and Grieser, F. (2005b). The optimisation of ultrasonic cleaning procedures for dairy fouled ultrafiltration membranes. *Ultrasonics Sonochemistry*, 12(1–2), 29–35.

Muthukumaran, S., Kentish, S. E., Stevens, G. W., Ashokkumar, M., and Mawson, R. (2007). The application of ultrasound to dairy ultrafiltration: The influence of operating conditions. *Journal of Food Engineering*, 81(2), 364–373.

Muthukumaran, S., Yang, K., Seuren, A., Kentish, S., Ashokkumar, M., Stevens, G. W., and Grieser, F. (2004). The use of ultrasonic cleaning for ultrafiltration membranes in the dairy industry. *Separation and Purification Technology*, 39(1–2), 99–107.

Narayan, A. V., Nagaraj, N., Hebbar, H. U., Chakkaravarthi, A., Raghavarao, K. S. M. S., and Nene, S. (2002). Acoustic field-assisted osmotic membrane distillation. *Desalination*, 147(1–3), 149–156.

New Logic Research (2007). http://www.vsep.com/index.html Accessed on April 24, 2007.

Noble, R. D., and Stern, S. A. (eds.) (1995). *Membrane separations technology: Principles and applications*. New York, NY, Elsevier.

Petala, M. D., and Zouboulis, A. I. (2006). Vibratory shear enhanced processing membrane filtration applied for the removal of natural organic matter from surface waters. *Journal of Membrane Science*, 269(1–2), 1–14.

Prazeres, D. M. F., and Cabral, J. M. S. (1994). Enzymatic membrane bioreactors and their applications. *Enzyme and Microbial Technology*, 16(9), 738–750.

Renner, E. (1984). Protein analysis of dairy products produced by ultrafiltration. *Special Publication – Royal Society of Chemistry*, 49, 201–205.

Rios, G. M., Belleville, M. P., Paolucci, D., and Sanchez, J. (2004). Progress in enzymatic membrane reactors – a review. *Journal of Membrane Science*, 242(1–2), 189–196.

Rodrigues, R. B., Menezes, H. C., Cabral, L. M. C., Dornier, M., Rios, G. M., and Reynes, M. (2004). Evaluation of reverse osmosis and osmotic evaporation to concentrate camu-camu juice (*Myrciaria dubia*). *Journal of Food Engineering*, 63(1), 97–102.

Simon, A., Gondrexon, N., Taha, S., Cabon, J., and Dorange, G. (2000). Low-frequency ultrasound to improve dead-end ultrafiltration performance. *Separation Science and Technology*, 35(16), 2619–2637.

Sivakumar, M., and Pandit, A. B. (2001). Ultrasound enhanced degradation of Rhodamine B: Optimization with power density. *Ultrason Sonochem FIELD; Ultrasonics Sonochemistry*, 8(3), 233–240.

Suslick, K. S. (1988). *Ultrasound; Its chemical physical and biological effects*. New York, NY, VCH.

Tarleton, E. S., and Wakeman, R. J. (1990). Microfiltration enhancement by electrical and ultrasonic force fields. *Filtration+Separation*, 27(3), 192–194.

Tarleton, E. S., and Wakeman, R. J. (1992). Electro-acoustic crossflow microfiltration. *Filtration+Separation*, 29(5), 425–432.

Teng, M. -Y., Lin, S. -H., and Juang, R. -S. (2006a). Effect of ultrasound on the separation of binary protein mixtures by cross-flow ultrafiltration. *Desalination*, 200(1–3), 280–282.

Teng, M. -Y., Lin, S. -H., Wu, C. -Y., and Juang, R. -S. (2006b). Factors affecting selective rejection of proteins within a binary mixture during cross-flow ultrafiltration. *Journal of Membrane Science*, 281(1+2), 103–110.

Thompson, L. H., and Doraiswamy, L. K. (1999). Sonochemistry: Science and Engineering. *Industrial and Engineering Chemistry Research*, 38(4), 1215–1249.

Vaillant, F., Cisse, M., Chaverri, M., Perez, A., Dornier, M., Viquez, F., and Dhuique-Mayer, C. (2005). Clarification and concentration of melon juice using membrane processes. *Innovative Food Science and Emerging Technologies*, 6(2), 213–220.

Villamiel, M., and De Jong, P. (2000). Influence of high-intensity ultrasound and heat treatment in continuous flow on fat, proteins, and native enzymes of milk. *Journal of Agricultural and Food Chemistry*, 48(7), 3068.

Wakeman, R. J., and Tarleton, E. S. (1991). An experimental study of electroacoustic crossflow microfiltration. *Chemical Engineering Research and Design*, 69(A5), 386–397.

Wang, X. -L., Li, X. -F, Fu, X. -Q., Chen, R., and Gao, B. (2005). Effect of ultrasound irradiation on polymeric microfiltration membranes. *Desalination*, 175(2), 187–196.

Weavers, L. K., Walker, H. W., Lamminen, M. O., and Chen, D. (2006). Ultrasonically cleaned membrane filtration system. *US Patent No. 7008540*, Ohio State University, USA.

Yuk, Y. J., and Youm, K. H. (2003). Enhancement of ultrafiltration performance using ultrasound. *Memburein*, 13(4), 283–290.

Zhu, C., and Liu, G. (2000). Modeling of ultrasonic enhancement on membrane distillation. *Journal of Membrane Science*, 176(1), 31–41.

Zou, H. F., Luo, Q. Z., and Zhou, D. M. (2001). Affinity membrane chromatography for the analysis and purification of proteins. *Journal of Biochemical and Biophysical Methods*, 49(1–3), 199–240.

Chapter 24
Industrial Applications of High Power Ultrasonics

Alex Patist and Darren Bates

1 Summary

Since the change of the millennium, high-power ultrasound has become an alternative food processing technology applicable to large-scale commercial applications such as emulsification, homogenization, extraction, crystallization, dewatering, low-temperature pasteurization, degassing, defoaming, activation and inactivation of enzymes, particle size reduction, extrusion, and viscosity alteration. This new focus can be attributed to significant improvements in equipment design and efficiency during the late 1990s. Like most innovative food processing technologies, high-power ultrasonics is not an off-the-shelf technology, and thus requires careful development and scale-up for each and every application. The objective of this chapter is to present examples of ultrasonic applications that have been successful at the commercialization stage, advantages, and limitations, as well as key learnings from scaling up an innovative food technology in general.

2 Introduction

Although ultrasonics have been used for years in research and diagnostics, major advances have been made in the last 5–10 years, turning this laboratory-based prototype technology into fully operational commercial processes throughout Europe and the USA. The applications for which high-power ultrasound can be used range from existing processes that are enhanced by the retro-fitting of high-power ultrasonic technology to the development of processes which up to now have not been possible with conventional energy sources. Section 2 starts with a discussion on the principal mechanism of ultrasound, followed by some key process parameters (Section 3). Sections 4 and 5 discuss a list of applications in the food industry,

A. Patist (✉)
Cargill Research, Wayzata, MN, 55391, USA
e-mail: alex_patist@cargill.com

H. Feng et al. (eds.), *Ultrasound Technologies for Food and Bioprocessing*,
Food Engineering Series, DOI 10.1007/978-1-4419-7472-3_24,
© Springer Science+Business Media, LLC 2011

followed by several examples of ultrasonic applications that have made it to commercial scale. Furthermore, some key learnings involving scale-up of an innovative technology in general are presented (Section 6).

3 Fundamentals of High-Power Ultrasound

The fundamental effect of ultrasound on a continuum fluid is to impose an acoustic pressure (P_a) in addition to the hydrostatic pressure already acting on the medium. The acoustic pressure is a sinusoidal wave dependent on time (t), frequency (f), and the maximum pressure amplitude of the wave, $P_{a,max}$ (Muthukumaran et al., 2006):

$$P_a = P_{a,max} \sin(2\pi ft) \tag{24.1}$$

The maximum pressure amplitude of the wave ($P_{a,max}$) is directly proportional to the power input of the transducer. At low intensity (amplitude), the pressure wave induces motion and mixing within the fluid, the so-called acoustic streaming (Leighton, 1994). At higher intensities, the local pressure in the expansion phase of the cycle falls below the vapor pressure of the liquid, causing tiny bubbles to grow (created from existing gas nuclei within the fluid). A further increase generates negative transient pressures within the fluid, enhancing bubble growth and producing new cavities by the tensioning effect on the fluid (Mason, 1998). During the compression cycle, the bubble shrinks and its contents are absorbed back into the liquid. However, since the surface area of the bubble is now larger, not all the vapor is absorbed back into the liquid, and thus the bubble grows over a number of cycles. Within a critical size range the oscillation of the bubble wall matches that of the applied frequency of the sound waves, causing the bubble to implode during a single compression cycle (Moholkar et al., 2000). This process of compression and rarefaction of the medium particles and the consequent collapse of the bubbles comprises the well-known phenomenon of cavitation, the most important effect in high-power ultrasonics. The conditions within these imploding bubbles can be dramatic, with temperatures of 5,000 K and pressures of up to 1,000 atm, which in turn produces very high shear energy waves and turbulence in the cavitation zone (Laborde et al., 1998; Suslick, 1988). It is the combination of these factors (heat, pressure, and turbulence), which is used to accelerate mass transfer in chemical reactions, create new reaction pathways, break down and dislodge particles (when cavitation in proximity of a solid surface), or even generate different products from those obtained under conventional conditions (Suslick, 1988).

When sound waves reflect on a solid surface or an air–water interface a standing wave can be formed. The acoustic pressure at the nodes is equal to zero, whereas at the antinode the acoustic pressure fluctuates from a maximum to a minimum. Leighton (1994) and Laborde et al. (1998) explain that bubbles smaller than the resonance size accumulate at the antinode, whereas bubbles larger than the resonance size accumulate at the node and consequently coalesce as they collide. This process

of bubble transport and growth at the nodes and antinodes is called microstreaming and is the main mechanism for ultrasonic degassing.

Ultrasound (i.e., mechanical waves at a frequency above the threshold of human hearing) can be divided into three frequency ranges:

- Power ultrasound (16–100 kHz)
- High-frequency ultrasound (100 kHz–1 MHz)
- Diagnostic ultrasound (1–10 MHz)

The work published by Lorimer and Mason (1987) shows that the frequency is inversely proportional to the bubble size. Therefore, low-frequency ultrasound (that is, power ultrasound 16–100 kHz) generates large cavitation bubbles resulting in higher temperatures and pressures in the cavitation zone. As the frequency increases the cavitation zone becomes less violent and in the megahertz range no cavitation is observed anymore and the main mechanism is acoustic streaming. While medical imaging operates at frequencies in the megahertz range (no cavitation), most industrial applications (processing of chemicals, food, as well as cleaning) operate between 16 and 100 kHz because cavitation can be produced within this frequency range.

The use of ultrasonics in industrial processes has two main requirements: a liquid medium (even if the liquid element forms only 5% of the overall medium) and a source of high-energy vibrations (the ultrasound). The vibrational energy source is called a transducer, which transfers the vibration (after amplification) to the so-called sonotrode or probe, which is in direct contact with the processing medium. There are two main types of transducers: piezoelectric and magnetostrictive. Piezoelectric transducers are the most commonly used in commercial scale applications due to their scalability, i.e., the maximum power per single transducer is generally higher than magnetostrictive transducers.

4 Process and Scale-Up Parameters

4.1 Energy and Intensity

Ultrasonic liquid processing can be described by the following parameters: amplitude (see previous section equation (24.1)), pressure, temperature, viscosity, and concentration of solids. The experimental outcome (e.g., % improved extraction yield and/or rate) is a function of the following:

1) Energy – the energy input per volume treated material (in kWh/L)
2) Intensity – the actual power output per surface area of the sonotrode (in W/cm^2)

The energy input is a function of power and flow rate and can be described as follows for continuous applications:

$$W_{\text{input}}(\text{kWh}/L) = W_{\text{spec}} = \frac{\text{Power of sonotrode (W)}}{Q\ (\text{L}/\ \text{min}) \times 60\ (\text{min}\ /h) \times 1000\ (\text{W}/kW)} \tag{24.2}$$

and for batch applications

$$W_{\text{input}}(\text{kWh}/L) = W_{\text{spec}} = \frac{\text{Power of sonotrode (W)} \times \text{treatment time (s)}}{3.6E6\ (\text{J}/kWh) \times \text{volume of treated material (L)}} \tag{24.3}$$

The energy density can be calculated by

$$W_{\text{density}}(\text{W}/\text{cm}^2) = \frac{\text{Power of sonotrode (W)}}{\text{Surface a rea of the sonotrode}\,(\text{cm}^2)} \tag{24.4}$$

Both energy and intensity are independent of scale and thus any ultrasonic process will be scalable using these two parameters (Hielscher, 2005). A very general relationship between flow rate and energy for several ultrasonic applications is shown in Fig. 24.1. It shows how the flow rate vs. energy relationship depends on the application. Ultrasonic pasteurization, for example, requires a great deal of energy per volume treated material and hence the maximum flow rate is relatively small (i.e., per kilowatt of energy). On the other hand, degassing requires a very small amount of energy, so much higher flow rates can be treated per kilowatt of ultrasonic energy.

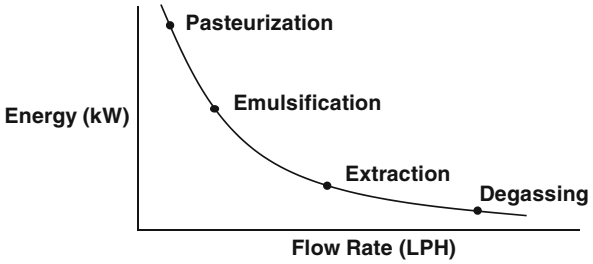

Fig. 24.1 Relationship of flow rate (l/h) vs. energy (kW) for several ultrasonic applications

4.2 Pressure

Increasing the external pressure (as controlled by the back pressure) increases the cavitation threshold and thus the number of cavitation bubbles is reduced (Muthukumaran et al., 2006). On the other hand, increasing the external pressure will increase the pressure in the bubble at the moment of collapse resulting in a more rapid but violent collapse (Lorimer and Mason, 1987). Therefore, increasing the back pressure can be an effective tool in intensifying the process without having to increase the amplitude (Hielscher, 2005).

4.3 Temperature and Viscosity

Temperature affects the vapor pressure, surface tension, and viscosity of the liquid medium (Muthukumaran et al., 2006). While increased temperature increases the number of cavitation bubbles, the collapse is "cushioned" or "dampened" by the higher vapor pressure. Cavitation bubbles form less easily in a highly viscous environment. Increased temperature decreases the viscosity allowing for a more violent collapse. Thus, there is an optimum temperature at which the viscosity is low enough to form enough violent cavitation bubbles; yet the temperature is low enough to avoid the dampening effect due to the vapor pressure.

It is clear that there are many process parameters affecting the process output and thus it takes time and effort to scale and fine-tune the process with the goal of achieving the maximum result with a minimum amount of energy (as that determines the number of transducers required for the commercial application).

5 Applications and Benefits

5.1 Summary of Applications

A broad range of ultrasonic systems and treatment conditions provide a diverse range of food application opportunities, as summarized in Table 24.1. The following sections will discuss the applications in more depth including details of the commercial system (where appropriate and allowed disclosure due to IP reasons).

5.2 Extraction

The extraction of organic compounds from plants or seeds has classically been based upon the judicious combination of solvent, heat, and/or agitation. This can be significantly improved by the use of high-power ultrasound, as the energy generated from collapsing cavitation bubbles provides greater penetration of the solvent into the cellular material and improves mass transfer to and from interfaces (Knorr, 2003; Li et al., 2004; Vinatoru, 2001; Vilkhu et al., 2008; Zhang et al., 2003). At higher ultrasonic intensities (i.e., W/cm^2), extraction processes can be further improved with the disruption of cell walls and the release of cellular materials. Patist et al. (2006), for example, showed that ultrasonics can be used to enhance the extraction of peel oil from citrus fruits. The fully commercial system uses several 16 kW systems in series to treat flow rates in excess of 36 m^3/h (see Table 24.2).

Cavitus Pty Ltd (2007) has developed commercial extraction systems using high-power ultrasound in the food and beverage industry. One particular example in the wine industry uses a 32 kW unit to treat 50 m^3/h of must for the extraction of grape color and anthocyanin during the fermentation process.

Table 24.1 List of high-power ultrasound applications in the food industry (references are listed in the appropriate section)

Application	Mechanism	Benefit
Extraction	Increased mass transfer of solvent, release of plant cell material (cavitational dislodgement)	Increased extraction rate and yield in solvent, aqueous, or supercritical systems
Emulsification/ homogenization	High shear micro-streaming	Cost-effective emulsion formation: reduced level of emulsifier, small particle size, and narrow distribution
Crystallization	Nucleation and modification of crystal formation	Formation of smaller crystals
Filtration/screening	Disturbance of the boundary layer	Increased flux rates and reduced fouling
Separation	Agglomeration of components at pressure nodal points	Adjunct for use in nonchemical separation procedures
Viscosity alteration	Reversible and nonreversible structural modification via vibrational and high-shear micro-streaming. Sono-chemical modification involving cross-linking and restructuring	Nonchemical modification for improved processing traits, reduced additives, and unique functionality
Defoaming	Airborne pressure waves causing bubble collapse	Increased production throughput, reduction or elimination of antifoam chemicals, and reduced wastage in bottling lines
Extrusion	Mechanical vibration, reduced friction	Increased throughput
Enzyme and microbial inactivation[a]	Increased heat transfer and high shear; direct cavitational damage to microbial cell membranes	Enzyme inactivation adjunct at lower temperatures for improved quality attributes
Fermentation[a]	Improved substrate transfer, CO_2 degassing and stimulation of living tissue, enzyme processes	Increasing production of metabolites, acceleration of fermentation processes
Heat transfer[a]	Improved heat transfer through acoustic streaming and cavitation	Acceleration of heating, cooling, and drying of products at low temperature

[a]At the time of publication the authors are not aware of any commercial scale installation of this application

Very recently, Balachandran and co-workers (2006) studied the effect of ultrasonics on supercritical extraction of ginger. Both rate and final yield were improved significantly. Since cavitational events in a supercritical fluid seem impossible due to the absence of liquid/gas phase boundaries, several other mechanisms, such as

acoustic streaming and the presence of gas pockets in the solid causing cavitational collapse, are proposed. Recently, it was shown that the same principles of mass transfer in extraction can be used in meat brining. Carcel and co-workers (2007) showed that above a critical ultrasonic intensity the uptake of brine solution into the meat was proportional to the applied ultrasonic intensity. At the highest level studied the total brine uptake was significantly higher than the initial water content of the meat.

5.3 Emulsification/Homogenization

If a cavitation bubble collapses near the surface of the phase boundary layer of two immiscible liquids, the resultant shock wave can provide very efficient mixing of the two layers. Relatively low energy input can result in the formation of very fine, highly stable emulsions (Canselier et al., 2002; Freitas et al., 2006). This has been well commercialized in the petrochemical, polymer, chemical, textile, cosmetics, and pharmaceutical industries and is now being developed in-line for food products such as fruit juices, mayonnaise, and tomato ketchup (Wu et al., 2000). Little, if any, additional emulsifier is required to maintain the stability of the system. For applications such as mayonnaise, an excellent white color is produced which reflects the small particle size and their narrow distribution (unpublished results). An obvious benefit of the ultrasonic emulsification process is that it can be installed in-line within the existing plant. In one particular commercial application the traditional homogenizer was replaced by ultrasonics, which allowed for a 50% reduction in emulsifier (in this case the most expensive ingredient). As a bonus the shelf-life was extended by several months. While the exact application cannot be disclosed here the system details are shown in Table 24.2.

Table 24.2 Business case examples of commercialized ultrasonic applications

Application	Description	Flow rate (m^3/h)	Power (kW)	Benefit (k$/year)	Payback time
Defoaming	Increased production capacity	>6	0.3	1,000	6 weeks
Emulsification	Reformulation and improved shelf-life	>7	32	500	1 year
Extrusion	Increased production capacity	Confidential	1	600	3 months
Extraction	Yield increase	>36	32	2,000	4 months
Waste treatment	Enhanced digestion and renewable energy	600	4	500	3 months

5.4 Crystallization

High-powered ultrasound can assist the crystallization process in several ways: influence the initiation of crystal nucleation, control the rate of crystal growth, ensure the formation of small and even-sized crystals, and prevent fouling of surfaces by the newly formed crystals (Luque de Castro and Priego-Capote, 2007; Virone et al., 2006). If such processes are not well controlled, nucleation and subsequent crystallization can occur randomly (often from small fluctuations in temperature and pressure), which generally produce a poor quality product. This can be of considerable financial significance in a large commercial process (McCausland et al., 2001).

Ultrasonic crystallization technology can be applied to foods where it can be used to control the size and rate of development of ice crystals in frozen foods (Chow et al., 2003). As food is frozen, small crystals form within the matrix. With conventional freezing, the time taken from the initiation of crystallization to complete freezing (the dwell time) can be lengthy, and then during storage the crystals can expand. With cellular materials, such as meats, fruits, and vegetables, the extended dwell time and crystal expansion soften and sometimes rupture cell walls, resulting in textural softening and the release of cellular liquid on thawing. Freezing using ultrasonics ensures rapid and even nucleation, short dwell times, and the formation of small, evenly sized crystals, greatly reducing cellular damage and preserving product integrity, even on thawing (Zheng and Sun, 2006). An added benefit from ultrasonically induced crystallization is the continuous cleaning effect from cavitation, which prevents encrustation of crystals on the cooling elements and ensures continuous heat transfer during the process.

5.5 Filtration and Screening

The application of ultrasound to filtration or screening processes can benefit the process in several ways. Ultrasound provides vibrational energy to keep particles in suspension and moving, leaving channels in the filter open and free for solvent elution. It also causes the filter or screen to vibrate, creating a "frictionless surface," allowing the liquid or smaller particles to pass through more readily (Telsonic Group, 2007). An additional advantage is an extension to filter life, as clogging and caking are prevented by continuous cavitation at the filter's surface. Ultrasonic oscillations are transmitted simultaneously to the filter and the material being treated, which improves the flow characteristics of the material (Grossner et al., 2005). All these factors are of significance to commercial filtration processes and several companies are offering ultrasonic filtration systems as an add-on to existing (vibratory) screens. More recently, the combination of ultrasound and membrane filtration has been investigated (Muthukumaran et al., 2005, 2006). While this area is still in its early phases of development, some promising results have been obtained in research labs and academia. The same principles as dead-end filtration apply and thus higher fluxes can be maintained for longer periods of time; in addition, the "cleaning-in-place" cycles can be conducted more efficiently (Feng et al., 2006).

5.6 Separation

A standing ultrasound force allows particles to aggregate to a node or antinode. The acoustic radiation force acts to drive the dispersed phase to either the nodes or antinodes of the stationary field and acts to hold the droplets in position (and consequently coalesce) relative to the bulk flow. This technology was shown to provide a novel principle for particle separation (Masudo and Okada, 2001). If high-power ultrasound is applied to an emulsion at low frequencies (<30 kHz), it can be used to split an emulsion into its component aqueous and oil phases (Gardner and Apfel, 1993; Pangu and Feke, 2004). The commercialization of this principle requires a great deal of development work and fine-tuning since high-power ultrasound can easily result in the opposite effect and yield a more stable emulsion or dispersion. Enhanced solid/liquid separation can be achieved in the wastewater industry where high-power ultrasound is used to degas the stream exiting the aerobic ponds. The removal of tiny air bubbles from the sludge enhances the settling rates significantly and allows for increased throughputs or the avoidance of capital expansions of the settling tank. This application has been commercialized on a global scale. Wastewater flows of over 10 m^3/min can be degassed effectively using 4+ kW of ultrasonic energy, depending on the type of wastewater (see Table 24.2).

5.7 Viscosity Alteration

Many food systems exhibit complex flow behavior and the viscosity is often determined by multiple factors such as pH, molecular weight of the protein, pectin, or polysaccharide, hydrogen bonding, and other inter- and intramolecular forces. Ultrasound can be applied to either increase or decrease the viscosity and, dependent on the intensity, temporary or permanent. Cavitation causes shear which in the case of thixotropic fluids causes a decrease in viscosity. This is often a temporary phenomenon. However, if enough energy is applied, the molecular weight may be decreased, causing a permanent viscosity reduction (Seshadri et al., 2003). Recently, Bates et al. (2006) showed that the opposite is also possible. In some vegetable purees the ultrasound actually allows for better penetration of moisture into the fiber network, which causes an increase in the viscosity of tomato puree. This application was commercialized to a full industrial scale and is unique in that it alters product functionality without reformulation.

5.8 Defoaming

Airborne ultrasonic technology is being applied commercially to achieve defoaming of carbonated beverages, fermentation systems, and other food processes where foaming adversely affects product quality or yields (Gallego-Juárez, 1998; Morey et al., 1999). Foaming problems can result in product losses and reduced efficiencies as production rates or volumes often have to be reduced. Since ultrasonic energy

dissipates quickly in the air, the applications of ultrasonics in the air are very limited. Nevertheless, the energy transmitted in the defoaming application is large enough to break a thin liquid film in the foam and thus provides a unique way of destroying foam without the use of mechanical breakers or by the addition of chemical antifoams, which may not be desirable in food processes. Cavitus Pty Ltd owns the technology and application of airborne ultrasonics and has commercialized several applications in the beverage/bottling industry. An example of an installation in the oilseed processing industry led to an increased throughput of 5–10%, which equated to a return on the investment of less than 2 months. The energy consumption of the ultrasonic defoaming system is extremely low, i.e., in the order of 300–600 W (Table 24.2).

5.9 Extrusion

A fairly recent development is the use of ultrasound in enhancing extrusion processes. The energy input provided by ultrasonic excitation of a metal tube or extrusion dye can be achieved by perpendicular attachment of the sonotrode onto the tube or dye. The vibration of the metal reduces the drag resistance and thus improves flow behavior (Akbari Mousavi et al., 2007; Knorr, 2004). Table 24.2 lists the business case for a commercial application, which unfortunately cannot be disclosed for confidentiality reasons.

5.10 Microbial Disinfection and Cleaning

Ultrasound has not only attracted considerable interest in the food industry due to its positive effects in processing, but more recently also due to its promising effects in food preservation. Knorr (2004) shows successful reduction of *E. coli* in liquid whole egg using ultrasound. Generally, most micro-organisms showed greater sensitivity to ultrasound at increased temperatures over 50°C (Sala et al., 1995; Villamiel and de Jong, 2000). Elevated temperature weakens the bacterial membrane, which enhances the effect of cavitation due to the ultrasound. "Ultrasonic pasteurization" at 50°C has the potential of preserving the quality of many food products in terms of physicochemical properties, color, and flavor compared to conventional pasteurization techniques at much higher temperatures.

Jiranek et al. (2008) recently discussed the use of ultrasonics in managing wine microbiology. Generally, a winemaker seeks to avoid higher temperatures because of the adverse effect it has on the flavor profile and color of wine. For this reason, the heating of wine to augment the effects of ultrasound would not be a preferred option. However, other points in the production process are routinely exposed to heat, e.g., the washing of fermentation tanks and barrels with hot water. Traditionally, wine barrels are cleaned using high-pressure, hot water sprays, which is only partly effective. Especially oak barrels could benefit from power ultrasound treatment in not only removing tartrate, but also killing the spoilage micro-organisms that are located

deep in the pores of the wood as well (Yap et al., 2007). Certainly wood barrels are not sterilized which explains the growth of the *Dekkera/Brettanomyces* spoilage organism, causing unpleasant odor compounds. Cavitus Pty Ltd has commercialized an automatic oak wine barrel cleaning system using a 4 kW ultrasonic transducer (Fig. 24.2). The cleaning result can be seen in Fig. 24.3 and the amount of microkill as a function of treatment time is shown in Fig. 24.4.

Fig. 24.2 Cavitus' commercial wine barrel cleaning and disinfection system

Fig. 24.3 Oak wine barrel before and after ultrasonic cleaning using Cavitus' proprietary ultrasonic cleaning system

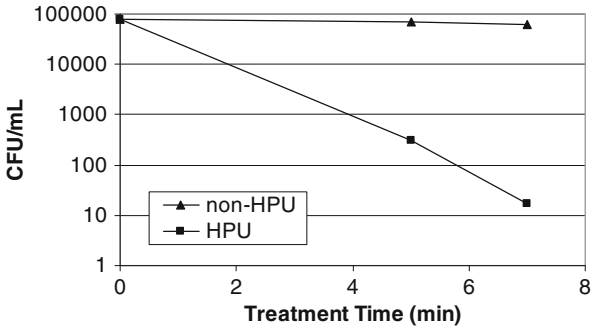

Fig. 24.4 Microbiological reduction of *Dekkera/Brettanomyces* by ultrasonics and conventional method (high-pressure/hot water sprays)

5.11 Fermentation

Several processes that take place in the presence of cells or enzymes are activated by ultrasonic waves. High-intensity ultrasound can rupture cells or denature enzymes; however, low-intensity ultrasound can improve mass transfer of reagents and products through the boundary layer or through the cellular wall and membrane (Pitt and Rodd, 2003; Sinisterra, 1992). Matsuura et al. (1994) showed an increase in the fermentation rate of sake, beer, and wine, when a relatively low-intensity ultrasound was applied during the fermentation. The proposed mechanism is that the ultrasound (a great degassing tool) drives off CO_2 produced during the fermentation, which normally inhibits the fermentation.

5.12 Heat Transfer

Cavitation can strongly affect the degree of heat transfer enhancement. Close to the boiling point of a liquid no cavitation occurs and acoustic streaming is the major factor in enhancing heat transfer rates, whereas at lower temperatures the effect of ultrasonic vibration is manifested through violent motion of cavitation bubbles (Kim et al., 2004). Very recently, the group of Gallego-Juarez (Fuente-Blanco et al., 2006) developed a novel ultrasonic drying process. Many food products (e.g., fruits and vegetables) are sensitive to heat, causing structural changes in the product after dehydration. The proposed system applies ultrasonic energy in combination with hot air to accelerate drying at room temperature, thereby preserving the integrity of the food product. The system is still in development but has great promise.

6 Commercialization

Ultrasonic processing is establishing itself as a significant food processing technology with the capability for large commercial scale-up and good payback on capital investment. Significant improvements in product quality, process enhancement, and cost reduction are achievable on a commercial scale. The reasons are summarized below:

Availability of high-amplitude/power units for large commercial operations: Manufacturers of high-power ultrasound equipment have been focusing on the design of large flow continuous treatment chambers (flow cells) causing the cost per volume of material treated to be reduced. A typical large flow chamber provides 8–16 kW of power for flows ranging from 5 to 500 l/min, depending on the application (see Fig. 24.5). Larger flow rates would require multiple systems in series or parallel.

Improved energy efficiency of the equipment: The efficiency of ultrasonic generators and transducers has been improved over the years, thereby reducing internal heating (and subsequent expensive cooling systems), which often causes system failure. Current systems have an energy efficiency of around

Fig. 24.5 Commercial 8 kW ultrasonic system used for pilot experiment in the field (feasibility stage of the project). The full-scale system will require multiple 16 kW transducers in series. Photo courtesy of Cavitus Pty Ltd

85%, which simply means that most of the power sent to the transducer is actually transferred into the medium.

Easy to install and/or retrofit systems: As mentioned earlier, due to improved efficiencies and the size of generator, cooling system and other parts, ultrasound is easily installed into an existing facility. If necessary, sound proof cabinets are available to reduce the noise generated by the cavitation (not by the ultrasound itself).

Competitive energy costs: Depending on the application, the amount of energy required per liter of material treated (defined as kWh/l, see Section 3.1) is comparable to any other unit operation in the industry (for example, homogenization, milling, and heat shock).

Low maintenance cost: One of the main benefits of ultrasonic technology is the absence of moving parts. The lack of rotors, seals, grease, etc., makes these systems particularly robust. The only part which requires replacement is the sonotrode (probe) which is in direct contact with the medium. Depending on the amplitude and the abrasiveness of the medium, the lifetime of a sonotrode ranges from 3 to 24 months.

Strong potential for intellectual property: While high-power ultrasonic systems become more and more standardized, the way the energy is applied to the medium (for example, flow cell design, number of transducers, piping arrangement) is unique for every application. Therefore, the potential to obtain patent protection is relatively large.

As a result, the technology has provided a strong economic business case in a range of food processing applications, which to date are only known by those involved in the application development, often due to confidentiality restrictions. A summary of the several business cases discussed in the previous section is provided in Table 24.2. The payback (defined here as investment cost over the benefit) is in general less than 1 year. Note that payback was used here as a simplified way to calculate the business case. Corporations generally use more sophisticated tools, such as net present value (NPV), internal rate of return (IRR), and return on investment (ROI) to evaluate the business case (Brealey et al., 2006).

7 Key Lessons in Commercializing Innovative Technologies

While the technology plays an important role in the implementation of an innovative food processing technology, there are some basic guidelines for making the project a success. Based on the authors' experience, a list of tips is given below:

– The technology has to have "$$$" and "Intellectual Property" appeal.
– The economics (total cost, payback, etc.) need to be well understood early on in the process. In other words, is the payback time acceptable to upper management?

In many industries the maximum payback time is shorter (for example, 2 years instead of 4 years) when the technology risk is higher.
- Build a road map to commercialization (including cost, time, and resources required). This helps manage expectations and ensures that management understands what it takes to commercialize the technology. A good approach is the so-called Stage-Gate™ process (Cooper, 2001), which focuses on both doing projects right and doing the right projects following a staged project management process from "ideation" to "launch" (note that Stage-Gate™ can be used for both new products and new processes).
- While it is important to get support from plant personnel, it is as important to keep decision makers in the loop and give them frequent project updates.
- Typically, the implementation of a new technology in an existing production facility means a temporary shutdown or production slow down. It is therefore critical that the plant manager and personnel understand the benefits of the implementation. In other words, plant "buy-in" will only be obtained if there is a "win-win" situation. This also emphasizes the importance of an "internal champion" of the project at the plant site, who can in turn delegate tasks to subcontractors (electricians, technicians, welders, engineers, etc.).
- Build a culture of recognizing each other for a job well done or going beyond the call of duty.
- Keep a positive attitude. As Sir Winston Churchill (1874–1965) said, "Success is the ability to go from one failure to another with no loss of enthusiasm."

While technology-related issues play a major part in the project, there are factors that are uncontrollable, yet may impact the last stage of the project, that is, the successful launch or full-scale implementation. Examples of mostly uncontrollable factors are as follows:

- The business is sold or ceases operation.
- The "internal champion" finds another job/resigns/retires. The transition of a new internal champion often results in project delays.
- A change of management and/or reprioritization of project portfolio. New management needs to be updated on existing projects, which may result in delays and the project being put on hold or even canceled.

These findings are all very important issues that need to be considered when commercializing an innovative technology. Therefore, often, the reason a new technology does not make it to commercialization is not related to the technology itself but due to the unexpected and uncontrollable factors listed above.

Last but not least, the following list of questions indicates an opportunity for better communication during the project, part of which is managing the expectations at all levels of management. Do not be surprised to hear these questions during start-up of the commercial installation:

– Can the technology be scaled up? Has this technology been implemented anywhere else?
– How reliable is ultrasonic technology? "...We want a patent, but we don't want to be the first to implement it..."
– What are the energy costs – will we need a nuclear power plant to run those units?
– What about spare parts? "Is there a 1–800 number we can call when the equipment breaks down?" Who, how, when...?

8 Conclusions

The considerable interest in high-powered ultrasound is due to its promising effects in food processing and preservation, such as higher product yields, shorter processing times, reduced operating and maintenance costs, improved taste, texture, flavor, and color, and the reduction of pathogens at lower temperatures. As one of the more advanced food technologies, it can be applied not only to improve the quality and safety of processed foods, but offers the potential for developing new products with unique functionality as well (as discussed in Section 4.7).

Commercial standard ultrasonic equipment is developing at great pace and no novel process for the application of ultrasound in industry is possible without ultrasonic equipment manufacturers willing to build new designs according to the requirements of customers. This implies that while the technology has great promise it will have to be carefully developed and scaled up for each single, unique application.

References

Akbari Mousavi, S. A. A., Feizi, H., and Madoliat, R. (2007). Investigations on the effects of ultrasonic vibrations in the extrusion process. *Journal of Materials Processing Technology*, 187–188, 657–661.

Balachandran, S., Kentish, S. E., Mawson, R., and Ashokkumar, M. (2006). Ultrasonic enhancement of the supercritical extraction from ginger. *Ultrasonics Sonochemistry*, 13, 471–479.

Bates, D. M., Bagnall, W. A., and Bridges, M. W. (2006). Method of treatment of vegetable matter with ultrasonic energy. *US patent application 20060110503*.

Brealey, R. A., Myers, S. C., and Allen, F. (2006). *Principles of corporate finance*, 8th edn. New York, NY, McGraw-Hill

Canselier, J. P., Delmas, H., Wilhelm, A. M., and Abismail, B. (2002). Ultrasound emulsification – An overview. *Journal of Dispersion Science and Technology*, 23, 333–349.

Carcel, J. A., Benedito, J., Bon, J., and Mulet, A. (2007). High intensity ultrasound effects on meat brining. *Meat Science*, 76, 611–619.

Cavitus Pty Ltd (2007). Applying high power ultrasonics to food and beverage processing. Adelaide, Australia. www.cavitus.com, *Australian patent application AU2007001958*.

Chow, R., Blindt, R., Chivers, R., and Povey, M. (2003). The sonocrystallization of ice in sucrose solutions: Primary and secondary nucleation. *Ultrasonics*, 41, 595–604.

Cooper, R. (2001). Winning at new products. In *The new product process: The stage-gate? game plan*, pp. 113–153, 3rd edn. Cambridge, MA, Perseus.

Feng, D., van Deventer, J. S. J., and Aldrich, C. (2006). Ultrasonic defouling of reverse osmosis membranes used to treat wastewater effluents. *Separation and Purification Technology*, 50, 318–323.

Freitas, S., Hielscher, G., Merkle, H. P., and Gander, B. (2006). Continuous contact and contamination free ultrasonic emulsification – A useful tool for pharmaceutical development and production. *Ultrasonics Sonochemistry*, 13, 76–85.

Fuente-Blanco, S., Riera-Franco de Sarabia, E., Acosta-Aparicio, V. M., Blanco-Blanco, A., and Gallego-Juárez, J. A. (2006). Food drying process by power ultrasound. *Ultrasonics*, 44, e523–e527.

Gallego-Juárez, J. A. (1998). Some applications of air-borne power ultrasound to food processing. In: Povey, M. J. W., and Mason, T. J. (eds.), *Ultrasound in food processing*, pp. 127–143. London, Blackie Academic and Professional.

Gardner, E. A., and Apfel, R. E. (1993). Using acoustics to study and simulate the coalescence of oil drops surrounded by water. *Journal of Colloid and Interface Science*, 159, 226–237.

Grossner, M. T., Belovich, J. M., and Feke, D. L. (2005). Transport analysis and model for the performance of an ultrasonically enhanced filtration process. *Chemical Engineering Science*, 60, 3233–3238.

Hielscher, T. (2005). Ultrasonic production of nano-size dispersions and emulsions. *Paper presented at 1st Workshop on Nano Technology Transfer*, ENS Paris, 14–16 December, Paris France.

Jiranek, V., Grbin, P., Yap, A., Barnes, M., and Bates, D. (2008). High power ultrasonics as a novel tool offering new opportunities for managing wine microbiology. *Biotechnology Letters*, 30(1), 1–6.

Kim, H. Y., Kim, Y. G., and Kang, B. H. (2004). Enhancement of natural convection and pool boiling heat transfer via ultrasonic vibration. *International Journal of Heat and Mass Transfer*, 47, 2831–2840.

Knorr, D. (2003). Impact of non-thermal processing on plant metabolites. *Journal of Food Engineering*, 56, 131–134.

Knorr, D. (2004). Applications and potential of ultrasonics in food processing. *Trends in Food Science and Technology*, 15, 261–266.

Laborde, J. L., Bouyer, C., Caltagirone, J. P., and Gerard, A. (1998). Acoustic bubble cavitation at low frequencies. *Ultrasonics*, 36, 589–594.

Leighton, T. G. (1994). *The acoustic bubble*. San Diego, CA, Academic.

Li, H., Pordesimo, L., and Weiss, J. (2004). High intensity ultrasound assisted extraction of oil from soybeans. *Food Research International*, 37, 731–738.

Lorimer, J. P., and Mason, T. J. (1987), Sonochemistry Part 1. The Physical Aspects. *Chemical Society Reviews*, 16, 239–274.

Luque de Castro, M. D., and Priego-Capote, F. (2007). Ultrasound assisted crystallization (sonocrystallization). *Ultrasonics Sonochemistry*, 14, 717–724.

Mason, T. J. (1998). Power ultrasound in food processing – The way forward. In: Povey, M. J. W. and Mason, T. J. (eds.), *Ultrasound in food processing*, pp. 103–126. London, Blackie Academic and Professional.

Masudo, T., and Okada, T. (2001). Ultrasonic irradiation: Novel principle for microparticle separation. *Analytical Sciences*, 17, 341–344.

Matsuura, K., Hirotsune, M., Nunokawa, Y., Satoh, M., and Honda, K. (1994). Acceleration of cell growth and ester formation by ultrasonic wave irradiation. *Journal Fermentation and Bioengineering*, 77, 36–40.

McCausland, L. J., Cains, P. W., and Martin, P. D. (2001). Use the power of sonocrystallization for improved properties. *Chemical Engineering Progress*, July, 56–61.

Moholkar, V. S., Rekveld, S., and Warmoeskerken, M. M. C. G. (2000). Modeling of the acoustic pressure fields and the distribution of the cavitation phenomena in a dual frequency sonic processor. *Ultrasonics*, 38, 666–670.

Morey, M. D., Deshpande, N. S., and Barigou, M. (1999). Foam destabilization by mechanical and ultrasonic vibrations, *Journal of Colloid and Interface Science*, 219, 90–98.

Muthukumaran, S., Kentish, S. E., Ashokkumar, M., and Stevens, G. W. (2005). Mechanisms for the ultrasonic enhancement of dairy whey ultrafiltration. *Journal of Membrane Science*, 258, 106–114.

Muthukumaran, S., Kentish, S. E., Stevens, G. W., and Ashokkumar, M. (2006). Application of ultrasound in membrane separation processes: A review. *Review of Chemical Engineering*, 22, 155–194.

Pangu, G. D., and Feke, D. L. (2004). Acoustically aided separation of oil droplets from aqueous emulsions. *Chemical Engineering Science*, 59, 3183–3193.

Patist, A., Mindaye, T. T., and Mathiessen, T. (2006). Process and apparatus for enhancing peel oil extraction. *US patent application 20060204624*.

Pitt, W. G., and Rodd, A. (2003). Ultrasound increases the rate of bacterial growth. *Biotechnology Progress*, 19, 1030–1044.

Sala, F. J., Burgos, J., Condon, S., Lopez, P., and Raso, J. (1995). Effect of heat and ultrasound on microorganisms and enzymes. In: Gould, G. W. (ed.), *New methods of food preparation*, pp. 176–204. London, Blackie Academic and Professional.

Seshadri, R., Weiss, J., Hulbert, G. J., and Mount, J. (2003). Ultrasonic processing influences rheological and optical properties of high methoxyl pectin dispersions. *Food Hydrocolloids*, 17, 191–197.

Sinisterra, J. V. (1992). Application of ultrasound to biotechnology: An overview. *Ultrasonics*, 30, 180–185.

Suslick, K. S. (1988). Homogeneous sonochemistry. In: Suslick, K. S. (ed.), *Ultrasound: Its chemical, physical, and biological effects*, pp. 123–163. New York, NY, VCH.

Telsonic Group. (2007). *Ultrasonic Screening Technology*. Bronschhofen, Switzerland, www.telsonic.com.

Vilkhu, K., Mawson, R., Simons, S., and Bates, D. (2008). Applications and opportunities for ultrasound assisted extraction in the food industry: A Review. *Innovative Food Science and Emerging Technologies*, 9, 161–169.

Villamiel, M., and de Jong, P. (2000). Inactivation of *Pseudomonas fluorescens* and *Streptococcus thermophilus* in trypticase soy broth and total bacterial milk by continuous-flow ultrasonic treatment and conventional heating. *Food Engineering*, 45, 171–179.

Vinatoru, M. (2001). An overview of the ultrasonically assisted extraction of bioactive principles from herbs. *Ultrasonics Sonochemistry*, 8, 303–313.

Virone, C., Kramer, H. J. M., van Rosmalen, G. M., Stoop, A. H., and Bakker, T. W. (2006). Primary nucleation induced by ultrasonic cavitation, *Journal of Crystal Growth*, 1, 9–15.

Wu, H., Hulbert, G. J., and Mount, J. R. (2000). Effects of ultrasound on milk homogenization and fermentation with yogurt starter. *Innovative Food Science and Emerging Technologies*, 1, 211–218.

Yap, A., Jiranek, V., Grbin, P., Barnes, M., and Bates, D. (2007). Studies on the application of high power ultrasonics for barrel and plank cleaning and disinfection. *The Australian and New Zealand Wine Industry Journal*, 22(3), 95–104.

Zhang, R., Xu, Y., and Shi, Y. (2003). The extracting technology of flavonoids compounds. *Food and Machinery*, 1, 21–22.

Zheng, L., and Sun, D. W. (2006). Innovative applications of power ultrasound during food freezing processes: A review, *Trends in Food Science and Technology*, 17, 16–23.

Chapter 25
Technologies and Applications of Airborne Power Ultrasound in Food Processing

Juan A. Gallego-Juárez and Enrique Riera

1 Introduction

Applications of ultrasonic waves are generally divided into two groups: low intensity and high intensity. Low-intensity applications are those wherein the objective is to obtain information about the propagation medium without producing any modification of its state. On the contrary, high-intensity applications are those wherein ultrasonic energy is used to produce permanent changes in the treated medium.

High power ultrasound is devoted to high-intensity applications. The limit between low and high intensities is very difficult to fix, but it can be approximately established for intensity values which, depending on the medium, vary between 0.1 and 1 W/cm^2.

The use of high-intensity ultrasonic waves in industrial processing is generally based on the adequate exploitation of a series of mechanisms activated by the ultrasonic energy such as heat, agitation, diffusion, interface instabilities, friction, mechanical rupture, and chemical effects. These mechanisms can be employed to produce or to enhance a wide range of processes such as plastic and metal welding, machining, and metal forming in solids or cleaning, atomization, emulsification and dispersion, degassing, extraction, defoaming, particle agglomeration, drying and dewatering, and sonochemical reactions in fluids.

The ultrasonic processes are very much dependent on the irradiated medium. In fact, a typical characteristic of high-intensity ultrasonic waves is their ability to produce different phenomena in different media in such a way that these phenomena seem to be opposite at times. This can be seen, for example, in the case of application of power ultrasound to liquid suspensions for particle dispersion and to gas suspensions for particle agglomeration. Such apparently contradictory behavior is clearly due to the different media where the acoustic energy is applied and, consequently, to the different mechanisms that are activated. In liquids, the great majority of the effects produced by power ultrasound are associated with cavitation, a phenomenon which is not possible to induce in gas or solid media.

J.A. Gallego-Juárez (✉)
Instituto de Acústica, CSIC, Serrano, 144, 28006 Madrid, Spain
e-mail: jgallego@ia.cetef.csic.es

H. Feng et al. (eds.), *Ultrasound Technologies for Food and Bioprocessing*, Food Engineering Series, DOI 10.1007/978-1-4419-7472-3_25,
© Springer Science+Business Media, LLC 2011

Another characteristic of high-intensity ultrasonic waves is their capacity to work synergistically with other forms of energy in order to promote, accelerate, or improve many processes. Thus, many practical applications of high-power ultrasound are not considered as exclusively ultrasonic processes, but rather as ultrasonically assisted processes.

The use of high-power ultrasound in industrial processing is a promising area which, in many aspects, remains closed. A large number of ultrasonic processes have been produced in the laboratory. Nevertheless, only a few of these processes have been introduced in the industry. Such a situation is particularly significant in those processes related with the food industry where the application of ultrasonic waves would incorporate many important advantages, such as noncontamination, deep action, efficiency, and cleanness.

Foodstuffs are, in general, inhomogeneous complex materials which usually contain gas, liquid, and solid phases. Therefore, it is frequently difficult to understand the different mechanisms provoked by the action of ultrasonic energy. In fact, many mechanisms of ultrasonic food processing are not well known, and this situation limits the possibilities of application in a field which appears as very promising. A strong effort in research about the basic mechanisms involved in any specific application is needed for efficient development in this area.

The future of power ultrasonics in food processing is also linked to the development of adequate industrial equipment. In fact, the commercial introduction of a new technology depends, in addition to its capability for solving real problems, on the design, operational simplicity, efficiency, and low energy consumption of the equipment used for the development of the process.

Airborne power ultrasound represents an example of a field of application to food processing that has not been sufficiently exploited. This is probably because of the problems already mentioned, i.e., lack of deep knowledge of the basic mechanisms involved and the difficulties in power ultrasonic technology. In fact, large-scale industrial applications require efficient transmission of energy and capacity in the acoustic generators to sonify large volumes.

Recently, as a consequence of the development of a new technology of high-power sonic and ultrasonic generators for radiation in air and in multiphase media (Gallego-Juárez et al., 1994, 2000, 2002) a series of ultrasonic applications at the laboratory and semi-industrial stages have been studied and developed.

This chapter deals with the main characteristics of the new ultrasonic technology for efficient airborne generation and presents a review of some applications in food processing developed by using this technology, such as defoaming, dehydration, and extraction.

2 Airborne Power Ultrasonic Technologies for Food Processing

For the efficient generation and application of high-intensity ultrasound to different media, it is necessary to design and develop high-power transducers specifically adapted to the requirements of each medium. Fluid media, particularly gases, present low specific acoustic impedance and high acoustic absorption. Therefore,

in order to obtain an efficient transmission of energy, it is necessary to achieve a good impedance match between the transducer and the medium, large amplitude of vibration, and high directional or focused beams for energy concentration. In addition, for large-scale industrial applications, high power capacity and extensive radiating area are required in the transducers.

There are few commercial power generators for airborne ultrasound and almost none of them cover all the above-mentioned requirements. For many years, the most common transducers for use in gases were aerodynamic systems of various kinds, such as whistles and sirens, in which the acoustic energy is provided by a gas jet (Allen and Rudnick, 1947; Hartmann, 1939). Although it is possible to yield large acoustic power with these generators, the efficiencies obtained are low, the sounds emitted are complex, and they present poor directivity and difficulty in reaching ultrasonic frequencies (Greguss, 1964).

At present, most high-power commercial transducers are based on the classical Langevin-type transducer which has many limitations for airborne applications. Therefore, new transducer technology is needed where the main points to be considered are increase in power capacity and efficiency, enlargement of the working area, and improvement of radiator design to reach, as much as possible, a uniform distribution of the acoustic field.

The recent development of a new technology based on stepped-plate transducers, which implement high power capacity, efficiency, and directivity, has opened new possibilities for airborne ultrasound and their applications in many industrial areas, particularly in food processing (Gallego-Juárez et al., 1999, 2005; Riera et al., 2004).

The stepped-plate transducers essentially consist of an extensive flexural vibrating plate radiator of stepped shape driven at its center by a piezoelectrically activated vibrator. The extensive surface of the plate radiator increases the radiation resistance and offers the vibrating system good impedance matching with the medium. The special stepped shape of the radiator permits, despite its flexural vibration, access to any configuration of the acoustic field by introducing adequate design in the profile of the plate surface. In this way, a high directional and/or focused radiator can be designed for energy concentration. Stepped-plate circular radiators axisymmetrically vibrating with diameters of up to 70 cm have been constructed (Fig. 25.1) (Gallego-Juárez et al., 1994).

Another version of this transducer model, adapted for specific industrial applications, uses rectangular plate radiators with double-stepped profile (Fig. 25.2). Rectangular plates offer a more uniform distribution of vibration, and therefore higher power capacity. In addition, the material needed for their construction (rolled titanium alloy) is more easily available than the forged titanium needed for the construction of circular plates. Two different versions of rectangular plate transducers have been designed and constructed: one with a plate of 0.3×0.6 m^2 for a power capacity of about 300 W and other with a plate of 1.8×0.9 m^2 for a power capacity of about 2 kW (Fig. 25.3) (Gallego-Juárez et al., 2001).

The main characteristics of the developed stepped-plate transducers are the following: efficiency of about 80%; beam width (at 3 dB) of 1.5°; power capacity up to 2 kW; and intensity levels reaching as high as 175 dB.

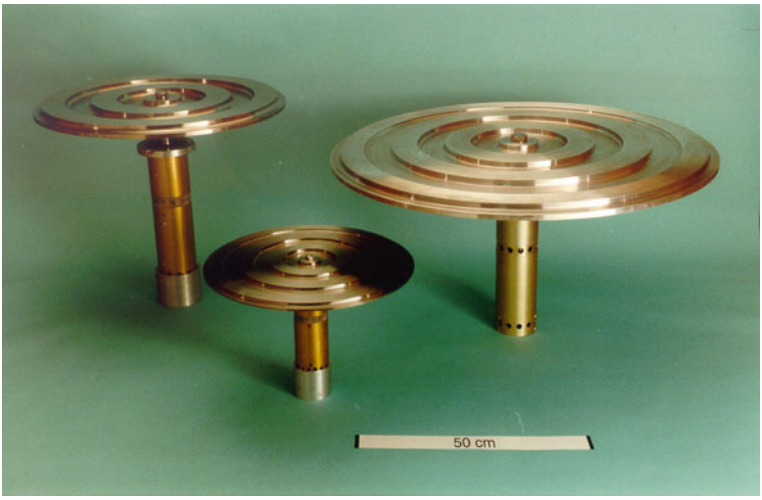

Fig. 25.1 Stepped-plate transducers

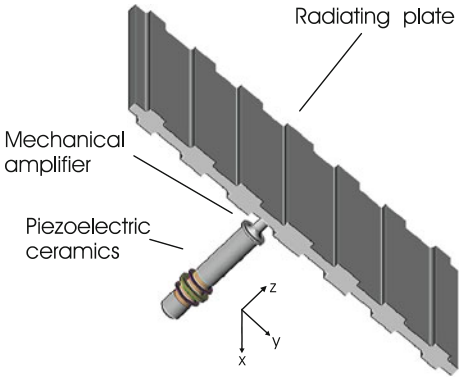

Fig. 25.2 Scheme of a rectangular plate transducer with double-stepped profile

The new transducers are driven by an electronic system especially designed to produce a signal lying permanently within their very narrow resonance frequency band. The electronic system is composed of an impedance matching unit, a power amplifier, and a frequency control device. Such devices were specifically developed to keep the power applied constant at the resonant frequency of the transducer during the process, independently of the variations of the acoustic impedance of the load and the resonant frequency of the transducer (Gallego-Juárez et al., 1994, 2005).

3 Applications in Food Processing

The new technology of high-power ultrasonic generators for fluids and for multiphase media has been successfully applied to some specific problems in food processing, such as

Fig. 25.3 Rectangular plate transducers

– defoaming in fermentation processes and in the filling operation of gassy beverages;
– dehydration of vegetables; and
– oil extraction with supercritical fluids assisted by ultrasound.

3.1 Ultrasonic Defoaming in Fermentation Processes and in the Filling Operation of Gassy Liquids

Foam is a dispersion of gas in a liquid in which the distances between the gas bubbles are very small. In fact, foam can be considered as the agglomeration of gas bubbles separated by a very thin liquid film. In a foam system the volume ratio of gas to liquid is very great and the bulk density approaches that of a gas. Foam generation may result from the aeration and agitation of liquids, from the vaporization of the liquid phase, and also from microbiological or chemical reactions that release gases. Foams are frequently undesirable in industrial processes because, in general, they cause difficulties in process control and in handling equipment. A typical example is in the fermentation industry, where foam represents one of the biggest problems. Therefore, there is a great interest in the destruction and/or control of foams.

Stability is one of the most important features of foam, since it determines the difficulty for its destruction (Viesturs et al., 1982). Foams can collapse naturally when

liquid drains from the upper to the lower layers. This process is opposed by the capillary pressure gradient along the height of the foam column that prevents the liquid running out. This means that there will be a critical height of the foam at which the drain processes vs. capillary pressure are balanced. Other relevant factors affecting the stability of foams are pH, molecular surface electrical charge, temperature, viscosity, and surface tension.

Several methods are used for defoaming that employ chemical and physical effects. Chemical defoaming methods employ antifoam agents that produce a decrease in surface tension. They are generally very effective, but they can cause a problem because of contamination during the process. Physical methods to solve this problem include trying to produce bubble rupture by thermal, electrical, or mechanical effects (Ghildyal et al., 1988).

3.1.1 Chemical Defoaming Methods

Chemicals used as antifoam agents produce a decrease in surface tension. They are usually very effective, but are generally forbidden in food and pharmaceutical industries because they contaminate the process.

3.1.2 Physical Methods

Physical methods employ thermal, electrical, and mechanical effects. Thermal breakers depend on the effect of temperature of the foam to produce the rupture of the bubbles. This method is based on the intensive expansion of the bubbles, the evaporation of the moisture and solvent causing the foam, a decrease in surface viscosity, freezing, and/or a reduction in surface tension. Some systems include the introduction of either a hot wire over the surface of the solution or a heating coil to heat the upper part of the reactor. Electrical methods depend upon the generation of an electric current passing through the foamy region to destroy the foam. The exact mechanism of this type of foam destruction is not well known. The activity may be based on the fact that the forces created by the current act differently on liquid and gas.

Mechanical methods are more widely used, mainly to overcome the disadvantages related with the use of antifoam agents. The collapse of bubbles is produced by mechanical shocks (rapid pressure changes, shear force, compressive force, impact force, suction, and centrifugal forces). Mechanical control of foam has been investigated in stirred vessels and bubble columns (Deshpaude and Barigou, 2000). Among the mechanical foam breakers, those with rotating parts, cyclones, impact sprays, nozzles, centrifugal basket, and vacuum systems are the most widely used. In general, the mechanical methods are effective only for coarse foams. In addition, many of them have significant disadvantages such as hygiene hazards and dilution of the product

3.1.3 Ultrasonic Defoaming

The use of the ultrasonic energy can be considered as a mechanical method based on the propagation of high-intensity ultrasonic waves, and it represents a clean means

of breaking foams without contact with the liquid. The destruction of foams by ultrasonic defoamers is assumed to be a combination of (a) the mechanical stress on the foam bubble surface produced by the high acoustic pressure; (b) impingement of radiation pressure on the bubble surface; (c) resonance of the foam bubbles; (d) interstitial friction causing bubble coalescence; (e) cavitation of the liquid film; (f) atomizing from the liquid film surface; and (g) acoustic streaming (Boucher and Weiner, 1963; Gallego-Juárez, 1999). The potential use of acoustic waves for foam breaking was first considered in the 1950s. Various types of acoustic defoamers were analyzed. The majority of those defoamers were based on aerodynamic acoustic sources of various types such as the Hartmann whistle and the rotatory siren. Nevertheless, such systems presented serious operating problems such as production of noise (they usually operated in the hearing frequency range), requirements for the controlled generation of high air flow, and the need for sterilization of such air flow for applications in food processing. As a consequence, the potential acoustic defoaming technology scarcely progressed after such early stages.

The new high-intensity ultrasonic defoamer is based on the use of a stepped-plate transducer to generate airborne ultrasound (Rodriguez et al., 1985). This system is a compact piezoelectrically activated device that neither requires air flow nor produces any disturbing noise, and may be used by the food or pharmaceutical industries without any restriction. In fact, this defoamer has been successfully applied to the control of excess of foam produced in fermentation processes and in the filling operation of carbonic beverages in high-speed canning and bottling lines (Gallego-Juárez, 1998). The experimental setup for canning and bottling lines involves the use of one or several focused transducers acting on the open surface of the can or the bottle to destroy the excess of foam (Fig. 25.4).

Another version of the ultrasonic defoamer (Gallego-Juárez et al., 2003) was developed for the treatment of foams produced in reactors. In this version, one or two directional or focused transducers are freely hung in a rotation system (Fig. 25.5). The rotation speed is electronically controlled and, due to centrifugal force, the angle of the transducer axis is changed according to the driving speed in such a way that the acoustic beam acting on the liquid surface will follow a predetermined path covering a large defoaming area. Different rotation systems have been developed for foam treatment in fermenters of up to 8 m in diameter.

The ultrasonic control of foam in reactors demonstrates that ultrasound is able to break older formed foam located at the surface much more effectively than freshly formed foam located close to the liquid. The main reason for this is that the older foam at the surface is less stable and lighter due to drainage and lower liquid content. The effect over the entire foam surface depends on how fast the foam rises as well as on the ultrasonic intensity at the focus.

3.2 Dehydration of Vegetables

An important process in the food industry is dehydration. Dehydration is a method for preserving foods. There are two basic conventional methods for dehydration, mechanical, and thermal. Mechanical dehydration is based on pressing or

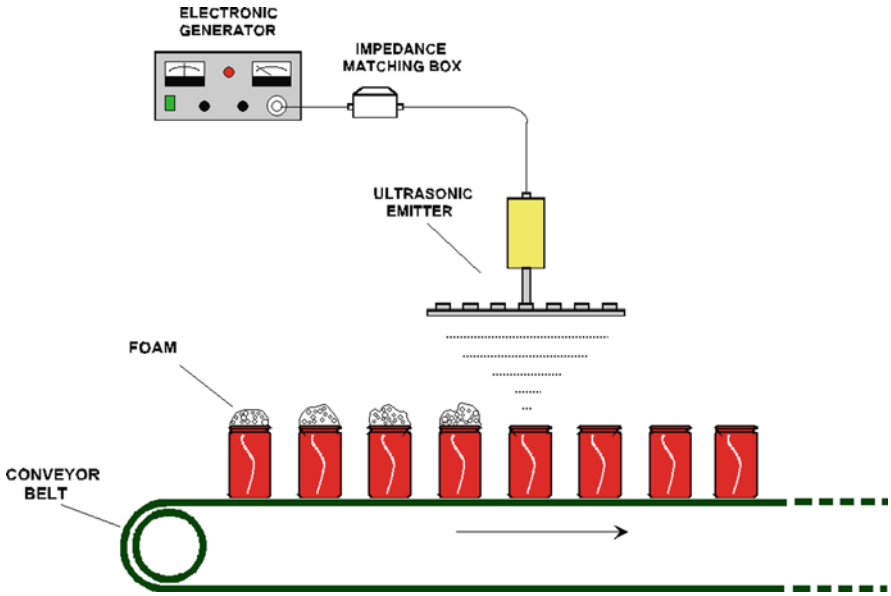

Fig. 25.4 Scheme of foam control in a canning line

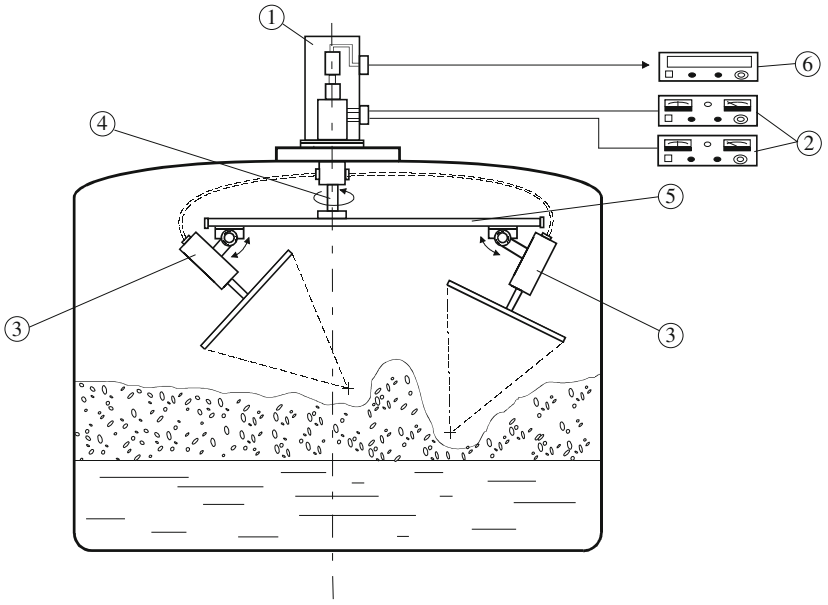

Fig. 25.5 Scheme of a twin set-focused transducer system for defoaming in reactors

centrifuging the material. In thermal dehydration or drying, the addition of energy in the form of heat is used to evaporate the liquid. Mechanical dehydration may be useful for the separation of moisture that is weakly attached, while thermal drying provides a more complete removal of any kind of moisture from the product.

The dehydration method suitable for each specific application is related to the attachment of the liquid with the solid material. In general, three types of attachment can be considered: chemical, mechanical, and physicochemical. For food dehydration, the present conventional systems employ two main procedures: hot air drying and freeze drying. Hot air drying is a widely used method, but it can produce deteriorative changes in food. Instead, in freeze drying, where food pieces are first frozen and then ice sublimates, product deterioration is negligible, but the process is expensive.

High-intensity airborne sonic and ultrasonic waves have been used to increase the drying rate of materials. The acoustically assisted hot air drying process permits the use of lower temperatures and may be useful for drying heat-sensitive materials (Fairbank, 1975; Seya, 1970).

On the basis of the new plate transducer power ultrasonic generators, a new ultrasonic technology for vegetable dehydration has been developed by using two experimental procedures: forced air drying assisted by airborne ultrasound and ultrasonic dehydration by applying ultrasound in direct contact with the material.

3.2.1 Forced Air Dehydration Assisted by Airborne Ultrasound

The application of airborne ultrasonic energy for drying materials has been explored for several decades. High-intensity airborne ultrasound introduces pressure variations at gas/liquid interfaces and, therefore, increases the evaporation rate of moisture. Moreover, in a forced air drying system, the air velocity influences the heat and mass transfer. Acoustic energy produces an oscillating velocity effect that can increase the drying rate at stable air velocity. In addition, high-intensity airborne ultrasound causes microstreaming at the interfaces which reduces the diffusion boundary layer, increases mass transfer, and accelerates diffusion. Therefore, the application of airborne acoustic energy can positively contribute to the drying process.

The application of the new stepped-plate generator as an airborne ultrasonic radiator, in combination with forced air at different temperatures, is a procedure aiming to efficiently use the synergistic effect of ultrasonic energy. The experimental system designed and constructed for airborne ultrasonic dehydration is shown in Fig. 25.6. It mainly consists of a hot air generator, a stepped-plate power ultrasonic transducer for 20 kHz with the corresponding electronic generator, and a flat plate parallel to the ultrasonic radiator, acting as a reflector for the formation of a standing wave and also as a sample holder. In addition, complementary sets of equipment to measure temperature, air flow velocity, and weight were used.

Experimental tests to characterize the system were carried out with vegetable samples: carrot slices of square (12 × 12 mm) or circular (14 mm in diameter) shape with 2, 4, and 8 mm in thickness. The samples were placed in the flat support

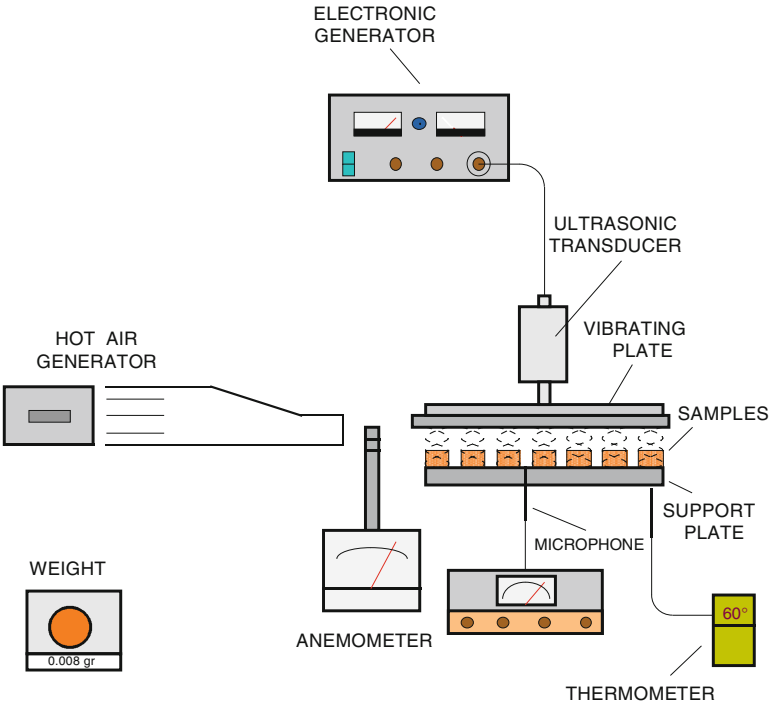

Fig. 25.6 Experimental setup for forced air drying assisted by airborne ultrasound

plate with their upper surface and contour free. Some representative results are presented in Figs. 25.7 and 25.8. Figure 25.7 shows the results obtained with forced air at 60, 90, and 115°C without and with ultrasound (acoustic pressure level applied at 155 dB). In all cases the size of the samples was 12 × 12 mm^2 section with 2 mm thickness. As can be seen, the effect of ultrasonic radiation is significant at low air temperature, and it diminishes when temperature increases. At the highest temperature (115°C), the ultrasonic effect was negligible. Dehydration curves are expressed in terms of moisture content on a dry basis (weight of water/weight of dry solid). The influence of acoustic pressure level can be observed in Fig. 25.8, where the results of tests conducted at higher intensity (acoustic pressure level of 163 dB) are shown. Comparison between Figs. 25.7 and 25.8 shows that the effect of increasing the acoustic pressure by about 8 dB allows the temperature of the air to diminish by 10°C, with little increase in flow velocity.

Other tests were conducted with the same type of samples by increasing air flow velocity up to 3 m/s. The results obtained showed that at this forced air speed the differences with and without ultrasound are less significant (Fig. 25.9).

Similar results were obtained with samples of circular shape and with different thicknesses.

From these results it can be stated that the application of airborne ultrasound is useful in increasing the efficiency of forced air drying processes. Nevertheless, this

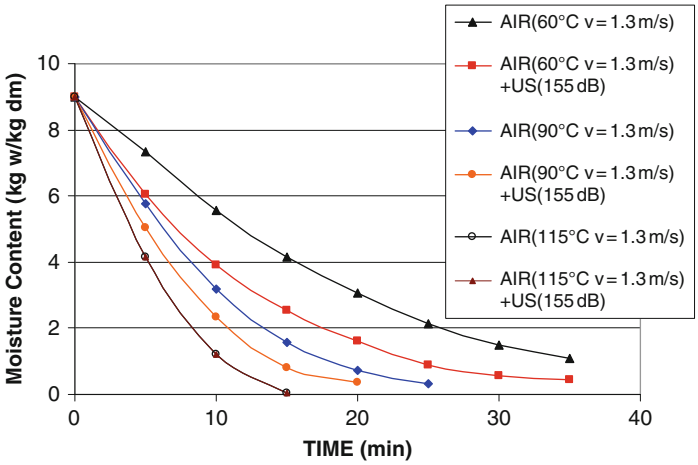

Fig. 25.7 Forced air dehydration kinetics of carrot slices at 1.3 m/s and various temperatures without and with airborne ultrasound (155 dB)

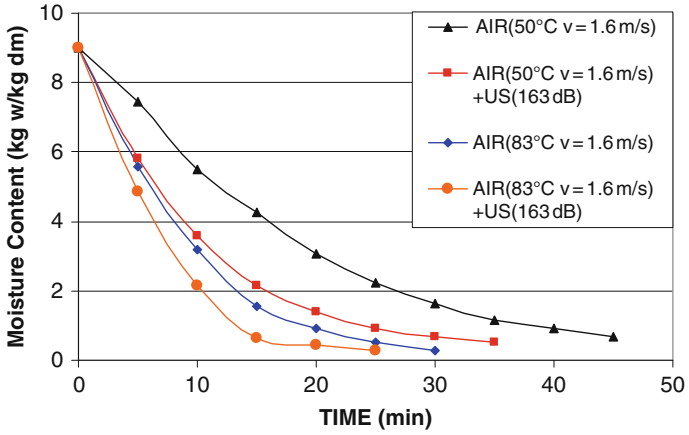

Fig. 25.8 Forced air dehydration kinetics of carrot slices at 1.6 m/s and various temperatures without and with airborne ultrasound (163 dB)

improvement seems to be relatively limited, and the use of airborne ultrasound could be restricted to specific products such as heat-sensitive materials and/or to special applications where rapid drying at low temperature is required.

3.2.2 Direct Contact Ultrasonic Dehydration

The main difficulty in dehydration by airborne ultrasonic radiation is the low penetration of acoustic energy in food material due to the mismatch between the acoustic

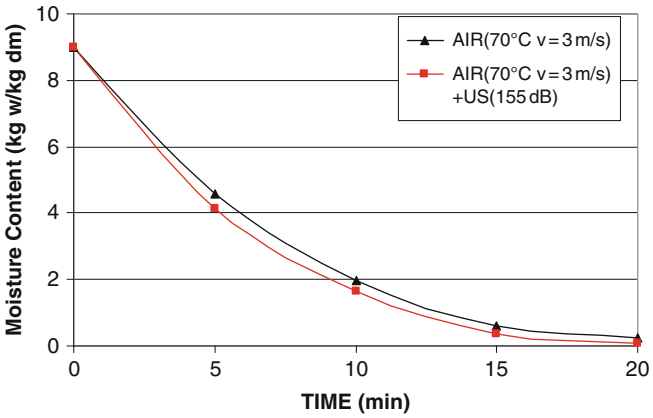

Fig. 25.9 Forced air dehydration kinetics of carrot slices at 3 m/s and 70°C without and with airborne ultrasound (155 dB)

impedance of air and that of the vegetable. In fact, the effectiveness of energy transfer between these two media very much depends on their acoustic impedances, defined as the product of the density by the sound speed in the material.

To increase energy transfer, a new procedure has been developed and tested in which ultrasonic vibration is applied in direct contact with the vegetable samples together with static pressure (Gallego-Juárez et al., 1996). Good acoustic impedance matching between the vibrating plate of the transducer and the food material favors the deep penetration of acoustic energy and increases the effectiveness of the process. The vegetable is subjected to high ultrasonic stresses which, due to the rapid series of contractions and expansions, produce a kind of "sponge effect" and a quick migration of moisture through natural channels or other channels created by the wave propagation, resulting in moisture release from the product. In addition, the production of ultrasonic cavitation inside the liquid may help the separation of the moisture strongly attached.

The experimental setup developed for the initial study of this process is presented in Fig. 25.10. The samples were placed on the surface of a support plate and the vibrating plate radiator of the transducer was kept in contact with the samples during treatment by applying static pressure. Air flow at 1 m/s and 22°C together with a suction system was also applied to facilitate the removal of moisture. The dehydration results obtained with carrot slices of circular shape with 2, 4, and 8 mm in thickness and 14 mm in diameter are shown in Fig. 25.11. It can be seen that the drying effect was remarkably improved by this process. In fact, the dehydration process is not only quicker and less energy consuming than forced air drying (with or without airborne ultrasound), but also more powerful: the final moisture content could be less than 1%. In addition, this process, which is basically due to mechanical action, perfectly preserves the quality of the product.

To interpret the experimental study, a mass transfer model was applied. This model is based on the use of the concept of effective diffusivity (D_e), which allows

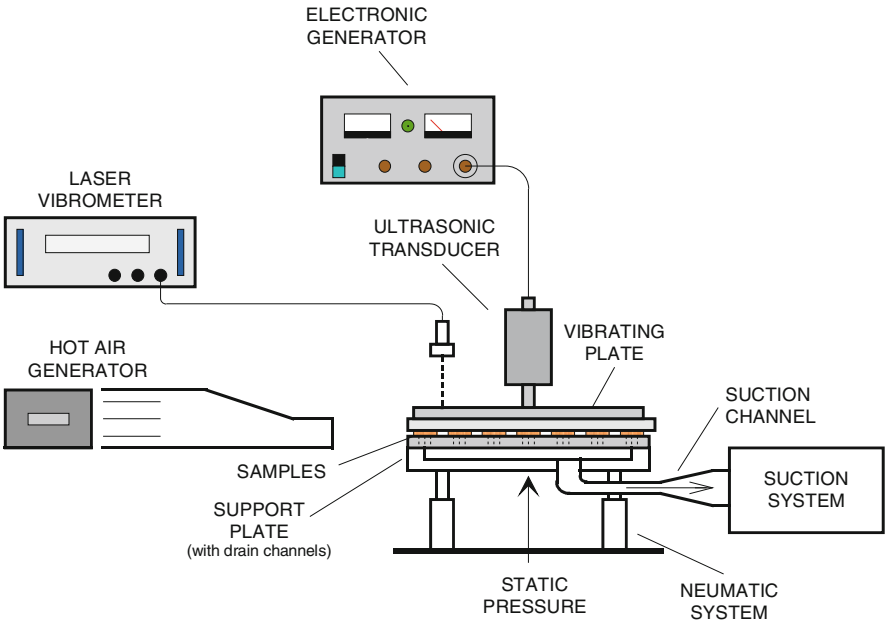

Fig. 25.10 Experimental setup for dehydration by direct contact ultrasonic vibration

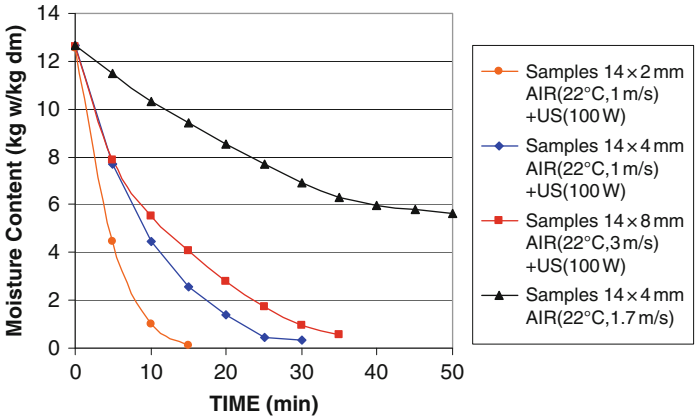

Fig. 25.11 Dehydration kinetics of carrot slices by direct contact ultrasonic vibration (100 W) and forced air at 22°C and various flow velocities. Comparison with forced air dehydration at 22°C and 1.7 m/s without ultrasound

us to describe the diffusion of moisture according to Fick's second law (Sablani et al., 2000):

$$\frac{\partial W}{\partial t} = D_e \nabla^2 (W) \tag{25.1}$$

where W is the moisture content on a dry basis (kg water/kg dry solid), D_e the effective diffusivity (m^2/s), and t the time.

Equation (25.1) can be integrated for different geometries and boundary/initial conditions. The solution of Equation (25.1) for a vegetable sample slice of thickness $2l$ is given by (Cranck, 1975)

$$W(t) = W_e + (W_o - W_e) \cdot \sum_{n=0}^{\infty} \frac{8}{(2n+1)^2 \cdot \pi^2} \cdot \exp\left(\frac{-D_e \cdot (2n+1)^2 \pi^2 t}{4\, l^2}\right) \tag{25.2}$$

where the subscripts indicate equilibrium (e) and initial conditions (o).

Drying kinetics were modeled using Equation (25.2), and the parameter D_e was calculated using a nonlinear regression method.

Dehydration curves and effective water diffusivity in apples and potatoes were calculated from Equation (25.2).

From the diffusional model, the effective water diffusivity coefficient was identified for experiments carried out at operational conditions. Identified D_e in these experiments in apples ranged from 2.93×10^{-08} m^2/s without ultrasound up to 8.84×10^{-07} m^2/s with ultrasound application and in potatoes from 2.2×10^{-08} m^2/s without ultrasound up to 1.37×10^{-07} m^2/s with ultrasound application.

For the extension of the new procedure to industrial applications, a multisample dehydration system capable of controlling the parameters of the process was developed (Gallego-Juárez et al., 2007). An example of this system is schematically presented in Fig. 25.12. It is constituted by the following parts: (a) treatment chamber; (b) ultrasonic power generator; (c) signals and power conditioner; (d) data acquisition unit; and (e) PC to monitor and control the parameters of the process. A depiction of the constructed dehydration system is shown in Fig. 25.13. The power ultrasonic generator is constituted by a rectangular plate transducer and an electronic unit for driving the transducer. In the design, the potential influence of the application of uniform pressure on the surface of the plate was also analyzed by FEM. No variation in the vibration mode of the plate was detected when static pressure was applied homogeneously to its entire surface (De la Fuente et al., 2006).

The drying process took place in the treatment chamber. The ultrasonic transducer was located at the upper part of the chamber. A parallelepipedic vacuum chamber, where the suction was applied, was fixed parallel to the transducer plate. Its upper porous surface acted as a multi-sample holder and also facilitated the removal of the moisture extracted from the samples. A pressure cylinder pneumatically controlled by a regulator was fixed at the bottom of the vacuum chamber and permitted the application of a constant force at the interface between transducer and samples. A forced air generator with flow rate and temperature control increased the removal of internal moisture, which was expelled to the lateral surfaces of the samples. The air velocity was controlled by PWM (pulse width modulation) and measured with a hot-wire anemometer in order to work at constant velocity. The temperature of the samples, measured with thermocouples, was recorded during the process and stored in a PC.

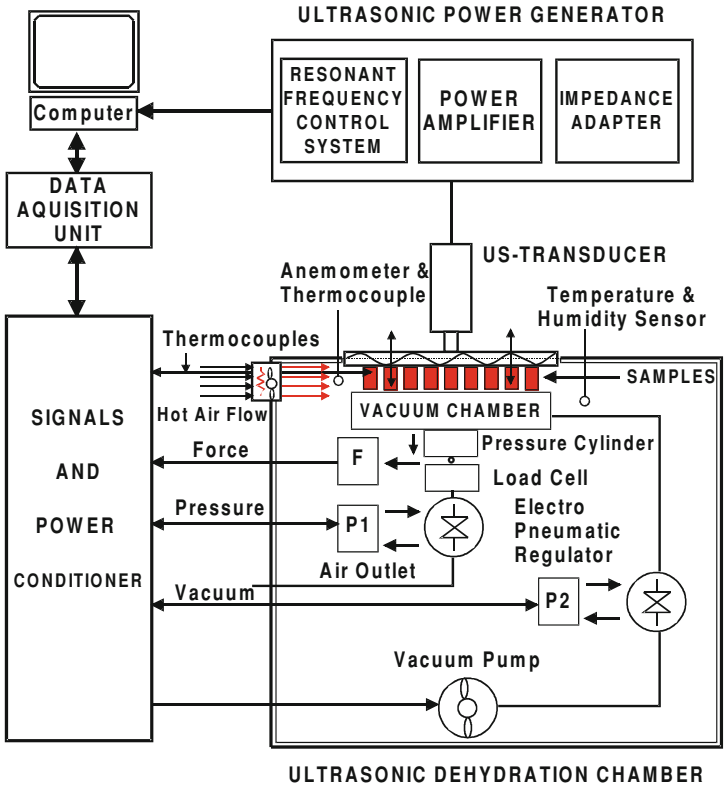

Fig. 25.12 Scheme of the direct contact multi-sample ultrasonic dehydration system

The electronic generator driving the ultrasonic transducer was composed of an impedance matching unit, a power amplifier, and a resonant frequency control system. This system was specifically developed to keep the power applied constant at the resonant frequency of the transducer during the process, independently of the variations of the acoustic impedance of the load. The ultrasonic generator has a maximum power capacity of about 250 W. The different parameters of the driving signal applied to the transducer (frequency, voltage, current, and phase) were continuously monitored and stored in a PC.

All the electro-mechanical and pneumatic devices installed in the treatment chamber were directly controlled by a PC by using specific software based on LabView® and Mathematica® codes.

The vegetable samples used for testing the dehydration system were carrots of cylindrical shape. The samples were cut into cylinders (24 mm in diameter and 8 mm in thickness). To prepare carrot samples for dehydration, some general rules were followed: choose tender vegetables, wash them, remove any damaged areas, and cut them into uniform-sized pieces. In addition, the samples were blanched for

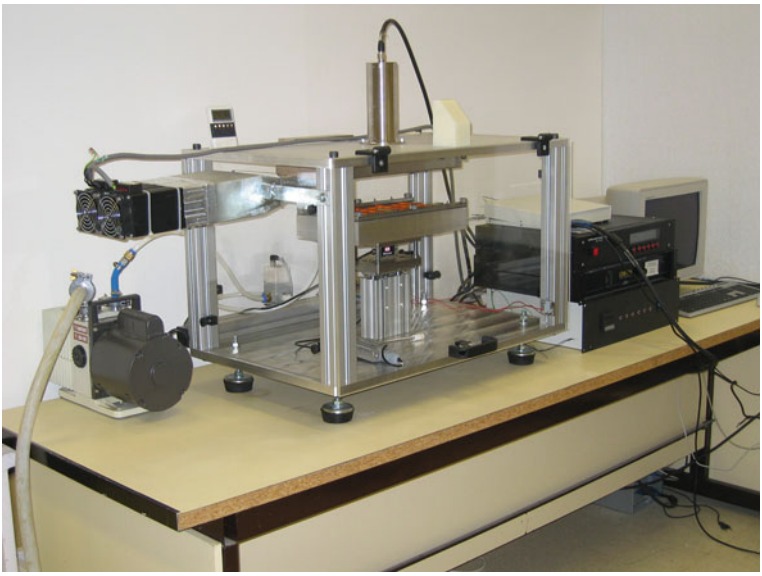

Fig. 25.13 Dehydration system

a certain amount of time in boiling water before being dried. This pretreatment was done to avoid enzyme attack and oxidation.

Experimental trials were carried out to study the influence of ultrasonic power (0, 25, 50, 75, and 100 W) in the kinetics of the dehydration process. In all tests the temperature and relative humidity were kept between 24 and 26°C and 30 and 46%, respectively. The applied static pressure was fixed at 0.06 kg/cm^2, the suction at 60 mbar, and the air flow velocity and temperature at 2 m/s and 30°C, respectively. Moisture content of samples was measured by weighing them at fixed intervals of 15 min. Figure 25.14 shows the evolution of the weight percentage (%) during the dehydration process of a set of 30 carrot samples with different applied ultrasonic powers. The curves obtained up to a maximum applied power of 100 W reveal a direct increase of the drying effect with the acoustic intensity, and no saturation was reached. This result confirms the significant role of ultrasonic intensity when other thermo-mechanical parameters (temperature, flow rate, and suction) are kept constant.

Another important characteristic to be considered in the performance of the multi-sample system is the homogeneity in the dehydration effect on all of the samples. To analyze such characteristics, a study on dehydration of various series of groups of 20 samples was carried out. This study consisted of measurements of the dewatering effect in each of the single samples along a process extending up to a point at which a 90% dehydration was reached during periodic time intervals. The results (Fig. 25.15) showed that the maximum dispersion in the dehydration effect among all the samples was about 12%. These results confirm the homogeneity in the dehydration action of the developed system.

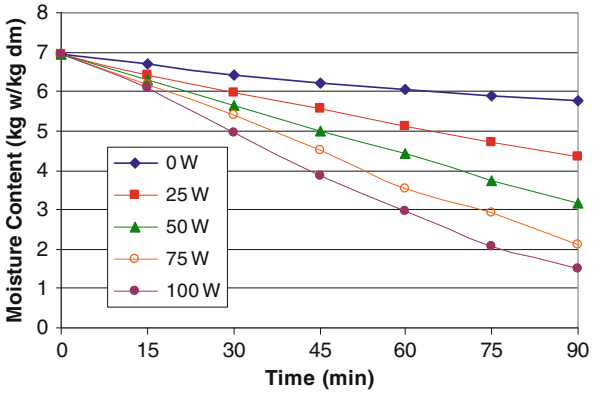

Fig. 25.14 Influence of ultrasonic power on the kinetics of direct contact ultrasonic dehydration process of carrot cylinders

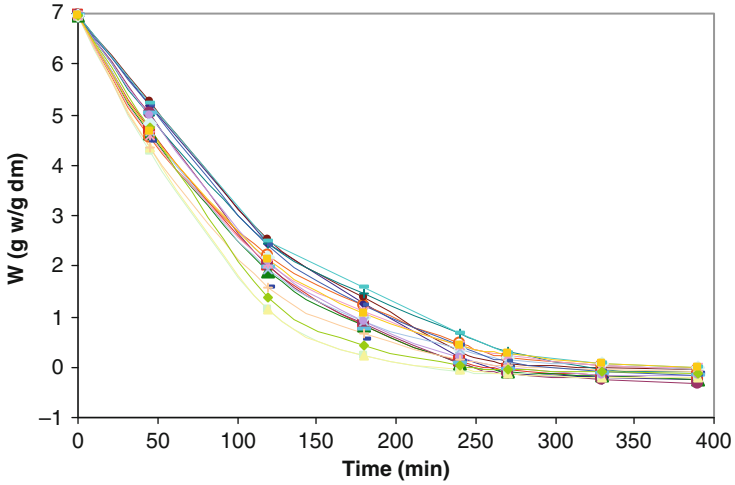

Fig. 25.15 Curves of direct contact ultrasonic dehydration of 20 carrot slices by using the multi-sample system

The new system constitutes the basic model to be scaled up for industrial applications.

3.3 Oil Extraction Processes with Supercritical Fluids Assisted by Power Ultrasound

Among the new opportunities for the food industry through new food processing technologies, power ultrasound is a promising and innovative method to assist in

the extraction of valuable compounds from food products. The efficiency of conventional techniques for extraction is based on the correct combination of solvent, temperature, and agitation (Mason, 1998; Mason et al., 1996). Supercritical fluid extraction (SFE) is a separation process based on the contact of a product containing the extractable compound with a solvent in supercritical conditions (King, 2002). The beneficial use of ultrasound in SFE is realized through its mechanical effects on the process: radiation pressure, acoustic streaming, compressions and rarefactions, and cavitation (Vinatoru, 2001). Such effects improve the extraction process by increasing the penetration of the solvent into the product and enhancing mass transfer to and from interfaces.

The use of supercritical fluids as extracting agents has been attracting wide interest for years and, in particular, supercritical carbon dioxide is considered nowadays as a very useful solvent in the extraction process because it is nontoxic, recyclable, cheap, relatively inert, and nonflammable (Balaban and Chen, 1992; Lang and Wai, 2001). Nevertheless, fixed bed SFE of oil from a solid matrix has a slow dynamic, even when solute-free solvent is recirculated. The use of power ultrasound represents a potentially efficient way to enhance mass transfer processes. In addition, this is probably the only practical way to produce agitation in SFE because of the inability of using mechanical stirrers.

As is well known, a *supercritical fluid* is a substance at a temperature and pressure above its thermodynamic critical point. It can diffuse through solids like a gas and dissolve materials like a liquid (Kodikowski et al., 1996). Fluids under supercritical conditions exhibit enhanced dissolving power and have transport properties that favor high extraction capabilities. In particular, supercritical fluids have relative lower viscosity and higher diffusivity than liquid solvents. Different substances have different critical temperatures and pressures. These properties are important in selecting appropriate fluid and operating conditions for application in SFE processes. Among all of the fluids studied, CO_2 nowadays remains the most commonly used for SFE applications because, in addition to its above-mentioned properties, its critical constants are low compared to other solvents ($T_c = 31.1°C; P_c = 73.8$ bar, $D_C = 0.468$ g/ml), and it is available in high purity at low cost. In particular, supercritical CO_2 is widely used in the extraction of essential oil from vegetable substrates.

The application of ultrasound in SFE has been proposed for both kinetics acceleration and yield improvement. In fact, an increase of about 10% in the yield of fresh wheat germ oil obtained in SFE assisted with ultrasound at 26.5 and 35 kHz was reported by Jun et al. (1997). The experiments were carried out on a laboratory scale with 50 g of two kinds of samples: wheat germ pieces and cylindrical granular samples (10 mm in height and 8 mm in diameter). The extraction pressure and temperature were 200–250 bar and 35°C, respectively. Each extraction experiment was performed over the course of 8 h. It was reported that ultrasound could penetrate into the solid material, caused micro-local turbulences within its interior, and decreased interparticle mass resistance. In addition, no decomposition of the oil was caused by power ultrasound since cavitation does not exist in supercritical fluids.

Better results were obtained by Riera et al. (2003, 2004) and Gallego-Juárez et al. (2005) on almond oil extraction by using supercritical CO_2 and 20 kHz power

ultrasound. The experiments were carried out in a pilot plant of SFE constituted by four stainless steel high-pressure extraction vessels 5 l in capacity, two separation vessels (a cyclone and a decanter), a diaphragm pump, and different sensors for monitoring and controlling the extraction temperature, pressure, and fluid flow rate (Fig. 25.16). The fluid used as a solvent in the extractor was supercritical CO_2. The ultrasonic transducer with a power capacity of about 100 W was installed in the upper part of the extractor vessel.

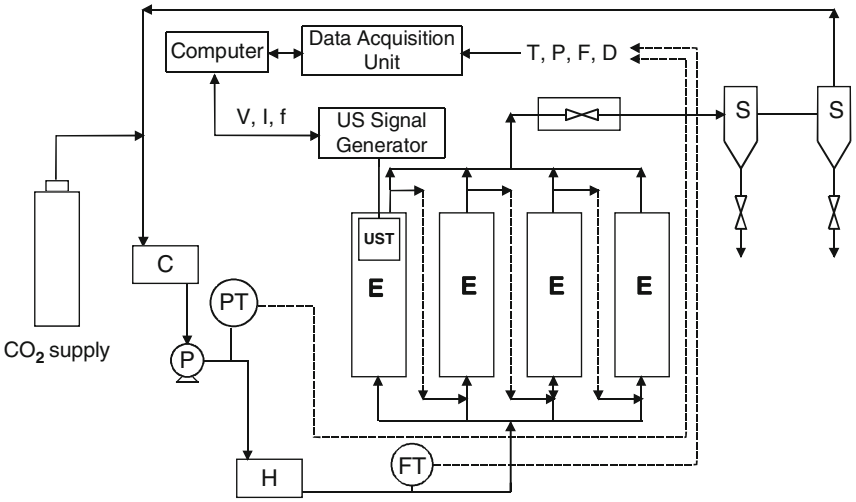

Fig. 25.16 Scheme of the experimental setup for ultrasound-assisted supercritical fluid extraction (USFE). Units: (E) extractors, (S) separators, (C) cooler, (P) high-pressure pump, (H) heater, (PT) pressure meter, (FT) flow meter, (UST) ultrasonic transducer. Electrical parameters: (V) voltage, (I) current. Extraction parameters: (T) temperature, (P) pressure, (F) CO_2 flow rate, (D) density

The experimental process was on oil extraction from ground almonds (55% oil content, wet basis) of different particle sizes (3–4 and 9–10 mm). The almonds, in an amount of 1,500 g, were placed in a basket inside the supercritical fluid extractor of 5 l in capacity, where the solvent was introduced at a flow rate of 20 kg/h. The solvent was CO_2 of 99% purity at 280 bar and 55°C. The average density reached was about 820 kg/m^3. The time for each trial was about 8 h and 30 min. To study and analyze the effect of ultrasound to assist supercritical extraction processes, all of the trials were carried out with and without ultrasound application. The results obtained with the application of the ultrasonic energy (a power applied to the transducer of 50 W) showed that the kinetics and the extraction yield were enhanced by 30 and 20%, respectively (see Fig. 25.17). It was experimentally shown that the initial stage of extraction, which is controlled by solute solubility, was less affected by ultrasound than the subsequent extraction stage, which is controlled by internal mass transfer. Moreover, the results showed that almond particulate size influences the extraction rate, with small particles favoring the ultrasonic action.

Balachandran et al. (2006a, b) studied the effect of power ultrasound during the extraction of pungent compounds from ginger. A power ultrasonic transducer

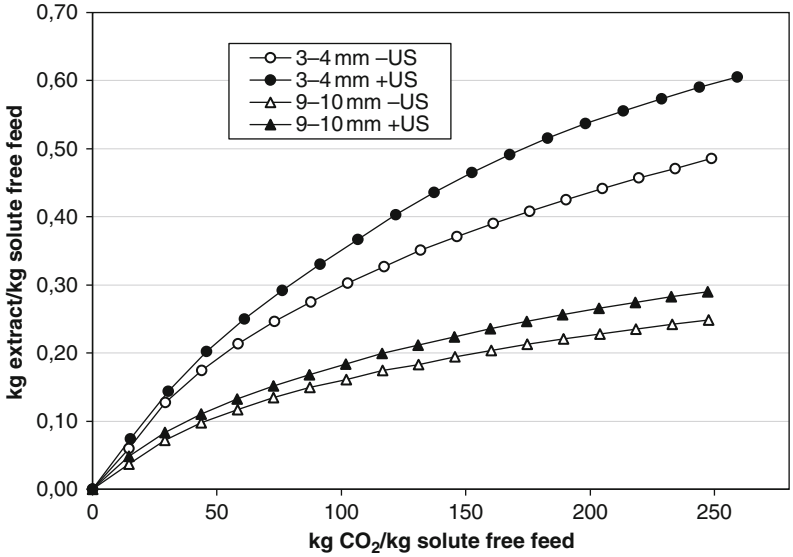

Fig. 25.17 Particulate almond oil extraction kinetics using supercritical CO_2 with and without ultrasound. Influence of particle size

operating at 20 kHz was applied to a laboratory-scale extraction vessel and the extraction of gingerols from freeze-dried ginger particles (4–8 mm) was monitored. The transducer was fitted externally to the wall of the extraction vessel and 300 W was applied during the trials. To maintain the temperature at 40°C the ultrasonic system and the extraction vessel were cooled in a water bath temperature controller (see Fig. 25.18). It was also found that by the application of ultrasonic energy, both the extraction rate and yield increased up to about 30% at 160 bar. The higher extraction rate was attributed to disruption of cell structures and to an increase in the accessibility of the solvent to the internal particle structure, which enhanced the intra-particle diffusivity.

Experiments were also performed at subcritical conditions below the CO_2 critical point (at liquid conditions 68 bar and 20°C). The influence of ultrasound was found to be similar in both cases (see Fig. 25.19). Therefore, it is apparent that the mechanism of intensification of mass transport due to physical effects caused by ultrasonic vibration may be used in both supercritical and subcritical conditions. The observed cellular damage could be caused by the rapid changes in fluid density induced by ultrasound, but also because the air pockets trapped within the ginger porous particles could expand under decompression and damage the cell walls of the particle.

Recently, Hu et al. (2007) investigated the solvent extraction of oil and coixenolide from adlay seeds using an experimental system similar to that used by Riera et al. (2005). Adlay seeds may be used as food for humans and in herbal medicine: both adlay oil and coixenolide are important components with many health benefits. Such components are normally obtained by mechanical (low yield) or chemical (organic solvents that can be harmful to human health and the environment)

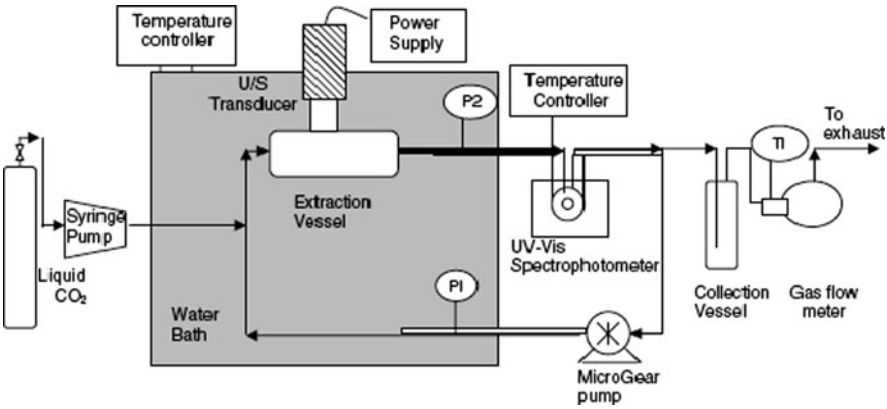

Fig. 25.18 Experimental setup for supercritical CO_2 extraction from ginger (from Balachandran et al., 2006a)

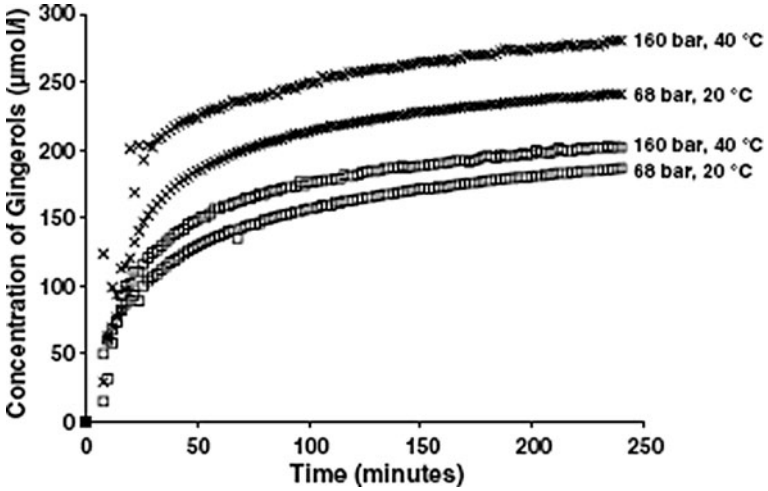

Fig. 25.19 Concentration of gingerols extracted vs. time for 4.3 mm particle size at different pressures and temperature conditions. x: with ultrasound, □: without ultrasound (from Balachandran et al., 2006a)

processes. To explore the ultrasound-assisted supercritical extraction (USFE) technique, a 20 kHz Langevin-type transducer was installed in the upper part of the extractor (1,000 ml pressurize vessel). The electrical powers applied to the transducers were set at 0, 50, 91, 97, and 110 W in different trials. The effect of ultrasound at various extraction temperatures (30–55°C) and pressures (100–320 bar) during treatment times of up to 4 h and 30 min, with CO_2 flow rates from 1.5 up to 4 l/h, was explored. An increase of 14% in the extracted yield from ground adlay seeds of 0.3–0.45 mm in diameter was obtained with ultrasound. The influence of the temperature and pressure values in the extraction yield was observed, as well as the extraction time and the CO_2 flow rate. Figure 25.20 shows that by using ultrasound,

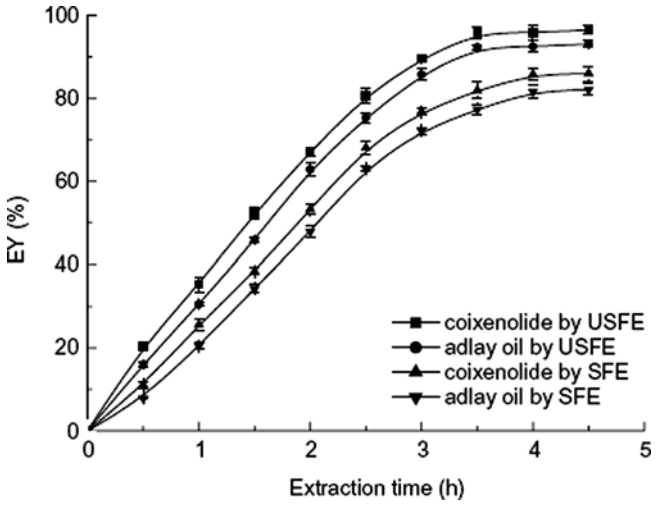

Fig. 25.20 Effect of extraction time on the yield of adlay oil and coixenolide: (●) adlay oil by USFE, (■) coixenolide by USFE, (▼) adlay oil by SFE, (▲) coixenolide by SFE at T=40°C and P=200 bar for USFE and T=45°C and P=250 bar for SFE. Other parameters: time = 3 h and 30 min, flow rate = 2.5 l/h, and ultrasound 110.5 W at 20 kHz (from Hu et al., 2007)

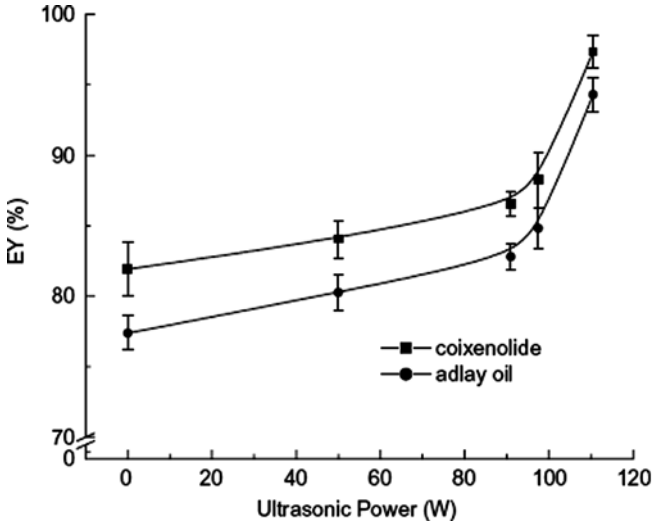

Fig. 25.21 Effect of power ultrasound on the yield of adlay oil and coixenolide: (●) adlay oil, (■) coixenolide. Other parameters: T=40°C, P=200 bar, time = 3 h and 30 min, flow rate = 3.5 l/h (from Hu et al., 2007)

more than 30 min in time are saved to obtain the same yield extracted, and the maximum yield is reached. The influence of the ultrasonic power level on the extraction process is shown in Fig. 25.21. The relevant conclusion is that the extraction time

and the CO_2 flow rate are reduced and the extraction yield is increased with the use of ultrasound.

Important efforts are presently being carried out (Riera et al., 2007) for the development of a pilot plant at the semi-industrial level, assisted by power ultrasound. To this purpose, new ultrasonic transducers for supercritical extraction processes in the frequency range from 18 kHz up to 50 kHz are under development.

4 Conclusions

It has been shown that airborne ultrasonic energy is useful to collapse surface foams, to dry vegetables, or to accelerate and enhance extraction processes in supercritical fluids. Until recently, such effects were simply laboratory curiosities or even unknown possibilities, but with the advent of powerful and efficient airborne ultrasonic systems with large radiating surfaces, pilot-scale applications have been realized. Such systems can introduce high acoustic energy into a large volume of gas, leading to the expectation that full-scale commercial applications will soon be available in the market place.

In food processing, a sustained growth of the use of high-intensity ultrasonic waves as a clean energy that is able to produce effects without deteriorating the quality of the food is to be expected.

References

Allen, C. H., and Rudnick, I., (1947). A powerful high frequency siren. *Journal of the Acoustical Society of America*, 19, 857–865.

Balaban, M. O., and Chen, C. S. (1992). Supercritical fluid extraction: Applications for the food industry. In: Hui, Y. H. (ed.), *Encyclopedia of Food Science and Technology*, vol. 4, pp. 2444–2449. John Wiley & Sons.

Balachandran, S., Kentish, S. E., and Mawson, R. (2006a). The effects of both preparation method and season on the supercritical extraction of ginger. *Separation and Purification Technology*, 48, 94–105.

Balachandran, S., Kentish, S. E., Mawson, R., and Ashokkumar, M. (2006b). Ultrasonic enhancement of the supercritical extraction from ginger. *Ultrasonics Sonochemistry*, 11, 471–479.

Boucher, R. M. G., and Weiner, A. L. (1963). Foam control by acoustic and aerodynamic means. *British Chemical Engineering*, 8, 808–812.

Cranck, J. (1975). *The mathematics of diffusion*. Oxford, UK, Clarendon Press.

De la Fuente, S., Riera, E., Acosta, V. M., Blanco, A., and Gallego-Juárez, J. A. (2006). Food drying process by power ultrasound. *Ultrasonics*, 44, e523–e527.

Deshpaude, N. S., and Barigou, M. (2000). Mechanical suppression of the dynamic foam head in bulk column reactors. *Chemical Engineering and Processing*, 39, 207–217.

Fairbank, H. V. (1975). Applying ultrasound to continuous drying process. *Ultrasonic International 1975 Conference Proceedings*, IPC Science and Technology Press Ltd, Guildford, UK, pp. 43–45.

Gallego-Juárez, J. A. (1998). Some applications of air-borne power ultrasound to food processing. In: Povey, M. J. W., and Mason, T. J. (eds.), *Ultrasonics in food processing*, pp. 127–143. London, Thomson Science.ISBN: 075140429.

Gallego-Juárez, J. A. (1999). High-power ultrasound. In: Webster, J. G. (ed.), *Wiley encyclopedia of electrical and electronics engineering*, vol. 9, pp. 49–59. New York, NY, Wiley.

Gallego-Juárez, J. A., Riera-Franco de Sarabia, E., De la Fuente, S., Rodríguez-Corral, G., Acosta-Aparicio, V. M., and Blanco-Blanco, A. (2007). Application of high power ultrasound for dehydration of vegetables: Processes and devices. *Drying Technology*, 25, 1893–1901.

Gallego-Juárez, J. A., Rodriguez-Corral, G., Acosta-Aparicio, V. M., Andrés-Gallego, E. Blanco-Blanco, A., and Montoya-Vitini, F. (2003). Sistema ultrasónico de desespumación mediante emisores con placa vibrante escalonada. *International Patent PCT/ES03/00465*.

Gallego-Juárez, J. A., Rodríguez-Corral, G., Gálvez Moraleda, J. C., and Yang, T. S. (1999). A new high intensity ultrasonic technology for food dehydration. *Drying Technology*, 17(3), 597–608.

Gallego-Juárez, J. A., Rodríguez Corral, G., Montoya-Vitini, F., Acosta-Aparicio, V. M., Riera-Franco de Sarabia, E., and Blanco-Blanco, A. (2005). Generador macrósonico para la desespumación industrial de líquidos por vía aérea. *International Patent, PCT/ES2005/070113*.

Gallego-Juárez, J. A., Rodríguez-Corral, G., Riera Franco de Sarabia, E., Campos Pozuelo, C., Vázquez Martínez, F., and Acosta Aparicio, V. M. (2000). A macrosonic system for industrial processing. *Ultrasonics*, 38, 331–336.

Gallego-Juárez, J. A., Rodríguez-Corral, G., Riera-Franco de Sarabia, E., Vázquez-Martínez, F., Acosta-Aparicio, V. M., and Campos-Pozuelo, C. (2001). Development of industrial models of high-power stepped-plate sonic and ultrasonic transducers for use in fluids. World Congress on Ultrasonics/IEEE International Ultrasonic Symposium, Atlanta 6–10 October 2001. *IEEE Ultrasonics Symposium Proceedings*, pp. 571–578.

Gallego-Juárez, J. A., Rodríguez-Corral, G., Riera-Franco de Sarabia, E., Vázquez-Martínez, F., Campos-Pozuelo, C., and Acosta-Aparicio, V. M. (2002). Recent developments in vibrating-plate macrosonic transducers. *Ultrasonics*, 40, 889–893.

Gallego-Juárez, J. A., Rodriguez-Corral, G., San Emeterio Prieto, J. L., and Montoya Vitini, F. (1994). Electroacoustic unit for generating high sonic and ultrasonic intensities in gases and interphases. *US Patent, no. 5,299,175*.

Gallego-Juárez, J. A., Yang, T., Vázquez Martínez, F., Gálvez Moraleda, J. C., and Rodriguez Corral, G. (1996). Procédé et dispositif de déshydratation. *International Patent no. WO9635340*, 14 November 96.

Ghildyal, N. P., Lonsane, B. K., and Karanth, N. G. (1988). Foam control in submerged fermentation: State of the art. *Advances in Applied Microbiology*, vol. 33, pp. 173–222. New York, NY, Academic.

Greguss, P. (1964). The applications of air-borne and liquid borne sounds to industrial technology. *Ultrasonics*, 2(1), 5–10.

Hartmann, J. (1939). Construction, performance and design of the acoustic air-jet generator. *Journal of Scientific Instruments*, 16, 140–149.

Hu, A., Zhao, S., Liang, H., Qiu, T., and Chen, G. (2007). Ultrasound assisted supercritical fluid extraction of oil and coixenolide from adlay seed. *Ultrasonics Sonochemistry*, 14, 219–224.

Jun, C., Kedie, Y, Shulai, C., Adschiri, T., and Arai, K. (1997). Effects of ultrasound on mass transfer in supercritical extraction. *4th International Symposium on Supercritical Fluids*, 11–14 May, Sendai, Japan, pp. 707–710.

King, J. W. (2002). Supercritical fluid extraction: Present status and prospects. *Grasas y Aceites*, 53(1), 8–21.

Kodikowski, A., Robertson, D. G., Aguiar-Ricardo, A. I., Popov, V. K., Howle, S. M., and Poliakoff, M. (1996). Probing vapour/liquid equilibria of near-critical gas mixtures by acoustics measurements. *Journal of Physical Chemistry*, 100, 9522–9526.

Lang, Q., and Wai, C. M. (2001). Supercritical fluid extraction in herbal and natural product studies – A practical review. *Talanta*, 53, 771–782.

Mason, T. J. (1998). Power ultrasound in food processing. In: Povey, M. J. W., and Mason, T. J. (eds.), *Ultrasound in food processing*, pp. 105–150. London, Blakie Academic and Professional.

Mason, T. J., Paniwnyk, L., and Lorimer, J. P. (1996). The uses of ultrasound in food technology. *Ultrasonics Sonochemistry*, 3, S253–S260.

Riera, E., Blanco, A., Acosta, V. M., Gallego-Juárez, J. A., Blasco, M., and Mulet, A. (2007). Prototype for the use of ultrasound in supercritical media. *Proceedings of the 19th International Congress on Acoustics ICA2007Madrid, CD Rom*, ULT-09-006-IP.

Riera, E., Gallego-Juárez, J. A., Montoya, F., Blanco, A., Mulet, A., Benedito, J. J., Peña, R., Golás, Y., Berna, A., Subirats, S., Blasco, M., and García, J. (2005). Separation or extraction method using supercritical fluids assisted by high-intensity ultrasound. *European Patent EP 1 547 679 A1*.

Riera, E., Golás, Y., Blanco, A., Gallego-Juárez, J. A., Blasco, M., García, J., and Subirats, S. (2003). *Effect of high-intensity ultrasound on the particulate almonds oil extraction kinetics using supercritical CO_2. 6th International Symposium on Supercritical Fluids*, 28–30 April, Versailles, France, Tome I, pp. 89–94.

Riera, E., Golás, Y., Blanco, A., Gallego-Juárez, J. A., Blasco, M., and Mulet, A. (2004). Mass transfer enhancement in supercritical fluids extraction by means of power ultrasound. *Ultrasonics Sonochemistry*, 11, 241–244.

Rodríguez, G., Gallego-Juárez, J. A., Ramos, A., Andrés, E., San Emeterio, J. L., and Montoya, F. (1985). High-power equipment for industrial defoaming. *Ultrasonics International 85 Conference Proceedings*, Butterworth, Guildford, Surrey, UK, ISBN 408 222 00X.

Sablani, S., Rahman S., and Al-Habi, N. (2000). Moisture diffusivity in foods. An overview. In: Mujumdar, A., and Arun, S. (ed.), *Drying Technology in Agriculture and Food Science*, pp. 35–50. Science Publishers, Inc.

Seya, K. (1970). Macrosonic drying. *Proceedings of the First International Symposium on High-power Ultrasonics, IPC Science and Technology*, Guildford, UK, pp. 136–140.

Viesturs, U. E., Kritapsons, M. Z., and Levitans, E. S. (1982). Foam in microbiological processes. In: A. Fiechter (ed.), *Advances in biochemical engineering*, pp. 169–224. Berlin, Springer.

Vinatoru, M. (2001). An overview of the ultrasonically assisted extraction of bioactive principles from herbs. *Ultrasonic Sonochemistry*, 8, 303–313.

Index

A

Acoustic cavitation, 13, 54–57
- chemical effects
  - primary radicals formation, 7–9
  - secondary radicals formation, 9
  - transient cavitation, 7
- chopped ultrasound, 54
- comparison with hydrodynamic cavitation reactors, 158–159
- defined, 2
- effects of sonoreactors, 183–185
- erosion by, 40
- fields (acoustics)
  - bubbly liquids, 44–45
  - calorimetric method (dissipative acoustics), 43–44
  - equation of linear acoustics, 41–42
  - non-dissipative acoustics, 42–43
- fields (bubble structures), 49
  - bubble layers (jellyfish and starfish), 50
  - bubble sizes and lifetimes, 51–52
  - clusters, 50–51
  - sonotrode cavitation and conical structures, 51
  - streamers and filaments, 50
- fields (forces exerted on bubbles)
  - added mass and viscous drag force, 49
  - primary Bjerknes force, 46–47
  - secondary Bjerknes force, 47–49
- fields (nucleation of bubbles), 45–46
- fields (simulation aspects)
  - continuum approach, 52–53
  - particle models, 53
  - unknowns, 52
- food ingredients modification, 347–348
- forced spherical single bubble, 18–19
  - radial oscillations, 19–26
  - rectified diffusion, 31–35
  - thermal effects, 26–31
- hydrodynamic cavitation analogy with, 157–158
- non-spherical oscillations, 36
  - collapses far from boundaries, 40–41
  - collapses near boundaries and erosion, 39–40
  - self-propulsion of non-spherical bubbles, 39
  - shape instabilities, 36–37
  - stability thresholds, 37–38
- physical effects, 2–7
  - boundary layers, 6
  - cavitation microstreaming, 4
  - inertial cavitation, 3
  - transient cavitation, 3–7
- quiet bubble
  - bubble ambient radius, 14–15
  - departure from spherical shape, 18
  - gas exchange with liquid, 17
  - radial equilibrium perturbations (free frequency), 16–17
  - radial mechanical stability (Blake threshold), 15–16
  - surface tension phenomenon, 14
  - translational motion, 18
- sonochemistry in food ingredients engineering, 240–242
- ultrasonic cleaning
  - cavitation formation mechanism, 548
  - frequency and cavitation abundance, 549–550
  - ultrasonic cavitations and surface cleaning, 550
- *See also* Controlled cavitation; Hydrodynamic cavitation; Ultrasonic cavitation

H. Feng et al. (eds.), *Ultrasound Technologies for Food and Bioprocessing*, Food Engineering Series, DOI 10.1007/978-1-4419-7472-3,
© Springer Science+Business Media, LLC 2011

Acoustic energy
density (AED), 108
effect on ultrasound-assisted hot air drying, 526–527
Acoustic microstreaming
food ingredients modification, 352
See also Streaming phenomena
Activation, *see* Enzymes activation/inactivation
Active power tracking (APT), 135–136
Aeration
controlled cavitation aspects, 202
See also ShockWave Power Reactor (SPR)
Afterbounces, *see under* Bubbles collapse
Aggregates formation, 389–390
Air
drying, *see* Ultrasound-assisted hot air drying
forced air dehydration assisted by airborne ultrasound, 625–627
ultrasonic inactivation of enzymes and, 395
velocity effect on ultrasound-assisted drying, 520–523
Airborne power ultrasound, 617–618
food processing applications, 620
dehydration of vegetables, 623–633
oil extraction processes with supercritical fluids, 633–639
ultrasonic defoaming in fermentation processes and in filling operation of gassy liquids, 621–623
technologies for food processing, 618–620
Alumina surface
Pd nanoparticles immobilized on, 429
Ambient radius
quiet bubble and, 14–15
See also Acoustic cavitation
Amorphous Fe nanocomposite
polystyrene, 426
Amplitude
ultrasonic waves influence on microbial inactivation, 323
See also Energy; Frequency; Intensity; Power
Anthocyanin, 575
Antioxidants
ultrasonic extraction and, 365
free radical scavengers, 398
See also Enzymes activation/inactivation; Food ingredients modification
Apple cider, 571
Apple juice, 570
Application system
in ultrasound-assisted hot air drying, 515
See also Transducers
Aqueous solutions
sonochemistry in, 245–247
See also Food ingredients engineering
Ascorbic acid, 578
Atomization, *see* Ultrasonic atomization
Average-phase-locked loop (APLL), 135

B

Bacterial inactivation mechanisms
MS/MTS, 308–311
See also Enzymes activation/inactivation; Manothermosonication (MTS)
Band-limited Hilbert transformer (BL-HT)
MMM technology, 135
Baths, 75
Bell peppers, 566
Beverages
milk as, 458
ultrasound applications in food processing
low intensity, 95
power ultrasound, 95
Biological systems
non-equilibrium thermodynamic theory for, 110–113
Biopolymer
molecular weight reduction of polymeric materials, 363–364
Bioprocessing, 141–583
cell disruption, 159–165
microbial disinfection, 165–168
See also Hydrodynamic cavitation; Ultrasonic membrane processing
Bjerknes force, 5
primary, 46–47
secondary, 47–49
See also Nucleation
Blake threshold
and rectified diffusion thresholds merging for small bubbles, 34–35
forced spherical single bubble, 23–25
radial mechanical stability
acoustic cavitation and, 16
quite bubble, 15
Blanching
conventional, 575
thermosonication, 575
Bovine serum albumin (BSA), 560, 564, 588
Bread, 95
Browning
nonenzymatic, 571
See also Color

Bubbles
acoustics phenomena fundamentals, 345–347
dynamics studies
bubble dynamics model improvements considering bubble/bubble and bubble/flow interactions, 152
cluster approach, 154–155
hydrodynamic cavitation reactors optimization based on, 149
simulations based on liquid continuum mixture model, 153
single cavity approach, 150–152
formation, 3–15
See also Acoustic cavitation
Bubbles collapse
afterbounces, 26
food ingredients modification nonlinearity and collapse, 348
forced spherical single bubble, 25–26
non-spherical collapses
far from boundaries, 40–41
near boundaries and erosion, 39–40
primary radicals formation, 7–9
secondary radicals formation, 9
sonoluminescence, 9–10
Bubbly liquids acoustics, 44–45

C

Cadmium chalcogenides (CdS), 435–436
Cake formation (ultrasonic membrane processing), 584
Calorimetric method
energy conservation and dissipation, 43–44
See also Non-dissipative acoustics
Carbon
nanofibers/polyurethane foam (CNFs/PU) composite, 428
Pt–Ru nanoparticles supported on carbon, 431
Carbon nanotubes (CNTs)
multi-walled (MWCNTs), 428
polymer-encapsulated carbon nanotubes by ultrasound initiated in in situ emulsion polymerization, 428
single-walled (SWNTs), 428
Catalysis
heterogeneous (sonochemical reaction), 251
See also Food ingredients engineering
CaviRex reactors, 176
See also Sonoreactors
Cavitation
cavitational yield, 156
defined, 2–141
inertial, 68
nuclei, 347
power ultrasound and, 82
See also Acoustic cavitation; Controlled cavitation; Hydrodynamic cavitation; Ultrasonic cavitation
Cavitation microstreaming, 352
See also Acoustic microstreaming
Cell disruption process, 159–165
See also Hydrodynamic cavitation
Ceria–zirconia-supported ruthenium, 432
Chalcogenides
cadmium (CdS), 435–436
copper (CuSe), 435
HgS and PbS nanoparticles, 435
lead (PbSe), 434–435
nanoparticles on silica submicrospheres, 433–434
metal chalcogenides with hollow spherical assembly, 436
zinc (ZnSe), 435
Chaos
forced spherical single bubble, 22–23
See also Cavitation
Cheese
power ultrasound processing, 461–462
ultrasound applications in food processing, 94
Chemicals
microbial inactivation aspects, 334–340
Chymosin, 449–462
See also Milk; Pasteurization
Clay nanocomposite
PMMA/montmorillonite, 425
polyurethane foam and, 425
PP and, 425
Cleaning
high-power ultrasound in, 545–557
membrane, 591–592
See also Ultrasonic membrane processing
microbial disinfection and industrial applications of high-power ultrasonics, 608–609
MMM technology applications, 136–139
precision, 550
ultrasonic cleaning
chemistry, 552–553
cleaning fluids selection, 553
equipment, 551–552

Cleaning (*cont.*)
mechanism, 554–557
particle removal, 555
power requirements, 551
redeposition prevention, 556–557
ultrasonic cavitations and surface cleaning, 550
ultrasonic cleaning mechanism
cavitation and micro-streaming, 546–547
cavitation formation mechanism, 548
frequency and cavitation abundance, 549–550
ultrasonic generation, 547–548
ultrasound applications in food processing, 98–99
See also Contaminants
Closed-loop control
MMM technology, 126
Clusters, 50–51
cluster approach, 154–155
See also Hydrodynamic cavitation
Cobalt nanoparticles, 409
See also Nanomaterials
Collapse, *see* Bubbles collapse
Color
parameter
browning, 571
lightness, 571
power ultrasound effect
milk pasteurization, 454–455
on food quality, 571–575
Compressibility
forced spherical single bubble, 20
liquid, 20
Concentration polarization, 584–585
See also Ultrasonic membrane processing
Condensation
elastic vibrations form, 66
single bubble (forced spherical)
thermal effects, 29–30
See also Evaporation
Conducting polymeric nanomaterials and composites, 426
PANI/nano-SiO_2, 428
polyaniline (PANI), 427
polypyrrole/Au nanoparticles, 428
polypyrrole/Pt nanoparticles, 428
Contaminants
inorganic, 554
insoluble particulate
hydrophilic, 553
hydrophobic substances, 553
organic, 554
particulate contaminants, 553
water insoluble, 554
water soluble, 554
See also Cleaning
Contamination-free sonoreactors, *see* Sonoreactors
Continuum approach
cavitation fields simulation, 52–53
Controlled cavitation, 191–208
aeration, 202
case study of cavitation using SPR, 203–204
emulsification, 201
gum/gel hydration, 201
mixing, 198
mixing thick liquids, 203
pasteurization, 198–200
production in SPR, 193–195
scale-free heating, 195–197
UV light using cavitation in SPR, 204–207
See also Acoustic cavitation; Hydrodynamic cavitation; Ultrasonic cavitation
Converging waves
acoustic waves, 175
cylindrical, 178–180
See also Sonoreactors
Copper, 413
chalcogenides (CuSe), 435
mixed oxide (CuO–ZrO_2 catalysts), 420
See also Nanomaterials
Co-solutes
ultrasonic inactivation of enzymes and, 397
Crossflow velocity effects
ultrasonic membrane processing, 590
Crystallization, 468
ice nucleation, 502–503, 505
industrial applications of high-power ultrasonics, 606
lipids, 272–273
reactive, 471
ultrasound applications in food processing, 97
See also Sonocrystallization
Curdling properties, 449
See also Milk; Pasteurization
Cutting, 211–234
conventional cutting principle, 213–215
practical aspects, 221–232
ultrasound-induced modifications cutting process, 217–221
See also Ultrasonic cutting

Cylinders
vibrating, 517–518
See also Ultrasound-assisted hot air drying

D
Dairy products processing
milk pasteurization, 447–448
enzymes, 449
physical–chemical characteristics, 451–455
proteins nutritional properties, 450–451
vitamins and minerals nutritional properties, 451
milk pasteurization (physical–chemical characteristics)
color, 454–455
density, 453
pH, 453–454
viscosity, 451–453
power ultrasound for, 445–446
cheese, 461–462
edible films, 463
microstructure of milk after sonication, 456–457
milk, 458–459
pasteurization of milk, 447–455
yogurt, 459–461
Defoaming
airborne power ultrasound food processing applications, 621–623
chemical defoaming, 622
physical methods, 622
ultrasonic defoaming, 622–623
industrial applications of high-power ultrasonics, 607–608
Dehydration, 623
direct contact ultrasonic, 627–633
forced air dehydration assisted by airborne ultrasound, 625–627
See also Drying
Denaturation
proteins, 371
See also Enzymes activation/inactivation
Density
milk pasteurization with power ultrasound, 453
Diagnostic ultrasound, 1
See also Power ultrasound
Diffusion, *see* Rectified diffusion
Digestibility (polysaccharides), 270–271
Dimeric enzymes, 390
See also Enzymes activation/inactivation
Direct contact ultrasonic dehydration, 627–633
Disinfection (microbial)
hydrodynamic cavitation applications, 165–168
industrial applications of high-power ultrasonics, 608–609
See also Cleaning
Diverging acoustic waves, 176
Drag force, 49
Drawing, 138
Drying
food drying process, 512–513
resistance control
external, 512
internal, 512
See also Dehydration; Ultrasound-assisted hot air drying

E
Edible
films, 463, 563, 565–566
oil, 567
Elastic vibrations forms
condensation, 66
rarefaction, 66
Electrical generators, 69
Electromagnetic (EM) waves, 68
Emitters forms
baths, 75
horns, 75
Emulsification
controlled cavitation aspects, 201
industrial applications of high-power ultrasonics, 605
Emulsion
polymerization (in situ), 428
stabilization, protein and, 254–256
See also Food ingredients engineering
Encapsulation
ultrasonic extraction and, 365–366
See also Food ingredients modification
Energy, 79
acoustic energy density (AED), 108
conservation (non-dissipative acoustics), 42–43
conservation (calorimetric method), 43–44
parameter (high-power ultrasonics in industrial applications), 601–602
See also Intensity; Power; Temperature
Enzymes, 258, 260–261
milk pasteurization with power ultrasound, 449
ultrasound treatments, 91–93

Enzymes (*cont.*)
and changes in food texture, 560, 564–566
mode of action in enzymes, 93
See also Food ingredients engineering; Proteins
Enzymes activation/inactivation
activation
biochemical effects, 389
enzyme release physical effects, 388
immobilized enzymes physical effects, 388
mass transfer and micro-mixing physical effects, 387–388
pretreatment procedures leading to enhanced enzyme activity, 388
basic principles, 369
inactivation (ultrasonic)
applications in food processing, 83, 91–93
enzyme concentration aspects, 396
kinetic inactivation considerations, 389
mode of action, 93
medium-related factors affecting ultrasonic inactivation of enzymes, 394
air, 395
antioxidants/free radical scavengers, 398
co-solutes, 397
enzyme concentration, 396
pH, 396–397
temperature, 395
ultrasound application, 394–395
mode of action (ultrasound), 392
free radicals-related effects on enzymes, 392–393
physical effects of sonication on enzymes, 393–394
oligomers
dimeric, 390
homohexameric, 391
tetrameric, 391
primary structure, changes in, 392
proteins denaturation by applied force, 371
secondary structure, changes in, 392
ultrasound in
aggregates formation, 389–390
basic principles, 369–371
kinetic activation considerations, 374–387
kinetic inactivation considerations, 374–389
mode of action, 392–394
oligomers breakdown, 390
physical effects, 372–373, 387–388
sonochemical effects, 373–374
See also Inactivation kinetics; Microbial inactivation; Thermosonication inactivation
Equilibrium radius, 15–16
Erosion
by acoustic cavitation, 40
See also Non-spherical oscillations
Evaporation
forced spherical single bubble thermal effects, 29–30
See also Condensation
External resistance (ER model), 519–520, 522
See also Ultrasound-assisted hot air drying
Extraction
food ingredients modification aspects, 355–358, 360–361, 363–366
industrial applications of high-power ultrasonics, 603–605
oil, 633–639
ultrasound applications in food processing, 97–98
See also Ultrasonic extraction
Extrusion
industrial applications of high-power ultrasonics, 608
MMM technology applications, 138–139

F

Fat globule
milk fat globule membrane (MFGM), 456–457
Fatty acid composition, 274–275
See also Lipids
Feedback loop, 131–132
Fermentation
airborne power ultrasound food processing applications, 621–622
industrial applications of high-power ultrasonics, 610
Ferrites
nanomagnetic oxide (ferrites) materials, 420–423
powders, 418
See also Nanomaterials
Filaments, 50
Films, edible, 463
Filtration
industrial applications of high-power ultrasonics, 606
See also Crystallization; Defoaming; Extraction; Extrusion; Separation

First-order kinetic models, 116–118
Flavors
  off-flavors, 570
  power ultrasound effect on, 566–571
  See also Food quality
Fluids, 348–350
  physical effects of sound on, 345
  See also Food ingredients modification; Streaming phenomena
Flux enhancement
  ultrasonic, 585–586
  See also Ultrasonic membrane processing
Foam
  foaming property, 99
  stabilization, 256
  See also Food ingredients engineering; Proteins
Food ingredients engineering, 239–277
  sonochemistry (fundamentals)
    basic sonochemical reactions, 242–251
    cavitation-driven chemical reactions, 240–242
  sonochemistry (in heterogeneous systems)
    heterogeneous catalysis, 251
    polymer degradation, 248–250
    polymer synthesis, 250
  sonochemistry (in homogeneous systems)
    aqueous solutions, 245–247
    organic solvents, 247–248
    thermolytic cleavage of water, 244–245
  ultrasound effect on functional properties of
    lipids, 271–275
    polysaccharide, 263–271
    protein, 252–262
  See also Power ultrasound, 239
Food ingredients modification
  acoustic microstreaming, 352
  bubble acoustics phenomena, 345–347
  cavitation, 347–348
  nonlinearity and collapse, 348
  physical effects of sound on fluids, 345
  practical ultrasonic separation, 352–355
  simultaneous extraction and modification
    and encapsulation, 365–366
    extraction and molecular weight reduction of polymeric materials, 363–364
    of antioxidant capacity and/or color, 365
  streaming phenomena, 348–352
    particle separation aspects, 351–352
    sound radiation pressure on sphere, 350–351
  ultrasonic extraction
    background, 355
    industrial extraction application and design, 361–363
    mechanisms and process development, 355–357
    process for functional compounds, 357–358
    separation of extracted components, 360
    simultaneous extraction and modification, 363–366
  ultrasonic opportunities for food industry, 358–360
  ultrasonic separation
    separation of extracted components, 360
Food processing, *see* Ultrasound applications in food processing
Food quality
  color, 571–575
  flavor, 566–571
  nutrients, 575–579
  texture, 560–566
  See also Food ingredients engineering; Food ingredients modification; Power ultrasound
Food seasoning, 535
  high power ultrasonic spray for, 535, 538–541, 543
    continuous atomization, 539–540
    registered pulsed spray, 540–543
  See also Ultrasound applications in food processing
Forced air dehydration
  assisted by airborne ultrasound, 625–627
  See also Drying
Forced spherical single bubble, *see under* Acoustic cavitation
Fouling
  membrane, 584
  See also Ultrasonic membrane processing
Fracture
  modification, 217–219
  See also Ultrasonic cutting
Free energy, 110
  See also Gibbs free energy
Free fatty acid (FFA), 566
Free frequency (radial equilibrium perturbations), 16–17

Free radicals, 449–453
related effects on enzymes activation/inactivation, 392–393
ultrasonic inactivation of enzymes
antioxidants/free radical scavengers, 398
Freezing, 496
preservation method, 495
ultrasound applications in food processing, 97
See also Ultrasound-assisted freezing
Frequency
influence on microbial inactivation, 324
power radiations and, 80–81
ultrasonic cleaning mechanism
frequency and cavitation abundance, 549–550
See also Intensity; Power
Friction
modification, 219–220
See also Ultrasonic cutting
Fruit juices, 571
Functional properties (food ingredients)
lipids, 271
crystallization, 272–273
fatty acid composition, 274–275
oxidative stability and rancidity development, 274
polysaccharides, 263–271
digestibility, 270–271
gelation, 270
immunology, 271
reactivity, 266–267
solubility, 265–266
thickening, 268–270
proteins, 252
emulsion stabilization, 254–256
enzyme activity, 258–261
foam stabilization, 256
gelation, 257–258
interfacial activity, 253–254
solubility, 252–253
thickening, 257
structural basis of observed modifications of protein functionalities, 261–262
Fungal enzymes, 449

G

Gas exchange
with liquid, 17
See also Acoustic cavitation
Gaseous cavitation cycle, 35
Gel, *see* gum/gel hydration
Gelation
polysaccharide, 270
protein, 257–258
See also Food ingredients engineering
Generators
for ultrasound-assisted hot air drying, 515
See also Transducers
Gibbs free energy, 110
Gold (Au), 412–413
nanoparticles on silica submicrospheres, 433
Au/alpha-Fe_2O_3 composite nanoparticles, 430
Au/Pd bimetallic nanoparticles, 414
nanoparticles in mesoporous silica, 431–432
polypyrrole/Au nanoparticles, 428
See also Nanomaterials
Gum/gel hydration
aspects, 201
See also controlled cavitation

H

Heat transfer
industrial applications of high-power ultrasonics, 610
See also High power ultrasonics
Heating
microbial inactivation
ultrasound and mild heating, 332–334
scale free, 195–197
See also Drying
Heinz and Knorr conception, 110
Hematite (alpha-Fe_2O_3)
nanosized hollow, 415
Heterogeneous systems
heterogeneous catalysis, 251
sonochemistry in
polymer degradation, 248–250
polymer synthesis, 250
See also Food ingredients engineering; Homogeneous systems
High frequency ultrasound, *see* Non-destructive ultrasound
High intensity ultrasound, *see* Power ultrasound
High molecular weight reduction of polymeric materials, 363–364
High power ultrasonics
in surface cleaning and decontamination, 545
cavitation and micro-streaming, 546–547

cavitation formation mechanism, 548
cleaning chemistry, 552–553, 557
cleaning chemistry and particles, 557
cleaning mechanism, 554–557
contaminants, 553
equipment, 551–552
frequency and cavitation abundance, 549–550
particle removal, 555
power requirements, 551
precision cleaning, 550
redeposition prevention, 556–557
ultrasonic cavitations and surface cleaning, 550
ultrasonic generation, 547–548
industrial applications of, 599
commercialization aspects, 611
commercialization aspects, lessons in, 612–614
crystallization, 606
defoaming, 607–608
emulsification, 605
extraction, 603–605
extrusion, 608
fermentation, 610
filtration and screening, 606
fudamentals, 600–601
heat transfer, 610
homogenization, 605
microbial disinfection and cleaning, 608–609
process and scale-up parameters, 601–603
separation, 607
viscosity alteration, 607
spray for food seasoning, 535, 538–541, 543
continuous atomization, 539–540
registered pulsed spray, 540–543
treatments and sonication effects, 81–82
High pressure homogenizer (HPH), 144–145
High speed homogenizer (HSH), 145–146
Hilbert transformer
band-limited (BL-HT), 134
Homogeneous systems
sonochemistry in
aqueous solutions, 245–247
organic solvents, 247–248
thermolytic cleavage of water, 244–245
See also Food ingredients engineering; Heterogeneous systems
Homogenization
industrial applications of high-power ultrasonics, 605
See also Extraction; Separation
Homogenizer
high-pressure (HPH), 144–145
high-speed (HSH), 145–146
Homohexameric enzymes, 391
Horns, 75
sonocrystallization reactor design, 472
Hot air drying, 511–513
See also ultrasound-assisted hot air drying
Hotspots, 81
Human milk, 459
Hydration, gum/gel, 201
Hydrodynamic cavitation, 141–170
analogy with acoustic cavitation, 157–158
applications
cell disruption, 159–165
microbial disinfection, 165–168
comparison with acoustic cavitation reactors, 158–159
future work aspects, 168–169
generation, 142–143
reactors configurations, 143
high-pressure homogenizer (HPH), 144–145
high-speed homogenizer (HSH), 145–146
liquid whistle reactors, 144
microfluidizers, 146
orifice plates setup, 147–149
reactors design
cavitational yield correlations development, 156
optimization, 149–155
reactors configurations, 143–149
reactors design optimization using bubble dynamics studies, 149
model improvements considering bubble/bubble and bubble/flow interactions, 152
cluster approach, 154–155
simulations based on liquid continuum mixture model, 153
single cavity approach, 150–152
See also Acoustic cavitation; Controlled cavitation; Ultrasonic cavitation
Hydroperoxide, 570
Hydrophilic particles, 553
See also Contaminants
Hydrophobic substances, 553

Hydrostatic pressure
effect on MS/MTS lethal effect, 296–297
Hydrothermal treatment
ultrasound-assisted, 417–418
nanomaterials (metal oxide), 417–418
Hydroxyapatite (HAP) nanoparticles, 437

I

Ice nucleation temperature, 502–505
Immobilized enzymes, 388
Immunology (polysaccharides), 271
In situ emulsion polymerization, 428
Inactivation kinetics, 115
first-order kinetic models, 116–118
non-linear inactivation models, 118–120
See also Enzymes activation/inactivation; Microbial inactivation; Thermosonication inactivation
Industrial applications (high-power ultrasound)
commercialization aspects
energy costs, competitive, 612
energy efficiency of equipment, improved, 611
high-amplitude/power units availability for large commercial operations, 611
installation ease, 612
intellectual property, strong potential for, 612
maintenance cost, low, 612
commercializing innovative technologies, lessons in, 612–614
crystallization, 606
defoaming, 607–608
emulsification, 605
extraction, 603–605
extrusion, 608
fermentation, 610
filtration and screening, 606
heat transfer, 610
high-power ultrasound fudamentals, 600–601
homogenization, 605
microbial disinfection and cleaning, 608–609
process and scale-up parameters
energy and intensity, 601–602
pressure, 602
temperature, 603
viscosity, 603
separation, 607
viscosity alteration, 607
Inertial bubbles
forced spherical single bubble
inertial oscillations, 25
thermal effects, 28–29
Inertial cavitation, 68
microbial inactivation, 322
physical effects, 3
power ultrasound and, 82–83
See also Non-inertial cavitation
Infrasound, 1
Inorganic contaminants, 554
Intellectual property, 612
See also High-power ultrasonics
Intensity
ultrasonic membrane processing and, 587–588
parameter and high-power ultrasonics in industrial applications, 601–602
See also Frequency; Power
Interactions
effect on MS/MTS lethal effect, 301–302
See also Microbial inactivation
Interfacial activity
protein, 253–254
See also Food ingredients engineering
Iron (Fe)
colloids, 409
Fe–FeC nanocrystalline particles, 434
nano-Fe into mesoporous titania pores, 431
nanocomposites
polystyrene/amorphous, 426
polystyrene/Fe_2O_3 nanocomposite, 425
oxides
Au/alpha-Fe_2O_3 composite nanoparticles, 430
nanosized hollow hematite (alpha-Fe_2O_3), 415

J

Jellyfish structure, 50

K

Kinetics, 115
enzyme, *see* Enzymes activation/inactivation
inactivation (kinetic models)
first order, 116–118
non-linear, 118–120
microbial inactivation
pasteurization, 108
sterilization, 108
power ultrasound processes, 107–108

L
Lactose
free milk, 458–459
recovery from whey (sonocrystallization case study)
experimental methodology, 476–477
operating parameters effect on lactose recovery and crystal habit, 477–481
process optimization using statistical analysis, 481–483
L-ascorbic acid, 578
Lead chalcogenides
PbS nanoparticles, 435
PbSe, 434–435
Lethal effect of ultrasonic waves under pressure, *see* Manothermosonication (MTS)
Linear oscillations
forced spherical single bubble, 20–22
thermal effects, 27
See also Radial oscillations
Lipase, 449
Lipids, 271
fatty acid composition, 274–275
lipids crystallization, 272–273
oxidative stability and rancidity development, 274
Lipolysis, 566–570
Liquid
bubbly, 44–45
compressibility, 20
continuum mixture model, 153
gas exchange with, 17
whistle reactors, 144
See also Acoustic cavitation; Hydrodynamic cavitation
Listeria monocytogenes, 447–448
Load parameter
MMM technology, 132–133
Low frequency ultrasound, *see* Power ultrasound
Low intensity ultrasound, *see* Non-destructive ultrasound
Lysosomal enzymes, 564
Lysosomes, 565

M
Manganese oxide
MnO_2 nanorods, 415
nanosized gamma-MnO_2, 415
nanosized hollow hematite (alpha-Fe_2O_3), 415
Manosonication (MS), 291
defined, 300
Manothermosonication (MTS), 313–314
defined, 300
environmental factors effect on MS/MTS resistance
factors prior to treatment, 302–305
factors simultaneous to treatment, 305–307
lethal effect of ultrasonic waves under pressure, 288–302
MS/MTS
bacterial inactivation mechanisms, 308–311
industrial processes, control of, 311–313
microbial inactivation kinetics, 289–292
microbial MS/MTS resistance, 292–294, 302–307
physical parameters effect on lethal effect, 294–302
physical parameters effect on MS/MTS lethal effect, 294
amplitude of ultrasonic waves, 295–296
hydrostatic pressure, 296–297
interactions, 301–302
temperature, 298–300
Mass transfer
enzyme activation kinetics, 387–388
ultrasound-assisted hot air drying, 513–514
Meat
colors, 575
tenderness, 565
Membrane processing, *see* Ultrasonic membrane processing
Mercury (HgS) nanoparticles, 435
Mesoporous
Fe-doped mesoporous TiO_2 powder, 424
nano-Fe into mesoporous titania pores, 431
silica
gold nanoparticles in mesoporous silica, 431–432
vesicles, 423
ZnS nanoparticle-assembled mesoporous structure, 424
See also Nanomaterials
Metal
chalcogenides with hollow spherical assembly, 436
phosphides, 437

Metastable zone (MZ), 470
Microbial disinfection
hydrodynamic cavitation applications, 165–168
industrial applications of high-power ultrasonics, 608–609
Microbial inactivation, 287–321
kinetics
pasteurization, 108
sterilization, 108
manothermosonication (MTS) for, 288–314
microbial MS/MTS resistance, 292–294
microbial MS/MTS resistance, environmental factors affect on, 302–307
MS/MTS bacterial inactivation mechanisms, 308–311
MS/MTS industrial processes, control of, 311–313
MS/MTS lethal effect, physical parameters effect on, 294–302
MS/MTS microbial inactivation kinetics, 289–292
microorganisms, 84–91
ultrasound action mechanisms, 322–331
future prospects, 340
inertial cavitation, 322
non-inertial cavitation, 322
ultrasonic waves, amplitude influence, 323
ultrasonic waves, external pressure influence, 324
ultrasonic waves, frequency influence, 324
ultrasonic waves, presence of impurities influence, 324
ultrasonic waves, temperature influence, 324
ultrasound and chemicals, 334–339
ultrasound and mild heating, 332–334
ultrasound and non-thermal physical factors, 339–340
See also Enzymes activation/inactivation; Inactivation kinetics; Thermosonication inactivation
Microfluidizers, 146
Micro-mixing, 387–388
Microorganisms (ultrasound treatments), 84–90
Aspergillus flavus, 84–86
B. subtilis, 86
Bacillus stearothermophilus, 85
E. coli, 85
Enterococcus faecium, 86
Lactobacillus acidophilus, 85
Listeria innocua, 86
Listeria monocytogenes, 85
Penicillium digitatum, 86
S. cerevisiae, 85–86
Salmonella, 85–86
ultrasonic mode of action in microorganisms, 90–91
Zygosaccharomyces bailii, 86
Microstreaming
acoustic, 352
cavitation, 4–352
ultrasonic cleaning mechanism, 546–547
See also Streaming phenomenon
Microwaves, 68.
See also Infrasound; Ultrasound
Milk
browning in, 571
microstructure after sonication, 456–457
milk fat globule membrane (MFGM), 456–457
power ultrasound processing
human milk, 459
lactose-free milk, 458–459
milk as beverage, 458
See also Yogurt
Milk pasteurization
physical–chemical characteristics
color, 454–455
density, 453
pH, 453–454
viscosity, 451–453
with power ultrasound, 447–451
enzymes, 449
proteins nutritional properties, 450–451
vitamins and minerals nutritional properties, 451
Minerals nutritional properties, 451
Mixing, 198
micro-mixing, 387–388
thick liquids, 203
See also Controlled cavitation
MMM technology, *see* Multi-frequency, multimode, modulated (MMM) technology
Molecular weight
reduction of polymeric materials, 363–364
Molybdenum oxide, 416
Montmorillonite clay nanocomposite, 425
Multi-frequency, multimode, modulated (MMM) technology, 125–140
applications, 136

ultrasonic cleaning, 136–137
ultrasonic drawing and extruding, 138–139
ultrasonic powder sieving and seed processing, 138
ultrasonic treatments and screening, 137–138
background and relevant theories
closed-loop control, 126
phase-locked loop (PLL), 128
pulse-width modulation (PWM) in power electronics, 128
operation mechanisms, 130
band-limited Hilbert transformer (BL-HT), 134
feedback loop benefits, 131–132
maximum active power tracking, 134–136
open-loop problems, 131
real-time load parameter estimation, 132–133
system components, 129–130
wideband technology, 125
Multi-walled carbon nanotubes (MWCNTs), 428
Myofibrillar protein, 564
Myofibrillar structure, 565

N

Nanoarrays TiO_2, 418
Nanocomposites, 425
Au/alpha-Fe_2O_3 composite nanoparticles, 430
carbon nanofibers/polyurethane foam (CNFs/PU) composite, 428
conducting polymeric nanomaterials and composites, 426
PANI/nano-SiO_2, 428
polyaniline (PANI), 427
polypyrrole/Au nanoparticles, 428
polypyrrole/Pt nanoparticles, 428
PMMA/montmorillonite clay nanocomposite, 425
polymer-encapsulated carbon nanotubes by ultrasound initiated in in situ emulsion polymerization, 428
polystyrene, 425–426
polyurethane foam/clay nanocomposite, 425
PP/clay nanocomposite, 425
SiO_2/PAPBA nanocomposite, 426
Nanocrystalline particles
Fe–FeC, 434
TiO_2, 418
ZrO_2, 418
Nano-Fe into mesoporous titania pores, 431
Nanomaterials, 405
bimetallic
Au/Pd nanoparticles, 414
Pt/Pd nanoparticles, 414
chalcogenides, 434
CdS, 435–436
CuSe, 435
HgS and PbS nanoparticles, 435
metal chalcogenides with hollow spherical assembly, 436
PbSe, 434–435
ZnSe, 435
hydroxyapatite (HAP) nanoparticles, 437
metal
cobalt, 409
copper nanoparticles, 413
Fe colloids, 409
gold nanoparticles, 412–413
noble metal, 410–412
ruthenium nanoparticles, 413
metal oxide, 414
MnO_2 nanorods, 415
molybdenum, 416
nanocrystalline TiO_2, 418
nanocrystalline ZnO_2, 418
nanosized gamma-MnO_2, 415
nanosized hollow hematite (alpha-Fe_2O_3), 415
nickel–zinc ferrite powders, 418
Sb_2O_3 nanobelts, 417
TiO_2 nanoarrays, 418
TiO_2 nanotubes and whiskers, 418
ultrasound-assisted hydrothermal treatment, 417–418
V_2O_5 nanowire bundles, 419
zinc oxide, 417
metal phosphides, 437
mixed oxide
CuO–ZrO_2 catalysts, 420
Gd_2O_3-doped CeO_2 nanoparticles, 419
nanomagnetic oxide (ferrites) materials
role of ultrasonic cavitation, 420–423
nanocomposites, 425
carbon nanofibers/polyurethane foam (CNFs/PU) composite, 428
conducting polymeric nanomaterials and composites, 426–428
PMMA/montmorillonite clay nanocomposite, 425

Nanomaterials (*cont.*)
polymer-encapsulated carbon nanotubes by ultrasound initiated in in situ emulsion polymerization, 428
polystyrene/amorphous Fe nanocomposite, 426
polystyrene/Fe3O4 nanocomposite, 425
polystyrene/Ni nanocomposite, 426
polyurethane foam/clay nanocomposite, 425
PP/clay nanocomposite, 425
SiO_2/PAPBA nanocomposite, 426
nanotubes, 437
nanowires, 437–438
porous materials, 423
Fe-doped mesoporous TiO2 powder, 424
mesoporous silica vesicles, 423
mesoporous TiO_2, 423
ZnS nanoparticle-assembled mesoporous structure, 424
supported/immobilized metallic nanoparticles, 429
Au/alpha-Fe2O3 composite nanoparticles, 430
ceria–zirconia-supported ruthenium, 432
gold nanoparticles in mesoporous silica, 431–432
metal (Pt, Pd, and Au) nanoparticles immobilization on TiO_2 surface, 431
nano-Fe into mesoporous titania pores, 431
Pd nanoparticles immobilized on alumina surface, 429
Pt on rutile TiO_2, 429–430
Pt–Ru nanoparticles supported on carbon, 431
SBA-15-supported Ru nanoparticles, 430–431
ultrasonic cavitation (nanomaterials preparation/formation), 408–432
cavitation generation, 407
bimetallic nanoparticles, 414
driving force responsible for nanoparticle formation, 407–408
metal nanoparticles, 409–414
metal oxide nanoparticles, 414–419
mixed oxide nanoparticles, 419–423
nanocomposites, 425–428
porous materials, 423–424
supported/immobilized metallic nanoparticles, 429–432
ultrasonic cavitation for production of, 406
ultrasound-assisted coating, 432
Ag nanoparticles on silica submicrospheres, 433
Au nanoparticles on silica submicrospheres, 433
chalcogenide nanoparticles on silica submicrospheres, 433–434
Fe–FeC nanocrystalline particles, 434
nano-Ni coating, 433
silver nanoparticles on nylon 6,6, 432
silver nanoparticles on wool fibers, 432
Nano-Ni coating, 433
Nanorods
MnO_2, 415
Nanotubes
SWCNTs, 437
TiO_2, 418
Nanowires, 437–438
V_2O_5 nanowire bundles, 419
Neglect it external resistance (NER model) , 519–522
See also Ultrasound-assisted hot air drying
Nickel
nano-Ni coating, 433
nickel–zinc ferrite powders, 418
polystyrene/Ni nanocomposite, 426
Noble metal, 410–412
See also Nanomaterials
Non-destructive technique (NDT), 84
Non-destructive ultrasound, 76
applications in food processing, 77, 93–95
beverages, 95
cheese and tofu, 94
overview, 77
See also Power ultrasound
Non-dissipative acoustics
energy conservation, 42–43
See also Calorimetric method
Nonenzymatic browning, 571
Non-equilibrium thermodynamics
theory for biological systems, 110–113
Non-inertial cavitation
microbial inactivation, 322
power ultrasound and, 82
See also Inertial cavitation
Non-linear inactivation models, 118–120
Non-linear oscillations
forced spherical single bubble
chaos, 22–23
non-linear resonances, 22

period doubling, 22–23
single bubble (forced spherical) thermal effects, 28
See also Linear oscillations
Nonlinearity
and collapse, 348
See also Food ingredients modification
Non-spherical oscillations
non-spherical collapses
far from boundaries, 40–41
near boundaries and erosion, 39–40
self-propulsion of non-spherical bubbles, 39
shape instabilities, 36–37
stability thresholds, 37–38
See also Radial oscillations
Non-thermal physical factors
ultrasound and, 339–340
See also Microbial inactivation
Nucleation
bubbles, 45–46
added mass and viscous drag force, 49
primary Bjerknes force, 46–47
secondary Bjerknes force, 47–49
ice, 502–505, *see also* Ultrasound-assisted freezing
Nutrients
power ultrasound effect on, 575–579
See also Food quality
Nylon
nylon 6, 6, 432
See also Nanomaterials

O

Off-flavors, 570
Oil extraction
processes with supercritical fluids, 633–639
See also Airborne power ultrasound
Oligomers
breakdown, 390
enzyme activation and inactivation
dimeric enzymes, 390
homohexameric enzymes, 391
tetrameric enzymes, 391
Open-loop problems
MMM technology, 131
Organic
contaminants, cleaning mechanism, 554
solvents, sonochemistry in, 247–248
Orifice plates
setup, 147–149
See also Hydrodynamic cavitation
Oxidative stability (lipids), 274

P

Palladium (Pd)
bimetallic nanoparticles
Au/Pd, 414
Pt/Pd, 414
nanoparticles immobilization
on alumina surface, 429
on TiO_2 surface, 431
Parametric instabilities
shape instability, 37
Particles models
cavitation fields simulation, 53
Particles removal
cleaning chemistry and particles, 557
defined, 555
mechanism, 555
See also Cleaning
Particles separation
particles much smaller than wavelength and larger than about 100 μm, 351–352
See also Streaming phenomena
Pasteurization, 108
controlled cavitation aspects, 198–200
milk pasteurization with power ultrasound, 447–448
enzymes, 449
physical–chemical characteristics, 451–455
proteins nutritional properties, 450–451
vitamins/minerals nutritional properties, 451
Pepsin, 449
See also Milk pasteurization
Period doubling, 22–23
pH
milk pasteurization with power ultrasound, 453–454
ultrasonic inactivation of enzymes and, 396–397
Phase-locked loop (PLL)
average (APLL), 135
MMM technology, 128
zero-phase-locked loop (ZPLL), 135
Phenolics, 575
Phosphides, 437
Piezoelectric (PZT) transducers, 547
Platinum nanomaterials
metal (Pt, Pd, and Au) nanoparticles immobilization on TiO_2 surface, 431
on rutile TiO_2, 429–430
polypyrrole/Pt, 428

Platinum nanomaterials (*cont.*)
Pt–Ru nanoparticles supported on carbon, 431
bimetallic (Pt/Pd), 414
PMMA/montmorillonite clay nanocomposite, 425
Polarization, *see* Concentration polarization
Poly(3-aminophenylboronic acid) (PAPBA), 426
Polyaniline (PANI), 427–428
Polymers
conducting polymeric nanomaterials and composites, 426
PANI/nano-SiO_2, 428
polyaniline (PANI), 427
polypyrrole/Au nanoparticles, 428
polypyrrole/Pt nanoparticles, 428
emulsion polymerization (in situ), 428
molecular weight reduction, 363–364
sonochemical reaction, 248–250
degradation
synthesis, 250
See also Food ingredients engineering; Polysaccharides
Polypyrrole/Au nanoparticles, 428
Polypyrrole/Pt nanoparticles, 428
Polysaccharides, 263–264
digestibility, 270–271
gelation, 270
immunology, 271
reactivity, 266–267
solubility, 265–266
thickening, 268–270
Polystyrene nanocomposites
polystyrene/amorphous Fe, 426
polystyrene/Fe_3O_4, 425
polystyrene/Ni nanocomposite, 426
Polyurethane foam
carbon nanofibers/polyurethane foam (CNFs/PU) composite, 428
clay nanocomposite, 425
Pore
blockage, 584
See also Ultrasonic membrane processing
Porous nanomaterials
mesoporous silica vesicles, 423
mesoporous TiO_2
Fe-doped mesoporous TiO_2 powder, 424
wormhole-like framework structures, 423
ZnS nanoparticle-assembled mesoporous structure, 424
Postmortem proteolysis, 564
Powder sieving
MMM technology applications, 138
Power
cavitation and, 82
electronics, PWM in, 128
high-power sonication effects, 81–82
MMM technology maximum active power tracking, 134–136
strength of treatment and, 78
strength of treatment measurement and frequency aspects, 80–81
power intensity, 80
vibrational amplitude, 79
ultrasonic cleaning power requirements, 551
See also Frequency; Intensity
Power ultrasound, 76–78–82
airborne, *see* Airborne power ultrasound
applications in food processing (beverages), 95
dairy products processing, 445–446
cheese, 461–462
edible films, 463
microstructure of milk after sonication, 456–457
milk, 458–459
pasteurization of milk, 447–455
yogurt, 459–461
defined, 1
food drying and, *see* Ultrasound-assisted hot air drying
food ingredients engineering, 239–277
lipids, 271–275
polysaccharides, 263–271
proteins, 252–262
sonochemistry fundamentals, 240–251
food quality and, 559
color, 571–575
flavor, 566–571
nutrients, 575–579
texture, 560–566
inertial versus non-inertial cavitation, 82–83
overview, 78
processes
kinetics aspects, 107–108
thermodynamic aspects, 107–115
thermodynamics, 107–115
non-equilibrium, 110–113
thermo-sonication, 108–109, 114–115
thermo-sonication inactivation

abnormality, 108–109
cut-off temperature for, 114–115
See also High power ultrasonics; Non-destructive ultrasound
PP/clay nanocomposite, 425
Precision cleaning, 550
Pressure
external pressure influence on microbial inactivation, 324
lethal effect of ultrasonic waves under pressure, *see* Manothermosonication (MTS)
parameter and high-power ultrasonics in industrial applications, 602
sonoreactors operating under pressure, 180–181
ultrasonic membrane processing aspects and, 588–590
See also Temperature
Primary Bjerknes force, 46–47
Primary radicals, 7–8
Process optimization
statistical analysis using, 481–483
See also Sonocrystallization
Protease, 449
See also Milk pasteurization
Proteins
denaturation by applied force, 371
functionality engineering by high-intensity ultrasound, 252
emulsion stabilization, 254–256
enzyme activity, 258–261
foam stabilization, 256
protein gelation, 257–258
protein interfacial activity, 253–254
protein solubility, 252–253
protein thickening, 257
structural basis of observed modifications of protein functionalities, 261–262
nutritional properties and milk pasteurization with power ultrasound, 450–451
ultrasound treatment and changes in food texture, 560, 564–566
See also Enzymes activation/inactivation; Food ingredients engineering
Proteolysis, 462–564
postmortem
Pulsed electric fields (PEF) waves, 68
Pulse-width modulation (PWM), 128

Q

Quality assurance
ultrasound applications in food processing
beverages, 95
bread, 95
cheese and tofu manufacturing, 94
product identification aspects, 96–97
See also Food quality, 560

R

Radial equilibrium
perturbations (Free frequency), 16–17
See also Acoustic cavitation
Radial mechanical stability (Blake threshold)
acoustic cavitation and, 15–16
Radial oscillations
forced spherical single bubble
bubble collapse, 25–26
dynamical Blake threshold, 23–25
inertial oscillations, 25
linear oscillations, 20–22
liquid compressibility effects, 20
non-linear oscillations, 22
Rayleigh–Plesset equations, 19–20
See also Linear oscillations
Radicals
cavitation chemical effects
primary radicals, 7–9
secondary radicals, 9
free radicals, 449–453
antioxidants/free radical scavengers, 398
related effects on enzymes activation/inactivation, 392–393
Radio frequency (RF) waves, 68
Radius
bubble ambient radius (quite bubble), 14–15
radial
equilibrium perturbations (Free frequency), 16–17
mechanical stability (Blake threshold), 15–16
Rancidity, lipids, 274
Rarefaction
elastic vibrations form, 66
Rayleigh–Plesset equations
radial oscillations (forced spherical single bubble), 19–20
Rayleigh–Taylor instability
shape instability, 36
shape instability thresholds, 37–38
Reactive crystallization, 471

Reactivity, polysaccharide, 266–267
Reactors, 75–76
sonoreactors, 175–189
ShockWave Power Reactor (SPR), 191–195
See also Hydrodynamic cavitation; Sonocrystallization
Rectified diffusion, 3–347
forced spherical single bubble
bibliography, 32–34
Blake and rectified diffusion thresholds merging for small bubbles, 34–35
physics, 31–32
threshold, 32, 34–35
Redeposition prevention, 556–557
See also Cleaning
Resonances
non-linear (forced spherical single bubble), 22
Ruthenium, 413
ceria–zirconia-supported ruthenium, 432
Pt–Ru nanoparticles supported on carbon, 431
SBA-15-supported Ru nanoparticles, 430–431
Rutile titanium oxide
Pt on, 429–430

S

Sb (Sb_2O_3) oxide nanobelts, 417
SBA-15-supported Ru nanoparticles, 430–431
Scale-free heating, 195–197
See also Controlled cavitation
Screening
industrial applications of high-power ultrasonics, 606
MMM technology applications, 137–138
Seasoning
snack food seasoning coating, 535–536
See also Ultrasound applications in food processing
Secondary Bjerknes force, 47–49
Secondary radicals formation, 9
Seed processing
MMM technology applications, 138
Separation
food ingredients modification
practical ultrasonic separation aspects, 352–355
streaming phenomena, 351–352
industrial applications of high-power ultrasonics, 607
See also Ultrasonic separation
Shape instabilities
non-spherical oscillations, 36–38
parametric instabilities, 37
Rayleigh–Taylor instability, 36
stability thresholds, 37–38
ShockWave Power Reactor (SPR), 191
case study of cavitation using SPR, 203–204
cavitation production in, 193–195
UV light using cavitation in SPR, 204–207
Sieving
MMM technology applications, 138
powder, 138
Silicon oxide
gold nanoparticles in mesoporous silica, 431–432
PANI/nano-SiO_2, 428
silica submicrospheres
Ag nanoparticles on, 433
Au nanoparticles on, 433
chalcogenide nanoparticles on, 433–434
SiO_2/PAPBA nanocomposite, 426
Silver (Ag)
nanoparticles on
nylon 6, 6, 432
silica submicrospheres, 433
wool fibers, 432
Simulations
based on liquid continuum mixture model, 153
See also Hydrodynamic cavitation
Single bubble (forced spherical), 18
radial oscillations
bubble collapse, 25–26
dynamical Blake threshold, 23–25
inertial oscillations, 25
linear oscillations, 20–22
liquid compressibility effects, 20
non-linear oscillations, 22
Rayleigh–Plesset equations, 19–20
rectified diffusion
bibliography, 32–34
Blake and rectified diffusion thresholds merging for small bubbles, 34–35
physics, 31–32
rectified diffusion threshold, 32
thermal effects
cavitation temperatures measurement, 31
inertial bubbles, 28–29
linear oscillations, 27
non-linear oscillations, 28
physics, 26–27

solvent evaporation and condensation, 29–30
sonochemistry relevance, 30–31
See also Acoustic cavitation; Non-spherical oscillations
Single bubble sonoluminescence (SBSL), 18
Single cavity approach, 150–152
Single walled carbon nanotubes (SWNTs), 428–437
Siren and whistle systems, 515–516
Small bubbles
Blake and rectified diffusion thresholds merging for, 34–35
Snack food seasoning coating, 535–536
conveyor belt, 536
tumble drum, 536
See also Ultrasound applications in food processing; Ultrasonic atomization
Sodium caseinate (SC), 565
Solids concentration, 590–591
Solubility
polysaccharide, 265–266
protein, 252–253
ultrasound applications in food processing, 99
See also Food ingredients engineering
Solvent
evaporation, 29–30
organic solvents, sonochemistry in, 247–248
Sonication
high-power, 81–82
milk microstructure after, 456–457
physical effects of sonication on enzymes activation/inactivation, 393–394
thermo-sonication inactivation
abnormality, 108–109
cut-off temperature for, 114–115
See also Manosonication (MS); Manothermosonication (MTS)
Sonochemistry, 176
enzyme activation and inactivation, 373–374
heterogeneous systems
heterogeneous catalysis, 251
polymer degradation, 248–250
polymer synthesis, 250
homogeneous systems
sonochemistry in aqueous solutions, 245–247
sonochemistry in organic solvents, 247–248
thermolytic cleavage of water, 244–245
in food ingredients engineering
basic sonochemical reactions, 242–251
cavitation-driven chemical reactions, 240–242
thermal effects (forced spherical single bubble), 30–31
Sonocrystallization, 467
future work aspects, 490–491
lactose recovery from whey (case study)
experimental methodology, 476–477
operating parameters effect on lactose recovery and crystal habit, 477–481
process optimization using statistical analysis, 481–483
literature overview, 483–490
mechanism, 469–472
metastable zone (MZ), 470
polymorphism aspects, 471
reactive crystallization, 471
reactor designs, 472–476
horns, 472
transducer, 473–475
Sonoluminescence
bubble collapse and, 9–10
See also Cavitation
Sonoreactors, 175–189
actual systems, 181–183
SR-31, 181–182
SR-42, 182
confined acoustic cavitation, powerful effects of, 183–185
costs of operation, 188
efficiency, 186–187
exclusive sonoreactor system, 177–178
SR-31, 177
SR-42, 177
known industrial sonoreactors, 177
CaviRex, 176
operating under pressure, 180–181
processing capacity, 187–188
processing conditions and versatility, 185–186
using cylindrical converging waves, 178–180
Sonotrodes, 75–176
cavitation and conical structures, 51
Sound, 350
physical effects on fluids, 345
See also Acoustic cavitation; Food ingredients modification; Streaming phenomena; Ultrasound

Sphere
sound radiation pressure on, 350–351
See also Streaming phenomena
Spherical oscillations, *see* Single bubble (forced spherical)
Spherical shape
departure from, 18
See also Acoustic cavitation
Sponge effect, 82
Spray for food seasoning, *see* Food seasoning
Stable cavitation, *see* Non-inertial cavitation
Starfish structure, 50
Statistical analysis
process optimization using, 481–483
See also Sonocrystallization
Steady streaming, 2
Stepped plates
transducers (airborne power ultrasound), 619
ultrasound-assisted hot air drying, 516–517
Sterilization, 108
Streamers, 5–50
Streaming phenomena
food ingredients modification, 348–352
particle separation aspects, 351–352
sound radiation pressure on sphere, 350–351
See also Acoustic microstreaming
Sunflower oil, 567–568, 570
Supercooling, 503–504
for ice nucleation, 504
See also Ultrasound-assisted freezing
Supercritical fluids
defined, 634
oil extraction processes with, 633–639
Supported/immobilized metallic nanoparticles, 429
Au/alpha-Fe_2O_3 composite nanoparticles, 430
ceria–zirconia-supported ruthenium, 432
gold nanoparticles in mesoporous silica, 431–432
metal (Pt, Pd, and Au) nanoparticles immobilization on TiO_2 surface, 431
nano-Fe into mesoporous titania pores, 431
Pd nanoparticles immobilized on alumina surface, 429
Pt on rutile TiO_2, 429–430
Pt–Ru nanoparticles supported on carbon, 431
SBA-15-supported Ru nanoparticles, 430–431
Surface activity
protein, 253–254
See also Food ingredients engineering
Surface cleaning, *see* Cleaning
Surface tension (quiet bubble), 14

T

Temperature
effect on
microbial inactivation, 324
MS/MTS lethal effect, 298–300
ultrasound-assisted hot air drying, 523–525
ice nucleation, 502–505
measurement (cavitation)
rectified diffusion, 32
thermal effects, 31
parameter for high-power ultrasonics in industrial applications, 603
thermo-sonication inactivation, cut-off temperature for, 114–115
ultrasonic inactivation of enzymes and, 395
ultrasonic treatments and, 81
See also Frequency; Power; Ultrasound-assisted freezing
Tenderness, 564–565
See also Food quality
Tetrameric enzymes, 391
Texture
power ultrasound effect on, 560–566
See also Food quality
Thawing, 97
Thermal effects
forced spherical single bubble
cavitation temperatures measurement, 31
solvent evaporation and condensation, 29–30
sonochemistry relevance, 30–31
thermal effects inertial bubbles, 28–29
thermal effects linear oscillations, 27
thermal effects non-linear oscillations, 28
thermal effects physics, 26–27
Thermodynamics
non-equilibrium thermodynamic theory for biological systems, 110–113
power ultrasound processes, 107
See also Acoustic energy density (AED)
Thermolytic cleavage of water
sonochemical reaction, 244–245
See also Food ingredients engineering

Thermosonication
blanching, 575
thermoultrasonication, 332
Thermosonication inactivation
abnormality, 108–109
cut-off temperature, 114–115
See also Enzymes activation/inactivation; Inactivation kinetics; Microbial inactivation
Thickening (polysaccharide), 268–270
Tissue orientation
ultrasound and, 505–507
See also Ultrasound-assisted freezing
Titanium oxide
mesoporous
Fe-doped, 424
nano-Fe, 431
wormhole-like framework structures, 423
metal (Pt, Pd, and Au) nanoparticles immobilization on TiO_2 surface, 431
nanoarrays, 418
nanocrystalline TiO_2, 418
nanotubes and whiskers, 418
Pt on rutile TiO_2, 429–430
ultrasound-assisted hydrothermal treatment, 418
Tofu
ultrasound applications in food processing, 94
See also Cheese; Milk
Total free amino acids (TFAAs), 566
Transducers, 75
airborne power ultrasound, 618–620
piezoelectric (PZT), 547
sonocrystallization reactor design, 473–475
ultrasound-assisted hot air drying, 515
Transient cavitation
chemical effects, 7
physical effects, 3–7
Translational motion, 18
Traveling wave, 67
Treatments
MMM technology applications, 137–138

U

Ultrasonic atomization
continuous atomization, 539–540
fundamentals, 536–538
registered pulsed spray, 540–543
ultrasonic atomizers for seasoning applications, 538
Ultrasonic cavitation, 347
cleaning mechanism, 546–547
for nanomaterials preparation, 408
bimetallic nanoparticles, 414
metal nanoparticles, 409–414
metal oxide nanoparticles, 414–419
mixed oxide nanoparticles, 419–423
nanocomposites, 425–428
porous materials, 423–424
supported/immobilized metallic nanoparticles, 429–432
for nanomaterials production, 406
driving force responsible for nanoparticle formation, 407–408
generation, 407
nanomagnetic oxide (ferrites) materials role of, 420–423
See also Acoustic cavitation; Controlled cavitation; Hydrodynamic cavitation
Ultrasonic cutting, 211–234
material properties and cutting performance, 224–228
homogenous and compact materials, 224
plant and animal tissues, 226
porous products, 225
practical aspects of ultrasonic cutting of foods, 221–223
cutting movement, 231–232
design parameters impact, 232
material properties and cutting performance, 224–228
material properties and secondary effects, 228–229
ultrasonic parameters, 229–231
ultrasound-induced modifications
fracture modification, 217–219
friction modification, 219–220
secondary effects, 220–221
Ultrasonic extraction
food ingredients modification
background, 355
extracted components separation, 360
functional compounds extraction, 357–358
industrial extraction application and design, 361–363
mechanisms and process development, 355–357
simultaneous extraction/modification, 363–366

Ultrasonic (*cont.*)
simultaneous extraction/modification, 363–366
and encapsulation, 365–366
antioxidant capacity and/or color extraction/modification, 365
polymeric materials molecular weight reduction, 363–364
Ultrasonic membrane processing, 583
concentration polarization, 584–585
crossflow velocity effects, 590
industrial scale module design, 592–593
membrane cleaning, 591–592
membrane fouling, 584–585
operating pressure effects, 588–590
related technologies, 594
solids concentration effects, 590–591
ultrasonic flux enhancement, 585–586
ultrasonic intensity effects, 586–588
See also Ultrasound applications in food processing
Ultrasonic pulse compression (UPC), 96
Ultrasonic separation, 355
extracted components, 360
See also Food ingredients modification
Ultrasound, 1
chemical effects
bubble collapse, 7–9
cavitation, 7–9
sonoluminescence, 9–10
chopped, 54
defined, 1
in food processing, *see* Ultrasound applications in food processing
microbial inactivation, 322–331
amplitude influence, 323
external pressure influence, 324
frequency influence, 324
future prospects, 340
inertial cavitation, 322
non-inertial cavitation, 322
presence of impurities influence, 324
temperature influence, 324
ultrasound and chemicals, 334–339
ultrasound and mild heating, 332–334
ultrasound and non-thermal physical factors, 339–340
physical effects
cavitation, 2–7
steady streaming, 2
types
diagnostic, 1
power, 1
See also Multi-frequency, multimode, modulated (MMM) technology; Power ultrasound
Ultrasound applications in food processing, 65–101
beverages
low intensity ultrasound, 95
power ultrasound, 95
cleaning, 98–99
crystallization, 97
diary, *see* Dairy products processing
energy, 79
extraction, 97–98
foaming property, 99
freezing, 97
general principles, 66–68
condensation, 66
high-intensity ultrasound overview, 78
high-versus low-intensity ultrasound, 76
low-intensity ultrasound overview, 77
rarefaction, 66
ultrasonic equipment overview, 69–76
inertial cavitation aspects, 68
low-intensity ultrasound, 93–94
microbial and enzyme inactivation, 83
enzymes, 91–93
microorganisms, 84–91
power, 78
cavitation and, 82
frequency, 80–81
high-power sonication effects, 81–82
inertial versus non-inertial cavitation, 82–83
power intensity, 80
vibrational amplitude, 79
power ultrasound, 82–95
quality assurance aspects
beverages, 95
bread, 95
cheese and tofu manufacturing, 94
product identification aspects, 96–97
solubility property, 99
temperature aspects, 81
thawing, 97
ultrasonic equipment overview, 69–76
electrical generator, 69
emitter (baths, horns, and sonotrodes), 75
examples, 75–76
Ultrasound-assisted freezing, 495
efficiency aspects
acoustic power influence, 500–502

influence on freezing rate, 496–500
ice nucleation temperature, 502–505
tissue orientation, 505–507
Ultrasound-assisted hot air drying, 511–513
main systems for
application system, 515
generator, 515
siren and whistle systems, 515–516
solid–gas applications, 515
solid–liquid applications, 515
stepped plates, 516–517
transducer, 515
vibrating cylinders, 517–518
process variables influence, 519
air velocity, 520–523
applied acoustic energy, 526–527
material structure, 528–531
temperature, 523–525
ultrasound effect on mass transfer, 513–514
Ultrasound-assisted hydrothermal treatment
nanomaterials (metal oxide), 417–418
Ultrasound-assisted supercritical extraction (USFE) technique, 637–638
See also Airborne power ultrasound
Ultraviolet (UV) light
using cavitation in SPR, 204–207
waves, 68

V
Vanadium oxide, 419
Vegetables dehydration
airborne power ultrasound food processing applications, 623–633
See also Drying
Velocity
crossflow velocity effects, 590
See also Ultrasonic membrane processing
Vibrating cylinders, 517–518
Vibrational amplitude
power measurement aspects, 79
See also Frequency; Power
Viscosity
high-power ultrasonics in industrial applications
viscosity alteration, 607
viscosity parameter, 603
milk pasteurization with power ultrasound, 451–453
viscous drag force and nucleation of bubbles, 49
Vitamins/minerals nutritional properties, 451
See also Pasteurization
Volatile fatty acids, 570
Vortex cavitation, 191

W
Water
thermolytic cleavage sonochemical reaction, 244–245
See also Food ingredients engineering
Whey
lactose recovery from (sonocrystallization case study), 476
experimental methodology, 476–477
operating parameters effect on lactose recovery and crystal habit, 477–481
process optimization using statistical analysis, 481–483
protein, 566
protein concentrate (WPC), 565–566
See also Milk
Whiskers (TiO_2), 418
Whistle systems, *see* Siren and whistle systems
Wideband technology, *see under* Multi-frequency, multimode, modulated (MMM) technology
Wines, 570–571
Wool
silver nanoparticles on wool fibers, 432
See also Nylon

Y
Yogurt, 560
power ultrasound processing, 459–461
See also Milk

Z
Zero-phase-locked loop (ZPLL), 135
Zinc (Zn)
chalcogenides (ZnSe), 435
nanocrystalline ZrO_2, 418
nickel–zinc ferrite powders, 418
oxide nanoparticles, 417
ZnS nanoparticle-assembled mesoporous structure, 424
zirconia
ceria–zirconia-supported ruthenium, 432
mixed oxide ($CuO–ZrO_2$ catalysts), 420
See also Nanomaterials